

PEDIATRIC
X-RAY DIAGNOSIS

Volume 2

*A Textbook for Students and Practitioners
of Pediatrics, Surgery & Radiology*

CONTRIBUTING AUTHORS

FREDERIC N. SILVERMAN, M.D.

*Professor of Pediatrics and Radiology, Cincinnati College of Medicine
Radiologist and Attending Pediatrician, Children's Hospital of Cincinnati*

DAVID H. BAKER, M.D.

*Professor of Radiology, College of Physicians and Surgeons, Columbia
University, Radiologist to the Babies Hospital, New York City*

WALTER E. BERDON, M.D.

*Professor of Radiology, College of Physicians and Surgeons, Columbia
University, Radiologist to the Babies Hospital, New York City*

JOHN DORST, M.D.

Professor of Radiology, Johns Hopkins University, Baltimore

BERTRAM R. GIRDANY, M.D.

*Professor of Radiology, School of Medicine, University of Pittsburgh
Radiologist to the Children's Hospital of Pittsburgh*

FRED A. LEE, M.D.

*Clinical Associate Professor of Radiology, School of Medicine, University of
California, Radiologist to Children's Hospital, Los Angeles*

CHARLES E. SHDPPNER, M.D.

*Professor of Radiology and Director of Radiologic Education, and
Director, Division of Diagnostic Radiology, University of Alabama, Birmingham*

6th EDITION

PEDIATRIC X-RAY DIAGNOSIS

by

JOHN CAFFEY

A B, MD (MD, Hon, University of Torino, Italy)

*Visiting Professor of Radiology and Pediatrics School of Medicine
University of Pittsburgh Roentgenologist, Children's Hospital of
Pittsburgh Professor Emeritus of Radiology College of Physicians
and Surgeons Columbia University Consultant Radiologist
Columbia Presbyterian Medical Center, New York City*

VOLUME 2

YEAR BOOK MEDICAL PUBLISHERS



INCORPORATED

35 EAST WACKER DRIVE • CHICAGO

COPYRIGHT © 1945 1950 1956 1961 1967 and 1972 BY
YEAR BOOK MEDICAL PUBLISHERS INC

All rights reserved. No part of this publication may be reproduced stored
in a retrieval system or transmitted in any form or by any means elec-
tronic, mechanical photocopying recording or otherwise without prior
written permission from the publisher

Published 1945

Reprinted 1946

Revised 1950

Revised, 1956

Revised 1961

Reprinted 1963

Revised 1967

Reprinted 1970

Revised November 1972

Reprinted, January 1973

Library of Congress Catalog Card Number 78-182005

International Standard Book Number 0-8151 1426-5

PRINTED IN U.S.A.

7.14-1
0.5-1

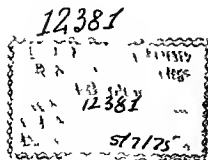


Table of Contents

VOLUME 2

SECTION 5	The Pelvis	717
The Pelvis	Normal	717
	Roentgen Appearance	718
	Normal Variations	719
	Congenital Malformations	730
	Diseases of the Pelvis	740
	Intrinsic Generalized Skeletal Dystrophies	740
	Fractures of the Pelvis	743
	Ischiopubic Osteochondrosis Juvenilis	743
	Osteitis of the Pelvic Bones	747
	Hypovitaminosis	747
	Coxa Vara and Coxa Valga	748

SECTION 6	The Urinary Tract	753
The Urinary	Normal Anatomy	753
Tract and	Normal Roentgen Appearance	757
Adrenal Glands	Excretory Urography	758
	Cystography	766
	Retrograde Urography	768
	Special Examinations	769
	Congenital Malformations	770
	Anomalies of the Kidneys	771
	Anomalies of the Renal Pelvis and Ureter	777
	Anomalies of the Bladder	782
	Anomalies of the Urethra	784
	Urinary Obstruction	785
	Roentgen Appearance at Different Levels	785
	Other Conditions Associated with Genitourinary Anomalies	793
	Urinary Calculi	795
	Trauma	798
	Urinary Infections	800
	Acute Infections	800
	Chronic and Recurrent Infections	801
	Neoplasms	805

VI / TABLE OF CONTENTS

	The Adrenal Glands	813
	Neoplasms	816
	Adrenal Insufficiency	818
SECTION 7	The Genital Tract	821
The Genital Tract	Methods of Examination	821
	Intersex	823
	Vaginitis	832
	Genital Tract Obstruction and Tumors	833
	Gynecologic Aspects of Imperforate Anus (Ectopic Anus)	835
	Bladder Exstrophy	839
SECTION 8	The Soft Tissues	847
The Extremities	Inflammations	849
	Neoplasms	850
	Calcification	851
	Foreign Bodies	853
	Interstitial Emphysema	857
	Muscular Dystrophies	858
	The Bones	873
	Normal Structure	873
	Roentgenographic Appearance	878
	Growth and Maturation	879
	Primary Ossification Centers	879
	Growth in Length	881
	Secondary Ossification Centers	881
	Constriction (Modeling)	885
	Velocity of Growth and Development	885
	Anatomic Variations	895
	Local	895
	Multiple Generalized and Scattered Normal Variants	900
	Diseases of Bone	963
	Generalized Undercalcification (Atrophy Rarefaction)	964
	Generalized Overcalcification (Hypertrophy Sclerosis)	965
	Focal Undercalcification	965
	Focal Overcalcification	966
	Constriction (Tubulation Modeling)	966
	<i>Transverse Lines of Park (Stress Lines of Park)</i>	969
	Alterations in Growth and Development	976
	Maturation of the Skeleton	977
	Congenital Malformations	978
	Congenital Intrinsic Dysplasias	998
	The Miscellaneous Intrinsic Dwarfs	1071
	Bone Lesions Due to Physical Agents	1082
	Fractures	1083
	Infections	1192
	Avitaminoses	1222
	Hypervitaminosis	1243
	Bone Tumors	1249

SECTION 9 The Vertebral Column

Bone Changes with Diseases of the Blood and Blood Forming Organs	1279
Skeletal Changes in the Endocrinopathies	1299
Bone Changes in Diseases of the Central Nervous System	1317
Bone Changes Associated with Cardiac Disease	1320
Bone Changes Associated with Diseases of Alimentary Tract	1320
Bone Changes Associated with Respiratory Disease	1320
Bone Changes Associated with Renal Disease	1321
Bone Changes Associated with Cutaneous Disease	1322
The Joints	1326
Normal Anatomy	1326
Normal Roentgen Appearance	1329
Diseases of the Joints	1331
Congenital Malformations	1332
Traumatic Changes	1332
Infectious Arthritis	1333
Bursitis	1336
Tuberculosis of Joints	1336
Rheumatic Fever	1337
Leukemic Arthritis	1337
Osteoarthritis (Hypertrophic Arthritis)	1338
Rheumatoid Arthritis	1338
Calcification of Cartilage and Joints	1346
Intermittent Hydrarthrosis	1348
Cysts and Neoplasms	1348
Normal Vertebral Column	1351
Anatomy	1351
Growth and Development	1352
Primary Ossification Centers	1353
Secondary Ossification Centers	1354
Roentgen Appearance	1355
Congenital Disturbances	1358
Malformations	1358
Systemic Dysplasias	1369
Achondroplasia	1369
Mucopolysaccharidoses	1369
Osteogenesis Imperfecta	1370
Osteopetrosis (Marble Bones)	1370
Traumatic Lesions	1372
Dislocations	1372
Fractures	1372
Traumatic Lesions in the Disks	1376
Traumatic Disorders of Growth	1377
Vertebra Plana (Calve)	1377
Adolescent Kyphosis (Scheuermann Schmorl Disease)	1381
Habitual Idiopathic Scoliosis	1383
Chronic Hypoxia	1383

VIII / TABLE OF CONTENTS

	<i>Calcification of Intervertebral Disks</i>	1385
	<i>Diseases Involving Vertebrae</i>	1387
	Infections	1387
	Nontuberculous	1387
	Tuberculous Spondylitis	1387
	Rheumatoid Arthritis	1391
	Syphilis	1391
	Hypovitaminoses	1391
	Vitamin D	1391
	Vitamin C	1391
	Marginal Lines	1392
	Endocrine Disorders	1392
	Reticulosis	1393
	Hemolytic Anemias	1393
	Leukemia	1393
	Cysts	1395
	Neoplasms	1395
	Primary Lesions	1395
	Secondary Neoplasms	1395
	Tumors of the Spinal Cord	1395
SECTION 10	<i>Special Procedures in Diagnosis</i>	1399
The Neonate and	Total Body Opacification	1399
Young Infant	Arteriography	1403
	Lymphangiography	1419
	Nuclear Medicine Isotopic Scanning	1422
	Ultrasound	1431
	Carbon Dioxide Contrast Studies	1431
	<i>The Chest</i>	1436
	Radiographic Technique	1436
	Factors Determining Fetal Lung Growth	1437
	The Newborn with Respiratory Distress	1438
	Surgical Conditions of the Newborn Chest	1459
	<i>The Gastrointestinal Tract</i>	1478
	The Fetal Gastrointestinal Tract	1478
	Gastrointestinal Tract in the First Hours of Life	1479
	Radiographic Evaluation of Newborns with Gastrointestinal Obstruction	1479
	Esophagus	1483
	Stomach	1492
	Duodenum	1495
	Small Bowel	1502
	Colon	1511
	Gallbladder, Bile Ducts, Liver	1531
	<i>The Genitourinary Tract</i>	1539
	Renal Function in Fetus and Newborn	1539
	Uroradiologic Procedures	1542
	Genitourinary Causes of Abdominal Masses	1547

TABLE OF CONTENTS / IX

	Hydronephrosis	1547
	Urethral Obstruction	1551
	Triad Syndrome (Prune Belly or Eagle Barrett Syndrome)	1554
	Vaginal Obstruction	1556
	Vascular Disturbances of the Neonatal Kidney and Adrenal	1557
	Adrenal Hemorrhage and Calcifications	1559
	Renal and Adrenal Tumors	1561
	Renal Cystic Disease	1565
	Screening Intravenous Pyelograms in Newborns with Anomalies	1570
SECTION 11	Artifacts and Natural Misleading Images	1573
Artifacts, Natural Misleading Images	Index	XI

VOLUME 1 (PARTIAL CONTENTS)

Section 1 THE HEAD AND NECK

Section 2 THE THORAX

Section 3 THE HEART

Section 4 THE ABDOMEN AND GASTROINTESTINAL TRACT

SECTION 5

The Pelvis

The Pelvis

Normal

THE ABDOMEN and the true pelvis are separated by the plane of the pelvic inlet which is determined by the promontory of the sacrum and the iliopectineal line. The bony pelvic girdle consists of the sacrum and coccyx behind, the arch of the pubes in front and the ischia, the parts of the ilia below the iliopectineal line and the pubic rami at the sides (Fig. 5-1).

The pelvis of fetus, infant and child are conspicuously small and funnel shaped, during the neonatal period the vertical diameter is elongated in proportion to the lateral and sagittal diameters. At birth the pelvic inlet tends to be more circular than in older age periods, also, the acetabular cavities are relatively larger and shallower and the obturator foramina are proportionately smaller and situated nearer together. The sacrum makes up a larger segment of the pelvic girdle during the first years and is situated higher in relation to the ilia than later. The infantile sacral promontory is less marked than in the adult. There is little change in the pelvic shape until the infant assumes the erect posture, when the sacrum descends between the ilia and the promontory becomes conspicuous. Pelvic growth is rapid during the first two years after which growth is slow until puberty. Postpuberal growth is principally epiphyseal.

Anatomists claim that sexual differences in pelves can be recognized as early as the 4th fetal month and are present at birth. The differential prenatal sexual characteristics are lost during the early rapid growth of the first two years of postnatal life. Reynolds found in a roentgen study of the pelvic girdle during the 1st year of life, that growth is most rapid from birth to 3 months, growth curves of boys and girls ran parallel. In boys the pelvic height was greater, the ilium broader and the ischiohiac space larger, girls showed greater bischial breadth, pubis length, sciatic notch and relative inlet breadth. The larger pelves were associated in boys, with earlier appearance of the ossification centers in the remainder of the skeleton and in both sexes, with earlier appearance of the first tooth. During childhood males and females have almost

identical pelves all are the anthropoid (dolichopelvic) type. The major sexual features do not reappear until after puberty. The time of appearance of the constant secondary epiphyseal centers is shown in Figure 5-2. Sometimes homologous centers on the two sides do not appear or fuse at exactly the same time, in cases of injury these unilateral normal secondary centers should not be mistaken for fracture fragments.

Fig. 5-1—Normal pelvis of a girl 10 years of age. The three major bones of the pelvis are still ununited. Cartilage covers the crest of the ilium, the body and inferior ramus of the pubic bone and the body and descending ramus of the ischium. These are the counterparts of the epiphyseal cartilages of the long tubular bones and secondary ossification centers appear in them during and after pubescence. The subchondral edges of all of these bones are not cortical walls but are provisional zones of calcification similar to those in the metaphyses of the long bones. (From Spalteholz.)



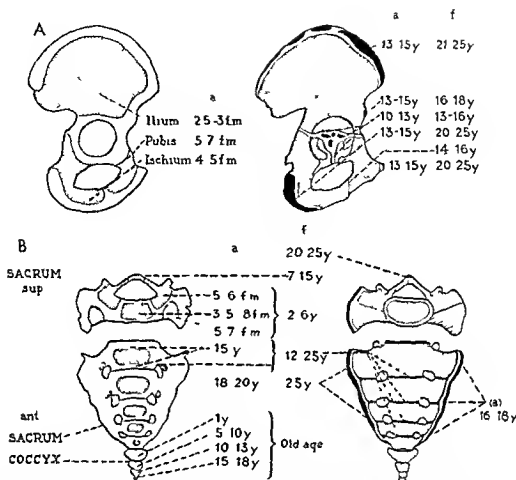


Fig 5-2.—Time of appearance of the secondary ossification centers in the innominate bone (A) and the sacrum (B) a = time of

appearance f time of fusion fm fetal months y years (Redrawn from Morris *Human Anatomy*)

In girls, the ossification centers in the crests of the ilia usually appear within six months of the onset of menstruation, it is possible that the beginning of ossification in the crests of the ilia of boys represents an analogous level of gonadal maturation

REFERENCE

- Reynolds E J The bony pelvic girdle in early infancy A roentgenometric study *Am. J Phys Anthropol* 3:321 1945

Roentgen Appearance

NORMAL SOFT TISSUES—In frontal projections, overlapping of the buttocks may be responsible for a vertical spindle shaped shadow of increased density which is superimposed on the symphysis pubis at or near the midsagittal pelvic plane (Fig 5-3, A) Axial projection of the shaft and head of the penis results in a surprisingly heavy, rounded shadow (Fig 5-3, B) which may suggest to the inexperienced observer a metallic foreign body in the rectum or bladder or in

tripelvic calcification Superimposition of the shadow of the penis on the bones of the pubic arch may give rise to shadows suggestive of localized osteosclerosis

Inconstant shadows of diminished density in the pelvis are cast by gas in the pelvic segments of the small intestine, colon and rectum Gas shadows superimposed on the pelvic bones produce local areas of diminished density which must not be confused with bone defects or bone destruction Residual barium foreign bodies and fecaliths in the appendix, colon and rectum all cast opaque pelvic shadows After excretory urography, residual contrast agent in the urinary channels may persist above the sites of obstruction

ABNORMAL SOFT TISSUES—As in other parts of the body, tumors cast shadows of increased density Dermoids and teratomas are not infrequently located in the buttocks The skeletal components of teratomas cast opaque shadows Occasionally dermoids contain tissue and fluid with a high fat content which casts a large shadow of diminished density Plugs of air-containing materials inserted into the vagina as



Fig. 5-3.—A, spindle-shaped shadow of increased density in the midpelvic plane caused by overlapping buttocks. B, heavy circular shadow cast by the penis projected in the axial plane.

menstrual absorbents cast a radiolucent image of the distended vaginal lumen and sometimes deform the bladder (Fig. 5-4). Opaque urinary stones and opaque appendiceal fecaliths should be considered when small opaque images are encountered. Myositis ossificans and interstitial calcinosis may be the source of opaque shadows derived from the pelvic walls. Calcifying tuberculous lesions in the urogenital system and in the pelvic lymph nodes are also responsible for intrapelvic opaque shadows. Pelvic phleboliths are rare in children, but are occasionally seen in association with pelvic hemangiomas.

REFERENCES

- Gross, R. E., *et al.*: Sacrococcygeal teratomas in infants and children, *Surg., Gynec. & Obst.* 92:341, 1951.
 Palumbo, L. T., *et al.*: Sacrococcygeal teratomas: Review of the literature; report of a case in an adult containing a glomus, *Ann. Surg.* 133:421, 1951.

NORMAL PELVIC SKELETON.—The roentgen appearance of the normal pelvis is depicted in Figure 5-5.



Fig. 5-4.—Radiolucent image of the vaginal lumen cast by air in a vaginal plug of menstrual absorbent.

During pubescence the secondary centers, illustrated in Figure 5-2, appear. Detail of a normal secondary center in the ilium as seen on roentgen films is shown in Figure 5-6.

Normal Variations

Bands of increased density form at the sites of growth and endochondral bone formation in the flat bones of the pelvis, just as they do in the long bones (Fig. 5-7); and they are produced by the same causal mechanisms as the transverse bands and lines in the metaphyses of the growing long bones.

The vascular markings in the ilium and ischium appear after the 3rd year and then may be conspicuous throughout childhood (Fig. 5-8); they should not be mistaken for destructive defects secondary to disease. The apophyseal center in the crest of the ilial wing often develops from several ossification centers which simulate fracture fragments (Fig. 5-9). The normally thin segments of the ilia, directly above the rims of the acetabula, cast normal images of dimin-

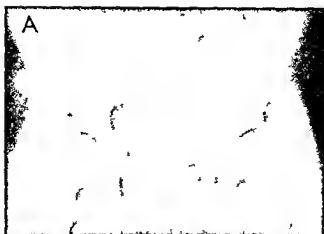


Fig. 5-5.—Normal roentgen appearance of the pelvis at different ages. **A**, at 3 months of age in a girl, the ischiopubic synchondroses are widely opened. The symphysis pubis is normally wide. The ossification centers in the femoral epiphyses have not yet appeared. **B**, at 5 years, the ilia are still separated from the ischia and pubic bones, but the ischiopubic synchondroses are almost completely closed; the lateral masses of the sacrum have

fused with their bodies; the scapulae are proportionately smaller and deeper than in **A**. **C**, at 14 years, the innominate bone is completely fused, and secondary centers are now visible in the crests of the ilia and in the inferior margins of the ischia (arrows). A small paraglenoid fosse indents the top of each sciatic notch.

Fig. 5-6—**A**, normal secondary epiphyseal center in the crest of the ilium of a girl 12 years of age. The edges of the striplike crestal center and the contiguous edge of the ilium are both normally irregular—often more irregular than in this normal patient. **B**,

apophyseal center on the inferior ramus of the ischium of an asymptomatic girl 15 years of age. The radiolucent strip between the apophyseal new bone and the edge of the ischium simulates a fracture line.

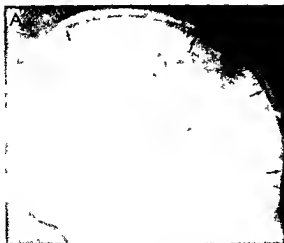




Fig 5 7 —Phosphorus bands in the flat bones and long bones of the pelvis and thighs. This patient was given large doses of yellow metallic phosphorus for four times at intervals of several months. Curved and straight phosphorus opaque bands have formed at all of the sites of cartilaginous growth and endochondral bone formation in a series of four corresponding to the four episodes of ingestion. The velocity of growth can be measured by the distances between the lines. It is clear that growth of the distal wings is much more rapid than growth of the base of the ilium and on the caudal edge of the ischium where the phosphorus bands are crowded together. At this age the longitudinal growth of the distal wings approximates that of the proximal ends of the femurs. Similar but less conspicuous bands form after the administration of lead bismuth and also during formation of the tines of Park in the long bones. (From Rubin.)

Fig 5 8 —Normal vascular markings in the pelvic bones. **A**, Y shaped tubular shadow (arrows) in the ilium of a boy 4 years of age. **B**, circular vascular foramen (arrow) in the body of the is-

chium of an asymptomatic girl 4 years of age. Sometimes several small circular foramina are present in the same site instead of a single large foramen as in this patient.

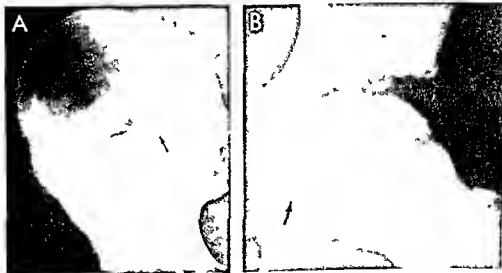


Fig 5 9 —Multiple independent ossification centers in the apophyseal cartilage of the crest of the ilium of a healthy girl 15 years of age which simulate comminuted fracture fragments.





Fig 5-10—Normal supra acetabular patches of rarefaction in a healthy boy 9 years of age. These normal patches have been confused by some with such destructive lesions as eosinophilic granuloma, leukemia, Ewing's neoplasm and other malignancies.

ished density which may be mistaken for areas of destruction (Fig 5-10).

Occasionally accessory secondary centers develop in the spine of the ischium and in the superior margin of the acetabulum (Fig 5-11). They are usually visible between the 14th and the 18th year after which they fuse with the main mass of the ischium and ilium respectively. Zander emphasized that the *ossae tomicae* of acetabuli is an ossification center—often a group of bony nodules—which appears during puberty in the anterior segment of the Y cartilage in the wall of the acetabulum. The roentgenologic os acetabuli in contrast is a single bony center which arises in the thick cartilage that forms the rim of the posterior segment of the acetabulum (Fig 5-12) during puberty after several years it normally fuses solidly

Fig 5-12.—Os acetabuli marginalis superior in the cartilaginous rim of the acetabulum of a girl 11 years of age. These normal separate marginal ossicles should not be mistaken for fracture fragments or calciferous foci in the soft tissues.



Fig 5-11—Accessory secondary pelvic ossification centers tracing of a roentgenogram. Ossicles in the rim of the acetabulum and in the tip of the ischial spine in a patient 14 years of age.

with the contiguous portion of the body of the ilium. For this posterior marginal ossicle Zander proposed the name os acetabuli marginalis superior. In some cases the marginal center in the acetabular rim persists as a separate ossicle—either unilateral or bilateral—and may be confused roentgenographically with chip fracture in the case of injury or with sequestrums or peritendinitic calcifications in the case of regional pain and inflammation. During puberty the strip of cartilage in the incisura acetabuli may cast a linear shadow of diminished density on the head of the femur which simulates fracture of the femoral head.

Ossification of the cartilage in the ischiopubic synchondrosis is extremely variable in both velocity and pattern. We found that bilateral fusion of the ischiopubic synchondroses is complete in about 5% of children at 4 years of age and in 82% at 12 years. Unilat

Fig 5-13—Irregular mineralization and swelling of the left ischiopubic synchondrosis in an asymptomatic boy 7 years of age. The osteoporotic swollen synchondrosis projects into the obturator foramen.





Fig 5-14—Early closure of the ischiopubic synchondroses in a normal girl 2 years of age. The rest of the skeleton had normal maturation.

eral swelling at the synchondrosis (Fig 5-13) was present in 57% of children at 7 years and bilateral swelling in 40% at 7 years. In some girls the ischiopubic synchondrosis may close as early as the 3rd year (Fig 5-14). We concluded that swelling preceded closure of the synchondrosis in most and perhaps all cases. The swellings lasted from one to three years. Irregular mineralization was present in about 8% of all cases between the ages of 4 and 11 years; it was never present without swelling and tended to develop in the more pronounced examples of swelling. We have seen the completely closed ischiopubic synchondrosis demineralize and swell and then fuse completely a second time in the absence of any clinical signs of disease at this site (Fig 5-15). Rarely an in-



Fig 5-16—Independent supernumerary ossification center in the ischiopubic synchondrosis of an asymptomatic boy 5 years of age.

dependent supernumerary ossification center may develop in the ischiopubic synchondrosis (Fig 5-16). Kaufmann observed a similar center in an infant 6 months of age. Junge and Heuck found swelling and irregular mineralization in 50% of 358 healthy children. They believed that excessive weight bearing on one side caused ipsilateral changes at the ischiopubic synchondrosis.

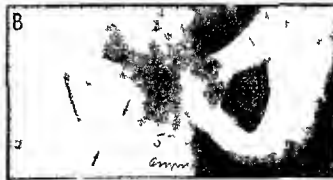
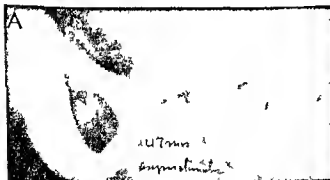


Fig 5-15—Demineralization and swelling of the ischiopubic synchondrosis after a first complete closure followed by a second complete closure. A, complete closure at 47 months of age. B, demineralization and swelling at 57 months. C, second complete closure at 69 months.



Fig. 5-17—Focal retarded ossification of the inferior ramus of the pubic and ischial bones on both sides in a girl 10 years of age. These were chance findings in the premenstrual excretory urography. Also, her sacrum was rotated upward and backward and its caudal four segments were hypoplastic.

Cases have been reported in which regional pain and tenderness and impaired locomotion were associated with irregular mineralization and swelling of the ischiopubic synchondrosis; this clinical picture and the associated roentgen finding have been called ischiopubic osteochondrosis, in the belief that it is analogous anatomically and pathogenetically to ischemic necrosis of the skeleton such as Perthes' disease in the head of the femur and Koehler's disease in the tarsal scaphoid. Apparently the prognosis has always been favorable in so-called ischiopubic osteochondrosis. The normally irregular mineralization in this area should be kept in mind when the question of early osteomyelitic or neoplastic destruction is raised. Devay suggested that stress fractures might cause some of these changes; this appears to be unlikely. We have seen one example of localized slowing of ossification of the ischial ramus (Fig. 5-17). Byers found normal bone and cartilage in a biopsy specimen.



Fig. 5-19—Patchy soap bubble rarefaction of the ischial ramus and tuberosity on the left with similar but much less marked changes at the same site in the right ischium of an asymptomatic boy 12 years of age. (Courtesy of Dr. R. Parker Allen, Denver, Colo.)

It should be emphasized that the medial edges of the bodies of the pubic bones are often irregularly mineralized in apparently healthy children.

Irregularities in the posterolateral edge of the ischium may also be observed occasionally during preadolescence; the lateral borders of the body of the ischium and its inferior ramus show marked irregularity both in the margin and in density (Figs. 5-18 and 5-19). We have seen one example of ischial irregularity with marked fluctuations on the two sides during the 11th and 12th years (Fig. 5-20). In two other asymptomatic boys the two sides were unequally affected (Fig. 5-21). In one of our patients some healing occurred during a period of six months (Fig. 5-22). It should be remembered that during growth and before fusion of the body of the ischium to its scale epiphysis along its under edge (see Figs. 5-1 and 5-2 A) this ischial edge is a provisional zone of calcification and is analogous to the provisional zones of calcification in the metaphyses of all of the long bones. It is not cortical wall made up of lamellar bone. In one of our patients an asymptomatic boy the ischial edges were normally smooth at age 10 years but deep irreg-

Fig. 5-18—Marginal irregularities (arrow) on the lateral edge of the descending ramus of the right ischium of a healthy boy 12 years old.



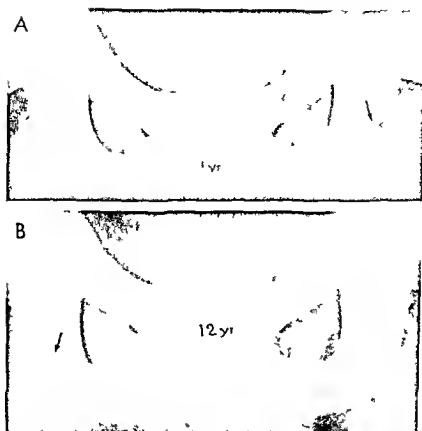


Fig. 5-20 —Bilateral fluctuating irregularities in density of the ischial tuberosities. In A, at 11 years of age, the left ischial tuberosity is irregular and poorly mineralized. In B, at 12 years of age,

the right ischial tuberosity is irregular and rarefied; the left tuberosity is now of normal density and has a smooth edge. These were chance findings in an asymptomatic boy.

Fig. 5-21 —Irregularities in both ischia of asymptomatic boys, 12 and 11 years of age. In A, the right ischium is irregularly rarefied at the tuberosity and slightly caudad into the ramus. The

tuberosity of the left ischium is evenly rarefied. In B, there is bubbly rarefaction in the site of the right tuberosity and caudad into the ramus.





Fig 5-22—Serial changes during six months of irregular mineralization of the right ischial ramus and body. This boy, 15 years of age, had had vague pains in the lumbar region of indefinite onset. A, on May 25, there is a large radiolucent defect in the

right ischium. B, on September 17, the defect has filled in. In part C, on November 8, the previously radiolucent segment is now sclerotic and the contiguous segment is slightly avulsed.

anterior were evident six months later. Large radiolucent defects are occasionally found in the inferior ramus of the ischium (Fig 5-23) of healthy children. In one of our patients, a man 22 years of age who had pain in the left buttock, normal cartilage was found in deep marginal ischial irregularities (Fig 5-24).

The lesser sciatic notches vary greatly in size in different individuals and on the two sides of the same individual (Fig 5-25). These notches are usually not visible during the first months of life, and increase in size and conspicuousness with advancing age.

It should be clear that the diagnosis of osteochondrosis juvenilis should be made with great reserve in these sites where irregular mineralization appears to be a normal anatomic variant in so many healthy asymptomatic children. In the pelvis these sites include the crest of the ilium, roof of the acetabulum, bodies of the pubic bones, ischiopubic synchondroses and the lateral aspect of the ischia. By the same token, when destructive lesions of inflammation and

Fig 5-23—Large sharply defined patch in the ischium of an asymptomatic girl 12 years of age. The nature of this variant was never determined.





Fig 5-24—Deep marginal irregularities in the left ischial tuberosity and ramus of a man 22 years of age who had completed

of penis in the left buttock for three months. Biopsy showed normal cartilage in the sites of the irregularities of the ischial edge.

neoplastic growth develop in these same sites, early roentgen diagnosis will be uncertain until the changes exceed the limits of normal variation.

Vertical clefts, unilateral and symmetrically bilateral, are found in the superior pubic ramus in about 1% of healthy newly born infants (Fig 5-26). Usually these radiolucent lines disappear completely during the first weeks of life. In one of our cases, the cleft persisted with marginal strips of sclerosis which simulated a fracture. Retarded and irregular mineralization of the pubic ramus may also be bilateral at birth and then gradually mineralize completely from several ossification centers during the first months of life (Fig 5-27). These findings indicate that sometimes the superior ramus of the pubic bones mineralize from several centers in the ramus rather than by the usual direct, even extension from a single primary ossifica-

tion center. It seems likely that the vertical radiolucent clefts seen radiologically represent bars of non calcified cartilage between the expanding ossification centers.

Iliac "horns" have been found in association with a wide variety of mesodermal and ectodermal defects. The "horns" are actually bony processes which project dorsad from the wing of each ilium (see Fig 8-841).

Failure of segmentation between the lateral masses

Fig 5-26—Congenital strip defect in the superior ramus of the pubis. These lesions may be unilateral or bilaterally symmetrical. A, at birth, there is a vertical band of diminished density in the middle third of the pubic ramus. B, at 6 months, at the same site there is a narrower radiolucent band which is now bordered by strips of increased density. The patient was always asymptomatic, and palpation disclosed no signs of fracture at this site.



Fig 5-25—Conspicuously deep and large lesser sciatic notches with sclerotic edges (arrows) in an asymptomatic boy 4 years of age.



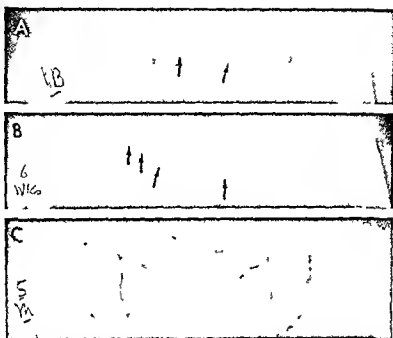


Fig 5-27—Retarded and irregular mineralization of both superior pubic rami. **A**, neonatal. In the pubic rami ossification is confined on each side to a round center. Most of the superior pubic rami are entirely radiolucent because ossification has not yet occurred. **B**, at 5 weeks. Ossification is now increased in both superior rami, but it is still incomplete and irregular. On the right side there are at least three large independent ossification centers with radiolucent clefts between them. **C**, at 5 months. The superior rami are evenly and extensively ossified, but there is still cartilage between the dorsal ends of the rami and their ischial bodies. The changes in the pubic bones are chance findings in a patient who also had bilateral dysplasia and dislocation of the hips.

ers with radiolucent clefts between them. **C**, at 5 months. The superior rami are evenly and extensively ossified, but there is still cartilage between the dorsal ends of the rami and their ischial bodies. The changes in the pubic bones are chance findings in a patient who also had bilateral dysplasia and dislocation of the hips.

of the 1st sacral segment and the transverse processes of the 5th lumbar is responsible for the variant known as sacralization of the 5th lumbar vertebra (Fig 5-28). In infants and children this condition is rarely associated with regional signs and symptoms. Vinke and White found that congenital narrowing of the lumbosacral space frequently accompanies sacralization of the 5th lumbar vertebra.

In rare cases bilateral sacrococcygeal ossicles resemble coccygeal ribs (Cornwell and Ramsey).

Defects in mineralization of the sacral neural arches are common in apparently normal infants and children. The adjoining neural arches of the 5th and 4th lumbar segments are often similarly affected (Fig 5-29). It should be emphasized that these imaging defects are not necessarily actual anatomic defects in

Fig 5-28—Sacralization of the 5th lumbar vertebra. **A**, in a boy 6 years of age. **B**, in a boy 11 years of age.



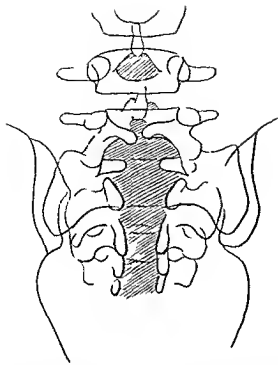


Fig 5 29 — Sacral spina bifida occulta in a patient 5 years of age. tracing of a roentgenogram. Wide midline defects are present in the neural arches in all levels of the sacrum. a narrow defect is visible in the 5th lumbar vertebra. It is probable that the neural arches are complete but incompletely ossified near the midsagittal plane. Actually these radiographic defects represent persistent synchondroses in the neural arches rather than defects warranting the name spina bifida occulta.

Fig 5 30 (left) — Normal irregular margins of the acetabulum in a boy 6 years of age.



the neural arches and for this reason "spina bifida occulta" is often a misleading name for them. The arch is usually intact anatomically, and the image defect represents a localized deficiency of ossification in cartilage rather than a gap in the arch itself. In many cases the defects seen during the early years of life disappear later owing to ossification of the cartilaginous segment, which looked like a defect in the arch radiographically. Sutow and Pryde pointed out that incidence of the radiographic defect diminishes with advancing age, in males from 22% at 7–8 years to 4% in adults and in females from 9% at 7–8 years to 1% in adults. Fawcitt found some degree of radiographic spina bifida occulta (usually incomplete ossification of the arch) in 82% of 500 English children. It is unlikely that these radiographic defects represent actual anatomic defects in this high incidence especially since Sutow and Pryde showed that they diminish substantially with advancing age.

During the 2nd, 3rd and 4th years the surface of the acetabular cavity becomes irregular and casts an indented tufted shadow (Fig 5-30). These normal irregularities disappear during the first half of the second decade and never reappear.

The superior iliac crest is smooth at birth but often becomes wavy and irregular after the 2nd or 3rd year (Fig 5-31). The ventral segment of the crest is always the most affected and in many cases the scalloping of the crest is confined to the anterior portions. Such crestal irregularities may persist until puberty (see Fig 5-2, A) after which they are obliterated by fusion of the crest of the ilium with the epiphyseal center. Segmental crestal ossification may resemble fracture fragments.

The paragenoid fossas of the ilia become evident

Fig 5 31 (right) — Normal marginal scalloping in the ventral segment of the iliac crest of an asymptomatic girl 6 years of age.



during adolescence one is often much larger than the other and the fossa may fail to develop on one side

REFERENCES

- Byers P D Ischio-public osteochondritis" A report of a case and a review J Bone & Joint Surg 45-B 694 1963
- Caffey J and Madell S H Ossification of the pubic bones at birth Radiology 67 346 1956
- and Ross, S E The ischiopubic synchondrosis in healthy children Am J Roentgenol 76 488 1956
- Comwell W S and Ramsey G H Unusual bilateral sacro-coccygeal ossicles, Radiology 68 70, 1957
- Del Duca, V Davis E V and Barroway J N Congenital absence of the sacrum and coccyx Report of two cases J Bone & Joint Surg 33-A 248 1951
- Devas W B Stress fractures in children J Bone & Joint Surg 45-B 528 1963
- Fawcitt, J Some radiological aspects of congenital anomalies of the spine in childhood and infancy Proc Roy Soc Med 52 331 1959
- Francis, C C Appearance of centers of ossification in the human pelvis before birth Am J Roentgenol 65 778 1951
- Friedman E Os acetabuli Am J Roentgenol 31 492, 1934
- Junge H, and Heuck, F Ischiopubic osteochondropathy With a contribution on the normal development of the ischiopubic junction during the period of growth Fortschr Geb Röntgenstrahlen 78 656 1953
- Karlitz J W Incidence of spina bifida occulta in children with and without enuresis Am J Dis Child 49 125 1935
- Kaufmann H J Historical note on the beginnings of Diagnostic Radiology at Basel's Children's Hospital and description of a new ossification center in the pelvic bones of a child Ann. paediat 199 175 1962
- Rubin P Dynamic Classification of Bone Dysplasias (Chicago Year Book Medical Publishers 1964)
- Sutow W W and Pryde A W Incidence of spina bifida occulta in relation to age Am J Dis Child 91 211 1956
- Vinke T H and White E H Congenital narrowing of the lumbosacral space Surg. Gynec & Obst 76 551 1943
- Zander G Os acetabuli and other bony nuclei, Acta rad 24 317 1943

Congenital Malformations

Persistence of the infantile type of pelvis is responsible for the generally contracted funnel pelvis in the adult Unilateral hypoplasia of one of the wings of the sacrum gives rise to the obliquely contracted pelvis

Fig 5 33 — Congenital regional hypoplasia of the left side of the sacrum (arrows) in a boy 6 years of age who had chronic pyuria



Fig. 5 32 — Hypoplasia of the sacrum with bilaterally contracted pelvis in a girl 10 1/2 years of age. Moderate coxa vara is present in both femurs A frontal and B lateral projections

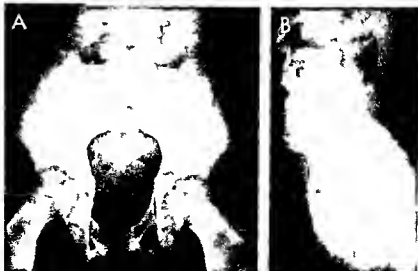




Fig 5-34—Separation of the symphysis pubis and lateral displacement of the pubic bones in a patient 2 months of age with exstrophy of the bladder

undergrowth of both wings produces the rare transversely contracted pelvis (Fig 5-32). This deformity has been recognized in films of the gravid uterus. Gross defects of the sacrum as well as hypoplasia are sometimes encountered (Fig 5-33).

In exstrophy of the bladder the pubic arch appears open and the centers of the pubic bones may be spread several inches apart (Fig 5-34). There is an associated compensatory alteration in the relative positions of the other pelvic bones. In some instances the inferior pubic rami appear to be hypoplastic and their mineralization is delayed. Separation and incomplete ossification of the pubic bones have also been found in association with imperforate anus. diastasis of the recti, deficiencies in the abdominal and pelvic musculature, and epispadias. Weiss and colleagues found that the degree of separation at the symphysis pubis correlates with the degree of epispadias. In slight epispadias the symphysis was normal and in the more severe degrees of epispadias separation at the symphysis was severe and in the most severe degree simulated the wide separation found in exstrophy of the bladder. In a few cases the pubic deficiencies have occurred without other anomalies.

Fig 5-35—A unilateral CDH in a girl 14 months of age. On the right side all three elements in Putz's triangle are visible: (1) hypoplasia of the acetabular roof with increase in its pitch; (2) hypoplasia of the femoral ossification center; (3) dislocation of the

Permanent delayed ossification of the pubic bones is common in cleidocranial dysostosis (Fig 79 C).

REFERENCES

- Blumel J *et al*: Partial and complete agenesis or malformation of the sacrum with associated anomalies. Etiologic and clinical study with special reference to heredity. A preliminary report. *J Bone & Joint Surg* 41 A:497, 1959.
Butterfield L J: Personal communication.
Weiss G *et al*: Epispadias. *Radiology* 90:85, 1968.

CONGENITAL DISLOCATION OF THE HIP (CDH) varies greatly in incidence among different peoples and in different regions. In the Nordics and the mixed white populations of the United States 1-2 per thousand newborns are affected. In large parts of Africa, India, China and Brazil CDH is virtually nonexistent. In a single European country such as Germany, Czechoslovakia, Hungary or Italy CDH is common in some parts and rare in others. In all countries CDH is more common in girls than in boys in the ratio of about 5:1, and it is 10 times as common after breech deliveries as cephalic, but the girl-to-boy ratio is reduced to 2:1. CDH is more common in dizygotic twins; in the

femur cephalad and laterad. The arrow points to a false acetabulum. B: dysplasia with dislocation of the left hip at 3 months of age. The left acetabular angle measures 48 degrees and the left femur is dislocated cephalad and laterad.

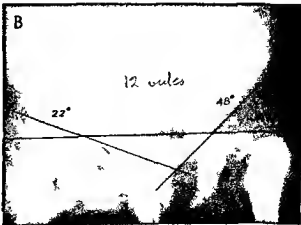
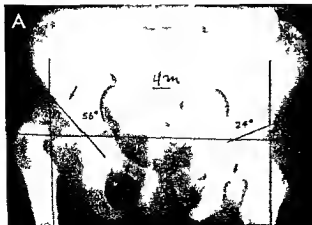


Fig. 5-36 — B lateral CHD in a girl 2 years of age. Putt's line is present on both sides. The right acetabular angle is enlarged to 36 degrees, the left to 44 degrees. The arrows point to bilateral false acetabula.



first born girl and in those born during the summer months CDH supposedly congenital has been reported in rabbits and several breeds of dogs.

Prenatal and perinatal relaxation of the capsule at the hip joint appears to be the basic lesion. Sudden stretching stresses on the capsule such as obstetrical manipulations during delivery (especially in breech presentation) or suspension of the newly born infant by its feet may initiate the dislocation. Limitation of abduction by restrictive clothing or by actual binding of the legs in adduction by Lapps and some American Indians may be responsible for the later onsets of acquired dislocations that lead to permanent dislocations when the joint capsules are hypotonic. Dysplasia of the acetabulum (increased acetabular angle), elongation of the capsule, femoral anteversion and contracture of the periaricular muscles are all secondary complications of primary hypotonia of the joint capsule. The high incidence of CDH in girls suggests a hormonal factor. The higher incidence in

children born during the winter months suggested to Salter that the tight covering of newborn infants with clothing and blankets during cold weather may be a causal factor.

Thieme and colleagues measured the urinary estrogen contents in 16 patients with congenital dislocation of the hip and 19 matched controls during the first six days of life and found no significant differences. Their findings do not support the suggestion of Andren that congenital dislocation of the hip is associated with disturbed estrogen metabolism in the fetus and newly born infant. Hiortorn and James concluded that one single clinical and radiographic examination is not enough; in some cases repeated examinations are essential during the first weeks and months. Among 6000 consecutive newly born infants Small found 24 cases of dislocation of the hip and of the 23 treated with the von Rosen splint 22 had excellent results.

In full dislocation of the hip the radiographic

Fig. 5-37 — A, unilateral dislocation of the hip in an untreated female child 7 years of age. B, the same pelvis after 22 months of thyroid treatment; no other therapy was given. The dislocation has almost completely disappeared; some deformity of the roof of the

acetabulum and flattening of the femoral ossification center are still visible. The generalized advance in maturation of the pelvis and femurs during the thyroid therapy is noteworthy.



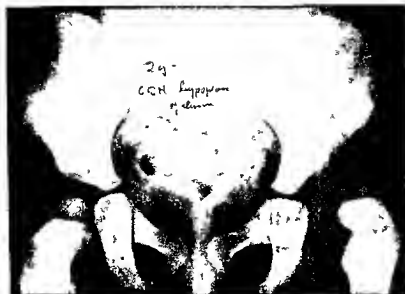
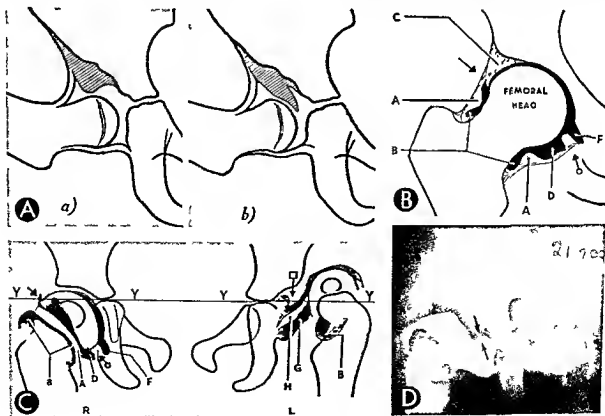


Fig 5 38 — Congenital dislocation of the hip with smallness of the ipsilateral left ilium in a girl 2 years of age

Fig 5 39 — Radiologic findings of infolding of the labrum in opaque arthrograms. *A*, schematic drawing which shows the normal labrum (*a*) and infolded labrum (*b*). *B*, schematic drawing of opaque contrast agent in a normal hip. *A* zona orbicularis. *B* ring of contrast agent around the femoral neck. *C* cartilaginous acetabular roof with fibrocartilaginous limbus dipping into the contrast agent. *D* puddle of contrast agent lateral to the transverse ligament. *F* contrast agent on the medial side of the transverse ligament. *arrow* edge of limbus. *arrow with circle* transverse ligament. *C*, schematic drawing of infolded labrum in

opaque arthrogram. The right hip is normal. The left hip shows the labrum infolded on the face of the acetabulum between the head of the femur and the articular surface of the acetabulum. *A*, *B*, *D* and *F* same as in *B*. *G* capsular isthmus. *H* ligamentum teres. *YY* horizontal lines thru *Y* cartilages. *arrow*, edge of limbus. *arrow with square* limbus infolded into joint. *arrow with circle* transverse ligament. *D*, actual opaque arthrogram showing the fitting defect between femoral head and acetabulum and the spinelike tilting defect (arrows) cast by the tip of the infolded labrum (*B* and *C* from Severin).



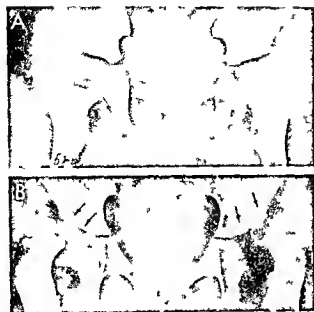


Fig 5-40 — Acquired bilateral dislocation of the hips in neuro-muscular disease. A, normal at 5 months of age. B, bilateral dislocation of the hips at age 5 years. The patient had meningo-encephalitis at 5 months of age, followed by persistent generalized spasmodic paraplegia.

changes present no difficulties in diagnosis, which is warranted when the three components of Putti's triad are present: shift laterad and cephalad of the femoral head, hypoplasia or absence of the femoral ossification center, and an increase in pitch of the acetabular roof toward the longitudinal axis of the body (Figs 5-35 and 5-36). In a cretin, all of these changes were present, and all of them disappeared after thyroid therapy and without local treatment of the dislocated hip (Fig 5-37). The ipsilateral ilium may be hypoplastic (Fig 5-38). Opaque arthrograms are useful in the

Fig 5-41 — Residual bilateral coxa plana after treatment of unilateral congenital dislocation of the hip. In A, at 2 years of age, the left hip is dislocated and dysplastic, but the right hip is normal. In B, at 5 years of age, and following successful reduction of the earlier dislocation of the left hip, coxa plana deformities are



demonstration of infolding of the labrum between the femoral head and the face of the acetabulum (Fig 5-39).

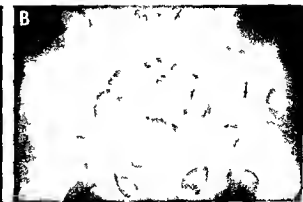
Acquired acute traumatic dislocation of the hip is rare; about four fifths of the dislocations occur in boys. Of the 18 patients followed to skeletal maturity by Donaldson, 11 recovered completely. In only 2 of 55 patients with so-called avascular necrosis did coxa plana develop later. Acquired dislocation of the hip may develop in neuromuscular disease (Fig 5-40).

Coxa plana (Fig 5-41) is a frequent complication of the treatment of CDH and occasionally a large metaphyseal defect will develop in a thickened femoral neck (Fig 5-42).

The methods for quantitating the degree of dislocation are shown in Figure 5-43. The ventrodorsal level of the displaced femoral head is shown best in the Chassard-Lapine projection, when patients are immobilized; this can be done best in the 45 degree frontal oblique projection as directed by Martz and Taylor. Slight degrees of excessive mobility at the hip and slight degrees of dislocation are always uncertain radiographically and clinically.

The monumental studies of CDH in the newborn by Andrén and von Rosen and by Palmén have proved convincingly that the only reliable clinical sign is the response to the Ortolani test, which actually demonstrates slipping of the femoral head in and out of the acetabulum as the femur is abducted and then adducted (provocative Ortolani). The experience of Andrén and von Rosen in Malmö, Sweden, indicates that CDH in the newborn was neither overdiagnosed nor underdiagnosed by the Ortolani test; in a study of more than 15,000 newborns, Palmén's report includes examination of 415,000 newborns, which constituted 49% of all births in Sweden through the years 1953 to 1960. Andrén and his associates found that CDH in newborns is associated with generalized relaxation of the infant and that laxity of the hip joint is the rule

evident in both femurs. The patient was treated by abduction and internal rotation for several months in plaster on both hips. Coxa plana is exceedingly rare or nonexistent in untreated dislocation of the hip.



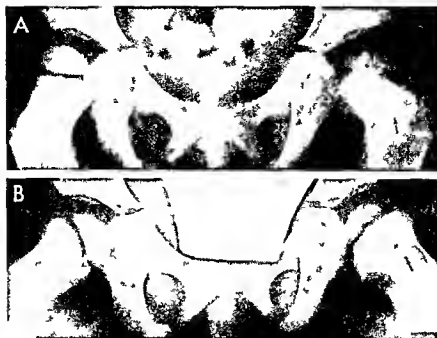


Fig 5-42.—Coxa plana residual to earlier dislocation of the left hip and its treatment. This girl 3 years of age had been treated in a plaster cast with 90 degrees of abduction of the left hip when she was 5 months of age. A, frontal projection on the femoral head is flattened and irregularly ossified. The arrow points to a meta-

physal defect in the anterior segment of the femoral neck. In B with the femurs in abduction and external rotation a large wedge-shaped metaphyseal defect is evident and the femoral neck is thickened in this projection. These findings simulate those of essential coxa plana (Legg-Perthes disease).

rather than limitation of abduction, which is characteristic of CDH in older infants. Andren attributes the relaxation of the newborns with CDH to their failure to metabolize and excrete in the urine the maternal hormones estrogen and relaxin.

The radiographic diagnosis of CDH in the newborn can be made only when actual dislocation of the femoral head is demonstrated by the method of Hilgenreiner (see Fig 5-43 A). Dysplastic changes in the acetabulum such as increase in the acetabular angle are not necessary and were usually absent in the huge Swedish studies. Von Rosen and Andren prefer the radiographic method which they devised for the newborn and is pictured in Figure 5-44, in which the infant's femurs are abducted 45 degrees, then rotated internally as far as can be done with light force and then extended. In the case of partial or complete dislocation, the extended line of the midlongitudinal axis of the femur crosses the ilium laterad and cephalad to the acetabulum; in contrast to normal hips this extended line crosses the acetabulum itself.

The early diagnosis and treatment of CDH in Sweden during the first days and weeks of life have made possible short periods of treatment of only a few weeks with the affected leg maintained in abduction and external rotation; the residual deformities have been practically nil.

In 1967 Palmén reported that 99% of all infants born in Sweden were delivered in general hospitals. All of these were tested routinely at birth by the Ortolani method, and all neonates with positive results of

the Ortolani test were given gentle prophylactic treatment. The new cases of CDH amounted to only 10 in the whole of Sweden in 1967, in contrast to more than 100 cases in 1952, when Ortolani testing and prophylactic treatment were started.

Salter and colleagues found that the femoral head was extremely vulnerable to therapeutically induced avascular necrosis and flattening during the first six months of life. They also found that true avascular necrosis of the femoral head developed in about 30% of infants under 30 months of age who had been treated for CDH. This figure was later reduced to 15% by the more frequent use of continuous traction and subcutaneous adductor tenotomy. Early diagnosis of doctor-induced necrosis of the femoral head depends on the following radiographic findings: (1) failure of appearance of the ossification center within one year after reduction; (2) failure of growth of an existing ossification center; (3) broadening of the femoral neck; (4) increased density of the ossification center; (5) residual deformity of the head and neck when reossification is complete. Undergrowth of the ilium and residual subluxation of the hip are associated findings. Salter and associates concluded that tight muscles, especially the adductors at the hip, and firm immobilization in the extreme abducted position cause pressure necrosis of the femoral head.

According to Finlay and associates and Barlow, the hip joint is unstable during the neonatal period: 4 to 11 per 1000 newborns exhibit clinical signs of dislocation, and 8 to 20 per 1000 signs of instability. How-

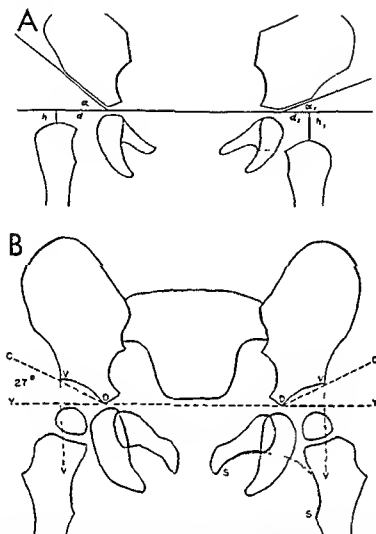


Fig 5-43 —A, Hilgenreiner's method for measuring the acetabular angles and amount of femoral dislocation before the femoral ossification centers appear. The horizontal line is drawn through the Y cartilages and is known as the Y-Y or Hilgenreiner's line. The oblique line parallel to the acetabular roof is drawn to intersect the Y-Y line; the angle between these lines is the acetabular angle. Vertical lines (h) are dropped from the Y-Y line to the middle of the superior edge of each femoral shaft; this measures the dislocation cephalad. The distance (d) from the in-

tersection of the roof line and h measures the lateral dislocation of the femur. In this figure, the right acetabular angle is increased to 40 degrees and the right femur is dislocated cephalad and laterad. B, hip measurements according to Martin. The basic pattern is the same as in A. The V-V lines are verticals dropped from the lateral ends of the acetabular roofs through the Y-Y line. The V-V lines, sometimes called Perkins lines, measure the lateral position of the femur. (From Martin.)

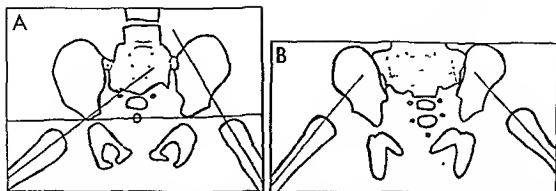


Fig 5-44—The Andrén von Rosen radiographic technique for identification of dislocation of the hip in the newly born. The projection is made in full frontal position with the central ray focused on the symphysis pubis. Both thighs are abducted 45 degrees then rotated internally as far as comfort permits. Lines are drawn through the midlongitudinal axes of both femurs and

then extended onto the ilia. In the normal hip the extended line will cross the acetabulum at some level. In the dislocated hip the extended line crosses lateral to and above the acetabulum and the inferior iliac spine. A, dislocation of the left hip. B, dislocation of both hips.

ever, in the United States and Western Europe, the incidence of actual CDH after the neonatal period is only 1 per 1000. It is manifest that 75% to 95% of the newborns with clinical signs of CDH and instability revert to normal without benefit of treatment during the first weeks of life.

REFERENCES

- Allen, R. P. Ischemic necrosis following treatment of hip "dysplasia." *JAMA* 180 153, 1962.
- Altman, W. S., and Morace, V. Laminography. An aid in the accurate localization in congenital dislocation of the hip. *Radiology* 78 19, 1962.
- Andrén, L. Pelvic instability in newborns with special reference to congenital dislocation of the hip and hormonal factors. A roentgenologic study. *Acta radiol., supp* 212 1982.
- Etiology and diagnosis of congenital dislocation of the hip in newborns. *Radiologie* 1 89, 1961.
- Barlow, T. G. Congenital dislocation of the hip. *Brit J Hosp Med* 2 571, 1968.
- Caffey, J., et al. Contradiction of the congenital dysplasia predislocation hypothesis of congenital dislocation of the hip through a study of the normal variations in the acetabular angles at successive periods in infancy. *Pediatrics* 17 632, 1956.
- Donaldson, W. F., et al. Traumatic dislocation of the hip in children. Final report by the Scientific Research Committee of the Pennsylvania Orthopedic Society. *J Bone & Joint Surg* 50-A 79, 1968.
- Furlay, H. V., et al. Dislocatable hip and dislocated hip in the newborn infant. *Brit Med J* 4 377, 1967.
- Herttonen, T., and James, U. Congenital dislocation of the hip. Experiences in early diagnosis and treatment. *J Bone & Joint Surg* 50-B 542, 1968.
- Martz, C. D., and Taylor, C. C. The 45-degree angle roentgenographic study of the pelvis in congenital dislocation of the hip. *J Bone & Joint Surg* 36-A 528, 1954.
- Palmen K. Preluxation of the hip joint. Diagnosis and treatment in the newborn and the diagnosis of congenital dislocation of the hip joint in Sweden during the years 1948–1960. *Acta paediat.*, Vol 50, supp 129, 1961.
- Diagnose und Behandlung der Preluxation an den Hüftgelenken der Neugeborenen. *Zschr. kind. Chir.* 4 228, 1967.
- Pinck, R. L., et al. Congenital dislocation of the hip. Determination of anterior posterior position of the femoral head in the Chassard Lapine view. *Radiology* 80 650, 1963.
- Salter, R. B., et al. Avascular necrosis of the femoral head as a complication of treatment of congenital dislocation of the hip in young children. A clinical and experimental investigation. *Canad J Surg* 12 44, 1969.
- Silverman, F. N. Current concepts in diagnosis and management of congenital dislocation of the hip. *Pediatrics* 34 554, 1964.
- Small, G. B. Congenital dislocation of the hip in the newborn. *J Bone & Joint Surg* 50-B 524, 1966.
- Smith, W. S., et al. Correlation of postreduction roentgenograms and thirty one year follow up in congenital dislocation of the hip. *J Bone & Joint Surg* 50-A 1081, 1968.
- Thieme, W. T., et al. Clinical examination and urinary estrogen assays in newborn children with congenital dislocation of the hip. *J Bone & Joint Surg* 50-B 546, 1968.
- Von Rosen S. Diagnosis and treatment of congenital dislocation of the hip joint in the newborn. *J Bone & Joint Surg* 44-B 284, 1962.

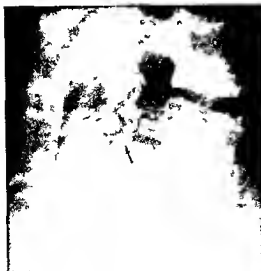
SPONDYLOLISTHESIS—This term is applied to dislocation of a vertebra, usually at the lumbosacral junction, where the body of the 5th lumbar slips anteriorly and caudad over the body of the 1st sacral. The dislocation itself is not, so far as is known, present at birth, but the primary causal factor is a congenital deficiency in the pars interarticularis of L-5. These weak fibrous, cartilaginous segments in the neural arch give way under the stress of increasing weight, excessive muscular pulls or local trauma and permit the body and the attached anterior segment of the divided neural arch of L-5 to slide forward and downward, leaving a portion of its neural arch behind. In some cases the separated posterior segment of the 5th lumbar neural arch may be crowded backward and downward. The defect in the neural arches may be present without anterior slipping of the body (spondylolysis). Spondylolisthesis appears most frequently in active adults during the third, fourth and fifth decades of life. In one of our patients it was recognized roentgenographically in the 5th year of life, when low back pain developed following a spanking. It is probable that spondylolisthesis is overlooked in children and that its incidence will be increased with more frequent and careful roentgen examinations of children.



Fig 5-45 — Defect in the pars interarticularis (arrow) of the neural arch of L5 (spondylolysis) which has permitted the body of L5 to slip forward (spondylolisthesis) on the body of S1

with low back pain and tenderness. The causal mechanism appears to be developmental and spondylolisthesis results from local weakness in the pars interarticularis (dysplasia) and then from stress on this weak segment induced by erect posture and normal lumbar lordosis of man.

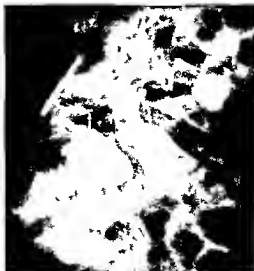
Fig 5-46 (left) — Early slight juvenile spondylolistheses with a narrow defect in the neural arch of L5 (arrow). The body of L5 and the attached anterior segment of its divided neural arch have slipped forward on the body of S1 but the bodies are not deformed save for a shallow defect posteriorly in the edge of S-1.



The roentgen signs of spondylolisthesis are best demonstrated in lateral projection. Frontal projections are not to be depended on for a conclusive diagnosis. The most important single finding is the anterior displacement of the 5th lumbar body and the attached anterior segment of its divided neural arch in relation to the 1st sacral which causes a break in the normal curves through the anterior and posterior surfaces of the vertebral bodies (Fig 5-45). The defect in the 5th lumbar arch appears as a wide gap between the anteriorly placed body and its neural arch. Examples of early slight spondylolisthesis and the late marked form are shown in Figures 5-46 and 5-47 respectively. The spinous process of L-5 may project backward beyond the tips of the spinous processes of the upper lumbar vertebrae which have moved forward with the displaced body of L-5. The magnitude of the displacement varies considerably in different patients. Meyerding's technique for measuring the degree of displacement is a satisfactory method for following the progress of the displacement and estimating therapeutic results (Fig 5-48). The position of the posterior edge of the 5th lumbar in relation to the 1st to 4th sacral quadrants indicates degree of displacement. In longstanding cases bony overgrowth may thicken the sacrum anteriorly. In frontal projections the overlapping of the 5th lumbar and 1st sacral segments casts a transverse shadow of increased density on the 1st and 2nd sacral segments. Sometimes the transverse processes of the caudally luxated 5th lumbar can be seen superimposed on the wings of the sacrum.

Cozen observed two patients in whom neither slipping of the vertebral body nor defects in the pars interarticularis were present at birth. In one of these

Fig 5-47 (right) — Late marked juvenile spondylolisthesis with a wide defect in the neural arch of L5 (arrows) and irregular destruction and sclerosis of its posterior inferior segment. The superior edge of S-1 is smooth but sclerotic.



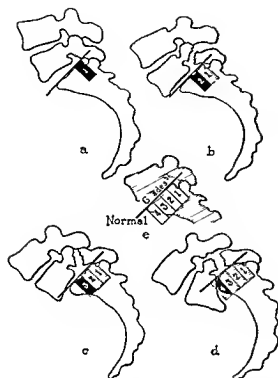


Fig 5-48—Meyerding's method of classifying the degree of spondylolisthesis

patients both of these features developed between the 5th and 7th years and in the other between the 10th and 13th years. In one of our patients the spine was normal at 9 months but there was a large defect in the pars interarticularis of the 4th lumbar vertebra (spondylolysis) at age 10 years (Fig 5-49).

Spondylolisthesis also occurs in levels above the lumbosacral junctions, especially at the 4th lumbar. I have seen lumbar and thoracic vertebral displacements in infantile and juvenile hypothyroidism (Fig 5-50) and achondroplasia. Retarded development and

hypoplasia of the articular processes appear to be the underlying cause.

In a review of the literature and report of a single case of cervical spondylolisthesis Niemeyer and Penning mentioned one patient 8 years of age in most reported cases spina bifida at the same level was associated.

Macnab pointed out that the 4th lumbar body may slip forward on the 5th lumbar body in the absence of a defect in the neural arch when there are dislocations at the articular facets of the diarthrodial joints

Fig 5-49—A normal spine at 9 months of age B spondylolysis at L4 vertebra at 10 years

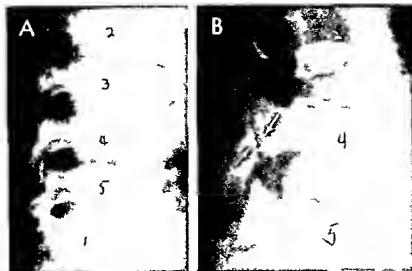




Fig. 5-50 — Spondylolisthesis above the lumbosacral junction. Hypoplasia and posterior displacement of the L1 segment with no defects in the pars interarticularis in a treated cretin 12 years of age.

He called this spondylolisthesis with intact neural arch and believed that when defects are not demonstrated radiologically in forward slipping of the 5th lumbar on the 1st sacral the neural arch may be intact at this level also and the ventral slipping result from dislocation of the dorsal joints.

Adkins showed that the pain of spondylolisthesis is due to compression of nerve roots. Prolapse of the disk is a rare complication.

Fig. 5-51 — Comparison of achondroplastic pelvis (A) and normal pelvis (B) at 8 months of age. In the achondroplastic all of the pelvic bones are too small and the cartilaginous parts relatively too large. The iliac wings are short but relatively wide and the under edges are long and flat with very small acetabular angles which approach zero. The greater sciatic notches are



In a family of 6 siblings 1 of whom had spondylolisthesis Wiltse found defects in the pars interarticularis in 5 of 101 direct relatives. In 36 patients with spondylolisthesis he found 26 examples of defects in the pars interarticularis without slipping of the vertebral body. In Wiltse's study spondylolisthesis was never present at birth and was rare prior to the 4th year of life. In the white race the incidence in males is twice that in females.

REFERENCES

- Adkins, E. W. O. Spondylolisthesis. *J. Bone & Joint Surg.* 37-B:48, 1955.
 Cozen, L. The developmental origin of spondylolisthesis. Two case reports. *J. Bone & Joint Surg.* 43-A:180, 1960.
 Kleinberg, S. Prespondylolisthesis: Its roentgenographic appearance and clinical significance. *J. Bone & Joint Surg.* 15:872, 1933.
 Macnab, I. Spondylolisthesis with intact neural arch: the so-called pseudospondylolisthesis. *J. Bone & Joint Surg.* 32-B:325, 1950.
 Meyerdind, H. W. Spondylolisthesis. *Surg. Gynec. & Obst.* 54:371, 1932.
 Niemeyer, T. and Penning, L. Functional roentgenographic examination in a case of spondylolisthesis. *J. Bone & Joint Surg.* 45-A:1671, 1963.
 Wiltse, L. L. The etiology of spondylolisthesis. *J. Bone & Joint Surg.* 44-A:539, 1962.

Diseases of the Pelvis

INTRINSIC GENERALIZED SKELETAL DYSTROPHIES

In the soft and delicate bony pelvis of *osteogenesis imperfecta* the sacrum is pushed forward and the side walls of the acetabula protrude inward, narrowing the true pelvis. These changes are usually asymmetrical; if scoliosis of the lower portion of the spine is present. The *achondroplastic pelvis* is broad and flat; the promontory of the sacrum is rotated forward and downward and the coccyx is rotated upward and

reduced to tiny stumps rounded at one end (arrows). The pubic and ischial bones are short and stubby; the ischial ramus tapers sharply at the ischopubic synchondroses, in contrast to the long gentle taper of the normal ischial ramus. These pelvic changes are sometimes more dramatic than those in the long bones.



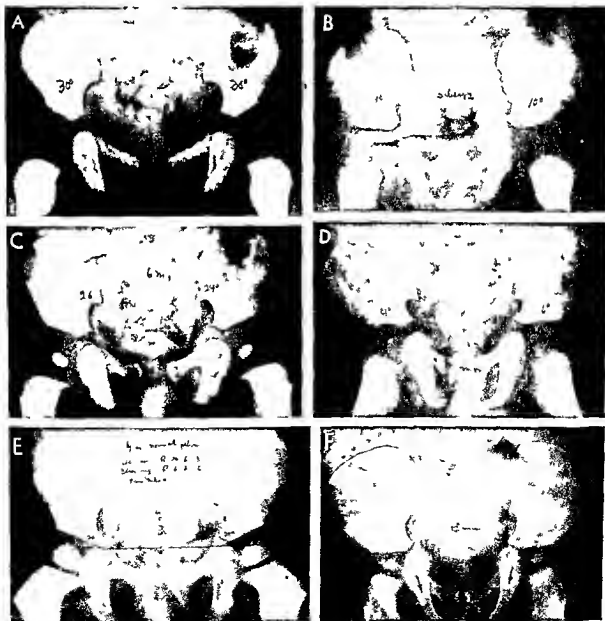
backward, resulting in a widening of the lumbosacral angle and a prominence of the sacrum and buttocks. The acetabular roofs are tilted toward the horizontal and are long, which is the converse of the findings in so-called congenital dysplasia of the hips, sometimes, in achondroplasia the acetabular angles approach zero (Fig 5-51) even in newly born infants. In *hereditary deforming dyschondroplasia* multiple exostoses are uncommon in the pelvic bones, we have seen a few needlelike exostoses projecting from the body of the pubic bones, and large bony masses have been found attached to the crest of the ilium. Timonen

described a primipara 24 years of age, in whom pelvic cartilaginous exostoses caused dystocia and fatal injury to the fetal head. The pelvis in *Morquio's disease* during growth is distinctive, the proximal ends of the femurs are incompletely ossified and the lower edges of the ilia are convex caudad. In *osteopetrosis* there is usually little or no significant change in the shape of the pelvis despite the marked generalized osteosclerosis. In many cases of cleidocranial dysostosis the pubic arch is incompletely ossified and partially invisible (see Fig 1-88 C).

In *mongoloidism* (Down's syndrome) during the

rami are usually hypoplastic with small girth and a long taper to the ischiopubic synchondroses. Ossification centers in the proximal epiphyseal cartilages appear later and remain smaller in mongoloids than in normal children.

Fig 5-52 — Pelvic changes in infantile mongoloidism. A and B, normal and mongoloid newborns. C and D, normal and mongoloid at 6 months. E and F, normal and mongoloid at 12 months. At all ages the ilia are large and flare laterad and acetabular angles are small. In mongoloids older than 9 months the ischial



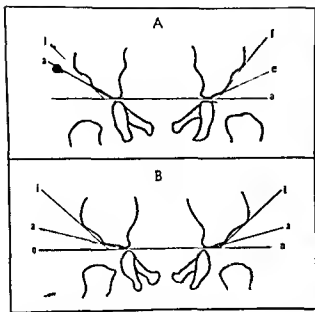


Fig 5-53 — Pelvic measurements in a normal newborn (A) and a mongoloid newborn (B). The acetabular angle is enclosed in the lines 2 and 3 and the iliac angle in the lines 1 and 2. Both of these angles are smaller than normal. Line 3 is drawn parallel to the face of the acetabular cavity. Line 1 is drawn through the two latero-most points on the lateral edge of the ilial wing below and above.

1st year of life the pelvis exhibits several stigmas which are diagnostic (Fig 5-52). The acetabular slopes are flattened and the ilia are large and flare laterad in the wings. These changes can be quantitated by the method of Caffey and Ross (Fig 5-53). In mongoloids the size of the acetabular angles varies between 7 and 25 degrees (average 16) and in normals between 12 and 37 (average 23). In mongoloids the iliac angle varies between 30 and 56 degrees (average 44) and in normals between 44 and 66 (average 55). The iliac index, which is the sum of the two acetabular angles and the two iliac angles divided by 2, varies in mongoloids from 49 to 80 degrees (average 60) and in normals from 65 to 97 degrees (average 81). Our findings proved diagnostic in about 4 of 5 mongoloids suggestive in about 1 of 5 and normal in 1 of 25. In Astley's more recent study the diagnostic significance and the limitations of the method appear to be similar to our own (Caffey and Ross).

After the 6th month the ischial rami become hypoplastic and usually by the 12th month they are elongated slender and have a long taper at their caudal ends. Coxa valga is common. The presence of an extra chromosome in mongoloid cells and the reduced absorption of vitamin A from the gut by mongoloids make possible the comparison of the incidence of mongoloid pelvis with incidence of these two objective signs of the syndrome which should increase the accuracy of its diagnosis.



Fig 5-54 — Pelvis of a gargoyle 2 years of age. The ilia are stenotic at their bases with short highly pitched acetabular roofs. These changes are the converse of those found in achondroplasia. The proximal ends of the femoral shafts are small and bent into severe varus deformities. In some cases of gargoylism (mucopolysaccharidoses) coxa valga is present but the changes in the pelvic bones of this patient are consistently present in gargoyles.

Characteristic pelvic changes in infantile mongoloids have also been reported by Kozłowski in Poland and by Nicolis and Sachetti in Italy. C. H. Lee and associates believe the diagnosis can be made best in newborns by demonstrating the trisomy of acrocentric short chromosomes in groups 21-22. Comprehensive considerations of the skeletal changes in mongolism are found in the paper of Rodighiero and Scapinelli. Currarino and Swanson found two ossification centers longitudinally placed in each manubrium sterni in 90% of mongoloids younger than 5 years and in 20% of normal infants and children of the same age. In a study of mongoloids younger than 2 years Rabinowitz and Moseley noted that the bodies of the lumbar vertebrae were increased in longitudinal diameter and diminished in ventrodorsal diameter also the ventral edges of these bodies were frequently concave.

In gargoylism some of the most diagnostic changes are found in the pelvis: the ilia are long and narrow with deep constrictions at their bases and the femurs are slender (Fig 5-54).

REFERENCES

- Astley R. Chromosomal abnormalities in childhood with particular reference to Turner's syndrome and mongolism. *Brit J Radiol* 36:2 1961.
- Auld R. M. et al. Vitamin A absorption in mongoloid children (a preliminary report). *Am J Ment Def* 63:1010 1959.
- Caffey J. Achondroplasia of the pelvis and lumbosacral spine. *Am J Roentgenol* 80:449 1958.
- and Ross S. Mongolism (mongoloid deficiency) during early infancy—some newly recognized diagnostic changes in the pelvic bones. *Pediatrics* 17:642, 1956.
- and Ross S. Pelvic bones in infantile mongolism. *Radiographic features*. *Am J Roentgenol* 80:458 1958.

- Curran G. and Swanson G. E. A developmental variant of ossification of the manubrium sterni in mongolism. *Radiology* 82 916 1964
- Kaufmann H. J. and Pelargonio S. Roentgenologic changes in the neonatal pelvis in mongoloidism. *Schweiz. med. Wchnschr* 87 1529 1957
- Kozłowski K. The value of x ray films of the pelvis in mongoloidism. *Pediat. polska* 35 881 1960
- Nicolis F. B. and Sachetti G. Evaluation of the morphologic changes in the pelvis in mongolism. *Minerva pediat* 12 1552, 1960
- A nomogram for the x ray evaluation of some morphological anomalies of the pelvis in the diagnosis of mongolism. *Pediatrics* 32 1074 1963
- Rabinowitz J. G. and Moseley J. E. The lateral lumbar spine in Down's syndrome. A new roentgen feature. *Radiology* 83 74 1964
- Rodighiero G. C. and Scapinelli R. Sulla alterazioni osteo-articolari del mongolismo (anomalía di Down). *Chin. or topica* 4 345 1962
- Sobel A. et al. Vitamin A absorption and other blood composition studies in mongolism. *Am J Ment Def* 62 642 1958
- Timonen S. Cartilaginous multiple exostoses in connection with labor. *Acta obst. & gynec. scandinav* 29 138 1949

FRACTURES OF THE PELVIS

Fractures of the pelvis may be single or multiple (Figs 5-53 and 5-56). Multiple fractures are common in automobile accidents. Breaks in one portion of the bony ring surrounding the obturator foramen are usually accompanied by a fracture in an opposite segment of the ring. Fracture lines in the floor of the acetabulum are usually difficult to demonstrate roentgenographically. Internal protrusion of the ischium may be a sequel of fractures in this area (Fig 5-57). Secondary epiphyses in the region of the iliac crests, ischial ramus, ischial spines and the rims of the acetabula should not be mistaken for fracture fragments in adolescents (see Figs 5-2 and 5-11). Traumatic separation of the symphysis or sacroiliac joints may ac-

company fractures. If there is little separation of the fragments and the plane of a fracture is oblique to the projection of the x rays (bevel fracture) it may be necessary to film the pelvis in several projections before the fracture is visualized. Stereoscopic films are essential for a satisfactory study of pelvic fractures; the entire pelvis must be included.

The scalelike epiphyseal ossification center of the ischium may be torn away from the main mass during ordinary athletic activities such as jumping and vaulting and even in sprinting races (Figs 5-58 and 5-59). In some cases the edge of the ischial body may also be injured and permanent deformities may develop secondarily. Avulsion fractures of the ilia and ischia occur in a variety of patterns (Figs 5-60 to 5-63).

REFERENCE

- Dunn A. W. and Morris H. D. Fractures and dislocations of the pelvis. *J Bone & Joint Surg* 50-A 1639 1968

ISCHIO-PUBIC OSTEOCHONDROSIS JUVENILIS

This lesion has been described by Van Neck (1924) and many others as a disorder of the ischio-pubic synchondrosis and its contiguous bones similar to Perthes' osteochondrosis of the ossification center in the proximal femoral epiphysis. We have never seen a convincing clinical case and the roentgen changes said to be characteristic of ischio-pubic synchondrosis are found in a considerable percentage of healthy asymptomatic older children (see Fig 5-13). We observed one girl for several years who developed limp and fever which lasted for two weeks and whose roentgenograms showed destruction of the inferior pubic ramus and large progressively destructive foci in the tibial metaphyses (Fig 5-64).

Fig. 5-55 — Multiple fractures of the pelvis (arrows)



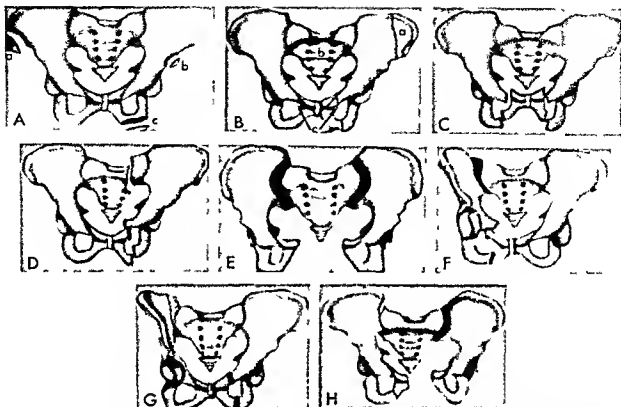


Fig 5-56 — Examples of pelvic fractures. A, avulsion fracture of the anterior superior iliac spine (a), anterior inferior iliac spine (b) and ischial tuberosity (c). B, stable fractures of the wing of the ilium (e), body of the sacrum (b) and in the pubic rami (c). C, straddle fractures of the pubic rami with distraction of the fragments. D, longitudinal unilateral shear fractures of the lateral process of the sacrum and pubic rami on the left side. E, widening

of both sacroiliac joints and separation of the symphysis pubis. F, lateral compression injury with fracture of the pubic rami on the side of the impact and widening of the sacroiliac joint on the same side. G, fracture (longitudinal) of the right iliac wing on the same side. H, total pelvic disruption with stable fractures of the pubic rami on the side of the impact. (From Dunn and Morris.)

Fig 5-57 — Displacement and internal protrusion of the right ischium following old pelvic fracture





Fig. 5 58 - Avulsion of the ischial apophysis and part of the lateral edge of the ischium with some ossification around a subperiosteal hematoma in a boy 18 years of age who was stricken with sudden pain in the ischial region during a sprint foot race (100 yd. dash). Residuals of this kind of injury may be visible radiographically for several years.



Fig. 5 59 - Fracture and avulsion of a fragment of the iliac wing in a healthy boy 16 years of age who felt a sharp pain above his right hip as he left the starting blocks in a sprint foot race (100 yd. dash).

Fig. 6 60 - Segmental avulsion fracture of the femur at the site of the anterior inferior spine of a boy 13 years of age.



Fig. 5 61 - Avulsion fracture of the apophysis of the ischium. A. This boy 14 years of age felt a sharp pain in the right buttock while jumping hurdles in a gymnasium. B. 10 days later he tripped and fell and again had sharp pain in the right buttock.





Fig 5-62. Avulsion fracture of the ischial apophysis (arrows) six months after the primary injury. This boy was 12 years of age.



Fig 5-63. Avulsion of the ischial apophysis (upper arrow) with a large comminuted fracture fragment widely displaced (lower arrow). The patient was age 15 years of age.

Fig 5-64. Osteochondrosis or low-grade destructive osteitis of one of the pubic bones and both tibias in a girl 7 years of age. A: destruction of the inferior ramus of the pubic bone (arrow) two weeks after onset of limp and fever. B: symmetrical destructive foci in the metaphyses of the tibias at the same time. C: four

years later the tibial lesions now occupy deep irregular zones in the middle segments of the tibial shafts. The epiphyseal ossification centers are not affected. The pubic lesions healed nine months after A was taken. At no time was there clinical evidence of disease of the tibiae.



REFERENCES

- Caffey J and Ross S E The ischiopubic synchondrosis in healthy children *Am J Roentgenol* 76 488 1956
- Corper F Osteochondrosis ischiopubica in childhood *Am J Dis Child* 56 957 1938
- Funk F J Jr Traumatic dislocation of the hip in children *J Bone & Joint Surg* 44 A 1135 1962
- Van Neck M Arch franco-belges de chir 27 238 1924
- Zeithin A A Osteochondrosis-osteochondritis ischiopubica *Radiology* 27 722, 1936

OSTEITIS OF THE PELVIC BONES

Osteitis of the pelvic bones is not uncommon it may occur alone or may be one of the sites of polyostotic skeletal infection. As in other bones the anatomic changes consist of destructive and productive lesions which cast shadows of diminished and increased density in a variety of patterns. The destructive features predominate in the early stages of the infection. Any portion of the pelvis may be affected in our patients the most frequent site of involvement has been on the margins of the acetabular cavity (Fig 5-65). The inflammatory reaction however may also begin on the crest of the ilium or on the borders of the sacroiliac joint. The pubic and ischial bones are involved by extension from the ischiopubic synchondrosis. Tuberculous and nontuberculous inflammations are similar roentgenographically. We have seen several instances of tuberculous cystic destruction of the body of the ischium (Fig 5-66). The asymmetrical hypoplasia of the pelvis which is residual to tuberculous of the ilium and sacroiliac joint during childhood is one cause of the obliquely contracted pelvis of Naegeli in the adult.

Fig 5-65 (left) — Chronic generalized pyogenic osteitis of the right ilium. The infection began in the margin of the acetabulum and later extended to all parts of the bone. The inflammatory destructive and productive changes cast patchy shadows of diminished and increased density respectively. The proximal epiphysis

OSTEITIS PUBIS has been reported in adults following pelvic surgery commonly suprapubic prostatectomy. Rarely similar destructive pubic lesions beginning at the symphysis on the medial edges of both pubic bones and extending into the pubic rami have been demonstrated in children. Alperin and Bender reported such a case in a Black boy 6½ years of age who had had no pelvic surgery prior to onset. This is a self-limited disorder which goes through a cycle of destruction and then repair usually with complete restitution of the pubic bones. However ankylosis of the symphysis pubis has followed in some cases. It is probable that the destruction in most cases results from traumatic ischemic necrosis rather than simple inflammation. If this be true the lesion could be classified as osteochondrosis juvenilis pubica. Purulent osteitis has been demonstrated in a few cases.

ISCHIAL OSTEITIS is a similar necrotic lesion limited to the ischial bones and follows urologic procedures such as suprapubic cystostomy.

REFERENCES

- Adams R J and Chandler F A Osteitis pubis of traumatic etiology *J Bone & Joint Surg* 35-A 685 1953
- Alperin J and Bender M J Osteitis pubis *Am J Dis Child* 88 227 1954
- Klinger M E and Levine J Ischial osteitis *New York J Med* 53 1579 1953
- Lavalle L L and Ham F C Osteitis pubis its etiology and pathology *J Urol* 66 418 1945

HYPOVITAMINOSIS

Following the deprivation of vitamin C the pelvic bones may show generalized osteoporosis a band of

of the femur is greatly enlarged and deformed. The ischium is displaced internally and hypoplastic from non use.

Fig 5-66 (right) — Localized destructive tuberculous osteitis in the body of the ischium.



increased density may be visible in the margin of the iliac crest in the more severe cases of scurvy. There are no significant sequels after healing.

In rickets the pelvic bones appear to be practically unaffected in some cases; in others they are markedly changed. During the active stage, generalized osteoporosis and irregular mineralization of the iliac crests are usually visible. In severe cases, the usual signs of healing found at the ends of the long tubular bones may be demonstrable in the iliac crests during the healing stage. In temperate zones and especially in Blacks, rickets used to be a common cause of pelvic deformities. In the adult, these deformities arise in infancy during the active phase of the disease when the pelvic girdle is softened, the deformities persist after the pelvis heals and hardens. The healed rachitic pelvis exhibits a variety of deformities, many of which cause dystocia. The pelvis may be generally diminished in size owing to retarded growth. The characteristic rachitic pelvis is flattened ventrally owing to the anterior displacement of the sacrum which also pulls the ischial spines forward owing to the traction of the sacrospinous ligaments. The sacrum becomes flat or may actually bulge anteriorly into the pelvis. The upward thrust of the femoral heads pushes in the walls of the acetabular cavities. Similar deformities develop in severe cases of renal rickets.

COXA VARA AND COXA VALGA

Both of these lesions can be best evaluated when the positions of the legs and feet are carefully controlled in the true anatomic position. The patient may be in either the recumbent or the erect position in full frontal projection. The inner edges of each leg and each foot must be parallel and in contact with their counterparts with the feet at right angles to the shanks. If this position is not maintained rigidly during filming, most children in recumbent position will externally rotate the legs which causes a spurious

coxa valga. The desired anatomic position is easily established and maintained by wrapping the shanks in Ace bandages and putting elastic bands around both feet.

Coxa vara is a deformity of the femur characterized by a decrease in the angle of the neck and shaft (normal angle varies between 120 and 140 degrees) beyond the lower limits of normal, owing to a caudal bending of the femoral neck (Fig. 5-67). In severe cases the neck may be depressed to a horizontal position or even beyond the horizontal. Coxa vara develops when the femoral neck is weakened, and there are many causal agents. Bilateral coxa vara is common in diseases associated with generalized weakening of the skeleton, such as rickets, osteomalacia, osteogenesis imperfecta and osteopetrosis (marble bones). The malformation is also seen in some of the congenital generalized dystrophies: achondroplasia, the dyschondroplasias of Ollier, Morquio and Hurler and the skeletal infantilism of hypothyroidism. Unilateral coxa vara may follow traumatic fracture of the femoral neck or pathologic fracture secondary to bone cysts, fibrous dysplasia, eosinophilic granuloma and osteitis. In some cases bilateral coxa vara has developed during early infancy, apparently owing to congenital failure of mineralization of the femoral necks. In all types of coxa vara, *limping gait is usually the principal clinical manifestation, and the condition must be differentiated from dislocation of the hip or hips.*

Blockey separates the congenital type of coxa vara associated with shortening and bowing of the femur, from infantile coxa vara in which the deformity develops after birth. He found trauma and fracture of normal weakened femurs to be the cause in the infantile type.

Coxa vara is readily detectable in the roentgen examination save in the youngest infants, in whom the roentgen diagnosis cannot be made satisfactorily. The femoral neck is shifted caudad from its normal obliquely upright plane toward the horizontal plane or

Fig. 5-67—Schematic drawing of coxa vara and coxa valga. A, normal angle of 125 degrees between the neck and the shaft; B, decreased angle of 90 degrees in coxa vara; C, increased angle of 165 degrees in coxa valga.

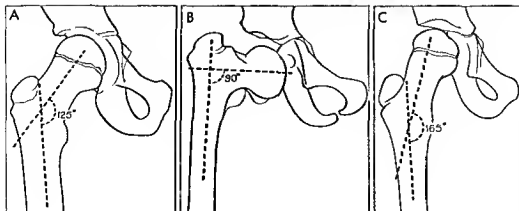




Fig 5 68 —B lateral rachitic coxa vara. A in a child 3 1/2 years of age. In addition to caudal bending of the neck, the terminal segment of the neck is not mineralized, which is responsible for weakening the neck. B the same patient at age 6. The rickets is now partially healed but the coxa vara is increased in comparison with A.

beyond (Fig 5-68). There is a corresponding shift cephalad of the greater trochanter which may ascend above the roof of the acetabulum in the more striking cases. When fracture of the femoral neck is secondary to local disease, the roentgen changes characteristic of the primary disease can usually be identified. When the obliquity of the neck is once shifted toward the horizontal, the strain of weight bearing on the deformed neck is correspondingly increased so that the coxa vara becomes progressively greater with increasing age.

Coxa valga is also a deformity of the femur but in contrast to coxa vara, the femoral neck is bent upward and outward so that the angle between the neck and the shaft is increased beyond the upper limit of normal of about 140 degrees (see Fig 5-67 C). Partial lateral dislocation of the femoral head out of the acetabular cavity is an almost invariable associated finding in the more severe cases. Coxa valga is common with lesions which predispose to atrophy or disuse of the structures contiguous to the hip, such as chronic injuries to the lower extremities and rheumatoid arthritis in the knees or ankles. Other common causes are the paralytic disorders such as muscular dystrophies (Fig 5-69) and postpoliomyelitic paralysis of the

leg. In a few cases we have seen the coxa valga deformity diminish after return of normal muscular function. Severe bilateral coxa valga is said to be a consistent finding in progeria (Hutchinson Gilford syndrome).

Protrusio acetabuli (Otto's pelvis) is a deformity produced by a variety of causes. In children it de-

Fig 5 69 —B lateral coxa valga in an asymptomatic boy 3 years of age. The angle between the neck and the shaft is increased to nearly 180 degrees on each side.



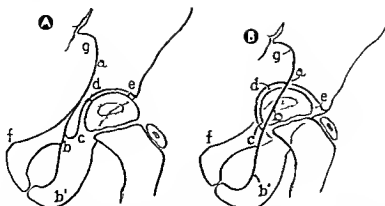


Fig 5-70 — A, normal acetabulum and B, protruded acetabulum. In B the protruded acetabular floor juts into the pelvis well

beyond the internal bony edge *fg*. The 'tear drop' figure (*ab-cd*) in A is obliterated in B. (From McEwen *et al*.)

velops in association with such longstanding and decalcifying diseases as rickets, rheumatoid arthritis, and hyperparathyroidism which weaken the acetabular floor (Fig 5-70). The acetabular cavity is deepened owing to thinning and molding of its walls. Otto first described the deformity in 1824. The lesion may be bilateral, usually in association with generalized osteomalacic diseases, or unilateral, in the case of local disease at one hip.

In the Schuller-Christian type of reticuloendotheliosis, large and small defects may be found in the pelvic bones (see Fig 1-155). Similar pelvic defects occur in eosinophilic granuloma (see Figs 1-156 and 1-157).

The pelvic girdle is swollen and osteoporotic in Mediterranean anemia (Cooley), in severe cases the

heavy struts may exhibit a radial fanlike pattern in the ilia.

REFERENCES

- Almond H G. Familial infantile coxa vara. *J Bone & Joint Surg* 38-B:539, 1956.
- Blockley N J. Observations on infantile coxa vara. *J Bone & Joint Surg* 51-B:106, 1969.
- Duncan G A. Congenital and developmental coxa vara. *Surgery* 3:741, 1938.
- Fairbank H A T. Infantile or cervical coxa vara, in: *The Robert Jones Birthday Volume: A Collection of Essays* (New York: Oxford University Press, 1928), p 225.
- Johanning K. Coxa vara infantum. I. Clinical appearance and etiologic problems. *Acta orthop scandinav* 21:273, 1951.
- McEwen C, *et al*. Protrusio acetabuli in rheumatoid arthritis. *Radiology* 66:33, 1956.

SECTION 6

*The Urinary Tract and
Adrenal Glands*

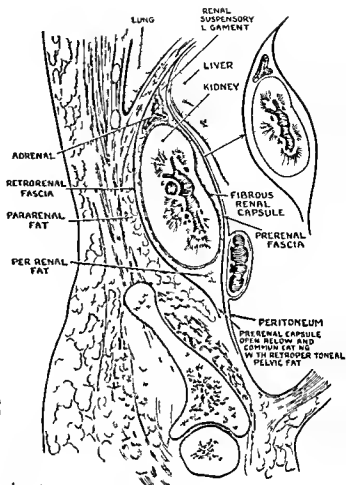


Fig 6.2 — The perirenal soft tissues in longitudinal section (From Campbell after Toldt)

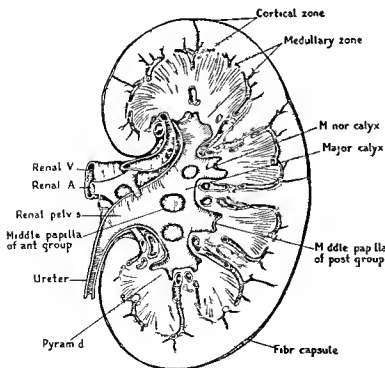


Fig 6.3 — Macroscopic anatomy of the kidney in longitudinal section (Redrawn from Kelly and Burnham)

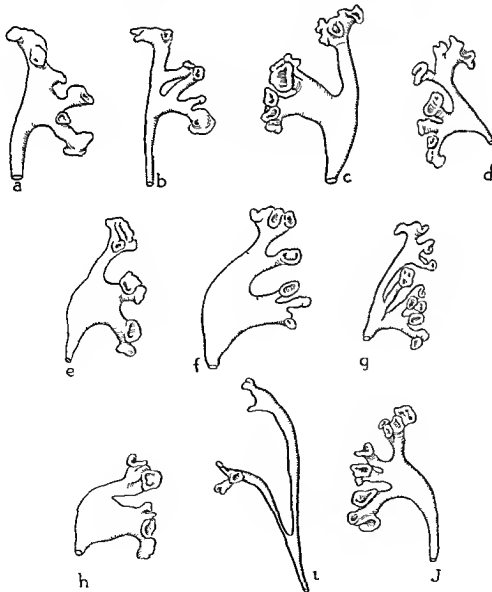
more than 1 cm in length is common, and proportionate differences are probably present in children. The macroscopic structure of the kidney and renal pelvis is shown in Figure 6-3. The renal parenchyma consists of an external granular cortical zone and an internal, radially striated medullary zone. Wedges of cortical substance project centrally through the medulla, dividing it into smaller segments, the renal pyramids. The cone-shaped pyramids radiate from the hilus with their bases directed peripherally, the apices or papillae jut centrally into secondary calices. The tips of the papillae are perforated by the straight tubules or papillary ducts (20–50 in number) which may be arranged in circular or stellate patterns. The cortex is thickest in the polar regions.

RENAL PELVIS—The renal pelvis is a funnel shaped collecting pouch with its base in the renal sinus, the

pelvic apex is directed medially, forward and downward into the ureter. During infancy most of the renal pelvis lies within the renal sinus, in childhood and later, about one half of the pelvis is outside the sinus (see Fig. 6-1). Usually the pelvis branches into three major calices which in turn subdivide into the minor calices. These subdivisions of the pelvis are highly variable in different individuals and on the two sides of the same individual (Fig. 6-4). Sphincteric mechanisms exist where minor calices join the major, where major calices enter the renal pelvis and at what can be considered the ureteropelvic junction.

According to Windholz, variable amounts of fat surround the renal pelvis within the kidney and may affect the configuration of the pelvis. The amount of fat reflects the general nutritional state much as does the perirenal fat, it is more abundant in well nour-

Fig 6-4 — Variations in the size and branchings of normal renal pelvis



ished adults than in the young, thin or undernourished "Spastic," empty calices may be due to compression by peripelvic fat if obesity is present. Increase in peripelvic fat has been described in atrophic lesions of the kidney.

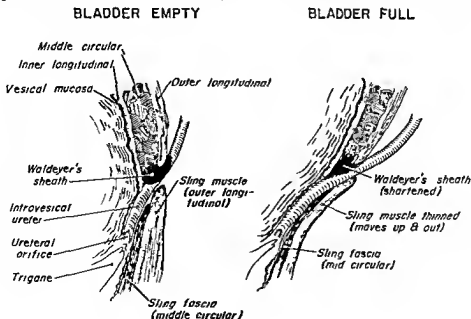
URETER—The tubular ureter begins at the apex of the pelvis and passes caudad to the bladder, traversing the bladder wall obliquely and terminating in the ureteral orifice at the superior lateral angle of the vesicular trigone. The ureters of infants are relatively shorter and wider than those of adults. The large normal ureteral sinus just above the crest of the ilium in infants should not be mistaken for an abnormal dilatation. The oblique course of the ureter through the bladder and its muscular attachments to, and support by, the wall of the bladder (Fig 6-5) are related to problems of vesicoureteral reflux and procedures designed to correct it. The stimulus to ureteral peristalsis seems to be a stretch reflex of the smooth muscle wall. Reflux may be potentiated by this mechanism when the ureterovesical junction is incompetent.

BLADDER—The urinary bladder is a muscular bag lined with mucous membrane. The size of the lumen varies markedly depending on the amount of urine present and the vesicular tone. In infants and children, the bladder is an abdominal organ; it does not attain its adult position on the pelvic floor until about the 20th year. As a consequence, anterolateral protrusions of the bladder through the inguinal rings occur with appreciable frequency in normal children under

the age of 1 year (see Fig 6-12). The high position of the bladder also facilitates suprapubic puncture for aspiration of urine or insertion of plastic catheters for pressure studies, injection of contrast agents and so on. The mucosal surface of the bladder is smooth when the bladder is fully distended. When the bladder is contracted, the mucosa is thrown into numerous folds or rugae which may be mistaken for muscular trabeculation in roentgenographic and cystoscopic examinations. The trigonal mucosa is firmly attached and is smooth in all normal conditions. The trigonal muscle is continuous with that of the internal sphincter and functions with it as a unit. The interureteric ridge represents the cephalic border of the muscle of the trigone. The muscle bundles of the bladder are now considered to be a complicated network with connections at all levels so that traditional division into three layers is not valid. True bladder sphincters probably do not exist, as the muscles of the bladder neck and posterior urethra are continuations of the complicated detrusor muscle. However, a circular fundus ring is present as a functional and anatomic structure and is derived from a circular layer of bladder muscle extending from just above the trigone down to the area anterior to the internal urethral orifice.

URETHRA—The urethra emerges from behind and above the most dependent portion of the inferior surface of the bladder. It is subdivided transversely in the male, into prostatic, membranous, bulbous and cavernous portions (Fig 6-6). In the female the ure-

Fig 6-5—Diagram of ureterovesicular junction showing bladder empty (left) and full (right). Note two sling layers supporting the intravesicular segment of the ureter. The ureter lies on these supporting structures but is not attached to them. Waldeyer's sheath, which does effect the ureteral wall to the bladder muscle, shortens as the bladder fills and anchors the ureter to the roof of the ureteral hiatus. (Modified from Hutch.)



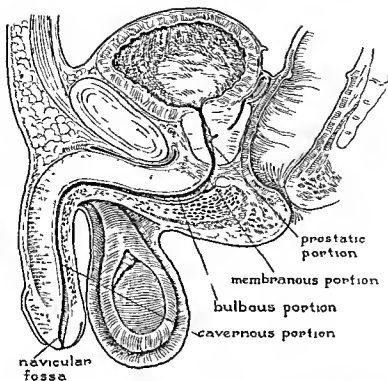


Fig 6-5 — The normal urethra showing the variations in caliber of the different segments

thra is relatively broad and short. The urethral muscles, continuous with the detrusor of the bladder, are arranged in an internal longitudinal and outer oblique or circular layer. In females, both extend the entire length of the urethra, terminating in fibrous tissue near the external meatus. In males, the inner longitudinal portion is practically limited to the posterior urethra.

The external sphincter is made up of striated muscle from the pelvic floor and extends a variable distance proximal and distal to the middle third of the female urethra. In the male, it is related to the prostatic and membranous portions. Details of bladder and urethral muscles can be found in the publications of Woodburne and of Tanagho and Smith.

REFERENCES

- Campbell M F. *Clinical Pediatric Urology* (Philadelphia: W B Saunders Company 1951)
- Cooperman L R, and Lowman R M. Fetal lobulation of the kidneys. *Am J Roentgenol* 92: 273, 1964
- Hodson C J, et al. Renal size in normal children. A radiographic study during life. *Arch Dis Childhood* 37: 616, 1962
- Hutch J A. Sacculi formation at the ureterovesical junction in smooth walled bladders. *J Urol* 86: 390, 1961
- Nelson J D, and Peters P C. Suprapubic aspiration of urine in premature and term infants. *Pediatrics* 36: 132, 1965
- Tanagho E A, and Smith D R. The anatomy and function of the bladder neck. *Brit J Urol* 38: 54, 1966
- Windholz F. The roentgen appearance of the central fat tissue of the kidney. Its significance in urography. *Radiology* 56: 202, 1951

Woodburne R T. The sphincter mechanism of the urinary bladder and the urethra. *Anat Rec* 1(41): 11, 1961

Normal Roentgen Appearance

In plain films of the abdomen, the edges of the kidney may be outlined when there is sufficient perirenal fat. The edges are better visualized in children over 5 years than in younger ones, and in infants.

The central fat tissue of the kidney (peripelvic fat) is visible, when present in adequate amount, as a roughly triangular area with a saw tooth base directed laterally. The irregular configuration of the base is produced by the extension of the peripelvic fat between the renal pyramids into the columns of Bertin. Visualization is enhanced during the nephrographic phase of excretory urography, laminagraphy at this time clearly delineates the fat shadow.

The approximate size, shape and position of the normal kidney can be estimated from plain films when visualization is satisfactory (Fig 6-7). Flattening of the lateral border of the upper half of the left kidney is common and has been attributed to pressure from the adjacent spleen. Occasionally the bladder is visualized on plain films as a water-density image between the gas filled loops of the bowel and the bony pelvis. The normal pelvis, ureters and urethra are not visible in plain films.

The channels of the urinary tract are visualized roentgenographically only after they have been filled with an opaque or radiolucent (gas) medium for contrast density. The contrast agents devised for excreto-

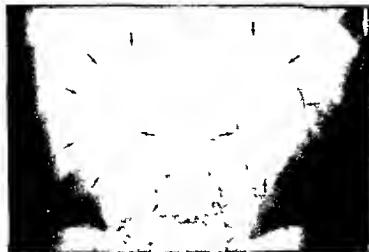


Fig 6-7 (above) — Roentgenographic appearance of normal kidneys in a patient 10 years of age. The edges of the kidneys are visible owing to the contrast of the marginal shadows of diminished density cast by the perirenal fat.

Fig 6-8 (right) — Normal excretory urogram in same patient as in Figure 6-7. The renal pelvis, bladder and portions of the ureters are shown. The portions not shown are in systole at the moment of exposure. Note the increased density (nephrogram) of the kidneys as the contrast material traverses the vessels and tubules.



ry urography have proved to be the most satisfactory for retrograde injection as well, owing to their high roentgen density, their freedom from local irritative action and their general lack of toxic effect when absorbed.

EXCRETORY UROGRAPHY

Organic compounds, containing varying amounts of iodine, can be injected into the blood stream, they are then selectively excreted by the kidney in sufficient concentration to render the channels of the urinary tract visible roentgenographically (Fig 6-8). The kidneys themselves also become more opaque during the excretion, owing to contrast material within the abundant capillaries as well as that flowing through the renal tubular system. Measurement of kidney size consequently becomes more certain during the nephrographic phase of excretory urography. O'Connor and Neuhauser have shown that increased density of the entire body can occur when large doses are injected rapidly; they believe this is a consequence of vascularity and flow rates of blood containing contrast material through various regions and organs of the body. Nonvascular masses (e.g., cysts, infarcts, etc.) in abdominal organs other than the kidney may be recognized by their relative radiolucency during this phase of intravascular loading. Excretion into the urine is by both glomerular filtration and tubular excretion; the triiodinated forms now in use are excreted mainly by glomerular filtration. In the blood, some degree of protein binding takes place, but, in general, the agents used for excretion in the urinary tract bind

poorly with albumin in comparison with those used for excretion in the biliary tract.

Although the radiographic contrast in the urine is dependent on the plasma concentration of the medium, the maximum urinary concentration of about 15 Gm/100 ml means that very high plasma levels can only cause an increasing osmotic diuresis without increasing the urinary concentration. Standan and associates, using very large doses (5 ml/kg), in infants demonstrated an elevation of serum osmolality which reached a peak 90 seconds after the injection and was associated with a measurable decrease in hematocrit. Fluid was apparently drawn into the vascular compartment from the extravascular spaces, causing hemodilution and relative hypoelectrolytemia. The

Fig 6-9 — The normal calyx showing its goblet shape in the filling phase (left) and emptying phase (right). (According to Narath.)



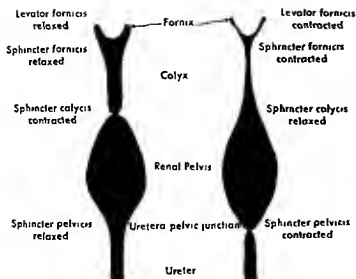


Fig 6 10 —Drawing illustrating the synchronous action of the muscles during the filling phase (left) and emptying phase (right) (According to Narath)

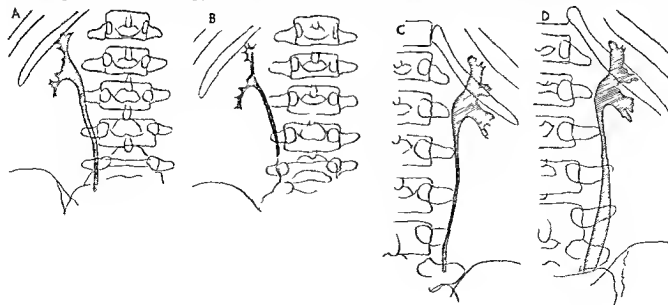
values tended to normalize within 15 minutes after the injection, but complete normality did not occur until 4 hours after the injection. Sodium salts of the iodine-containing compounds are apparently more toxic to cerebral and myocardial tissues than are the methylglucamine salts, especially during rapid injections as in angiography. Benness and subsequently others have shown that the sodium compounds are associated with less diuresis than the methylglucamine compounds and may provide better visualization of renal pelvis and their divisions. No recognizable difference in the diagnostic quality of roentgenographic examinations with methylglucamate diatrizoate and with a mixture of sodium and methyl

glucamate diatrizoate could be found by Nogrady and her associates in very young infants.

The urine is transported in the urinary duct system by descending peristaltic contractions beginning in the renal pelvis; urinary movements are controlled by sphincteric action at several levels (Figs 6-9 and 6-10). The physiologic changes in the shape and caliber of the urinary channels during the systolic and diastolic phases of these movements, and local segmental contractions, have been described in detail by Narath; they should be taken into account in the estimation of abnormal dilatations and stenoses (Fig 6-11). With the substances now available, papillary ducts are occasionally delineated as fine streaks in the tips

Fig. 6 11 —Tracings of excretory urograms showing the physiologic changes in shape and volume during systolic and diastolic phases of contraction. A, the renal pelvis of a girl 7 years of age showing the diastolic or collecting phase. B, the same renal

pelvis 10 minutes later during the systolic or emptying phase. C, the right ureter in systolic phase in a patient 11 years of age. D, 10 minutes after C was taken, the ureter is in the normally dilated diastolic phase.



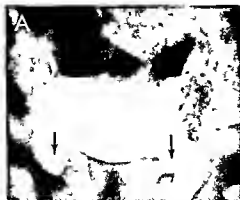


Fig 6-12.—Transitory hernias of the bladder (bladder ears) in normal infant A, bilateral (arrows) in a healthy infant 4 months of age B, unilateral (arrow) in a healthy infant 3 months

of age (Figs 6-12 and 6-13 courtesy of Drs R Parker Allen and Vergi Condon Denver Colo)

of the pyramids invaginating the minor calices. The passage of peristaltic waves down the ureter produces transient discontinuities in the column of contrast laden urine within it. At certain levels the discontinuities are more persistent because of contiguity to anatomic structures. These levels include the site where the ureter crosses the psoas muscle, the site of crossing the iliac vessels and, in the female, a site possibly related to the position of the broad ligament. During the accumulation of contrast material and urine in the bladder, the vesicular shadow gradually becomes more opaque, increases in volume and changes shape. Transitory herniation of the bladder (" bladder ears ") can be seen in normal infants when the bladder is incompletely distended (Figs 6-12 and 6-13). Superimposition of material in the rectum may cause confusing shadows.

Excretory urography is one of the most valuable procedures in pediatric roentgenology and is the only radiographic approach to many pediatric problems. Its use is indicated in any patient in whom visualization of the urinary tract is desirable (except for a few contraindications mentioned later). It is a routine procedure in the investigation of urinary tract infection, hematuria, dysuria, enuresis and albuminuria.

Fig. 6-13.—Transitory fling of hernia of the bladder (bladder ears) in a healthy infant 3 months of age A, frontal and B, later



Patients with obscure abdominal pain, malformations of the external genitalia and especially, abdominal tumors also may benefit from excretory urography. Whenever contrast agents are injected into the blood stream for nonurologic reasons, as for angiography of any body area, a film of the abdomen obtained within 30 minutes may provide unexpected diagnostic dividends. Excretory urography demonstrates function better than retrograde urography and is simpler and safer, the detail of the renal pelvis and their finest divisions is very clear. Excretory urography is in itself a rough test of renal function, both of glomerular filtration and of tubular excretion. However, renal pelvises of different sizes will have different radiodensities with the same concentration of contrast material (Fig 6-14); moreover, a paradoxical increase in density may occur when renal blood flow is diminished on one side, as in some instances of renal hypertension. The diminished glomerular filtration on the affected side results in a relatively increased tubular resorption of water and a spurious increase in concentration of the contrast material. Amplatz has recommended the intravenous administration of urea in a large volume of saline to exaggerate the differential renal blood flow in unilateral renovascular disease. The

at projection. The ventral extension of the bladder ear is well shown in B.



Fig. 6-14—Normal difference in appearance on the left and right sides in a normal child 40 months of age. The larger left pelvis casts a more dense shadow because it contains more contrast material than the smaller right pelvis although concentrations of contrast material are probably similar on the two sides. Variations in density from side to side may reflect physiologic alterations in size of the pelvis due to muscular activity.

urea and saline are injected after a large dose of contrast material has produced good renal opacification. The kidney with adequate glomerular filtration will flush out the dense contrast material; the kidney with poor circulation, presumably responsible for the hypertension, will be unable to respond to this increased water load. Lesperance and associates recorded both false positive and false negative observations when comparing intravenous urography and urea diuresis with selective renal arteriography for the identification of hypertension presumably due to renal artery stenosis.

The excretory method formerly was considered hazardous and usually was unsatisfactory when renal function was poor, as indicated by an elevated nonprotein nitrogen content of the blood. Experience with the newer triiodinated compounds and with the large doses utilized in cardiac and vascular examinations together with careful deliberate study of individuals with nitrogen retention has indicated not only that the risk apparently is less than believed but that important diagnostic information can be obtained in conditions previously considered outside the province of excretory urography. Larger doses of contrast material are now being used with rapid injections and with repetition once or even twice during an examination in which contrast excretion is initial

ly inadequate and if adverse reactions are being encountered they are rarely reported. Fatal overdoses of contrast medium in infants have been associated with grossly excessive dosage. As in any medical procedure the risks in a given case must be weighed against the benefits but the improving relationship between risk and benefit would seem to enhance the scope of excretory urography.

Careful studies of the effect of high dose urography in individuals with impaired renal and hepatic function have indicated that diagnostic examinations can be performed with doses not greater than 2 ml/kg. Higher doses not only do not provide improved urine concentration of contrast medium but are associated with unpleasant systemic sensations.

The availability of hubless needles and plastic catheters and the training of physicians in techniques of venipuncture make obsolete the use of subcutaneous or intramuscular injections of contrast agents for excretory urography. Usually a small vein can be found in the scalp, the dorsum of a hand or foot or the volar aspect of the wrist. Even in a grossly obese or edematous infant a satisfactory vein can be isolated by surgical exposure. In the newborn the umbilical vessels provide an additional route for careful introduction of contrast agents for both angiography and excretory urography.

A rigid routine for the sequence of film exposures is not essential in excretory urography. At the Cincinnati Children's Hospital a preliminary film is made with a tape containing opaque metal markers adjacent to the patient corresponding to marks made on the patient's skin (Fig. 6-15). When the preliminary film is inspected prior to the intravenous injection the radiologist indicates to the technician the numbers between which the kidneys are found. The first film is then exposed with the x-ray beam limited by the collimator to the area between these numbers. This film is exposed approximately 3 minutes after the injection is completed and is usually helpful only for visualization of the kidneys and pelves rather than the ureters and bladder. The second film usually taken at 8 or 10 minutes includes the entire area of interest again, and each film is inspected before the time for the subsequent film is decided. In this way, variations of technique to take advantage of special projections, decisions to inject a second dose of contrast material and other maneuvers to obtain adequate information from a single examination can be accomplished just as the radiologist modifies his gastrointestinal examination with spot films, special projections and so on. In fact fluoroscopy and cine fluoroscopy should be utilized whenever indicated in excretory urography as well as in gastrointestinal examinations.

Nogardy and Dunbar observed delayed concentration and prolonged excretion of urographic contrast medium in the 1st month of life. Optimal visualization of the upper urinary tract occurred at 1-3 hours after the intravenous injection of the contrast material.



Fig. 6-15—Radiation-sparing use of collimator in excretory urography. In A, preliminary film, the vertical lead numerals are on a tape attached to the table top; corresponding marks are made on the child's skin. In B, the 3 minute film, the renal out-

lines were between numerals 2 and 5, so the technician restricted radiation to this area. C, the 8 minute film, concludes the entire series to show ureters and bladder.

al. In infants under 1 month of age, after the initial total body opacification films are obtained, films at 1, 2, and 3 hours may provide more information than films at 10 or 15 minute intervals during the first hour.

A prolonged nephrogram in infants and children following intravenous injection of contrast agents may be a consequence of precipitation of Tamm Horsfall protein within the renal tubules and transitory block. This possibility is supported if there is an initial flash filling of the pelvicalyceal system and then a dense nephrogram which may become progressive up to 24 hours. The Tamm Horsfall protein is produced in the renal tubules and is precipitated by hypertonic solutions such as urine containing contrast material. During the recovery phase, the conduit system again becomes visible and large amounts of the protein are found in the urine. In the interval of relative anuria, affected children rarely show any adverse signs or symptoms.

The large amount of gas normally present in the small intestine of the infant is a troublesome factor which interferes with satisfactory visualization in many cases. This gas is derived principally from swallowed air and may appear suddenly and increase before or during the examination. Elaborate preliminary dietary and evacuant measures to reduce intestinal gas before the examination are usually ineffective. In children over 5 years of age, fluid intake should be limited during the 12 hours preceding the injection. Limitation of fluids in infants during the 1st month of life and in children under 5 years is ineffective and not wise, as the discomfort caused by thirst induces crying and swallowing of air. For very young infants, and even for older children, it is helpful to have an intravenous needle in place prior to the

preliminary film, a saline drip is maintained at a slow enough rate to keep the needle open, and subsequent injections can be made into the tubing or through a three-way stopcock in the system without disturbing the child. Should a systemic reaction take place, the vascular compartment is immediately available for medication.

Dosage with the diatrizoate compounds in relation to body weight is appreciably higher in infants and children than in adults. Doses recommended by MacEwan and colleagues are 10 ml up to 6 months of age, 10–15 ml from 6 months to 2 years, and 15–30 ml from 2 years to adulthood. The amounts are frequently doubled in infants and younger children, especially when preparation has been poor and second injections have been used with success a few hours after an initial injection had failed. Standan and associates recommended doses up to 5 ml/kg in young infants; we seldom use more than 2 ml/kg, although this same dose has been repeated after about 15 minutes. In adults, visualization was not improved with doses above 2 ml/kg, and severe discomfort occurred regularly after 4 ml/kg. It is difficult to ascertain whether infants are less susceptible to discomfort with large doses or less able to express their discomfort. The contribution that unrecognized discomfort might make to the subsequent course of a sick infant is unknown, notwithstanding the immediate satisfactory condition of infants given the larger doses.

Since Matthei reported the advantage of distending the stomach with air immediately after an intravenous injection of contrast material for visualization of the kidneys, most pediatric departments have arranged to provide a feeding for an infant or a beverage for an older child. The liquid not only quiets the child and diminishes crying, thus facilitating the



Fig. 6-16 Effect of liquid feeding after intravenous injection of contrast material in excretory urography. In A the patient is in the prone position. The opaque material in the right side of the abdomen is residual barium from an enema given the previous day. The amount of gas present would seem to preclude satisfactory visualization of the kidneys. In B taken 17 minutes after intravenous

injection of contrast material the child is swallowed with the formula offered as soon as the injection was completed. Gas distends the stomach displaces the intestinal gas and provides excellent visualization. This patient should be maintained in supine position to impede passage of gas from the stomach.

examination but also acts as a water trap for the air swallowed with it so that much of the stomach is greatly distended and the detail of the renal pelvis can be seen as through a window (Fig 6-16). Berdon and associates recommend the prone position for examination routinely; we have found it of value as an additional position when excessive gas is present with the child supine (see Fig 3-81).

Infusion drip pyelography is rarely required in children. If indications exist a satisfactory result can be achieved with a dose of 4 ml of the 50 or 60% solution per kg of body weight diluted with an equal volume of 5% dextrose. The mixture is allowed to flow by gravity into the vein as rapidly as possible through a needle as large as feasible (hopefully 18 or 20 gauge). Films are exposed when approximately half of the dose of contrast material has been infused and again at completion of the infusion. Subsequent films may be obtained as indicated by the degree of opacification achieved and the extent of delineation of the collection system.

The renal pelvis, ureters and bladder are generally filled with some urine at the time excretion of contrast material begins. Nogrady and Dunbar have shown conclusively that the excreted contrast material much heavier than the urine tends to settle under the residual urine which forms a layer over the con-

trast material. These findings are exaggerated when there is pathologic dilatation of the urinary tract and an increased amount of retained urine. As a consequence the most dependent superior and posterior calices of the kidney seem to fill first and with greatest concentration in the child who is lying on his back (Fig 6-17). Furthermore spurious narrowing of the ureteropelvic junction can be produced by contrast material spilling over in a thin stream from the dilated pelvis into the dilated ureter, both of which are at a lower level than the ureteropelvic junction. Dependent layering of contrast material in the bladder in a recumbent child may also give a very false idea of its size and shape (see Fig 6-22). The rapid injection by ureteral peristalsis of contrast-containing urine into a bladder containing radiolucent urine gives rise to the jet phenomenon (Fig 6-18). Although this has been considered by some to be abnormal, Dunbar's studies indicate that it is a normal phenomenon. The transitory herniations of the incompletely filled bladder through the inguinal canals known as bladder evers are a normal variation in the 1st year of life (see Figs 6-12 and 6-13). Frequently the concentration of excreted contrast material in the bladder is sufficient for visualization of the urethra in films taken during voiding (Fig 6-19). The specific gravity of urine is spontaneously increased at times to unusually



Fig 6-17 — Differences in outflow tract with the patient supine (A) and prone (B) 25 minutes after intravenous injection of contrast agent. In A the calyces and infundibula are heavily opacified but pelvis and ureter are not opacified. In B the calyces and infundibula are weakly opacified but the pelvis and a long proximal segment of the ureter are opacified. (From Elkin)

Fig 6-18 — Jet phenomenon during excretory urography. Penaltic wave has emptied the upper portion of the ureter and forced urine and contrast material out the ureteral orifice. Streaming of heavy contrast laden urine through residual urine in bladder causes jet. Arrow indicates probable site of ureteral orifice.



high values as long as contrast material is present within it. The contrast agents in urine may also produce a black copper reduction reaction like that which occurs in alkaptonuria.

Excretory urography is generally safe but may be hazardous in some circumstances. Several deaths attributable to the technique have been reported. Anaphylactoid shock is thought to be the cause of most of the immediate deaths, injury to vital organs by the iodine is the usual explanation for the delayed deaths. Tests for hypersensitivity to the contrast material have not been helpful in identifying patients who will have reactions. Intradermal, ocular, sublingual and intravenous tests have been used in various clinics. It is imperative to ask whether the patient has had any reactions with previous injections and if there is any history of asthma or other allergic manifestations. If so, diagnostic procedures other than intravenous urography may have to be considered, but if the intravenous examination is of significant importance it may be undertaken with careful precautions. Preliminary administration of antihistamines has been suggested; an emergency tray should always be at hand and should contain anticonvulsant drugs, antihistamines, respiratory stimulants and instruments for artificial respiration, thoracotomy and heart massage. Urinary reactions usually respond to epinephrine (Fig 6-20); with severe anaphylactoid reactions the only hope is to maintain circulation and an adequate airway.



Fig 6-19 Normal voiding urethrograms. A after excretory urography. B after urethral catheterization and cystography. C erect lateral position for voiding urethrogram.



Fig 6-20—Reaction to intravenous urography. Between 3 m nute (A) and 8 m nute f m (B) severe ureteral developed. Epinephrine was given subcutaneously just before B was made. C n cal response was satisfactory and the 20 m nute f m (C) was taken to complete the examination. The nephrogram (B) after

good pelvic visualization (A) suggests that marked spasm of smooth muscle of the pelvis and ureter took place during the reaction but was relieved by the time the 20 m nute f m was exposed.



REFERENCES

- Allen R P and Condon V R Transitory extraperitoneal hernia of the bladder in infants (bladder ears) *Radiology* 77 979 1961
- Amar A D Limited area urographic films to reduce radiographic exposure *J Urol* 89 506 1963
- Amplatz K Two radiographic tests for assessment of renovascular hypertension A preliminary report *Radiology* 79 807 1962
- Ansell G Fatal overdose of contrast medium in infants *Brit. J. Radiol* 43 395 1970
- Askin J et al Indications for excretory urography in children *Pediatrics* 20 1033 1957
- Benness G T Urographic excretion study contrast agents *Australasian Radiol* 12 245 1968
- Berdon W E Baker D H and Leonidas J Advantages of prone positioning in gastrointestinal and genitourinary roentgenologic studies in infants and children *Am J Roentgenol* 103 444 1968
- Davidson A J et al An evaluation of the effect of high-dose urography on previously impaired renal and hepatic function in man *Radiology* 97 249 1970
- Doyle F H et al Large dose urography Is there an optimum dose? *Lancet* 2 964 1967
- Elkin M The prone position in intravenous urography for study of the upper urinary tract *Radiology* 76 961 1961
- Friman Dahl J Normal variations of the left kidney Anatomical and radiologic study *Acta radiol* 55 207 1961
- Grainger R G Radiologic Contrast Media in MacLaren J W (ed.) *Modern Trends in Diagnostic Radiology* (4th ed London Butterworth & Co Ltd 1970) Chap 15
- Hinkel C L Opacification of the renal pyramids in intravenous urography *Am J Roentgenol* 78 317 1957
- Kalmon E H Albers D D and Dunn J H Ureteral jet phenomenon *Radiology* 65 933 1955
- Kurlander G J and Smith E E Total body opacification in the diagnosis of Wilms' tumor and neuroblastoma A note of caution *Radiology* 69 1075 1967
- Lasser E C et al The significance of protein binding of contrast media in roentgen diagnosis *Am J Roentgenol* 87 338 1962
- Lee B and Schoen I Black-copper reduction reaction simulating alkaptonuria occurrence after intravenous urography *New England J Med* 275 268 1966
- Lesperance J Saitel J and Barcelo R Valeur de l'urographie endoveineuse avec epreuve de diuresis osmotique (wash-out) dans le diagnostic et l'evaluation de l'hypertension reno-vasculaire *Ann. radiol* 11 127 1968
- MacEwan D W Dunbar J S and Nogrady M B Intravenous pyelography in children with renal insufficiency *Radiology* 78 893 1962
- Matthet L P Improved pediatric excretory urography *J Urol* 64 417 1950
- Narath P A Renal Pelvis and Ureter (New York Grune & Stratton Inc 1951)
- Nevin I N Cline F A and Haug T M Forceful ureteral spurt Common roentgen manifestation of urinary tract infection in children *Radiology* 79 933 1962
- Nogrady M B and Dunbar J S Delayed concentration and prolonged excretion of urographic contrast medium in the first month of life *Am J Roentgenol* 104 289 1968
- et al Clinical comparative study of meglumine and sodium diatrizoate (Renografin 60) and meglumine diatrizoate (Hypaque-M 60) in pediatric urography *J Canad. A Radiologists* 19 210 1968
- O'Connor J F and Neuhauser E B D Total body opacification in conventional and high-dose intravenous urography in infancy *Am J Roentgenol* 90 63 1963
- Olsson O and Jonsson G Roentgen Examination of the Kidney and Ureter in *Handbuch der Urologie* *Encyclopedia of Urology* Vol. V/1 *Diagnostic Radiology* 1 365 (Berlin Springer Verlag 1962)
- Pendergrass E P et al Further consideration of deaths and unfavorable sequelae following the administration of contrast media in urography in the United States *Am J Roentgenol* 74 262 1955
- Standan J R et al Osmotic effects of methylglucamine diatrizoate (Renografin 60) in intravenous urography in infants *Am J Roentgenol* 93 473 1965
- Wendth A J Jr Drip infusion pyelography *Am J Roentgenol* 95 269 1965
- Williams D I Paediatric Urology (New York Appleton Century Crofts Inc 1968)

CYSTOGRAPHY

Examination of the bladder by filling it with contrast material is a valuable procedure at any time and especially when there is lower urinary tract obstruction or evidence of impaired renal function. A catheter is inserted under sterile precautions; advantage should always be taken of the position of the catheter to obtain urine for culture and analysis. The same substances used for excretory urography can be diluted up to twice their volume with distilled water; they are better tolerated than is sodium iodide and some of the older preparations devised for retrograde examination. Contrast material is allowed to flow in under gravity pressure until the patient has a desire to void or until objective evidence of impending voiding is noted. This evidence may be irritability, straining, dorsiflexion of the great toes as described by Kjellberg or actual voiding around the catheter. Ideally filling should be observed by intermittent imaging in intensification fluoroscopy and pathologic changes if they are noted should be recorded by cinefluoroscopic methods. In this way one can differentiate between low pressure reflux and high pressure (during voiding) reflux which may have some bearing on management and prognosis. Adequate examination can, however, be performed with serial spot filming and 70 mm and 90 mm cameras may be the recording apparatus of choice. The introduction of pulsed radiation has greatly diminished radiation dose. Pressure can be recorded through an additional small catheter even during voiding. Bryndorf recommended transabdominal bladder puncture and introduction of a small plastic tube through the needle which is then with drawn over the tube for voiding cystography in young infants. Filling of the bladder is better controlled and voiding films can be obtained at will. The method would seem to be especially valuable in instances of infravesical obstruction which do not permit easy retrograde passage of a catheter. The method would also permit the recording of pressures throughout the procedure and the tubing can be left in place for supra pubic drainage. Extensive abnormal dilatation of the urinary tract with reflux can often be demonstrated by cystography when excretory urograms made just before or after show little or no pathologic change (Fig 8-21). With the high doses he has recommended in excretory urography Dunbar obtains adequate

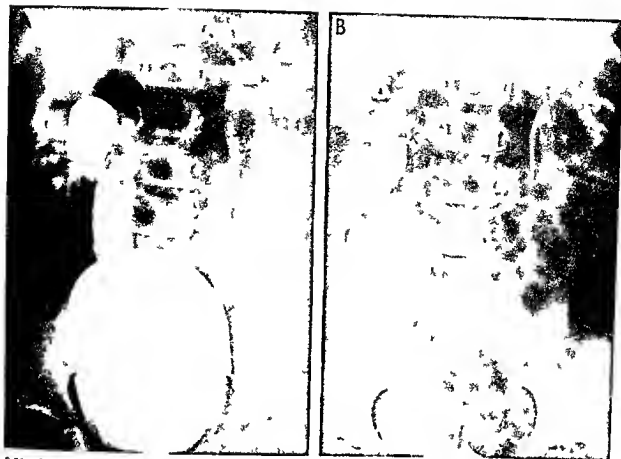


Fig. 6-21—Contrast radiographs of upper urinary tracts. A, excretory and retrograde pyelography. B, lateral pyelograms and ureterectasis demonstrated by retrograde cystography in a girl 2 years of age who had had pyuria for several months. B, the same

upper urinary tract opacified by excretion urography 2 days later in which no dilatation of the ureters and pelvis is evident. Dilatation of the kidneys believed to be due to hypotonia caused by chronic infection.

densities of contrast material in the bladder for voiding cystourethrograms at the completion of an excretory urogram.

At Cincinnati Children's Hospital it is routine to precede the introduction of the contrast material by an injection of 5 cc of 10% (Ascendol) Lipiodol through the catheter as recommended by Young. If emptying of the bladder is not complete during the examination a follow up film 24 hours later shows whether the child was unable to empty the bladder completely in the interval or whether he was only unable to do so at the time of the examination (Fig. 6-22). The normal child will have no residual Lipiodol in the bladder in a film taken 24 hours after it has been introduced. Residual Lipiodol indicates that there has been continuous residual urine throughout the period between examinations and reflux not apparent during the examination may be recognized from the presence of opaque oil in the ureters or pelvis.

Although cine films demonstrate the mechanics of micturition a spot film taken during voiding provides anatomic delineation of fine valve structures and

other changes which cannot be detected in the individual frames of a film strip. The momentary interruption of the motion picture film to obtain the spot film has not been objectionable in our hands and the spot film has provided fine detail which is lacking in the movie.

In the enthusiasm for examination of the lower urinary tract by this valuable technique one should not lose sight of the direct radiation being received by the gonads.

When voiding cystourethrography is undertaken in the recumbent female the vagina fills almost invariably during the examination (see Fig. 6-57). Examinations done in the erect position are easier for older children and eliminate this occasionally confusing shadow. The placing of a towel or pad between the labia will also prevent vaginal reflux. A true lateral or steep lateral oblique position is required to demonstrate the structures of interest in a voiding cystourethrogram.

Double contrast cystography is said to provide detail of bladder mucosa not achieved by standard techniques.

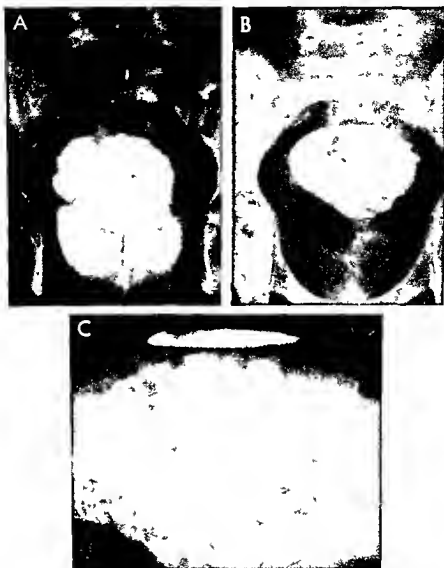


Fig 6-22—Use of Ascendent Lipiodol in cystourethrography. **A**, globules of Ascendent Lipiodol outline the dome of the bladder while diatrizoate contrast medium outlines the dependent portion of the bladder. **B**, film of the abdomen 24 hours after cystourethrography. Residual Lipiodol still outlines the bladder

dome. **C**, lateral horizontal beam film corresponding to **A**. The Ascendent Lipiodol floats on the radiolucent urine while the heavier diatrizoate agent settles in the dependent portion of the bladder under the radiolucent urine layer. The patient had meatal stenosis and residual urine.

RETROGRADE UROGRAPHY

With the improved detail provided by the excretory contrast agents now available, fewer retrograde examinations are being made. Ureteral catheterization for determination of differential renal function, for differential cultures and for anatomic demonstration in instances of unilateral nonfunction still has an important role in diagnosis. The various types of artifacts produced by retrograde examination—air bubbles, pyelocanalicular and pyelosinus back flow and sinolymphatic and sinovenous absorption—should not be forgotten because they will occur on the occasion

of retrograde examination. But other anatomic abnormalities are sufficiently well demonstrated by excretory studies to require no additional description here.

Retrograde urethrograms have been made much more feasible in the male by the technique described by Lucaya. A plastic catheter is inserted 1–2 cm into the external urethral meatus and is fixed in position with the orifice sealed by allowing collodion to drop over the area. The collodion dries almost immediately, leaving a thin film covering the glans and extending onto the catheter just outside the meatus (Fig 6-23). Urologic contrast agents can then be injected from a syringe attached to the end of the catheter well out

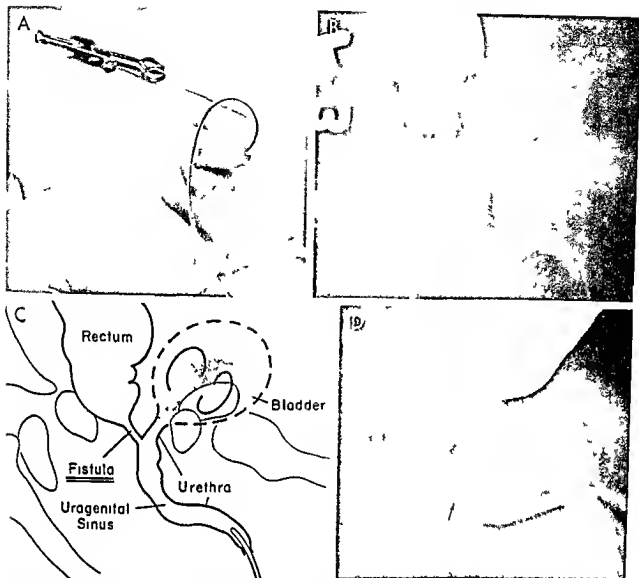


Fig. 6-23—Retrograde urethrography. Lucaya technique. A the plastic catheter has been inserted about 2 cm into the urethra and is held in place by collodion which covers the catheter and the glands. The prepuce has fallen forward obscuring the glans; a drop of dried collodion is suspended from it. B spot film during retrograde injection in an infant with imperforate anus. Filling defects in the urethra are produced by meconium which also has filled the bladder and posterior urethra, interfering with flow into

these structures. The major portion of the contrast agent flows through the fistula into the rectum. The diagnosis is therefore imperforate rectum with rectourethral fistula. C, diagram of B. D, imperforate anus was the clinical diagnosis. Inverted film showed gas extending below the pubococcygeal line. The retrograde urethrogram demonstrates a patent fistula and the diagnosis is imperforate rectum. Arrow indicates the area of the external sphincter. (A courtesy of Radiology.)

side the field of radiation. The injection is monitored fluoroscopically and spot films or cine films are obtained as indicated. The technique has been extremely valuable in infants in whom retrograde passage of a catheter for cystography could not be accomplished and has been particularly helpful in the identification of rectourethral fistulas in association with congenital atresia of the anus. It should have application following urethral trauma. At the completion of the procedure the edge of the collodion film is gently lifted with a fingernail; the remainder peels away easily, permitting spontaneous voiding and registration of voiding cystourethrography as well.

SPECIAL EXAMINATIONS

AORTOGRAPHY AND RENAL ANGIOGRAPHY—These procedures in infants and children are best carried out by passage of a catheter to the proper level of the aorta from the femoral artery. Transabdominal puncture is generally unsuccessful until the late teens because of the relative small size of the aorta and its straight position along the anterior border of the vertebral column before that age. Even in very young infants, percutaneous techniques have proved feasible, but considerable skill is required in the cannulization of their minute vessels. Reports on transfemoral arte-

rography in infants should be carefully reviewed for all aspects of the technic of examination. The examination should be concluded as quickly as possible because the incidence of occlusive complications increases with the time that the catheter remains within the artery. During the 1st week of life the passage of a catheter into the umbilical artery provides a ready and relatively safe route of access to the aorta. The possibility that a clot within the umbilical artery will be dislodged and pushed into the iliac artery from whence embolization into the femoral can take place cannot be overlooked especially if there is difficulty in passing the catheter. In such cases retrograde brachial injection may be used for examination of the descending aorta and its branches. Renal arteriovenous fistulas following percutaneous biopsies have been demonstrated by angiography (see Figs 6-68 and 6-81). Whenever radiographic studies are undertaken subtraction technics can be used to provide greater security in the recognition of vascular patterns.

NEPHROTOINOGRAPHY—Following the rapid injection of a relatively large amount of contrast material into the renal artery or aorta (and even into the vascular compartment on the venous side) the renal parenchyma becomes opaque probably due to the flooding of the extremely well vascularized tissue of the kidney with the contrast agent. The massive opacification of the kidney is called a nephrogram and the contrast tends to disappear as excretion into the pelvis takes place. If at the time of this diffuse flush the kidney contains nonvascularized structures such as a cyst or a less regularly vascularized tumor these structures are outlined by the more opaque vascularized kidney parenchyma. Body section roentgenography has been utilized in adults to demonstrate radiolucent areas surrounded by radiodense vascularized renal tissue; there has been little experience with this technic in children but in appropriate instances the method may have value.

RADIOISOTOPE SCAN—In instances of unequal renal function and especially when there is a possibility of renal hypertension from a unilateral hypoplastic and poorly vascularized kidney the renal blood flow on the two sides can be compared by the injection of iodized substances excreted promptly and exclusively by the kidneys which have been made radioactive by the addition of iodine-131 or to minimize radiation iodine-125. Such a procedure with appropriate instrumentation may result in appreciably less radiation to the child than would an excretory urogram or an aortogram. However the procedure should not be undertaken unless there is available instrumentation of high sensitivity capable of measuring accurately over very small areas.

ULTRASOUND—Ultrasonic technics using probes devised for echoencephalography and echocardiography may provide an additional diagnostic tool. Experience with this modality is extremely limited in children but in adults particularly in combination

with radioisotopic scans it has proved of value in differentiating cystic from solid lesions.

REFERENCES

- Bennett A R and Wiener S N. Intrarenal arterial venous fistula and aneurysm. A complication of percutaneous renal biopsy. *Am J Roentgenol* 95:372, 1965.
- Dalrymple G V et al. A rapid method for producing subtraction technic roentgenograms. *Radiology* 89:934, 1967.
- Deslattes D T, Ruttenberg H D and Hoffman R B. Percutaneous catheterization in children. *Radiology* 87:119, 1966.
- Freimanis A K and Asher W M. Development of diagnostic criteria in echographic study of abdominal lesions. *Am J Roentgenol* 108:747, 1970.
- Hanasee W and Shinno J M. Second-order subtraction with simultaneous bilateral carotid internal carotid injections. *Radiology* 86:334, 1966.
- Holm H H. Ultrasonic scanning in the diagnosis of space occupying lesions of the upper abdomen. *Brit J Radiol* 44:24, 1971.
- Howry D H. A brief atlas of diagnostic ultrasonic radiologic results. *Radiol Clin North America* 3:433, 1965.
- Jensen J Th. Double contrast cystography. A new contrast medium and simplified technique. *Acta Radiol (diag)* 10:337, 1970.
- Kaufman H J (ed). *Progress in Pediatric Radiology*. Vol III. Genito-urinary Tract. (Basel: S Karger, 1970).
- Kjellberg S R, Encoson N O and Rudhe U. *The Lower Urinary Tract in Childhood*. (Chicago: Year Book Medical Publishers Inc, 1957).
- Lucaya J. A simple technique of retrograde urethrography in male infants. *Radiology* 102:402, 1972.
- MacEwan D W and Rosenthal L. Assessment of excretory urography and radioisotope renal scanning in diseases of the kidneys. *Radiology* 86:1010, 1966.
- McDonald P. Arterio-venous fistulae following percutaneous renal biopsy. *Australasian Radiol* 10:124, 1966.
- Nebesar R A et al. Arteriography in infants and children with emphasis on the Seldinger technique and abdominal diseases. *Am J Roentgenol* 106:61, 1969.
- Obenchain T G et al. Complication rate of selective cerebral angiography in infants and children. *Radiology* 95:669, 1970.
- Seltzer R A, Kereiakes J G and Saenger E L. Radionuclide exposure from radioisotopes in pediatrics. *New England J Med* 271:84, 1964.
- Wellman H N, Kereiakes J G and Bransom B M. Total and partial body counting of children for radiopharmaceutical dosimetry data, in: *Medical Radionuclides: Radiation Dose and Effects* (Washington D C: U.S. Atomic Energy Commission, 1970) p 133.
- Williams D I. *Pediatric Urology*. (New York: Appleton Century Crofts Inc, 1968).
- Young B W, Anderson W L and King G C. Radiographic estimation of residual urine in children. *J Urol* 75:263, 1956.

Congenital Malformations

Malformations of the urinary tract are among the most common congenital abnormalities found in infants and children; they are frequently multiple and bilateral. With many of the malformations there is no dysfunction and the patients are asymptomatic. However obstruction of urine flow and predisposition to infection are common concomitants of urinary tract malformation and the ingenuity of modern surgical procedures as well as the potency of anti-infectious drugs make mandatory the early recognition



Fig 6-24—Solitary kidney associated with imperforate anus and hemivertebra deformity of L5. Megacolon from anal stricture consequent to surgery in the newborn period has displaced the bladder and caused obstruction of the solitary ureter as well as the bladder.

tion of potentially harmful deviations from normal development.

Knowledge of the embryology of the urinary tract enhances the understanding of most malformations, this information is well described in available texts, so that only the basic concept of union of a nephrogenic and a ureterogenic component need be mentioned here. The secretory portion, the nephrons, is derived from the metanephrogenic blastema, which appears before, and is subsequently influenced by the excretory portion derived from the ureteric bud. The latter portion gives rise to the ureters, the renal pelvis

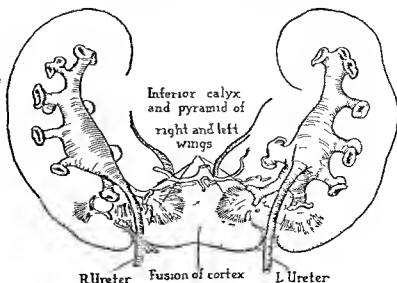
and collecting tubules of the pyramids, and these structures are most accessible to roentgenographic investigation.

ANOMALIES OF THE KIDNEYS

ANOMALIES OF NUMBER—When one kidney is absent, the ipsilateral ureter is atretic, rudimentary or absent. Absence of the uterovesical orifice and lack of development of the adjacent portion of the trigone are noted on cystoscopy. The adrenal gland is said to be absent in about one third of the cases of unilateral renal agenesis or hypoplasia and, when present, has an abnormal shape. The solitary kidney is almost always hypertrophied, it may be ectopic. A solitary kidney is not unusual in association with lumbar vertebral deformities, especially when there is also an imperforate anus (Fig 6-24). Supernumerary kidneys are rare, but there are reports of as many as six functioning kidneys and ureters.

ANOMALIES OF FORM—Sometimes the lobulations of the infantile kidney persist into older childhood and adult life. Flattening by pressure of adjacent normal organs, such as the spleen, has been alluded to. Anomalies of fusion of the two kidneys give rise to distorted structures described as disks, doughnuts, horseshoes and the like. The best known and most easily recognized is the horseshoe kidney, in which the lower poles of the two kidneys are fused (Figs 6-25 and 6-26); rarely, the upper poles are united and the lower poles separate. In the more common variety the kidneys are at a lower level than usual, and the lower poles are directed toward the spine. The ureteropelvic junctions face forward or even laterad, and the ureters curve forward over the connecting bridge of renal parenchyma and swing toward the midline below it. The upper calices usually are directed laterad in relatively normal fashion, but the lower calices almost always project both medially and laterally.

Fig 6-25—Horseshoe kidney showing fusion of the inferior poles, spreading apart of the superior poles and failure of rotation. The renal pelvis enter the kidneys on their anterior aspect. (Redrawn from Kelly and Burnam.)



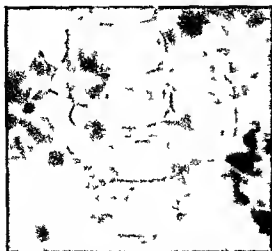


Fig 6-26 ~Horseshoe kidney. The long axes of the pelves are parallel or converge toward the lower poles, which are united. The upper calyces are directed laterally in normal fashion; the lower are directed medially.

when viewed in the frontal plane. Obstructive changes in the pelves are not unusual. The position of horseshoe kidneys, like that of other ectopic kidneys, makes them vulnerable to trauma, so that contact sports are best avoided by affected individuals.

ANOMALIES OF POSITION—An ectopic kidney is one which has never occupied a normal position and it should be distinguished from a dislocated kidney, which has attained but not maintained its normal position. Ectopia, usually unilateral, may be axial

(cephalad or caudad) or medial. Caudal ectopia is most common, and the ectopic kidney may be in the bony pelvis in the iliac fossa or merely low in the abdomen (Fig. 6-27). Cephalad ectopia is seen in association with foramen of Bochdalek diaphragmatic hernias; the kidney may actually obstruct the hiatus and prevent migration of the bowel and other viscera. Medial ectopia is often called crossed ectopia or crossed dystopia.

The ectopic kidney may be solitary, fused with the opposite kidney (Fig. 6-28), or completely separated from it. Its ureterovesical orifice is usually in normal position. Malrotation is almost invariable in ectopic kidneys. During its ascent out of the pelvis, the kidney normally turns mediad on its long axis, and the renal pelvis is rotated from an anterior to medial position. Renal rotation is usually completed during the eighth week of fetal life. Interference with ascent apparently interferes also with rotation. Anomalous vascular supply is usually present in renal ectopia; it probably represents persistence of caudal vessels, which disappear during normal ascent of the kidney. They can be demonstrated by aortography.

In mobile kidney fixation is incomplete, usually due to defects in fascial attachment, and the kidney is free to move around its pedicle. Caudal ptosis, on assumption of the erect position, is more common than medial ptosis in lateral recumbency, but both may be associated with episodes of pain and even obstructive changes in the pelvis. The degree of normal mobility must be considered before attributing symptoms to minor or even moderate renal migration on change of position. The left kidney, lacking the

Fig 6-27 ~Ectopic kidney in a boy 5 years of age, in whom a mass was felt in the abdomen on routine examination. In A, the ectopic right pelvis is low and malrotated. It could be distorted

but in B, the normal configuration of the pelvis and calyces is clear. The ureteropelvic junction faces forward, instead of anteromedially as on normal left sides.





Fig 6-28 — Crossed renal ectopia. The left kidney has its own ureter, but is probably fused at its upper pole with the lower pole of the malrotated right kidney.

Fig 6-29 — Effect of prone and supine positions on pelvic visualization and apparent position of kidneys. In A, supine position, the right renal pelvis is obscured; both pelves are at the level of the 2nd lumbar vertebral body and 2nd lumbar interspace. In B, prone position, the intestinal gas is displaced later

and improving visualization of both pelves. The left seems displaced downward slightly while the right is now fully an interspace height. Note the change in the projected shape of the bladder. The subject was a girl 6 months of age.



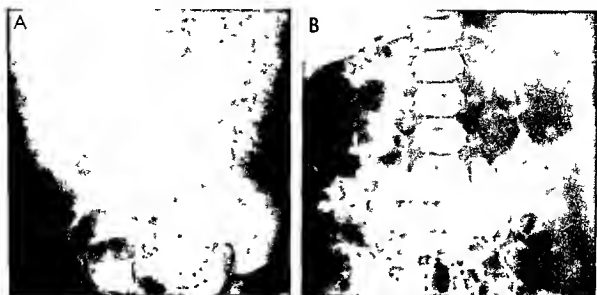


Fig 6-30 — Congenital cystic disease type uncertain. A, at 4 months the streakiness and collection of contrast medium in the pararenchyma suggest renal tubular ectasia. The elongated pelves raised the question of polycystic disease. B, at 5 years and 4

months only the elongated pelves are seen and the diagnosis of polycystic disease seems more likely. This patient probably has infantile polycystic disease.

support of the liver, appears to tip forward and "migrate" caudally in the prone position to a greater degree than does the right (Fig 6-29).

ANOMALIES OF STRUCTURE—Parenchymal lesions of congenital origin fall into two main groups: dysplasias (aplasias and hypoplasias) and cystic malformations. It is often difficult to separate the two on either pathologic or radiologic grounds. Certain patterns can be identified roentgenographically but other features such as inheritance may have to be considered in diagnosis.

Aplasia is characterized by the presence of a small malformed kidney structure with little or no urographic evidence of function. In the most severe and fortunately most rare, forms there are one or several small cystlike, often calcified formations of different sizes in the area occupied by or traversed by the kidney during its development. **Hypoplasia** is characterized by local or regional underdevelopment but with some ability to excrete contrast material. The hypoplastic kidney contains primitive renal elements and even tissues normally foreign to the kidney, such as cartilage and striated muscle. Almost identical histologic and radiographic changes have been noted in atrophic pyelonephritis (see p 777) and the cause and effect relationship between malformation (dysplasia) and infection is far from clear (see also p 801). Except in the newborn, signs of infection may be expected in association with dysplasia, although the reverse is not always the case. The high frequency of 'dysplasia' in females has been offered as evidence of noncongenital factors in its genesis because of the known high frequency of infection in females.

Oligomeganephronia is a French term introduced

Fig 6-31 — Renal tubular ectasia in a newborn infant with bilateral masses in the abdomen. The large kidneys are diffusely opacified except where noncommunicating cysts produce filling defects. The pelves are poorly seen but are stretched and resemble those in Figures 6-32. A contrast material in the bladder shows good concentration. This film was taken 24 hours after intravenous injection of contrast material. First delineation of the kidneys occurred 3 hours after injection and slowly increased.



by Royer and his colleagues to describe a form of renal hypoplasia in which there are too few nephrons and each is greatly enlarged. Radiographically the kidneys may be small and function poorly. In rare instances the number of calices may be reduced. The antemortem diagnosis is made by renal biopsy.

Cystic disease of the kidney appears in several forms, some of which appear to be distinct entities, some of which are classified with difficulty, and some of which have features common to both groups. From the radiologic standpoint, bilateral renal masses in

the newborn infant which do not transilluminate (hydronephrosis) and which are not demonstrable on excretory urography are most frequently the infantile multicystic dysplastic type in which the entire substance of the kidney appears to be replaced by dilated tubular cysts. If retrograde studies are undertaken the pelvis may be stretched somewhat, as in adult polycystic disease, but more frequently they have a normal appearance. Most children with this condition die shortly after birth, but some may survive into childhood. Delayed excretion of contrast material is

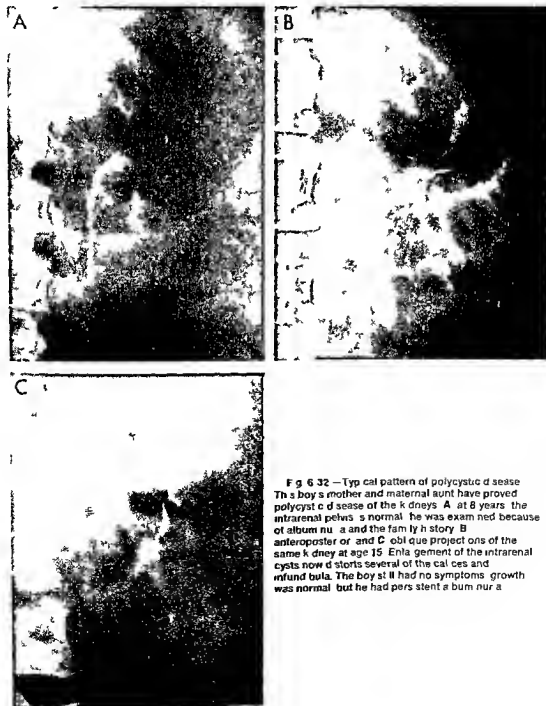


Fig. 632—Typical pattern of polycystic disease. The boy's mother and maternal aunt have proved polycystic disease of the kidneys. A, at 8 years, the intrarenal pelvis is normal; he was examined because of albuminuria and the family history. B, anteroposterior, and C, oblique projections of the same kidney at age 15. Enlargement of the intrarenal pelvis now distorts several of the calices and infundibula. The boy at 18 had no symptoms; growth was normal, but he had persistent hematuria.



Fig 6-33 —Classical polycystic disease with elongated calices in a 13½-year old boy who also had spondyloepiphyseal dysplasia tarda. Note the platyspondyly.

common in the latter children and nephrograms due to accumulation and concentration of contrast material in the dilated tubular structures may be seen best in films taken 8-12 and even 24 hours after the injection (Figs 6-30 and 6-31). It is this form which was reported as renal tubular ectasia by Reilly and Neuhäuser. The association of cystic changes in the liver in some of these cases may lead to hematemesis from ruptured esophageal varices due to portal hypertension as the initial manifestation. Cystic changes are occasionally described in the lungs, pancreas and ovaries.

The adult form of congenital polycystic disease is strongly familial and frequently passes unnoticed in childhood. However, excretory urography in a child with progressive renal failure occasionally may disclose renal enlargement, not so great as that in the infantile form of polycystic disease, but enlargement associated with elongation and distortion of the individual calices (Figs 6-32 and 6-33). Frequently by the time this degree of distortion has taken place the renal function is so impaired that anatomic delineation requires retrograde examination. Multiple small cysts may cause minimal enlargement and minimal distortion yet interfere significantly with renal function. The bilateral nature of the condition and the strong familial history are helpful diagnostic points. renal biopsy may be necessary for conclusive diagnosis. Intermediate forms in which there are associated hepatic symptoms and even medullary cystic disease (Fig 6-34) of the type seen in adults have been described but are relatively uncommon. Polycystic renal disease has been mentioned as an associated malformation of von Hippel-Lindau disease.

Fig 6-34 —Schematic diagrammatic depiction of distortion of the renal tubules and the formation of small and large cysts, some of which communicate directly with the renal pelvis. (From Evans.)

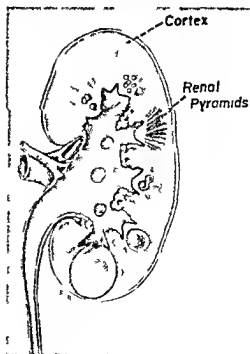




Fig 6-35—Large calyceal diverticulum (arrows) in a girl 10 years of age. excretory urogram. This diverticulum did not fill during retrograde urography.

In the newborn infant, a unilateral abdominal mass is most frequently caused by a hypoplastic multicystic kidney. In such cases, the ureters are commonly atretic and the vessels are abnormal so that no function is identified on the affected side in excretory urography. Multicystic kidneys also occur in older children and are characteristically unilateral. Solitary cysts are rarely seen in children, but when they are they present as intrarenal masses distorting the adjacent pelvis. Nephrography and especially nephrotomography have been useful in adults in differentiating a cyst from tumor, but in most instances the identification of a mass within the renal substance warrants definitive diagnosis by exploration. Calyceal diverticula (Fig 6-35), or pyelogenic cysts, are probably of infectious rather than congenital origin. They are seen most frequently with chronic atrophic pyelonephritis (see Fig 6-71). Focal areas of pyelonephritis break down, perhaps discharging into the pelvis. Subsequently they epithelialize presumably from the pelvis. Gross changes in size are seldom encountered in serial examinations. They communicate with the pelvis but fill variably on excretory and retrograde examinations.

ANOMALIES OF THE RENAL PELVIS AND URETER

Doubling of the ureter and the pelvis outside of the renal hilus is one of the most frequent of urinary tract anomalies. Several varieties of duplication are shown in Figure 6-36. The caudal of the two renal pelvises is usually the larger, the smaller cephalic pelvis often has a tubular shape resembling the continuation of the ureter. As can be seen from the drawings, how-

ever they are occasionally of equal size, and rarely the cephalic pelvis may be the larger. Multiple subdivisions of the pelvis have been described.

A nonfunctioning second pelvis may be suspected on excretory urography when the functioning pelvis lacks a full complement of calices and is unusually remote from one pole of the kidney. Most frequently it is the cephalic pole which is involved, and the configuration of the incomplete caudal pelvis and calices has been described as a "wilted flower" (Fig 6-37). Retrograde filling is often required for roentgenographic proof.

The ureter may branch and become a double tube at any level between the bladder and the renal pelvis (Figs 6-38 and 6-39). When the duplications of the ureter are separate throughout their course, the ureter from the caudal renal pelvis enters the vesicular trigone in the normal position and the orifice of the ureter derived from the cephalic pelvis enters caudal to it. The lower end of a single or supernumerary ectopic ureter may open into the bladder, urethra, vestibule, vagina, rectum, the ejaculatory duct or the vas deferens and seminal vesicle. These structures represent Mullerian duct derivatives in the female and Wolffian duct derivatives in the male. Occasionally a dilated ureter and the vas form a palpable multilocular cystic mass involving the seminal vesicle. Renal hypoplasia or dysplasia may be associated (Fig 6-40). Ectopic orifices are usually obstructed, and dilatation of the affected ureter is common. Some of the most severe obstructions are encountered in what has been called "ectopic ureterocele." This condition actually represents an ectopic ureteral orifice from a ureter whose most distal portion traverses the sphincter of the bladder (Figs 6-41 and 6-42). The muscular



Fig. 6-40 — Ureteral ectopy in the vas deferens associated with renal dysplasia in a youth 18 years of age who had recurrent right-sided pain. In A, excretory urogram, the right kidney is not delineated. The right herningone was absent on cystoscopic examination. In B, on incision into the vas deferens exposed in

the right scrotum during surgery, the dysplastic kidney presents as a cystic mass communicating with the vas deferens. Dilatation of the seminal vesicle and adjacent portions of the vas deferens obstructs (congenital?) in the right ejaculatory duct. (Courtesy of Dr. Courtney Parsinger.)

Fig. 6-41 — Diagram of ectopic ureterocele. The upper pole drains the dysplastic kidney parenchyma. Its ureter burrows submucosally in the wall of the bladder, bulging in the cavity of the bladder, and traverses the bladder sphincter.

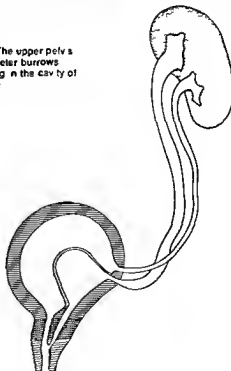




Fig 6-42.—A, ectopic ureterocele simulating gas in the rectum. Duplication of the pelvis is definite on the right side. B, diagram of diagnostic features. A, lumen of urinary bladder. H, nonopacified left ectopic ureterocele. E, nonopacified cephalic

pelvis. M, opacified caudal pelvis of left kidney. L, ureter from caudal pelvis of left kidney. P, cephalic pelvis and P₂, caudal pelvis of the right kidney.

tone of this structure, as well as the effect of the detrusor contraction when the sphincter is relaxed causes a severe degree of obstruction. The dilated ureter, which passes in the wall of the bladder from the region of the normal ureterovesical orifice to the bladder neck, is supported externally by the thick muscular wall of the bladder but is covered internally only by bladder mucosa. Dilatation of the ureter therefore produces a large herniation within the bladder which has been called a ureterocele. It has been estimated that as many as 80% of the "ureteroceles" in infants and children are of this variety, the incidence in girls is four times or more than in boys. Serious urinary tract symptoms usually occur in the 1st year of life. The portion of the kidney drained by the ectopic ureter is almost invariably dysplastic and management usually requires removal of the abnormal portion of the kidney together with the ureter whose intravesicular portion is "uncapped." Ericsson clarified the problem of ectopic ureterocele, and his publications should be consulted for details. The infrequent adult type of ureterocele, with its "spring onion" or "cobra head" appearance at the ureterovesi-

cular junction, its small size and its usual lack of association with dilatation of the ureter, can be identified by its characteristic appearance. Some trigonal cysts almost certainly represent ectopic ureteroceles whose cephalic and caudal portions have degenerated during fetal life. They present as fluid-filled cystic structures bulging into the lumen of the bladder from the trigone and usually causing severe obstruction of the bladder outlet.

In the female most ectopic ureteral orifices other than those associated with "ectopic ureteroceles" are incontinent as well as obstructive. They present clinically, therefore, with what passes for diurnal and nocturnal enuresis.

Congenital malformations of the ureter commonly are associated with obstructive manifestations and are discussed later in detail under this heading. Strictures are most common at the ureteropelvic junction or the vesicular orifice in the trigone, but may occur at any level. The condition described as "high insertion of the ureter" is thought by Williams to result from asymmetrical distention of an obstructed pelvis. The layering effect of excreted contrast material

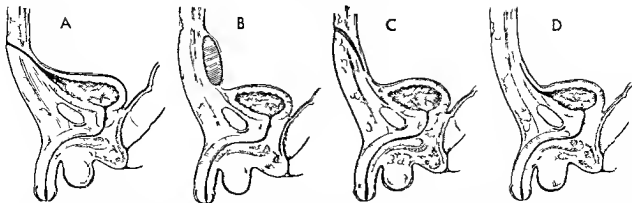


Fig 6-43 —Patency of the urachus and urachal remnant. A: patent urachal canal connecting the umbilicus and bladder. B: urachal cyst with both ends of the urachal canal closed and the

lumen dilated with epithelial exudate. C: urachal remnant open at the umbilicus and closed at the vesical end. D: urachal remnant open at the vesical end and closed at the umbilicus.

may preclude adequate visualization of the ureteropelvic obstruction unless films are taken with the patient prone as well as in the routine dorsal recumbent positions (see Fig 6-17). Rarely mucosal valves are present within the lumen and may or may not be associated with obstruction. The mucosa itself is involved and the muscularis does not extend into the valves.

As a result of anomalous development of the inferior caval system of veins, one or both ureters may pass behind venous structures which produce compression and proximal dilatation of the ureter. The most common anomaly is seen on the right side where the ureter passes behind the inferior vena cava at a level between the third and the fifth lumbar vertebral body; the distal portion of the ureter is medially placed and not dilated, but the proximal portion and the pelvis are.

ANOMALIES OF THE BLADDER

URACHAL ANOMALIES — The allantoic canal between the umbilicus and the bladder is normally completely obliterated by the time of birth. However, it may remain open through its entire course or it may close at either end (Fig 6-43; see also Figs 4-3 and 4-4). When both ends close and the intermediate segment remains open, a large or small urachal cyst may develop and become filled with exudate from the epithelial lining. Patent urachal remnants are situated in the midsagittal plane of the abdomen between the bladder and the umbilicus and are clearly delineated by opaque substance injected into the orifice at the umbilicus or into the bladder (Fig 6-44). Retrograde injections through draining orifices in the umbilicus should be done only with as clean a technique as possible and with urologic agents suitable for injection into the blood stream. At times it is impossible to tell before an injection whether the minute draining orifice represents an incompletely obliterated allantoic canal, an omphalomesenteric duct, or an umbilical vein.

Large closed urachal cysts cannot be visualized by retrograde injection and present only as a mass of water density displacing the intestines away from the anterior abdominal wall and occasionally impinging on the bladder from above.

DIVERTICULA — Diverticula of the bladder are usually associated with obstruction; they are produced by mucosal herniation through defects in the muscular wall and are actually pseudodiverticula. Contraction of the bladder usually causes distention of the diverticulum even when obstruction is not present, and reflux of urine from the diverticulum into the bladder during the relaxation phase is a cause of false residual urine. Superimposition of the filled diverticulum on the filled bladder may preclude its identification in films taken in only one projection. Cinefluorographic examinations are probably most valuable in identifying the position and nature of diverticula. A common

Fig 6-44 —Patent urachal remnant (arrows) extending cephalad from the summit of the bladder to the umbilicus. Cystogram in lateral projection.



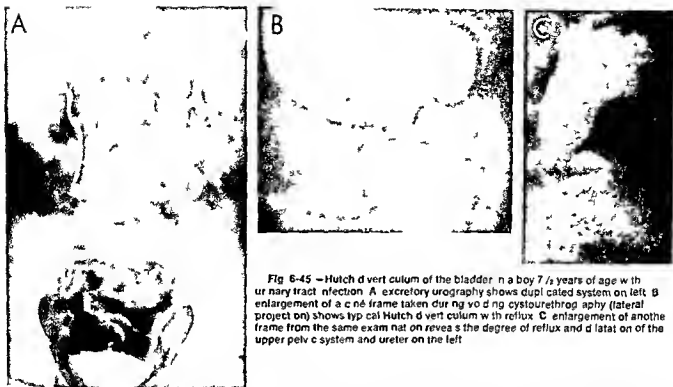


Fig 6-45—Hutch diverticulum of the bladder in a boy 7 1/2 years of age with urinary tract infection. A, excretory urography shows duplicated system on left. B, enlargement of a cine frame taken during voiding cystourethrography (lateral projection) shows typical Hutch diverticulum with reflux. C, enlargement of another frame from the same examination reveals the degree of reflux and dilatation of the upper pelvic system and ureter on the left.

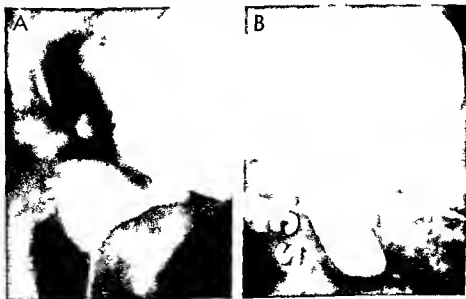
site of diverticula has been adjacent to the ureterovesicular junction, and the incorporation of this junction in the diverticulum sac has been recognized on many occasions. Hutch suggested that many of these diverticula are a consequence of congenital or acquired deficiencies of the muscular structures surrounding the oblique canal through which the ureter enters the bladder (see Fig 6-5). Occasionally these

diverticula fill only during voiding (Fig 6-45). Their significance lies in the fact that surgical correction with re-insertion of the ureter into the bladder through a new oblique channel is required for elimination of the urinary signs and symptoms related to such a diverticulum and the reflux commonly associated with it.

EXSTROPHY—The radiologic features of this condi-

Fig 6-46—Posterior urethral valves proved at surgery in two infants less than 1 week of age. A, severe obstruction and marked bladder trabeculation. The urethra filled only when pressure was made on the abdomen. Congenital urethral stricture

was suspected but valves were found at surgery. B, severe obstruction, but the bladder is not decompensated. This is the more typical appearance of posterior urethral valves.



tion, which is usually diagnosed on inspection are separation of normally mineralized pubic bones and secondary changes in the upper urinary tract. A surprisingly large number of children may have a relatively normal upper urinary tract so that surgical procedures involving closure of the bladder when feasible or, more frequently, the production of an ileal bladder may have much to offer. Occasional instances of pubic separation with diastasis recti and ventral hernia possibly represent incomplete forms of the anomaly, when the skeletal manifestations are identified. Examination of the urinary tract is usually desirable (see Fig. 5-34).

TRICONAL CYSTS—These structures have been described in relation to ectopic ureteroceles.

ANOMALIES OF THE URETHRA

Most urethral anomalies, whether in male or female, are important because of the associated obstruction. Some such as hypospadias and epispadias, are best diagnosed clinically but are indications for evaluation of the upper urinary tract because of frequently associated abnormalities. Fistulous communications with the rectum are discussed under anal atresia (see Fig. 4-227) and fistulous communications with the vagina are described later in the section on the reproductive system. Congenital structures of the urethra occur almost exclusively in the male, in the prostatic urethra they are indistinguishable from posterior urethral valves of the diaphragm type (Fig. 6-46). The most common form of posterior urethral valve is a fold of mucosa running from the veru montanum to the lateral walls of the urethra. Rarely urethral valves are found in the female and may re-

semble, radiographically, posterior urethral valves in the male. Anterior urethral valves are less common than posterior ones and occur almost exclusively in the male. Urethral polyps are rare. Diverticula occasionally are found in the male, rarely in the female. The concealed diverticulum opens into the floor of the penile urethra and is surrounded by the corpus cavernosum (Fig. 6-47), therefore, it is not usually recognized on clinical inspection. Vestigial structures such as a persistent utricle, may simulate a posterior urethral diverticulum. According to Williams, true urethral diverticula do not occur in the female in childhood.

Duplications of the urethra are uncommon. A complete accessory channel may be present, or it may be blind at one or both ends, or it may communicate at one or both ends with the normal channel (Fig. 6-48). In the female a complete double urethra may cause urinary incontinence. Meatal stenosis in the male is a clinical observation and is most often a consequence of ammoniacal dermatitis and poor hygiene. In the female, meatal stenosis is of uncertain significance. It is discussed in the following section on urinary tract obstructions.

Most of the anomalies of the urethra are associated with obstruction of urinary flow. As a consequence there are frequently enlargement and trabeculation of the bladder with reflux into and dilatation of the upper urinary tract as well as other features of obstruction: urinary retention and superimposed infection which are described in the appropriate sections.

REFERENCES

- Alken C. E. *et al.* (ed.) *Handbuch der Urologie*. Encyclopedie of Urology VII/1 Malformations (Berlin: Springer Verlag, 1968).

Fig. 6-47 (left)—Diverticulum in the floor of the pendulous urethra in a voiding urethrogram made in oblique projection.



Fig. 6-48 (right)—Duplication of the urethra in which a narrow dorsal urethral channel (arrows) joins with an obstructed primary posterior urethra.



- Campbell M F. *Clinical Pediatric Urology* (Philadelphia: W B Saunders Company 1951)
- Carter J E and Lirenman D S. Bilateral renal hypoplasia with oligomeganephronia. *Oligomeganephronic renal hypoplasia*, *Am J Dis Child* 120:537 1971
- Curran G., and Winchester P. Position of the kidneys relative to the spine with emphasis on children. *Am J Roentgenol* 95:409 1965
- Ericsson, N O. Ectopic ureteroceles in infants and children. *A clinical study*. *Acta chir scandinav* supp 197 1954
- and Ivarmark, B I. Renal dysplasia and urinary tract infection. *Acta chir scandinav* 115:58 1958
- Evans J A. Medullary sponge kidney. *Am J Roentgenol* 85:119 1961
- Gross R E., and Bill A H. Concealed diverticulum of the male urethra as a cause of urinary obstruction. *Pediatrics* 14:148 1948
- and Moore T C. Duplication of the urethra. Report of two cases and summary of the literature. *Arch Surg* 60:749 1950
- Grossman H., Winchester P H and Chisari, F V. Roentgenographic classification of renal cystic disease. *Am J Roentgenol* 104:319 1968
- Hutch, J A. *The Uterovaginal Junction* (Berkeley: Calif University of California Press 1958)
- Kelly H A. and Burnham C F. *Diseases of the Kidneys, Ureters and Bladder* (2d ed. New York City: D Appleton & Co 1922)
- Landau S J., and Lattimer J K. Functional closure of bladder exstrophy. *Pediatrics* 31:433 1963
- Longino L A. and Martin L W. Abdominal masses in the newborn infant. *Pediatrics* 21:596 1958
- Lowman, R M. Waters L L. and Stanley H W. The roentgen aspects of congenital anomalies in the umbilical region. *Am J Roentgenol* 70:883 1953
- Lundin, P M. and Olow I. Polycystic kidneys in newborns, infants and children. A clinical and pathological study. *Acta paediat* 50:180 1961
- Mitchell G E. Makhluh Z. and Fritelli G. Congenital urethral valve in the female. *Radiology* 89:690 1967
- Osathanondh, V. and Potter E L. Pathogenesis of polycystic kidneys. *Arch. Path.* 77:459 1964
- Parks R E., and Chase W E. Retrocaval ureter. Report of two cases diagnosed preoperatively in childhood. *Am J Dis Child* 82:442, 1951
- Reilly B J. and Neuhauser E B D. Renal tubular ectasia in cystic disease of the kidneys and liver. *Am J Roentgenol* 84:546 1960
- Robenstein, M. Meyer R. and Bernstein J. Congenital abnormalities of the urinary system. *J Pediatr* 58:356 1961
- Spangler E B. Complete triplication of the ureter. *Radiology* 80:790 1963
- Stephens F D. *Congenital Malformations of the Rectum, Anus and Genito-Urinary Tracts* (Edinburgh: E & S Livingstone Ltd 1963).
- Vanhouste J J. Ureteral ectopia into a Wolffian duct remnant (Gartner's ducts or cysts) presenting as a urethral diverticulum in two girls. *Am J Roentgenol* 110:540 1970
- Wyatt, G M. and Lanman T H. Calculus in an urachus. Report of a case with enuresis. *Am J Roentgenol* 63:673 1940
- Wyrens R G. Calyceal diverticula or pyelogenic cysts. *J Urol* 70:358 1953

Urinary Obstruction

Numerous lesions and agents within and contiguous to the urinary tract lead to obstruction of the urinary channels (Fig 6-49). Obstruction causes urinary stasis and this in turn, favors the perpetuation of infection. Investigators do not agree concerning

the roles of infection and obstruction alone but since both are in many instances amenable to therapy and either is apparently worse when the other is also present an attempt will be made to partition their individual contributions to the radiologic features. The principal structural changes caused by urinary obstruction are dilatation and elongation of the urinary channels above the level of the obstruction. The pattern and the magnitude of these changes are determined by the level and the nature of the obstruction and the presence or absence of infection.

When obstruction is of long standing and there is considerable dilatation of the pelvis and calices excretion of intravenously injected contrast material may be so delayed that films taken within the first hour after the injection do not demonstrate shadows of contrast material. In some instances the papillary ducts which normally are perpendicular to the long axis of the alux are forced into a position parallel to the circumference of the dilated calix. Collection of contrast material in these circumferentially oriented papillary ducts contrasts in density with the urine distending the calix so that initially the position of the dilated calix is outlined by a ring or crescent of increased density (Fig 6-50). When late films are obtained (two to three and five hours after the injection) the accumulation of contrast material in the dilated calices is sufficient for the mixture of urine and contrast material to be recognized. Even when the crescentic silhouette presents initially delayed films in instances of obstruction or suspected hydronephrosis or both may permit delineation of the dilated pelvis although additional procedures are often required for identification of the nature of the obstructing lesion.

ROENTGEN APPEARANCE AT DIFFERENT LEVELS

Obstruction to the calices with consequent caliectasis or hydrocalix is most commonly due to pelvic stones. Rarely scarring following trauma or infection may produce infundibular stenosis. Both renal arteries and renal veins may produce indistinguishable impressions. These are most common at the base of the superior group of calices (Fig 6-51). Not only is the affected calix larger and its fornices blunter than adjacent normal calices but contrast medium tends to remain in it while the others empty in normal fashion.

OBSTRUCTION AT THE URETEROPELVIC JUNCTION — Isolated ureteropelvic obstruction occurs more commonly in older children than in infants. It is often bilateral although of unequal degree on the two sides. Urologists generally agree that dilatation due to this type of obstruction affects the extrarenal portion of the pelvis first and that dilatation of the calices occurs relatively late. Lower urinary tract obstruction on the other hand is said to spare disproportionate dilatation of the calices and to spare the pelvis. Experience with cine cystourethrography which permits

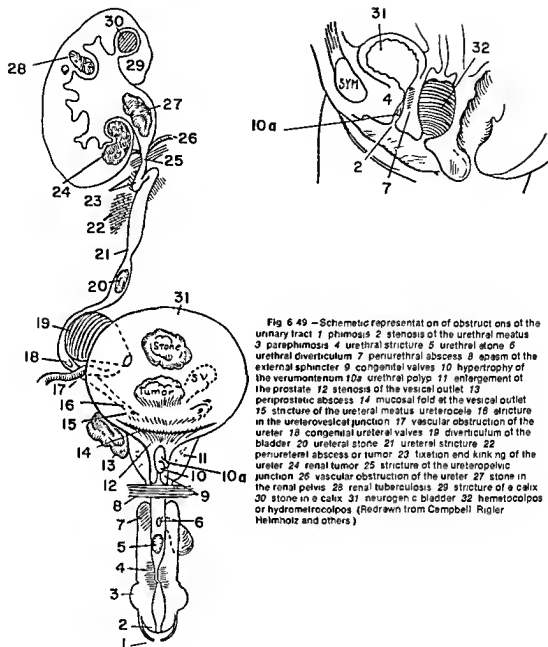


Fig 6 49 —Schematic representation of obstructions of the urinary tract 1 phimosis 2 stenosis of the urethral meatus 3 paraphimosis 4 urethral stricture 5 urethral stone 6 urethral diverticulum 7 periurethral abscess 8 spasm of the external sphincter 9 congenital valves 10 hypertrophy of the verumontanum 10a urethral polyp 11 enlargement of the prostate 12 stenosis of the vesical outlet 13 periprostatic abscess 14 mucosal fold at the vesical outlet 15 stricture of the ureteral meatus ureterocele 16 stricture in the ureterovesical junction 17 vascular obstruction of the ureter 18 congenital ureteral valves 19 diverticulum of the bladder 20 ureteral stone 21 ureteral stricture 22 periureteral abscess or tumor 23 fixation and kinking of the ureter 24 renal tumor 25 stricture of the ureteropelvic junction 26 vascular obstruction of the ureter 27 stone in the renal pelvis 28 renal tuberculosis 29 stricture of a calix 30 stone in a calix 31 neurogenic bladder 32 hematoecolpos or hydrometecolpos (Redrawn from Campbell, Rigler, Helmholtz and others)

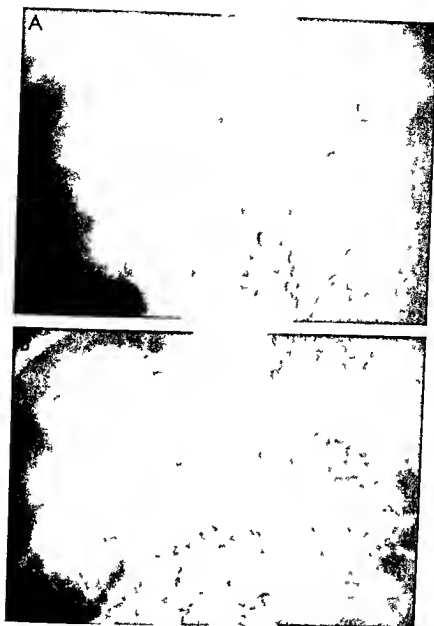


Fig 5-50 — Crescent sign in hydronephrosis. In A, at 5 minutes, the normal left pelvis is clearly seen. On the right, opaque rings outline the dilated calices. Some contrast material can be seen in dependent portions of the dorsal calices. In B, at 30 min-

utes, the contrast material has been flushed out of the left pelvis but it has accumulated in the enormous right pelvis. Compare with A for size and location of individual calices. This sequence also illustrates the value of delayed films in hydronephrosis.



Fig 6-51 —Dilatation of the superior calyx on the right cause unknown. Possibly it was due to pressure by an extrinsic vessel although scar from a prior inflammatory reaction is not excluded.

There was no history of calculus. Contrast material was retained in the calyx after other calyces and pelves on both sides had emptied almost completely.

study of the dynamics of the urinary collecting and conduit systems suggests that this differentiation is not regularly valid. Structures which appear to be normal at one moment are observed to distend to pathologic proportions the next. The degree of activity at the instant of radiographic exposure determines the form of the roentgen image. Size alone of the renal pelvis is not an indication of ureteropelvic obstruction because of the great range of variation in the volume of the normal renal pelvis. Extrinsic pressure from anomalous vessels is quite common; most frequently the vessel is a separate artery from the

aorta to the lower pole of the kidney (Fig 6-52). Extrinsic adhesions by themselves or associated with an aberrant vessel may narrow the lumen, producing pyelectasis. Nonobstructing adhesions may be responsible for the appearance of kinks when the kidneys are displaced downward during deep inspiration. True extrinsic obstructions produce constant narrowing. According to Williams, so-called high insertion of the ureter is a consequence of obstruction and asymmetrical dilatation of the pelvis rather than a primary cause of pyelectasis, although it subsequently may contribute to persisting obstruction. Actual stenoses at the ureteropelvic junction are found which may be associated with adhesions or aberrant vessels or both. Lich suggested that fine mucosal valves are responsible for intrinsic obstruction; these cannot be demonstrated radiographically and require special fixation of the intact ureteropelvic junction and serial histologic sections for their demonstration. At times the obstruction is of a degree which permits a slow normal urine flow to proceed without clinical signs or symptoms; if there is rapid urinary flow the narrowed segment is inadequate and the pelvis proximal to it dilates and causes pain. This has been referred to as hydration hydronephrosis and may be identified at times only by repeating what appeared to be normal excretory urography under conditions which enhance renal filtration rates.

URETERAL AND URETEROVESICAL OBSTRUCTION — Depending on the level of obstruction, a segment or the entire ureter may be distended. In addition to the ureteral dilatation and elongation, the renal pelvis is distended. Nevertheless, in many instances of ureteral dilatation, and particularly when there is dilatation of the lower urinary tract, the pelvis and calyces appear to be spared.

Localized ureteral obstruction may be caused by iliac lymphadenopathy. Characteristic features as described by Marshall and Schmittman include (1) pain in the flank without significant urinary symp-

Fig 6-52 —Deep localized indentation at the ureteropelvic junction by an ectopic blood vessel (arrows) with only slight evidence of dilatation.





Fig. 6-53 — Neurogenic uropathy in a girl 9 years of age with manngocoe and clubbed feet referred from the orthopedic clinic because of growth failure. A: sacral spine bifidum with scoliosis.

loss and pelvic deformity. B: cystogram showing trabeculated bladder and bilateral reflux. Compare with Figure 6-55.

diverticula) and often vesicoureteral reflux with dilatation of the upper urinary tract (Fig. 6-53). The dilated ureters of bladder neck obstruction or infravesical obstruction are relatively atonic in comparison with the active peristalsis of equally dilated ureters in the megacystis megaureter syndrome of unknown etiology. Bladder neck obstruction probably plays no part in the megacystis syndrome and the ability of the bladder to empty its lumen completely even though marked reflux into ureters takes place is a characteristic finding. Production of an excessive volume of dilute urine may play a role in some instances of the megacystis syndrome. Refilling of the collapsed bladder from the dilated ureters often requires multiple voidings before all of the bladder content can be discharged to the outside.

URETHRAL OBSTRUCTIONS—*Congenital obstructions* of the urethra are usually associated with proximal dilatation of the urinary tract and destruction of the kidneys. Although conceivably susceptible to diagnosis by retrograde urethrography or suprapubic cystourethrography, urethral obstructions are seldom seen in viable infants. These obstructions are usually in the proximal portion of the urethra; distal urethral obstructions are thought to represent temporary obstructions because the upper urinary tract is frequently normal.

Fibroelastosis of the prostate is discussed in the preceding section.

Posterior urethral valves cannot be identified ade-

quately by retrograde urethrography requiring voiding urethrography for their demonstration. Failure to encounter obstruction on passage of a catheter or even on cystoscopic inspection is common because the thin mucosal folds are easily displaced just as the cusps of the aortic valve are displaced by the blood during cardiac systole. During voiding as in cardiac diastole the direction of fluid pressure brings the valve leaflets together to impede the flow (Fig. 6-54). Children with posterior urethral valves may have almost as much upper urinary tract dilatation and kidney destruction as those with urethral obliteration (Fig. 6-55); however, the ability of the urinary tract to recover and the relative ease with which this obstructing lesion can be relieved warrant early surgical removal of the valves. Normal folds extending both proximally and distally from the verumontanum should not be confused with pathologic valves (Fig. 6-56). The folds are occasionally seen when the posterior urethra is dilated as a consequence of more distal obstruction.

Hypertrophy of the verumontanum is mentioned as a cause of obstruction more frequently than it probably occurs. It is quite possible that other associated obstructive lesions have been overlooked when this structure of variable size appears prominent in children with infravesical obstruction. Frates and DeLuca reported two instances of *urethral polyps*, one with recurrence six years after original excision. The polyps were attached to the verumontanum and



Fig. 6-54 (left) — Marked dilatation of the prostatic urethra (arrows) due to valves in the posterior urethra. The ureters and renal pelvises on both sides were dilated. Lateral oblique voiding cystogram.



Fig. 6-55 (right) — Posterior urethral valves — same patient as in Figure 6-54. The patient had been thought to have neurogenic uropathy because no obstruction was found on cystoscopy and retrograde urethrogram. The cystogram shows extensive reflux and trabeculated bladder. Compare with Figure 6-53 B.

Fig. 6-56 — Normal mucosal folds in the male posterior urethra. The constrictor urethralis and prostatic collum may be thrown

into relief when the urethra is dilated and are confused with posterior urethral valves. (From Callander.)

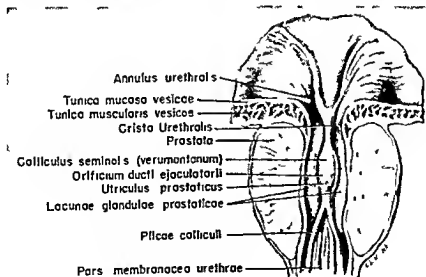




Fig. 6-57 — Meatal stenosis in a girl 6 years of age with recurrent pyuria. Two spot films taken during cinecystourethrography. The external orifice (meatus) is narrow and the urethra above it is

dilated by the vigorous bladder contraction. The prominent bladder neck (internal sphincter) is secondarily hypertrophied.

moved from the bladder outlet to the urethra on cystography and voiding cystourethrography respectively. The upper urinary tract may be normal on excretory urography.

Meatal stenosis in the female achieved considerable popularity as a cause of recurrent urinary tract infection during the past decade. Clinical and radiologic features for identifying stenosis have been described. The caliber of the meatal orifice has been evaluated by the size of the largest catheter or sound it will easily pass. Standards in relation to age have now been published but are not universally accepted. Mean values obtained by Immergut and colleagues

follow 0 to 4 years, 15.1 F, 5 to 9 years, 17 F, 10 to 14 years, 21.4 F, and 15 to 20 years, 26.2 F. It is not clear whether meatal stenoses are due to muscular spasm, fibrosis, other factors or to a combination of causes. Nevertheless voiding cystourethrography in patients with recurrent urinary tract infection has disclosed a large group of children with dilatation of the urethra proximal to the meatus who have enjoyed freedom from recurrent infection for the first time only after mechanical dilatation of the meatus. Radiographic abnormalities in the urethra may persist unchanged, but residual urine and ureteral reflux disappear following the procedure. A prominent bladder neck is commonly associated with the urethrographic pattern of meatal stenosis (Figs. 6-57 and 6-58). It has been suggested that the primary abnormality is bladder neck hypertrophy with poststenotic dilatation of the urethra, but it is much more likely that hypertrophy, if present, is a manifestation of general detrusor hypertrophy. Multiple studies of pressure and flow relationships in children with normal urinary tracts and those with what has been considered abnormal urethral dilatation have not demonstrated consistent reproducible results. The subject was reviewed in considerable detail by Krøigaard. Krøigaard uses the term "urethral dysfunction" to designate urethral dilatation in females of the type shown in Figure 6-57. Support for the concept that this configuration does represent a deviation from normal is provided from several sources. Kjellberg and associates failed to identify this configuration in any of the normal females they investigated during their pioneer study of the lower urinary tract. Headstream allowed me to review the films of the 100 normal females he examined in a study of reflux, and in none of these is there a urethra with this configuration. Although Headstream's films are single exposures during the act of voiding, it is unlikely that not a single patient would show the dilatation if it were as common in normal females as has been suggested by Shopfner. Confirmation or refutation of Shopfner's statistics is urgently needed to help resolve the question of the signifi-

Fig. 6-58 — Same patient as in Figure 6-57 after meatotomy and dilatation. The urethra shows a gradual narrowing from above downward; there is no abnormal dilatation and the hypertrophy of the bladder neck has disappeared. In all films, tilting of the vagina behind the urethra is a normal finding in recumbent voiding films.



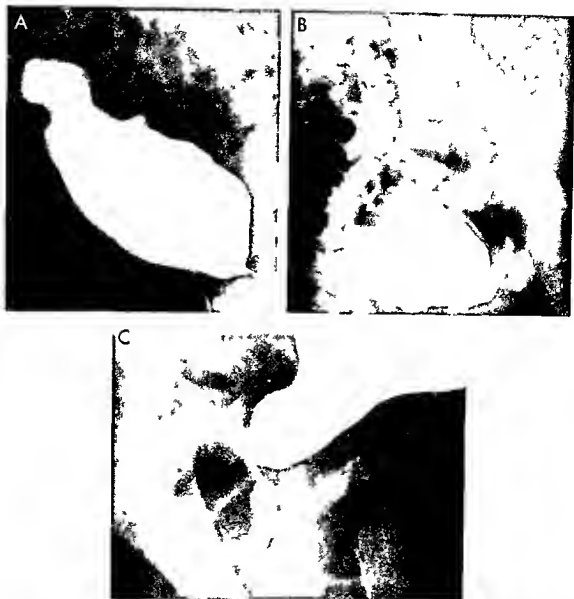


Fig 6.60—Urologic complications in congenital absence of the abdominal muscles in a boy 8 months of age. **A**: cystogram shows the faccid bladder adherent to the anterior abdominal wall, especially in the area of the apical dilatation, which probably represents a urachal remnant. There was no urachal fistula. **B**: excretory urogram 24 hours after **A** shows residual Lp odor, which, from failure to empty the bladder, has refluxed into the dilated ureters and pelves, especially on the left. **Renal function**

is good notwithstanding the hydronephrosis and hydroureter. **C**: voiding urethrogram (Crédé) at completion of cystogram. The post-void urethra is dilated to the level where the external sphincter is found. Although a valve is suggested, none was found. The appearance of a fundus ring is simulated; there was no active bladder contraction at the time the contrast medium was manually expressed.

greater than anticipated frequency with Wilms' tumor. Hereditary nephropathy occurs in association with osteo-onychodysplasia (nail patella syndrome). Bilateral renal hypoplasia has been described in association with a lateral displacement of the nipples.

REFERENCES

- Blanc, W. A., and Baens, G. Ear malformations, abnormal facies and genitourinary tract anomalies. *Am J Dis Child* 100:781, 1960.
- Eagle, J. F., Jr., and Barrett, G. S. Congenital deficiency of abdominal musculature with associated genitourinary abnormalities. A syndrome. Report of nine cases. *Pediatr* 6:721, 1950.
- Fleisher, D. S. Lateral displacement of the nipples: a sign of bilateral renal hypoplasia. *J Pediatr* 69:806, 1966.
- Leahy, M. S. The hereditary nephropathy of osteo-onychodysplasia. Nail patella syndrome. *Am J Dis Child* 112:237, 1966.
- Müller, R. W., Fraumeni, J. F., Jr., and Manning, M. D. Association of Wilms' tumor with aniridia, hemihypertrophy and other congenital malformations. *New England J Med* 270:922, 1964.
- Potter, E. L. Facial characteristics of infants with bilateral renal agenesis. *Am J Obst & Gynec* 51:885, 1946.
- Silverman, F. N., and Huang, N. Congenital absence of the abdominal muscles associated with malformation of the genitourinary and alimentary tracts. Report of cases and review of literature. *Am J Dis Child* 80:91, 1950.
- Smith, D. W., et al. The no. 18 trisomy syndrome. *J Pediatr* 60:513, 1962.
- . The D, trisomy syndrome. *J Pediatr* 62:326, 1962.

Urinary Calculi

Urinary stones vary greatly in size, shape, location, number and radiopacity (Figs 6-61 and 6-62). Calculi are not rare in early life, and uric acid stones are fairly

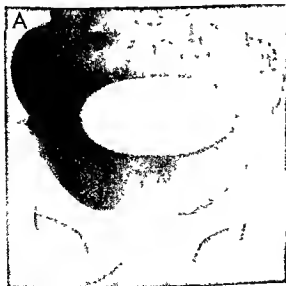
frequent in the neonatal period. Large calculi may be found in the bladder and kidneys during the 1st year of life. Most of the stones are composed of a mixture of salts. Uric acid and urate calculi are the most common type, phosphate and oxalate stones vary in frequency in different series. Oxalate stones are more common in Denmark and the United States than in England, where phosphate stones are most often seen. About 75% of the urinary stones are in the bladder, but they may be found in any part of the urinary tract. Migration of the stones from a cephalad to a more caudal level is common.

Only radiopaque stones are visible in plain films of the abdomen and pelvis. The density of a stone is directly proportional to its calcium content. Diffuse calcification in the pyramids of the kidney, commonly referred to as nephrocalcinosis, usually results from renal tubular disease associated with hypercalcemia (Fig 6-63). Cystinuria, a familial defect of tubular resorption, usually produces renal intrapelvic calculi. The deposition of calcium in the kidney, in both cystinuria and cystinosis, may lead to total renal failure. Calculi are found following prolonged recumbency and with hypervitaminosis D; they may also develop around foreign bodies inserted into the bladder. In oxalosis, oxalate deposits are found in the kidney (Fig 6-64), and oxalate stones can occur in the conduit system. Calcifications are occasionally associated with renal tubular ectasia. Intraluminal calculi can cause obstruction proximal to their point of lodgment and perpetuate obstruction by the production of secondary strictures (Fig 6-65).

The images of urinary calculi must be differentiated from other dense images cast by foreign bodies and opaque intestinal contents, calcifying abdominal and

Fig 6-61 — A, large radiopaque stone in the bladder of a boy 5 years of age. Concentric lamellations were visible in the original film. B, multiple intrapelvic (staghorn) calculi in a boy 10 years of

age. Arrow indicates several stones from the right pelvis that have passed to the lower ureter.



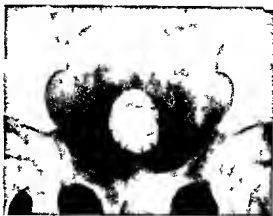


Fig 6 62.—Typical calcium oxalate stone in the bladder lumen of a girl 12 1/2 years of age

Fig 6 63 (left)—Bilateral renal calcification in a 16-year-old boy who had hypochloremic acidosis and renal rickets

Fig 6 64 (right)—A 10-year-old boy with oxalosis. Note diffuse calcifications of small kidneys. Six months after examination after

passage of a stone revealed growth failure, small kidneys, hypertension, and elevated blood urea nitrogen level. Oxalate crystals were found in bone marrow; oxalate excretion was greatly increased above normal.



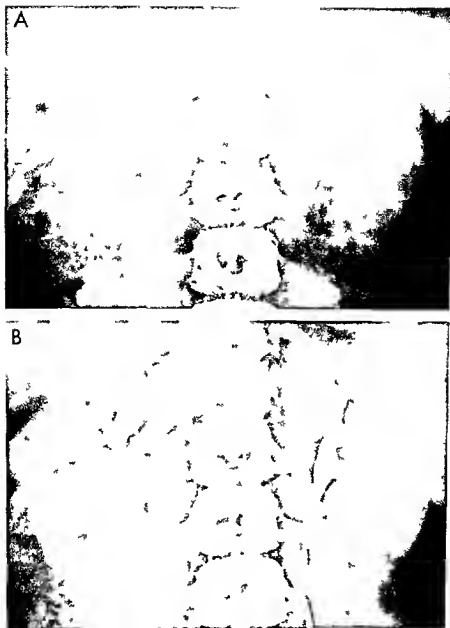


Fig 6-65 - Stone in the renal pelvis. A, plain film of the abdomen. In B, during excretory urography, the stone is a most obli-

terated because of density of the excreted contrast agent. Moderate to severe pelvic obstruction is present.



Fig 6-65 (left) — Hypoplastic twelfth rib superimposed on the dense shadow of a renal stone. Tracing of a roentgenogram.

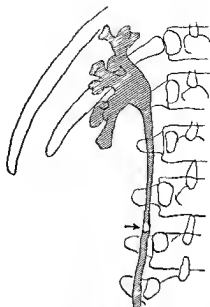


Fig 6-67 (right) — Excretory urogram showing a small radiolucent shadow in the ureter. Human tracing of roentgenogram. Such filling defects may be caused by nonopaque stones and blood clots.

pelvic tuberculous lymph nodes calcified tuberculous foci in the urinary and genitourinary tracts and phleboliths. Rudimentary ribs and atypical vertebral processes superimposed on the kidneys may cast opaque images which can be confused with renal calculi (Fig 6-66). Calcification in neuroblastoma, calcification or even bone formation in Wilms' tumor or in retroperitoneal teratomas and calcification in other tumors in the vicinity of the kidneys must be differentiated from renal calculi. Lateral and oblique projections may be essential to the accurate interpretation of opaque images in the abdomen and pelvis. Spot films taken during image intensification fluoroscopy are valuable. The diagnosis of urinary calculi should not rest on roentgen findings alone; negative findings in plain films do not necessarily exclude nonopaque urinary calculi.

In urograms radiolucent urate stones appear as filling defects in the opaque shadow of the contrast material in the urinary channels (Fig 6-67). Sometimes absorption of the radiopaque contrast medium into an originally radiolucent stone renders it opaque in later examinations. Air bubbles in the opaque contrast material injected during retrograde urography and blood clots resemble the filling defects caused by nonopaque calculi. Major features during excretory urography of acute obstruction due to stone are (1) delayed appearance of contrast on the affected side, (2) an enlarged kidney on the affected side with exaggerated nephrogram, and (3) delayed emptying of an enlarged pelvis and ureter proximal to the stone.

Wyatt and Lanman reported calculus formation in a urachal cyst in an enuretic boy 7 years old. Following excision, the enuresis was said to have improved. The excised urachal remnant was not only calcified but in part ossified.

REFERENCES

- Albright, F. and Reifenstein, E. C. Jr. *The Parathyroid Glands and Metabolic Bone Disease. Selected Studies* (Baltimore: Williams & Wilkins Company, 1948).
- Anderson, W. A. D. Renal calcification in infancy and childhood. *J. Pediatr.* 14:375, 1939.
- Basa, H. N. and Emanuel, B. Nephrolithiasis in childhood. *J. Urol.* 95:749, 1966.
- Lonsdale, K. Human stones. *Science* 159:1199, 1968.
- Myers, N. A. A. Urolithiasis in childhood. *Arch. Dis. Child.* 32:48, 1957.
- Salk, J. O. and Abeshouse, B. S. Calcification, ossification and cartilage formation in the kidney. *Am. J. Roentgenol.* 83:125, 1962.
- Wyatt, G. M. and Lanman, T. H. Calculus in the urachus: report of case with enuresis. *Am. J. Roentgenol.* 43:673, 1940.

Trauma

Radiographic examinations in instances of renal trauma are important for diagnosis, management and follow-up. Plain films of the abdomen are helpful in identifying or excluding other visceral injuries in addition to providing presumptive evidence of unilateral injury. Frequently scoliosis, concave toward the injured side, is present; scoliosis may be reflex due to

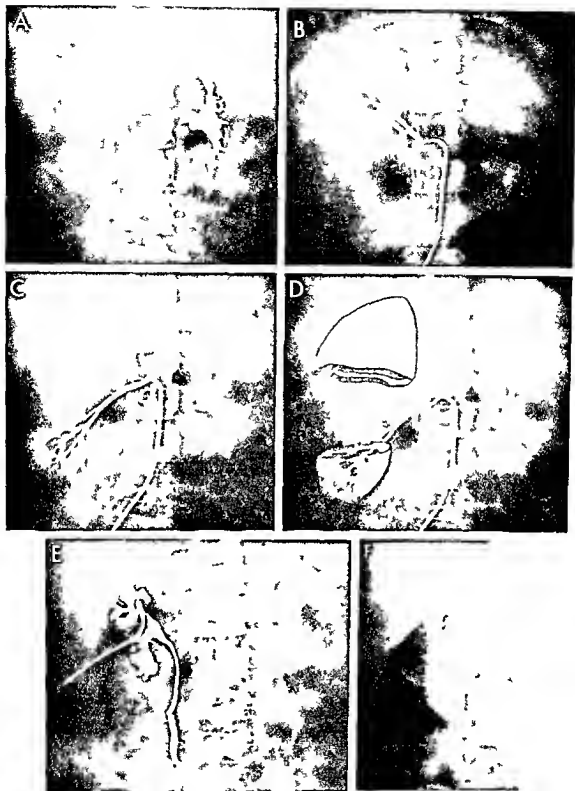


Fig. 6-68 — Renal laceration in a 5-year old girl due to a sliding accident. A: immediate pyelogram shows extravasation of urine and contrast agent on the right. B: selective right renal arteriogram shows a relatively small vessel going to the upper half of the kidney. C: a second small artery originating half a vertebral body lower supplies the lower pole. The upper pole functions well. D: drawing of the kidney split between two separate renal ar-

teries supplied superimposed on a later film in the series. This interpretation was confirmed at surgery when the halves of the kidney were reunited. E: film made after injection through nephrostomy tube after surgical repair. F: excretory urogram nine months after surgery. The child was clinically well without hypertension.

muscle injury and may obliterate the normal psoas muscle shadow without renal injury. Differences in the definition of the perirenal fat shadows on the two sides may indicate perirenal hemorrhage. Further more fractures of ribs or transverse processes in the area of the kidneys may provide indications of the force of the injury.

Excretory urography is of great value: the only contraindication is severe shock in which case exploration of the abdomen may be necessary without further radiographic examination. Retrograde urography is best restricted to instances in which excretory examination is inadequate to demonstrate the nature and extent of injury. Renal injuries can be divided conveniently into contusions, fractures or ruptures and tears of the renal vessels or ureter. With contusions and minor fractures the excretory urograms may be normal but more frequently there is incomplete filling of the pelvis on the affected side. Sometimes the defect of filling is a consequence of blood clots within the pelvis. More severe ruptures especially those extending to the renal pelvis are associated with extravasation of urine and contrast material. With vascular injuries the kidney usually cannot be visualized and immediate surgery may be indicated. The excretory examination is of primary value in demonstrating a functioning kidney on the side opposite the injury. Aortography and selective renal arteriography are valuable in selected cases (Fig. 6-68). The frequency of asymptomatic tumors in children always warrants consideration of susceptibility to injury because of the tumor and bizarre configurations of the pelvis should be looked upon with considerable suspicion.

As a rule renal ruptures show excellent healing tendencies. Deformities of the pelvis and calices due to atrophy and scarring have been reported but are usually recognized within one to two years after the injury. Follow up examinations after this interval are desirable in all instances of known renal injury. Hypertension may occur supposedly because of the compressing effect of a perinephric hematoma.

Indirect injury to the bladder can lead to total or partial rupture which may be extra- or intraperitoneal. Extraperitoneal rupture causes displacement of the lumen of the bladder away from the site of the accumulation of blood and urine. Intraperitoneal rupture produces the signs of free fluid in the abdomen which cannot be differentiated from other causes of free fluid without contrast visualization of the bladder when extravasation of the contrast medium can be demonstrated.

Urethral injuries mostly contusions and ruptures occur with pelvic fractures or straddle injuries. The region most subject to injury because of maximal fixation to the pelvic structures is that near the external sphincter. Retention of urine in the bladder and

extravasation of contrast material on retrograde urethral injection are diagnostic.

REFERENCES

- Palavattana C, Graham S R, and Silverman F N. Delayed sequelae to renal injury in childhood. *Am J Roentgenol* 91:659 1964.
Perry L, and Forsythe W E. Renal trauma in childhood. *JAMA* 182:709 1962.

Urinary infections

Regardless of whether the urinary tract is infected directly by direct extension from other infection or by hematogenous lymphatic or retrograde urinary routes any condition favoring urinary stasis predisposes to initial infection as well as its recurrence and perpetuation. The radiographic signs of infection therefore are those frequently associated with or complicated by those of obstruction. It has long been a general rule that the first episode of infection in a male and the second in a female constitute indications for urologic investigation. It now appears that proved bacilluria in a specimen of urine obtained during mid voiding (clean catch specimen) is an equally good indication. Studies have shown that cystography provides a satisfactory diagnosis in about 50% of the cases and about twice as often as excretory urography alone. Combination of these techniques provides a satisfactory diagnosis in 85-90% of the cases. The need for complete urologic evaluation was pointed out by Steele and associates who found only 52% of children hospitalized for urinary infection alive and free from disease 10-20 years after the initial diagnosis.

ACUTE INFECTIONS

ACUTE PYELONEPHRITIS may cause no changes whatever in the upper urinary passages on excretory urography. Occasionally poor filling of the renal pelvis on the clinically affected side may be an indication of irritability or spasm. Linear streaking of pelvis and ureters was observed by Gwinn and Barnes in association with acute and recurrent urinary tract infection. Poole and associates support this observation but it is clear that streaking can occur without disease. Periodic pyuria may be the only evidence of recurrent acute pyelonephritis.

With RENAL ABSCESS or CARUNCLE the renal outline may be deformed by the inflammatory swelling in addition to demonstrating the few changes seen in acute pyelonephritis. Often the spine is curved with the concavity on the side of the perirenal abscess. The difficulty in obtaining the co-operation of young children should be kept in mind in evaluating spinal curvatures. Fixation of the kidney in its bed by the inflammatory reaction can be demonstrated sometimes by a relatively long exposure taken during breathing or by separate exposures one in inspiration and one

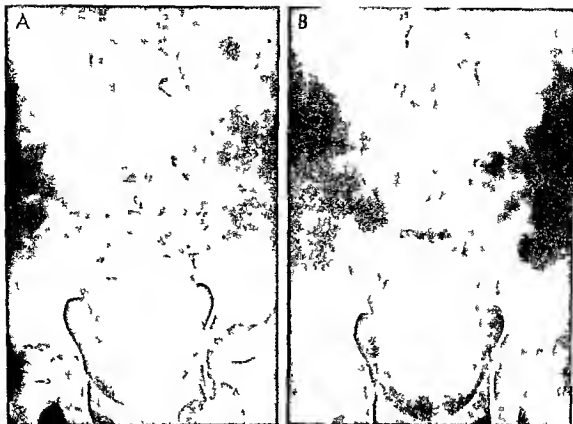


Fig. 6-69 Pyelonephric abscess. In A during excretory urography no diagnostic features are noted. In B exposure was made during breathing. The right renal pelvis is distorted as a result of

distortion by pyelonephric inflammation and other structures are blurred by motion.

in expiration. Both of these maneuvers are undertaken in conjunction with excretory urography. In the first instance, during breathing, the pelvis on the affected side is clearly demarcated because of its fixation, while the pelvis on the healthy side is blurred due to motion (Fig. 6-69). In the second instance, the pelvis on the healthy side is displaced to a greater degree than that on the affected side on comparison of the two films.

In ACUTE CYSTITIS, the bladder wall is frequently observed to be thick when outlined by contrast material within it and gas in adjacent small bowel loops. In addition, gross irregularities in the mucosa may indicate sites of edema or hemorrhage, or both. Type 11 adenovirus has been isolated from the urine of children with hemorrhagic cystitis, and a significant rise of antibody titer was found in these children on comparison with control subjects.

CHRONIC AND RECURRENT INFECTIONS

CHRONIC PYELONEPHRITIS is one of the commonest infections of the urinary tract. Anatomically, it is characterized by coarse focal scarring with areas of normal or hypertrophied kidney between. As the scar-

ring progresses with repeated infection, the kidney becomes contracted and marked by coarse depressions on the external surface. Calices in the area of infection and scarring become blunted and distorted and ultimately are drawn out with the contraction of the scar toward the depression on the surface (Fig. 6-70). Hodson has shown that in normal circumstances a line connecting the fornices of the several calices forms a smooth curve paralleling the border of the kidney. In pyelonephritis, the dilated blunted calix in an affected area produces a bulge in this line just at the point where the renal outline is depressed (Fig. 6-71). Compensatory hypertrophy may be observed on the healthy side when chronic atrophic pyelonephritis has produced significant renal loss on the other (Fig. 6-72). Often the condition is bilateral. At times it is difficult to differentiate renal atrophy due to infection from infection in a hypoplastic dysplastic kidney (Fig. 6-73). Many investigators believe that renal dysplasia is present in most individuals with pyelonephritis and predisposes to the infection. Bilateral chronic pyelonephritis may be confused radiographically with congenital cystic disease, particularly when infection has been present in the latter.

The association of obstruction, urinary tract dilata-



Fig 670—Chronic pyelonephritis in a 5-year-old boy with exstrophy of the bladder. Black arrows indicate blunted and distorted calices or calyceal diverticula. White arrows indicate indentations of the renal surface opposite. Nowhere else is the parenchyma so thin as in the areas of the pyelonephritic scarring.

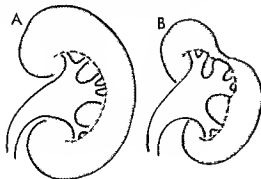
tion residual urine and vesicoureteral reflux with chronic pyelonephritis has been argued pro and contra for almost any given combination. There is no doubt that dilatation and infection may occur without obstruction, as Shopfner maintains. It is equally true however that they do occur with obstruction and are exaggerated by obstruction. From a practical point of view, all of these features play some role in the initiation and perpetuation of urinary tract infection and when found require therapy appropriate to the pathology. The problem is to separate the factors. Shopfner's insistence on conservative management has much to support it but in the presence of unequivocal obstruction or progressive anatomic changes surgical intervention can be of equal importance.

Obstruction leads to dilatation proximal to it and

stasis. Urine is a good medium for bacterial growth so that stasis and residual urine favor propagation of organisms. Studies on adult females in whom residual urine volume was measured using ^{131}I Hippuran indicate that residual urine volumes of as little as 1–10 ml were associated with difficulty in treating urinary infection. Mechanical incompetence of the ureterovesical junction due to obstruction, muscular fatigue or malformation involving the intramural portion of the ureter permits the introduction of infected urine into the upper urinary tract. The individual's own colon is generally accepted to be the most common source of infection but the route of infection has been debated with probably all of the theories containing some degree of truth. Support for the ascending route of infection has been provided by the almost constant presence of organisms in the distal urethra which implies the possibility of retrograde introduction of organisms both into the bladder and upward in the ureters. Eighty percent of recurrences of urinary tract infection in females have been shown to be related to reinfection with a new organism (type variation). Females possibly may be particularly susceptible to infection partly because the urine in the male has a lower pH and a higher osmolality factors which inhibit bacterial (*Escherichia coli*) growth.

Animal experiments indicate that when reflux normally exists in certain species the incidence of pyelonephritis after bladder inoculation closely parallels the frequency of reflux. In species which do not exhibit frequent reflux, bladder inoculation is followed by pyelonephritis only when artificial vesicoureteral reflux is produced. Injection of coliform organisms into the blood stream of animals does not produce infection of the kidneys partly because of dilution of the inoculum and partly because of the magnitude of the flow of blood through the kidneys. Only if there is some impediment to blood flow is

Fig 671—Diagram of renal changes in chronic pyelonephritis. In the normal kidney (A) a line connecting the tips of the calices parallels the edge of the kidney. In the diseased kidney (B) scarring has led to dilatation of the affected calix and narrowing of adjacent parenchyma. The edge of the kidney no longer conforms to a line connecting tips of the calices and is actually indented at the site of atrophy. (After Hodson.)



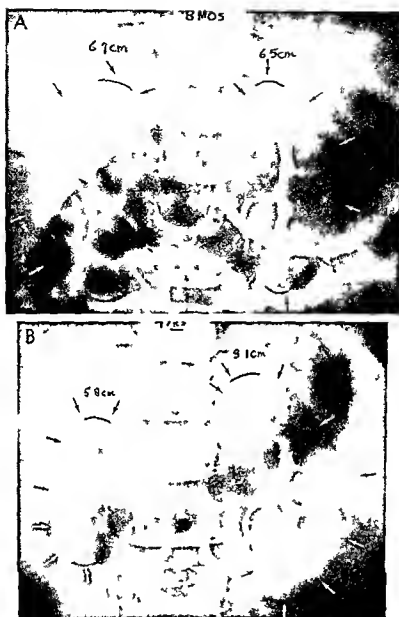


Fig. 672.—Serial studies in recurrent urinary tract infection. A at 8 months. The cystogram showed reflux but the nephrovenous pyelogram was abnormal only in demonstrating possible calyceal diverticulum on the left. This girl had had two previous documented urinary tract infections. B nephrovenous pyelogram at 7

years of age after irregular medical management. Only obvious infections were treated, mostly without control of sensitivity of organisms. The left kidney is normal for age and has grown 46 cm. The right kidney has actually decreased in size 0.9 cm. Its calyces are clubbed and loss of parenchyma is obvious.

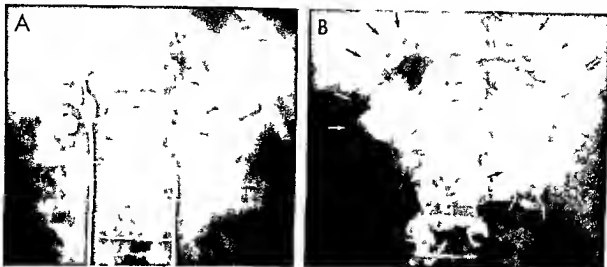


Fig 6-73 — Chronic pyelonephritis. In A, the right kidney is small, and the left is large. Irregular calyceal dilatation and variable cortical thickness are also seen. In B, calyceal deformities are confirmed on retrograde examination. Variations in thickness of

renal parenchyma on the left are due to regular scarring and asymmetric compensatory hypertrophy. The right kidney could be atrophic or hypoplastic or could represent the results of hypoplasia and atrophy.

infection easily produced via the intravenous route. Some maintain that reflux is always pathologic in human beings when reflux is present from whatever cause it is logical to assume a pathogenesis of pyelonephritis similar to that in animals.

Measurements of renal size in serial examinations of patients with recurrent urinary tract infection are of value in assigning priorities to various forms of therapy. Continued increase in size of the kidneys with age is probably the best indication that management is adequate. Distortions of the pelvis or the renal outline provide supporting radiologic indications but like definite atrophy they indicate that serious loss of parenchyma has occurred. Curran¹⁰ has provided a simple estimate of renal size by noting that the length of the first four lumbar vertebral bodies corresponded to the length of the normal kidney plus or minus 1 cm throughout childhood except for the first year and a half of life when the kidney length was greater. Hodson and associates have related kidney length to stature. Frieden¹¹ and associates have developed a renal index comprised of the product of the length and width of the kidney divided by the body surface area; this may be the most accurate radiographic measurement of renal size.

URINARY TUBERCULOSIS — Infection of the urinary tract with tubercle bacilli may occur during the early bacteremic phase of the primary infection, organisms from the blood stream lodge in the kidney from which the rest of the urinary tract and sometimes the genital tract are infected by direct canalicular spread. The diagnosis of tuberculosis of the genitourinary tract is best established by the isolation of tubercle bacilli from the urine or the observa-

tion of tubercles in the course of endoscopy or biopsy.

There are no pathognomonic or characteristic roentgen signs of tuberculosis of the genitourinary tract but the roentgen examination is helpful in demonstrating the site, size and character of the tuberculous lesions and some of their complications. In plain films the larger calcifying lesions cast opaque images. Localized inflammatory spasm may cause stenosis and obstruction in the calices or the pelvis. In the early phases of urinary tract tuberculosis urograms may be normal.

URETHRITIS — Irregularity of the caliber of the urethra and urethral spasm during voiding were formerly thought to favor the diagnosis of urethritis. Longitudinal striations due to thickened mucosa have often been reported; they are comparable to the linear streaking of pelvis and ureters described by Gwynn and Barnes in upper urinary tract infection. With associated clinical signs and symptoms the mucosal irregularities may warrant consideration of the diagnosis but current opinion is that the diagnosis is not a radiologic one. Irregularity of contraction of the urethra during voiding can be caused by factors other than local irritation and is commonly seen when the examination is emotionally disturbing to the patient.

URETERITIS CYSTICA and **CYSTITIS CYSTICA** conditions characterized by cystic proliferation of the urinary mucosa owing to chronic infection are seen less often in children than in adults but when seen demonstrate the identical pattern. The cystic (or proliferative) mucosal lesions tend to disappear with time if infection is controlled. Their inflammatory origin and spontaneous resolution are reminiscent of the benign inflammatory juvenile polyp of the colon.

REFERENCES

- Allen, T D. Pathogenesis of urinary tract infections in children. *New England J Med* 273 1421 and 1472 1965
- Asscher A W *et al*. Urine as a medium for bacterial growth. *Lancet* 2 1037 1966
- Curran G. Roentgenographic estimation of kidney size in normal individuals with emphasis on children. *Am J Roentgenol* 93 464 1965
- Ericsson N O and Ivarmark B. Renal dysplasia and pyelonephritis in infants and children. *Arch Path* 66 255 and 264 1958
- Friedenberg M J *et al*. Roentgen size of normal kidneys. Computer analysis of 1286 cases. *Radiology* 84 1022 1965
- Guze L B and Reeson P B. Experimental pyelonephritis. I. Effect of ureteral ligation on course of bacterial infection in kidney of rat. *J Exper Med* 104 803 1956
- Gwynn J L and Barnes G R Jr. Striated ureters and renal pelvis. Preliminary report. *Am J Roentgenol* 91 666 1964
- Hinkle N H, Partin, J C and West C D. Diagnosis of acute and chronic pyelonephritis in children. *Am J Dis Child* 100 333 1960
- Hodson C J. The radiological contribution toward the diagnosis of chronic pyelonephritis. *Radiology* 88 857 1967
- *et al*. Renal size in normal children. *Arch Dis Child* 37 616, 1962.
- Johanning P W and Marshall V F. Question of urethral reflux in female patients. *J Urol* 85 584 1961
- Kaufmann H J (ed). *Progress in Pediatric Radiology Vol III Genitourinary Tract* (Basel: S Karger 1970)
- Kunin C M. The natural history of recurrent bacteriuria in school girls. *New England J Med* 282 1443 1970
- , Deutscher R. and Paquin A Jr. Urinary tract infection in school children. Epidemiologic clinical and laboratory study. *Medicine* 43 91 1964
- Latimer J K. A roentgenographic classification of tuberculous lesions of the kidney. *Am Rev Tuberc* 67 604 1953
- Mahoney S A and Persky L. Observations on experimental ascending pyelonephritis in rat. *J Urol* 89 779 1963
- Shand D G *et al*. Relation between residual urine volume and response to treatment of urinary infection. *Lancet* 1 1305 1970
- Shopfner C E. Urinary tract pathology with sepsis. *Am J Roentgenol* 108 632 1970
- Smellie J M *et al*. Clinical and radiological features of urinary infection in childhood. *Brit M J* 2 1222, 1964
- Sommer J L. Experimental pyelonephritis in the rat with observations on ureteral reflux. *J Urol* 86 375 1961
- Stamey T A *et al*. Antibacterial nature of prostatic fluid. *Nature London* 216 444 1968
- Steele, R E Jr, Leadbetter G W Jr and Crawford J D. Prognosis of childhood urinary tract infection. The current status of patients hospitalized between 1940 and 1950. *New England J Med* 269 683 1963
- Sunshine H. Prevention of ascending pyelitis by intact ureterovesical junction. Experimental study. *J Urol* 92 351 1964

Neoplasms

It has been estimated that genitourinary neoplasms account for 25% of the malignancies found in children. This figure would be greater if neuroblastoma were included (see the following section on the adrenal glands)

WILMS TUMOR—The commonest tumor of the kidney and the perirenal tissues is the Wilms embryoma or nephroblastoma. More than 80% of Wilms tumors are found in children under 5 years of age and 70% in children under 3 years. Occasionally the tumor is present in the fetus. The frequency of bilateral

Fig 674—Bilateral Wilms tumor. In A at 2 years the right renal pelvis is filled cephalad by the large tumor. Its lower half. The right kidney was excised and Wilms tumor was proved microscopically. In B at 3 1/2 years the left side of the abdomen is

filled with a large mass which displaces a dilated renal pelvis caudad. This tumor responded temporarily to x-ray radiation and chemotherapy. (Courtesy of Dr Henry Penk, Salt Lake City Utah)



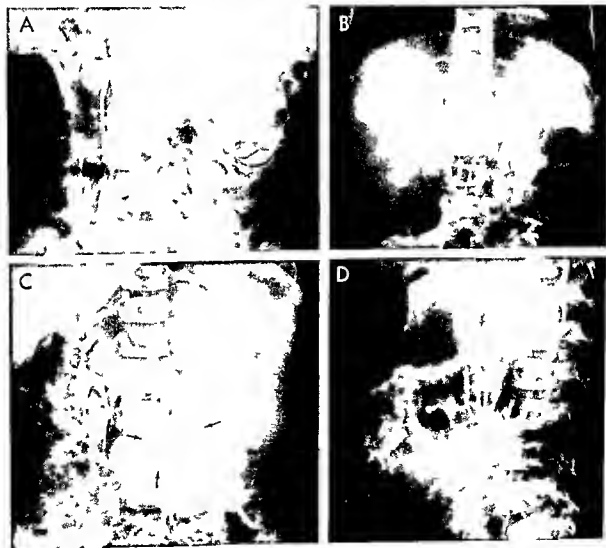
Wilms tumors is only now being appreciated (Fig 6-74). The curability of this tumor may be greater than previously considered inasmuch as late pulmonary metastases may originate from a previously unrecognized tumor of the apparently healthy kidney. The implications with respect to a transabdominal surgical approach in which both kidneys can be carefully inspected and palpated are obvious.

The roentgen appearance of a Wilms embryoma varies with its size and position. Plain films disclose a water density mass displacing gas-filled loops away from the area of tumor; the posterior location is frequently well demonstrated in lateral projection. Calcification is occasionally found and rarely actual bone

formation is present. In excretory urograms the renal pelvis is distorted (Fig 6-75). Any intracapsular renal mass tends to distort the renal pelvis to a degree greater than it displaces it from its normal position. The overwhelming frequency of Wilms embryoma as an intracapsular tumor in comparison with other tumors makes this feature almost diagnostic. Only extremely large tumors or tumors which obstruct the vascular pedicle cause failure of visualization of the pelvis of the affected kidney. Obstruction of the ureter or ureteropelvic junction may produce distorting and complicating pyelectasis. Lateral projections are important for identification of a stretched, flattened pelvis lying on the anterior aspect of a large tumor

Fig 6-75—Variations in form of the renal pelvis with Wilms tumor. A: in a 6-year-old boy with downward displacement and distortion. B: in a 16-month-old boy with upward displacement and distortion. C: in a 3½-year-old girl with medial displacement

and stretching (arrows). D: same patient as in C, lateral projection. The pelvis is displaced anteriorly and must be flattened against the anterior surface of the tumor.



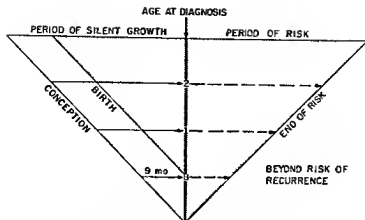


Fig 6-76 — Prognosis in Wilms' tumor. Assuming that metastatic tumor grows at the same regular rate that the primary tumor did prior to diagnosis (period of silent growth), the patient can be

considered free from tumor if no recurrences are found by the time he is twice his age at the time of diagnosis plus 9 months (twice the period of silent growth). (After Collins et al.)

because in frontal projection, only pyelectasis or hydronephrosis may be suggested. When a Wilms' tumor occurs in a horseshoe or an ectopic kidney, the diagnosis may be extremely difficult. We have recently seen two instances of Wilms' tumor on the affected side of children with hemihypertrophy. Muller called attention to the frequent association of Wilms' tumor with anuria as well as hemihypertrophy. The association has been confirmed by several investigators. Boxer reported the finding of a Wilms' tumor in a child before the onset of recognizable hemihypertrophy. On the other hand, Roggensack and McAlister observed bilateral enlargement of the kidneys which was thought to be a Wilms' tumor in a child with hemihypertrophy but was proved not to be. Recent reports have appeared of neonatal renal tumors which are confused with Wilms' tumors but which apparently can be differentiated on gross and histologic grounds. They are thought to be benign hamartomas and to require neither radiation therapy nor chemotherapy after surgical removal. In one series, the only infants who did not survive succumbed to the complications of radiation and chemotherapy. It is possible that the favorable prognosis of Wilms' tumor in infancy in comparison with that in later life is heavily weighted by the inclusion of patients with the benign lesion. Careful histologic evaluation of tumors removed from the newborn is obviously indicated before cytotoxic physical and chemical agents are prescribed.

Metastases of Wilms' tumor are characteristically to the lung but occasionally lytic bone lesions are found as well. Scoliosis and alterations in the form of vertebral bodies have been described in survivors treated by surgery and radiation. The addition of potent antibiotics such as Actinomycin D seems to have assisted materially in the management of these patients. Collins and co-workers postulated that the rate of growth of a given Wilms' embryoma is constant for the primary tumor and for its metastases in a given individual. Assuming that the first tumor cell

could not have been present for more than the child's age plus nine months at the time the tumor was clinically recognized, they suggested that metastatic cells should reach the same size and level of clinical recognition by the time the child is nine months older than double the age at which the tumor was recognized (Fig 6-76). This theory has been better than 95% correct in predicting the time within which metastases will be identified if they are going to occur following removal of a tumor.

Fig 6-77 — Large calcifying neuroblastoma which originated in a right paravertebral ganglion and displaces the right kidney, renal pelvis, and ureter laterad. The renal pelvis is rotated about 90 degrees on its longitudinal axis, and the normal pelvis and ureter are slightly dilated. A large patch of tightly packed focal calcification is outlined by the arrows. (Courtesy of Dr R. Parker Allen, Denver, Colo.)



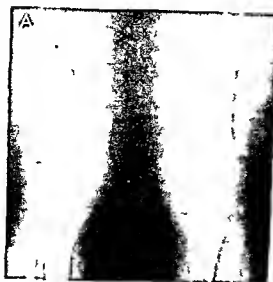


Fig 6-78 —Destructive metastases in the long bones of a 3 year old girl with an adrenal neuroblastoma. A upper and B lower extremities. The metastases appear at the ends of the major long bones as far as the lesions seen in leukemia. Clinical arthritis was present for four months before the examination. Note subperiosteal reaction along the shaft of the radius.



Retropertitoneal fibrosarcomas may simulate Wilms tumor both in their location and in the distribution of the metastatic lesions.

Angiographic investigations of Wilms tumors have demonstrated primary supply of the tumor via the renal artery whose branches are stretched and distorted and associated neovascularity. The initial enthusiasm for evaluation of intracapsular tumors by this technique has faded somewhat and often the procedure can represent nothing more than a diagnostic overkill. However, in atypical instances the examination may be useful and it is wise to consider angiographic investigation in all instances of abdominal mass even though it is ultimately undertaken in only a few.

NEUROBLASTOMA (sympathicoblastoma) is the second most common abdominal neoplasm in childhood. It is the most common neoplasm apart from leukemia but the occurrence of at least 25% of these tumors in extra abdominal locations obliges it to take second place to Wilms embryoma with respect to incidence in the abdomen. The tumor is described here because of its importance in differential diagnosis of Wilms embryoma. About 80% of neuroblastomas are found in children under 2½ years of age and many neuroblastoma like masses are found in situ in routine autopsies of infants dying of other causes. In plain films of the abdomen it frequently cannot be differentiated from Wilms tumor although the ten-

dency to diffuse calcification is somewhat more prominent in sympathicoblastoma than in Wilms tumor (Fig 6-77 and see Fig 6-91). Erosion of contiguous bones, enlargement of intervertebral foramina and separation of ribs on the affected side may indicate the neural origin and extension to the spinal canal. Metastases are most frequent to the retropertitoneal

Fig 6-79 —Advanced metastatic adrenal neuroblastoma showing productive as well as destructive changes in the calvaria of a girl 2 years of age.

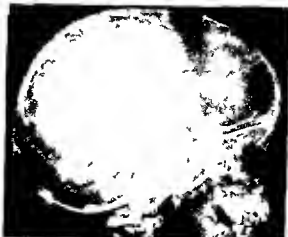




Fig 6-80 —Neuroblastoma displacing the left kidney. Faint calcification is visible within it. Note coarse bone trabeculation in the ilia. Same patient as in Figure 6-78.

Fig 6-81 —Neuroblastoma in a girl 6 years of age. A, aortogram shows the right renal artery stretched as it supplies the displaced right kidney. Large suprarenal arteries course around and into the suprarenal tumor. B, selective injection of the right



lymph nodes, but radiographically, metastases are recognized in the skull and appendicular skeleton (Figs 6-78 and 6-79) and in the liver. The hepatic metastases often calcify. Widening of the paraspinous stripe may be an important clue that extension of a neuroblastoma has taken place. The skeletal metastases are osteolytic and are indistinguishable from those produced by leukemia. The frequency of skeletal metastases makes bone marrow aspiration a valuable diagnostic aid. Radiologic examination often indicates the optimal site for bone marrow aspiration. In excretory urograms, the tumor tends to displace the kidney from its normal position, producing more displacement of its pelvis than distortion, because the tumor lies outside the renal capsule and invasion of the kidney is a relatively late phenomenon (Figs 6-80 to 6-83). Occasionally, a neuroblastoma is indistinguishable from a Wilms tumor (Fig 6-84).

The recognition that tumors of sympathetic nerve cell origin produce abnormal amounts and types of catecholamines which are excreted in the urine has provided an important chemical aid in determining the probable nature of a mass as well as providing a guide for therapy and early evidence of recurrence or metastases. The catecholamines apparently account for the frequency of circulatory hypertension in children with neuroblastomas and for occasional diarrhea. Their relationship to the syndrome of opsoclophoric artery shows its contributions to the tumor supply and indicates that the celiac axis and its branches are all displaced into the left side of the abdomen.



Fig 6-82—Neuroblastoma which originated in the paravertebral sympathetic ganglion on the left side and displaced the left kidney and renal pelvis and ureter to the left. The left pelvis is also rotated on its longitudinal axis, but there is little or no compression of the pelvis or obstruction to flow through the left pelvis and its ureter (Figs 6-82 to 6-84 courtesy of Dr R Parker Allan, Denver, Colo.)

nus and occult neuroblastoma is uncertain because most of the children reported with this combination in whom catecholamine studies have been undertaken have not demonstrated elevations. Opsoclonus is a condition of irregular spontaneous eye move-

Fig 6-83—Large metastatic neuroblastoma in a left adrenal paravertebral lymph node (secondary to a primary in the adrenal) which lifts the left kidney and its renal pelvis cephalad and displaces the lower pole of the left kidney and its renal pelvis laterad. The kidney is rotated slightly on its longitudinal axis. The renal pelvis and ureter are not compressed.



Fig 6-84—Unusual compression, partial obstruction and lateral displacement of the left kidney and renal pelvis by an intra-adrenal neuroblastoma. These radiographic findings are more common in Wilms' tumor than in adrenal neuroblastoma.

ments, often accompanied by myoclonic jerks of the face and body and cerebellar ataxia. Its occurrence in the first years of life has been associated in several instances with the subsequent incidental finding of a neuroblastoma, most seem to be localized, but metastatic disease has been reported. Psychomotor retardation has been a common feature in these children (Fig 6-85). Prognosis is uncertain. Instances of recovery from extensive metastatic disease are recorded. There is some evidence that extra-adrenal tumors have a better prognosis than intra-adrenal tumors. Such factors as ease of diagnosis when tumors are not deep in the abdomen may play a role. Immunolog-

Fig 6-85—Ganglioneuroblastoma in an 11-year-old girl who was studied for ataxia with opsoclonus at 2 years of age. Calcification in the paravertebral area remained unchanged over 9 years. Catecholamine level in the urine were never elevated. Surgical extirpation was done at age 11.





Fig 6-86—Suprarenal teratoma producing downward displacement of the right kidney comparable to that seen in neuroblastoma. Compare with Figures 6-75 A, 6-80, 6-81 and 6-84.

ic studies of patients with neuroblastoma, particularly of those who have recovered, have suggested the presence of factors having lethal reactivity to neuroblastoma cells. Further investigations of the biologic mechanisms of regression of neuroblastoma may open new therapeutic channels.

RETROPERITONEAL TERATOMAS may produce displacements similar to both Wilms tumors and neuroblastomas. The condition can be diagnosed with certainty only when definite formed skeletal components or dental structures can be recognized within the water-density mass. The fact that bone formation can occur in Wilms embryoma should not be overlooked. Retroperitoneal sarcomas may simulate neuroblastomas as well as Wilms tumors (Fig 6-86).

MUCOSAL EPITHELIAL TUMORS of the urinary passages are uncommon in children. Diagnosis depends on removal of tissue for histologic study. In **TUBEROUS SCLEROSIS**, hamartomatous growths within the kidneys may present a radiologic picture suggesting multiple cystic lesions and particularly multicystic disease (Fig 6-87). The tumors are not malignant and seldom are a primary cause of death.

SECONDARY TUMORS—Leukemia and lymphoma may cause diffuse infiltration of the renal parenchyma and enlargement of these structures. Not only may the kidneys become palpable, they may present as an abdominal mass. The renal pelvis on excretory urography are generally enlarged; the appearance is a magnification of the normal structure rather than a dilatation of the type seen in hydronephrosis or the distortion produced by stretching over a solitary tumor. Enlargement of the kidney and stretching of the otherwise normal calices and pelvis may also occur in the glucose-6-phosphatase deficiency form of glycogen storage disease. In this form, the enzyme normally present in the kidney and liver is lacking, and deposition of glycogen takes place in areas where normally enzyme activity prevents its accumulation. The distortion of the pelvis can be seen in excretory

urograms. Presumably renal changes do not occur in the other forms of glycogen storage disease.

REFERENCES

- Beckwith J B and Parnell E V. In situ neuroblastomas. A contribution to the natural history of neural crest tumors. *Am J Pathol* 43:1089, 1963.
- Benzing W Jr. Wilms tumor of infancy and childhood. *Radiology* 58:674, 1952.
- Bill A H. Studies of the mechanism of regression of human neuroblastoma. *J Pediatr, Surg* 3:727, 1968.
- Bray P F et al. The coincidence of neuroblastoma and acute cerebellar encephalopathy. *J Pediatr* 75:983, 1969.

Fig 6-87—Tuberous sclerosis. The renal pelvises are distorted by hamartomas.



- Brissaud H E and Beauvais P. Opsoclonus and neuroblastoma. *New England J Med* 280:1242, 1969.
- Collins V P, Loeffler R K, and Tilvey H. Observations on growth rates of human tumors. *Am J Roentgenol* 76:988, 1956.
- Davidson, M, Tolentino Y, and Sapir S. Opsoclonus and neuroblastoma. *New England J Med* 279:948, 1968.
- DiGeorge A M and Harley R D. The association of aniridia, Wilms tumor, and genital abnormalities. *Arch Ophthalmol* 75:796, 1966.
- Eklöf O and Gooding C A. Paravertebral widening in cases of neuroblastoma. *Brit J Radiol* 40:358, 1967.
- Gowdey J F and Neuhauser E B D. Roentgen diagnosis of diffuse leukemic infiltration of the kidneys in children. *Am J Roentgenol* 60:13, 1948.
- Gross R E, Farber S, and Martin L W. Neuroblastoma-sympathicoma: A study and report of 217 cases. *Pediatrics* 23:1179, 1959.
- Jagasia K H et al. Bilateral Wilms tumors in children. *J Pediatr* 65:371, 1964.
- Kincaid O W, Hodgson J R, and Dockerty M B. Neuroblastoma: A roentgenologic and pathologic study. *Am J Roentgenol* 78:420, 1957.
- Lattimer J K, Melicow M M, and Uson A C. Wilms tumor: A report of 71 cases. *J Urol* 80:401, 1958.
- Lawlor J B, Lattimer J K, and Wolff J A. Wilms tumor in a horseshoe kidney. *Pediatrics* 23:354, 1959.
- Lusted L B, Besse B L, Jr, and Fritz R. The intravenous urogram in acute leukemia. *Am J Roentgenol* 80:608, 1958.
- Mandeville F B. Calcification in sympathicoblastoma (neuroblastoma). *Radiology* 53:403, 1949.
- Martin L W and Kloecker R J. Bilateral nephroblastoma (Wilms tumor). *Pediatrics* 28:101, 1961.
- Miller R W, Fraumeni J F, Jr, and Manning M D. Association of Wilms tumor with aniridia, hemihypertrophy, and other congenital malformations. *New England J Med* 270:922, 1964.
- Richmond H and Dougall A J. Neonatal renal tumors. *J Pediatr Surg* 5:413, 1970.
- Silver H K and Gruskay F L. Syndrome of congenital hemihypertrophy and elevated urinary gonadotropins. *Am J Dis Child* 93:559, 1957.
- Solomon G E and Chutman A M. Opsoclonus and occult neuroblastoma. *New England J Med* 279:475, 1968.
- Voorhes M L and Whalen J P. Role of catecholamine excretion in diagnosis and treatment of neuroblastoma. Report of 2 cases. *Radiology* 83:92, 1964.
- Waisman J and Cooper P H. Renal neoplasms of the newborn. *J Pediatr Surg* 5:407, 1970.

MISCELLANEOUS MASSES—In severe dehydration with hyperelectrolytemia, blood in renal veins may thrombose just as blood clots in the dural sinuses. Under these conditions, the kidneys become greatly enlarged and present as masses in the abdomen. Hematuria is invariably associated with renal vein thrombosis. The condition may occur as a unilateral mass as well. In these circumstances, the clinical pattern is very much the same, but excretory urography demonstrates failure of function only on the affected side. Retrograde examination demonstrates a relatively normal renal pelvis. In angiographic studies, the renal arteries are attenuated; there may be a prolonged nephrographic phase or no visualization of the renal parenchyma at all. We have seen one instance in an older child during recovery from a severe burn, in this instance the thrombus was in the renal vein and could be removed surgically. In the infantile form, the thrombi are throughout the small venous structures of the kidney and not susceptible to surgical removal. Nahum and associates reported the development of calcification in nonfunctioning kidneys following renal vein thrombosis in infancy. In one case, renal hypertension supervened but was relieved following removal of the atrophic calcified kidney.

REFERENCES

- Nahum H, Gubler J P, and Rod er J. Thrombose veineuse renale unilatérale du nouveau né. *Ann radiol* 12:293, 1969.
- Scanlon G T. The radiographic changes in renal vein thrombosis. *Radiology* 80:208, 1963.

The Adrenal Glands

THE NORMAL ADRENALS cannot be seen clearly in conventional films—they become visible only when they contain adequate amounts of calcium or after air has been injected into the perirenal space or after contrast material has been injected into its arterial supply.

Calcium salts are deposited in the adrenals in a variety of conditions. Large amounts are occasionally seen in the adrenals of healthy infants (Fig 6-88) and children (Fig 6-89) who have apparently never had adrenal insufficiency. The pathogenesis of these lesions is obscure; it is possible that they represent sequelae to extreme degrees of physiologic neonatal in-olution or to unrecognized neonatal adrenal hemorrhages. The large fetal adrenals normally undergo extensive necrosis and atrophy during the first weeks of life after which the massive fetal cortex is replaced by the smaller permanent cortex and the adrenals shrink to their normal infantile size. During this physiologic neonatal shrinkage there is no clinical or

chemical evidence of adrenal insufficiency. Massive adrenal hemorrhage in the newborn may present as a tumor mass or with signs suggesting exsanguination. Prolonged neonatal jaundice has been emphasized as an occasional feature. Renal displacement similar to that in neuroblastoma can occur. High-dose intravenous urography and total body opacification may demonstrate the relatively radiolucent hemorrhagic area. Marginal calcification can occur as early as 10 days after the sudden appearance of the tumor and becomes progressive thereafter (Fig 6-90). Rarely the hematoma can become infected.

Calcification occurs pathologically in tumors such as neuroblastoma (Fig 6-91 and see Fig 6-77) and pheochromocytoma. Calcification in enlarged adrenal glands can be massive in Wolman's disease (familial cholesterolosis) (Fig 6-92). Clinically the patients have poor weight gain, vomiting, diarrhea, and hepatosplenomegaly. Signs of adrenal insufficiency are usu-

Fig 6-88—Adrenal calcification in a 2-year-old girl who had had neonatal sepsis and convulsions.



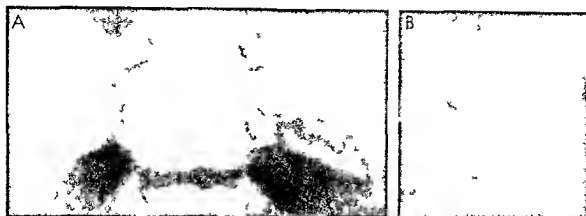


Fig 6 89 —Adrenal calcification: an incidental finding in a healthy boy 22 months of age. A: anteroposterior projection. B: lateral projection showing adrenal configuration.

Fig 6 90 —Calcification in suprapubic hematoma in a 19 day old boy who had microscopic hematuria at 5 days of age. The right adrena mass was thought to be an enlarged kidney unit in

the venous pyelography showed normal pelvis and calyces. Calcification was first noted on the 10th day of life.



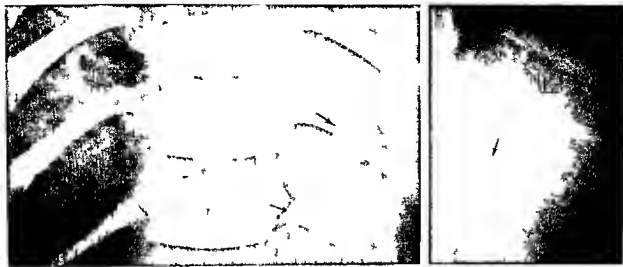


Fig 6-91 — Different types of calcification in sympathoblastoma of the adrenals. A: two large discrete masses of calcium

ally present. In contradistinction to Niemann-Pick disease, with which it can be confused because of the hepatosplenomegaly and foam cells in bone marrow and many other tissues, the brain is only mildly involved. The cholesterol content of the liver and spleen is increased to many times normal.

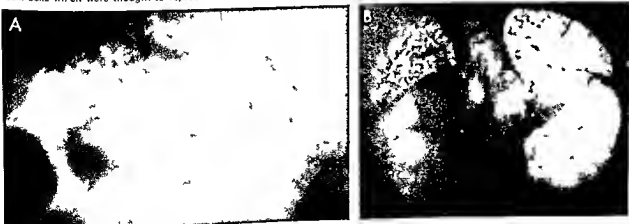
Pneumograms of the perirenal space are more valuable in adults than in children, but they can be helpful in the investigation of adrenal pheochromocytoma (Fig 6-93). The outstanding contraindication to retroperitoneal pneumography is suspected neuroblastoma because of the danger of dissemination, since neuroblastoma is the most common adrenal tumor in children. Retroperitoneal pneumography should not have a significant role in pediatric radiologic diagnosis. The examination should be limited to carefully selected patients, and the air injection should be made by an experienced surgeon under aseptic precautions. In

density in a relatively small tumor. B: numerous scattered calciferous foci in a large neoplasm.

the presence of large pheochromocytomas, the adjacent kidney and renal pelvis may be rotated displaced caudad and deformed. Large accessory pheochromocytomas outside the perirenal space and the retroperitoneal tissues have in at least two cases impinged on and deformed the duodenum. Volhard actually demonstrated such a mass after a barium feeding; in one case, when the duodenum was outlined with barium. A confirmatory radiographic sign is evidence of left ventricular hypertrophy in films of the heart, a characteristic of longstanding hypertension.

Aortography may be of considerable value in the diagnosis of pheochromocytomas because of the abundant blood supply, but they are not invariably diagnostic. The aortogram is preferred to selective arteriograms because unsuspected tumors may be demonstrated by the blush, which occurs as the

Fig 6-92 — Massive bilateral adrenal calcification in a girl 2 months of age who exhibited some signs of adrenal insufficiency. At necropsy, many of the tissues showed accumulation of foam cells, which were thought to represent Niemann-Pick disease.



ease. In retrospect, this patient almost certainly had Niemann-Pick disease. A film of abdomen during life. B: film of the kidneys and adrenals after they had been removed en masse.

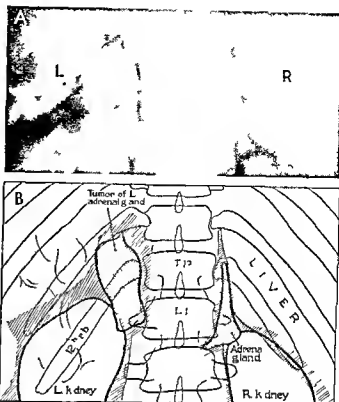


Fig 6-93 —Pneumogram of the perirenal spaces which shows a normal adrenal on the right side and an adrenal tumor on the left side. The tumor was excised and proved to be a pheochromocytoma. A, Film of the abdomen after insufflation of the perirenal spaces. B, tracing of A. (Courtesy of Dr. G. F. Cohn.)

vascular tumor is perfused. When however there is reason to believe that the tumor resides in the organs of Zuckerkandl selective injection of the inferior mesenteric artery may provide more diagnostic features. Arteriography has not been exceptionally valuable in the study of other adrenal tumors in childhood but it may have a place even if it only shortens the operative time by contributing to the surgeon's diagnostic security. On the other hand Alfidi and colleagues have found arteriography of adrenal neoplasms of considerable value in adults.

Neoplasms

Primary tumors of the adrenal can be subdivided into medullary and cortical groups. The clinical symptoms and signs each presents depend on whether or not they have endocrine function and the nature of the endocrine function. Radiographically therefore they are identified by their local characteristics as masses and by the demonstration of calcification when present. Supportive evidence may be sought by identification of appropriate responses to endocrine secretion such as alterations in skeletal maturation and size configuration of the heart, external genitalia and so on. A classification of adrenal tumors is shown in Table 6-1.

Neuroblastoma has been discussed in relation to

Wilms' embryoma (p. 805). Ganglioneuromas occasionally occur in the adrenal gland; they may appear as calcified or noncalcified mass lesions much like neuroblastomas. Abnormal excretion of catecholamines was first recognized in association with ganglioneuroma and ganglioneuroblastoma. Instances have been recorded in which symptoms simulating celiac disease with chronic severe diarrhea have resolved

TABLE 6-1 —CLASSIFICATION OF ADRENAL TUMORS*

Cortical tumors
Adenoma (hormonal or nonhormonal)
Carcinoma (hormonal or nonhormonal)
Hyperplasia (hormonal)
Medullary tumors
Pheochromocytoma (paraganglioma)
Neuroblastoma
Ganglioneuroma
Cysts
Pseudocysts
Lymphangiomatous cysts
Connective tissue tumors
Neurofibroma
Fibroma
Lipoma
Hemangioma
Secondary tumors
Metastatic or direct extension

*From Meyers, M. A. *Diagnosis of the Adrenal Glands*. Radiologic Diagnosis (Springfield, Ill.: Charles C. Thomas Publisher, 1963).

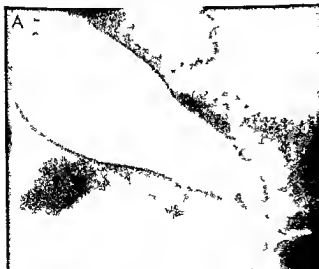


Fig 6-94—Vag nogram after injection of Lp iodol into a hypospadiac urethral opening; the patient proved to be a female pseudohermaphrodite with congenital bilateral cortical hyperplasia of the adrenals. A, frontal; and B, lateral projection.

following surgical removal of the functioning sympathetic neural tumor. Angiographic studies of ganglioneuroblastomas generally show appreciably less vascularity than and at times almost total avascularity in comparison with the abundantly vascularized neuroblastomas.

Cortical adenomas may be hormonal or nonhormonal. Nonfunctioning adenomas are rare and are usually nonmalignant. Functioning adenomas like carcinomas generally cause Cushing's syndrome.

Fig 6-95—Urogenital sinus demonstrated in a female pseudohermaphrodite with the adrenogenital syndrome. A catheter passed regularly only into the urethra and could not be introduced into the minute opening to the vagina. Opaque oil was introduced into the bladder where it floats in droplet form on the retained urine. The tip of a Foley catheter was introduced into the small

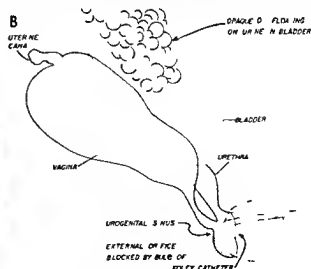


though occasionally the adrenogenital syndrome is associated with carcinoma. Patients with manifestations of both Cushing's syndrome and the adrenogenital syndrome frequently have an adrenal carcinoma. Mass lesions, calcified or uncalcified, are the chief radiologic features, but tumors of appreciable size have been found on surgical exploration which could not be identified radiographically before surgery. Associated radiologic findings in Cushing's syndrome are osteoporosis, cardiomegaly, as a consequence of hypertension and adiposity. Skeletal maturation is not advanced.

Adrenal hyperplasia in infants and children generally causes somatic changes that are reflected in roentgenographic studies, although the first suspicion of abnormal adrenal function usually arises from clinical observations. In boys, adrenal hyperplasia produces precocious puberty, and what has been termed macrogenitosomia praecox. In girls, it results in virilism. If present before birth, the infant girl is born as a female pseudohermaphrodite. In both sexes, hypertrophy of the androgenic zone of the cortex may compromise adrenal function, and signs of adrenal insufficiency may develop and lead to sudden death.

Roentgenographic features are related to the skeletal system, heart, reproductive organs, and the adrenal glands themselves. Although skeletal maturation is always advanced when the disease is first recognized after the first few months of life, the skeletal maturation of the newborn infant is generally retarded. In all instances, growth acceleration accompanies the acceleration of maturation, but growth ceases early because of premature fusion of the epiphyseal ossification centers and their shafts. During treat-

ment of the urogenital sinus, the orifice was blocked by pressure of the inflated balloon, and urographic contrast material was injected. The urethra was distended, but most of the contrast material passed into the vagina and even into the cavity of the uterus. A spot film during injection. B, diagrammatic representation of A.



ment with cortisone the rate of skeletal growth is reduced to a greater degree than the rate of skeletal maturation. If maturation is maintained commensurate with the age the length of the bones is diminished at the time of union of primary and secondary ossification centers of bone. If the length of the bones is maintained at the expected rate the relatively accelerated skeletal maturation causes premature fusion of the primary and secondary centers. In either event the treated individual in adulthood is significantly shorter than the average adult. The heart is small as in Addison's disease; this is probably a consequence of diminished blood volume. In the genital apparatus hypertrophy of the clitoris or the penis is pronounced anomalies of the vaginal orifice are common in newly born girls in whom what appears to be a hypospadiac urethral orifice actually represents a urogenital sinus. This communicates internally with a recognizable vagina. Retrograde injection of contrast substance into the urogenital sinus (Figs 6-94 and 6-95) is of value in demonstrating the presence of a vagina. The technic of gonitography is discussed in detail in Section 7.

Cysts, connective tissue tumors and secondary tumors of the adrenal glands are rare in children.

Adrenal Insufficiency

Weens and Golden demonstrated radiologic evidence of pyloric and duodenal obstruction in two vomiting infants. At necropsy in both there was no evidence of organic obstruction but there was a pronounced deficiency of cortical tissue in the adrenal glands. In the adrenogenital syndrome especially in the salt losing type similar functional cortical deficiency may be produced by overgrowth of the androgenic zone (zona reticularis). The diagnosis of the salt losing adrenogenital syndrome has been correctly suggested in infants with vomiting and dehydration when films of the abdomen showed what appeared to be a gasless intestinal tract and a disproportionately

large phallic shadow. Dehydration of any cause may be associated with a relatively gasless alimentary tract. Correction of the dehydration usually causes the gas pattern of the abdomen to revert to normal.

Although calcifications in the adrenals are found in about 25% of the adults with Addison's disease we have not observed calcification in the three instances of juvenile Addison's disease which we have seen.

REFERENCES

- Alford, R. J., Gilt, W. M. Jr. and Klein, H. J. Arteriography of adrenal neoplasms. *Am J Roentgenol* 106:635, 1969.
- Crocker, A. C. et al. Wolman's disease. Three new patients with a recently described lipidosis. *Pediatrics* 35:627, 1965.
- Cushing, H. and Wolbach, S. B. The transformation of a malignant paravertebral sympatheticoblastoma into a benign ganglioneuroma. *Am J Path* 3:203, 1927.
- Favara, B. E., Akers, D. R. and Franciosi, R. A. Adrenal abscess in a neonate. *J Pediatr* 77:682, 1970.
- Grumbach, M. M. and Wilkins, L. The pathogenesis and treatment of virilizing adrenal hyperplasia. *Pediatrics* 17:418, 1956.
- Jarvis, J. L. and Seaman, W. B. Idiopathic adrenal calcification in infants and children. *Am J Roentgenol* 82:510, 1959.
- Malter, I. J. and Kochler, P. R. Angiographic findings in pheochromocytoma of the organs of Zuckerkandl. *Radiology* 97:57, 1970.
- Meyers, M. A. *Diseases of the Adrenal Glands. Radiologic Diagnosis* (Springfield, Ill.: Charles C. Thomas Publisher, 1963).
- Rose, J. et al. Prolonged jaundice as presenting sign of massive adrenal hemorrhage in newborn. *Radiology* 98:963, 1971.
- Snyder, C. H. and Vick, E. H. Hypertension in children caused by pheochromocytoma. *Am J Dis Child* 73:581, 1947.
- Sobel, E. H. et al. Functioning adrenal tumors in childhood. *Am J Dis Child* 88:733, 1953.
- Steinbach, H. L. et al. Extraperitoneal pneumography. *Radiology* 59:167, 1952.
- Weens, H. S. and Golden, A. Adrenal cortical insufficiency in infants simulating high intestinal obstruction. *Am J Roentgenol* 74:213, 1955.
- Wolman, M. et al. Primary familial xanthomatosis with involvement and calcification of the adrenals. *Pediatrics* 28:742, 1961.

SECTION 7

The Genital Tract

The Genital Tract

LESIONS OF THE genital tract are uncommon in infants and children, and clinical signs of congenital malformations may be delayed until puberty or marriage. Vaginitis is the most common acquired disease. Although limited in value, radiographic examination is important in some patients because it can lead to early treatment and preservation of future sexual and reproductive functions.

Too often radiologic examination of urogenital structures is performed only as a final resort although it is less traumatic and frequently yields more exact information than digital palpation, catheterization, endoscopy or surgical exploration. Therefore it should often be done as a primary procedure. Many times the other procedures become unnecessary after the radiographic findings are known.

Indications for radiographic examination of the genital tract are distinct but are restricted to lesions which produce variations of densities in the plain roentgenogram and contain abnormal passages that can be demonstrated with contrast material. Its usefulness is therefore determined by the nature of each individual lesion.

Radiographic examinations should be limited by the foregoing indications because the young and especially their gonadal tissues, are highly sensitive to ionizing radiation. However, when indicated adequate examinations should not be omitted because of concern about radiation injury. Inadequate radiographic information may be more dangerous than the radiation hazard. For example, surgical removal of a functional vagina and uterus because they were not identified by radiologic study is more injurious than the potential radiation injury of diagnostic radiology.

Congenital and acquired abnormalities of the genital system commonly involve the urinary and intestinal tracts because the fetal and postnatal structures of all three are intimately related. Pelvic masses originating in the genital tract interfere with bladder function. An abnormal organogenetic development

which leads to ectopic anus may affect the genital and urinary tracts. Bladder exstrophy frequently is associated with genital and intestinal tract abnormalities. Consequently, awareness that the three systems and their diseases are interrelated will reduce the risk of diagnostic mistakes.

Procedures utilized in examining the genital tract of children include the plain abdominal roentgenogram, cystourethrography, intravenous pyelography, vaginography and genitography. Pelvic pneumography, hysterosalpinography and pelvic arteriography usually are not necessary. A major problem is restraint of the young patients, but this is not insurmountable. Common deterrents to accurate radiologic diagnosis include examinations without valid indications, the radiologist's incomplete knowledge of basic principles and inadequate immobilization of younger patients.

Methods of Examination

Simple abdominal pelvic roentgenography is the basis for radiologic evaluation of any disorder of the genital tract. Images must be of the highest quality so that soft tissue, calcium and fat are clearly distinguishable. Frontal and lateral views with the patient in erect, recumbent and decubitus positions may be required to establish the location of a foreign body or mass. Precise and proper interpretation of abdominal pelvic roentgenograms, may make further procedures unnecessary. Preliminary information is often provided from the plain films, which direct other roentgen procedures to a final accurate diagnosis.

The other examinations are classified as special procedures only because they involve the introduction of contrast agents, usually opaque. The principles and techniques are similar to those applicable to study of the gastrointestinal tract. Fluoroscopy and spot filming allow proper positioning of the catheters, controlled injection into cavities, accurate detection of normal and morbid structures and precise positioning of the patient for spot film recordings. Blind injection, blind filming and flash visualization with the overhead tube are condemned.

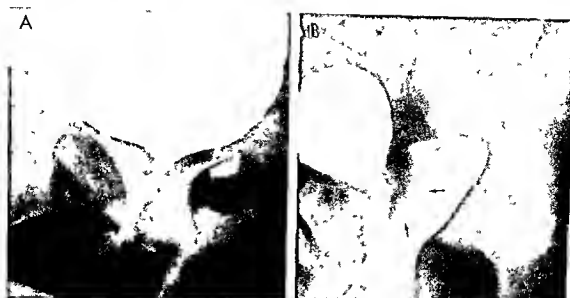


Fig 7-1 — A girl 4 years of age had had intermittent pyuria for one year. Fever with the pyuria at onset did not persist. Vaginal reflux during the voiding phase of cystourethrography reveals an unsuspected vaginal foreign body. A, reflux has only partly filled

the vagina during early voiding and the foreign body is not visible. B, full vaginal filling by reflux during the late stages of voiding reveals a 1.5 cm ovoid defect in the upper vagina which was a plastic bead (arrow).

Maximal information can be expected from cystourethrography. The essence of this method is fluoroscopy, which allows the radiologist to control later procedures. Displacement of the bladder and urethra often reveals the position and size of masses which arise in the genital structures. Passages between the urinary, genital and intestinal tracts are sometimes filled during voiding when they cannot be located by catheterization and retrograde injection. Vesicoureteral reflux during cystourethrography may delineate nonobstructive hydronephrosis and maldevelopments of the upper urinary tract which have not been demonstrated by intravenous pyelography.

Intravenous pyelography supplies data concerning renal function and structure. Dysplasia and other malformations of the kidney are common with abnormalities involving the caudal end of the embryo. The renal status is sometimes more significant than the combined lower urinary, genital and intestinal disease in determining ultimate prognosis. Intravenous pyelography is sometimes unsatisfactory in the newborn period owing to the immature kidney's inability to filter and concentrate the contrast agent as effectively as the kidney of the older infant, child and adult. In this case, re-examination in three to six months frequently supplies the renal evaluation not possible in the neonatal period. Vesicoureteral reflux, when it occurs, is also helpful in evaluating the structure of the neonatal upper urinary tract.

Vaginography alone is helpful in the evaluation of vaginitis because a foreign body may be the cause. Under fluoroscopic control it is a simple matter to inject contrast agent into the vagina. A Foley catheter inserted just inside the introitus with the balloon in-

flated prevents leakage. Seventy percent of females have vaginal reflux as a normal phenomenon during voiding cystourethrography, and it often provides a vaginogram that detects abnormalities not otherwise demonstrated (Fig 7-1). Vaginography combined with cystourethrography and genitography is most

Fig 7-2 — Ambiguous external genitalia of a 1 month old infant. There is a phallus and scrotum but no gonads are palpable. A single perineal opening exists at the base of the phallus (arrow). There may be pits, depressions and dimples which must be probed to prove that they are not true openings but simply simulate them.



TABLE 7.1—GYNECOLOGIC DISORDERS AMENABLE TO RADIOLOGIC DIAGNOSIS

- 1 Intersex
- 2 Vaginitis
- 3 Genital tract obstruction
- 4 Tumors
- 5 Developmental aspects of imperforate anus
- 6 Developmental aspects of bladder exstrophy

valuable in disorders which require demonstration of all the internal genital passages

Genitography is a procedure for the diagnosis of the intersex patient, and the term implies visualization of all genitourinary passages in a coordinated and correlated manner. It is to be distinguished from simple vaginography, hysterography, cystography and urethrography. The object of genitography is, as the name implies, to observe all internal channels. One technic or a combination of two methods may be employed in performing adequate genitography: (1) the flushing technic, and (2) the multiple catheter technic. Fluoroscopy is essential in both methods. One is cautioned against blind catheter insertion, blind injection and blind filming without fluoroscopy.

In genitography, the radiologist must first inspect the genitalia and perineum for external openings. The usual lesion is a single opening either at the base of the phallus or in the perineum (Fig. 7.2). For the flushing technic, the tip of a blunt nosed syringe is inserted in the genital tract opening and the glass barrel is pressed firmly against the perineum to obtain a leakproof seal. Contrast agent is then flushed into the external opening. The goal is to flush the contrast agent into all the internal passages. The disadvantage of inserting a catheter and instilling contrast agent is restriction of visualization to the cavity containing the catheter, without delineation of other cavities.

To avoid this error, when the flushing technic fails the multiple catheter technic is used to probe the genital opening with multiple catheters under fluoroscopy. The aim is to direct catheters and enter cavities which cannot be flushed or are only partly filled or did not remain filled sufficiently long for spot film demonstration by the flushing technic. When more than one passage is found, simultaneous injections are made in each one via the catheters. When only one passage is found the catheter is withdrawn to a point just inside the external opening, the perineal skin is held tightly around the catheter, and the contrast agent is again flushed. These methods usually result in delineation of all the internal genital passages.

The most satisfactory contrast agent is a 50% solution of sodium or meglumine diatrizoate. It is convenient to work with and fills the passages readily. On the other hand, it will leak around the syringe and drain out of the passages easily. In this event, the oily agents can be used, although they are viscous and hard to work with. The aqueous agent should be tried

first, then, if unsuccessful, the oily medium be employed. A 20% solution of sodium diatrizoate (Hypaque) is satisfactory for cystourethrography.

Disorders of the genital tract listed in Table 7-1 have proved amenable to radiologic diagnosis.

Intersex

The ultimate sex of an individual is moderated by morphologic, hormonal and sociopsychologic factors. Hampson and associates classified these into seven variable components (Table 7-2). Harmony and consistency of these components are required for an individual to be unisexual. Primarily there is a need for unity between genital structure and gender.

Gender is indicated by a person's behavior. It is the psychosexual performance of an individual. If it is male, the individual must be able to function organically as a male. Gender must match genital structure. A conflict in which one type of normal genital structure of either sex is coupled with the opposite gender results in psychiatric intersex (transsexualism, transvestism, homosexuality). A conflict in which ambiguous genital anatomy is coupled with gender of either sex results in structural intersex.

Resolution of the clinical aspect of morphologic intersex requires: (1) prompt assignment of a sex in accordance with genital structure, (2) establishment of the gender role to match the anatomic capabilities as nearly as possible, and (3) subsequent treatment, if necessary, to improve and make the anatomic capabilities as compatible as possible. Unnecessary delay of decision causes anxiety, concern, suspicion and gossip on the part of friends, relatives, siblings and parents.

An intersex problem is recognized at birth when ambiguous external genitalia are detected by visual inspection. Of the internal genitalia knowledge of the gonads is not essential, but the nature of the internal genital passages must be known to establish anatomic capability. Genitography is the simplest and easiest method of identifying the internal genital passages. It supplies information not available by catheterization, rectal palpation, endoscopy and surgical exploration.

TABLE 7.2.—THE VARIABLE COMPONENTS OF SEX

COMPONENT	VARIABLES	
1 Chromosomal	Chromatin positive (XX) Chromatin negative (XY)	Morphologic Intersex
2 Gonadal	Testis Ovaries	
3 Internal genital anatomy	Neither or both Müllerian (female) Wolffian (male)	
4 External genital anatomy		
5 Hormonal	Androgenic Estrogenic	Effect at puberty Governed by 3 & 4 Governed by 6
6 Rearing	Sex assignment	
7 Gender	Sex orientation	

TABLE 7-3—STUDIES UTILIZED IN FINAL EVALUATION OF ERRORS IN SEXUAL DIFFERENTIATION

- 1 Sex chromatin pattern
- 2 External genital anatomy
- 3 Internal genital anatomy
- 4 Urinary hormonal excretion
- 5 Gonadal nature by biopsy

tion—information that assures the assignment of a sex in accordance with the anatomic capabilities rather than with chromosomes, gonads and hormones. A good guiding principle is that it is easier to transform a sexually ambiguous person into an acceptable female than into a male. Therefore, usually a vagina of any size in the absence of absolutely normal male external genitalia is an indication for the assignment of the female sex regardless of the chromosomes, gonads and hormones.

The data in Table 7-3 are useful for evaluation of an intersex problem but, with few exceptions, they can await genitography and assignment of a practical sex. Chromosomes, gonads and hormones play little if any role in the assignment of a practical sex, in the determination of gender and consequently in the clinical solution of intersex problems. Errors in the management of intersex problems have been difficult to avoid because of the erroneous belief that the assigned sex must accord with chromosomes and gonads.

At what age is the gender role established and when can the sex of rearing be effectively changed? The questions are academic and insignificant if a practical sex is assigned early and gender is in accordance with structural potentials. In this event there is no need for a change in the pattern of sex rearing. For genitography to take its deserved place in intersex diagnosis, radiologists should be familiar with normal sexual differentiation, the altered prenatal development responsible for the genitographic types and the classification of genitographic types.

NORMAL SEXUAL DIFFERENTIATION—Genetic, tes-

ticular and androgenic determinants are responsible for embryologic development and sexual differentiation (Grumbach, Hoffenberg, Jones). These determinants can be thought of as inductors, each of which has its own specific action. They are shown in simplified form in Table 7-4.

Primary (genetic) inductors carried by both the sex chromosomes and the autosomes of the ovum and sperm determine the differentiation of the primordial gonad into an ovary or a testis. Chromosomal abnormalities and gonadal dysgenesis, as in Klinefelter's (XXY) and Turner's (XO) syndromes, are the result of abnormal primary induction.

Secondary induction determines the nature of the internal genitalia and therefore has special significance for genitography. Early intrauterine castration of certain animals is invariably followed by feminine genital tract differentiation, even if the gonads were destined to become testes (Jost). Whether or not ovaries are present, Mullerian (female) growth will occur in the absence of a functioning testis. The presence of testes determines Wolffian (male) growth. A single testis is capable of directing growth on its own side. Thus there is only a male secondary inductor and its action is local, not hormonal. The lateralized true hermaphrodite is the best illustration of this local action. These intersexual individuals have a testis on one side and an ovary on the other, with the Wolffian development restricted to the testicular side. Secondary induction is repressive to female and stimulative to male internal genital development. Incomplete secondary induction in the fetus accounts for male pseudohermaphrodites who have vaginal and uterine remnants of varying size.

Tertiary induction is responsible for masculinization of the lower genital tract. Removal of one embryonal testis does not alter masculinization of the urogenital sinus and external genitalia. Therefore pervasive and not locally acting inductors are responsible for tertiary induction. These pervasive inductors are androgens because masculinization of the lower genital tract of females occurs after exposure to androgens, through either medication or adrenal corti-

TABLE 7-4—SEXUAL DIFFERENTIATION

INDUCTOR	DETERMINES	NORMAL	ABNORMAL
Primary—genetic, from ovum and sperm	Gonadal primordium	Ovaries Testes	Turner's Klinefelter's True hermaphrodite
Secondary—presence of testes (local)	Male internal genitalia	Absence—Normal female Presence—Normal male	Male pseudohermaphrodite (Mullerian duct remnants)
Tertiary—hormonal androgens from testes or extra gonadal source	Male external genitalia	Absence—Normal female Presence—Normal male	Female pseudohermaphrodite Adrenal cortical Iatrogenic Idiopathic With anal atresia

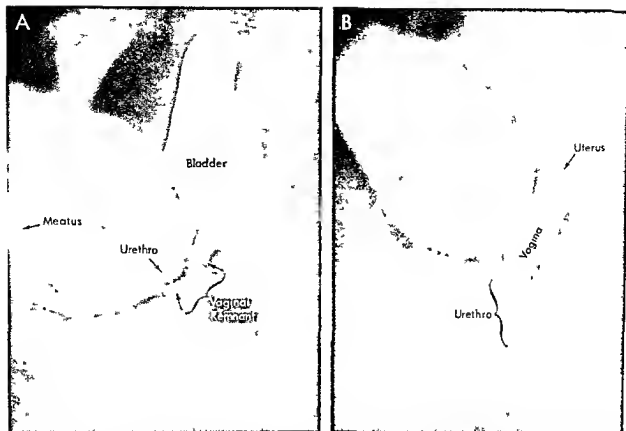


Fig 7-3—One-month old individual with a phallus and a small perineal opening at its base. Male sex was assigned at birth. **A**, gonitography at 1 month of age shows a short male type urethra and small vaginal remnant. Adrenal cortical hyperplasia was proved by electrolyte and hormone studies. Severe tertiary induction by androgen from the adrenal cortex has repressed growth of the vagina and caused partial male differentiation of the external genitalia. The sex was changed to female and treatment started for adrenal hyperplasia. **B**, at 20 months the vagina has grown to normal size illustrating the repressive effect on vaginal growth by androgen before its elimination by treatment. Demonstration

of the uterus at this time indicates that the excessive androgen had no effect on female differentiation of the internal genitalia but did inhibit their growth. The postnatal growth of the urogenital sinus and Mullerian duct structures under proper hormone therapy is intriguing. It represents growth of embryonic structures during the postnatal period which should have occurred in utero. The tragic consequences of the male sex assignment in an individual who has potential for female growth and development of the internal genitalia is obvious. A vagina of almost any size is usually an indication for assignment of the female sex.

cal hyperplasia. Such an effect is responsible for female pseudohermaphroditism. Excessive tertiary induction of a male fetus causes either no deviation from normal male external genitalia or virilization of it.

Thus far only differentiation of the genital structure has been considered, but growth is also a factor since the size of the structures has clinical importance. Little is known about the relationship of the inductors to growth, however, clinical experience has shown that androgens (tertiary induction) are important stimulants to the growth of the male genital tract and repressants to the growth of the female genital tract (Fig 7-3).

In summary all human beings will develop along female lines if there is no testicular tissue, that is, secondary and tertiary induction. Imperfect secondary and tertiary induction permits the presence of vaginal and uterine remnants with incomplete masculinization of the external genitalia. Androgen is the

prime factor responsible for growth of the genital structures.

EMBRYOLOGY—Embryologic development of the genital tract is controlled by the genetic, testicular and androgenic determinants mentioned in discussion of normal sexual differentiation. When the human embryo is 6–8 weeks old (15–20 mm length) the anatomy of the genital tract is exactly the same for male and female, that is, there is an indifferent state (Fig 7-4, A). At the time of the indifferent state, the important urogenital structures include the cloaca, Wolffian and Mullerian ducts, gonadal primordium, genital tubercle, labioscrotal folds and genital swellings. In the absence of secondary and tertiary induction (the presence of ovaries) Mullerian duct development progresses and the Wolffian ducts regress (Fig 7-4, B–D). In the presence of secondary and tertiary induction (the presence of normal testicles) Wolffian

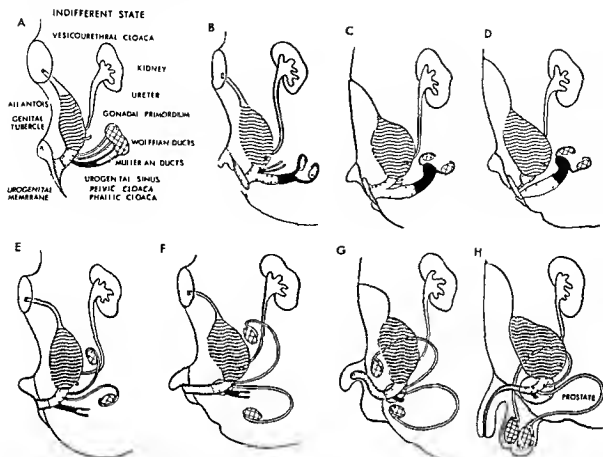


Fig 7-4—Diagrammatic sketches of sequential changes in the anatomy as the indifferent state is converted into that of a normal female and male. Careful attention to these dynamic changes in the fetal anatomy is important because they explain the anatomic findings of the neonate. B, C and D depict development of the vagina, vulva, vestibule and uterus from the urogenital sinus and Mullerian ducts. E, F, G and H outline the sequential development of the penis, scrotum, urethra, vas deferens and

prostate. Absence of testes (i.e. absence of secondary tertiary induction) causes development of normal female anatomy whereas presence of testes (i.e. presence of secondary and tertiary induction) causes a normal male. Deficient and/or incomplete secondary and tertiary induction may result in any of the intermediate types between the indifferent state of A and the normal female and male anatomy of D and H.

duct development progresses and the Mullerian ducts regress (Fig 7-4 E-H).

The Mullerian ducts lie side by side between and caudal to the Wolffian ducts, the four ducts ending in the pelvic portion of the urogenital sinus and forming the genital cord. In the male the Mullerian ducts atrophy but traces of their caudal portions fuse to form the utriculus in the floor of the prostatic portion of the urethra. In the female the Wolffian ducts atrophy, persistent portions are known as Gartner's ducts. They may persist as isolated segments as far as the hymen.

The cloaca is subdivided into three portions: (1) a vesicourethral portion continuous with the allantois; (2) an intermediate narrow channel, the pelvic portion, into which the Wolffian and Mullerian ducts open; and (3) a phallic portion closed internally by the urogenital membrane (Fig 7-4 A). The second

and third parts together constitute the urogenital sinus. The caudal portion of the vesicourethral cloaca incorporates the ends of the ureteral diverticula and gives rise to the base of the bladder and the proximal urethra as far down as the intermuscular incisura (Shopfner and Hutch). The remainder of the vesicourethral portion forms the body of the bladder; its apex is prolonged to the umbilicus as a narrow channel (the urachus) which later is obliterated and becomes the middle umbilical ligament.

The pelvic part of the urogenital sinus becomes the posterior urethra of the male and the entire female urethra. Absence of secondary and tertiary induction in the female permits vaginal development by formation of a diverticulumlike outgrowth of the pelvic urogenital sinus epithelium which invades the area of the Mullerian ducts. It is continuous with, and pushes before it, the Mullerian ducts which by this

time have formed the uterus and fallopian tubes (Fig 7-4, B) Progressive growth and enlargement of the vagina, coupled with rearrangement of the pelvic portion of the urogenital sinus which occurs with flattening and elongation of the phallic portion, causes the vagina and urethra to open separately into the vulvar vestibule which is simultaneously being created by the phallic portion of the urogenital sinus (Fig 7-4, C and D)

Secondary and tertiary induction in the presence of testes inhibits the epithelial outgrowth from the pelvic urogenital sinus and the Mullerian ducts gradually regress to the minute utrunculus masculinus The Wolffian ducts grow, elongate and accompany the testes in their migration to the scrotum (Fig 7-4, E-H)

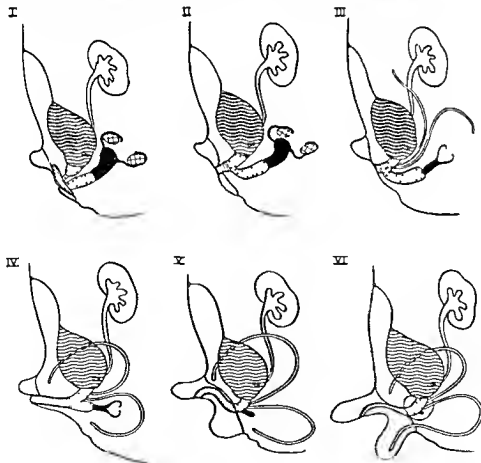
Like other parts of the genital system the external genitalia pass first through a period of indifference In the female a deep groove forms around the phallus and separates it from the other structures The tissue at the sides of the phallus grows caudad as the labioscrotal folds and genital swellings which ultimately form the labia majora and minora the phallus itself

becomes the mons pubis and clitoris The phallic part of the urogenital sinus is vertically flattened and elongated between the labioscrotal folds to become the vulvar vestibule In this manner separate openings for the urethra and vaginal orifices are created in the vulvar vestibule (Fig 7-4, B-D)

In the male the early changes are similar, but the phallus undergoes much greater development as it is pushed ahead by the phallic portion of the urogenital sinus The terminal part of the phallus representing the future glans becomes solid the remainder, which is hollow, is converted into a longitudinal groove by absorption of the urogenital membrane and thus creates the first opening of the urogenital sinus to the exterior It becomes elongated simultaneously as labioscrotal fusion converts it into the male urethra by the action of tertiary induction (Fig 7-4, E-H) The genital swellings extend around and between the urogenital sinus and the anus to form the scrotal area, during the changes associated with descent of the testicles this area is drawn out to form the scrotal sacs As in the female, the urogenital membrane undergoes absorption, forming a groove on the under

Fig 7 5 - The six types of genitographic anatomy determined by the nature of the internal genital passages Correlation of the

identification code with that of Figura 7-4 shows the embryologic origin of the anatomic components



surface of the phallus, this groove is then incorporated by labioscrotal fusion to form the male urethra.

CLASSIFICATION OF GENITOGRAPHIC TYPES—Classification of genitographic findings as first presented (Shopfner 1964) was based on the information obtained from genitography performed in 25 individuals with ambiguous genitalia (Fig. 7.5).¹⁸ The objective of the classification is to assist the radiologist in interpreting genitographic findings. It is not based on and has no relation to other classifications of intersex that have been proposed (Spence Wilkins 1957), they are based on gonadal biopsy and chromatin patterns whereas the genitographic classification is based on the anatomy of the internal genital passages which indicates the practical sex.

Experience with the classification now includes 78 patients, and it remains as valid as when originally proposed. No attempt is made to depict or predict gonadal and genetic sex from the classification because they are not important in the assignment of a practical sex. Genitographic findings affirm the existence of a vagina and/or urogenital sinus and shows the relationship of the urethra to them. It is important to demonstrate only the passages which communicate with the exterior, since the presence of a urogenital sinus and vagina of almost any size is an indication for female sex assignment because it is easier to transform a sexually ambiguous person into an acceptable female than into a male. The classification does not include those rare instances of true hermaph-

roditism and male pseudohermaphroditism with atretic or hypoplastic structures that do not communicate with the exterior of the body.

It is convenient to think of intersex anatomy in terms of deviation from a normal female since in the fetal period all humans develop as females in the absence of testes. All changes from the normal female represented by the six types of genitographic anatomy are varying degrees of masculinization caused by imperfect secondary and tertiary induction.

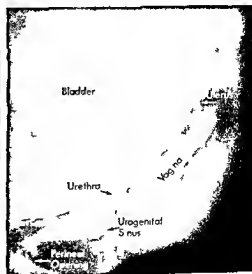
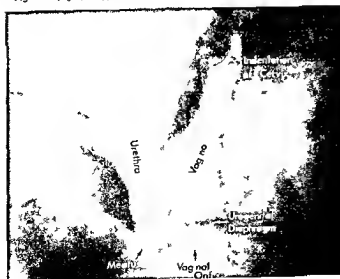
Type I is simple clitoral hypertrophy. It represents masculinization of the phallus, but all other structural aspects are female (Fig. 7.5). No labioscrotal fusion occurs; therefore labial development is normal. The phallic urogenital sinus is flattened and elongated into a vulvar vestibule and the urethra and vagina have separate openings into it. Vaginal development is complete, and genitographic demonstration of it in the neonatal period is an indication for assignment of the female sex (Fig. 7.6). These individuals have a uterus and ovaries which make it possible for them to bear children. Sex life is adequate as a female. Subsequent treatment is not always necessary, but if it is only a simple revision of the phallus is required. This should be postponed until after puberty when the adult anatomic structures are fully developed and an accurate appraisal of the revision needs is possible.

Type II represents additional masculinization which involves the urogenital sinus in addition to the phallus as in type I (Fig. 7.5). Partial labioscrotal fu-

Fig. 7.6 (left)—Type I anatomy. This 4 year old individual was being reared as a girl, but the mother was concerned because the child appeared to have a penis. There were a phallus, labia majora, labia minora and vulvar vestibule. A female urethra opens into the vestibule, behind which is a normal sized vagina capped superiorly by the indentation of the uterine cervix. A vagina of any size is indicated for assignment of the female sex, and fortunately it was assigned at birth to this child.

Fig. 7.7 (right)—Type II anatomy. This 38 year old male

has a phallus with a single opening at its base. The urogenital sinus receives the urethra and vagina separately. Partial filling of the uterus has occurred. The vagina indicates female anatomic capabilities, but the individual is forced to lead the life of a male because the sex of rearing was improperly assigned at birth. He is actually a female who has been masculinized by mild adrenal cortical hyperplasia. Gonadal chromosomal and hormonal evaluations indicated the female nature. (From Shopfner Radiol Clin North America 5:151 1967.)



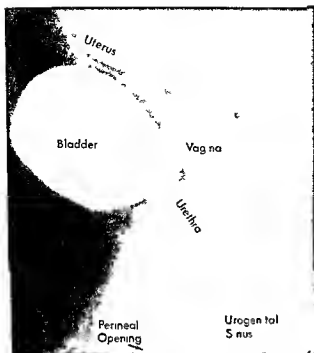


Fig 7.6.—Type III anomaly. In this 1 week old individual with ambiguous genitalia there was a phallus and a single urogenital opening in the perineum. Genitography shows a short urogenital sinus with most of it incorporated into a longer male urethra. Extending posteriorly is a fully formed vagina capped by a normal uterus. This anomaly is an indication for the female sex assignment. Gender is properly established as female if the sex is assigned promptly at or shortly after birth. In this patient the female sex was assigned despite a male chromatin pattern and intra-abdominal testes. Administration of hormones to induce female secondary sex characteristics after testicular tissue is removed assures a sexually adequate female from the anatomical standpoint.

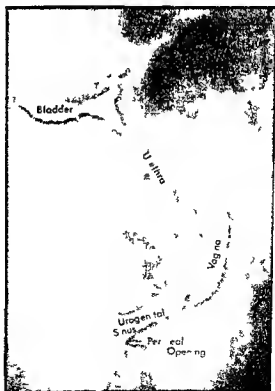
sion has occurred and there is a single perineal opening at the base of the phallus. It is the opening of the urogenital sinus which has been elongated by tertiary induction (Fig 7-4). Vaginal development is complete and its opening into the urogenital sinus is posterior to the female type urethra (Fig 7-7). Female sex assignment should be made on the basis of the fully developed vagina. These individuals are usually the result of masculinization of a female fetus by androgens which may come from the adrenal cortex or from androgenizing hormones administered during the first trimester of pregnancy. In this event the ovaries and uterus are normal. These individuals lead sexually acceptable lives as females and are fertile. The only treatment necessary is possible revision of the phallus and perineal opening at or near the time sexual function is anticipated.

Additional masculinization produces individuals with type III genitographic anatomy (Figs 7-5 and 7-6). The natural and irresistible development along female lines is partly inhibited by incomplete secondary and tertiary induction. There is a phallus with a single opening either at its base or in the perineum.

The urogenital sinus is short and remains about as it was in the fetal indifferent state. Vaginal and uterine development were not inhibited so they exist as fully developed structures. The phallus cannot function adequately as a penis in spite of numerous surgical procedures. On the other hand, the vagina, with little or no surgical revision, permits adequate sexual function as a female. Therefore, and despite the possibility that the chromatin pattern and gonads are male, the female sex should be assigned. Testicular tissue should be excised and female hormone therapy administered at puberty. These individuals can be emotionally adequate as females if this gender is established at birth; of course they will be sterile.

Type IV represents more masculinization (Fig 7-9). A phallus exists with a single opening usually at its base. The phallic urogenital sinus has been progres-

Fig 7-9.—Type IV anatomy. This 2 month old infant had a male sex assignment at birth on the basis of a phallus. However the parents were concerned that something was wrong with the penis because the urine came from a hole in the perineum. At the time of genitography there was a phallus and a single urogenital opening in the perineum. Anatomic structures are the same as for type III except that the urethra is longer, vaginal size is smaller and there is no indication of a uterus. Chromatin pattern and gonads were male, indicating a male pseudohermaphrodite. However the sex was changed to female because construction of a penis did not seem possible. Sterility will exist because testicular tissue is to be excised and female hormones administered so that female secondary sex characteristics develop at puberty. A vagina of almost any size is a valid medical indication for female sex assignment because it is easier surgically to make an acceptable female than an acceptable male.



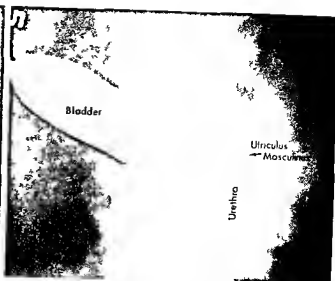
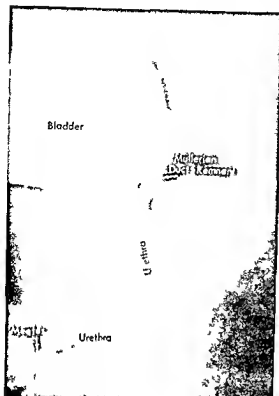


Fig 7 10 (left) - Type V anatomy. This 15 month old patient had hypospadias with the urethral meatus on the shaft of the hypoplastic penis just above where it joined with the scrotum and penneum. There were undescended testicles, the right one palpable in the groin and the left one not palpable. The urethra is distinctly shortened but male in type and the Mullerian duct remnant comes from the midportion of the posterior urethra. This child is committed to be a male but faces the formidable difficult and usually unsuccessful attempt at reconstruction of a penis. It should be recognized that objectives in the surgical repair of hypospadias are to create a urethra that drains as nearly as possible at the end of the penis. There are no surgical techniques reconstructive or grafting which can create a sexually functioning penis.

Fig 7 11 (above) - Type VI anatomy. This 15 month old patient has hypospadias with the urethral meatus just behind the glans. An utricle masculinus exists which is a little larger than average. The individual is committed to be a male and his sexual outlook is optimal because a penis sufficiently well developed to have the urethra near the glans requires little surgery and functions adequately from the sexual standpoint.

sively elongated into a longer male type urethra. Vaginal and uterine structures exist but are hypoplastic. These individuals are usually male pseudohermaphrodites. However, the presence of a vagina is an indication for the assignment of the female sex. It is a formidable task to reconstruct the penis whereas it is a simple matter to revise and remodel the hypoplastic vagina into a functional female sexual makeup. These individuals require castration and female hormone therapy for development of female secondary sex characteristics at puberty. They will be sterile.

Types V and VI represent different degrees of what is clinically known as hypospadias. A phallus of variable size exists and in type V the urethral meatus opens anywhere from the midpenile shaft to the base of the phallus. There is a Mullerian duct remnant which actually consists of an enlarged utricle masculinus (Fig 7 10). There is no vagina. The Mullerian duct remnant originates higher from the posterior urethra at the site of the embryological genital cord.

Type VI is a milder form of hypospadias with the urethral meatus opening in a more distal location

along the shaft of the penis. The Mullerian ducts have undergone complete regression so that they persist as the normal utricle masculinus which may or may not be filled on genitography (Fig 7 11). Patients with either type V or type VI usually have undescended testicle on one or both sides. It is important to demonstrate the Mullerian duct remnant because it differentiates between male pseudohermaphroditism and lateralized true hermaphroditism. The lateralized true hermaphrodite frequently has a hypoplastic uterus and tube in the hernial sac accompanying the undescended testicle. The presence of a Mullerian duct structure opening into the posterior urethra indicates that the patient is not a lateralized true hermaphrodite because the Mullerian duct structures cannot form the enlarged utricle masculinus and in addition the hypoplastic uterus and tubes in the hernial sac.

Types V and VI usually receive a male sex assignment because the phallus is fairly well developed and a scrotum of some type exists. However, a female sex assignment should be seriously considered in individuals who have minimal penile development and a

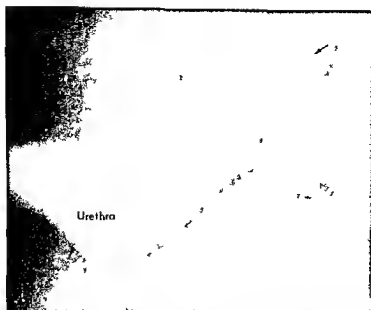


Fig 7 12 —This 9 year old patient had testicles in the groin and third degree hypospadias at birth. He had had five surgical procedures for reconstruction of the penis and urethra. Physical inspection revealed an irregular fibrotic 3 in long structure which resembled a penis more because of its location than because of its appearance. A reflection of the difficulty of surgical reconstruction of the penis and urethra is the genitographic appearance seen here. The urethra is a saccular atonic structure which has little resemblance to a normal urethra. Reactive spasm

from the retrograde injection prevents filling of the posterior urethra but a Mullerian duct structure (type V) does fill (arrow). An objective of reconstructive surgery must be to create a sexually adequate penis and this is not now possible with severe hypospadias. Most individuals who have hypospadias with the urethral opening in the proximal half of the phallus (penis) have a better prospect as females from the standpoint of urinary and sexual reconstruction.

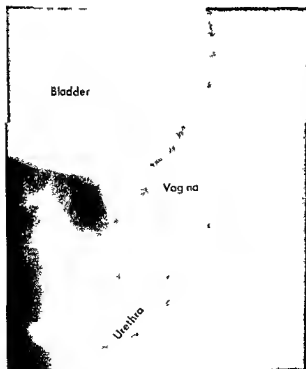


Fig 7 13 —In this 6 year old patient with hypospadias the urethral opening was at the base of the phallus. The left testicle was palpable in the inguinal canal but one could not be palpated on the right. Genitography shows a shortened hypospadiac urethra and fully developed vagina. The anatomy is functionally that of a female but this individual is being asked to lead the life of a male without the anatomic capability. Genitography performed at birth prevents entrance of contrast medium into the principle of assigning sex in accordance with anatomic capability rather than chromosomes and gonads should be followed.

severe hypospadiac urethral opening even though there is no significant vaginal development. It is extremely difficult to reconstruct a sexually adequate penis in a severely hypospadiac individual whereas it is relatively easy to reconstruct a vagina that will make a sexually adequate female (Fig 7 12). Sex and gender assignment should be established at birth to permit female psychosexual adaptation. In addition to the vaginal reconstruction, testicular tissue must be excised and female hormones administered at puberty. Individuals with type V and VI anatomy who receive a female sex assignment will be sterile as is the case in types III and IV.

We emphasize again the purpose of genitography is not to predict genetic and gonadal sex but to permit the assignment of a practical sex in accordance with the structural capabilities. Specifically, it establishes the existence of a vagina and/or urogenital sinus and shows the relationships of the urinary tract. It is not recommended that genitography replace previously used diagnostic methods. It is to be used in conjunction with all other methods in achieving a final and precise diagnosis. Genitography should take precedence over other diagnostic methods in order to assure a prompt sex assignment in accordance with anatomic capabilities at birth. Patients with so-called hypospadias should have genitography to prevent the common occurrence of a severely hypospadiac male with a normally developed vagina being assigned a male sex (Fig 7 13).

Fig 7 14 (left) — A 9 year old girl had had a vaginal discharge for several weeks. A marble is in the vagina. The vaginal location of a foreign body can be definitely established with lateral views and if necessary, vaginography.

Fig 7 15 (right) — In a girl 7 years of age with pus in the urine, physical examination showed purulent granulation tissue around

Vaginitis

A vaginal foreign body may be present when an infant or child has persistent inflammation and discharge. Schaeffer found 9 instances (3%) of foreign body in 302 patients with vaginal discharge. A bloody discharge and foul odor strongly suggest a foreign body. Vaginal foreign bodies can be detected by rectal palpation combined with rectovaginal examination, vaginoscopy and radiographic examination. The last is often done as a final resort. Reluctance of physicians to refer patients for radiologic examination often results in delayed diagnosis and inadequate treatment. Radiologic study should be a primary diagnostic procedure in all girls with subacute or chronic vaginitis. It is more accurate and less traumatic than either vaginoscopy or digital examination of the rectum or vagina.

Radiologic examination of the patient with vaginitis secondary to a foreign body begins with anteroposterior and lateral views of the abdomen and pelvis. They will detect and localize opaque foreign bodies (Fig 7 14). An opaque vaginogram is then indicated in the event an opaque foreign body is not detected. During fluoroscopy it is a simple matter to insert a small catheter into the vagina and distend it with opaque material. It is seldom necessary to inflate the balloon of a Foley catheter to keep the opaque material within the vagina. A syringe with its tip inserted

the urethra at menses, injected vulvar mucosa and yellow foul smelling vaginal discharge. Vaginography demonstrates a wedge of cloth which is negatively filling defect (left arrow) and a piece of dried nongelatin which is a near density (right arrow) because the hollow lumen is filled with contrast agent.



just inside the vagina and the glass barrel pressed firmly against the perineum to obtain a leakproof seal can also be used to instill the opaque material. Conventional spotfilms adequately demonstrate the anatomy and pathology (Fig 7 15)

Genital Tract Obstruction and Tumors

Genital tract obstructions and tumors are discussed together because each presents as an abdominal mass which has risen from the pelvis into the abdomen. Imperforate hymenal membrane partial vaginal aplasia vaginal atresia and combined vaginal and uterine atresia cause varying degrees of genital tract obstruction with accumulation of excretions above which produce the mass. Sometimes these abnormalities do not become clinically manifest until the menarche; in only a few instances do symptoms and physical findings appear during the first week of life as hydrocolpos (Fig 7 16)

Fetal factors explain genital tract obstruction (see Fig 7-4). The urogenital sinus is a hollow structure from its earliest existence, but the paired Mullerian ducts are solid structures which fuse together and become canalized. Their failure to canalize results in uterine atresia of varying degrees. Localized atresia at or near the cervix causes uterine dilation which presents as an abdominal mass. The commonest type of genital tract obstruction is, however, a simple im-

perforate hymenal membrane caused by failure of resorption of that portion of the urogenital membrane which covers the urogenital sinus.

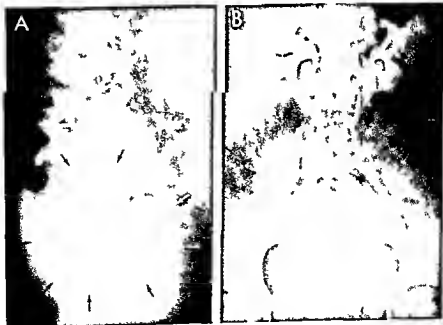
The radiologist first inspects the perineum and urogenital structures. An imperforate hymenal membrane is found in over 90% of the patients.²² Anteroposterior and lateral projections of the abdomen reveal the soft tissue mass. The abdominal mass, in combination with an intact hymenal membrane which bulges downward on abdominal pressure, is usually sufficient to establish the diagnosis. Needle aspiration via the vaginal membrane and replacement with a similar quantity of opaque medium makes the dilated vagina and uterus visible and conclusively establishes the diagnosis of hydrocolpos. Hysterectomy has been done mistakenly in some children in absence of an accurate diagnosis.

Tumors of the genital tract often are first observed as abdominal masses. Teratoma of the ovary is the only tumor with an incidence high enough to warrant discussion here. It is important to recognize that they may rise out of the pelvis and suggest an abdominal rather than a pelvic origin (Fig 7 17).

The objectives of radiographic examination are to establish location, origin, diagnostic features such as calcium and fat densities, and relationship to contiguous structures (Fig 7 18). Cystourethrography and intravenous pyelography are usually the only additional diagnostic methods necessary after plain films

Fig 7 16 The 12 year old girl had an abdominal mass. The hymen was imperforate and bulged into the vulvar vestibule. A cystogram lateral projection shows ante- and superior displacement of the bladder by the midline mass (arrows). The mass is cone-shaped and has the same appearance as that caused by the fecal mass of constipation. B, intravenous pyelogram shows lateral deviation, kinking and mild distention of the ureters due to shortening of the capsule to the bladder by its ante- and superior displacement. If desired, perforation of the hymen followed by injection of contrast agent can be done to document the vaginal and uterine distention which causes the mass. (Courtesy of D. R. Parker, Allen, Denver, Colo.)

g am shows lateral deviation, kinking and mild distention of the ureters due to shortening of the capsule to the bladder by its ante- and superior displacement. If desired, perforation of the hymen followed by injection of contrast agent can be done to document the vaginal and uterine distention which causes the mass. (Courtesy of D. R. Parker, Allen, Denver, Colo.)



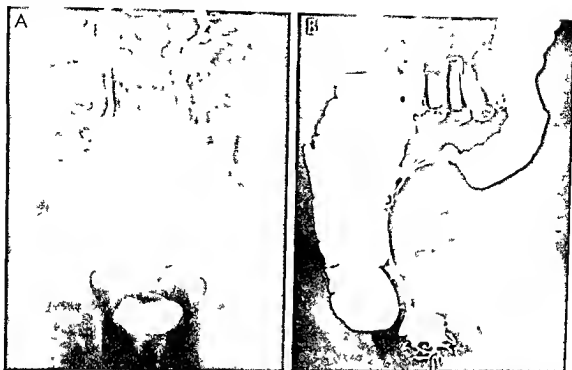


Fig 7-17—In a 5-year-old girl a lower abdominal mass suddenly developed two days before hospitalization. She had backache when urinating. Plain abdominal films, intravenous pyelograms, and films after barium enema were obtained. A representative film of the intravenous pyelogram shows the large abdominal mass compressing the ureters. There is no calcification in the

mass. B, barium enema reveals the mass compressing the sigmoid colon, but the rectum is in a normal position. This information may be interpreted to indicate that the mass did not arise in the pelvis. It is important to recognize that pelvic masses rise out of the pelvis to simulate an abdominal organ. The mass was a cystic ovarian teratoma.

Fig 7-18—In a 12-year-old girl a suprapubic mass was detected during examination because of constipation. This scout film as a preliminary to barium enema shows bilateral calcifications (arrows) some resembling teeth, characteristic of teratoma. No additional films were exposed. Surgical exploration confirmed the ovarian origin and teratomatous nature of the masses.



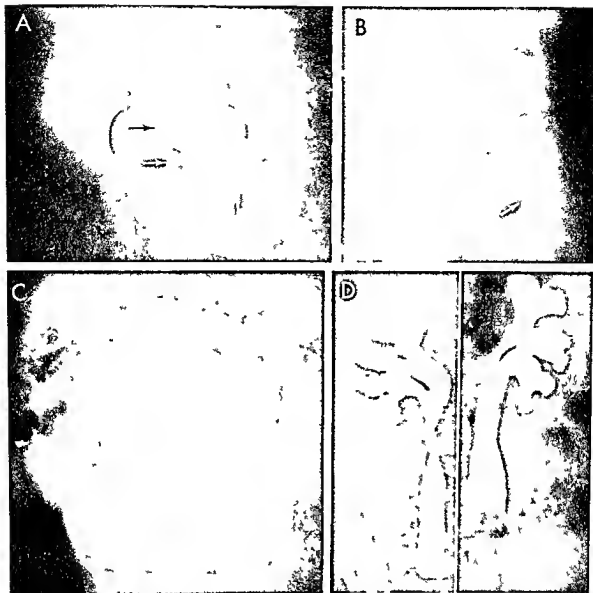


Fig 7 19—Abdominal protuberance and a lump over the tail bone prompted the mother of this 2 year old child to seek medical attention. A, anteroposterior and B, lateral projections show sacral hypoplasia and an (black arrow) irregular clump of calcification (white arrow) associated with a mass which extends up into the abdominal cavity and posteriorly to the buttocks area. C, nonobstructive hydronephrosis is the roentgen manifestation of ureteral and renal maldevelopment which existed initially. Exami-

nation a year after surgical excision of the mass (a teratoma) showed no improvement and confirmed the nonobstructive nature of the hydronephrosis. Nevertheless bilateral cutaneous ureterostomies were performed. D, hydronephrosis persists 1½ years later to the same degree as initially. The maldevelopment and nonobstructive nature of the hydronephrosis is indicated by its persistence after removal of the mass and the ureterostomies.

of the abdomen are obtained. These examinations assist in the location of the mass and also reveal the relationship and nature of the urinary tract structures which are important because they occasionally reveal maldevelopment equal to or exceeding the significance of the pelvic tumor. A pelvic mass occupying space normally reserved for the bladder and ureters interferes with and prevents their development. As a consequence, some patients with pelvic masses present maldevelopment of the upper urinary tract

which is manifested radiologically as nonobstructive hydronephrosis (Fig 7 19).

Gynecologic Aspects of Imperforate Anus (Ectopic Anus)

A careful review of fetal development shows that imperforate anus is not a primary condition but is secondary to more basic pathology—an ectopic anus. Prior to the 5th fetal week, the cloaca is a single

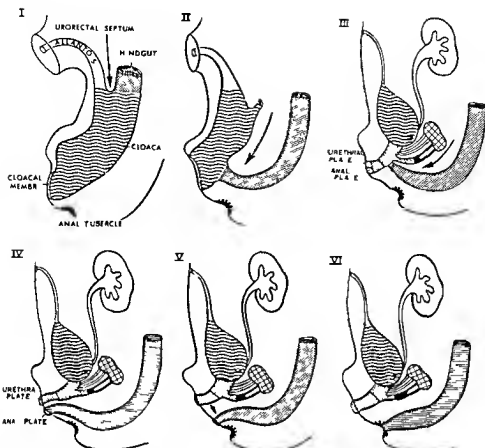


Fig 7 20—Embryology of ectopic anus. Following the cross hatching code in I through the progressive stages of urorectal septum descent. In II–VI illustrates the dynamic action involved in rectal and urogenital development. Arrest of urorectal septum

descent in any stage results in the clinical types of ectopic anus (Fig 7 21). An ectopic anus in the location of stage III causes persistence of the urogenital sinus in females and creates the important gynecologic problem of proper sex assignment.

structure into which the ureter, Wolffian duct, Mullerian duct, and hindgut enter (Fig 7 20 I). Dynamic action of the urorectal septum separates the hindgut from the urogenital structures; some embryologic motivator causes it to migrate in a caudal direction and separate the cloaca into the dorsally placed rectum and ventrally placed urogenital sinus. Progressive downward descent of the urorectal septum pushes the hindgut before it, taking it from a location high on the posterior wall of the cloaca near the openings of the urogenital structures down to a point of complete separation when it reaches the cloacal membrane (Fig 7 20 II, III & IV). Separation of the hindgut from the urogenital sinus is followed by union of the anal plate and the rectum, which then continue their migration together across the perineum to reach the definitive site of the anus (Fig 7 20 V). This point is marked by the anal tubercles, which have been independently developing. A union of the rectum and anal tubercles creates the anus at its definitive site (Fig 7 20 VI).

Failure of adequate migration of the urorectal septum down the posterior wall of the cloaca leads to an abnormal connection between the pars pelvina of the urogenital sinus and the rectum. In this event the urogenital sinus persists in the female and an ectopic anus is created which opens anywhere along the path of caudal descent of the urorectal septum, but usually at the superior or inferior extremity of the persistent urogenital sinus. This explains the so-called high vaginal and posterior fourchette fistula traditionally described in females with imperforate anus. Strictly speaking, this is not a fistula but an ectopic anus and it communicates not with the vagina but rather with a persistent urogenital sinus. Hence the surgical problem with imperforate anus is determination of the structure of the internal genital passages, assignment of a practical sex in accordance with anatomic capabilities, and the preservation of these structures for future sexual function.

Forty-eight patients with imperforate anus were studied by the principles mentioned above: the clinical

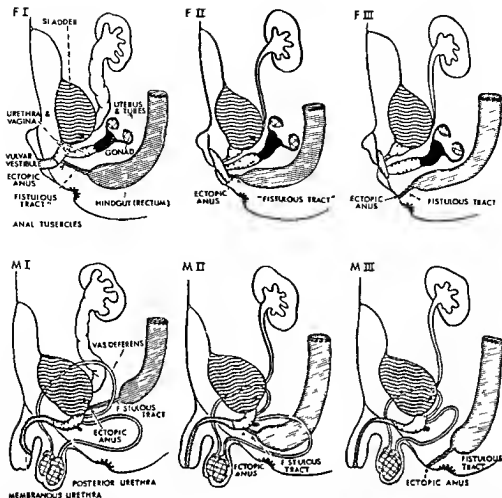


Fig. 7.21 — Clinical types of ectopic anus are derived from arrest of the urorectal septum descent during the embryologic stages shown in Figure 7.20. A female without a perineal anus as

shown in type F III will have an anus either in the posterior fourchette (type F II) or in a persistent urogenital sinus (type F I).

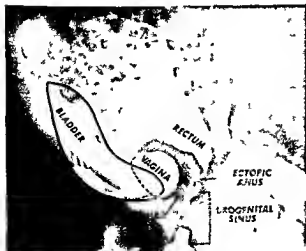


Fig. 7.22. — This girl was referred with a diagnosis of imperforate anus and third degree hypospadias. Arrest of urorectal septum descent at stage III of embryologic development (Fig. 7.20) results in type F I ectopic anus (Fig. 7.21). The rectum opens into the urogenital sinus, which also receives the vagina and urethra. The tip of the syringe is in urogenital sinus just inside the perineal opening. (From Shopfner South M J 88:712 1965.)

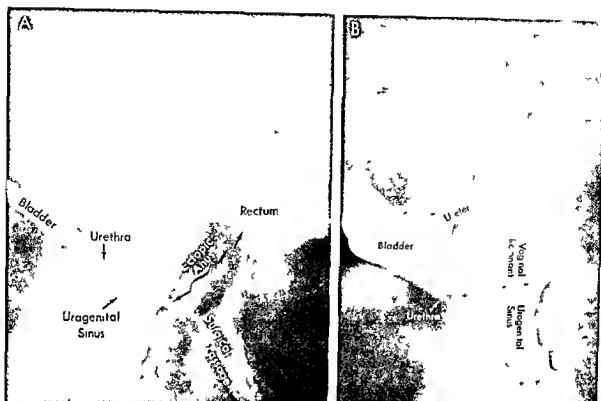


Fig 7 23 —A girl 7 years of age had severe constipation and a fecaloid vaginal discharge which had persisted since severance of a presumed rectovaginal fistula and pull-through of the rectum at 1 year of age. A single perineal opening, considered to be vagina, was situated 1.5 cm anterior to the surgically created anus. A catheter outlines the passage created by the surgical pull-through. It communicates with a greatly dilated rectum via the fistula. The remnant of the ectopic anal tract connects the surgical passage and rectum with the urogenital sinus. Failure to

resect and utilize the ectopic anal tract in the anastomosis invariably results in severe constipation because it cannot transmit feces. B, entrance of the bladder and urethra to the urogenital sinus is shown to advantage by flushing injection of the anterior perineal opening. A nonobstructive hydronephrotic ureter is demonstrated by reflux. Extending above the urethral entrance to the urogenital sinus is a small remnant of the vagina. The remainder of the vagina and the uterus were surgically removed at 1 year of age. (From Shopfner, *Seminars Radiol* 4:218, 1969)

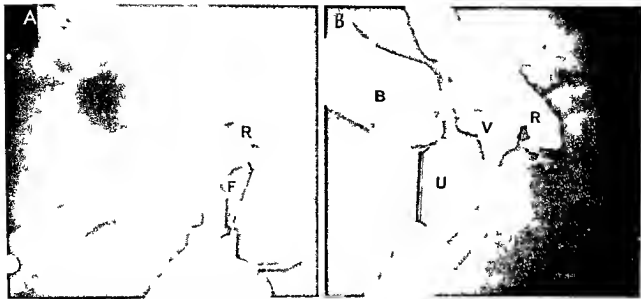


Fig. 7 24—This newborn girl had imperforate anus and no ectop canal in the perineum. Separation of the labia and inspection of the vulvar vestibule revealed an ectop canal in the posterior fourchette. A flush ng injection of the ectop canal opening demonstrates the fistula (F) leading to the rectum (R) (type F I).

ectop canal of Fig. 7 21). Descent of the urorectal septum below the pelvic port on of the urogenital sinus allows normal development of female genitalia. B. Injection via catheters in the vagina (V), urethra (U) and bladder (B) shows the exact anatomic status and assures preservation of these important urogenital passages.

types of ectopic anus are shown in Figure 7 21. Types F I & F II are the only ones in which a female complication exists. Arrest of urorectal septum descent when the rectum communicates with the urogenital sinus results in persistence of the latter structure (Fig. 7 22). In this event there is a single perineal opening that may lead some examiners to consider the infant a hypospadiac male. Demonstration of the persisting urogenital sinus is imperative to prevent removal of the uterus at the time of surgical treatment because of ignorance as to the exact nature of the structures which persist (Fig. 7 23). If no male female genitalia are present and there is no ectop anus in the perineum, an anus will exist in the posterior fourchette (Fig. 7 24). Recognition of the exact anatomic status as shown by genitography assures proper management of the imperforate anus and preservation of the healthy internal genital passages.

Bladder Exstrophy

Exstrophy of the bladder is almost always an associated genital abnormality. It is a rare lesion occurring only once in every 30 000 births, which amounts to a total of 200 such infants born each year in the United States. Consequently the experience of one physician or clinic with this lesion is limited, as a result emphasis is apt to be placed on the bladder anomaly while the significant lesion in the genital tract is overlooked.

There are three objectives in management of the patient with bladder exstrophy. Preservation of renal

function is the most important one. The next objective is to provide for comfort and social acceptability which in essence means either closure or excision of the exposed bladder and provision of some kind of urinary control, natural or otherwise. Third is the assignment of a sex in accordance with the anatomic potentials of the patient. There is no need for hasty repair of the bladder defect because small infants survive this anatomic inconvenience very well. Surgery should be postponed until the child has grown enough for adequate evaluation of renal development and determination of the internal genital passages. Williams has indicated that these children are far more likely to die of surgery than of any other cause and that improvement in the conditions of life rather than the simple mechanical closure of the defect in the bladder is the standard by which treatment should be judged.

Embryologically bladder exstrophy is caused by failure of the mesoderm to form the abdominal wall musculature by growing downward and medially between the ectoderm and endoderm. The embryologic defect occurs very early in fetal life, when the fetus is 2–4 weeks of age, and consequently affects the development of the urogenital tract, which does not commence until the fetal age of 6–8 weeks. The cloacal membrane extends from the yolk sac all the way down to the caudal end of the embryo (Fig. 7 25 I). It consists of layers of ectoderm and endoderm and is the only covering for the cloaca. Shortly thereafter the mesoderm begins to grow down and medially to form the abdominal musculature which will eventu-

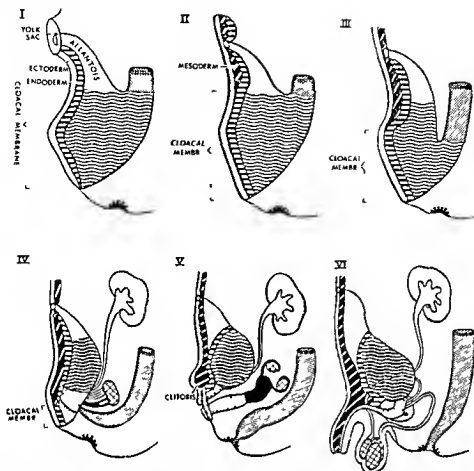


Fig 7 25 — At the fetal age of 2 and 4 weeks the only covering over the allantois and cloaca is the cloacal membrane which consists of a layer of ectoderm and another of endoderm (I). Progressive downward and medial growth of mesoderm from the primitive streak replaces and pushes down the cloacal membrane. The mesoderm forms the definitive abdominal wall musculature which at first covers only the allantois (II). Arrest of mesodermal growth at this point results in complete bladder *exstrophy* or so-called *ectopic cloaca*. In this event all structures originating and communicating with the cloaca open to the exterior. Progressive growth of the mesoderm eventually takes it down to cover the vesicourethral portion of the cloaca and form

the genital tubercle (III and IV). The cloacal membrane at this stage covers only the portion of the cloaca destined to become the phallic and pelvic urogenital sinus. From the condition in IV there develops either the normal female (V) or the normal male (VI) anatomy. Note that the mesoderm is responsible for development of the clitoris and root of the male urethra as well as the anterior abdominal wall. Arrest of mesodermal growth accounts for the following clinical types of bladder *exstrophy*: (1) arrest of mesodermal development at stage II (2) incomplete bladder *exstrophy* (III) (3) epispadias of the male and bidid clitoris of the female with diastasis recti (IV). (See Fig 7 26.)

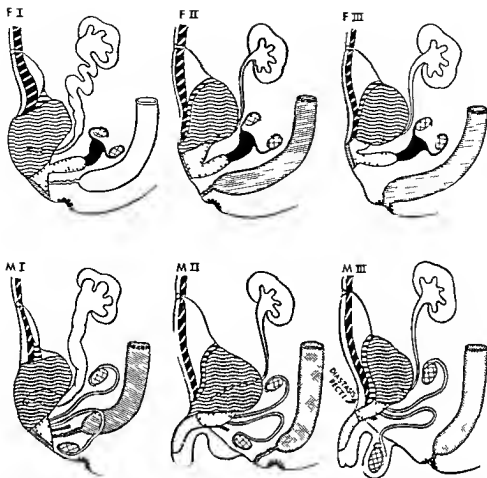


Fig 7 26.—Clinical types of bladder exstrophy traced directly from the embryologic type (Fig 7 25) Female types are shown in F I, F II and F III and male types in M I, M II and M III Arrest of mesodermal development as in types F I and M I results in arrest of mesodermal development of embryologic stage II (Fig 7 25 II) Mesodermal development has progressed only for a short distance below the yolk sac The entire cloaca is exposed to the exterior Therefore the ureteral, vaginal, urethral and rectal apertures all open to the exterior Further descent of the mesoderm covers much of the bladder but a small amount of it is exposed (F II and M II) In addition the root of the penile urethra is exposed resulting in epispadias and the posterior urethra

formed by the pelvic urogenital sinus is exposed In the female (F II) both urethra and vagina open to the exterior In both male and female the position of the ectopic anus is variable but usually it is in a penile site Further descent of the mesoderm causes all of the definitive bladder to be covered either by abdominal musculature (F III) or by a layer of skin If mesodermal development extends down to the level of the genital tubercle but does not meet in the midline in the female this leads to the clinical condition of bifid clitoris (F III) and in the male is the classic epispadias with or without astasia recti (M III) Failure of symphysis pubis development with separation of the pubic bones is a constant finding in all clinical types

ally cover the cloaca destined to become the bladder (Fig 7 25 II) As the mesoderm grows down it pushes before it the cloacal membrane which ultimately comes to cover the cloaca which is to become the definitive urogenital structures (Fig 7 25 III and IV) It is important to recognize that the mesoderm also forms the genital tubercle and symphysis pubis Schematic sequential sketches in Figure 7 25 show these changes from the time when only cloacal membrane covers over the cloaca to the full development of the female (Fig 7 25, V) and male normal anatomy (Fig 7 25 VI)

Arrest of the medial and downward descent of the mesoderm during any one of the intermediate stages

I—VI, results in the clinical types of bladder exstrophy shown in Figure 7 26 If no mesoderm develops all of the urinary and genital structures are exposed to the exterior (Fig 7 26 F I and M I) If partial mesoderm development occurs only a small part of the bladder is exposed but the urethra and genital structures open to the exterior (Fig 7 26 F II and M II) Further descent and migration of the mesoderm results in complete coverage of the bladder and genital structures but with the condition of epispadias in the male and bifid clitoris in the female (Fig 7 26 F III and M III)

The female internal genital passages must be preserved so that the individual can pursue a reasonably normal sexual life All openings contained in the ab-

Fig 7 27 —A newborn with anastrophy of the bladder is the patient male or female? The answer is the responsibility of the radiologist who must first explore the deformed mass of abdominal wall for urogenital openings. Three were found in the area of the arrow. Figure 7 28 is the genitogram of this patient (type F I of Fig 7 26) (Figs 7 27 and 7 28 from Shoptner, *Radiol Clin North America* 5:151, 1967.)



Fig 7 28 —Genitogram of the patient in Figure 7 27. A catheter is in the opening indicated by the upper and middle arrows of Figure 7 27, which are the urethra and vagina respectively. Injection of opaque material into these catheters shows the bladder and a normal sized vagina displaced anteriorly and su-

periorly. A third catheter has been inserted in the opening indicated by the lower arrow in Figure 7 27, and opaque material shows an ectopic anus with a long fistulous tract leading to the rectum (type F I of Fig 7 26). C and D are radiographs of A and B respectively.

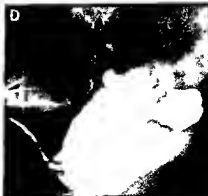
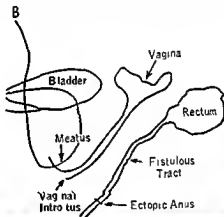
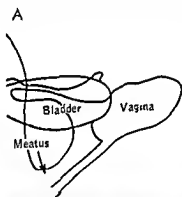




Fig. 7 28 —Bladder exstrophy in a 1 1/2 month old infant. The anus was in normal position. There was no penis, but at the lower margin of the deformed abdominal wall was a single opening (arrow). Injection of contrast agent into the opening showed it to be the posterior urethra. No vagina existed. In this case a female sex assignment is advisable because male sex function is impossible to attain by reconstruction when external structures are simple to construct a vagina.

dominal wall defect must be explored for identification of urogenital structures so that they can be recognized and preserved (Figs 7 27 and 7 28). A vagina of almost any size is an indication for the assignment of female sex. The patient who does not have a vagina and therefore is male but lacks anatomic capability presents a difficult problem (Fig 7 29). If reconstruction of the genitalia cannot create a functional penis, rearing of the infant as a female is mandatory. The true nature of all external openings should be ascertained and the vagina identified. Reconstruction of the penis is a formidable and discouraging task.

Fig. 7 30 —Teratoma of the testicle with several calcified components.



Fig. 7 31 —Bilateral calciferous masses in bilateral ovotestes in a patient 16 years of age who although brought up as a girl has never menstruated. The calcifications (arrows) are in bilateral ovotestes and a segment of the epididymis on one side with no evidence of ovarian tissue. This true hermaphrodite has the mosaic sex chromosome pattern of XYXO. (Courtesy of Dr Arthur Robinson, Denver, Colo.)

because eventual production of a sexually adequate and fertile male is rarely achieved when the penis is severely maldeveloped. Maldevelopment of the scrotum and undescended testicles are common associated malformations in the male patient. These defects are manifest on physical examination.

Teratomas of the testicle can be recognized radiographically when they contain calcified ossified elements (Fig 7 30). Bilateral calcification in the ovotestes can be identified in plain films (Fig 7 31). When the vaginal process is open in an inguinal hernia, calcifying meconium peritonitis may extend into the scrotum and be visible in plain films.

REFERENCES

- Allan, F. D. *Essentials of Human Embryology* (2nd ed. London: Oxford University Press, 1969).
- Bleischmidt, E. *The Stages of Human Development before Birth* (Philadelphia: W. B. Saunders Company, 1961).
- Gans, S. L., and Friedman, N. B. Some new concepts in the embryology, anatomy, physiology, and surgical correction of imperforate anus. *West. J. Surg.* 69:34, 1961.
- Gorlando, S. W. *Vaginitis: Diagnosis and treatment*. Clin. Med. 73:33, 1966.
- Gray, H. *The Anatomy of the Human Body* (28th ed. Philadelphia: Lea & Febiger, 1968).
- Grumbach, M. M., et al. Chromosomal sex in gonadal dysgenesis (ovarian agenesis): Relationship to male pseudohermaphroditism and theories of human sex differentiation. *J. Clin. Endocrinol.* 15:1161, 1955.
- Hamblen, E. C. The assignment of sex to an individual. Some enigmas and some practical clinical criteria. *Am. J. Obst. & Gynec.* 74:1228, 1957.
- Hampson, J. G., et al. Hermaphroditism: Recommendations concerning case management. *J. Clin. Endocrinol.* 16:547, 1956.

- Hoffenberg R and Jackson W P Sex chromatin and Intersex *J Clin Endocrinol* 17 454 1957
- Jones H W Jr and Scott W W (ed) *Hermaphroditism Genital Anomalies and Related Endocrine Disorders* (Baltimore: Williams & Wilkins Company 1958)
- Jost A Embryonic Sexual Differentiation (Chapter 2 in Jones and Scott)
- Schauffler G C *Pediatric Gynecology* (4th ed Chicago: Year Book Medical Publishers Inc 1958)
- Shoppner C E Cystourethrography *M Radiog & Photog* 47 1 1971
- Cystourethrography An Evaluation of Method *Am J Roentgenol* 95 468 1965
- Cystourethrography Methodology 16 mm movie distributed by Institute for Pediatric Radiology 4148 N Cleveland Ave Kansas City Mo 64117
- Genitography in Intersexual states *Radiology* 82 664 1964
- Clinical evaluation of cystourethrographic contrast media *Radiology* 88 491 1967
- Gynecologic roentgenology In children *Seminars Roentgenol* 4 218 1969
- Roentgenologic evaluation of imperforate anus *South M J* 88 712 1965
- Roentgen demonstration of the ectopic anus associated with imperforate anus *Radiology* 84 464 1965
- Urinary tract pathology associated with constipation *Radiology* 90 865 1968
- Radiology in pediatric gynecology *Radiol Clin North America* 5 151 1967
- and Hutch J A The normal urethrogram *Radiol Clin North America* 6 165 1968
- Spence H M *et al* Anomalies of external genitalia in infancy and childhood *J Urol* 93 1 1965
- Wilkins L The Diagnosis and Treatment of Endocrine Disorders in Childhood and Adolescence (2nd ed Springfield, Ill: Charles C Thomas Publisher 1957)
- *et al* Hermaphroditism Classification diagnosis selection of sex and treatment *Pediatrics* 16 287 1955
- Williams D I *Urology in Childhood* (Berlin: Springer Verlag 1958) p 98
- Winter C C Exstrophy of bladder A re evaluation of the treatment *J Urol* 93 700 1965

SECTION 8

The Extremities



Fig 8-2—Normal compression image (arrows) to the lateral wall of the femurs of a healthy boy 5 1/2 years of age. This normal image must not be mistaken for a tumor or an abscess or for early cortical thickening of the femur. We have not been able to identify the structure anatomically but we believe it to be the segment of the vastus intermedius muscle in direct contact with the lateral wall of the femur. In this boy, as is usually true, the images are bilaterally symmetrical in left and right thighs.



Fig 8-4—Radial fluorescent fatty staining of the muscular mass contiguous to the femur just below the greater trochanter in a 10-year-old boy who was weak in both thighs. The changes were bilaterally symmetrical and probably located in the vastus lateralis muscle near the site of attachment to the femur. We see uncertainty of the clinical significance of these fatty changes because we have seen them in normal children as well as those suffering from weakness and from muscular diseases.

with the thickness of the tissue. For this reason the thicker portions of the soft tissues cast denser shadows than the thinner portions.

According to Stuart and Sobel the thickness of the subcutaneous tissue increases during the first nine months of life, then decreases abruptly until the 30th month, and then even more slowly until about the 69th month, when the actual thickness is on the average about one-half as great as at 9 months. During the period between 66 months and 11 years the thickness remains unchanged, but at the onset of puberty

between 11 and 13 years there is a substantial accumulation of subcutaneous fat. During childhood girls have more subcutaneous tissue than boys. In healthy growing individuals of the same sex and age the

Fig 8-3—Tubular shadows of water density cast by blood vessels in the more radiolucent subcutaneous fat in an infant.



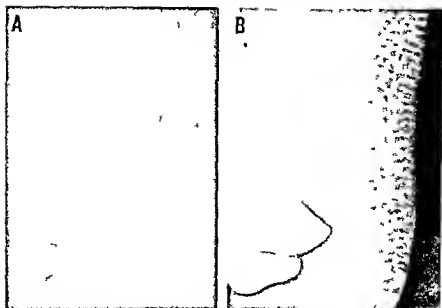


Fig 8-5—Edema of the soft tissues of the thigh showing coarsening and exaggeration of the connective tissue reticulum of the subcutaneous fat. A: roentgenogram. B: drawing of A. The

appearance is caused by fluid of water density in the connective tissue septums surrounding the more radiolucent fat lobules.

greatest variability in the amount of subcutaneous fat occurs during infancy and at pubescence.

In healthy children there is often a muscular strip of water density which runs along the lateral edge of the femur beginning at the lower edge of the greater trochanter (Fig 8-2). This normal muscular mass must not be confused with tumors or abscesses. In poliomyelitis the fat may be increased in this muscular mass to a degree which produces a radiolucent stippling and striping (Fig 8-4).

REFERENCES

- Frantzell A. Soft tissue radiography. Technical aspects and clinical applications in the examination of limbs. *Acta radiol. supp* 85 1951.

Melot G J. Roentgenologic examination of the soft tissues. Technical considerations. *study of axillary region*. *Am J Roentgenol* 46 189 1941.

Stuart H C and Sobel E H. The thickness of the skin and subcutaneous tissue by age and sex in childhood. *J Pediatr* 28 637 1946.

Inflammations

Inflamed soft tissue structures are usually swollen and edematous. The increase in thickness of the inflamed part is responsible for a greater absorption of x rays and a more dense regional shadow. When the inflamed part lies contiguous to the subcutaneous fat, the inflammatory exudate extends into the connective tissue reticulum and thickens the individual trabeculae. This is recorded roentgenographically as a subcu-

Fig 8-8—Abscess of the soft tissues of the thigh with a sinus tract (arrows) extending from the deeper muscular masses to the skin. The neighboring fatty layer is moderately edematous.

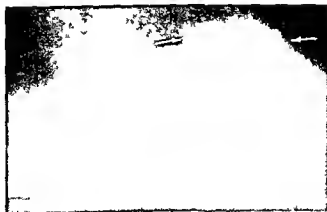


Fig 8 7 — Hemangioma of the elbow and forearm. The soft tissues are swollen and individual vessels can be seen on the periphery embedded in the subcutaneous fat



aneous reticular pattern of increased density. Extravasated blood and noninflammatory edema fluid in the subcutaneous layers produce a similar roentgen appearance (Fig 8 5). Localized inflammatory masses cast shadows of increased size and density with varying degrees of coarsening of the subcutaneous reticulum. Inflammatory sinus tracts running through the subcutaneous fatty layer are often visible, owing to the heavier density of their walls (Fig 8 6). When the portal of entry of a primary tuberculous infection is located in the skin, the swollen regional nodes during the exudative phase and prior to calcification may be visible as shadows of increased density. Enlarged nontuberculous nodes cast similar shadows in the soft tissues.

Neoplasms

Neoplasms of the soft tissues generate shadows of water density similar to those cast by the tissue from which the new growth originated. A tumor appears as a shadow of increased density owing to a regional thickening of the part. The heavier edges of the neoplasms are visible when they project beyond the normal external surface of the part and are outlined by

the contrast density of a more radiolucent layer of fat. The size, shape and location of many soft tissue tumors can be determined with a fair degree of accuracy. Encapsulated tumors exhibit well defined smooth edges; the margins of infiltrating tumors are poorly defined and poorly visualized.

Hemangiomas and lymphangiomas are common tumors in the extremities of infants and children. When the edges of these tumors are in contact with a strip of overlying fat, the individual peripheral vessels appear as multiple tubular shadows embedded in the more radiolucent fat (Fig 8 7). Large blood and lymph vascular neoplasms are often associated with hypertrophy of the extremity affected. Ward and Horton found that congenital arteriovenous fistulas are common in large hemangiomas and nevi. The exact morphology of the larger arteriovenous fistulas is best demonstrated by vasography. The presence of fistulas is usually indicated by elevation of the cutaneous temperature and increase in the oxygen saturation of the venous blood from the part as well as by regional hypertrophy of the bones and soft tissues. In the case of extensive infantile and juvenile varicosities, however, the regional bones and soft tissues are normal or may be hypoplastic.

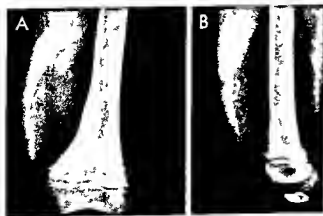


Fig 8 8 — Large radiolucent lipoma in the lateral part of the right thigh which partially surrounds the distal segment of the femur and displaces and compresses muscular masses in a girl 4 1/2 years of age. Local swelling pain and tenderness were present but there was no evidence of compression of blood vessels.

Lipomas with a high fat content cast shadows of the same density as the normal fat which is equal to that of the surrounding nonfatty soft tissues. Lipomas appear roentgenographically as sharply demarcated round or oval shadows of diminished density (Fig. 8-8 and also see Fig. 2-350). Lipomas may compress peripheral nerves, especially at the elbow where they cause radial nerve paralysis. Unexplained radial nerve deficiencies warrant radiographic study of the elbow and careful inspection of the compressing lipomas. Lipomas with a low content of fat are invisible or poorly visualized. Rarely there is a diffuse increase in the adipose tissue in a part of an extremity in which the muscular bundles are surrounded and separated by thick layers and masses of hyperplastic fat (Fig. 8-9). The amount of connective tissue reticulum varies in different fatty tumors. In some teratomas sacs filled with fatty fluid may cast shadows of diminished density identical with those cast by solid lipomatous masses.

Total lipodystrophy is characterized primarily by total absence of body fat. The absence may be congenital or acquired. The cause and causal mechanisms are obscure. According to Wesenberg and associates radiographs of the extremities demonstrate

the absence of subcutaneous fat and slight compensatory increase in the muscular masses. The shafts of the bones are overconstricted with flared ends and relatively large epiphyseal ossification centers. Bone age is consistently and markedly advanced. The third ventricle has appeared to be large in some pneumograms. Excretory urograms have been normal in some patients but have shown large kidneys with stretched renal pelvises in others.

REFERENCES

- Barber K. W., et al. Benign extraneural soft tissue tumors of the extremities, causing compression of nerves. *J Bone & Joint Surg* 44-A:98, 1962.
Goldman W., et al. Radial nerve entrapment—a case report. *Radiology* 87:522, 1966.
Wesenberg R. L., et al. The roentgenographic findings in total lipodystrophy. *Am J Roentgenol* 103:154, 1968.

Calcification

Calciferous masses in the soft tissues cast opaque shadows of a density similar to that of bone (specific gravity 1.9). They are visible in shadows of water density as well as those of fat density. Lime may be deposited in traumatic or infectious or neoplastic necrotic foci in any of the soft tissues.

Cutaneous calcification is rare in infants and children and roentgen techniques are rarely used in its identification. Calcifying epitheliomas are often invisible although palpable. The larger of these small tumors which tend to develop in the fascial and cervical regions frequently have sufficient lime in them to be visualized radiographically. These benign calcifying epitheliomas (pilomatrixomas) extend from the skin surface into the subcutaneous levels as dilated follicular crypts. They may be as large as 3 cm in diameter.

REFERENCE

- Bingul O., et al. Pilomatrixomas (calcifying epitheliomas) in children. *Pediatrics* 30:233, 1962.

SUBCUTANEOUS FAT—Calcinosis universalis a rare disorder of infants and children is a term applied to calcifications which begin in the subcutaneous fat but later involve other connective tissues such as muscles, ligaments and tendons. Bauer, Marble and Bennett found the calcareous material to be made up of calcium phosphate and calcium carbonate in proportions similar to those of normal bone and of other types of abnormal calcifications in the soft tissues. The earliest structural change appears to be the deposition of finely divided particles of lime around the periphery of otherwise normal fat cells. This initial deposition of lime is not preceded by inflammation, infarction, necrosis or hemorrhage in the fat. The entire fat lobule may eventually be replaced by lime and then a foreign body reaction sets in which brings about fibrosis, giant cell formation and slight round cell infiltration. Small calcareous nod-

Fig. 8-8—Roentgenogram and lipomatous shadows of the third and fourth digits with roentgenogram of less degree of the third metacarpal and perhaps the fourth metacarpal of an otherwise healthy boy 2 years of age.



ules coalesce into larger masses which may break through the skin and then be extruded from it (Fig 8 10) Inflammation appears to play no part in this process The fat in the pericardium, mesentery omentum and perirenal spaces is not affected Later, however, calcification extends to the connective tissues between the muscles—to the fascial sheaths tendons ligaments and nerves The internal organs escape completely save for the mesenteric lymph nodes, which were calcified in one case

The findings in the roentgen examination depend on the stage of the disease in which the patient is examined In children calcific foci are visible in the subcutaneous fat and neighboring connective tissues (Fig 8 11) During infancy, in contrast calcifications are usually limited to the subcutaneous fat (Fig 8 12) and should not be mistaken for congenital cutaneous osteomas In one of our patients cutaneous calcification was first noted clinically in the scrotum and there was extensive scrotal calcification when he was first seen by us at 11 months This is interesting because the scrotum is said to be the one segment of the skin which has no subcutaneous fat, this is true in

Fig 8 10—Calcinosis universalis (interstitial) in a boy 10 years of age Photograph shows several types of lesions: subcutaneous nodules perforating calcific masses and residual cutaneous defects and scars after extrusions of the lime masses (From Bauer *et al*)



Fig 8 11—Lateral projection of the knee and thigh showing lobulated calcifications in the subcutaneous fat in front of the femur of a boy 10 years of age The lesions are limited sharply below In addition to the subcutaneous fat calcification may be present in the superficial layers of the quadriceps muscle (calcinosis universalis?)

the adult at least, whose scrotal subcutaneous tissue is made up of the muscular dartos Cutaneous calcifications were reported in one patient 5 weeks of age with calcinosis universalis In a black girl 12 years of age Davis and Moe found that calcinosis universalis responded favorably to edathamil disodium We have seen one patient in whom severe and scattered calcinosis universalis disappeared spontaneously and completely without treatment between the 5th and 9th years of life

Calcinosis circumscripta is characterized by calcifications in the subcutaneous fat only, this disorder is much rarer than calcinosis universalis

REFERENCES

- Bauer W, Marble A, and Bennett G A Further studies in a case of calcification of the subcutaneous tissue ("calcinosis universalis") in a child *Am J M Sc* 182:237 1931
- Leustyna J A, and Hassan H I Interstitial calcinosis *Am J Dis Child* 107:96 1964

Neonatal subcutaneous fat necrosis (pseudoscierema) is found in otherwise healthy infants who

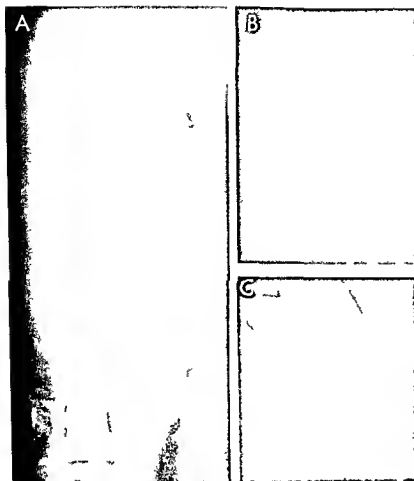


Fig 8-12.—Calcinos subcutanea in an infant 9 months of age. A, calciferous foci in the subcutaneous tissues of the leg. B, extensive fat deposits in the scrotum probably in the dartos. C, calcareous plaques in the scrotum and penneum.

Fig 8-13 Calcifying subcutaneous fat necrosis in the thighs of an infant 47 days of age





Fig 8-14—Generalized subcutaneous fat necrosis in an infant 5 months of age who was thriving otherwise. The subcutaneous fat of the right arm and forearm is extensively calcified in a diagnostic lobulated pattern. Similar changes were present in the skin of both arms, both legs, the abdomen and pelvis. The skin of the head was not affected. (Courtesy of Dr. R. Parker Allen, Denver, Colo.)

exhibit hard plaques in the skin. The cheeks, shoulders and thighs are sites of predilection; the cause is unknown, but it is believed that obstetric trauma plays a secondary causal role. Usually there are no systemic symptoms; the temperature is not increased. Sometimes the indurated cutaneous patches are slightly hyperemic. The prognosis is good and the subcutaneous lumps gradually disappear in the course of several weeks without ulceration or scars. During the late healing stage, large and small calciferous foci may be demonstrable in the roentgen film (Figs 8-13 and 8-14).

In two neonates who had been immersed in ice water in the treatment of neonatal asphyxia, Duhn and associates observed subcutaneous fat necrosis and massive calcifications without hypercalcemia that appeared two and five weeks after the immersions. Focal subcutaneous calcifications developed in all parts of the skin except in parts of the head which were not immersed. At age 6½ months the calcifica-

tions had been resolved except in some large plaques in the buttocks in one patient. In the second patient a substantial resolution of the calciferous foci was evident at 4 months.

REFERENCES

- Duhn R, et al: Subcutaneous fat necrosis with extensive calcification after hypothermia in two newborn infants. *Pediatrics* 41:661, 1968.
Kendall N and Ledis S: Sclerema neonatorum successfully treated with corticotropin (ACTH). *Am J Dis Child* 83:52, 1952.

Ehlers Danlos syndrome is a rare but striking disorder with two main pathogenic mechanisms: excessive elasticity of the skin and excessive friability of the skin and its blood vessels. These mechanisms produce the clinical features of looseness, scarring and ecchymoses in the skin and hyperextensibility of the joints. In an infant girl with Ehlers Danlos syndrome, Lees and colleagues found multiple stenoses of the pulmonary arteries and tortuous systemic ar-

Fig 8-15—Ehlers Danlos syndrome in a girl 18 years of age. There are multiple calciferous nodules in the subcutaneous fat of the upper arm. Similar shadows were demonstrated in the subcutaneous fat of all four extremities. The hands, feet, head and trunk were free from calcifications. A sister 16 years of age exhibited similar calcifications with similar distribution. (Courtesy of Dr. J. F. Holt.)



teries The radiologic changes in 100 patients with Ehlers-Danlos syndrome were described by Beighton and Thomas in all anatomic systems of the body They pointed out the serious potential hazards of angiography, owing to the friability of the tissues of the great arteries, particularly Subluxation of the joints with dislocation at the shoulders and of the patellas, and flat feet are the most common changes in the skeleton Regional tumors often develop over the more superficial bones and numerous nodules usually appear in the subcutaneous fat Dental anomalies and skeletal dysplasias such as radioulnar synostoses and delayed ossification of the cranium have been reported in some cases The patients are normal at birth, but during the 1st year easy bruising and easy breaking of the skin become evident Holt demonstrated large numbers of calcareous foci in the subcutaneous fat of two girls 18 and 16 years of age (Fig 8-15) It is likely that these calcifications had been present for a long time before roentgen examinations were made There is no record of roentgen examinations in younger patients, but calcific nodules in the subcutaneous fat should be looked for in infantile and juvenile patients

Arthrochalasia multiplex congenita is a name designed by Hass and Hass to describe overfascidity in multiple joints without associated hyperelasticity of the skin They consider this a primary disease of the mesenchyme with genetic transmission

REFERENCES

- Beighton P, and Thomas, M L. The radiology of the Ehlers-Danlos syndrome, *Clin Radiol* 20:354 1969
 Lees M H, et al Ehlers Danlos syndrome with multiple pulmonary artery stenoses and tortuous systemic arteries *J Pediatr* 75:1031, 1969
 McKusick, V A. *Heritable Diseases of Connective Tissue* (2nd ed, St Louis C V Mosby Company 1960)

FIBRODYSPLASIA OSSIFICANS PROGRESSIVA WITH MICRODACTYL (myositis ossificans progressiva) is a disorder of the mesodermal tissues in which scattered inflammatory foci first appear and proliferate in fibrous tissue—the intramuscular fascia and the tendons and ligaments Tender warm swellings are usually first noted in the neck and back of the thoracic wall, the onset may be as early as the 4th week of life After several weeks the tenderness and signs of inflammation disappear and the inflammatory tumors shrink and gradually become ossified The muscles are involved secondarily from the contiguous fascial coverings and then go through the same course of inflammation, necrosis and ossification After variable periods new foci appear in other parts of the body, and progressive changes continue until most of the connective tissue and muscle in the body are ossified and most of the joints are ankylosed The tongue, heart, larynx, diaphragm and sphincters are said to be never involved During the early months and years of the disease, lesions are largely confined to the neck

and trunk, and the extremities are relatively or absolutely free The skin is usually exempt as well as the anterior abdominal wall, eye and perineum The converse is usually the case for the subcutaneous calcifications of calcinosis universalis

One of the puzzling and diagnostic features of progressive myositis is the high incidence of associated congenital deformities of the big toes and the thumbs which are apparently completely unrelated to the myositis In our cases the first metacarpals were hypoplastic in addition to the hypoplasia of the phalanges in the first digits, the first metatarsals, in contrast, were normal in the presence of hypoplasia of the phalanges of the great toes The middle phalanges of the fifth digits of the hands have also been hypoplastic in some cases

Laboratory investigation provides no findings of positive diagnostic value except an increase in the phosphatase activity of the affected muscles during their early inflammatory stage, some specimens taken at biopsy have shown a phosphatase activity 1000–1500 times that of normal muscle Samples of bone and cartilage from older myositic lesions have also shown a much higher phosphatase activity than normal bone from the ribs

During the earliest phase of the disease and before the formation of extraskeletal bone, roentgen examination shows only soft tissue swellings of water density, the anomalies of the great toes and thumbs are, of course, present from birth In some cases extensive bone formation is already evident in the muscles by the end of the 1st year of life (Fig 8-16) In older patients the calcareous masses often show a pattern and texture which suggests normal bone detail (Fig 8-17) The distal segments of the extremities, the forearms and shanks, are characteristically uninvolved

The cause of progressive myositis is unknown and there is no known effective treatment The course is an inevitable, slow, progressive one in the extent of the involvement and increasing loss of motor function until the patient is practically helpless Notwithstanding extensive and severe ossifications in the connective tissues, patients may live on into the sixth and seventh decades of life Often during the course there are sudden shrinkages in volume of the soft tissue swellings which, to the inexperienced observer, may suggest beneficial effects if the patient happens to be under some special treatment These unpredictable remissions in the swellings are natural phenomena and occur commonly in untreated patients Surgical intervention to relieve ankylosis may aggravate the local lesions in the connective tissues

Lockhart and Burke treated a girl 7 years of age with corticotropin with indifferent results We were unable to halt the progress of the disease in a boy 7 years of age who was treated early in the course of many lesions with the combination of adrenal corticosteroids, x radiation and potassium iodide

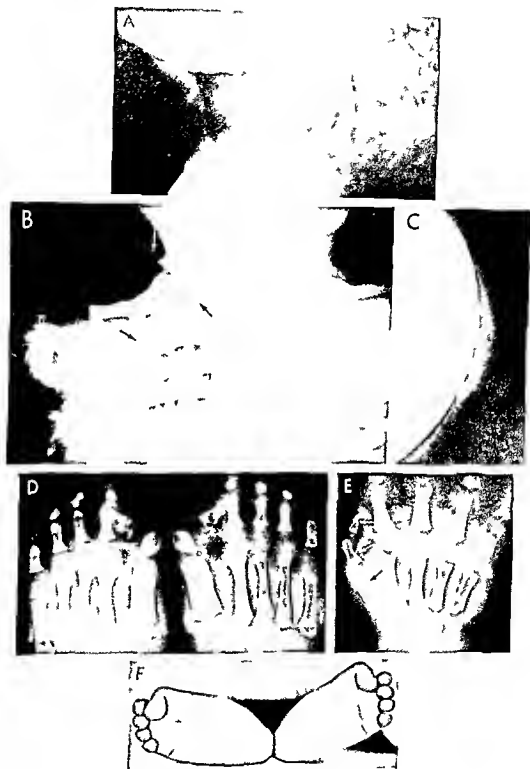


Fig 8-16 — Descript on on fac ng page



Fig 8-17—Juvenile progressive myositis ossificans in a girl 9 years of age who had had swellings in the neck and back since age 4. A tubular mass of calcium density is seen in the position of the ligamentum nuchae (arrows). The texture and shape of the calcareous mass resemble those of a tubular bone with cortex, medullary cavity and spongiosa. The similarities in the nuchal calcifications in this patient and the younger one shown in Figure 8-6 are striking.

REFERENCES

- Fairbank H A T Myositis ossificans progressiva. *J Bone & Joint Surg* 32 B 108 1950
 Lockhart J D, and Burke F G Myositis ossificans progressiva. Report of a case treated with corticosteroids (ACTH). *Am J Dis Child* 87 626 1954
 Wilkins W E, Reagan E M, and Carpenter G K Phosphate studies in biopsy tissue in progressive myositis ossificans. *Am J Dis Child* 49 1219 1935

Acute and chronic pyogenic myositis and cellulitis may sometimes be associated with sufficient necrosis in the subcutaneous connective tissues and underlying muscles to result in late residual calcifications which can be seen radiologically. These phenomena have been reported in one case of long standing destructive staphylococcal cellulitis and myositis associated with hypergammaglobulinemia. It is probable that more careful follow up radiologic examinations after destructive cellulitis would demonstrate more calcification of this origin.

Muscular calcifications after poliomyelitis have

been noted in several patients. Although tens of thousands of patients have been observed early and late in the disease, muscular calcifications have been reported in only eight. It is also puzzling that all but one of these eight patients were adults, the single exception was an adolescent girl 12 years of age. The mechanism of calcification after poliomyelitis is probably the same as in all muscular calcifications—necrosis with increased alkalinity of the dead tissues and the deposition of lime in them. Trophic neural factors are thought to be responsible for the atrophy or death of the muscles. In some cases the process goes on to actual ossification. Calcareous masses have been demonstrated in the muscles at the shoulders and hips, often bilateral masses, and in the thighs and hands.

Measles encephalomyelitis followed by calcification of the para articular tissues at the hips in a girl 5 years of age was studied by Jacobs 10 months after the viral infection. The calcifications were gradually and completely resorbed during the next three years without special treatment. It is probable that more para articular calcifications would be found in patients paralyzed by viral infections of the central nervous system if these patients were examined more frequently by radiography during the later paralytic stages of the disease.

REFERENCES

- Costello F V, and Brown A Myositis ossificans complicating anterior poliomyelitis. *J Bone & Joint Surg* 33 B 894 1951
 Freiberg J A Para articular calcification and ossification following acute anterior poliomyelitis in an adult. *J Bone & Joint Surg* 34 A 339 1952
 Jacobs P Reversible ectopic soft tissue calcifications following measles encephalomyelitis. *Arch Dis Childhood* 37 40 1962
 Larsen L L, and Wright H H Para articular ossification: a complication of poliomyelitis. *Radiology* 69 103 1957
 Liberson M Soft tissue calcifications in cord lesions. *JAMA* 152 1010 1953

Acute idiopathic calcifying myositis—Occasionally massive muscular calcifications appear many weeks after the onset of acute fever with generalized lymphadenopathy and regional signs of pain, tenderness and limitation of motion owing to muscular spasms in the regions of the hips and knees. The muscular calcifications and disabilities may persist for months after acute signs have subsided (Fig 8-18). Local myositis ossificans is common following regional thermal necrosis of muscular masses (Fig

Fig 8-18—Infantile progressive myositis ossificans in a patient 11 months of age. During the 4th week of life it was noted that the infant could not turn his head toward a nursing bottle. At the same time tender swellings appeared in the neck and back. These later became hard and non tender. At 11 months the extremities were free from nonskeletal calcifications save for a few tiny foci in one arm and one shank. A, massive calcifications in the regions of the ligamentum nuchae and left sternocleidomastoid

muscle. B, large calcareous masses in the left axilla and at the sternocleidomastoid. The left clavicle is deformed and dislocated. C, large soft tissue swelling with small calcific area at its base in the occipital segment of the scalp. D, symmetrical hypoplasia and deformity of the phalanges of the great toes. E, symmetrical hypoplasia and deformities of the phalanges of the thumbs and first metacarpals. F, deformed great toes. There were no calcific foci in the feet.



Fig 8 18 — Acute idiosyncratic myositis ossificans with residual calcifications in the gluteal muscles (biopsy) six months after onset of acute pain and tenderness in the hips and knees with limitation of motion and fever with generalized hypertrophy of lymph nodes. The patient, a boy, was 5 1/2 years of age at onset. Similar calcifications developed in both buttocks and were still present 18 months after onset with limitation of motion although fever had disappeared more than one year before.

8 19) Johnson found myositis ossificans in three patients who had been extensively burned. The sites of ossification in the muscles did not always coincide with the sites of the burns.

REFERENCE

Johnson J H T. Atypical myositis ossificans. *J Bone & Joint Surg* 39-A 189 1957.

Dermatomyositis is characterized by fever and inflammatory changes in the skin and underlying muscles. It is more common in children than adults, although it is rare at all ages. The muscular lesions are usually located in the extremities and cause local weakness, tenderness, induration and swelling. The cutaneous changes are variable; they may be erythematous, petechial, urticarial or edematous. Residual calcifications may develop in the necrotic foci in the subcutaneous fat and muscles during healing and be visible roentgenographically years after the acute disease has subsided (Fig 8-20).

Shelley and Vaughan described a progressive musculocutaneous dystrophy in which the intermuscular septums and possibly the muscles themselves calcified recurrently over long periods. Their case may represent an unusually extensive and longstanding example of chronic and recurrent dermatomyositis. The disorder appeared during the first weeks of life. We have observed a similar patient who exhibited



Fig 8 19 — Local myositis ossificans in the right gluteal muscles of a girl 11 years of age who had suffered a third degree burn of the right buttock six years before.

progressive calcifications in the fat and muscles during a period of seven years, but the onset was during the 3rd year (Fig 8 21). Mills and Mathews reported chronic nonspecific inflammation in the lungs of a 52 year old woman who had classic dermatomyositis.

REFERENCES

Langmead F S. Relationship between certain rare diseases. Generalized scleroderma, calcinosis, dermatomyositis and myositis fibrosa. *Arch. Pediatr* 40 112 1923.

Fig 8 20 — Cluster of small shadows of calcium density (arrow) which is a residual of a painful lesion of active dermatomyositis five years before. Similar calcifications developed in two sites in the upper arm. The patient was 13 years of age when this film was made.



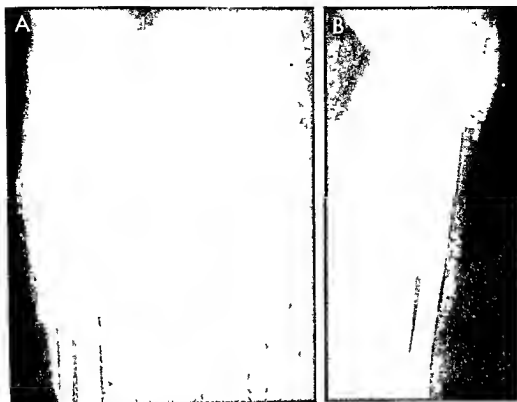


Fig 8-21 —Chronic progressive recurrent dermatomyositis in a boy 10 years of age who began to exhibit inflammatory changes

in the skin and muscles during his 3rd year. A, frontal and B, lateral projections

- Mills E S and Mathews W H. Interstitial pneumonitis in dermatomyositis. *JAMA* 160 1467 1956
- Shelley D C, and Vaughan J O. Juvenile type of Winer syndrome. Progressive musculocutaneous dystrophy observed for 18 years. *J Pediatr* 38 559 1951
- Wedgewood R J P et al. Dermatomyositis. Report of 26 cases in children with discussion of endocrine etiology. *Pediatrics* 12 447, 1953

REFERENCES

- Cammer W F P et al. Contracture of the vastus intermedius in children. Report of two cases. *J Bone & Joint Surg* 45-B 370 1963
- Lotke P A. Ossification of the Achilles tendon. Report of seven cases. *J Bone & Joint Surg* 52 A 157 1970

Progressive fibrosis of the vastus intermedius muscle in children is a cause of limited knee flexion and elevation of the patella. One or both legs may be affected. In one of our patients, the volume of the affected thigh muscles was reduced; these changes were clearly visible radiographically. The patella is usually smaller and elevated on the affected side. In electromyography, the rectus femoris and vastus intermedius show little or no activity. Chronaxie reactions are normal. The clinical and microscopic pictures are those of progressive fibrous degeneration. It is possible that this syndrome is a viral myositis which sometimes involves groups of muscles. It is easily mistaken for postpoliomyelitic paralysis and degeneration, regional cerebral palsy and limited amyoplasia arthrogryposis.

Ossification of the Achilles tendon has occurred in children as young as 9 years (Lotke). Trauma and surgery are common precursors. The lesion is usually asymptomatic, if it becomes painful, a fracture through the ossified mass should be suspected.

Traumatic localized myositis ossificans (myositis ossificans circumscripta) may follow a single severe injury (Figs 8-22 to 8-24) or repeated slight injuries. The principal pathogenic factor is laceration of the periosteum and displacement of the torn periosteum with its bone-forming cells away from the shaft. Extensive local myositis ossificans may complicate traumatic dislocations of the joints, especially posterior dislocations at the elbows. Occupational myositis ossificans results from frequent recurring slight injuries to one region of the body during long periods until local masses of bone appear in the traumatized muscles—these lesions probably result from a true metaplasia of local connective tissue cells into osteoblasts rather than laceration and displacement of periosteum. Such muscular ossification is so far as we know, unknown in infants and children. Several types have been described in adults: toe dancers' bone in the soleus; fencers' bone in the brachialis anticus, and riders' bones in the subischial soft tissues.

Massive localized calcification of muscles and ten-



Fig 8-22—Local traumatic myositis ossificans in a girl 12 years of age who suffered a painful injury several months before. It seems likely that laceration of the tibial periosteum and displacement of it are responsible for the ectopic bone formation.

dons may follow the severe convulsions and muscular injuries of tetanus (Fig 8-25).

REFERENCES

- Lewin P. *The Skeletal Muscles and Tendon Apparatus: Semimembranosus, Bursae and Fasciae*. In: Brennemann's Practice of Pediatrics (Hagerstown Md. W F Prior Company 1945) Vol 4 chap 37.
 Williams G. Saddle tumors. *Radiog & Clin Photog* 22:29 1946.

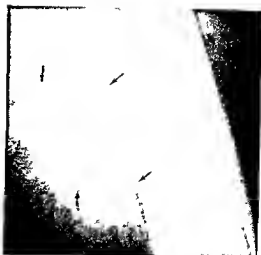


Fig 8-23—Traumatic myositis ossificans (microscopic diagnosis) associated with traumatic cortical thickening of the femur in a boy 10 years of age four months after a single kick in the thigh. The cortical wall of the femur is thickened externally and at the same level a large rounded mass with slight calcification is visible in the contiguous muscular mass.

Parasitic muscular calcifications are rare in the United States. The major involvements in trichinosis are in the diaphragm and the intercostal muscles. Individual dead calcified larvae are too small (0.5 mm) to be detected roentgenographically.

Miscellaneous muscular calcifications—Occasionally calciferous foci are visualized in the muscles when there is no known antecedent disease which could have caused them. It is probable that necrotic myositis passes unrecognized in several illnesses which are characterized by pain and tenderness in the extremities. Kean and Grocott demonstrated



Fig 8-24—Traumatic myositis ossificans. A, of the left gluteus medius five weeks after a heavy fall on the left hip followed by local pain, tenderness, muscular spasm, fever, and increased sedimentation of erythrocytes. B, of the brachialis anticus muscle five weeks after dislocation of the elbow.



Fig 8-25 (left) — Massive calcification of the iliopsoas tendon and muscle of a boy 9 years of age who had recovered from tetanus three years before. The morbid anatomy and pathogenesis of this lesion are not known, but it is possible that the calcification resulted from necrosis at this site secondary to tetanic contractions and possibly hemorrhage. There were no other known injuries and surgery had not been done in this region. A tender swelling

was palpable, but motion at the hip was only slightly limited. (Courtesy of Dr. Roman Marcinia, Wrocław, Poland.)

Fig 8-26 (right) — Ossification of the subcutaneous tissues of the left shank of an infant 6 months of age secondary to thrombophlebitis of the left saphenous vein which had been catheterized 30 days before this film was made. The film was made the day the mother noticed swelling and tenderness of the left shank.

numerous toxoplasma [pseudocysts] in the muscles of the tongue, cheeks, chest, legs and back in a fatal case of infantile toxoplasmosis. In the event of recovery after toxoplasmosis, the possibility of late calcareous foci in the muscles should be kept in mind.

Chronic venous insufficiency in the legs secondary to thrombophlebitis is said to be a common cause of extensive subcutaneous ossification in adults. In an infant 8 months of age we have seen extensive calcification of the shank which was evident clinically and radiographically four weeks after inflammation of the saphenous vein began. The phlebitis was secondary to catheterization for intravenous fluid therapy. So far as is known, calcium solutions were not injected (Fig 8-26). According to Lippman and Goldin, the ossification represents metaplasia of the tissues between the skin and the muscles. They found no evidence of fat necrosis.

REFERENCES

- Kean, B. H., and Grocott, R. G. Congenital toxoplasmosis. *JAMA* 136:104, 1948.
Lippman, H. S., and Goldin, R. R. Subcutaneous ossification of the legs in chronic venous insufficiency. *Radiology* 74:279, 1960.

CALCIFICATIONS IN LYMPHOID TISSUES of the extremities are rare in comparison with the calcifications in lymph nodes which are present so frequently with tuberculosis in the neck, thorax and abdomen. When, however, the primary tuberculous focus is in the skin, the regional nodes in the extremities may become calcified. Regional calcifying lymphadenitis

regularly follows vaccination with BCG. We have seen extensive calcifications in the axilla and groin of infants who had disseminated hematogenous tuberculosis. O'Connor, Golden and Auchincloss visualized calcified *Filaria bancrofti* in subcutaneous lymph nodes and vessels. It seems likely that lymphatic calcifications would develop in histoplasmosis and coccidioidomycosis in the same fashion as in tuberculosis.

REFERENCE

- O'Connor, F. W., Golden, R., and Auchincloss, H. Roentgen demonstration of calcified *Filaria bancrofti* in human tissues. *Am J Roentgenol.* 23:494, 1930.

Fig 8-27 — Arteriosclerosis of the upper extremity in an infant 5 months of age with hyperparathyroidism. Similar calcification was present in the arteries of the lower extremities, the neck and the heart (necropsy).

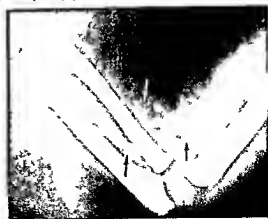




Fig 8-28 — Two round phlebectas in varicosities in the foot of a girl 10 years of age

VASCULAR CALCIFICATIONS are relatively rare during early life. We have seen calcification in the medium-sized arteries in one infant who had hyperparathyroidism (Fig 8-27). Similar calcifications have been observed in renal rickets and hypervitaminosis D and in association with hydramnios. However, there are many other cases which are unexplained and hypercalcemia is not essential to this type of arteriosclerosis, which differs from adult arteriosclerosis in that there is no intimal damage in the former. Round phlebectas are not uncommon in infantile and juvenile varicosities (Fig 8-28) and may appear after radiation therapy. Fine intravascular calcifications accompany some hemangiomas (Fig 8-29).

Fig 8-29 — Small intravascular calcification in a hemangioma of the hand and wrist of a boy 8 years of age. Calcification is also visible in the soft tissues of the forearm.



REFERENCES

- Andersen D H and Schlesinger E R. Renal hyperparathyroidism with calcification of the arteries in infancy. *Am J Dis Child* 63:102, 1942.
- Field M H. Medial calcification of the arteries of infants. *Arch. Path.* 42:607, 1946.
- Lipman B L *et al*. Arteriosclerosis in infancy. *Am J Dis Child* 82:561, 1951.
- Moran J J and Steiner C G. Idiopathic arterial calcification in a 5-year-old girl. *Am J Clin. Path.* 37:521, 1962.
- Weens A H and Marin C A. Infantile arteriosclerosis. *Radiology* 67:168, 1956.

CALCIFICATIONS IN THE NEURAL TISSUES are limited so far as we know to the multiple calcareous neurofibromatosis found in two infants by Holt at the University of Michigan (Fig 8-30). Multiple lesions were also present in the long bones. Neurofibromatosis was demonstrated by biopsy. In both cases, follow-up examinations made several months later showed that both the calciferous tumors and the skeletal defects had disappeared. More complete study of the biopsy specimens from these two cases later indicated that these tumors in both bones and skin were made up almost exclusively of fibrous tissue and small blood vessels. Fibromatosis is preferable to neurofibromatosis in their description. Agnieszka also reported the disappearance of multiple subcutaneous and intra-muscular neurofibromas by the 17th month in an infant who exhibited neurofibromas as early as the 7th week of life.

Para-articular calcifications have been observed in a large number of paraplegic adult patients in the

Fig 8-30 — Multiple fibromatosis with numerous small and large calcareous masses in the soft tissues of the leg of an infant 5 months of age. There are also large bony defects in the femur and tibia shafts. (Courtesy of Dr J F Holt)





Fig 8-31 — Calcium gluconate under the sheath and out along the sciatic nerve of an infant 7 weeks of age from another hospital who had had calcium gluconate injected into both buttocks in intramuscular treatment of tetany of the newborn on the 2nd day of life. At the 10th week all of the calcium gluconate had disappeared and there were no calcifications.

lower extremities. These calcifications are probably secondary to inflammatory necrosis of the soft tissues rather than to a specific trophic effect of the paraplegia. In children, pararticular calcifications have been demonstrated in association with severe paralysis due to poliomyelitis and measles encephalomyelitis. Adult diabetics may show calcific foci in the soft tissues which also appear to result from inflammatory necrosis and the deposition of lime during healing. Diabetic children apparently do not suffer this complication.

Pararticular calcifications are common in rheumatoid arthritis after treatment with large doses of vitamin D.

Opaque agents such as calcium gluconate which are injected into the gluteal muscles in therapy are occasionally injected into the sciatic nerve as well. The calcium in the nerve casts an opaque tubular shadow (Fig 8-31) in the position of the sciatic nerve and may extend over a distance of 8–10 cm. In one of our patients, such intraneural injection caused no immediate or late disability and the calcium gradually and completely disappeared over a period of about three months.

REFERENCES

- Agnew, A. An unusual case of neurofibromatosis in an infant, *Maandschr. kindergeneesk.* 18:347 1950.
Combs, M. A. Sciatic nerve injury in infants, *J. A. M. A.* 173:116 1960.
Holt, J. F. and Wright, E. M. Radiologic features of neurofibromatosis, *Radiology* 51:649 1948.
Ward, W. C. Pararticular calcification in lower extremities of paraplegic patients, *Am. J. Roentgenol.* 56:717 1946.

CALCIFICATION OF ARTICULAR AND PERIARTICULAR TISSUES with the formation of large tumors near the joints has been observed in a number of young individuals and sometimes in siblings. The tumors are

cystic and often filled with a milky fluid. Surgical removal cures the disorder.

REFERENCES

- Inclan, A. Tumoral calcinosis, *J. A. M. A.* 121:490 1943.
Thomson, J. E. M. and Tanner, F. H. Tumoral calcinosis, *J. Bone & Joint Surg.* 31 A:132 1949.

Foreign Bodies

Opaque foreign bodies of sufficient size can be readily detected. Needles or portions of needles are by far the most common. Fragments of lead containing glass are also clearly visible in the more radiolucent density of the skin and muscles (Fig 8-32). Opaque preparations made from mercury bismuth and calcium and injected subcutaneously or intramuscularly (Figs 8-33 and 8-34) may remain visible for years after their introduction. Intramuscular injections of all calcium preparations should be avoided because calcium solutions may precipitate in the tissues and cause extensive necrosis and ulceration. Small opaque foreign bodies may be invisible in the standard heavily penetrated films made for the demonstration of bone detail and become visible only in special soft tissue exposures made with lower voltage (Fig 8-35).

Most nonopaque foreign bodies are invisible in the deep soft tissues because they have the same water density of these surrounding soft tissues. Wooden lead pencils, however, contain enough gas in the

Fig 8-32 — Large broken splinter of leaded opaque glass in the forearm of a girl 7 years of age.

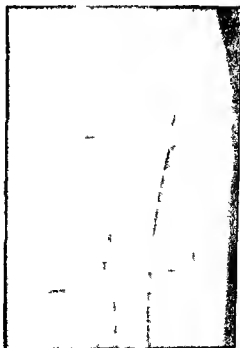




Fig 8-33 - Calcium gluconate in the buttocks of an infant 43 days of age

soft wood to make them more radiolucent than the surrounding tissues and their graphite cores (Fig 8-36)

Metallic foreign bodies in soft tissues may remain at the original site of introduction or they may move long distances with little or no disability to the patient. Such was the case in one of our patients, a girl 4 who had a Steinmann fixation pin inserted in the treatment of congenital dislocation of the hip (Fig 8-37). The pin was inserted into the medullary cavity of the left femur at 4 months of age and then had mi-

Fig 8-34 - Opaque calcium gluconate in the soft tissues at the elbow following leakage at this site during intravenous injection in the treatment of an infant 21 days of age



Fig 8-35 - Small opaque foreign body in the soft tissues of the ankle, invisible in A, taken for bone detail but clearly visible in B which was made for soft tissue detail with a light penetration

grated to the right side of the abdomen at 7 months to the right side of the pelvis and hip at 8 months and to the right hip and thigh at 8½ months. This migration occurred without pain or disability of any kind. It was removed without difficulty. Migration of foreign bodies which are sharp and slender as is the Steinmann pin is more common and extensive than with blunt broader foreign bodies. In our case it is likely that the regional resorption of bone permitted the pin to start moving and it was then driven on by both gravitational forces and local muscular forces. Usually there are remarkably few clinical signs of migration but in some cases migration into critical structures such as large arteries and veins has resulted in death. For this reason sharp migrating bodies should be removed as soon as their movement is detected.

Superimposed shadows from the overlying soft tissues and soft shadows of foreign bodies in the soft tissues must be taken into account in every film made of any part of the body as shown in Figures 8-31 to 8-36. They frequently simulate fractures of the bones (Figs 8-38 to 8-41).

Following subcutaneous injections of insulin fat necrosis is a possible complication. Repeated injections of antibiotics at a single site have caused local

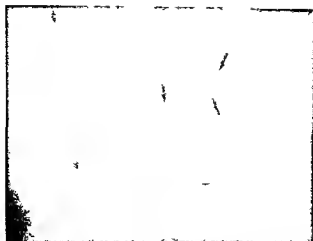


Fig 8-36—Wood-graphite pencil (lead pencil) in the soft tissues of the buttock of a boy 14 years of age who sat down on the sharp end of an ordinary wooden pencil which penetrated clothing and skin deeply into one buttock and then broke below the level of the skin. There are two radiopaque lines

one wood of the pencil which contains considerable gas (arrows) and an intermediate strip of a greater than water density. A represents the core of graphite. (Courtesy of Dr. Richard A. Lake City, Utah.)

Fig 8-37—Migration of a Steinmann pin from the medullary cavity of the left femur at age 4 months (A) to the right side of the abdomen at 7 months (B) to the right side of the

thigh at 8 1/2 months (C). The pin was removed. The patient was always asymptomatic.



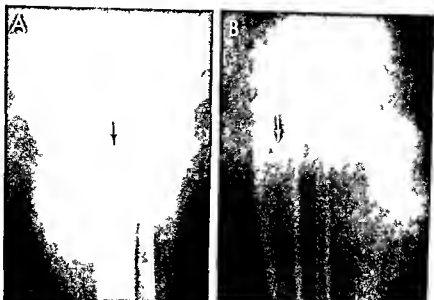
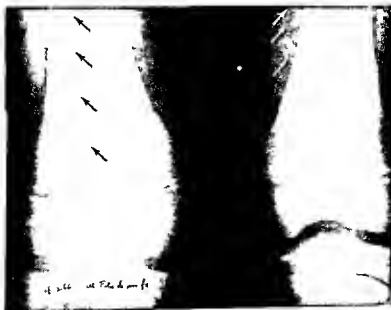


Fig 8 38 —Pseudotransverse fracture of the tibia shaft due to a circular groove in the overlying skin caused by an encircling and constricting rubber band. The radiolucent transverse strip of demineralized density which simulates a fracture is cast by the air in the cutaneous depression under the rubber band. This boy

3½ years of age had been treated for clubfoot and his leg had been in a plaster cast for three months. When the cast was removed the rubber band in the cutaneous air-filled cleft was found. **A**, anteroposterior and **B**, lateral projection.

Fig 8 39 —Fatty strips of demineralized density superimposed on the femoral shaft simulate longitudinal fracture lines. The patient was a healthy boy 12 years of age. In the right femur superimpo-

sition of the longitudinal fatty strips is complete in the left femur it is incomplete.



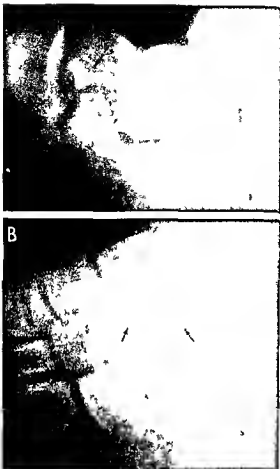


Fig 8-40—Glass foreign body in the foot which simulates a fracture fragment of bone or a bony bridge between the sustentaculum of the calcaneus in lateral projection (A) or the scaphoid in (B) lateral oblique projection. This boy 12 years of age had a painful swelling anterior to the internal malleolus. The opaque glass foreign body was removed at exploratory surgery.

Fig 8-41—A small layer of radiolucent intra-articular gas superimposed on the floor of the lateral articular facet of the tibia which simulates a transverse fracture line in an asymptomatic boy 14 years of age. The intra-articular gas accumulated because the knee joint was suddenly stretched during positioning of the patient and represents an antivecum effect.



Fig 8-42—Large local defect in the lateral head of the incept muscle in the left arm of a girl 8 years of age. The muscular defect is filled with a local overgrowth of subcutaneous fat. Antibiotics had been injected at this single site many times.

necrosis of muscle (Fig 8-42). The mineral oil which was injected intramuscularly as a carrier in camphorated oil caused thousands of intramuscular and subcutaneous foreign body fibromas during and after the pandemic of influenza during 1917 and 1918.

REFERENCES

- Harle T S and Beard E E. Migration of Steinmann pins. *Am J Roentgenol* 100:542, 1967.
- Lewis R W. The roentgenographic study of glass and its visibility as a foreign body. *Am J Roentgenol* 27:853, 1932.
- Von Hofe F H and Jennings R E. Calcium deposition following the intramuscular administration of calcium gluconate. *J Pediatr* 8:348, 1936.

Interstitial Emphysema

Gas in the soft tissues casts a shadow of diminished density. Air may be introduced through a wound or gas may be generated in the part by gas-producing bacteria. Small amounts of air are commonly introduced during hypodermoclysis. Air which enters the soft tissue spaces of the neck and mediastinum through perforations in the trachea and esophagus

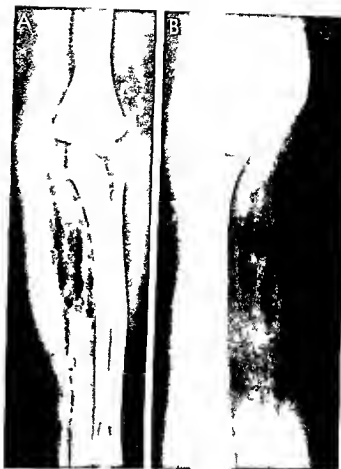


Fig 8-43 — A Interstitial emphysema of the arm and forearm secondary to pneumothorax and interstitial emphysema of the neck, shoulder and upper arm of an asthmatic boy 4 years of age. The emphysema developed during a severe attack of asthma. B Local interstitial emphysema in the forearm due to local laceration of the skin. The radiolucent gas images are confined to the superficial layers of the soft tissues.

may extend into and be diffusely distributed through the fascial spaces of the arm and hand (Fig 8-43).

After traumatic laceration the presence of gas in the neighboring soft tissues always raises the question of gas gangrene. Filler and associates pointed out that widely spread gas in the soft tissues with widely spread subcutaneous crepitation developed in their patients without any evidence of infection clinically or bacteriologically when extensive debridement and amputation were not done. They suggested that the gas which enters the soft tissues from local lacerations is in the main subcutaneous in contrast to the gas generated in clostridial infection which lies deep within the muscular masses with considerable edema of the skin and superficial soft tissues.

Regional subcutaneous and prevertebral emphysema may follow traumatic dental procedures and traumatic injection of air after lumbar puncture.

REFERENCES

- Filler R M *et al*. Post traumatic crepitation falsely suggesting gas gangrene. *New England J Med* 278:758, 1968.
 Porath S and Golding J. Subcutaneous emphysema following dental procedures. *Radiology* 91:954, 1968.

Muscular Dystrophies

The size, shape and density of the muscular masses are modified in both the primary and the secondary myopathies. When there are congenital absences of muscles or groups of muscles there are corresponding defects in the shadows of the muscles. In *protoplasia congenita* (arthrogryposis congenita or congenital anterior poliomyelosis) the fetal muscle fails to grow adequately with resultant contracture deformities at the major and sometimes minor joints. Current hypotheses favor either defective formation or degeneration of the anterior horn cells in the spinal cord as the probable cause. The microscopic findings in the muscles and spinal cord are not pathognomonic of this disease. Although agenesis and hypertrophy of muscle fibers are consistently present, some normal muscle fibers are also present. In the spinal cord the anterior horn cells may be reduced in both size and number. The articular capsules may be thickened and the articular tissues fibrous. The articular cartilages are usually normal. The clinical findings in arthrogryposis include classic contractures and deformities at the joints and muscular deficiencies. The humeri at

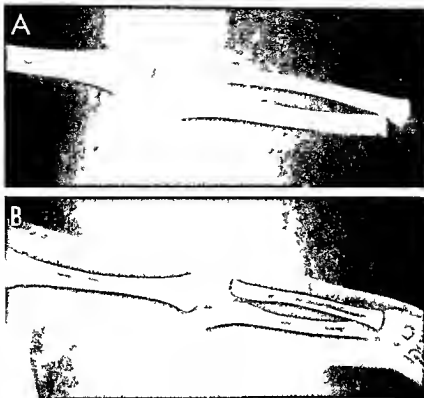


Fig 8-44 - Extreme muscular deficiency in amyoplasia congenita (arthrogryposis congenita) in an infant 3 months of age. A: roentgenogram. B: drawing of A. The muscular masses are so

atrophic that they are identified with difficulty. Compare the atrophic muscular masses in this patient with the normal muscular bundles in Figure 8-1.

the shoulder are usually adducted and internally rotated. The bones of the knees may be fixed in flexion or extension, the wrists in flexion and ulnar deviation, and the fingers in flexion with convergence. The femurs at the hips are flexed, externally rotated and abducted. At all affected joints, movements are limited. Owing to the muscular deficiencies, the extremities are small in caliber, although there is considerable hypertrophy of fat, which is compensatory. Radiographic examination discloses the deformities at the joints and muscular deficiencies and the compensatory hypertrophy of fat (Figs 8-44 and 8-45). The bones are small in caliber and flare at the ends due to the central overconstriction of nonuse and disuse. The patellas may be rudimentary or absent. Hyperextension at the hip in utero was found radiographically in one case of amyoplasia by Epstein.

In a review of 41 cases, Poznanski and La Rowe found that breech deliveries occurred in one half of their patients. Occasionally the disease is familial. They mentioned a similar neuromuscular disease in chickens and calves. In their 41 patients, both upper and lower extremities were affected in 20, lower extremities only in 17, and upper extremities only in 4. The feet were clubbed in two-thirds of the patients. Other more common deformities were flexion contractures of the hand (22/33), dislocation at the hips

(17/37), flexion contractures at the knees (13/25), scoliosis (14/35). The most common deformity in the skull was hypoplasia of the mandible (4/17). Contractures were present at birth. The muscular masses are

Fig 8-45 - Webbing of the knee and absence of the patellar ossification center in a boy 5 years of age who suffered from a primary myopathy, probably amyoplasia congenita (arthrogryposis congenita). The tibial ossification center is deformed.



diminished with regional compensatory increase in the subcutaneous and the intramuscular fat. Mental development was normal in most of the 41 patients. The clinical manifestations rather than the radiographic and microscopic should determine the diagnosis.

REFERENCES

- Epstein B S. Radiographic identification of arthrogryposis congenita in utero. *Radiology* 77:108, 1961.
 Friedlander H L. *et al*. Arthrogryposis multiplex congenita. *J Bone & Joint Surg* 50-A:89, 1968.
 Poznanski A K. and La Rowe P C. Radiographic manifestation of the arthrogryposis syndrome. *Radiology* 95:353, 1970.

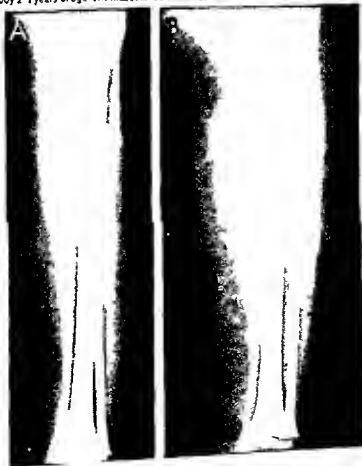
IN THE INFANTILE MUSCULAR ATROPHIES such as congenital amyotonia (Oppenheim's disease) and the Werdnig Hoffmann type of primary myopathy the smallness of the muscular bundles and their infiltration by fat as well as the reciprocal hypertrophy of the

subcutaneous fat can all be beautifully demonstrated in films (Fig. 8-46). The consistent reciprocal or compensatory hypertrophy of the fatty tissues in the presence of muscular atrophy makes clinical estimation of the size of the muscular bundles by external measurement of the part not only inaccurate but highly misleading. Roentgen examination is much more exact in the estimate of muscular mass and the changes in muscular volume following injury or treatment. During the late stages of muscular atrophy the fatty content of the muscular masses may be greater than the volume of the residual muscular tissues themselves (Fig. 8-47).

Pseudohypertrophic muscular dystrophy is characterized in its early stages by simple enlargement of the muscular masses but later large amounts of fat appear in the fascial spaces and in the muscles (Fig. 8-48). Kaufmann found thickening of the fibular shaft ventrodorsally relative to the ventrodorsal diameter of the companion tibia; this sign has not been

Fig. 8-46 — Primary muscular atrophy. A. amyotonia congenita (Oppenheim's disease) in a boy 3 years of age. The muscular bundles are small and broken up by shadows of fat density; the subcutaneous fat is oversubstant. B. Infantile muscular atrophy (Werdnig Hoffmann) in a boy 2 1/2 years of age. The muscular bundles

are shrunken but show no roentgen evidence of fatty infiltration or fatty degeneration. There is great hypertrophy of the subcutaneous fatty layer which is even a little thicker than the normal thickness. The fibular shadows in the thickened fat are cast by blood vessels.



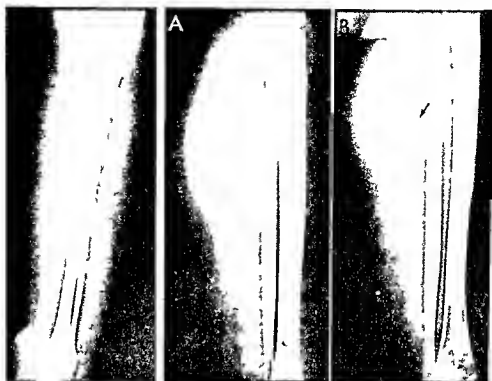


Fig 8-47 (left) - Severe infantile muscular atrophy (Werdnig-Hoffmann) in a boy 8 years of age. Practically all of the shrunken muscular mass has been replaced by fat, so that the atrophic muscles are barely visible in the fat. The subcutaneous fat is greatly increased and it is obvious that external measurements of the circumference of the leg would give a misleading idea of the amount of muscular tissue actually present owing to the compensatory thickening of the fat.

Fig 8-48 (right) - Pseudohypertrophic muscular dystrophy. A, at a relatively early phase of the disease when the enlarged muscular mass is made up of hypertrophic muscle and fibrous tissue in a boy 6 years of age. B, at a relatively late stage when the enlarged muscular mass is beginning to show fatty degeneration and infiltration in another patient 10 years of age.



Fig 8-49—Postpoliomyelitic fatty replacement and reduplication of the gastrocnemius soleus group of the right leg of a girl 8½ years of age who had had acute poliomyelitis six years before. The bones and muscles in the right shank are hypoplastic and atrophic. A, poliomyelitic muscles in the right shank; B, normal muscles in the left leg.

present in many of our patients. Kaufmann's patients all had the pseudohypertrophic form of progressive muscular dystrophy.

In the acquired muscular atrophies the injured muscles show the same shrinkage and fatty infiltration and perhaps fatty degeneration which have been shown in the primary myopathies. In postpoliomyelitic paralyses the muscular atrophy and fatty changes are probably best demonstrated by the roentgen method (Fig. 8-49). The atrophy of disuse in the muscles secondary to the "cast treatment" of fractures and osteomyelitis is also easily recognizable in roentgenograms (Fig. 8-50).

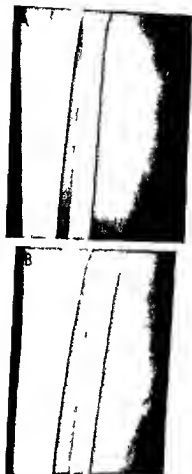


Fig 8-50—Acquired muscular atrophy and fatty infiltration following application of a cast in treatment of osteomyelitis. A, normal left leg; B, right leg which had been in a cast and shows the accumulation of fat between and possibly in the fibers of the soleus and gastrocnemius.

REFERENCES

- Giedan R. B., and Danowski T. S. Muscular dystrophy II. Radiologic findings in relation to severity of disease. *Am. J. Dis. Child* 91:339, 1956.
- Kaufmann H. J. A new roentgen sign in pseudohypertrophic muscular dystrophy. *Am. J. Roentgenol.* 89:970, 1963.
- Leviton B., and Nathanson L. The roentgen features of muscular dystrophy. *Am. J. Roentgenol.* 73:226, 1955.
- Petkoff G. T. et al. Myopathy due to the administration of therapeutic amounts of 17 hydroxycorticosteroids. *Am. J. Med.* 26:891, 1959.

The Bones

Normal Structure

IN THE EXTREMITIES there are three kinds of bones: the elongated tubular bones, the round bones in the wrists and ankles, and the sesamoids, the small bones in the tendons and articular capsules. Functionally a growing tubular bone is made up of three segments: the diaphysis, the paired roetaphyses, and paired epiphyses at each end of the diaphysis (Figs 8-51 to 8-53). Apophyses and secondary cartilaginous masses which grow out obliquely from the main axis of the diaphysis contribute nothing to the longitudinal growth of the shaft. The apophyses ossify and fuse with the shaft in the same way and about the same time as the epiphyses fuse with it at maturity.

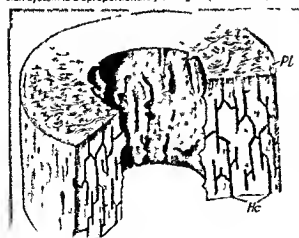
The bones are composed chemically of a matrix of collagen and collagenous fibers in which apatite crys-

tals are deposited. The skeletal tissues are exceedingly strong and highly resistant to all kinds of mechanical stresses, and at the same time are active metabolically, especially during the growing period. Bones are supplied by an abundant complex of arteries, veins, and nerves in the cortical walls and in the medullary cavities and also in the epiphyses and metaphyses. The skeleton serves as a semirigid frame on which the soft tissues are supported, and the individual bones provide multiple levers for the insertion of ligaments and tendons. The relatively rigid walls of the cranium and thoracic cage act as protective shields for the brain and intrathoracic organs. Skeletal calcium is a reservoir from which calcium may be drawn to satisfy the fluctuating calcium needs of other tissues. The medullary cavities of the bones are the sole postnatal sites for the formation of blood. The usual sites for the foramina of the nutrient arteries to the shafts are shown in Figure 8-54.

The diaphysis of the shaft (the part which grows through) is the elongated intermediate segment between the metaphyses which it separates. The diaphysis elongates at each of its ends from growth of the epiphyseal cartilages away from each other. During growth a long bone is a tube closed at each end by the transverse cartilage plate. Its central cavity or medullary canal is filled with red and fatty marrow, and with cancellous bone in its terminal segments. Its cortical walls are made up of peripheral layers and longitudinally directed Haversian osteons. In the ends of the marrow cavities there is a lattice of varying degrees of tightness made up of spongy bone, the terminal spongiosa. The spaces between the branches of the lattice communicate directly with one another and with the central main space of the medullary cavity. The peripheral or marrow spongiosa is a thin sheet of spongy bone between the inner edge of the cortex and the outer edge of the marrow which extends the length of the marrow cavity.

The periosteum covers the external edge of the cortical wall. It is made up of an outer layer of densely packed collagenous fibers arranged parallel to the cortical edge with similarly arranged fibroblasts. The

Fig. 8-51—Schematic representation of the lamellar arrangement in the cortex of a tubular bone. The concentric lamellae of the Haversian systems are indicated as well as the communicating Haversian canals (Hc). The external edge of the cortex is made up of the peripheral lamellae (Pl). In the diagram the Haversian system is disproportionately enlarged. (From Clark.)



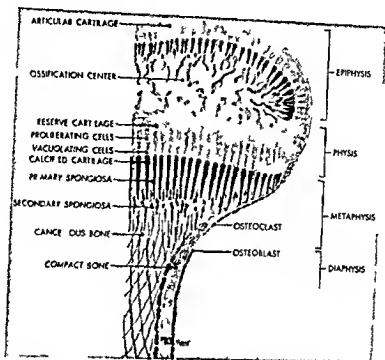


Fig 8-52 — Growth units of the epiphysis, metaphysis, and diaphysis and the rat anatomical counterparts according to Rubin who

defined the metaphysis as the segment of funnel on the condensation (From Rubin)

inner periosteal layer during growth consists of several sheets of osteoblasts in a much looser connective tissue whose fibers are directed perpendicular to the cortical surface. This inner envelope—the osteogenetic layer—deposits progressively new layers of subperiosteal bone on the outer edge of the cortex. This weaker layer of the periosteum is usually the site of traumatic separation and subperiosteal hemorrhage. The tough outer fibrous envelope also limits the migration of osteoblasts externally and prevents them from extruding into the contiguous tissues. The periosteum binds itself to the underlying cortex by the centrally directed fibers of Sharpey; these are less numerous and shorter in children than in adults and thus much less effective as binders of the periosteum to the cortex.

The epiphyses (the segments which grow upon) are cartilaginous caps which lie beyond the metaphyses at both ends of the bone. Secondary ossification centers develop in all of them except some of the epiphyses of the phalanges, metatarsals and metacarpals.

The cartilage plate is a transverse disk of cartilage whose function is epiphyseal on its juxta-articular side and metaphyseal on its shaftward side. These two different transverse segments of the cartilage plate are sharply different both structurally and functionally (Figs 8-55 to 8-57). The several transverse subdivisions of the epiphyseal metaphyseal plate are

not sharply limited but they are useful in the understanding of bone and cartilage growth and in the classification of several intrinsic acquired and inherent lesions which are dependent on growth. The cartilage plate is active metabolically and is richly supplied with blood. Longitudinal growth is exclusively epiphyseal in origin. Rubin classifies the epiphyseal segment of the cartilage plate as the physis.

The metaphysis (the segment of changed growth) contributes nothing to longitudinal growth but is responsible for removal of cartilage, its reconstruction and the formation of the primary spongiosa and the medullary cavity—the layering of endosteal bone on the cartilage cores of the residual lattice.

The blood supply of a growing bone consists of several circulatory subsystems (Brookes). Many macroscopic and microscopic arteries perforate the cortex and then continue on through their branches into the marrow and into the trabeculae of spongy bone. The compacta of the cortical walls is riddled with blood vessels which differ functionally from the more superficial vessels of the periosteal vascular bed. The medullary supply begins as the principal nutrient artery which perforates the shaft at the foramen for the nutrient artery and then divides into proximal and distal branches which supply through their progressively subdividing branches the marrow and the metaphyses. Near both ends of the diaphysis perforating arteries pierce the thin cortical shell at this level.

el and supply marrow and the peripheral metaphyseal terminal segment. The metaphyseal arteries terminate in straight branches which penetrate the necrotic cartilaginous columns. The epiphyses are supplied by their own arteries which branch from local arteries near the joints and enter the cartilage through the foramina nutricia. They then subdivide and these small branches supply the longitudinally proliferating cartilage cells in the cartilage plate, the epiphyseal ossification center and the articular cartilage. The perichondral vessels are superficial and never penetrate deeply into the cartilage plate. They supply the osteoblasts in the perichondral ring which are re-

sponsible for the latitudinal growth of the epiphyseal cartilage. This latitudinal growth is appositional, in contrast to the interstitial longitudinal epiphyseal growth in the cartilage plate.

The blood vessels and the blood supply are of primary importance in the normal growth of bone and in all of the lesions, both congenital and acquired, which develop during growth. Normal osteogenesis is dependent on the blood itself for all of the essential metabolites—proteins, fats, sugars, salts, vitamins and endocrine solutes. Normal osteogenesis is also directly dependent on the presence of an adequate number of osteoblasts which are probably derived in large part

Fig 8-53—The macroscopic components of a normal tubular bone and their roentgeno counterparts. A roentgenogram and the longitudinal section of the right tibia of a child 2 years of

age. *eoc* epiphyseal ossification center; *pzc* provisional zone of calcification and cartilage plate.

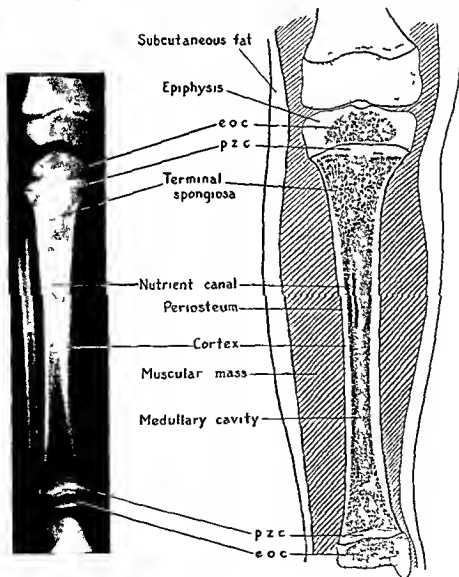


Fig 8 54 — Schematic representation of the position of the nutrient canals in the long bones (Modified from Hodges)

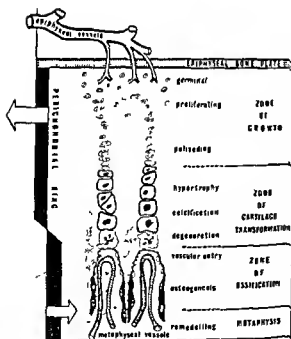
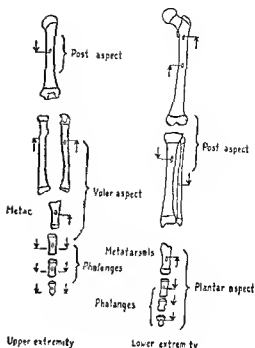


Fig 8 55 — Schematic drawing of a longitudinal section of cartilage plate—the epiphyseometaphyseal junction. The subdivisions are not actually as clearly defined as represented. The epiphyseal segment at the top is supplied by the epiphyseal arteries. The exact limits of the shaftward side of the epiphysis and the epiphyseal side of the metaphysis are still controversial. In the drawing the metaphysis is labeled to begin at the level of the remodeling. From a strictly functional standpoint it could just as well be located at the level of hypertrophy and beginning death of the cartilage cells. This would fit the meaning of the word metaphysis—the segment of changed growth. The zone of growth is made up of three different layers of cartilage cells; it is the only zone in which longitudinal growth occurs. In the zone of cartilage transformation the quality of the cartilage cells changes and the ground substance calcifies; but there is no longitudinal growth. In the zone of ossification the metaphyseal arterial loops invade the cartilage, destroy most of it and endosteal bone is formed on the edges of the residual lattice of this partially destroyed cartilage. (From G Hertel and Gilbert.)



Fig. 8-58—Longitudinal section of the cartilage plate of a puppy a few weeks of age. A, longitudinal section of cartilage columns made up of longitudinal stacks of flattened chondrocytes in different phases of germation. The reserve cartilage is a shallow segment at the top where the cartilage cells are scattered in random and tend to be round. The next layer of cells is more enlarged and multiply and are seen in various stages of mitosis and division. These cartilage cells enlarge as one progresses shaftward (downward in this section) the nucleolus fragment and the protoplasm becomes vacuolated and degenerates leaving

empty lacunae in many cases. At the very bottom invasion of the arterial loops of the metaphyseal arteries is visible. B, longitudinal section of the cartilage plate on its edge where it is joined with the perichondrium and perichondrial ring of osteoblasts. In the upper levels the round reserve cartilage cells are growing transversely in contrast to the longitudinal growth of the cartilage rows. This faecal growth is appositional. In contrast to the interstitial growth in the longitudinal rows. (Courtesy of Dr. Robert B. Greer, Children's Hospital, Pittsburgh.)

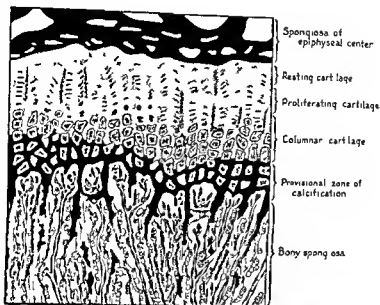


Fig 8-57—Microscopic elements of the epiphysis and metaphysis in the cartilage plate. The epiphysis extends shaftward to the level of the hypertrophic vacuolated columnar cartilage cells. The metaphysis extends from the above level shaftward through the level where the black cartilage cores in the spongiosa hang

as stactactres from the roof of the medullary cavity and terminate and endochondral bone is complete. (Modified from Ingalls, but the definition of the boundness of the epiphysis and metaphysis are my own, not Ingalls's—J.C.)

from endothelium cells of the marrow capillaries and sinuses (Trueta, 1968). It is likely that all of the inherent dysplasias of the skeleton are caused, either primarily or secondarily, by deficiencies (hypoplasias) and excesses (hyperplasias) of blood supply and endothelium derived osteoblasts.

REFERENCES

- Brookes M. Blood supply of bone. *Mod. Trends Orthopedics* 4:91, 1964.
 ———. Cortical vascularization and growth of fetal tubular bones. *J. Anat.* 97:597, 1963.
 Clark, W. E. L. *Tissues of the Body* (2nd ed., Oxford: Clarendon Press, 1945).
 Cockshot, W. P. Dactylitis and growth disorders. *Brit. J. Radiol.* 36:19, 1963.
 Crook, H. V. *The Blood Supply of Lower Limb Bones in Man* (London: E. & S. Livingstone Ltd., 1967).
 Dodds, G. S. Row formation and other types of arrangement of cartilage cells in endochondral ossification. *Anat. Rec.* 46:385, 1930.
 Johnson, L. C. The kinetics of skeletal remodeling. A further consideration of theoretical biology of bone. *Birth Defects (orig. art. series)* 2:66, 1966.
 LeCrox, P. *The Organization of Bones* (Philadelphia: Blakiston Company, 1951).
 Park, E. H. The imprinting of nutritional disturbances on growing bone. *Pediatrics* 33 (supp.):815, 1964.
 Rang, M. (ed.) *The Growth Plate and Its Disorders* (London: E. & S. Livingstone, Ltd., 1969).
 Rubin, P. *Dynamic Classification of Bone Dysplasias* (Chicago: Year Book Medical Publishers, Inc., 1964).
 Trueta, J. *Studies of the Development and Decay of the Human Frame* (Philadelphia: W. B. Saunders Company, 1968).
 ———, and Morgan, J. D. Vascular contributions to osteogenesis. *J. Bone & Joint Surg.* 42-B:97, 1960.

Röntgenographic Appearance

The calcified portions of a growing bone cast opaque shadows of calcium density, the noncalcified components cast shadows of a lesser water density (Figs 8-58 and 8-59, and see Fig 8-53). The heavily mineralized compact cortex casts the heaviest shadow, a long fusiform strip of increased density which tapers off toward the end of the shaft on each side of the medullary cavity. The central spongiosa at the

Fig 8-58—Large nutrient canal in the ulna of a normal infant 10 days of age projected in profile. Tracing of a roentgenogram. The proportionately thick cortex and narrow medullary canal are characteristic of the physiologic sclerosis of the newborn.

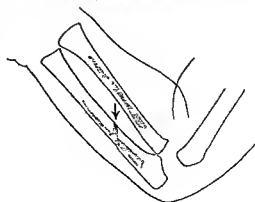




Fig 8-59—Double canals through the medial cortical wall of the femur for the nutrient arteries of a normal newly born infant

ends of the shaft is recorded in the film as a tightly meshed network of linear shadows which is always partially obscured by the heavier superimposed shadows of two layers of cortex. The peripheral spongiosa fuses with the central spongiosa at the ends of the bones, on the borders of the medullary canal the peripheral spongiosa may give rise to a roughening of the internal surface of the cortex or may be invisible.

The nutrient canals appear as defects in the cortices (Fig 8-58, and see Fig 8-53). When a nutrient

canal is projected in profile, its oblique channel through the cortex can be clearly demonstrated (Fig 8-59). In other projections the nutrient canals are partially or completely obscured by the heavy shadow of the cortex surrounding them. The calcified cartilaginous disk interposed between the shaft and the epiphyseal ossification center, the provisional zone of calcification, casts a transverse band of increased density across the end of the shaft. The ossification centers appear as rounded or ovoid shadows of opaque bone density in the lighter water density of the surrounding uncalcified cartilage, their margins are denser than the reticular central portions.

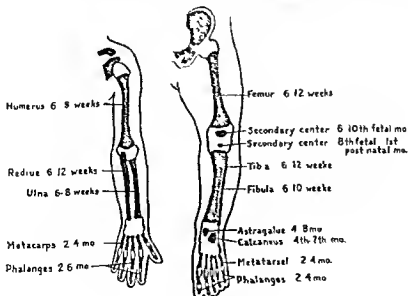
The uncalcified portions of a growing bone cast shadows of water density similar to that of the surrounding soft tissues. The shadows of the peripheral uncalcified portions of the epiphyseal cartilage fuse with those of the soft tissues. The strip of uncalcified cartilage interposed between the epiphyseal ossification center and the end of the shaft, sometimes called the epiphyseal plate, appears as an intermediate strip of water density. The periosteum, bone marrow and intrasosseous vessels are invisible roentgenographically. Fatty marrow has a diminished density in comparison with red marrow, this difference is not detectable in the standard films made with the technical factors used at the present time.

Growth and Maturation

PRIMARY OSSIFICATION CENTERS

Near the end of the second month of fetal life, the embryonal cartilaginous skeleton has already been

Fig 8-60—Time schedule for the appearance of the primary ossification centers in the shafts of the long bones and in the tarsal bones during fetal life



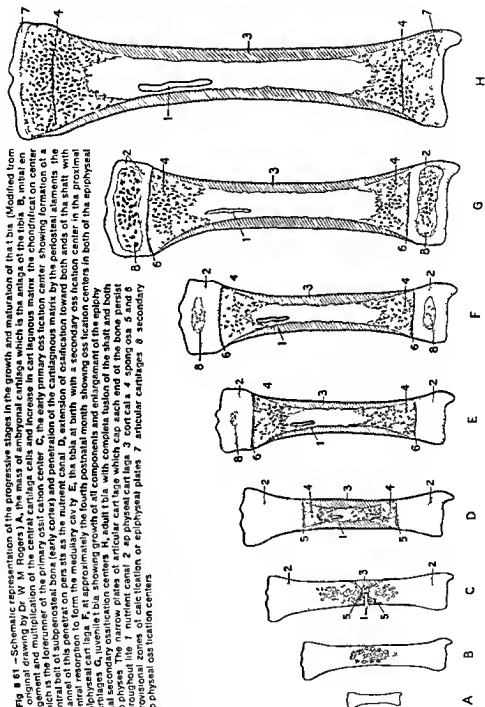


Fig. 8-61 — Schematic representation of the progressive stages in the growth and maturation of the tibia. (Modified from an original drawing by Dr. W. M. Rogers.) A, the mass of embryonal cartilage which is the anlage of the tibia. B, initial enlargement and multiplication of the central cartilage cells and increase in cartilaginous matrix. The chondrocytes on center which is the forerunner of the primary ossification center. C, the early primary ossification center showing formation of a central part of subperiosteal bone (early cortex) and penetration of the cartilaginous matrix by the perosteal elements. The central part of this penetrates on perasts as the nutrient canal. D, extension of ossification toward both ends of the shaft with central resorption to form the medullary cavity. E, the tibia at birth with a secondary ossification center in the proximal epiphyseal cartilage. F, at approximately the fourth postnatal month showing ossification centers in both of the epiphyseal cartilages. G, juvenile tibia, showing growth of all components and enlargement of the epiphyseal centers. H, adult tibia, with complete fusion of the shaft and both epiphyses. The narrow plates of articular cartilage which cap each end of the bone persist throughout life. 1. Nutrient canal. 2. Apophyseal cartilage. 3. Cortical area. 4. Spongy area. 5 and 6. Provisional zones of calcification or epiphyseal plates. 7. Articular cartilages. 8. Secondary epiphyseal ossification centers.

subdivided into its principal segments which are the forerunners of the bones of the extremities. All of the primary ossification centers for the tubular bones appear during fetal life (Fig. 8-60). A primary ossification center is formed by the deposition of a transverse disk of lime in the cartilaginous matrix at approximately the center of the embryonal shaft following the hypertrophy and vacuolization of the local cartilage cells (Fig. 8-61). The center of this segment is almost immediately absorbed and becomes the primary marrow cavity or medullary canal. This absorption is associated with the ingrowth of penosteal arteries. The calcified cartilaginous disks on the proximal and distal sides of the primary cavity become the preparatory zones of calcification which follow the advancing proliferating cartilage toward the proximal and distal ends of the shaft during growth. The cortical defect resulting from the penosteal ingrowth persists as the nutrient canal. Concurrently with these changes within the cartilage a compact cylinder of peripheral bone, the cortex, is being laid down under the periosteum which surrounds the primary ossification center.

Ray and colleagues showed that in rats which had had early excision of the pituitary and thyroid glands the injection of thyroxine caused marked stimulation of maturation and only moderate increase in growth. In contrast, the injection of pituitary growth hormone caused marked increase in dimensional growth of the bones but no increase in maturation. The combined administration of thyroxine and pituitary growth hormone restored the balance between growth and maturation.

REFERENCE

- Ray, R. D., et al. Growth and differentiation of the skeleton in thyroidectomized hypophysectomized rats treated with thyroxine, pituitary growth hormone, and the combination. *J. Bone & Joint Surg.* 36-A: 94, 1954.

GROWTH IN LENGTH

The elongation and ossification of a tubular bone are the result of the synchronous continuing action of several independent but co-operative phenomena which constitute endochondral bone formation (see Figs. 8-55 to 8-57). The cells within the proliferative cartilage multiply continually and are given off away from the cartilage toward the shaft. The addition of these constantly accumulating new cells lifts the cartilage away from the shaft and increases its length. At the same time and advancing with the proliferation, the oldest of the proliferating cartilage cells degenerate and lime is deposited in their matrix to form a thin, rigid, transverse disk—the preparatory zone of calcification. Coincidentally with the deposition of calcium in this preparatory zone, the shaftward eroded or thus calcified plate is being continually eroded and reamed out into a honeycomb of cartilaginous

trabeculae separated by the marrow spaces. This honeycomb or lattice serves as a temporary scaffold on which a shell of endosteal bone is deposited by osteoblasts. As growth proceeds, the branching endosteal shell enveloping the cartilaginous scaffold gradually becomes thicker and the cartilaginous core inside the bony shell becomes smaller until the central core of cartilage ultimately disappears, leaving a lattice of solid endosteal bone, the spongiosa (see Fig. 8-57). The central intermediate portions of the spongiosa are later resorbed to form the medullary canal.

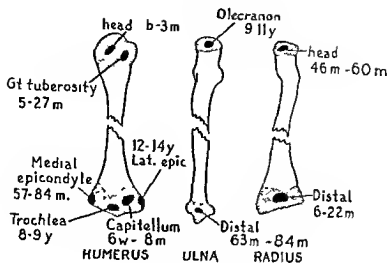
The thickness of the cortex and the shaft increases as the result of the deposition of compact bone on the external surface of the cortex by the overlying osteogenic layer of the periosteum. Channels are formed in the cortex by osteoclastic resorption, and these become the Haversian and the Volkmann canals through which the medullary blood vessels pass. The width of the medullary cavity increases concurrently with increase in the caliber of the shaft owing to the simultaneous continuing absorption of the innermost cortical layers. In this way the caliber of the shaft, the thickness of the cortex and the size of the medullary cavity are maintained in proper balance during the period of growth.

SECONDARY OSSIFICATION CENTERS

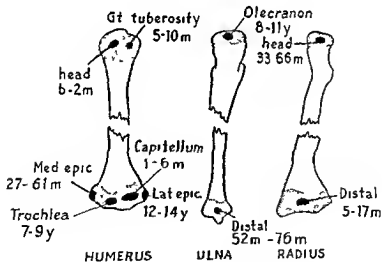
The epiphyses are ossified and enlarged by essentially the same process of endochondral bone formation as that described for the lengthening of the shafts except that it is three dimensional. The secondary centers usually appear after birth, except those in the distal epiphyses of the femurs and less frequently those in the proximal epiphyses of the tibiae. With increasing age the bony penetration advances into the cartilage in all directions from the initial focus, it is almost an invariable rule that velocity of penetration is greater on the articular border of the ossification center than on its diaphyseal border. Penetration continues until the edges of the cartilage are reached. The disk of cartilage interposed between the shaft and the ossifying epiphyseal center, the cartilage plate diminishes progressively in thickness until it disappears completely at the completion of growth, when the epiphysis and the diaphysis fuse into a mature bone. On the articular surfaces of the epiphyses, however, strips of cartilage persist into adult life as the articular cartilages. The time schedule for the appearance of the secondary centers is shown in Figures 8-62 and 8-63. Multiple ossification centers normally develop in both epiphyses of the humerus and the proximal epiphyses of the femur (head and two trochanters).

Normal ossification of the epiphyseal ossification center is often not an even, uniform process especially during its early phase and during periods of rapid growth and ossification. Instead of a single center, several fine bony foci may appear first, and these fuse

BOYS



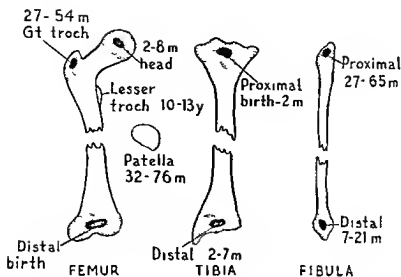
GIRLS



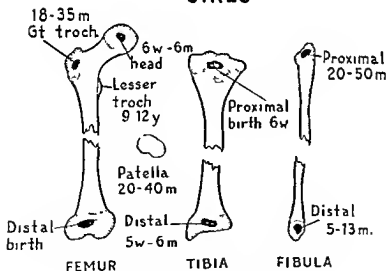
m = months y = years b = birth

Fig 8 62A—Time schedule for appearance of secondary epiphyseal ossification centers in the upper extremity (Figs 8 62A and 8 62B modified from Vogt and Vickers)

BOYS



GIRLS



w = weeks, m = months

Fig 8 62B —Time schedule for appearance of secondary epiphyseal ossification centers in the lower extremity

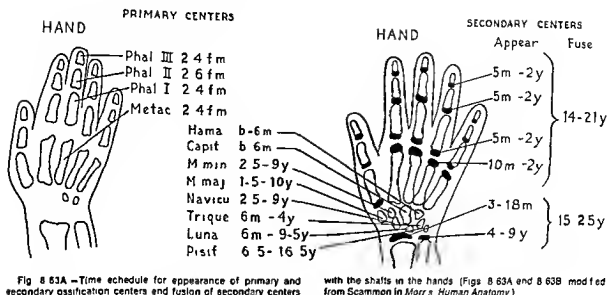
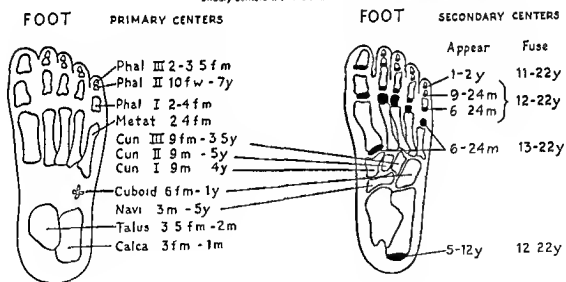


Fig 8 63B —Time schedule for appearance of primary and secondary ossification centers and fusion of secondary centers with the shafts in the feet



fm = fetal months, m = post natal months; y = year

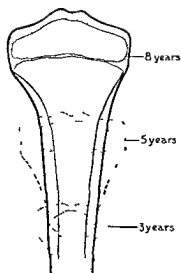
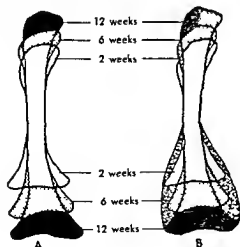


Fig 8-64 —Growth and configuration of the tibia with advancing age. The progressive concentric constriction of the shaft away from the wider epiphyseal plate is shown schematically in superimposed tracings of roentgenograms.

later into a single large bony center which may remain uneven in density and irregular on the margins for many months before it becomes uniform in density and smooth on the edges. During such stages of normal irregularities the diagnosis of osteochondrosis or epiphysitis should not be made because the epiphyseal ossification center is irregular in density or rough on the edges.

Fig 8-65 —A, normal modeling of a long bone. With progressive growth there is progressive constriction of the shaft away from the terminal flares of the shaft at both ends. B, failure of modeling. The ends of the shafts are swollen and clubbed owing to failure of progressive constriction. (From Drey.)



CONSTRICTION (MODELING)

During the period of growth in addition to the constant increase in length and breadth the shaft is being continually molded or reshaped to produce its final form. The mechanism responsible for these changes in shape has been called modeling or tubulation. One of the most conspicuous features of modeling in many tubular bones is the progressive concentric contraction of the shaft behind the wider advancing terminal segment (Fig 8-64). Modeling is responsible for the flaring of the ends of many of the tubular bones. Significant errors in configuration of the shafts develop in most of the diseases affecting the growing skeleton (Fig 8-65).

REFERENCES

- Clark W E L. *The Tissues of the Body* (2d ed. Oxford: Clarendon Press 1945), p 60.
 Drey L. Failure of modeling of bone. *Radiology* 61:643, 1953.
 Ingalls T H. Epiphyseal growth. Normal sequence of events at the epiphyseal plate. *Endocrinology* 29:710, 1941.
 Park E A. Bone growth in health and disease. *Arch Dis Childhood* 29:369 and 369, 1954.
 Scammon R E. In *Morris Human Anatomy* (10th ed. Philadelphia: The Blakiston Company 1942).
 Trueta J and Amato V P. The vascular contribution to osteogenesis. III. Changes in growth caused by experimentally induced ischemia. *J Bone & Joint Surg* 42 B:571, 1960.

VELOCITY OF GROWTH AND DEVELOPMENT

METHODS OF APPRAISAL—The velocity of the longitudinal growth of tubular bones can be most accurately measured in serial roentgenograms. Mareš determined the length of the tubular bones in healthy subjects from age 1 year to 12 years (Table 8-1). She found that girls' bones elongate more rapidly than those of boys. The reader should consult the tables of Mareš published in 1955 for more comprehensive and detailed statistical treatment of normal growth in length of the tubular bones. Stuart Hill and Shaw reported that the tibial shaft tends to be slightly longer in girls after the 2nd year, the head of the tibia, in contrast, is consistently wider among boys. It is well established that the quantities of longitudinal growth derived from each of the two ends of a tubular bone are unequal. For example, in the arm the ends of the humerus, radius and ulna near the elbow grow less than their counterparts near the shoulder and the wrist. In the leg the ends of the femur, tibia and fibula near the knee grow more than their counterparts near the hip and ankle. Digby and others found that in the femur approximately 70% of the total growth occurs at its distal end and in the tibia 55% of total growth occurs at its proximal end.

Green and Anderson published tables for the average growth of the femur and tibia in boys and girls

TABLE 8-1—AVERAGE VALUES FOR LENGTH OF SHAFT IN CENTIMETERS

AGE Yr	1	2	3	4	5	6	7	8	9	10	11	12
Humerus	106	130	148	165	179	193	207	220	232	245	258	270
Radius	79	97	111	123	131	144	153	163	172	181	190	199
Ulna	90	109	124	137	149	159	168	178	187	196	207	217
Femur	135	171	198	224	248	271	293	315	334	352	368	383
Tibia	109	140	162	184	203	221	239	258	275	292	309	326
Fibula	105	136	162	182	201	219	237	254	271	287	302	318

older than 5 years which they used in estimating the quantity of growth which would be lost after surgical arrest of longitudinal growth in the unaffected leg done for the purpose of equalizing the lengths of the two legs one of which was shortened owing to poliomyelitic paralysis

The radial and ulnar shafts of 100 white boys and 100 white girls were measured by Ghantus at 3 9 12 18 and 24 months. The average length and the range for each age was tabulated. These tables are valuable for estimation of the degree of acceleration or retardation in growth of these bones at any age prior to the 25th month. Ghantus found that the average lengths of the two bones in boys were consistently greater than in girls of the same age. During the 1st year the rate of growth of the shafts of both bones was greater in boys the converse was true during the 2nd year.

The studies of Wilson and associates indicate that newborns who have suffered fetal growth retardation grow at normal velocity during the first four to six weeks after birth if a superimposed illness does not intervene.

We lack adequate data for the rates of growth and the relative sizes during different age periods of several features of tubular bones other than longitudinal growth. There are no satisfactory standards for the changes in configuration in proportionate thickness of compacta and medullary canal in the magnitude and distribution of the spongiosa and in the size and position of the nutrient canals at different age levels. Bonnard measured diaphyseal diameters in relation to the long axis of the metacarpal bones during infancy and childhood.

Growth can be retarded locally by the use of staples at the metaphysis which bind the primary and secondary ossification centers together and prevent longitudinal expansion of the tissues between them mechanically (Blount and Zeier). In some cases reduced growth in the distal femoral metaphysis is compensated for by increased growth in the companion tibial metaphysis across the knee joint so that total shortening of the entire leg is not as great as the shortening in the distal femoral metaphysis. Growth has been stimulated successfully by the implantation of metallic and ivory screws in the metaphysis which cause increase in blood supply to the part (Pease). Ivory blocks have been similarly implanted with successful stimulation of growth in many cases.

REFERENCES

- Anderson M et al. Distribution of lengths of the normal femur and tibia in children from 1 to 18 years of age. *J Bone & Joint Surg* 46-A: 1197 1964.
 Blount W P and Zeier F. Control of bone length. *JAMA* 148: 451 1952.
 Bonnard C D. Cortical thickness and diaphyseal diameter in relation to the long axis of metacarpals during infancy and childhood. *Helvet paed et acta* 5: 445 1968.
 Maresh M M. Linear growth of the long bones of the extremities from infancy through adolescence. *Am J Dis Child* 89: 725 1955.
 Pease C N. Local stimulation of growth of long bones. *A preliminary report*. *J Bone & Joint Surg* 34-A: 1 1952.
 Wilson M C et al. Postnatal bone growth of infants with fetal growth retardation. *Pediatrics* 40: 213 1967.

VELOCITY OF OSSIFICATION—The progressive stages of ossification during advancing age are shown schematically in Figure 8-61. Numerous roentgenographic methods have been proposed for assessing the skeletal age according to the time of appearance, the size and the differentiation of the ossification centers. The charts and diagrams of Scammon of Hodges and of Camp and Culley depict the time schedule of skeletal maturation from fetal until adult life. Skeletal age is only one measure of the maturational level of an individual in the final over all clinical estimate of maturation the skeletal age must be correlated with several other findings including the mental development motor performance nutritional status race height and weight.

The reason that healthy skeletons vary so greatly is the wide diversity genetically of the healthy child population in the United States and especially in New York City. The healthy child population is made up of heterogeneous individuals who differ widely in color racial constitution and development size and structure who have lived and still live in widely different environments in regard to food climate housing and exercise. Although bone maturation can be used successfully in the measurement of the general development of large groups of infants and children it may be highly misleading in estimating the general development of single individuals in these same groups.

Fetal and neonatal—The time of appearance of the primary centers in the tubular bones prior to birth and the number present at birth are shown in Figure 8-60. All of the primary centers have appeared and

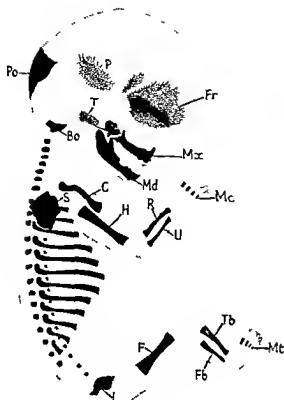


Fig 8-66 —The primary ossification centers in the fetal skeleton. Drawing of a 13 week embryo which had been cleared in glycerin after the bones had been stained with Alizarin. The centers for the following bones are shown: frontal *Fr*; parietal *P*; postoccipital *Po*; basioccipital *Bo*; temporal squamosa *T*; maxilla *Mx*; mandible *Md*; clavicle *C*; humerus *H*; radius *R*; ulna *U*; metacarpals *Mc*; acapula *S*; ilium *I*; femur *F*; tibia *T*; fibula *Fb*; metatarsals *Mt*; ribs and vertebrae not labeled. Magnification $\times 2\frac{1}{2}$ approximately (From Clark).

are well developed into diaphyses by the thirteenth fetal week except some of the primary centers for the shafts of the phalanges in the hands and feet (Figs 8-66 and 8-67). O'Rahilly and Meyer demonstrated the maturation of the fetal skeleton in a radiographic study made after impregnation of the skeleton with silver chloride. The principal clinical interest in the fetal centers is associated with the diagnosis of prematurity. Ossification begins in the distal epiphysis of the femur during the last two months of gestation, and this secondary center is present in all full term females and in 96% of males at birth. Absence of ossification centers in the distal femoral epiphyses at birth is presumptive evidence of prematurity. The presence of an ossification center in the distal femoral epiphysis is not however, unquestionable evidence of maturity at birth, for Schrieber and associates found visible ossification centers radiographically in 64 of 124 infants at birth, all of whom appeared to have been born prematurely. The center in the proximal epiphysis of the tibia, on the other hand, is present in but approximately two-thirds of full term infants, its absence at birth cannot, therefore, be used as a criterion of prematurity. In his anatomic study of 500 fetuses Hill found a distinct sex linked lag in the development of the male fetal skeleton after the seventh lunar month. The ossification centers for the humeral head, the coracoid process, the capitate and the hamate occasionally appeared during the last months of fetal life. The center for the body of the hyoid was present in 59% of newborns and appeared as early as the fifth fetal month in some cases. The reader should also consult the paper of Menees and Holly for the frequency and the distribution of ossification centers in the newborn infant. Their study was based on a roentgenographic study of 500 normal living newborns. Race as well as sex may be a factor in

Fig 8-67 —Early fetal ossification according to Mall. A, On the 49th day. B, On the 73rd day.

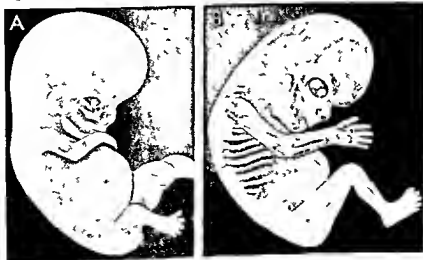


TABLE 8.2 - PRESENCE OF EACH OF 10 CENTERS OF OSSIFICATION (RIGHT SIDE) IN ROENTGENOGRAMS OF 1 112 NEWBORNS*
DISTRIBUTED ACCORDING TO RACE, SEX AND WEIGHT AT BIRTH†

CENTER OF OSSIFICATION	Less Than 2 000		2 000-2 499		2 500-2 999		3 000-3 499		3 500-3 999		4 000 or more	
	Total	%	Total	%	Total	%	Total	%	Total	%	Total	%
Calcaneus	11	100.0	15	100.0	34	100.0	113	100.0	88	100.0	35	100.0
White boys	6	100.0	24	100.0	49	100.0	111	100.0	54	100.0	21	100.0
White girls	11	100.0	26	100.0	75	100.0	100	100.0	45	100.0	14	100.0
Negro boys	14	100.0	32	100.0	103	100.0	101	100.0	22	100.0	4	100.0
Negro girls												
Talus												
White boys	11	79.7	15	100.0	34	100.0	113	99.1	88	100.0	35	100.0
White girls	6	83.3	24	100.0	49	100.0	111	100.0	54	100.0	21	100.0
Negro boys	11	90.9	26	100.0	75	100.0	100	100.0	45	100.0	14	100.0
Negro girls	14	100.0	32	100.0	103	100.0	101	100.0	22	100.0	4	100.0
Distal epiphysis of femur												
White boys	11	9.1	16	75.0	34	85.3	113	100.0	88	100.0	35	100.0
White girls	6	50.0	24	91.7	49	98.0	112	100.0	54	100.0	21	100.0
Negro boys	11	38.2	26	88.5	75	90.7	100	94.0	45	100.0	14	100.0
Negro girls	14	50.0	32	93.8	103	99.0	101	100.0	22	100.0	4	100.0
Proximal epiphysis of tibia												
White boys	11	0.0	16	18.8	34	52.9	113	78.8	88	84.1	35	97.1
White girls	6	0.0	24	54.2	49	75.5	112	85.7	54	80.7	21	80.5
Negro boys	11	0.0	28	38.5	75	62.7	100	76.0	45	80.0	14	92.9
Negro girls	14	14.3	32	40.6	103	78.7	101	88.1	22	88.4	4	100.0
Cuboid bone												
White boys	11	0.0	16	6.2	34	14.7	113	29.8	88	44.3	35	60.0
White girls	6	0.0	24	37.5	49	57.1	112	65.2	54	70.4	21	78.2
Negro boys	11	0.0	26	23.1	73	43.6	100	58.0	44	68.2	14	100.0
Negro girls	14	21.4	32	37.5	103	68.0	101	78.2	22	81.8	4	75.0
Head of humerus												
White boys	11	0.0	13	7.7	29	13.8	62	41.9	51	49.0	22	59.1
White girls	4	0.0	18	5.6	31	25.8	74	41.9	38	69.4	15	88.7
Negro boys	11	0.0	23	0.0	66	15.2	78	27.6	31	48.4	11	03.8
Negro girls	13	0.0	28	10.7	88	22.7	78	52.8	18	38.9	1	100.0
Capitate bone												
White boys	11	0.0	15	0.0	33	0.0	112	8.0	88	15.9	34	17.6
White girls	8	0.0	24	0.0	47	14.9	106	15.1	53	20.8	21	38.1
Negro boys	11	0.0	26	7.7	73	16.4	96	20.8	42	26.2	13	30.8
Negro girls	14	0.0	32	12.5	101	19.8	101	41.8	22	40.9	3	100.0
Hemate bone												
White boys	11	0.0	15	6.7	32	6.2	112	6.2	87	10.3	35	11.4
White girls	6	0.0	24	0.0	47	10.8	108	13.7	53	20.8	21	32.3
Negro boys	11	0.0	26	16.4	73	18.4	96	17.7	43	44.2	14	28.6
Negro girls	14	0.0	32	9.4	101	22.5	100	41.0	22	54.5	3	66.7
Third cuneiform bone												
White boys	11	0.0	16	0.0	34	0.0	113	2.7	88	2.3	33	3.0
White girls	6	0.0	24	0.0	49	0.0	111	0.0	54	5.6	21	9.5
Negro boys	11	0.0	26	3.8	74	8.1	100	15.0	43	14.0	14	14.3
Negro girls	14	0.0	32	6.2	103	13.8	101	18.8	22	18.2	4	25.0
Head of femur												
White boys	11	0.0	16	0.0	33	0.0	107	0.0	76	0.0	30	0.0
White girls	5	0.0	21	0.0	49	0.0	105	1.0	52	0.0	20	0.0
Negro boys	11	0.0	25	0.0	75	0.0	99	0.0	43	0.0	14	0.0
Negro girls	14	0.0	31	0.0	100	1.0	98	1.0	21	0.0	4	0.0

*258 white boys 267 white girls 371 Negro boys 376 Negro girls
†From Chart A. Am. J. Dis. Child. 77:355 1953

fetal maturation, Dunham and her co-workers found the ossification center of the cuboid to be present more frequently in newborn black infants than in white newborns.

In the study of Kelly and Reynolds, carpal centers appeared first in black females and later in black males, white females and then white males in that order.

Christie studied skeletal maturation in 1 112 singly born, newly born, premature and mature infants and tabulated his data according to birth weight, sex and race (Table 8-2). He found that skeletal development in the newborn varies directly with birth weight. Black infants were consistently more advanced than white infants of the same weight and sex. Female neonates were consistently more advanced than male infants of the same weight and race.

Postnatal—Ideally, films of the entire skeleton should be studied before the skeletal age is estimated. In daily clinical practice the time-consuming, expensive roentgen examination of all of the bones cannot be carried out except in special cases. For this reason a small and convenient segment of the skeleton commonly the hand and wrist is considered representative of the entire skeleton in the assessment of skeletal age. It should be borne in mind that there is a potential error in this practice. Unfortunately the velocity of ossification may not be uniform in different regions of the skeleton of a single healthy child or in the analogous portions of skeletons of different healthy children of the same age who are apparently equally advanced in nonskeletal features of maturation. Homologous parts of the two sides of the same skeleton may show considerable differences in de-

velopment, and there may even be discrepancies in the maturational levels of different bones in a small structure such as the hand. Dreizen and colleagues, in a radiographic study of the hands of 450 children, found identical bilateral symmetry of bone maturation in only 117 children. As a rule, the secondary epiphyseal centers of the tubular bones exhibit a more uniform development than do the primary centers of the small round bones of the wrists and ankles. This phenomenon is demonstrated in Figure 8-68. Late ossification of a center is usually not associated with permanent morphologic changes.

Notwithstanding the potential errors just discussed, roentgenograms of the hands offer the most accurate practical method for assessing skeletal age. The schematic diagrams of Vogt and Vickers (Fig. 8-69) are specially useful because they show clearly the wide range for normal at all ages in both sexes. The children who were used in this study were a healthy group from which abnormal children were excluded by careful clinical investigation. For children older than 6½ years and thus not included in the chart of Vogt and Vickers the standards of Greulich and Pyle are recommended. During the first months of life the knee and foot are more satisfactory for appraisal of skeletal age because more centers appear at an early age than in the hand. Stuart's diagrams (Fig. 8-70) have exceptional advantages during the first year owing to the use of the short age interval of three months.

Sontag, Snell and Anderson proposed that the entire left side of the skeleton should be used for the estimation of skeletal age in patients younger than 5 years, and they published tables showing the total number

Fig. 8-68—Disparity in maturation of the round bones in the left and right wrists of a healthy boy 3 years of age, in whom maturation of the epiphyseal ossification centers in the tubular bones of the same hands is identical. There are four centers in the left wrist and seven in the right. The four carpal centers in the left wrist agree with the boy's chronological age and with maturation

of the tubular bones in both hands. These findings demonstrate the principle that the carpal bones are much more erratic in development than the tubular bones in this patient as has been shown repeatedly in large groups of healthy infants and children.



BOYS

90th PERCENTILE (Advanced)



50th PERCENTILE (Average)



10th PERCENTILE (Slow)



Fig 8 69A - Normal maturation of the bones of the hands in boys. The wide range of normal at all age levels and sexual differences are noteworthy (Figs 8 69A and 8 69B from Vogt and Vickers)

GIRLS

90th PERCENTILE (Advanced)



50th PERCENTILE (Average)



10th PERCENTILE (Slow)



Fig 8 69B — Normal maturation of the bones of the hands in girls

BOYS

GIRLS

PERCENTILE

PERCENTILE

10th

50th

90th

10th

50th

90th



birth



3 mos



6 mos



9 mos



12 mos



Fig 8 70 — Normal maturation of the bones of the feet from birth to 1 year (According to Stuart)

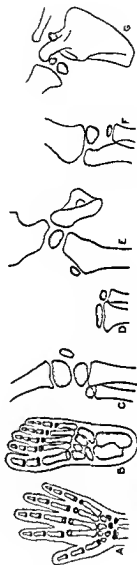
TABLE 8.3—NUMBER OF OSSIFICATION CENTERS AT DIFFERENT MONTHS OF AGE*

GIRLS

BOYS

AGE, Mo	AV. NO. CENTERS - M	RANGE OF VARIATION					RANGE OF VARIATION				
		M - 3 σ	M - 2 σ	M - σ	M + σ	M + 3 σ	M - 3 σ	M - 2 σ	M - σ	M + σ	M + 3 σ
1	48	19	0	29	67	96	105	0	28	86	95
2	57	20	0	37	77	107	117	0	39	85	120
3	65	20	0	45	65	115	125	0	51	101	139
4	89	28	0	61	117	159	173	0	57	113	151
5	98	24	0	74	122	156	170	0	64	124	164
6	112	24	0	88	136	172	164	0	72	132	188
7	125	20	0	98	154	196	212	0	87	143	184
8	130	17	0	113	147	173	161	0	94	155	191
9	136	17	0	109	183	204	217	0	98	161	204
10	152	35	47	117	190	240	257	0	103	187	223
11	158	32	62	128	190	238	254	0	111	197	235
12	165	49	16	142	214	268	282	0	124	225	251
13-15	199	63	10	151	262	357	386	0	137	256	313
16-18	235	84	0	171	339	485	507	0	158	296	434
19-21	255	84	0	215	319	445	487	0	164	338	469
22-24	323	92	47	231	415	553	599	0	179	378	510
25-27	368	55	203	313	423	508	523	0	196	327	459
28-30	396	84	146	314	462	608	650	0	204	340	481
31-33	441	48	297	321	393	489	585	0	214	356	502
34-36	485	58	311	340	427	543	630	0	229	388	556
37-42	495	69	288	322	426	564	668	0	237	407	595
43-48	506	49	419	443	517	615	689	0	241	417	571
49-54	593	55	428	455	536	646	731	0	259	401	543
55-60	618	35	513	530	583	700	723	0	268	429	573

*from Fiskmark, O. Acta paediatrica, vol. 33 suppl. 1 1946



Secondary centers in one side of the skeleton which are counted in the Eigenmark method: A, hand; B, foot; C, knee; D, wrist; E, hip; F, shoulder; G, elbow.

of secondary centers normally present in the left side of the skeleton at different ages from 1 to 60 months. In a careful study of a larger group of normal infants and children and with a more elaborate statistical evaluation of his data, Elgenmark (Table 8.3) confirmed the validity of Sontag's tables and the usefulness of the method. The technique is easy and inexpensive: the left side of the body, including the scapula is filmed, and all of the secondary centers present are counted, the number present is then compared with the number which should be present according to age, in the table, and it is readily manifest whether the patient has the normal number of centers, or too few or too many. The centers include all of the epiphyseal ossification centers in the long tubular bones of the legs, arms, hands and feet, the round bones of the tarsus and carpus, and the coracoid of the scapula. In older children the center for the greater trochanter of the femur must also be included in the count.

In an attempt to establish skeletal criteria for the onset of adolescence, Buehl and Pyle found that ossification appeared in the crest of the ilium within six months of the menarche (12.9 years) in two-thirds of 130 girls studied. These authors suggested that the age of inception of crestal ilial ossification in the male represents a maturational level analogous to the female maturational level at the menarcheal date. In males, ilial ossification appeared, on the average, at 14.5 years, or 1.6 years later than in females. In the proximal phalanx of the second digit of the hand, fusion of the epiphyses with the shaft also began near the menarcheal date, in the majority of girls this fusion began after the onset of the menstrual flow.

In the small bones of the wrists and ankles there is a great variability in the time of appearance and the order of appearance of the primary centers. Robinow found that in the same individual the secondary centers in the epiphyses of the tubular bones of the hands and feet often show wide discrepancies in comparison with the primary centers in the tarsals and carpals. These discrepancies between round bones and epiphyseal centers sometimes make it difficult or impossible to appraise the skeletal age according to the standards of Vogt and Vickers. Todd or Flory. Robinow made the interesting suggestion that two categories of skeletal age be established, "round bone skeletal age" and "epiphyseal skeletal age."

In a study of the variability in the order of appearance of the ossification centers of the bones of the hands and the wrists in 75 boys and 79 girls, Garn and Rohmann found that even the least variable children diverged substantially from the median sequence for the group. The sequence of appearance of the triquetrum and the trapezium and trapezoid bones differed in boys and girls. Deviant ossification patterns did not appear to be due to illnesses in these children. They also found that the hand wrist ossification count was not a precise measurement of the

developmental progress of the whole individual but was significant in the identification of growth abnormalities in groups of individuals. In a later analysis of the hand wrist development of 300 children with Silverman, they found the 10 most consistent secondary centers for appearance time to be in this diminishing order: distal phalanx, third finger, distal phalanx, fourth finger, proximal phalanx, second finger, third metacarpal, distal phalanx, fifth finger, distal phalanx, second finger, middle phalanx, fourth finger, fifth metacarpal, proximal phalanx, fifth finger, and middle phalanx, second finger. These findings confirm Robinow's conclusion that the sequence of the round bones in the wrist is more variable and therefore less useful than the sequence of appearance of the centers in the epiphyseal cartilages of the tubular bones of the hands. Surprisingly, the radial epiphyseal center was more variable than the epiphyseal centers in the small tubular bones of the hand.

In many older children there is a fair correlation between skeletal age before adolescence and ultimate adult height. Bayley and Pinneau published useful tables for predicting final adult height from skeletal age as determined from films of the hand. They claimed that after the 9th year juvenile skeletal age and mature height correlate in the degree of 0.86. The principal error in the method is the difficulty in estimating skeletal age accurately. The younger the subject, the greater the error of prediction. However, in boys older than 14 years and in girls older than 12 years, Bayley and Pinneau found that they could predict the mature height within 1 inch in approximately two-thirds of cases.

The method of Acheson which measures maturity from the differential features of the bones at different ages and expresses maturity in "maturity units" (Oxford units) rather than units of time promises to solve the difficulties in this problem.

The reader is referred to the paper of Falkner for an exceptionally clear and authoritative discussion of the basic principles of human development and of the methods available for its study. Biometry and statistics are presented simply and with refreshing clarity.

REFERENCES

- Acheson R. M. A method of assessing skeletal maturity from radiographs. *J Anat* 88:498, 1954.
- Bayley N., and Pinneau S. R. Tables for predicting adult height from skeletal age. *J Pediatr* 40:423, 1952.
- Christie A. Prevalence and distribution of ossification centers in the newborn infant. *Am J Dis Child* 77:355, 1949.
- Christie A., et al. The estimation of fetal maturity by roentgen study of osteal development. *Am. J Obst & Gynec* 60:133, 1950.
- Clark W. E. L. *The Tissues of the Body* (2d ed., Oxford: Clarendon Press, 1945) Fig. 37, p. 83.
- Dreizen S., et al. Bilateral symmetry of skeletal maturation in the human hand and wrist. *Am J Dis Child* 93:122, 1957.
- Danham E. C., Jenns R. M., and Christie A. Consideration of race and sex in relation to growth and development of infants. *J Pediatr* 14:156, 1939.

- Elgeemark O Normal development of the ossific centers during infancy and childhood. *Clinical roentgenologic and statistical study* Acta paediat. vol 33 supp 1 1946
- Falkner F The physical development of children. A guide to growth charts and development assessments and a commentary on contemporary and future problems. *Pediatrics* 29:441 1962
- Francis C C, Werle P P and Behm A The appearance of centers of ossification from birth to five years. *Am J Phys Anthropol* 24:273 1939
- Gallagher J R Various aspects of adolescence. *J Pediatr* 39:532 1951
- Garn F M and Rohmann C G Variability in the order of ossification of the bony centers of the hand and wrist. *Am J Phys Develop* 18:219 1960
- et al The number of hand wrist centers. *Am J Phys Develop* 18:293 1960
- Greulich W W and Pyle J S *Radiographic Atlas of Skeletal Development of Hand and Wrist* (2nd ed. Stanford Calif. Stanford University Press 1959)
- Harding V S V A method of evaluating osseous development from birth to 14 years. *Child Devel* 23:247 1952
- Hill A H Fetal age assessment by centers of ossification. *Am J Phys Anthropol* 24:251 1939
- Hoerr N L et al *Radiographic Atlas of Skeletal Development of the Foot and Ankle* (Springfield Ill. Charles C Thomas Publisher 1962)
- Kelly H J and Reynolds L Appearance and growth of ossification centers and increases in the body dimensions of white and Negro infants. *Am J Roentgenol* 57:477 1947
- Mall F P On ossification centers in human embryos less than 100 days old. *Am J Anat* 5:433 1905-06
- Menees T O and Holly L E Ossification in the extremities of new born. *Am J Roentgenol* 28:399 1932
- O Rahilly R and Meyer D B Roentgenography of the fetal skeleton. *Am J Roentgenol* 76:455 1956
- Park E A Bone growth in health and disease. *Arch Dis Childhood* 29:269 1954
- Robinson M Appearance of ossification centers. Groupings obtained from factor analyses. *Am J Dis Child* 64:229 1942
- Sawtell R W How children grow. *Univ Iowa Studies in Child Welfare* 5:7 1931
- Scammon R E in Morris Human Anatomy (10th ed. Philadelphia. Blakiston Company 1942).
- Sontag L W, Snell D and Anderson M Rate of appearance of ossification centers from birth to the age of five years. *Am J Dis Child* 58:949 1939

Anatomic Variations

LOCAL

There are numerous anatomic variants in the growing skeleton which closely simulate the destructive and productive lesions caused by disease. The diagnostician must be familiar with the sites of these variants, their character and the age of their appearance and disappearance if he is to evaluate films accurately and if he is not to give children diseases which they do not have. Air trapped between the fingers may simulate fractures when superimposed on phalanges (Fig. 8-71). Full knowledge of these common variants is much more important and useful than knowledge of the roentgen signs of the diseases themselves. I am convinced that many of the so-called cases of infantile and juvenile osteochondritis or osteochondritis described in the literature are actually examples of unrecognized and wrongly interpreted normal varia-



Fig. 8-71—Strips of air trapped between the fingers in lateral oblique projection are superimposed on the proximal phalanges of digits three and four and simulate longitudinal fractures in them. The patient was an asymptomatic girl 2 years of age. The bones were normal of course. (Frontal projection.)

tions in the bones rather than ischemic necrosis. The cases of Perthes disease are of course excepted. However, it is exceedingly difficult to differentiate slight changes due to stress from normal variants (Figs. 8-72 to 8-74).

Metaphyseal cuppings without conical epiphyseal ossification centers, both single and double, are occasionally found in the phalanges of apparently healthy children (Fig. 8-75). In an otherwise healthy girl of 22 months the terminal segments of the thumbs and fingers were elongated owing to enlargements of the epiphyseal ossification centers of the distal phalanges (Fig. 8-76). These changes were bilaterally symmetrical and might be classified as congenital malformations rather than normal variants.

During the first decade of life the epiphyseal ossification centers in the proximal epiphyses of the metacarpals are roughly hemispherical. During the 9th, 10th and 11th years the sides of the ossification centers become flattened and even cupped on their medial and lateral sides (Fig. 8-77). This lateral flattening and cupping begins characteristically in the fifth metacarpal and is usually more pronounced on the lateral than on the medial side of the hand. The other metacarpals become flattened and cup progressively from lateral to medial sides of the hand and during later years the cupping is more marked on the lateral sides of the metacarpals. This metaphyseal flattening

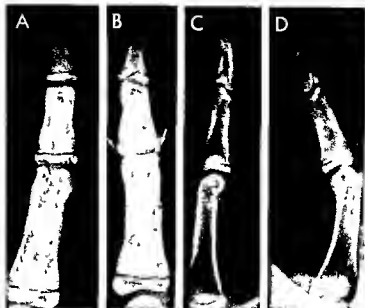


Fig 8-72 —Pseudofracture of the epiphyseal ossification center. In B, frontal projection, the middle phalanx of the third digit (arrow) is smaller and not fully extended. As a result, the radiolucent strip of the cartilage plate is superimposed obliquely on the body of the epiphyseal ossification centers. The second digit in

A frontal projection is not swollen and is fully extended so the cartilage plate is not superimposed on its epiphyseal ossification center and there is no false fracture. In C, lateral projection of the second digit, the finger is fully extended, the partial flexion of the third digit is shown in D, lateral projection.

Fig 8-73 —A, spurious marginal fractures of the epiphyseal ossification centers of the middle phalanges of the second and fourth digits due to slightly oblique superimposition of the radiolucent cartilage plate on the epiphyseal ossification centers of the middle phalanges of the second and fourth digits (arrows). The patient was a healthy girl 13 years of age. B, false fractures of the epiphyseal ossification centers (arrows) of the middle phalanges due to slight flexion of the proximal interphalangeal joints which cause superimposition of the radiolucent cartilage plate on their epiphyseal ossification centers.

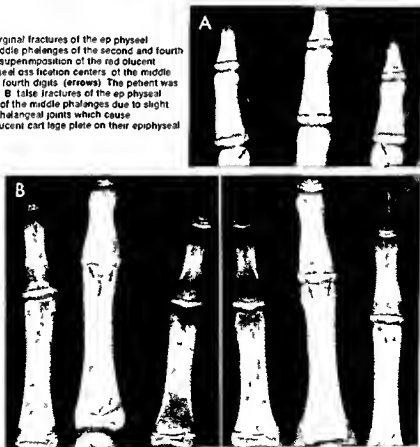




Fig 8-74—Spurious fractures in the epiphyses of the centers of the middle phalanges of the second third and fourth digits caused by oblique superimposition of the ends of the radiolucent cartilage plates on the bony epiphyseal ossification centers.



Fig 8-75—Uneven cupping of the proximal metaphyses of the fourth and fifth digits in an asymptomatic boy 5½ years of age. The cuppings are double in the middle phalanx of the second digit and the proximal phalanges of the fourth and fifth digits. Shallow metaphyseal cuppings are present in the proximal ends of all of the metacarpals. The epiphyseal ossification centers are not cone-shaped.

Fig 8-76—Bilateral symmetrical enlargements of the epiphyseal ossification centers of all of the distal phalanges in both hands of an otherwise healthy girl 22 months of age. These hypertrophies are probably attributable to hyperemia of the epiphyses.

seal ossification centers due to congenital hypertrophy of the epiphyseal arterioles which supply these enlarged epiphyseal ossification centers in the distal phalanges.





Fig. 8-77—Lateral flattening and cupping of the epiphyseal ossification centers of the metacarpals of a boy 13 1/2 years of age. The cuppings are deeper on the lateral sides in each meta-

carpal but both sides of the epiphyseal ossification centers are cupped in metacarpals 2 and 5. The cups become progressively deeper as age advances to adulthood.

of the epiphyseal ossification centers is prominent and is a consistent finding during adolescence and its degree of involvement is a good measure of age during adolescence.

REFERENCES

- Kochler A. *The Borderlands of the Normal and the Early Pathological in the Skiagram* (New York: William Wood & Company 1928).
- Pyle J. A. *The meaning of normal*. *Lancet* 1:1 1947.

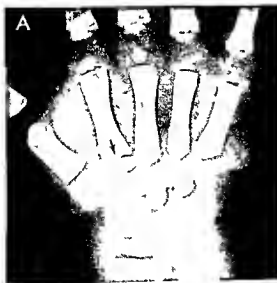
HAND AND WRIST—In the basal phalanx of the thumb and in the middle phalanges of the other fingers small oval sharply defined defects are frequently visible; these represent the nutrient foramina to the shafts of these bones. They are rare in the distal

or proximal phalanges save in the thumb. Similar radiolucent defects in the round carpal bones cast by nutrient foramina may be mistaken for cysts or destructive foci. The middle and terminal phalanges of the fifth digits are said to be hypoplastic in a small fraction (1/100) of normal children. In Down's syndrome (mongoloidism) a large proportion of patients have a similar hypoplasia which is responsible for the curvature of the fifth digit; one of the consistent stigmas of the disease. The radiographic appearance of the mongoloid hand was reported by Telford Smith in July 1896; only a few months after Röntgen had reported the discovery of x-rays. Cretins and achondroplasts occasionally show the same hypoplasias.

Extra and false epiphyseal ossification centers may appear in the proximal epiphyseal cartilages of

Fig. 8-78—Accessory and false secondary ossification centers in the proximal epiphyseal cartilages of the metacarpals of normal infants. A, in the second metacarpal of an infant 12 months of age; a similar accessory center was present in the other hand.

B, false centers in the second, third, fourth and fifth metacarpals of a child 2 years of age; similar false centers were present in the other hand.



the second, third, fourth and fifth metacarpals and metatarsals, where usually the cartilages are ossified progressively by extension of the edge of the shaft in a smooth transverse edge. Extra or supernumerary ossification centers appear well out beyond this edge as individual bony foci which then grow peripherally and finally fuse with the advancing edge of the shaft. The false centers are merely rods of bone which extend off the edge of the shaft into the cartilage and simulate partially fused ossification centers when their proximal ends swell into a mushroom shape or their bases constrict near their junction with the shaft. Examples of these variants are shown in Figures 8-78, 8-161, 8-569, 8-817 and 8-818. Lee and her colleagues called this phenomenon, in the second and fifth metacarpals, "metacarpal notching" and found no correlation between the notching and either stature or maturation, in a comparison of these features in children without notching. It should be emphasized that the term "pseudoepiphyseal" for accessory or pseudo-ossification center is a misnomer, there

is no such anatomic entity as a pseudoepiphyseal.

In studies of the maturation of the phalanges of the toes by Stanley M. Garn of the Fels Research Institute, absence of epiphyseal ossification centers (EOC) had a surprisingly high incidence in the middle phalanges and a less high but substantial incidence in the distal phalanges. This incidence of absence was higher in girls, tended to be familial, which indicated a strong genetic influence, and was clearly sex linked. Absence of EOC led to fusion of primary centers of the shafts frequently. In the middle phalanges of girls, EOC were absent in 99%, 70, 24 and 1% in the fifth, fourth, third and second toes respectively, and in boys in 98%, 54, 16 and 2% respectively. In the distal phalanges of girls, EOC were absent in 31%, 1 and 1% in the fifth, fourth and third toes, and in boys in 35%, 1 and 0.5% respectively.

In asymptomatic children there is a wide variation in the density of the epiphyseal ossification centers of the phalanges: some may be sclerotic when others are less dense (Fig. 8-79). The diagnosis of osteochon-

Fig. 8-79 — Physiologic sclerosis of the epiphyseal ossification centers in the phalanges of asymptomatic children. A, of the distal phalanges of digits 2, 3, 4 and 5 of a girl 8 years of age. B, in the terminal phalanges of digits 2 and 5 of a boy 6 years of age.

C, symmetrical sclerosis in both hands, digits 3, 4 and 5 of the middle phalanges of a girl 5 years of age. These sclerotics do not warrant the diagnosis of sclerotic epiphyses when pain or limitation or swelling appears in the hands.

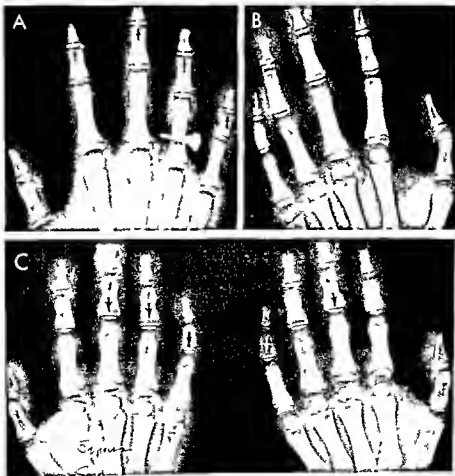




Fig 8-80—Transitory internal thickening of the cortical walls of the metacarpals in the newly born (arrows). The first metacarpal is thickened on its ulnar side, while the second and third bones are thickened on the radial sides. These regional thickenings disappear gradually during the first weeks after birth.

dritis or epiphysitis is not warranted on the basis of this healthy sclerosis. It seems likely that the changes in Staples's patient represented healthy sclerosis rather than osteochondritis.

The neonatal metacarpals present distinctive thickenings of their cortical walls. In the first metacarpal the medial wall is thicker than its lateral cortical wall and the converse is true of the second metacarpal (Fig 8-80). After the first weeks of life the originally thinner medial (ulnar) cortical wall of the second metacarpal becomes thicker than its lateral (radial) counterpart. The transitory early thickening of the lateral (radial) cortical wall of the second metacarpal is probably due to stress from prenatal position of the hand. Lateral and medial cupping of the epiphyseal ossification centers (Fig 8-81) first becomes evident

Fig 8-81—Late lateral and medial cupping of the sides of the epiphyseal ossification centers in the metacarpals of a healthy girl 13 years of age.

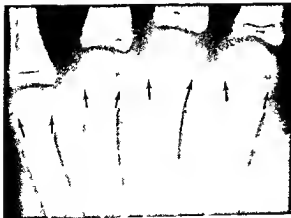


Fig 8-82—Accessory ossicle, the epilunatum, in an asymptomatic girl 16 years of age.

in girls at about 10 years of age and in boys at 12-13 years. Gann and associates found medullary stenosis of the metacarpals in 74 of 2065 native healthy women of Central America, 18-45 years of age. The highest incidence was found in Costa Ricans (66/1000).

The lunate may show two centers early (Fig 8-82) which may fuse later or persist as separate ossicles, lunate and epilunatum. Sometimes the lunate and triquetrum fuse and give rise to a spurious fracture line at their site of fusion (Fig 8-83). Minaar suggested that this fusion represents a persistence of a primitive characteristic in African (Negro) peoples. The hook of the hamate, which is invisible during the early years of childhood, should not be mistaken for a separate ossicle or a fracture fragment when it becomes conspicuous prior to adolescence (Fig 8-84). The pisiform, the smallest carpal bone and the last to

Fig 8-83—Fusion of the lunate and triquetrum in an asymptomatic 17 years of age in a case of injury that caused a fracture line.





Fig 8 84—Hook of the hamate in an asymptomatic boy 12 years of age. The normal uncinate process should not be mistaken for a fracture fragment or an accessory ossicle. The hook of the hamate is not visible on roentgenography during infancy and early childhood because it is not mineralized. The third arrow is directed at a rounded sesamoid bone in the tendon of the flexor pollicis longus and is adjacent to the first metacarpophalangeal joint.

appear often ossifies from several small foci (Fig 8-85) and it may remain granular for years after it first appears. The diagnosis of osteochondrosis juvenilis of the pisiform should be made with caution. In the earliest stages of their development the multangulars may be rough and irregular (Fig 8-86) in healthy infants who show no local signs of disease. Ravelli described binuclear ossification of both multangular bones and of the semilunar bone in a boy 6 years of age. In a second patient a girl of 6 the greater multangulars only exhibited double ossification centers.

A comprehensive detailed summary of anomalies in

Fig 8 85—Normal irregular mineralization of the pisiform. A, first multiple bony foci in the pisiform of an asymptomatic boy 9



Fig 8 86—Normal irregular mineralization of the greater multangular in a girl of 2 years.

the carpal bones was made by O Rahilly (Fig 8-67) and his data are recommended to the reader for the identification of rare anomalies of fusion, accessory ossicles, accessory sesamoids, bipartite bones, and anomalies caused by mechanical stresses of disease. O Rahilly concluded that some of the postnatal accessory ossicles are formed prenatally because nodules of hyaline cartilage have been found in embryos at sites corresponding to the sites of the ossicles found postnatally.

During the first months of life the distal ends of the ulnar and less frequently the radial shafts may present a cupped transverse surface instead of the customary straight transverse surface seen in most infants. Physiologic cupping of this type should not be misinterpreted as rachitic cupping. We have seen defects in the proximal metaphysis of the radius which were apparently due to repeated slight stress

years of age. B, granular pisiform in an asymptomatic boy 12 years of age.



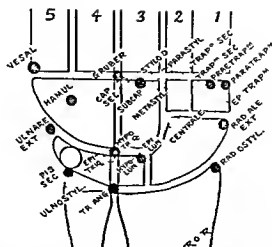
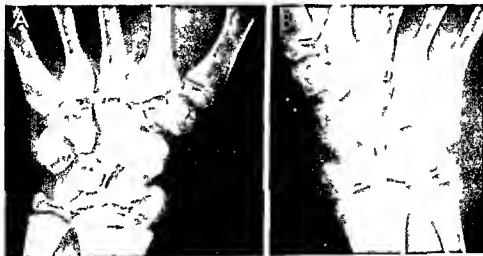


Fig. 8-87—Accessory bones in the right hand according to O'Rahilly. The palmar aspect of the right hand is drawn schematically with the more dorsally situated ossicles shown in broken outline.

ca. ly with the more dorsally situated ossicles shown in broken outline.

Fig. 8-88—Metaphyseal defect in the lateral segment of the metaphysis of the right radius in a girl 10 years of age who was an expert cellist and had reputedly practiced several hours daily for

several years. This could perhaps be classified more properly as a stress defect than a nonmelvarient. (A) right hand and wrist; (B) left hand and wrist.



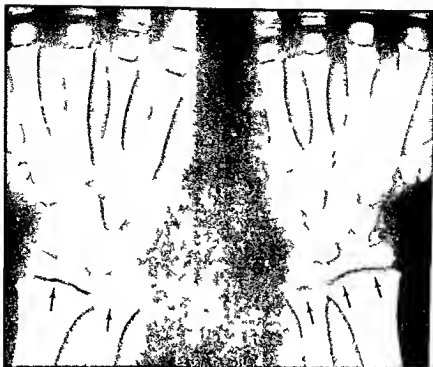


Fig. 8-89—Physiologic wavy irregular lines in the distal metaphyses of the radius and ulna in an asymptomatic 10 years of age; none of the other bones showed similar changes

over several years (Fig. 8-88). During the latter half of childhood the radius and ulna may terminate in wavy irregular surfaces (Fig. 8-89) in normal children whose other bones show normally smooth diaphyseal ends. We have seen some healthy children who before and during adolescence showed multiple bony foci in the cartilage between the shaft and the epiphyseal ossification center (Fig. 8-90) possibly these

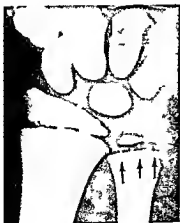
foci represent calcifications in the portions of the cartilage contiguous to the channels of the epiphyseal arteries but so far as we know these calcifications have not been studied anatomically. Separate ossification centers for the styloid of the ulna are not uncommon (Fig. 8-91) and they should not be mistaken for fracture fragments.

The number and distribution of the sesamoids of

Fig. 8-90 (left)—Small independent bony foci in the epiphyseal cartilage of the ulna of a healthy rapidly growing girl 9 years of age.

Fig. 8-91 (right)—Separate secondary epiphyseal ossification centers for the styloid in the distal epiphyseal cartilage of the ulna of an

asymptomatic boy 11 years of age. Ossicles of this type should not be mistaken for fracture fragments in case of injury. Such separate ossification centers may later fuse with the main epiphyseal ossification center or may persist throughout life as separate ossicles.



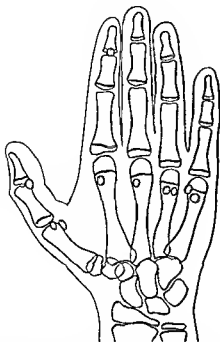


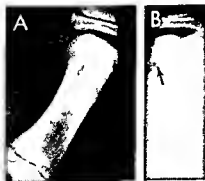
Fig 8 92 —The location and distribution of the constant and nonconstant sesamoid bones of the hands. Five sesamoids are of almost constant occurrence: the pair at the base of the thumb which appear just before adolescence; the single sesamoid most distal in the thumb; and the solitary sesamoid at the bases of the second and fifth digits. Five additional sesamoids are shown.

the hands are shown in Figure 8 92. The sesamoids are usually identified clearly radiographically but when they are partially superimposed on the neighboring metacarpal they may simulate fracture fragments (Fig 8 93).

REFERENCES

Lachman E. Pseudo-epiphyses in hand and foot. *Am J Roentgenol* 70:149, 1953, editorial.

Fig 8 93 —Sesamoid superimposed on the metacarpal simulates a fracture fragment. In A, lateral projection, the smooth sesamoid is seen in its entirety. In B, lateral oblique projection, the sesamoid is superimposed on the edge of the first metacarpal at the level of the normal notch and simulates a small rough fracture fragment.



- Lee M M C et al. Relation of metacarpal notching to stature and maturational status of normal children. *Invest Radiol* 3:95, 1968.
- Minaar A B de V. Congenital fusion of the lunate and trapezoidal bones in the South African Bantu. *J Bone & Joint Surg* 34 B:45, 1952.
- O'Rahilly R. A survey of carpal and tarsal anomalies. *J Bone & Joint Surg* 35-A:626, 1953.
- Epitriquetrum, hypotriquetrum and lunotriquetrum. *Acta radiol* 39:401, 1953.
- Developmental Deviations in the Carpus and Tarsus. In De Palma A F (ed.) *Clinical Orthopaedics* (Philadelphia: J B Lippincott Company, 1957) Vol 10, p 9.
- Ravelli A. Ossification of the multangular bones. *Fortschr Geb Röntgenstrahlen* 83:852, 1955.
- Schreiber M H et al. Reliability of the distal femoral epiphyses as a measure of maturity. *Am J Obst & Gynec* 83:1249, 1962.
- Smith T T. A peculiarity in the shape of the hands in idiots of the mongol type. *Pediatrics* 2:315, 1896.
- Staples O S. Osteochondritis of the epiphyses of the terminal phalanges of the fingers. *J Bone & Joint Surg* 25:917, 1943.
- Wauh R L and Sullivan F. Anomalies of the carpus with particular reference to bipartite scaphoid (navicular). *J Bone & Joint Surg* 32-A:682, 1950.
- Weinert P. Ein Beitrag zur Frage der Pseudo-epiphysen. *Anat. Anz.* 99:1, 1952.
- White E H. Bilateral congenital fusion of the carpal capitate and hamate. A case report. *Am J Roentgenol* 52:406, 1944.

FOREARM —Ridges on the middle third of the shaft of the ulna and radius are sometimes prominent and cast narrow peripheral shadows suggestive of cortical thickening. Owing to a more delicate and less opaque spongiosa, the lateral half of the radius is more radiolucent than the medial half. The widely meshed spongiosa in the proximal end of the ulna normally casts a widely spaced reticular shadow which should not be mistaken for bone destruction. Canals for the nutrient artery are visible in the olecranon process in 15-20% of healthy children (Figs 8-94 to 8-96). Variations in the thickness of the cortical wall and in the spongiosa of the proximal end of the ulna may simulate fracture lines (Fig 8-97). This healthy defect should be remembered when the question of destructive disease is raised at this site. The spongiosa in the proximal end of the radius is, in contrast, thick and coarse.

ELBOW —The several secondary epiphyseal centers can be satisfactorily identified only after two projections have been visualized (Fig 8-98). In frontal projections the center or centers in the olecranon are superimposed on the humerus and are poorly seen. The trochlear center is consistently irregularly mineralized and always develops from several small foci (Fig 8-99). Single and multiple secondary ossification centers in the olecranon epiphyseal cartilage may simulate fracture fragments (Figs 8-100 and 8-101). The lateral epicondyle does not fuse directly with the humeral shaft as the medial epicondyle does but instead fuses first with the neighboring epiphyseal ossification center the capitulum; then their fused mass fuses with the end of the humeral shaft (Fig 8-102). In cases of injury the position of the various centers

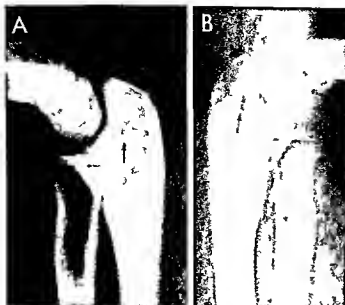
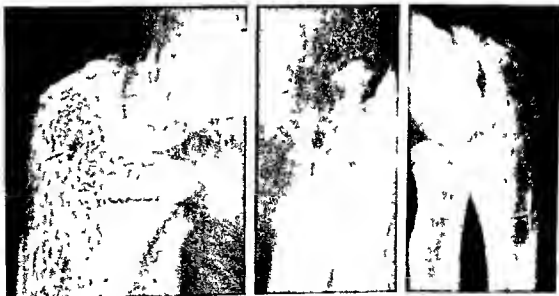


Fig 8-94 —Bilateral symmetrical nutrient canals in the olecranon process in the ulnas of a healthy girl 10 years of age

Fig 8-95 (left) —Detail of the canal for the nutrient artery of the olecranon of a healthy girl 9 years of age. The oval bony edge is sclerotic, which differentiates the foramen from the ordinary destructive lesion.

Fig 8-96 (center) —Unusually large foramen for the nutrient artery of the ulna with unusually sclerotic margin. There were no foramina in the olecranon of the other ulna. This asymptomatic boy was 14 years of age.

Fig 8-97 (right) —Longitudinal strip of diminished density (arrow) in the proximal end of the ulna which simulates a longitudinal fracture. Longitudinal grooves and ridges in the cortical wall and longitudinal defects in the spongiosa are responsible for changes of this type. This was an asymptomatic boy 14 years of age.



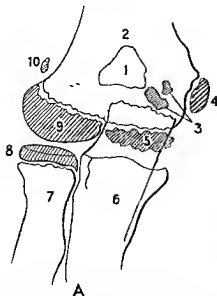


Fig 8 98 — Normal secondary epiphyseal ossification centers at the elbow. **A**, frontal projection. **1** olecranon fossa **2** shaft of the humerus **3** centers of the olecranon process **4** medial epicondyle **5** trochlea **6** shaft of the ulna **7**

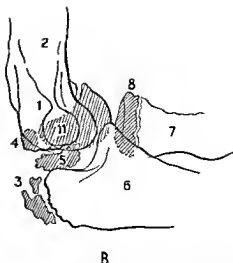
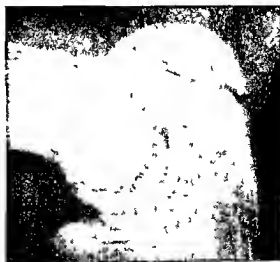


Fig 8 98 — Normal secondary epiphyseal ossification centers at the elbow. **B**, lateral projection. **1** olecranon fossa **2** shaft of the humerus **3** centers of the olecranon process **4** medial epicondyle **5** trochlea **6** shaft of the ulna **7** capitulum of the radius **8** caputulum of the radius **9** capitulum of the humerus **10** lateral epicondyle **11** lateral projection of the distal humerus

Fig 8 99 — Normal irregular ossification center of the trochlea of a healthy boy 13 years of age. The irregular ossification of the trochlea persists throughout the growth period and should always be recognized as a normal variant. Actually it is the norm. The capitulum, in contrast, ossifies uniformly as it expands during the growth period.



Fig 8 100 — Synchondrosis of a partially fused angle. Normal secondary ossification center of the olecranon which simulates an incomplete fracture line. The patient was a healthy boy 13 1/2 years of age.



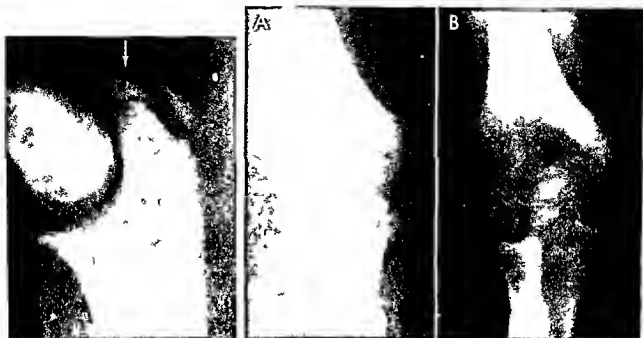


Fig 8 101 (left) —Multiple ossification centers in the olecranon epiphysis which simulate multiple fracture fragments at the elbow. The patient was a healthy boy 11 years of age.

Fig 8 102 (right) —The lateral epicondyle center is independent of both the capellum and the shaft in A, at 11 years. It has

already fused with the capellum in B, at 12 1/2 years, and these combined ossification centers will later fuse with the shaft. The medial epicondyle center is fusing directly with the shaft in A and B. In B the trochlea is normally irregular.

Fig 8 103 (left) —Frontal projections of the right (A) and left (B) elbows of an asymptomatic girl 11 years of age. The ossification center for the right lateral epicondyle (arrow) is large and has been present for several months. On the left, this ossification center has not yet appeared.

Fig 8 104 (right) —Frontal projection of the right elbow of a healthy girl 11 years of age. The lower arrow points to a small smooth independent image of bone density at the level of the trochlea. The upper arrow points to the medial epicondyle.





Fig 8-105 (left) —False longitudinal oblique fracture line in the medial epicondyle of the humerus of a healthy boy 15 years of age. The radiolucent line is cast by the superimposed radiolucent shadow of the cartilage plate between the ossification center of the epicondyle and the bony side wall of the humerus. Also there is a small rounded independent mass of bone at the lower pole of the epicondyle which could be mistaken for a fracture fragment.



Fig 8-106 (right) —False fracture line and fragment at the lower pole of the medial epicondyle of the humerus (upper arrow) of a healthy boy 10 years of age, cast by an accessory ossification center and its radiolucent synchondrosis at the lower pole. The lower arrow points to an accessory center of the trochlea.

should be carefully identified before epiphyseal laceration and displacement have been excluded.

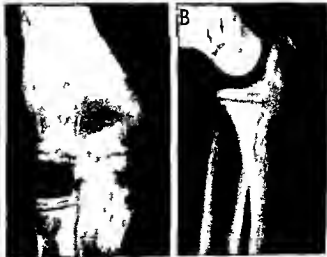
The ossification center for the lateral epicondyle on one side may appear several months before its normal counterpart on the other side (Fig 8-103) and be mistaken for a fracture fragment in the case of injury at this elbow. A small smooth independent center for the trochlea may simulate a fracture fragment (Fig 8-104). Accessory ossification centers in the epicondyles of the humerus also simulate fracture fragments.

Fig 8-107 (left) —Multiple ossification centers in the lateral epicondyle of the humerus which could be mistaken for comminuted fracture fragments after injury to the elbow. This healthy boy was 12 years of age.



(Figs 8-105 to 8-107) The radiolucent cartilage plate the dorsal segment of which is more proximal than the ventral segment often casts a transverse strip of diminished density in the lateral half of the humerus which simulates a fracture line (Fig 8-108). Air trapped in the transverse and curved wrinkles of the skin cast radiolucent strip images which may be confused with fracture lines (Figs 8-109 to 8-111). Rarely a sesamoid bone develops in the triceps tendon (patella cubiti). The secondary ulnar centers are char-

Fig 8-108 (right) —A false transverse fracture line just proximal to the capitulum of the humerus, cast by the dorsal segment of the radiolucent cartilage plate, which is situated more proximal than the ventral segment. A frontal and B lateral projection. The patient was a healthy boy 12 years of age.



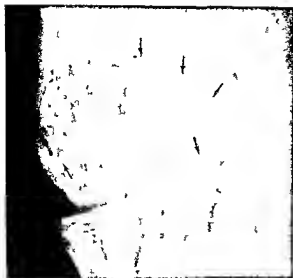


Fig. 8-109 (left) —Curved line of diminished density (3 arrows) simulates a supracondylar fracture line in the medial half of the end of the humerus. This radiolucent line is cast by a wrinkle of skin behind the elbow during full extension of the elbow and then compression against the cassette which traps air in the wrinkle. The other arrows are directed at (1) the radiolucent cleft between the lateral epicondyle and the shaft cast by the partially closed radiolucent synchondrosis (2) the radiolucent synchondrosis of the trochlea (3) the radiolucent synchondrosis of the medial epicondyle superimposed on part of the main body of the epicondyle. This healthy girl was 10 years of age.

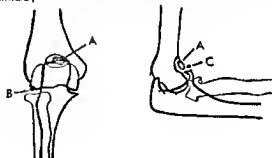


Fig. 8-110 (right) —Curved radiolucent band superimposed on the medial half of the end of the humeral shaft which simulates a fracture with substantial distraction of the fragments. The band extends 15–20 mm beyond the medial edge of the bone and is obviously not a fracture line. It is cast by a radiolucent strip of air trapped in a curved wrinkle of skin behind the elbow during extension. The wrinkling is caused by full extension and compression against the cassette. This asymptomatic boy was 6 years of age.

Fig. 8-111 —Transverse band of radiolucent air trapped in a cutaneous wrinkle which is superimposed on the supracondylar level of the end of the humeral shaft and could be mistaken for a transverse supracondylar fracture in the case of injury to this elbow. The patient was a healthy girl 20 months of age.



Fig. 8-112.—Rare accessory ossicles of the elbow. A entecubital bone B peritrochlear bone C accessory coronoid (From Schwarz)



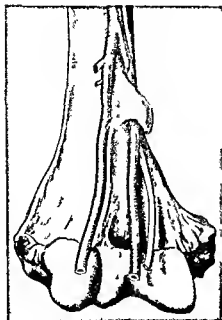


Fig. 8-113—Drawing of the supracondylar process on the anterior surface of the humerus which shows the relation of the process to the brachial artery and its branches and the median nerve (From Barnard and McCoy)

characteristically rough occasionally the radial and humeral centers present irregular edges and a granular texture in asymptomatic children Schwarz pointed out that there are less common anomalous ossicles

Fig. 8-114—The supracondylar process. A and B in a healthy child 5 years of age. In A the frontal projection on the process superimposed on the shaft of the humerus casts a small opaque formless image (arrow). In B lateral projection a short thick

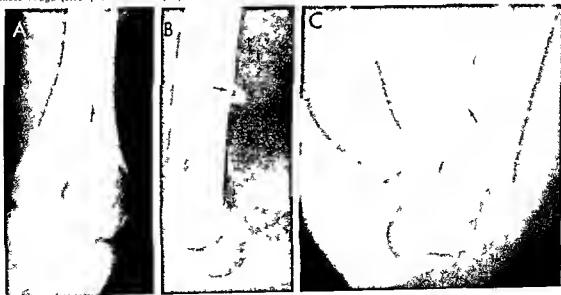
hooklike bony mass extends ventrad off the ventral edge of the humeral shaft. C the supracondylar process is often bilateral and varies little in its longitudinal position on the humeral shaft in different individuals. This boy was 3 years of age.

at the elbows—the antecubital bone the paratrochlear bone and the accessory coronoid (Fig. 8-112). In the distal end of the humerus the bony septum which separates the olecranon fossa behind from the coronoid fossa in front varies in thickness and casts a shadow of variable density. Extraradiolucency in this area should not be mistaken for bone destruction. Occasionally the septum is perforated or absent and a supratrochlear foramen is present; this foramen is said to be more frequent in primitive peoples. The supracondylar process is a vestigial structure which projects from the medial aspect of the anterior surface of the humeral shaft (Fig. 8-113). This process is said to be present in about 1% of persons of European stock; only in rare instances is it associated with clinical signs, usually median nerve neuralgia. The process is not well seen in frontal projections of the humerus but in lateral and especially oblique projections is clearly visualized as a beaklike exostosis in front of the anterior humeral edge (Fig. 8-114). The supracondylar process may be connected below with a tendinous band which extends to the medial epicondyle and an anomalous insertion of the pronator teres when this band is calcified it outlines the supracondylar foramen.

REFERENCES

- Barnard L. B. and McCoy S. M. The supracondylar process of the humerus. *J. Bone & Joint Surg.* 28:845, 1946.
 Habbe J. E. Patella cubiti: A report of 4 cases. *Am. J. Roentgenol.* 48:513, 1942.
 Iannaccone G. and Banilla M. Die zystenartigen Gebilde

hooklike bony mass extends ventrad off the ventral edge of the humeral shaft. C the supracondylar process is often bilateral and varies little in its longitudinal position on the humeral shaft in different individuals. This boy was 3 years of age.



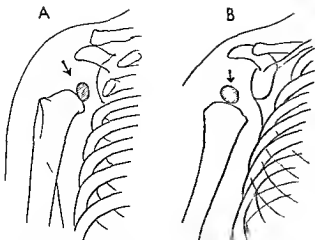


Fig 8-115—Factitious shift in position of the normally eccentric proximal ossification center of the humerus caused by rotation of the bone. A, anatomic position of the humerus with the ossification center in the medial segment of the epiphysis. B, with the humerus in internal rotation, the ossification center appears to be displaced laterad. Tracings of roentgenograms. The patient was 8 months of age.

am Proximalende der Ulna, Fortschr Geb Röntgenstrahlen 64:598, 1956

Levine M. A. Patella cubiti. J Bone & Joint Surg 32 A:686, 1950

Schwartz G. S. Bilateral antecubital ossicles (fabella cubiti) and other accessory bones at the elbow. Radiology 69:730, 1957

Caution should be used in the diagnosis of displacement of the proximal humeral centers for they are normally eccentric. The first center to appear develops in the medial half of the epiphysis. When the arm is rotated internally this eccentric center shifts to a factitious lateral position (Fig 8-115). Internal

rotation of the humerus causes the shadow of the bicipital groove and its companion tubercular ridges in the proximal segment of the humerus when the humerus is rotated externally and these structures are seen in profile. They are not visible when the humerus is in anatomic position because they are superimposed on the heavy shadow of the shaft. A, in a healthy infant 9 months of age with

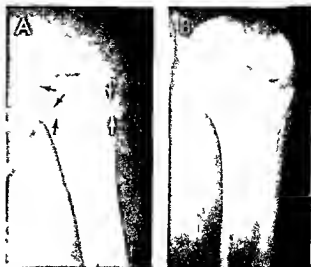
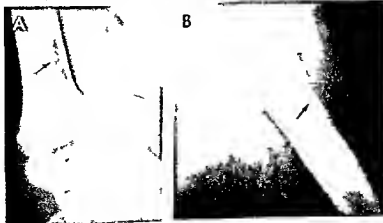


Fig 8-116—A, false fracture (arrows) of the humeral neck on internal rotation to 90 degrees. B, there is no fracture line in anatomic position. The radiolucent cartilaginous plate at the end of the shaft is not a straight plate transverse to the long axis of the shaft but is tented with the apex well above the pitched anterior and posterior segments. The anterior pitch is wider and deeper than the posterior and it is the image of the segment below the posterior end of the shaft which casts the factitious fracture line.

rotation is the characteristic position of the humerus in Erb's palsy and the importance of rotation as a cause of spurious malposition of the ossification center should be considered before diagnosing epiphyseal displacement.

At the proximal end of the humerus the radiolucent cartilaginous strip between the head and shaft is continuous but the lateral segment lies distal to the medial segment (Fig 8-116 A). When the humerus is

the arm elevated (abducted) over the head and the anterior wall of the humerus rotated into a lateral position. B, in an infant 12 months of age with the arm partially abducted and its anterior wall rotated into the lateral position. This normal depression and its radiolucent shadow must not be mistaken for destructive lesions of inflammatory or neoplastic origin.



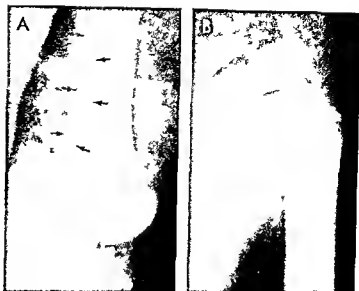


Fig 8-116 — The normal shadow of the bicipital groove in the proximal end of the humerus. A: the humerus in full abduction and external rotation; the groove appears as a shadow of diminished density. B: the same humerus in anatomic position; the groove is invisible because it is superimposed on the heavy shadow of the humeral shaft.

internally rotated 90 degrees the two radiolucent strips—the medial segment proximal and the lateral segment distal—may suggest an epiphyseal plate and a fracture line (Fig 8-116 B) to the unwary.

The bicipital groove in the anterior surface of the proximal end of the humeral shaft varies greatly in different individuals but may be sufficiently deep even during the first months of life to cast a shadow of diminished density when the anterior surface of

Fig 8-119 — End of one bicipital ridge which simulates a spur or a localized traumatic thickening. The patient was an asymptomatic boy 4 1/2 years of age.



the shaft is projected in profile (Fig 8-117); this groove shadow should not be mistaken for a destructive lesion. In some oblique projections the two tubercular ridges which parallel the groove overlap and the crest of one of the ridges gives the spurious appearance of localized cortical thickening (Figs 8-118 and 8-119).

Fromson and Alfred found a large partite sesamoid bone in the subscapularis tendon of a man 28 years of age.

Cocchi demonstrated that the lesser tuberosity has a secondary ossification center of its own which makes its first appearance during the 3rd year and then fuses with the humeral head during the 6th and 7th years. This third ossification center in the proximal epiphyseal cartilage of the humerus is best seen when the arm is rotated externally and abducted to a right angle; the central beam of x rays is directed into the axillary fossa with the roentgen tube parallel to the sagittal diameter of the thorax and inclined 10 degrees caudad.

REFERENCES

- Cocchi, U. Zur Frage der Epiphysenossifikation des Humerusköpfes. Das Tuberculum minus. *Radiol clin* 19:18, 1950.
 Fromson H. and Alfred K.S. Sesamoid bone in the subscapularis tendon. *J Bone & Joint Surg* 43-A:881, 1961.

FEET — Phalanges and metatarsals — Accessory ossification centers may develop in the distal phalanx of the great toe (Fig 8-120). Normal dysplastic splitting of the cartilaginous plate may produce a factitious fragment fracture at the base of the shaft of the distal phalanx, great toe (Fig 8-121). The foramen and canal for the nutrient artery of the proximal phalanx of the great toe is usually visible in both frontal

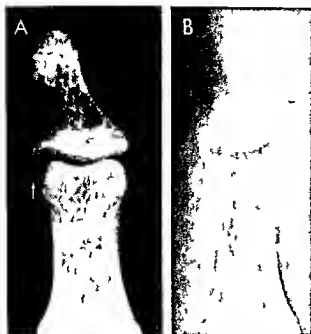


Fig 8-120—Accessory ossicle in the styloid process laterally of the distal phalanx of the right great toe of a girl 14 years of age.

Fig 8-121—The right (A) and left (B) great toes in a frontal projection. There is an accessory ossification center in the epiphyseal cartilage (arrow) in B. The cartilage plate is epiphysal and a small triangular segment of the metatarsal simulates a fracture fragment. The patient was a healthy girl 11 years of age.

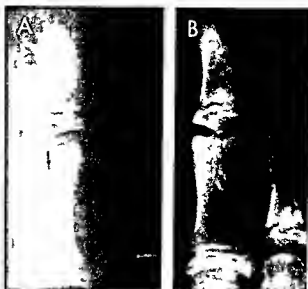
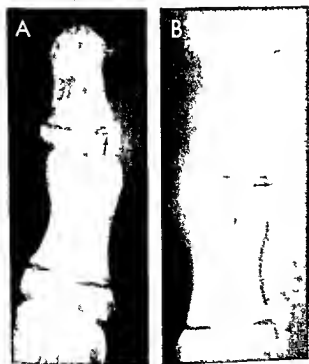


Fig 8-122—The foramen (A) in frontal projection and the canal (B) for the nutrient artery of the shaft of the proximal phalanx of the great toe should not be mistaken for a lesion or fracture line. This asymptomatic girl was 12 years of age.

and lateral projections (Fig 8-122). In the great toes remnants of the cartilage plate of the proximal phalanx may be responsible for false fracture fragments and fracture lines (Figs 8-123 and 8-124). The incomplete synchondrosis at the distal end of the first metatarsal may simulate a fracture (Fig 8-125). The secondary centers in the epiphyseal cartilage of these small tubular bones often develop from several fine bony foci and normally they may cast irregular shadows with rough edges for several years after they first appear (Fig 8-126). Secondary centers may never appear in the epiphyses of the distal phalanges of the third, fourth, and fifth toes.

The conical epiphyseal ossification centers (mistakenly called cone-shaped epiphysis by some) of the pedal phalanges are shown in Figures 8-127 and 8-128. Cone-shaped epiphyseal ossification centers are also encountered in the phalanges of the fingers (Fig 8-129). In a study of the radiographs of the feet of 1800 normal London school children, Venning found that conical ossification centers (CEO) occurred in the proximal phalanges in 26% of girls and 8% of boys aged 4 through 10 years and in 13% of girls and 4% of boys aged 11 through 15 years. The lower incidence in older children suggests that the cone-shaped centers fuse earlier than the normal disk-shaped type. When only one phalanx had a cone-shaped center, it was always in the third toe, and when there was more than one cone-shaped center, they were located in descending order of frequency, in the third toe, fourth, second, and fifth toe. Cone-shaped centers are almost always distributed bilaterally in symmetrical patterns. The shafts associated with markedly cone-shaped centers tend to be short.



Fig 8 123 (left) Frontal projections of the great toes. **A**, right; and **B**, left. In **A**, a small, angular mass of bone is cut off from the main mass of the phalanx by an oblique radio-ulnar synchondrosis. In **B**, an incomplete radio-ulnar synchondrosis notches the proximal phalanx on its lateral edge near its distal end. This healthy boy was 12 years of age.

Fig 8 124 (right) Frontal projections of the left great toe at age 5 years (**A**) and at 10 years (**B**). In **A**, a normal appearance.

tion center is present in the proximal epiphysis of the proximal phalanx, but in **B**, two years later, the same center is bifid. It is manifest that this center did not develop from two centers and the two masses of bone do not represent two centers with a synchondrosis between them, which has always been present. The splitting of this center developed between the 8th and 10th years of life. The causal mechanism is uncertain. The patient was an asymptomatic boy who had had no recognized injuries.

Fig 8 125 Incomplete synchondrosis of a false accessory epiphyseal ossification center which simulates a transverse fracture at the distal end of the left first metatarsal. The view is from

the findings in the right metatarsal of this asymptomatic boy 11 years of age. **A**, frontal; **B**, oblique; and **C**, lateral projection.

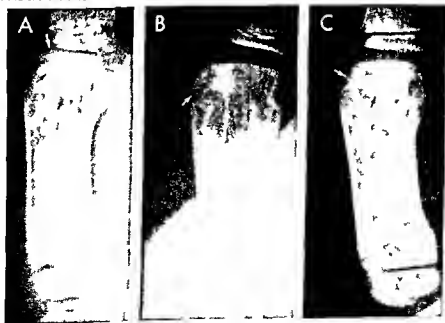




Fig. 8-126—Symmetrical fissuration of the secondary ossification centers in the proximal epiphyses of the basal phalanges of the great toes of an asymptomatic boy 11 years of age. The fissures between the segments of each center must not be mistaken for fracture lines.

ures between the segments of each center must not be mistaken for fracture lines.

Fig. 8-127—Symmetrical bilateral conical or belt-shaped epiphyseal ossification centers in the proximal phalanges of the second, third and fourth toes of both feet of an asymptomatic girl 8 years of age. The contiguous distal end of each shaft is recessed to receive its elongated ossification center. The epiphyseal ossification centers in the basal phalanges of the first and fifth toes are the normal flat shallow transverse disks usually present in all of the phalanges. In the middle and distal phalanges of toes 2, 3, 4 and 5 the primary and secondary ossification centers have fused in a single bony mass.



Fig. 8-128—Cone-shaped epiphyseal ossification centers in the middle phalanges of the second and third toes of an asymptomatic boy 14 years of age. The bases of the shafts contiguous to these centers are deeply notched to receive the apex of the cones. In the middle phalanges of toes 4 and 5 the epiphyseal ossification centers have already fused with the shafts. The epiphyseal ossification centers of the distal and proximal phalanges are normally shaped.

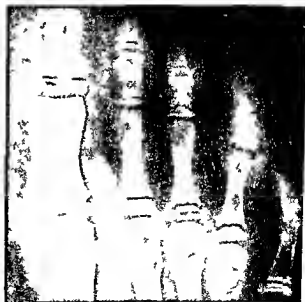




Fig 8-129—Cone shaped epiphyseal ossification centers in the distal phalanges of fingers 2, 3, 4 and 5. In fingers 4 and 5 the cones are not as long and the recesses for them in the bases of their shafts are not as deep as in fingers 2 and 3. The findings were similar in the two hands.

Hertzog and associates found cone-shaped epiphyseal ossification centers (there is no such entity as a cone-shaped epiphysis) to be common in the phalanges of the fingers in normal populations. The inci-

Fig 8-130—Lateral oblique projection of the left foot showing a normal localized depression in the lateral cortical wall (arrow) of the left third metatarsal in an asymptomatic boy 8 years of age. A similar depression was present in the right third metatarsal. This normal variant should not be confused with destructive lesions or traumatic depressions of the cortical wall. This depression occurs in a substantial percentage of all normal third metatarsals.



Fig 8-131—A sharp cleft (arrow) in the cortical wall at the proximal end of the fourth metatarsal of a healthy boy 14 years of age. This notch is seen in a substantial percentage of asymptomatic healthy fourth metatarsals during adolescence. A, frontal and B, lateral projections.

dence was 9% in Guatemalan girls and less than 1% in girls in southwestern Ohio. These malformed epiphyseal ossification centers were often associated with reduced length of the companion diaphysis and premature fusion of the epiphyseal ossification center with its shaft.

During the second half of childhood, a normal depression occasionally appears on the lateral cortical walls of the third metatarsal (Fig 8-130) which can be confused with bone destruction or a depressed fracture. Occasionally clefts and notches of the cortical walls at the proximal ends of the metatarsals are encountered in asymptomatic children (Fig 8-131).

Fig 8-132—Symmetrical marginal irregularities in the tips of the shafts of the first metatarsals in an asymptomatic girl 7 years of age. These findings were made because a rock had fallen on the outside of the right foot. (Courtesy of Dr. Alfred Berns, Syracuse, N.Y.) These lesions may result from stress ischemic necrosis due to hypoxia, which does not cause recognizable chondroinhibitions. Kessel and Bonney found similar bone changes in association with hallux (see Fig 8-133).





Fig 8-133—Normal scale ossification center in the apophysis at the proximal end of the fifth metatarsal of a healthy boy 12 years of age. When this center fails to fuse normally later with the metatarsal shaft the independent mature ossicle is called the os vesalianum. A faint transverse fracture line in the end of the shaft is located directly opposite the ossification center.

Fig 8-134 (left)—Normal healthy irregular ossification in the secondary epiphyseal ossification center (arrows) at the base of the fifth toe of a boy 10½ years of age who had injured the other foot two years before. A, the injured foot with a single evenly ossified ossification center. B, asymptomatic foot with multiple healthy small ossification centers in the epiphyseal cartilage at the base of the proximal phalanx of the fifth toe (arrows).

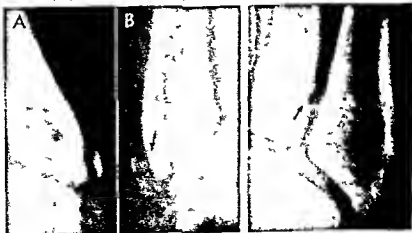
Fig 8-135 (right)—The fourth (left) and the fifth (right) right

Cone shaped ossification centers and other minor anomalies of the bones in the hands were studied in healthy British children aged 1–15 years by de lauriza and Tanner. They found that in some there were no residual deformities (group A), in others, slight malformations did result (group B), and others were associated with the development of specific pathologic skeletal syndromes (group C).

Accessory ossification centers in the proximal epiphyseal cartilages of the metatarsals are common and usually have no recognizable clinical significance, as in the hand, they are most common in cretins. We have seen one example of irregular mineralization of the distal tips of the shafts of the first metatarsals (Fig 8-132) in a black girl who appeared to be healthy and was asymptomatic.

During puberty a scalelike secondary center may appear in the proximal epiphyseal cartilage of the fifth metatarsal (Fig 8-133). This may persist throughout life as a separate ossicle, usually it fuses with the shaft after a few years and completely disappears. In the case of injury to the foot it should not be mistaken for a fracture fragment or an example of osteochondrosis juvenilis (Figs 8-134 and 8-135). Fusion of two of the metatarsals at their bases may occasionally be demonstrated roentgenographically when there are no clinical signs of metatarsal dysfunction. In some cases the os metatarsium may be the cause of hallux valgus. Bipartite sesamoids are not uncommon and the fissure between the parts should not be mistaken for fracture of the sesamoid (Fig 8-136). The facing edges of the bipartite sesamoids are often irregular, and in case of injury in this region the radiologist cannot differentiate develop-

metatarsals in lateral oblique projection. The scale epiphyseal ossification center at the proximal end of the fifth metatarsal is developing from several small ossification centers which could be mistaken for a cluster of fracture fragments in the case of regional traumatic injury. The arrow on the fourth metatarsal is directed at a small notch on its lateral cortical wall. This healthy boy was 12 years of age.



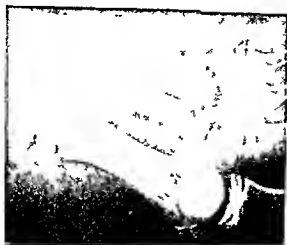


Fig 8-136 (left) —Normal bipartite sesamoid at the base of the great toe of an asymptomatic girl 13 years of age. This normal developmental variant should not be mistaken for fracture of the sesamoid in the case of local injury. The companion sesamoid superimposed on the shaft of the first metatarsal appears as an opaque circular mass which is not fissured.



Fig 8-137 (right) —Bipartite sesamoid superimposed on the distal end of the first metatarsal of an asymptomatic boy 13 years of age. The facing edges of the two parts of the sesamoid are irregular and are highly suggestive of fracture with distraction, but the parts had never been injured and there were no local signs of disability.

mental bipartism from fracture (Fig 8-137). The number and sites of the pedal sesamoids are shown in Figure 8-162. In the two feet the number, size and pattern of the sesamoid bones are frequently different.

REFERENCES

- Henderson R S. Os metatarsaleum and a possible relationship to hallux valgus. *J Bone & Joint Surg* 45-B:117, 1963.
 Hertzog K P et al. Cone-shaped epiphyses in the hand. Population frequencies, anatomic distribution and developmental stages. *Invest. Radiology* 3:433, 1968.
 Huhay C A. Sesamoid bones of the hands and feet. *Am J Roentgenol* 61:493, 1949.
 de Iturriza J R and Tanner J M. Cone-shaped epiphyses and other minor anomalies in the hands of normal British children. *J Pediatr* 75:265, 1969.
 Roche A F and Sunderland S. Multiple ossification centers in the epiphyses of the long bones of the human hand and foot. *J Bone & Joint Surg* 41-B:375, 1959.

Venning P III. Cone-shaped epiphyses of the proximal phalanges. *Am J Phys Anthropol* 19:131, 1961.

Tarsal bones are arranged in two rows: the proximal row is made up of the calcaneus and talus, and the distal row consists of the cuboid and the three cuneiforms. The navicular is interposed between the talus and the cuneiforms, but on the lateral side of the foot the calcaneus comes into direct contact with the cuboid. There are a number of variants of the tarsal bones which are important in roentgen diagnosis, such as normal roughening of the edges, normal irregularities in density during early phases of ossification, and in the apophysis of the calcaneus, normal sclerosis during all phases of its development.

The calcaneus is the largest of the tarsal bones and has several normal features which need careful roentgen consideration. After the first months of life

Fig 8-138 —Lateral projections of the two heels of a healthy girl 17 years of age. The calcaneal apophyses are normally sclerotic, and in B the fissure in the lower one is also normal. The

black arrow points to a secondary apophyseal center which appears during the prepubescent period.





Fig 8-139 —The apophyseal secondary center in 45 degree views on. In A in an asymptomatic girl 10 years of age the center is located well away from the posterolateral edge of the body of

the calcaneus as a separate small ossicle. In B in an asymptomatic boy 15 years of age the ossicle is fusing with the edge of the body of the calcaneus.

the posterior edge is rough. The apophysis is often normally fragmented from its earliest phases and is characteristically sclerotic during its entire developmental phase (Figs 8-138 to 8-140). When the calca-

neus is viewed in lateral oblique projections the normal fissures in the apophysis are superimposed on the dorsal end of the calcaneal body and may simulate multiple fracture lines (Fig 8-141). It is obvious that

Fig 8-140 —Normal roentgen features of the growing calcaneus and its apophysis in asymptomatic children. A irregular dorsal margin in a boy 3 years of age before the appearance of the apophyseal ossification center. B irregular but sclerotic apo-

physeal center in a boy 10 years of age the normal dorsal margin of the calcaneal mass is deeply jagged. C normally sclerotic apophyseal center in a girl 10 years of age the margins of the calcaneal body end of its apophysis are relatively smooth.



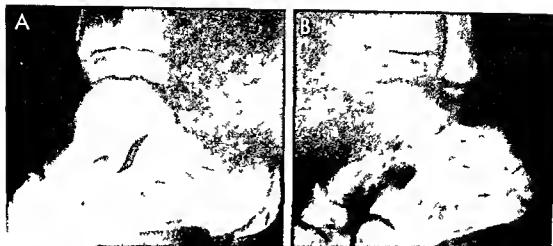


Fig. 8 141 —The left calcaneus of a healthy girl 10 years of age. In A, lateral projection, the apophysis of the calcaneus is normally sclerotic and fissured. In B, lateral oblique projection,

the fissured apophysis is superimposed on the dorsal edge of the body and simulates fracture lines in the body.

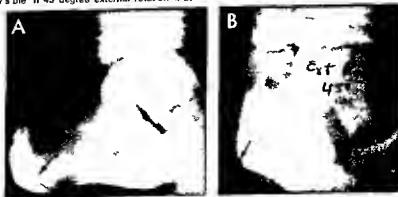
Fig. 8 142 —Double ossification centers in the body of the calcaneus on each side of an infant 20 months of age. The infant was normal and films were made only because of an injury

to the left ankle a few hours before. We have seen similar double ossification centers in the body of the calcaneus in mongrels and in gorgoyle (mucopolysaccharidoses type I).



Fig. 8 143 —Calcaneus secundarius in the trochanteric process on the lateral wall visible in full lateral (A) or frontal projections.

invers on (B) is visible in full lateral (A) or frontal projections.



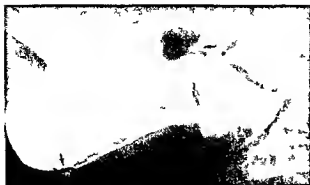


Fig 8-144 —Small round smooth calcaneal secundarius (arrow) in the center of the space between the calcaneus, cuboid, scaphoid and talus. lateral oblique projection. The patient was an asymptomatic boy 12 years of age. The posterior arrow points to a center in the apophysis. Similar ossicles were present in the other foot.

the roentgen diagnosis of disease of the apophysis on the basis of irregularity in density, roughening of its edges or sclerosis is always uncertain because these features are all present in the healthy apophysis. In the case of painful heel the diagnosis of sclerotic apophysitis is an irrational one because the normal calcaneal apophysis is always sclerotic.

Occasionally the body of the calcaneus may ossify from two independent centers rather than the usual single center, the strip of cartilage between these two ossification centers just prior to their fusion may sug-

gest fracture (Fig 8-142). We have seen this variant in normal infants, gargoyles and mongoloids. A secondary ossification center in the tip of the trochlear process on the lateral wall of the calcaneus may suggest a chip fracture when the foot is projected in 45 degree external rotation with inversion (Fig 8-143). The trochlear process fails to develop in some children but it may be so large in others that it suggests an exostosis.

The calcaneus secundarius lies in the center of the space between the calcaneus, talus, cuboid and scaphoid (Fig 8-144). It varies greatly in size and form from circular, triangular and rectangular. At times it may form a part of a bridge between the calcaneus and scaphoid (calcaneoscaphoid coalition) or between the calcaneus and the cuboid (calcaneocuboid coalition). It is rarely visible radiographically before the 12th year. We have seen a deep notch in the caudal edge of the calcaneus and a large sharply defined defect in the base of the sustentaculum tali in healthy children (Figs 8-145 and 8-146).

In full lateral projection of the foot a pseudocystic radiolucent circle or triangle (Figs 8-147 and 8-148) is visible in approximately 10% of children older than 7 years. This radiolucent image is cast by a normal deficiency of spongy bone at this site.

The increased ivorylike density of the apophyseal center which is often used mistakenly as a sign of apophysitis when the heel of a child is painful was found to be a normal feature of the calcaneus in both heels of all healthy children (Ross and Caffey). Ossifi-



Fig 8-145 (above) —In this lateral oblique projection of the left foot the caudal edge of the calcaneus is deeply notched near an independent ossification center in the apophysis. The apophysis at the proximal end of the fifth metatarsal is made up of two large ossification centers. The patient was an asymptomatic girl 14 years of age.

Fig 8-146 (below) —A large sharply defined oval defect at the base of the sustentaculum tali of a healthy boy 14 years of age. The nature of the defect was not determined. We suspected a large foramen for the nutrient artery or one of its branches.





Fig 8-147 (left) — Normal pseudocystic circle or triangle in the calcaneus of a healthy boy 10 years of age. The segmental radiolucency is due to local normal deficiency of spongy bone.



Fig 8-148 (right) — Small, sharply defined pseudocystic radiolucency in the body of the calcaneus of a healthy boy 8 years of age. This image may represent a large ectopic nutrient canal or local defect in the spongiosa.

cation began in the apophyseal center between the ages of 4 and 6 years in healthy girls and 4 and 9 years in healthy boys. Roughness of the edges, especially the dorsal edges, and fissuration of the main mass were common features in healthy children of both sexes. In the study of Shopfner and Coin the normal sclerotic density of the apophysis diminished with non use and absence of weight bearing due to fracture immobilization or neuromuscular disease. The appearance time and growth of the apophyseal center were delayed by the absence of weight bearing.

In longitudinal radiologic studies of normal children Harding found that a secondary center in the calcaneal apophysis developed consistently above the main apophyseal (see Figs 8-138 and 8-139). This center is useful in the estimate of skeletal age because it appears late after most of the centers have already appeared. This secondary apophyseal center rarely appeared before age 10 in girls and age 11 in boys and usually between 10½ and 12 years in girls and between 11½ and 13½ years in boys. After its appearance it quickly fuses with the main apophyseal center, which has already fused with the body of the calcaneus.

REFERENCES

- Harding V V. Time schedule for the appearance and fusion of a second accessory center of ossification of the calcaneus. *Child Devel* 23:181, 1952.
- Ross S E and Caffey J. Ossification of the calcaneal apophysis in healthy children. Some normal radiographic features. *Stanford M Bull* 15:224, 1957.
- Shopfner C E and Coin C G. Effect of weight bearing on the appearance and development of the secondary calcaneal epiphysis. *Radiology* 86:201, 1966.
- Sirry A. The pseudocystic triangle in the normal os calcis. *Acta radiol* 36:516, 1951.

The *talus* has but one common variation of clinical importance: an accessory ossicle, the *os trigonum* (Fig 8-149) often develops in the posterior process

This separate center may later fuse with the main mass of the talus or persist throughout life as an independent ossicle. In oblique projections the *os trigonum* may be superimposed on the body of the talus and simulate a sequestrum (Fig 8-150). *Os supratolare* on the crest of the nose of the talus can be mistaken for a chip fracture (Fig 8-151). In some cases the roughness of the edge of the ossicle and the deformity of the underlying edge of the talus suggest that stress may be an important factor in the generation of the *os supratolare* (Fig 8-152). In others, especially pread-

Fig 8-149 — Normal apophyseal ossification center (arrow) in the dorsal process of the talus in a healthy boy 11 years of age. The radiolucency between the body of the talus and the ossification center is a normal synchondrosis, not a fracture line. When the synchondrosis persists after the normal age for its fusion with the body of the talus, the persistent ossification center is called the *os trigonum*.



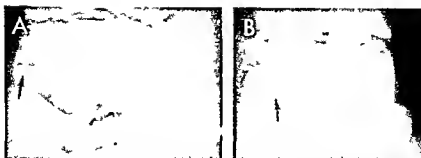


Fig 8-150 —A, normal os trigonum (arrow) in full lateral projection. B, normal os trigonum (arrow) in oblique projection and superimposed on the main mass of the talus. This patient, 7 years of age, had local swelling, redness, and heat of this ankle with fever and a high erythrocyte sedimentation rate. At another hospital the image in oblique projection was interpreted by a

bone specialist to represent a sequestrum of destructive osteomyelitis and exploratory drainage and excision advised. This plan was canceled when the interpretation of normal os trigonum in oblique projection was made in consultation. Two days later the heart dilated and a diastolic murmur appeared which indicated the diagnosis of rheumatic arthritis and rheumatic carditis.

Fig 8-151 —Os supratarsale on the dorsal edge of the talus just proximal to the talocalcaphal joint. A, at 13 years; and B, at 18 years in an asymptomatic girl.

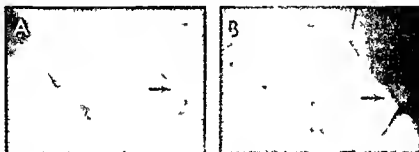


Fig 8-152 (left) —Large rough or asperate bone with associated thickenings of the underlying edge of the talus in an asymptomatic girl, 15 years of age. We believe that many of these small bony changes in the feet are due to stress from imbalanced feet rather than simple dysplasia.



Fig 8-153 (right) —Large supranavicular bone which seems to be partially fused with the main mass of the navicular itself. This appears to be an accessory ossification center in the periphery of the navicular cartilage. Similar changes were present in the other foot. This asymptomatic boy was 8 years of age.



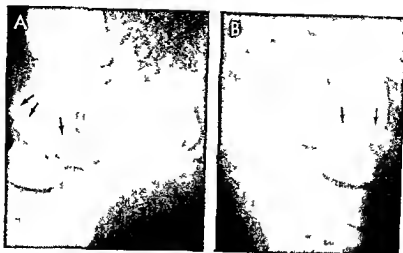


Fig 8-154—Double ossification centers for the talus bones of a boy 7 years of age who had always had weak feet. The independent centers for the talus heads are flattened longitudinally

olescent children the os supranaviculare in the periphery of the navicular cartilage is incompletely fused (Fig 8-153) but may fuse later. If this center does not fuse later it becomes an os supranaviculare. We have seen one example of bilateral separate ossification centers for the heads of the talus bones (Fig 8-154) in a boy 7 years of age who had badly ballanced feet. The heads of the talus bones were flattened and the edges were mushroomed beyond the contiguous bone and were overlapped in comparison to

and spread transversely well beyond the usual limits. These variations may be due to the abnormal stresses in these poorly ballanced feet.

the contiguous naviculars. It is possible that these were stress deformities in addition to the presence of separate ossification centers. Factitious roughening of the superior edge of the talus may be caused by its superimposition on the cartilage plate and the edge of the provisional zone of calcification of the epiphyseal ossification center of fibula in lateral projection (Fig 8-155).

REFERENCE

- Gottlieb C and Berenbaum S L: Pine bone accessory ossicle on the dorsum of the astragalus—often bilateral. *Radiology* 55:423, 1950.

Fig 8-155—Factitious roughening of the superior edge of the talus (lower arrows) of a healthy boy 12 years of age due to superimposition of the provisional zone of calcification of the fibula on the center in lateral projection. The upper arrow points to a segment of the radiolucent cartilage plate of the tibia which could be mistaken for a fracture line.



The tarsal navicular exhibits several important and frequent variations which are of great clinical interest. The primary ossification center appears during the 2nd year. It is during this early phase that irregular mineralization is the rule (Fig 8-156) and the normal irregularity in some cases persists for months and even years in children who are free from symptoms. It is not uncommon for mineralization to be regular in one tarsal navicular and irregular in its fellow in the other foot.

The os tibiale externum is the best known and one of the most important variants in the foot. It lies behind and above the tuberosity of the navicular in the tendon of the posterior tibial muscle. This ossicle is a true sesamoid in a tendon. It begins as a nodule of cartilage which later ossifies and becomes visible radiographically in 10–15% of all children (Fig 8-157). It is usually bilateral and may be bifid. After the 10th year of life the os tibiale externum may grow out of the posterior tibial tendon in large part and coalesce with the contiguous navicular to lose its sesamoid status. The fibrochondroid anlage of the ossicle may never ossify to become visible radiographically. The navicular tuberosity and the os tibiale externum often



Fig 8-156—Normal irregular medial salient on and flattening of the distal navicular (arrow) of an asymptomatic boy 3 years of age. The second arrow is directed at the fissure shadow between

separate ossification centers in the proximal epiphysis of the first metatarsal. A, frontal and B lateral projections.

become swollen and painful in flat feet especially during puberty when growth is rapid. Swelling of the tuberosity and of the os tibiale externum may lift the tendon of the posterior tibial muscle from its insertion on the medial side of the navicular.

Occasionally a small mass of bone is found free in the soft tissues dorsad to the superior edge of the navicular, the os supranaviculare (Fig 8-158 A). It is possible that some of these independent ossicles are fragments of stress fractures rather than purely developmental anomalies. A longitudinal radiolucent strip in the navicular itself may simulate a fracture line (Fig 8-158 B). The infranavicular bone, which develops dorsad to the navicular-cuneiform joint, is usually smaller than the os supranaviculare.

The cuboid during the earliest phases of its ossification in the last fetal and the first postnatal months is often composed of multiple fine ossification centers (Fig 8-159) which later slowly fuse to form a single

bony mass. This irregularity in ossification and density has no known clinical significance and should not be interpreted roentgenographically as evidence of disease in the case of injury or infection of the foot. In a study of newly born Indian (Asian) infants, Bhargava and Garg found that centers for the cuboid were visible in approximately one-half of 160 males and 140 females. Some of these cuboids had two, three, and four ossification centers, usually bilaterally symmetrical. Their study indicates that the cuboids in Indian infants at birth are more mature than in white infants, approximating the more mature cuboids of the American Negro (Christie). In the more mature cuboid bone, the ridge for the insertion of the long plantar ligament and the groove for the tendon of the peroneus longus muscle should not be mistaken for traumatic impaction and deformity (Fig 8-160).

The three cuneiforms begin to ossify between the 1st and the 5th year; one or all of them occasionally

Fig 8-157—Os tibiale externum in an asymptomatic boy 11 years of age. A, frontal and B lateral projections.



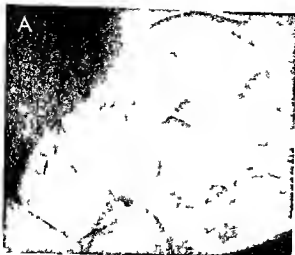


Fig 8-158 - A. Os supranavicular above and behind the navicular of an asymptomatic 13 years of age. B. longitudinal radiolucent strip in the right navicular which simulates a fracture



There is a small strip was present in the left navicular. Oblique lateral projection

Fig 8-159 - Normal bilateral regular mineralization of the cuboids of an asymptomatic infant 3 days of age. The left cuboid contains nine or 10 separate small bony centers. The right cuboid

is a single relatively large bony mass of regular density and rough on the edges



Fig 8-160 - Lateral oblique projection of the right foot of an asymptomatic girl 15 years of age. The upper arrow is directed at a radiolucent strip cast by the cartilage between the proximal end of the second metatarsal and the distal edge of the middle cuneiform. The lower arrow points to a ridge for the attachment of the long plantar ligament distal to which lies the groove for the tendon of the peroneus longus muscle. The radiolucent strip to the left has been mistaken for a fracture line and the ridge to the right in the cuboid for an impacted fracture



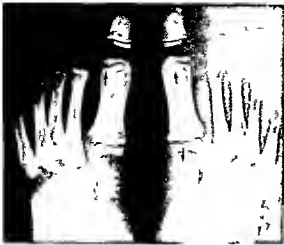


Fig 8-161 —B lateral Irregular density of the medial cuneiform bones of an asymptomatic boy 5 years of age. The distal ends of the shafts of the first metatarsals are also irregularly ossified in a fashion which suggest incompletely fused accessory epiphyseal ossification centers. Irregular mineralization of this kind is so common in asymptomatic children that one can conclude that the irregularities are healthy developmental variants rather than abnormal necroses (osteochondrosis juvenilis). They disappear without treatment.

may show rough edges (Fig 8-161) in children who are healthy and have no clinical evidence of local disease in the feet.

The common accessory ossicles of the feet are depicted schematically in Figure 8-162.

Fig 8-162 —Normal supernumerary ossicles of the feet. A, ventrodorsal and B, lateral projections. 1 os tibiale externum 2 processus uncinatus 3 os intercuneiforme 4 pars paronea metatarsalia 5 cuboideum secundarium 6 os peroneum 7 os

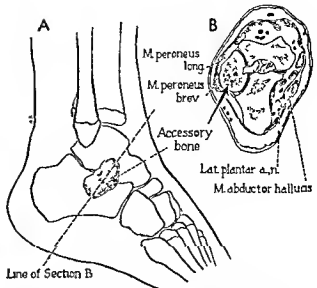
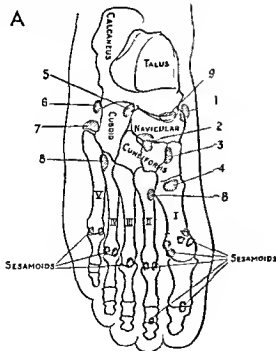
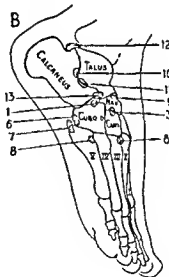


Fig 8-163 —Drawing of the anomalous os talocalcaneum (From Hirschtik)

8 os intermetatarsale 9 accessory navicular 10 talus accessorius 11 os austeniaculum 12 os trigonum 13 os caninus secundarius

Hirschtik found a large anomalous bone which arises from the base of the talus and articulates with the calcaneus. It is the os talocalcaneum.



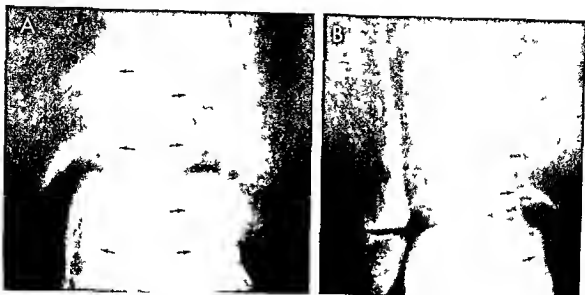


Fig 8-164—A, visualization of both edges of the Achilles tendon of a healthy 10-year-old boy. B, visualization of the medial edge only of the Achilles tendon of an asymptomatic boy 9 years of age.

articulated with the talus above and the calcaneus below (Fig 8-163) for which he suggested the name *os talocalcaneus*. This is probably an example of incomplete talocalcaneal coalition. The multiple accessory ossicles on the medial side of the first cuneiform which were described by Zimmer proved to be sesamoids in the tendon of the tibialis anticus. The reader should consult the paper of O'Rahilly for a comprehensive description of the rarer tarsal anomalies.

REFERENCES

- Christie A. Prevalence and distribution of ossification centers in the newborn infant. *Am J Dis Child* 77:355, 1949.
 Hirschtik A. B. An anomalous tarsal bone. *J Bone & Joint Surg* 33-A:907, 1951.
 O'Rahilly R. A survey of carpal and tarsal anomalies. *J Bone & Joint Surg* 35-A:686, 1953.
 Zimmer E. A. Skellettelemente medial des Cuneiforme I. *Acta radiol* 34:102, 1951.

DISTAL ENDS OF TIBIA AND FIBULA—The medial edges of the Achilles tendons are often visible in frontal projections of the ankles. They appear as longitudinal strips of water density which are concave medially. They cross the tibial cartilaginous plate and the cartilage space between the tibia and the talus to fuse with the calcaneal bones (Fig 8-164). Separate accessory ossification centers are common in the cartilages of the medial malleolus of the tibia and less common in the lateral malleolus of the fibula (Figs 8-165 to 8-167). In a study of 100 healthy children aged 6–12 years, Powell found that 20% had independent ossification centers in the medial malleoli of the tibia. Bilateral centers were present in 13%. In contrast, separate epiphyseal centers were found at the distal

ends of the fibulas in their lateral malleoli in but 1% (Fig 8-168). Selby found in the internal malleoli of the tibiae extra centers in 47% of girls and 17% of boys. Bilateral centers occurred in 90% of girls and 20% of boys. The average age of time of appearance was 7.6 years in girls and 8.7 years in boys. In all children the extra centers had fused with the main mass of the tibial epiphyseal center by the 12th year. These physiologic variants should not be confused with fracture fragments; the ossicles may be unilateral or bilateral. The lateral surface of the tibial shaft is reg-

Fig 8-165. Separate ossification centers in the medial malleolus of the distal tibia epiphyses cartilage of an asymptomatic 19-year-old girl. This was an accessory ossicle in the other foot. This ossicle must not be mistaken for a fracture fragment.



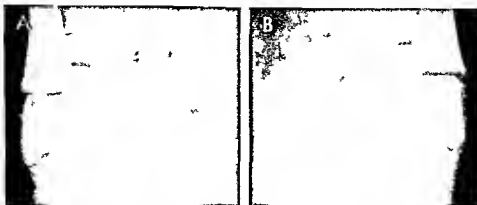


Fig 8 166 —B lateral accessory epiphyseal ossification centers in the medial malleoli of the tibia. In A, right tibia a single large extra ossification center is present. In B, left tibia the area multiple smaller ossification centers which could be confused

with comminuted fracture fragments or so called osteochondrosis juvenilis (schematic necrosis). This asymptomatic boy was 8 years of age.

Fig 8 167 —Accessory ossification centers in the lateral malleolus of the fibula. A, small separate center (arrow) in the fibular styloid of an asymptomatic girl 11 years of age. B, large ossifica-

tion center (arrows) of the fibular styloid of an asymptomatic boy 12 years of age. The other fibular styloid did not have an analogous secondary center.

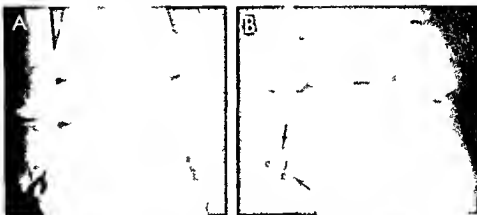


Fig 8 168 —Inset, accessory center in the distal epiphysis of the fibula whose superior radiolucent synchondrosis suggests transverse fracture in frontal projection (A) but is seen to be a

smooth rounded center in a deep smooth notch in lateral oblique projection (B). This patient was a boy 10 years of age.

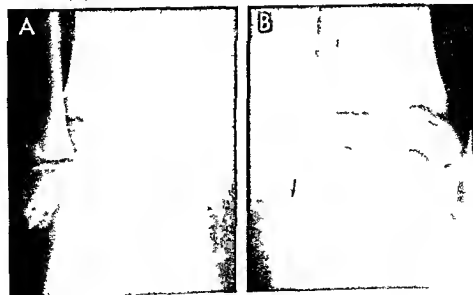




Fig. 8 169—Normal foveal notch in the lateral tibial wall of an asymptomatic boy

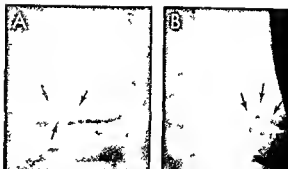


Fig. 8 170—Protuberance of the epiphyseal ossification center into the metaphysis which forms the tenon of a mortise and radiographically simulates a fracture fragment. The patient was an asymptomatic boy 10 years of age. A frontal and B lateral projections

Fig. 8 171—Tenon of the mortise of the epiphysis and shaft which simulates a fracture fragment because a segment of the radiolucent cartilage plate is superimposed on it in lateral projection (B) at a more proximal level. The girl 2 1/2 years of age was asymptomatic

tion (B) at a more proximal level. The girl 2 1/2 years of age was asymptomatic

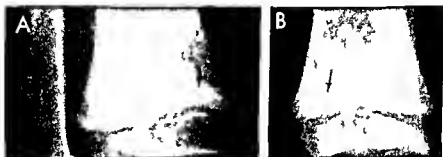


Fig. 8 172.—Tenon of the mortise between the epiphyseal ossification center and the shaft which simulates a fracture fragment because the radiolucent cartilage plate is superimposed on it at

different levels in the two projections. A frontal and B lateral. The pseudofragment is usually long ventrodorsally in this asymptomatic boy 7 1/2 years of age

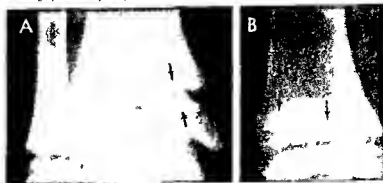




Fig 8-173 (left)—False longitudinal fracture of the distal end of the tibia (arrows) caused by the interference phenomenon of rays from two bodies which neutralized each other. The patient was an asymptomatic girl 14 years of age.

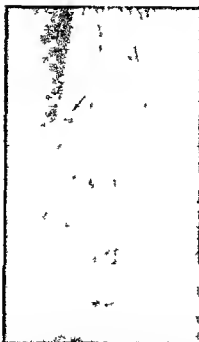


Fig 8-174 (right)—Tunnels (arrow) through the medial cortical wall of the tibia for the perforating perosteal vessels which simulate cortical fractures. This asymptomatic boy was 14 years of age. The nature of the tunnels was not proved anatomically.

ularly grooved to form the fibular notch (Fig 8-169) for reception of the fibular shaft. Sometimes the medial surface of the fibular shaft is cupped at the level which is in contact with the tibia.

Factitious extra ossicles in the cartilage plate at the distal end of the tibia are common in asymptomatic children (Figs 8-170 to 8-172).

Fig 8-175—A, extra ossicle in a notched marginal recess in the lateral segment of the distal fibular metaphysis in an asymptomatic boy 9 years of age. Similar changes were present in the right fibula. In case of injury, this little variant ossicle must not be mistaken for a fracture fragment or osteochondroma. **B**, similar ossicle with notch in an asymptomatic boy 10 years of age.



One should be familiar with the interference phenomenon of light rays and x rays when the rays from two contiguous bodies meet and tend to neutralize each other (Fig 8-173). Occasionally the tunnels through the cortex which carry the perforating perosteal arteries are visible (Fig 8-174) and simulate fine cortical fractures.

The provisional zone of calcification in the distal fibular metaphysis may be notched shaftward and a

Fig 8-176—Accessory ossicle in the distal metaphysis of the fibula in an asymptomatic boy 13 years of age. In this older boy the ossicle is larger and is already fusing with the epiphyseal ossification center and not with the shaft.



Fig 8 177 —Tiny fibular ossicle invisible in frontal projection (A) but clearly visible in lateral oblique projection (B). This asymptomatic boy was 15 years of age.



Fig 8 175 —The fibular metaphyseal ossicle which appears to be single in frontal projection (A) but is seen to be composed of a cluster of small ossification centers in lateral oblique projection (B). This asymptomatic boy was 14 years of age.

tiny extra ossicle may develop in the notch (Figs 8 175 and 8-176) this variant should not be confused with fracture or osteochondrosis dissecans. We have seen this variant ossicle in its indentation in the shaft in a variety of patterns (Figs 8 177 to 8 181). Sometimes in lateral projection of the ankle the radiolucent cartilage plate of the fibula superimposed on the tibial ossification center suggests a fracture (Fig 8 182). This notching is usually bilateral. In older children aged 14–16 years an extra ossicle may appear lateral to the lateral end of the fibular cartilage-shaft

junction (Fig 8 183). The malleolar fossa in the medial face of the fibular ossification center resembles a patch of destruction when viewed in oblique projection (Fig 8 184).

The distal third of the tibial shaft is a common site of benign cortical defects (Fig 8 185).

PROXIMAL ENDS OF TIBIA AND FIBULA —In the proximal segment of the lateral wall of the tibia visualization of the anterior tibial crest displaced laterad owing to slight external rotation of the tibial shaft should not be misconstrued as abnormal localized

Fig 8 179 (left) —Large rounded fibular ossicle in a deep recess; the ossicle does not project beyond the edge of the shaft. The patient was an asymptomatic boy 9 years of age.

Fig 8 180 (right) —Small fibular ossicle in the caudal segment of a deep sharply defined metaphyseal notch. This asymptomatic boy was 11 years of age.





Fig 8-181 — Fibular ossicle associated with accessory center in the tip of the lateral malleolus of an asymptomatic girl 12 years of age



Fig 8-182 — The radiolucent cartilage plate of the fibula is superimposed on the tibia (arrows) simulating a short transverse fracture line in lateral projection. This asymptomatic boy was 13 years of age. At the ventral end of the tibial shaft, a rounded bony protrusion appears to suggest a tendon of the mortise with the recessed cup of the mortise on the edge of the ossification center. This is the converse of the mortise deformities in Figures 8-170 to 8-172.

Fig 8-183 — Independent ossification center in the cartilage on the edge of the distal end of the left tibial shaft which apparently will fuse with the fibular shaft directly and not with the epiphyseal ossification center in an asymptomatic boy 15 years of age. A similar ossicle was present in the same position on the right fibula.



Fig 8-184 — Malleolar fossa (lower arrow) which is not well seen in frontal projection (A) but is clearly seen in oblique projection (B) in an asymptomatic girl 10 years of age.

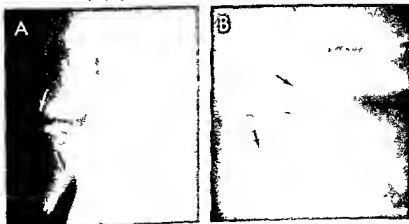
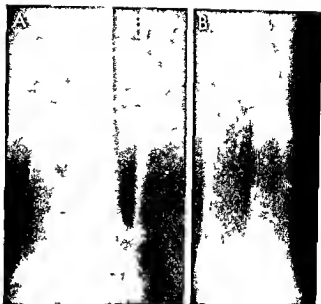


Fig 8 185 —Multiloculated benign cortical defect in the distal end of the left tibial shaft (not proved microscopically) A frontal and B lateral projections The patient was a boy 15 years of age

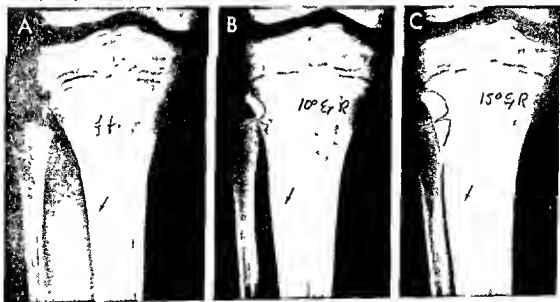


cortical thickening (Fig 8 186) The cortical defect on the posterior aspect of the shaft near the junction of the upper and middle thirds represents the nutrient canal (see Fig 8 53 p 875) The snout like tibial tuberosity which projects from the anterior surface of the proximal epiphysis and hangs down in front of the shaft is an extremely variable structure which ossifies irregularly (Figs 8 187 and 8-188) A separate

ossicle usually appears in the distal end of the process to fuse with the process and form the tibial tubercle Not infrequently a deep notch in the shaft below and behind the tip of the process is responsible in frontal projections for a narrow strip of diminished density (Fig 8 189) located a few centimeters below its proximal end. The remarkable variability in the size shape and texture of the tibial tuberosity and tubercle in

Fig 8 186 —Spurious thickening of the lateral cortical wall of the tibia of a boy 10 years old due to external rotation of the leg A, full frontal projection on the lateral and medial cortical walls are approximately equal in thickness B and C, 10 and 15 degrees of rotation respectively the lateral cortical wall becomes progres-

sively thicker as external rotation is increased The thickening is due to the fact that the anterior tibial crest comes progressively more into profile on the lateral edge of the shaft as the tibia is rotated externally This phenomenon cannot be demonstrated roentgenographically during the first years of life



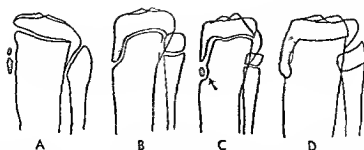


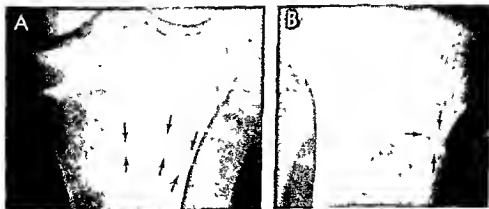
Fig 8-187 —Normal variations in the size and configuration of the anterior tibial process (Modified from Koehler)



Fig 8-188 —Irregular ossification of the anterior tibial process of an asymptomatic girl 12 years of age. Similar changes were present in the other anterior tibial process. There is no avulsion of the pseudofracture fragments or thickening of the patellar tendon as is usually the case in Osgood-Schlatter disease.

Fig 8-189 —Radiolucent shadow of the notch on the anterior surface of the tibia which the anterior tibial process overlies. The peripheral portions of this depression in the tibial shaft which are not covered by the opaque anterior tibial process appear as a

strip of diminished density in the anteromedial segment of the tibia. This shadow is never visible in infants and younger children. A, frontal; and B, lateral projections of the tibia of a boy 13 years of age.



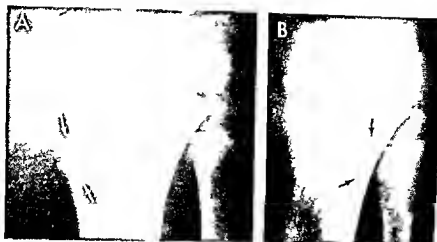


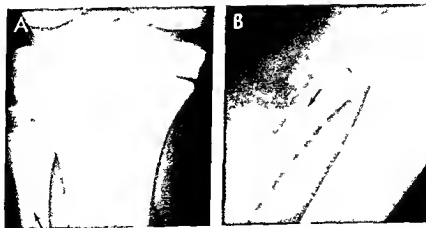
Fig 8-190 — Asymptomatic cortical defect in the posteromedial aspect of the tibia of a healthy boy 9 years of age. A, frontal; and B, lateral projections.

different persons and in the same person on the two sides warrants considerable reservation before a diagnosis of fracture or osteochondrosis juvenilis tibialis (Osgood Schlatter disease) is made. Local tenderness and swelling of the soft tissues in front of the tubercle and the lifting of the process anteriorly away from the shaft are helpful clinical and roentgen features pointing to injury. The margins of the proximal tibial ossification center are usually smooth but in younger children the lateral and medial aspects may show characteristic physiologic marginal irregularities in health.

Large numbers of healthy asymptomatic children show cystlike shadows in the tibiae, fibulae and the femurs when the shadow is projected *en face* but when the same shadow is seen in profile the anatomic change responsible for the shadow is seen to be a superficial cortical defect (Figs 8-190 and 8-191).

In our experience these shadows never appear during the first two years and they tend to disappear during late childhood. Rarely similar shadows are found in the distal ends of the tibiae and fibulae. The cystlike shadow may be unilocular or multilocular; usually its edges are sclerotic and sharply defined. The cause and the pathogenesis of the tissue changes responsible for the cortical defect are not well known because there have been few opportunities to study them clinically or anatomically. Some biopsies have shown that the cortical defect is filled with fibrous tissue. In one of our patients a painful cortical defect was filled with cartilage. Ordinarily the demonstration roentgenographically of these cortical defects has no clinical significance and one should be careful not to misconstrue them as sites of inflammatory or neoplastic destruction. There is no known correlation of these shadows and the disorders of skeletal growth.

Fig 8-191 — Asymptomatic cortical defect in the posterior wall of the fibula of a healthy girl 10 years of age. A, frontal; and B, lateral projections.



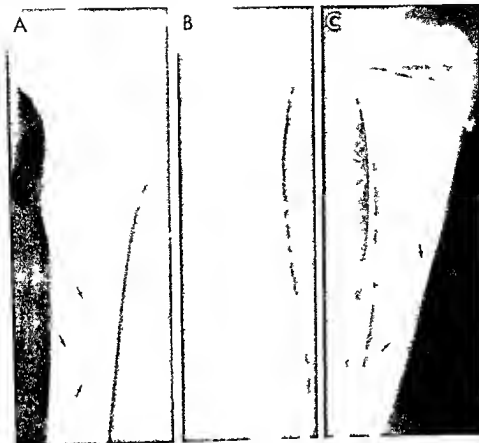
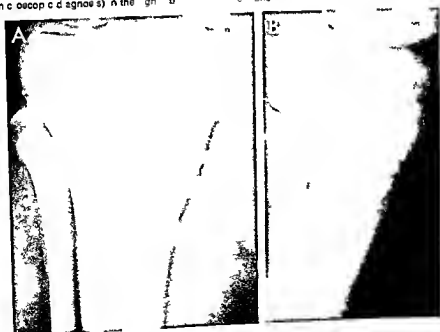


Fig 8192—Healed opaque cortical defects show proximal third of the left femur. A: Anterior and B: lateral views.

medial healed opaque cortical defects through the ventral aspect of the femur. C: Anteroposterior view.

Fig 8193—Legg-Calvé-Perthes disease (osteochondritis of the femoral head) in the right femur. A: Anterior and B: lateral views.

medial aspect of the femur. A: Anterior and B: lateral views.



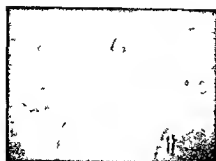


Fig 8 194 —Asymptomatic transitory axostosis at the medial end of the proximal tibial metaphysis of a healthy boy 6 years of age. Small bony spines like this one may appear at this site in healthy children during the 5th and 6th years of life, produce no clinical signs and disappear after three to four years.

Occasionally small shadows of increased density are found in the tibial shafts of asymptomatic pubescent girls (Figs 8 192 and 8 193). They are cast by localized internal thickenings of the cortex and the peripheral spongiosa; they do not represent focal accumulations of the spongiosa far out and free in the medullary cavity. Their clinical significance is not known; they may represent physiologic sclerosis of the cortex or may be residuals of local cortical disease which passed unrecognized clinically during the active phase. We have not had the opportunity to make longitudinal studies on any of these patients so are not familiar with the progressive changes and the ultimate outcome. During the last half of childhood a small bony spine may appear at the medial end of the proximal tibial metaphysis (Fig 8 194) persist for two, three or four years and then disappear spontaneously without having produced clinical signs of any kind.

We have seen several examples of unexplained ra-



Fig 8 195 —Unexplained metaphyseal defect (arrow) in the left tibia of an asymptomatic boy 6 years of age. A similar defect was present at the same site at age 12, and the bones had failed to grow longitudinally in the affected segment at the medial end of the metaphysis. This radiolucent defect probably represents segmental failure of resorption of uncalcified cartilage from the cartilage plate. We believe that the causal mechanism is local oligemia of the metaphyseal arteries on the metaphyseal side of the cartilage plate.

diolucent defects in the medial segments of the tibial metaphyses (Fig 8 195). The tendon of the mortise center at the proximal end of the tibia produces a false fracture fragment (Fig 8 196) much as it does at the distal end of the tibia. Small amounts of intra-articular gas in the knee joints superimposed on the margin of the epiphyseal ossification center may cast a transverse radiolucent strip that simulates a fracture line (Fig 8 197).

The intercondylar eminence is usually bifid, with medial and lateral tubercles (spines) which vary considerably in size and shape; this causes no interference in joint function. Occasionally the intercondylar eminence is tripartite, with three instead of two tubercles or spines. The base of the eminence sometimes presents sharply defined segments of rarefaction (Fig

Fig 8 196 —False fracture fragment (arrows) in the proximal end of the tibia caused by superimposition of the radiolucent strips of the cartilage plate on the tendon of a mortise which pro-

jects from the metaphysis into a cup at the base of the epiphyseal ossification center. A, frontal; and B, lateral projections. This asymptomatic girl was 6 years of age.

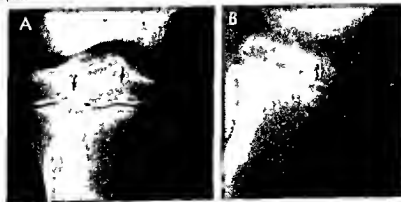




Fig 8 197 —The left knee of an asymptomatic boy 16 years of age, frontal projection. A transverse radiolucent strip of gas density is superimposed on the edge of the tibial epiphyseal line on center (arrow) which simulates a fracture line and fracture fragment. The gas is in the joint because sudden separation of the joint during positioning of the leg has increased the intra articular pressure which in turn sucked gas into the articular fluids and tissues and prevented a vacuum—an ent vacuum phenomenon.

Fig 8 198 —Discrete rarefaction of the lateral epiphysis in an asymptomatic boy 18 years of age.



Fig 8 199 —Fabella the normal sesamoid in the lateral head of the gastrocnemius muscle of a healthy boy 15 years of age. This usually appears during adolescence is inconstant and should not be confused with a fracture fragment, a phlebolith or a foreign body. We have seen two examples of a small ossicle embedded in the edge of the lateral condyle of the femur (Figs 8-200 and 8-201) which could be mistaken for a fabella. However, its lower position and its location partially buried in the edge of the lateral condyle of the femur makes its identification as the cyamella certain. According to Kaplan this rare sesamoid has been encountered in dissections of the human knee. It is probably related



to 196). It is said that the medial spines are larger when osteochondrosis dissecans is present in the medial condyle.

FABELLA—This is an inconstant sesamoid bone in the lateral head of the gastrocnemius muscle which is visible in the lateral projections of the knee of adolescent children. The fabella is common in Negroes and is more common in males than females in the ratio of about 4:1. In frontal projections the fabella is not clearly visualized because it is obscured by the heavier shaft of the femur on which it is superimposed. In lateral projections it appears as a small oval shadow of calcium density in the soft tissues behind the knee joint (Fig 8-199). The fabella should not be mistaken for a free body in the joint, a fracture fragment, a phlebolith, or a foreign body. We have seen two examples of a small ossicle embedded in the edge of the lateral condyle of the femur (Figs 8-200 and 8-201) which could be mistaken for a fabella. However, its lower position and its location partially buried in the edge of the lateral condyle of the femur makes its identification as the cyamella certain. According to Kaplan this rare sesamoid has been encountered in dissections of the human knee. It is probably related



Fig 8-200—A left sesamoid (cyamella) is partially embedded in the edge of the lateral femoral condyle of an asymptomatic boy 16 years of age. This ossicle appears to be in the position of the head of the popliteus muscle near its attachment



origin on the lateral condyle of the femur. This is the normal position for the rare sesamoid of the popliteus, the cyamella. B: Right fabella in the lateral head of the gastrocnemius in its normal position well separated from the femur itself.

Fig 8-201—Cyamella sesamoid in the popliteal tendon in the popliteal groove of the lateral femoral condyle of an asymptomatic boy 12 years of age.



developmentally to the femorofibular disk of four footed animals and is located in the tendon of the popliteus (Haines). So far as we have been able to discover this rare ossicle has not been demonstrated before in radiographs of human bones.

REFERENCES

- Haines R W. The tetrapod knee joint (grey squirrel). *J Anat* 76:291-1941:42.
 Kaplan E B. Surgical approach to the lateral (peroneal) side of the knee joint. *Surg Gynec & Obst* 104:346-1957.
 Powell H D W. Extra center of ossification for the medial malleolus in children. Incidence and significance. *J Bone & Joint Surg* 43-B:107-1961.
 Ravelli A. X ray appearance of the proximal end of the tibia. *Fortschr Geb Röntgenstrahlen* 82:48-1955.
 Selby S. Separate centers of ossification of the tip of the internal malleolus. *Am J Roentgenol* 86:496-1961.

PATELLA—The patella is the large sesamoid bone on the anterior aspect of the knee joint in the tendon

of the quadriceps muscle. It is best seen in lateral projections. Ossification normally develops from several small foci; the healthy patella is often granular and the edges may be irregular during childhood (Figs 8-202 and 8-203). Owing to the physiologic irregularity of mineralization, the diagnosis of osteochondrosis of the patella on the basis of granular osteoporosis should be made with caution. Following fusion of the granular centers in the lower half of the patella, a second irregular center of ossification may develop later in the superior half of the bone. The strip of radiolucent cartilage between the upper and lower ossification centers casts a shadow of diminished density which might be mistaken for a fracture line.

The patella is displaced cephalad during the progressive shortening due to fibrosis of the vastus intermedius muscle and also when the patellar tendon is shortened following injury.

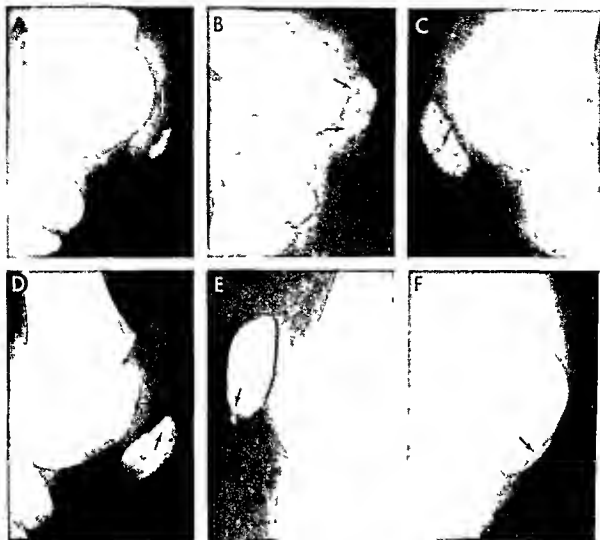


Fig. 8-202.—Normal variations in size, shape and density of the patella at different ages in healthy children. **A**, small irregular patella of a boy 5 years of age. **B**, multiple irregular centers in a girl 6 years of age. **C**, generalized granular texture with partial segmentation in a girl 8 years of age. **D**, irregularity in density of

the superior third of the patella of a boy 8 years of age. **E**, small separate ossicle at the inferior pole of the patella of a boy 11 years of age. **F**, scalloped marginal ossicles on the anterior edge of the patella of a girl 9 years of age.

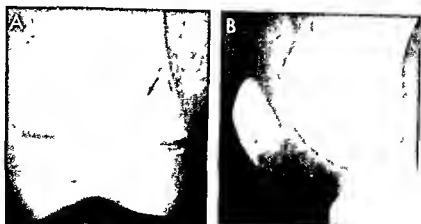
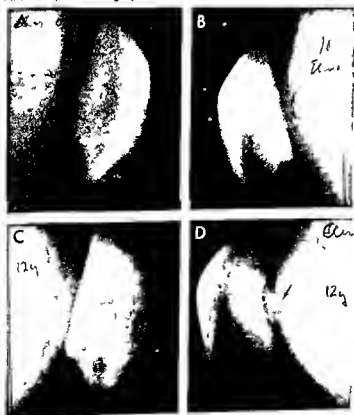


Fig 8-203 — Marginal segmentation of the patella of an asymptomatic boy 10 years of age. In A, frontal projection, the separate

ossicle is clearly visible, but is invisible in B, lateral projection, because it is superimposed on the main mass of the patella.

Fig 8-204 — Lateral projections of the knees of an asymptomatic boy at 10 years (A and B) and at 12 years (C and D) with extra ossification centers in the lower pole of the right patella at

10 years and on the dorsal edge of the left patella at 12 years, which suggests osteochondrodysplasia.



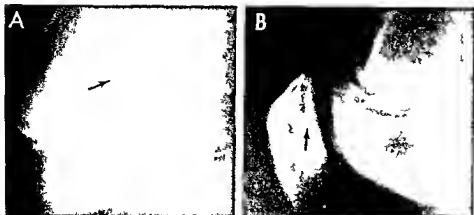


Fig 8-205—Left knee of an asymptomatic girl. A frontal and B lateral projections. In both projections a radiolucent defect is

visible near the upper pole and on the dorsal edge of the patella.

In one of our patients an asymptomatic boy 12 years of age an extra center appeared on the dorsal edge of the left patella which resembled osteochondrodis dissecans (Fig 8-204). The fossas on the dorsal edge of the patella develop at various cephalocaudal levels and they may be empty of bony centers (Fig 8-205) or filled with one or more accessory centers (Fig 8-206).

REFERENCE

Sontag L. W. and Pyle S. I. Variations in the calcification pattern in the epiphyses. *Am. J. Roentgenol.* 45:50, 1941.

Fig 8-206—Lateral projection of the left knee of an asymptomatic boy 12 years of age. The long indentation on the dorsal edge of the patella is filled with two accessory ossification centers.



FEMUR.—The ossification center in the distal epiphysis increases in size and extends laterally rapidly during the 2nd to the 6th year. During this interval of rapid growth the lateral and medial margins are commonly irregular and ragged (Fig 8-207). In lateral projection normal femoral ossification centers may present a rough fringed-like margin (Fig 8-208 A). We found an accessory ossification center at the proximal ventral superior angle of the greater femoral condyle of an asymptomatic boy (Fig 8-208 B). In older children marginal mineralization of the femoral condyles is characteristically uneven and is often associated with independent ossification centers beyond the edge of the main mass of the bone (Fig 8-209). These irregularities are located on the dorsal and caudal walls of the condyles and are best seen in lateral and tunnel projections when they may be only faintly visible in standard frontal projections. These normal marginal roughenings of the dorsal walls of the condyles and their independent marginal ossicles have been mistaken for osteochondritis dissecans and superfluous surgical treatments instituted. Our studies indicate that conspicuous irregularities of this kind occur in approximately 30% of all healthy children when the knees are examined in tunnel and lateral projections. Similar but less marked changes are often simultaneously present in the edges of the proximal tibial epiphysis. These irregularities should be recognized as normal anatomic features and not misconstrued to be the result of rickets, trauma or infection. The pattern and distribution of these extra-normal independent ossification centers in the distal femoral epiphyseal cartilage is shown schematically in Figure 8-210.

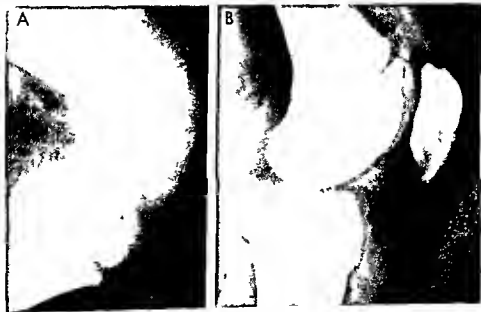
During late childhood when the intercondylar fossa becomes deeper, lateral projection of the distal femoral epiphysis shows the anterior segment to be more radiolucent than the remainder of it (Fig 8-211). Its posterior segment is more opaque because posteriorly the intercondylar fossa is deeper than it is anteriorly and for this reason, with the femur in lateral projec-



Fig. 8-207—Normal irregular mineralization on the margins of the ossification centers in the distal epiphyses of the femur of a boy 3 years of age.

Fig. 8-206—A, lateral projection of the left knee of an asymptomatic boy 3 1/2 years of age. The femoral condyle has a rough fringed edge due to partial fusion with several marginal accessory ossification centers in the contiguous epiphyseal cartilage. Similar marginal centers were present at both ends of the ossi-

cation center in frontal projection. B, small triangular independent accessory ossification center at the proximal ventral edge of the greater condyle (arrow) of an asymptomatic boy 13 years of age. Smaller scale accessory centers are also visible at the ventral edge (lower pole) of the patella.



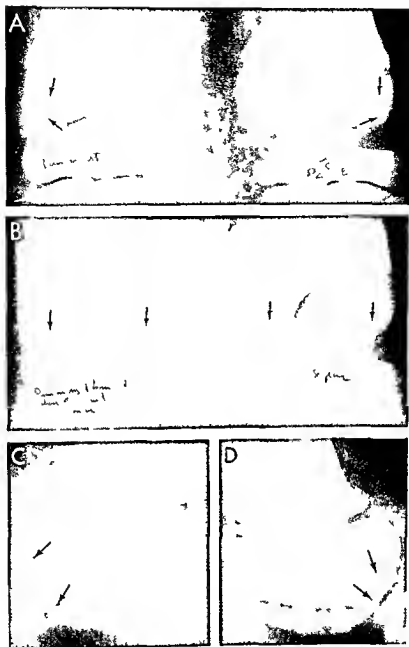


Fig. 8-209 — Knees of a boy 10 years of age in frontal (A) tunnel (B) and lateral projections (C and D). The right knee had been slightly and indefinitely painful for two days only. The left was always asymptomatic. In the frontal projection the margins of the condyles are smooth but the texture of the condyles is

slightly irregular (arrows). In both tunnel and lateral projections there are deep marginal irregularities in the dorsal edges of the condyles. Independent marginal ossification centers can be seen in the cartilage well beyond the edge of the main mass of the condyles.

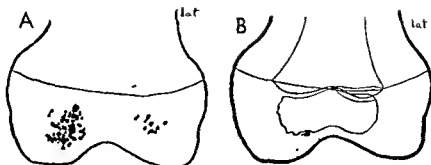


Fig 8-210 —A, sites of focal extra-ossification centers in the left distal femoral epiphyseal cartilages of 291 children recorded on tracings of an adult femur. B, tracing of the distal ends of a child's femur superimposed on a tracing of the distal end of an

adult femur which shows an accessory ossification center in the cartilage of the epiphysis just beyond the caudal edge of the main ossification center as a black dot. The dotted line indicates the projected growth of the accessory center. (From Rosenberg.)

Fig 8-211 —Normal radiolucent inferior segment of the distal femoral epiphysis of a girl 5 years of age as seen in lateral projection. It is more radiolucent than the posterior segment because the rays traverse only two opaque walls: the medial wall of the medial condyle and the lateral wall of the lateral condyle.

Posteriorly where the intercondylar notch is deeper the rays traverse four opaque walls: the lateral and medial walls of both condyles. The arrows point to an opaque sclerotic band cast by the floor of the intercondylar notch. A, frontal end; B, lateral projections.

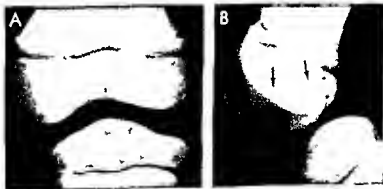


Fig 8-212 —Normal popliteal groove (arrow) in the posterolateral wall of the lateral femoral condyle of an asymptomatic girl 11 years of age.



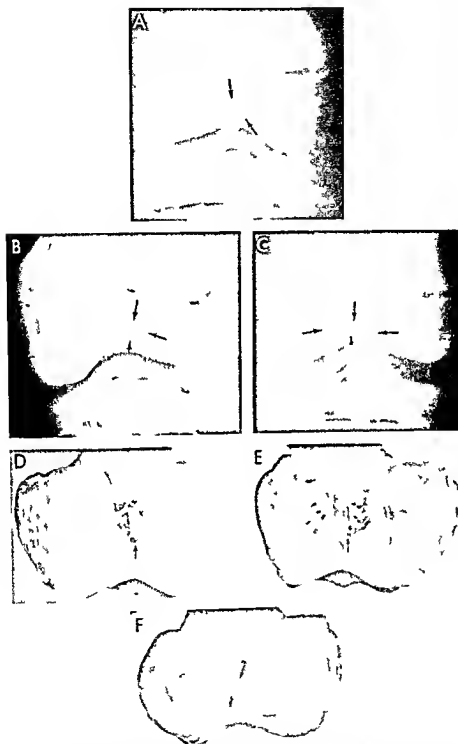


Fig. 8-213 — Normal radiolucent shadow of the nutrient foramen of the distal femoral epiphysis (arrows) on the posterior wall of the intercondylar fossa. A, poorly defined foramen in a boy 7

years of age. B, sharply defined foramen in a girl 11 years of age. C, long transverse foramen in a girl 10 1/2 years of age. D, E and F, photographs of nutrient foramina in adult femurs.

tion the x rays must traverse four opaque walls the lateral and medial walls of each of the two condyles. In the anterior segment where the intercondylar fossa is shallow there are only two opaque walls to be traversed by the rays the lateral wall of the outer condyle and the medial wall of the inner condyle.

The popliteal groove is a normal marginal defect which appears on the posterolateral aspect of the outer condyle in the prepubertal period (Fig 8 212). This groove carries the tendon of the popliteus muscle; it is never visible during infancy or early childhood.

The nutrient foramen of the distal femoral epiphysis has received little attention roentgenographically but it is often clearly visible in frontal projections of the distal femoral epiphysis in children older than 4 years (Fig 8 213). It should not be mistaken for a destructive lesion when there are local clinical signs of disease in or around the knee.

REFERENCES

- Caffey J. et al. Ossification of the distal femoral epiphysis. *J Bone & Joint Surg* 40-A: 647, 1958.
 Ribbing S. On the cause of osteochondrosis dissecans. *Acta radiol.* 25: 732, 1944.
 Rogers W. M. and Gladstone H. Vascular foramina and arterial supply of the distal end of the femur. *J Bone & Joint Surg* 32-A: 868, 1950.

Marginal irregularities of the medial cortical wall of the femur near its distal end are common between 10 and 15 years (Simon). Sometimes constriction at the same level and on the same side is reduced. In some cases these irregularities are the precursors of benign cortical defects. The anomaly is three times as

Fig 8 214—False fracture lines (arrows) at the distal end of the femur cast by the superimposed radiolucent image of the cartilage plate at a more proximal level. Similar changes were present at the proximal end of the tibial shaft. This was a healthy girl 10 years of age.



common in boys as in girls. Mature bones do not show this irregularity.

REFERENCE

- Simon H. Medial distal metaphyseal femoral irregularity in children. *Radiology* 90: 258, 1968.

False fracture lines may be superimposed on the distal end of the femoral shaft due to superimposition of the radiolucent cartilage plate at two different levels (Fig 8 214). These marginal fusions of accessory ossification centers with the caudal edge of the femoral condyle may be invisible in standard frontal projections and clearly visible in tunnel projections (Fig 8 215). Rarely an accessory ossification center develops in the epiphyseal cartilage contiguous to the lateral edge of the epiphyseal ossification center (Fig 8 216). Frequently small transitory exostoses appear and soon disappear on the medial cortical wall of the distal end of the femoral shaft (Figs 8 217 and 8 218).

Cortical femoral fibrous defects similar in all respects to the defects already described in the tibia and fibula are even more common in the distal metaphysis of the femur. Cortical defects have however not been found in the epiphyses. Two defects may be present in one femur or single defects may be found in each of the femurs. In rare instances the same

Fig 8 215—Fusion of marginal accessory ossification centers with caudal edge of the femoral condyle. A visible frontal projection (A) but clearly visible in tunnel projection (B).

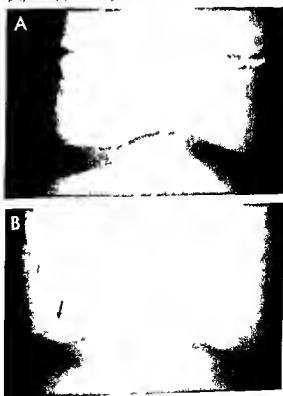
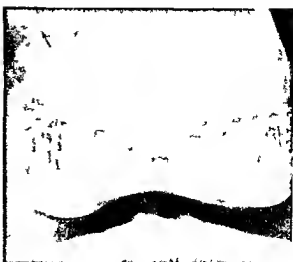




Fig. 8-216 (left) —Accessory medial ossification center (arrow) contiguous to the medial edge of the epiphyseal ossification center of the right femur of an asymptomatic girl 13 years of age. Injury to the medial collateral ligament has been associated with the appearance of this accessory center in some cases.

Fig. 8-217 (right) —Transitory small exostoses on the medial edge of the femoral shaft of a boy 10 1/2 years of age.



child may show multiple defects in the femurs, tibiae and fibulae. The size of the defects is variable; some are only a few millimeters in diameter while others may be several centimeters.

When projected *en face* the defects cast a round or oval radiolucent vacuolated cystlike shadow which is always shown to be a shallow superficial defect in the cortex when it is projected in profile. These femoral lesions have not been seen in children younger than 18 months and are usually best developed after the 5th and 6th years. They disappear during the later years of childhood or persist into adult life and are not uncommon in young adults. During their earliest phase they are usually small and poorly defined; also at this time they are usually located very near the end of the shaft and often extend to the primary zone of calcification, either abutting or overlapping it (Fig. 8-219).

Early and viewed in profile the typical cortical defect is a superficial radiolucent patch (Fig. 8-220). Cortical defects are exceedingly rare in the ventral cortical wall of the femurs (Fig. 8-221). Early the cortical defects begin consistently as an erosion on the external edge of the cortical wall (Fig. 8-222). I have never seen the initial erosion begin on the inner edge of the affected cortical wall. Endochondral bone formation is apparently never disturbed in the presence of these defects, which points to their probable cortical rather than endochondral origin. Older lesions are located deeper in the shaft, are larger, better defined, are often multilocular with fluted sclerotic borders (Fig. 8-223). The difference in the full face and the profile projection is shown in Figure 8-224. Formation of transverse lines in the same metaphysis is apparently not especially affected by the presence of the cortical defect (Fig. 8-225).



Fig. 8-218 —False fracture lines and fragments in the metaphysis of the distal end of the left femur due to images of the radiolucent cartilage plate at different longitudinal levels superimposed in both lateral (A) and frontal (B) projections. This healthy boy was 13 years of age.



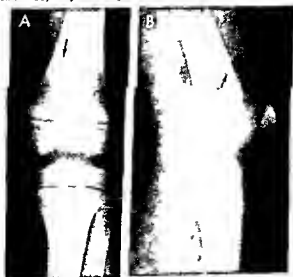
Fig. 8 219 (left) - Small poorly defined cortical defect in the medial segment of the femoral metaphysis of a healthy boy 5 years of age. A small benign cortical defect was also present in the medial cortical wall of the tibia.

Fig. 8 220 (right) - Early superficial benign cortical defect in

the lateral cortical wall of the right femur of an asymptomatic boy 10 years of age. In all of our early examples of cortical defects the cortical wall appears eroded from the outside rather than impinged on and expanded from the inside.

Fig. 8 221 - Benign cortical defect in the ventral cortical wall of the left femur of an asymptomatic boy 10 years of age. **A**,

frontal; and **B**, lateral projections. The ventral position is a great exception.



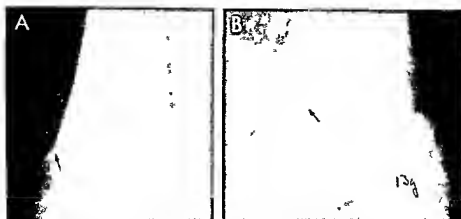
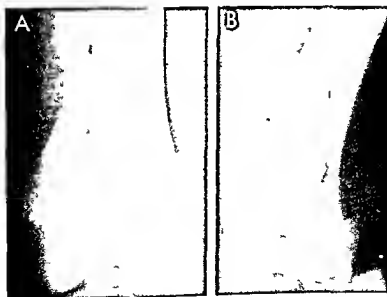


Fig 8 222.—Benign cortical defect at age 8 years when it was small (A) and at 13 years (B) when it was greatly enlarged. In A the cortical wall appears to be eroded and depressed from the outside probably from the periosteum rather than from over

growth and pressure from within the medullary cavity. In B the end of the shaft has extended caudad and the cortical defect is located more cephalad than it is in A. This patient was an asymptomatic boy.

Fig 8 223.—Large multilocular cortical defect at a relatively deep level in the shaft and well away from the epiphyseal cartilage of the femur of an asymptomatic boy 11 years of age. The two projections show that the defect is superficial and largely confined to the cortex without involving the spongiosa. This defect lies in the posteromedial arc of the compacta; it is multilo-

cular and the sclerotic fluted margins are well shown in both films. Directly over the defect a thin layer of cortex bulges externally but general tubulation of the shaft is not disturbed. All of these features suggest that the lesion originated from the cortex rather than from the growing cartilage. A, frontal and B, lateral projections.



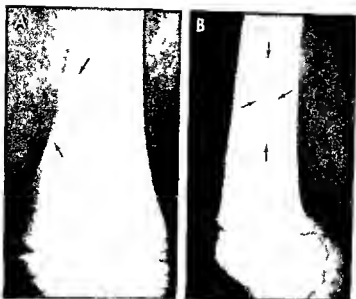


Fig 8-224 — Cortical defect in the medial wall of the femur of an asymptomatic boy 6 years of age. In A, frontal projection on the defect is seen in profile and appears as a superficial lesion in the

medial cortical wall. In B, lateral projection on the defect is seen en face and presents a cystic appearance roentgenographically.

Fig 8-225 — Oval cortical defect in the femur of an asymptomatic boy 9 years of age associated with transverse lines in the spongiosa at the same level of the shaft. The underlying transverse lines are not deformed in the site of the cortical defect because they represent linear scleroses in the spongiosa which are unaffected by the overlying cortical lesion.



Fig 8-226 — Concurrent migration shaftward and opacification of a linear cortical defect at A, 7 years; B, 8 years; C, 9 years. In the evolution of these defects opacification always begins in the segment farthest from the epiphyseal cartilage.



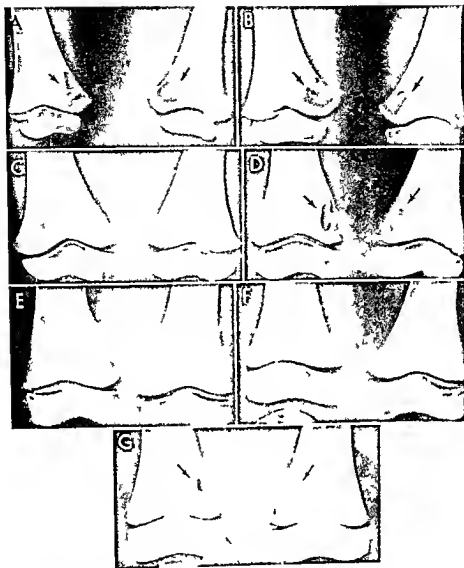


Fig. 8-227 — Fluctuating identical courses in two symmetrically placed femoral defects A at 21 months B at 34 C at 47 D at 59 E at 72 F at 83 and G at 95 months. Both defects disappeared

spontaneously at 47, 72 and 83 months to recur at the same sites at 59 and 95 months

The course of these defects is highly variable especially in the femurs. Most of them gradually shift away from the end of the shaft with advancing age and shrink in size until they become invisible. Many during the same time gradually become opaque first in their shaftward segments and later in whole (Fig. 8-226). Others may persist in the exact site of their origin at the end of the shaft for many years. Others may completely disappear from year to year with recurrences from year to year in the exact site of their origin (Fig. 8-227). Large defects may break up into several smaller segments and then these segments may fluctuate in size and shape and in relative position. This remarkable lability of cortical defects is one of their most characteristic features, one which dif-

ferentiates them from all the known lesions of growing bones.

Occasionally the early superficial cortical defect is present in one bone and the older deeper defect in another bone at the same time (Fig. 8-228). During healing some defects migrate toward the end of the shaft and leave a sclerotic internal thickening of the cortical wall—a sclerotic trail of new bone formation along the trail of their migration (Fig. 8-229). In their late phase of healing these defects do form bone (see Fig. 8-226); they are osteogenic in the healing phase.

Cortical defects in the femurs can be demonstrated roentgenographically in a surprisingly high percentage of normal asymptomatic children older than 3 years. Sontag and Pyle found them in approximately



Fig 8-228—Benign advanced multiloculated defect in the tibia and single early superficial defect in fibula (arrow). It is likely that the large deep tibial defect began as a superficial defect similar to the superficial defect in the fibula. The patient was 5 years of age. Microscopic diagnosis of fibrous defect was made by Dr Henry L. Jaffe, New York.

one-half of the normal boys they examined and in about one-fifth of the normal girls. In our serial studies of the bones at the knees, defects were found at one or more ages in 40% of boys and 30% of girls. Cortical defects were present in 34 of 54 siblings from 20 families studied by Selby. This means that the presence of such femoral shadows in children who are abnormal need carry no implication of destructive disease in the femur even when there are clinical signs of disease in and around the knee. Also these defects and their cystlike shadows need have no clinical significance when found in patients who have diseases which cause multiple and generalized destructive changes in the long bones, such as leukemia, eosinophilic granuloma, polyostotic osteomyelitis, syphilis, tuberculosis, and osteitis fibrosa cystica. It is also manifest that in view of the fact that these defects are common in all children, they will be found by chance in a considerable number of children who have growth disturbances and such disorders as Osseous Schlatler disease and Perthes disease when there is no causal relationship between the femoral defect which is developmental and the disease found in association with it. When the significance cannot be satisfactorily evaluated, biopsy will be necessary for a conclusive diagnosis.

Radiologically, cortical defects may be confused with bone cysts, eosinophilic granuloma, localized fibrous dysplasia, localized osteitis fibrosa cystica, intracortical (Brodie's) abscess, aneurysmal bone cyst, subperiosteal desmoid, or periosteal chondroma.

In single films, cortical defects are similar to the nonosteogenic fibromas of Jaffe and Lichtenstein. It may be that cortical defects are the earlier and

smaller phase of nonosteogenic fibromas. They are apparently identical microscopically. Jaffe observed a patient who presented a cortical defect in the femur at 9½ years of age which had converted to a nonosteogenic fibroma 3½ years later, radiographically.

The morbid changes and the tissues in the site of the defect which are responsible for it are not well known. Hatcher made block biopsies in several patients and he found the site of the roentgen defect filled with a mass of fibrous tissue which occupied a smooth-walled cavity in the bone. The external segment of the cavity was covered by periosteum which fused with the fibrous mass below it. In the words of connective tissue were many multinucleated cells and with them some lipid-containing macrophages.

Marek provided a detailed description of the gross structural changes. He found grayish-white localized thickening of the periosteum over the site of the cortical defect with projection of the internal end of the periosteal fibroma through the defect for a short distance into the medullary cavity. The basic lesion was a localized thickening of the periosteum inward which was directly continuous with the overlying periosteum. There was no overhang of the cortical edges and no marrow elements in the periosteal thickening.

Fig 8-229—Large cortical defect in the medial and dorsal cortex of the right femur of an asymptomatic boy 11 years of age. The arrows point to a long strip of thickened cortex which represents new bone formation in the site of the path of migration of the defect toward the end of the shaft as the epiphysis grows distalward. Bone formation is the rule in the sites of healing cortical defects and the term nonossifying fibroma is a misnomer.

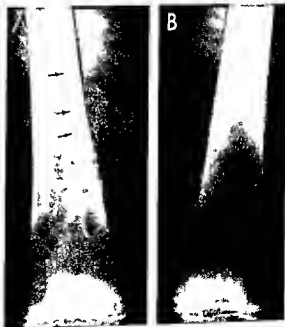




Fig 8-230 — Large multiloculated benign cortical defect with a pathologic fracture in a girl 8 years of age. Injury was denied. This fracture healed rapidly with abundant callus.

Pathologic and traumatic fractures through cortical defects are rare, but they have been seen occasionally through large defects in the distal third of the tibial shaft (Fig 8-230).

REFERENCES

- Caffey J. On fibrous defects in cortical walls of growing bones. In Levine S Z (ed): *Advances in Pediatrics* (Chicago: Year Book Medical Publishers Inc, 1955) Vol VII, p 13.
- Hatcher C H. The pathogenesis of localized fibrous lesions in the metaphyses of long bones. *Ann Surg* 12:1016, 1945.
- Jaffe H L. Aneurysmal bone cyst. *Bull Hosp Joint Dis* 11:3, 1950.
- . Tumors and Tumorlike Conditions of the Bone and Joints (Philadelphia: Lea & Febiger, 1959), p 81.
- and Lichtenstein L. Nonosteogenic fibroma of bone. *Am J Path* 18:205, 1942.
- Kimmelstiel R and Rapp I. Cortical defects due to perosteal desmoids. *Bull Hosp Joint Dis* 12:286, 1951.
- Lichtenstein L and Hall J E. Periosteal chondroma. A destructive benign cartilage tumor. *J Bone & Joint Surg* 34-A:691, 1952.
- Marck F M. Fibrous cortical defect (periosteal desmoid). *Bull Hosp Joint Dis* 16:77, 1955.
- Nicoli R. Etiology of bone cysts in children. *Helvet. chirurg. acta* 20:268, 1960.
- Selby S. Metaphyseal cortical defects in the tubular bones of children. *J Bone & Joint Surg* 43-A:395, 1961.
- Soutag L W and Pyle S I. The appearance and nature of cystlike areas in the distal femoral metaphysis of children. *Am J Roentgenol* 46:185, 1941.

physiologic variations in the spongiosa which are without clinical significance.

Localized external thickenings of the dorsal cortical wall of the femur at its distal end develop in about

Fig 8-231. Longitudinal striations in the distal end of the femoral shaft of an asymptomatic girl 11 years of age. The anatomic changes responsible for these striations were not proved roentgenographically; they appear to represent longitudinal striations of the metaphyseal spongiosa.



Longitudinal striations in the distal femoral metaphysis, both radiolucent and opaque, are not so common as cortical defects (Fig 8-231). These striations are found in children who are asymptomatic and do not give a history indicative of earlier local disease in the femur. For this reason, they are believed to be

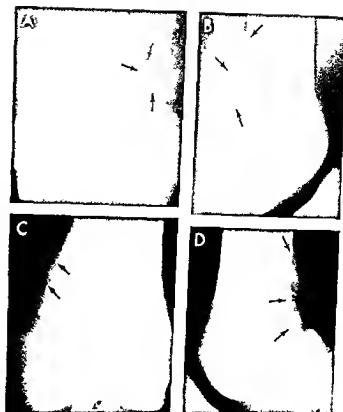


Fig 8-232.—Symmetrical localized cortical thickenings of the dorsomedial cortical walls of the distal ends of the femurs of a boy 18 years of age. The films were made because pain developed in the left knee a week before after a fall from a bicycle. The right knee was normal. A and B: frontal and lateral projections of the right knee. C and D: frontal and lateral projections of the left knee.

Fig 8-233.—Normal irregular condylar ridges on the distal cortical wall of the femur of a boy 15 years of age who had had pain behind the left knee (A) for several weeks. The question of osteogenesis imperfecta was raised because of the abnormal irregular thickening. When films of the right knee were made and the irregular bony ridge was disclosed on the right side as well (B) the diagnosis of osteogenesis imperfecta was abandoned.

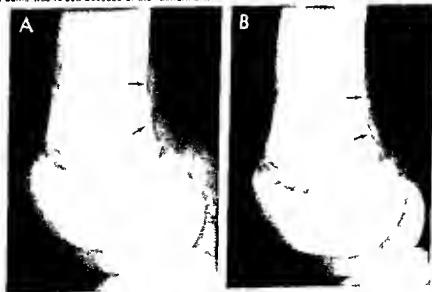




Fig 8-234—Long, thick, irregular overgrowth of the planum popliteum of a healthy boy 14 years of age. This external thickening has raised the question of osteosarcoma in some cases. In three biopsy study showed normal bone.

20% of healthy adolescents (Allen) and should not be confused with early osteogenic sarcoma which is common in the same site. In some cases these thickening are bilaterally symmetrical (Figs 8-232 and 8-233). They vary in length from 3–5 cm in children from 12–16 years of age (Fig 8-234). The foramina and canals for the nutrient arteries are often visible in both projections (Fig 8-235).

REFERENCE

- Allen D H: A variation in the diaphyseal development which simulates the roentgen appearance of primary neoplasia of bone. *Am J Roentgenol* 69:940, 1933.

The ossification centers of the trochanters, large and small, develop from multiple foci, and these structures are usually irregularly mineralized during much of the growth period (Figs 8-236 and 8-237). The physiologic irregularity in density makes it necessary to use caution in the diagnosis of osteochondrosis, fracture, or osteitis of the femoral trochanters. Optimal visualization of the smaller trochanter is obtained when the leg is rotated externally; internal rotation is the optimal position for visualization of the greater trochanter.

The best view of the femoral neck is obtained with the leg rotated slightly inward. The neck is foreshortened by outward rotation of the leg, and fractures and deformities are easily overlooked in this position. The proximal end of the shaft commonly shows a roughened margin. The irregularities on the edges of the femoral ossification center and the provisional zone of calcification directly opposite it suggest one or more transitory extra ossification centers (Fig

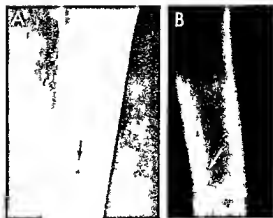


Fig 8-235—Superior (A) and lateral (B) projections of the femur. In A the foramen casts a small circular radiolucent image. In B the canal perforates the anterior cortical wall and could be interpreted as a cortical fracture line. Small foramina and canals were present in the other femur at the same level in this asymptomatic boy 3 1/2 years of age.

8-238). The marginal defect in the medial side of the proximal femoral epiphyseal ossification center (Fig 8-239) is the fovea capitis femoris. The proximal femoral epiphysis may sometimes be found divided into two portions by a jagged band of lesser density. This results from ossification of the epiphyseal cartilage from two centers rather than the normal one.

Fig 8-236—Normal irregularities in density of the shaft adjacent to the trochanters and the secondary center in the greater trochanter of the femur in an asymptomatic boy 5 years of age.



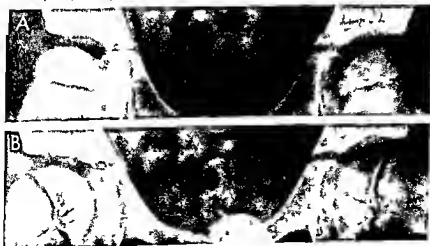


Fig. 237—Normal irregularities in density and margins of the proximal end of the femur in an asymptomatic boy 9 years of age. **A**, frontal projection with the femur adducted. Arrows are directed at areas of uneven density and grooves near the greater and lesser trochanters, cartilage-shaft junction and summit of the proximal epiphysis where the fovea capitis is seen as a shadow of diminished density. There are three secondary centers in the lesser trochanter. The flattening on the medial aspect of the proximal epiphysis is physiologic and should not be misconstrued as early coxa plana. **B**, frontal projection with the femur abducted and rotated axially. Arrows point to areas of uneven density in the femoral shaft and pubis.

ow of diminished density. There are three secondary centers in the lesser trochanter. The flattening on the medial aspect of the proximal epiphysis is physiologic and should not be misconstrued as early coxa plana. **B**, frontal projection with the femur abducted and rotated axially. Arrows point to areas of uneven density in the femoral shaft and pubis.

Fig. 238—Symmetrical irregular ossification in the proximal metaphyses of the femurs of a child 5 1/2 years of age who limped slightly on the left side only. In **A**, the irregularities are not clearly

seen. In **B**, in which the femurs are abducted, the arrows point to symmetrical segments of irregular ossification and possibly accessory multiple ossification centers in the metaphyses.



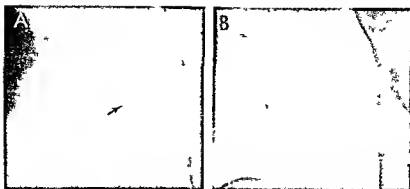


Fig. 8-239 — The fovea capitis femoris (arrow) is characteristically visible in standard frontal projection (A) but is not visible

when the femur is externally rotated and abducted into the frog position (B). The patient was a healthy boy 15 years of age.

Fig. 8-240 — Factitious splitting of the femoral head in an asymptomatic girl 4 years of age. In A, frontal projection, the femoral head image is normal. In B, lateral, externally rotated position, the femoral head image is divided longitudinally into

two unequal segments by a strip of decreased density which represents the synchondrosis between the two ossification centers which developed one behind the other in the ventrodorsal direction.

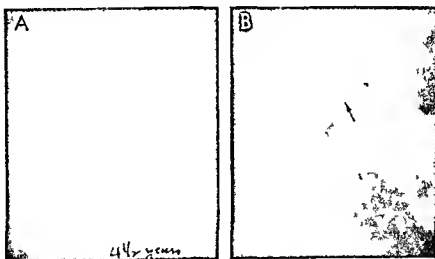




Fig. 8-241 (left) —Normal fetal osteosclerosis of the femur due to internal thickening of the cortex (arrows) with corresponding diminution in caliber of the medullary cavity. At approximately the middle of the thickened cortical segment the canal for the nutrient artery is seen.

Fig. 8-242 (middle) —Normal osteosclerosis of the newborn. A, forearm of an asymptomatic infant 14 days of age. The radius and ulna, especially the proximal two-thirds, are sclerotic owing to disproportionately thick cortices and correspondingly narrow medullary cavities. The nutrient canal of the ulna is projected axially and casts a small oval shadow of diminished density (arrow); the nutrient canal of the radius, in contrast, is projected in profile and casts a short tubular shadow of diminished density

where it traverses the compacta (arrow). B, forearm of an asymptomatic girl 6 years of age. In comparison with A, the cortices are relatively thin and the medullary cavities wide. The nutrient canals are not visible because they are small in relation to the thicker cortex of childhood.

Fig. 8-243 (right) —Diffuse thickening of prematurity in a nonsyphilitic premature infant 6 months of age. The blood of both parents and of the infant gave negative react one to Wassermann and Kahn tests on several occasions. It is noteworthy that there is no roentgen evidence of recent or old rickets in the metaphysis. Unrecognized repeated trivial trauma is a probable cause.

center (Fig. 8-240). The two proximal femoral ossification centers, one on each side, are often unequal in size during the 1st year in healthy infants; this fact invalidates many diagnoses of congenital dysplasia of the hip on the basis of relative smallness of this ossification center on one side. Also occasionally one or both of the proximal femoral ossification centers may develop in a flattened contour which simulates coxa plana when the patient is actually healthy and never shows signs of clinical coxa plana.

MULTIPLE GENERALIZED AND SCATTERED NORMAL VARIANTS

OSTEOSCLEROSIS OF THE NEWBORN —The long tubular bones of fetuses, premature infants and newborn mature infants often appear to be sclerotic roentgenographically (Figs. 8-241 and 8-242) in comparison with older bones. This sclerosis is due to proportionately thicker cortical bone and more abundant spongiosa during fetal and neonatal periods (see Fig. 8-58)

In some cases the medullary cavities appear to be almost completely obliterated by the internal thickening of the cortex. The sclerotic changes disappear gradually during the first weeks of life; this phenomenon has not been studied carefully. As far as is known, neonatal sclerosis has no pathologic significance. Correlations of the magnitude of neonatal physiologic skeletal sclerosis with the magnitude of physiologic anemia of the first months of life and the anemia of prematurity would be of interest. The nutrient canals are relatively large during the neonatal period.

CORTICAL THICKENING OF PREMATUREITY can be demonstrated roentgenographically in more than half of all premature nonsyphilitic infants (Fig. 8-243). The exact cause and pathogenesis of these lesions are not known nor is it known why so many premature infants do not show them. Malmberg showed that intensive prophylaxis with large doses of vitamin D will prevent the formation of these cortical thickenings in all but a few cases, and he concluded that rickets was the sole or at least a partial causal factor. From a

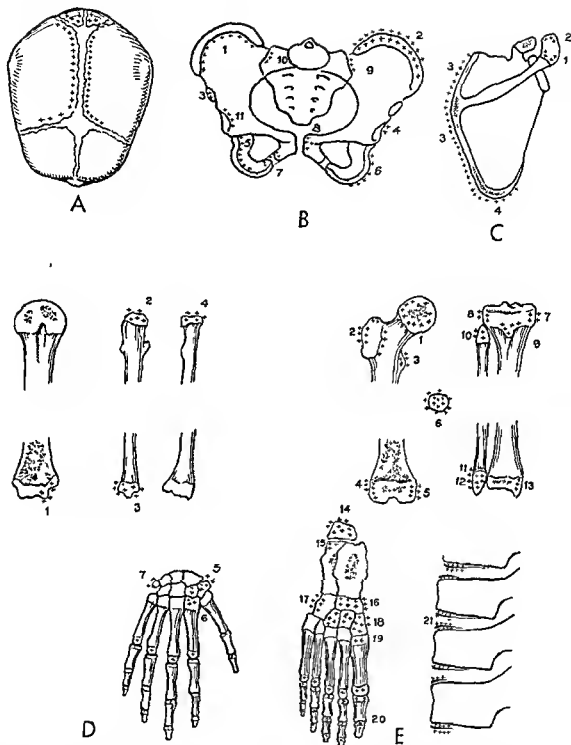


Fig. 8-245 — Common sites of normally irregular mineralization in the growing skeleton, marked by crosses. Details of many are illustrated in preceding figures, beginning with Figure 8-78.

A, cranium. During the first weeks of life and continuing for several months, edges of the bones at the great sutures are commonly irregular, and in many infants deep fissures extend

from the sutures into the bodies of the bones. Irregularities are also common on the edges of the temporal suture, not shown here.

B, pelvis. 1 crest of ilium 2 secondary center in crest of ilium 3 secondary center of anterosuperior spine 4 os acetabuli 5 body of ischium 6 secondary center of ischium 7 →



Fig. 8-246 — An elongated sclerotic strip in the humerus which in a single projection suggests an enostosis of the cancellous bone in the center of the medullary cavity. In two projections however this proved to be attached to the inner edge of the dorsal cortical wall of the humerus over a long distance. A second and possibly better explanation of this image is that it represents the late calcified stage of a fibrous cortical defect which was radiolucent earlier. The patient 11 years of age had never had clinical signs at this site.

REFERENCES

- Ferguson A B. Calcified medullary defects in bone. *J Bone & Joint Surg* 29:58 1947.
 Kim S K. Bone islands. *Radiology* 99:77 1968.
 Laurence W, and Franklin E L. Calcifying enchondroma of long bones. *J Bone & Joint Surg* 35-B:224 1953.
 Steel H H. Calcified islands in medullary bone. *J Bone & Joint Surg* 32-A:405 1950.

THICKNESS OF THE EPIPHYSEAL PLATES —The calcified cartilaginous disks and the contiguous tightly meshed cartilaginous spongiosa which cast the transverse bands of increased density across the ends of the shaft vary considerably in thickness in healthy children of the same age and in the same child at different ages. The exact significance of these differences in thickness is not known and the subject needs more study. In our experience the epiphyseal plates tend to be proportionately thicker during the 2nd to 5th years (Fig. 8-248). In the diagnosis of "lead lines" one should use a wide normal range for the epiphyseal plate shadow during this age period.



Fig. 8-247 — Normal focal sclerosis in the calcaneus. A, numerous small foci in an asymptomatic boy 12 years of age. B, single large focus in an asymptomatic boy 12 years of age. The arrow at the base of the fifth metatarsal points to a normal apophyseal center which is developing from two foci in this patient.

Diseases of Bone

One, several or all of the component parts of a growing tubular bone may be diseased, corticalis, spongiosa, epiphyseal plates and medullary cavity may be involved singly or in combination. Local lesions may be limited to the shaft or one of the epiphyses, but in generalized diseases similar abnormalities are usually found in corresponding portions of the shafts and the epiphyseal ossification centers. The external configuration may be modified or remain normal. The density of the entire bone or any part of it depends on the calcium content and the amount of calcium containing tissue. The compact bone of the cortex is responsible for most of the shadow cast by a long tubular bone, the shadow of the

ischium and pubis at the ischiopubic synchondrosis 8 body of pubis 9 ilium at sacroiliac joint 10 sacrum at sacroiliac joint 11 iliac edge and roof of the acetabular cavity

C, scapula 1 and 2 secondary centers of acromion process 3 secondary center of vertebral edge 4 secondary center of inferior angle

D, upper extremity 1 secondary center of trochlea always irregular 2 and 3 proximal and distal epiphyseal centers of ulna 4 proximal epiphyseal center of radius 5 greater and lesser metacarpals 6 constant center of second metacarpal 7 pisiform

E, lower extremity 1 proximal metaphysis of femur 2 and 3

secondary center and edges of shaft at the greater and the lesser trochanter 4 and 5 lateral and medial edges of distal epiphyseal center of femur 6 patella 7 and 8 medial and lateral edges of proximal epiphyseal center of tibia 9 secondary center in anterior tibial process 10 proximal epiphyseal center of tibia 11 and 12 distal metaphysis and distal epiphyseal center of tibia 13 internal malleolus of distal epiphyseal center of tibia 14 apophysis of calcaneus 15 primary center of calcaneus 16 navicular 17 cuboid 18 cuneiform 19 proximal epiphyseal center of first metatarsal 20 epiphyseal centers of phalanges 21 marginal centers of the spine.

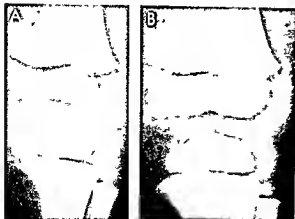


Fig 8-248—Normal absolute and relative increase with advancing age in depth of the metaphyseal bands which represent normal primary zones of calcification and the normal contiguous tightly meshed cartilaginous and bony spongiosa. A, normal bands in a child at 9 months. B, normally deeper bands in same child at 37 months.

normal spongiosa is relatively faint and severe spongiol changes must develop before they become visible roentgenographically. Increased density results from increased concentration of calcium or thickening of the calciferous tissues, decreased density is due to diminution of calcium content or thinning of calciferous tissues. Disease alters calcium content by destroying the normal equilibrium between deposition and resorption of calcium salts. Diminished calcium content and likewise roentgen density may be due to increased resorption or decreased deposition of calcium, increased calcium content, and increased roentgen density, result from increased deposition or decreased resorption of calcium.

A "dynamic" classification of the diseases of growing bones was proposed by Philip Rubin of Rochester, N.Y. He observed, in careful studies of radiation induced dysplasias, that each of the four growth units of a tubular bone—the epiphysis, physis, metaphysis and diaphysis—had its own specific function in the determination of the shape and size of the bone. He assumed from this observation that disturbance in growth in each segment could cause but a single malformation of the bone and that each malformation could result only from disturbed growth in a single segment. This is a brilliant and challenging hypothesis, but its validity cannot be tested satisfactorily until we know more about how normal bones grow and until the classification has stood the test of time and experience. We know that it is valid for some of the simpler disturbances of growth such as achondroplasia, Pyle's disease, multiple cartilaginous exostoses and enchondromas. Its validity is not so certain for the dystrophies and dysostoses, and even the variants of simpler dysplasias such as the hypoplastic and hyperplastic types of achondroplasia.

GENERALIZED UNDERCALCIFICATION (ATROPHY, RAREFACTION)

Generalized undercalcification results from the loss of lime and protein in the cortex and spongiosa; this is a common skeletal change in many chronic diseases in infancy and childhood. The severe rarefaction seen in osteogenesis imperfecta is due to a congenital failure of subperiosteal and cancellous bone production. Regional bone atrophy follows such conditions as poliomyelitic paralysis, fracture, osteomyelitis, arthritis, Erb's palsy, muscular dystrophy and others in which there is disuse of a part of the skeleton for a long period. Generalized rarefaction develops in chronic indigestion in which there is diminished absorption or increased excretion of calcium. In longstanding infections, the increased metabolic rate in conjunction with faulty digestion contributes to skeletal atrophy. Pressure atrophy of the corticals and spongiosa develops in Cooley's Mediterranean anemia owing to overgrowth and expansion of hyperplastic bone marrow. In scurvy, osteoblastic activity is inhibited and there is generalized failure of deposition of bone. Two factors are responsible for the rarefaction of vitamin D rickets: faulty absorption of lime from the intestines and a lowered threshold for its excretion through the kidneys. Excessive renal excretion of phosphorus and calcium is the basic cause of the loss of lime from the skeleton in hyperparathyroidism.

Fig 8-249—Diffuse undercalcification and rarefaction of the tibia and fibula of a girl 2 1/2 years of age who had calic disease. The cortical walls are thin owing to loss of compacts on their internal aspects and the medullary cavities are correspondingly dilated. The spongiosa is faint owing to its low lime content, but the spongiol pattern is coarsened by loss of shadows of the finer secondary trabeculae.



The roentgen signs of generalized rarefaction include cortical thinning and a decrease in the size and number of the trabeculae in the spongiosa (Fig 8-249). Concentric constriction of the shaft (over configuration) and thickening of the epiphyseal plates are common associated findings in rarefaction. Often during the development of generalized rarefaction the spongiosa and nutrient canals become more conspicuous because the cortex becomes thinner and less dense. Transverse bands of diminished density may be found on the shaftward side of the thickened epiphyseal plates in some cases of severe generalized rarefaction. Analogous submarginal bands of diminished density are often found in the small bones and epiphyseal centers of the same patients. Generalized rarefaction develops in many diverse morbid states; its presence has little specific diagnostic value.

Geiser and Trueta produced rarefaction of the calcaneus of rabbits consistently soon after this bone was relieved of its normal muscular compressing forces. When the same bones were again subjected to the stresses and strains of normal muscular action, new bone was consistently generated. During the phase of progressive rarefaction the vascularity of the rarefying calcaneus was greatly increased.

GENERALIZED OVERCALCIFICATION (HYPERTROPHY SCLEROSIS)

Generalized overcalcification may be due to excessive bone production or diminished resorption of cor-

tex or spongiosa. Cortical thickening is the usual cause of diffuse overcalcification. External cortical thickening is a common feature of healing in osteitis scurvy and rickets and of hypertrophic pulmonary osteoarthropathy. Diffuse internal cortical thickening of a tubular bone is a rare cause of bony sclerosis; we have seen it in the tibia of a child who had extensive congenital varicosities of the lower extremities. Internal cortical thickening has been found in sickle cell anemia of adults. Diffuse thickening of spongiosa is an exceptional cause of bone sclerosis but may occur in such rare conditions as congenital osteopetrosis, fluorine poisoning, and sclerotic leukemia.

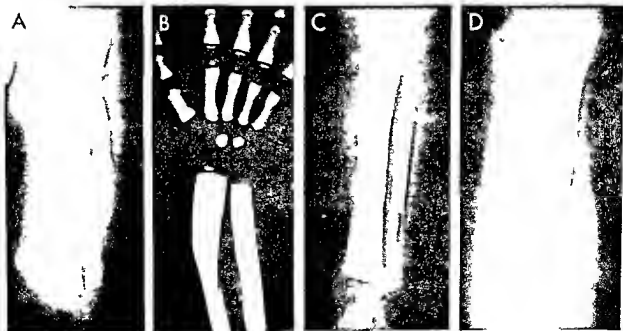
The roentgenographic features of generalized sclerosis are shown in Figure 8-250. The density is diffusely increased. The corticis may be uniformly thickened or it may be stratified. In osteopetrosis the heavy shadow of the thickened spongiosa fuses with the cortex and obliterates the line of demarcation between corticis and spongiosa.

FOCAL UNDERCALCIFICATION

Local resorption of the cortex and spongiosa develops at the site of injury or infection of a bone. The portions of a bone contiguous to cellulitis or arthritis may become demineralized during the active phase of the adjacent inflammation. In localized and scattered fibrous dystrophies the sites of fibrosis appear roentgenographically as shadows of diminished density. Localized hyperplasias of the intraosseous reticu-

Fig 8-250—Diffuse overcalcification in: A, healing scurvy; B, osteopetrosis; C, syphilitic osteitis; D, healing rickets. Cortical overcalcification is also found in callus formation after fracture and in involucrum formation after infection. The cortex is also

thickened externally in infantile cortical hyperostosis, hypertamnosia, and Engelmann's disease, and internally in prenatal bowing of the long bones.



endothelial tissues may destroy and replace bone and give rise to bony defects. Primary and secondary osteolytic neoplasms produce bony defects in a similar manner. Defects in the epiphyseal ossification centers result from infection, ischemic necrosis and cretinoid dysgenesis. In many of the destructive lesions, marginal bone production develops during the later phases of healing. Sudeck described an unusual type of atrophy which develops following major or trivial injuries to the joints. Within four to six weeks the bones distal to the injured joint show marked demineralization and atrophy.

The cortical defects of the femur, tibia and fibula described in the preceding chapter are excellent examples of localized undercalcification of unknown origin.

FOCAL OVERCALCIFICATION

Localized increases in the cortex and spongiosa are common features of localized osteitis, traumatic subperiosteal hematoma, callus formation, rickets, hypervitaminosis A, scurvy, infantile cortical hyperostosis, Engelmann's disease, hyperphosphatasemia (Caffey) and prenatal bowing of the long bones. Long-standing cellulitis, varicosities and neoplasms near tubular bones may also give rise to localized overcalcifications in these bones. In the flowing periostitis of Léri, the same side of several bones in an extremity exhibits cortical thickening. Transverse lines in the

ends of growing bones are cast by transverse disks of thickened spongiosa. Analogous submarginal cancellous thickenings develop at the same time in the small bones and the epiphyseal ossification centers.

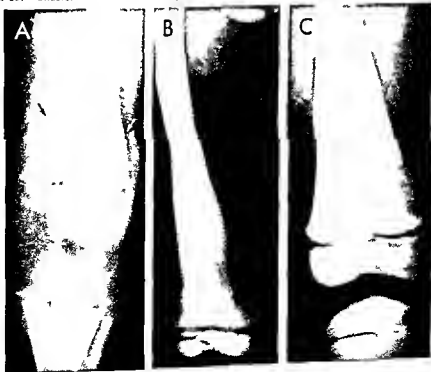
REFERENCES

- Bauer W, Aub J C and Albright F: Studies of calcium and phosphorus metabolism. 5. A study of the bone trabeculae as a readily available reserve supply of calcium. *J Exper Med* 49: 145, 1929.
 Geiser M and Trueta J: Muscle action, bone rarefaction and bone formation. An experimental study. *J Bone & Joint Surg* 40-B: 282, 1958.
 Key A J: Local bone atrophy. *Am J Roentgenol* 30: 34, 1933.
 Stevenson F H: The osteoporosis of immobilization in recumbency. *J Bone & Joint Surg* 34-B: 256, 1952.
 Sudeck P: Ueber die entzündliche Knochenatrophie. *Arch f kl u Chir* 62: 147, 1900.

CONSTRICTION (TUBULATION MODELING)

With few exceptions in the tubular bones the ends of the shaft are wider than the middle and there is a progressive concentric decrease in the caliber of the shaft as one passes from the end toward the middle of the bone (see Fig 8-64). The growth factors responsible for normal terminal flaring and intervening stenosis have been called modeling or tubulation. Morbid processes in growing bones may modify configuration in one of two directions—underconstriction and overconstriction.

Fig 8-251—Underconstriction in: A, healing rickets; B, osteoporosis; C, after recovery from lead poisoning.



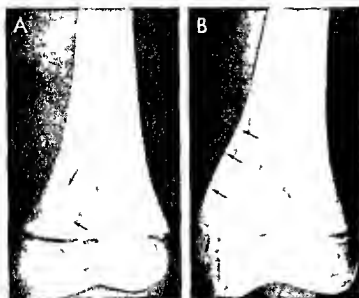


Fig. 8-252.—Unilateral failure of tubulation due to injury at biopsy. A, frontal projection of the femur at 5 years of age. There is a large cortical defect (arrows) in the metaphysis, but both cortical walls are normally concave. A biopsy was done a few days after this film was made. B, frontal projection of the same femur three years later. The shape of the femur is now abnormal owing to the external convexity of the medial wall which previously was normally concave. The lateral, ventral and dorsal walls of the femur were all normal. Cases of this kind demonstrate clearly that tubulation is a function of the cortical wall and is independent of proliferation of cartilage at the growth zone and of endochondral bone formation.

Fig. 8-253.—Failure of constriction of the proximal half of the humeral shaft associated with two cartilaginous exostoses in the same levels. The patient was a boy 2 years of age.

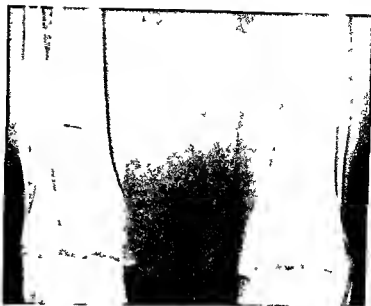


UNDERCONSTRICTION—Underconstriction or failure of modeling of the long bones is illustrated in Figure 8-65. It is characterized by shallowness of the usually concave lateral borders, in marked examples, the concave outline may become straight or even convex (Fig. 8-251). Many of the diseases of growing bone modify constriction and inhibit it if the morbid process continues for any length of time. Tubulation may fail after local mechanical injury to the cortical wall (Fig. 8-252). Diminished constriction or failure of constriction is conspicuous in the cartilaginous dystrophies (Figs. 8-253 and 8-254), osteopetrosis, late lead poisoning, neoplasms, fibrocystic disease of the pancreas, healing rickets, healing scurvy, healing fractures and old productive osteomyelitis. In Cooley's Mediterranean anemia the cortical walls are spread apart diffusely by the expanding hyperplastic marrow, which reduces or obliterates the normal middle constriction and results in swollen rectangular shapes for the tubular bones. In reticuloendothelioses such as Gaucher's disease the long bones, especially the distal ends of the femurs, become swollen in a similar fashion owing to hyperplasia of the reticuloendothelial cells. In many cases of dysostosis multiplex (Hurler's syndrome), generalized failure of tubulation is a conspicuous roentgen finding, and in Pyle's disease, failure of tubulation and the resultant splaying of the ends of the long tubular shafts are the principal roentgen features.

Generalized enlargements of the shafts due to distention of the medullary cavities may also be a late feature of infantile cortical hyperostosis in which the cortical walls may be reduced to paper thinness.

OVERCONSTRICTION—This is the reverse of underconstriction. As one passes from the end of the shaft toward the middle there is an excessive progressive concentric constriction, the concave curves become

Fig 8 254 — Local failure of constriction on the distal end of the lateral cortical wall of the right tibial shaft associated with a rounded cartilaginous exostosis which impinges on the tibia and causes segmental widening and flattening of this bone also. This boy was 15 years of age.



deepened and the terminal segment of the shaft flares widely in contrast with the stenosed intermediate segments (Fig 8 255). Most of the constriction takes place at the expense of the medullary cavity; the cortical walls, in contrast, are relatively little affected. Overconfiguration is found in longstanding paralytic and pseudoparalytic conditions such as rheumatoid arthritis, old poliomyelitis, muscular dys-

Fig 8 255 — Postpoliomyelitic overconstriction of the left radius and ulna of a girl 8 1/2 years of age who had had acute poliomyelitis at age 5. Comparison of analogous bones in the two forearms shows that the left radius and ulna are of smaller caliber than the counterparts on the right and flare more at the ends. The loss of volume of these bones is due almost entirely to loss of volume of the medullary cavities; the cortical thickness of the bones is practically the same on the two sides.



Fig 8 256 — Cupping of the right distal femoral metaphysis in a boy 13 years of age who had acute poliomyelitis at age 4 and severe permanent paralysis of the muscles in the right leg. The metaphysis of the right femur is deeply cupped and spread and the shaft is shortened. The cartilage plate is thinned and obliterated in its central segment where the shaft and epiphyseal ossification centers have apparently fused. The intercondylar notch in the femoral epiphyseal ossification center is deepened. The right tibial epiphyseal ossification center is also enlarged, but its metaphysis is not cupped. The joint space at the right knee is deepened. All the bones in the right leg are retarded and the muscular masses are small owing to the longstanding atrophy and hypoplasia of muscles.



trophy birth palsies congenital malformations of the spinal cord and brain and other like disorders

Curran in a study of 250 unselected postpolio-myelitic patients found metaphyseal cupping in 22. The bones at the knees were affected in 3 patients in the other 19 metaphyseal cupping and shortenings developed in the metatarsals. We have seen severe metaphyseal cupping with shortening of the distal end of the tibia (Fig 8 256) nine years after the onset of paralysis of the leg

REFERENCES

- Bakwin H and Krida, A. Familial metaphyseal dysplasia, *Am J Dis Child* 53 1521 1937
 Curran G. Premature closure of the epiphyses in the metatarsals and knees *Radiology* 87 424 1966
 Drey L. Failure of modeling of bone *Radiology* 61 645 1953
 Jansen M. *Dissociation of Bone Growth* (London Oxford University Press 1928).
 Keith A. Studies of the anatomical changes which accompany certain growth disturbances of the human body *J Anat* 54 101 1919

TRANSVERSE LINES OF PARK (STRESS LINES OF PARK)

Opaque transverse lines (hereafter referred to as TL) across the terminal segments of growing long bones are found in healthy and sick children at all ages. They never cause local signs or symptoms. TL may be present at birth in full term infants and in prematurely born as well which shows that they also develop in the fetus. They cannot appear after growth

is completed but they may form late during childhood and then persist into adult life. Marginal lines of increased density in the round and flat bones are the counterparts of TL in long bones and they develop simultaneously with them

Usually TL are distributed symmetrically throughout the skeleton and occupy identical sites in the corresponding bones on the two sides of the body (Fig 8 257). TL are thickest at the ends of bones which grow most rapidly (sternal ends of ribs both ends of femurs and tibias) where they also lie deepest in the shafts. At the bone ends of slowest growth (proximal ends of radii and ulnas) TL do not form at all or are exceedingly thin and lie at the very end of the shaft directly under the provisional zone of calcification. Radiographically however there are many exceptions to these usual patterns of uniform and symmetrical distribution. TL may be present in the bones of the legs and absent in the bones of the arms and vice versa; they may be conspicuous at the knees and invisible at the ankles or they may be conspicuous in the distal ends of the radii and barely visible or invisible in the distal ends of the ulnas.

TL parallel almost exactly the contours of the provisional zones of calcification which they underlie. When several TL are present at the end of a shaft they parallel one another (Fig 8 258). The lines nearest the end of the shaft are ordinarily the thickest and widest. Older lines deeper in the shaft are thinner, less distinct and usually defective at their ends. Occasionally a line may be broken into many small segments instead of being a continuous unbroken strip. Rarely long segments of a TL may be absent in its

Fig 8 257 — Transverse lines of Park in the ends of the femoral and tibial shafts of a boy 4 years of age. The transverse lines are located deeper in the shafts of the femurs because the longitudi-

nal growth is greater at the distal ends of the femurs than in the proximal ends of the tibiae.

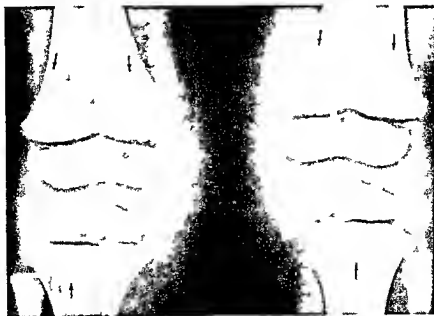


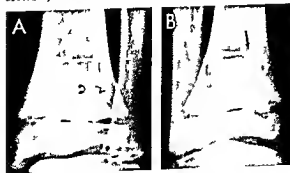


Fig 8-258—Multiple transverse lines of Park in a patient 11 years of age who was and apparently had been healthy

middle third. A line may appear to be complete in frontal projection but be seen as a large defect in lateral projection (Fig 8-259).

The exact cause of the formation of transverse lines is not known with certainty, but they appear to develop whenever a growing animal is subjected to stress of sufficient degree over sufficient time, especially such stresses as starvation and fever. Stresses to pregnant women may induce TL in the bones of the fetus growing in utero. Sontag concluded that the TL which develop in the infant during the neonatal period are due to the nutritional stress of its shifting from placental nutrition and oxygenation to those of

Fig 8-259—Incomplete transverse line of Park in the distal end of the tibia of a boy 10 years of age. In A, frontal projection, the line appears to be complete, although its medial portion is not as distinct as the rest. In B, lateral projection, the line is defective ventrally (arrow). It is manifest that transverse lines must be visualized in all three dimensions before they can be accurately evaluated.



the alimentary tract and lungs. Endocrine adjustments at birth may also be a cause in the neonate. Harris produced TL experimentally in growing animals by starvation. Park and his colleagues induced TL in rats by feeding diets deficient in protein and fat but high in carbohydrate.

A reasonable hypothesis for the causal mechanism is persistence of the excessive cartilaginous scaffold due to transitory oligemia of the metaphyseal arteries owing to the slowed blood flow through them.

The anatomic change which casts the TL in a radiograph are shown in Figure 8-260. It consists of transversely directed bony trabeculae in a thin stratum

Fig 8-260—Three-dimensional view of Park's transverse line made in a study with a binocular dissecting microscope from a preparation cleared with water-glass according to the method of Spalteholz. The transverse line is composed entirely of bone in transversely disposed trabeculae which are identical with the bone in the normal longitudinally disposed trabeculae above and below it. The transversely disposed trabeculae are formed independently of the action of the proliferative cartilage in the epiphysis and never went through a cartilaginous phase. (Courtesy of Dr. Edwards A. Park, Baltimore.)

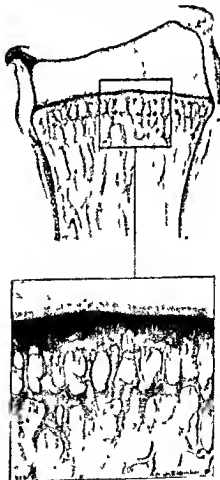




Fig 8-261—The generation of transverse lines of Park under the proliferating cartilage whose growth was accelerated by chronic hyperemia incidental to osteomyelitis of the left tibia. Transverse lines developed at all cartilage-shaft junctions. In the left tibia the lines are deeper in the shaft than its fellow in the right tibia (5 mm as compared with 3 mm) which proves that growth

of the left tibia was accelerated. The left tibial transverse lines are thicker than the lines in the right tibia which proves that longitudinal growth of the bone was accelerated during generation of the transverse line. The lines in the two femurs are each 7 mm from the ends of the shaft.

tum which extends entirely across the medullary cavity and exactly parallels the provisional zone of calcification above it and runs at right angles to the normal longitudinally directed trabeculae.

Transverse lines have been called lines of arrested growth or growth arrest lines in the belief that they developed during periods of slowed or stopped growth. However in several cases radiographic findings indicated that these lines were formed during periods of accelerated growth because in cases in which there was a difference in the velocity of growth on the two sides of the body the TL which formed in the more rapidly growing bone was buried deeper in the shaft and was thicker than its counterpart which developed at the same time in the corresponding bone which was growing more slowly on the other side (Fig 8-261). As with so many problems of this kind it fell to the talents of a great investigator in this case Dr Edwards A. Park whose penetrating studies and canny interpretations of the microscopic changes in the metaphyses in both health and disease have taught many of us the basic knowledge in this field to clarify the confusions and seeming inconsistencies. Dr Park's studies indicate that longitudinal growth arrest of a growing bone is a prerequisite to the formation of a TL in it and that longitudinal growth stops initially or is slowed in every instance. During this initial phase of growth stoppage or slowing the local osteoblasts form a thin transverse bony template directly on the underside of the zone of proliferative cartilage which is visible microscopically but is so thin that it is invisible radiographically. This primary thin bony template is formed exclusively by local osteoblasts without the aid of proliferating cartilage

cells. It is only when longitudinal growth in the proliferating cartilage is resumed during what Dr Park calls the recovery phase that a resurgence of the activity of the local osteoblasts on the template thickens it to several times its original depth and it becomes visible in a radiograph as a TL. At the same time a pent up regrowth of the proliferative cartilage occurs and buries the TL deeper in the shaft. It is clear that the TL seen by radiologists are formed during periods of accelerated growth which follow the initial phase of arrested growth. These facts resolve the seeming paradox in Figure 8-261. In view of his findings Dr Park suggested that we abandon such terms as lines of arrested growth and growth arrest lines because they are "positively bad as descriptive terms." He estimated that "1/10 or in some cases 1/100 of the completed transverse stratum which we see radiographically represents growth during the recovery phase when longitudinal growth has been resumed." He proposed the term *postarrest lines*. I prefer the term *transverse line of Park* in recognition of his splendid researches and scholarly writings on the metaphyseal phenomena during growth—a token appreciation of this knowing seeker and finder of the truth and wise and gentle teacher. If one were to select a term indicative of the cause of TL *stress transverse lines* would be appropriate.

A comprehensive review of the transverse lines and bands will be found in the article by Garm and associates published in 1968.

REFERENCES

- Elliot M. M., Souther S. P. and Park, E. A. Transverse lines in the x ray plates of long bones of children. *Bull. Johns Hopkins Hosp.* 41:364 1927.

Folbs R H Jr and Park E A. Some observations on bone growth with particular respect to zones and transverse lines of increasing density in the metaphysis. *Am J Roentgenol* 68:709 1952

Garn S M *et al*. Lines and bands of increased density. Their implication to growth and development. *Radiog & Photog* 44:58 1968

Park E A. The imprinting of nutritional disturbances on growing bone. *Pediatrics supp* May pt II 815 1964

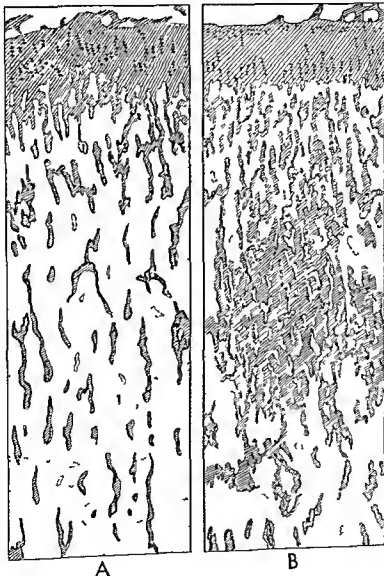
Sontag L W. Evidences of disturbed prenatal and neonatal

growth in bones of infants aged one month. *Am. J Dis Child* 55:1248 1938

LEAD BANDS—Following the ingestion of lead or its inhalation over long periods thick transverse white bands develop in the ends of the shafts of growing bones. The morphologic change which casts these bands in the radiograph is entirely different from that of Park's stress lines. The proliferative cartilage is not

Fig 8-262—Structural changes in the spongiosa which cast the transverse band shadows in the ends of the growing shafts. A and B are sections of the proximal ends of the femoral shafts of two growing dogs littermates killed at 86 days of age. Animal A received no bismuth and the section shows a normal femoral metaphysis. Animal B received 200 mg of elemental bismuth, a four intramuscular injections of 50 mg each on the 67th, 74th, 81st and 88th days of life, and films of the bones showed deep opaque bands in all of the growing metaphyses. The section of

B's femur shows the radiopaque longitudinal trabeculae to be enormously increased and the radiolucent marrow spaces correspondingly reduced in the levels of the shaft which cast the heavy transverse shadows. The lead and bismuth lesions are actually chondroscleroses. The proliferative cartilage zones at the top are not affected. Phosphor films have a different morphology and pathogenesis. It is also noteworthy that the overabundant spongiosa produced by bismuth has no or only very thin coverings of endosteal bone.



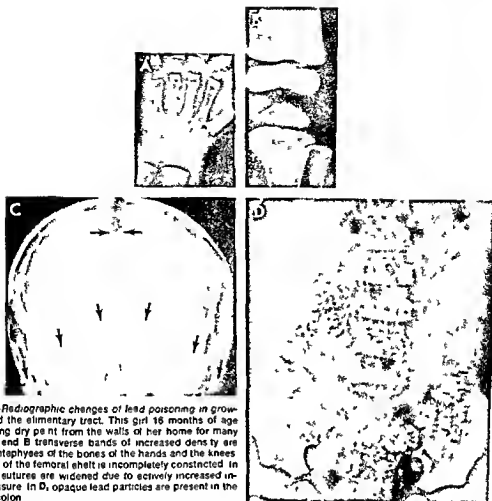


Fig 8-263—Radiographic changes of lead poisoning in growing bones and the alimentary tract. This girl 18 months of age had been eating dry pe nt from the walls of her home for many months. In A and B transverse bands of increased density are seen in the metaphyses of the bones of the hands and the knees. The distal end of the femoral shaft is incompletely constricted. In C, the cranial sutures are widened due to actively increased intracranial pressure. In D, opaque lead particles are present in the lumen of the colon.

affected so long as longitudinal growth is not slowed and a transverse template does not form. The level of the white band is filled with an excessive number of longitudinal cartilaginous trabeculae closely crowded together, and called the trabecular thicket by Park (Fig 8-262). These trabeculae are made up of calcified thick cartilaginous cores covered by thin sleeves of endosteal bone almost devoid of osteoblasts. The morbid anatomy of the lead band and the bismuth band is similar. This calcified thicket occupies space normally filled with more radiolucent marrow and is due to failure of normal thinning out of cartilaginous trabeculae, 90% of which are usually removed during normal growth. In lead and bismuth bones less than 20-30% are removed. The depth of the lead bands correlates directly with the duration of poisoning and velocity of growth in each metaphysis (Fig 8-263). From the morbid anatomy one would suspect that the basic causal mechanism for lead and bismuth lines is oligemia of the metaphyseal segment of the cartilage plate due to chronic reduced flow of arterial blood in the terminal metaphyseal arteries.

It should be remembered that lead bands are not generated rapidly enough to be visualized during the earliest phase of lead poisoning and that they form more slowly in older children. Sartain and associates have demonstrated the advantages of chemical diagnosis over radiographic in children, especially the excessive excretion of lead in the urine following a dose of versenate. In chronic infantile and juvenile plumbism lead bands are almost constant findings. The diagnosis of lead poisoning should not rest solely on the identification of lines in the skeleton; it should be based on the history of ingestion or inhalation of lead and the demonstration of excessive amounts of lead chemically or spectrographically in the urine, blood and sometimes the skin. Patients poisoned by lead are usually anemic long before the lead band appears in the bones, and the red blood cells are stippled prior to the appearance of the bands. Heavy transverse bands may be found in apparently healthy children (Fig 8-264) which are identical roentgenographically with the lines which appear in the bones during chronic lead poisoning and for this reason

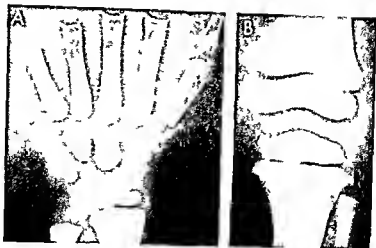


Fig 8-264—Idiopathic thick transverse bands of increased density in the terminal segments of the shafts of an asymptomatic boy 4 years of age. There was no clinical or laboratory evidence that suggested lead or bismuth poisoning and he had never ingested phosphorized cod liver oil. There had been no recognized illnesses to which these lines could reasonably be attrib-

ed. Transverse lines of this magnitude are common in apparently normal children between the ages of 2 and 6 years. The diagnosis of lead poisoning cannot be made from the roentgen changes alone; all chronic cases of plumbism are, however, characterized by heavy transverse bands in the metaphyses of growing bones.

roentgen findings must always be given only secondary weight in the diagnosis of lead poisoning. Several erroneous diagnoses have been made on the false assumption that heavy transverse bands in growing bones are pathognomonic of lead poisoning. Many patients with lead poisoning exhibit roentgen signs of increased intracranial pressure and occasionally opaque lead containing material is visible in the intestinal tract.

The lead band is gradually buried deeper in the shaft with the passing of time and during this process it interferes with constriction of the shaft, reducing constriction so that the leaded metaphyses are wider than normal (see Fig 8-251, C). This terminal widening of the shafts may persist for months or years following clinical recovery from lead poisoning, but then it slowly disappears. Pease and Newton were impressed with the resemblance of these lead widenings at the ends of the bones to the splaying of the bones which characterize Pyle's disease. It seems unlikely that lead poisoning is related causally to Pyle's disease because the lead lesions are transitory and Pyle's lesions are permanent, and so far as is known no patient with Pyle's disease has been poisoned with lead.

It seems probable that now the most important source of lead poisoning in children is the old glazing window putty which dries and breaks off in sticks several inches long that simulate candy bars. This old putty has a high content of lead. Palmisano and associates pointed out that illegally produced alcohol is the most common cause of both acute and chronic lead poisoning in the southeastern United States. Pregnant women are of course exposed to this hazard and both mother and her fetus may suffer from lead poisoning from this source.

REFERENCES

- Caffey J. Clinical and experimental lead poisoning. Some roentgenologic and anatomic changes in the growing bones. *Radiology* 17:957, 1931.
- Lead poisoning associated with active rickets. Report of a case with the absence of lead lines in the skeleton. *Am J Dis Child* 55:798, 1938.
- Gordon I and Whitehead T P. Lead poisoning of an infant with lead nipple shields. Association with rickets. *Lancet* 2:647, 1949.
- Palmisano P A, et al. Untaxed whiskey and lead exposure. *J Pediatr* 75:889, 1969.
- Park E A, et al. Shadows produced by lead in x-ray pictures of the growing skeleton. *Am J Dis Child* 41:485, 1931.
- Pease C N, and Newton G B. Metaphyseal dysplasia due to lead poisoning. *Radiology* 79:233, 1962.
- Sartain P, et al. Absence of lead lines in bones of children with early lead poisoning. *Am J Roentgenol* 91:597, 1964.

BISMUTH BANDS—Bismuth affects the growing skeleton in the same manner as lead and bismuth bands have the same roentgen features as lead bands. In our experience, bismuth bands have been encountered exclusively in children who were receiving bismuth for the treatment of syphilis. During the treatment of syphilitic pregnant women, some of the bismuth injected into the mother crosses the placenta to the fetal circulation and is transported to the fetal skeleton where bismuth bands may develop (Fig 8-265). These bismuth changes may closely simulate several types of syphilitic osteochondritis and caution should be used in the diagnosis of infantile syphilitic osteochondritis when the mother has been treated with bismuth during pregnancy. There is no convincing evidence that silver and mercury produce skeletal changes similar to those of lead and bismuth. If arsenic produces any change at the cartilage-shaft

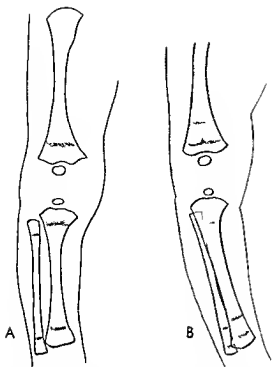


Fig 8-265—Tracings of roentgenograms of two cases of bismuth bands in the neonatal skeleton which followed maternal bismuth therapy. A, film made the 10th day of life, showing single bismuth bands deep in each end of the tibia. A single course of six injections of bismuth was given the mother between the 165th and the 214th day of gestation. B, film made the 5th day of life, showing double bismuth bands in each end of the tibia. This mother received two courses of bismuth, one during the sixth lunar month of gestation and the second during the ninth lunar month.

junction, its effect does not develop with the doses used in the treatment of infantile syphilis. Gold solution is used in the treatment of juvenile rheumatoid arthritis. We have observed the development of transverse lines in a few cases followed roentgenographically, but we are not sure that the gold was the only factor in their generation. Radiographically they resemble the stress lines of Park.

REFERENCES

- Caffey, J. Changes in the growing skeleton after the administration of bismuth. *Am J Dis Child* 53:56, 1937.
 Russin, L. A., and Stadler, H. E. The bismuth lines in the long bones in relation to linear growth. *J. Pediatr.* 21:211, 1942.
 Whitridge, J., Jr. Changes in the long bones of newborn infants following the administration of bismuth during pregnancy. *Am. J. Syph., Gonorr. & Ven. Dis.* 24:223, 1940.

RADIUM BANDS—In growing rats following the administration of radium chloride, Thomas and Bruner found heavy terminal bands of increased density in the ends of the shafts. We have not seen descriptions of the skeletal changes in human infantile or juvenile radium poisoning. Therapeutic roentgen irradiation of the cartilage-shaft junction produces heavy thick transverse lines locally; this effect is not found in corresponding nonirradiated portions of the same skeleton. They appear to be similar to the stress lines of Park.

PHOSPHORUS BANDS—The protracted ingestion of metallic phosphorus (yellow phosphorus) produces deep bands of increased density in the ends of growing shafts. The phosphorus band is made up of a bundle of fine transverse lines (Fig 8-266). The pathogenesis of the phosphorus lesion is considerably different from that of the lead effect. As with lead, the phosphorus shadow is cast by a thickening of closely packed overnumerous longitudinal trabeculae which result from failure of the normal thinning out of trabeculae. In contrast to the lead and bismuth trabeculae, the phosphorus trabeculae are made up of solid bone or small central cartilaginous cores surrounded by heavy sleeves of endosteal bone on which the osteoblasts swarm in large numbers. The phosphorus thickets are osteosclerotic, whereas lead and bismuth thickets are chondrosclerotic. Phosphorus bands have been found most frequently in rachitic and tuberculous children being treated with phosphorized cod liver oil. There is no evidence pointing to retardation of

Fig 8-266—Deep stratified phosphorus transverse bands in the bones of a girl 4 years of age who had been taking phosphorized cod liver oil by mouth for several months. She had osteogenesis imperfecta. Increases in density are also visible in the cortical walls and peripheral spongiosa.



longitudinal growth of the shafts during the formation of phosphorus bands

Marginal phosphorus bands were produced in the occipital and sphenoid bones experimentally by feeding yellow phosphorus to growing rats (Sgarbi and Gans). From the structural change one might conclude that the causal mechanism of the phosphorus bands is chronic hyperemia of the metaphyseal side of the cartilage plate due to excessive blood flow in the terminal metaphyseal arteries

REFERENCES

- Hess, A. E., and Weinstock, M. The value of elementary phosphorus in rickets. *Am J Dis Child* 82:483, 1926
 Phemister, B. D. The effect of phosphorus on growing and diseased bone. *J A M A* 70:1737, 1918

TRANSVERSE LINES OF DIMINISHED DENSITY—These are not as common or as conspicuous as the lines of increased density with which they may be associated. Rarefied transverse lines underlie and sometimes alternate with lines of increased density in such diseases as scurvy, syphilis and leukemia. A transverse stratum of defective loose spongiosa casts the shadow of diminished density visible in the roentgen film. In the level of transverse rarefaction, microscopically only a few thin longitudinal trabeculae can be seen widely separated from one another by the increased volume of marrow spaces (Park). Paucity of opaque trabeculae which are radiopaque in an excess of marrow spaces which are radiolucent is responsible for the transverse radiolucent line.

ALTERATIONS IN GROWTH AND DEVELOPMENT

The great variation in the length of the long bones in apparently normal individuals precludes the interposition of a sharp line of demarcation between normally short and abnormally short, and normally long and abnormally long. The extreme types of undergrowth are recognized without difficulty and are grouped under the generic label of dwarfism. Extreme overgrowth is usually known as gigantism. It is much less common than dwarfism. The average normal lengths of the different long bones at various age levels are recorded in Table 8-1 (p. 886). Deviations in either direction which exceed 10% of the average length lie outside the normal range and are considered abnormal. Idiocy and imbecility are often characterized by smallness of stature, maturation of the skeleton may be normal or delayed in such circumstances.

GENERALIZED UNDERGROWTH (DWARFISM)—The demarcation between normal small stature and dwarfism is an arbitrary one. According to McCune, dwarfism connotes conspicuous shortening of the long axis of the body, and the diagnosis of dwarfism is justified when the defect in stature approximates three times the standard deviation of average height.

There are many causes for generalized undergrowth of the long bones. The most common conditions include long standing severe constitutional diseases such as infections, malnutrition, diabetes and anemia, organic disorders of the heart, liver, intestines and kidneys, thyroid and pituitary deficiencies, cartilaginous hypoplasias and dystrophies, osteogenesis imperfecta, and severe rickets with shortening of the bones. Shortening of the spine may be the cause of both acquired and congenital dwarfism. In Morquio's disease dwarfism is due largely to shortening of the trunk which is secondary to congenital flattening of the vertebral bodies, in patients with multiple hemivertebrae the trunk is short owing to congenital absence and hypoplasia of the vertebral bodies but the long bones in the extremities are normal in length. Congenital mental retardation is usually associated with retarded longitudinal growth with good, had or indifferent nutrition. The syndromes associated with aberrations in the chromosomes—in the sexual as well as the somatic chromosomes—are usually characterized by deficiencies in longitudinal growth.

It is doubtful that "true immature dwarfism" ever occurs in which the individual has proportionate growth and maturation at all ages and whose only abnormality is a lack of dimension. Neither hypogonadism nor hypoadrenocorticism necessarily results in deficiency of growth or development, but moderate dwarfism is the rule in ovarian agenesis. The common type of so-called primordial dwarf (Gilford's atelosis type 2) is thought to be due to panhypopituitary deficiency. These dwarfs are normal at birth but grow and develop slowly, growth and maturation of the skeleton are delayed at all postinfantile age levels and skeletal growth and maturation may not be complete until the fifth decade. Puberty may be delayed until middle life. Roentgen examination discloses the retarded growth and maturation of the skeleton—the soft tissues of the extremities are often folded and appear excessive in comparison with the shortened long bones. Bilateral dislocation of the patella was observed in one of our patients of this type, it was apparently due to excessive length of the patellar and quadriceps tendons.

GENERALIZED OVERGROWTH (GIANTISM)—Generalized overgrowth during infancy and childhood is due to excessive secretion of the eosinophilic cells in the anterior part of the pituitary gland. Such infantile and juvenile giants show rapid growth over a prolonged period with normal or delayed skeletal maturation and retardation of sexual development. Hypergonadism and hyperadrenocorticism may be characterized early by overgrowth and accelerated development of the skeleton but the early overgrowth is temporary, the actual growth period is so shortened that the ultimate result is total undergrowth and dwarfism.

Cerebral gigantism is the name given to a syndrome by Sotos and colleagues which includes mental retardation, excessively rapid growth during the first four years of life, accelerated maturation of the skeleton

early pubescence acromegalic features and clumsy poorly co-ordinated movements. In radiographs the ventricular spaces in the brain were slightly dilated and the pituitary fossa were normal.

Hemihypertrophy may be congenital or acquired unilateral or crossed and total or incomplete. True congenital total hemihypertrophy signifies enlargement of all of one side of the body including head thorax abdomen pelvis and extremities and all of the tissue components—cutaneous neural muscular and vascular. This malformation has been found in fetuses and is present at birth. The cause is unknown in complete twinning and neurofibromatosis have been suggested as causal mechanisms. Roentgen examination discloses excessive bulk of both soft tissues and bone on the affected side. Maturation on the larger side is occasionally accelerated. Hemihypertrophy is said in most cases to lessen gradually with advancing age and disappear during early adult life. Silver and his co-workers reported elevation of urinary gonadotropins in congenital hemihypertrophy.

LOCALIZED UNDERGROWTH—This prevails when local lesions retard or destroy the proliferation of the epiphyseal cartilage. Destruction of the cartilage or reduction of its blood supply is usually caused by local trauma infection or neoplasm.

LOCALIZED OVERGROWTH—Such an overgrowth of long bones is encountered in many conditions that are accompanied by longstanding hyperemia of the part and increased blood supply to the growing cartilage. Among the most common agents are chronic osteitis including the tuberculous type chronic arthritis neoplasms healing fractures chronic hemophilic hemarthrosis and regional arteriovenous fistulas. Pronounced local and regional overgrowth of both bones and soft tissues have been found in patients with chronic infantile cortical hyperostosis. Regional overgrowth of this type may persist for more than two years.

REFERENCES

- Caffey J. On some late skeletal changes in chronic infantile cortical hyperostosis. *Radiology* 59 651 1952.
 Dennison W M. Unilateral limb lengthening associated with hematoxylin osteitis in childhood. *Arch. Dis Child* 27 54 1952.
 Halperin G. Normal asymmetry and unilateral hypertrophy. *Ann. Int. Med.* 48 676 1931.
 McCune D J. Dwarfism. *Clinics* 2 380 1943.
 Moehlig R C. Progeria with nanism and congenital cataracts in a five year old child. *J. A. M. A.* 132 640 1946.
 Rossi E. Le tableau clinique du Status Bonnevie. *Uthrich d'après le cas du Kinderspital de Zurich*. *Helvet. paediat. acta* 1 134 1945-46.
 Silver H K. Asymmetry short stature and variations in sexual development. *Am. J. Dis Child.* 107 490 1964.
 Sotos J F et al. Cerebral gigantism in childhood. A syndrome of excessively rapid growth with acromegalic features and a nonprogressive neurologic disorder. *New England J. Med.* 271 109 1964.
 Talbot N B et al. Progeria. Clinical metabolic and pathologic studies in patients. *Am. J. Dis Child.* 69 267 1945.
 — et al. Dwarfism in healthy children. Its possible relation to emotional, nutritional and endocrine disturbances. *New England J. Med.* 236 783 1947.

- and Sobel E. Endocrine and other factors determining the growth of children. *Advances Pediat.* 2 238 1947.
 Wagner R White P and Bogan I K. Diabetic dwarfism. *Am. J. Dis Child* 63 354 1942.
 Ward J and Lerner H H. A review of the subject of congenital hemihypertrophy and a complete case report. *J. Pediat.* 31 403 1947.

MATURATION OF THE SKELETON

GENERALIZED ACCELERATION—The principal conditions of infancy and childhood which are characterized by advanced development of the skeleton are cortical neoplasms of the adrenals (adrenogenital syndrome) and hypergonadism (Fig. 8-267). Precocious puberty and advanced skeletal development have been found in a few cases of intracranial neoplasms and cysts and hepatomas. In excessively obese children bony maturation is moderately accelerated. It is rarely if ever retarded. In the interesting syndrome described by McCune and Bruch which is composed of unilateral hyperpigmentation of the skin and scattered fibrosis of the skeleton maturation of the entire skeleton is accelerated in female patients only.

It must be emphasized that there is not a good correlation between skeletal and mental development. In some instances of mental retardation skeletal maturation is accelerated. This is not infrequently the case in mongoloidism. Bone age is not a sound basis for the estimation of intellectual abilities or potentials. In my opinion it should not be used in the mental grading of school children.

GENERALIZED RETARDATION OF MATURATION—Such retardation in the long bones is found in many of the conditions which cause undergrowth. The most conspicuous retardation of maturation occurs in congenital hypothyroidism. Cranio-pharyngiomas in and above the pituitary fossa are usually accompanied by delayed maturation of the long bones. The appearance time of the epiphyseal ossification centers is frequently delayed in severe constitutional disease such as Cooley's Mediterranean anemia poorly controlled diabetes mellitus celiac disease and poorly compensated congenital cardiac disease. In cerebral hypoplasia and mongolism the maturation of the skeleton may be at any level from markedly retarded to normal. Francis believed that the schedule of maturation is delayed temporarily in many acute illnesses such as the common contagious diseases allergic attacks gastrointestinal upsets and upper respiratory infections. Sontag and Lipford on the other hand found no delay or alteration in the appearance time of the secondary centers which could be attributed to acute infantile or juvenile diseases. Dreizen and colleagues found fusion of primary and secondary ossification centers in the hand to be delayed in chronic malnutrition.

LOCALIZED ACCELERATION OF MATURATION—The development of the secondary centers is advanced by the same local agents which stimulate excessive

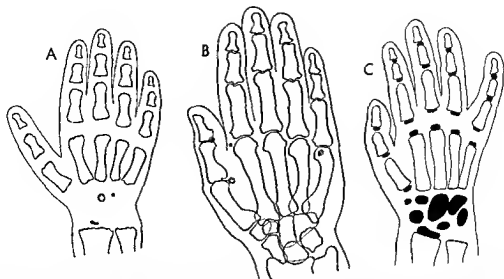


Fig 8 267 — Epiphyseal maturation. A retarded maturation in an untreated cretin whose chronological age is 7 years but whose skeletal age is 6 months. The secondary epiphyseal centers have not yet appeared except for the tiny center in the radial epiphysis. B accelerated maturation in a boy with hypergonadism whose chronological age is 7 years but whose skeletal age is 20

years. All of the secondary epiphyseal centers have appeared grown and fused with the shafts, giving the appearance of adult bones. Sesamoids are visible near the distal ends of the first and fifth metacarpals and near the distal end of the first phalanx of the thumb. C average maturation at 8 years. Tracings of roentgenograms.

growth in length listed in the discussion of localized overgrowth.

LOCALIZED RETARDATION OF MATURATION—Local destructive lesions may delay or stop the development of the epiphyseal centers in any portion of the extremities. As is the case with localized retardation of growth the most important agents are local trauma infection and neoplasm. Exposure of the proliferating cartilage to roentgen irradiation inhibits and in sufficient dosage arrests the appearance of the epiphyseal center.

REFERENCES

- Banks S W, Krigten W and Compere E L. Regeneration of epiphyseal centers of ossification following destruction by pyogenic or tuberculous infection. *JAMA* 114 23 1940.
- Compere E L and Adams C O. Studies of longitudinal growth of long bones. I. The influence of trauma to the diaphyses. *J Bone & Joint Surg* 19 922 1937.
- Dreizin S *et al*. The effect of prolonged nutritive failure on epiphyseal fusion in the human hand skeleton. *Am J Roentgenol* 78 461 1957.
- Francis C C. Factors influencing appearance of centers of ossification during early childhood. *Am J Dis Child* 58 817 1939.
- Lipschultz O. The end results of injuries to the epiphyses. *Radiology* 28 223 1937.
- Sontag L W and Lipford J. The effect of illness and other factors on the appearance pattern of skeletal epiphyses. *J Pediatr* 23 391 1943.

CONGENITAL MALFORMATIONS

APLASIA AND HYPOPLASIA—The cause and pathogenesis of congenital deviations in skeletal develop-

ment are not well understood. Penrose stated that experimental infection of fertile chicken's eggs with virus of influenza has produced defects in the skeleton. Entire bones or portions of bones in a great variety of patterns may fail to form in the membranous anlage during the early fetal weeks. These have been classified by O Rahilly and by Frantz and O Rahilly according to the embryonic somatic origin of the limb (Fig 8 268). O Rahilly stated that the aplasias and hypoplasias in the major long bones occur in the following descending order of frequency: fibula, radius, femur, ulna and humerus. Since the clinical studies of maternal rubella by Gregg which indicated that maternal virus infection crosses the placenta, infects the fetus and may produce a variety of fetal malformations, one must consider fetal virus infection as a possible cause of congenital malformations of the skeleton. Lefort and Lynch described defective development of the phalanges of the toes of a newborn whose mother was covered from head to foot with chickenpox during the eighth week of the gestation.

Thousands of deformed infants were born in West Germany of mothers who had ingested thalidomide (alpha [N-phthalimido] glutamide) during the sensitive first trimester of pregnancy. Most of these deformed infants had phocomelia (seal flipper) of the arms and legs and also according to Taussig occasional dysplasias of the digestive, cardiovascular and nervous systems. Phocomelia, according to O Rahilly's classification is an intercalary deficiency of the intermediate parts with persistence of the proximal and distal elements. Congenital absence or hypoplasia may be associated with hypoplasia and deform

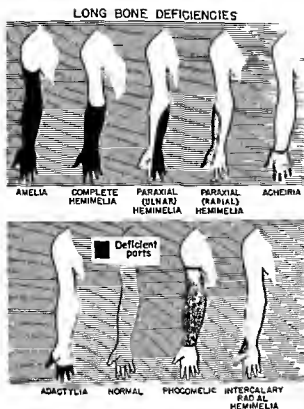


Fig. 8-268.—Types of skeletal defects in the extremities according to the classification of O'Ran. The defects may be transverse or longitudinal or they may be interposed transversely between normal structures as in phocomelia or interposed longitudinally as in intercalary radial hemimelia. (From O'Reilly.)

ity of the first metacarpal, the trapezium, radius and phalanges of the thumb (Davison). Symmetrical aplasia of the radius with congenital megakaryocytopenia has been found in 12 patients (Toenz). 2 examples have been reported in siblings, a boy and girl (Shaw and Olver).

Dysmelia is a term coined by Wiedemann to indicate a spectrum of malformations characterized by undergrowth, both partial and complete of the tubular bones of the extremities, ranging from isolated peripheral hypoplasias to complete absence of an extremity. The term was first applied to the malformations caused by thalidomide during the period 1958–1962. Ectromelia was considered by Henkel and Willert to include all degrees of hypoplasia of the radius and ulna with their peripheral bony rays and the humerus and femur. Phocomelia signifies those degrees of dysmelia in which there are no long bones between the shoulder girdle and the hand and the pelvic girdle and the foot. Amelia includes total absence of the extremity. The new classification of Wiedemann (see Henkel and Willert) gives detailed significance to the teratologic sequences and specific structure losses. In the distal and proximal types of ectromelia the distal and proximal parts of the limb

are hypoplastic. In axial ectromelia the distal as well as the proximal part of the limbs are hypoplastic.

With increasing severity, more parts of the bones become involved in the distinct sequence. Henkel and Willert reported on 287 malformed children with 557 defective arms and 136 defective legs. In the arm, the milder lesions were confined to the radial ray of the hand. Then follows, with increasing extent, radial hypoplasia and when the radius is absent or has fused with the ulna the humerus becomes involved. In the leg, in contrast in the mild cases of tibial hypoplasia the femur may also be involved. The tibia need not be absent and its remnants need not be fused before the femur becomes hypoplastic. In addition, isolated hypoplasia of the femur does develop in which the bones in the shank and feet are not affected. Isolated defects of the humerus, in contrast to the femur have not been described. In both phocomelia and amelia the shoulder and pelvic girdles may be impaired.

Reductions in the hand and fingers depend directly on the degree of hypoplasia of the arm bones. The number and the size of the remaining phalanges is inversely related to the degree of hypoplasia in the arm. The most severe hypoplasias in the hand occur in phocomelia. The reductions in the hand begin at the thumb and extend progressively from the radial toward the ulnar sides, the index, middle and ring fingers may be absent in phocomelia.

The same principles apply in the reductions in the foot bones in dysmelia of the legs but the interdependence is much less consistent, a nearly normal foot may be associated with severe malformations in the bones of the shanks and thigh. When the foot is affected hypoplasia extends progressively from the distal toward the tibial ray. Solitary malformation of the tibial ray, corresponding to hypoplasia and triphalangism of the radial ray, appears to be exceedingly rare.

The malformations in dysmelia show a specific pattern and obey a specific set of principles. They are not random defects. The individual bones vary in the degrees of their hypoplasias (thumb, radius, ulna, humerus and femur). These malformations are classified according to the segment of the limb and the skeletal parts affected, the degree of undergrowth—(hypoplasia, partial hypoplasia and total aplasia) and the presence or absence of fusion of bones. On the basis of these criteria, dysmelia was described in five main types: distal form of ectromelia, axial form of ectromelia, proximal form of ectromelia, phocomelia and amelia.

In the axis malformation in dysmelia involving the forearm and hand the radius and radial digits (first and second) are always affected. Hypoplasia of the humerus in the axial type is never a solitary lesion but is combined with hypoplasias of the radius and radial digits. The humerus, radius and radial ray of the hand are combined in an axis malformation in the upper limb. This same combination may also oc-

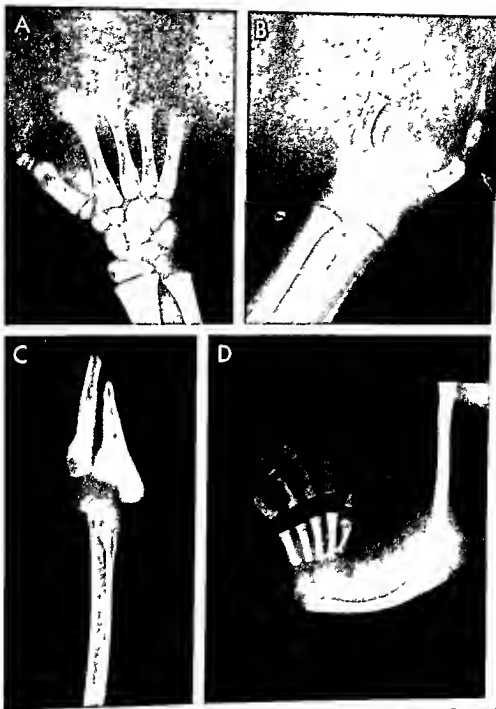


Fig 8-269—Congenital aplasia and hypoplasia of the skeleton. **A**, aplasia of the phalanges. **B**, aplasia and hypoplasia of the digits and metacarpals. **C**, total aplasia of the hand and partial aplasia of the forearm. **D**, congenital absence of the radius with club-hand. A similar malformation was present in the other arm. According to O'Rahilly's classification, **A** represents incomplete adactylia in a terminal medial deficiency, **B**, incomplete adactylia

in a terminal deficiency of the central type, **C**, incomplete transverse hemimelia, **D**, paraxial (longitudinal) radial hemimelia of the complete type with hypoplasia of the bones of the thumb and first metacarpal. In **D**, the trapezium and navicular are probably also hypoplastic or absent, but they cannot be evaluated in this young hand before their ossification.

cur in the leg, in which the femur, ulna and tibia of the foot are hypoplastic. In the severe type the ulna and fibula are the only long bones which persist. They are not subject to the hypoplastic tendency and are either present in toto or absent until the stage of phocomelia is reached. The ulna and fibula may, however, show secondary changes due to absence or deformity of their companion parallel bone.

Fusion of adjacent bones is another feature of dysmelia. This does not signify excess of bone formation because skeletal elements are usually hypoplastic when they undergo fusion. Fusion occurs in parallel bones (carpals, tarsals, metacarpals, metatarsals, radius and ulna) or in the bones arranged longitudinally (phalanges, humerus and ulna). In the leg, synostosis is limited largely to bones in the foot.

Maturation of remaining skeletal elements is characteristically retarded, which is usually most pronounced in the skeletal parts nearest the defects. Occasionally bony centers and structures which should have appeared during early childhood will appear much later. Some ossification centers remote from the defects may also appear late.

In all cases of dysmelia of the legs the changes are bilateral. In the arms this was also true, except in 14 radial types. In most cases of dysmelia the changes are symmetrical as well as bilateral. Most patients with dysmelia of the arms (219 of 287) had normal legs. When the arms were phocomelic or amelic. None of the 68 patients with dysmelia of the legs had normal arms. However, almost all possible combinations of patterns in the upper and lower extremities have been reported, and gross exceptions should be expected in sporadic cases of dysmelia. The foregoing stausness relate largely to thalidomide induced dysmelia.

Warkany and Schraffenberger produced syndactylism and osseous fusion of the humerus and radius by exposing fetal rats to x rays on the thirteenth day of gestation. Multiple malformations of the skeleton have been reported from the same laboratory in fetal rats whose mothers were fed a faulty diet. Multiple congenital malformations of the skeleton in the offspring of a mother who had been poisoned by coal gas during the seventh week of gestation were explained by Bette on the causal basis of the hypoxia to which the fetus had been exposed. In postnatal life a great variety of complete and partial skeletal defects in the extremities have been identified, regional hypoplasia of the soft tissues is commonly associated (Fig. 8-269). In some cases the hands and feet are attached directly to the trunk. In amnioplasia congenita the fibulae and patellas may be absent. The experience in Germany suggests that the fetus may be sensitive to other drugs and possibly foods ingested by the mother during the early weeks of gestation.

HYPERPLASIA—Congenital enlargement of bone may involve a portion or all of one extremity, and in some cases one half of the body (*hemihypertrophy*). Regional hypertrophy of the soft tissues is always

associated. Congenital localized gigantism is most common in the hands and feet (Fig. 8-270).

MALESCIMENTATION—The skeletal primordium is subdivided during the first fetal weeks, at the stage of chondrification. Errors in segmentation are often inherited; they are responsible for many of the important congenital malformations of the skeleton, particularly in the hands and feet (Fig. 8-271). Roentgen examination often provides useful information for the plastic surgeon in the treatment of these conditions. Fusion of the proximal ends of the radial and ulnar shafts is the commonest error of segmentation of the large long tubular bones (Fig. 8-272). Proximal radioulnar synostosis has been found in five of nine cases of the excessive sex chromosomal syndrome of the XXXXY type and in two of the other cases there were malformations at the proximal ends of the radius and ulna on one or both sides. Cleveland and associates on the other hand, found XYY chromosomal patterns in two prepubertal boys who also had radioulnar synostosis. In the case of radioulnar synostosis of Card and Strachman, the bones were independent of each other at age 6 weeks and fused together at 6 months.

Undersegmentation or fusion of the bony anlage may result in absence of articular spaces (Fig. 8-273), this is most commonly found in the interphalangeal joints and the radioulnar articulations. In the wrist and ankle the small bones exhibit a variety of abnormal patterns. Failure of longitudinal segmentation of the phalanges is responsible for *syndactylism*.

Congenital spastic flat feet—Undersegmentation or fusion of tarsal bones has been given the special designation of coalition and is often an important feature of spastic and painful flatfoot. The fusions may be bony, cartilaginous or fibrous, singly or in combination. Talocalcaneal coalition may obliterate the subtalar joint completely or in part. In some cases of talonavicular coalition the bones form a single bony mass with no suggestion of a joint at their usual level of articulation (Fig. 8-274). Waugh described an interesting example of coalition between the cuboid and scaphoid which caused spastic flatfoot. In Lamb's case the talus, calcaneus and navicular were all fused into one bone. Inversion and eversion are usually both limited when the tarsal bones are fused.

The Shrewsbury mark (*Symphalangism*) signifies fusion of phalanges as well as of tarsal and carpal bones (Fig. 8-275). These fusions are familial and genetic, in one family in Virginia studied by Cushing more than 25% of the members were affected. In Great Britain the descent of the phenotype has been traced back in several families through several generations to the Earl of Shrewsbury, who died in 1453. It is believed that most of the cases in Great Britain and the United States stem from this single source. One pedigree of this genetic skeletal syndrome provided the first example of dominant Mendelian inheritance in human beings (Farabee. Papers of the Peabody

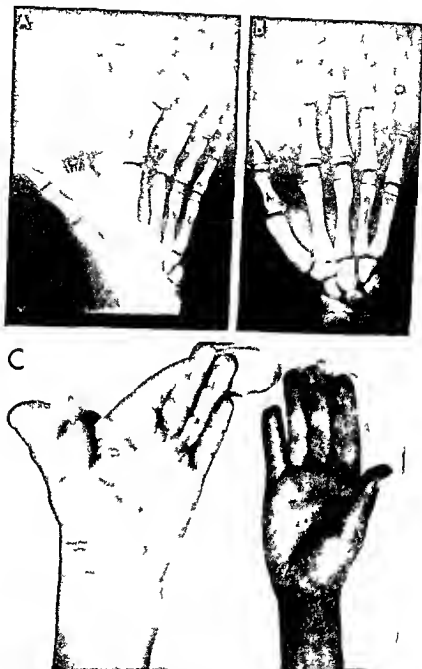


Fig 8-270 Part a congen a hypertrophy of the left hand **A**, in addition to the bony hypertrophy of the first and second digits the entire marked hypertrophy of the tissues and generalized

hypertrophy of the hand and forearm **B** the normal right hand **C** photograph of **A** and **B**

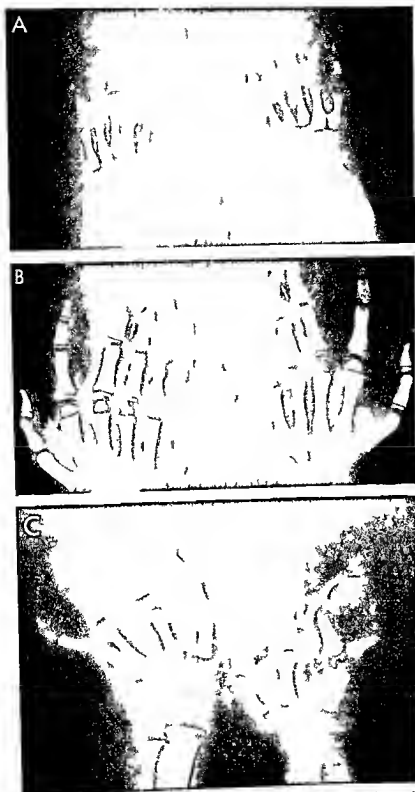


Fig 8-271 Congenital errors in segments on with multiple errors in size and shape. A, oversegments on of the digits and metacarpals in both feet of an infant 6 months of age. B, bilateral

symmetrical faure of segments on of the distal phalanges of the third and fourth digits in a boy 8 years of age. C, irregular segments on and hypoplasia of the phalanges and metacarpals

Fig 8 272 — Congenital proximal radial-ulnar synostosis with hypoplasia of the forearm and hand of a boy 19 months of age

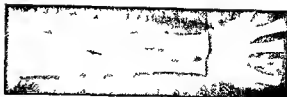
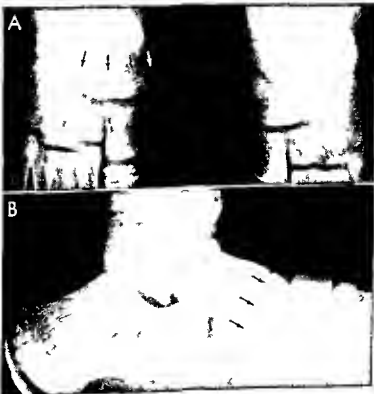


Fig 8 273 (above) — Congenital bilateral fusions of the second metatarsals and the middle cuneiforms (arrows) of a boy 4 1/2 years of age

10 years of age. A: Anteroposterior and B: lateral projections. On the right side the tarsus and navicular form a single bony mass with no intervening joint. The series of arrows mark the approximate position for the normal articular cleft.

Fig 8 274 (below) — Congenital talonavicular coalition in a boy



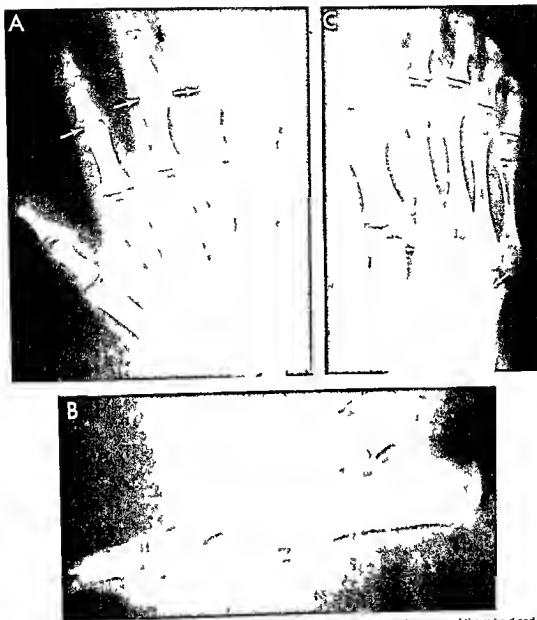


Fig. 8-275 — Familial congenital coalition of joints (the Shrewsbury family). **A** Symmetrical absence of joints (symphalangism) between the middle and proximal phalanges of both hands in a girl 5 years of age who had had stiff fingers and toes since birth. The epiphyseal ossification centers of the middle phalanges of fingers 2, 3, and 4 and possibly 5 fused distally with the distal ends of the corresponding proximal phalanges. In **B** lateral projection

the joint between the calcaneus and the cuboid and the talocalcaphaloid joint are obliterated. In **C** frontal projection, the joints which bind the middle and lateral cuneiforms to the second and third metatarsals are obliterated. A younger sibling had dental calcifications in the hands and feet, and many other direct and collateral relatives had similar deficiencies of joints. (Courtesy of Dr. R. Parker Allen, Denver, Colo.)

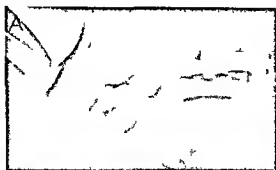
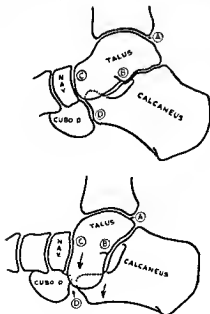


Fig 8-276—Progressive coalescence of the calcaneus and cuboid. A, at 8 months of age, the calcaneus and cuboid have separate independent ossification centers. B, at 3 1/2 years, these same centers are almost completely fused and they were completely fused in redog ephe made at 6 years of age. The coalescence in this foot is associated with total aplasia of the 4th and 5th toes. 4th and 5th metatarsals and the lateral cuneiform.

Fig 8-277—Schematic drawing of internal derangement of the tarsal bones in flatfoot with plantar flexion of the talus. A, ankle joint. B, subtalar joint. C, talaronavicular joint. D, calcaneocuboid joint. (From Haveson.)

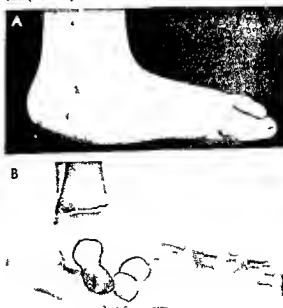


Museum Harvard University p 3 1905) Multiple coalitions may be present in a single foot (Fig 8-276). During the prefusion stage of the coalitions the bones are separate entities which fuse later. Apert's syndrome (premature synostoses of the sutures and syndactylism and polydactylism) has been associated with carpal and tarsal coalitions in a few cases.

Heiple and Lovejoy found bilateral talocalcaneal bridges, one complete and one incomplete in a pre-Colombian Indian skeleton dating from approximately 1000 A.D. They concluded that the anomaly is a very ancient one in which the responsible genes are widely distributed among the races of man. The most common synostosis between the carpal bones is that between the lunate and the triquetrum according to Szalesky and associates. The anomaly is usually asymptomatic and may be unilateral; it may be sporadic or familial. The tarsus is usually normal. Pisiform hamate fusions were found in an incidence of about 0.5 by Cockshot in Ibadan. He pointed out that the distal portion of the flexor carpi ulnaris must have been cartilaginous at one time to explain this anomaly.

Congenital vertical talus (Fig 8-277) is an uncommon but well known feature of severe rigid flat feet in infants and children. It occurs in otherwise healthy newborns and also in association with other congenital malformations, especially amyotonia congenita and spina bifida. The radiologic findings in the feet

Fig 8-278—Congenital vertical talus with severely flattened and pronated feet. A, the foot externally of a child 6 years of age tends to be "boat shaped" with the point of the heel lifted. The great toe is plantar flexed in compensation for elevation of the first metatarsal. B, redograph showing the vertical position of the talus fitting of the dorsal segment of the calcaneus and dorsiflexion of the forefoot with elevation of the bases of the metatarsals. (From Lloyd Roberts and Spence.)



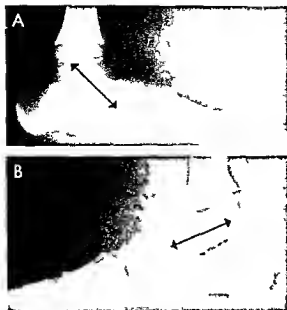


Fig 8-279—Plantar flexion of the talus in idiopathic acquired lateral flatfoot in a boy 4 years of age. Lateral projections during weight bearing of **A**, the plantarflexed talus, and **B**, normal left foot. The talus is rotated on its transverse axis with its ventral end down and dorsal end up in comparison with the congenital type of vertical talus in Figure 8-278. Flexion of the talus is not as marked and the scaphoid and calcaneus have not followed the ventral end of the talus caudad.

are similar in all cases and include rotation of the talus on its transverse axis toward a vertical position with the ventral end down equinus position of the calcaneus and dorsiflexion of the forefoot (Fig 8-278). In severe cases the talus is lined up with the long axis of the tibia, and may be constricted in its middle. Plantar flexion of the talus is also found in some cases of idiopathic acquired flatfoot (Fig 8-279) but the talus does not reach a truly vertical position and talonavicular separation does not develop in the acquired variety.

The difference in the displacement at the talonavicular joint differentiates clubfoot (*talipes equinovarus*) and congenital vertical talus. In clubfoot the talonavicular joint is displaced caudad and medial in congenital vertical talus it is displaced cephalad and laterad and the navicular bone lies on the *dorsum* of the head or neck of the talus (Eyre-Brook). The radiographic diagnosis of congenital vertical talus can be made conclusively only by demonstration of the high dorsal position of the navicular on the head or neck of the talus.

Oversegmentation gives rise to supernumerary carpal and tarsal metatarsals and metacarpals and polydactylism. Excessive segmentation proximal to the wrists and ankles is rare.

Irregular segmentation produces a bizarre pattern of malformed small bones in the hands and feet.

REFERENCES

- Badgley E. E. Coalition of calcaneus and navicular. *Arch. Surg.* 15:75 1927.
- Card, R. Y. and Strachman J. Congenital ankylosis of the elbow. *J. Pediatr.* 46:81 1955.
- Chambers C. H. Congenital anomalies of the tarsal navicular with particular reference to calcaneonavicular coalition. *Brit. J. Radiol.* 23:580 1950.
- Cleveland W. A. et al. Radioulnar synostoses: behavioral disturbances and XYY chromosomes. *J. Pediatr.* 74:103 1969.
- Cockshott W. P. Pisiform-hamate fusion. *J. Bone & Joint Surg.* 51-A:778 1969.
- Conway J. J. and Cowell, H. R. Tarsal coalition. Clinical significance and roentgenographic demonstration. *Radiology* 92:799 1969.
- Davidson E. R. Congenital hypoplasia of the carpal scaphoid bone. *J. Bone & Joint Surg.* 44-B:816 1962.
- Duraswami P. K. Experimental causation of congenital defects and its significance in orthopedic surgery. *J. Bone & Joint Surg.* 34-B:646 1952.
- Eyre-Brook A. L. Congenital vertical talus. *J. Bone & Joint Surg.* 49-B:618 1967.
- Frantz C. H. and O'Rahilly R. Congenital skeletal limb deficiencies. *J. Bone & Joint Surg.* 43-A:1202 1961.
- Ganhoed G. W. et al. Symphalangism and tarsal coalition: a hereditary syndrome. *J. Bone & Joint Surg.* 51-B:278 1969.
- Harold A. J. Congenital vertical talus in infancy. *J. Bone & Joint Surg.* 49-B:634 1967.
- Heiple K. G. and Lovejoy C. E. The antiquity of tarsal coalition. *J. Bone & Joint Surg.* 51-A:979 1969.
- Henkel L. and Waldert H. G. Dysmelia: A classification and pattern of malformations in a group of congenital defects in the limbs. *J. Bone & Joint Surg.* 51B:399 1969.
- Ingalis T. H. and Curley F. J. Principles governing the genesis of congenital malformations induced in mice by hypoxia. *New England J. Med.* 257:1121 1957.
- Kite J. H. Congenital metatarsus varus. *J. Bone & Joint Surg.* 49-A:388 1967.
- Lusby H. L. J. Navicular cuneiform synostosis. *J. Bone & Joint Surg.* 41-B:150 1959.
- Murphy H. S. and Hanson C. C. Congenital humeroradial synostosis. *J. Bone & Joint Surg.* 27:712, 1945.
- O'Rahilly R. Morphological patterns in limb deficiencies and duplications. *Am. J. Anat.* 69:135 1951.
- Sel J. M. and Grand N. R. Cubo-navicular synostosis. *J. Bone & Joint Surg.* 41-B:149 1959.
- Shaw S. and Oliver R. A. M. Congenital hypoplastic thrombocytopenia with skeletal deficiencies in siblings. *Blood* 14:374 1959.
- Simmons E. H. Tibialis spasticus varus with tarsal coalition. *J. Bone & Joint Surg.* 47-B:533 1965.
- Szabosky A. T. et al. Anomalous fusion between lunate and triquetrum. *J. Bone & Joint Surg.* 51-A:1001 1969.

- Taussig H B A study of the German outbreak of phocomelia the thalidomide syndrome JAMA 180 1106 1962
 Von Murralt R H Limitation of supination of the forearm Fortschr Geb Röntgenstrahlen 81 497 1954
 Waugh W Partial cubonavicular coalition as a cause of spastic flat foot J Bone & Joint Surg 39 B 520 1957

CONGENITAL CLUB FEET (TALIPES EQUINOVARUS) is a common and important malformation which may be bilateral or unilateral. It occurs approximately in 1 per 1000 births and is about twice as common in boys as in girls. The deformity affects the entire foot and has three components: inversion of the entire foot on its longitudinal axis with the medial side cephalad and the lateral side caudad (talipes) plantar flexion of the foot at the ankle (equinus) and adduction of the forefoot on the hindfoot (metatarsus varus). These deformities are all obvious and best appreciated by direct inspection, palpation and tests of passive movement for function. Everything which can be demonstrated radiographically is better seen and evaluated by clinical methods. Radiographic findings are confirmatory and secondary and should be disregarded if they conflict with the clinical findings. Elaborate radiographic procedures with fine measurements of the comparative relationships of the different bones in the foot are usually meaningless and of ten misleading because the feet cannot be put in identical positions in different examinations.

The diagnosis should be made clinically in the newborn and it is immediately imperative to differentiate the rigid clubfoot from the flexible clubfoot which needs only mild or no treatment. This differentiation can be made only by careful palpation of the

Fig 8 280—Congenital metatarsus varus (one third clubfoot) in a boy 2 months of age. The forefeet are adducted on the hindfoot. The distal ends of the talus bones are displaced medially in a fashion similar to that of flatfoot. In full clubfoot the calcaneus rotates under the talus so that the spread between the distal ends of the talus and the calcaneus often reduced to near zero.



foot and stimulation of the peroneal muscles. Radiographs are superfluous in this differentiation. The radiographic demonstration of spina bifida dislocation of the hip and amyotonia congenita (arthrogryposis) indicates a worse prognosis and more difficult treatment.

METATARSUS VARUS—The forefoot is bent medially on the hindfoot in the horizontal plane only. The heel is in normal position as is the rest of the foot. Metatarsus varus is sometimes called incomplete clubfoot or one third clubfoot. This lesion should be identified in the newborn because it is obvious on inspection (Fig. 8 280). The differentiation of rigid metatarsus varus which needs immediate treatment from the milder and more mobile types can be made only on careful palpation. Radiographs are not needed for either diagnosis or treatment. The film shows adduction of the forepart of the foot, distraction of the talus and calcaneus—the converse of talipes equinovarus. This deformity occurs in a wide spectrum of severity from rigid metatarsus varus to mobile moderate and mild degrees which recover spontaneously. In cases of doubt no harm is done by waiting from four to six weeks to decide whether treatment is needed.

CALCANEVALGUS FOOT is uncommon. The deformity is the converse of true clubfoot, talipes equinovarus. The entire foot is everted instead of being inverted on its longitudinal axis (valgus); the entire foot is dorsiflexed instead of being plantarflexed (calcaneus) and the forefoot is not adducted on the hindfoot. The dorsum of the foot lies parallel to the lateral aspect of the shank and the heel projects laterally. The passive movements of the foot are free or even excessive except plantar flexion, which is limited by the tight anterior tibial tendon. Radiographs are not needed for either diagnosis or treatment when the feet have been carefully examined clinically.

EXAGGERATED FETAL POSITION FOOT simulates the calcaneovalgus foot. It is dorsiflexed at the ankle but the calcaneus is not in valgus and the dorsiflexion can be reduced to 90 degrees or more by passive motion. This is not a rigid deformity but is a functional shortness and tightness of the anterior tibial tendon due to excessive dorsiflexion of the feet in utero. Radiographs are not essential in diagnosis or treatment.

CAVUS FOOT (see Fig 8 644) is discussed in the section on weak feet.

REFERENCES

- Ferguson A B Jr Orthopedic Surgery in Infancy and Childhood (2nd ed. Baltimore: Williams & Wilkins Company 1963)
 Kite J H Congenital metatarsus adductus J Bone & Joint Surg 49-A 388 1967
 Ryder C T Orthopedic problems of the newborn infant, Bull. Sloane Hosp. Women 6 9 1960
 Settle G W Anatomy of congenital talipes equinovarus: 16 dissected specimens J Bone & Joint Surg 45-A 1341 1963

APLASIA AND HYPOPLASIA OF THE FIBULA—The fibula of all of the larger tubular bones is the most

frequently absent or too small. The fibular aplasia syndrome includes absence or hypoplasia of the fibula with ventral and medial bowing of the compartment and pitting of the skin over the summit of the tibial bowings talipes equinovarus absence of one or two of the lateral rays of the foot and absence or fusion of one or more tarsal bones. This primary pattern may be altered and the syndrome may vary from mere hypoplasia of the proximal end of the fibula to total aplasia of the fibula and multiple malformations and deficiencies in other bones. The ipsilateral femur is usually shortened and development is retarded in the proximal end of the femur and its opposing ilium.

REFERENCE

Coventry M. B. and Johnson E. W. Jr. Congenital absence of the fibula. *J Bone & Joint Surg* 34-B 646 1952

APLASIA AND HYPOPLASIA OF THE TIBIA which are about five times as common on the right as on the left side are rare defects. About one-quarter of the cases are bilateral. The associated foot is commonly deformed in an equinovarus pattern; the foot may contain all of its components or the toes and metatarsals may be aplastic, hypoplastic or fused and in excessive number. The muscles of the shanks are grossly deficient and cutaneous dimples are present. Congenital dislocation of the hip, atresia and cleft palate and hypospadias have been associated in some patients. Hemivertebrae have been present in a few of our patients.

REFERENCE

Ferguson A. D. and Scott R. B. Congenital absence of the tibia. *Am J Dis Child* 64 84 1952

Fig 8 281—Congenital bilateral hypoplasia of the femurs of an infant 4 days of age. A, both thighs are shortened; the proximal end of the right femur was palpated cephalad to the acetabulum. B, the right femur is visible because it is not yet mineralized; the roof of the right acetabular cavity is hypoplastic—a dys-

APLASIA AND HYPOPLASIA OF THE RADIUS are usually associated with radial deviation of the hand (see Fig 8 269 D). The first metacarpal and the phalanges of the thumb may also be hypoplastic or absent. Similar deformities develop in association with hypoplasia and absence of the ulna, but the ulnar club hand is deviated to the ulnar side and the third, fourth and fifth fingers and third, fourth and fifth metacarpals are small or absent. According to the classification of Frantz and O'Rahilly, the plane of demarcation between radial and ulnar hemimelia runs through the longitudinal axis of the second digit (see Fig 8 268).

Judith and associates described nine patients with the syndrome of hypomegakaryocytic thrombocytopenia and bilateral absence of the radius (TAR). In three unrelated families and four other single patients in unrelated families. In their survey of the literature they found twenty seven additional examples of the syndrome. Most of the bleeding episodes occurred during the 1st year of life, although late bruising and menorrhagia were common. Occasionally long bones in the arms other than the radius were absent, but in all cases the fingers and thumbs were present.

APLASIA AND HYPOPLASIA OF THE FEMUR gives rise to marked external deformities with shortening of the thigh (Figs 8 281 and 8 282); it may be unilateral or bilateral and associated with congenital dislocation of the hip or congenital coxa vara. Golding showed in follow up studies that the congenital short incompletely mineralized and bowed femur of the neonatal period later exhibits congenital coxa vara when the proximal bent end of the femur becomes mineralized and visible roentgenographically (Fig 8 283).

ULNAR DYMELIA or double ulna is much less com-

mon than the association of congenital dislocation of the hip. The left femur is short and bent; its proximal end is not mineralized and probably is deformed in a congenital coxa vara deformity. The left acetabular cavity is normally deep and its roof is not dysplastic.

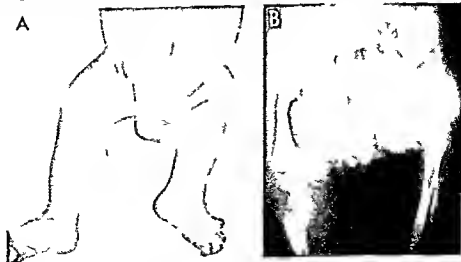




Fig. 8 282 — Prenatal bowing of the femurs which are also hypoplastic with transverse fracture and pseudarthrosis at the crest of the ensartion in the left femur. The patient a newly born infant was normal otherwise. (Courtesy of Dr. Gene Triano Harrisburg Pa.)

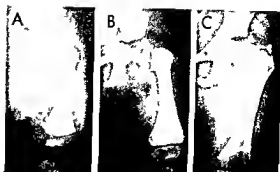
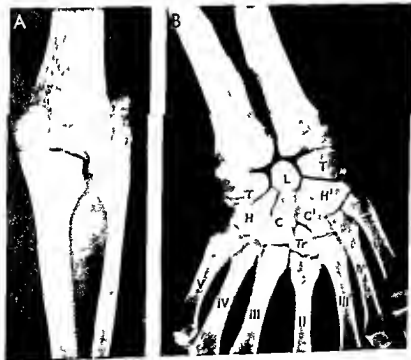


Fig. 8 283 — Congenital short femur with congenital coxa vara. A early stage in which the proximal end of the femur is not mineralized. B later intermediate stage with partial mineralization of the femur. C, later stage with more complete mineralization of the bent femur in which the coxa vara deformity is visible. (From Goldberg.)

Fig. 8 284 — Ulnar dysplasia in the left forearm of a man 39 years old who was born with seven fingers and no thumb in the left hand. The right forearm and hand were normal. In A, two ulnas with well developed olecranon processes articulate with the humerus which has no capitulum. In B, there are nine carpal bones: the capitates, hamates and triquetrals are paired. The

lunata and trapezoid are solitary. But one pisiform is evident on the reader's left. There are seven metacarpals: two each of the third, fourth and fifth, and a single second metacarpal. All of the fingers had three normal phalanges. Movements of the wrist and fingers were limited. (Figs. 8 284 and 8 285 from Hairsch et al.)



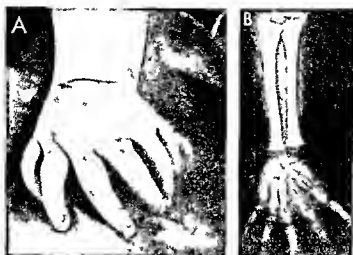


Fig. 8 285 — Infantile ulnar dimelia. In A, photograph of the hand at 3 weeks of age, there are seven fingers. In B, radiograph of the hand and forearm at 4 years of age, the ulnas are paired.

mon than absence of the radius and ulna. Nine examples had been described in which both bones in a single forearm were ulnas prior to 1960 when three new examples were reported. Usually there are seven digits but no thumb (Fig. 8 284). The carpal bones were excessive in number, with double sets on each side of the hand which included triquetral, capitate and base of the 5th metacarpal. The trapezoid, lunate and pisiform were single in each wrist. In a young patient 4 years of age, maturation was advanced (Fig. 8 285). In the remarkable patient of Laurin and colleagues both

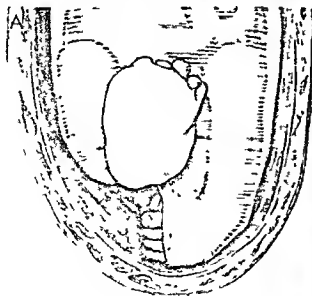
the distribution of the excessive number of carpal bones is characteristic and the fingers all have three phalanges. Two of the extra fingers and metacarpals were excised at 9 months of age.

radiuses were absent and there were two ulnas in each forearm and both tibias were absent and there were two fibulas in each shank.

REFERENCES

- Harrison R. G. *et al.* Ulnar dimelia, *J. Bone & Joint Surg.* 42-B 549, 1960.
 Judith G. H. *et al.* Thrombocytopenia with absent radius, *Medicine* 48 411, 1969.
 Laurin C. A. *et al.* Bilateral absence of the radius and tibia with bilateral reduplication of the ulna and fibula, *J. Bone & Joint Surg.* 46-A 137, 1964.

Fig. 8 286 — Protrusion of fetal parts through the amniotic membrane as a cause of congenital contraction rings in the extremities. A, schematic drawing of the hypothetical fetal position.



tion with the amniotic membrane cross lined B, actual deformity of the protruding foot and ankle in photograph (From Browne).

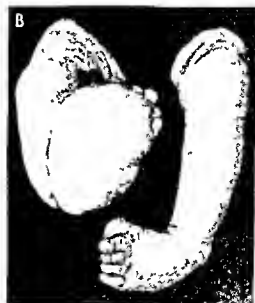




Fig 8 287 — Incomplete prenatal amputation of the shank with deep annular constriction of the soft tissues and shadowing of the ventral cortical wall of the tibia at the same level. Soft tissues of the hands and feet presented several annular constrictions and there was a large defect in the scapula. A: photograph of the shanks. B: radiograph of left shank made the 6th day of life.

Pinzile D. *et al*. Double ulna with symmetrical polydactyly. Case report. *J Bone & Joint Surg* 46-B 69 1964.
Sandraw R. E. *et al*. Hereditary ulnar and fibular dimelia with peculiar facies. *J Bone & Joint Surg* 52-A 367 1970.

RING CONTRACTIONS OF THE EXTREMITIES were at one time believed to be due to contracting amniotic adhesions but a more reasonable explanation appears to be localized focal deficiencies (Streeter) possibly due to localized ischemia. Penetration of the amniotic membranes by various parts of the fetal body—digits, limbs or other parts—causes ring defects the edges of which produce ring constrictions on the protruding parts (Fig 8 286). In Gypta's patient a large constriction ring encircled the pelvis. In the case of complete prenatal amputation the amputated part is found loose in the amniotic fluid completely separated from the deformed stump. In the case of incomplete amputations there are deep scar ring circular furrows in the soft tissues sometimes

with constriction of the underlying bone at the same level (Figs 8 287 and 8 288).

REFERENCES

- Browne D. The pathology of ring constrictions. *Arch Dis Childhood* 32 517 1957.
———. Ring constrictions. *Proc Roy Soc Med* 56 159 1963.
Cypta M. L. Congenital annular defects of the extremity and trunk. *J Bone & Joint Surg* 45-A 571 1963.
Kohler H. G. Congenital transverse defects of the limbs and digits (intrauterine amputations). *Arch Dis Childhood* 37 263 1962.
Streeter G. L. Focal deficiencies in fetal tissues and their relation to intra uterine amputations. *Contributions to Embryology* no. 125 (Washington D.C. Carnegie Institution of Washington 1930).

CONGENITAL PSEUDARTHROSIS is a rare pathological fracture which is followed by nonunion and false motion at the site of fracture. The primary lesion is localized fibrous degeneration of bone of unknown cause. The fracture and pseudarthrosis are not neces-

Fig 8 288 — Examples of complete and incomplete congenital amputations with constriction rings in the thighs to arms and toes. (From Streeter.)





Fig 8-289—Fibrous dysplasia (microscopic diagnosis) in the tibia 24 hours after birth. A, frontal; and B, oblique projection. The medullary cavity is dilated by a huge radiolucent mass with thin overlying cortical wall which has been broken in at least two sites. (Courtesy of Dr. Boyd G. Holbrook, Salt Lake City, Utah.)

sarily present at birth but usually appear during the first eighteen months of life. Lloyd Roberts and Shaw pointed out that the café-au-lait patches in the skin and nodular neurofibromas often are not present at birth and their absence during early infancy is not conclusive evidence against the diagnosis. They advised early bone grafting to prevent fracture and deformity. The principal external deformities are anterior angulation of the shank, usually near the junction of the distal and middle tibial thirds and shortening of the part. The tibia is the most commonly affected bone, but pseudarthrosis has also been found in the fibulas, clavicles and femurs. In some cases the complete picture of pseudarthrosis is present at birth; in others there is no deformity at birth and the fracture and deformities develop later. One should differentiate congenital and infantile pseudarthrosis. Scott described a patient who exhibited localized fibrous degeneration of the tibia on the 14th day of life but did not show fracture and pseudarthrosis in the fibula until 12 months later, and in the tibia until 30 months later. Fetal pseudarthrosis and fetal bowing of the tibia may develop in the same tibia independently of each other. According to McFarland, fetal fracture is exceedingly rare, if it ever occurs, he believed that it should be classified as a fatigue fracture. The break may take place during or immediately after birth, or several weeks or months later. Aegerter, among several others, emphasized the importance of neurofibro-



Fig 8-290—Congenital pseudarthrosis, the early primary fibrous lesion (arrows) on the 14th day of life, before fracture. The distal ends of the tibia and fibula are bent laterad and probably varus fractures and pseudarthrosis were not identified in the fibula until 12 months later and in the tibia until 20 months later. (From Scott.)

matosis in congenital pseudarthrosis. Boyd and Sage, on the other hand, believed that pseudarthrosis of the congenital type and associated with a local cystic defect is due basically to local prenatal fibrous dysplasia (Fig. 8-289).

Fig 8-291—Congenital pseudarthrosis of the tibia in a newly born infant. There is a long radiolucent fibrous segment which is broken in its upper levels. Angulation is just beginning to develop. The distal fragment is pointed and sclerosed at its upper end. The proximal fragment is cupped at its lower end and the cup fits over the point to form a false joint. The fracture and its deformity are secondary to the fibrosis, which must have begun many weeks or even months before birth.



Van Nes separated the lesion into three clinical types: the true congenital pseudarthroses which are present in the tibia at birth; the pseudarthroses that follow spontaneous fractures through cystic lesions in the tibia after birth; and pseudarthroses which result from postnatal or congenitally weak, sclerotic and curved tibias. In each of these the pseudarthrosis is secondary to congenital segmental dysplasia of the tibia which is too weak for ordinary stress of fetal and early postnatal life.

Röntgen examination early discloses the primary change—the radiolucent area of fibrous degeneration in the affected shaft (Fig. 8-290). Following the fracture, a line or band of decreased density is seen between the ends of the fragments; the tissue responsible for this shadow is avascular connective tissue which permits motion between the fragments. During the later stages of pseudarthrosis (Fig. 8-291) the distal end of the proximal fragment is sharpened and becomes sclerotic while the proximal end of the distal fragment is deformed into a wide shallow cup. Prognosis is bad in untreated patients. Colonna stated that surgical treatment is rarely successful in patients younger than 8 years.

REFERENCES

- Boyd H B and Sege F P: Congenital pseudarthrosis of the tibia. *J Bone & Joint Surg* 40-A:1245 1958.
 Lloyd Roberts G C and Shaw N E: The prevention of pseudarthrosis in congenital kyphosis of the tibia. *J Bone & Joint Surg* 51-B:100 1969.
 Scott C R: Congenital pseudarthrosis of the tibia. *Am. J. Roentgenol.* 42:104 1939.
 Van Nes C F: Congenital pseudarthrosis of the leg. *J Bone & Joint Surg* 48-A:1467 1966.

FANCONI SYNDROME consists of the basic elements of anemia, leukopenia and thrombocytopenia and a number of inconstant anomalies. The most common associated anomalies in the skeleton include aplasia and hypoplasia of the thumbs and first metacarpal bones; absence of the calcaneal bones; syndactylism; microcephaly and ectopia of the external auditory canals. A second and entirely different Fanconi syndrome is characterized by cystinosis and refractory rickets, often of the most severe type.

REFERENCES

- Fanconi G: Familiäre infantile perniciöse Anämie (perniciöse Blutbild und Konstitution). *Jahrb. f. Kinderh.* 117:257 1927.
 Kunz H W: Hypoplastic anemia with multiple congenital defects (Fanconi syndrome). *Pediatrics* 10:286 1952.

PRENATAL BOWING OF LONG BONES—Faulty fetal position is an important cause of a variety of congenital malformations of the head, neck and trunk such as localized depressions of the calvaria, asymmetries of the face, hypoplasia and asymmetry of the mandible, congenital torticollis and localized depressions of the ribs and sternum. In the extremities, congenital



Fig. 8-292—Prenatal bowing of the radius, hypoplasia of the ulna and pitting of the regional skin in the forearm associated with radial humeral synostosis in a newly born infant.

dislocation of the hip, posterior dislocation of the knee and clubfoot may all result from cramped fetal positions in which the supporting tissues of the joints, the muscles, tendons and articular capsules are over-stretched. Localized deformities of individual bones from faulty packing of the fetal extremities are not uncommon. Anterior tibial kyphosis is the most completely studied of these types of lesions. The bones of the arms are said to be rarely affected by faulty fetal posture. We have seen one example of prenatal bowing

Fig. 8-293—Prenatal bowing of the legs on the 17th day of life. Both thighs are symmetrically bowed laterally. The right shank is bowed laterally and ventrally, but the left shank is straight. Bowing deformities were also present in the arms and to arms.



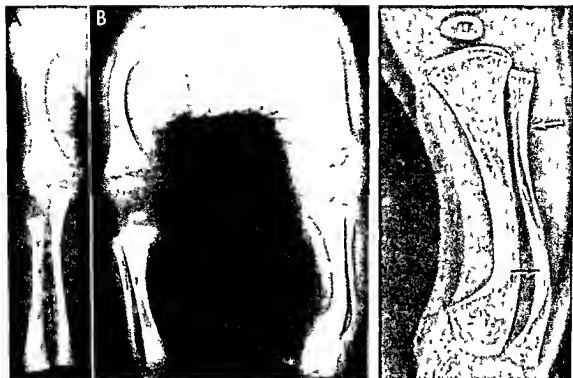


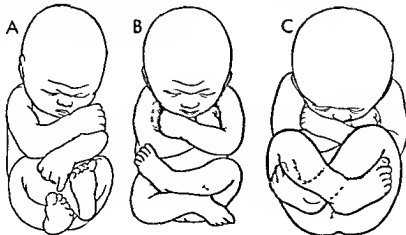
Fig. 8 294 (left) — Prenatal bowing of the long bones of an infant 5 days of age. **A**, the right humerus is bowed and thickened the bones of the forearm are thickened in their middle thirds. **B**, both femurs are thickened and bowed laterad, both tibias are thickened and bowed laterad and ventrad with the tibial changes greater on the left side.

Fig. 8 295 (right) — Schematic drawing of the left tibia and fibula of Figure 8 294. The tibia is bowed laterad and the cortical wall

on the inside of the curve is greatly thickened internally with corresponding decrease in volume of the medullary cavity. The cortical wall on the outside of the curve is thin. In the fibula there is a double curve and the cortical segment on the inside of each curve is thickened internally. Internal thickening of the cortex on the concave side of the curve is characteristic of all prenatally bowed bones.

Fig. 8 296 — Schematic drawing of probable faulty fetal positions responsible for prenatal bowing. **A**, normal fetal position. **B**, abnormal fetal position, each hand impinges on its opposite humerus and each foot on its opposite femur in a fashion which makes possible the transmission of the uterine forces through the impinging part onto the humeri and femurs and causes mechanical pressure affects in the bones, bowing and cortical

thickening. **C**, similar to **B** except that the right shank is folded over the left one. It is this difference in position of the two shanks which is responsible for the asymmetries in the bowings and thickenings of the two tibias. In this case the right tibia would be bowed laterad and ventrad because the right tibia is folded over the left one.



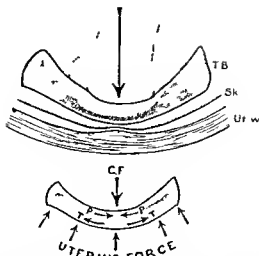


Fig. 8-297—Schematic diagram of the pressure and tension which operate on the tubular bones in prenatal bowing. The heel transmits a compressing force to the near wall of the femur end bends and thickens the femur at the site of the pressure impact. The far wall of the curve, however, is under tension and is thinned rather than thickened. The skin caught between the

summit of the bony curve and the uterine wall undergoes pressure atrophy and dimples. CF, compressing force of fetal part P, pressure on the near wall of the bony tube. T, tension on the far wall of the bony tube. TB, tubular bones. Sk, skin. Ut w, uterine wall.

ing of the radius, hypoplasia of the companion ulna and pitting of the skin associated with radiohumeral synostosis (Fig. 8-292). This suggests that faulty fetal position may also be a causal factor in the fusion or failure of segmentation of fetal joints.

Prenatal symmetrical bowing and thickening of the humeri and femurs with asymmetrical inconstant bowing and thickening of the bones of the shanks and

forearms (Figs. 8-293 to 8-295) have been described (Caffey), all apparently secondary to faulty packing and molding of the fetal extremities in the uterus (Figs. 8-296 and 8-297). In one of our patients the ribs as well as the tibias and one femur were bowed (Fig. 8-298). Associated cutaneous stigmata of pressure dimples and pits in the skin (Fig. 8-299) are often present; they are usually located over the summits of

Fig. 8-298 (left) Prenatal bowing of both tibias and femurs (A) and the lower ribs (B) on both sides in an infant 3 weeks of age.

Fig. 8-299 (right) Deep cutaneous dimple over the apex of the curvature of a severely bowed tibia. The patient was 17 months old.

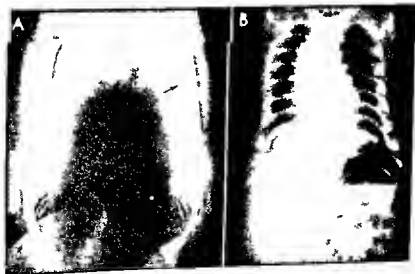
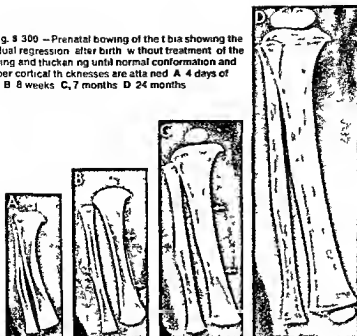


Fig. 8 300 — Prenatal bowing of the tibia showing the gradual regression after birth without treatment of the bowing and thickening until normal conformation and proper cortical thicknesses are attained. A 4 days of age B 8 weeks C 7 months D 24 months



the curvatures in the deformed bones. The prenatal bowings and thickenings tend to regress shortly after birth, in some cases regression is complete by the end of the 2nd year (Fig 8 300) but in others marked bowings have persisted as late as the 7th year (Fig 8 301) it is probable that the more severe deformities

of this nature may persist into adult life. In Gordon's patient the prenatal crossed leg position of 'comfort' persisted as late as the 12th postnatal month (Fig 8-302). In Weller's case of hypophosphatasia of the newborn multiple symmetrical dimples of the skin were present in the forearms and shanks in the ab-

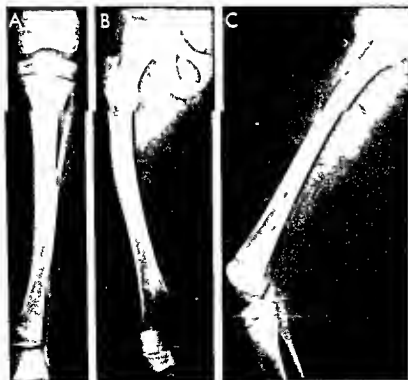
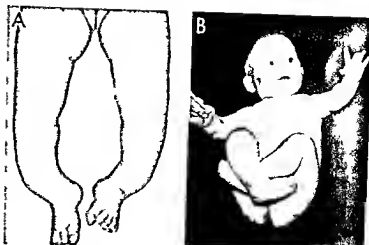


Fig. 8 301 — Residual prenatal bowing and thickening of the long bones at 7 1/2 years of age. This is the patient whose bones are shown at age 5 days in Figure 8 294. A left tibia B and C frontal and lateral projections of the left femur

Fig 8 302 — Prenatal bowing of the tibiae at the 12th postnatal month. A photograph of the bowed shanks in approximately anatomical position. B spontaneous maintenance of normal fetal cross-legged position on which is probably a long standing position of comfort. (From Gordon)



sence of bowing of the underlying bones. The dimples do not appear to regress with advancing age. In retrospect it is clear that prenatal bowings of the bones in the extremities have been confused with rachitic bowings in some cases.

REFERENCES

- Angle C R. Congenital bowing and angulation of the long bones. *Pediatrics* 13 193 1904.
 Bedgley C E. *et al*. Congenital kyphoscoliotic tibia. *J Bone & Joint Surg* 34-A 349 1952.
 Browne D. Congenital deformities of mechanical origin. *Proc Roy Soc Med* 29 1409 1936.
 Caffey J. Prenatal bowing and thickening of the tubular bones with multiple cutaneous dimples in the arms and legs. A congenital syndrome of mechanical origin. *Am J Dis Child* 74 543 1947.
 Chapple C C and Davidson D T. A study of the relationship between fetal position and certain congenital deformities. *J Pediatr* 18 483 1941.
 Conway T J. Prenatal bowing and angulation of the long bones. A description of its occurrence in a brother and sister. *Am J Dis Child* 95 305 1958.
 Gordon G C. Congenital Deformities (London: E. & S. Livingstone Ltd. 1961).
 Krida A. Congenital posterior angulation of the tibia. A clinical entity unrelated to pseudarthrosis. *Am J Surg* 82 98 1951.
 Middleton D S. Studies on prenatal lesions of striated muscles as a cause of congenital deformity. I. Congenital tibial hypoplasia. II. Congenital high shoulder. III. Myodystrophia foetalis deformans. *Edinburgh M J* 41 401 1934.
 Weller S V D. Hypophosphatasia with congenital dimples. *Proc Roy Soc Med* 52 637 1959.
 Williams E R. Two congenital lesions of the tibia: congenital angulation and congenital pseudarthrosis. *Brit J Radiol* 16 371 1943.

CONGENITAL INTRINSIC DYSPLASIAS

CONGENITAL CARTILAGINOUS DYSPLASIAS — Achondroplasia — This is a generalized symmetrical disease of the skeleton in which longitudinal interstitial growth of epiphyseal cartilage is decreased and latitudinal appositional growth of epiphyseal cartilage is not affected. Subperiosteal bone formation is also not affected.

In microscopic studies of specimens from the cartilage rim of the iliac crests and the proximal cartilage plates of the fibulas of seven living typical achondroplasts, Posen found normal cartilage in the growth plates of the iliac crests. In the fibular growth plates, however, growth was stunted and the proliferating cartilage cells were disposed in clusters which were separated by wide septums of fibrous matrix. The resorption of which appeared to be slow and irregular. Rimoin and associates made similar studies at the sternal ends of the ribs and the iliac crests and found



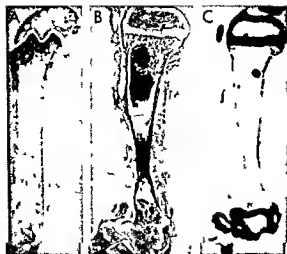
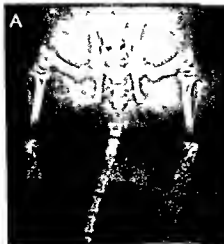


Fig 8-304 — Experimental achondroplasia in rats. A, radiograph of a long bone after injection into a rat of bone-seeking isotope (plutonium) showing its localization in the most active metabolite sites in the bone: the provisional zone of calcification and metaphyseal foci, but no deposition in cartilage. B, section of long bone of rat stained with hematoxylin-eosin. C, radioautograph of a section of long bone of a rat treated intraperitoneally with large doses of ^{225}Ac , a cartilage-seeking isotope, which shows maximal localization in resting and proliferative cartilage. In contrast to A, there is no deposit on or in the provisional zones of calcification or metaphyseal bony foci (Figs. 8-304 and 8-305 courtesy of Dr. Philip Rubin, Rochester, N.Y.).

regular, well organized endochondral bone formation. They concluded from the nearly normal findings that the basic causal mechanism at these sites in achondroplasia is a reduction in the velocity of longitudinal growth. These two important studies indicate that samples of bone used for diagnosis in achondroplasia should not be taken from the iliac crests, the sternal ends of the ribs or the proximal ends of the fibulas.

Fig 8-305 — Radiographs of pelvis and legs of A, a rat treated with cartilage-seeking isotope ^{225}Ac which shows shortenings and



deformities in the long bones similar to those of human achondroplasia. B, control untreated litter mate.

Achondrogenesis is thought by some to be a separate entity; radiographically, it appears to me to be a severe type of thanatophoric achondroplasia. The tubular bones are short and proportionately thick. These primary disturbances in cartilaginous growth result in shortened, bowed extremities, a relatively elongated trunk, a large head with flattened nose and prominent buttocks caused by an upward tilt of the sacrum (Fig. 8-303). The cause of fetal achondroplasia is unknown; instances of familial transmission have been recorded. Inheritance is primarily dominant, but occasionally other types occur. Phenotypic achondroplasia is a remarkably consistent syndrome which results from the action of a single mutant gene; about 90% of parents of achondroplasts are normal. Matings between achondroplasts and normals have resulted in about 50% achondroplastic offspring. Non-achondroplastic parents rarely have had more than one achondroplastic offspring. Two achondroplasts mate only rarely. Infants born of such matings usually have severe skeletal changes and die during the first weeks of life (thanatophoric achondroplasia). Durrant-Swami produced an achondroplasia-like disorder in chicks by the injection of insulin into the yolk sac on the fifth day of incubation and also by the injection of thallium on the fifth day. In Rubin's beautifully designed experiments with the radioactive isotope of sulfur (^{35}S) which was injected in large doses into the peritoneal cavities of rats 3 weeks of age, achondroplasia-like changes were produced consistently in the long tubular bones (Figs. 8-304 and 8-305). He produced similar but hyperplastic achondroplasia-like changes by carefully controlled external irradiation of the proliferative cartilage zones in long tubular bones.

Kaufmann differentiated three types of achondroplasia in fetuses and newly born infants according to the changes in the cartilage. In the *hypoplastic form*, which is the most common, each metaphysis shows

deformities in the long bones similar to those of human achondroplasia. B, control untreated litter mate.



an approximately uniform diminution in cartilaginous proliferation, in the *hyperplastic type* diminished cartilaginous growth is irregular, resulting in thick, broad, mushroomlike terminal bony segments which overhang the middle portions of the shaft. This hyperplastic form is much commoner during the first months of life than later. The rare *malacic type* is characterized by softening of the cartilage; this is a pathologic rather than a clinical entity.

Langenskiöld believed that the growth disturbance in achondroplasia is due to the formation of a perosteal disk in the metaphysis of each bone—a metaplasia of the local connective tissue so that compact bone is formed prenatally within the epiphyseal plate by cells which normally migrate from the center of the cartilage and usually do not take on bone-forming properties until they are incorporated into the perosteum as osteoblasts.

Transverse fibrous and bony bands were produced experimentally in the metaphyses of growing rabbit bones by Trueta and Trios by the application of pressure longitudinally on the ends of the bones. These bands are similar to those which are found in the metaphyses of achondroplastic human bones and they raise the question of the causal relationship of excessive pressure in utero and the development of achondroplasia in the fetus.

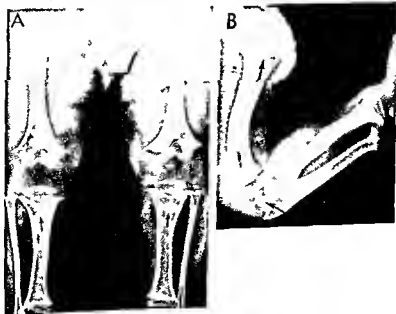
The roentgen features of the *hypoplastic type* are

shown in Figures 8-306 to 8-308. The tubular bones are short but their caliber is approximately normal. The cortices are normally thick; the medullary canals and spongiosa are not affected. The tuberosities for muscular attachments are enlarged and the normal curves exaggerated. The epiphyseal plates are smooth or only slightly irregular. In the distal ends of the femurs and proximal ends of the tibias the epiphyseal ossification centers are sometimes partially buried in the shafts owing to marginal overgrowth of the ends of the shaft around them. This causes a cupped or ball and socket appearance of the metaphyses at the knees. The fibula is frequently proportionately elongated in comparison with the tibia; the excessive caudal extension of the fibula may cause inversion of the foot and serious disability which requires osteotomy of the fibula for correction. The epiphyseal ossification centers appear late and are small during early life. The hands and feet are broad and stubby, the trident deformity of the digits may or may not be present, the carpal and tarsal are often quite irregular in outline.

Hypochondroplasia is a type of short limbed dwarfism in which there is only slight clinical deformity and moderate dwarfism with some features which suggest achondroplasia. Some patients are said to lack rhizomelia or root shortening of the extremities which is one of the cardinal signs of typical achondro-

Fig 8-306—Typical severe achondroplasia in a boy 6 years of age. In the legs (A) the long tubular bones are shortened with relatively greater shortenings of the femurs than of the tibias. The fibulas are relatively overlong in comparison with the tibias and they overlap the tibias in the ankle. All the ends of the shafts are cupped and their epiphyseal ossification centers fill the cup in a shallow ball and socket pattern. The epiphyseal ossification centers are all small. The arrows point to local rarefaction of the

terminal segments of the tibial shafts at the knees due to shallowness of the tibial shafts at this level. In B a similar change is evident in the arm where the humerus is disproportionately shortened in relation to the shortened bones of the forearm. The arrow is directed at the sharp projection on the proximal end of the ulnar shaft. This feature is a common one which has not usually been described in achondroplasia.



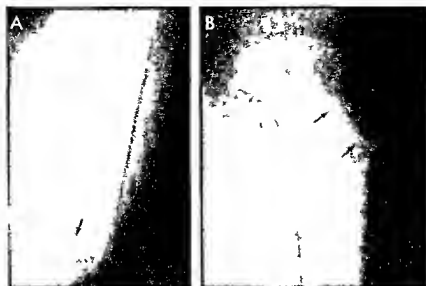


Fig 8 307 —A, deformity at the proximal end of the growing ulnar shaft of an achondroplastic boy 6 years of age. B, the oblique face of the ventral edge of the proximal end of the tibial shaft which reduces the diameter of the proximal end of the tibial

shaft in its ventrodorsal axis and accounts for the rereflexion of the proximal ends of the tibial shafts in frontal projection (see Fig 8 306 A)

Fig 8 308 —Cupping of the metaphyses of the femurs at the knees and the tibiae at the ankles in an achondroplastic boy 6½ years of age. In addition to cupping of the metaphyses, the bones are short, the metaphyses are widened, and the epiphyseal ossification centers are overlarge and bulge into the cupped metaphyses. The epiphyseal ossification centers fuse prematurely with the cupped metaphyses. Similar changes were present in the radius and ulna at the wrist and in the humerus at the shoulder on both sides.



plasia, and other secondary relatively unimportant achondroplastic features such as depression at the base of the nose and trident hands. The latter are, of course, not present in many classic achondroplasts. Clinical diagnosis is said to be especially difficult in the newly born. The most diagnostic radiographic features are said to develop in the extremities, even there, however, the radiographic changes are said to be absent during infancy and early childhood. The ratios of the lengths of the tibia and femur and the radius and humerus in older children disclose usually, but not invariably, mild mesomorphic shortening of the middle segments. Elongation of the fibula, shortening and flaring of the ulna and cupping of the dorsal edges of the vertebral bodies are believed to be earliest radiographic changes. Owing to the vagueness of both clinical and radiographic signs of this entity, it probably will continue to be considered a variation of normal or mild type of achondroplasia, by many. A sufficient population has not been adequately studied for establishment of satisfactory diagnostic criteria. Kozlowski pointed out that the absence of mixed examples of achondroplasia and hypochondroplasia in the same families favors the argument that hypochondroplasia is an independent entity and not a mild phenotype of achondroplasia. It should be emphasized that from the radiographic findings alone, the conclusive differentiation of achondroplasia and hypochondroplasia is exceedingly difficult, if not impossible, in many young patients.

A feature of achondroplasia which has generally been overlooked is the disproportionate elongation of the hands and feet in relation to the rest of the extremities. This is due to the large amounts of cartilage in the carpal and tarsal bones and in the ends of

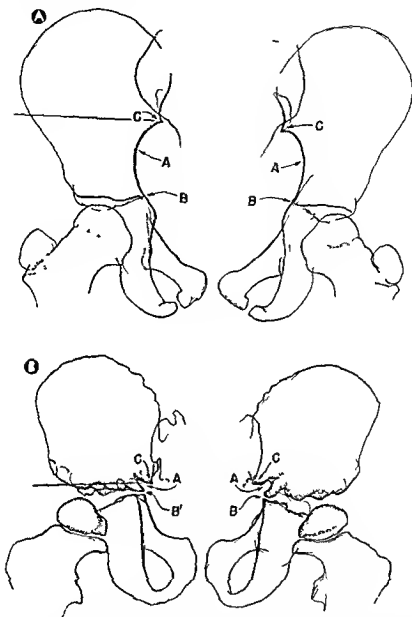


Fig. 8-309 — Comparison of normal (A) and achondroplastic (B) pelvises at 5 years of age in tracings of radiographs. In B the sacrum is narrow and articulates low on the ilia; the transverse and oblique pelvic diameters are shortened. The ilia are shortened longitudinally owing to undergrowth of the iliac bases and to a

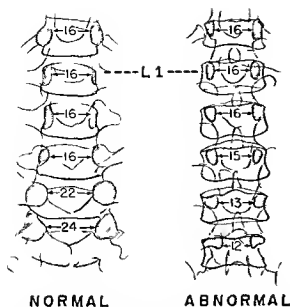
less degree of undergrowth of the iliac wings, which are also squarer. The iliac bases are stepped. The greater sciatic foramen is reduced to a narrow slit just above the Y cartilage. A and A' are the greater sciatic foramina; B and B' are the Y cartilages; C and C' are the inferior iliac spine.

the metacarpals, metatarsals and the phalanges. The spine is relatively elongated for the same reason—the excessive amounts of cartilage in the many vertebral bodies.

The distinctive features of the rarer hyperplastic type are the wide flaring of the ends of the shaft and the funguslike irregularities which project from the terminal margins. The margins of the neighboring

epiphyseal ossification centers are usually smooth in contrast with the tufted edges of the diaphyses.

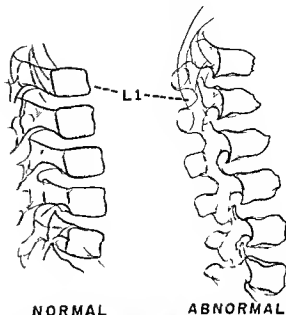
In many cases the radiographic changes in the pelvis and lumbar spine (Figs. 8-309 to 8-311) are highly diagnostic and helpful in differentiating achondroplasia from such diseases as hypophosphatasia, metaphyseal dysostosis, juvenile rickets and gargoylism. In actual practice the diagnostic problem of achon-



NORMAL

ABNORMAL

Fig. 8-310—Comparison of normal and achondroplastic lumbar spines in tracings of radiographs made in frontal projection at 24 months of age. The normal spine flares from top to bottom and the L 5 segment is the widest. The achondroplastic spine tapers from top to bottom and the L 5 body is the narrowest. The numbers on each space measure the interpediculate space in each segment which is a measure of the transverse diameter of the spinal canal at that level. In the normal spine the spinal canal is widest at L 5. In the achondroplastic spine in contrast the spinal canal is narrowest at the L 5 segment.



NORMAL

ABNORMAL

Fig. 8-311—Comparison of normal and achondroplastic spines in tracings of radiographs made in lateral projection at 24 months of age. The pedicles are shaded and at all levels are shortened to less than one-half in the achondroplastic which indicates that the spinal canal is flattened to less than one-half its normal depth. The dorsal edges of the achondroplastic bodies are slightly concave. The ventral ends of some of the vertebral bodies in the achondroplastic are rounded into bullet-nosed deformities. The intervertebral spaces are deeper and the vertebral bodies smaller in the achondroplastic.

droplasia is most crucial and most frequent in the newly born infant (Figs 8-312 and 8-313).

In the most severe type of fetal achondroplasia, the shortness of the ribs and the smallness of the thoracic cage cause crowding of the lungs and interfere with their normal expansion. This in turn impairs normal oxygenation of the blood, induces dyspnea and hypoxia, and often death within the first hours of life. In some cases respiration does not begin and the infant is born dead (see discussion of thanatophoric dwarfism). Impingement of the edges of the small foramen magnum on the medulla is also an important cause of early death, especially in prenatal deaths.

According to Cohen and associates the most important neurologic complications of achondroplasia are moderate communicating hydrocephalus and compression of the spinal cord from kyphosis at the level of the L-12 and S-1 segments.

The cupping of the metaphyses in many younger achondroplastics (Fig. 8-308) suggests impairment of the arterial blood supply to the epiphyseal arterioles which supply the longitudinally growing cartilage in the cartilage plate, this impairment being due primarily to congenital hypoplasia of these arterioles. It seems likely that this mechanism of the oligemia of the longitudinally proliferating cartilage is the fundamental cause of achondroplasia and several other

cartilaginous dysplasias characterized by longitudinal undergrowth of bone.

Metatrophic dwarfism is a term designed by Maroteaux and associates to name a type of short limbed dwarf characterized by wide flaring of the metaphyses (Fig. 8-314) in which longitudinal cartilaginous growth is retarded but latitudinal cartilaginous growth is excessive. In the newborn the most conspicuous changes in the long bones are the wide flarings at the metaphyseal levels with shortening, cupping and terminal flarings of the trumpetlike expansions. The ossification centers for the vertebral bodies are mere transverse strips of calcium density between deepened radiolucent intervertebral spaces. Mild kyphoscoliosis is present at birth and becomes progressively more severe with advancing age despite treatment. The spinal canal in the lumbar levels does not taper progressively as is the case in the typical achondroplastic lumbar spine. The pelvic bones show achondroplastic-like changes—shortening of the ilia at their bases with deepening and narrowing of the sciatic notches but little or no change in the ischia and pubic bones. The skull, however, is normal. According to Larose and Gay, with advancing age the long bones grow more rapidly than would be expected in achondroplasia and the kyphosis becomes more pronounced so that the patient who was a short



Fig 8-312.—Achondroplasia In the legs on the 2nd day of life. **A**, normal legs. **B**, achondroplastic. The achondroplastic bones are shortened, but their caliber is little affected save for absence of the normal terminal flares. The femoral ossification centers in the distal epiphyseal cartilages are not present in the achondroplastic.

and the ends of the shafts tend to be straight or oblique rather than rounded as in the normal. The lateral tibial cortical walls are thickened in the achondroplastic, and the fibulas are overlong and overlap on the ankles.



Fig 8-313.—Achondroplasia of the spine on the second day of life. **A**, normal; **B**, achondroplastic. All of the bony elements in the vertebrae are smaller in **B**, and the cartilaginous elements are larger. The intervertebral spaces are deeper and the small vertebral bodies tend to be rectangular. The sharp angulation at the lumbosacral junction in the achondroplastic before weight bearing is noteworthy.



Fig 8-314—Hyperplastic larval achondroplasia at 6 days of age (metatropic dwarfism). A, shortening and flaring of the convex ends of the shafts in the arms and legs. The disproportionate increase in the transverse diameters of the epiphyseal cartilages and metaphyses and ends of the shafts is the most striking deformity in the shortened long bones. The tubular bones in the hands are unusually large. B, severe vertebral plana in the thoracolumbosacral segment with reciprocal deepening of the intervertebral spaces. The spinal segments are not flattened. Only the

ossification centers of the bodies are flattened. The first cervical segment is displaced forward. This displacement probably compresses the cervical spinal cord and contributes to respiratory failure, muscular weakness and early death. Absence of kyphoscoliosis is noteworthy. C, the small caliber thorax is due to undergrowth of the ribs, which is also an important factor in early death. The sternal ends of the ribs are widened. D, normal skull. The lack of severe vertebral flattening in the cervical spine is well shown in this film as so.

limbed dwarf with a relatively long trunk during the first months of life is converted into a relatively long limbed dwarf with shortened kyphoscoliotic trunk. Knock knee is usually severe and persists despite treatment. Skeletal maturation is normal or slightly delayed.

REFERENCES

- Beales R K. Hypochondroplasia. Report of five kindreds, *J Bone & Joint Surg* 51 A 728 1969
- Caffey J. Achondroplasia, in Brennemann's Practice of Pediatrics (Hagerstown Md. W F Prior Company Inc 1945) Vol IV chap 28
- Achondroplasia of the pelvis and lumbosacral spine. Some radiographic features. *Am J Roentgenol* 80 458 1958
- Cohen M E et al. Neurological complications of achondroplastic children. *J Pediatr* 71 367 1967
- Dandy W E. Hydrocephalus in chondrodystrophy. *Bull Johns Hopkins Hosp* 32 1 1921
- deGroot J W C. Two atypical cases of chondrodysplasia, *J Pediatr* 39 715 1951

- Duraiswami P K Experimental cause of congenital defects Its significance in orthopedic surgery J Bone & Joint Surg 34 B 646 1952
- Kaufmann E Untersuchungen über die sogenannte foetale Rachitis (Chondrodystrophia foetalis) (Berlin Georg Reimer 1892)
- Kozłowski K Hypochondroplasia, Polish Rev Radiol 24 450 1965
- Langenskiöld A Normal and pathological bone growth in the light of the development of cartilaginous foci in chondrodysplasia, Acta chir scandinav 85 367 1947
- Langer L C et al Achondroplasia Am J Roentgenol 100 12 1967
- Larose J H and Gay B B, Jr Metatrophic dwarfism Am J Roentgenol 106 156 1969
- Marie P L achondroplasie dans l'adolescence et l'âge adulte Presse méd 8(2) 17 1900
- Maroteaux P and Lamy M Les chondrodystrophies génétiques (Paris L Expansion Scientifique Française 1960)
- et al The metatrophic dwarfs Arch f Kinderheilk 173 211 1966
- Morch E T Opera ex Domo Biologiae Hereditariae Humanæ Universitatis Hafniensis (Copenhagen Elias Munksgaard 1941) Vol III
- Noonan C D Antenatal diagnosis of achondroplasia with comment on Devels halo sign Am J Obst & Gynec 10 929 1968
- Parrot M J Sur la malformation achondroplasique et le dieu Ptah Bull Soc d anthropol de Paris 1(3d ser) 296 1878
- Ponseti I V Skeletal growth in achondroplasia J Bone & Joint Surg 52-A 701 1970
- Rimoin D L et al Endochondral ossification in achondroplastic dwarfism New England J Med 283 728 1970
- Rubin P et al Radiation induced dysplasias of bone Am J Roentgenol 82 206 1959
- Silverman F N and Briennen S Errors in diagnosis of achondroplasia, Acta radiol (diag) 6 305 1967
- Trueta J and Trios A The vascular contribution to osteogenesis IV The effect of pressure on the epiphyseal cartilage of the rabbit J Bone & Joint Surg 43-B 800 1961
- Spondyloepiphyseal dysplasia (pseudoachondroplastic type)** is the name given by Lamy and Maroteaux to a syndrome in three dwarfs who resembled achondroplasts but differed from achondroplasts in these respects onset of dwarfism was delayed beyond the 20th month noninvolvement of the head and face more severe and more irregular changes in the metaphyses and the epiphyseal ossification centers of the long bones and irregular hypoplasia of the bodies of the vertebrae which resulted in wedge-shaped bodies with a central anterior extension in the lower thoracic and lumbar levels These patients appeared to be of normal stature and free from deformities until late in their 2nd year Lamy and Maroteaux pointed out the difficulty of differentiating their syndrome from our cases of hyperplastic achondroplasia In our cases of hyperplastic achondroplasia the dwarfism develops in utero and is well advanced during the early months of life (Fig 8-315) The spine is affected commonly in classic achondroplasia at birth (see Fig 8-313) and the epiphyseal ossification centers are hypoplastic (see Fig 8-306) and may be irregular (Fig 8-316) For these reasons we prefer to call the irregular types of achondroplasia, hyperplastic achondroplasia, rather than spondyloepiphyseal dysplasia (pseudoachondroplastic type) When and if it is proved on valid evidence from both clinical and radiographic examinations that there is an achondroplasia-like disease which begins after birth and as late as the end of the 2nd year such cases should be considered entities separate from both standard achondroplasia and the hyperplastic type of achondroplasia.
- Ford and colleagues described three dwarfs who

Fig 8-315—Hyperplastic wedge-shaped achondroplasia with universal vertebral plana in an infant 5 months of age. Radiographs made at 2 weeks of age were said to have been similar. In A characteristic changes are present in the pelvic bones and

femurs in B a of the vertebral bodies as a flattened caphalocaudally. The early age at onset excludes the diagnosis of the spondyloepiphyseal dysplasia of Lamy and Maroteaux.

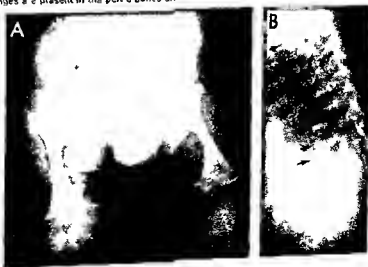




Fig 8 316 — Achondroplasia calcificans congenita in an infant 2 days old. All of the talus the margins of the calcaneus and metatarsals of the tubular bones show characteristic irregular spotty and stringy sclerotic calcification. Maturation is retarded and the tubular bones are short and heavy.

resembled the patients of Lamy and Maroteaux in several features.

Maroteaux and associates attempted a new and more elaborate classification of the spondyloepiphyseal dysplasias in 1968. They pointed out that in this group, most patients are normal until after the 2nd year of life. They arbitrarily excluded several spondyloepiphyseal diseases from the classification in which vertebral, epiphyseal and metaphyseal lesions were present. The diseases which are included are divided into three sections dependent on the predominance of involvement of the epiphysis or vertebrae or metaphyses. The authors pointed out the many difficulties in their classification. Some of the entities included do not really qualify neatly for their design. The criteria for differentiation of the various entities are vague and the radiographic differences in different supposed entities are those of degree and position rather than of quality. The fact that in some of these diseases the sites of the disease and their nature change with advancing age also invalidates their accurate classification or even the diagnosis of spondyloepiphyseal dysplasia. Until larger populations of patients with these diseases are studied more adequately from clinical, radiographic, metabolic and genetic standpoints it is unlikely that elaborate classifications of these indefinite entities will be helpful in their radiographic identification.

In 29 patients who had *spondyloepiphyseal dysplasia congenita*, according to the standards of Spranger and Langer, small stature was consistently present

and present at birth. Already at birth ossification of the bones in the extremities, pelvis and spine was retarded. During later childhood the metaphyses were affected, often severely, which suggests that a more adequate name for this entity would be *spondyloepiphyseometaphyseal dysplasia congenita*. The spine, pelvis and femoral heads were the sites of the most striking radiographic changes in older children. Maturation was retarded in all parts of the skeleton. The spine was shortened at all ages, and this shortening is a major factor in the clinical appearance. The tubular bones in the hands were not shortened. The shortening of the extremities was not more marked at their roots in the femur and humerus. Retinal detachment and myopia were common complications.

Spondyloepiphyseal dysostosis (Kozłowski, Maroteaux and Spranger) is a bone disease which appears between 1 and 4 years of age in which the chief loss of stature is in the spine and trunk. In the radiographic examination, the vertebral and pelvic changes include unusual vertebra plana and an achondroplasia-like pelvis. In the long bones the principal changes are in the metaphyses, which are incompletely and irregularly mineralized. These changes simulate those in metaphyseal dysostosis and rickets. The vertebral changes are similar to and overlap the changes of spondyloepiphyseal dysplasia in Morquio's disease. However, slit lamp examinations disclosed no opacities in the corneas, and excretion of urinary polysaccharides was normal. In this vague field of spondyloepiphyseal and spondyloepiphyseal dysplasias, one cannot be sure whether all cases represent a single genetic entity with a wide range of phenotypic variations or whether two or more distinct entities are involved.

REFERENCES

- Ford N, et al. Spondylo-epiphyseal dysplasia (pseudoachondroplastic type). *Am J Roentgenol* 86:462, 1961.
- Kozłowski K, et al. Spondylo-metaphyseal dysplasia. *Presse med* 75:2759, 1967.
- Maroteaux P and Lamy M. Les formes pseudoachondroplastiques des dysplasies spondyloepiphyseales. *Presse med* 10:383, 1959.

Mesomelic dwarfism (*dyschondrosteosis*) is commonly associated with bilateral Madelung deformity. This type of dwarfism was first described as *dyschondrosteose* by Léri and Weill in 1929. Its inheritance in the families of Lamy and Maroteaux suggests dominant genetic transmission. Stature is reduced and the middle segments of the extremities (forearms and shanks) are reduced disproportionately in relation to the root segments (upper arms and thighs). These disproportions are the converse of the "root" or rhizomelic disproportions in typical achondroplastic extremities and serve to differentiate these two dysplasias. Felman and Kirkpatrick reported nine cases of isolated Madelung's deformity and six of the Léri-Weill syndrome of dyschondrosteosis. In their cases of



Fig. 8 317—Madelung's deformity in mesomelic dwarfism (dyschondrosteosis of Léri and Weil). The forearms in frontal (A) and lateral (B) projections of a stunted girl 12 years of age. In A each shortened radius is bowed laterad. Each distal end of the radius is tipped toward the distal and of its companion ulna which leaves a V shaped space between them. The carpal bones

have shifted into the space with the lunate wedged into the apex of the V and the navicular contiguous to the lateral slope of the V and the triquetrum against the medial slope of the V. In B each radius is bent dorsad and each ulna is displaced dorsad out of its normal articular contact with the radius at the wrist.

Madelung's deformity, the age of onset varied between 11 and 20 years. Pain at the wrist was the only clinical complaint.

The radiographic changes are most pronounced and most diagnostic in the forearms and wrists (Fig. 8 317). In the forearms, the radius and ulna are both shortened but the ulna more than the radius. The ulna is dislocated dorsad at the distal radioulnar joint and the radius is bowed laterad and dorsad. The distal ends of each radius and ulna are tipped toward each other, which leaves a V shaped space between them. The carpal bones are shifted proximally into the inter radioulnar space with the lunate wedged in the apex of the V and the navicular and triquetrum contiguous to each sloping wing of the V. The tibia and fibula are shortened absolutely and in proportion to the femur. In some cases apparently the root bones (femur and humerus) have also been shortened. The bones in the hands and feet are normal. The axial skeleton is normal.

REFERENCES

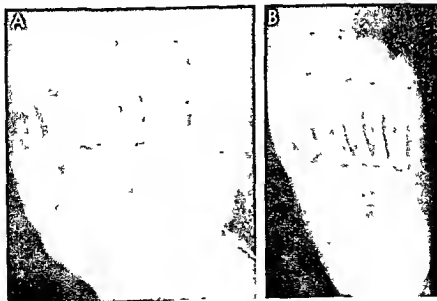
- Berdon, W. E. et al. Dyschondrosteosis (Léri-Weill syndrome). Congenital short forearms. Madelung type wrist deformities and moderate dwarfism. *Radiology* 85:677, 1965.
- Felman, A. H. and Kirkpatrick, J. A. Madelung's deformity. Observations in seventeen patients. *Radiology* 93:1037, 1969.
- Kozłowski, K. et al. Spondylometaphyseal dysplasia. *Presse méd.* 75:2796, 1967.
- Lamy, M. and Maroteaux, P. Les chondrodystrophies génétiques (Paris). L'Expansion scientifique française, 1961, p. 33.
- Langer, L. O. Dyschondrosteosis: a hereditary bone dysplasia with characteristic roentgenographic features. *Am J Roentgenol* 95:178, 1965.
- Finlay, D. and Hermann, W. G. Mesomelic dwarfism (dyschondrosteosis of Léri and Weil). *J A.M.A.* 193:1056, 1965.
- Spranger, J. W. and Langer, L. O. Spondyloepiphyseal dysplasia congenita. *Radiology* 94:313, 1970.
- Chondrodystrophia calcificans congenita**—This name has been applied to two conditions which should be clearly differentiated. In some classic achondroplasts, always fetuses and infants, mineralization of the epiphyseal cartilages and round bones may be irregular and spotty (Fig. 8 316). This irregularity is merely a variant in the severer types of classic achondroplasia in young subjects and does not warrant a separate name. This irregularity in miner-

Berdon, W. E. et al. Dyschondrosteosis (Léri-Weill syndrome). Congenital short forearms. Madelung type wrist deformities and moderate dwarfism. *Radiology* 85:677, 1965.



Fig 8-318 —Chondrodystrophia calcificans congenita in a boy 17 days of age who had no manifestations of achondroplasia. All of the secondary centers of the femurs and tibiae show extensive punctate calcifications. The patellae show similar extensive calcifications. normally lime does not appear in the patellae in boys until about the 32d month. The symmetrical small sclerotic foci ventral to the proximal tibial metaphyses may represent focal calcification of the synovial membrane of the knees. At necropsies much of such calcification has been found in the articular tissues as well as epiphyseal cartilages. All of the metaphyses and the entire diaphyses are normal; there are no changes suggestive of achondroplasia.

Fig 8-319 —Chondrodystrophia calcificans congenita in the newborn bones of the hands (A) and of the feet (B). The fine focal increases in density are present in the epiphyseal cartilages of the tubular bones and also in the tarsal and metatarsal bones. Many of



alization in achondroplasia is never seen after the first two or three years of life.

In Conradi's chondrodystrophia calcificans congenita punctata, irregular mineralization may also develop in fetuses and infants who are not achondroplastic and who apparently have no abnormalities save calciferous stippling of the growing cartilage (Fig 8-318). Unfortunately this condition has been called chondrodystrophia calcificans congenita, although it is wholly unrelated to and has a much different prognosis from chondrodystrophia foetalis (achondroplasia) with which it has been commonly confused. The characteristic change is the focal and often premature deposition of lime in masses of degenerating connective tissue in the growing cartilages in the sites of both primary and secondary ossification centers (Fig 8-319). Borovsky and Arendt reported calcification of the synovial tissues as well. In contrast to achondroplasia, there may be no shortening of the tubular bones, and maturation of the epiphyses and round bones is accelerated rather than retarded. Chondrodystrophia calcificans congenita is not confined to the tubular bones in the extremities, the sternum, scapulae, vertebrae and ribs, ilia and ischia may all be affected (Fig 8-320). In 2 cases we have seen massive deposits of lime in the neck which appeared to be in or near the hyoid bone and the laryngeal cartilages. Regional and local hypoplasias of the skeleton are not uncommon in this disease, such congenitally short bones remain short permanently and after the punctate calcification of the cartilage has long disappeared. Hemivertebrae dysplasia and dislocation of the hip, and clubfoot have all been

the affected tubular bones are shortened and widened. Multiple calciferous foci are visible in the proximal ends of the second and third metacarpals where normally epiphyseal ossification centers never appear.

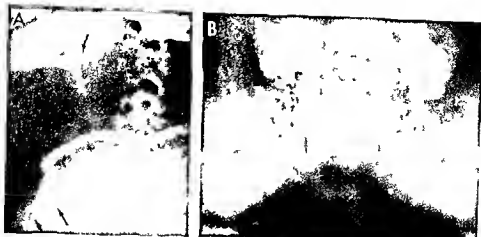


Fig. 8 320 — *Chondrodystrophia calcificans congenita* in the neck, thorax and pelvis of a boy 17 days of age. A, punctate and irregular mineralization of the sternum, hyoid bone and cervical spine. The top arrow points to a mass of lime in or near the hyoid

bone and laryngeal cartilage. B, irregular punctate calcifications in epiphyses of the femurs, tibiae and lateral masses of the sacrum.

complications of this cartilaginous dystrophy. Bilateral congenital cataracts are frequently present; they were found in 9 of 42 cases studied by Mosekilde. Cutaneous thickenings have been observed in several patients. Optic atrophy has been reported in a few. In

Fig. 8 321 — Universal coronal cleft vertebra of the thoracic and lumbar segments of the spine in a boy at 11 days of age who also had severe generalized *chondrodystrophia calcificans congenita*. All of the vertebral bodies are split into dorsal and ventral segments by radiolucent bars of cartilage.



the skin, follicular atrophoderma, incontinentia pigmenti and ichthyotic hyperkeratoses have been described. Calcifications in the cartilaginous rings of the trachea have interfered with tracheal endoscopy.

Prognosis is good for complete recovery without residual deformities or shortened stature provided that initially there were no gross deficiencies or deformities of individual bones. The roentgen signs of spotty calcification have completely disappeared after two or three years in patients who have been followed in serial studies. Licht and Jesiotr found in a man 24 years of age, incomplete dorsal sclerosis and flattening of vertebral bodies at all cervical, thoracic and lumbar levels which they attributed to congenital *chondrodystrophia calcificans*. The rest of the skeleton was normal radiographically. The reasons for attributing these spinal changes to this congenital disease are not clear. Some of the most extensive and the most long standing cases of coronal cleft vertebra have also included *chondrodystrophia calcificans congenita* (Fig. 8 321).

Silverman followed one patient who had typical *chondrodystrophia calcificans congenita* at birth to the 17th year, when radiographic findings were suggestive of multiple epiphyseal dysplasia. It seems likely that this same course might occur in other patients: early *chondrodystrophia calcificans congenita* followed by multiple epiphyseal dysplasia.

We have seen two infants whose radiographic changes in the extremities were typical of *chondrodystrophia calcificans congenita* but whose clinical, radiographic, microscopic and serologic findings all indicated acquired calcifying arthritis and chondritis secondary to bacteremias. The first patient was well until the 24th month when her knees, ankles and wrists swelled and became red and hot. She had fever. Inflammatory fluid in large amounts was withdrawn from the left knee joint; bacteria did not grow from

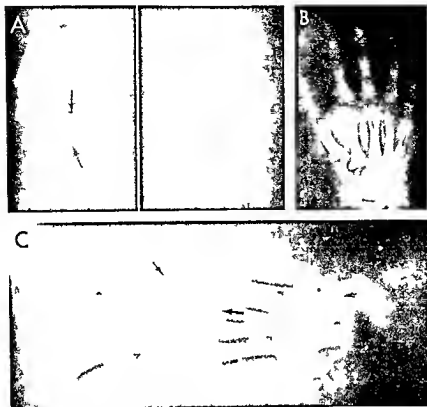


Fig. 8-322 — Calciferous masses at the knees (A), wrist (B) and ankles (C) of a girl 28 months of age who had had clinical arthritis at these sites for four months. The femoral distal ossification centers are much too small and relatively too small in comparison with the tibial centers opposite them. This child had been

exposed to several sick calves, proved to have the polyarthritides of swine influenza at necropsy and whose hocks showed calcifications much like those in this patient. (Courtesy of Dr. R. Parker Allan, Denver, Colo.)

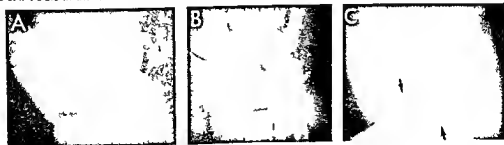
this fluid in standard cultures. At 27 months the radiographic changes were typical of chondrodystrophia calcificans (Fig. 8-322) and in later biopsy specimens the articular tissues were thickened and calcified and the epiphyseal cartilages inflamed and calcified. This patient had been exposed for several months to a number of calves which had clinical swellings of several joints and at postmortem studies were

proved to have calcifying arthritis and infection by the organism of swine influenza (*Erysipelothrix rhusiopathiae*).

The wrist of the second patient became so swollen on the 3rd day of life that it was put in splints to combat pain. At the 7th month widely scattered calciferous foci were demonstrated (Fig. 8-323). At 3 years the serum agglutination titer against *Listeria micro-*

Fig. 8-323 — Calcifications of the wrists and ankles of a girl who had acute clinical arthritis of the left wrist on the 3rd day of life and a protective cast was applied for several weeks. A, the left wrist at 7 months of age, similar but less pronounced calcifications were present at the other wrist. B, at 43 months the sclerotic mass is still visible in the left wrist. C, the left ankle at 7

months shows extensive calcifications. Similar changes were present in the right ankle. At 46 months faint residual calcifications were still visible at the ankles. The knees never became visibly calcified. Seroagglutination tests at 43 months yielding agglutination titers of 1:2500 to *L. monocytogenes*.



cytogenes was 1:2500. A biopsy specimen taken from the left wrist showed dense fibrous tissue with interspersed calcific foci.

In Coughlin's study of the cadaver of an infant who had had classic radiographic and clinical signs of chondrodystrophia calcificans congenita the joint spaces were filled with dense vascularized connective tissue which contained foci of lime-containing bone. Calciferous foci were also found in the thickened synovium and at one site in the synovial membrane an appreciable mass of calcified material was located inside the joint capsule.

These data all suggest that acquired calcifying arthritis—acquired in utero or as late as the 24th month of life—produces radiographic changes which are identical to those found in classic chondrodystrophia calcificans congenita. In our two patients *Erythrasiopathia* of swine influenza and *L. microcytogenes* appeared to be the causal agents. It seems probable to me that all cases of chondrodystrophia calcificans have similar causes. Cataracts in a substantial number of patients, frequent hypoplasias and deformities of individual bones and calcification of laryngeal cartilages all point to a systemic affection probably a bacteremia or viremia rather than simple dysplasia of the epiphyseal cartilages. Obviously such patients need to be studied carefully from the standpoint of infection of blood and joints and in the cases of congenital disease, from the standpoint of the maternal blood stream infection with transplacental infection of the fetus.

Ray and Wedgwood reported in 1964 six cases of neonatal infection with *L. microcytogenes* in Seattle Wash., an area where this infection had never before been suspected. None of the six neonates had arthritis.

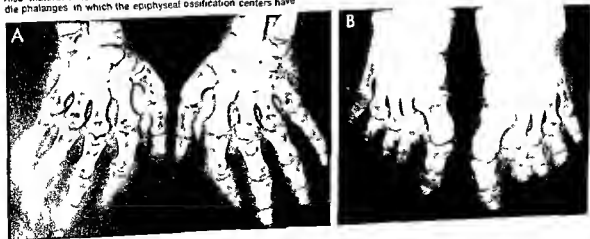
Fig 8-324—Peripheral dysostosis in the hands and feet of a boy 9 years of age. Maturation is accelerated in the tubular and the round bones. All of the tubular bones are shortened; the shortening becomes less marked distally with the greatest shortening in the metacarpals and the least in the distal phalanges. Also, maturation is more advanced distally in the distal and middle phalanges in which the epiphyseal ossification centers have

REFERENCES

- Comings D E *et al*: Conradi's disease. *J Pediatr* 72:63 1968.
 Coughlin E J Jr *et al*: Chondrodystrophia calcificans congenita. Case report with autopsy findings. *J Bone & Joint Surg* 32 A:938 1950.
 Josephson B M: Chondrodystrophia calcificans congenita. Report of a case and review of the literature. *Pediatrics* 28:425 1961.
 Ray C G, and Wedgwood R J: Neonatal listeriosis. Six case reports and a review of the literature. *Pediatrics* 34:378 1964.
 Silverman F N: Epiphyseal dysplasias. Protean entities. *Amer radiol* 4:633 1961.

Peripheral dysostosis is characterized clinically by short broad hands and feet. The cardinal radiographic findings are shortening of the metacarpals and metatarsals, the proximal and middle phalanges are also shortened but to a less degree and cupped at their metapophyseal levels with conical epiphyseal ossification centers (Fig 8-324). The round bones in the wrists are normal in size and shape but accelerated in maturation. Affected individuals are short in stature but otherwise normal. Newcombe and Keats found the middle phalanx of the second finger (index) conspicuously shortened and notched, which produced an ulnar curvature of this second digit. Both the phalangeal and the metacarpal and metatarsal involvements are variable in different patients and in the same hands and feet, but the metacarpal shortenings are usually the most severe. Transmission is thought to be genetic and as an autosomal dominant. Skeletal maturation has been advanced in most patients. Garces and associates found no disturbances in the pituitary-adrenal-gonadal axis in the function of the thyroid, pancreas or in growth hormone responsiveness. In addition to the short and stubby hands and feet, some patients

are ready fused with the proximal phalanges. The cone-shaped epiphyseal ossification centers are visible in the second to fourth middle and proximal phalanges and the second to fifth metacarpals with corresponding cupping of the ends of the opposite shafts. The styloid process of the ulna is elongated and thickened. (Courtesy of Dr. Edward B. Singleton, Houston, Tex.)



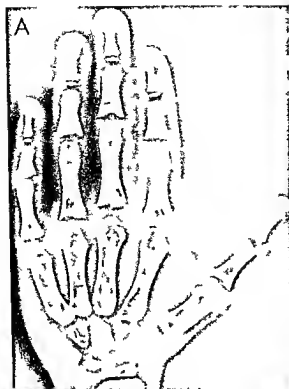


Fig. 8 325.—Trichorhophalangeal syndrome. A. In a girl 7 years of age the proximal ends of the middle and proximal phalanges are abnormal. The base of these phalanges are cupped and spread. There are no epiphyseal ossification centers in the middle phalanges except in the fifth digit. Cone-shaped ossification centers fill the cups at the proximal ends of the proximal phalanges of digits 1, 2, 3, and 4. The ossification centers in the



distal phalanges are sclerotic except in the first digit. The epiphyseal ossification centers in the metacarpals all appear to be fusing prematurely. This is also the case in the proximal phalangee. B. In a woman 49 years of age, all of the proximal ends of the middle phalanges are cupped and spread and the articular cartilages are thin. The fifth metacarpal is shortened distally and metacarpal is normal. (Courtesy of Dr. B. R. G. Rany.)

have had flat nasal bridges and highly arched palates.

One would suspect from the cupping of the metaphyses and the conical epiphyseal ossification centers that the primary causal mechanism of peripheral dysostosis is chronic oligemia, probably congenital of the epiphyseal arterioles which supply the longitudinally proliferating cartilage cells in the cartilage plate.

REFERENCES

- Cohen P., and Van Crevelde S. Peripheral dysostosis. *Brit. J. Radiol.* 36:761, 1963.
- Garces L. Y. et al. Peripheral dysostosis: Investigation of metabolic and endocrine functions. *J. Pediatr.* 4:730, 1969.
- Newcombe D. S. and Keats T. E. Roentgenographic manifestations of hereditary peripheral dysostosis. *Am. J. Roentgenol.* 106:178, 1969.
- Singleton E. B. et al. Peripheral dysostosis. *Am. J. Roentgenol.* 84:499, 1960.
- Walker N. Peripheral dysostosis. *Ann. radiol.* 7:326, 1964.

Fig. 8 326.—Face in trichorhophalangeal syndrome. In a boy 10 years of age. Alopecia, large mouth, large pear-shaped nose, large everted ears and large mandible. The proximal and middle metacarpals were dysplastic at the proximal ends.



Trichorhophalangeal syndrome is made up of three elements: sparse and slowly growing hair, large pear-shaped nose with long vertical groove in the upper lip, and phalangeal dysplasias which include cupping of the metaphyses and conical epiphyseal

ossification centers which result in shortening of the phalanges (Figs 8 325 and 8 326)

The epiphyseal centers fuse early with their shafts maturation of the phalanges is accelerated Maturation of the metacarpals and carpals may be normal or accelerated In the adult hand the proximal edges of the phalanges are indented and spread Similar

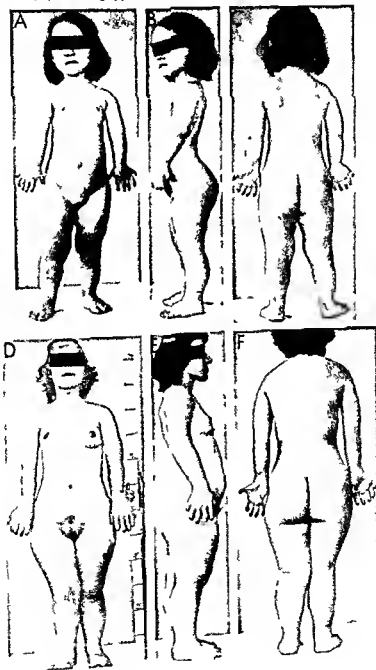
changes may be found in the pedal phalanges but they are not as frequent or as marked as those in the manual phalanges

REFERENCES

- Gledion A. Das tricho-rhino-phalangeale Syndrom Helvet paediatr acta 21 475 1966
Girdany B R Unpublished data.

Fig 8 327 —The external appearance of E1 s-Van Creveld syndrome In a girl A B and C at 4½ years of age D E and F, at 19 years Stature is reduced head and trunk are approximately normal The thorax is small and scapules are high placed Poly-

dactyly is evident There is a heavy growth of hair on the scalp eyebrows eyelashes and pubic region The arms and legs are short owing principally to shortening of the segments distal to the elbows and knees



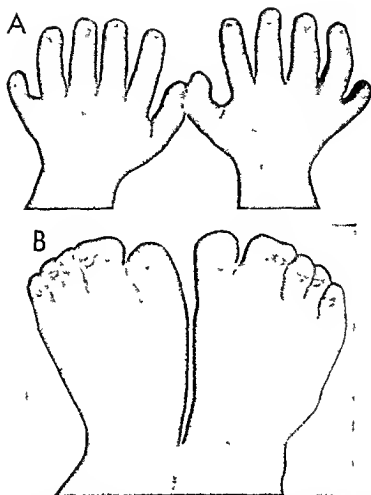


Fig 8-328—Polydactyly and syndactyly in Ellis-Van Creveld syndrome in a girl 28 months of age. All of the nails are hypoplastic and tend to be spoon shaped with the dorsal aspects

Pleonosteosis (Farber's lipogranulomatosis) is a vague clinical syndrome with variable changes in the skin, facies and skeleton. The skin of the hands, forearms and face may be thickened. The face has a mongoloid cast owing to upward tilting of the lateral segments of the palpebral fissures. The tubular bones of the hands and feet are shortened and thickened, with especially broad phalanges in the thumbs and great toes. The principal changes are widely scattered in connective tissues. Many of the younger patients, in several reports, resemble gargoyles.

REFERENCES

- Léri, A. A congenital and hereditary disease of ossification. *Familial pleonosteosis*. Bull et mém Soc méd hôp Paris 45 1228, 1921.
 Rukavina J G, et al. Leri's pleonosteosis. A study of a family with review of the literature. *J Bone & Joint Surg* 41 A 397, 1959.

Chondroectodermal dysplasia (Ellis-Van Creveld) is characterized by chondrodysplasia and shortening of the tubular bones, ectodermal dysplasia, polydac-

tyly and sometimes congenital malformation of the heart. McIntosh in 1933 described a patient showing all the cardinal features of the disorder, 2 additional cases were reported in 1940 by Ellis and Van Creveld. In 1962 Ellis and Andrew reviewed 36 previously reported cases, added 2 cases of their own and in their addendum added 2 more cases for a total of 40 reported cases. They did not include Ferrero's case, which is reputedly the first example of the syndrome from South America. McKusick found this disorder in one or more members of twenty three families of Amish descent in Lancaster County, Pennsylvania.

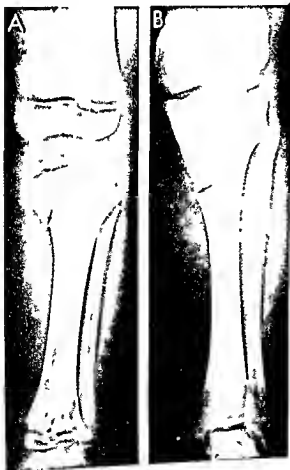
Diagnosis can be made on inspection of the patient, who has a cylindrical, narrow thorax which flares at its base, loss of stature owing to shortening of the legs, principally distal to the knees, and shortening of the arms, principally distal to the elbows (Fig. 8-327), short and stubby hands with polydactyly and sometimes syndactyly (Fig. 8-328), and hypoplasia and dysplasia of the teeth (Fig. 8-329) and the nails of the fingers and toes. Hypotrichosis of the scalp was present in one patient and congenital malformation of the

concave. The skin of the hands is veined in the so-called marbled pattern.



Fig 8-329.—Dental dysplasia in Ellis-Van Creveld syndrome. These are the deciduous teeth of a girl 4½ years of age.

Fig 8-330—A, the shank in Ellis-Van Creveld syndrome in a girl 4½ years of age. The tibia and fibula are short and heavy. The proximal end of the tibia is widened and a small exostosis projects from its medial side. The proximal tibial metaphysis is bridged cephalad and capped by a small, deformed and malplacated epiphyseal ossification center opposite the medial slope of the metaphyseal ridge. The distal tibial metaphysis is irregularly mineralized. The fibula is not disproportionately long in relation to the tibia as is the case in achondroplasia. B, the same bones at age 19. The epiphyseal cartilage has disappeared in the tibial metaphyses and growth is complete in these still short and heavy bones. The exostosis on the medial tibial wall is still present. The tibial epiphyseal ossification center is still flattened and has a deepened articular facet on its lateral side.



heart in two patients reported by Ellis and Van Creveld. In all patients the ectodermal dysplasia has been of the hydrotic type without disturbances in the function of the sweat and sebaceous glands. Intelligence has been normal in all cases. The clinical manifestations are present at birth but become more conspicuous with advancing age.

In the roentgen examination the most constant findings are shortening and deformities of the tibia and fibula (Fig 8-330) and of the radius and ulna (Fig 8-331) and shortening of the tubular bones of the hands and feet with polydactyly and massive fusion of the carpal bones (Fig 8-332). Also all cases have shown hypoplasia and ectopia of the proximal tibial ossification centers with angulation deformity of the contiguous tibial metaphysis (see Fig 8-330). Oligemia of the epiphyseal arteries which supply the epiphyseal side of the cartilage plate is a probable causal mechanism for the undergrowth of proliferating cartilage cells and shortness of the bones.

Ridging of the proximal end of the tibial shaft with hypoplasia and medial shift of the contiguous ossification center opposite the shorter medial slope of the ridge is one of the most consistent changes in the skeleton at all ages. In the extremities the tubular bones become progressively shorter centrifugally from the trunk toward the tips of the fingers and the toes. This is the converse of the pattern of shortenings in achondroplasia. The most peripheral bones—the phalanges—also show markedly accelerated maturation and this is more pronounced in the distal and middle phalanges than in the more proximal basal phalanges. Maturation is moderately accelerated in the metacarpals and metatarsals but in less degree than in the phalanges.

Fig 8-331—The arm of a girl 4½ years of age with Ellis-Van Creveld syndrome. The radius and ulna are short and heavy; the proximal end of the ulna is swollen, while the proximal end of the radius is hypoplastic. The converse is true at the distal ends of these bones. The radius is dislocated out of the elbow, apparently owing to the disproportionate shortness of the ulna. The humerus is bowed but is shortened less than the bones in the forearm.





Fig 8-332—Ellis Van Creveld syndrome in the hands of a girl 28 months of age. The capitate and hamate bones are fused into a large single mass. There are six metacarpals; the extra hypoplastic 6th is partially segmented from the 5th. The hypoplastic 6th digit has but two phalanges, the distal and proximal. The proximal phalanges are slightly widened, and the slightly cone-shaped epiphyseal ossification centers project into and are beginning to fuse with their contiguous shafts, especially in the

thumb. The middle phalanges are markedly widened with disproportionately large epiphyseal ossification centers which are cone-shaped, and the rapexes project into the cupped bases of the contiguous shafts. The terminal phalanges are hypoplastic with relatively huge epiphyseal ossification centers which are attached to the shafts by narrow bony stalks. These hands present the paradox of retarded growth of the shafts and accelerated maturation of the epiphyseal ossification centers.

The femur and humerus may be bowed as well as shortened. In one patient an exostosis projected from the medial aspect of the proximal tibial metaphysis. Dental hypoplasia and dysplasia are visible in films of the upper and lower maxillas; the former is usually underdeveloped while the latter is enlarged, which

produces malocclusion. The spine is normal roentgenographically.

The importance of undergrowth of the ribs and the reduction of vital capacity caused by the long narrow thorax was not fully appreciated until 1958, when Smith and Hand stated that "the greatly diminished

Fig 8-333—The small restrictive chest in chondroectodermal dysplasia. A, photograph of an infant dead on the 10th day of life. The thorax is disproportionately long and small in circumference in the upper levels, above the resistance of the liver and spleen; it is pinched on both sides. (From Smith and Hand.) B, radiographs of another patient at the age of 10 months. The tho-

rax is elongated and small in all transverse and ventrodorsal diameters. The ribs are short and the costal cartilages relatively long. The large costochondral junctions impress the underlying lung and produce long peripheral longitudinal strips of compression atelectasis. The ribs flare laterad over the liver (arrow).



volume of the thorax (Fig 8-333) would appear to have been sufficient to cause disastrous effects on pulmonary function. In addition to the smallness of the long tubular thorax the anterolateral segments of the chest wall were depressed and the sternum bulged forward in one patient. During the entire respiratory cycle Smith and Hand found that the ribs remained fixed and breathing was exclusively diaphragmatic. Maroteaux and Savart observed that in severe cases dyspnea due to reduced thoracic volume and reduced vital capacity may dominate the clinical picture. They emphasized the similarity of the inadequate thoracic cage of chondroectodermal dysplasia to the asphyxiating thoracic dystrophy of Jeune (Arch franç pédiat 12:886 1964).

Kelzer and Schilder observed a woman 21 years of age who exhibited the cartilaginous cutaneous and cardiac dysplastic elements of the syndrome but who lacked polydactyly.

The two infant patients of Smith and Hand exhibited all of the four major components of the syndrome; they both succumbed to progressive cardiac failure. One of these infants was a Negro.

Classic examples of the Ellis Van Creveld syndrome have been found in high incidence in the Old Amish populations of Pennsylvania and Ohio by McKusick.

Maroteaux and Lamy found increase of urinary chondroitin sulfate in some of their patients. Gatti and associates studied two patients, a brother and a sister who had lymphopenic hypogammaglobulinemia as well as ectodermal dysplasia.

REFERENCES

- Caffey J. Chondroectodermal dysplasia (Ellis Van Creveld syndrome). Report of three cases. *Am J Roentgenol* 68:875 1952.
- Ellis R. W. B. and Andrew J. B. Chondroectodermal dysplasia. *J Bone & Joint Surg* 44-B:626 1962.
- and Van Creveld S. A syndrome characterized by ectodermal dysplasia, polydactyly, chondrodysplasia and congenital morbus cordis. *Arch Dis Childhood* 15:65 1940.
- Ferrero N. A. et al. Chondro-ectodermal dysplasia (Ellis-Van Creveld syndrome). Report of a case and review of the literature. *J Bone & Joint Surg* 43-A:1290 1961.
- Gatti R. A. et al. Hereditary lymphopenic agammaglobulinemia associated with a distinctive form of short limb dwarfism and ectodermal dysplasia. *J Pediatr* 75:675 1969.
- Hannitsian A. S. et al. Infantile thoracic dysplasia—a variant of the Ellis Van Creveld syndrome. *Pediatrics* 71:855 1967.
- McKusick V. A. et al. Dwarfism in the Amish. I. The Ellis Van Creveld syndrome. *Bull Johns Hopkins Hosp* 115:306 1964.
- Maroteaux P. and Savart P. Asphyxiating thoracic dysplasia. Radiological study. The relationship with the syndrome of Ellis and Van Creveld. *Ann Radiol* 7:332 1964.
- Smith H. L. and Hand A. M. Chondroectodermal dysplasia (Ellis Van Creveld syndrome). Report of two cases. *Pediatrics* 21:298 1958.

Diastrophic (twisted) dwarfism is the name given by Lamy and Maroteaux to a syndrome which resem-

bles both achondroplasia and gargoylism in some of its clinical and radiographic features. The major clinical findings include dwarfism with shortened extremities, disproportionately shortened forearms and shanks, equinovarus feet, short broad hands with uneven shortening of the fingers, ectopic thumbs (hitchhiker thumbs), severe lumbar lordosis with prominence of the buttocks, variable degrees of scoliosis, swellings of the larger joints with limitation of motion, short tense tendons, orbital hypertelorism and swelling of the external ears and protruding upper teeth which overbite on the lower teeth (Fig 8-334). In radiographs the radius and ulna are shortened disproportionately and there are shortening of all long bones, multiple deformities of the bones of the hands and feet and swellings of the ends of tubular bones, especially the proximal ends of the femurs in which the heads are swollen beyond the limits of the acetabular cavities (Fig 8-335). Kyphosis of the cervical spine is common during infancy. The sacrum is tipped up and back. Cleft palate and deformities of the external ear have been present in some cases. The syndrome has occurred in siblings and thus has raised the question of genetic transmission. Consanguinity appears to have been a factor in one family.

REFERENCES

- Lamy M. and Maroteaux P. La nanisme diastrophique. *Presse med* 68:1977 1960.
- Stover C. N. et al. Diastrophic dwarfism. *Am J Roentgenol* 89:914 1963.
- Taybi H. Diastrophic dwarfism. *Radiology* 80:1 1963.

Chondromatosis—In this group there are two primary errors in growth: abnormality in the direction of growth of isolated bits of proliferating cartilage and tumor formation. When segments of proliferating cartilage grow longitudinally from the cartilage plate they produce exostoses. When islands of uncalcified cartilage persist in the metaphysis and hypertrophy they expand to become enchondromas. The former are probably caused by overcirculation (hyperemia) in the penchondral ring arteries and the latter by segmental oligemia of the terminal metaphyseal arteries on the epiphyseal side of the metaphyseal plate.

In more than half the cases of external chondromatosis or inherited multiple exostoses, exostoses are found in one of the parents as well as in the child. Fathers are affected about three times as frequently as mothers. In several families the disease has been traced through more than two generations. The principal lesions are bony projections from the ends of the shafts near the cartilage-shaft junctions, the terminal segments of the affected shafts are usually swollen exhibiting failure of normal constriction. There is a wide variation in the form of the scattered exostoses; they may be large or small, broad or narrow, long or short, rough or smooth, blunt or sharp (Fig 8-336). The epiphyseal ossification centers are normal. The longitudinal axes of the exostoses are almost invari-

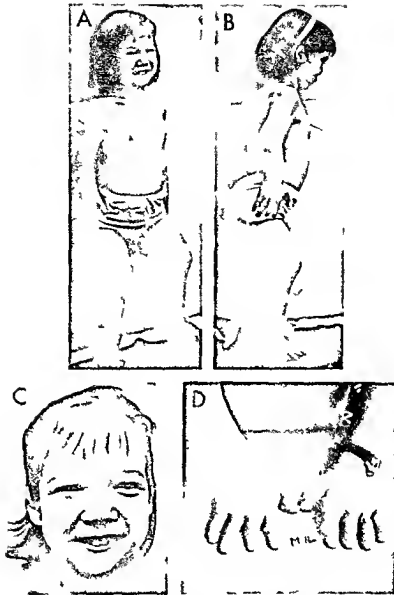


Fig. 6-334—Osteoplastic dwarfism in a girl 9 years of age whose sister 7 years of age had similar deformities and radiographs findings. In A and B the major deformities include lordosis with prominence of the buttocks, scoliosis, swelling at the larger joints, disproportionate shortness of the forearms and shanks, and bilateral club feet of the talipes equinovarus pattern. Abduction of the arms at the shoulders is limited by tightness of the soft tissues of the thorax, and the elbows are held in semi-

flexion. In C, the face is wide at all levels with broad flat nose, orbital hypertelorism, huge upper maxilla, and maxillary prominences and long narrow palpebral fissures. The upper central canines overbite on the lower lip. The deformed right ear is visible in both B and C. In D, the forearms are shortened and the hands and fingers short and broad; the 2nd and 3rd fingers are disproportionately shortened. (Courtesy of Dr. Hooshang Tayb, San Francisco.)

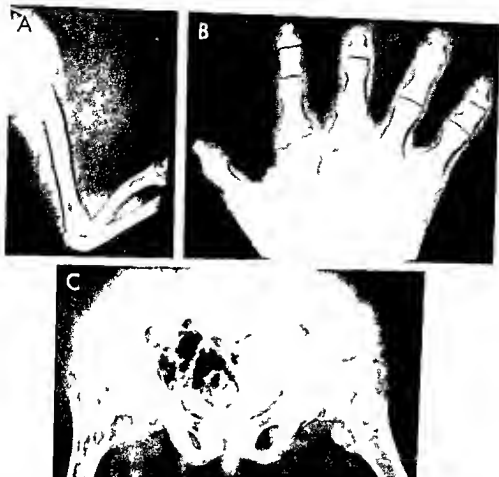


Fig 8-335 — Radiographic findings in dwarfism. In the arms (A) the bones in the forearm are disproportionately shortened, and the radius is bowed. At the shoulder, elbow, and wrist the ends of the long bones are swollen. In B, hypoplasia and dysplasia deform the tubular bones of the hand. The 2nd and 3rd

fingers are shorter than the 4th finger. In the pelvis (C) the swollen ends of the femurs articulate into abnormal acetabular cavities while the articular cartilages are greatly thinned. On the right severe coxarthrosis is present, and on the left pronounced coxarthrosis.

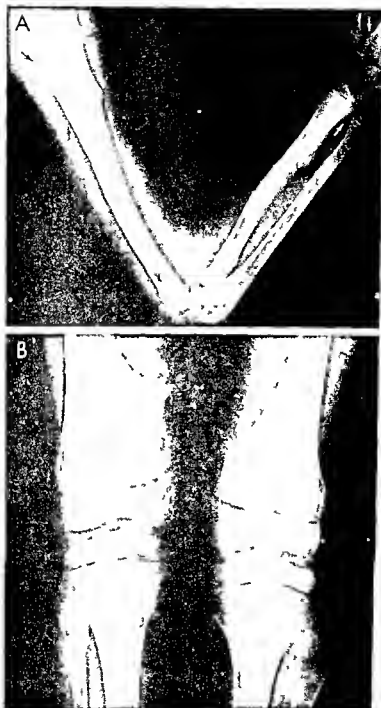


Fig. 8-336—External inherited chondromatosis in a boy 8 years of age showing multiple multiform exostoses. A, upper and B, lower extremity. Broadening and features of constriction of

the terminal segments of all the shafts are evident. The exostoses produced neither clinical deformity nor disability. The father also had multiple exostoses.



Fig 8-337—Diminished growth of the ulna in extensive hereditary chondromatosis. The ulna is shortened at the distal end and the epiphyseal plate is tipped into an oblique plane. Bowing of the radius and early ulnar deviation of the hand were already evident in the original film.

bly directed away from the nearest joint. Any of the tubular bones may be affected; the exostoses are commonly largest and most numerous near the knee joints and are least common and smallest at the elbows where the bones grow longitudinally very little.

Fig 8-338—Two large cartilaginous exostoses: one extending laterally off a rib and the other medially off the inner edge of the scapula plate. The boy was 14 years old.



The cranium rarely shows even small exostoses; the ribs (see Fig 2-62), vertebrae and flat bones, particularly the scapulas, are involved in some cases.

La Croix found that the exostoses shift epiphyseal ward during growth. In a study of the relation of the exostoses to transverse lines in the same bones, he explained the shift on the basis of the drag of the growing periosteum on the base of the exostosis.

The longitudinal growth of the shafts may be normal or reduced. The distal end of the ulna is the most common site of reduction of longitudinal growth and deformity. Occasionally the two sides of the same epiphyseal plate grow unequally, which causes obliquity of the columnar cartilage and a shortening of this bone because of a change in direction of growth of cartilage (Fig 8-337). The reduced longitudinal growth of the ulna causes bowing of the radius, which continues to grow normally and deviation of the hand at the wrist toward the ulnar side. Sometimes the radial head is dislocated at the elbow. Similar reduction in growth of the fibula causes medial bowing of the tibia with knock knee and valgus ankle. The most pronounced secondary growth changes occur in the bones in the extremities, which are the smallest in caliber: the ulna and fibula. Direct impaction of a growing exostosis onto a contiguous bone may produce local cupping and bowing of that bone. We have seen large exostoses of the femur disappear spontaneously in two patients.

In most of Solomon's patients, stature was reduced due to undergrowth of the bones of the legs during puberty. In one-half of his patients the forearm was shortened and bowed due to undergrowth of the distal end of the ulna and radiohumeral dislocation at the elbow developed in about 10%. In about one in six patients the hands were broad and short and the digits were deformed due to undergrowth of metacarpals and phalanges. Exostoses in the spine caused scoliosis and pelvic and thoracic deformities developed secondary to exostoses in the ilia, scapulas, ribs and clavicles (Figs 8-338 and 8-339).

Cartilaginous exostoses are never present in the newly born infant; they begin to appear during the first half of the 2nd year. We have seen one boy with distinct exostoses of the middle and proximal phalanges of the third digit at 8 months of age. At 8 years cartilaginous exostoses were visible in several other phalanges and at the distal ends of the radius and ulna; the rest of the skeleton was not examined radiographically.

A radiolucent patch of diminished density is cast at the site of a cartilaginous exostosis in axial projection due to loss of cortical wall (Fig 8-340).

The exostosis is a local out-pouching of the cortex and is capped by a layer of proliferating hyaline cartilage which generates endochondral bone from its under side. The exostoses probably result from groups of cells in the periosteum which retain their normal chondrogenic power after their displacement from the proliferating cartilage into the periosteum.



Fig 339—Multiple cartilaginous exostoses of the pelvic bones of a boy 14 years of age. Bony masses project off the iliac crests, the ventral and dorsal edges of the iliac wings and the lateral edges, and the edges of the acetabular roofs. The necks and shafts of the femurs are swollen due to failure of construction and possibly enchondromas.

(Langenskiöld) Following adolescence when growth of the exostoses ceases, the cartilaginous caps disappear or are reduced to narrow strips of nonproliferating cartilage.

These exostoses are potentially malignant, especially in adults. Chondrosarcomatous degeneration has been reported in several cases. Solitary exostosis simulates the individual lesions of multiple exostoses.

Fig 3340—Cartilaginous exostosis of the right tibia which produces an image of diminished density in frontal projection (A) but thickness of the bone at the same site in axial projection (B).



morphologically and roentgenographically. Murphy and Blount found cartilaginous exostoses in the sites of radiotherapy 6.9 and 11 years later. Of 288 chondrosarcomas studied in adults by Henderson and Dahlin, 25 had developed in the sites of earlier cartilaginous exostoses, and 15 of these were of hereditary multiple type. Only 4 of these chondrosarcomas had developed in the sites of enchondromas.

We have seen typical multiple cartilaginous exostoses in femurs and tibias of American Indians unearthed in one of the islands off Santa Barbara, California. Archeologists estimated that the artefacts with which the bones were found indicated that these Indians lived about 800 A.D.

REFERENCES

- Cardis, R. Concerning two cases of multiple cartilaginous exostoses. *Radiol Clin* 30:209, 1961.
- Henderson, E. D. and Dahlin, C. D. Chondrosarcoma of bone—a study of 288 cases. *J Bone & Joint Surg* 45-A:1450, 1963.
- Jacobson, S. A. Contribution to the pathogenesis of multiple hereditary osteochondromatosis. *Am J Cancer* 39:220, 1940.
- Jaffe, H. L. Hereditary multiple exostosis. *Arch Path* 36:335, 1943.
- Keith, A. Studies in the anatomical changes that accompany certain growth disturbances of the human body. *J Anat.* 54:101, 1919, 20.
- Lacroix, P. Sur la migration des exostoses au cours de la croissance. *Rev d'orthop* 36:20, 1950.
- Langenskiöld, A. Normal and pathological bone growth in the light of the development of cartilaginous foci in chondrodysplasia. *Acta chir scandinav* 95:367, 1947.
- Murphy, F. D. Jr. and Blount, W. P. Cartilaginous exostoses following irradiation. *J Bone & Joint Surg* 44-A:662, 1962.
- Solomon, L. Hereditary multiple exostoses. *J Bone & Joint Surg* 45-B:292, 1963.

The radiolucent patch in A is due to loss of opaque dorsal cortical wall associated with thickening of the more radiopaque marrow cavity.

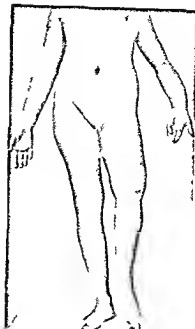


Fig. 8-341—Unilateral shortening deformities of the arm and leg in Ollier's multiple internal chondromatosis

Fig. 8-342—Roentgen findings in the patient pictured in Figure 8-341. A, left forearm showing shortening and irregularity in density of the radius and ulna. The radius is bowed and the hand deviates toward the ulna. The external configuration of both bones is abnormal owing to failure of constriction of the

shafts. B, left leg showing deformity and irregularity in density of the femur. The tibia and fibula are stippled and resemble the Abers-Schanberg type. Marked stippling was visible in the left ilium. The bones in the right arm and leg were normal.



Stock, P., and Barrington A. Hereditary Disorders of Bone Development, *Eugenics Laboratory Memoir 22* (London University of London, Francis Galton Laboratory for National Eugenics, 1925).

In *internal chondromatosis*, or Ollier's dyschondroplasia, multiple enchondromas of the shafts of the tubular bones are irregularly distributed in the skeleton but tend to be unilateral and characteristically produce shortening deformities of the affected bones (Fig 8-341). The cartilaginous roasses, according to Langenskoold, represent a persistence of cartilage cells in the cortex which normally, after their development in the epiphyseal plate, are transformed into osteoblasts and normally produce cortical compact bone. The ends of the involved bones are irregularly dilated, irregularly mineralized and grossly deformed (Figs 8-342 and 8-343). Occasionally the *spongiosa* in the area of the chondroma is stippled or streaked longitudinally. The epiphyseal ossification centers are often hypoplastic and deformed. In many cases, multiple enchondromatosis is limited to the bones of the hands and feet (Fig 8-344).

Maffucci's syndrome is a combination of multiple enchondromas and multiple cavernous hemangiomas in the same individual. The association appears to be fortuitous. Distribution of both of these hamartomatous proliferations is asymmetrical, usually the tumors are limited to one side. The viscera are not affected. The hemangiomas are located in the soft tissues, often the subcutaneous soft tissues. The hemangiomas may overlie enchondromas or normal bone. The hands and feet are the most severely and the most frequently affected, but bones in all parts of the skeleton have contained enchondromas. The bone lesions and their deformities are identical with those found in Ollier's disease. Elmore and Cantrell estimated that the malignant conversion occurs in 19% of patients who have Maffucci's syndrome.

REFERENCES

- Elmore, S M., and Cantrell W C. Maffucci's syndrome. Case report with a normal karyotype. *J Bone & Joint Surg* 48-A 1607, 1966.
- Jansen M. Dissociation of Bone Growth (*Exostoses and Enchondromata*) in Ollier's Dyschondroplasia and Associated Phenomena (Robert Jones Birthday Volume) (London Oxford University Press 1928) p 43.
- Mahomer H R. Dyschondroplasia, *J Pediatr* 10 1 1937.
- Ollier L. Dyschondroplasia. *Lyon méd* 38 23 1900.
- De la dyschondroplasia. *Bull Soc de chir de Lyon* 3 22, 1900.
- Voorhoeve, N. L'image radiologique non encore décrite d'une anomalie de la squelette. *Acta radiol* 3 407 1924.

Osteopathia striata is the name applied by Fairbank to a disorder of the growing skeleton characterized by longitudinal streaking of the metaphyses and ends of the shafts. Voorhoeve described the condition first in 1924. The changes are usually most conspic-

uous in the distal ends of the femurs. In Bloor's patient (Fig 8-345), fine longitudinal striations were present bilaterally in the ends of the shafts without other changes of dyschondroplasia, such as osteopikilosis or irregularities in the metaphyses. The lengths of the striated segments in the different ends of different bones are directly proportional to the velocities of growth in the different bones, they are longest at the sites of most rapid growth, the distal ends of the femurs. In the iliac wings, the striations are in a fanlike pattern. The bones at the base of the skull have been thickened and sclerosed in some cases. The patients present no consistent clinical picture and usually are asymptomatic insofar as skeletal manifestations are concerned. Osteopathia striata may exist alone or be an element in Ollier's disease. Longitudinal streaking of the ends of the shafts also develops during periods of rapid growth and also during periods of rapid demineralization of the bones.

REFERENCES

- Bloor D. A case of osteopathia striata, *J Bone & Joint Surg* 36-B 261 1954.
- Fairbank H A T. Osteopathia striata, *J Bone & Joint Surg* 32 B 117 1950.
- Voorhoeve N. L'image radiologique non encore décrite d'une anomalie du squelette, *Acta radiol* 3 407 1924.

Multiple epiphyseal dysplasia is a familial disease in which the significant changes are in the epiphyseal ossification centers and the round bones, the primary ossification centers in the shafts are not affected. It was first recognized by Fairbank in 1935 and has been detected with increasing frequency. The epiphyseal centers and the round bones are small, rough, irregularly calcified and often flattened into angular contours (Fig 8-346). The ends of the shafts relatively are unaffected, although they may be spread and concave in compensation for the deformities in the contiguous ossification centers. Pain and stiffness in the hips and knees are the principal complaints and later lead to disturbances in gait. Stature may be shortened in severe cases owing to the flattening deformities at the hips, knees and ankles. The digits are short and thick with blunt ends. With advancing age the tendency is to disappearance of mottling and fragmentation of the epiphyseal centers, but deformities persist. Crippling osteoarthritis in the weight bearing joints is a serious common late complication. In several instances the disease has been familial.

In some cases, chondrodystrophia calcificans congenita appears to have been the initial stage of multiple epiphyseal dysplasia (Silverman). The "hereditary multiple epiphyseal changes" of Ribbing resemble multiple epiphyseal dysplasia in some respects. Generalized smallness of ossification centers and delayed appearance have been associated with bilateral coxa plana in several families studied by Girdany. Monty met this same problem in the study of several mem-

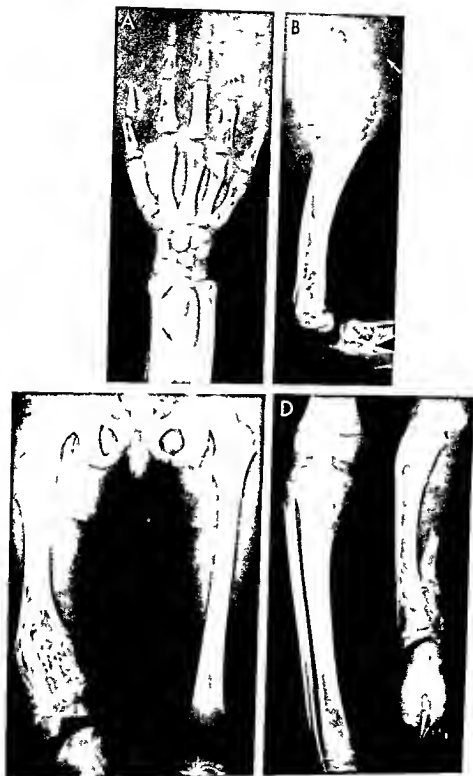


Fig. # 343 - A D Description of fac ng page



Fig. 8-343—Generalized aneurysmal bone cysts (Ollier's dyschondroplasia) in a girl 5 years of age. All bones were affected save those in the skull and vertebral column, the two clavicles and sternum. **A**, multiple aneurysmal bone cysts in the phalanges and first metacarpal of the left hand. There are long radiolucent strips of cartilage in the enlarged shaft of the radius. **B**, in the right arm multiple defects are visible in all long tubular bones whose terminal segments are enlarged owing to failure of ossification. **C** and **D**, in the legs the right tibia and femur are shortened, deformed and defective owing to enclosed masses of cartilage. In

the widened distal femoral and proximal tibial metaphyses there are both stippled and striped patterns of sclerosis. Most of the right tibia had been excised. **E**, all bones of the pelvis show rounded and elongated defects, the sites of aneurysmal bone cysts. **F**, thorax, frontal projection. There are multiple bony defects in the enlarged sternal ends of several ribs (arrows). The vertebral edge of the right scapula is roughened and shows a large defect which is probably the site of an aneurysmal bone cyst. The bones on the right side of the body were more affected than those on the left side.



Fig 8 344 — Multiple enchondromas limited to the phalanges and metacarpals in a girl 13 years of age. The rest of the skeleton was normal. The radiolucent enchondromas have replaced the spongiosa and distended the medullary cavities. In severe cases expansion of the enchondromas causes axial bowing of the shaft and atrophy of the overlying cortex.

Fig 8 345 — Osteopetrosis in a girl 13 years of age. A, longitudinal striations in the long bones. B, radiolucencies in the ilia (Redrawn from Brody).

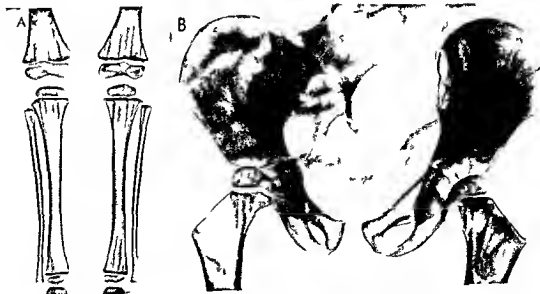




Fig. 8-346—Multiple epiphyseal dysplasia in an infant. A, Irregular and premature ossification of the epiphyseal ossification centers of the femur, tibia and patella at 4 days of age. An irregular ossification center is also visible anterior to the tibia, probably in the joint capsule. The shaft of the femur is broken in its distal third. B, Irregular and premature ossification in the epiphyses of the humerus, radius and carpal bones at 6 months of age. C, Irregular and premature ossification in the manubrium and gladi-

olus of the sternum with unusual coronal clefts in the vertebral bodies at 49 days of age. D, Irregular and premature ossification in the body of the hyoid bone (arrow), cervical vertebral segments, proximal epiphyseal cartilages of the humerus (two arrows) and manubrium of the sternum at 4 days. E, Similar irregular and premature ossification in the costal cartilage and sternum at 4 days. (Courtesy of Dr. F. N. Silverman, Cincinnati.)

bers of one family—the differentiation of bilateral coxa plana from multiple epiphyseal dysplasia.

Congenital hypoplasia of the branches of the epiphyseal arteries which supply the epiphyseal ossification centers and the arteries to the carpal and tarsal bones and the associated chronic oligemia of these bony structures may be responsible for their undergrowth and irregular growth.

Felman studied three patients, father, son and daughter, who were dwarfs and who had extensive epiphyseal dysplasia scattered throughout the skeleton with severe vertebral deformities which began during childhood. The femoral heads were eventually

destroyed almost completely and the femoral necks virtually disappeared. With advancing age the caudal thoracic and cephalic lumbar vertebrae became irregularly ossified and wedged. The spine became sharply scoliotic at the thoracolumbar level. It was most pronounced in the father.

REFERENCES

- Christensen, W. R. et al. Dysplasia epiphysealis multiplex. *Am. J. Roentgenol.* 74:1059, 1955.
Clément, R. Dystrophie polyépiphyseaire. Dysplasie épiphyseaire multiple ou unique. *Semaine Hop. d. Paris* 83:3353, 1932.

- Fairbank H A T Dysplasia epiphysealis multiplex *Brit J Surg* 34:225 1947
- Felman A H Multiple epiphyseal dysplasia Three cases with unusual vertebral anomalies *Radiology* 93:119 1969
- Freiberger R H Multiple epiphyseal dysplasia, *Radiology* 70:379 1958
- Girdany B R Personal communication
- Jackson W P U *et al* Multiple epiphyseal dysplasia Its relation to other disorders of epiphyseal development, *Arch Int Med* 94:886 1954
- Monty C P Familial Perthes' disease resembling multiple epiphyseal dysplasia *J Bone & Joint Surg* 44-B:565 1962
- Ribbing S The hereditary multiple epiphyseal disturbances and the consequences for the ontogenesis of local malacia—particularly osteochondrosis dissecans *Acta orthop scandinav* 24:286 1955
- Shepard E Multiple epiphyseal dysplasia, *J Bone & Joint Surg* 38-B:458 1956
- Silverman F N Epiphyseal dysplasias Protean entities *Ann Radiol* 4:833 1961
- Waight W Dysplasia epiphysealis multiplex in three sisters *J Bone & Joint Surg* 34-B:82 1952

Dysplasia epiphysealis hemimelica (tarsoepiphyseal aclasia Trevor's disease) is a rare condition which causes swellings in the extremities, usually on the inner and outer aspects of the knees and ankles. The swellings are bony hard and the neighboring soft parts are not involved. Gait becomes clumsy owing to the limitations of motion at the knee and ankle. Knock knee, bowed knee and flatfoot are commonly associated. Painful 'locking' of the knee has occurred in a few cases, and regional atrophy of muscles has developed. At exploration the swellings are found to be made up of bone covered with epiphyseal cartilage. The edges may be smooth or rough. Microscopically hypertrophic normal cartilage is found surrounding the extra masses of bone, in which normal endochondral bone formation is taking place. In single lesions the findings are similar to those of solitary osteochondroma.

Diagnosis depends on the radiographic changes (Fig 8-347). The findings are limited to the epiphyses or parts of the epiphyses lying on one side of a single limb. The absence of changes in other epiphyses is diagnostic.

REFERENCES

- Kittiekamp D B *et al* Dysplasia epiphysealis hemimelica. A report of fifteen cases and review of the literature *J Bone & Joint Surg* 48-A:746 1966
- Saxton H M and Wilkinson J A Hemimelic skeletal dysplasia, *J Bone & Joint Surg* 46-B:608 1964

Metaphyseal dysostosis (Jansen's disease) is characterized by spreading, cupping and defective irregular mineralization in the metaphyses of the tubular bones (Fig 8-348) and to some degree the edges of the flat bones, especially the ilia. The round bones of the wrists and ankles and the epiphyseal ossification centers are characteristically smooth. Blood chemistry is normal and renal function unimpaired. In the severe type, which resembles the hyperplastic type of achon-

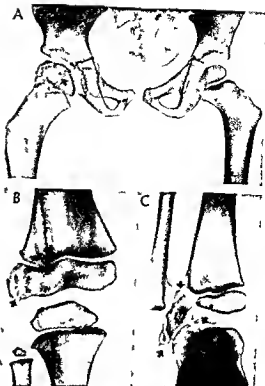


Fig 8-347—Dysplasia epiphysealis hemimelica of Fairbank or Trevor's disease in a boy 8½ years of age. A, the lateral half of the proximal femoral ossification center is enlarged and irregularly increased in density with coxa valga. B, the lateral half of the distal femoral epiphyseal center is irregularly ossified and enlarged. C, the overgrowth of cartilage and bones between the tibia and fibula has separated them. The overgrowth appears to be made of two parts: an osteochondroma extending off the distal tibial epiphysis laterally and caudad, and a larger osteochondroma of the iliac which extends laterally and cephalad. The tibial ossification center is defective in its lateral segment. The separate individual lesions appear to be osteochondromas. The multiplicity and their distribution in the lateral aspects of the bones of one leg warrants the diagnosis of dysplasia epiphysealis hemimelica. (Redrawn from Fairbank.)

dropsia in some respects the spine and thoracic bones are normal (Fairbank) and from the photograph in Jansen's paper, the head appears to be normal. In Holt's patient severe rarefaction of the cranial bones which was present on the 4th postnatal day had disappeared by the 6th month (Fig 8-349). In contrast, the changes in the metaphyses of the long bones increased with advancing age (Figs 8-350 and 8-351). Ozonoff noted similar findings in his patient 7 weeks of age. A striking feature of metaphyseal dysostosis is the smooth edge of the epiphyseal ossification center in contrast to the rough edge of its contiguous metaphysis. The milder types of metaphyseal dysostosis can be differentiated from the milder types of refractory rickets and of hypophosphatasia by biochemical means only. In the milder types which are much more common the radiographic changes simu-



Fig 8-348 — Metaphyseal dysostosis (Jansen type). A, external ricketslike deformities in a Chinese boy 7 years of age. He is dwarfed and has multiple deformities in the extremities, chest and pelvis. Other than moderate frontal bossing, the head appears to be normal. B, severe irregularities in metaphyseal ossification with normal smooth ossification in the contiguous epiphyseal ossification centers (A and B from Cameron et al.). C, Jansen's patient at 10 years of age. The swellings at the end of the long bones and the bowing deformities are suggestive of rickets. The arms are too long for achondroplasia. The hypotonic feet are badly deformed. The patient was 12 in. under height. (From Jansen.)



Fig 8-349—Metaphyseal dysostosis. In **A**, lateral projection of the head on the 4th day of life, the parietal squamosal and the parietal bones are rarefied with a wide-meshed reticulated texture. The mandible is severely affected. The cartilaginous bones

at the base of the skull are thickened. In **B**, at 6 months of age, ossification of the entire skull is normal save for an unusually wide innominate synchondrosis. (Figs 8-349 to 8-351, courtesy of Dr John F. Holt, Ann Arbor, Mich.)

Fig 8-350—Metaphyseal dysostosis of the hands and wrists. Progressive increase in the metaphyseal changes in the tubular bones in the hands and wrists with advancing age. In **A**, at 12 months of age, the metaphyses are irregularly ossified, cupped and spread in a ricketslike fashion. The terminal phalanges are hypoplastic. In **B**, at 23 months, the metaphyseal changes are more marked and deeper, with striking smoothness of the epi-

physeal ossification centers and round bones in the wrists. In **C**, at 54 months, the metaphyseal changes are still more pronounced; the round bones and epiphyseal ossification centers remain smooth. In the distal ends of the ulna there is a deep and thick and transversely radiolucent band which is devoid of bone although a broad terminal band has ossified irregularly.



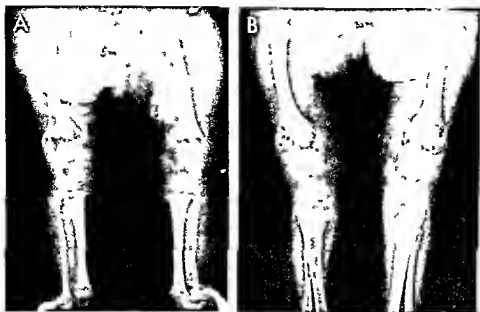


Fig 8-351.—Metaphyseal dysostosis of the lower extremities at A, 5 months and B, 35 months of age. The metaphyseal lesions have increased in size and irregularity of density with advancing

age. In contrast the edges of the epiphyseal ossification centers are smooth.

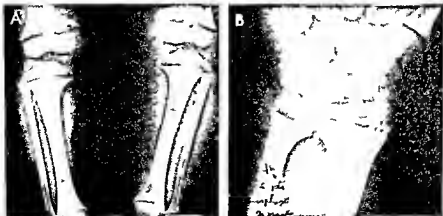
late those of refractory rickets and the late phase of hypophosphatasia. In one of our milder cases (Fig 8-352) the patient was treated for refractory rickets despite normal serum chemistry with massive dose of vitamin D, and she developed severe signs of vitamin D poisoning. Lenk of Israel reported this mild type of metaphyseal dysostosis in a dwarfed deformed girl 2 years of age whose five forerunners, all male, had similar clinical deformities.

In the light of available evidence an uneven con-

genital hypoplasia of the epiphyseal arteries which supply the epiphyseal plate could cause an uneven oligemia to the longitudinal proliferating cartilage cells and thus impair their growth irregularly. This seems at present to be the most reasonable primary causal mechanism for metaphyseal dysostosis.

Gram studied a remarkable patient whose radiographic changes in the skeleton suggested the severe type of metaphyseal dysostosis but whose chemical changes in the blood serum—hypercalcemia and

Fig 8-352.—Metaphyseal dysostosis of the milder ricketslike type in a girl with bowed legs and lateral coxa vara. A, the legs at 3 years; B, the wrist at 4 years. Serum phosphate, calcium and phosphatase activity were normal in many serial examinations over several years. Microscopic changes in the costochondral junctions contained much osteoid suggestive of rickets. The patient, however, reacted normally to large doses of vitamin D.



which are usually well tolerated in refractory rickets with signs of severe renal damage. In these films all of the larger metaphyses are irregularly and incompletely ossified with some spreading and cupping. The epiphyseal ossification centers in contrast are evenly ossified with smooth edges. All of these changes are found commonly in refractory rickets and in the juvenile type of hypophosphatasia.



Fig. 8 353.—The scattered uneven metaphyseal dysostosis of Kozłowski and Zychowicz. A) of the metaphyses not shown here, were normal. In A, all of the metaphyses at the knees and ankles show deep, regular ossification. In B, ossification in the metaphyses is irregular and maturation accelerated in the phalanges. The edges of the round bones and epiphyseal ossification

centers in contrast are smooth. The proximal femoral epiphyseal ossification centers are each developing from two independent unfused centers. The patient is a Polish girl 5 years of age. (Courtesy of Dr. Kazimierz Kozłowski and Czesław Zychowicz, Poznań, Poland.)

hypophosphatemia—suggested hyperparathyroidism

A large Mormon family studied by Stephens in 1943 had 41 members in four generations who were affected by a bone disease which at the time suggested a variant of achondroplasia. The data on this family now in the light of more knowledge are more suggestive to me of the mild and moderate types of metaphyseal dysostosis.

Scattered metaphyseal dysostosis (Fig. 8 353) was found in a Polish girl 6 years of age by Kozłowski and Zychowicz. Severe metaphyseal lesions were present in the bones of the hands and at the knees, but there were few or no changes in the bones in other parts of the skeleton. Kozłowski and Budzinska described two patients in whom metaphyseal and epiphyseal dysostoses were present in both the metaphyseal changes dominated.

The experience of the last 35 years has shown conclusively that the severe metaphyseal dysostosis of Jansen is a rare disease and the milder types are relatively common and that it may affect numerous members of a family through several generations.

REFERENCES

- Cameron J A P et al. Metaphyseal dysostosis. Report of a case. *J Bone & Joint Surg* 36-B 622 1954
- de Haas H N et al. Metaphyseal dysostosis. A late follow up of the first reported case. *J Bone & Joint Surg* 51 B 290 1969
- Dent C E and Normand I C S. Metaphyseal dysostosis type Schmid. *Arch Dis Childhood* 39 44 1964
- Evans R and Caffey J. Metaphyseal dysostosis resembling vitamin D refractory rickets. *Am J Dis Child* 95 581 1958
- Fairbank H A T. Metaphyseal Dysostosis. Atlas of Generalized Affections of the Skeleton (Baltimore: Williams & Wilkins Company 1953)
- Gram P B. Metaphyseal chondrodysplasia of Jansen. *J Bone & Joint Surg* 41 B 951 1959
- Jansen M. Ueber atypische Chondrodystrophie. *Achondroplasia und ueber eine noch nicht beschriebene angeborene Wachstumsstörung des Knochensystems. Metaphysäre Dysostosis*. *Ztschr Orthop Chir* 61 255 1934
- Kozłowski K and Zychowicz C. Metaphyseal dysostosis of mixed type in a female child. *Am J Roentgenol* 88 443 1962
- and Budzinska A. Combined metaphyseal and epiphyseal dysostosis. *Am J Roentgenol* 97 21 1966
- Lenk R. Hereditary metaphyseal dysostosis. *Am J Roentgenol* 76 569 1956
- Müller S M and Paul L W. Roentgen observations in familial metaphyseal dysplasia. *Radiology* 83 665 1964
- Ozonoff M B. Metaphyseal dysostosis of Jansen. *Radiology* 93 1047 1969
- Rosenbloom A L and Smith D W. The natural history of metaphyseal dysostosis. *J Pediatr* 66 857 1965
- Stephens S E. An achondroplastic mutation and the nature of its inheritance. *J Hered* 34 229 1943

The cartilage hair hypoplasia of McKusick is a genetic disease found first in 77 dwarfed individuals in the Amish population of Pennsylvania. The hair of the scalp and of the eyebrows is sparse, fine and blond, and the bones present changes characteristic of the Schmidt type of metaphyseal dysostosis, with retarded maturation of the bones. Megacolon and manifestations suggestive of the malabsorption syndrome were found in some of these patients.

Lux and associates described two children with cartilage hair hypoplasia who also suffered from chronic respiratory infections and had unusually severe reactions in the course of varicella. Studies of their immune reactions indicated chronic neutropenia secondary to failure of myeloid maturation. Both had persistent lymphopenia, reduced and delayed cutaneous hypersensitivity and one had delayed rejection of a cutaneous allograft.

REFERENCES

- Lux S E, et al. Chronic neutropenia and abnormal cellular immunity in cartilage-hair hypoplasia. *New England J Med* 282:231 1970.
- McKusick, V A, et al. Dwarfism in the Amish. II. Cartilage-hair hypoplasia. *Bull Johns Hopkins Hosp* 116:285 1965.

Metaphyseal dysostosis with pancreatic insufficiency and/or blood dyscrasia (pancreas blood bone disease) has been described in several dwarfed children. The pancreatic deficiency is exocrine in origin and the blood changes are characterized as variable anemia, neutropenia and thrombocytopenia. Some patients originally had a diagnosis of cystic fibrosis of the pancreas. All unusually short patients with cystic fibrosis of the pancreas should have their skeletons searched radiographically for metaphyseal dysostosis. Metaphyseal dysostosis has been first recognized in some of these patients radiographically, because of enlargements of the sternal ends of the ribs.

REFERENCE

- Taybi, H. Metaphyseal dysostosis and the associated syndrome of pancreatic insufficiency and blood disorders. *Radiology* 93:563 1969.

Osteopetrosis congenita (marble bones Albers-Schonberg disease)—This is a rare generalized dysplasia of the skeleton characterized by persistence of the calcified cartilaginous matrix which is normally destroyed during growth. As a result, the marrow spaces and the medullary cavity are diminished in volume or are never formed, being replaced by the excessive calcified cartilaginous matrix (Fig. 8-354). The compact bone of the cortex is hypoplastic and poorly differentiated. The spongiosa is a more or less solid calcified cartilaginous matrix in contrast with its normal spongy cancellated structure, the paucity of marrow spaces in the thickened or solid spongiosa leaves little room for blood formation in the skeleton. The cause of this condition is unknown, heredity appears to play a part.

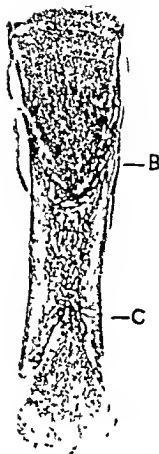


Fig. 8-354—Necropsy specimen of metacarpal in axial section in generalized severe congenital osteopetrosis. The marrow cavity is filled with calcified chondro-osseous matrix which is responsible for the marblelike densities in the radiologic images of the bones. (From Cohen.)

The diagnosis becomes manifest on roentgen examination. The entire skeleton shows a generalized but uneven heavy amorphous sclerosis in which the individual components—cortex, epiphyseal plates, spongiosa and medullary cavity—are obliterated (Fig. 8-355). Invariably there is failure of constriction of the shafts and they appear swollen and splayed at the ends. In some cases multiple transverse (Fig. 8-356) and in others multiple longitudinal striations of uneven density streak the ends of the shafts. We have seen one remarkable set of films in which the changes suggested a limited scattered type of generalized osteopetrosis (Fig. 8-357). Slipping of epiphyses and pathologic fractures especially at or near the proximal ends of the femurs are not infrequent complications, the bones in osteopetrosis are made up largely of calcified cartilage and are brittle rather than strong. During the first months of life rickets may be an added complication (Fig. 8-358), in our case the rickets healed promptly during administration of vitamin D. Of all of the bones of the body, the



Fig 8-355 (left) — Osteopetrosis congenita in a boy 4 years of age, showing the diffuse amorphous sclerosis, failure of constriction of the shafts and the miniature inset in the tibia. A — upper and B — lower extremity

Fig 8-356 (right) — Transverse wavy striations in the wide terminal segments of sclerotic bones of an infant 5 months of age with osteopetrosis congenita

Fig 8-357 — Regional osteopetrosis tarda of the long bones in the right radius (A) and in the femur, tibia and fibula at the knee (B). Osteopetrosis-like changes are present in an otherwise normal skeleton. These were chance findings in films made of the skeleton as a check after a head injury in a girl 4 years of age (Courtesy of Dr. Charles N. Pease, Chicago).



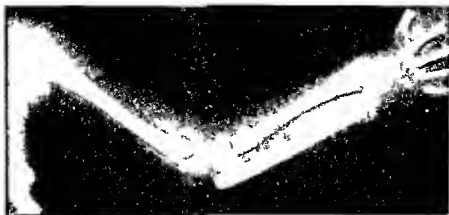


Fig 8-358—Osteopetrosis congenita and healing rickets in an infant 5 months of age

mandible is usually the least affected which is a helpful diagnostic feature in the differentiation of osteopetrosis and Pyle's disease during the first months of life.

Protracted hypoplastic anemia, thrombocytopenia, splenomegaly, hepatomegaly and hyperplasia of the lymph nodes are constant findings in severe cases. The anemia is aregenerative and is due to the crowding out of the marrow by overabundant calcified cartilage and fibrous tissue. Hemopoietic centers persist and become hyperplastic in the spleen, liver and lymph nodes in compensation for the loss of marrow in the skeleton. Massive hemorrhage due to thrombocytopenia and intercurrent infection are the usual causes of death.

Osteopetrosis tarda in contrast to osteopetrosis congenita develops during the first years of life and is a much milder disease. The morbid anatomy in the bones is similar in the two types. In the tarda form, however, sclerosis is limited to the ends of the bones and the margins of the epiphyseal ossification centers in round bones (Fig 8-359). The central segments of both tubular and round bones and of the epiphyseal ossification centers which are formed prior to onset of the disease are normally radiolucent and contain normal amounts of spongiosa. The sclerotic ends of the shafts are enlarged due to failure of constriction (funnelization). The sclerosis is due to persistence of excessive spongiosa and failure of cavitation or tubulation. The cranium presents a small number of Wormian bones. The radiolucent insets which represent the bone formed prior to onset are often clearly seen in the metacarpals (Fig 8-360). Patients with the tarda type may survive into the sixth and seventh decades. Hypercalcaemia has been suggested as a cause of osteopetrosis.

From a structural standpoint osteopetrosis is a persistence of excessive amounts of calcified cartilage and primary spongiosa. In view of the fact that the end loops of the nutrient artery at the metaphyseal side of the cartilage plate play a major role in the

normal destruction of the primary spongiosa, it is reasonable to assume that a congenital deficiency of these terminal branches of the nutrient artery and resultant chronic oligemia on the shaftward side of the cartilage plate are the primary causal mechanisms in osteopetrosis tarda. One must assume that these mechanisms do not begin to operate until after or near birth in the tarda type.

REFERENCES

- Cohen J. Osteopetrosis. Case report, autopsy findings and pathological interpretation. *Failure of treatment with vitamin A*. J Bone & Joint Surg. 33-A:923, 1951.
- Fairbank, H. A. T. Osteopetrosis generalisata. J Bone & Joint Surg. 30-B:337, 1948.
- Rubin P. *Dynamic Classification of Bone Dysplasias* (Chicago: Year Book Medical Publishers, Inc. 1964).

CONGENITAL PERIOSTEAL DYSTROPHIES—*Osteogenesis imperfecta*—This condition also known as Lobstein's disease, fragilitas osseum and osteopsathyrosis is characterized by defective formation and differentiation of subperiosteal and endosteal bone. The growth and differentiation of the epiphyseal cartilage are not seriously disturbed. Diminished osteoblastic activity has been considered the probable causal mechanism by most authors. Owing to the defective cortex and spongiosa, the shafts are weak and fracture easily. Following fracture, the formation and resorption of callus are normally rapid. In severe cases, multiple angulation and bowing deformities of the extremities are almost invariable sequels. In milder cases, the only abnormality may be the tendency to fracture; there may be no deformity after callus formation. Blue sclerae are the rule in patients with late onset of fractures, but are absent in many congenital cases. Otosclerosis and deafness sometimes accompany the brittle bones and blue sclerae.

Odontogenesis imperfecta (hereditary opalescent dentin) is found in association with osteogenesis imperfecta, or alone without skeletal disease. It is often familial and can be recognized by the opalescent

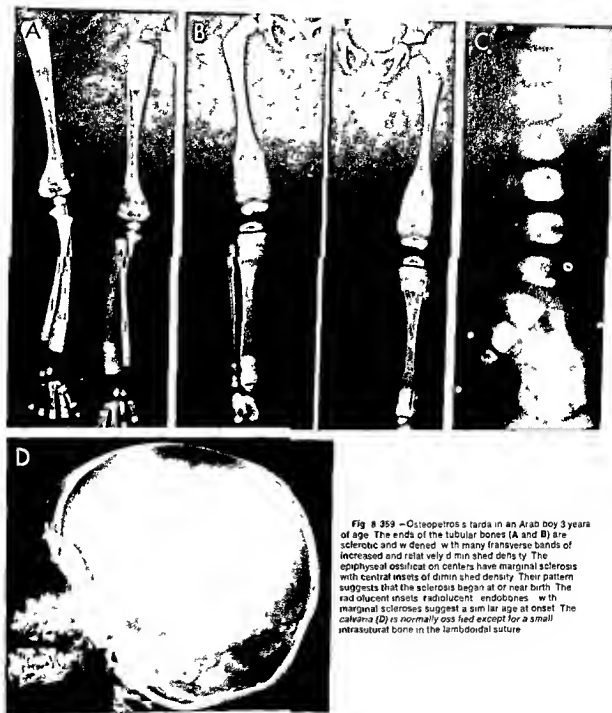


Fig 8-359—Osteopetrosis tarda in an Arab boy 3 years of age. The ends of the tubular bones (A and B) are sclerotic and widened, with many transverse bands of increased and relatively diminished density. The epiphyseal ossification centers have marginal sclerosis with central insets of diminished density. Their pattern suggests that the sclerosis began at or near birth. The radiolucent insets radiolucent endobones, with marginal sclerosis suggest a similar age at onset. The calvaria (D) is normally ossified except for a small intrasutural bone in the lambdoid suture.



Fig 8-360—Osteopetrosis tarda in a girl 3 years of age. The radiolucent insets in the shafts of the metacarpals represent bone formed in utero prior to onset of the disease. The sclerotic segments are longer in the distal ends of the shafts because there is more growth at the distal than at the proximal ends. Also the carpal bones and bony centers in the epiphyses show no radiolucent insets because these bones were formed extra utero and after the disease had been present for several months (Courtesy of Drs Frances B Toomey and Harold Rosenbaum Lexington Ky)

amber appearance of the teeth especially when a light is placed behind the teeth and their translucency is conspicuous. The teeth tend to be small and are deformed, both deciduous and permanent teeth are affected. The dentin is the principal site of morphologic change, with poor calcification and disorderly pattern of tubules. Roentgenograms of the teeth show obliteration of pulp chambers and root canals. The roots are thin, short and pointed. Severe crumbling and loss of enamel give the appearance of rampant canines although as a rule there is little actual caries.

Several clinical and pathologic classifications of osteogenesis imperfecta have been made according to age at onset and severity. The disease has been found in fetuses, infants, children and adults. The congenital type is the commonest and most severe form, dozens of fractures may occur in utero particularly in the ribs. It is clear that all of the different types represent variants and phases of the same basic condition. Consanguinity is often associated and a genetic abnormality is apparently responsible for many cases. The severe congenital form of the disease is said to be recessive in its transmission; the late type is usually dominant.

Follis found the basic mechanism in osteogenesis imperfecta to be faulty conversion of early reticulum

fibers into adult collagen fibers in the corium of the skin, scleras, corneas and in the skeleton. Callus formation may be normal or excessive; excessive callus may persist and cause deformities. Hilton reported familial hyperplastic callus formation in the absence of osteogenesis imperfecta; radiotherapy proved helpful in the early painful stages.

Hemorrhagic disease has been found in osteogenesis imperfecta several times (Siegel), suggesting that this is not a chance association.

The essential roentgen findings are hypoplasia and thinning of the cortex and a scanty spongiosa (Fig 8-361). In the absence of fractures it is impossible to differentiate osteogenesis imperfecta from simple generalized atrophy in the long bones. The central segments of the shafts are narrowed and the ends flare excessively. Fractures vary, depending on the severity of the disease. In the congenital type, dozens of fractures may be present at birth (Fig 8-362), in older mild cases long intervals may intervene between single fractures. The multiple fractures give

Fig 8-361—Congenital osteogenesis imperfecta in a girl 2 years of age. Numerous fractures were present elsewhere in the skeleton in the tibia shown here; there are no fractures but the basic deficiency of cortex and spongiosa is evident. Constriction of the tibia is excessive; the ends flare at each end of the narrow intermediate segments. The similarity of these findings and the atrophy of disuse is noteworthy.



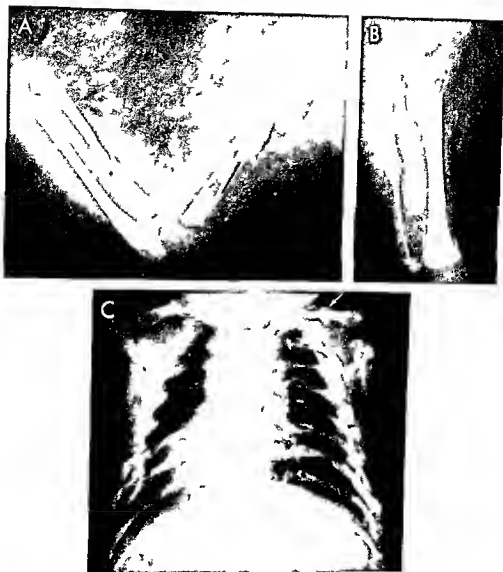


Fig 8-362—Congenital osteogenesis imperfecta in a 12-month-old child showing multiple fresh and old fractures in the arms (A), legs (B), and thorax (C).



Fig 8-363 —Osteogenesis imperfecta in a boy 8 1/2 years of age. There are multiple bowing and angulation deformities secondary to old fractures. The proximal half of the humerus shows the honeycomb pattern of rarefaction which develops in the fractured

bones but is never seen in unfractured bones. This honeycomb phenomenon has never been observed by us in fetal or infantile bones but is common during later childhood and adult life in osteogenesis imperfecta.

Fig 8-364 —Osteogenesis imperfecta. Mosaic rarefaction of the dorsal segments of the parietal bones of an infant 3 months of age.

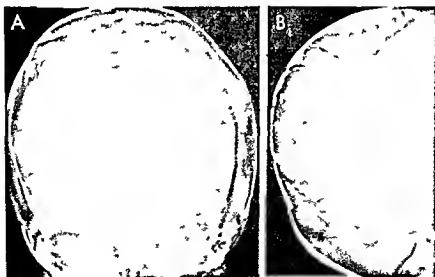




Fig 8-365—Osteogenesis imperfecta. Failure of constriction of the distal ends of the femoral shafts after fractures led to bursitis and synovitis of the ends of the femurs of this 12½ year old girl. We believe that the severe muscular weakness in such pa-

tients is largely responsible for failure of constrictions of the shaft because of loss of the normal moulding effect of healthy muscles during bone growth.

rise to extensive deformities and callus may be responsible for regional and local segments of sclerosis (Fig 8-363). In the otherwise osteoporotic bones, irregular mineralization of the calvaria (mosaic rarefaction, Fig 8-364) is often of great assistance in diagnosis when the changes in the long bones are equivocal (see p 1041) and may during the first years of life be the most diagnostic change.

Bizarre residual deformities due to failure of constriction after fractures (Fig 8-365) and due to cortical thickening and ossification of interosseous membranes (Fig 8-366 A and B) develop in some cases. Prenatal bowing of the long bones is a common complication of osteogenesis (Fig 8-366 C).

The hydrolysates of the collagens from normal bone and normal sclera contain large amounts of the amino acid proline which is not found in the hydrolysates of collagens from other parts of the body (Cannuggia *et al*). This common high proline content of skeletal and scleral collagens suggests that it may be responsible for the frequent association of scleral and skeletal lesions in osteogenesis imperfecta.

Distinct clinical and roentgen improvement has been observed in some cases following the onset of puberty especially in girls. This has led to the treatment of younger girls with ovarian extracts with some promising results. Testosterone might be tried therapeutically in boys who have osteogenesis imperfecta.

Bakwin and Eiger described a puzzling patient with fragile bones but with macrocranium and dilatation of the marrow spaces in the skull and in the unfused tubular bones of the hands.

Solomons and Styner found the levels of inorganic

pyrophosphates increased in the serum and urine of 28 patients who had osteogenesis imperfecta. In 4 the oral administration of magnesium oxide or magnesium sulfate reduced the pyrophosphate levels in both serum and urine significantly. The effect on the radiographic appearance of the bones was not mentioned.

REFERENCES

- Cannuggia, A. *et al*. On the pathogenesis of fragilitas osseum. *Panminerva med* 3:67, 1961.
- Fairbank, H. A. T. Osteogenesis imperfecta. *J Bone & Joint Surg* 30-B:164, 1948.
- and Baker, S. L. Hyperplastic callus formation with or without evidence of fracture in osteogenesis imperfecta. *Brit J Surg* 36:1, 1946.
- Folliot, R. H. Jr. Osteogenesis imperfecta. A connective tissue diathesis. *J Ped* 41:713, 1952.
- McKusick, V. A. *Hentable Diseases of Connective Tissue* (2nd ed., St. Louis: C. V. Mosby Company, 1960).
- Solomons, C. C. and Styner, I. Osteogenesis imperfecta. Effect of magnesium administration on pyrophosphate metabolism. *Calcif Tissue Res* 3:318, 1969.

Meloreostosis of Léri is a rare disease which usually affects one side of the bones on one side of the body commonly in one lower extremity but it is also seen in the spine at all levels, the skull, ribs and facial and pelvic bones. Lester found changes suggestive of this disease in a right fibula which was estimated to be about 1500 years old. Regional pain with both swelling and atrophy of the overlying soft tissues and stiffness of the neighboring joints are the common clinical manifestations. Diagnosis depends on the radiographic demonstration of the peculiar longitudinal sclerosis of parts of the bones (Fig 8-367). The sclerotic strip extends from the pelvic bones to

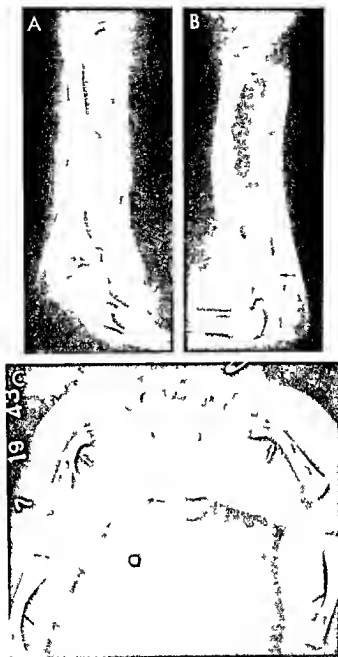


Fig 8-366 Osteogenesis imperfecta. A and B changes in the radius of a girl 12 1/2 years of age. The cortical walls are thickened and the interosseous membrane between the radius and ulna is partially calcified or ossified to form incomplete bony bridges. The ventrad position of the proximal end of each radius suggests that they are dislocated ventrad. The complete bony bridges at

the proximal end of one radius (B, arrow) appear to be holding the proximal end of the radius forward. See similar changes in infantile cortical hyperostosis (Fig 8-696). C, severe prenatal bowing of the femurs and tibiae of an infant 2 weeks of age. The cortical wall is thickened on the concave (compression) side of the bend.



Fig 8-367—Melorheostosis of Léri in a girl 10 years of age that involved the bones of the extremities and thorax. The longitudinal white stripes on the medial sides of the long bones from

pelvis to toes as well as the round bones (flat bones, patella (a sesamoid bone) and the short tubular bones of the foot) in which the bones in the medial ray are affected (Redrawn from Muzz).

the toes and although interrupted at the joints seems to flow down the bones of the leg as molten wax flows down the side of a candle or honey down the side of a stick. The sclerotic thickening is all internal and it reduces the volume of the medullary cavity. The overlying soft tissues may be reduced owing to fibrosis and muscular atrophy or thickened by lymphedema, scleroderma and hemangioma. Melorheostosis has been present at birth in several cases and is believed to be a congenital dysplasia. However the changes are slight in patients younger than 3 years of age but the hyperostosis increases with age. Campbell and colleagues published films of the skeleton of patients 2 and 3 years of age. Fractures and malignant degeneration of the affected bones have not been recorded. In the case of Gillespie and Siegel, cutaneous and subcutaneous changes were present at 1 month of age but the underlying bones were normal radiographically. Obliterative endarteritis is a common microscopic finding. The sclerotic strips of bone observed radiographically are made up of mature Haversian bone mixed with osteoid and fibrous tissue. The causal agent and causal mechanism are unknown. Treatment is not effective.

REFERENCES

- Campbell C J *et al*: Melorheostosis. A report of the clinical, roentgenographic and pathological findings in fourteen cases. *J Bone & Joint Surg* 50-A:1281, 1968.
 Gillespie J G and Siegel J A: Melorheostosis. *Len, Am J Dis Child* 55:1273, 1958.
 Lester C W: Melorheostosis in a prehistoric Alaskan skeleton. *J Bone & Joint Surg* 49-A:142, 1967.

Morris J *et al*: Melorheostosis. Review of the literature and report of an interesting case with 19 year follow up. *J Bone & Joint Surg* 45-A:1191, 1963.

THE MUCOPOLYSACCHARIDOSES have been classified into six types (McKusick) on the basis of their clinical, genetic and biochemical features. Brante apparently first used the term "mucopolysacchondrosis" (hereafter referred to as MPS) in 1952 after he had found that in the tissues of gargoyles the fibroblasts throughout most of the collagen tissues were swollen and filled with granular water soluble material which had characteristic findings after metachromatic staining. Collagenous tissues including cartilage, fasciae, tendons, blood vessels, cardiac valves, meninges, muscles, osteocytes, chondrocytes and corneas were all similarly affected. Kupffer cells in the liver, reticulum cells in the spleen and lymph nodes and epithelial cells in the kidney and in several endocrine organs contained similar deposits with similar staining properties. The ganglion cells in both central and peripheral segments of the nervous system were swollen but the deposits in the swollen ganglion cells were made up largely of water insoluble lipid gangliosides with little or no MPS. Gangliosides were found in small amounts by Brante in the epithelium of the renal tubules, reticulum cells in the spleen, in the corneal cells and in the connective tissues of the blood vessels and cardiac valves of gargoyles.

In 1957 and 1958 Dorfman and Lorincz and also Meyer and his associates demonstrated excessive amounts of mucopolysaccharides, chondroitin B sul-

fate and heparitin sulfate in the urine of gargoyles and so provided a valuable diagnostic test. In 1961 Meyer studied two patients who excreted heparitin sulfate only. In the same year Lamy and Maroteaux reported the excretion of keratosulfate only in a Morquio dwarf. In 1963 the same authors reported the excretion of chondroitin B sulfate only in a single patient. Sanfilippo and associates in 1963 confirmed Meyer's finding of solitary urinary excretion of heparitin sulfate in several gargoyles and pointed out that mental retardation was unusually severe in such patients. The somatic changes, however, were relatively mild.

Current knowledge of the different types of disturbances in mucopolysaccharide metabolism provides a biochemical classification of entities previously called Hunter-Hurler disease, Morquio's disease, hypochondrodystrophy, gargoylism and dysostosis multiplex, names largely based on clinical and radiographic findings. In the following discussion of mucopolysaccharidosis we have followed the classification of McKusick.

Prenatal diagnosis of MPS is possible by studying the fetal cells in the amniotic fluid removed after transabdominal amniocentesis. After culture in vitro these cells present two diagnostic features. They incorporate radioactive sulfate into their mucopolysaccharides and they stain differentially with toluidine blue. In a study of three patients Madsen and Linker concluded that vitamin A in large doses is detrimental to patients who suffer from MPS.

REFERENCES

- Brante G. Gargoylism. A mucopolysaccharidosis. *Scandinavian J Clin & Lab Invest* 4:43 1952.
- Dorfman A and Lorincz A E. Occurrence of urinary acid mucopolysaccharides in the Hurler syndrome. *Proc Nat Acad Sci* 43:443 1957.
- Fralatoni J C, et al. Intrauterine diagnosis of the Hurler and Hunter syndromes. *New England J Med* 280:686 1969.
- Madsen J A, and Linker A. Vitamin A and mucopolysaccharidosis. A clinical and biochemical evaluation. *J Pediatr* 75:843 1969.
- McKusick V A. Heritable Disorders of Connective Tissue (3rd ed. St Louis: C V Mosby Company 1966) p 35.
- Meyer K, et al. Excretion of sulfated mucopolysaccharides in gargoylism (Hurler's syndrome). *Proc Soc Exper Biol & Med* 97:275 1958.
- Maroteaux P, and Lamy M. La maladie de Morquio. Étude clinique, radiologique et biologique. *Presse méd* 72:2091 1963.
- Sanfilippo S J, et al. Mental retardation associated with acid mucopolysacchariduria (heparitin sulfate type). *J Pediatr* 63:837 1963.

Mucopolysaccharidosis (MPS I) combined chondroitin B sulfatemia and heparitin sulfatemia (Hurler's syndrome)—This type is made up largely of patients who were called gargoyles prior to biochemical classification. They are dwarfed and retarded mentally. Deafness is often severe and is progressive. The usual clinical manifestations include large hydrocephalic type of head, ugly, coarse and sometimes

puffy facies, prominent supraorbital ridges, large nostrils with enlarged turned up nasal tips, sunken nasal bridge (saddle nose) with nasal obstruction, large thick everted patulous lips, large and sometimes protruding tongue, steamy clouding of the corneas, thick and long eyelashes and eyebrows (Figs 8-368 to 8-374). The teeth are small and widely spaced. The neck is short. The scapulas tend to be highly and widely spaced. Cardiomegaly and cardiac murmurs are common. Shallow kyphosis of the spine near the thoracolumbar junction appears early, sometimes during the first months of life. Abduction of the arms at the shoulders may be limited to 90 degrees, due in part to severe varus deformity at the proximal end of the humerus. The hands are broad with stubby, thick fingers held in semiflexion at rest. The ankles are often stiff after rest when patients may walk on their toes. Respiratory movements may be inhibited by limitation of costal movements at the costovertebral joints. The skin may be lumpy due to deposits of mucopolysaccharides, and many gargoyles are covered with excessive but fine lanugolike hair. Diagnostic clinical signs are usually not present at birth but develop slowly during the first year.

Metachromatic granules in the circulating leukocytes (Reilly granules) are present in only a few patients. Pearson and Lorincz found mucopolysaccharide

Fig 8-368.—Typical gargoyle facies (MPS I) of a boy 4½ years of age. The head is large, face large, the nasal base depressed, the tip of the nose enlarged, the nostrils are large, the upper lip is long and both lips are thick, the teeth are widely spaced, the mandible is large, and the neck is short.



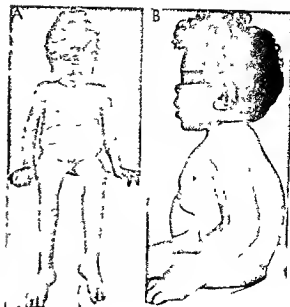


Fig 8-369 — Hurler's syndrome (MPS-1) A, frontal and B, lateral views of a boy 4 years of age who exhibited marked skeletal changes of the osteoporic type (see also Fig 8-378)

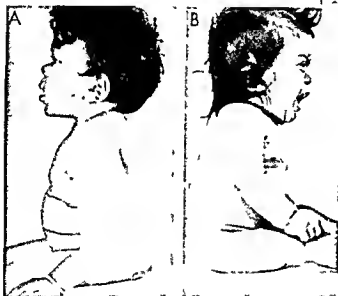


Fig 8-370 — A, gargoylism (MPS-1) boy 4 1/2 years of age and B, gargoylism (MPS-1) girl 20 months of age with shallow kyphoses at the lower thoracolumbar levels. The short neck, large ears, sunken bases of noses, large nasal lips and thick, long lips are also evident.



Fig 8-371 — Mucopolysaccharide (MPS-1) swelling of the upper gums which extend caudad below the biting edge of the widely spaced teeth and interfere with the chewing of food in a gargoylism girl 8 months of age.



Fig 8-372. Limitation of abduction of the arms to about 90° in a boy with Gaucher's disease (MPS 1) aged 2 months. The angle of the shoulder and the width of the chest are shown and the wide spacing of the teeth.

Fig 8-374. Gaucher's disease (MPS 1) boy A, a 8 years old with a small head, large ears and characteristic nose and lips. Both cheeks were asymmetrical (not evident on this picture). B, a 8 years old the co-

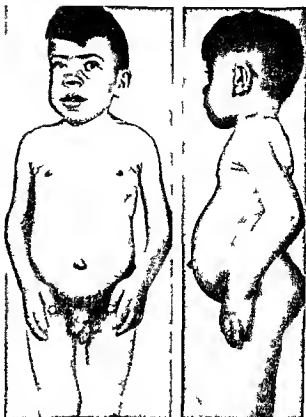


Fig 8-373. Gaucher's disease (MPS 1) boy 9 years of age with a large abdomen, a protruding umbilicus, a large, wide, fleshy hands and fingers, typical faces, short neck and large ears. The incomplete extension of the joints produces a crouching stance. The shoulders are high, wide and square.

nease is opaque and miliary. Hypertrophic sclerosis is evident on the face and scalp. Uterine polyps and chondrosarcoma were not observed and it is possible that he is an example of mucopolysaccharidosis type 5.





Fig 8-375 (left) —Gargoyle (MPS I) hand and wrist at 3 1/2 years of age. Similar changes were present in the other hand and wrist. All of the tubular bones are shortened and widened. Their cortical walls are thin and the medullary cavities large and distated. The metacarpals except the first are pinched and pointed at their proximal ends. The fifth metacarpal is the most affected. The phalanges are all pointed and rounded at their distal ends. The distal phalanges are hypoplastic. The epiphyseal ossification centers are small and appear late. The round bones in the wrist are small. Bone age approximates that for a healthy child of 12–15 months. The distal end of the radius is tipped toward the distal end of the ulna, which is also oblique.

Fig 8-376 (right) —Hand and foot of a gargoyle (MPS I) 2 years of age. Changes in the tubular bones of the hand are similar

to those in Figure 8-375. However, the metacarpals are pinched and pointed at both ends with tiny ossification centers at the pinnacles of the pinched segments distally. The distal phalanges are markedly hypoplastic, the primary center in the distal phalanx of the second digit has not yet appeared. In the foot, the tubular bones are elongated and slender with pinching and pointing of metatarsals 2, 3, and 4. Metatarsal 5 is relatively widened. In all, the cortical walls are thin and the medullary cavities are distated. The pedal phalanges are all of the same caliber and their distal ends are pointed. The middle and distal phalanges are markedly hypoplastic and slow in appearance time. The stenoses of the tubular bones in the feet were a mirror to those in the proximal halves of the femurs and bases of the ilia.

ride granules in macrophages of the bone marrow however, in 17 of 18 consecutive patients with Hurler's syndrome. The incidence of metachromatic granules in bone marrow of the less common types of MPS will not be known until after more patients are studied.

The radiographic changes in the bones appear to be due to malfunction of the osteoblasts and chondroblasts secondary to accumulation of mucopolysaccharides in them. The principal radiographic findings are shown in Figures 8-375 to 8-386. Metaphyseal changes are characteristically slight. In the shafts of the long bones however, the distinctive changes are due to disturbed modeling which early produces shafts of increased girth with thick cortical walls and narrow medullary cavities but the cortical walls are thin and the marrow cavities dilated later. Reduced growth of the proliferative cartilage is responsible for the dwarfism. Asymmetrical growth in the length of the two sides of the same shaft particularly at the distal ends of the radius and ulna, often tip the ends of these shafts toward each other. Overconstriction

results in pointed conoidal proximal ends of the metacarpal bones which are also sometimes hooked and flattened on one side. During the early years the tubular bones of the hands may show the most diagnostic changes. The distal ends of the phalanges are usually rounded or pointed and the terminal phalanges are hypoplastic and may ossify late. Adequate studies of the feet have not been made.

Radiographic changes in the skull vary greatly in different patients. The hydrocephalic type is the most common (see Fig 1-91). The calvaria is enlarged and digitations of the sutures are elongated. The pituitary fossa is often elongated ventrodorsally into a J shape due to long recesses under the anterior clinoid processes. An arachnoid cyst may enlarge and deform the pituitary fossa. Flattening of the condylar process of the mandible near the molar teeth may be present.

In the spine a shallow thoracolumbar kyphosis is the rule due to hypoplasia of the bodies of the first or second lumbar segments. In lateral projections the upper anterior segment of these bones is usually defective, which produces the 'hook' vertebra at the

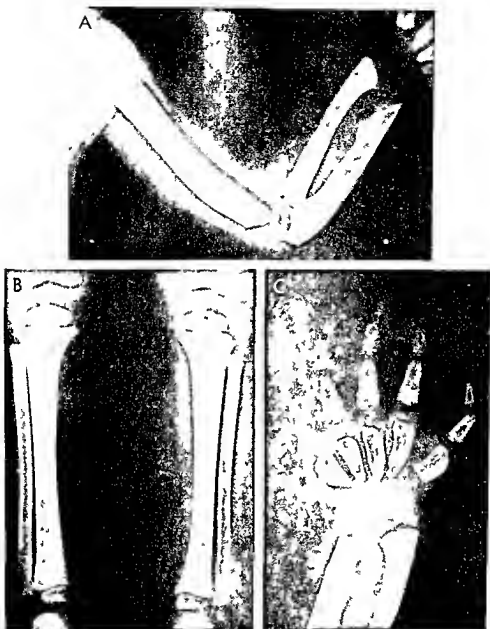


Fig 8-377 — Hurler's syndrome (MPS I). Characteristic roentgen changes in a girl 20 months of age. **A**, upper extremity showing marked swelling and tapering of the short stubby shafts; the corticalis is thick. **B**, lower extremities in which there is minimal swelling of the shafts and no chondrodystrophic changes. **C**,

hand: the pointed metacarpals are broad at the distal ends and taper in the proximal direction, which is responsible for the triangular outline with the apex directed proximally. The ends of the radius and ulna taper and are tipped toward each other.



Fig 8-378 —Osteoporotic type of Hurler's syndrome in a boy 9 years of age. The cortical in all the bones is thin and the spongy area appears to be defective. Contrast the thin osteoporotic

shafts in this case with the thickened sclerotic shafts in Figure 8-377.

Fig 8-379 (left) —Humeral varus of the proximal terminal segment of the humerus of a gargyle (MPS 1) 30 months of age.
Fig 8-380 (right) —Bilateral proximal ankylosis of the femoral

shafts of a gargyle 120 months of age. The base of each humerus narrowed. The bones of the hands and arms were dwarfed.





Fig 8-381 (above) —Spatulate ribs pinched at the vertebral ends but flaring laterad and dilated and blunt at the sternal ends in a gargoye (MPS 1) girl 20 months of age.

Fig 8-382 (right) —Stenoses of the bases of the tibia which create a false enlargement of the acetabular cavities and increase the acetabular angles. The proximal ends of the femurs are markedly stenosed and these slender bones are bent into severe varus deformities. At about the level of the trochanters the femoral shafts begin to increase in girth and at midshaft they are beginning to approach normal caliber. The patient is a girl who was a gargoyle (MPS 1) 20 months of age.



Fig 8-383 —Deep indentations (upper arrows) in the lateral masses of the 1st and 2nd sacral vertebrae of a gargoyle (MPS 1) boy 5 years of age. The lowest arrow points to stenosis of the base of the ilial wing. (Courtesy of Dr. John Lane, Little Rock, Ark.)



Fig 8-384 —Hypoplasia of the 1st lumbar body (MPS 1) with slight distraction dorsad with the apex of the kyphosis at this level. The pedicles are elongated slender and irregularly mineralized. The dorsal edges of the lumbar bodies are concave dorsad.



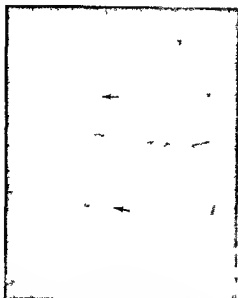


Fig 8 385 - Small rarefied pedicles with deeply concave dorsal edges of the lumbar vertebral bodies of a gargoyle (MPS 1) boy 8 years of age. These changes are similar to those of increased intraspinal pressure caused by local intraspinal tumors

apex of the kyphosis (see Figs 9 38 and 9 39). In many older gargoyles the pedicles are slender and rarefied and the dorsal edges of the bodies especially in the lumbar levels are curved (convex ventrad). In one of our patients the upper edges of the lateral masses were deeply scalloped (Fig 8 385).

In the shoulder girdle the scapula is rarefied and appears to be ballooned out with thin cortical walls. The clavicles may be thickened in their medial halves

Fig 8 386 - Sclerosis and irregular destruction of the lateral half of the clavicle in a severely retarded and dwarfed gargoyle 11 years of age (MPS 1). The scapula is swollen and sclerotic and the acromion process is sharpened. Similar changes were present in the other shoulder bones. (Courtesy of Dr. Marvin Davies, Denver, Colo.)



and stenosed and hooked in their lateral halves (Fig 8 386 and see Fig 2 67). The ribs are characteristically swollen in the same fashion as the other long tubular bones and they narrow the intercostal spaces correspondingly (see Fig 2 67). The ends of the ribs are stenosed while the intermediate segments are widened and often present a blade-like or spatulate contour (Fig 8 381).

In the pelvis the most conspicuous change is the hypoplasia and stenosis of the bases of the ilia which give rise to factitious enlargement of the acetabula (Figs 8 381 and 8 382). This is one of the most characteristic and constant skeletal signs of MPS. The pubic and ischial bones although slightly dilated are relatively little affected.

In the long bones of the extremities the basic changes are errors in modeling of the diaphyses which result in swollen shafts with varying degrees of cortical thickness and thinness and varying degrees of stenosis and dilatation of the medullary canals. One or both ends of the shafts may be pinched and pointed generally the end of the shaft which grows the less is the more pinched. The ends of the shafts of parallel bones may be bent toward or away from each other due to unequal longitudinal growth in the neighboring proliferative cartilages of each parallel bone. The epiphyseal ossification centers appear late and are small but not necessarily deformed. One of the most interesting and characteristic features of the growing gargoyle skeleton is the stenosis of the proximal halves of the femurs in association with stenosis of the bases of the ilia. In contrast the distal ends of the femurs are usually only slightly affected and this is true of the tibiae. However in the feet the metatarsals may be elongated and slender when the metacarpals are broad and stubby (see Fig 8 377). Usually the tibiae are the least affected of all the tubular bones; they may be normal when advanced changes are present in bones of the arms, ilia, femurs and bones of the hands and feet. The most striking and consistently diagnostic changes are usually found in tubular bones of the hands and the ilia even in the mildest cases. The neonatal and early infantile patients and their bones have been studied in but a few cases. We observed the evolution of the clinical manifestation and radiographic changes in the skeleton in one patient from birth through the 18th month (Figs 8 387 to 8 389). During the first weeks the tubular bones were elongated and slender but external cortical thickening was evident as early as the 8th day in one patient. This external thickening increases the girth of the bones and thickness of the cortical walls temporarily but is soon compensated for by a reaming out of the thickened cortical walls after several months this resulted in thin cortical walls around dilated medullary cavities with pinched, pointed and cone-shaped ends of the short broad shafts the classic gargoyle changes. The varus deformity in the proximal end of the humerus develops from this shrinking, pinching



Fig. 8-387 —Gargoyle (MPS-1) infant at age 4 months (A and B) and at 16 months (C and D). The large nasal tips and nostrils are suggestive at 4 months and class c at 16 months. The depressions

at the ankles were present at birth and we believed they were due to prenatal compression secondary to faulty fetal position of the feet.

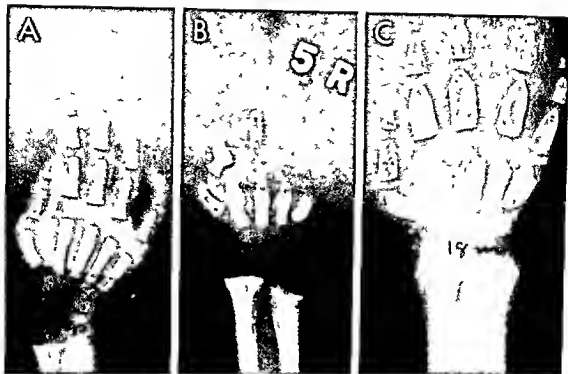
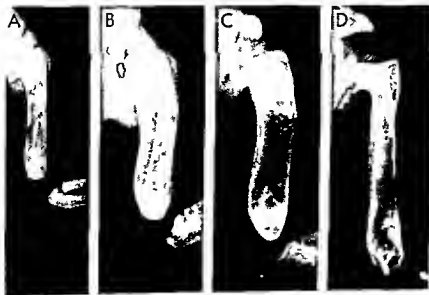


Fig. 8-388 —Progressive changes (MPS-1) in the bones of the hand and forearm at 8 days (A), 10 weeks (B) and 18 months (C). In A the tubular bones in the hand are elongated and slender. The radius and ulnar shafts are covered by faint cloaks of calcium density. In B all of the metacarpals are thickened externally by excess of new cortical bone. The thin external layers on the radius and ulna are also thicker and more easily seen. In C the metacarpals are now broad and short and pinched at both ends; their cortical walls are thin and medullary cavities are dilated. The phalanges are sharpened at their distal ends only. The terminal phalanges are hypoplastic. Bone age is retarded. Same patient as in Figure 8-387.

us and ulna are also thicker and more easily seen. In C the metacarpals are now broad and short and pinched at both ends; their cortical walls are thin and medullary cavities are dilated. The phalanges are sharpened at their distal ends only. The terminal phalanges are hypoplastic. Bone age is retarded. Same patient as in Figure 8-387.

Fig. 8-389 —Progressive changes (MPS-1) in the right humerus at 8 days (A), 4 months (B), 6 months (C) and 18 months (D). In A the dorsal cortical wall is thickened. In B this thickening has increased. In C the cortical thickening has disappeared and now the cortical walls are thin and the medullary cavities dilated. The epiphyseal ossification center (arrow) is well behind the shaft, the end of which is beginning to bend dorsad and mediad. The distal end of the shaft is now pinched and pointed. In D the prox-

imal end of the shaft is bent sharply backward and made into a 90° varus deformity with the second epiphyseal ossification center lying directly above its superior edge. The entire shaft is now constricting, especially in the proximal half. The varus deformity at the proximal end of the humerus is largely responsible for the limitation of abduction at the shoulders in many gargoyles. Same patient as in Figures 8-387 and 8-388.



process at the proximal ends of the shafts (Fig 8-389). The stenosis at the base of the ilia in the proximal halves of the femurs also became evident during the first year.

The severe, moderate and mild skeletal changes in the different types of MPS in different patients with the same type of MPS in siblings and in patients with pseudomucopolysaccharidosis and the lipomucopolysaccharidoses are all illustrated and discussed in the excellent paper by Spranger and Schuster. They found the changes in bones of the hands, pelvis and spine to be the most characteristic of the different types.

Among eight cases in younger infants reported by Landing and associates as "familial neurovisceral lipoidosis" one had radiographic changes in the skeleton similar to those in one of our infant gargoyles. Landing's patients, however, had gangliosides in their tissues rather than polysaccharides. It should be emphasized that none of Landing's patients had classic severe gargoyle changes in their skeletons. More recently Scott and co-workers studied one infant who had radiographic skeletal changes similar to ours and they found polysaccharides in the renal epithelium. They also found the alkaline phosphatase activity of the serum to be unusually high (364 King Armstrong units). O'Brien defined generalized gangliosidosis as a storage disease characterized by cerebral degeneration and death during the first two years of life and by the storage of gangliosides in the brain and viscera and the storage of mucopolysaccharide in the viscera only. The mucopolysaccharide is structurally similar to keratosulfate. Iannaccone and Capotorti discussed two female infants, 1 day and 6 months of age, who had severe classic skeletal changes of Hurler's disease. The urinary excretion of mucopolysaccharides was normal, the blood findings were normal and there was no histochemical or microscopic evidence of the accumulation of mucopolysaccharides or lipids in the tissues. The nature of the storage material was not determined. It is now clear that there are several storage disorders which simulate gargoylism clinically and radiographically but differ from it chemically.

REFERENCES

- Caffey J. Gargoylism (Hunter-Hurler disease, dysostosis multiplex, lipochondrodystrophy). Prenatal and neonatal lesions and their early postnatal evolution. *Am J Roentgenol* 67:715, 1952.
- Hurler G. Ueber einen Typ multiplex Abartungen vorwiegend am Skelettsystem. *Ztschr Kinderheilk* 24:220, 1919.
- Iannaccone G and Capotorti L. Contribution to the so-called syndrome "pseudo-Hurler". *Ann radiol* 12:355, 1969.
- Landing B H et al. Familial neurovisceral lipoidosis. *Am J Dis Child* 108:503, 1964.
- O'Brien J. Generalized gangliosidosis. *J Pediatr* 75:167, 1969.
- Pearson H A and Lorincz A E. A characteristic bone marrow finding in Hurler's syndrome. *Pediatrics* 34:281, 1964.
- Scott C R, et al. Familial visceral lipoidosis. *J Pediatr* 71:357, 1967.
- Spranger J and Schuster W. Classifiable and nonclassifiable mucopolysaccharidoses (types classiques et variantes). *Ann radiol* 12:365, 1969.

Steinbach H L et al. The Hurler's syndrome without abnormal mucopolysacchariduria. *Radiology* 90:472, 1968.

Mucopolysaccharidosis (MPS 2) chondroitin B sulfatase and heparitin sulfatase (Hunter's syndrome) is differentiated from MPS-1 by its limitation to the male sex, absence of corneal clouding, milder mental retardation, longer survival rate and better auditory acuity. It is believed that most of the gargoyles who survive until middle and old age are of this type. The radiographic skeletal changes are similar to those but often less marked than in MPS-1. It is estimated that MPS-1 is five times as common as MPS-2 (McKusick).

REFERENCE

- Njaye A. A sex limited type of gargoylism. *Acta paediat* 33:267, 1946.

Mucopolysaccharidosis (MPS 3) heparitin sulfatase only (Sanfilippo syndrome) was first identified by Meyer chemically in 1961 and was studied clinically by Sanfilippo and his associates in a larger group of patients. Sanfilippo recognized that the mental retardation was unusually severe but the somatic changes were relatively mild. Clouding of the cornea and signs of cardiac disease were rare. In the same group Langer found radiographic changes in the skeleton similar to those in MPS-1 but milder, with the most diagnostic slight findings in the hands, pelvis and spine. Loss of stature is moderate or slight and in some cases stature may be above the average (Lamy and Maroteaux). Owing to the lack of convincing diagnostic clinical signs it is probable that in many of these severely retarded children MPS is never detected and they have been confined to homes for the mentally retarded under the diagnosis of unexplained mental retardation. Urinary screening tests for polysaccharides of all mentally retarded children will probably correct this error and give us a much better knowledge of the incidence of MPS-3.

REFERENCES

- Langer L O. The radiographic manifestations of Hurler's mucopolysaccharidosis of Sanfilippo. *Ann radiol* 7:315, 1964.
- Sanfilippo S J et al. Mental retardation associated with acid mucopolysacchariduria (heparitin type). *J Pediatr* 63:837, 1963.

Mucopolysaccharidosis (MPS 4) keratosulfatase only (Morquio's disease)—This disease is much less common than any of the three MPS's just described and differs substantially in the radiographic changes in the bones. It is obvious now that disease as defined by Morquio and Brailsford on clinical and radiographic grounds has long been grossly overdiagnosed. In 1961 Maroteaux and Lamy identified keratosulfate in the urine of a Morquio dwarf and in the same year Zellweger and associates found mucopolysacchariduria and opacities in the corneas of



Fig. 8-390—Characteristic deformities in Morquio's disease.
(From Morquio, 1935)

their patients they proposed the name Morquio-Ullrich disease. The Morquio dwarf is normal mentally. The corneal changes come on late in MPS-4; in most cases they are not visible to the unaided eye until late in childhood. The cardinal clinical and radiographic signs as described originally by Morquio are still valid for older patients. Morquio's patients were aged 14 (girl), 8, 15 and 19 years. The disproportionate shortness of the spine due to universal vertebra plana is responsible for most of the diagnostic deformities which include a normal head on a short neck. The thorax, abdomen and pelvis are all shortened in contrast to the relative long extremities (Fig. 8-390). The ventral thoracic wall attempts to lengthen normally but is anchored to the shortened spine, and in compensation the sternum and costal cartilages bulge forward in the upper thoracic levels to produce one of the most characteristic features of the Morquio dwarf. Stature is always reduced primarily due to the shortness of the spine. The short spine may be straight kyphotic or lordotic. Scoliosis of significant degree is rare in children. Knock knee develops early and is usually severe in young patients and crippling in older ones. All patients have flattened weak feet which become crippling deformities in later years. Generalized and regional muscular weaknesses develop as age advances. In some patients this has been attributed to spinal compression at the levels of the 1st and 2nd cervical vertebrae secondary to hypoplasia of the dens of the 2nd cervical vertebra and dislocation of the dens dorsad. In one of Morquio's original patients, now about 50 years of age (examined by us

in December 1967) the lower extremities were spastic with almost complete loss of muscular power. Muscular power in his arms and hands, in contrast, was normal. Swellings at the sternal ends of the ribs are suggestive of a rachitic rosary in some patients and eversion of the lower ribs sometimes produces a groove similar to Harrison's groove of rickets. Mentality is normal. Facies are not characteristic but in some older patients the mouth is wide and the lips are thick, cheek bones are large and prominent. Although the joints are not stiff, many patients assume the semiflexed stance of MPS-1, especially at the hips.

The radiographic changes in the skeleton have always been difficult to evaluate accurately because of the marked variations at different ages and because until recently the clinical diagnosis was uncertain owing to our ignorance of such supporting signs as dental dysplasias and corneal opacities and of the diagnostic chemical finding of urinary excretion of keratosulfate. Langer and Carey studied 10 Morquio dwarfs radiographically at varying ages from 15 months to 52 years, whose corneas were inspected for opacities and one half of whom had urinary tests for mucopolysaccharides and all of whom had all their teeth inspected for dysplasias. The findings were positive in all of the patients so examined: pointed dental cusps and lamellations of the enamel were present in 8 of the 10 patients; the other 2 had lost their teeth from dental caries. Both deciduous and permanent teeth had gray crowns with pitted enamel which was thin and often flaked off. In this relatively large group of Morquio dwarfs and with the advantages of chemical tests and accurately defined clinical signs, Langer and Carey were able to establish the detailed skeletal changes in Morquio disease. They found the most consistent and most characteristic changes to be in the spine, pelvis, hands and wrists. The vertebral bodies were oval in the young child and become elongated and flattened ventrad in the older child; they then became rectangular and flattened in the adult. The intervertebral spaces were deepened at all ages. Actual vertebral plana was never well developed in young children. During the 1st year the bases of the ilia were narrowed owing to hypoplasia of the bone on the edges of the acetabular cavities, whose upper edges were roughened. With advancing age this ilial stenosis increased with factitious enlargement of the acetabular cavities, and at the same time the femoral necks began to lose their angles and the femoral heads began to flatten. These processes continued until the femoral heads were resorbed completely and the femoral necks were thickened.

Changes were present in the hands and wrists early in life when they simulated the mild changes of MPS-1 (gargoylism). In the younger child the epiphyseal ossification centers in the round bones of the wrists were small and appeared late, but they were not deformed. The pinched appearance of the proximal ends of the metacarpals and distal ends of the phalanges was present early; this is identical with the

corresponding changes in MPS-1. The tipping of the ends of the ulna and radius also simulated MPS 1, the differential diagnosis of MPS 1 and MPS-4 cannot be made radiographically in many patients during the first years of life from the changes in the hands alone. In the older child flattening of the epiphyseal ossification centers and the angular contours in the round bones became evident while the proximal ends of the metatarsal shafts were losing their cone shaped deformities. These changes were most characteristic in the older child. In the adult the most striking change was the disappearance of some of the carpal bones which were present earlier. In one of Morquio's original patients at 50 years of age (observed by Soto in Montevideo) all carpal bones were invisible radiographically. The epiphyseal changes were not prominent after fusion of the primary and secondary ossification centers. Tipping of the ends of the radius and ulna into oblique planes persisted into adult life. It is probable that some of the marginal epiphyseal changes in older patients are due to stress rather than to simple dysplasia. During early life the metaphyseal changes dominate the picture.

In the large tubular bones errors in modeling may produce increases in their girth with large medullary cavities similar to but less marked than those in MPS 1. Hypoplasia of the odontoid process with dorsal dislocation of the 2nd cervical vertebra is often found in patients with generalized muscular weakness. Widened ribs may narrow the intercostal spaces. The final diagnosis in the skeleton must rest however on the changes in the spine, pelvis and hands. During the first years of life the radiographic skeletal changes simulate those of MPS 1 so closely that differentiation is best based on identification in the urine of the appropriate mucopolysaccharide, keratan sulfate.

REFERENCES

- Blaw M E. and Langer L O. Spinal cord compression in Morquio-Brailsford disease. *J. Pediatr.* 74: 593 1969.
 Brailsford J F. Chondro-osteodystrophy. Roentgenographic and clinical features in a child with dislocation of the vertebrae. *Am J Surg* 74: 404 1929.
 Langer L O Jr. and Carey L W. The roentgenographic features of hS mucopolysaccharidosis of Morquio (Morquio-Brailsford's disease). *Am J Roentgenol* 97: 1 1968.
 Maroteaux, P., and Lamy L. Hurler's disease. Morquio's disease and related mucopolysaccharidoses. *J. Pediatr.* 67: 312 1965.
 Morquio L. Sur une forme de dystrophie osseuse familiale. *Arch de méd d enf* 32: 129 1929 38: 1 1938.
 Soto J A. Personal communication.
 Zellweger H., et al. Morquio-Ullrich's disease. Report of two cases. *J. Pediatr.* 59: 549 1961.

Mucopolysaccharidosis (MPS 5) chondroitin sulfate B sulfaturia (Schnee's disease) is said to be characterized by peripheral clouding of the corneas which is the cardinal clinical finding. Mentality is normal or superior and the stature is normal or moderately reduced. The joints are stiff, hair is excessive

and the hands may be flexed. McKusick found aortic regurgitation in some patients. The radiographic changes in the growing skeleton are not known.

REFERENCE

- Schnee H G. et al. A newly recognized forme fruste of Hurler's disease (gargoylism). *Am J Ophthalmol* 53: 753, 1962.

Mucopolysaccharidosis (MPS 6) chondroitin B sulfaturia only (Lamy-Maroteaux) is characterized by short stature which becomes evident at about 2 years of age. At the same time knock knee, lumbar kyphosis and high ventral protuberance of the sternum and costal cartilages begin to become apparent. Thick lips with large nostrils and enlarged nasal tips suggest the facies of Hurler's disease. Semiflexion is the rule at all of the large joints and in the joints in the hands. Liver and spleen are enlarged. Mentality is normal during the first ten years of life at least. Radiographic skeletal changes are similar to those in MPS-1 but are usually less severe. Bilateral coxa plana and coxa valga were present in one of McKusick's patients. The corneas become cloudy early. Metachromatic granules have been found in the polymorphonuclear leukocytes and lymphocytes. These patients excrete large amounts of chondroitin B sulfate in the urine; this polysaccharide only is excreted in excess.

REFERENCES

- Maroteaux P. and Lamy M. Hurler's disease. Morquio's disease and related mucopolysaccharidoses. *J. Pediatr.* 67: 312 1965.
 — et al. Une nouvelle dysostose avec élimination urinaire de chondroïtine sulfate. *B. Presse méd.* 71: 849 1963.
 McKusick, V A. et al. The genetic mucopolysaccharidoses. *Medicine* 44: 445 1965.

Rheumatoid type of MPS — Winchester and associates using tissue cultures of cutaneous fibroblasts claimed to have identified a new MPS in which the changes in the skeleton simulated those of rheumatoid arthritis. Their two patients were siblings of a consanguineous marriage. The facies suggested gargoylism and there were focal opacities in the peripheries of the corneas. Mucopolysaccharides were not found in excess in the urine.

REFERENCE

- Winchester P. et al. A new acid mucopolysaccharidosis with skeletal deformities simulating rheumatoid arthritis. *Am J Roentgenol* 106: 121 1969.

Mannosidosis — Kjellman and co-workers studied a patient with a storage disorder in the central nervous system in whom biochemical tests demonstrated a deficiency of the enzyme alpha mannosidase in the liver. Some of the clinical findings suggested gargoylism, but the radiographic changes in the skeleton were slight and not diagnostic.

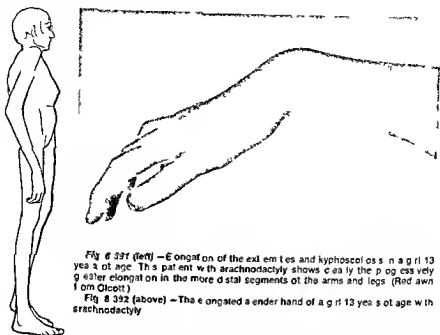


Fig 8-391 (left) — Elongation of the extremities and kyphoscoliosis in a girl 13 years of age. This patient with arachnodactyly shows clearly the disproportionately greater elongation in the more distal segments of the arms and legs (Redrawn from Olcott).

Fig 8-392 (above) — The elongated slender hand of a girl 13 years of age with arachnodactyly.

REFERENCE

- Kjellman B *et al*: Mucopolysaccharidosis. A clinical histopathological study. *J Pediatr* 75:366, 1969

Fucosidosis was disclosed in two siblings whose parents were cousins by Durand and colleagues. They concluded that this was a new type of neurovisceral disease. Both patients underwent severe progressive mental retardation and gradual loss of muscular power which progressed to spasticity and decorticate rigidity, emaciation, thickening of the skin, excessive sweating, and cardiomegaly. Respiratory infections were common. The boy died at 4 years and the girl at 5 years. Glycolipids accumulated in the skin, lymphocytes, and other tissues. Chemically, the basic defect appears to be an absence of α -L-fucosidase. The hearts were enlarged radiographically; skeletal findings were not reported.

REFERENCE

- Durand P *et al*: Fucosidosis. *J Pediatr* 75:665, 1969

Marfan's syndrome — This is characterized by elongation of the tubular bones, especially those in the hands and feet; hypoplastic and hypotonic musculature and diminished subcutaneous fat. At least half the patients have had bilateral dislocation of the ocular lenses and contracted pupils which do not respond to mydriatics. The latter is due to absence of the dilator muscle. Congenital cardiac disease has been present in about one third of reported cases.

Marfan's syndrome is simulated in many of its features by homocystinuria, namely, ectopia lentis, aortic

aneurysm and the skeletal changes. Adler and Nyhan reported arachnodactyly in a patient who suffered from keratosis follicularis spinulosa decalvans. The available evidence suggests that this complex is fundamentally an anomalous development of the mesoderm which begins early in fetal life. The kyphoscoliosis (Fig 8-391) found in many cases is secondary to muscular weakness. In two cases of arachnodactyly, Landucci found the manifestations of Ehlers-Danlos syndrome.

Diagnosis is usually manifest after direct inspection of the hands and feet, which are elongated (Fig 8-392). The roentgenogram discloses a relative and absolute elongation of the phalanges, metatarsals, and metacarpals; the other long bones are usually also elongated, but the proportionate elongation increases progressively from the shoulder to the fingertips and from the hip to the toes (Fig 8-393). The corticulus is diffusely thin and the spongiosa delicate. Maturation is normal or advanced. The pulmonary emphysema and pulmonary cysts found in many young patients are due, according to Bolande and Tucker, to weakness of the interstitial supporting tissues of the lungs.

REFERENCES

- Adler R C and Nyhan W L: An oculocerebral syndrome with aminoaciduria and keratosis follicularis. *J Pediatr* 75:436, 1969.
Bercason G S and Serra M T: Mucopolysacchariduria in Marfan's syndrome. *Fed Proc*, Vol 18, part 1, March, 1959 (abst 749).
Bolanle R P and Tucker A S: Pulmonary emphysema and cardio-respiratory lesions as a part of Marfan's syndrome. *Pediatrics* 33:356, 1964.

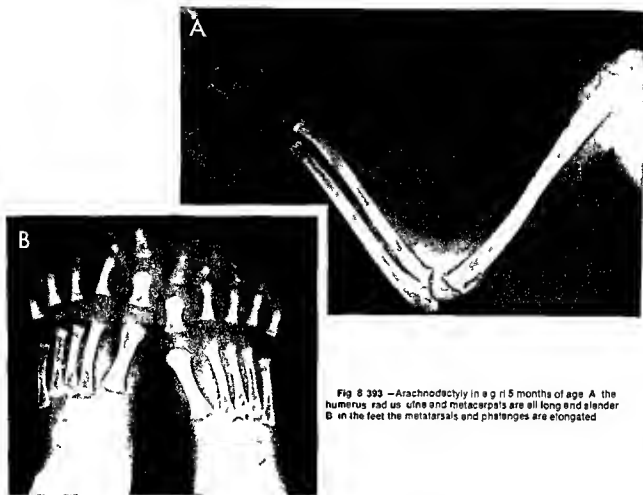


Fig 8-393—Arachnodactyly in a girl 5 months of age. A, the humerus, radius, ulna, and metacarpals are all long and slender. B, in the feet the metatarsals and phalanges are elongated.

McKusick V. A. Heritable Disorders of Connective Tissue (3rd ed. St. Louis: C. V. Mosby Company, 1966).
 — et al. The genetic mucopolysaccharidoses. *Medicine* 44: 445, 1965.

Cleidocranial dysostosis has two principal radiographic components: hypoplasia of the clavicles and slow and incomplete ossification of the calvarium (see Figs 1-87 and 1-88). Associated deficiencies of ossification in the pelvis and spine are common. Roentgen examination of the entire skeleton will show associated anomalies in the tubular bones of many of these patients. In a report on 70 cases, Jackson recorded dysplasias in both ectodermal and mesodermal structures—teeth, facial bones, sternum, scapulae, vertebrae, pelvic bones, long bones, metacarpals and phalanges, as well as in the calvaria and clavicles. Complete or submucous cleft palate has been present in some patients. The number of teeth may be excessive and simulate a third eruption. The paranasal sinuses are often small or absent. The mastoid processes are said to be small and poorly pneumatized owing to the weakness and lack of molding by the sternocleidomastoid muscles.

REFERENCE

Keats T. E. Cleidocranial dysostosis. Some atypical roentgen manifestations. *Am J Roentgenol* 100: 71, 1967.

Osteopoikilosis (spotted bones)—The salient features of this condition are multiple sclerotic foci in the ends of long bones and scattered stippling in round and flat bones (Fig 8-394). Small focal sclerotic shadows are cast by local thickenings of the spongiosa; the overlying cortex is normal. All except the cranial bones may be affected. Osteopoikilosis is symptomless; the diagnosis is usually made fortuitously in the x-ray examination. Several members of the same family may be affected; the condition is transmitted genetically. Many cases of spotted bones have been described in children and Green mentioned fetal and neonatal examples of this syndrome. Osteopoikilosis is not a residual of chondrodystrophia calcificans congenita. Lenticular fibromas of the skin have been found in a few cases of osteopoikilosis (Curth). With increasing age the lesions may disappear completely or they may increase in size and number. The lesions fluctuate in adults, but not as rapidly as in children.



Fig 8 394—Osteopetrosis in a healthy boy 12 years of age. **A**, right hand. **B**, left hand. Numerous sclerotic foci of varying sizes are visible in the shafts of the phalangeal ossification centers and

round and flat bones. The boy was asymptomatic, and films of his skeleton were made only because osteopetrosis had been demonstrated in his mother. (From Holly.)

Fig 8 395—Combined osteopetrosis and metapneostosis in a boy 18 years of age. **A**, osteopetrosis of the proximal ends of the femurs and all of the pelvic bones. Smear opaque spotting was present in the tibia, humerus, radius, and carpal bones on both sides and in some of the vertebrae. **B**, metapneostosis of the humerus, radius, and radial side of the ulna. The ectosteal layer

the thickenings and sclerosis of the bones flow through and past the elbow joint. The same flowing effect was evident at the wrist, where the ectosteal and thickenings were confined to the carpal bones on the radial side of the hand and to the first and second metacarpals and the phalanges in the first and second digits.



In one patient, we have seen osteopoikilosis and melorheostosis associated (Fig 8-395), it is possible that these two rare syndromes have the same pathogenesis

REFERENCES

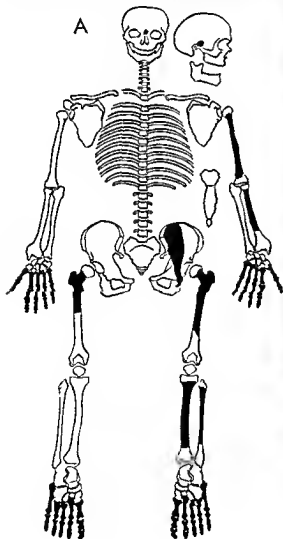
- Archer, M. C., and Fox, K. W. Osteopoikilosis. Report of two new cases. *Radiology* 47 279, 1946
 Curth H. O. Dermatofibrosis lenticularis disseminata and osteopoikilosis. *Arch. Dermat & Syph.* 30 552, 1934
 Fairbank, H. A. T. Osteopoikilosis. *J Bone & Joint Surg* 30-B 544, 1948
 Green, A. E., et al. Melorheostosis and osteopoikilosis with review of the literature. *Am. J. Roentgenol.* 87 1096, 1962.
 Hinson, A. Familial osteopoikilosis. *Am J Surg* 45 566, 1937
 Holly, L. E. Osteopoikilosis. A five year study. *Am J Roentgenol.* 36 512 1936

- Nather, F. B. Osteopoikilosis. Report of four cases. *Am. J. Roentgenol* 35 495, 1936
 Wilcox, L. F. Osteopoikilosis (disseminated condensing osteopathy). *Am J Roentgenol* 27 580 1932

Osteodystrophia fibrosa (McCune Albright), polyostotic fibrous dysplasia—This bizarre condition is characterized by predominantly unilateral fibrosis of the skeleton and hyperpigmentation of the skin, in females, maturation is accelerated and puberty is precocious. The pathogenesis is obscure, although there is some evidence that the dystrophy is of neurogenic origin. Osteodystrophia fibrosa has not been found in embryos, or infants, our youngest case was recognized at the age of 3 years. It is becoming evident as more cases are studied that mild forms may

Fig 8-396—Osteodystrophia fibrosa in a boy 3 years of age. A, map of the skeleton showing patchy, predominately left sided involvement. B, forearm showing dilatation and cystic rarefaction of the left radius. C, lower extremities showing streaky rare-

faction of the proximal end of the left tibia and swelling and elongation of its shaft in comparison with the right tibia. The middle third of the left fibula is also irregularly osteoporotic and dilated. D, hyperpigmentation confined to the left arm and shoulder



be limited to one bone and that skeletal fibrosis may develop without hyperpigmentation of the skin. Islands of cartilage in the fibrous tissue, once thought to be characteristic of the disease, were found in only 14% of cases by Harris and colleagues, and these cartilage islands were limited to sites of earlier fracture or trauma. The cartilage islands are probably residues of abortive callus formation rather than foci of primary cartilage proliferation. The femur is almost invariably involved and usually shows the most extensive lesions. Aarskog and Tveterras studied a girl who developed the signs of Cushing's disease at 1 month of age. Total excision of both adrenals was done at age 4 months. The clinical picture of McCune Albright syndrome became evident during the 8-44 months after the excision.

The roentgen findings vary depending on the severity of the disease. The fibrotic areas appear as scattered patches of irregular rarefaction, which are predominantly unilateral (Fig. 8-396) in the shafts of the tubular bones and in the flat bones and the round bones of the wrists and ankles. The epiphyses are not affected. The lower extremities are the sites of the most frequent and extensive involvement. The affected shafts are often elongated and dilated. The cortices overlying the fibrosis are eroded from the internal aspect, sometimes to the point of pathologic fracture. The fibrosis occasionally invades proliferating cartilage at the ends of the shaft, interfering with growth and producing deformities. Cystic radiolucent areas of varying size may be interspersed in the areas of fibrosis. In females, the maturation of the entire skeleton is accelerated; the bones not affected by the fibrosis show the same acceleration as those extensively fibrosed. Following adolescence, there may be a tendency to subsidence of the fibrosis, but this is not complete, and the lesions do not disappear.

This disease has commonly been mistaken for hyperparathyroidism. There are no conclusively differential roentgen features in these two conditions. In osteodystrophia fibrosa, the lesions are scattered in hyperparathyroidism, the osteoporosis is usually generalized. In osteodystrophia fibrosa, the lesions are unilateral or predominantly so, and chemical findings in serum are always indicative of a normal calcium metabolism.

REFERENCES

- Aarskog D and Tveterras E: McCune Albright's syndrome following adrenalectomy for Cushing's syndrome. In *Infancy Pediatrics* 73:89, 1968.
- Albright F *et al*: Syndrome characterized by osteitis fibrosa disseminata, areas of pigmentation and endocrine dysfunction with precocious puberty in females. *New England J Med* 216:727, 1937.
- Harris WH *et al*: The natural history of fibrous dysplasia. *J Bone & Joint Surg* 44-A:928, 1962.
- Lichtenstein L: Polyostotic fibrous dysplasia. *Arch. Surg* 36:874, 1938.
- and Jaffe H L: Fibrous dysplasia of bone. *Arch. Path* 33:777, 1942.
- McCune D J and Bruch H: Osteodystrophia fibrosa. *Am. J Dis Child* 54:806, 1937.

Localized or monostotic fibrous dysplasia of bone has become a common diagnosis in recent years. The anatomic and radiologic changes are similar to those in polyostotic fibrous dysplasia but are confined to a single bone. The other features of the syndrome described by McCune and by Albright are not present. Lesions are most common in the craniofacial bones, ribs, vertebrae and the long bones, especially the radius (Fig. 8-397). The earliest radiologic change is a loss of density in the sites where bone is being replaced by fibrous tissue and cartilage (see Fig. 8-764). Later the whole shaft may exhibit a ground glass rarefaction with dilatation of the medullary cavity and internal atrophy of the cortical walls in the levels of the fibrocartilaginous hyperplasia. Diagnosis depends on the microscopic findings of fibrotic whorls in which there are scattered islands of osteoid tissue and uncalcified cartilage. Solitary lesions usually respond well to curettage and packing with bone chips.

Fig. 8-397 — Fibrous dysplasia of the proximal half of the radius (arrow) in a girl 6 years of age whose skin was not hyperpigmented. The proximal half of the right radius is dilated and the cortical walls are thinned. The affected segment has a mottled ground glass rarefied appearance. A biopsy specimen showed fibrous dysplasia.



REFERENCES

- Gould M. D. *et al*. Fibrous dysplasia of bone. *Am. J. M. Sc.* 234 590 1957
 Jaffe H. L. Fibrous dysplasia of bone. *Bull. New York Acad. Med.* 22 558 1946
 Strassburger P. *et al*. Fibrous dysplasia of bone. *J. Bone & Joint Surg.* 33-A 407 1951

Engelmann Camurati disease (progressive diaphyseal dysplasia)—In 1929 Engelmann described a boy 8 years of age who had symmetrical sclerotic swellings of the long bones in the extremities (Fig. 8-398). In the humerus and femur the more distal parts of the shafts were affected in contrast the proximal segments of the ulna, radius and tibia were sclerotic. None of the known causes of bone sclerosis could be identified in his patient. The lesions were limited to the shafts the epiphyseal ossification centers and metaphyses were not involved. The ribs, vertebrae and pelvis remained free from the disease but the base of the skull was thickened and sclerotic. In 1922 Camurati had described similar changes in the bones of the legs of a boy 7 years of age and also in his father.

The principal clinical manifestation is a waddling gait which became evident in one patient on the first attempt at walking but did not appear in another patient until the 6th year. The time of first appearance of the roentgen changes is not known and it is not

Fig. 8-398—Malnutrition, muscular atrophy and slender extremities in Engelmann's patient, a boy 8 years of age. (From Engelmann.)



certain whether this is a congenital or acquired disease. The causal agent is wholly unknown. Malnutrition is usually an associated finding and all patients have tired easily especially in the legs notwithstanding the fact that initial muscular power before the fatigue may be surprisingly good. These patients either run with great difficulty or refuse to run. The muscles of the legs are characteristically small. Intellectual and motor development other than gait have been normal.

A review of all patients shows that the basic lesion in the tubular bones is a long spindle-shaped sclerotic thickening of the cortical walls (Fig. 8-399) which involves the intermediate segment of the shaft and produces both internal and external swelling of the cortical walls. The former reduces the caliber of the corresponding segment of the medullary canal. The metaphyseal zones at the ends of the shafts and the ossification centers in the epiphyses are not affected. With advancing age the sclerosis and thickening extend in both directions and the bones themselves become overlong. The bones of the hands and feet, the ribs, scapulas and pubic bones are not affected. The base of the cranium, cervical vertebrae and clavicles have been sclerotic in some cases and normal in others. Specimens taken from the shafts in the sites of the roentgen sclerosis have shown nonspecific cortical and endosteal hyperostosis.

Gurdany found three examples of the disease in one family—a mother, her brother and her son. The mother was asymptomatic but showed sclerotic changes in her bones. Her brother who as a child was so weak that he walked with difficulty and could not run, became normally strong during adolescence and was healthy and earned out heavy labor as an adult; his bones were also sclerotic. The son at the age of 12 was still weak and showed characteristic changes in the skeleton. In a fourth patient 11 years of age improvement in muscular power began after rigorous physiotherapy although this child had shown progressive muscular weakness during the previous nine years. Gurdany's findings suggest that the muscular weakness improves and disappears in the early years of the second decade but the bone changes persist into adult life. In the case of Stronge and McDowell muscular weakness persisted throughout life until the 28th year.

Mikity and Jacobsen observed an adult from age 22 to 54 and found no progression in the bone lesions; his muscular development and function appear to have been normal all this time.

REFERENCES

- Camurati, M. Di un caso di osteite simmetrica ereditaria degli arti inferiori, *Chir. org. movimento* 6 662, 1922.
 Engelmann G. Osteopathia hyperostotica sclerotisans multiplex infantilis. *Fortschr. a. d. Geb. d. Röntgenstrahlen* 39 1101 1929.
 Gurdany B. R. Engelmann's disease (progressive diaphyseal dysplasia): a nonprogressive familial form of muscular dystrophy with characteristic bone changes. *Clin. Orthop.* 14 102, 1959.



Fig. 8-399 —Classic Engelmann's disease in a girl 4 years of age who did not begin to walk until 16 months of age and still had a clumsy waddling gait and was slow in beginning movements. A, B and C in the long bones the cortical walls are thickened internally as well as externally which produces concurrent increase in the growth of the bones and constriction of their medullary cavities at the same levels. The terminal segments of the shafts and epiphyseal ossification centers are conspicuously unaffected. The cortical thickenings extend nearer to the elbows and knees than to the wrists and ankles. D in the pelvis the bodies of the ischia show some thickening and sclerosis. E, in

the skull the membranous bones of the calvaria and cartilaginous bones of the base are irregularly thickened and sclerosed but the bones of the face in contrast are normal. At age 10 this girl is said to have had repeated tests for alkaline phosphatase activity in the serum and all yielded normal values. She had become very weak and muscles had become atrophic. At this time the findings in radiographs of her skeleton and skull which had become very thick are said to have resembled hyperphosphatasia more than Engelmann's disease. (Courtesy of Dr. Louis R. P. ley, Roanoke, Va.)

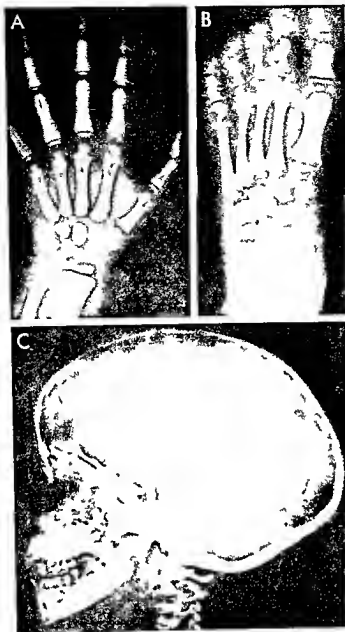


Fig. 8-400.—Benign familial idiopathic osteosclerosis in the hand (A), foot (B) and skull (C) of an asymptomatic girl 3 years of age. In the shafts of the tubular bones the cortical walls are thickened internally at the expense of the marrow cavities, which are narrowed. The external shape of these bones is normal. The epiphyseal ossification centers and the round bones in the wrist and ankle are sclerotic because the opaque spongiosa is increased

and its mesh is tightened at the expense of the radiolucent marrow spaces. Maturation is normal. In the skull the cartilaginous base is sclerotic but the membranous calvaria, except the occipital squamosa, is not affected. In the eight members of this family the degree of bony sclerosis appeared to vary directly with the age of the individual.

Lennon E A *et al* Engelmann's disease Report of a case with review of the literature *J Bone & Joint Surg* 43-B 273 1961

Pyknodysostosis (Lamy Maroteaux) is a generalized sclerosis of the skeleton which resembles osteopetrosis radiographically but differs from it in several important respects. The distal phalanges of the fingers and toes are short and the tips of the fingers and toes are clubbed and have large nails which run over the tips onto the distal edges. More important anemia, thrombocytopenia and splenomegaly do not develop in pyknodysostosis and the prognosis is good. It is possible that pyknodysostosis is a separate entity but it may be a mild variant of osteopetrosis. In some cases the sutures and fontanelles have remained large, the mandible has been hypoplastic with widened mandibular angle, the teeth have been dysplastic and ectopic and the clavicles have been rudimentary.

Fig 8-401—Diffuse sclerosis of the bones in the forearm (A) and shank (B) of a healthy girl 3 years of age. In the shafts the cortical walls are thickened internally with compensatory narrowing of the medullary cavities. In the round bones of the wrist and ankle and the large sesamoid bone and patella the sclerosis is due to excess of spongy bone with reduction of the radiolucent marrow spaces. The external shape of these bones is normal as are growth and maturation.



REFERENCES

- Elmore S Pyknodysostosis A review *J Bone & Joint Surg* 49 A 153 1967
Kajli T *et al* Pyknodysostosis *J Pediatr* 69 131 1966
Shuler S E Pyknodysostosis *Arch Dis Childhood* 38 620 1963

Benign idiopathic familial osteosclerosis (Figs 8-400 to 8-404) occurs in infants, children and adults. This is a radiographic phenomenon in persons who are unaware of the changes in the bones, have no complaints and have normal findings on physical examination. Results of standard laboratory tests have been normal. In particular phosphatase activity in the serum is normal. So far as I know, their life spans are not shortened and they lead active carefree lives until the radiographic changes in the skeleton are demonstrated. The radiographic change is a diffuse increase in the density of the bones without increase in caliber or change in the shape of the tubular or round bones. The changes in older patients are usually most marked in the skull, with thickening of both tables of the calvaria at the expense of the depth of the diploic cavity. The converse is true in children in whom the cranial bones are the least affected. In the other bones there is no deformity of construction and maturation is normal. The clinical endocrine functions are normal, although there is some suggestion that the bone changes increase with age. In the tubular bones the basic change is a generalized internal thickening of the cortical walls with a corresponding compensatory narrowing of the medullary cavity. In the epiphyseal ossification centers in the round bones during growth, the increase in density is due to tightening and thickening of the spongiosa at the expense of the medullary cavity.

REFERENCE

- Russell W J *et al* Idiopathic osteosclerosis A report of six related cases *Radiology* 90 70 1968

Hereditary multiple diaphyseal sclerosis (Ribbing) is a familial skeletal dyscrasia which resembles Engelmann's disease in some respects, but has not been identified prior to adolescence. Paul, however, found clinical and roentgen findings characteristic of Engelmann's disease in the infant son of a father who exhibited Ribbing's disease and whose brother had similar lesions. This suggests that Ribbing's disease may be the adult form of Engelmann's disease.

REFERENCES

- Paul L W Hereditary multiple diaphyseal sclerosis *Radiology* 60 412 1953
Ribbing S Hereditary multiple diaphyseal sclerosis *Acta radiol* 31 522 1949

Pyle's disease (idiopathic symmetrical spaying of the long bones)—In 1931 Pyle described a boy 5



Fig 8-402 (left) — Diffuse sclerosis of the shafts and epiphyseal ossification centers of the bones at the knees of an otherwise healthy girl 11 years of age. At these levels in the bones the sclerosis appears to be due to excess of opaque spongy bones



with deficiency of radiolucent marrow spaces in both the shafts and the epiphyseal ossification centers

Fig 8-403 (right) — Diffuse sclerosis of pelvic bones and both femurs of an asymptomatic girl 13 years of age. The sacrum is relatively not affected

Fig 8-404.—Severe sclerosis of the skull of an otherwise healthy woman 39 years of age. The frontal squamosa parietal bones and occipital squamosa are thickened and sclerotic. The diploic spaces appear to be obliterated. The frontal sinuses are small. Pneumatization of the ethmoids body of the sphenoid and temporal bones was normal



years of age who came to him because of knock knees which had been noted one year before. The boy was tall for his age and save for the deformities of the knees was said to be "in the picture of health." There were no thoracic deformities. The long bones in the extremities were all enlarged to palpation but were not tender, there was some limitation of extension at the elbows. Roentgen examination disclosed spreading of the ends of all the tubular bones in the extremities (Fig 8-405). In the femur, radius and ulna spreading was more marked at the distal ends and in the humerus in the proximal two-thirds, both ends of the tibia were about equally affected. In the widened segments of the shafts the cortex was thinned but the spongiosa was normal. At surgical exploration the periosteum appeared normal but the cortex offered too little resistance to a bone chisel. The bones healed normally following biopsy. Pyle concluded that failure of normal constriction—failure of shaping or modeling—was responsible for the symmetrical increase in caliber of the shafts at many sites.

Typical severe changes in the tubular bones of the extremities and flattening of the vertebral bodies of a boy 12 years of age are shown in Figure 8-406. The mandibular swelling and expansion of the pubic and ischial bones in a girl 13 years of age are portrayed in Figure 8-407. Symmetrical bilateral dilatation of the medial halves of the clavicles is evident in a man 23 years of age (Fig 8-408). Mori and Holt stated that cranial changes are common in Pyle's disease principally symmetrical hyperostoses of the calvaria and mandible and ocular hypertelorism (Fig 8-409) with retarded pneumatization of the paranasal sinuses. In the newborn the skeleton is generally sclerotic, with a radiographic picture which resembles osteopetrosis.

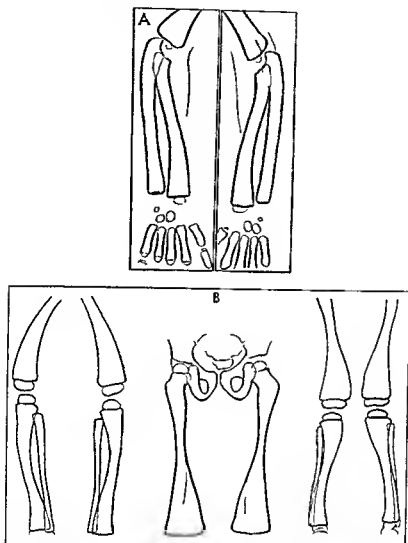


Fig. 8-405 - Congenital splaying of the shafts (Pyle's disease) in a boy 5 years of age. A - arms. B - legs. Spreading is most con-

spicuous in the distal portions of the femurs, radii and ulnas. Both ends of the tibia are splayed. (Redrawn from Pyle.)



Fig 8-406.—Severe class C Pyle's disease in the extremities with universal vertebral plana in a boy 12 years of age. A, B, C, D, splaying of the ends of the shafts and thinning of the cortical walls in the diaphyseal segments of the tubular bones in the extremities.

E, sclerosis and flattening of all of the vertebral bodies (Figs 8-406 to 8-408 courtesy of Dr. Bertam R. Gandy, Pittsburgh).

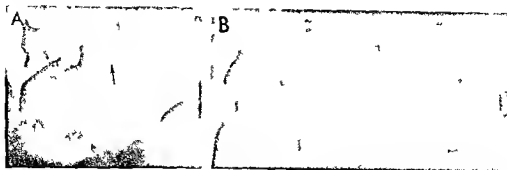


Fig. 8-407 — Mandibular and pelvic changes in Pyle's disease in a girl 13 years of age. A, the ramus and body of the mandible are swollen and the usually spiculated endoprocess is distended

Fig. 8-408 — Spaying of the medial ends of the clavicles of a man 23 years of age who had Pyle's disease



However, with advancing age the growing ends of the shafts begin to lose their heavy density and the medullary cavities become visible until, after a few years, the density of the bones is approximately normal, but the shafts fail to constrict and never attain normal shape and caliber. In the newly born infant with Pyle's disease the mandible is said to be more sclerotic than in osteopetrosis, in which the mandible may not be severely affected. Blindness associated with optic atrophy may occur during early infancy.

Fig. 8-409 — Facial appearance of two boys 6 years of age who had classic Pyle's lesions in the long bones. Both exhibit marked ocular hypertelorism, flattening of the base of the nose and dental defects. The nasal bridges are extremely broad in one face



into a bunt hump. B, both pubic and schal bones are swollen but the epiphyseal separation is normal. The ramus of the pubic bones and the schal ram

Urteaga and Mosely found the classic changes of Pyle's disease in parts of a skeleton recovered from an ancient cemetery in Peru.

Theoretically, Pyle's disease could be due to chronic hyperemia of the perichondral ring of osteoblasts which causes chronic overgrowth latitudinally from the epiphyseal cartilage. Hyperemia in this hypothesis is due primarily to congenital hyperplasia of the arteries to the perichondral ring.

Gorlin and colleagues argue that metaphyseal dysplasia (Pyle's disease) and craniometaphyseal dysplasia (Jackson) are separate entities. In their study of films of the skull of Pyle's original patient and two patients' brothers of their own they found only slight thickening of the calvaria. They did not find the frontal paranasal and occipital hyperostosis and sclerosis which they apparently consider mandatory for the diagnosis of craniometaphyseal dysplasia.

REFERENCES

Bakwin H. and Knida R. Familial metaphyseal dysplasia. *Am J Dis Child* 53:1521, 1937.

the mouth is open secondary to nasal obstruction which produces an empty facial expression. Thickening and enlargement of the frontal squamosa are evident in both photographs. (From Mo and Hot).

- Feld H *et al* Familial metaphyseal dysplasia *Radiology* 65 206, 1955
- Gorlin R J *et al* Pyle's disease (familial metaphyseal dysplasia) A presentation of two cases and an argument for its separation from craniometaphyseal dysplasia *J Bone & Joint Surg* 52-A 347 1970
- Hormel M B *et al* Familial metaphyseal dysplasia *Am J Roentgenol* 70 413 1953
- Jackson W P U *et al* Metaphyseal dysplasia, epiphyseal dysplasia and diaphyseal dysplasia and related conditions *Arch Int Med* 94 871 1954
- Kowins C Familial metaphyseal dysplasia (Pyle's disease), *Brit J Radiol* 27 670 1954
- Mori P A and Holt J F Cranial manifestations of familial metaphyseal dysplasia *Radiology* 66 335 1956
- Pyle E A case of unusual bone development *J Bone & Joint Surg* 13 674 1931
- Urteaga O and Mosely J E Craniometaphyseal dysplasia (Pyle's disease) in an ancient skeleton from the Mochea culture of Peru *Am J Roentgenol* 99 712 1969

Fibrogenesis imperfecta is a rare entity described in two adults. The principal radiographic finding is a deficiency and wide spacing of the trabeculae of the spongiosa which produce a coarse pattern suggestive of a fishnet (Golding)—a fishnet rarefaction. The radiographic changes are most pronounced in the bones and the parts of the bones near joints. Excretion of calcium in the urine and feces was excessive in one patient. The basic microscopic finding is a diffuse deficiency of collagen fibers in newly formed bone matrix of lamellar bone.

REFERENCE

- Golding F C *Fibrogenesis imperfecta*, *J Bone & Joint Surg* 50-B 619 1968

THE MISCELLANEOUS INTRINSIC DWARFS

In addition to the primary intrinsic hypoplasias of the skeleton which we have just discussed there are several individual types of dwarfism in which the primary growth disturbance appears to be in non-skeletal tissues and the skeletal disturbance is secondary or at least not dominant.

PROGERIA (SENILE DWARF) is a rare and distinctive type of generalized undergrowth with a peculiar combination of dwarfism and premature aging. There are no mild or even moderate examples; this appears to be an all-or-none disease. The diagnosis can be made immediately on inspection (Fig 8-410). At birth the patient is near normal in weight and normal in appearance. He grows normally until about the end of the 1st year when both normal growth and gain in weight slow down never to be resumed. At the end of the first decade the size attained approximates that of a normal child 3 years of age. Intelligence varies but it is often normal and may be superior. The skeleton matures normally. Joints become swollen and bent and the arteries harden. Death comes during the first or second decade usually owing to coronary sclerosis.

In radiographs the long bones are shortened and

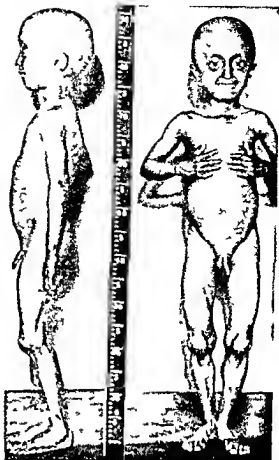


Fig 8-410—Progeria in a black boy 8 years of age. He is height equivalent of a normal boy 2½ years of age. The ears are normal on the scalp. Eyebrows and eyelids. The bald dome of the head is relatively large in relation to the small face and mandible. The end of the nose is pinched owing to hypoplasia of the nasal cartilages. The pinched beaked faces suggest the profile of a bird and these mandibles are sometimes exhibited as the bird-faced boy in circus sideshows. The malnourished appearance is due to an almost complete absence of subcutaneous fat. The upper lip is beaked and the angles of the mouth are elevated in a perpetually grin. (From Cooke.)

overconstricted in their central segments with flares at the ends. The calvaria is thin and relatively large and the diploic space is absent or very shallow. The face is small with disproportionate smallness of the mandible. From the outset the clavicles are small in caliber and rarefied; during childhood they may disappear in part or in toto due to progressive fibrosis. Oronoff and Clemett observed complete fibrous resorption of the clavicles during a period of four years. The posterior segments of the upper four ribs on each side disappeared radiographically during and shortly after the same period. Vascular markings and Wormian bones are conspicuous in the large thin calvaria. The anterior fontanel closes slowly. Bilateral severe coxa valga is said to occur in all patients.

REFERENCES

- Cooke J V The rate of growth in progeria With report of two cases J Pediat 42:26 1953
- Gabr M *et al* Progeria A pathologic study J Pediat 52:70 1960
- Kozlowski K Radiologic study of a case of senile dwarfism (progeria) Ann radiol 8:92 1965
- Ozonoff M B and Clemett A R Progressive osteolysis in progeria, Am J Roentgenol 100:75 1967
- Schwartz E Roentgen findings in progeria, Radiology 79:411 1962

THE BRACHMAN DE LANGE SYNDROME has two major components dwarfism and mental deficiency and several associated anomalies which include macrobrachycephaly excessive hair generally with a low hairline at the forehead and heavy eyebrows which are confluent at their medial ends and long heavy eyelashes a pug nose low set ears short arms and legs bent fifth fingers proximally set thumbs and

Fig 8-411—Facies of the Brachman-de Lange syndrome in four patients, age 3, 5 and 4 months and 5 years. The hair of the scalp and face is excessive and the hairline is lowered onto the forehead. The heavy eyebrows are confluent medially. The base of the nose is sunken and the nostrils are large and flared. The

marbled skin. The diagnosis is usually first suspected and finally made from the characteristic facies (Fig. 8-411). Mental retardation is severe usually imbecilic in degree. Stature is reduced about 20% and head size by 15%. Radiographic findings are important only as an excluding agent of other diseases (Fig. 8-412). The microcephaly, bent fingers, ectopic thumbs, retarded maturation of the epiphyses and delayed dental development can all be seen satisfactorily in radiographs. Chromosome counts have been normal as have metabolic and endocrine tests. Brachman's report in 1916 (Jahrb Kinderh 84:225 1916) is probably the first recorded description of this syndrome.

In one of our patients the tubular bones in the arms and legs were stenosed due to loss of width of the medullary cavities; the terminal phalanges of the fifth digits were deformed in the Kumer fashion; the middle phalanges of the second digits were hypoplastic as were the first metacarpals (Fig. 8-413). The

upper lip is deepened between the nose and mouth; the lips are thin and the upper lip is beaked; the nasal sagittal plane. The angles of the mouth are bent caudad; the grimace expression. (From Placak *et al*.)



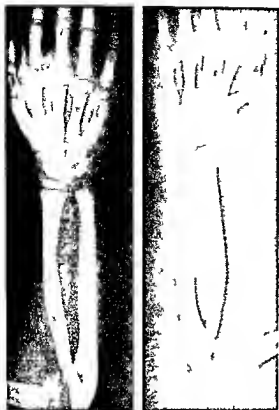


Fig 8-412 — In a Brachman de Lange dwarf a girl 5 years of age the thumbs are hypoplastic phalanges in both thumbs hypoplastic first metacarpals and hypoplastic bent proximal ends of the radius which appear to be dislocated dorsad

proximal phalanges of the great toes were hypoplastic and dysplastic. Three of the patients of Pashayan and associates and of Kurlander and De Myer had other characteristic clinical and radiographic features of the syndrome but were not mentally retarded.

REFERENCES

- Jervis G A and Stimson C W DeLange syndrome The Amsterdam type of mental defect with congenital deformations *J Pediatr* 63:634 1963
- Kurlander G J and De Myer W Roentgenology of the Brachman-de Lange syndrome *Radiology* 88:101 1967
- Lee F A and Kenny F M Skeletal changes in the Cmel de Lange syndrome *Am J Roentgenol* 100:27 1967
- Pashayan H et al Variability in the de Lange syndrome Report of three cases and genetic analysis of fifty four families *J Pediatr* 75:853 1969
- Ptacek L J et al The Cornelia de Lange syndrome *J Pediatr* 63:1000 1963

COCKAYNE'S SYNDROME is a rare combination of dwarfism and mental retardation (Fig 8-414) which begins during the 2nd year of life. Deafness and retinal atrophy were present in both of Cockayne's patients. The facies is characteristic due to loss of subcutaneous fat, sunken eyes, depressed nose, large lower jaw, and wrinkled and irregularly pigmented skin. The arms, legs, hands, and feet are disproportionately large. The head is small. In radiographs the tubular bones in the hands are short and broad in

contrast to the normal tubular bones in the feet. The calvaria is small and thickened secondary to cerebral hypoplasia. In one girl the lateral edges of the ilia were upped beyond the longitudinal axis of the body to make the iliac angles greater than 90 degrees. This iliac deformity is the converse of the iliac deformity of Down's syndrome (mongoloidism) in which the iliac angles are decreased.

In a girl 9 years of age who suffered from Cockayne's dwarfism, Fujimoto and associates found hyperproteinaemia, fasting hyperinsulinemia, and renal insufficiency with acidosis. She did not respond normally to a challenge with normal growth hormones and an intravenous infusion of arginine, which suggests that the undergrowth is not due to inability to produce growth hormones.

REFERENCES

- Cockayne E A Dwarfism with retinal atrophy and deafness *Arch Dis Childhood* 11:1 1936
- Fujimoto W Y et al Cockayne's syndrome *J Pediatr* 75:881 1969
- MacDonald W B et al Cockayne's syndrome: An hereditary familial disorder of growth and development, *Pediatrics* 25:997 1960

FETAL DWARFISM is characterized by short body length and low birth weight in comparison with gestational age. Fetal dwarfs with small heads, narrow



Fig 8-413 A B achman de Lange dwarf. A: Knees deformed by the distal phalanx of the fifth digit and hypoplasia of the middle phalanx. hypoplasia of the middle phalanx of the second digit and dysplasia and hypoplasia of the first metacarpal. B and C: smallness in caliber of long bones due to stenosis of the

medullary cavities in the bones of the arms and legs, especially. Severe coxa vara is present in the femurs. This boy was 10 years of age. Skeletal maturation was delayed to the equivalent of 4-5 years. These findings are similar to those in the Kenny dwarf.

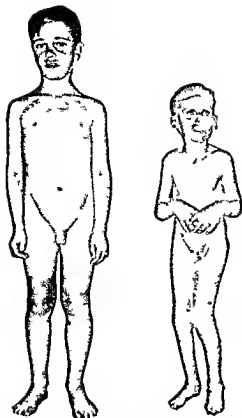


Fig 8-414 —Cockayne's type of dwarfism in a boy 10 years of age and a normal boy of the same age. Short stature, shveled faces, macrocephaly, large ears and lower jaw, and disproportionately large hands and feet are all evident. (From MacDonald et al.)

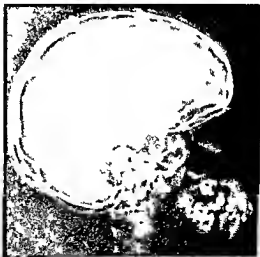
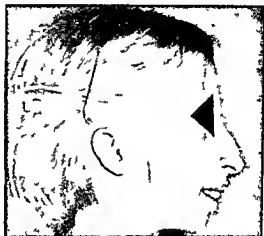


Fig 8-415 —Fetal dwarf of the bird-headed type. The height of this girl 10 years of age approximates the average for a healthy girl 5 years of age. Her head is too small, the face long and narrow, eyes are large, nose long and protruding like a beak, and the nasofrontal angle is obliterated (see lateral view). Lips are thick and everted and the lower jaw is small and pointed. (From Szalay.)

pinched facies, prominent eyes, sharply angled small lower jaws, and long beaklike noses (Fig 8-415) seem to belong to a special group and have been called the bird-headed dwarfs by Seckel. Radiographic examination discloses the smallness of all parts of the body and retarded bone maturation.

REFERENCES

- Black J. Low birthweight dwarfism. *Arch Dis Childhood* 36:633, 1961.
- Seckel H, P, C. Bird-headed dwarfs. (Springfield, Ill: Charles C Thomas Publisher, 1960).
- Warkany J, et al. Intrauterine growth retardation. *Am J Dis Child* 102:249, 1961.

Silver's syndrome is a type of fetal dwarfism with congenital hemihypertrophy, elevated urinary gonadotropins, and a variety of anomalies of sexual development. Hemihypertrophy differentiates the Silver complex from the other types of fetal dwarfism and the diagnosis is not tenable without congenital asymmetry. Miller and associates reported Wilms' tumor and aniridia with other malformations in association with hemihypertrophy. Copple and Duncan found

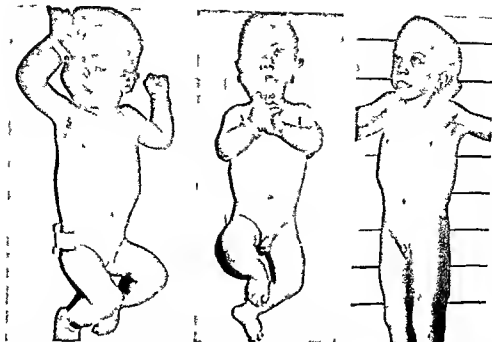


Fig 8-416—Three S-L-O dwarves at 10 and 9 months and 5 years of age. All are dwarfed and mentally retarded and have hypoplastic incompletely formed external genitalia. The heads

are small, noses are depressed with large anteverted nostrils, alveolar ridges in the upper maxillas are wide and lower jaws are small. (From Smith et al.)

adrenal carcinoma in a patient with congenital hemihypertrophy. Radiographs confirm the smallness of all parts of the patient; bone maturation is retarded. The hemihypertrophy is visible radiographically and occasionally the larger side shows more advanced bone maturation.

The regional hypertrophies associated with some neurofibromas, hemangiomas, arteriovenous fistulas and lymphangiomata have so little in common with congenital asymmetries and fetal dwarfism that they present no problems in differential diagnosis.

REFERENCES

- Copple P J and Duncan, W G III. Congenital hemihypertrophy and adrenal carcinoma. *Am J Dis Child* 111:420 1966.
 Miller R W et al. Association of Wilms' tumor with anuridia, hemihypertrophy and other congenital malformations. *New England J Med* 270:922 1964.
 Silver H K. Congenital asymmetry, short stature and elevated urinary gonadotropin. *Am J Dis Child* 97:768 1959.
 Szalay G C. Intrauterine growth retardation versus Silver's syndrome. *J Pediatr* 64:234 1964.

The S-L-O DWARVES of Smith, Lemli and Opitz were retarded mentally and microcephalic and had hypoplasia and incomplete maturation of the external genitalia. The empty facies were dominated by prominent eyes, wide depressed noses with large anteverted and flaring nostrils, wide alveolar ridges in the upper jaws and small lower jaws (Fig. 8-416). Two of three

patients had pyloric stenosis. Normal skeletal maturation and rotational errors of one kidney were shown in radiographs.

REFERENCE

- Smith D W et al. A newly recognized syndrome of multiple congenital anomalies. *J Pediatr* 64:210 1964.

The RUBENSTEIN-TAYBI DWARF (Figs. 8-417 and 8-418) is characterized by short stature, mental retardation, skeletal retardation, large and broad thumbs and great toes, microcrania, highly arched palate, bulbous nasal tip and large nostrils and antimongoloid slant of the palpebral fissures. Superficial hemangiomas are common in the skin of the forehead and nape. Reflexes are usually hyperactive and the testes may be undescended. In radiographs, widening of the phalanges in the thumbs and great toes and skeletal retardation are evident.

REFERENCES

- Johnson C F. Broad thumbs and broad great toes with facial abnormalities and mental retardation. *J Pediatr* 68:942 1966.
 Rubenstein J H and Taybi, H. Broad thumbs and toes and facial abnormalities. A possible mental retardation syndrome. *Am J Dis Child* 105:589 1963.

The KENNY DWARF has the following characteristics: reduced stature, retarded skeletal maturation, normal mentality, congenital stenoses of the medulla

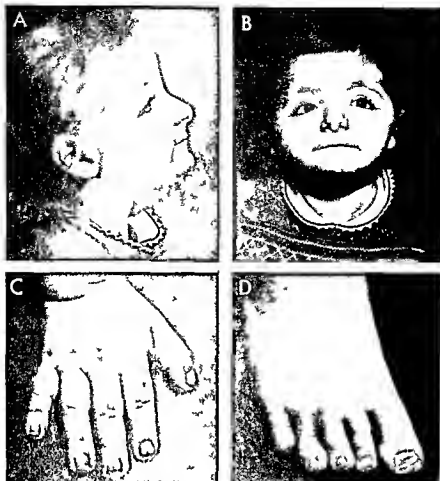


Fig 8-417—Rubinstein-Taybi dwarfism. 4 years of age. The caudal end of the nose and the nostrils are large and prominent.

The ears are large. The ends of the fingers and toes are enlarged and flat (Figs 8-417 and 8-418 from Johnson).

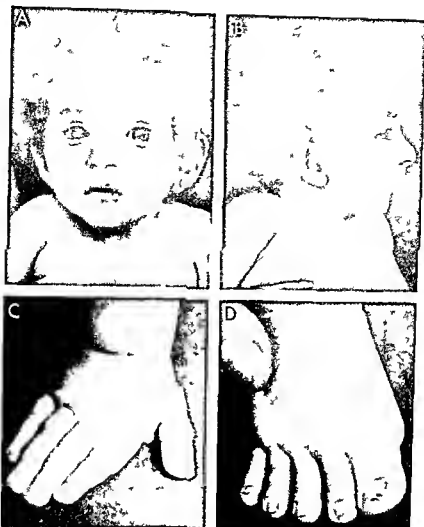


Fig 8-418.—Rubinstein Taybi dwarfism in a Mexican boy 8 months of age. The nose and nostrils are as large as the ears.

The ends of all fingers and toes are enlarged except the second and flattened.

ry spaces in the tubular bones and calvaria, coupled with transitory hypocalcemic spasmodophilia. The typical radiographic changes in a dwarfed mother and her dwarfed son are depicted in Figures 8-419 and 8-420. The dwarfism is proportionate throughout the skeleton in both patients. The dwarfed mother menstruated normally after her 12th year and conceived three times. She gave birth to one normal son. The hypocalcemia was not satisfactorily explained; it might have been caused by episodic hypoparathyroidism or episodic hypercalcaemia. A third example of this syndrome was described by Frech and McCalister. Epstein and associates discovered hereditary stenosis of the long bones in a father and son who however had no other manifestations of the Kenny dwarf. Garn and associates found medullary stenosis of the metacarpals in 6% of healthy Costa Rican

women. We have seen severe generalized stenosis of the long bones in one de Lange dwarf.

REFERENCES

- Caffey J. Congenital stenosis of the medullary spaces and the calvaria in two proportionate dwarfs: mother and son coupled with transitory hypocalcemic tetany. *Am. J. Roentgenol* 100:1 1967.
- Epstein, C. J. et al. Hereditary dysplasia of bone with kyphosis, contractures and abnormally shaped ears. *J. Pediatr* 73:379 1968.
- Frech R. S. and McCalister W. H. Medullary stenosis of the tubular bones with hypocalcemic convulsions and short stature. *Radiology* 91:457 1968.
- Garn, S. M. et al. Medullary stenosis in Central America. In Report of the Department of Growth and Genetics, Fels Research Institute, Yellow Springs, Ohio, January 1968.
- Kenny F. M. and Lunarelli, L. Dwarfism and cortical thickening of the tubular bones. Transient hypocalcemia in mother and son. *Am. J. Dis. Child* 111:201 1966.

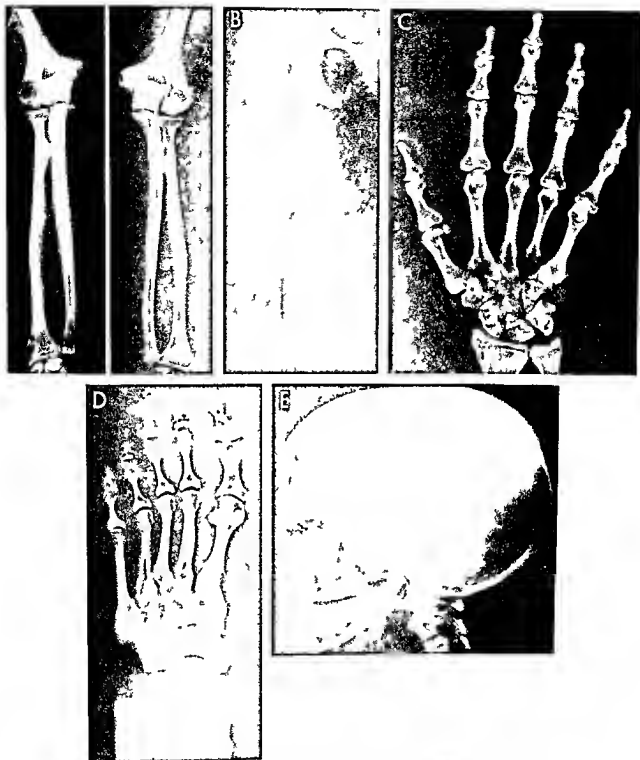


Fig 8-419 — Kenny dwarf. Congenital stenosis of the medullary cavities in the bones of a dwarfed mother at 41 years of age. A, humerus; B, femur; C, hands; D, feet; E, calvaria.

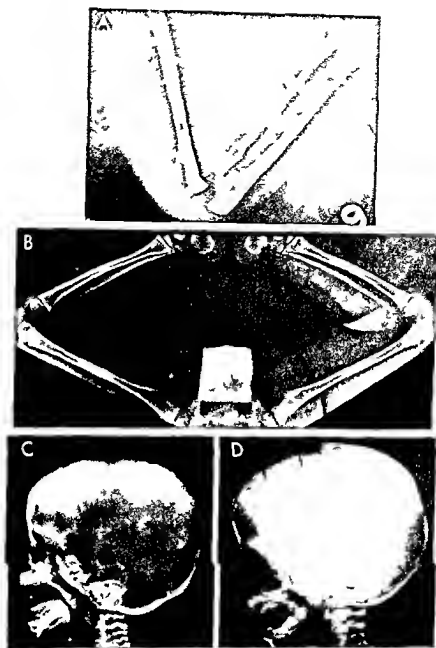


Fig 8-420 Sterosis of the medullary spaces in the son, 29 months of age, of the mother in Figure 8-419. A, arms; B, legs; C, caudal at 14 days; and D, at 29 months.

THANATOPHORIC DWARFISM described by Maroteaux and associates resembles severe achondroplasia anatomically and radiographically in the fetus and newly born infant in many ways. Maroteaux and colleagues believe that the high frequency of fetal death and death in newly born infants during the first hours of life, the very severe changes in the long bones and the absence of these kinds of changes in families with less severe types of achondroplasia warrant the classification of this condition as a separate entity. The most conspicuous clinical findings include high incidence of deaths in utero and during the first hours after birth, short limbed dwarfism, large head, small face, flattened nose and large fontanels. The skin and subcutaneous tissues are excessive in the extremities and the muscles are generally hypotonic.

In radiographs the bones of the extremities are disproportionately short and incurved near their ends. The hands and feet are disproportionately large although their tubular bones show changes similar to those in the extremities. The ribs are short and the costal cartilages elongated proportionately. The thorax is small in caliber at all levels because of under growth of the ribs. This smallness of the thorax reduces respiratory amplitude and vital capacity and induces hypoxia, which is thought to be the cause of the early postnatal death. Smallness of the foramen magnum may also be an important cause of early death, especially prenatal death. Cyanosis is the rule. The vertebral bodies are flat and very thin with dis

proportionately deep intervertebral spaces between the small flat ossification centers in the vertebral bodies.

The mechanism of genetic transmission has not been finally determined. Until more convincing evidence accumulates which indicates that the entity is not just a severe rapidly fatal type of achondroplasia, we prefer to call this condition thanatophoric achondroplasia. Langer and associates presented radiographic findings which they claimed differentiate thanatophoric dwarfism from severe achondroplasia. The changes in their patients were quantitative and not qualitative and are therefore of uncertain differential value. Both parents of their four patients were normal as were those of seventeen to whom they referred.

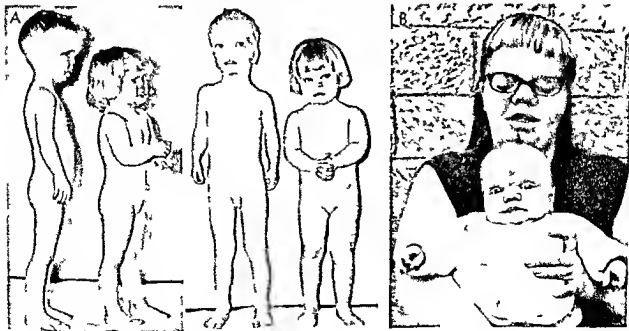
REFERENCES

- Maroteaux P. *et al*. Le nanisme thanatophore. *Presse med* 75:2519, 1967.
Langer L. O. *et al*. Thanatophoric dwarfism. *Radiology* 92:285, 1969.

ROBINOW SILVERMAN SMITH DWARFS are short limbed and have depressed noses and bulging foreheads (Fig. 8-421). They differ from achondroplasts because the extremities are more shortened in the forearms and shanks than in the root segments, the upper arms and thighs, the hands are normal, the orbits are widely spread, palpebral fissures are widened and the teeth are malaligned. Radiographically

Fig. 8-421—Robinow Silverman Smith dwarfs. A, two children, 55 and 35 months of age, with mesomelic shortening of the legs and arms due to shortening of the forearms and shanks. Inferior ball distances are increased and palpebral fissures are widened. The foreheads bulge forward and the nasal bridges are depressed and wide. The lateral segments of the lower limbs are depressed

exposing an undue amount of tibiae. The nostrils are large and lower jaws small. B, mother and infant, 2 months of age. Crowded malalignment of the teeth is visible in the mother, and the infant has characteristic deformities of the head and face. (From Robinow *et al*.)



they lack the cardinal achondroplastic features of rhizomelic (root) shortening of the arms and legs progressive caudal stenosis of the interpediculate spaces of the lumbar vertebral bodies and stenosis of the greater sciatic notches. Both sexes were affected. Both clinical and radiographic changes are present at birth but are not progressive.

REFERENCE

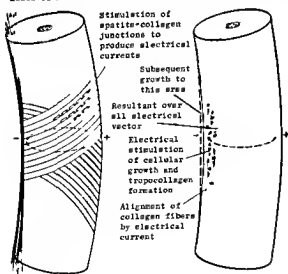
- Robinow M, Silverman F N and Smith H D. A newly recognized dwarfing syndrome. *Am J Dis Child* 117: 645 1969

Bone Lesions Due to Physical Agents

Stress effects of the electrical potential in bone may explain some of the localized thickenings and thinning of the cortical walls of tubular bones after recurrent trauma and overload. In Becker's view, the generation of electrical currents in bone under stress is explained by the transducer action of myriads of natural apatite-collagen diodes. In bone bent by the stress of overload the concave (compression) side becomes electrically negative and the convex (tensile) side becomes electrically positive. A significant and measurable current flows from the negative to the positive side. During stress of overload the

Fig 8 422—Schematic picture of both halves of a self contained electrical control system of a bone under a bending stress. At the left, the major stress line activates the apatite-collagen PN diodes and produces many small local electrical currents all oriented in the same direction, which produce an overall electrical vector between the negative concave compression side and the positive tension side. On the right, these local vectors stimulate deposition of newly formed collagen along the lines of stress, and the overall vector stimulates the osteoblasts in the negative segment. New bone is formed in the negative concavity or aligned with the collagen fibers longitudinally and parallel to the vector forces. (From Becker.)

Lines of mechanical stress



bone thickens on the concave (compression) side which is negative electrically and becomes thin on the convex (tensile) electrically positive side (Fig 8-422). The implantation of battery powered but powerful electrodes adjacent to the cortical wall and inside the medullary cavity of normal bone also results in massive local cortical thickening on the side of the negative electrode. Twenty days after the electrodes were removed the earlier cortical thickenings were resorbed. Microscopic examination of the thickened bone induced electrically, showed an accelerated rate of mitosis of local osteoblasts at the site of the negative electrode which probably explains the cortical thickening at this site. Increase in the blood supply of the concave side with decrease in the blood supply in the convex side may be the primary cause of the cortical thickenings.

REFERENCE

- Becker R O. The electrical control of growth processes. *Resident Physician* p 69 April 1968

Electrical trauma to bone results from several possible mechanisms according to Brann and Moseley. Pure secondary mechanical trauma may cause fractures and displacements from sudden muscular contractions which are induced by direct electrical stimulation of the muscles after electrical injury to the brain or spinal cord. Compression fractures of the vertebral bodies are induced by this mechanism when it causes severe flexion contractions of the spinal column. Focal and regional bone necrosis may be due to direct overheating of the bone. The growing epiphyseal cartilages are especially susceptible to this thermal factor. Fine fractures (fibrillations) are probably due to local thermal evaporation at the site of contact of the electric current and the bone. Cortical thickenings have been found in children only similar to the cortical thickenings which develop after severe burns as well as failure of tubulation of growing bones. The discrete patches of rarefaction and the radiolucent holes found in some bones have not been satisfactorily explained.

REFERENCE

- Brann L B and Moseley J F. Bone changes following electrical injury. Case report and review of the literature. *Am J Roentgenol* 97: 682 1966

Bone lesions due to excessive cold are seen most often in the fingers and are due to frostbite. The epiphyses of growing bones are especially vulnerable to cold and exposed epiphyses may be completely destroyed and disappear. Longitudinal growth of the affected bone is of course stopped or reduced. The terminal phalanges are customarily the most exposed to cold and the most frequently injured by it (Fig 8-423). The epiphyses in the phalanges of the thumbs are usually protected from cold by flexion of the thumbs into the palms of the hands and then cover of the thumbs by flexion of the fingers around them. In a

Florkiewicz L. and Kozłowski, K. Symmetrical epiphyseal destruction by frostbite Arch Dis Childhood 37 51 1962.
 Thelander H E. Epiphyseal destruction by frost bite J Pediatr 36 105 1950

FRACTURES

Mechanical stress and injury to healthy growing bones produce a variety of lesions and deformities—fractures and dislocations of the shafts, lacerations and compression of the cartilage plates with displacement of the fragments, fractures of the epiphyseal ossification centers, cupping of the metaphyses secondary to injury to the epiphyseal arteries, enchondromas of uncalcified cartilage due to injury to the metaphyseal arteries, cortical thickenings (traumatic involucrum) with and without fractures of the shafts and infarctions at the levels of the metaphyses. All of these traumatic lesions may be present singly or in a variety of combinations. Residual errors in modeling and growth of the shafts and epiphysis, both over and underconstruction and over and undergrowth may develop later. The actual direction of growth may be altered in the case of residual abnormal position of a terminal fragment which contains the proliferating cartilage. When growing bone is injured and there is an associated chronic paralytic disorder such

Fig 8-424—Effects of excessive heat on growing bones. A, external cortical thickening and destruction of cartilage at the ankles of a boy 5 years of age. B, fusion of the tibiae due to external cortical thickenings 5 years after a third degree burn at the site. C, para-articular calcifications in the soft tissues of the hips following regional burns of the soft tissues. (From Evans and Smith.)

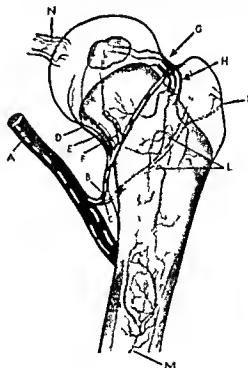


Fig 8-423—Destruction of the epiphyseal cartilages of the terminal phalanges of fingers 2-4 of a boy 5 years of age who had had severe frostbite two years before. Similar changes were present in the bones of the other hand. Thelander's description of fingers from frostbite in that it changes are usually confined to the proximal and middle phalanges. (Courtesy of Dr. Kazimierz Kozłowski, Royal Alexander Hospital for Children, Sydney, Australia.)

patient 10 months of age Falk found external cortical thickenings of the phalanges and of the fifth metatarsal and the neighboring ulna as well. In Thelander's patient 9 years of age who had suffered frostbite two and one-half years before the epiphyseal cartilages had disappeared completely and growth had been stopped permanently in the frozen epiphyses.

Injuries due to excessive heat usually follow burning of both the soft tissues and the bones. Regional radiographic changes in the bones include rarefaction, cortical thickenings, destruction of the epiphyses and the formation of osteophytes (Fig 8-424). The burned necrotic para-articular and juxtaosteal soft tissues may calcify later. Ankylosis of the joints may follow destruction of the articular cartilages.

REFERENCES

- Bigelow D R. and Ritchie G W. The effects of frostbite in childhood. J Bone & Joint Surg 45-B 122 1963.
- Evans E B. and Smith J R. Bone and joint changes following burns. A roentgenographic study. J Bone & Joint Surg 41 A 785 1959.
- Falk, W. Beiträge zur Pathogenese und Klinik akuten entzündlicher Knochenerkrankungen im Kindesalter. Ann. paediat. 173 23, 1949.

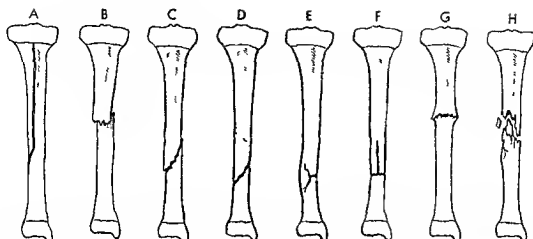
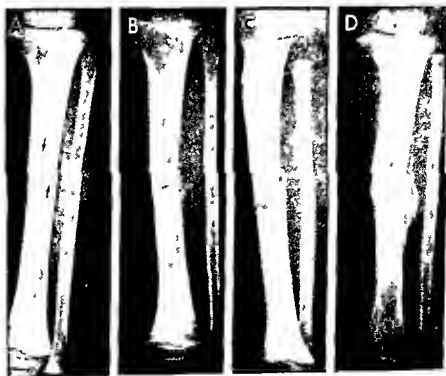


Fig 8 425 — Classification of fractures according to the course and nature of the fracture line. A, longitudinal; B, transverse; C,

oblique; D, spiral; E, incomplete transverse; F, longitudinal transverse; G, transverse impacted; H, comminuted.

Fig 8 426 — Fracture of the tibia in a boy 19 months of age. A, simple oblique fracture in a film made a few hours after the injury; B, 16 days after A, and without treatment, a wide branched fissure-fracture and slight angulation deformity have developed

in the original film, a small amount of callus was visible; C, a lateral projection of B; D, three weeks after B and C were made, a long fusiform incompletely mineralized mass of callus surrounds the ends of the fracture fragments.



as postpoliomyelitic paralysis or myelomeningocele with paralyzed muscle, bizarre residual deformities of the shafts are common, owing to absence of the usual molding and compressing effect of normal muscles around a broken growing bone. Severe secondary deformities may follow injury to the blood supply of growing bone when the bone itself is not injured. These residual deformities of growth do not appear after injuries to mature bone.

The site, frequency and nature of traumatic bone lesions are all conditioned by the age of the patient. The fetal bones, effectively protected from external trauma by the amniotic fluid and thick uterine wall, are rarely traumatized, save by penetrating injuries such as gunshot and knife wounds. However, chronic intrauterine stresses operating on the fetus in faulty position may cause changes in the fetal bones and cause the disorder we call "prenatal bowing of the long bones" and several local deformities, especially of the mandible and facial bones. During parturition and most frequently in breech deliveries, a wide variety of traumatic lesions may be induced—fractures of the shafts and epiphyseal cartilages, traumatic involucra and dislocations, especially at the hips. The latter may also be triggered by stretching of the joint capsules immediately after birth when the neonate is inverted and held by the heels, head down, to promote drainage of the respiratory tract. The most common obstetric fractures are those in the skull and the clavicles.

During the first postnatal year fractures are relatively rare. Multiple severe fractures do develop, however, when the mother falls on the child or during automobile accidents. Sliding sides of cribs are special sources of injuries to the bones of the legs and arms of infants. Most willful assaults on children occur during the first two years of life and cause the clinical problem which is called the "battered baby" or "battered child" syndrome, in which fractures and dislocations and traumatic involucra often offer the first diagnostic lead. After age 2 the radius is the most commonly fractured single large bone, the high incidence of these fractures continues and increases until adolescence. Fractures of the phalanges and metacarpals are common after the 1st and 2nd years. "Toddler's fracture" of the distal half of the tibia is common during the period between the 2nd and 5th years. Throughout childhood, fractures of the clavicle are common. During later childhood, fractures occur in all parts of the skeleton, many of them induced by the popular juvenile sports such as football, basketball, baseball, sking, sledding, skate-board hopping and horseback riding. At all ages, however, the automobile is the principal killer andcripler of children and smasher of the skeletons of healthy children. The serious hazards of snowmobiles to children are already evident.

A schematic depiction and classification of fractures of the shaft of a long bone are shown in Figure 8-425, according to the location, course and number

of fragments. The typical serial radiographic changes in an untreated transverse oblique fracture of the tibial shaft are depicted in Figure 8-426.

BONES OF THE HANDS are frequently broken in children in a variety of ways and are similar to the traumatic lesions in the other parts of the skeleton. Injuries to the cartilage plates, between the ends of the shafts and their epiphyseal ossification centers, are common in all of the tubular bones of the hands, with dislocation of the epiphyses to which tags of the fractured shafts are often attached. The distal phalanges are especially exposed to trauma in games played with a ball and in closing doors, particularly automobile doors (Figs 8-427 to 8-429). The shafts of the other phalanges and metacarpals may be fractured at any level and also at their cartilage plates (Figs 8-430 to 8-435). Metacarpal fractures are shown in Figures 8-436 to 8-438. The proximal end of the shaft of the first metacarpal and its cartilage plate are occasionally injured, but the true Bennett fracture with disruption of the metacarpo-trapezium joint is rare in children.

Carpal bones are rarely broken prior to adolescence because, during early childhood, these ossification centers are surrounded and protected by thick cushions of cartilage. In older children, the navicular is occasionally broken (Figs 8-439 to 8-442).

BONES OF THE FOREARM are broken frequently. In our experience, the shaft of the radius is fractured more often than any other large bone in the skeleton,

Fig 8-427—Comminuted crush injury to the distal phalanx of the thumb. The shaft has two long longitudinal fracture lines. The cartilage plate is lacerated transversely and the epiphyseal ossification center is impacted on one side of the shaft. An automobile door slammed on the thumb of this boy 6 years of age.





Fig 8 428 (left) — A t anverse hyperextens on fracture of the cartilage plate at the proximal end of the distal phalanx of the 3rd digit with longitudinal fracture of the epiphyseal ossification center and dorsal avulsion of the epiphyseal segment which also has a teg of the end of the shaft attached to it. This girl was 12 years of age. B avuls on hyperextension fracture of the dorsal

segment of the fused epiphyseal ossification center of the distal phalanx. 3 digits left hand of a boy 13 years of age.

Fig 8 429 (right) — Oblique fracture through the shaft and epiphyseal ossification center and transverse laceration of the cartilage plate of the distal phalanx. 4 digits of a boy 15 years of age (Salter cartilage plate injury type IV).

Fig 8 430 (left) — Angle fracture at the base of the shaft of the middle phalanx. 4th digit. The epiphyseal ossification center is displaced slightly laterally due to transverse laceration of its cartilage plate. Also A, immediately after the injury and B 20 days later when distraction of the cartilage plate and also the shaft fracture fragment are more clearly seen. (Salter cartilage plate injury type II).

Fig 8 431 (right) — Cartilage plate injury at the proximal end of the proximal phalanx of the 4th digit with oblique impact on the displaced ossification center on the broken end of the shaft, and a 90° rotation of the broken shaft on its long axis. Probably a Salter type I injury to the cartilage plate with unusual displacement and rotation of the shaft in its epiphyseal ossification center. This girl was 11 years of age.

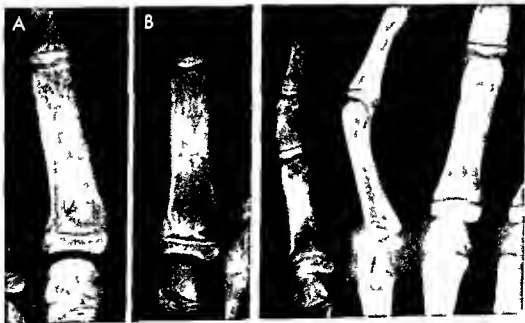




Fig 8-432 (left) - Angle fracture at the base of the proximal phalanx of the thumb with a tag of the broken shaft attached to the epiphyseal ossification center. Both are displaced medially (Salter type II injury).

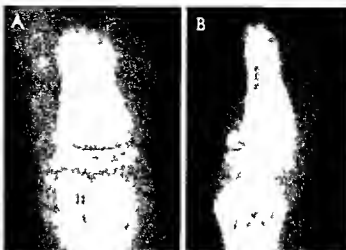


Fig 8-433 (right) - Angle fracture at the base of the distal phalanx of the left thumb. The cartilage plate appears to be broken also and transversely and the epiphyseal ossification center is displaced dorsally along with the angular tag of the shaft (Salter type II injury to the cartilage plate and shaft). This boy was 9 years of age. A, frontal and B, lateral projections.

Fig 8-434 - Fracture of the base of the proximal phalanx of the 3rd digit (arrow) and the shaft (oblique spiral) of the 2nd metacarpal (arrow). The phalangeal deformity is a Salter type II with marked displacement of the smaller fragment. This girl was 15 years of age.



Fig 8-435 - Fracture (arrows) of the epiphyseal ossification center of the 5th digit with transverse laceration of the cartilage plate and lateral displacement of the lateral epiphyseal fragment. This is a Salter type III injury to the cartilage plate and epiphyseal ossification center.



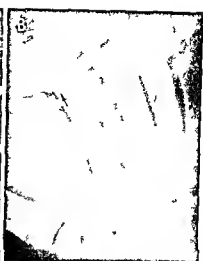


Fig. 8-436 (left) — Spiral fracture of the shaft of the 3rd metacarpal without injury to the cartilage plate. The boy was 10 years of age.

Fig. 8-437 (right) — Impacted fracture at the distal end of the

shaft of the 2nd metacarpal. This appears to be an angulated fracture at the end of the shaft with a tag of the shaft attached to the slightly displaced epiphyseal ossification center. The boy was 12 years of age. A: frontal; and B: lateral oblique projections.

Fig. 8-438 (left) — Angle fracture at the proximal end of the 1st metacarpal which appears to run into the cartilage plate. This might have developed into a Bennett fracture with displacement of the trapezium metacarpal joint of an adult. It is probably a Salter type II injury of the cartilage plate. The girl was 11 years of age.

Fig. 8-439 (right) — Transverse fracture of the carpal navicular of a boy 11 years of age. The fragments are separated owing to slight ulnar deviation of the hand at the wrist.



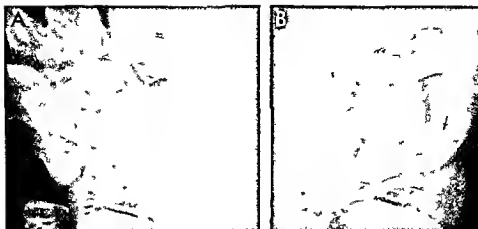


Fig 8-440.—Fracture of the navicular which is visible immediately after the injury (A) but is marked by a sclerotic band (arrow) of opaque internal callus 21 days later (B). Both films were

made with the hand in ulnar deviation. The boy was 13 1/2 years of age.



Fig 8-441.—Horizontal transverse fracture of the navicular of a boy 14 years of age who had fallen on his hand and then had pain in the wrist with point tenderness over the navicular.

Fig 8-442.—Schematic drawing of the different types of breaks in relation to arterial circulets on navicular fractures. A, fracture between the two sources of arterial blood, with good prognosis because each fragment has a satisfactory arterial supply.

B and C, fractures at the central end and the proximal levels in which the blood supply of the proximal segment is impeded or lost. (From Cave.)





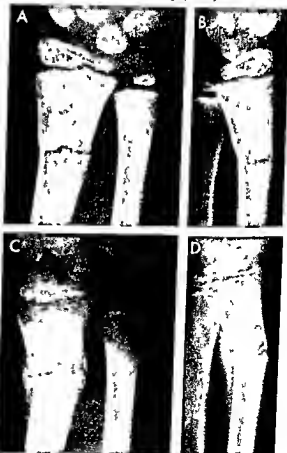
Fig 8-443—Calcification of the intraosseous membrane during healing of a fracture in the midshaft of the ulna of a girl 16 years of age

and the distal third of the radial shaft is fractured much more often than the middle and proximal thirds. The epiphyseal ossification center in the distal radial epiphysis is rarely broken. Radial fractures do not become common until after the 2nd year of life but these absolute and relative high incidences of these fractures continue until adolescence. Of 100 consecutive fractures of the distal third of the radius that we studied with Dr Jocelyne Ledesma 67 occurred in boys and 33 in girls. All but 1 of these fractures were transverse or obliquely transverse. Only 2 were comminuted. The edges of the fragments were both smooth and rough and occasionally jagged. Compaction of the fragments was more common than distraction in the ratio of 61:31, in 8 distraction was so slight that its recognition was doubtful radiographically. The ulna was also broken in its distal third in 37 of these patients. The cartilage plate of the radius was injured and deformed in 16 of the 100 cases. 11 of these were Salter type 2 deformities and 5 were Salter type 1. The distal radial fragment was usually dorsiflexed. A fracture line was not visible in 48 of 61 impacted fractures and incompletely visible in 13. In follow up radiographic examinations made three to four weeks after the original examination of impacted fractures which had invisible fracture lines, opaque internal callus outlined what appeared to have been complete transverse clefts through the radial

shaft. From this experience and others, we believe that incomplete fractures in the distal third of the radius are rare. Midshaft fractures of radius or ulna more commonly the ulna may be followed by calcification of the intraosseous membrane (Fig 8-443).

Distraction fractures in the distal third of the radius are readily seen radiographically owing to the radiolucent gap between the edges of the fragments which represents the soft tissues and fluid between the edges of the fragments (Fig 8-444). When the

Fig 8-444—Transverse fracture of the distal third of the radius with moderate longitudinal distraction. On A and B, frontal and lateral projections made immediately after the injury. In A, a transverse radiolucent strip separates the fracture fragments. The lateral and dorsal ends of the fracture line are closed because the distal fragment is flexed slightly laterad and dorsad. The medial and ventral ends of the fracture lines are widened. In C and D, made 30 days later, the flexion deformities of the distal fragment are increased and the fracture line is widened by the increased flexion in comparison with A and B, also by resorption of bone calcium from margins of both fragments. Substantial opaque external callus and some opaque internal callus have formed on the flexion or compression side of the fracture line. This relative increase in callus on the flexion side is probably due to its relative increase in blood supply. Opaque callus is not visible on the tensile or stretch side of the shaft, probably owing to its relative vascularity. There may be, and probably is, substantial nonopaque callus which is invisible radiographically.



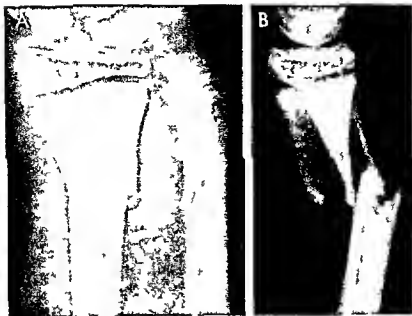
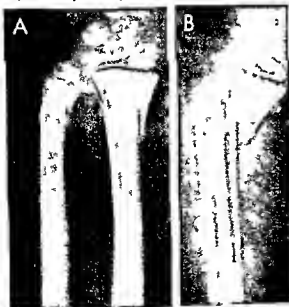


Fig 8-445 —Transverse fracture of the radial and ulnar shafts at the same level. In A, frontal projection there is no fracture line at the junction of the radial fragments but there is a deep transverse sclerotic band caused by overlap of the radial fragments which is clearly seen. In B, lateral projection in the ulna

the distraction fracture causes the standard transverse band of diminished density between the fragments because there is no overlap and the fragments are distracted from each other longitudinally.

Fig 8-446 —Transverse fracture of the distal thirds of the radius and ulna with deep overlap of fragments in both bones. The distal fragments have been displaced dorsad and slightly latered then pulled proximally several millimeters to produce the overlap. Both distal fragments are foreshortened in the frontal projection due to the oblique projection caused by the dorsiflexion. The girl was 7 1/2 years of age. A, frontal and B, lateral projections.



fragments are displaced and then drawn toward each other longitudinally so that the terminal segments of the fragments overlap. The zone of overlap causes a transverse sclerotic band due to the greater absorption of the x-rays by the two overlapping terminal segments in one of the projections. The depth of the overlap determines the depth of the sclerotic transverse band (Figs 8-445 and 8-446). Inversion of the broken edges of the fragment may also cause additional but usually thinner transverse sclerotic bands (Figs 8-447 and 8-448). During healing, opaque callus formation becomes evident first and is more abundant on the compression (flexion) side while the stretch (tension) side remains free of ossified callus (Fig 8-449). This is probably due to relative hyperemia on the compression side and relative oligemia on the tensile side. A severe injury to the cartilage plate of the radius with simultaneous fracture of the ulna is shown in Figure 8-450.

Impacted fractures of the distal third of the radius are the rule and they produce a variety of deformities in which the fracture line may be absent or incompletely demonstrated (Figs 8-451 to 8-455). We have seen one example of striking rarefaction of the distal fragment during healing in which there was a deep inversion of the cortical edge of the distal fragment (Fig 8-456). Impacted fractures may be invisible in the frontal projection (Fig 8-457).

In several cases in which impacted fractures have the early appearance of being incomplete, films made after healing three to four weeks later show transverse strips of opaque internal callus. These indicate

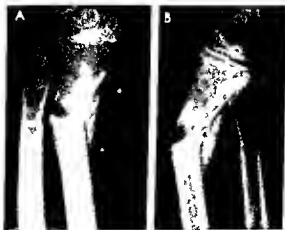
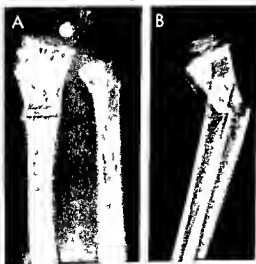


Fig 8-447 — Transverse fracture of the distal third of the radius with an unusual transverse radiolucent fracture band between the fragments and an additional transverse band of increased density on the proximal edge of the distal fragment due to deep inversion of its distal edge. **A**, frontal; and **B**, lateral projections. The distal fragment is palmar flexed and also flexed medially. The cortical wall is fractured on the tensile lateral side where there is a wide gap between the cortical edges of the two fragments. The radiolucent band tapers toward the ulna and disappears when

the medial cortical wall is reached. The latter is buckled slightly externally but there is no visible break in its continuity. The image of the cartilaginous plate of the radius is partially obliterated due to being tilted from its usual transverse position into the oblique by dorsiflexion of the entire distal fragment. Five months later the entire distal fragment was resorted possibly secondary to injury to the periosteal arteries followed by local ischemia of the cortex (see Fig 8-458).

Fig 8-448 — Transverse fracture of the distal thirds of the radial and ulnar shafts with irregular sclerotic strips in the radius and sclerotic patches in the ulna due to inversion of the edges of the fragments. Also, some small comminuted fragments are present in both **A**, frontal; and **B**, lateral projections. There are additional double sclerotic lines due apparently to inversion of two broken fragments of the inverted edge of the distal fragment on the dorsal compression side of the dorsiflexed distal fragment. The patchy scleroses on the edge of the ulnar fragment cannot be satisfactorily evaluated because this fragment is inadequately seen in lateral projection (**B**). The lateral cortical wall of the radius is buckled externally at the level of the fracture line and the medial cortical wall to a lesser degree.

Fig 8-449 — Transverse fracture of the distal third of the radial shaft with marked lateral flexion in **A**, and dorsiflexion in **B**, 28 days after injury and treatment in a plaster cast. Opaque callus has accumulated in large amounts on the lateral and dorsal concave sides of the radius (compression on sides of the flexed distal fragment). On the convex tensile sides there is striking absence of external opaque callus; there is also little or no opaque internal callus in the medial and ventral halves of the fracture line (the convex tensile or stretched sides). In **A**, the cartilage plate is obliterated owing to the oblique position due to dorsiflexion. One must bear in mind that nonopaque callus is invisible radiographically and substantial amounts of it may be present and unappreciated radiographically. This boy was 9 years of age.



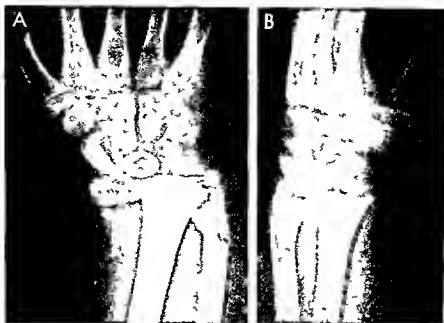


Fig 8-450.—Injury of the cartilage plate at the distal end of the radial shaft with simultaneous fracture of the ulnar shaft. The cartilage plate of the radius is completely lacerated transversely and the ossification center is displaced along with the wrist and hand laterad and dorsad. A small tag of the shaft is attached to

the displaced radial epiphyseal ossification center (Salter injury type II). The fragments of the ulna are slightly distracted and its distal fragment is flexed laterad. This boy 10 years of age fell from a platform onto his hand. A, frontal and B, lateral projections.

Fig 8-451.—Transverse fracture of the distal third of the radius with impaction of the fragments and dorsiflexion and slight lateral flexion of the distal fragment. The styloid process of the ulna (A, arrow) is broken and a small distal styloid fragment is displaced laterad. The edges of both fragments are spiculated and a jagged transverse sclerotic line crosses the lateral half of the broken radial shaft. This is due to inversion of the edge of the cortical wall. The image of the epiphyseal plate is partially closed due to tipping of its usual transverse plane into an oblique plane secondary to its dorsiflexion. This boy was 12 years of age. A, frontal and B, lateral projections.

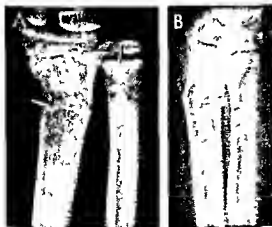


Fig 8-452.—Impacted fracture of the distal third of the radius with partial obliteration of the fracture line in both A, frontal and B, lateral projections. Due to inversion of the edge of the dorsal cortical wall (B). In A the cortical walls are buckled externally at both lateral and medial sides and most of the fracture line itself is obliterated. The central transverse strip of increased density distal to the poorly seen fracture line is due to the inverted edge of the distal fragment posteriorly (B). A faint ventrodorsal fracture line extends ventrad and caudad in steplike course from the posterior inverted cortical edge forward across the medullary cavity and through the ventral cortical wall at a lower level. This boy was 9 years of age.

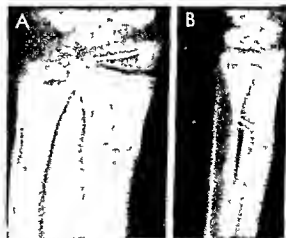




Fig 8-453—Trauma to the distal third of the radius with external buckling of the lateral cortical wall and only slight local deformity of the underlying spongiosa. A fracture line is not visible. This boy was 7 years of age. Films 22 days later disclosed internal callus which extended the full width of the shaft, indicating that a complete but invisible transverse fracture had been present.



Fig 8-454—Impaction fracture of the distal third of the radial shaft without a fracture line in either frontal (A) or lateral (B) projection. In A there is a barely discernible shallow bulge of the lateral cortical wall (arrow). At the same level in B the ventral cortical wall is buckled internally. The findings are conclusively diagnostic in both projections but could be uncertain from the frontal projection alone. This girl was 2 years of age.

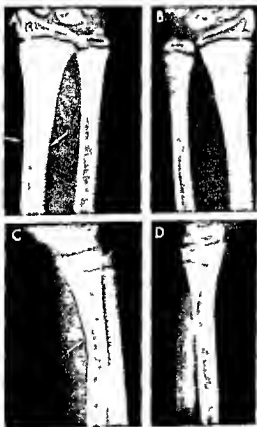


Fig 8-455—Impacted greenstick fracture in the distal third of the right radial shaft with slight lateral bulging of the cortical walls in A (frontal projection) and dorsally on the distal fragment in C (lateral projection) but without suggestion of fracture line in either projection. B and D: The normal left side. This boy was 12 years of age.

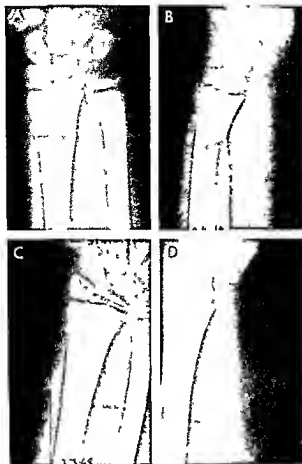


Fig 8-456 — Fracture of the distal third of the radial shaft with deep inversion of the edge of the distal fragment and later rarefaction of the distal fragment probably due to injury to the periosteal arteries at the level of the inversion and chronic ischemia of the cortical walls of the distal fragment. A, frontal and B, lateral projections obtained immediately after the injury. C and D, made five months later.

that impacted fractures without earlier radiographic fracture lines are actually complete and extend across the entire transverse and ventrodorsal diameters of the shafts (Figs 8-458 to 8-461).

Midshaft fractures of the radius are usually visible and readily detectable in roentgenograms (Fig 8-462). These fractures are rarely longitudinal or comminuted with marked displacement of the fragments.

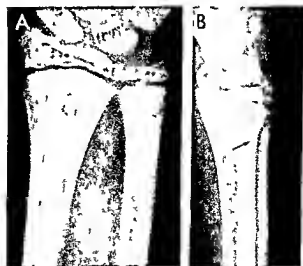
Fractures of the proximal third of the radius and ulna are of several varieties. Breaks in the proximal part of the ulna are often accompanied by ventral dislocation of the radius at the elbow (Monteggia's fracture-dislocation, Figs 8-463 and 8-464) when the injury occurs with the elbow in extension. When the elbow is injured in flexion, however, the radius is dislocated dorsad (reversed Monteggia's fracture, Fig 8-465). Different types of fractures at the proximal end of the radius and ulna are shown in Figures 8-466 to 8-474.

Shortening of one of the forearm bones by fracture often causes fracture of the other bone or dislocation at the distal or proximal radioulnar joint (Fig 8-475). When the ulna is broken and shortened in its middle or proximal third, the radial head may be dislocated forward or backward to produce the Monteggia fracture. When the radius is broken in its middle or proximal third and shortened, the distal radioulnar joint dislocates to produce the Galeazzi fracture.

The fat pads at the elbow in the olecranon fossa (dorsal) and the coronoid fossa (ventral) are frequently displaced out of the fossa during traumatic injuries and become clearly visible in radiographs made in lateral projections of the elbows (Fig 8-476). The anterior fat pad in the coronoid fossa is often visible in normal elbows as a thin strip of radiolucent fat density ventrad to anterior edge of the humeral shaft. All of the pads are extracapsular in some patients (Norell) and partially intracapsular in others, but are always external to the synovial layer. Flexion at the elbow increases displacement of the fat pads. The two anterior fat pads (coronoid and radial) are superimposed on each other when they are displaced forward and viewed in lateral projection. Demonstration of the dorsal olecranon fat pad behind the humerus always indicates an abnormality, usually increased intra-articular pressure and distention of the articular capsule by fluid, often blood after trauma or pus in pyarthrosis. The neighboring bones need not be injured. The tendon of the triceps muscle is also displaced forward when the fat pad is displaced forward by the fluid distended joint.

Partial dislocation of the radial head alone is a common clinical diagnosis but is rarely demonstrable

Fig 8-457 — Fracture at the distal end of the radial shaft which is invisible in frontal projection (A) but presents a diagnostic indentation of the cortical wall in lateral projection (B). There is no fracture line. This girl 12 years of age had fallen on her outstretched hand.



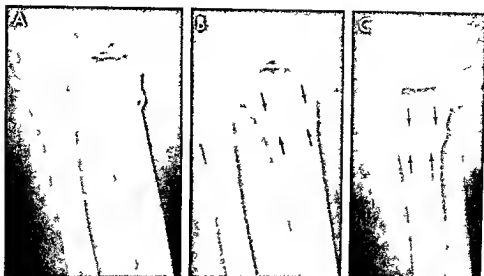
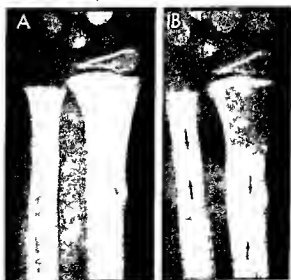


Fig 8-458—Compacted transverse fracture near the distal end of the left radial shaft. In A, made 3 hours after the injury, the lateral cortical wall of the radius is buckled externally but its medial wall appears to be intact and there is no deformity on the medial aspect. In B and C, made 22 days later, buckling of the lateral cortical wall has disappeared but a transverse band of increased density at the same level (the band of opaque intracallus (arrows)) indicates that a complete transverse fracture has

healed. Both transverse in B (frontal projection) and ventrodorsal in C (lateral projection). The dorsal cortical wall is buckled dorsally as it was in lateral projection made immediately after the injury. This boy was 7 years of age. Our findings during healing of fractures of the radius and ulna indicate that there are few, if any incomplete fractures, even when a fracture line is not visible in the radiograph.

Fig 8-459—Fracture of the distal ends of the radius and ulnar shafts. In A, the immediate film, an impacted buckled fracture of the radius is clearly visible, but the ulnar shaft is not sufficiently deformed for a diagnosis of fracture. In B, made 40 days later, a

transverse band of increased density (band of opaque intracallus) marks the fracture site in the ulna as well as the radius. This boy was 7 1/2 years of age.



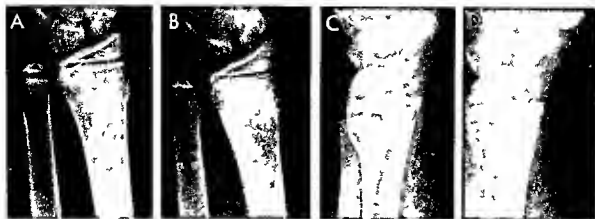


Fig 8-460.—Torus fracture of the distal end of the radial shaft without radiolucent fracture line in the immediate films (A and C frontal and lateral projections). In the same projections made

27 days later (B and D) there is a transverse band of increased density (opaque internal callus) which indicates that the fracture originally extended the full width and depth of the shaft.

Fig 8-461.—Impacted fracture of the radius. In A, obtained immediately after injury, the radial shaft is buckled externally but the ulna appears to be normal. In B, 41 days later, a faint but conclusive transverse band of increased density in the ulnar shaft indicates opaque internal callus. External cortical thickening is visible in both shafts at the level of the fracture in the radius and proximal to the fracture in the ulna. This boy was 7 1/2 years of age.



Fig 8-462.—Fracture in the middle thirds of the radius and ulna with dorsiflexion of the distal fragments. This girl was 10 years of age. A, frontal and B, lateral projections of the left forearm.



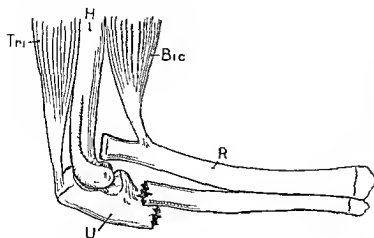


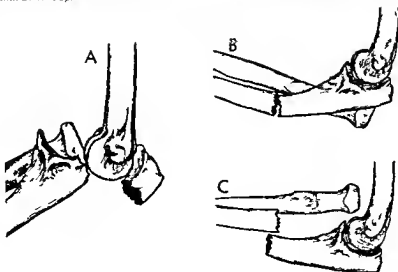
Fig 8-463 (above) —Schematic drawing of Monteggia's injury. The ulnar is fractured transversely and shortened. The radial head is dislocated ventrad. The biceps pulls the radial head forward when the injured orbicular ligament is weakened. The triceps pulls the proximal ulnar fragment dorsad.

Fig 8-464 (right) —Radiographic findings in Monteggia's fracture. Complete transverse fracture and shortening of the ulnar shaft in its middle third with ventral displacement of the radial head by the biceps muscle. This boy was 10 years of age.



Fig 8-465 —Fracture dislocations at the elbow. A, transverse fracture of the olecranon process with forward dislocation of the unfractured radius and the distal ulnar fragment. B, fracture of the shaft of the ulna with dorsal displacement of the unfractured

radius (reversed Monteggia fracture). C, fracture of the ulnar shaft with forward displacement of the unfractured radius (standard Monteggia fracture). (Figs 8-465 and 8-466 from Keon Cohen.)



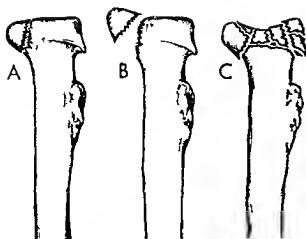


Fig 8 466 —Fractures at the proximal end of the radius. A, longitudinal with slight distraction. B, longitudinal with marked distraction. C, comminuted.

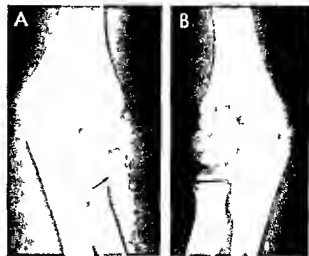


Fig 8 467 —Transverse fracture through the cartilage plate of the right radial head with lateral and caudal displacement of the epiphyseal ossification center (A, arrow). A small tag of shaft is attached to the displaced epiphysis indicating Salter type II injury to the cartilage plate. This girl was 7 years of age. A, right and B, left elbows in frontal projection.

Fig 8 468 —Fractures at the proximal end of the ulna. A, transverse fracture of the olecranon with slight distraction. B, transverse fracture of the olecranon with wide distraction. C, comminuted fracture of the olecranon. (From Keon Cohen.)

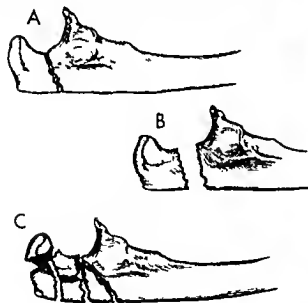


Fig 8 469 —Transverse fracture of the proximal third of the right ulna with slight displacement and rotation of the fragments. The proximal fragment is comminuted. The radius is displaced ventrad which warrants diagnosis of Monteggia's fracture. This boy was 15 months of age. A, frontal and B, lateral projection.

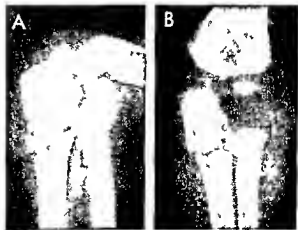




Fig 8 470 (left) —Break in continuity of the edge of the semilunar notch, either a short fracture line or a dysplastic marginal defect. This girl was 14 years of age.



Fig 8 471 (right) —Impacted fracture of the proximal end of the ulna, the olecranon, which was visible in lateral projection. This girl was 4 1/2 years of age.

Fig 8 472 —Submarginal fracture of the end of the olecranon process of the ulna with marginal scalloped fragment attached to the apophysis. The dorsal fat pads (arrows) are displaced dorsally. This girl was 11 years of age.



Fig 8 473 —Slight comminuted fracture at the proximal end of the right radius. The lateral cortical wall (arrow) is slightly buckled medially but there is no fracture line. This boy was 14 years of age.

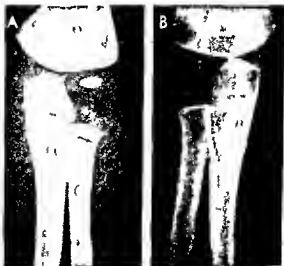


Fig 8-474 — Sagittal section on end separation of the cartilage plate of the radius with a triangular shaft fragment attached (lower arrow). Upper arrows are directed at the transverse radiolucent strip cast by the cartilage plate of the humerus. This is not a fracture line. The boy was 13 years of age.



Fig 8-475 — Effect of midshaft fracture of the radius or ulna on the elbow and wrist joints. In Monteggia fracture of the ulna, the radial head is dislocated at the elbow. In Galeazzi fracture of the

radius, the ulna is dislocated at the wrist. When the radius and ulna are fractured simultaneously, these dislocations do not occur. (From Rickert and Cordell.)

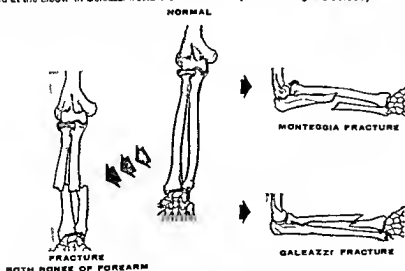




Fig 8 476 — Displacement of the olecranon fat pad dorsad out of the olecranon fossa and the coronoid fat pad ventrad out of the coronoid fossa after injury and acute swelling at the elbow. The bones are normal. Acute distention of the elbow joint due to acute traumatic hemarthrosis is the probable cause of displacement of the fat pads.

radiographically. It occurs chiefly in children between 2 and 6 years following excessive traction when the child is suddenly lifted by its arm. It is often reduced spontaneously by attempts to move the bones at the elbow. Theoretically the radial head is displaced out of the elbow joint when it is pulled through the orbicular ligament by traction and then is maintained in an ectopic position by contraction of the fibers of the

Fig 8 478 — Supracondylar fracture of the right humerus with characteristic displacement of the distal fragment dorsad in lateral projection (C). A, frontal projection; B, frontal projection shows complete transverse fracture of the right humeral shaft proximal to the con-

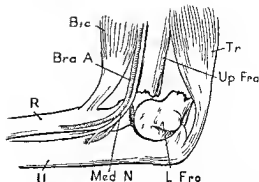
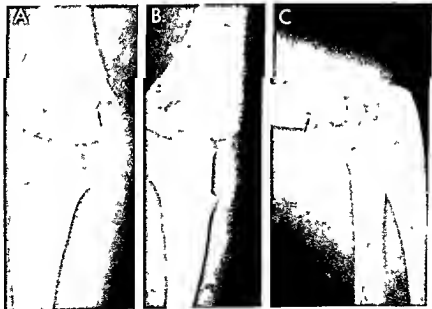


Fig 8 477 — Morbid anatomy of supracondylar fracture of the humerus. Schematic drawing. The proximal fragment displaced forward may puncture the brachial vessels and/or injure the median nerve. Bic, biceps; Bra A, brachial artery; R, radius; Tr, triceps; Up Fra, upper fragment; L Fra, lower fragment; Med N, median nerve; U, ulna.

ligament. Although we have examined the elbows radiographically in scores of such cases, we have not been able to demonstrate the dislocation. The radiographic technicians probably reduce this dislocation consistently before the film is exposed by their manipulations of the elbow while positioning the patient.

FRACTURES OF THE HUMERUS are most common in its distal third and of the fractures of the bones at the

dylea, with some distraction of the fragments. B shows the normal unfractured left humerus in frontal projection. This boy was 3 years of age.



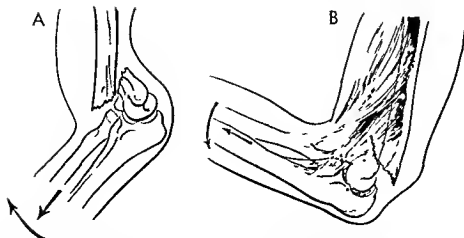


Fig 8-479 — Supracondylar fractures. A, standard supracondylar fracture of the humerus in which the distal fragment is dis-

placed backward. B, rare flexion supracondylar fracture in which the distal fragment is displaced forward (From Cave)

elbow, the supracondylar and diacondylar fractures of the humerus are by far the most frequent and important. In most cases these fractures are of the "flexion type," in which the distal fragment is displaced dorsad. The "extension type," in which the distal fragment lies anterior to the proximal fragment, is less common and is reduced with far greater difficulty (Figs 8-477 to 8-479). Simple, uncomplicated supracondylar fractures are shown in Figure 8-480. Diacondylar fractures with dislocation at the elbow in Figure 8-481. In C of Figure 8-481, the margin of the humeral shaft is broken as well as the capitellar ossification center, but without dislocation of the bones and with only slight displacement of the fragments. A variety of fractures of the distal third of the humerus is shown in Figure 8-482. Fracture of the lateral segment of the end of the humerus which produces a fragment made up of the humeral capitellum and its lateral epicondyle, which is avulsed laterad and rotat-

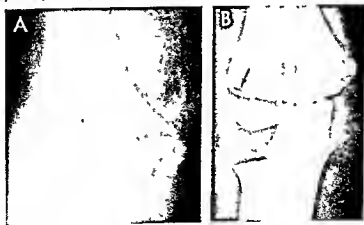
ed sometimes more than 90 degrees (Fig 8-483), should be treated by open reduction if closed reduction is not readily accomplished.

The medial epicondyle is often broken, avulsed and displaced with an attached cortical fragment in a wide variety of positions (Fig 8-484). The radiographic findings in fracture of the medial epicondyle and slight avulsion of a tag of the shaft and the epicondylar ossification center are shown in Figure 8-485. Fracture of the lower pole of the medial epicondyle center itself with avulsion of a small caudal fragment is depicted in Figure 8-486. Substantial regional swelling of the soft tissues is characteristic of this injury, and the fracture can be suspected radiographically, before the ossification center appears from the local soft tissue swelling alone.

Occasionally the distal fragment of a transverse supracondylar fracture is not displaced dorsad (Fig 8-487).

Fig 8-480 — A, supracondylar fracture with impacted fragments proximal and distal to the transverse fracture line. In lateral projection (not shown) the distal fragment was displaced dorsad a flexion injury. This boy was 9 years of age. B, submargin-

short fracture on the lateral side of the distal end of the humeral shaft with only slight displacement of the peripheral scale-like fragment.



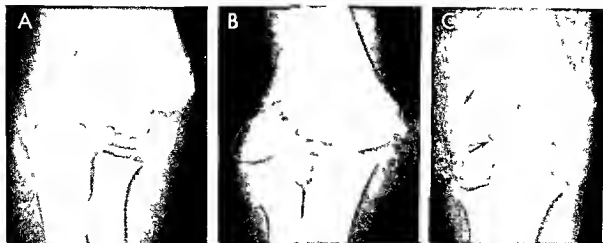
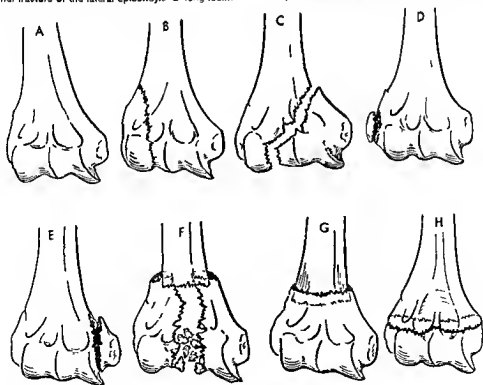


Fig 8-481 — A, supracondylar fracture with dislocation of the radius and ulna medially. The capitellum is avulsed, rotated and displaced medially. B, supracondylar fracture of the lateral epicondyle with avulsion of the epicondylar fragment attached to the

capitellum which is also avulsed, rotated and displaced laterally. C, supracondylar marginal fracture of the lateral end of the humeral shaft and longitudinal fracture of the capitellum with avulsion. The radius and ulna are not displaced.

Fig 8-482 — Different patterns of fractures of the distal end of the humerus. A, normal humerus. B, supracondylar oblique longitudinal fracture of the lateral epicondyle and capitellum. C, supracondylar oblique fracture of the medial epicondyle and trochlea. D, longitudinal fracture of the lateral epicondyle. E, longitudinal

fracture of the medial epicondyle. F, transverse fracture of the shaft and longitudinal supracondylar fracture with comminution. G, simple impacted supracondylar fracture of the shaft. H, transverse supracondylar fracture (Figs 8-482 and 8-483 from Cava).



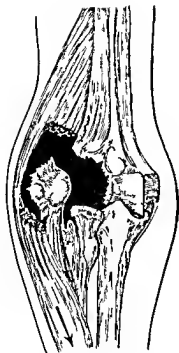


Fig 8-483 — Fracture of the lateral segment of the end of the humeral shaft with avulsion of the cephalum and lateral epicondyle. The fragment is also rotated more than 90°.

The proximal end of the humerus may be broken by direct blows on the upper arm or indirectly by falls backward with the arms extended and adducted onto the hand or elbow. The traumatic force thrusts cephalad through the humeral shaft. The deformity after fracture is largely determined by the level of fracture relative to the levels of insertions of the deltoid muscle (abductor), pectoralis major muscle (adductor and internal rotator) and abduction and rotation of the muscles of the rotator cuff (Fig 8-488). A transverse fracture at the level of the surgical neck but with slight displacement of the fragment is shown in Figure 8-489. A partial distraction and partial impaction fracture is shown in Figure 8-490. According to Dameron and Reibel, traumatic separation of the three epiphyseal ossification centers in the proximal epiphysis of the humerus has not been reported. We have seen one example (see Fig 8-552 A).

BONES IN THE LOWER EXTREMITIES are broken much less frequently than those in the upper extremity and their treatment and healing are complicated by weight bearing.

In the feet there are several ossicles which simulate fracture fragments; these should be considered before the diagnosis of fracture fragment is made. Opaque foreign bodies also may be driven into the soft tissues when the foot is injured and simulate bony fracture fragments radiographically.

The pedal phalanges are frequently fractured by the fall of heavy objects on them and in children by stubbing the toes when barefoot. Fracture of a single phalanx usually causes only transient minor disability. Reduction of broken distal and middle phalanges is usually unnecessary. Fractures of the proximal

Fig 8-484 — Fracture and avulsion of the medial epicondyle. A with slight distraction. B with more distraction and the epicondylar fragment at the level of the joint. C enfolded into the joint.

D with lateral subluxation at the elbow and the broken epicondyle deeper in the joint. (From Keon Cohen.)

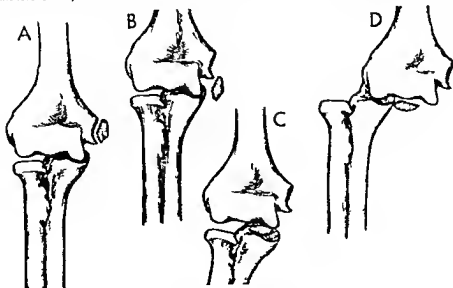




Fig 8 485—Avulsion of the ossification center of the medial epicondyle with a tip of attached shaft (Salter injury to cartilage plate type II). This boy 12 years of age had sharp pain and region

of swelling at the elbow while pitching baseball (Little League age group)

Fig 8 486—A, fracture of the lower pole of the ossification center of the medial epicondyle with avulsion caudad of a small fragment. The regional soft tissues are swollen. This boy was 11

years of age. B, avulsion fracture of the medial epicondyle (arrow) with massive swelling of the regional soft tissues in a boy 8 years of age



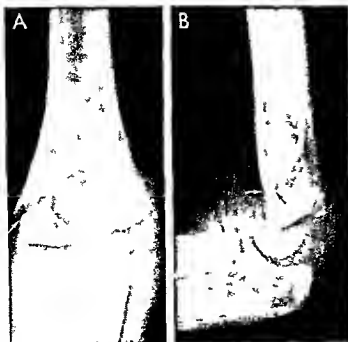


Fig 8487—Supracondylar transverse fracture of the humeral shaft without dorsal or ventral displacement of the distal fragment. A: Anteroposterior projection shows the transverse supracondylar fracture line. B: Lateral projection shows the distal fragment in normal position. The girl was 4 years of age.

Fig 8488—Fractures at the proximal end of the humerus with characteristic deformities. A: Adduction of proximal fragment due to pull of the pectoralis major when the fracture is between insertions of the pectoralis major and deltoid muscles. B:

abduction of the proximal fragment when the fracture is distal to insertion of the deltoid muscle. C: Adduction and rotation of the proximal fragment when the fracture is proximal to insertion of the pectoralis major and the rotator cuff. (From Cave.)

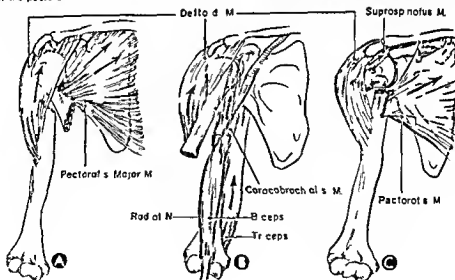




Fig 8-489 — Transverse jagged fracture of the surgical neck of the humerus of a girl 6 years of age. The fracture line is at the level of insertion of the pectoralis major.

phalanges however if untreated may result in disabling flexion deformities.

Metatarsal fractures are also frequently caused by falling objects. They are relatively rare in children but are important occupational hazards for adults.

The transverse fracture at the proximal end of the shaft of the fifth metatarsal is perhaps the most common metatarsal fracture in older children (Fig 8-491). It is called Jones's dancing fracture. This transverse fracture should not be confused with the normal scale apophysis and its synchondrosis on the lateral aspect of this bone. The second and third metatarsals are occasionally the site of stress or fatigue fractures (Fig 8-492).

Fractures of the tarsal bones are relatively rare in children because their ossification centers are protected by elastic coats of cartilage. In severe injuries however one or several of the tarsal bones may be broken simultaneously (Figs 8-493 to 8-495). Fractures of the calcaneus and talus are the most important clinically because they are both weight-bearing bones. It has been estimated that the superior articulating edge of the talus carries more weight per square millimeter of surface than any other bone. The calcaneus fractures in a variety of patterns. Fractures of its tuberosity are readily treatable in contrast to the difficulties in treating the crush comminuted fractures which extend into the subtalar joint. The talus receives almost all of its blood through its neck, and in fractures of the neck the talar body is especially prone to ischemic necrosis. The greater part of the talar surface is composed of seven avascular articular cartilages and traumatic arthritis is a frequent sequel of talar fracture. Avulsion fracture of the tuberosity of the navicular is caused by excessive stress through the tendon of the tibialis posterior muscle. Fracture fragments of the tuberosity of the navicular should be carefully differentiated from the normal variant in the tendon, the os tibiale

Fig 8-490 — Transverse fracture at the level of the surgical neck of the humerus with the ventral inferior segment of the fracture line widened due to distraction of the fragments and the dorsal superior segment impacted. A, frontal and B, lateral projections.

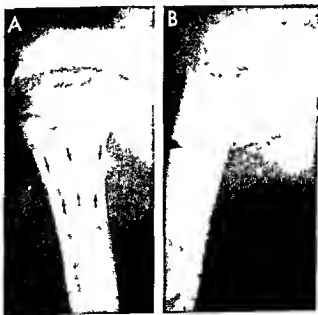




Fig 8-491 — Transverse fracture at the proximal end of the 5th metatarsal of a girl 10 years of age. In A, immediately after a twisting injury, the arrow is directed at the incomplete transverse fracture. The independent small mass of bone lateral to the end of the shaft is the normal apophyseal center. In B, 34 days later, the fracture line is widened and the apophyseal center is more completely fused. Fusion has probably been accelerated by the local chronic hyperemia induced by the fracture. This is known as Jones's dancing fracture.



Fig 8-492 — March or fatiguel stress fracture in the 2nd metatarsal of a girl 5 years of age.

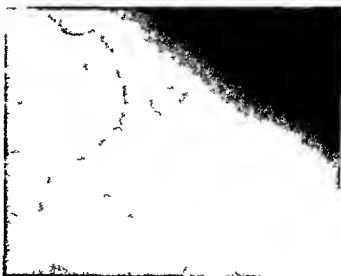


Fig 8-493 — Fracture of the tarsal scaphoid with displacement of the superior fragment dorsad. The larger inferior segment is not dislocated. This boy 7 1/2 years of age fell from his bicycle and the foot was stuck by the pedal.



Fig 8-494 — Multiple fractures of the tarsal bones of a boy 13 years of age. The posterior arrow is directed at a fracture line at the base of the sustentaculum of the calcaneus. The anterior arrow points to the fracture fragment of the tuberosity of the navicular. The large fragment of the navicular is also fractured and compressed.



Fig 8-495 — Avulsion fracture of the dorsal edge of the calcaneal tuberosity and swelling of the contiguous Achilles tendon of a boy 6 years of age. There was a tender swelling above the level.

Fig 8-496 — Fracture of the accessory center in the medial malleolus of the right tibia of a boy 8 years of age who had twist-

ed his right ankle (A). The accessory center in the left medial malleolus (B) is normal. Lateral oblique projections.



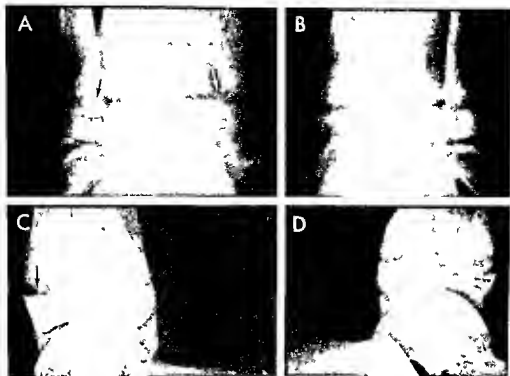


Fig 8-497 — Transverse laceration of the cartilage plate of the right tibia of a boy 13 years of age who had twisted his right ankle a week previously. A, frontal and C, lateral projections of the injured right ankle. B, frontal and D, lateral projections of the

normal left ankle. The cartilage plate of the right tibia is deepened due to distraction of the fragments longitudinally. There is however no displacement of the fragments transversely or varus/valgus (Salter type I injury to the cartilage plate).

externum. Fractures of the cuboid and the cuneiforms usually cause minor disabilities; they are, of course, sometimes associated with breaks in other tarsal bones.

Fractures of the distal tibial and fibular epiphyses are common and important clinically. Inadequate treatment of these fractures may result in permanent crippling deformities. The bone injury is usually acquired in sudden turning or twisting movements during ordinary activity, such as stepping on a pebble or slipping on icy or grassy surfaces and particularly in the sudden stopping on one foot in athletic games. The foot is suddenly fixed and the inertia of the heavier leg and body above the ankle generates excessive stresses on the ends of the tibia and fibula which, depending on the position of the foot, lacerate single or multiple ligaments at the ankles and break the bone and cartilage in the epiphyses in a variety of patterns. We have found lateral oblique projections of the ankles, as well as frontal and lateral projections essential for adequate visualization and evaluation of injuries at the ankle (Figs 8-496 to 8-502).

Fractures of the tibial and fibular shafts are also common. In infants and children repair and regrowth of the injured bone tissue are so vigorous that most of these fractures can be treated without resort to open surgery. All athletic games in which high

running speed is essential, with dodging and sudden stops and turns, are liable to induce fractures of the tibial and fibular shafts, especially football, basketball and soccer. Skiing has become a common cause of tibial fractures in older children. Bumper injuries by automobiles are responsible for many of the most severe compound and comminuted fractures which often do not respond well to treatment. It should be remembered that a fracture in the distal segment of the tibia may be associated with a companion fracture in the proximal segment of the fibula (Fig 8-503). The radiographic examination should always include the entire shafts of both bones in both legs and films of the knees and ankles as well. Fractures of the fibular shaft without fracture of the tibia usually heal readily. Wide distraction of the fragments delays healing, especially in the distal third of the tibia where blood supply is relatively meager. Fractures in the proximal segment of the tibia are relatively uncommon. In injuries at the knee, lacerations of the ligaments and menisci are much more common and important than fractures of the bone itself. Some variations in the types of fractures of the tibial and fibular shafts, according to Cave, are shown in Figure 8-504 and radiographic findings in Figures 8-505 to 8-510. Fractures which are invisible or barely visible in films made immediately after injury may later show

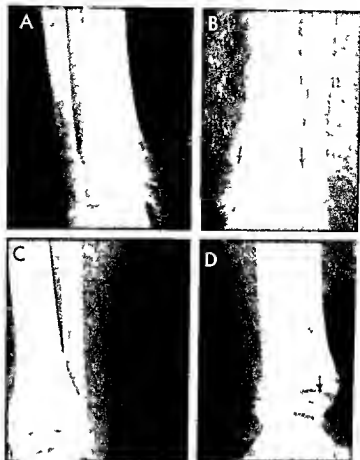


Fig. 8-498—Transversal laceration of the cartilage plate of the left tibia of a boy 15 years of age who had twisted his ankle a few hours before. **A**, frontal and **C**, lateral projections of the normal right ankle. **B**, frontal and **D**, lateral projections of the injured left

ankle. The cartilage plate of the tibia is deepened due to distraction of the fragments in **B** and **D**, and the apophyseal ossification center is displaced dorsad in **D**. (Salter type I injury to the cartilage plate.)

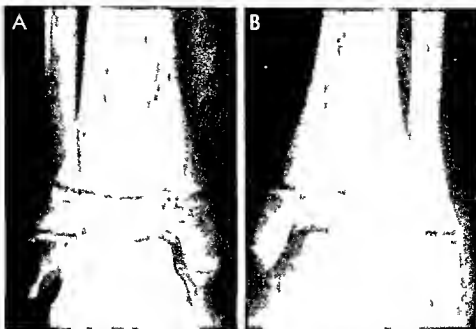
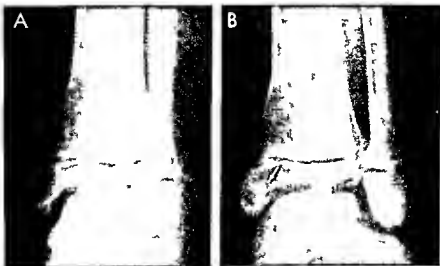


Fig 8 499 —Fracture at the base and medial side of the medial malleolus of the left tibia of a boy 14 years of age who wrenched his ankle and foot A normal right ankle in frontal projection B injured left ankle The medial segment of the left

cartilage plate is deepened and the malleolar fragment displaced medially due to distraction. The mortise at the ankle is enlarged and weakened (Satter type III injury to the cartilage plate.)

Fig 8 500 —In frontal projection (A) the findings are normal. In lateral oblique projection (B) a longitudinal fracture line is clearly visible (arrow) in the medial segment of the tibial epiphyseal ossification center. One cannot evaluate injuries to the ankles

satisfactorily without lateral oblique as well as frontal and lateral projections. This boy 13 years of age sprained his left ankle and had point tenderness over the medial malleolus.



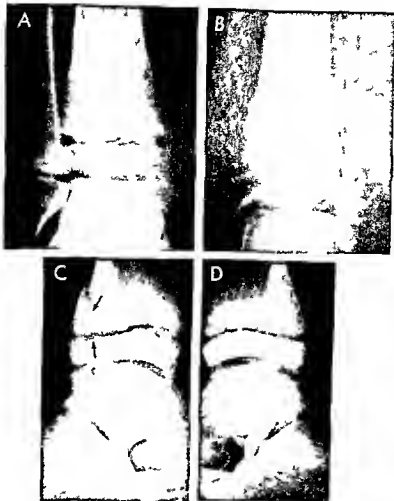


Fig. 8-501 — Laceration of the cartilage plate with distal longitudinal fracture at the end of the tibial shaft of a girl 11 years of age who had fallen on her right ankle. In A, frontal and C, lateral projections of the injured right ankle, the tibial cartilage plate is deepened due to longitudinal displacement of the fragments. In C,

the distal fragment of the tibial shaft, which was not visible in frontal projection, is so clearly delineated (Salter type II injury to the cartilage plate). B, frontal, and D, lateral projections of the uninjured left ankle.

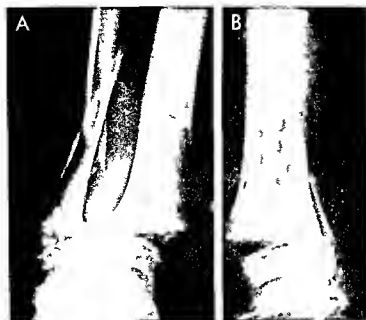


Fig 8-502 —Transverse laceration of the cartilage plate of the right tibia of a boy 12 years of age with lateral and ventral displacement of the epiphyseal ossification center. The fibular shaft is broken obliquely and the tip of the proximal fragment is broken off the main mass of the cephalic fragment—a comminuted fracture of the fibula. The lesion in the tibia is a Salter type I injury to the cartilage plate. A, frontal and B, lateral projections.

Fig 8-503 —Comminuted oblique spiral fracture of the distal third of the left tibial shaft with comminuted oblique fracture of the proximal third of the left fibular shaft of a boy 14 years of age. A, frontal and B, lateral projections.



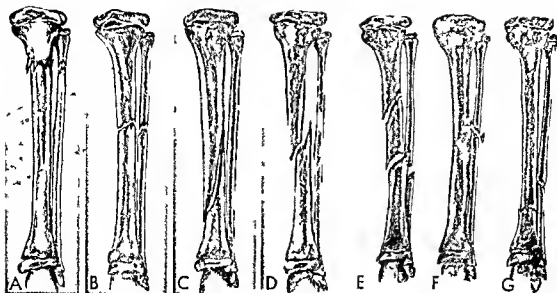
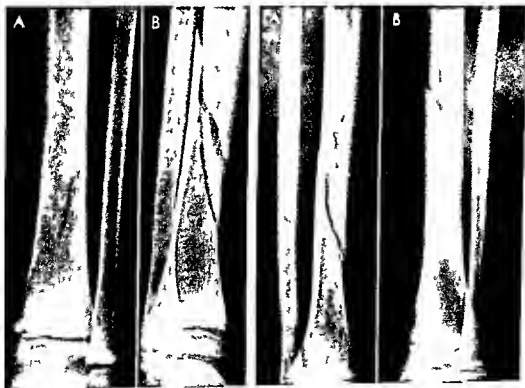


Fig 8 504 —Varieties of diaphyseal fractures of the tibia and fibula. (Modified from Cave.) Stable transverse fractures: proximal A; midshaft B; Unstable oblique fractures: long oblique C;

short oblique D; Unstable segmental fractures: comminuted E; comminuted F; Stable transverse fracture: distal G.

Fig 8 505 (left) —Long oblique spiral fracture of the right tibia of a boy 10 years of age who was hit by a toboggan sled. In A (lateral projection) only a short caudal segment is visible. In B (distal lateral projection) the true extent of the long oblique spiral fracture with distraction of the fragments is now visible.

Fig 8 506 (right) —Long oblique spiral fracture in the distal half of the left tibia in which different levels of the fracture line are visible in the different projections. A: lateral and B: frontal. The boy 15 years of age fell while skating.



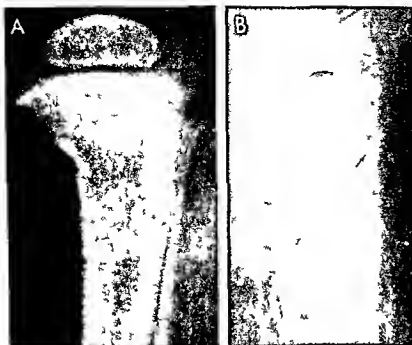


Fig 8-507—A, frontal and B, lateral projections of impacted fracture of the ventromedial wall of the proximal tibial segment of a girl 11 months of age who was flung against the back seat in an automobile accident.

Fig 8-508—Longitudinal fracture of the distal segment of the tibial shaft of a boy 8 years of age. The fracture is visible in

frontal (A) and oblique (B) projections but is clearly visible in the lateral (C) projection.



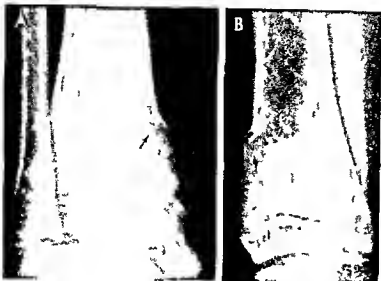


Fig 8-509 Compacted torus fracture in the distal third of the tibial shaft with external buckling of the medial and ventral cortical walls but no fracture line. A frontal and B lateral projections.

opaque callus which makes the diagnosis of earlier fracture certain (Fig 8-511). Toddler's fracture in the tibia of children 15 months to 5 years of age may be invisible in some projections and visible in others. They must always be carefully sought because most of them are hairline fractures (Figs 8-512 to 8-514). Transverse fracture of the tibial shaft at the same level with comminution of the fibula is shown in Figure 8-515. Long oblique fractures of the tibial shaft may be invisible in frontal projection and be conspicuous with substantial distraction of the fragments in lateral projection (Fig 8-516).

Stress fractures (march or fatigue fractures) in children are commonly located in the proximal segments of the tibial shaft (Fig 8-517). They occur more rarely in the distal third of the tibia also (Fig 8-518). A stress fracture develops in normal bone during normal use without external injury. Excessive endogenous traumas repeated slight overloads of the bones and bending and stretching strains cause distracted stress fractures. Pain may precede the appearance of radiographic signs of fracture by several weeks. Exuberant callus may simulate inflammatory and malignant tumors. The fibula has been affected in a few cases. The stresses of excessive running, skating and swimming cause stress fractures in children. I saw one example in a child who practiced tap dancing several times a day for several months. In the tibia stress fractures are usually transverse in the proximal third of the shaft. The fracture line is usually obliterated in part by opaque internal callus and local thickenings externally of the cortical wall. Painful lump is the common complaint; pain increases with activity during the day and disappears promptly when the leg is at rest. The local bony swelling is usually slight but may be sufficiently large

Fig 8-510—Comparison of torus fractures of the distal segments of the tibia and fibula at different longitudinal levels: the lateral cortical wall of the left tibia and the medial cortical wall of the fibula just cephalad to it are buckled externally. The boy 17 months of age had fallen off a chair.



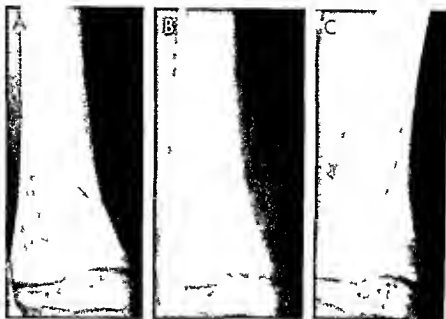


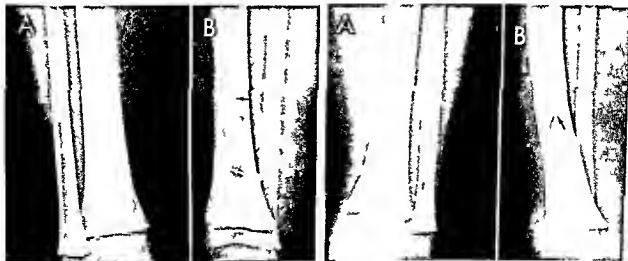
Fig. 8-511—Invisible, or barely visible fracture of the medial cortical wall in the distal segment of the right tibia in a film made immediately after the injury (A). Twenty-eight days later localized opaque internal callus is evident in both frontal (B) and lateral (C)

projections. The fact that the opaque callus does not extend entirely across the medullary cavity in three dimensions suggests that the original fracture was incomplete. This boy was 5 years of age.

Fig. 8-512 (left)—Toddler's fracture in a boy 4 1/2 years of age who had refused to walk or bear weight on the right foot after twisting the right leg 24 hours before. In A frontal projection the findings are normal. In B lateral projection there is a long oblique hairline fracture (arrows) in the distal third of the tibial shaft. Such fractures are easily missed radiographically and ob-

lique views should be obtained when clinical evidence suggests toddler's fracture.

Fig. 8-513 (right)—Toddler's fracture in a boy 3 1/2 years of age who had refused to bear weight on the left foot for about 12 hours. In A frontal projection the findings are normal. In B lateral projection a short oblique fracture line is visible.



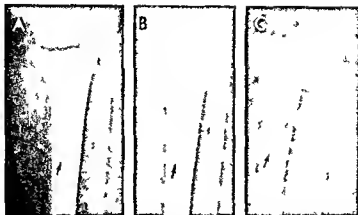


Fig 8 514 — Toddler's fracture in the proximal segment of the tibial shaft which was invisible or barely visible in A made immediately after the boy 30 months of age stopped walking and refused to move the left leg. In B made a few minutes later and af-

ter some manipulation the fine fracture line is visible. In C made about three hours later after application of a plaster cast the fracture line is wider and more clearly visible owing to the slightly increased distraction of the fragments.

Fig 8 515 — Transverse fracture of the tibial shaft with transverse comminuted fracture of the fibular shaft at the same level. A frontal and B lateral projections.

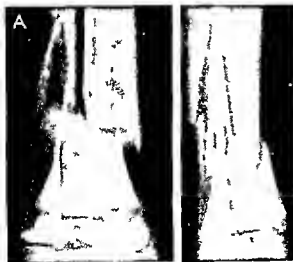


Fig 8 516 — Long oblique unstable fracture of the tibial shaft is practically invisible in frontal projection (A) but is clearly visible with substantial distraction of the fragments in lateral projection (B). This boy was 5 years of age.





Fig 8-517—Stress fracture of the tibia (arrows) of a boy 8 years of age. In A, frontal projection, a transverse band of increased density marks the site of fracture. In B, lateral projection, the dorsal cortical wall only appears to be affected. This fracture appears to be incomplete.

Fig 8-518—Transverse stress fracture in the distal third of the right tibial shaft of a boy 6 1/2 years of age. There is no fracture line. A transverse opaque strip of external callus marks the site of the fracture. Both above and below the fracture the cortical walls are slightly thickened.



Fig 8 519 — Transverse fracture of the intercondylar eminence with incomplete separation of the fragments in a boy 7 years of age who had been struck by an automobile fender **A** frontal and **B** lateral projections

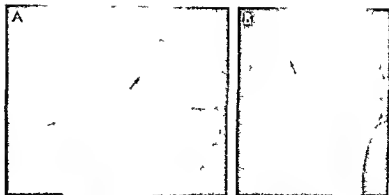


Fig 8 520 — Distract on transverse fracture of the cartilaginous plate of the left tibia (Salter injury type II) with deepening of the space between the end of the shaft and base of the epiphyseal ossification center but without fracture of the shaft or its caudally

displaced epiphyseal ossification center (B) Compare the normal shallowness of the cartilaginous plate of the uninjured right side (A) of this boy 15 years of age

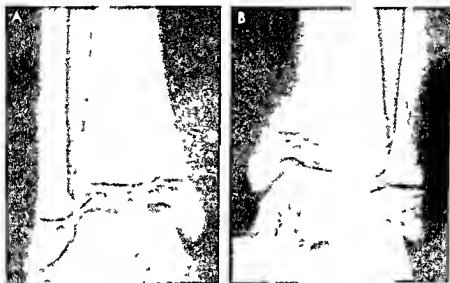


Fig 8 521 — Chip fractures of the lateral cortical walls of the tibia near the end of the shaft. In **A** frontal projection the fracture fragments are barely visible but are clearly visible in **B** lateral

oblique projection. This boy 12 years of age had twisted his right ankle





Fig 8-522 — Marginal fracture of the ventral superior edge of the patella with distraction of the flake fragment. This boy was 13 years of age.

to be palpated. Stress fractures have been described in the distal third of the fibula; they tend to occur in the younger children. Some reported cases may be simple cortical post-traumatic thickenings rather than fractures with callus formation. I have seen one example of stress fracture of the tibia associated with a benign cortical defect. Some have been confused

with productive osteitis and Ewing's sarcoma. In England some children have developed stress fractures in the humerus from bowling during cricket games. In javelin throwers the ulnas are said to be vulnerable to stress fractures. So far as I know, and surprisingly, stress fractures in the bones of the arms have not been reported. In juvenile baseball pitchers stress fractures have developed in the metatarsals in several children and in the pedal sesamoids in a few. The femoral necks are frequent sites of stress fractures in young army recruits from excessive marching. The normal variations at the juvenile ischiopubic synchondrosis have led to erroneous diagnosis of stress fractures at this site. After complete immobilization in a cast, stress fractures in the long bones usually heal in 8–12 weeks.

Fractures of the proximal tibial epiphysis are rare except in the newly born and from automobile accidents (Fig 8-519).

Fractures of the fibular shaft usually heal without significant deformity or disability. Full weight bearing can usually be tolerated after two weeks. Injuries to the distal cartilage plate are not uncommon (Fig 8-520). Oblique projections may be necessary for satisfactory visualization of some of the superficial cortical fractures of the shaft (Fig 8-521).

Fractures of the patella should not be confused with the several normal variations during growth which simulate fractures, especially the polar fractures (Fig 8-522). Transverse fractures through the middle of the patella due to sudden excessive contraction of the quadriceps femoris muscle are rare in children, as are comminuted crush fractures caused by blows on the patella which drive it onto the femoral condyle. The patella may be displaced (Fig 8-523) owing to endogenous disturbances of stress equilibrium.

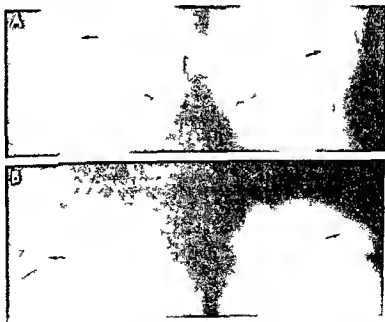


Fig 8-523 — B lateral dislocation of the patella as lateral anteroposterior (A) and skyline (B) projections. This girl 15 years of age also had idiopathic juvenile scoliosis and bilateral knock knee. The patellar dislocation was probably incidental to endogenous disturbances in stress equilibrium at the knees due to abnormal stresses induced by knock knee and scoliotic deformities.



Fig. 8-524 This boy 15 years of age had been injured during a football game a few hours earlier. In A, taken before manipulation, there is no evidence of injury. In B, made a few minutes later after manipulation under general anesthesia, deepening of the

cartilage plate and displacement of the epiphysis are clearly evident. This is a transverse fracture of the cartilage plate. Salter type I injury. (From Smith.)

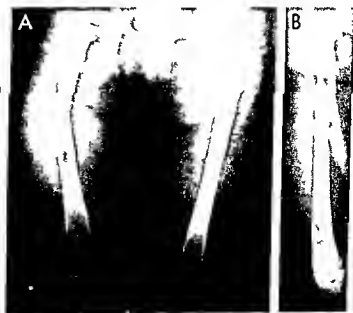


Fig. 8-525 Long oblique fracture of the proximal half of the right femur with wide displacement of the fragments. A, frontal; and B, lateral projections. The proximal fragment is fixed laterally and medially. The distal fragment is a so-called "butterfly" fragment and is surrounded by massive hematoma of the thigh of a boy 3 years of age.

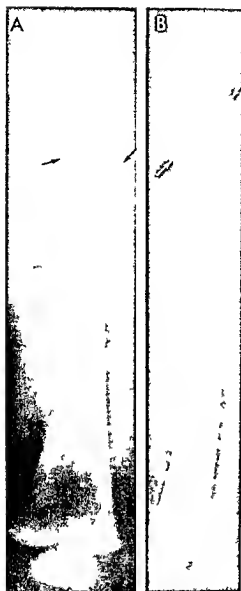


Fig 8-526 — Transverse impacted fracture of the femur of a girl 7 months of age who was thrown against the front seat in an automobile accident. A, frontal; and B, lateral projections.

um such as excessive traction by the shortened quadriceps femoris in spastic paralyses.

Fractures of the femur occur at all levels but are less common than fractures of the tibia. Fractures of the distal epiphysis are rare if one excludes marginal fractures of the medial condyle which are called osteochondroses dissecans. Occasionally the distal cartilage plate is lacerated transversely and the epiphysis may be displaced (Fig 8-524). Fractures of the femoral shaft are often associated with wide distractions of the fragments (Figs 8-525 and 8-526). Large amounts of callus are common in fractures of the femoral shaft. Occasionally however in younger patients the displacement of the fragments is minor

(Fig 8-527). Avulsion fractures of the trochanters usually offer no special problem in diagnosis (Fig 8-528). In comparison with older patients the femoral necks are fractured infrequently in children but they may occur at any age even in the newly born when the neck is cartilaginous and invisible radiographically. The course of the fracture varies from the nearly horizontal to oblique and nearly longitudinal. Impaction of these fragments is common.

Injuries to the proximal cartilage plate with traumatic separation of the femoral capital epiphysis are rare but do occur after violent injuries (Fig 8-529). Rathbun found only 4 previous examples which were illustrated with radiographs prior to 1962 when he reported 13 cases. It is interesting that of his 13 ex-

Fig 8-527 — Short oblique fracture in the middle third of the femoral shaft with only slight distraction of the fragments. The fracture line is much better seen in frontal projection (A) than in lateral projection (B), although a fine break in the dorsal cortical wall is clearly evident. This girl was 18 months of age.





Fig 8-528 —Avulsion fracture of the left lesser trochanter of a boy 15 years of age. The sclerotic fragment of the lesser trochanter is displaced medially and cephalad.

amples with complete separation of the epiphysis coxa plana developed in but 1 and bony union occurred at the fracture site in 12 cases.

Fractures of the capital femoral epiphysis are rare because throughout childhood the bony center is protected by a mantle of elastic cartilage. In our study of Legg Perthes coxa plana the early consistent radiographic change was a marginal fracture of the epiphyseal ossification center and traumatic separation of the edge of the center from its overlying cartilage. It is probable that marginal stress fracture of the center due to overload on its superior ventral edge is the primary causal mechanism in most cases of Legg Perthes disease.

REFERENCES

- Berkheide R D. Stress fractures in children. *Am J Roentgenol* 91:588 1964.
- Brogdan B G and Crow N E. Little Leaguers' elbow. *Am J Roentgenol* 83:671 1963.
- Blick E M. Structural patterns of callus in fractures of the long bones. *J Bone & Joint Surg* 30-A:141 1948.
- Bledsoe R E and Izenmark J L. Displacement of fat pads in disease and injury at the elbow. *Radiology* 73:717 1959.
- Caffey J. The early radiographic changes in the essential coxa plana. Their significance in pathogenesis. *Am J Roentgenol* 103:620 1968.
- Cave E F. *Fractures and Other Injuries* (Chicago: Year Book Medical Publishers Inc 1958).
- Dameron T B and Rebel D B. Fractures involving the proximal humeral epiphyseal plate. *J Bone & Joint Surg* 51-A:289 1969.
- Devas M B. Stress fractures in children. *J Bone & Joint Surg* 45-B:528 1963.
- Keon Cohen B T. Fractures at the elbow. *J Bone & Joint Surg* 48-A:1023 1966.
- Leviton J and Colloff B. *Roentgen Interpretation of Fractures and Dislocations* (Springfield Ill: Charles C Thomas Publisher 1956).

Fig 8-529 —Avulsion of the right lateral femoral epiphysis due to laceration of the proximal cartilage plate of the femur of a boy 3 years of age who had fallen from a second story window and refused to walk afterward. In A, made immediately after injury, the findings are normal except for some deepening of the right

cartilage plate. In B, made with the femur in abduction and external rotation, dislocation and displacement of the femoral head of the right femur are clearly visible. (See type I injury of the cartilage plate.) (From Wikstrom.)



- Madsen E T. Fractures of the extremities in the newborn. *Acta obst. et gynec. scandinav* 34:41 1955
- Norell H G. Roentgenologic visualization of the extracapsular fat. Its importance in the diagnosis of traumatic injury to the elbow. *Acta radiol* 42:205 1954
- Penrose J H. The Monteggia fracture with posterior dislocation of the radial head. *J Bone & Joint Surg* 33-B:65 1951
- Rathbun A H. Fractures of the neck of the femur in children. *J Bone & Joint Surg* 44-B:528 1962
- Rickling F W and Cordell L D. Unstable fracture-dislocations of the forearm. *Arch. Surg* 96:999 1968
- Smith L. Concealed injury to the knee. *J Bone & Joint Surg* 44-A:1659 1962

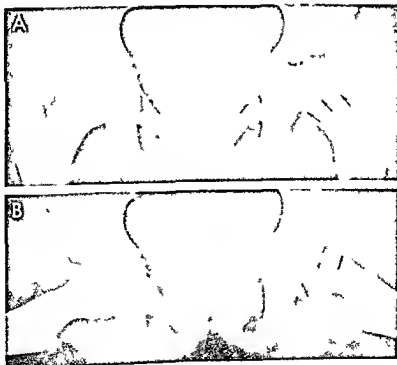
SLIPPING OF THE CAPITAL FEMORAL EPIPHYSIS is rare in children younger than 9 years. The exact causal agent and mechanisms are not known although trauma and stress appear to be important factors. The slipping may develop suddenly after severe injury to an apparently normal child or gradually without preliminary traumatic episode. In most cases limp, pain and limitation of motion at the hip begin during such ordinary activity as walking or running. There are no constitutional signs. Boys are more frequently affected than girls; one or both femurs may be involved. Andren and Borgstrom found a high incidence from June to September and suggested that the caus-

al agent is aminonitriles in the milk of cows which have been out to pasture on green fodder during these four months. Ponseti and McClintock produced epiphyseolysis by feeding aminonitriles (sweet peas) to experimental animals. LaCroix and Verbrugge concluded from a study of sections of the entire head-neck femoral junction that the primary structural changes are fibrous degeneration of the cartilage plate which weakens it and permits it to slip gradually medially and dorsad. One explanation for the sharp age limitation of the lesion is the shift from a somewhat horizontal plane to a more oblique vertical plane of the cartilage plate during adolescence which increases the stress of weight bearing and permits easier slipping. Johnston and colleagues suggested that during adolescence there is a suboptimal retention of calcium which causes incomplete mineralization of the femoral neck that leads to slipping of the femoral head on the shaft. The diagnosis rests on the radiographic changes which disclose thickening of the cartilage plate with varying degrees of displacement of the femoral head dorsad and medially (Fig 8-530). The quantitative differentiation of the medial and dorsal slipping can be demonstrated by Klein's method (Fig 8-531).

Trueta has stated that the transverse radiolucent band at the cortical shaft junction represents a local

Fig 8-530—Slipped femoral epiphysis of a boy 10 years of age who sprained his foot one year before, began to limp and became much worse a few weeks before this study. In A, frontal projection with the femurs in adduction, the epiphyseal plate of the left femur is thickened in a pattern which at one time suggested the pre-slipping phase of slipped femoral epiphysis. In

B, with the femurs abducted and rotated externally, the head is slipped caudad and dorsad in relation to the femoral neck but is still in normal relationship with the acetabular cavity. It is clear in these films that the diagnosis of pre-slipping phase should never be based on films made with the femurs in adduction alone.



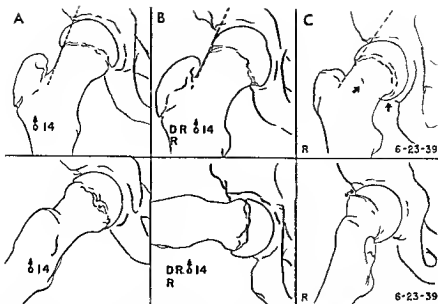


Fig. 8-531 — Klein's method of differentiating medial and dorsal slipping of the femoral head. A normal femur B medial slipping of the femoral head in relation to a line which is the projection of the lateral edge of the femoral neck as seen in frontal

projection C posterior slipping which is often invisible in frontal projection but is clearly visible in lateral projection (see arrow at cartilage shaft junction) (From Klein et al.)

Fig. 8-532 — Failure of normal modeling of the shaft after fracture in association with paralysis of the muscles of the leg. Fracture of the distal end of the femoral shaft in a boy whose leg was paralyzed. A at 20 months exuberant thick external callus has formed with extensive cortical thickening at the fracture site (ar-

rows) B at 25 months the callus and cortical thickening have disappeared but the distal fragment is distended with a wide medullary cavity and thin cortical walls. This boy had lumbosacral spina bifida with meningocele.



increase in the medullary vascular sinuses with a reciprocal reduction of local spongy bone

REFERENCES

- Andren, L., and Bergstroem, K. E. Seasonal variations in the epiphyseolysis of the hips and the possibility of an alimentary causal factor. *Acta orthop. scandinav.* 28 22, 1958.
- Johnston J. A., et al. Epiphyseolysis. *Am J Dis Child* 92 347 1956.
- Klela, A. et al. Roentgenographic features of slipped capital femoral epiphyses. *Am J Roentgenol.* 66 361 1951.
- LaCroux P. and Verbrugge J. Shipping of the upper femoral epiphysis. A pathologic study. *J Bone & Joint Surg.* 33-A 371 1951.
- Ponseti V. and McClintock R. Pathology of shipping of the upper femoral epiphysis. *J Bone & Joint Surg.* 38-A 71 1956.
- Shea, D., and Mankin H. J. Slipped capital femoral epiphysis. *J Bone & Joint Surg.* 48-A 349 1966.
- Trueita, J. Studies on the Development and Decay of the Human Frame (Philadelphia: W. B. Saunders Company 1968).
- Salter R. B. and Harris W. R. Injuries involving the epiphyseal plate. *J Bone & Joint Surg.* 45-A 587 1963.

REFERENCE

TRAUMATIC CUPPING OF THE METAPHYSES has developed in several of our patients months and years after their original injuries (Fig. 8-535). The cupping is due to undergrowth or stoppage of longitudinal growth of the rows of cartilage cells on the epiphyseal side of the cartilage plate. This undergrowth is apparently due not to direct injury to the cartilage plate but to traumatic thromboses and chronic reduction of blood flow in the terminal arterioles of the epiphyseal arteries which supply the proliferating cartilage. The cup forms because the central segment of the bone grows slower longitudinally than does its peripheral segment and coracal wall. In many cases the central segment of the cartilage plate fuses earlier with the shaft and longitudinal growth is stopped prematurely and permanently. Prolonged immobilization of the affected part appears to be the principal cause of the oligemia in the epiphyseal arteries. Prolonged immobilization is induced both by paralysis of contiguous muscles and by therapeutic restraints such as casts, bandages and frames. Compensatory overgrowth of the epiphyseal ossification center customarily produces a triangular cone-shaped epiphyseal ossification center. It should be emphasized that this deformity of the ossification center is secondary to failure of growth of the proliferating cartilage in the cartilage plate.

REFERENCES

- Caffey J. Some traumatic lesions in growing bones other than fractures and dislocations. Clinical and radiographic features. *Brit J Radiol.* 30 225 1957.
- . Traumatic cupping of the metaphyses in growing bones. Late residuals after earlier injury. *Am J Roentgenol.* 108 451 1970.

TRAUMATIC CORTICAL THICKENINGS are often the most prominent radiographic signs of trauma in growing bones and are never well developed in mature bones. Such thickenings are relatively most marked in the bones of the newly born. Their thick

BONE INJURIES ASSOCIATED WITH PARALYTIC DISORDERS —The most common of the paralytic disorders associated with bone injuries is meningomyelocele secondary to spina bifida. In paralytic limbs fractures of the long bones are followed by severe metaphyseal changes and persistent deformities of the shafts (Fig. 8-532). Gyepes and associates reported that all of the spinal cord lesions they observed were in the lumbar levels. The radiographic changes were most marked at the ankles and knees. They included deep transverse bands of rarefaction in the metaphyseal levels and demineralization of the provisional zones of calcification weakening of the ends of the shafts with cortical thickenings and slipping of some of the epiphyses and multiple fine fragmentations. Surprising by the contiguous epiphyseal ossification centers were not affected. Also at the ankles the fibulas remained intact in the presence of severe changes in the tibias. This suggests that the changes in the bones are due to stress rather than to trophic disturbances. Hyposensitivity to pain is one of the causes of high frequency of bone injuries in these patients.

REFERENCE

- Gyepes M. T. et al. Metaphyseal-epiphyseal injuries with spina bifida and meningoceles. *Am J Roentgenol.* 95 168 1965.

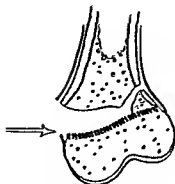
INJURIES TO THE CARTILAGE PLATE were classified by Salter and Harris (Figs. 8-533 and 8-534) in a pattern which is convenient and useful from a radiographic standpoint. Serious deformities and crippling may follow these injuries. Traumatic separations occur consistently at the same level. The line of cleavage in the cartilage plate is across the level where the columnar cartilage cells and their lacunae are maximal and where the amount of tough collagenous matrix is minimal (see Fig. 8-57). This of course is the level at which the resistance to shear force is the least. As a result the proliferating carti-

Type I



Separation of epiphysis

Type II


Fracture-separation
of epiphysis

Type III


Fracture of part
of epiphysis

Type IV


Fracture of
epiphysis and
epiphyseal
plate

Bony union
and resultant
premature
closure

Type V


Crushing of
epiphyseal
plate

Premature
closure

Fig. 8-533—Injuries to the cartilage plate classified according to Salter and Harris. Type I: complete transverse laceration of the cartilage plate with longitudinal distraction and some transverse displacement of the epiphysis. The bone itself is not broken. Prognosis is good. Type II: incomplete transverse laceration of the cartilage through a variable distance associated with oblique fracture of the contiguous shaft with a triangular tag of shaft attached to the displaced epiphysis. Prognosis is good. Type III: short incomplete transverse laceration of the cartilage plate with a longitudinal fracture extending through the epiphyseal ossification center toward the joint. This usually occurs in cartilage

plates of the tibia. Prognosis is bad if the epiphyseal fracture is not reduced with smooth joint surfaces. Type IV: oblique longitudinal fracture extending from the articular cartilage through the epiphyseal ossification center across the cartilage plate and through a short segment of the metaphysis through the cortical wall. This type is most frequently seen at the lateral condyle of the humerus. Perfect reduction is essential for a good prognosis. Type V: segmental crushing of the cartilage plate, often followed by closure of the plate prematurely and stoppage of growth. (From Salter and Harris.)



Fig 8 534—Injury to the cartilage plate at the distal end of the left femur of a boy 11 years of age. The medial segment of the cartilage plate is lacerated transversely and the lateral segment is broken obliquely and longitudinally (Salter type II injury to the cartilage plate).

ness and extent vary inversely with age. Traumatic cortical thickenings are often the most conspicuous radiographic findings in so-called battered children; their presence is often the most important single radiographic manifestation which makes it possible for the radiologist to identify traumatic injury to a child when it is denied or has been unrecognized by parents. The thickenings are similar in cases of intentional assault by adults and of purely accidental injuries. They are of no value in the decision as to whether the injured child was actually beaten by another person or incurred an accidental injury for which no one is responsible. They were, however, a major factor in my first radiographic identification of the unrecognized traumatized child in the early 1930s and which I first described in 1946. The radiographic nature of the lesions is illustrated in detail in the later discussion of the multiple bone injury syndrome (see Figs 8 542 to 8 559).

REFERENCES

- Caffey J. Multiple fractures in the long bones of infants suffering from subdural hematoma. *Am. J. Roentgenol.* 56:163, 1946.

Some traumatic lesions in growing bones other than fractures and dislocations. Clinical and radiographic features. *Brit J Radiol.* 30:225, 1957.

PATHOLOGIC FRACTURES in generalized bone diseases are due to changes which modify the relative amount of structural materials of the bones (according to Chalmers the relative amounts of organic and inorganic matrices) by the changes in design and the shape of the bone and by reduction of the total amount of bone present. Changes in these three features singly or in combination may weaken the bone and increase its potential for fracture. Normal bones have remarkable strength and high resistance to potential breaking forces of several kinds: tension, compression, shear, and torsion. For example, their tensile strength greatly exceeds that of granite and their compression strength equals that of granite. Normal bone also has remarkable resistance to repetitive loading. Chalmers quoted Lee and Evans to the effect that the second metacarpal could be subjected to 2 million repeated loadings of 15 lb each before it would break. Younger bones, owing to their elasticity, absorb the force of sudden impact and the soft tissues which surround bone also provide effective cushions which increase resistance to forces of sudden impact.

Fig 8 535—Traumatic metaphyseal cupping of the knees and shanks in frontal and lateral projections. The girl 18 months of age had suffered multiple fractures of both femurs and left tibia at 5 months of age when abused and beaten by her mother. Residual metaphyseal cupping is present in both bones at the left knee and at the distal end of the left tibia. At the left knee the femur and tibia are shortened and apayed and the joint space is deepened in the femur and proximal end of the tibia. The epiphyseal ossification centers are enlarged; the cartilage plates are thin and appear to be fusing with the shafts in the central segments of the cupped cartilaginous plate. The deformities are greatest at the distal end of the femur and least at the distal end of the tibia.



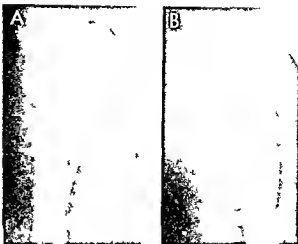


Fig 8 536 --A postfracture cyst of the right fibular shaft of a boy 14 years of age B fresh splinting fracture after a severe fall 61 days later a radiolucent cystic image has developed in the fracture site

In osteogenesis imperfecta the bones are weaker than in any other disease because the organic and inorganic matrices are deficient the structural design of the bone is disarranged and the amount of bone is reduced In scurvy the organic bone matrix is reduced In rickets and hypophosphatasia the mineral matrix is deficient and the bone mass reduced In osteopetrosis and polyostotic fibrous dysplasia the structural design is disarranged In hyperparathyroidism the structural design is disturbed and the bone mass reduced in osteoporosis also the bone mass is reduced

REFERENCE

Chalmers J Metabolic bone disease in relation to fractures
Mod Trends Orthopedics 4 208 1964

POSTFRACTURE CYST of the fibula was demonstrated in a boy 15 years of age by Levine and associates The right tibia and fibula were injured in an automobile accident and simple fractures were demonstrated radiographically without evidence of cyst formation in the broken fibula Four months later a cystic swelling was present at the site of the fibular fracture Eight months after injury the cystic lesion had continued to expand with erosion of contiguous bone At surgical exploration the cyst was found to be an encapsulated hematoma the periosteum formed part of the cyst wall There were no cysts in other parts of the skeleton The authors suspected that a false aneurysm or local arteriovenous fistula had formed The radiographic appearance simulated that of an aneurysmal bone cyst We have seen a cystic image develop at the site of a fracture in several cases (Figs 8 536 and 8 537)

REFERENCE

Levine B S et al Evolution of a post fracture cyst of the fibula, J Bone & Joint Surg 51 A 163 1969

PARENT INFANT TRAUMA SYNDROME (PITS CAFFEY KEMPE SYNDROME BATTERED CHILD SYNDROME) —In growing bones there are three important traumatic radiographic changes in addition to fractures and dislocations injuries to the cartilage plate cupping of the metaphyses and external cortical thickenings The last named in association with small peripheral cortical fractures at the metaphyseal levels were the principal findings which made possible my first recognition of PITS radiographically The cortical metaphyseal fragments are present immediately following

Fig 8 537 —Postfracture cyst in the distal third of the radial shaft 20 weeks after injury to a girl 9 years of age A transverse band of increased density marks the site of the earlier fracture line A eccentric sharply defined radiolucent patch is the site of the cyst which was filled with blood and a few multinucleated giant cells surrounded by spongy bone when explored surgically



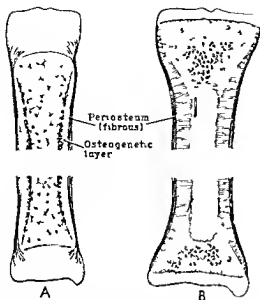


Fig 8-538 - Schematic drawings of the differences in periosteums and their attachments to the underlying cortex in young bones (A) and adult bones (B). In the growing younger bone the fibrous external layer of the periosteum is relatively shallow and delicate, with sparse and short Sharpey's fibers; the osteogenic layer is thick (see stippled layer). In growing bones, however, the periosteum is tightly anchored at both ends by heavy extensions into the epiphyseal cartilages. The loosely attached, highly vascularized young periosteum is easily torn from its underlying cortex and free subperiosteal bleeding is common and copious, which lifts the bone-forming layers away from the cortex to form an external shell of new bone. In the adult bone, the periosteum is largely fibrous with reduced vascularization, but with many heavy and long Sharpey's fibers which bind the periosteum tightly to the cortex the whole length of the shaft. As a result, in the adult after injury, bleeding is rare under the periosteum, and when it occurs it does not lift the periosteum as is the case in young bone.

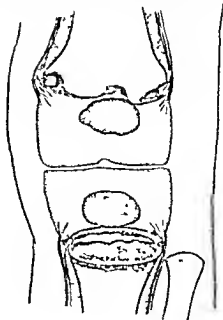
the injury and permit the immediate radiographic diagnosis of trauma. In contrast, the extra shells of cortical thickenings do not become visible radiographically until 7-14 days after injury, although subperiosteal soft tissue swellings, the precursors of the cortical thickenings, may be immediately visible radiographically. Traumatic metaphyseal cuppings develop slowly, and these changes are usually not diagnostic until after many weeks or several months. Subdural hematomas have been present in 10-25% of patients who have had multiple injuries to the long bones. Fractures and thickenings of the cranial bones and the flat bones at the shoulder girdle and pelvis may or may not be present. Marked changes are often present in the bones with surprisingly little evidence of injury to the overlying skin. Ecchymotic cutaneous lesions are present sometimes; these were described in detail by Sussman. Retinal hemorrhages and papilledema have been reported by Gilles and Mann. In 1971 Silverman reviewed the nonskeletal lesions.

The anatomic counterparts of the radiographic lesions are shown schematically in Figures 8-538 to 8-

540. The tightness of the periosteum on the shaft is compared in young and old bones in Figure 8-538. The looseness of the periosteum in younger bones is due to the relative shortness and paucity of Sharpey's fibers. The tighter terminal attachments of the periosteum in the terminal segments of the shaft and of perichondrium and the contiguous epiphyseal cartilage respectively are responsible for avulsion of the metaphyseal fragments (Fig 8-539). The progressive changes in the formation of traumatic involucria (cortical thickenings) are shown in Figure 8-540. These progressive temporal changes make it possible for the radiologist to estimate the age of these lesions and, when lesions of different ages are present in the different bones of the same patient, to suggest that there have been two or more traumatic episodes. Figure 8-541 shows the sequential changes in a single bone, the tibia, of a patient who was accidentally injured. The metaphyseal fragments are clearly seen in A (12 hours after injury), which makes the diagnosis of trauma a practical certainty several days before the cortical thickenings became visible. The cortical thickenings and metaphyseal fragments occur in a great variety of patterns (Figs 8-542 to 8-559).

Traumatic involucria and metaphyseal fragments induced by obstetric injuries during breech deliveries are shown in Figures 8-560 to 8-563; they resemble

Fig 8-539 - Schematic drawings of the tight terminal attachments of the periosteum and perichondrium which are responsible for the frequent metaphyseal fragmentation after injury to young growing bones. In the femurs, small chunks of metaphyseal bones have been torn from the periphery of the shaft. In the tibia, a large single fragment has been avulsed and then lifted, hinge fashion, toward the epiphyseal cartilage to overlap on it and produce the characteristic bucket-handle deformity of trauma.



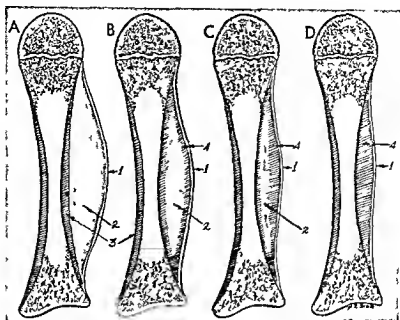


Fig. 8-540—Schematic drawings of the sequential changes in the formation of traumatic cortical hyperostosis. **A**, the first stage: the traumatic force has loosened the periosteum and caused bleeding which has lifted the periosteum away from the cortex. **1**, periosteum; **2**, hematoma; **3**, normal cortex; **4**, periosteal new bone. **B**, a peripheral shell of bone is being formed over the hematoma by the lifted periosteum. **C**, the new shell has contin-

ued to thicken while the hematoma continues to be resorbed. **D**, all of the hematoma has been resorbed with the gradual thickening of the cortex, where the new thick shell has now fused with the old underlying cortex. With the passing of time the cortical thickening is resorbed although it may last for several years in older patients. The mechanism of new bone formation is similar to that of cephalohematoma (see Fig. 1-93).

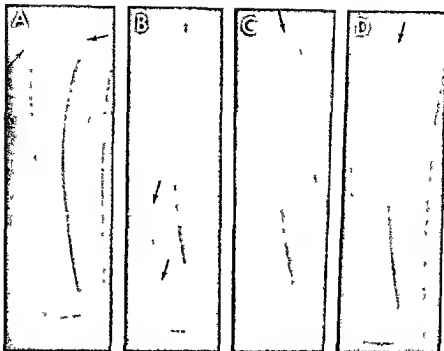


Fig 8 541 — Sequential changes in traumatic infantile hyperostosis in a patient 3 weeks of age. A. 12 hours after injury. There is no evidence of cortical hyperostosis because it is too soon after injury for the necessary bone formation. There are two chip fracture fragments at the proximal end of the tibial shaft near the cartilage-shaft junction where the periosteum is most tightly bound to the underlying cortex and primary zone of calcification. B. 7 days after injury. The ventral cortical wall is now thickened externally over its entire length excepting a short distal terminal segment. This thickening represents new subperiosteal bone laid down between the cortex and the raised periosteum.

teum. C. at 13 days. Ventral and dorsal cortical thickenings are deeper and more opaque than before. The chip fracture fragments are blending with the shaft. D. at 19 days. The cortical sheath of new bone is thicker and more opaque and the fracture fragments are fused with the tibial shaft.

The mother fell on this infant while carrying it across a all puppy floor — a pure accident with no elements of wilful neglect or evil intent, but she did not admit that the child had been injured until after a good prognosis was evident. She was ashamed to be responsible for an accident to her child, whom she loved dearly.

Fig 8 542 (left) — Severe traumatic fragmentation of the provisional zones of calcification of an infant 8 months of age.

Fig 8 543 (right) — Multiple metaphyseal cortical fragments at the distal ends of the radius and ulna of a boy 6 months of age.



who suffered from congenital insensitivity to pain. The changes induced by trauma are alike in patients insensitive to pain and those who are sensitive to pain.

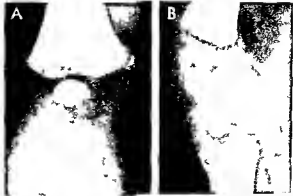


Fig 8 544 — Right knee of an infant 30 months of age. **A**, frontal, and **B**, lateral projections. Small metaphyseal cortical fracture fragments are visible on the proximal side of the right femur directly above the proximal edge of the right tibial shaft on the caudal edge of the femur in **A** and in front and behind the tibia in

B. The diagnosis of traumatic injury was made radiographically but was rejected by the clinicians and by the court. The mother, a psychopath, strangled this infant to death several weeks later. (Courtesy of Dr R Parker Allen, Denver, Colo.)



Fig 8 545 — Multiple metaphyseal cortical fracture fragments at the distal end of the left femur and proximal ends of both tibiae. The right femur is dislocated out of the right acetabulum by hemarthrosis, and there is a large traumatic involucrum on the proximal end of the right femur. In contrast to the other bones, the distal metaphysis of the right femur is normal. This boy, 8 months of age, was beaten by an attendant in a nursery.

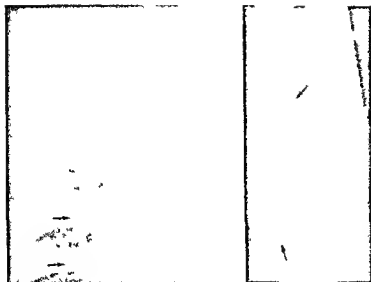


Fig 8-546 —Fragments of the proximal zones of calcification of the left femur and tibia and fractures of two ribs of an infant 10 weeks of age whose mother finally confessed to having beaten her because of incessant crying. There were also multiple fractures of the calvaria and bilateral subdural hematomas. The mother had taken excellent care of two siblings, 4 and 6 years of age, who had never been beaten or abused in any way according to the father.

Fig 8-547 —Traumatic avulsion of cortical metaphyseal fragments and possible separation of the proximal zone of calcification of both femurs and both tibias of a boy 3 1/2 months of age. The medial cortical walls of the femurs are thickened externally. Also, the left humerus was broken in its middle third where considerable opaque callus had formed. At the proximal end of the left tibia separation of a cortical rim of bone produces a buckshot hand deformity.

Fig 8-548 —Large traumatic cortical involucrum with a relatively thin shell of bone around a thick subperiosteal hematoma which suggests relatively recent formation in companion with that in Figure 8-549. The distal femoral epiphysis is lacinated and its ossification center is displaced laterad and dorsad (Sellar type injury to the cartilage plate). This boy was 5 months of age. Figs 8-548 and 8-549, courtesy of Dr. Frederic N. Silverman, Cincinnati.



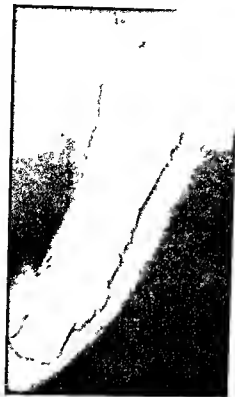


Fig 8-549—Large traumatic cortical involucrum with relatively thick bony walls and relatively thinner radiolucent mass of blood between it and the edge of the old cortical wall (compare with Fig 8-548 in which the mass of blood is large and the involucrum wall comparatively thin). This pattern of more peripheral bone and less blood centrally suggests an older lesion than that in Figure 8-548. This boy was 9 months of age.

Fig 8-550—Traumatic Involucra in the femurs. In the right femur the involucrum is thick and irregular with relatively deep radiolucent strips between it and the underlying cortex. In contrast, the involucrum in the left femur is thin and smooth with relatively thinner radiolucent strips of superficial blood. Severe metaphyseal changes are present in both ends of the tibia and include a deep "bucket handle" deformity at the distal end of the right tibia, probably caused by avulsion of a rim of the cortical bone at this level. The different types of traumatic lesions were all present at the same time in a girl 5 months of age who was said to have been beaten by her sister 4 years of age.





Fig 8 551 —Massive irregularly ossified traumatic cortical involucre in all bones of the arms and legs with generalized avulsed metaphyseal cortical fragments and dislocations at both

elbows and fractures of the left humerus. The boy 15 months of age was said to have been beaten with a bull whip by his drunken father.

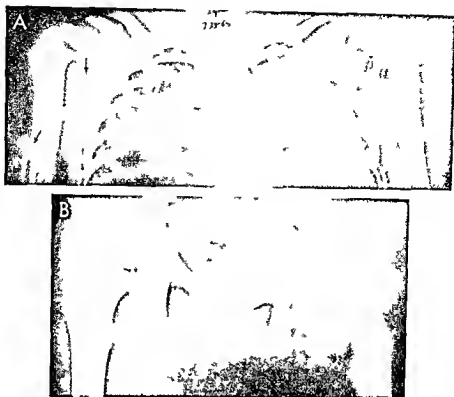
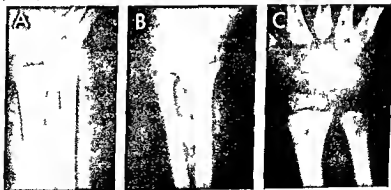


Fig 8-852—The multiple bone injury syndrome. **A** separation of the epiphyseal ossification centers from the proximal end of the left humeral shaft (Satter type I injury to the cartilage plate) evulsed fracture fragment of the right scapula and localized cortical thickening on the lateral aspect of the right humeral shaft of a girl 2 years of age. The type of injury at the metaphysis at the proximal end of the left humerus was not satisfactorily determined. The cause of these injuries was also not learned. The la-

ther said that she had fallen out of bed that morning, which is probably not true because the acromioclavicular joint at the proximal end of the left humerus would require more time than a few hours to develop. **B** fracture of the left femoral neck and pathological destruction at the left hip. Pus and blood were aspirated from the left hip joint. It seems likely that one of these radiographic changes were produced by injuries sustained several weeks and months before these films were made.

Fig 8-853—The multiple bone injury syndrome with persistent traumatic changes in the right radial distal metaphysis. **A** at age 4 months a small fracture fragment is visible on the ulnar side of the distal end of the radius. **B** at 2 years the radial metaphysis is incompletely and irregularly ossified. **C** at 5 years the zone of metaphyseal irregularity is deeper than at age 2. The companion

ulnar metaphysis is normal. The boy weighed only 28 lb and was 35 in. long at 5 1/2 years of age. Although he was neglected, a conclusive story of trauma was not obtained, but the radiographic changes probably were all due to mechanical injury and possibly parental assault.



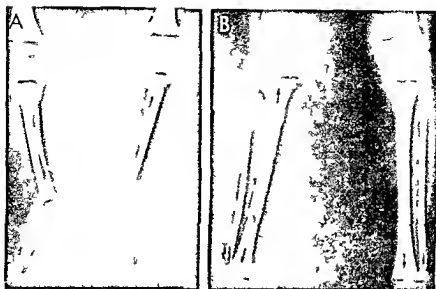


Fig 8-554 - Persistent traumatic metaphyseal changes in both ends of the tibiae. A - at 14 months all of the metaphyses at the knees and ankles show traumatic contractions and a large traumatic involucrum covers the proximal half of the left tibia shaft. B - at 5 1/2 years marked metaphyseal changes are still present at

the proximal metaphyses of the right tibia. In contrast to the normal metaphyses at the proximal end of the left tibia. The distal tibia metaphyses are also irregularly ossified, but the femoral metaphyses are normal. This is the same patient as in Figure 8-553.

Fig 8-555 - Lateral projection of a lumbar segment of the spine at 5 1/2 years of age (same patient as in Figs 8-553 and 8-554). The kyphosis is shallow with the apex at the L12 segment. The bodies of T10 through L2 are deformed due to defects at the superior or anterior angles with narrowing of the intervertebral spaces at these levels. The arrows are directed at the site of fracture fragments between T11 and T12.

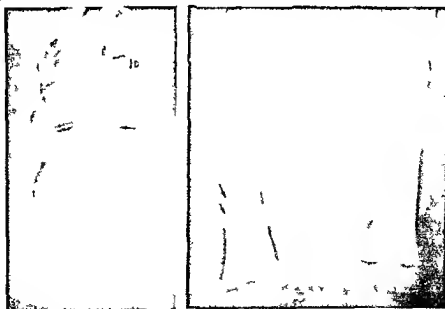


Fig 8-556 - Residual failure of constriction at the distal end of the right femur of a boy 20 months of age after resorption of a traumatic involucrum. The right leg was first injured six months before. The distal third of the right femoral shaft is widened, its medullary cavity dilated and its lateral wall bulges externally (arrows). (See failure of tubulation of femoral biopsy in entry Fig 8-252.)



Fig 8 557 —Residual shortening, cupping and spreading at the distal end of the right femur of a girl 30 months of age who suffered multiple injuries to the bones and also subdural hematoma during the 6th to 9th month of life. Growth in the central segment of the proliferating cartilage has stopped but has continued on the edges which has resulted in cupping and spreading of the end of the diaphysis with shortening and enlargement and fusion of the shaft and enlargement and fusion of the epiphyseal ossification center.

Fig 8 558 —This massive traumatic external cortical thickening of the femur formed during four weeks after this boy 9 months of age was supposedly thrown out of bed by a sibling. The right thigh was said to have impacted on the sharp edge of a table leg. A relatively small amount of blood, the narrow radiolucent strip between the outer edge of the cortical wall and the inner edges of the newly thickened cortex, is still present. The distal epiphyseal ossification center (Salter type I injury to the cartilage plate) is displaced dorsad, as seen in lateral projection (B) and there is a small avulsion fracture fragment at the dorsal angle of the tibial metaphysis. A fracture fragment is also evident at the ventral end of the tibial metaphysis.



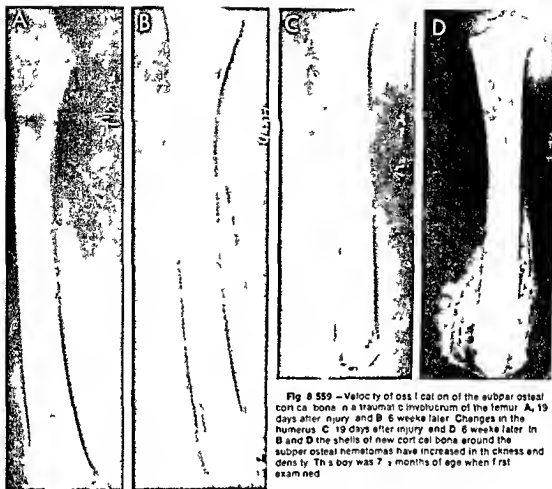


Fig 8 559 —Velocity of ossification of the subperiosteal cortical bone in a traumatic involucrum of the femur. A, 19 days after injury, and B, 6 weeks later. Changes in the humerus. C, 19 days after injury, and D, 6 weeks later. In B and D the shells of new cortical bone around the subperiosteal hematomas have increased in thickness and density. This boy was 7 1/2 months of age when first examined.

Fig 8 560 —Neonatal contusion of the tibia. A, on the 1st day of life the bones appear to be normal, although there were swelling and tenderness above the ankle. B, at the age of 10 days, a

deep localized thickening of the tibial cortex is now evident. C, at the age of 102 days, the cortical thickening is still visible. Tracings of roentgenograms.

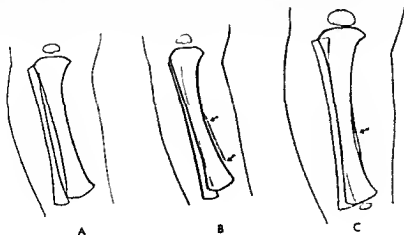


Fig 8-561 — Neonatal subperiosteal contusion of the distal end of the femur on the 14th day of life. A delicate shell of new bone lies external to the medial aspect of the cortex; it represents bone which has been formed under the raised periosteum and over a subperiosteal hematoma caused by obstetric trauma during breech extraction. There were similar roentgen changes in the other femur.



Fig 8-562 (left) — Neonatal contusion of the femur with massive cortical thickening and lateral displacement of the ossification center of the distal epiphysis on the 14th day of life. The patient was delivered by breech extraction and a soft mass was evident in the right thigh soon after birth; this swelling gradually became smaller and harder. At no time was the skin over the swelling discolored. The rest of the skeleton was normal roentgenographically. **A**, frontal; and **B**, lateral projection.

Fig 8-563 (center) — Neonatal contusion of the femur with long massive external cortical hyperostosis on the 26th day of life in a patient delivered by breech extraction. Traumatic lesions of this kind, especially when multiple, have been confused with syphilis of the diaphyses, scurvy and infantile cortical hyperostosis.

Fig 8-564 (right) — Infantile contusions of the radius and ulna with long massive external cortical thickenings one month after the infant, 4 months of age, was jerked upward by the arm to prevent him from falling off a table. The forearm became swollen a few hours after the injury. At first the mother denied that the patient had suffered injury at any time, but told of the injury on direct questioning in the x-ray department after this film was made. This case illustrates the unreliability of the history of trauma to infants by mothers and nurses when the usual causal history of trauma is taken. These traumatic obstetric and accidental lesions are identical radiographically with those caused by willful abuse.

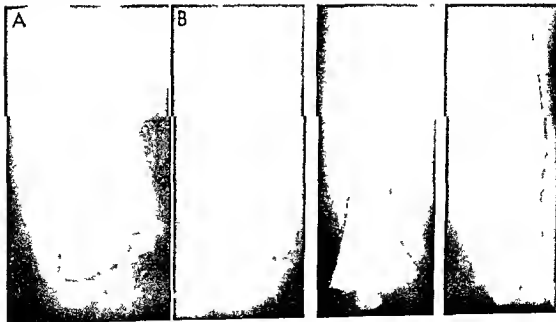




Fig 8-585 — Juvenile contusion of the femur with a large, delicate, foamy cortical thickening four weeks after a football injury to the thigh: the patient, aged 14, fell on the upturned cleats of his blocking back after being tackled. In comparison with infantile lesions, the cortical thickenings in juveniles and adults form more slowly and are more confined to the exact site of injury to the periosteum because the periosteum is more tightly attached to the shaft in older persons. A, frontal; and B, lateral projections.

the traumatic lesions encountered in infants after birth and in children. The most rapidly forming, most extensive and thickest traumatic involucri, relatively, develop in the injured newborns. The changes in Figures 8-541 and 8-564 developed after denied but accidental injuries; they are identical radiographically with the traumatic changes that develop after wilful assault of older children by adults. The extent of the involucrium is more limited in older children (Fig 8-565, compare with the extensive neonatal involucrium in Fig 8-563). Free bone fragments may be seen in the soft tissues. Symmetrical cortical thickenings (Fig 8-566) of the fibulas have been due to excessively tight lacing of boots in several patients. The reader is referred to my report of 1957 for detailed descriptions and a wide variety of these lesions in their clinical settings. Examples of possible idiopathic traumatic cortical thickenings are shown in Figure 8-567, and examples of traumatic cortical thickenings of the phalanges in Figures 8-568 and 8-569.

The high diagnostic value of these skeletal changes has been proved over many years. Absence of radiographic bone changes does not, of course, exclude parent infant abuse. The radiographic lesions in the



Fig 8-566 — Symmetrical external thickening of the lateral cortical walls of the fibulas of a boy 4 years of age who had worn tightly laced boots for several months. Cortical thickenings of this kind have been called stress fractures of the fibulas; erroneously we believe, in some cases.

Fig 8-567 — Symmetrical thickenings of the lateral cortical walls of the femur of an asymptomatic infant 3 months of age. Trauma was denied in the history. Lesions of this type found in many asymptomatic infants, especially premature, are probably due to trivial, unrecognized trauma incidental to dressing, bathing, and even gentle play to the loosely attached, highly vascular, delicate periosteum of the very young.





Fig. 8-568—Residual fusiform swelling of the middle and basal phalanges of the 3rd digit of a girl 2 years of age whose hand had been caught in a door and injured five months before. Traumatic changes of this kind have been confused with the fusiform digital swellings and cortical thickening of the phalanges found in rheumatoid arthritis.

long bones which are induced during parturition especially in breech deliveries simulate the skeletal changes of parent infant trauma. Many premature (low birth weight) and some normal full term infants develop smooth cortical thickenings during the 1st year of life. These should not be confused with traumatic involucriums of parental trauma.

Radiographic study of the bones discloses the site, number, nature and approximate age of the bone lesions. Radiographic changes are often present in the absence of local clinical signs. It is clear that this roentgen test of the skeleton for signs of trauma in parent traumatized young infants not only identifies the traumatic origin of the lesion but provides information that is valuable in several other ways. Positive evidence of changes in the skeleton when presented to the parents has on several occasions persuaded them to confess the truth and such evidence is a deterrent to further trauma by guilty parents who do not admit their guilt. At necropsies in cases in which traumatic injury is suspected or the cause of death is unknown, complete radiographic examination of the skeleton is mandatory. There is no single test for disease in the total diagnostic field of pediatrics which identifies the causal agent and provides as much other useful information. We include such valuable time honored procedures as the tuberculin Schick Wassermann and Kahn tests and the chemical and immunologic serologic tests for disease agents. In the same breath we emphasize that the radiographic skeletal changes do not identify the perpetrator of the trauma or his motive.

Most of the skeletal lesions result from traction (stretch) stresses rather than impact (compression) stresses. They are induced by stretching and shearing

forces in the periosteum and on the tendinous and ligamentous attachments to the growing bones rather than by direct compression of a hit from a parent's hand or kick from his foot. The high frequency of traction lesions indicates that the infant is commonly grabbed and held by the extremities during shaking which often causes whiplash stresses on the head and neck and repeated fast stretching and then squeezings of the brain and intracranial blood vessels which account for the high incidence of subdural hematoma and probable bruising of the brain itself. In the extremities the soft tissue stretching and squeezing are aggravated by the resistant counter forces of the infant as he twists and squirms.

A summary of current knowledge of the parent infant trauma syndrome indicates that it has a high incidence although the exact incidence is unknown. Kempe estimated in 1971 that 15 000-25 000 infants and children are significantly injured in the United States each year. The parent infant injuries are largely in the group younger than 3 or 4 years. The syndrome apparently has similar incidences in Canada, Western Europe and Australia. The prevalence of PITS in Eastern Europe, Russia, the Middle East and Africa is not known to me. I have seen a few examples in American Indians and films of several cases have been sent me from South America. Dr. Mazloum Osman investigated the frequency of PITS at the Children's Hospital, Alexandria, Egypt and encountered no cases during the three years 1966-71. Our resident physicians from India and Iran report that the syndrome has not been recognized in their countries. The English have recognized the syndrome officially in their National Society for the Prevention

Fig. 8-569—Multiple metaphyseal fragmentations (arrows) with sclerosis and thickenings in the cortices of the tubular bones in a boy 5 years of age who had made a practice of slamming the door of a refrigerator on one hand and then the other many times each day for several months. He seemed to enjoy the practice and was later found to be insensitive to pain in the basal phalanges. There are extra epiphyseal ossification centers in the distal epiphyseal cartilages (arrows); these were believed to be owing to the chronic hyperemia induced by the repeated trauma during long periods. Similar changes were present in the bones of the other hand.



of Cruelty to Children in a Department for Battered Child Research. However, statistics are inadequate in all parts of the world. It is possible that many cases of idiopathic subdural hematoma and brain injuries are residuals of unreported parent infant trauma and also spastic cerebral disease, idiopathic hydrocephalus and microcephaly and idiopathic mental retardation. If so, effective prevention of parent infant trauma would decrease these miserable and costly disorders substantially. We hope that penetrating studies of these important aspects of PITS will be made.

The cause of PITS is intentional assault of infants by mothers usually but occasionally by parent substitutes and others to whom infants are exposed in their own homes. The basic pathogenesis is fitful loss of self control by the distraught mother owing to excessive stresses of a hostile impoverished environment, a mother unprepared for marriage, child bearing and child rearing. She succumbs momentarily to the combat fatigue in a hopeless struggle with overwhelming odds.

The victims are normal infants commonly 12 months old or younger who are usually well fed, well clothed and clean. The incidence of parent infant trauma is however higher in premature, unwanted, deformed and adopted infants and in multiple-birth infants, those with a step-parent and those resident in foster homes. It is possible that provocative demanding infants are traumatized more than normal infants.

Usually assaulters are mothers and to a much lesser degree fathers or parent substitutes of all races, all religions and from all social, educational, economic and cultural levels from a wide and uniform geographic distribution. Customarily the parents are of normal intelligence and as a group with few exceptions they suffer from the same neuroses, the same character and emotional problems in the same range and degree as any randomly selected group of the same size and from the same milieu (Galdston). No stereotype psychotic has been identified. According to Kempe, in 5% one parent is a delusional psychotic and in 5% one is an arrogant psychopath.

Curative treatment is exceedingly difficult and usually impossible by a single physician in the office, hospital or outpatient department. Social service follow ups, psychiatric counseling and wordy advice do not eliminate the basic causes—the hostile impoverished environment and its heavy stresses on a beleaguered mother in despair. The mother and her family need immediate substantial material and emotional support. This has apparently been done most effectively by Galdston's method of "protective intervention" which provides day care ten hours a day, five days a week. Personal and telephone consultations are provided to parents on demand and they have group meetings at the center in the evenings. In an experience with 43 infants cared for at an average of five months each, not a single patient has been reinjured during the nights at home and the

two days he has remained at home over the weekend.

Preventive treatment which should be the goal of everyone could be achieved by the application of knowledge and resources currently available. Young mothers and fathers need training in the practical aspects of the optimal care of their infants before they are born. Unwanted pregnancies could be prevented by proper contraceptive control and/or sterilization of one or both parents on demand. Unwanted pregnancies could be terminated by abortion on demand. The major need in prophylaxis of parent infant trauma is full recognition of the primary, important social and economic service the child bearing, child rearing mother provides the community and a generous reward to her for her valuable contributions to society. She produces nurtures and rears the most valuable product in our Gross National Product but is consistently undervalued, underpaid and overworked. Her task demands 24 hours a day, 365 days a year during several years. Her emoluments should outrank such dilettante workers as electricians, truckers and plumbers. Perhaps these realistic values cannot be achieved short of the organization of a Union for Motherhood which could become the largest in membership, the strongest in social and economic power and the most persuasive in political clout.

The following conclusions on PITS seem reasonable in the year 1971: (1) Because of its high incidence, substantial mortality and morbidity and late cerebral complications, PITS is probably the most important discovery of a new pediatric disease in the past 50 years and certainly the most important infantile disease ever discovered by radiographic examination. (2) The deep impacts of the discovery of this syndrome in medicine, law, social practices, politics, communication services (press, radio, television) are unparalleled in the history of pediatric discoveries. (3) Intentional, vigorous and even mild casual shaking of younger infants with phibole skulls is probably a much more important cause of cerebral and cerebrovascular disease with serious later residuals than is now appreciated. (4) This disease could be largely eliminated now by proper prophylactic measures currently available. (5) The liberation of the child bearing, child rearing mother in the prevention of PITS could serve as the spearhead for the liberation of women generally.

The elements of the syndrome are epitomized in the following threnody:

A Clinical Lament

Poor forlorn babe, barely started in life
But victim already of cruel family strife
Your parents' tongues locked in silence
Hush untold tales of secret violence
When we flush your flesh with sad and streams
Sick bones shine clear in truthful gleams
It's shake, shake and shake more than bash and batter
That bruise brain, bones and dura mater
Remember your mother is not a fiend partaken
Just your mom in distress by the world forsaken

J.C.

REFERENCES

- Astley R. Multiple metaphyseal fractures in small children. *Brit J Radiol* 26:577 1953
- Bakwin H. Roentgenologic changes in the bones following trauma in infants. *J Newark Beth Israel Hospital* 3:17 1952
- Multiple skeletal lesions in young children due to trauma. *J Pediatr* 49:7 1956
- Barta, R. A. Jr. and Smith N. J. Wilful trauma to young children: a challenge to the physician. *Clin Pediatr* 2:545 1963
- Caffey J. Synchysis of the skeleton in early infancy. The non-specificity of many of the roentgenographic changes. *Am J Roentgenol* 42:637 1939
- *Pediatric X-ray Diagnosis* (1st ed. Chicago: Year Book Medical Publishers Inc. 1945) p. 753
- Multiple fractures in the long bones of children suffering from chronic subdural hematoma. *Am J Roentgenol* 56:163 1946
- Some traumatic lesions in growing bones other than fractures and dislocations: clinical and radiological features. *Brit J Radiol* 30:225 1957
- Significance of the history in the diagnosis of traumatic injury to children. *J Pediatr* 67:1000 1965
- The parent infant traumatic stress syndrome (Caffey-Kempe syndrome) (battered babe syndrome). The First Annual Neuhauser Presidential Address of the Society for Pediatric Radiology. *Am J Roentgenol* 114:217 1972
- Elmer E. *Children in Jeopardy* (Pittsburgh: University of Pittsburgh Press 1967)
- Fairburn A. C. and Hunt, A. C. Caffey's third syndrome—a critical examination of the battered baby. *Med Sci & Law* 4:123 1964
- Galdston R. Observations on children who have been physically abused and their parents. *Am J Psychiat* 122:440 1965
- Violence Begins at Home. Presented at the annual meeting of the American Academy of Child Psychiatry. Denver, Colo. Oct. 17 1970
- Gil D. G. Physical abuse of children: Findings and implications of a nationwide survey. *Pediatrics* 44 (supp) 857 1969
- Gilles M. J. and Mann T. R. Funds of battered babies. *Lancet* 2:268 1967
- Guthkelch A. N. Infantile subdural hematoma and its relationship to whiplash injuries. *Brit M J* 2:430 1971
- Helfer R. E. and Kempe C. H. (ed.) *The Battered Child* (Chicago: University of Chicago Press 1968)
- Ingraham F. D. and Heyl H. L. Subdural hematoma in infancy and childhood. *JAMA* 112:198 1939
- Kempe C. H. et al. The battered child syndrome. *JAMA* 181:17 1963
- Pediatric implications of the battered babe syndrome. *Arch Dis Childhood* 40:28 1971
- Silverman F. N. The roentgen manifestations of unrecognized skeletal trauma in infants. *Am J Roentgenol* 56:163 1953
- Personal communication 1971
- Snedecor S. T. et al. Traumatic ossifying periostitis of the newborn. *Surg Gynec & Obst* 61:387 1935
- Some obstetrical injuries to the long bones. *J Bone & Joint Surg* 31A:378 1949
- Sussman S. J. Skin manifestations of battered child syndrome. *J Pediatr* 72:95 1968
- Tardieu A. Étude médico-légale sur les services et mauvais traitements exercés sur des enfants. *Ann hyg publ et méd lég* 13:361 398 1860
- West S. Acute periosteal swellings in several young infants of the same family probably rachitic in nature. *Brit. M J* 1:856 1888
- Wooley R. V. Jr. and Evans W. A. Jr. Significance of skeletal lesions in infants resembling those of traumatic origin. *JAMA* 158:539 1955

FOCAL STRESS FRACTURES AND STRESS DEFORMITIES OF THE EPIPHYSES, ROUND BONES AND METAPHYSES (formerly called ischemic necrosis and osteochondrosis juvenilis) constitute a group of widely scattered and unrelated independent lesions in the growing skeleton which are characterized radiographically by focal fractures and compression of the provisional zones of calcification and their underlying spongy bone. Many of them pass through a series of progressive radiographic changes which include sclerosis, flattening, fibrous replacement of the sclerotic bone and reossification of the fibrous tissue with complete healing but often severe crippling deformity as well. These cyclic changes may continue over a period of three to five years. The degree of deformity and disability depends on the duration and degree of the stress to which the softened fibrous parts are subjected. The exact causal agents and mechanisms are not known although excessive simple mechanical endogenous stress appears to play an important role in all of them.

The traditional causal hypothesis suggests that impairment to the local arterial blood supply is the primary cause which reduces the flow of essential nutrients and oxygen to the growing bone and plays the primary causal role and induces ischemic infarction. Our observations in coxa plana and the findings of Blount in tibia vara indicate that deformity and sclerosis follow fracture in Perthes coxa plana and that there is no necrosis in Blount's tibia vara. Boznan proposed that the primary injury and causal mechanism might be direct mechanical compression of the convex edges of epiphyseal ossification centers and of round bones (provisional zones of calcification during growth) which does not immediately damage the whole bone but merely affects its edges. According to Boznan the necrosis which follows is secondary to the original compression—compression of bone is the sole underlying cause of all these diseases. He also pointed out the frequency of microscopic compression fractures of the cancellous trabeculae. Crock, a meticulous student of the precise blood supply of growing bones, commented in 1967 that the significance of the blood supply as a causal mechanism in Perthes disease remains unclear. Johnson concluded that a dense femoral head following injury does not necessarily mean a necrotic head; that specimens of Osgood-Schlatter disease rarely show any evidence of necrosis and that the explanation of osteochondrosis dissecans as an infarctive process is unsatisfactory.

Except for Blount's tibia vara, the juvenile stress lesions are more common in boys than in girls, rarely develop before age 3 or after age 12 and are exceedingly rare in Black children. Each of these several independent lesions are often designated by the name or names of its discoverers (Fig. 8-570); this has given rise to bewildering plethora of eponyms. Developmental focal irregularities in ossification which of course are not necrotic and not significant clinically are found at the same sites where many of these

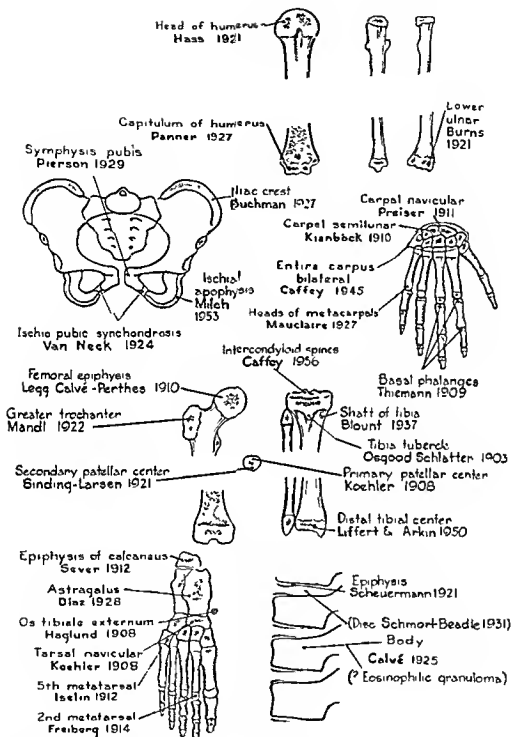


Fig. 6 570 - Schematic drawing of the growing skeleton showing the sites of the juvenile osteochondroses (focal ischémie

neccroses) names of the discoverers of the different lesions and the years during which each les on was first reported

stress lesions develop (see Fig 8-245) This has led to frequent errors in diagnosis and the sentencing of many healthy children to unnecessary long term, expensive and emotionally damaging treatment. Some of the supposed "ischemic necroses," such as Sever's disease of the calcaneal apophysis and Van Neck's disease of the ischiopubic synchondrosis, are now conceded to be medical myths. Kochler's disease of the tarsal navicular is an exceedingly rare entity which simulates the normal irregular sclerosis and hypoplasia of this bone. Hypoplasia and irregular sclerosis of the tarsal navicular are normal development features in at least 20% of all healthy children.

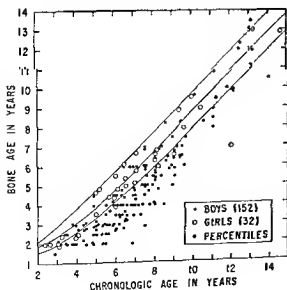
REFERENCES

- Bozman E J: Compression of cancellous bone, *Am J Surg* 53:532, 1941
 Crock H V: The Blood Supply of the Lower Limb Bones in Man (Edinburgh: E & S Livingstone, Ltd, 1967), p 88
 Goff, C W: Legg Calve Perthes Syndrome and Related Osteochondroses of Growth (Springfield, Ill: Charles C Thomas, Publisher, 1954)
 Johnson L C: Morphologic Analysis in Pathology in Frost, H M (ed): Bone Biodynamics (Boston: Little Brown & Company, 1964)
 Kung E D J: Localized Rarefying Conditions of Bone (London: Edward Arnold & Co, 1935)

Legg's stress fracture of the femoral head (Legg Perthes Calve disease) is one of the most common acquired crippling lesions of childhood and is often

Fig 8-571—The retarded skeletal maturation of essential coxa plana according to Girdany and Osman. All values are below the median or fifty percentile and the majority are well below the third percentile. The probability of this being a random pattern is less than one in a million. (From Girdany and Osman.)

BONE AGE VS CHRONOLOGIC AGE IN PERTHES' DISEASE



followed by disabling osteoarthritis 10-30 years later. It is by far the most important of the focal stress lesions. If one excludes Legg's stress fracture, the importance of the whole group diminishes by 80-90%. This lesion develops in children between age 3 and 12, with maximal incidence at 6-8 years. Boys are affected four to five times as frequently as girls. In about 1 in 10 patients the changes are bilateral. Black children are rarely affected. The patients are generally clinically healthy, but bone maturation is consistently and often severely retarded. Among 184 patients Girdany and Osman found that no patient had a bone age greater than the median age and most were below the 3 percentile of a normal population (Fig 8-571). Legg's coxa plana is occasionally familial and may affect several generations (Fig 8-572). Coxa plana (mere flattening of the femoral epiphyseal ossification center) has been found fortuitously by us in association with a wide variety of clinical disorders: congenital dislocation of the hip, hypothyroidism, pituitary dwarfism, juvenile rickets, Gaucher's disease, hemophilic hemarthrosis of the hip, gargoylism, Morquio's disease, achondroplasia, the congenital adrenogenital syndrome, celiac disease, the rheumatic state, diabetes mellitus, carcinoma of the thyroid, sickle cell anemia, aregenerative anemia, familial fibrosis of the jaws, multiple epiphyseal dysplasia and Fabry's disease. Most of these are probably chance associations. However, in Morquio's disease and multiple epiphyseal dysplasia coxa plana is a consistent finding. It is also likely that many of the examples cited above, except Morquio's disease, are developmental in origin, such as Meyer's dysplasia of the epiphyseal ossification center in the proximal femoral epiphyses, without the progressive flattening and destructive characteristic of Legg Perthes coxa plana. The coxa plana associated with congenital dislocation of the hip is not Legg Perthes disease, but probably is a late sequel due to previous treatment during the early months before the epiphyseal ossification center of the femur ossified. The metaphyseal lesion of Perthes' coxa plana rarely appears with congenital dislocation of the hip. The coxa plana of sickle cell anemia affects older children and usually does not progress through the standard cyclic changes of essential coxa plana. This is also true of several other of the disorders mentioned above.

The principal clinical signs are limp and pain and limitation of motion at the hip. Sometimes pain is referred to the inside of the ipsilateral knee, for this reason, films of the hips should be made when a child has pain at the knee. These signs may last for a few days or several months. They are often inconstant. At the onset they are commonly slight and vague. In some cases an exact date of clinical onset is not recognized by the patient or his parents. Radiographic changes are in many cases far advanced when the clinical onset is first detected, indicating that radiographic changes have been present long before the clinical signs became appreciated. Occasionally radi

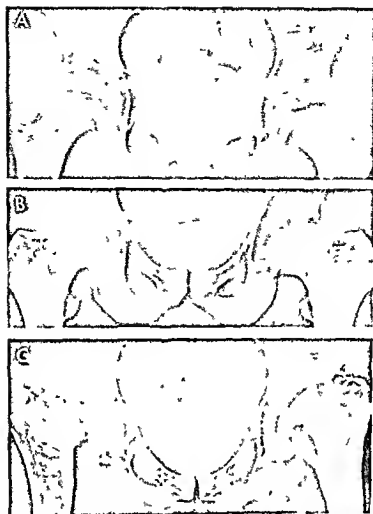


Fig. 8-572 - Familial coxa plana in three generations. A, in a boy 6 years of age. B, in his father 32 years of age. C, in the paternal grandfather 60 years old in whom severe residuals of coxa magna, widening of the femoral necks, distalation of the acetabular cavities and destruction of their roofs and marked

thinning of the articular cartilages demonstrate the late painful sequelae in patients who may be asymptomatic during the second, third and sometimes the fourth decades. (Courtesy of Dr. Bertram R. Girdany, Pittsburgh.)

ographic changes are discovered by chance in patients who had no clinical signs or signs for only a few days or hours (see Fig. 8-586). There are no constitutional signs and standard laboratory findings are normal. In 1964, 87 new cases of coxa plana were reported in the entire population of the Commonwealth of Massachusetts by Molloy and MacMahon. They estimated that the annual incidence rates peaked between the ages of 4 and 8 years and were about five times as high in boys as in girls. Their cumulative-to-15-years-of-age attack rates were 1/740 boys and 1/3700 girls. Of 74 patients with adequate records, 1 was Black. The mean birth weight of the affected children was smaller than that of controls.

Prognosis is uncertain even after most skillful treatment. Early age at onset improves the prognosis.

Regardless of treatment, results are better in patients whose lesions appear from age 3-5 years than in those in whom the first signs appear at 6-8 years. The value of different types of treatment is controversial. Complete healing with varying degrees of deformity occurs spontaneously regardless of treatment and the degree of deformity. Few (perhaps less than 10%) of the patients recover with normal femoral heads and normal acetabular cavities. Despite complete healing during childhood, the patients may suffer from painful crippling osteoarthritis during the third and fourth decades of life owing to progressive destruction of the articular cartilage on both sides of the hip joint due to misfit of the enlarged and deformed healed femoral heads into the now too small acetabular cavities. Better results have been reported by a few surgeons after surgical treatments which

provide deeper and more complete coverage of the femoral head by the acetabular roof.

The microscopic changes during the earliest phase of the disease are unknown. Jonsater found high grade necrosis of both bone and bone marrow in his initial stage¹ which appears to be later radiographically than the earlier marginal fracture and flattening stage of Caffey. In the more advanced stages of the active disease microscopic examination discloses massive necrosis of spongy bone with multiple fractures and distortions of dead trabeculae which are scattered along with some bone powder in the fibrous tissue of the compressed medullary spaces. During the reossification phase new bone is deposited on the dead trabeculae (Bobechko and Harns).² The late residual gross deformities are not associated with necrosis because healing is complete in the latest stage after three to five years. The radiolucent defects in the metaphyses appear after the primary stage of marginal fracture and are made up of tongues of radiolucent uncalcified cartilage (Ponseti)³ which replace the more radiopaque spongy bone and in some cases a segment of the radiopaque ventral cortical wall. There is no necrosis at the site of the radiolucent metaphyseal defect, but often the uncalcified cartilage hypertrophies to form an enchondroma in the medullary cavity of the femoral neck.

The causal agent and mechanism have not been satisfactorily demonstrated. Many hypotheses have been advanced including local ischemic necrosis due

to impairment of arterial blood flow, inflammation, vitamin D deficiency, thyroid deficiency, idiopathic lateral dislocation of the femoral head, torsion of the femoral neck, increased declivity of the acetabular roof, thickenings of the soft tissues at the level of the femoral neck, and direct marginal compression and local fracture of the femoral ossification center. The first named has long been the most popular although it has little other than circumstantial evidence to support it. Our findings during what appears to be the very earliest radiographic phase of the lesion support the last named hypothesis—direct compression and fracture of the edge of the femoral ossification center by the acetabular roof owing to lateral idiopathic displacement of the femoral head which leads to segmental overload on the edge of the femoral head. This is a stress fracture and is usually due to repeated long standing compression of the displaced femoral head (Calot)⁴ against the overhanging segment of the acetabular roof. The traumatic forces involved are largely endogenous, although occasionally coxa plana appears to develop after a single episode of excessive external stress as in a sudden twist during running or ice skating. The secondary necrosis which follows primary fractures is due to progressive compression of the medullary cavity rather than primary injury to the retinacular arteries. Waldenstrom⁵ apparently saw marginal fractures and possibly intraepiphyseal gas in some of his patients observed early in the disease. Burrows⁶ saw subchondral fissures during the

Fig 8-573—Coxa plana in the early dislocation phase prior to the fracture phase. This boy 5 years and 5 months of age had been limping for three weeks on his left leg. The left femur lies 4 mm farther laterad in its acetabular space than does the right femur. Also the dislocation laterad is reflected in the overlap of the epiphyseal ossification center on the ischium which is less in

the left hip in both A, standard, and B, frog projections. There is no sclerosis, fracture or flattening. In some similar very early examples the affected femoral ossification center was smaller than in the normal femur. In this patient seven months later flattening and sclerosis of the left femoral head were marked.

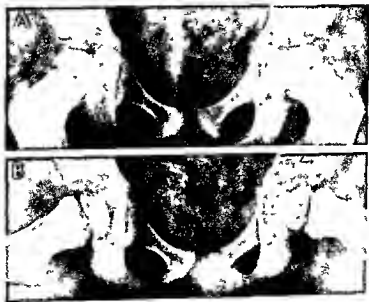
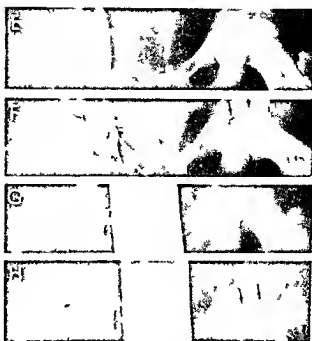




Fig 8-574 — Early radiographic findings in coxa plana. A, standard and B, frog positions, immediately after painful injury to the hip in a football game and onset of right adducted limp. There is no evidence of flattening or sclerosis but the right femoral head is slightly laterally tilted. C, frog position 13 months later, the right and 10 mm on the left. In C and D, 10 months later, the femoral head is fractured in the upper lateral quadrant and a strip of gas density intervenes between the fragments. In E and F, six months



after the femoral epiphyseal ossification center is diffusely sclerotic and slightly flattened and the fracture is clearly visible in G and H. Nine months later flattening and sclerosis of the right epiphyseal ossification center have increased and the fracture line has been obliterated. The large radiolucent metaphyseal defects are now visible in both positions. The fracture clearly preceded both flattening and sclerosis. Also, the metaphyseal lesions were not present in the earlier films of this series.

first phase of coxa plana prior to collapse. Edgren found submarginal radiolucent strips which appear to be marginal fractures of the femoral epiphyseal ossification centers in 43 patients. Coxa plana did not develop in Rathjiff's patients who had complete traumatic separation of the femoral heads. The smallness of the femoral ossification center suggests that the femoral head has been displaced at the hip for weeks and months before primary fracture occurs and that Calot was correct in his conclusions during the 1920s that the slight dislocation is the earliest radiographic change in essential coxa plana. Coxa plana develops frequently after prolonged treatment with adrenocortical steroids.

The radiographic findings depend on the stage of the disease in which the radiographic examination is made. The earliest or "dislocation" phase is characterized sometimes by smallness as well as slight lateral displacement of the femur—Waldenström's sign (Fig 8-573). In the second or "fracture" stage a marginal fracture line is clearly visible as well as the dislocation of the head in the anteromedial superior quadrant of the epiphyseal ossification center (Figs 8-574 to 8-578). The fracture line is only partially visi-

ble or is often invisible in the standard frontal projection with the femurs adducted, but it is clearly visible widened and elongated in the Lauenstein or "frog" position. The latter should be used regularly in all phases of the disease. In all of our cases the early fracture line had disappeared on the second examination made 4–12 months later (Fig 8-579). Flattening and sclerosis were absent when fracture was already well developed and seemed to follow the appearance of the fracture line in the anterior segment of the epiphyseal ossification center, the earlier site of the fracture (Figs 8-580 and 8-581).

These features appeared first in the same segment as the fractures, both increased with advancing time as the fractures disappeared. We attribute the flattening to weakening of the edge of the epiphyseal ossification center at the fracture site by simple compression of this weakened ossification center by the overlying acetabular roof. The sclerosis was also ipsilateral with the fracture and was characteristically marginal during its earliest phase. The very earliest sclerosis is due, we believe, to local compression which crowds and tightens the mesh of the opaque spongiosa into a smaller space, with compensatory local shrinkage



Fig 8 575 —Early fracture stage of essential coxa plana of the left femur of a boy 10 years of age who had limped and had pain in the left hip for six weeks. In **A**, standard frontal projection, the left femur is displaced laterad 3 mm in its acetabular cavity and the superior edge of the epiphyseal ossification center is slightly

flattened. In **B**, frog position, a submarginal radiolucent fracture line extends across the top of the epiphyseal ossification center and the superior fragment is less dense than the inferior fragment. Fracture here clearly precedes flattening and generalized sclerosis of the epiphyseal ossification center.

Fig 8 576 —Coxa plana in early fracture stage prior to flattening and sclerosis. This boy 6 1/2 years of age had been limping on his right leg for a few weeks. In **A**, standard projection, the right femur is dislocated laterad 2 mm; this is also evident in the greater overlap of the left femoral head and femoral neck on its ischium. The right femoral epiphyseal ossification center is not flattened or sclerotic. In **B**, frog projection, a wide submarginal

fracture line is seen in the anterolateral segment of the epiphyseal ossification center. There is no metaphyseal lesion. This is an example of substantial fracture before flattening or sclerosis. Failure of visualization of the fracture line in the standard projection (**A**) is also noteworthy. The right femur progressed through the typical cyclic changes of coxa plana in the next three years.



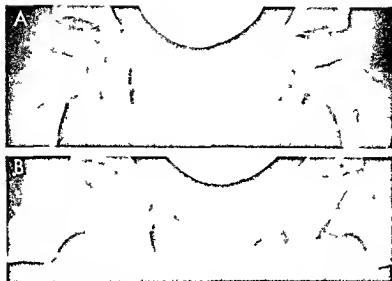
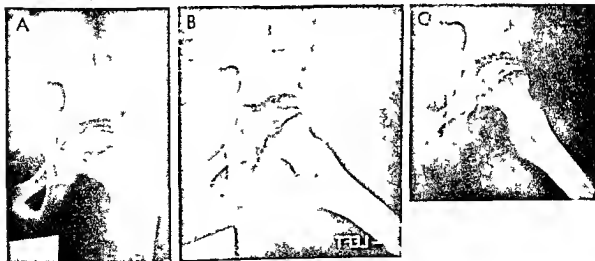


Fig. 8-577—Coxa plana in early fracture stage with slight flattening and sclerosis. This girl 5 1/2 years of age had limped and had pain at the right hip for some weeks. In A, standard projection there is no fracture. The epiphyseal ossification center, however, is displaced laterad 3 mm, evident also from the increased overtop of the left femur on its ischial/acetabular edge. In B, frog position,

on a clear submarginel fracture line parallels the superior/entrolateral edge of the epiphyseal ossification center. Its bright black density suggests that there may be gas between the edges of the fracture fragments. This is an example of segmental fracture, a prior to flattening and sclerosis invisible in standard position (A) but clearly visible in frog position (B).

Fig. 8-578—Essential coxa plana in early fracture stage with minimal flattening and sclerosis. A, standard; and B, frog positions made at the same time. C, frog position later than B. In A, a short fracture line is seen under the superior/lateral edge of the epiphyseal ossification center, which is slightly flattened. In B, the fracture line is longer and wider than in A, clearly the spongiosa as well as the provisional zone of calcification is broken.

The fractures in the superior/entrolateral segment with little or no sclerosis in any part of the epiphyseal ossification center. In both films the metaphysis is normal. In C, the fracture line is shortened and the antrolateral superior segment sclerotic and slightly flattened. Now there is a sharply outlined defect far forward in the metaphysis directly under the fractured segment above in the epiphyseal ossification center. (From Lewis.)



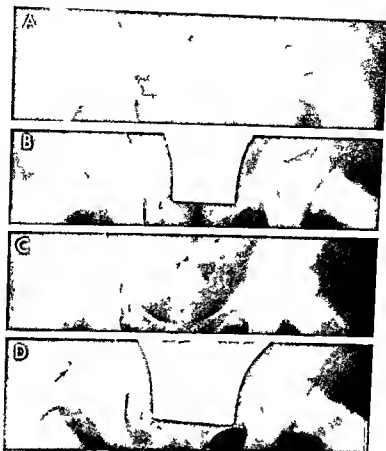


Fig. 8-579—A and B: films of a girl 6 years of age who had limped for four weeks on the right side. In A: standard position the right apophyseal ossification center is small and diffusely sclerotic but there is no fracture line. In B: frog position a submarginal fracture line is clearly visible in the anterolateral aspect of the distal radius. In C and D: five months later there is no fracture line in the standard position and the apophyseal ossification center has flat-

tened and become more sclerotic. Also, a small defect is now present in the ventral segment of the metaphysis directly under the ventral segment of the apophyseal ossification center. In all of our cases the early fracture disappeared as the apophyseal ossification center flattened and became more sclerotic and the metaphyseal defect appeared.

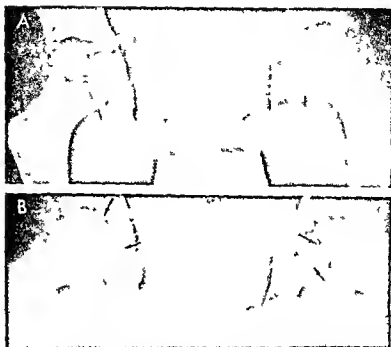
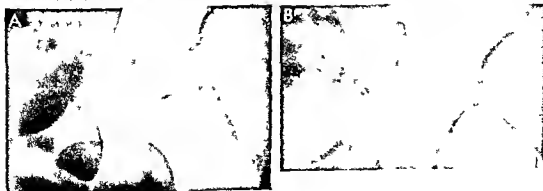


Fig 8580—Early segmental and marginal sclerosis in a boy 4 years of age who had limped on the left leg for three weeks. In A, standard position, the left epiphyseal ossification center is displaced laterally but there is no sclerosis or flattening. In B, frog position, the left epiphyseal ossification center is smaller than the right and displaced laterally. The anterolateral superior lateral quadrant is flattened and the margins of the flattened segment are sclerotic, but the rest of the epiphyseal ossification center is normal in density. We believe this early sclerosis represents

compression but not necrosis. Near the flattened edge of the epiphyseal ossification center, a fracture line extends forward and down from the summit. In the right hip, a long curvilinear strip of bright black density outlines the edges of the femoral articular cartilage below it and the acetabular articular plate above it. This is gas in the articular space and is due to the ant vacuum effect following displacement of the articular space by stress of traction and twist on the right hip to obtain the frog position. (Courtesy of Dr. William McCalister, St. Louis.)

Fig 8581—Invisible early fracture with total sclerosis of the epiphyseal ossification center in standard position (A) and true segmental and marginal sclerosis associated with early segmental fracture and flattening in frog position (B). This boy 7 years of age had been limping on his right leg for about three months. In A, the right epiphyseal ossification center is displaced laterally and appears to be diffusely and totally sclerotic. A fracture is not visible. However, in B, the anterosuperior segment of the epiphyseal ossification center is flattened and sclerotic and a short

fracture line is visible near its upper edge. The sclerosis in the frog position, in contrast to that in standard position, is marginal and confined to the entire or broken flattened segment of the epiphyseal ossification center; the dorsal part of which is not flattened or sclerotic. The central portion of the epiphyseal ossification center is not sclerotic. The films demonstrate the futility of attempting to evaluate the changes in early coxa plana without the frog position.



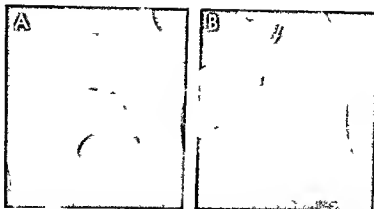


Fig 582.—Example of anterior segmental involvement only relatively late in the disease and demonstration of the advanced stages of frog position. This boy 3 years of age had had pain in the right hip and limped on the right side for several weeks. In A, standard position, there is no flattening or sclerosis. In B, frog position, the anterior segment of the epiphyseal ossification center

appears to be fragmented and is irregularly mineralized. In contrast, the dorsal segment is normal and remained normal throughout the course of the disease. The lesion is in the resorption stage; the fragmented appearance is due to multiple small ossification centers, not to fracture. Without the frog position, none of the important features of this lesion can be seen.

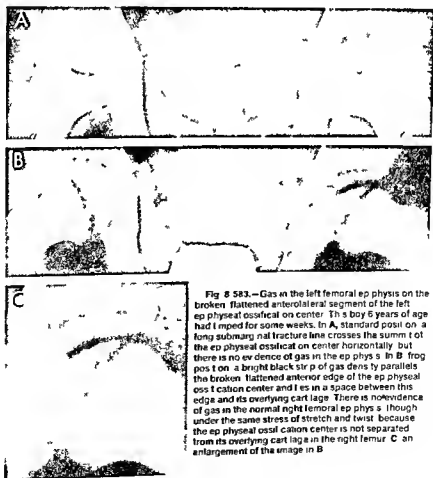


Fig 583.—Gas in the left femoral epiphysis on the broken, flattened anterolateral segment of the left epiphyseal ossification center. This boy 6 years of age had limped for some weeks. In A, standard position, a long submarginial fracture line crosses the summit of the epiphyseal ossification center horizontally, but there is no evidence of gas in the epiphysis. In B, frog position, a bright black strip of gas density parallels the broken, flattened anterior edge of the epiphyseal ossification center and lies in a space between this edge and its overlying cartilage. There is no evidence of gas in the normal right femoral epiphysis (though under the same stress of stretch and twist, because the epiphyseal ossification center is not separated from its overlying cartilage in the right femur). C, an enlargement of the image in B.

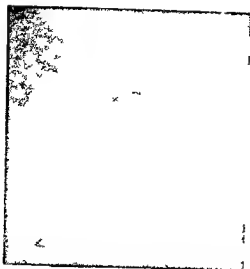


Fig 8-584—Gas in the cleft between fracture fragments and also in a narrow septal space between the broken flattened edge of the epiphyseal ossification center and its overlying cartilage. The bright black strip of gas is clearly visible between the fracture fragments at the base and follows a wavy course toward the summit. This boy 4½ years of age had limped for three months.

of the more radiolucent medullary spaces. The compression does impair the blood flow into the medullary space of the ossification center because it increases resistance to arterial inflow. Total sclerosis of the epiphyseal ossification center is rare and in more than 8% of cases a dorsal segment of variable size persists unaffected throughout the disease (Fig 8-582). Among 25 cases O'Gara found 20 in which destruction was limited to the anterior part of the epiphyseal ossification center, 5 in which the entire center disappeared, and none in which the posterior segment only was affected.

Intraepiphyseal gas was demonstrated in several cases early but only in association with the primary fracture and directly peripheral to it (Figs 8-583 and 8-584). The gas is visible only in the frog position and of course only in the affected femur. It is confined strictly to the segment of the fracture and flattening. It appears to fill a space between the edges of the overlying cartilage and the broken edge of the epiphyseal ossification center which normally are in direct contact with each other. The space is due to separation of the two edges and appears to be limited to the segment of compression and fracture of the edge of the center. In some cases gas was also visible deeper in the ossification center between the faces of the fracture fragments. The sudden stretch and twist applied to the hip where the legs are placed in frog position suddenly dilate this space of separation, and as the space dilates the interspace pressure is reduced and gas is instantly sucked into the expanding space and prevents a vacuum. It is probable that water vapor, oxygen, nitrogen, and carbon dioxide make up the gaseous content. This is the same suck-

ing antevacuum mechanism which fills the articular spaces at the hips and shoulders when these joints are suddenly stretched during their positioning for radiographic examination (see Figs 8-851 to 8-853).

Metaphyseal defects are always radiolucent in contrast to the sclerosis in the neighboring epiphyseal ossification center (Figs 8-585 to 8-587). In punch biopsies from two patients Ponseti found that these radiolucent metaphyseal images were cast by masses of uncalcified cartilage enchondromas. We have found radiographically that they replace the more opaque cancellous bone and the superior segment of the more opaque ventral cortical wall of the femur. They are nearly always located well forward in the metaphysis directly under the site of maximal compression and fracture of the epiphyseal ossification center. Ponseti concluded that they must be derived

Fig 8-585—Metaphyseal defect in corse plane. This boy 5½ years of age had limped for about three months. In A, standard position, the left epiphyseal ossification center is flattened and distally sclerotic. The medial half of the metaphysis contains a large radiolucent patch. In B, frog position, on the side of the epiphyseal ossification center is flattened to a sharp angle anteriorly and its ventral edge is roughened and probably crumpled. Directly beneath the compressed ventral end of the epiphyseal ossification center in the metaphysis is a radiolucent patch which is now anterior and extends directly off the center plate. This medial ventrally located mass is an enchondroma made up of radiolucent uncalcified cartilage which has not been resorbed and has hypertrophied. In both projections the femur is distally sclerotic laterally in the labrum cavity.

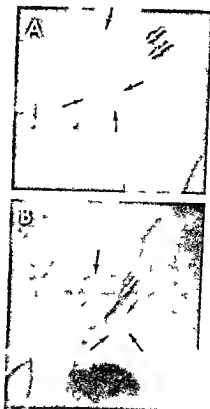
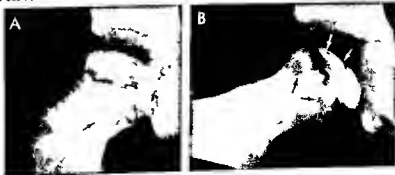




Fig 8 586 —Coxa plana in the late stage of flattening and fibrous replacement with double metaphyseal lesions. This boy 5 years of age began to limp only 24 hours before this film was made. Although the radiographic changes suggest that the disease has been present in the right femur for many months. The right epiphyseal ossification center is flattened and irregularly sclerotic. The cartilage space of the joint is increased. Two large radiolucent patches extend caudad directly off the cartilage plate deeply into the metaphysis. The femoral neck is widened and the right femur dislocated laterad in its acetabulum (Waldenström sign). The scapular roof is roughened.

from the proliferating cartilage of the epiphysis. He also found fibrillations in the cartilage plate itself. It seems reasonable to conclude that the compressing force is transmitted through the anterior segment of the weakened fibrillated cartilage plate where it disrupts the normal mechanism of endochondral bone formation and permits islands and tongues of uncalled cartilage which normally would die and be resorbed to persist and to be displaced and grow caudad into the metaphyseal levels of the medullary cavity where they proliferate to produce sizable enchond

Fig 8 587 —Double metaphyseal defect one ventral and one dorsal. This boy 5 years of age had limped for about two months. In A, standard position, the epiphyseal ossification is flattened and irregularly sclerotic. A large radiolucent defect occupies a large part of the metaphysis and extends far caudad from the cartilage plate almost to the intertrochanteric line. In B, frog position, the epiphyseal ossification center is irregularly sclerotic



dromas which we see as radiolucent patches. The defects last for several months or years. In one of our patients a substantial radiolucent metaphyseal defect was still visible 19 years after the active disease had subsided.

The later cyclic changes which follow the first phases of slight dislocation and segmental fracture present one of the most diagnostic serial radiographic patterns of all diseases in the growing skeleton (Fig 8 588). Although the early fracture disappears completely after a few months, the early lateral dislocation may persist for months or years. The cartilage plate usually increases in thickness while the flattening and sclerosis are extending from the original anterolateral quadrant and sclerosis may appear to be total in standard frontal projections. However, frog projections show that the dorsal part of the epiphyseal ossification center is usually spared and need not become sclerotic or flattened even during the latest phase (see Fig 8 582). As the center flattens progressively, sclerotic bone is replaced by radiolucent fibrous tissue (fibrous replacement) which then begins to ossify from several foci. These new bony foci enlarge and fuse until the entire epiphyseal ossification center is completely reconstituted with normal spongy bone. This complete healing occurs in untreated as well as treated patients and regardless of the type or degree of deformity. The complete cycle of lateral displacement, fracture, necrotic compression, destruction, fibrous replacement and reossification consumes three to five years. As the neck of the femur thickens, it forms a larger base (coxa lata) with which the ossification center must fuse later, so in compensation the center itself widens into a larger epiphyseal ossification center called coxa magna. This enlarged flattened femoral head is often much too large for its acetabular cavity and this misfit causes compression molding and enlargement of the acetabular cavity. Stress changes of sclerosis, irregular mineralization and eversion of the acetabular rim

and flattened. Its anterior segment is flattened to a sharp point and a fracture line is visible just under the upper edge. A sharply defined radiolucent defect is located in the very ventral end of the metaphysis (arrows) and directly under the most severe flattening (compression). In addition, a wide and deep radiolucent patch (arrows) occupies the whole dorsal metaphyseal segment.

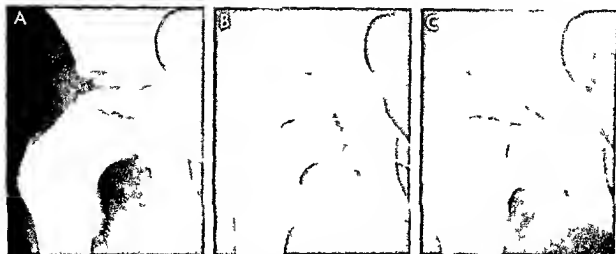
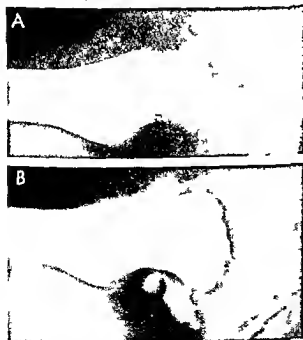


Fig 8-588—This boy had limped and had pain in the right knee for about 4 months. In A, 8 months after onset, flattening of the epiphyseal ossification center is marked and its medial and lateral parts are radiolucent because they are being replaced by radiolucent vascular fibrous tissue. The metaphysis is normal. In B, 18 months after onset, a radiolucent patch is evident in the metaphysis (arrows) directly below the cartilage plate. The multiple bony patches of the epiphyseal ossification center are made up of residual shreds of sclerotic bone and new bony centers which indicate beginning reossification. In C, 56 months after onset, a large radiolucent patch is still evident in the metaphysis; the neck has widened progressively since A, and the flattened epiphyseal ossification center is completely healed and widened to fit onto the widened neck. The acetabular cavity is enlarged.

Fig 8-589—Perthes coxa plana in a boy 6 years of age. In A, standard lateral projection on the epiphyseal ossification center is flattened and reduced to two small fragments in the late stage of fibrous replacement. In B, lateral projection on injection of opaque contrast agent, the joint space is well outlined and shows that the cartilaginous head has a smooth edge and is approximately hemispherical with no evidence of flattening of its edge or deformity of the cartilaginous part of the femoral head. Only the epiphyseal ossification center is abnormal in the first phases of essential coxa plana.



may also become visible at the same time. Meanwhile in the metaphysis radiolucent patches or more commonly a single patch may appear two to three months after the original fracture phase, characteristically adjacent to the cartilage plate. This small defect may continue to grow to substantial size, and sometimes it becomes separated from the cartilage plate by a narrow zone of normal spongy bone. The metaphyseal defects may disappear after a few months or may persist for many years. After complete healing, abnormal stresses on the deformed femur may produce coxa vara deformity in the neck and mushrooming of the femoral head onto the neck. Opaque arthrograms show that the cartilaginous head is not flattened even when the ossification center is in the late stage of flattening and fibrous replacement (Fig 8-589).

We have observed one patient who had clinical signs of Perthes disease whose femoral ossification center had a submarginal fracture in its superior lateral quadrant. The fracture was however dorsal instead of in the usual ventral portion. For two years the fracture line persisted but flattening and sclerosis of the head did not develop and metaphyseal lesions did not appear (Fig 8-590). This atypical fracture would probably have been called osteochondritis dissecans under the old classification, had it been located in the margin of the distal femoral ossification center. The findings in this patient suggest that fracture in the ventral portion of the epiphyseal ossification center is essential for progressive development of flattening and sclerosis.

Meyer's dysplasia of the femoral head (Fig 8-591) simulates necrotic coxa plana in some of its features

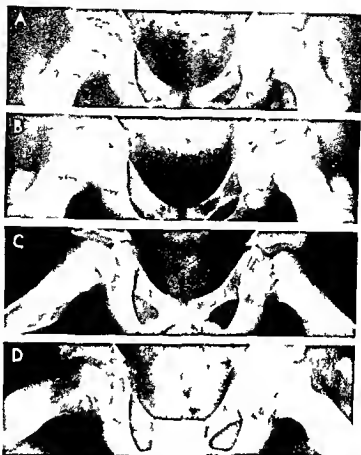


Fig 8-590—Lateral marginal fracture of the epiphyseal ossification center of the left femur of a boy 7 years of age (A and C). The fracture line persisted for two years (B and D) without development of fattening and sclerosis of the femoral head and other standard progressive complications of Perthes' disease.

The fracture fragment is in the dorsal segment of the epiphyseal ossification center rather than in the usual anterior position, which suggests that the ventrodorsal position of the fracture is important in prognosis.

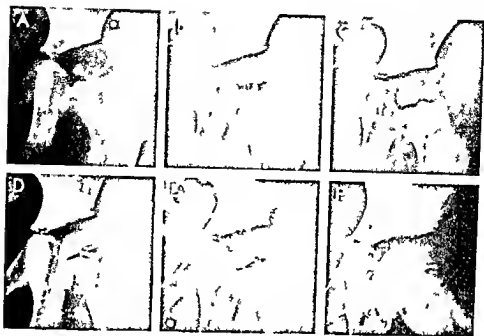


Fig. 8-591—Serial changes in Meyer's dysplasia from 2 to 10 years of age. At age 2 (A) and 3 (B) the femoral epiphyseal ossification is small and irregularly mineralized and is made up of multiple ossification centers. At 3 years and 10 months (C) the mu-

ltiple centers have fused into a single slightly flattened mass. At ages 4, 6 and 9 (D, E, F) the flattened center has rounded into a roughly hemispherical center with normal density and texture. This patient was not treated. (From Meyer.)

and has led to serious overdiagnosis of necrotic coxa plana or Perthes' disease. Meyer estimated that 10% of his cases of coxa plana were of the dysplastic type rather than the true necrotic type. As in Perthes' disease, skeletal maturation is retarded in all parts of the skeleton. Clinical signs are usually mild or absent according to Meyer. In all of our cases the radiographic changes were found by chance in patients who had no signs or symptoms in the hips. In Meyer's dysplasia, femoral bony nuclei appear late and are small and granular at about 2 years of age. The serial bony changes improve with advancing age and finally disappear after three to four years. At the beginning the femoral epiphyseal ossification center is made up of several independent bony foci rather than a single normal large ossification center. The granular centers gradually grow and coalesce into larger centers and finally fuse into a single slightly flattened center. The epiphyseal ossification center is never sclerotic although false sclerosis may be produced by superimposition of two or more centers which are of normal density. In contrast in Perthes' necrotic coxa plana a normal displaced femoral bony nucleus deteriorates due to fracture, flattening, necrosis and fibrous replacement and may be completely destroyed during the first two years to be followed by permanent thickening of the femoral neck, coxa magna, coxa vara and mushrooming of the femoral head. The only residual in Meyer's dysplasia is slight or moderate coxa plana in which the epiphyseal ossification center is of nor-

mal density and texture. In Meyer's disease there is no dislocation of the femur and no metaphyseal defect also 42% of the cases are bilateral. In contrast to the usual 10% in Perthes' coxa plana. The dysplasia begins during the 2nd year of life and usually has disappeared by the end of the 6th year. The course of Meyer's dysplasia is destined from the outset for progressive improvement and complete healing without residuals. The course of Perthes' disease in contrast is destined from the outset to progression through variable degrees of fracture, flattening, necrosis, fibrous replacement and complete reossification with residual deformities of various types and degrees. Meyer's dysplasia needs no treatment. Perthes' disease could benefit from treatment but in too many cases treatment does not modify the course of the lesions significantly. Of Meyer's cases 6 of 30 (20%) converted from benign dysplasia to necrotic coxa plana (Perthes' disease).

In our experience Meyer's lesion has usually been discovered by chance in patients who had no signs or symptoms at the hips but whose hips were included in exposures during such examinations as barium enemas, excretory urograms or films of the abdomen or pelvis (Fig. 8-592).

The improved visualization of the early fracture line achieved by slightly increasing the degree of abduction and external rotation of the femurs is shown in Figure 8-593. In one of our patients who had infantile osteomyelitis of the femur and pyarthrosis

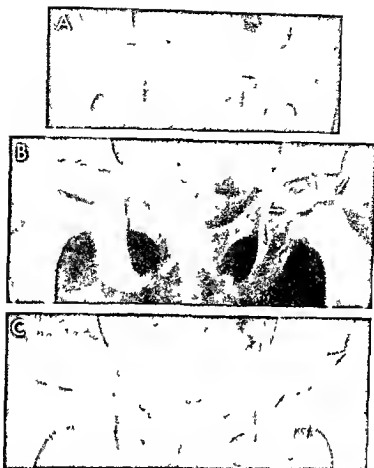


Fig 8 592 —Meyer's dysplasia of the left femoral epiphyseal ossification center. This boy at 60 months of age developed pain and distention of the abdomen. He had had a positive skin reaction to tuberculin early and the first film (A) at 60 months was made in search for calcifying tuberculous lymph nodes. The left femoral epiphyseal ossification center is small, flattened and irregular in density.

regular in density in B at 65 months and C at 66 months (the left epiphyseal ossification center is still flattened but has regained normal density and texture). Five years later he was normal clinically and his hips were normal radiographically. He was not treated for coxa plana.

Fig 8 593 —Early marginal subchondral fracture in the ectrotic dead head which is just beginning to flatten. The fracture is much better seen with the femur in the abducted, externally rotated position (B). This boy, 8 years of age, had been limping for only one week. These early fractures would disappear early and are never seen in the late phases.

tated position (B). This boy, 8 years of age, had been limping for only one week. These early fractures would disappear early and are never seen in the late phases.



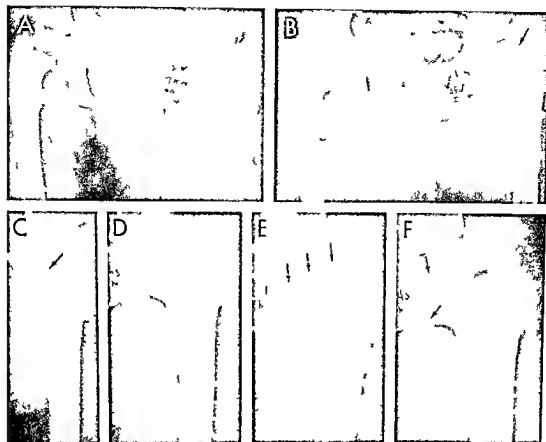


Fig 8-594—Acquired coxa plana and coxa vara secondary to acute staphylococcal osteitis of the femur and acute pyarthrosis of the hip with pathologic dislocation. A, at 12 months of age seven weeks after onset of pain in left leg and hip and fever. A deep segment of the femoral metaphysis is destroyed, the ossification center sclerotic and the femur dislocated laterally with involucrum already evident on the lateral cortical wall. B, at 13 months, the sclerotic center is shrunken and fragmented, the deep metaphyseal defect persists and involucrum is again visible. C, at 14 months, the epiphyseal ossification center has disappeared and the metaphyseal defect is closing. D, at 23 months, the femoral center is still inviable, the metaphyseal defect is visible, but the valgus deformity is beginning to appear with widening of the femoral neck. E, at 31 months, the epiphyseal ossification center is reossifying from the acetabulum and the valgus deformity has increased. F, at 43 months, the femoral center is againular and flattened and the end of the femoral shaft is widened medially. Coxa plana and coxa vara are now clearly evident. The femoral ossification center is disappeared and ramified inviable for 11 months then ossified and flattened to form

peaked and the metaphyseal defect is closing. D, at 23 months, the femoral center is still inviable, the metaphyseal defect is visible, but the valgus deformity is beginning to appear with widening of the femoral neck. E, at 31 months, the epiphyseal ossification center is reossifying from the acetabulum and the valgus deformity has increased. F, at 43 months, the femoral center is againular and flattened and the end of the femoral shaft is widened medially. Coxa plana and coxa vara are now clearly evident. The femoral ossification center is disappeared and ramified inviable for 11 months then ossified and flattened to form

of the hip, the serial radiographic changes simulated some of the serial changes in Perthes' coxa plana (Fig 8-594).

REFERENCES

- Bobechko W and Harris W. The radiographic density of avascular bone. *J Bone & Joint Surg* 42 B 629 1960.
- Bozsan E J. Compression of cancellous bone. *Am J Surg* 53 541 1941.
- Burrows H J. Osteochondritis juvenilis. *J Bone & Joint Surg* 41 B 455 1959.
- Caffey J. The early radiographic changes in essential coxa plana. Their significance in pathogenesis. *Am J Roentgenol* 103 620 1968.
- Calot F. L'orthopédie indispensable aux praticiens (Paris: N. Maloine 1926).
- Calve J. Sur une forme particulière de pseudocoaxalgie greffée sur déformations caractéristiques de l'extrémité supérieure du fémur. *Rev chir* 30 54 1910.
- Cruess R. L. et al. Aseptic necrosis following renal transplantation. *J Bone & Joint Surg* 50-A 577 1968.
- Edgren W. Coxa plana. The importance of the metaphyseal changes for the final shape of the proximal part of the femur. *Acta orthop scandinav* suppl 84 1965.
- Freund E. Zur Deutung des Röntgenbildes der Pertheschen Krankheit. *Fortschr Geb Röntgenstrahlen* 42 435 1930.
- Girdany B R and Osman M C. Longitudinal growth and skeletal maturation in Perthes disease. *Radiol Clin North America* 6 245 1968.
- Jonsäter S. Coxa plana: a histopathologic and arthrographic study. *Acta orthop scandinav* suppl 12 1953.
- Legg A T. An obscure affection of the hip joint. *Boston M & S J* 162 202, 1910.
- Lewis R W. *The Joints of the Extremities* (Springfield, Ill.: Charles C. Thomas Publisher 1954).
- Meyer J. Dysplasia epiphysealis capitis femoris. *Acta orthop scandinav* 34 183 1964.
- Molloy M K and MacMahon B. Incidence of Legg Perthes disease (osteochondritis deformans). *New England J Med* 275 988 1966.
- and MacMahon B. Birth weight and Legg Perthes disease. *J Bone & Joint Surg* 49 A 498 1967.
- O'Garra J A. The radiographic changes in Perthes disease. *J Bone & Joint Surg* 41 B 465 1959.

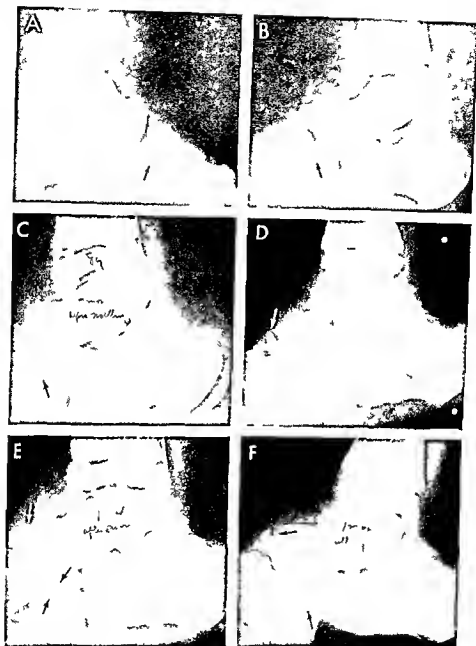


Fig 8-595—Progressive Koehler's disease in a girl 18 years of age who suffered from dysautonomia (Riley Day syndrome) and diminished sensitivity to pain. In **A**, 2 months before onset of convulsions, the tarsal scaphoid is normal. **B**, 2 days after onset, the scaphoid is flattened and sclerotic. The cartilage space between scaphoid and head of the talus has deepened. In **C**, 10

weeks after onset, the scaphoid is now flattened to water-thinness but has expanded peripherally. Patches of sclerotic bone have become radiolucent and presumably represent fibrous replacement. **D**, 7 months after onset, flattening and peripheral expansion persist with irregularity of density. After the first two weeks, she had no pain or limp.

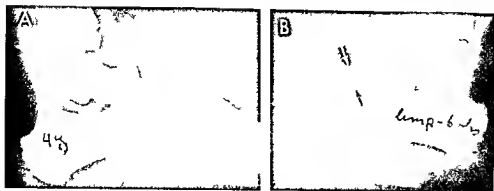


Fig 8 596 — This girl 4 years of age had been limping for six weeks after hurting the left foot. The left tarsal scaphoid is too small, too flat and irregularly sclerotic in this patient, the affected tarsal scaphoid is on the same side as the injury in a single

examination, one cannot be sure whether this represents a chance finding of developmental dysplasia of the tarsal scaphoid (Karp's dysplasia) or traumatic necrosis of the tarsal scaphoid (Kochler's disease).

Perthes G. Ueber Arthritis deformans juvenilis. Deutsche Zeitschrift für Chirurgie 107:111, 1910.

Fonsetti J V. Legg-Perthes disease. Observations on pathological changes in two cases. J Bone & Joint Surg 38-A:739, 1956.

Rathbun A H C. Traumatic separation of the upper femoral epiphysis in young children. J Bone & Joint Surg 50-B:757, 1968.

Rydell N W. Forces acting on the femoral head prosthesis. A study on strain gauge supplied prostheses in living persons. Acta orthop scandicavica 38:1966.

Trueta J. The normal vascular anatomy of the human femoral head during growth. J Bone & Joint Surg 39-B:358, 1957.

— Studies in the Development and Decay of the Human Frame (Philadelphia: W B Saunders Company, 1968).

Waldenström H. The first stages of coxa plana. J Bone & Joint Surg 20:559, 1938.

Stress compression (focal sclerosis) of the tarsal scaphoid (Kochler's disease) was first described by Kochler in 1908, two years before the original description of coxa plana. One of his three patients had retarded skeletal maturation. Progressive destructive Kochler's disease in which the tarsal scaphoid is normal in the beginning then progresses through a cycle of flattening, sclerosis, fibrous replacement and reossification analogous to that in coxa plana is exceedingly rare (Fig 8 595). I have encountered but a single example in radiographs in over 40 years. A limp is usually the first clinical sign, followed by local pain and tenderness and sometimes swelling in the mid tarsal region. Complete healing is inevitable and occurs in all patients without residual deformity of the tarsal scaphoid or residual disability. Treatment does not modify the course although it may relieve severe pain which is also rare. Both treated and untreated patients recover completely without residuals.

The rare destructive necrotic Kochler's disease described above is often simulated radiographically by purely developmental dysplastic changes in the tarsal scaphoid which include late appearance time for the bony nucleus, slow growth, smallness, flatness and irregular sclerosis (Figs 8 596 to 8 598). In the dysplastic type the scaphoid is abnormal from the

very start and always improves with advancing age. Radiographic changes are unrelated to the severity and duration of the clinical manifestations. In patients with limp and pain of a few days or hours the radiographic changes may be marked and may seem to have been present for many weeks or months. Se-

Fig 8 597 — This boy 5½ years of age twisted one ankle (A) a few days before this film was made. In the foot that was not twisted (B) the scaphoid is too small, too flat, sclerotic and irregularly ossified. Presence of the scaphoid lesion in the foot which was not twisted suggests that it could represent the developmental dysplasia (Karp) rather than traumatic necrosis of Kochler.

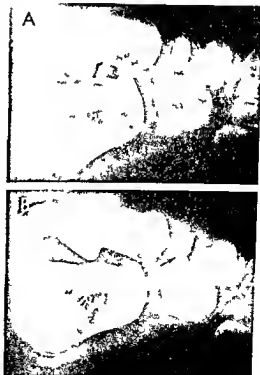




Fig 8 598 —This boy 8 years of age twisted his right ankle six hours before this film was exposed. Both tarsal scaphoids are too small, too flat and irregularly sclerotic. It is unlikely that the recent trauma was the cause in view of the brief duration and the

changes in both scaphoids. History and radiographic findings suggest that the bilateral lesions in the naviculars represent Karp's developmental dysplasia rather than Koehler's traumatic necrosis.

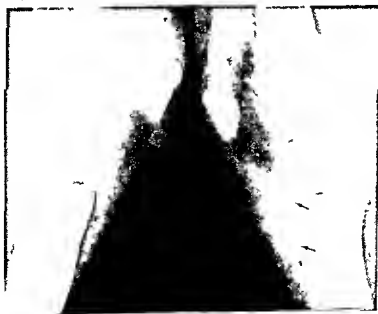
vere dysplastic radiographic changes may be present in one or both of the tarsal scaphoids in the absence of clinical signs and are often found in the foot contralateral to an injury, or unexpectedly when the feet are examined radiographically in skeletal surveys for generalized disease. The course of these dysplastic lesions found most frequently by chance is always in the direction of improvement regardless of treatment until the tarsal scaphoid achieves normal size, shape and density. Normality is usually attained two to three years after the first radiographic examination.

This developmental type of deformity and sclerosis

Fig 8 599 —Probable Osgood-Schlatter injury prior to ossification of the anterior process of the left tibia of a girl 6 years of age. The pretibial soft tissues and caudal end of the patellar ligament are thickened. Local pain and swelling followed injury to

(Karp's dysplasia) of the tarsal scaphoid was fully appreciated by Karp in his radiographic study of the feet of 50 children (25 girls) examined every six months between the ages of 9 and 54 months. He found the average age of appearance of ossification to be 18-24 months in girls and 24-30 months in boys. The bony nucleus of the tarsal scaphoid was frequently small, flat, irregular and sclerotic in healthy children, especially in boys in whom the scaphoid ossification appeared late. Waugh confirmed most of Karp's findings. In his patients the degree of deformity and irregularity varied considerably and the most severe changes simulated those in Koehler's disease. Waugh

the left knee several days before this study. It is possible that swelling of the anterior infrapatellar bursa contributes to thickening of the pretibial soft tissues.



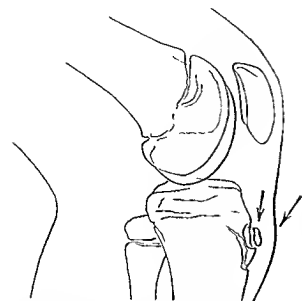


Fig 8 600 - Injury to the tibial tubercle (Osgood Schlatter disease) in a boy 12 years of age. A fragment of the tibial process is lifted off the shaft and the overlying soft tissues are swollen. Tracing of a roentgenogram.

found slow growth and irregular ossification in the tarsal scaphoid in 30% of his normal boys and 20% of normal girls.

The high incidence of slow growth and irregular ossification in children who appear to be normal otherwise makes it obvious that the radiographic diagnosis of Koehler's traumatic destructive disease can be made satisfactorily only in serial examinations in which progressive destruction is demonstrated.

REFERENCES

- Karp M G. Koehler's disease of the tarsal scaphoid. An end result study. *J Bone & Joint Surg* 19:84 1937.
 Koehler A. Roentgenology (London: Bailliere Tindall & Cox 1928) p 114.
 Waugh W. The ossification and vascularization of the tarsal navicular and their relation with Koehler's disease. *J Bone & Joint Surg* 40-B 765 1959.

Osgood Schlatter lesion (trauma to the soft tissues at the tibial tubercle) - This condition is characterized by local pain, tenderness and swelling over the tibial tubercle with limp and disability in running or climbing stairs. It is met with most frequently in children between 10 and 15 years, particularly in active boys who participate in rugged sports. The roentgen signs include fragmentation and displacement of the fragments away from the shaft with swelling of the overlying soft tissues (Figs 8 599 to 8-602). The diagnosis should not be based on mere irregularity in density of the tibial tubercle; this is a common physiologic variant and is present in a wide variety of patients in considerably more than half of asymptomatic

adolescent children (see Fig 8 187). There are often marked discrepancies in the pattern of mineralization of the two tibial tubercles of a single asymptomatic child.

Hughes believed that the primary lesion is a partial traumatic separation of the ligamentum patellae from the tibial tubercle (Fig 8 603) rather than direct injury and necrosis of the tubercle itself. This concept is based on the practically constant early roentgen demonstration of soft tissue swelling of the tibial tubercle and thickening of the ligamentum patellae, with later roentgen demonstration of ossification in the distal end above the ligamentum patellae. Distention of the inferior infrapatellar bursa between the tibia and patellar tendon may also be a major source of local thickening of the soft tissues. Rapp and Lazerte found neither bone necrosis nor degeneration microscopically in 19 specimens taken from 17 patients who had clinical and radiographic Osgood Schlatter disease. They did find progressive avulsion of a small fragment of the bony apophysis of the tibial tubercle which they attributed to rapid increase in linear growth and accidental injury to the patellar tendon.

These and other studies indicate that the primary Osgood Schlatter lesion is simple local fracture of the anterior tibial process and injury to the soft tissues at the site of insertion of the patellar tendon into the tib-

Fig 8 601 - Osgood Schlatter lesion in a boy 13 years of age one day after injury to the left knee. An avulsed fragment of the tibial tubercle lies loose in the swollen soft tissues in front of the anterior tibial process. Its presence one day after injury indicates that it is a fracture fragment, not heterotopic bone in the swollen patellar tendon. A, right and B, left knee.





Fig 8 602 (left) —Osgood Schlatter injury in a boy 13 years of age who hurt his knee a month before. The base of the patellar tendon is thickened and a small independent part of bone lies in front of a depression on the ventral edge of the anterior tibial process from which it was probably avulsed one month ago (logo iron attachment).

ia during rapid growth with heterotopic bone formation in the tendon. At biopsy in many cases simple low grade tendonitis of the patellar tendon has been found with heterotopic bone formation in the inflamed tendon. The clinical signs of this lesion usually develop without known precedent trauma.

REFERENCES

- Holstein A *et al*: Heterotopic ossification of the patellar tendon. *J Bone & Joint Surg* 45-A:656 1963
 Hughes E S R: Osgood Schlatter's disease. *Surg Gynec & Obst* 86:323 1948
 Osgood R B: Lesions of the tibial tubercle during adolescence. *Boston M & S J* 148:113 1903
 Rapp S H and Lazerte G: Clinical pathological correlation in Osgood Schlatter's disease. *South M J* 51:909 1958

Fig 8 604: Fragmentation and avulsion of the lesser trochanter of the femur (arrows) in a boy 15 years of age who had



Fig 8 603 (right) —Osgood Schlatter injury in a girl 16 years of age. A: no malright knee. B: left knee with a small mass of bone at the base of the patellar tendon. This appears to be a mass of ectopic dysplastic bone in the patellar tendon, not a fracture fragment of the anterior tibial process which is intact.

Traumatic avulsion of ossification centers is occasionally seen at the lesser trochanter of the femur (Fig 8 604) and at the apophysis of the ischium. The former usually follows heavy stress on the iliopsoas muscle and tendon; the latter follows sharp contraction of the hamstrings during jumping.

REFERENCES

- Malch H: Ischial apophysis lysis. *Bull Hosp Joint Dis* 14:188 1953
 Stayton C A Jr: Ischial epiphysiolysis. *S Am J Roentgenol* 76:1161 1956

Stress compression (focal sclerosis) of the tarsal bones —The cuneiform bones, especially the medial

lateral pain but surprisingly little disability for 10 days since he first experienced the pain after kicking a soccer ball.





Fig 8-605 — This boy never had symptoms or signs in the feet or ankles. A. at 6 years of age both scaphoids and both medial cuneiforms are small, sclerotic and irregularly ossified. B. at 8 years and without treatment, all four bones are normal. The clinical facts suggest that the lesions at age 6 represent slow and irregular developmental dysplasia rather than traumatic necrosis.

cuneiform may show smallness, deformity and sclerosis when the tarsal scaphoids are similarly affected (Fig 8-605). We have also found the cuneiform changes only in asymptomatic patients without involvement of the tarsal scaphoids (Fig 8-606). In all of our patients the cuneiform changes have disappeared without treatment over a period of two to three years. The radiographic and clinical findings suggest that the changes in the cuneiforms are developmental and dysplastic in origin rather than traumatic and necrotic.

Stress compression (focal sclerosis) of the heads of the talus bones is exceedingly rare. We have seen but one case in which the patient was asymptomatic and we have classified it as a possible normal variant (see Fig 8-154).

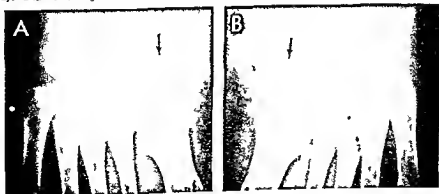
Stress compression (focal sclerosis) of the apophysis of the calcaneus (Sever's disease) from a radiographic standpoint appears now to be a medical myth. From its first appearance in childhood to fusion time after adolescence the calcaneal apophysis is consistently and diffusely sclerotic with irregular margins and usually some radiolucent fissures (synchondroses) which divide this ossification center into several parts and radiate to its margins. Since this is true in all healthy children it is true in all children who have painful heels. The diagnosis of destruction of the calcaneal apophysis therefore should never be made on the normal findings of sclerosis, irregular edges and fissuration (see Figs 8-138 and 8-140).

REFERENCE

Sever, J. W. Apophysitis of the os calcis. *New York M J* 95: 1025, 1912.

Fig 8-606 — Slow, irregular growth and ossification of both medial cuneiforms in a boy 4 years of age who had limped on the right leg for two days. B: lateral changes and short duration of

calcaneal signs suggest developmental and slow, irregular dysplasia rather than traumatic necrosis of the medial cuneiform bones.



Stress compression of the proximal end of the tibia (Blount's tibia vara) is a local disturbance of growth of the medial and dorsal segments of the proximal tibial metaphysis, epiphysis and epiphyseal ossification center. The changes may appear at any time between the 1st and 12th year. When the changes appeared in infancy, Blount identified them as the infantile type, when they appeared after the sixth year, he classified them as the adolescent type. The infantile type is six to eight times as frequent as the adolescent. Only 2 of Blount's 19 patients were males, in other series, however, the males have predominated. The cardinal clinical sign in all cases is the unilateral or bilateral bowing of the legs. In most cases of tibia vara, the physiologic bowed leg of infants, a normal residual of normal fetal position, increases with advancing age and instead of disappearing progressively to a straight leg or slight normal knock knee in girls, converts into severe tibia vara without evident cause. In bilateral bowing, the deformity on one side may disappear spontaneously. Limp is the principal clinical manifestation, but waddling is the rule with bilateral involvement. Pains in the ipsilateral knee, ankle or foot may develop due to local stresses and strains. In tibia vara, the tibia is bent abruptly medially and caudad at the proximal metaphyseal level, in contrast to the shallow bowing of

the entire tibia in physiologic bowed leg. This abrupt angulation of the medial cortical wall although clearly visible radiographically, is difficult to identify on the physical examination, especially in children with fat legs. However, the medial swelling of the tibia may be palpable. In Blount's patients internal rotation of the tibia, genu recurvatum and flatfoot were consistent associated findings. In testing for stability of the affected knee, Blount found excessive mobility on medial strain and normal mobility on lateral strain. Rarely, the joint swells from intra articular effusion, which is painful. In older patients, shortening of the ipsilateral shank is common.

The causal agent is not known, but it must be local in origin. The most reasonable explanation seems to be either primary weakness of the lateral supporting structures of the knee or secondary weakness due to chronic application of excessive stress on the normal supporting structures during too early walking and weight bearing. These factors increase the mobility at the knee, of the tibia on the femur, which results in the tibia meeting femoral condyles obliquely and in a shift laterad when the force of weight bearing is applied. The lateral tibial shift overloads the mediolateral segment of the tibia and bends it medially and caudad, which eventually forms a large and often hooked spur. The cartilage plate is also bent caudad in its

Fig 8 697 (left) — Blount's tibia vara in a girl 2½ years of age who had pronounced lateral bowing of the left leg. In A, frontal projection on the medial end of the tibial ossification center is flattened into a slope in place of the normal convex curve at this site. This is hypoplasia of the medial segment of the bony nucleus rather than destruction by ischemic necrosis. The metaphysis is widened medially by a broad horizontal spur which is roughened on its medial edge where the previously bony terminal segment of the spur has been replaced by a radiolucent calcified cartilage. The lateral cortical wall is not bent at the level of the medial wall. In B, lateral projection spurs project dorsad from the dorsal wall of the femoral and tibial shafts.

Fig 8 698 (right) — Tibia valgus. In A, frontal projection the lat-

eral end of the femoral ossification center is cut off by a straight longitudinal plane in place of the normally convex rounded contour. The lateral segment of the metaphysis is bent caudad into a lateral spur. In B, lateral projection spurs project dorsad from the dorsal walls of the femur and the tibia. This boy 2 years of age was normal at birth but developed knock knee which became accentuated after he started to walk. Tibia valgus is the converse of tibia vara and develops in the posterolateral segment of the tibia because the weak supporting structures on the lateral side of the knee permit the tibia to shift medially on the femoral condyles and the lateral segment of the tibia is overloaded during walking and weight bearing.

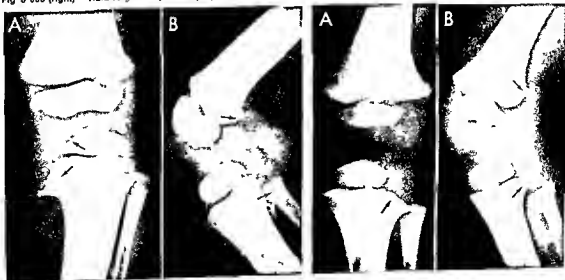
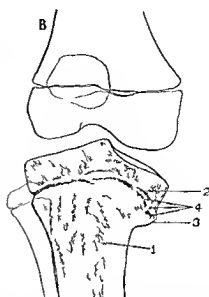




Fig 8 609 —Sharp bending of the medial segment of the tibial metaphysis caudad and medially in tibia vara. The medial segment of the tibial shaft is bent on center has followed the metaphysis caudad. The medial femoral condyle is hypertrophied in compensation for the tibial deformity. This girl 10 years of age was bow-



legged on the right side. The straight right cortical wall of the tibia is noteworthy. B is a tracing of A. 1, medially bowed shaft; 2 and 3, medially and caudally bent tibial shaft on center and tibial metaphysis; 4, regular ossification center and early closure of the medial segment of the bent cartilaginous plate.

Fig 8 610 —Bilateral Blount's tibia vara. In A, at 18 months, bilaterally symmetrical sharp caudally hooked spurs extend medially off the medial metaphyses. Similar but less marked spurs extend medially and cephalad off the medial metaphyses of the femur. In B, at 26 months, the ends of the spurs now have reg-

ular margins and the terminal segments have been replaced by radiolucent uncalcified cartilage. The cartilaginous replacement of bone in the tips of the spurs is secondary and follows spur formation.

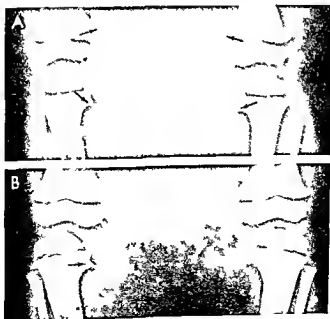




Fig 8-611—B lateral bowed legs with tibia vara and femora vara in incompletely healed rickets in a boy 3 1/2 years of age

medial segment which changes the plane of growth from the normal longitudinal to oblique longitudinal. With further growth the proximal end of the tibia becomes progressively shorter in its medial dorsal segment. The beaklike spur which projects medially from the metaphysis represents overgrowth at right angles to the principal stress plane. Microscopic examinations have shown no evidence of ischemic necrosis. The loss of bone at the tip and in the body of the medial spur is due to replacement of spongy and cortical bone by radiolucent uncalcified cartilage which results from irregular advance of the cartilage in endochondral bone formation—a true dysplasia followed by hypertrophy of islands of uncalcified cartilage but without necrosis. The ectopic masses of uncalcified cartilage in the metaphysis in Blount's tibia vara are analogous in both nature and pathogenesis to the metaphyseal enchondromas in Legg-Perthes coxa plana.

The radiographic findings in the fully developed lesions are diagnostic in themselves. The most difficult diagnostic problem is to distinguish the conversion from physiologic bowed legs to tibia vara in the younger patients. Often this is impossible in a single film but can be clearly seen in serial examinations. The principal distinction is the abrupt angulation medially of the medial cortical wall with a straight lateral cortical wall in Blount's tibia vara in contrast to the gradual curve of both medial and lateral cortical walls in physiologic bowed legs. Also the apex of the angulation is near the proximal metaphysis of the tibia in tibia vara; the apex of the bend is much farther distal in the middle third of the bone in physiologic

bowing. The epiphyseal changes are not well developed in young patients.

Typical radiographic changes in the infantile type are shown in Figures 8-607 to 8-613. Reversed tibia vara or tibia valga is portrayed in Figure 8-608; this patient had knock knees. In Figure 8-609 the medial segment of the tibial metaphysis is bent caudad. The end of the medial beak is replaced by uncalcified cartilage between 18 and 26 months of age in Figure 8-610. Tibia vara and femur vara of rachitic origin are shown in Figure 8-611. Involvement of the femurs as well as the tibia is depicted in Figure 8-612. In the patient of Langenskiöld and Riska the lesion progressed from physiologic bowing to tibia vara.

REFERENCES

- Blount, W. P. Tibia vara: osteochondrosis tibiae. *J Bone & Joint Surg* 19:1, 1937.
 Goldring, J. S. R., and McNeil Smith, J. D. G. Observations on the etiology of tibia vara. *J Bone & Joint Surg* 45-B:320, 1963.
 Langenskiöld, A., and Riska, E. B. Tibia vara (osteochondrosis tibiae). *J Bone & Joint Surg* 46-A:1405, 1964.

Stress sclerosis of the patella is difficult to identify roentgenographically owing to the normal irregular mineralization of the patella during all phases of its growth (see Figs. 8-202 and 8-203) and the normal differences in size and density of the two patellas in asymptomatic children. The patella may of course be the site of destructive disease, and it is claimed that

Fig 8-612—Blount's tibia vara at the left knee showing typical changes in the tibial ossification center and metaphysis with irregular radiolucent cartilage replacement of the medial part of the tibial spur. Similar but less marked changes are present in the femoral ossification center and metaphysis. Accessory ossification centers are present in the tip of the femoral metaphyseal beak and the medial flattened end of the femoral ossification center.



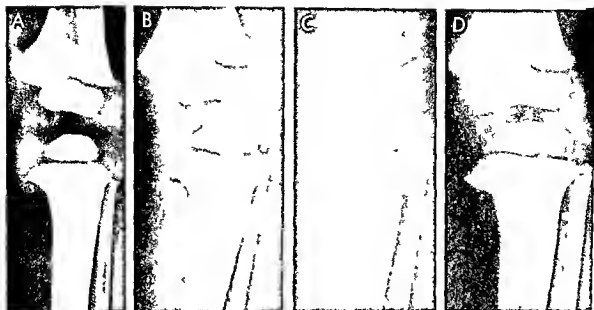


Fig 8-613 —Progressive changes in Blount's disease. A at 17 months the medial segment of the tibial metaphysis is widened and sharpened into a short beak or spur which is bent slightly caudad. B at 26 months the spur is longer, sharper and more bent. A red fluorescent strip on its upper edge represents non-

calcified cartilage. C at 32 months the amount of cartilage is increased and the spur thickened. D at 38 months the beak of the spur is displaced caudad possibly owing to trauma; the medial edge of the ossification center is flattened and the femur has shifted medially in the tibia.

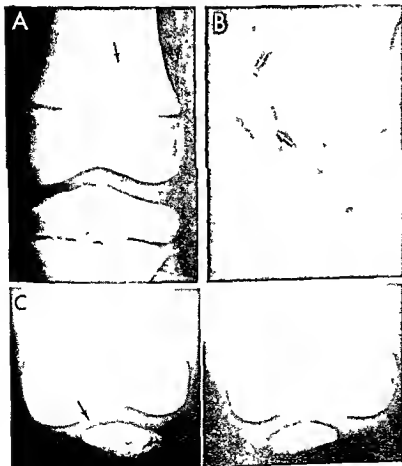


Fig 8-614 —Irregular sclerosis of the patella in a boy 9 years of age who had pain and swelling in the left knee after a fall on the knee one year before. The knee was swollen and motion limited; there was a scar in the skin over the left patella. The patella is swollen, irregularly mineralized and sclerotic. A, frontal; and B, lateral projection. C, cephalocaudal projection of both knees during flexion.



Fig 8-615—Irregular mineralization of the dorsal edge of the right patella of a boy 15 years of age who had pain in the right knee for several weeks. The arrow is directed at the irregularly mineralized dorsal edge of the right patella. The dorsal edge of the left patella is in contrast smooth. At surgical exploration and on microscopic examination ischemic necrosis was found on the dorsal edge of the right patella.

the destruction may be osteochondritic in nature—*ischemic necrosis*. Osteochondrosis of the primary patellar center was described by Koehler in 1908. Osteochondrosis of the secondary patellar centers has been known as Sinding-Larsen disease since 1921. We are of the opinion that the diagnosis of osteochondrosis of the patella is made altogether too often by roentgenologists. We reserve this diagnosis to cases in which the patella is sclerotic in association with appropriate clinical signs (Fig 8-614). In most cases of supposed roentgen patellar osteochondrosis the roentgen changes are equally marked on the two sides

when the clinical signs are limited to one side. This was true in the two cases reported by Sinding-Larsen.

We have seen two examples of irregular mineralization of the dorsal edge of the patella (Fig 8-615).

REFERENCES

- Jungmann J. Osteochondritis of the patella. *Brit J Radiol* 17:305, 1944.
 Koehler A. Über eine häufige bisher anscheinend unbekannte Erkrankung einzelner kindlicher Knochen. *München med Wchnschr* 45:1923, 1908.
 Sinding-Larsen C, M F. A hitherto unknown affection of the patella in children. *Acta radiol* 1:171, 1921.
 Wolf J. Larsen-Johansen disease of the patella. *Brit J Radiol* 23:335, 1950.

Stress sclerosis of the ossification center in the proximal tibial epiphysis following a crush injury was reported by Siffert and Arkin in 1950. This is said to be the first recorded example of this lesion. I have seen a similar case through the courtesy of Dr. Bertram R. Girdany at the Children's Hospital, Pittsburgh.

Stress fracture and sclerosis of the intercondylar spines of the proximal tibial epiphysis (Fig 8-616) is another example of fracture on the edge of an epiphyseal ossification center associated with sclerosis, which has not been previously recorded.

REFERENCES

- Robertson D. E. Post-traumatic osteochondritis of the lower tibial epiphysis. *J Bone & Joint Surg* 46-B:212, 1964.
 Siffert R. S. and Arkin A. M. Post-traumatic aseptic necrosis of the distal tibial epiphysis. Report of a case. *J Bone & Joint Surg* 32-A:691, 1950.

Osteochondrosis of the capitulum of the humerus (Panner's disease) is a rare lesion usually encountered in boys between the ages of 8 and 16 years. Klein's patient was however a girl who had local pain and radiographic changes at 2 years of age. Clinical manifestations are usually mild and limited; they include vague local persistent pain in the affected elbow and moderate limitation of movement. Radiographically the capitulum is diffusely sclerotic with a submarginal radiolucent strip next to a shallow

Fig 8-616—Fracture and sclerosis of the tibial spines in a boy 12 years of age who had had intermittent pain in the knee for several weeks.



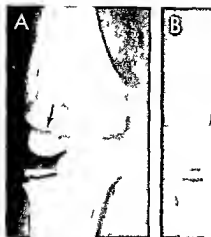
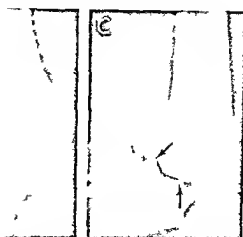


Fig 8 617 — Panner's osteochondrosis juvenis of the capitellum of the humerus of a boy 10 years of age who had had local pain and moderate limitation of motion at the left elbow for three months. In A, normal right elbow in frontal projection, the capitellum is smooth and of uniform density. In B, the affected el-



bow the capitellum has irregular margins and its general density is uneven. In C, lateral projection of the left elbow, a fine shell of bone surrounds the capitellum beneath which there is a compartment of diminished density. (Courtesy of Dr. Paul R. Milgman, Salt Lake City, Utah.)

sclerotic shell of bone (Fig 8 617). The radiographic findings have been similar in all patients with a similar course of progressive changes. Flattening and massive destruction of the capitellum are rare. Radiographic evidence of complete healing is the rule without residual deformity or disability. Complete healing occurs without elaborate treatment.

REFERENCES

- Elward, J. E. Epiphysitis of the capitellum of the humerus. *JAMA* 112:705, 1939.
 Klein, E. W. Osteochondrosis of the capitellum (Panner's disease). *Am. J. Roentgenol.* 88:466, 1962.
 Panner, H. G. An affection of the capitellum humeri resembling Calve-Perthes disease of the hip. *Acta radiol.* 8:617, 1927.
 Smith, M. G. H. Osteochondritis of the humeral capitulum. *J. Bone & Joint Surg.* 46-B:50, 1964.

Osteochondrosis of the radial head is said to have been first observed by Brailsford in 1935. It has the same radiographic elements as the other osteochondroses—fragmentation, sclerosis and shrinkage of the affected center, with clinical and radiographic recovery after two to three years. *Coxa plana* may be associated.

REFERENCE

- Trias, A. and Ray, R. B. Juvenile osteochondrosis of the radial head. *J. Bone & Joint Surg.* 45-A:576, 1963.

Miscellaneous focal aseptic necroses—Space does not permit description of all of the different sites of aseptic necrosis depicted in Figure 8 570. In such bones as the patella, pisiform, anterior tibial process, femoral trochanters, cuneiforms, ischopubic synchondrosis and the calcaneal apophysis, where physiologic irregular mineralization is an almost constant

feature during growth, it is extremely difficult to identify or exclude aseptic necrosis on the basis of the roentgen examination. One of the most convincing lesions is the swelling and fragmentation of the os tibiale externum (Fig 8 618), which is associated with clinical swelling and local pain and tenderness (Haglund's disease). Keats and Wheeler observed a boy 10 years of age who had limitation of motion at both shoulders and destruction and deformity of the humeral epiphyseal ossification centers and portions of the contiguous metaphyses. In all portions of the growing skeleton, unless local signs or symptoms are present, it is hazardous to base the diagnosis of necrosis on foci of irregular mineralization visible in roentgenograms, because nearly all such irregular mineralization in asymptomatic children is of developmental rather than of necrotic origin.

Fig 8 618 — Osteochondrosis of the right os tibiale externum (Haglund's disease) in a boy 11 years of age. Both feet were painful and tender. Swelling was palpable and visible on the medial side of the right foot. The os tibiale on the right side (arrows) is large and regularly ossified. There is an os tibiale on the left side, but it is small, smooth and evenly ossified.



REFERENCES

- Hall T D Osteochondritis of the greater trochanteric epiphysis *J Bone & Joint Surg* 40-A 644 1958
- Harbin M and Zollinger R Osteochondritis of the growth centers *Surg Gynec & Obst* 51 145 1930
- Keats T E and Wheeler P C Osteochondritis A description of two unusual sites of involvement *Am J Roentgenol* 89 1250 1963
- Meistrup D B Osteochondritis of the internal cuneiforms *Am J Roentgenol* 58 329 1947

Multiple focal irregular scleroses—Foci of osteoporosis and irregular mineralization may be found in more than one site Koehler's lesion of the tarsal navicular Perthes' disease of the femur and Van Neck's lesion at the ischiopubic synchondrosis were present simultaneously in one of our patients Roentgen examination of the entire skeleton of every patient with supposed solitary irregular sclerosis would undoubtedly disclose that multiple irregular scleroses are not as rare as now believed Owing to the high frequency and the wide distribution of physiologic focal irregular mineralization (see Fig 8 245) multiple roentgenographic findings are to be expected For example most

patients with Perthes' disease exhibit irregular mineralization of the patella and calcaneal apophysis because the last named two bones are irregularly mineralized in most children Multiple spotted epiphyses are not uncommon in hypothyroidism chondrodystrophia calcificans congenita dyschondroplasia and Hurler's syndrome in all of the four conditions the focal irregular mineralization is developmental in origin

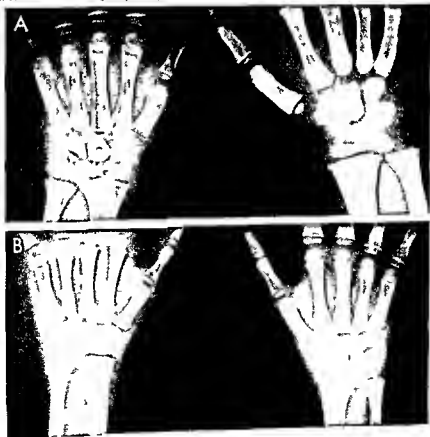
REFERENCES

- Martin W C and Roesler H Multiple manifestations of subchondral necrosis *Am J Roentgenol* 30 861 1931
- O'Donoghue A F O'Donoghue E S and Zimmerman W W Bilateral osteochondritis of the tarsal navicular and first cuneiform *J Bone & Joint Surg* 30-A 780 1948

Multiple sclerosis of the phalangeal ossification centers (Thiemann's disease) is a localized necrosis of the epiphyseal ossification centers of the phalanges in the hands and feet The condition was first described by Thiemann in 1909 The proximal phalanges of the middle fingers of both hands are most often affected but the other phalanges may be in

Fig 8 519—Symmetrical progressive bilateral multiple necroses of the carpal bones A 10 months after injury to the left hand all of the carpal bones are shrunken irregularly osteoporotic and

scale of end deformed B 18 months after A the carpal bones in both wrists now show a similar type of degeneration even though there was never recognized injury to the right hand



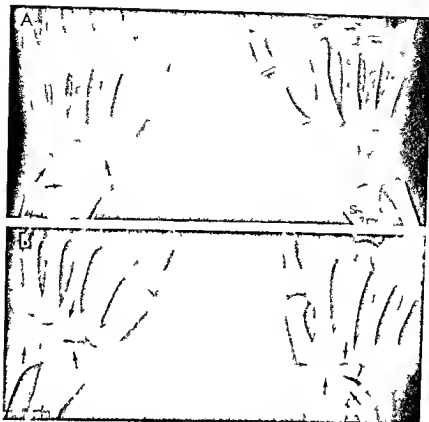


Fig 8-620—Idiopathic familial multiple carpal necrosis in son, father and grandfather. A: wrists of a boy 7 years of age with loss of cartilage and marginal sclerosis and subchondral necrosis in all of the carpal bones of one wrist (arrows). Joint spaces are also narrowed at the carpometacarpal and carpometacarpal joints. The radial center shows marginal sclerosis and subchondral necrosis similar to those in the carpal bones. The other wrist is normal.

The affected wrist had been painful for four months, it had not been injured and there were no signs of rheumatoid arthritis elsewhere. B: bilateral carpal necrosis in the father who is said to have had progressive deformities in the wrists and ankles since childhood. The grandfather had similar carpal deformities at the wrists. (Courtesy of Dr. Rafael Alfonso and the James Law Center, Kansas Hospital, Baltimore, Md.)

involved in a variety of patterns, often asymmetrically in the two hands. The syndrome has been observed only during late childhood and adolescence. Frostbite has apparently been a cause of some cases (see Fig 8-423) but as a rule the lesions develop without evident cause.

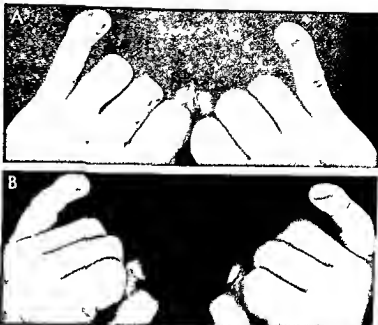
It should be borne in mind that sclerosis of the epiphyseal ossification centers of the phalanges is physiologic in healthy children (see Fig 8-79) and should not be confused with Thiemann's disease, which is essentially destructive. Sclerosis alone is normal even in multiple centers and should not be diagnosed as osteochondritis.

REFERENCES

- Florkiewicz L. and Kozlowski K. Symmetrical epiphyseal destruction by frostbite. Arch. Dis. Childhood 37:51 1962.
- Shaw E. W. Avascular necrosis of the phalanges of the hands (Thiemann's disease). JAMA 156:711 1954.
- Staples O. S. Osteochondritis of the epiphyses of the terminal phalanx of the fingers. J. Bone & Joint Surg. 25:917 1943.
- Thiemann H. Juvenile Epiphysenstörungen. Fortschr. Geb. Röntgenstrahlen 14:79 1909.

Bilateral carpal necrosis—We have had under observation for a number of years a curious case of bilateral multiple necroses of the carpal bones (Fig 8-619). Necrosis, fragmentation and shrinkage of all of the carpal bones in the left wrist were identified following an injury to the left hand when it was caught and severely jammed between the rollers of a clothes wringer on a washing machine. Several months later almost identical roentgen changes appeared in the right wrist, although the right hand had not been injured at any time. The bizarre involvement of both wrists after injury to the left hand alone is difficult to explain and has not been explained. Martel and co-workers observed bilateral carpal necrosis with partial destruction of contiguous portions of the metacarpals in a child 4 years of age who had rheumatoid arthritis. We have also seen multiple carpal necroses which developed without known injury (Fig 8-620) in a child whose father had severe bilateral carpal necroses said to have developed without conspicuous injury. The grandfather is said to have had similar clinical deformities at the wrists. The same phenomena were present in five members of one family in

Fig 8 621 — Bilateral idiopathic swellings of the terminal segments of the 5th fingers with radial and ventral deviation (Kirner's disease) in siblings — girls aged 14 (A) and 19 years (B). These swellings were painless, were not inflammatory and had appeared gradually during the last half of childhood (Figs 8 621 and 8 622 courtesy of Dr Eugene Blank.)



three of its generations observed by Thieffry and Sorrel Dejerine.

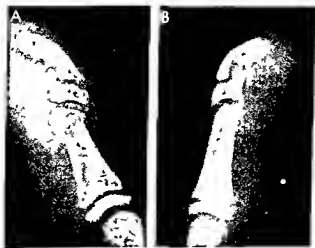
Torg and associates described three of six siblings who had multiple necroses in the carpal and tarsal bones which became progressively more severe as age advanced. Laboratory tests failed to detect any disorder of calcium or phosphorus metabolism. The authors concluded that inheritance was recessive. Microscopic changes in the bones were diagnostic.

REFERENCES

- Martel, W. *et al*. Roentgenologic manifestations of rheumatoid arthritis. *Am. J. Roentgenol.* 88:400, 1962.
 Thieffry S. and Sorrel Dejerine J. Special kind of idiopathic hereditary and familial osteolysis appearing in early infancy with later spontaneous stabilization. *Presse med.* 66:1838, 1958.
 Torg J. S. *et al*. Hereditary multicentric osteolysis with recessive transmission. A new syndrome. *J. Pediatr.* 75:243, 1969.

Fig 8 622 — Kirner's deformity. A, lateral radiograph of a girl 14 years of age shows swelling of the soft tissues and irregular ventral edge of the shaft of the terminal phalanx, which is bent ventrad on itself and angulated ventrad at its junction with the epiphyseal cartilage. In B, the 5th finger of her brother 16 years of age shows similar changes, but in addition a mortise pattern of the joint has developed between the shaft and its epiphysis.

physis. In B, the 5th finger of her brother 16 years of age shows similar changes, but in addition a mortise pattern of the joint has developed between the shaft and its epiphysis.



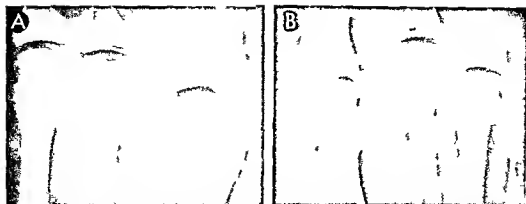


Fig. 8-623—Freiberg's osteochondrosis or fracture of the distal end of the 2nd and/or 3rd metatarsal. In A, the distal end of the shaft of the 2nd metatarsal is partially destroyed and presents a squared end of irregular density. This patient was a girl 14

years of age. In B, the distal end of the 3rd metatarsal in a boy 15 years of age is deformed and fragmented. The 2nd metatarsal is affected in about 75% of cases.

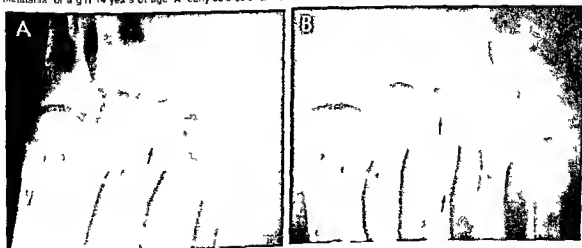
Turner's disease (bilateral swelling and bending of the terminal segments of the fifth fingers) affects the soft tissues at the tips of the fingers as well as the terminal phalanges. The cause is unknown. The marginal irregularities in the shafts of the phalanges suggest bone necrosis, and for this reason we classify it under the ischemic necroses. In Blank's family seven affected members in three generations; the lesions were not present at birth and the soft tissue swellings of the fingers were evident when the phalanges were still not deformed. Painless swellings appeared at the ends of the fifth fingers in one patient at about the 8th year of life. The clinical and radiographic changes are shown in Figures 8-621 and 8-622. The swellings are painless but may interfere with digital skills such as typing, sewing and the playing of musical instruments. The diseased phalanges stabilize in their abnormal position with resid-

ual shortening and incurving. In some patients skeletal maturation has been retarded. Girls have been affected more frequently than boys. There is no treatment.

Clinodactyly (curvature of a finger in the mediolateral plane) may be directed to the radial or the ulnar side of the hand. It is most common as radial bending of the fifth finger at the distal interphalangeal joint. It is usually due to hypoplasia of the middle phalanx of the fifth digit, which is shorter on its radial side. Approximately 60% of mongoloids have this deformity. *Camptodactyly* signifies permanent flexion of one or more fingers usually the fifth finger and always at an interphalangeal joint and at no other joint. The reader is referred in this connection to the comprehensive paper by Poznanski and associates for detailed description of the different deformities of the fingers.

Fig. 8-624—Progressive changes in Freiberg's fracture of the 3rd metatarsal of a girl 14 years of age. A, early stages; B, 48

days later, beginning collapse of bony replacement and thickening of the cortical wall.



REFERENCES

- Blank E and Gurdany B R. Symmetric bowing of the terminal phalanges of the fifth fingers in a family (Kürner's deformity) *Am J Roentgenol* 93:367 1965
- Kaufmann H J and Taillard W F. Bilateral incurving of the terminal phalanges of the fifth fingers. An isolated lesion of the epiphyseal plate. *Am J Roentgenol* 86:490 1961
- Poznanski A K *et al*. Clinodactyly and camptodactyly. Kürner's deformity and other crooked fingers. *Radiology* 93:573 1969
- Staehli L T *et al*. Bilateral curving of the terminal phalanges of the little fingers. *J Bone & Joint Surg* 48-A:1171 1966

Freiberg's fracture (ischemic necrosis of the head of the second metatarsal) is about four times as common in girls as in boys, occurs commonly between the 8th and 17th years and develops in the right and left foot with equal frequency. The same kind of lesion is also found in the head of the third metatarsal. It is rarely bilateral (in 3 of 80 of Smilhe's patients). It is commonly found in association with march fractures in the metatarsals of the same or other foot. The primary lesion is a superficial fissure fracture in the edge of the epiphyseal ossification center followed by ischemic necrosis and then repair which often includes overgrowth at the site of injury. The course is similar to that of Perthes' coxa plana in which there are long periods of destruction followed by long periods, many months of repair. Radiographic findings depend on the stage in which the lesion is examined. Early the only finding is widening of the contiguous joint space without evidence of fracture of the edge of the ossification center. Later absorption of cancellous bone causes the dome of the articular cartilage to sink into the shaft and the dead bone is sclerotic. The head of the third metatarsal then becomes squared and flat and often enlarged (Figs

Fig 8-625—Freiberg's fracture of the epiphyseal ossification center of the 2nd metatarsal. 12 hours after onset of pain in the 2nd toe of a girl 14 years of age. Injury was denied.



8-623 to 8-625). Freiberg's deformity may persist in this late deformed state into old age.

REFERENCES

- Freiberg A H. Infracture of the second metatarsal bone. A typical injury. *Surg Gynec & Obst* 19:191 1914
- Koehler A. On the first announcement of the typical disease of the second metatarsophalangeal joint, München med. Wchnschr 71:109 1924
- Smilhe I S. Freiberg's infracture (Koehler's second disease). *J Bone & Joint Surg* 39-B:580 1957

Osteochondrosis dissecans (marginal stress fracture) occurs principally in young adults; is rare in children and is nearly nonexistent in infants. The juvenile lesion is rarely found in children younger than 12 years. Morphologically there is a marginal defect in the edge of the bone directly under the epiphyseal cartilage which is contiguous to the articular cartilage. The overlying cartilage is cracked and sometimes defective. A piece of the broken cartilage and bone may be separate from the edge and be extruded into the joint cavity to act as a loose body. Chondral and osteochondral fractures are the primary lesions in nearly all cases, with complete or incomplete separation of the fracture fragment. Local necrosis of bone and cartilage is secondary. The thicker cartilaginous layer which envelops the smaller ossification centers of younger persons probably prevents injury to the underlying bone. The clinical picture is characteristically mild, inconstant and intermittent. History of trauma is often lacking. Localized pain, tenderness and limitation of motion in the neighboring joint are common clinical manifestations. Often the mild clinical signs are unilateral when distinct radiologic changes are bilateral. Green and Banks found the incidence in males three times that in females. Of 36 lesions in their 27 cases, 32 were in the condyles of the femurs at the knees, three in the bones at the elbow and one in the talus. Ray reported changes in the superior edges of the talus and stated that the bones at many joints might be similarly affected—at the shoulder, elbow, hip, wrist and metatarsophalangeal joints. The clinical problem is largely the identification of this lesion in the femoral condyles; about one-third of the cases are bilateral. Velayos and associates demonstrated multiple marginal fragmentations of the medial femoral condyles in a girl 17 years of age after protracted administration of adrenocorticosteroids in the treatment of sarcoidosis.

The diagnosis is usually not made unless there are confirmatory radiologic changes. These consist of a marginal defect in the subchondral bone on the edge of the ossification center near the joint surface (Figs 8-626 to 8-632). An independent particle of normal looking or sclerotic bone may be seen in the craterlike marginal defect or loose in the articular cavity. In proved cases, osteochondrosis of the femoral condyles has almost always been located on the anterolateral edge of the medial condyle. When the marginal irregularities are on the dorsal edges and especially on the

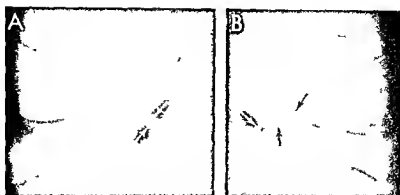


Fig 8-626 - Osteochondrosis dissecans. A, marginal subchondral bone destruction on the under edge of the medial femoral condyle. Within the cupped defect is a smaller wedge of bone density which suggests partial separation of an independent necrotic part. This boy 11 years of age had had mild intermittent

pain in the knee without disability. B, marginal defect in the under edge of the medial femoral condyle with partial extrusion of a loose necrotic fragment into the knee joint. This boy 12 years of age had had a painful knee for six weeks.

Fig 8-627 - Bilateral stress compression fracture (osteochondrosis dissecans) of the medial condyles of both femurs. This girl 14 years of age had had pain in the left knee for five days. The caudal edge of the medial condyle of the left femur (B) is broken and a small slightly sclerotic fragment tilts a small gap recess. At the same site on the edge of the medial condyle of the

right femur (A) there is a marginal transverse fracture line with only slight distraction of the fragments. There were no clinical signs at the right knee. These stress shearing or compression fractures characteristically develop in the medial segment of the caudal edge of the medial condyle.

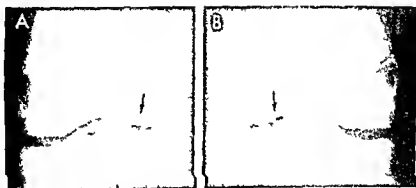


Fig 8-628 - Shearing or compression stress fractures (osteochondrosis dissecans) of the medial femoral condyle of a girl 14 years of age who had had intermittent pain at the left knee for several weeks. In A, frontal projection, a small oval and slightly

sclerotic fragment is seen near the caudal edge of the medial condyle and appears to fit into a sharply circumscribed defect. In B, lateral projection, the fragment in its hollow is situated well forward on the medial condylar edge.

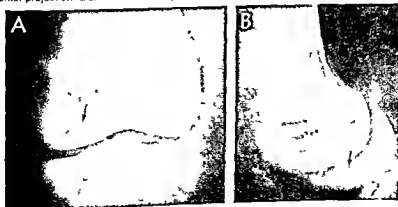




Fig 8-629 — Loose bony fragment of a marginal stress fracture of the medial condyle in the suprapatellar bursa after separation and migration from the caudal edge of the medial femoral condyle. The site of fracture following shear or compression stress (osteochondrosis dissecans) in a girl 16 years of age. (Proved on surgical exploration.)

lateral condyle the probabilities are high that marginal irregularities represent normal developmental variants in healthy children. Tunnel projections give maximal visualization of these dorsal variants and increase the error of overdiagnosis of osteochondrosis dissecans (see Fig 8-209) when the changes are erroneously evaluated. Furthermore, approximately 20% of healthy girls and 30% of healthy boys have marginal irregularities on the posterior condylar wall which are identical radiologically with many of the findings in so-called femoral osteochondrosis dissecans, even to the presence of independent ossicles on the margins beyond the main mass of the ossification center. I am convinced that these normal condylar variations (see Fig 8-210) are commonly called osteochondrosis dissecans when children actually have no bone disease but do have painful and tender lesions in neighboring soft tissues. Independent bony centers may develop in the peripheral portion of the epiphyseal cartilage beyond the edge of the main ossification center and then fuse with the main center as it grows toward and onto the smaller bony nucleus and simulate osteochondrosis dissecans radiographically (see Figs 8-209 and 8-210).

Spontaneous gradual disappearance of the normal variants without treatment may last for many months. Van Demark and Edelstein both pointed out the good natural prognosis in contrast to the need for surgical treatment of adults.

Talar lesions are usually associated with local pain and tenderness but occasionally characteristic marginal defects are encountered on the superior edge of the talus in patients who are asymptomatic (see Fig 8-631). Trauma, pure and simple without vascular injury appears to be the sole cause. In most cases the trauma appears to be minor and repeated. It is usually endogenous and due to repeated internal compression or shearing stresses rather than to conspicuous single exogenous injury. The radiographic changes are located on the superior curved edge of the talus, either medial or lateral, and consist of marginal indentations which may or may not contain a bone fragment. Talar lesions are rare before age 15.

Osteochondrosis dissecans of the distal end of the first metatarsal may be unilateral or bilateral. The destructive lesion is in the end of the shaft, not in a secondary epiphyseal center as is the case in most of the osteochondroses (Fig 8-633). It resembles some of the destructive foci found in the ends of the metatarsals (see Fig 8-132). Kessel and Bonney believe that the primary lesion is rigid hyperextension of the great toe on the first metatarsal with secondary destruction of this bone.

Burrows has pointed out that osteochondrosis (osteochondrosis) has been widely used as a convenient label for any perplexing radiographic change in epiphyseal ossification centers in any part of the growing skeleton. According to Burrows this error has been consistently supported by the misconceptions of the pathology of these lesions promoted by Lenche and Polcard and in my opinion by radiologists and orthopedic surgeons unfamiliar with the normal variations in the normal images of epiphyseal ossification centers. Anatomic proof of the nature of these lesions has been inadequate because of the rarity of direct observations of most of them during surgery. Since Fairbanks's convincing observations it has been clear that osteochondrosis dissecans represents a fracture and its sequelae. We are indebted to Burrows for reminding us that Sir James Paget demonstrated by

Fig 8-630 — Stress marginal fracture of the medial condyle of the femur, standard position. The fracture fragment is not visible, but the marginal defect is clearly demonstrated.



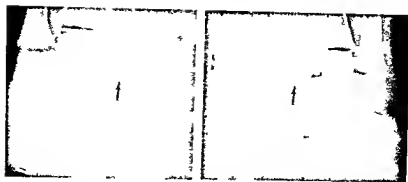


Fig 8 631 —Marginal stress fractures of the defects on the superior edges of the talus of chance findings in a boy 12 years of age who signs at the ankles. They are probably residues

V
C
AG

healing or compression of talus stress fractures (osteochondrosis dissecans) after disappearance of the fracture fragments themselves

direct observation during surgical exploration of the femoral head represents a simple marginal fracture of the peripheral fragment

PEEF

- Burrows H J Osteochondritis juvenilis J Bone & Joint Surg 41 B 455 1959
- Caffey J et al Ossification of the distal femoral epiphysis J Bone & Joint Surg 40-A 647 1958
- Edelstein G M Osteochondritis dissecans with spontaneous resolution J Bone & Joint Surg 36-B 343 1954
- Fairbanks H A T Osteochondritis dissecans Br J Surg 21 67 1933
- Green W T and Banks H H Osteochondritis dissecans in children J Bone & Joint Surg 35-A 26 1953
- Hay B M Two cases of osteochondritis dissecans affecting several joints J Bone & Joint Surg 32 B 348 1950
- Kessel L and Bonney C Hallux rigidus in the adolescent J Bone & Joint Surg 40-B 686 1962
- Paquet J Production of some loose bodies in joints St Bartholomew's Hosp Rep 6 1 1870
- Pick M P Familial osteochondritis dissecans J Bone & Joint Surg 37 B 142 1955

- Ly R B Osteochondritis dissecans of the talus J Bone & Joint Surg 29 607 1947
- Ly R B Hereditary multiple epiphyseal disturbance and consequences for the autogenesis of focal malaciations particularly osteochondritis dissecans Acta orthop scand 24 286 1955
- Ly R B and Hughes R Osteochondritis dissecans of the elbow joint J Bone & Joint Surg 32 B 348 1950
- Ly R B Osteochondritis dissecans Loose Bodies in Joints Etiology Pathology and Treatment (Edinburgh E & S Livingstone Ltd 1960)
- Ly R B Demark R E Osteochondritis dissecans with spontaneous healing J Bone & Joint Surg 34-A 143 1952
- Ly R B et al Arthropathy associated with steroid therapy Ann Int Med 64 759 1966

BOWLEG is caused in part by mechanical stress. In this deformity the knees are separated from each other when the legs are placed in anatomic position

Fig 8 633 Marginal subchondral necrosis (osteochondrosis dissecans or fracture) of the distal end of the 1st metatarsal of a boy 12 years of age who had had pain in his leg on for about three weeks. The lesion is in the shaft not in an epiphysis. The arrows point to the radiolucent subchondral defect. (Courtesy of Dr W. Am. Cevs Denver Colo.)

Fig 8 632 —Marginal stress fracture (osteochondrosis dissecans) of the talus of a boy 15 years of age who had had pain and tenderness of the right ankle for several weeks. A smooth oval mass of bone (arrow) fits into a smooth indentation on the upper edge of the talus near its lateral extremity. Injury was denied





Fig. 8 634 —Bowleg deformities. **A** tunnel projection of the knees of a boy 20 months of age showing upward tilting of the medial ends of the femoral shafts with downward tilting of the lateral ends of the tibial shafts. This projection reflects the deformities in the posterior halves of these bones. **B** in a boy 30 months of age the tibiae and femurs are bowed laterad below

and above the knees. The medial ends of the metaphyses are spurred and beaked and the femoral ossification centers taper medially. The medial cortical walls of the tibiae through which the greatest lines of force are projected are thickened. There is no avoidance of recent or old necks.

Fig. 8 635 —Bilateral idiopathic bowed legs in a boy 22 months of age. The arrows point to the medial and dorsal beaking of the femoral and tibial metaphyses at the knees. The increased stress of weight bearing has also thickened the medial and dorsal cortical walls of the tibiae inward. The femoral ap-

physal ossification centers are much too small, especially in their medial halves, which are under a greater stress of weight bearing when the legs are bowed. After correction of bowed legs these stress phenomena disappear after several months.

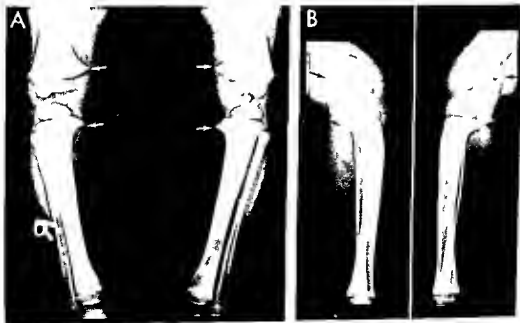




Fig 8-636. Spontaneous conversion of bowed legs to knock knees. A at 21 months both femurs and both tibiae bowed

at age 42 months. B the same patient at 42 months exhibits severe symmetrical knock knees with widening at the ankles.

There are many obvious causes: rickets, prenatal bowing and occasionally trauma. Most cases have no evident cause and are idiopathic. It seems probable that muscular imbalances and postural stresses during growth are much more important causally than actual disease in the bones. Both clinician and radiologist should bear in mind that most bowleg deformities in infants and younger children are transitory and after two to three years disappear without treatment.

In the radiologic examination the tibial shafts are bowed laterad in their upper two-thirds with spurring and beaking of the medial aspects of the ends of the shafts. In almost all cases there is an associated but less marked ventral bowing of the shafts at the same levels at which the lateral bowings occur. The posterior aspects of the metaphyses are also beaked dorsad. The medial and posterior cortical walls of the tibiae on the inside of the curves are thickened (Figs 8-634 and 8-635). The medial halves of the tibial and femoral epiphyseal ossification centers are often wedge-

shaped and taper to a point medially. We have seen many cases in which the clinical diagnosis of bowlegs was made but which showed straight bones radiologically. This clinical error is due to examining the legs when they are slightly abducted and externally rotated instead of in the anatomic position.

We have seen one example of spontaneous conversion of bowed legs into knock knees (Fig 8-636) and another of unilateral bowed leg with knock knee on the opposite side (Fig 8-637).

The bowings are usually more marked in the tibiae but occasionally the bowing is due almost exclusively to lateral bowing of the distal segment of the femurs (Fig 8-638). Anterior bowing of the femur with dorsal spurring is also present. In some unilateral cases the femur is spurred and the femoral epiphyseal ossification center is hypoplastic and sharpened medially which simulates the tibial changes in unilateral tibia vara (Fig 8-639).

Radiographs should always be made when the patient is bearing weight to obtain the radiographic pic-



Fig 8-637 (left)—Right knock knee and left bowleg in a boy 2 1/2 years of age. In bowleg the medial cortical walls are bent laterad and thickened and the lateral cortical walls are thinned. The converse is true in knock knee. Also in knock knee the lateral cortical wall of the fibula is thickened, suggesting substantial weight bearing by this bone.

Fig 8-636 (right)—Femoral bowed legs, endogenous stress fracture at the knees without weight bearing. **A**, frontal projection

shows marked bowlegs in which the tibiae are straight and both femurs are bowed abruptly laterad near their distal ends (femora vara). The femoral epiphyseal ossification centers are small and flattened on the medial halves. In **B**, lateral projection, the right tibia is straight but the femur is bowed ventrad near its distal end and a spur projects dorsad from the same level of the femoral shaft. When possible, frontal projection of the leg should be obtained with the patient standing and the ankles in apposition.

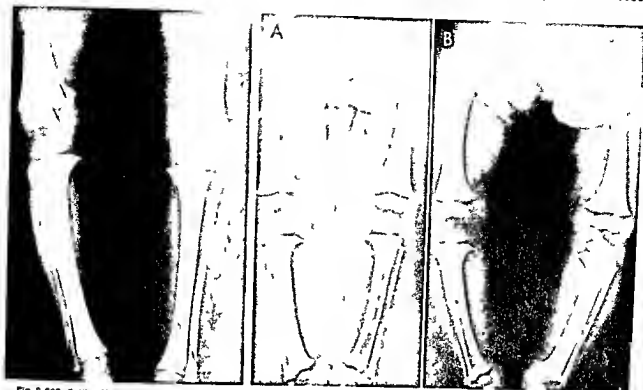


Fig. 8-639 (left) — Unilateral bowleg. The right femur is bowed more than the tibia and the medial part of the femoral epiphyseal ossification center is hypoplastic and sharpened medially. The right tibia is slightly everted medially at the metaphyseal level and its medial cortical wall thickened. This deformity could be properly called femoral vara corresponding to Blount's tibia vara. This boy was 3 years.

Fig. 8-640 (right) — Bowed legs of a girl 12 months of age who

started to walk at 8 months. In A, recumbent position, the tibiae and femurs are bowed but the legs are not bowed because the knees and ankles are in apposition. In B, erect position during weight bearing and with ankles in apposition, the legs are bowed with a gap of 12 cm at the knees. The real clinical deformity of bowed legs is shown most accurately radiographically when the patient is erect and weight bearing.

ture in the same position and degree as the clinician sees them in his physical examination (Fig. 8-640).

REFERENCES

- Holt J F *et al* Physiological bowing of the legs in young children JAMA 154:390 1954
 Sherman M Physiologic bowing of the legs South M J 53:830 1960

KNOCK KNEE (IDIOPATHIC) is a deformity of the legs in which there is a bowing or angulation medial at the level of the knees. When the thighs are placed in the anatomic position the shanks deviate laterad so that there is a wide gap between the ankles, which should touch each other in the anatomic position. Weakness of the medial ligament of the knee and the vastus medialis muscle are the common primary causes. Many healthy infants and younger children have transitory knock knee which disappears without treatment. Geppert found that the maximal degree of this functional knock knee occurred during the 3rd year of life. In measurements on 239 subjects he found the normal maximal range of separation at the

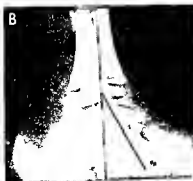
ankles to be 1.5 cm during the 1st year, 3.0 cm during the 2nd, 3.5 cm for the 3rd, 2.0 cm for the 4th and 5th, and 1.5 cm for the 6th year. Knock knee is functional in older girls and women owing to the greater width of the pelvis and thus the greater interarticular distance at their hips. Knock knee may complicate and follow flatfoot and other conditions characterized by regional muscular weakness. In some cases of refractory rickets, severe knock knee, both unilateral and bilateral, develops. MacEwan and Dunbar found that physiologic knock knee developed during the 3rd year when the tibias straightened following the physiologic bowing of the first two years. Knock knee became maximal at the 4th year, when the malleolar gap exceeded 2 in. In some children. By the end of the 6th year physiologic knock knee had disappeared, even in some children who had had malleolar gaps as large as 4 and 5 in., without treatment of any kind.

The radiologic examination may disclose no changes in the bones or a lateral bending of the tibias in their distal halves and medial bowing of their proximal halves with thickening of the lateral cortical walls (Fig. 8-641)—the converse of the changes in bowleg.

Fig. 8 641 — Bilateral idiopathic knock knee in a girl 4 years of age. The lower halves of the tibiae are bent laterad owing to the medial bowing of their upper halves. There is a wide gap between the ankles when the thighs and knees are in anatomic position. The lateral cortical walls of both tibiae, through which the principal lines of force are transmitted in this deformity, are thickened (arrows). This is the converse of the cortical thickenings in bowleg.



Fig. 9 642 — Severe bilateral flatfoot with plantar flexion of the talus bones and rotation of the first metatarsals medially. **A**, frontal; and **B** and **C**, lateral projections. The boy 5 years of age had had flat feet since birth and always walked with difficulty.



The radiographic examination should be made during weight bearing to determine the actual functional degree of knock knee.

REFERENCES

- Geppert T V. Physiological knock knee. *Am J Dis Child* 83:154, 1952.
MacEwan D W and Dunbar J S. Radiologic study of physiologic knock knee in childhood. *J Canad A Radiologists* 9:59, 1958.

FLAT FEET are probably the most common orthopedic problem in the growing child. In many cases they result from persistence of the physiologic pronation of the early infantile feet into later childhood with stretching of the ligaments on the medial side of the ankle—the deltoid calcaneotibial and posterior talocalcaneal ligaments. The usual clinical findings include the flattened contours of the plantar arches, pigeon-toed gait and pain in the foot and leg. On standing, the calcaneus extends laterad from under the talus into a valgus position and the medial side of the foot becomes prominent where the head of the talus is displaced medially. Radiographic findings are shown in Figure 8-642. Films of the feet should always be made during weight bearing (Fig. 8-643).

The special types of flat feet are better recognized by clinical than by roentgen means. They are all characterized by shift of the ventral end of the talus caudad and medially.

PES CAVUS is the converse of flatfoot; its longitudinal plantar arch is deepened and the deformity is easily recognized clinically. The changes in the cavus foot are almost always secondary to lesions in the spinal cord such as congenital malformations and poliomyelitis. Internal derangements in the cavus foot include rotation of the calcaneus on its transverse axis with the front end up, rotation of the talus counterclockwise on its transverse axis into a more



Fig. 8-643—Severe congenital flatfoot with plantar flexion of the talus. A, normal foot at 7 years of age. B, rocker flatfoot at 7 years of age. The calcaneus is rotated clockwise on its transverse axis with the ventral end down and the dorsal tuberosity (heel) up, and the talus is rotated into a vertical position with its ventral end down and the dorsal end up. The scaphoid has not followed the end of the talus caudad as in Figure 8-642 but articulates with the ventral edge of the ectopical talus. The metatarsals are lifted slightly into a shallow equinus position. The longitudinal arch not only is flattened but has gone beyond flatness into a convex plane.

Fig. 8-644—Postpoliomyelitic paralytic pes cavus in a boy 11 years of age. The plantar arch is deepened. The calcaneus is rotated counterclockwise on its transverse axis toward a vertical

position with its ventral end up and the dorsal tuberosity down, while the talus is rotated counterclockwise but toward a more horizontal position with the ventral end up and dorsal end down.



horizontal position with its front end up, plantar flexion of the metacarpals into the equinus position and some degree of dorsiflexion of the phalanges into the cockup toe position (Fig 8-644)

INFECTIONS

Hematogenous osteitis or osteomyelitis is preponderantly a disease of the growth period, infantile and even neonatal cases are not uncommon. Bacteria are the common inflammatory agents, but growing bones may also be invaded by viruses, spirochetes, fungi and yeasts. The radiographic changes are very similar regardless of the infecting agent.

PYOGENIC HEMATOGENOUS OSTEOMYELITIS—This is actually a panosteitis in which all parts of the infected bone are involved, the marrow spaces, however, are usually first infected, and early extension to other bony components follows. The organisms lodge most frequently in the terminal capillary loops in the spon-

giosa near the end of the shaft and infect the juxta-epiphyseal marrow spaces (Fig 8-645). Less frequently the infection is implanted in an epiphysis by way of the articular and cortical arteries or in the corticalls of the shaft through the periosteal vessels. A small focus of purulent necrosis or abscess develops in the soft tissues of the marrow, this is followed by local decalcification and destruction of the spongiosa and overlying corticalls. When many organisms lodge in the end of the shaft multiple focal abscesses are generated and multiple foci of bone destruction develop which coalesce later.

The increased pressure of the local subepiphyseal inflammation may drive the infection into several channels of lesser tension (Fig 8-646). The commonest route of spread is by direct extension through the Haversian canals of the overlying cortex to the subperiosteal space, where the periosteum is lifted off the cortex by the formation of a subperiosteal abscess.

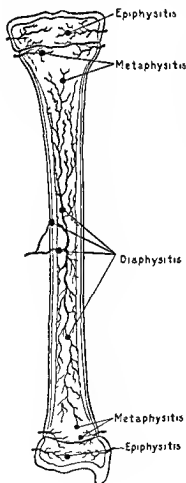
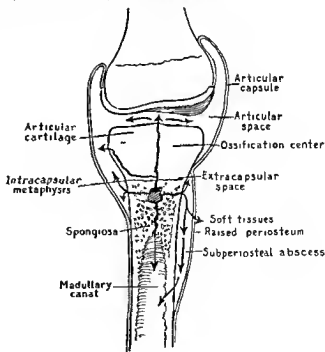


Fig 8-645 (left) —Schematic representation of the arterial channels through which invading bacteria enter the growing bone and the sites of primary implantation. (Modified from Hertzler.)

Fig 8-646 (below) —Schematic representation of the pathways through which infection spreads in the bone after hematogenous implantation in the metaphysis and of the formation of the primary metaphyseal abscess. When the infected metaphysis is intracapsular the articular space is infected by extension through the terminal segment of the cortex. In the case of an extracapsular metaphysis a subperiosteal abscess is formed at the same level but the articular space is not infected. (Modified from Hart.)



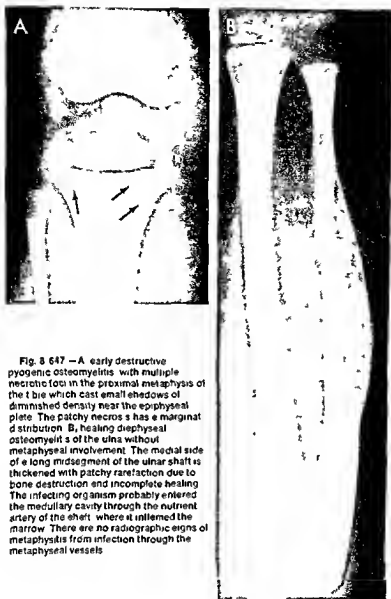


Fig. 8-647 — A, early destructive pyogenic osteomyelitis with multiple necrotic foci in the proximal metaphysis of the tibia which cast small shadows of diminished density near the epiphyseal plate. The patchy necrosis has a margined distribution. B, healing diaphyseal osteomyelitis of the ulna without metaphyseal involvement. The medial side of a long midsegment of the ulnar shaft is thickened with patchy rarefaction due to bone destruction and incomplete healing. The infecting organism probably entered the medullary cavity through the nutrient artery of the shaft where it inflamed the marrow. There are no radiographic signs of metaphysitis from infection through the metaphyseal vessels.

The periosteum itself then may rupture, with extrusion of the infection into the overlying soft tissues. Ordinarily the subperiosteal abscess is limited at one end by the neighboring epiphyseal plate and the firm fixation of the latter to the periosteum and perichondrium. Pus from the subperiosteal abscess may be forced back into the medulla at variable levels of the shaft and set up secondary foci of infection in the marrow tissues. The articular tissues may be infected by rupture of the periosteum when the metaphysis is intracapsular or by extension through the epiphyseal plate into the cartilage and thence onto the synovial surface. The metaphysis, the medullary canal in the middle of the shaft, the epiphysis and the cortex may be infected singly or in combination, concurrently or at intervals.

Repair begins with localization of the infection and the reduction of intraosseous and subperiosteal tension. The cells of the osteogenic layer of the elevated periosteum begin to deposit a shell of new bone (involucrum) over the subperiosteal abscess and after a few weeks a thick bony sleeve envelops the affected segment of the shaft, in the case of extensive lesions almost the entire shaft may become encased in involucrum. Defects in the involucrum—the cloacas—permit the continued discharge of the inflammatory products from the bone. The underlying old cortex begins to die following its separation from the periosteum which eliminates its principal cortical blood supply. The dying and dead bone is covered with granulation tissue. The dead segment or sequestrum may be completely detached, fragmented and discharged.



Fig 8 648 — Concurrent destructive contiguous epiphysis and metaphysis in a boy 3 years of age. Lesions dual changes three months after onset. Shortly after onset purulent fluid was aspirated from the left knee. The metaphyseal lesion appeared several weeks after changes had appeared in the epiphyseal ossification center.

through the cloacas in particles of varying size. Large sequestrums may persist until removed surgically, partially detached sequestrums may be resorbed in place. After several weeks the new cortex or involucrum begins to contract, may become lamellated and slowly changes in the direction of normal structure and contour. The defects in the spongiosa are gradually repaired but often distortion and sclerosis of the cancellous bone are evident for years. In infants healing is more rapid and more complete than in children. Sclerosis and peripheral hypertrophy of the corticulis and shaft can usually be detected many years after subsidence of the infection. If the infection becomes chronic destruction, sclerosis and sequestration may continue indefinitely.

In younger infants pyarthrosis and dislocation of the hip are common complications of osteomyelitis of

the femur, ilium or ischium singly or in combination.

Röntgen findings — It should be emphasized that there are no roentgen changes in the earliest stage of marrow infection and prior to decalcification and destruction of macroscopic quantities of the spongiosa. Significant bone destruction usually does not appear until late in the second week of the disease. Following the roentgen negative early phase roentgen examination is invaluable in determining the location and extent of bone destruction, involucrum formation, sequestrum formation, discharge and resorption and the secondary growth disturbances. The demonstration in a film of regional soft tissue swelling near the site of bone tenderness and pain is only presumptive evidence of infection of the underlying bone. Swelling of the soft tissues signifies simply local cellulitis either with or without osteomyelitis.

The first roentgen sign is the appearance of one or more small shadows of diminished density which are cast by foci of bone necrosis (Fig 8 647). This necrosis may be limited to a small area near the end of the shaft or occupy a considerable portion of the shaft when first detected. Sometimes focal destructive changes develop in the epiphyseal ossification center and in a segment of the metaphysis directly opposite (Fig 8 648). In this case the destruction in the epiphyseal center was evident for several weeks before the metaphyseal destruction became visible. After the second or third weeks involucrum appears and casts a strip of increased density outside of and parallel to the shaft. The extent of the involucrum is directly proportional to the extent of the subperiosteal abscess; it may be limited to the end of the shaft or cover the greater portion of it (Fig 8 649). The margins of the involucrum are usually irregular and multiple defects are often visible. With the passing of time the involucrum becomes thicker and less irregu-

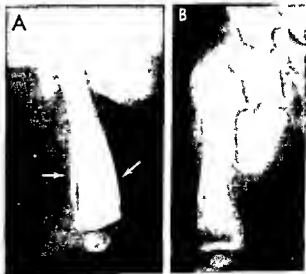


Fig 8 649 — Healing osteomyelitis showing involucrum formation. A: early involucrum limited to the distal end of the femur. New layers of corticulis are visible on the anterior and posterior aspects of the shaft. B: massive irregular involucrum which surrounds and obscures most of the shaft of the femur. The proximal end of the femur is destroyed. The femur is dislocated out of the acetabulum. Several loose sequestrums are visible in the soft tissues.



Fig 8-650 — Massive sequestrum on the radius in situ. A moderately thin wrinkled involucrum (arrows) surrounds the underlying dead sclerotic cortex.

lar. The dead portions of the old shaft or sequestrums cast a sclerotic shadow owing to the higher mineral content caused by shrinkage and disappearance of the soft tissues after death. Sequestrums vary in size from large segments of dead compacta to tiny particles (Fig 8-650). They may be located wholly inside the involucrum or be found partially extruded through cloacas or loose outside in the neighboring soft tissues (Fig 8-651).

Treatment with antibiotics early modifies the roentgen picture of acute osteomyelitis: the destructive features are lessened so that involucrum formation is sometimes the earliest and most conspicuous roentgen finding (Fig 8-652). During the administration of

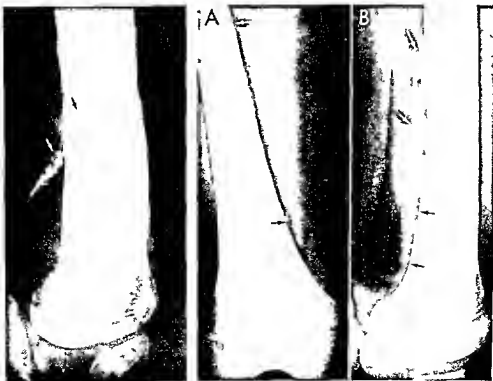
antibiotics even large sequestrums may be resorbed spontaneously in the soft tissues without benefit of surgical drainage (Fig 8-653). It should be remembered that there is always a lag between clinical recovery and roentgen improvement in osteomyelitis treated by antibiotics: the roentgen changes may continue to increase for weeks after the infection has completely subsided clinically.

A ball and socket type of residual shortening deformity may develop at the cartilage-shaft junction when the osteomyelitic agents kill the growing cartilage cells in the central segment of the proliferating cartilage so that a peripheral rim of healthy cartilage cells continues to grow beyond the central segment of

Fig 8-651 (left) — Partial extrusion of a moderately large sequestrum through sclerotic thick involucrum.

Fig 8-652 (right) — Acute hematogenous osteomyelitis of the femur treated with penicillin from onset. A: frontal and B: lateral

projections made three weeks later. Although a thick involucrum has formed on the dorsal cortical wall, there is little evidence of destruction and none appeared in later films made over several months.



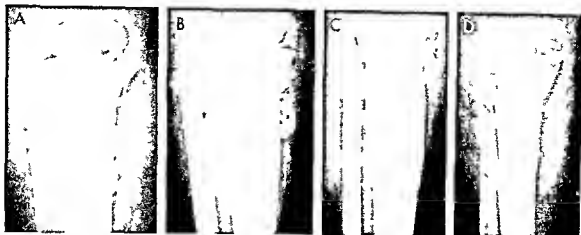


Fig 8-653 — Resorption of small and large sequestrums in soft tissues during penicillin treatment and without benefit of surgical drainage. A, destructive osteitis in the proximal tibial metaphysis.

B, multiple loose sequestrums in the soft tissues one week after A. C, D, lateral projection of B. D, six weeks later the sequestrums have disappeared but the tibial metaphysis is still deformed.

the epiphyseal ossification center and bury it into the deformed end of the shaft (Fig 8-654). We have seen similar lesions follow trauma and scurvy and they have been reported as residuals of vitamin A poisoning. Cupping of the ends of the shafts with enlargement and premature fusion of ossification centers

Fig 8-654 — Residual deep cupping of the distal femoral metaphysis following acute osteomyelitis. This deformity appears to be due to destruction of the proliferating cartilage cells in the central segment of the cartilage segment with suppression of longitudinal growth in the center of the shaft but with continuing growth on the periphery so that the ossification center is gradually buried into the concave face of the shaft. A, acute osteomyelitis of the juxtaepiphyseal metaphysis at 9 months of age with the enlarged ossification center almost completely buried in the cup and beginning to fuse prematurely with the shaft. We have seen similar cupping of the distal end of the femur following trauma, scurvy, and vitamin A poisoning.

with their shafts at the knees were observed in three patients following prolonged immobilization and manipulations in the treatment of congenital dislocation of the hip (Botting and Scrase). This same cupping and premature fusion deformity in the growing metaphysis has also been found in sickle cell anemia, postpoliomyelitic states, and chronic poisoning by vitamin A and may be residual to traumatic injuries to the knees. The same phenomena at the knees have also been observed as complications and sequelae to inflammatory diseases at the hip, such as tuberculosis, chronic arthritis, and osteomyelitis and slipping of the upper femoral epiphysis.

When a segment of the metaphyseal arteries is occluded by inflammation in the medullary cavity, a long tongue of radiolucent uncalcified cartilage may persist and hypertrophy to elongate with growth, casting a narrow radiolucent strip of diminished density which extends shaftward from the cartilage (Fig 8-655). Such strips are reminiscent of the changes in infantile hypophosphatasia, and they may be due to local segmental hypophosphatasia caused by the local oligemia in the metaphysis in this patient.

Localized Osteomyelitis—Some pyogenic infections are sharply localized and are of low virulence. Only a small patch of necrosis develops which is surrounded by a sclerotic capsule of spongy bone (Fig 8-656). In the early stages the cavity is filled with purulent exudate; later this is replaced by granulation tissue. Localized infection of this type is commonly referred to as Brodie's abscess or silent focus (Phemister). The clinical manifestations are usually mild and the condition often remains unrecognized during its early stages. One should be cautious in the diagnosis of Brodie's abscess in the distal ends of the femurs and proximal ends of the tibiae, where physiologic defects in the cortex may cast small cystic shadows similar to those cast by localized inflammatory



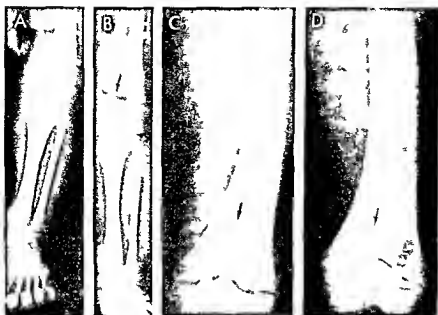


Fig. 8-655 Osteomyelitis at the distal end of the femur with residual long radiolucent tongue of uncalcified cartilage which extends shaftward off the cartilage plate. A and C at 4 weeks of age; point tenderness and fever suggested osteomyelitis at the distal end of the femur. B and D at 6 weeks; a small segment of

the metaphysis is radiolucent and part of the tongue is still at the distal end. The tongue of uncalcified cartilage is presumably due to segmental failure of normal destruction of cartilage plate caused by local osteomyelitis which led to reduced blood flow in the terminal branches of the metaphyseal arteries.

Fig. 8-656 Broad abscesses (metaphyseal abscesses) in the distal femoral metaphysis (upper arrow) and in the metaphysis of the calcaneal body (lower arrow) of a boy 12 years of age.



Fig. 8-657 Chronic sclerosing osteomyelitis (Garrod's) in the distal end of the humerus of a boy 4 years of age. The anterior aspect of the cortex is thickened internally and externally. Changes of this nature should also raise the question of osteoid osteoma in which the destructive nidus is concealed in the surrounding dense bone.



foci (see Fig 8-219) Brodie's abscess is defined by Waldvogel as primary subacute pyogenic osteomyelitis. It is usually localized in the metaphysis. The increase in density around the radiolucent, lytic center represents local marginal increase in spongy bone and sometimes thickening of contiguous cortical bone.

Diffuse sclerosing osteomyelitis (Garré's disease, osteomyelitis sicca)—This is characterized by diffuse bone production with little or no bone destruction or sequestrum formation. The lesion is usually limited to the cortex, which is thickened externally or internally over a variable distance (Fig 8-657). The cause is thought to be a low grade infection. The roentgen changes in Garré's disease resemble those in osteoid osteoma. These conditions usually cannot be differentiated conclusively without biopsy.

Infantile osteomyelitis—This differs in several important respects from osteomyelitis in children. The infantile disease is much milder clinically, and prognosis for rapid complete recovery is usually excellent. The thin, less compact cortices of infants permits earlier spread to the subperiosteal space, and the more delicate, loosely attached periosteum permits earlier subperiosteal abscess formation and rupture into the soft tissues. These factors all favor early spontaneous decompression and drainage of the shaft, thus preventing much of the necrosis which develops in thicker, less easily decompressed, older bones. Sequestrums are absorbed more rapidly and completely in infants.

During infancy, there is a peculiar type of osteomyelitis which is not seen in older patients. The chief complaint and presenting physical findings are 'lumps in the neck, chest and extremities' which appear suddenly in an infant who shows little or no constitutional signs of severe infection. There is so little local inflammatory reaction in the swellings and constitutional reaction that osteomyelitis is not suspected until roentgen examination shows the bone lesions. In the trunk, both clavicles and several ribs may be infected and in the extremities, all of the bones proximal to the knees and elbows. Suppurative

arthritis at the hips, shoulders and elbows is commonly associated. The spine and bones in the peripheral segments of the extremities are conspicuously spared. Although prognosis for recovery is good, serious multiple crippling deformities are common in the proximal ends of the humeri and the distal ends of the femurs, owing to the early destruction of proliferating metaphyseal cartilage cells. In a case of this type reported by Yakovac and colleagues, the infecting organism was a nonphotochromogenic mycobacterium (*Bacillus*).

Complications—The important complications and sequelae include arthritis, fractures, dislocations and growth disturbances. The growth disturbances which result from infections in the tubular bones of the hands have been described in detail by Cockshott; they represent his large experience with such lesions in Nigeria. The frequency of secondary joint infection depends largely on the anatomic relationship of the articular capsule, periosteum, metaphysis and epiphyseal plate (Fig 8-658). Secondary arthritis is common when the infected metaphysis is intracapsular, as in the hip joints. During infancy, in the presence of purulent arthritis of the hip, the femur may be dislocated out of the acetabular cavity. Primary infection of the synovium from the blood stream apparently precedes osteomyelitis in many cases. Follow up roentgenograms in cases of supposed primary synovitis, however, may disclose lesions in the neighboring epiphyses or metaphyses which were not evident in films made in the early acute phase of the infection. Pathologic fractures may occur during the early stage of bone destruction or later if there is insufficient involucrum formation. Either elongation or shortening of the affected bone may be the sequel of osteomyelitis. When there is no destruction of the epiphyseal cartilage but growth is stimulated by the chronic hyperemia of the part, elongation results; acceleration of epiphyseal maturation occurs in the same circumstances. Shortening is due to actual inflammatory destruction of the proliferating cartilage cells. Shortening is often attended by marked deformities, dislocations and disturbances in mechanical

Fig 8-658—Diagram showing the importance of the position of the articular capsule in the spread of infection from the metaphysis into the articular space. A, both sides of the metaphysis

are extracapsular. B, both sides are intracapsular. C, one side is intracapsular and the other side extracapsular.

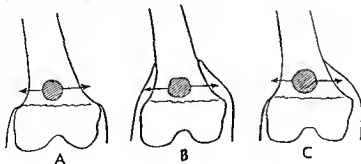




Fig 8-659 - Pyogenic epiphysitis in the proximal end of the femur of an infant 4 months of age. The large peripherally located area of destruction is visible in the dorsal segment of the epiphyseal ossification center.

function owing to changes in the inclination of the opposing articular surfaces.

Epiphysitis - The epiphysis may be infected alone or with the diaphysis. The area of necrosis in the epiphysis casts a shadow of diminished density (Fig 8-659). Secondary infections of the joint are common but not invariable; the articular cartilages may be destroyed and the joint space narrowed. Pyogenic epiphysitis may be marginal and resemble the marginal destruction which is characteristic of tuberculous epiphysitis. Tuberculous and chronic pyogenic epiphysitis cannot be conclusively differentiated by roentgen findings alone.

Osteomyelitis of the patella is more common in children than adults but infection of the cartilaginous patella of infants and younger children is exceedingly rare. Evans described four examples in children 5-11 years of age. Inflammatory signs - swelling, pain, and redness - develop in the prepatellar tissues. Radiographic findings of destructive followed by productive changes are similar to those found in other inflamed bones. Effusions into the knee joint and its contiguous bursae are common complications.

REFERENCES

- Baylin, G. J. and Glenn, J. C. Jr. Soft tissue changes early in acute osteomyelitis. *Am J Roentgenol* 58:142, 1947.
 Blanche, D. W. Osteomyelitis in infants. *J Bone & Joint Surg* 34-A:71, 1952.
 Botting, T. D. J. and Scrase, W. H. Premature epiphyseal fusion at the knee complicating prolonged immobilization for congenital dislocation of hip. *J Bone & Joint Surg* 47-B:280, 1965.
 Cass, J. M. Staphylococcus aureus infection of the long bones in the newly born infant. *Arch Dis Childhood* 15:55, 1940.
 Cockshott, W. P. Dactylitis and growth disturbances. *Brit J Radiol* 36:19, 1963.
 — and MacGregor, M. Osteomyelitis variola. *Quart J Med* 27:369, 1958.

- Dalldorf, G. Viruses and human cancer. *Bull New York Acad Med* 36:19, 1960.
 Evans, D. K. Osteomyelitis of the patella. *J Bone & Joint Surg* 44-B:319, 1962.
 Garsche, R. Osteomyelitis in infants following bone marrow puncture. *Schweiz med Wchnschr* 81:1131, 1951.
 Gilmour, W. N. Acute hematogenous osteomyelitis. *J Bone & Joint Surg* 44-B:841, 1962.
 Green, W. T. Osteomyelitis in infancy. *JAMA* 105:1835, 1935.
 Hart, V. L. Acute hematogenous osteomyelitis in children. *JAMA* 108:524, 1937.
 Hendrickse, R. G. and Collard, P. Salmonella osteitis in Nigerian children. *Lancet* 1:80, 1960.
 Hertzler, A. E. *Surgical Pathology of the Diseases of Bones* (Chicago: Lakeside Press, 1930).
 Markowa, J. Dystitis produced experimentally in mice by the virus of tick borne encephalitis. *J Bone & Joint Surg* 44-B:722, 1962.
 Phenuster, D. B. Silent foci of localized osteomyelitis. *JAMA* 82:1311, 1924.
 Wilson, J. C. and McKeever, F. M. Bone growth disturbance following hematogenous acute osteomyelitis. *JAMA* 107:1188, 1936.
 Yakovac, W. C. et al. Fatal disseminated osteomyelitis due to an anonymous mycobacterium. *J Pediatr* 59:909, 1961.

TUBERCULOSIS - Hematogenous metastasis of tubercle bacilli to the skeleton may take place early during the active phase of the primary complex in the thorax or later from postprimary tuberculous foci. After implantation in the bone, an immediate active inflammatory reaction may develop or the bacilli may be dormant for years until activated by local factors such as trauma to the bone or joint. All or a single component of a growing bone may be affected. The synovial surface may be infected before the bones are involved; the infection may then spread from the joint to the contiguous epiphysis and metaphysis.

Tuberculosis produces a chronic inflammatory reaction in the bones which is similar in its macroscopic aspects to chronic pyogenic osteomyelitis. Local necrosis of the intraosseous soft tissues develops at the site of implantation and is then followed by regional decalcification and destruction of the osseous tissue itself. Spread of the infection from the focus in the bone takes place through the same pathways as those described in the pathogenesis of pyogenic osteomyelitis. When the synovium is infected first, the subchondral bone necrosis which develops secondarily in the contiguous epiphysis is usually marginal in its distribution in the noncontact portions of the articular surfaces.

During infancy and early childhood, when the cartilages are relatively thicker and the epiphyseal ossification centers smaller, direct transfer of the infection from the joint to the bone is not as common as in later childhood and adolescence, when the epiphyseal cartilages are thinner and the ossification centers are correspondingly larger. For the same reasons, infection of the opposing epiphyses of a joint is not as common in infants and children as in adults. The articular cartilages are preserved longer in tuberculous osteitis and arthritis than in pyogenic arthritis owing

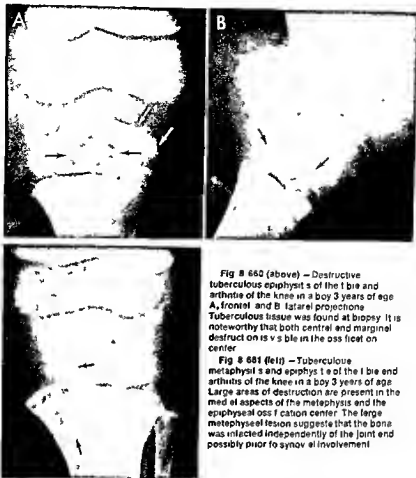


Fig 8 660 (above) — Destructive tuberculous epiphysitis of the tibia and arthritis of the knee in a boy 3 years of age. **A**, frontal; and **B**, lateral projections. Tuberculous tissue was found at biopsy. It is noteworthy that both central and marginal destruction is visible in the ossification center.

Fig 8 661 (left) — Tuberculous metaphysitis and epiphysitis of the tibia and arthritis of the knee in a boy 3 years of age. Large areas of destruction are present in the medial aspects of the metaphysis and the epiphyseal ossification center. The large metaphyseal lesion suggests that the bone was infected independently of the joint and possibly prior to synovial involvement.

to the lack of a destructive proteolytic ferment in tuberculous exudates. Sinus formation and cold abscesses are common in tuberculous osteitis. involucrum formation and sequestration are not as conspicuous as in pyogenic osteomyelitis.

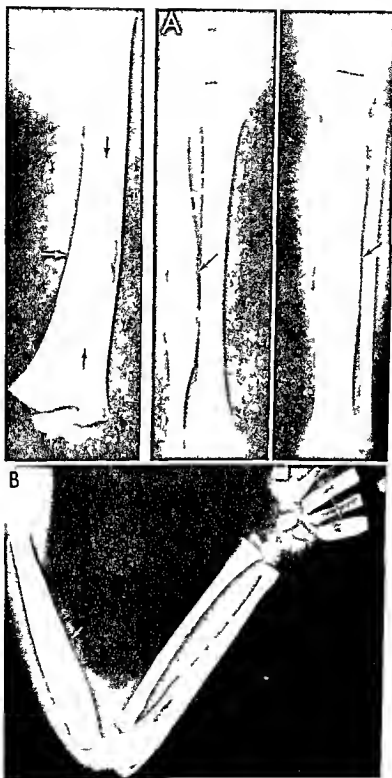
Röntgen appearance — The roentgen findings in skeletal tuberculosis are similar to those of chronic pyogenic osteomyelitis in all of the principal features. From the roentgen appearance alone a conclusive diagnosis of tuberculosis is not justified. Pyogenic and tuberculous lesions are found at the same sites in the growing bone; they produce the same pattern of

bone destruction and production. Persistence of the joint space and presence of cold abscess favor the diagnosis of tuberculosis but are by no means pathognomonic. Extensive sequestration favors the diagnosis of pyogenic osteomyelitis. Bone neoplasms, particularly Ewing's sarcoma, often resemble chronic osteitis pyogenic or tuberculous so closely that these three conditions cannot be clearly differentiated without biopsy. The conclusive identification of these chronic bone lesions is too important to be left to statistical speculations by even the most expert observers. Shrewd roentgenographic interpretation may

Fig 8 662 (left above on facing page) — Tuberculous diaphysitis of the femur in a boy 21 months of age. In the middle third of the shaft is a long segment of cystic rarefaction (arrows). The inner surface of the overlying cortex is eroded and a narrow layer of involucrum covers the shaft externally. Epiphyses and metaphyses are not affected. Disseminated tuberculosis was demonstrated at necropsy.

Fig 8 663 — Benign multiple tuberculous diaphysitis in a boy 18 months of age, with cold abscesses on the dorsal surfaces of the hands. **A**, lower extremities. The left tibia and right tibia are

swollen. The medullary canals are dilated and the overlying cortices are thickened by involucrum formation. **B**, left upper extremity. The distal half of the humerus is swollen into a sausage-shaped contour and the cortex is thickened. The medullary canal is dilated and exhibits cystic rarefaction. The proximal half of the ulna is swollen, dilated and irregularly cystic. Its cortical surface is thickened. The 5th left metacarpal is swollen and irregularly osteoporotic. All of these lesions healed slowly but completely. In 2 1/2 years later the skeleton appeared to be normal.



Figs. 8-662 and 8-663. Descriptions on facing page

prove correct in a satisfying percentage of a large group of cases and, notwithstanding, be catastrophically incorrect in a single case.

Metaphysitis and epiphysitis—These are characterized roentgenographically by patches of diminished density with and without regional sclerosis in the juxtaepiphyseal segment of the shaft and in the ossification center (Figs 8-660 and 8-661). These shadows are cast by defects and thickenings of the affected spongiosa and overlying corticalls. Small or large segments of involucrum may surround the metaphyseal lesions. When the joint is involved the increased synovial fluid and thickening of the articular tissues cast a diffuse shadow of increased density. Atrophy of disuse is a constant feature of the bones when movement has been limited for more than a few weeks. The location of the destructive lesions in the metaphyses and epiphyses is usually marginal but may be central. The joint space is characteristically well retained in the early phases of tuberculous arthritis, early narrowing of the articular space favors the diagnosis of pyogenic infection (Phemister).

Tuberculous diaphysitis—Not infrequently the tuberculous inflammation in a long bone is limited to the intermediate segments of the shaft and the metaphyses and epiphyses are not affected. Thus diaphyseal reaction probably results from original implantation of the infection near the nutrient canals, in some cases, however, the shaft involvement may merely be a residue of an earlier metaphysitis which has been buried deeper in the shaft owing to later growth of the epiphyseal cartilage away from an initial metaphyseal lesion. Tuberculous diaphysitis is usually not associated with conspicuous clinical signs and spontaneous complete healing is the rule. Long segments

of the shaft exhibit destructive and productive changes (Figs 8-662 and 8-663). The cortex may be eroded on its internal surface and thickened externally. In massive lesions the medullary cavity is widely dilated and the shaft has a spindle shaped external contour with a diffuse central rarefaction. Sometimes these sharply defined rarefactions present the roentgen appearance of cysts, which has given rise to the term "cystic tuberculosis of bone," a superfluous and misleading designation for destructive tuberculosis of the shafts. In other cases the productive changes dominate and the bone appears sclerotic owing to the extensive cortical thickening. In the short bones of the hands and feet this same lesion is called *spina ventosa* (Fig 8-664).

Growth disturbances are not uncommon in bone tuberculosis. Shortening and elongation result from the same mechanisms as those described for pyogenic osteomyelitis. Single and multiple transverse lines develop frequently.

An important complication and sequel of tuberculosis and other lesions at the hip is premature fusion of the primary and secondary ossification centers at the distal end of the same femur and at the proximal end of its opposing tibia. This stops growth and often leads to crippling shortening. The femur may fuse without concomitant fusion of its companion tibia. Dobson encountered ipsilateral fusions at the knee in 23% of all patients younger than 15 years. Kestler cited examples of hip disease other than tuberculosis, in which premature fusion developed at the ipsilateral knee. Pathogenesis is obscure. It has been suggested that early fusion results from rupture of the epiphyseal plates due to loss of the supporting spongiosa and cessation of endochondral bone formation in the affected metaphyses.

Curran found premature fusion of the epiphyseal ossification centers of the metatarsals and of the femur and tibia at the knee to be a common sequel of polyomyelitis. The cupping of the metaphysis and overgrowth and premature central fusion of the epiphyseal ossification center were similar to the findings in trauma, vitamin A poisoning (see Fig 8-729) and after purulent metaphysitis (see Fig 8-654). Slee studied 28 patients who had premature fusion of the epiphyseal ossification centers in the knee, 11 had tuberculosis of the ipsilateral hip, 13 had polyomyelitis of the legs, and 4 had been treated for congenital dislocation of the hip. All patients had had prolonged immobilization of the legs and the bones were rarefied. This experience suggests that therapeutic complete immobilization of the legs should be as brief as possible.

Krieger and associates reported two cases of chronic inflammatory disease in the lungs and bones which appeared to be due to atypical mycobacteria.

Sarcoidosis—This condition also known as Besnier Boeck disease, is a chronic granulomatous inflammation which affects the bones of children occasionally and of infants rarely. The causal agent has

Fig 8-664—Tuberculous diaphysitis (*spina ventosa*) in a boy 2 years of age. Cystic swelling of the 5th metacarpal and destructive changes in the 1st phalanx of the 1st digit are evident (arrows). *Spina ventosa* is of historical interest because it was the first lesion described roentgenographically in a child (by Feilchenfeld in May 1896).



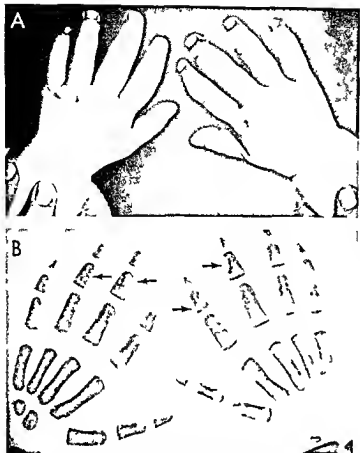


Fig 8-665—Sarcoidosis of the hands of a child 2 years of age. A photograph showing the fusiform swelling of the digits. B roentgenogram showing the foamy rarefaction of the phalanges (From News and Hardwick)

not been established. Some pathologists hold that sarcoid is a non-necrotic form of tuberculosis; others believe that it is a peculiar reaction to the tubercle bacillus, while others are of the opinion that sarcoidosis is a specific reaction to an unknown virus. The skin, lungs and lymphatic structures may be affected as well as the bones.

The most characteristic skeletal lesions are small destructive cystic areas in the distal end of the phalanges, metacarpals and metatarsals (Fig 8-665). Extension to the neighboring joint spaces and cold abscesses are said not to occur; the overlying cortex is rarely thickened. The differential diagnosis of sarcoidosis and tuberculous diaphysitis is always difficult roentgenographically and remains uncertain in some cases even after biopsy.

REFERENCES

- Curran G. Premature closure of the epiphyses in the metatarsals and knees. A sequel of polyomyelitis. *Radiology* 87:424, 1966.
- Donovan M S and Sosman M C. Tuberculosis of the greater trochanter and its bursa. *Am J Roentgenol* 48:719, 1942.
- Gill C G. Cause of discrepancy in length of limbs following tuberculosis of the hip in children. Arrest of growth from premature central closure of epiphyseal cartilages about the knee. *J Bone & Joint Surg* 26:272, 1944.
- Hardy J B and Hartman J R. Tuberculous dactylitis in childhood. A prognosis. *J Pediatr* 30:146, 1947.
- Kneger I et al. Atypical mycobacteria as a probable cause of chronic bone disease. Report of 2 cases. *J Pediatr* 65:340, 1964.
- News G H and Hardwick C. Besnier-Boeck's disease in an infant. *Arch Dis Childhood* 14:78, 1939.
- Petter C K and Medelman J P. Tuberculosis of the shafts of the long bones: clinical and roentgenological study with report of 8 cases. *Am Rev Tuberc* 32:285, 1935.
- Phemister D B. Changes in the articular surfaces in tuberculous and in pyogenic infections of joints. *Am J Roentgenol* 12:1, 1924.
- and Hatcher C H. Correlation of pathological and roentgenological findings in diagnosis of tuberculous arthritis. *Am J Roentgenol* 29:736, 1933.
- Slee G C. Premature fusion knee epiphyses. *J Bone & Joint Surg* 48-B:589, 1966.
- Waldvogel F A et al. Osteomyelitis. A review of clinical features, therapeutic considerations and unusual aspects. *New England J Med* 282:198 and 360, 1970.

OSTEITIS DUE TO VIRAL INFECTIONS has not been conclusively proved. The osteomyelitis which may complicate smallpox and is rarely seen in association with chickenpox and measles is usually due to secondary pyogenic organisms from the skin lesions. In cat scratch fever, osteolytic lesions in the skeleton were found in the ilium of a boy 5 years of age by Adams and Hundman, and in the neck of the femur



Fig 8-666 — Large oval sharply defined defect in the lemur of a boy 4 years of age who had had cat scratch fever for 51 days (Redrawn from Collipp and Koch)

(Fig 8-666) of a boy 4 years of age by Collipp and Koch. In the radiographic and anatomic study of Eeckels and Seynhaeve the bone lesions of smallpox—necrosis and resorption followed by fibrosis—were believed to be due to ischemia and necrosis secondary to regional proliferative arteritis rather than to the direct bacterial and viral inflammation of bone.

Cochran and colleagues studied an Irish boy 3 weeks of age who was vaccinated and developed a severe local reaction at the site of inoculation on the left deltoid region. A few weeks later the left scapular region became swollen and the patient then went through a typical clinical and radiographic course of infantile cortical hyperostosis. In this case the infant suffered from the two diseases—vaccinia and infantile cortical hyperostosis successively—or the vaccinia virus caused infantile cortical hyperostosis.

REFERENCES

- Adams W C and Hindman S M. Cat scratch disease associated with osteolytic lesion. *J Pediatr*. 44:665 1954.
Blattner R J. Comments on current literature. Bone and joint involvement in virus disease. *J Pediatr*. 67:144 1965.

- Cochran W et al. Bone involvement after vaccination against smallpox. *Br J J* 2:285 1963.
Collipp P J and Koch R. Cat scratch fever associated with an osteolytic lesion. *New England J Med*. 260:278 1959.
Eeckels R and Seynhaeve V. Bone lesions due to smallpox. *Arch Dis Childhood* 39:591 1964.

OSTEITIS DUE TO FUNGUS INFECTIONS is being recognized with increasing frequency especially in generalized coccidioidomycosis and histoplasmosis. The radiologic changes are similar to those in chronic pyogenic osteitis and tuberculosis of bone. The principal clinical findings are usually single or multiple painful and tender subcutaneous swellings which exhibit little or no increase in local heat. One or several of any of the bones may be affected. Contrary to earlier opinion, fungus infections of the skeleton do not in themselves connote severe disease with certain death.

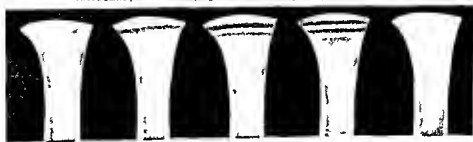
Blastomycosis in children produces chronic inflammatory reactions in the skin, lungs and bones. Gill and Gerald found distinctive inflammatory changes in the calvaria radiographically in three of their six cases in children.

REFERENCES

- Allen J H Jr. Bone involvement with disseminated histoplasmosis. *Am J Roentgenol*. 89:250 1959.
Burner J W and Smart S. Osseous coccidioidomycosis. A chronic form of dissemination. *Am J Roentgenol*. 76:1052 1956.
Dykes J et al. Coccidioidomycosis of bone in children. *Am J Dis Child* 85:34 1953.
Gill J A and Gerald B. Blastomycosis in childhood. *Radiology* 91:965 1966.
Klingberg W G. Generalized histoplasmosis in infants and children. *J Pediatr* 36:728 1950.

INFANTILE SYPHILIS—The reaction of growing bone to syphilitic infection is not unlike that of other chronic infections in many respects. The spirochetes are implanted in the metaphyses and diaphyses and produce destructive and productive changes in the areas of destruction the marrow cells and bone are replaced by syphilitic granulation tissue. The outstanding characteristic of infantile syphilis is the multiple bone involvement. In severe cases nearly all of the metaphyses are affected, but in milder cases

Fig 8-667 — Diagrammatic representation of the types of transverse striping of the metaphysis found in infantile syphilis. These same patterns of striping are found in many nonsyphilitic conditions.



the changes may be limited to two or three bones usually the tibia, femur and humerus.

In addition to the local inflammatory changes caused by the spirochetes trophic changes develop in the metaphyses which are due to the nonspecific generalized effect of a severe disease on endochondral bone formation. These trophic changes are seen at the cartilage shaft junctions and are responsible for the transverse-band appearance of the metaphyses in roentgenograms (Fig 8-667). Thickening of the epiphyseal plate and atrophy of the juxtaepiphyseal spongiosa are the anatomic equivalents of the transverse shadows. The transverse striped appearance of the metaphysis is an almost constant phenomenon in all severe diseases during the fetal period and early infancy. It is not pathognomonic and not diagnostic of syphilis, although almost all patients with active infantile syphilis show some of these trophic metaphyseal changes. Moreover, the administration of bismuth to the mother during pregnancy produces transverse bands of increased and diminished density in the metaphyses of the nonsyphilitic fetus which simulate the trophic transverse striping found in syphilitic fetuses and newborns (see Fig 8-265).

Engeset and co-workers emphasized that the principal changes in bone syphilis are deviations of the normal growth processes rather than specific destructive and productive changes due to syphilitic inflammation. They found little evidence of formation of a specific syphilitic granulation tissue in bones. They agreed with Parrot's conception of the metaphyseal changes in syphilis as nutritional (*dystrophie syphilitique*) rather than inflammatory. They suggested that the older terms implying inflammation such as osteochondritis, periostitis and diaphysitis be replaced by terms indicative of purely dystrophic causation such as osteochondropenostosis or Parrot's syphilitic dystrophy.

Röntgen appearance—Characteristically the syphilitic inflammation appears irregularly diffuse involving the diaphysis and both metaphyses of each of the several bones affected (Fig 8-668). A curious and conspicuous feature of skeletal syphilis is the absence of involvement in the epiphyseal ossification centers even when the most marked productive and destructive changes are visible in the adjacent shafts. Granular osteoporosis of the ossification centers is a normal finding during the first months of life and should not be interpreted as abnormal in syphilitic infants.

Metaphysitis—The juxtaepiphyseal segments of the shaft are usually the earliest sites of involvement and a variety of changes develop in different cases and in the same case during different stages of the disease. Rarely the metaphyses appear normal roentgenographically. In other cases only the trophic transverse striping of the metaphysis is evident. The destructive lesions may be limited to foci of rarefaction in the corners between the end of the shaft and the epiphyseal plate (Fig 8-668). In other cases a deep terminal layer of spongiosa in the metaphysis is

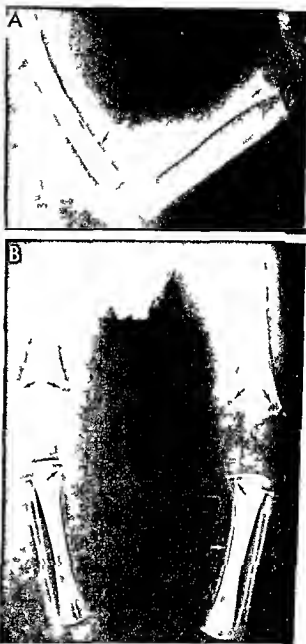


Fig 8-668 Syphilitic panostitis in an infant 5 weeks of age. A, upper extremities; B, lower extremities. Focal destructive changes are visible in the metaphyses, and the shafts are cloaked in an exte layer of subperiosteal bone.

destroyed which casts a deep uniform band shadow of diminished density extending the full width of the shaft (Fig 8-669). In severe cases large lateral metaphyseal defects may extend deep into the shaft (Fig 8-670). The cortex overlying these metaphyseal defects may be destroyed or thickened. Lateral metaphyseal defects may be found in many bones. At the proximal ends of the tibiae they are almost without



Fig 8 669—Syphilitic metaphysitis in a premature infant 1 month of age showing deep segments of diminished density in the ends of the shafts. The spongy bone in these segments has been replaced by radiolucent syphilitic granulation tissue. **A** upper extremity. **B** lower extremities.

fail located on the medial aspects when they are symmetrical on the two sides they are known as Wimberger's sign. The Wimberger lesions are often accompanied by symmetrical defects on the medial aspects of the distal end of the femurs.

Pathologic fractures through destructive metaphyseal lesions are not uncommon. The terminal fragment of the shaft with attached epiphysis may be displaced anteriorly, posteriorly or laterally and impacted into the shaft (Fig 8 671). A remarkable feature of congenital syphilis is the complete healing and normal growth without residual deformities of these fractured and deformed metaphyses. Rectitution of the normal alignment of the fragments takes

place without application of orthopedic appliances. The synovial tissues appear to be immune to syphilitic infection during early infancy.

Occasionally the juxtaepiphyseal edge of the epiphyseal plate is serrated and exhibits numerous prongs or spines which project into the epiphyseal cartilage (Fig 8 672). Thus jagged appearance is usually absent in mild cases and may not be present when severe changes are present in the shaft. Park and Jackson showed that the individual projections in the saw tooth metaphysis are due to local extensions of calcification into the cartilage surrounding hypertrophied longitudinal cartilage canals. The syphilitic saw tooth metaphyses may be closely simulated roentgenographically by the irregularly mineralized epiphyseal plate of early rickets.

Diaphysitis—The long segment of the shaft interposed between the terminal metaphyses may be unaffected or show extensive destructive and productive changes. Scattered focal cortical destruction gives rise to a patchy moth eaten rarefaction (Fig 8 673). In some cases the medullary canal is dilated into a fusiform contour (Fig 8 674) similar to that seen in cystic tuberculous diaphysitis (see Fig 8 663). Productive diaphysitis is evidenced by subperiosteal cortical thickening which is confined to one end of the shaft in some cases and extends the entire length of

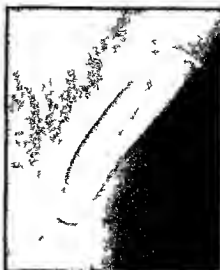
Fig 8 670—Bilateral symmetrical destructive syphilitic metaphysitis of the proximal ends of the tibiae (Wimberger's sign) in an infant 2 months of age. On the medial aspects of the tibiae (arrows) are large areas of destruction of spongy bone and its overlying cortex. In the left tibia the medial segment of the epiphyseal plate is partially destroyed.





Fig 6 671 (left) -Destructive syphilitic metaphysitis of the radius and ulna with infiltration and impact on an infant 6 weeks of age

Fig 6 672 (right) -The saw tooth or zigzag metaphyseal line



syphilitic infant 4 weeks of age. Fine spines projecting from the distal end of the shaft of the ulna into the epiphyseal cartilages produce a serrated appearance on the epiphyseal margin of the epiphyseal plate

Fig 6 673 (left) -Scattered destructive syphilitic diaphysitis in the radius and ulna. Multiple areas of destruction in the spongy bone and cortex are responsible for the extensive moth eaten rarefaction



Fig 6 674 (right) -Destructive diaphysitis in a syphilitic infant 3 months of age showing distal and thickening of the shafts

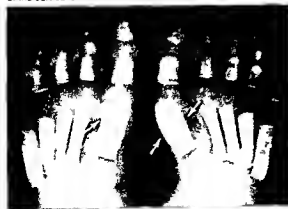




Fig 8-675—Diffuse productive syphilitic diaphysitis. A: single layer of hyperplastic cortex in a syphilitic infant 6 months of age. B: laminated subperiosteal thickening in a syphilitic infant 6 months of age.

the shaft in others. The cortical thickening may be deposited in a solid single layer or may be lamellated (Fig 8-675). Hyperplastic subperiosteal diaphysitis is simulated in prematurity, healing rickets, neonatal multiple contusions, infantile cortical hyperostosis, and in several unidentified nutritional states. Residues of cortical thickening commonly persist for months after the infection has subsided and the destructive foci have disappeared.

Fig 8-676—Hyperplastic syphilitic diaphysitis in an infant 6 months of age. The 1st metatarsal in each foot shows thickening of the corticalis.



Small bones—The metacarpals, metatarsals, and phalanges on occasion exhibit the same changes as the longer tubular bones (Fig 8-676). In the carpal and tarsal bones, however, roentgenograms rarely show syphilitic changes.

Healing syphilis—During the treatment of young infants with antisyphilitic drugs, the skeletal changes involute slowly over periods of several weeks or months in contrast with the rapid subsidence of clinical manifestations such as snuffles and cutaneous eruptions after a few days or weeks of treatment. The metaphyseal bands of increased and diminished density are buried progressively deeper into the ends of the shafts and gradually fade out. The areas of destruction become smaller and the cortical thickenings are slowly resorbed; the latter may persist for more than a year. During the first three or four weeks of treatment, however, the destructive foci often become temporarily larger and the thickened cortex becomes thicker notwithstanding the treatment and the concurrent improvement in clinical manifestations. This initial transitory exaggeration of the skeletal lesions develops in our experience during penicillin as well as during arsenical treatment.

Diagnosis—During fetal life and the first postnatal weeks, syphilitic lesions are usually confined to the metaphyses and consist of transverse bands of increased and diminished density which cannot be satisfactorily differentiated from the trophic changes found frequently in many nonsyphilitic fetuses and infants. Destructive metaphyseal lesions are most common in the period between the 1st and 8th months; they usually heal during the first six months spontaneously or following treatment. Diaphysitis is rare during the fetal and neonatal period; it usually appears after the 1st month and may persist into the second half of the 2nd year. Relapses in the skeleton are rare between the 2nd and the 6th year.

As mentioned previously, none of the syphilitic skeletal lesions is conclusively diagnostic in itself. Syphilis, however, is the only disease except pyogenic bacteremia which produces polyostotic inflammatory lesions during the early months of life. The pyogenic bacteremias can usually be identified from the clinical and bacteriologic findings without difficulty. The diagnosis of syphilis should be based on the evaluation of all of the findings—clinical, serologic, and bacteriologic. The transverse striped appearance of the metaphyses is an unreliable diagnostic sign. In the tubular bones of the hands and feet, syphilis and tuberculosis produce similar changes; these two conditions can be differentiated in the light of tuberculin skin tests and serologic tests for syphilis.

JUVENILE SYPHILIS—When the syphilitic infant survives, the bones heal completely. Postinfantile lesions probably result from reactivation of latent infections which were originally implanted in the fetal bones. During childhood, inflammatory reactions may appear in any of the tubular bones; the tibiae



Fig. 8-677—Diffuse syphilitic diaphysitis in a girl 5 years of age. The cortex of the tibia and fibula is thickened. The areas of rarefaction in the thickened layers of cortex are due to focal gummatous destruction.

however, are most frequently affected. As in all bone infections, the inflammatory changes in juvenile syphilis may be both destructive and productive. The most characteristic finding is diffuse or localized subperiosteal thickening of the cortex (Fig. 8-677). Thickening of the anterior aspect of the proximal half of

Fig. 8-678—Cortical thickening and lamellation in chronic pyogenic osteitis (proved).



the tibia is responsible for the saber shin deformity, one of the important clinical stigmas of syphilis tarda. The corticalis is usually thickened externally, but occasionally it may hypertrophy internally and encroach on the underlying medullary cavity. Gummas in the hyperplastic syphilitic cortex may cast small shadows of rarefaction. Syphilitic, tuberculous and chronic pyogenic diaphysitis resemble each other, and they usually cannot be differentiated satisfactorily from the roentgen findings alone. The lamellated or onion peel appearance of the thickened corticalis is not pathognomonic of syphilis, for it may be a feature of nonsyphilitic osteitis (Fig. 8-678).

Secondary pyogenic infection of the neighboring soft tissues, joints and the bone itself may develop into gummatous osteitis owing to the extension of pyogenic organisms to these tissues following gummatous perforation of the skin. Charcot joints are rare in juvenile syphilitics, the roentgen changes are identical with those found in the acquired syphilis of adults. There are no significant roentgen changes in the bones associated with chronic syphilitic hydrarthrosis (Clutton joints).

REFERENCES

- Ceffey, J. Changes in the growing skeleton after the administration of bismuth. *Am J Dis Child* 53:56, 1937.
- Syphilis of the skeleton in early infancy. The non specificity of many of the roentgenographic changes. *Am J Roentgenol* 42:637, 1939.
- Engsted A. et al. On the significance of growth in the roentgenological skeletal changes in early congenital syphilis. *Am J Roentgenol* 69:542, 1953.
- McLean S. Roentgenographic and pathologic aspects of congenital osseous syphilis. *Am J Dis Child* 41:130, 1931.
- Correlation of roentgenographic and pathologic aspects of congenital osseous syphilis, with particular reference to the first months of life. *Am J Dis Child* 41:363, 1931.
- Correlation of roentgenologic picture with gross and microscopic examination of pathologic material in congenital osseous syphilis. *Am J Dis Child* 41:607, 1931.
- Correlation of clinical picture with osseous lesions of congenital syphilis as shown by x rays. *Am J Dis Child* 41:887 and 1128, 1931.
- Osseous lesions of congenital syphilis. Summary and conclusions in 102 cases. *Am J Dis Child* 41:1411, 1931.
- Park, E. A., and Jackson, D. A. The irregular extensions of the end of the shaft in the x ray photograph in congenital syphilis with pertinent observations. *J Pediatr* 13:748, 1938.

MISCELLANEOUS INFECTIONS—The skeleton may be involved in a number of rare infectious diseases such as leprosy, echinococcosis, yaws, sporotrichosis, blastomycosis and actinomycosis. The diagnosis must usually be based on the clinical and microscopic findings rather than on the roentgenographic evidence. The roentgenographic examination is invaluable in demonstrating the site and extent of such lesions but there is nothing specifically characteristic in their roentgen appearance. The roentgen picture is similar to that found in chronic pyogenic osteitis and tuberculous inflammation of bone. Allen, for example, in a

study of histoplasmosis found productive and destructive changes in the bones which simulated those found in syphilitic infants

REFERENCE

Allen J H Jr Bone involvement in disseminated histoplasmosis *Am J Roentgenol* 82:250 1959

NEONATAL TRANSPLACENTAL RUBELLA SYNDROME originally thought to be limited to multiple congenital malformations of the eyes and heart is now known to include thrombocytopenic purpura, neonatal dwarfism, hypertrophy of the liver and spleen and radiographic changes in the skeleton (Fig 8-679). Among Rudolph's group of 25 patients from Houston, Tex., more than half had bone changes. Their exact nature is not known; they may be inflammatory or trophic, either singly or in combination. The recovery of po-

tent virus at birth and as late as 18 weeks after birth in combination with active thrombocytopenia and purpura and hypertrophy of the liver and spleen indicate that the lesions in the bones could represent active inflammation of bone. Metaphyseal trophic changes are, however, often found in noninfectious diseases such as hemolytic disease of the newborn (see Fig 8-791). Viral osteitis in rubella or morbilli contracted after birth is all but unknown.

Rudolph and associates concluded that the bone changes in rubella are due to metabolic and nutritional disturbances rather than direct inflammation of the bone. Reed, after microscopic study of metaphyseal rarefactions, suggested that disturbance of growth rather than inflammation is the probable cause of the metaphyseal rarefaction seen in radiographs. Massive calcification of the periphery of both cerebral hemispheres was found by Harwood-Nash and associates in an infant 9 days of age who had longitudinal striping of the metaphyses which suggested prenatal rubella (see Fig 1-240).

Graham and colleagues and others found that the radiographic changes in the skeleton were similar in prenatal rubella and prenatal cytomegalic inclusion disease. It is probable that similar skeletal changes occur in all fetal viral infections. The changes are trophic rather than inflammatory and simulate the changes in prenatal syphilitic infections (syphilis) and prenatal dystrophy such as hypophosphatase.

Fig 8-679—Radiographic changes in the bones of a newborn due to transplacental rubella infection. **A**, on the 3rd postnatal day the ilium, ischium, femur, tibia and tibia are irregularly mineralized with large and small scattered patches of rarefaction. Deep transverse terminal bands of rarefaction longitudinally streaked occupy the metaphyseal zones. The absence of cortical thickening is noteworthy. The mother had typical clinical rubella during the first trimester of the pregnancy. The infant, born after gestation of 40 weeks, had thrombocytopenic purpura. Rubella virus was isolated from throat swabs. Serologic tests for syphilis were negative for infant and mother. **B**, on the 62nd postnatal day the bones are normal radiographically. (Courtesy of Dr Aaron R. Reuser, Elmhurst, N.Y.)



REFERENCES

- Alford C A et al Virologic and serologic studies in human products of conception after maternal rubella, *New England J Med* 271:1275 1964
Graham B C et al Rubella like bone changes in congenital cytomegalic inclusion disease *Radiology* 84:39 1970
Harwood-Nash D C et al Massive calcification of the brain in a newborn infant *Am J Roentgenol* 108:528 1970
Rabinowitz J G et al Osseous changes in rubella embryopathy *Radiology* 85:494 1956
Reed G B Jr Rubella bone lesions *J Pediatr* 74:208 1969
Rudolph A J et al Transplacental rubella infections in newborn infants *JAMA* 191:834 1965
— et al Osseous manifestations of the congenital rubella syndrome *Am J Dis Child* 110:428 1965

INFANTILE CORTICAL HYPEROSTOSIS is a disorder affecting the skeleton and some of its contiguous fascias and muscles. The cause is unknown and the pathogenesis obscure. It is discussed here under skeletal infections because many patients have severe and protracted fevers and in most, erythrocyte sedimentation is increased. Another feature suggesting an infectious origin is the occasional presence of a cellular pleural or extrapleural exudate in association with contiguous costal hyperostoses. The intense early polymorphonuclear reaction in the periosteum contiguous to fascias and muscles is also highly suggestive of infection.

The presence of acute inflammatory changes in the periosteum (Eversole et al) the apparent immunity

engendered early in most cases, the demonstration by Daldorf of a virus which has an affinity for the mandible as well as other bones of hamsters infected with a filtrate from human tumors, the failure of the disease to respond to antibiotics and sulfonamides, all favor a viral causal agent for infantile cortical hyperostosis, probably transmitted through the placenta at variable phases of gestation, possibly from fibroid tumors in the maternal uterine wall. Some of the features also raise the question of an allergic reaction in the collagen tissues, especially the striking response to adrenal corticosteroids and the high sedimentation rates. The almost explosive onset in some cases suggests angioneurotic edema, an intensely pruritic disease, but pruritus does not occur in infantile cortical hyperostosis. The articular tissues apparently have not been affected.

In a study of multiple biopsy specimens from one patient, Sauterel and Rabinowicz were impressed by the hyperplasia of collagen fibers and their fibrinoid degeneration. They concluded that the disease is primarily an early extra articular collagen reaction in the cortex of the bones and in the contiguous striated muscle, fibrous tissue and blood vessels. If this hypothesis is correct, infantile cortical hyperostosis is the first example of prenatal collagen disease. There are, however, many other possible causal agents which need investigation, these should include all of the factors introduced into human living which might poison a pregnant woman and then her fetus by way of the placenta, such as increased use of tobacco by pregnant women, sedative drugs—in fact all types of drugs used during gestation—cosmetics, soaps, home-cleansing agents and furniture polishes, pesticides for the home and for pets to which pregnant women are exposed and the host of new preparations and materials continuously entering the home in the interest of better living.

The actual development of classic infantile cortical hyperostosis following vaccinia in one infant should always be remembered in a consideration of causal mechanisms and agents.

Thrombocytopenia was reported in three patients by Pickering and Cuddigan. They questioned the use of adrenocorticosteroids in the treatment of patients with high platelet counts.

We have seen one example of thickening of the mandible and swelling of the perimandibular soft tissues in a kitten which simulated infantile cortical hyperostosis closely in radiographs. If the cat is susceptible to this disease, it could provide many new avenues of investigation.

Since it was first clearly recognized and named during 1945, infantile cortical hyperostosis has been widely reported, especially in the United States, where several cases have been observed in almost every large clinic. It has occurred in all manner of circumstances—in cities and rural communities in all kinds of climates in all seasons of the year, in all racial strains, in poverty and luxury, among the pri-

mitive and the cultured. The incidence in males and females is approximately equal, but there is a striking age limitation. In my opinion, there are no valid cases in which the onset has occurred later than the 5th month of life. DeToni concluded in 1943 that the disease was congenital. Several cases have been recognized in utero. On the other hand, most patients have been well for several weeks after birth and before the onset, in some of these, the skeletons were normal radiographically before the disease appeared clinically. The average age at onset is about 9 weeks.

Morbid anatomy has been studied in biopsy specimens, there are no recorded necropsy studies on valid examples of the disease. The hyperostoses are made up of normal immature lamellar bone with no subperiosteal hemorrhage. The periosteum is usually greatly thickened and shows numerous mitotic figures with a sticky mucouslike edema.

Eversole, Holman and Robinson made the most comprehensive microscopic studies of biopsy specimens both early and late in the disease. They found that early, the lesion is confined to the periosteum, is actually intraperiosteal, consisting of numerous foci of polymorphonuclear leukocytes—an acute inflammatory reaction in a richly cellular, overactive periosteum. The swollen, mucoid periosteum loses its peripheral limiting fibrous layer and blends with the contiguous overlying fascias, muscles and tendons and disappears temporarily as an identifiable structure microscopically, blended with the overlying connective tissues and the underlying osteoid trabeculae which have extended peripherally into the periosteum. At the same time, focal resorption of some superficial layers of the underlying cortex takes place, so far as I know, this early destructive cortical lesion has not been observed radiographically. It is during this early acute phase, when the periosteum is richly cellular and has fused with neighboring structures that it resembles osteosarcoma.

In the subacute phase, the periosteum re-establishes itself as an entity, with a peripherally limiting sheet of fibrous tissue beyond the new bone which has formed from the ectopic osteoid trabeculae, so that the latter becomes truly subperiosteal. In the late or remodeling stage, the extra peripheral bone is gradually removed. In radiographs, it is clear that this process always begins from the inside, resulting in dilation of the medullary cavity as the thickened cortical wall is reamed out from the inside, and then remodeling shrinks the dilated thin walled shaft.

Often the changes in the periosteum extend directly into the contiguous fascia. The bone marrow is characteristically fibrotic, without abnormal cells. Neither bacteria nor viruses have been cultured from the affected tissues, nor have serologic tests disclosed reactions to infections. Sherman and Hellyer found obliterating intimal proliferation in the small arteries in the region of the bone and fascial lesions. Some believe that these arterial proliferations are the primary changes which lead to hypoxia in the regional

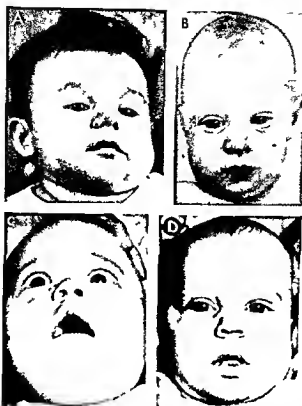


Fig 8-680—Facies in infantile cortical hyperostosis. In all cases the changes have appeared before the 5th month of life. **A** unilateral swelling of the left cheek and left side of the jaw in an infant 12 weeks of age—five weeks after its first appearance. **B** unilateral swelling of the right cheek and right side of the jaw in an infant 15 weeks of age—eight weeks after first appearance. **C**

b lateral swellings of cheeks and jaw in an infant 6 months of age—five weeks after their first appearance. **D** bilateral swellings of cheeks and jaw in an infant 12 weeks of age—four days after their first appearance. Hyperostosis of the mandible was not visible in films made at this time but became visible in later films. The cervical lymph nodes were not enlarged.

soft tissues and bone which in turn react to hypoxia by hyperostosis and soft tissue swelling.

The occurrence of the disease in siblings, in twins, and in cousins has raised the question of familial and possibly genetic transmission. The immunity of all infants older than 5 months would in itself prevent concurrent familial infections. In twins, triplets, or quadruplets, Veller and Laur reported the disease in an infant 9 weeks of age whose father had productive perostitis of unknown origin when he was 4 weeks of age in 1929. This father was the prime case of infantile cortical hyperostosis described by Roske in 1930. Tampas and associates observed this disease in ten members of two generations of the same family during a period of 14 years. They also demonstrated that cortical thickenings in the skeleton may persist or recur into adult life, as in one of their patients who presented pronounced thickenings at age 25. Holman and Gerrard claimed that several members of the family of one of their infant patients had also had the disease—one of two siblings, father and mother, three maternal aunts, and the history

suggested that four siblings of the grandparents had been affected as well as one of their first cousins.

There are but three manifestations common to all patients: hyperirritability, swellings of the soft tissues, and cortical thickenings of the underlying bones. The soft tissue swellings appear suddenly at the onset and present a painful, wooden hardness during the active phases of the disease. They are always deeply situated and never extend into the subcutaneous fat. Early the swellings may be exquisitely tender but are never overly warm or discolored (Figs 8-680 and 8-681). In Figure 8-682 the massive deep swelling in the muscular masses in the left shank is seen. Such swellings represent the extension of the primary intraperiosteal reaction into the overlying connective tissues. They appear clinically before the hyperostoses become visible roentgenographically; they subside and lose their tenderness long before the hyperostoses become invisible roentgenographically. These swellings involute slowly without suppuration; sometimes they recur suddenly in their original sites or in new sites either during or after the subsidence



Fig. 8-681 — Swelling of the forearm and recurrent swelling of the right side of the face in an infant 5 months of age. The facial swelling first appeared at age 2 months; the forearm became swollen at age 3 months. The mandible and both bones in the forearm showed massive hyperostoses at the time this photograph was made (see Fig. 8-689). All cervical axillary and epitrochlear lymph nodes were normal.

of the swellings which appeared at the onset of the disease. The uneven protracted clinical course of the disease with unpredictable remissions and relapses is one of its most characteristic features and one which makes the evaluation of therapeutic agents uncertain.

Among 24 patients, Minton and Elliot found edema and swellings around the orbits in 8. One patient had unilateral proptosis. The authors estimated that periorbital swellings around the orbits were evident before the mandibular swellings in 6 patients.

Fever has developed in all patients with the exception of a few younger infants; in two of our patients the temperature was carefully measured in all stages of the disease and fever was never found. Other clinical features, present in some patients but lacking in others, have been pallor, painful pseudoparalysis and rhesus. The most constant positive laboratory findings are increased sedimentation rate of erythrocytes and increased phosphatase activity of the blood serum, during active phases of the swellings and fever; these two laboratory findings are usually present. Hemoglobin and the number of red blood cells were reduced in more than half of our patients. Other laboratory studies have given uniformly normal results. The results of serologic tests for both bacterial and viral infections have been consistently negative. All attempts to culture bacteria from the tissues and fluids of these patients have failed. A complement fixation test for mumps was performed in one case and gave a normal reaction. Campbell and Turner found pronounced renal aminoaciduria in one patient during the acute phase; it subsided promptly during treatment.

Fig. 8-682 — Soft tissue swelling in infantile cortical hyperostosis in an infant 4 months of age. The deep muscular mass in the left shank is increased in volume and its edges are shaggy, which suggests the extension of fluid or cellular proliferation into the interlobular septums of the subcutaneous fat. Although the cartilaginous patella does not contain an ossification center, it is enlarged and its edges are shaggy.



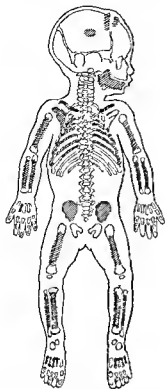


Fig 8-683—Schematic drawing of distribution of the skeletal lesions in infantile cortical hyperostosis. The sites of hyperostosis are shaded. The mandible, clavicles and ulnas are affected most frequently. Hyperostosis in the vertebrae, round bones of the wrists and ankles and phalanges have not been observed. Pleurisy has been found only in younger infants who had associated costal thickening.

Fig 8-684—Ipsilateral hyperostosis of the right scapula and eventration of the right side of the diaphragm in a patient 9 weeks of age who had classic infantile cortical hyperostosis. The face and jaws had been swollen for 10 days and movements at the right shoulder limited for three weeks. We have seen ipsilateral scapular sclerosis and eventration of the diaphragm in three patients; in one the eventration was still marked at 5 years of age; four years after all of the bone lesions had disappeared.

Cortical hyperostoses have been demonstrated in all of the tubular bones of the skeleton except the phalanges and vertebral bodies. Of the flat bones the mandibles, scapulas, ilia, parietals and frontals have all shown sclerosis and thickenings (Fig 8-683). Scapular lesions have usually been unilateral and have always appeared during the first half of the 1st year (see Fig 2-58). In a few instances the scapular hypertrophy and sclerosis of infantile cortical hyperostosis have been mistaken for malignant neoplasm by those unfamiliar with infantile cortical hyperostosis and radical surgical removal of the entire shoulder girdle advised. In the interesting example reported by Clement and Williams, a hard swelling on the right side of the nose was the first clinical sign and the right nasal bone was swollen and sclerotic in radiographs. Exophthalmos developed early in one patient observed at the University of Michigan. Ipsilateral eventration of the diaphragm developed in two of our patients who had scapular hyperostoses (Fig 8-684). In only a single patient have we seen bilateral massive hyperostosis of the ilia (Fig 8-685); in this case the pubic and ischial bones were not affected. Of all of the bones the mandibles, clavicles and ulnas have been involved the most frequently. The mandibular lesions frequently fluctuate widely in extent and activity and roentgenographically have been mistaken for purulent osteitis and surgical drainage advised (Fig 8-686). Clavicular lesions may be unilateral or bilateral. The ulnas are the most commonly affected of all the bones in the extremities and are often extensively sclerosed when the companion radii are normal (Fig 8-687).

Cortical hyperostoses are usually most prominent in the lateral arcs of the ribs (Fig 8-688). In the lower extremities distribution is asymmetrical and in the arms and legs the larger hyperostoses often present conspicuous marginal irregularities (Figs 8-689 and



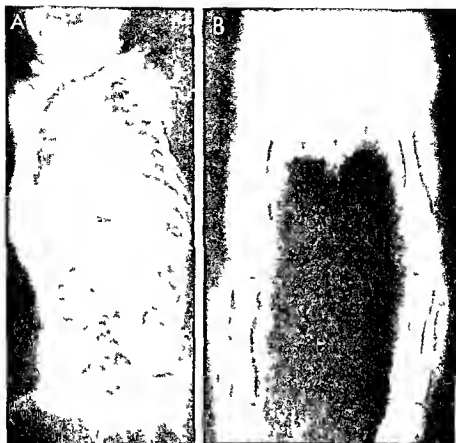


Fig 6585 — B lateral massive thickening and sclerosis of the ilia in an infant 2 months of age who had unusually severe skeletal involvement. All of the ribs are affected save the 1st left, and the right ribs are more affected than the left. A hyperostoses in

the mandible, both clavicles and scapulae, ribs, and ilia. The vertebral bodies and the pubic and ischial bones are conspicuously spared. B hyperostoses in both ilia and all bones in the legs.

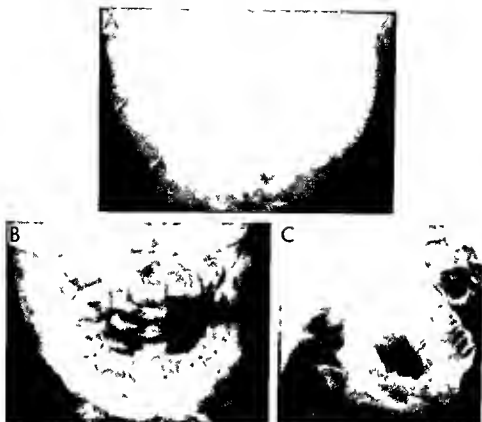


Fig. 866—Mandibular hyperostoses. Massive cortical thickenings of the mandible of an infant 6 months of age whose facial swellings first appeared during the 4th week of life. **A**, mouth

closed. **B**, mouth open. **C**, massive mandibular hyperostosis in an infant 7 weeks of age whose facial swelling first appeared during the 4th week of life.

Fig. 867—Massive cortical hyperostoses in the ulna and humerus. The ulna is often conspicuously involved when the radius is unaffected. As in this patient, we have never seen the con-

verse—radial hyperostosis with normal ulna. In this patient as in others, the metacarpals and phalanges were not thickened. Axillary and epitrochlear lymph nodes were normal.



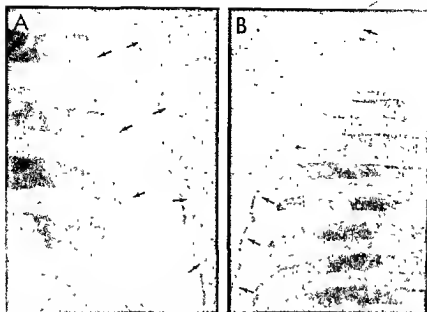


Fig. 8-688.—Costal hyperostoses. **A**, early bilateral multiple thickenings of the ribs with underlying pleural exudate in an infant 14 weeks of age. **B**, older multiple costal hyperostoses in an

infant 5 months of age. The lamellations are a sign that the hyperostoses are old and beginning to involute.

Fig. 8-689.—Massive cortical hyperostoses in tubular bones of the extremities. **A**, in the legs of an infant 14 weeks of age. The arrows point to thick swellings in the soft tissues of the thigh. **B**, in the forearm of an infant 5 months of age (shown in Fig. 8-

681). In all of these hyperostotic bones there is striking absence of the metaphyseal changes almost invariably present in infantile scurvy and syphilis. The coarse and deep marginal irregularities in many of the hyperostoses are noteworthy.





Fig. 8 690 (left) — Deep marginal irregularities in thick femoral hyperostoses in an infant 4 months of age in whom facial swelling and mandibular thickening first appeared in the 2nd month of life. Arrows point to small marginal hyperostoses in the ilium (Courtesy of Dr. J. B. Elderback, Portland, Ore.)

Fig. 8 691 (right) — Parietal hyperostosis in an infant 4 months of age. The other parietal, mandible, clavicles and several ribs showed hyperostoses (Courtesy of Dr. R. K. Whipple, Providence, R. I.)

8 690) Thickenings in the calvaria have been identified in several patients (Fig. 8 691), and it seems likely that many inconspicuous lesions in the calvaria have been overlooked. Cortical thickenings on the margins of the anterior fontanel may simulate bulging of the fontanel owing to increased intracranial pressure. The residual thickenings of earlier unrecognized cortical hyperostoses may be the explanation of some of the thickenings at the anterior fontanel which are seen occasionally in asymptomatic children. In one patient 3 months of age, massive thickenings and sclerosis developed in the ilia (Fig. 8 692).

So far as I know, hyperostoses in the round bones, phalanges and the vertebral column have not been described. In the interests of accurate differential diagnosis it should be remembered that, in contradistinction to rickets and scurvy, the lesions of infantile cortical hyperostoses are confined to the shafts, and the metaphyses and epiphyseal ossification centers are normal roentgenographically. Clinical and roentgen recovery is usually complete after several weeks or months; hyperostoses are usually invisible within 12 months after the swellings in the soft tissues and the fever have subsided. Sometimes the hyperostoses disappear within three months. During healing the cortical thickenings may become lamellated; we have never seen lamellation early in the disease.

The serial changes in the formation of the hyperostoses are quite different from those of scurvy, osteomyelitis and trauma. In the last named lesions, a thin

shell of bone forms first over the soft tissue swelling, separated from the shaft by a deep strip of water density. In infantile cortical hyperostosis, new bone formation begins in the soft tissue swelling directly contiguous to the original cortex, becomes progressively more dense and then is capped later by a dense shell of limiting bone. Eversole, Holman and Robinson found this to be true in microscopic sections of biopsy specimens.

It is possible, even probable, that most of the mild cases of infantile cortical hyperostosis are overlooked clinically and are never examined radiographically. After a short course of milder fever, these patients recover without a satisfactory diagnosis. Slight swellings of the mandible are exceedingly difficult to palpate in the deep subcutaneous fat of the infantile jaw, as are deep slight swellings of the ribs and long bones in the extremities. Many of the unexplained cortical hyperostoses encountered radiographically in well infants may be residuals of earlier and mild unrecognized infantile cortical hyperostosis. Some of these are also, of course, due to unrecognized trauma.

The distribution of the bone lesions is one of the most diagnostic features of infantile cortical hyperostosis. If the disease were ever confined to one bone, other than the mandible, it would be impossible to identify it with certainty. In our experience, cortical hyperostosis of this type in one bone is usually due to trauma, except in the mandible. There is great need for a specific cutaneous, serologic or chemical test.

I have seen one example of bilateral focal destruction of the frontal squamosa (Fig. 8 693).

Chronic infantile cortical hyperostosis — Occasionally active disease may persist and recur inter-

Fig. 8 692 — Massive marginal hyperostoses on the lateral edges of the iliac wings. The lesions stop short of the faces of the acetabular cavities and crests of the ilia. The patient, 6 weeks of age, had classic signs of the disease with thick hyperostoses in the mandible and several long bones (Courtesy of Dr. W. P. Yarbrough, Greene, Miss.)

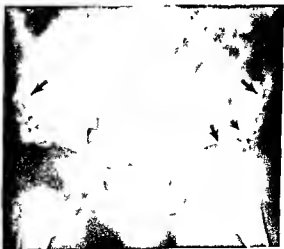




Fig 8-693 — Extensive bilateral multiple destruction in both sides of the frontal squamosa and thickening and sclerosis of the horizontal plates of the frontal, upper maxilla and mandible of an

infant 3 months of age. A, frontal and B, lateral projections (Courtesy of Dr. Virgil Condon, Salt Lake City, Utah)



Fig 8-694 — Residual dilatation of the medullary cavity with thinning of the cortical walls in the sites of earlier thickening due to hyperostosis 18 months after onset of the disease in a black girl 15 months of age. A, the affected right leg. B, the left leg, which was never affected. The right femur shows the same dilatation as in the tibia and fibula, but its hyperostoses are only partially resorbed. At 32 months these abnormal bones had reshaped themselves and their cortexes had thickened to normal proportions.



Fig 8-695—Multiple costal cortical hyperostoses with resudual bony bridges between the 5th and 6th and 6th and 7th left ribs. **A**, at 4½ months (four weeks after onset during the active phase with multiple bilateral hyperostoses in the ribs and a long fluid strip of water density along the inner edges of the ribs which

suggests either intrapleural or extrapleural fluid. **B**, at 9 months after subsidence of all general and local manifestations, there is still more dilatation of the ribs and bridges of bone have formed (arrows).

persistently for years with crippling deformities in the extremities and markedly delayed muscular and motor development. In long standing cases the hyperostoses appear to be reamed out from the inside producing a thinwalled bone with a large medullary cavity (Fig 8-694). These swollen delicate bones then slowly reshape themselves into normal contours with gradual concomitant thickenings in the cortical walls. When excessively large hyperostoses affect

parallel neighboring bones such as the ribs or the radius and ulna, pressure may kill the contiguous periosteums with local fusion of the cortical walls which act as interosseous bridges (Fig 8-695). When the radius and ulna are brought under such stresses the radial head may be dislocated with serious loss of function (Fig 8-696). Scott reported such a case of radioulnar synostosis with dislocation of the radial heads. Ventral bowing of the tibiae may persist well

Fig 8-696—Residual bony bridges between each radius and ulna. **A**, massive cortical thickenings of the radiuses and ulnas at 4½ months of age. Pressure from the external thickenings has forced the radial heads latered out of the elbows. **B**, at 12½ months (nine months after onset) all affected bones are still greatly swollen, owing largely to dilatation of the medullary cavities, although there are still residues of the earlier cortical thick-

ening. The radial heads are still dislocated and the radial shafts are now anchored in this ectopic position by solid bony bridges between them and the ulnar shafts—a single bridge on the right and three on the left. At 32 months these bridges were still intact although they had diminished slightly in caliber. It is possible that these bony bridges represent ossification of the interosseous membrane.



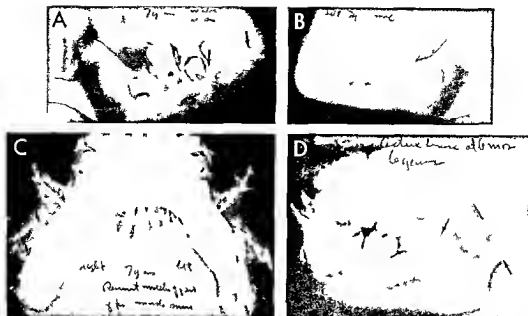


Fig 8-697—Late residual changes in the mandible in chronic recurrent infantile cortical hyperostosis. A and C residual thickening and sclerosis of the right side of the mandible in a patient 7 years of age who had the disease diagnosed initially at 3 months of age. Arrows point to the mandibular thickening which came and went at intervals of four to six months with recurrences of

fever, pain and swelling on the right side of the face. The rest of the skeleton had no recurrences. B, normal left side of the mandible. D, late alveolar projection of the mandible of a boy 6 years of age who last had active disease at age 6 months. The usually sharp sclerotic alveolar processes sclerosed and swollen into a blunt hump.

into the 4th year from early infantile hyperostosis of the ventral cortical walls of the ribs.

In one case the disease persisted recurrently in the mandible and the soft tissues of the jaw from early infancy into the 7th year of life. During the 3rd month the mandible, both clavicles and several ribs became thickened. The clavicular and costal lesions cleared after a few weeks but swellings in the jaw recurred at irregular intervals with persistent sclerosis and thickening of the mandible which was still marked when the patient was last seen at 7 years (Fig 8-697). In the puzzling case of Altman and Pomerance the radiographic changes suggested both infantile cortical hyperostosis and Engelmann's disease but clinical evidence and the findings at biopsy did not support either of these diagnoses.

Treatment did not appear to be very important in the early mild cases. When however chronic and fatal cases began to appear it became obvious that early effective treatment was highly desirable. Fortunately corticosteroids became available at about the same time these agents have proved remarkably effective in all forms and all stages of the disease. Often the clinical signs disappear and the sedimentation rate of the erythrocytes falls to normal after two or three days of treatment with the steroids. We treat all patients in a daily dosage of about 100 mg of cortisone for a minimum of 10–14 days then taper the dose to prevent rebound reactions which have been

severe in some cases in which cortisone has been stopped suddenly.

Bose reported the first cases from India in 1962.

REFERENCES

- Alberti C P et al: De Toni Caffey Silverman syndrome in the classification of the periosopathies of childhood. *Ann Radiol Diagnost* 35:443, 1962.
- Altman H S and Pomerance H H: Chronic polyostotic periostitis of unknown etiology. *Pediatrics* 28:719, 1961.
- Barba W P II and Frenks D J: The familial occurrence of infantile cortical hyperostosis in utero. *J Pediatr* 42:141, 1953.
- Bennett H S and Nelson T R: Prenatal cortical hyperostosis. *Brit J Radiol* 26:47, 1953.
- Bose S K: Infantile cortical hyperostosis. Report of two cases. *J Indian Ped Soc* 1:99, 1962.
- Caffey J: Infantile cortical hyperostosis. *J Pediatr* 29:541, 1946.
- On some late skeletal changes in chronic infantile cortical hyperostosis. *Radiology* 59:651, 1952.
- and Silverman W A: Infantile cortical hyperostosis. *Am J Roentgenol* 54:1, 1945.
- Infantile cortical hyperostosis. A review of the clinical and radiographic features. *Proc Roy Soc Med* 50:347, 1957.
- Caffey's enigmas. *JAMA* 176:495, 1961 (editorial).
- Campbell D J and Turner E: Aminoaciduria in a case of infantile cortical hyperostosis (Caffey's disease). *Am J Clin Path* 38:97, 1962.
- Clement A R and Williams J H: The familial occurrence of infantile cortical hyperostosis. *Radiology* 80:409, 1963.
- Dalldorf G: Viruses and human cancer. *Bull. New York Acad. Med.* 36:795, 1960.

- Eik, S. Infantile cortical hyperostosis. Development of a case in utero. *Acta paediat* 44 (supp 103) 135 1955
- Eversole, S. L., Jr., Holman, G. H., and Robinson, R. A. Hitherto undescribed characteristics of the pathology of infantile cortical hyperostosis (Caffey's disease). *Bull Johns Hopkins Hosp* 101 80, 1957
- Gerrard, J. W., et al. Familial infantile cortical hyperostosis. *J Pediatr* 59 543 1961
- Holman, G. H. Infantile cortical hyperostosis. A review. *Quart Rev Pediatr* 17 24 1962
- Meadows, J. L., and Weens, H. S. Infantile cortical hyperostosis. *Acta radiol* 42 43, 1954 (6 cases, all in blacks)
- Minton, L. R., and Elliot, J. H. Ocular manifestations of infantile cortical hyperostosis. *Am J Ophthalm* 64 902, 1967
- Pickering, D., and Cuddigan, B. Infantile cortical hyperostosis associated with thrombocythemia. *Lancet* 2 464, 1969
- Roske, G. Eine eigenartige Knochenkrankung im Säuglingsalter. *Monatsschr Kinderh* 47 385, 1930
- Sauterel, L. Infantile Cortical Hyperostosis, a New Collagen Disease (?). Thesis, Faculty of Medicine, University of Lausanne Geneva 1962
- , and Rabinowicz, T. A new etiological view of infantile cortical hyperostosis. *Ann. radiol* 4 211, 1961
- Scott, E. P. Infantile cortical hyperostosis. Report of an unusual complication. *J Pediatr* 62 782 1963
- Sidbury, J. B., Jr., and Sidbury, J. B. Infantile cortical hyperostosis. An inquiry into the etiology and pathogenesis. *New England J Med* 250 309, 1954
- Smyth, F. S., et al. Periosteal reaction fever and irritability in young infants. A new syndrome? *Am J Dis Child* 71 333, 1946
- Tampas, J. P., et al. Infantile cortical hyperostosis. *JAMA* 175 491, 1961
- Van Buskirk, F. W., et al. Infantile cortical hyperostosis. An enquiry into its familial aspects. *Am. J Roentgenol* 85 613, 1961
- Voller, K., and Laur, A. Etiology of infantile cortical hyperostosis (Caffey's syndrome). *Fortschr Geb Röntgenstrahlen* 79 446, 1953
- Wilson, A. K. Infantile cortical hyperostosis. A review of the literature and report of a case without mandibular involvement. *Clin Orthop* 62 209 1969

Idiopathic cortical hyperostosis (Goldbloom) was observed in two unrelated children, 10 and 14 years of age, who had fever, pain and tenderness in bones and stopped walking. The serum gamma globulin content in one patient was increased with an increase in the IgG fraction. Plasma cells were overabundant in the bone marrow. The cortical walls were thickened externally in the long tubular bones and in the mandible. These radiographic changes subsided gradually over several months after the fever subsided. The mandibular involvement and the nature of the individual lesions raised the question of infantile type of cortical hyperostosis in older children.

REFERENCE

- Goldbloom, R. B., et al. Idiopathic periosteal hyperostosis with dysproteinemia. A new clinical entity. *New England J Med* 274 873 1966

Cortical hyperostosis—external thickening of the cortical walls—was associated with hyperphosphatemia in two children described by Melhelm and associates. In a boy 9 years of age, Burrows found cortical thickenings associated with infectious mononucleosis.

REFERENCES

- Burrows, F. G. Transient periosteal reaction in an illness diagnosed as infectious mononucleosis. *Radiology* 98 291 1971
- Melhelm, R. E. et al. Cortical hyperostosis with hyperphosphatemia. A new syndrome (?). *Pediatrics* 77 986, 1970

AVITAMINOSES

RICKETS—This disease of infancy and childhood is characterized by the failure of calcification of growing cartilage and bone. The principal causes are deprivation of the short ultraviolet radiations of sunlight and deficiency of vitamin D in the food. Unknown constitutional factors in different individuals also play an important causal role in the individual susceptibility to rickets and in the vitamin D requirements for its cure. Prematurity is an important predisposing factor. In a small proportion of cases of rickets the primary defect is in the patient's metabolism rather than in his environment. Cases of endogenous rickets of this type are usually associated with long standing renal failure, chronic acidosis and more rarely hepatic and pancreatic disease. Contributory causal factors include the quantities and ratios of calcium and phosphorus in the diet, the velocity of growth of the individual and the ultraviolet ray filtering power of the atmosphere. Failure of calcification and the demineralization of the growing skeleton are due to an insufficient supply of the inorganic compo-

Fig 4-391—Mild early rickets in an infant 3 months of age. The provisional zones of calcification at the distal ends of the ulna and radius are irregularly mineralized and frayed. The distal end of the ulna is cupped, but the distal end of the radius is straight. Slight spreading of the distal ends of both bones is evident. The shafts are diffusely osteoporotic and the texture of the shafts is coarse. There are no visible changes in the proximal end of either bone, where growth is slower than at the distal end.



nents of bone in the blood and body fluids the organic phosphate concentration of the serum is reduced to less than 35 mg/100 cc of serum but the blood calcium is unaffected except in cases of rachitic tetany. The main action of vitamin D is to promote absorption of calcium from the gut and in severe vitamin D deficiency rickets calcium absorption from the intestine is so reduced that there is little or no calcium in the urine.

Roentgen findings—These are the shadow images of the gross structural changes. In its earliest stage rickets is not detectable roentgenographically. histologic changes are evident in the bones and chemical changes develop in the blood serum several weeks prior to the appearance of conclusive roentgen changes. The distal ends of the ulna and radius are the optimal sites for the demonstration of the earliest lesions. significant changes are often visible in the ulna when the radius appears to be normal. The principal diagnostic features are the rarefaction and irregular fraying of the provisional zone of calcification (Fig 8 698). The normally sharply defined provisional zone of calcification fades out undistinctly into the soft tissue density of the adjacent epiphyseal cartilage. The affected metaphyses may be concave and slightly widened. Cupping of the distal end of the ulna in younger infants is not necessarily abnormal for it has been observed in some nonrachitic infants during the first months of life. Significant changes in the shaft are often absent when changes are first detected in the metaphysis. rarefaction of the shaft becomes evident a few weeks later. The early metaphyseal changes offer great difficulty for conclusive evaluation; they are best interpreted in retrospect from serial films.

In more advanced stages the roentgen findings are pathognomonic and the diagnosis can be made immediately on inspection of the films. The diagnostic signs are similar to those in the early stage; they are merely more marked. The shadow of the provisional zone of calcification is absent and the terminal segment of the shaft—the rachitic metaphysis—is partially or totally invisible (Fig 8 699). this is seen only in rickets. Owing to the nonvisualization of the uncalsified rachitic metaphyses at each end of the shaft the visible calcified portion of the shaft is shortened longitudinally for the same reason the space between the visible end of the shaft and its neighboring epiphyseal ossification center is deepened. Thus abnormally deep radiolucent shadow between the epiphyseal ossification center and the end of the shaft is cast by the intermediate rachitic zone and is pathognomonic of rickets. The end of the shaft is smooth in some cases and irregularly frayed in others. When the fraying is long and longitudinally parallel the pattern resembles the bristles in a brush.

The end of the shaft may be straight or hollowed out into a concave cuplike central depression. Cupping is common in both ends of the fibula and the distal ends of the ulna and tibia. the distal end of the

radius is far less frequently affected than the distal end of the ulna. These concavities however are never found in the bones at the elbows and rarely in the bones at the knees. Cupping and spreading of the ends of the shafts are regularly absent in some of the severest cases of rickets—the atrophic type (Fig 8 700) in which poor muscular power permits little activity of the extremities. In well nourished rachitic infants with relatively good muscular power who crawl and walk cupping and flaring of the ends of the shaft are common features. In all cases cupping and spreading become more conspicuous roentgenographically when the disease is partially healed (Fig 8 701).

The changes in the shaft develop concurrently with those in the metaphyses. The entire shaft shows a diffuse rarefaction caused by the loss of lime. The cortex is thin and its texture coarsened (Fig 8 700). The mesh of the spongiosa coarsens owing to the complete decalcification and disappearance of the finer secondary trabeculae when the cortex is markedly thinned the underlying spongiosa is more conspicuous because the heavy superimposed shadow of the normal cortex has been partially removed. Green stick fractures of the cortex are not uncommon even in moderately severe cases. Sometimes sharply defined radiolucent transverse bands or *Umbauzonen* are found in the shafts (Fig 8 702) these are more common in juvenile rickets. Their anatomic structure has not been adequately studied.

The epiphyseal ossification centers and the carpal and tarsal bones show roentgen changes similar to those in the tubular bones. The margins of these rounded bones which are analogous to the provisional zones of calcification of the tubular bones disappear and the spongiosa becomes osteoporotic. In severe cases the ossification centers may become invisible during the active stage of rickets and reappear when they are recalcified during healing.

The first evidence of healing is the reappearance of the provisional zone of calcification (see Fig 8 699). The recalcified provisional zone of calcification casts a transverse linear shadow of increased density in the rachitic metaphysis beyond the visible end of the shaft at a level the epiphyseal plate would have reached had there been no rickets. The radiolucent rachitic metaphysis interposed between the newly calcified provisional zone of calcification and the visible end of the shaft is still not mineralized and casts a shadow of soft tissue density. As healing continues the new provisional zone of calcification thickens into a transverse band at the same time the metaphyseal spongiosa is gradually recalcified and fills in the previously radiolucent intermediate rachitic zone and the shadow of the metaphyseal spongiosa fuses with that of the provisional zone of calcification. This recalcification of the terminal segments of the shaft produces a false appearance of rapid increase in length of the shaft. Analogous changes develop concurrently in the epiphyseal ossification centers a

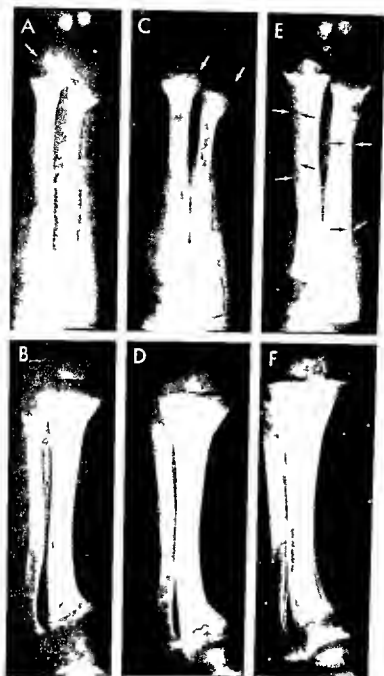


Fig 8 699 Descri pt on on fac ng page



Fig 8 700—Severe atrophic or hypoplastic rickets in a black infant 16 months of age. Limbs of necropsy specimens of femur and tibia. The ends of the shafts are not deeply frayed and there is no cupping and spreading. Absence of these features is characteristic of atrophic rickets. Coarsening or trabeculation of the entire shafts is clearly demonstrated. It is due principally to loosening of the lamellar structure in the cortices rather than to coarsening of the spongiosa. This coarse texture is marked in the middle third of the shafts where there is little or no spongiosa.

marginal ring shadow of increased density appears which gradually thickens and fuses with the central mass owing to a gradual increase in density of the submarginal zone. In the shaft the spongy mesh becomes more sharply defined and more delicate. Healing of the cortices is usually slower and less conspicuous roentgenographically. When, however, thick layers of osteoid have been deposited under the

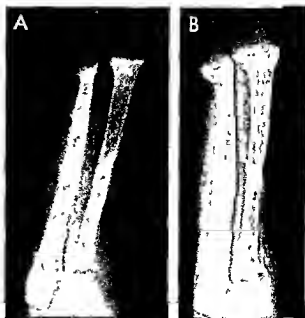


Fig 8 701—Exaggeration of cupping and spreading during the healing stage of rickets. A, typical atrophic rickets prior to treatment and healing. B, 16 days after inception of treatment the partially recalcified healing metaphyses show marked increase in cupping and spreading. The length of the shafts also appears to be increased because the previously invisible metaphyseal caps on the ends of the shafts have now become visible.

periosteum in the peripheral layers of the compacta, recalcification of this osteoid discloses a diffuse cortical envelope which may be of uniform density or lamellated (Fig 8 699, E). The cortical changes in healing rickets often simulate those of syphilitic productive diaphysitis (osteopenostitis).

Occasionally the direction of recalcification of the rachitic metaphysis is reversed, it begins on the shaftward margin of the metaphysis and progresses from the middle end of the shaft toward the epiphyseal cartilage, the provisional zone of calcification thus is calcified last and after the metaphyseal elements have become opaque (Fig 8 703). In other rare

Fig 8 699—Advanced hyperplastic rickets showing active and healing stages in the forearms (A, C and E) and legs (B, D and F). A, active stage before treatment. The shafts are diffusely osteoporotic, coarse in texture, and greenstick fractures are visible in the middle thirds. Distal ends of both bones are spread frayed and cupped. Provisional zones of calcification are invisible. The radial epiphyseal center is a small shadow barely visible (arrow). The zone between the ossification center and the visible end of the shaft is deepened. The shafts appear to be short because the terminal rachitic metaphyses are invisible.

B, active stage in the tibia and fibula. The changes are analogous to those in the radius and ulna. The middle third of the fibula exhibits a greenstick fracture. Both ends of the fibula are cupped. The deep intermediate rachitic zone between the proximal end of the tibia and its epiphyseal center is well shown. Deformity and change in inclination of the distal tibial metaphysis are evident and growth is proceeding in a plane oblique to the long axis of the shaft.

C and D, healing after 34 days of treatment. C, in the forearm the provisional zones of calcification are partially recalcified and located well beyond the ends of the shafts where they appear as transverse lines of increased density. D, in the tibia and fibula findings are similar to those in C. Apparent increase in length of the shafts in comparison with B is due to recalcification of the rachitic metaphyses in each end of the bones which were invisible during the active phase. Increased spreading of the ends of the shafts is due to the same phenomenon.

E and F, healing after 63 and 94 days of treatment respectively. E, in the forearm previously rachitic metaphyses are completely recalcified and radiolucent intermediate rachitic zones have disappeared. Ossification centers are sharply defined and in normally close proximity to the ends of the shafts. Recalcification of the subperiosteal osteoid has produced a thick opaque envelope of cortex which surrounds the shafts (arrows). F, the tibia and fibula exhibit changes similar to those in E except that the subperiosteal cloaking is not so conspicuous.



Fig 8-702—Symmetrical transverse radolucent bands (Umbauzone) in ulnar shafts

cases scattered foci of calcification appear at different levels in the rachitic metaphysis and healing is effected by the enlargement and coalescence of these foci.

Rachitic sequelae—Complete healing and restoration of normal structure are the rule in rickets even when severe changes are present during the active stage. Distortion and sclerosis of the spongiosa in the

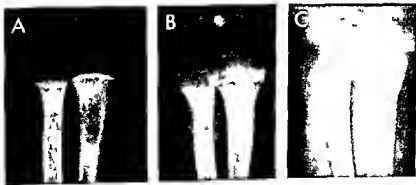
levels affected during the active disease are common after healing and usually remain visible in the same level of the shaft for years (Fig 8-704). Central rarefaction of the ossification centers also persists in many cases. Cortical thickening of the segment of the bone involved during the active stage may remain evident for years after healing is completed particularly on the concave surfaces of curvature deformities. Most of the bowing and angulation deformities result from displacement of the epiphyseal cartilage during the active stage which gives rise to a change in its inclination and a change in the direction of its growth. Growth proceeds in the direction of the deformity instead of in the direction of the longitudinal axis of the shaft (Fig 8-705). Angulation deformities may also be secondary to pathologic fractures early during the active stage. The commonest deformities in the lower extremities are knock knee, bowleg and saber shin.

Juvenile rickets—The roentgen findings are similar to those in the infantile type. Roentgenographically one cannot differentiate the various types of juvenile rickets, refractory vitamin D rickets and endogenous rickets present the same roentgen picture (Figs 8-706 and 8-707).

The different types of protracted infantile and juvenile rickets which are not due to deficiency of vitamin D, can best be classified according to the type of renal dysfunction which causes them. Dent established two main types. The renal glomerular type is associated with impaired glomerular filtration and found in patients with chronic glomerular nephritis, congenital hypoplasia of the kidneys or congenital cystic kidneys or gradual destruction of renal parenchyma behind congenital obstructive lesions in the lower urinary tract. In such cases there is proteinuria with retention of urea, phosphate and creatine. In tubular rickets—in contrast the glomerular filtrate is normal but there is a failure of resorption of one or more components of this filtrate by the renal tubules.

Fig 8-703—Healing of rachitic metaphyses. The recalcification appears to spread from the end of the shaft toward the epiphyseal plate instead of from the epiphyseal plate toward the end of the shaft. A: Before treatment. B: 13th day of healing. C: 34th day of healing. The apparent reversal of the direction of healing

is actually due to cupping of the epiphyseal plate. In this case deposit on of lime in the provisional zone of calcification on the floor of the cup near the end of the shaft is responsible for the tactious appearance of diaphyseal healing.



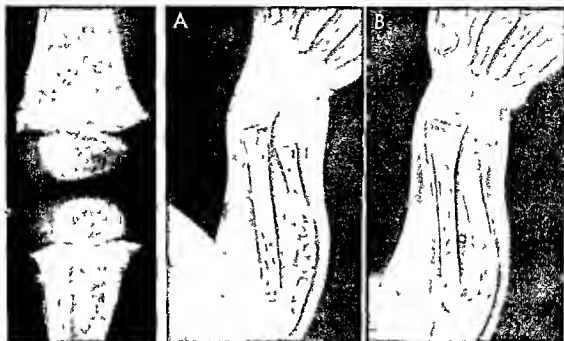


Fig 8 704 (left) — Chemoirring of the ends of rachitic shafts due to recalcification of distorted and deformed spongiosa for long healing

Fig 8 705 (right) — Pathogenesis of curvature deformities of the long bones in rickets: drawings of roentgenograms. A, active rickets in a patient 20 months of age. The distal halves of the shafts appear to be straight. The middle third of the ulna is

bowing externally in the site of the multiple greenstick fractures. B, healing stage 60 days after A. Angulation deformities are now evident at the junction of the calcifying metaphyses and the shaft. Before calcification on the angulations were present but were invisible. The bowing deformity in the middle third of the ulna persists.

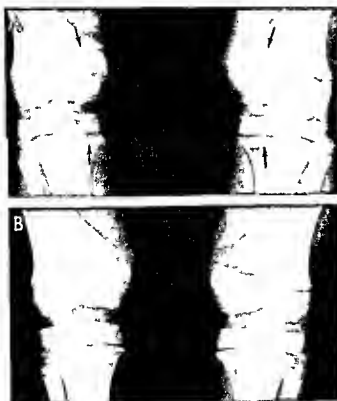


Fig 8 706 — Active refractory rickets in a girl 9 1/4 years of age who had bilateral severe symmetrical knock knees. The serum phosphate value was diminished, serum calcium normal and serum phosphatase activity increased. All metaphyses showed long-standing rachitic changes, most marked in the femurs and tibias. It is noteworthy that only the medial segments of these metaphyses are affected (A). B, the same knees nine months after massive treatment with vitamin D: healing is complete, serum phosphate and serum phosphatase activity were normal at this time. Numerous transverse lines deform the spongiosa in the terminal segments of all shafts.

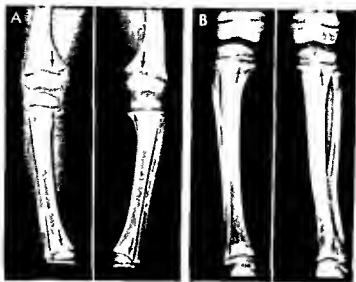


Fig. 8-707—Shift of a segment of active rickets with shift in the longitudinal axis of weight bearing in the tibia. A, at 4 years and 9 months, bilateral bowed legs with active rickets confined to the medial segments of the femurs and tibias at the knees. B, at 6 years and 7 months following corrective osteotomy to the left tibia, the active rickets have shifted to the lateral segment of the tibial metaphysis because the longitudinal axis of weight bearing has shifted to the lateral segment in an overcorrection.

which has converted a bowed leg to a knock knee and the medial segment has healed because it has been relieved of maximal weight bearing. For the same reason, the lateral cortical wall of the left tibia has thickened and the medial wall has become thinner. In the uncorrected right tibia, maximal weight bearing is still on the medial segment and the active rickets persists in the medial segment, and its medial wall remains thickened.

The radiographic changes in these different types of rickets are similar, except that the signs of secondary hyperparathyroidism may be present as well, in the glomerular type of renal rickets (see Fig. 8-824).

Dent described six types of tubular rickets according to their type of tubular dysfunction and in ascending order of severity of this dysfunction. They are all characterized by low values for serum phosphate and a high value for the clearance of phosphate from the serum. In juvenile cystinosis, cystine crystals in the kidneys induce damage to the renal tubules and renal rickets in the skeleton. Renal damage secondary to the disturbed copper metabolism in Wilson's disease causes a rare type of renal rickets. Dent and colleagues described one patient with a most severe type of vitamin D resistant rickets and severe myopathy whose response to high doses of vitamin D was spectacularly good, clinically as well as biochemically. Ordinary vitamin D doses, of course, had no effect. Owing to the exceptionally good response to treatment, the authors concluded that this type of rickets is distinct clinically and biochemically from the usual 'vitamin D resistant rickets' which does not respond so well to massive doses of vitamin D.

In the simplest type of 'tubular rickets' the sole deficiency is either the impaired resorption of phosphate from the glomerular filtrate by the proximal convoluted tubule or decreased intestinal absorption of calcium, which causes hyperplasia and increased secretion of the parathyroids which in turn is respon-

sible for the hypophosphatemia and rickets. Such patients are usually in good health save for the rickets and complicating mechanical deformities. These are usually mild and rarely appear until after weight bearing begins. Treatment should be started as soon as the diagnosis is made to prevent stress deformities. These patients rarely if ever achieve normal stature even in the circumstance of early and successful treatment of the chemical changes in the serum and the radiographic changes in the bones. They respond satisfactorily to large doses of vitamin D and the disease is usually called 'refractory' or 'resistant' rickets. Hypophosphatemia, however, can rarely be completely corrected without poisoning the patients who are usually dwarfed before treatment is started and dwarfed when adult age is reached after otherwise successful treatment. The term 'phosphate diabetes' has been used by some. This type is truly endogenous and genetic, in the comprehensive studies of familial hypophosphatemia by Winters and colleagues in North Carolina, the disease was found to be nearly always inherited and usually congenital. They also found an interesting sexual factor in that hypophosphatemic males usually had severe or moderate rickets while hypophosphatemic females tended to have mild or no rickets.

In a study of 36 patients with familial hypophosphatemic vitamin D-resistant rickets, McNair and Suckler found that the principal clinical manifestation was shortness of stature. This shortening was

limited to the legs. Shortness of equal degree was found in both sexes and was not related quantitatively to the phosphorus content of the serum or to deformities alone. Neither height nor deformity nor hypophosphatemia was improved with massive doses of vitamin D. The phosphatase activity of the serum was reduced by treatment. Vitamin D intoxication was a constant hazard during therapy.

In simple familial hypophosphatemic rickets, Ko and Fellers feel that the bone changes cannot be ascribed to a renal defect but are due to some change in the vitamin D metabolism which reduces absorption of calcium from the alimentary tract. Sheldon and colleagues observed interesting rachitic twins in whom failure of absorption of aminoacids and glucose developed long before failure of resorption of phosphate appeared. Serum acid phosphatase activity however was high early and before the appearance of radiologic evidence of rickets.

In addition to these renal types of rickets, rickets may develop in the malabsorption syndromes in which vitamin D is lost owing to diarrhea and in some types of hepatic and biliary disease in which vitamin D-bearing fat is not absorbed or is poorly absorbed.

The radiographic findings in all kinds of renal and refractory rickets are similar to one another and similar to vitamin D deficiency rickets. In juvenile rickets of all kinds, the medial segments of the femoral and tibial metaphyses at the knees are often affected when other portions of the skeleton exhibit no diagnostic changes.

It is well to remember that metaphyseal dysostosis (see p. 1030) simulates rickets radiologically but is characterized by normal concentrations of phosphate and calcium in the serum.

REFERENCES

- Albright F *et al*. Rickets resistant to vitamin D therapy. *Am J Dis Child* 54:629 1937.
- Dent C E. Rickets and osteomalacia from renal tubule defects. *J Bone & Joint Surg* 34-B:266 1952.
- *et al*. Hereditary pseudo-vitamin D deficiency rickets. *J Bone & Joint Surg* 50-B:708 1968.
- Engfeldt B *et al*. Primary vitamin D resistant rickets. III. Biophysical study of skeletal tissue. *J Bone & Joint Surg* 38-A:1323 1956.
- Fraser D. Clinical manifestations of genetic aberrations of calcium and phosphorus metabolism. *JAMA* 176:281 1961.
- Harrison H E. Primary vitamin D resistant rickets. *J Pediatr* 64:618 1964.
- Ko K W., and Fellers F X. On the mechanisms of simple familial hypophosphatemic rickets. *Proc 31st Ann Meet Soc Pediatr Res* 1961 (abst.).
- McNair S L. and Stuckler G B. Growth in familial hypophosphatemic vitamin D-resistant rickets. *New England J Med* 281:511 1969.
- Malmberg N. Occurrence and significance of periosteal proliferation in the diaphyses of premature infants. *Acta paediatr* 32:626 1945.
- Park E A. Some aspects of rickets. *Canad M A J* 26:3 1932.
- Observations on the pathology of rickets with particular reference to the changes at the cartilage-shaft junctions of growing bones. *Harvey Lect* 34:157 1938.
- Sheldon W *et al*. A familial tubular absorption defect of glucose and aminoacids. *Arch. Dis Childhood* 36:90 1961.
- Winters R W *et al*. A genetic study of familial hypophosphatemia and vitamin D resistant rickets with a review of the literature. *Medicine* 37:97 1958.

Rickets and prematurity—Poor retention of minerals by prematures, the loss of the usual deposition of calcium and phosphorus in the skeleton which occurs in term infants during the last months of gestation and the rapid growth of prematures are responsible for the frequent occurrence and early development of rickets in prematures. Eck and co-workers found that all premature infants are born with rarefied metaphyseal zones which gradually blend with the generalized osteoporosis which develops 10–13 weeks after birth. Later double cortical contours become visible which they attributed to improved mineralization. We believe that many of the double cortical contours in prematures are due to trivial trauma to their loosely attached periosteum. Eck found no correlation between double cortical contours in roentgenograms and mineral concentrations in the blood serum. The basic radiographic changes in the rickets of prematurity and the rickets of infancy and childhood are similar.

REFERENCE

- Eck S *et al*. Prematurity and rickets. *Pediatrics* 20:63 1957.

MILKMAN'S SYNDROME of pseudofractures is characterized by symmetrically bilateral clefts of diminished density in both tubular and flat bones. In adults the commonest sites of these lesions are the axillary edges of the scapulas, ribs, pubic rami and upper ends of the femurs. In adults the syndrome is invariably associated with osteomalacia of some type. In children, Milkman's clefts are rare save during active rickets when the bones of the forearms are often involved (see Fig. 8-701). We have seen classic Milkman's lesions in one case of oxalosis (see Fig. 8-829).

The pathogenesis has long been a puzzle because none of the proposed explanations accounted for the bilateral symmetry, the consistent predilection for certain sites in the skeleton and the clefts at sites where there is little or no mechanical stress such as the axillary scapular margins. Le May and Blunt in anatomic dissections of three cadavers found that the sites of the clefts are commonly grooved and crossed by neighboring arteries. They concluded that the clefts were caused by local vascular stresses on the partially demineralized bone—local pulsating arterial erosion. Steinbach and colleagues confirmed these findings in arteriographic studies in living patients suffering from osteomalacia. In rickets, Milkman's clefts (*Umbauzone* of Looser) disappear when the rickets heals (see Figs. 8-701 and 8-702).

REFERENCES

- Albright F *et al* Osteomalacia and late rickets Relation ship between osteomalacia and Milkman's syndrome *Medicine* 25 399 1946
- Le May M and Blunt J W Jr A factor determining the location of pseudofractures in osteomalacia *J Clin Invest* 28 521 1949
- Magilligan D J and Dulligan P J Jr Milkman's pseudofractures A form of osteomalacia, *J Bone & Joint Surg* 34 A 170 1952
- Milkman L A Multiple spontaneous idiopathic symmetrical fractures *Am J Roentgenol* 32 622 1934
- Steinbach H L *et al* A mechanism of the production of pseudofractures in osteomalacia (Milkman's syndrome) *Radiology* 62 388 1954

HYPOPHOSPHATASIA resembles rickets clinically and to some degree radiographically and microscopically although it is an independent entity with no abnormal changes in the phosphate and calcium concentrations in the serum. The three cardinal diagnostic features are diminished activity of alkaline phosphatase activity in the blood serum and many tissues irregular and incomplete ossification of cartilage and

of growing bone in roentgenograms and microscopic sections and increased urinary excretion of phosphorylethanolamine. Fraser classified the disease as an inborn error which is determined genetically and he believes that the basic lesion is a defect which reduces the calcificability of the organic bone matrix. Transitory hypercalcemia is common in all cases and permanent hypercalcemia in severe cases. This is said to be the first identification of a genetic enzyme deficiency of any kind. The diagnosis can be established satisfactorily by demonstration of the low phosphatase activity in the serum and by the detection of phosphorylethanolamine in the urine. Curran and associates stated that this amino acid has been found in the urine in all patients in whom adequate examinations have been made.

Clinical and radiographic findings depend on the age of the patient. During the first days of life the calvaria is soft and the bones in the extremities are bowed and angulated. Radiographic examination discloses a generalized rarefaction of the skeleton but with regional excessive rarefaction of the bones of

Fig 8708 Early infantile changes in hypophosphatasia. A and B at 2 months of age the shafts are shortened and spread at the ends with irregular ossification of the metaphyses which simulate rickets and achondroplasia. Both femurs are bowed laterad in the middle thirds which probably represents prenatal bowing. C and D at 26 months the defective and irregular ossification of the metaphyses characterised by deep segmental defects which is the most diagnostic feature of the disease. The contiguous epiphyses ossification centers and round bones are not affected. The edges are smooth. E the calvaria is deformed and the digital markings increased due to premature synostosis of the sutures.

calvaria of the metaphyses characterised by deep segmental defects which is the most diagnostic feature of the disease. The contiguous epiphyses ossification centers and round bones are not affected. The edges are smooth. E the calvaria is deformed and the digital markings increased due to premature synostosis of the sutures.

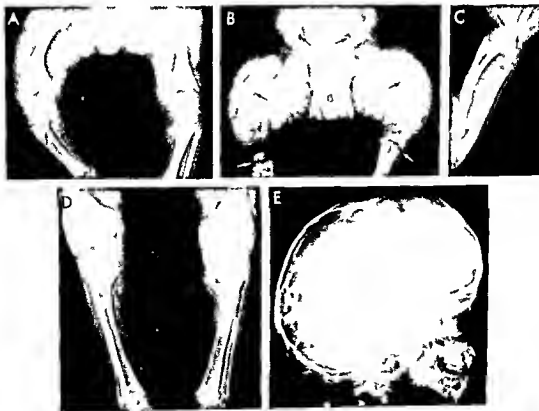




Fig. 8-709 — Hypophosphatasia in a boy 3 years of age. In A the sharp deep metaphyseal defects (arrows) in the humerus and ulna are characteristic of hypophosphatasia and differentiated

from standards of rachitic changes. In B the sternal ends of the ribs are cupped and splayed; these costal changes simulate rachitic rosary both clinically and radiographically.

the calvaria and the metaphyses of the long bones. These changes in the calvaria simulate osteogenesis imperfecta; the metaphyseal lesions simulate achondroplasia and rickets; and the bowings in the long bones appear to be identical with those found in prenatal bowing of the long bones due to faulty fetal position (Figs. 8-708 and 8-709). Weller found cutaneous dimples over the summits of the bowings in the long bones to be similar to the cutaneous dimples associated with congenital bowings of the long bones not associated with hypophosphatasia. Kelsey made the same observations. In his patient at birth the bones of the legs were bowed but the metaphyses were normally mineralized; at 4½ months of age flared rickets-like metaphyseal changes had appeared. In this patient the disease appeared to become more severe as age advanced, which is the converse of the usual course. In older children the skeletal changes are much less marked and are usually confined to shallow terminal metaphyseal zones of irregular calcification which are identical radiographically with the changes found in juvenile rickets and metaphyseal dysostosis (see Fig. 8-352 and p. 1030). These diseases in older children can be satisfactorily differentiated by the chemical changes in the serum and urine.

Pseudohypophosphatasia is a term coined by Scriver and Cameron to describe a disease that resembles hypophosphatasia clinically and radiographically but lacks the low alkaline phosphatase activity in the plasma. However, hypercalcemia and phosphorethanolaminuria were consistently present in their patient, a girl 3 months of age. The authors concluded that a phenotype of classic hypophosphatasia does exist in the presence of normal alkaline phosphatase activity in the plasma.

REFERENCES

- Curran G. *et al.* Hypophosphatasia, *Am J Roentgenol* 78:392 1957
- Fraser D. Hypophosphatasia, *Am J Med* 22:730 1957
- Calcium and phosphorus metabolism, *JAMA* 176:281 1961
- Kelsey D. C. Hypophosphatasia and congenital bowing of the bones, *JAMA* 179:157 1962
- Rathbun J. C. Hypophosphatasia: a new developmental anomaly, *Am J Dis Child* 75:822 1948
- Rosenthal I. M. *et al.* Tissue alkaline phosphatase in hypophosphatasia, *Am J Dis Child* 92:183 1960
- Scaghone R. B. and Lucey J. F. Further observations on hypophosphatasia, *Am J Dis Child* 92:403 1956
- Scriver C. R. and Cameron D. T. Pseudohypophosphatasia, *New England J Med* 281:604 1969
- Weller S. V. D. Hypophosphatasia with congenital dimples, *Proc Roy Soc Med* 52:637 1959

FAMILIAL CHRONIC HYPERPHOSPHATASEMIA with immaturity and hypermetabolism of growing membranous bone is a rare genetic disease. Two siblings have been affected in four of the ten families described to date. Gestation and parturition have been normal. One patient was underweight at birth. Other wise all newborns were considered normal. The first clinical signs have been detected from age 3 to 18 months. They include progressive enlargement of the head. The facial bones have remained normal clinically in all but one patient. Progressive loss of muscular power with delayed and clumsy walking or failure to walk with swelling and bowing of the extremities (Fig. 8-710) and recurrent pain have been features in all patients. Muscular dysfunction and stricture have not been studied adequately. The pains have been attributed to microfractures of the long bones. The neck and trunk have been shortened owing to universal flattening of the vertebral bodies. Mental and endo-

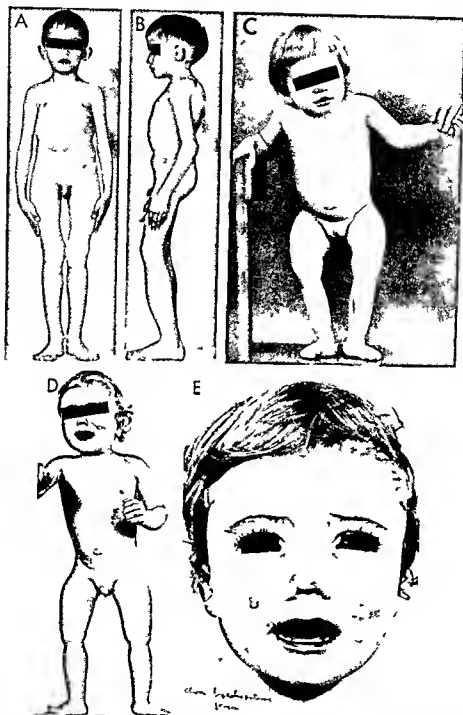


Fig 8-710—Clinical appearance of patients of hypophosphatasia showing similarity of clinical appearance of different ages. **A** and **B**, a boy 6 years of age in whom the calvaria is large, trunk short, thighs thickened and bowed laterad and the shanks thickened and bowed ventrad. His loss of stature is due to universal vertebral plana. The arms and legs are held in semiflexion. He died at

age 18 (see text). **C**, similar changes in a girl 2 1/2 years of age (From Swoboda). **D**, a boy 18 months of age whose trunk is not short; he did not have vertebral plana. (Courtesy of Dr. John Sutcliffe). **E**, bilateral palatal swellings of the upper maxilla of the boy in **D**.

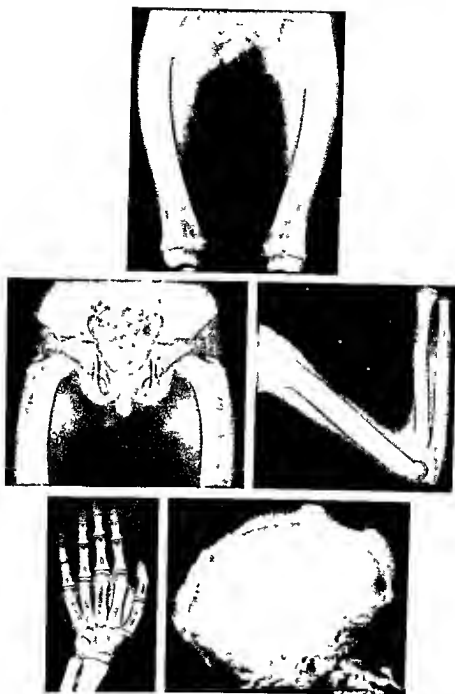


Fig 8.711 — Chronic familial hyperphosphatasemia in a boy 6 years of age. In all of the long bones the volume is increased owing to thickening of the cortical walls. At the proximal ends of the femurs the thickenings taper and disappear at the metaphyses. The pelvic bones are not affected. The femurs are bowed laterally; the rest of the long bones are straight. The new endochondral bone in the metaphyses and on the edges of the ossification

centers in the epiphyses is normal everywhere. In the skull the facial bones are not affected but the calvaria is thickened owing to deepening of the diploic space. In addition, there are numerous large and small independent patches of sclerosis. These cranial changes resemble those of the McCune-Albright syndrome.

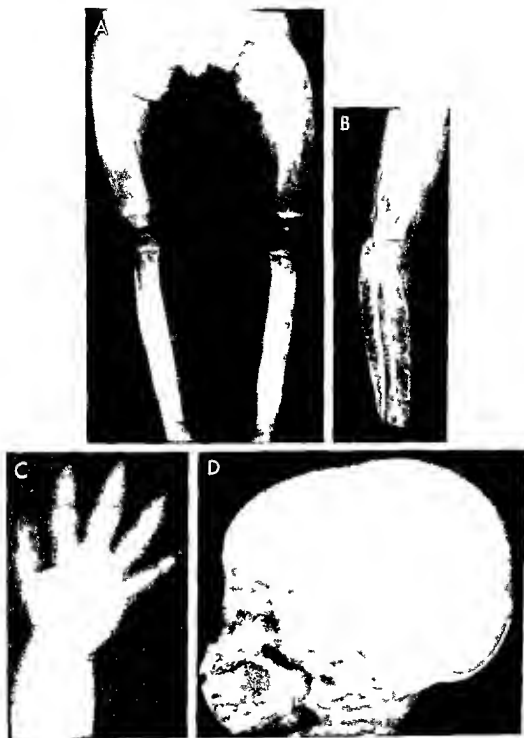


Fig 8 712 See desc pt on on page 1235

crine development have been normal. Menarche was normal in one girl. Deciduous teeth were shed prematurely in two patients. Angioid streaks were found in the ocular fundi in three older patients and senous visual and auditory losses were detected in several, it seems likely that some loss of vision and/or hearing occurs in all older patients. Sustained high blood pressure was present in three patients, it was not recorded in several. In one older patient (18 years), yellowish cutaneous patches characteristic of xanthoma elasticum were found in the neck and one shoulder.

Both alkaline and acid phosphatase activity in the serum was increased and sustained over several years. Peptides were excreted in massive amounts in the urine of several patients. Serum and urinary acid levels were increased in the few patients in which tests were made. The high phosphatase values indicate increased activity of osteoblasts and osteoclasts—concurrent overproduction and overdestruction of bone. The excess of urinary peptides suggests increased metabolism of collagen. The elevated serum and urinary acid values signify increased cellular turnover, probably of osteoblasts and the connective tissue cells in the medullary cavity.

The radiographic changes in the skeleton are illustrated in Figures 8-711 to 8-714.

Three of the 14 reported patients have died. The two early deaths were apparently due to acute infections of the lung at 3 years and of the meninges at 4 years. The sole necropsy was done on the boy (A and B of Fig. 8-710) who died at age 18 by Dr. Sumi Mitsudo. In addition to characteristic changes in the membranous skeleton, she found pseudoxanthoma elasticum of the skin, endocardium, retina and arteries, and a massive cerebral hemorrhage. The enlarged heart weighed 400 Gm. Severe arterial sclerosis was found in several organs. The intramuscular arterial changes and chronic muscular hypoxia may explain the severe muscular weakness and pain that distressed several patients. This boy whose hyperphosphatasemia persisted until death had had recorded arterial hypertension for more than 12 years. In the thickened calvaria a mosaic pattern of thickened cement lines was indistinguishable from the mosaic pattern in adult Paget's disease.

Although the findings in patients suffering from this syndrome produce in toto one of the most conclusive-

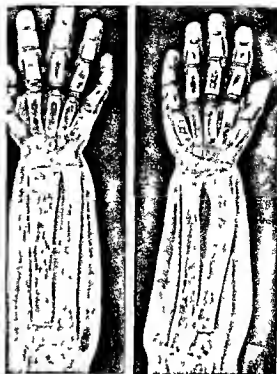


Fig. 8-713—Typical severe changes of chronic hyperphosphatasemia in the hands and forearms of an Austrian girl 2 years of age. The radiuses and ulnas show the same increases in width, dilatation of medullary cavities and thin streaked cortical walls with no evidence of compact Haversian bone. The differential pattern of changes in the phalanges and metacarpals is almost identical with those in Figure 8-712. A relatively large whitish patch in the shaft of the right radius suggests an infarct. This lesion has as far as is known not been studied microscopically. (Courtesy of Dr. A. Swoboda.)

ly diagnostic pictures in pediatrics, all of them show similarities to adult Paget's disease, Engelmann's craniodiaphyseal dysplasia, osteogenesis imperfecta and possibly Van Buchem's disease. In my opinion all of these are readily excluded by the clinical, chemical, radiographic or pathologic features either singly or in combination. In Paget's disease, for example, onset is rare before the 30th year and skeletal involvement is local, regional and asymmetrical. In chronic hyperphosphatasemia onset is between the

—Fig. 8-712—Typical severe changes of chronic hyperphosphatasemia in an infant 2 years of age. A: the femurs are bent laterally and tibias ventrally. The shafts are enlarged and radioluculent with widely meshed streaky cortical walls and no evidence of compact cortical bone. The dilated shafts (osteoclastasia) are about the same caliber at all levels owing to failure of normal metaphyseal constrictor (funnelization). The provision zones of calcification at the ends of the shafts are normally calcified. The epiphyseal ossification centers are normal in size but are rarefied probably due to reduced use. B: marked similar changes are present in the arm bones. In addition, the dilated rarefied segments in the distal third of the humeral shaft raise the question of cyst formation. C: in the hands and forearms at 14 months the middle and proximal phalanges of digits 2-5, the proximal phalanx of

digit 1 and the 1st metacarpal are thickened externally and sclerotic with narrowed medullary cavities. The other metacarpals are rarefied with thin cortical walls and dilated medullary cavities. These metacarpophalangeal differences are present in some degree in all patients and are in my experience not found in other diseases. D: in the calvaria at 3 months the frontal squamosa and parietal bones are thickened but rarefied and streaked by what appears to be primary fibrous bone. In sharp contrast the bone in the occipital squamosa is normally sclerotic and compact. This bone is of cartilaginous origin. The membranous mandible is also thickened streaky but rarefied. The teeth are normally sclerotic. (Courtesy of Drs. Harold Rosenbaum and Robert D. Shepard, Lexington, Ky.)

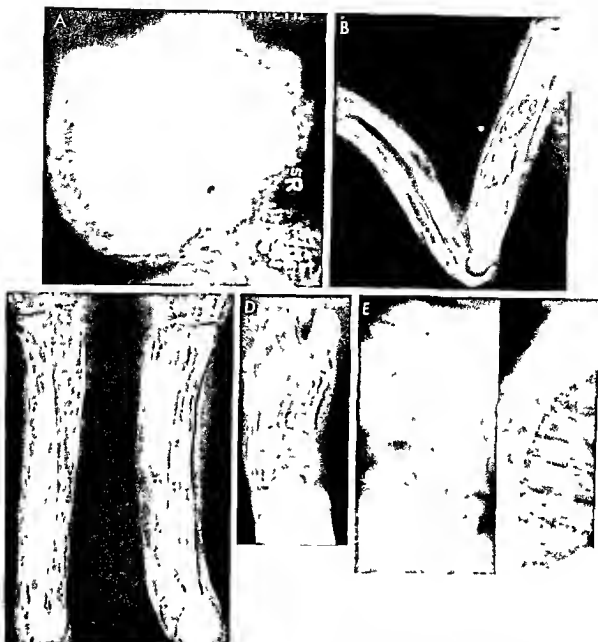


Fig 8-714—Severe typical changes of chronic hyperphosphatasemia in a girl 19 years of age. **A**, the calvaria is markedly thickened in frontal, parietal and occipital segments. There are countless large and small rounded whitish (cottonball) images, the microscopic nature of which is not known. The facial bones appear to be normal. **B**, the bones in the arm are bowed, widened, dilated but rarefied, with poorly defined, widely meshed cortical walls. Two large whitish patches in the humerus suggest infarctions, similar to the whitish image in the radius in Figure 8-713. **C**, the tibiae and fibulae present similar but more severe changes plus individual transverse sclerotic streaks at several longitudinal levels which suggest microfractures. These lesions (not studied

microscopically) could be strips of sclerosis on the edges of dilated perforating canals for the perforating arteries. Failure of normal constriction of the middle segments of the shafts with normal flares in the terminal metaphyseal levels is striking. **D**, typical changes in the tubular bones of the feet. The relative sclerosis in the proximal phalanx, 1st digit and 1st metacarpal resembles the minimal changes in preceding figures. **E**, severe universal vertebra plana in the thoracic and lumbar levels of the spine. The lumbar bodies are flattened into bilateral concave disks with expansion of the companion intervertebral disks into bilateral convex disks. (Courtesy of Drs. David H. Baker and Walter E. Berdon, New York.)

3rd and 18th month and skeletal involvement is universal and symmetrical in membranous parts of the skeleton. In Engelmann's disease the ends of the shafts are not affected and the bony cortical thickenings are made up of compact Haversian bone. In osteogenesis imperfecta the calvaria is thin and presents a mosaic rarefaction in radiographs and there is no evidence of the accelerated turnover of bone or bone collagen microscopically or chemically. Van Buchem patients have not been identified prior to the 20th year: the bones are sclerotic rather than rarefied; the facial bones are severely and consistently affected and the sclerotic bony thickenings are made up of compact mature Haversian bone.

REFERENCES

- Alderman M H and Frimpter G W. Inherited bone disease with glycylproline peptiduria, *Abstr Clin Res Proc* 16: 295 1968.
- Bakwin H and Elger M S. Fragile bones and macrocranium *J Pediatr* 49: 558 1956.
- et al. Familial osteoectasia with macrocranium *Am J Roentgenol* 91: 609 1964.
- Caffey J. *Pediatric X-ray Diagnosis* (5th ed). Chicago: Year Book Medical Publishers 1967. p 983.
- Familial Hyperphosphatasemia with Ateliosis and Hypermetabolism of Membranous Bone in Kauffmann H J (ed) *Progress in Pediatric Radiology* Vol 4 (Basel Switzerland: S Karger AG Distributed in the U.S. by Year Book Medical Publishers Inc. Chicago 1972).
- Choremis C et al. Osteitis deformans (Paget's disease) in an 11 year old boy *Helvet paediatr acta* 13: 185 1958.
- Eyring E J and Eisenberg E. Congenital hyperphosphatasia. A clinical, pathological and biological study of two cases *J Bone & Joint Surg* 50-A: 1099 1968.
- Fancom G et al. Osteocalcalasia desmalis familiaris *Helvet paediatr acta* 19: 279 1964.
- Halliday J. A rare case of bone dystrophy *Brit J Surg* 37: 52 1949.
- Marshall W C (for Moncreff A. A.). Chronic progressive osteopathy with hyperphosphatasia, *Proc Roy Soc Med* 85: 238 1962.
- McKusick V A. Heritable Disorders of Connective Tissue (3rd ed. St Louis: C V Mosby Company 1966) p 421.
- Mitsudo S M. Chronic idiopathic hyperphosphatasia associated with pseudoxanthoma elasticum *J Bone & Joint Surg* 53-A: 503 1971.
- Seakins J W T. Peptiduria in an unusual bone disorder: isolation of two peptides *Arch Dis Childhood* 38: 215 1963.
- Snapper I. Paget's Disease (Osteitis Deformans) in *Medical Clinics on Bone Diseases* (New York: Interscience Publishers 1949).
- Stemmermann G N. An histologic and histochemical study of familial osteoectasia (chronic idiopathic hyperphosphatasia), *Am J Path* 43: 641 1966.
- Straskey E et al. On Paget's disease with leontiasis ossea and hypothyroidism starting in early childhood *Ann paediatr* 199: 393 1962.
- Swoboda W. Hyperostosis corticalis deformans juvenilis *Helvet paediatr acta* 13: 292 1958.
- Thompson R C Jr et al. Hereditary hyperphosphatasia. Study of three siblings *Am J Med* 47: 209 1969.
- Wagner J M and Solomon A. Hyperostosis corticalis infantilis (Paget's disease) *South African M J* 43: 754 1969.
- or boiled milk. It is the heating of cow's milk to reduce the bacterial content which destroys vitamin C in sufficient amount to lead to clinical scurvy. In such circumstances the addition of orange juice or ascorbic acid to the diet prevents scurvy easily and effectively. In nearly all cases the appearance of manifest scurvy is preceded by a prodromal asymptomatic interval of four to six months. There are no authentic cases of symptomatic or roentgenographic scurvy in infants younger than 3 months. During the first weeks of life skeletal syphilis has been misinterpreted as skeletal scurvy in roentgenograms. In Burns's report of scurvy in an infant 2 months of age the findings are better explained in my opinion on the basis of trauma than by deficiency of vitamin C.
- Dennis and Mercado reported the development of typical radiographic changes of scurvy in the bones of a girl 16 months of age during a six month course of aminopterin therapy. These bone changes disappeared slowly when aminopterin was withdrawn and vitamin C administration begun. Hematuria and clinical signs of scurvy did not accompany the bone lesions. Engest reported scurvy like changes in the bones of hypothyroid infants both before and after treatment with vitamin C. The metabolic defects in scurvy and in tyrosinosis, an exceedingly rare anomaly of protein and amino acid metabolism, are similar. In the films of the skeleton of a girl who had tyrosinosis the typical changes of active scurvy were present. These did not of course respond to the administration of ascorbic acid. The films were seen through the courtesy of Drs Marvin Daves and R Parker Allen of the University of Colorado.
- Knowledge of the morbid anatomy of scurvy is surprisingly meager except that relating to the skeleton. Lack of intercellular cement substance in the endothelial layer of the capillaries is supposedly the cause of the hemorrhagic tendency; the blood clotting mechanism is not significantly altered. The hemorrhages which may take place in any organ or tissue have been found at necropsy to be associated with edema and with hydrops of the serous cavities.
- The basic skeletal changes are due to the suppression of normal cellular activity both productive and destructive in the growing bones. The noncellular activities such as the deposition of lime in the provisional zone of calcification and internal resorption (hausteresis) of the corticis and spongiosa are not disturbed. This disruption of the normal balance of productive and destructive forces results in generalized atrophy of the cortex and spongiosa and at the same time an increase in the thickness of the provisional zones of calcification.
- At the cartilage-shaft junction (metaphyses) the proliferating cartilage cells are markedly diminished in number and their mitosis and growth are reduced. On the epiphyseal side of the provisional zone of calcification deposition of lime continues in the cartilaginous matrix while on the opposite side (the diaphyseal) destruction of the provisional zone is dimin-

INFANTILE SCURVY — Scurvy is caused by deficiency of the accessory food factor vitamin C or ascorbic acid. Infantile scurvy is found almost exclusively in babies who are fed formulas containing pasteurized

ished or stops. As a result lime piles up deeply and the provisional zone of calcification becomes thickened. In roentgen films this thickened calcified epiphyseal disk casts a heavy transverse shadow but it is not as strong physically as its shadow suggests. Actually it is brittle rather than strong and often presents fissures and fractures. The calcified cartilaginous trabeculae just beneath the thickened zone are irregular in size and irregularly disposed in a random network having lost much of their normally longitudinal parallel pattern. These trabeculae are bare of endosteal bony coating and like the provisional zone are brittle rather than hard and fracture easily. Transverse fractures through the brittle calcified cartilaginous plate and its attached lattice give rise to epiphyseal displacements and separations.

When the heavy provisional zones of calcification project laterad beyond the usual limits of the shaft they form spurs and provide one of the most diagnostic roentgen features of scurvy. Early ossification under the raised periosteum in the angle between the provisional zone of calcification and the periosteal attachment is another cause of spur formation. The trabeculae just beneath the cartilaginous lattice are sparse, small and poorly mineralized. This atrophic layer between the sclerotic provisional zone and the heavier spongiosa deeper in the shaft casts a transverse band of diminished density in the roentgenogram which has been called the scurvy line. Unilateral or bilateral defects in the spongiosa and cortex just below the provisional zone of calcification may permit incomplete separation of the plate from the shaft owing to subepiphyseal marginal clefts. These clefts appear roentgenographically as the corner or angle sign of scurvy. All of these metaphyseal changes appear earliest and are most marked at the sites of most rapid growth and most active endochondral bone formation, especially at the stemal ends of the ribs, the distal end of the femur, the proximal end of the humerus, both ends of the tibia and fibula and the distal end of the radius and ulna.

In the shaft the spongiosa becomes atrophic; this is responsible for the ground glass texture in the roentgenogram. This ground glass appearance is also found in many types of bone atrophy of non-scurvitic origin. The cortex gradually becomes thinner as the disease progresses until it may be reduced to one-fourth or one-fifth its original thickness. In the ter-

minal segments of the shaft where the cortex is normally exceedingly thin the cortex may disappear roentgenographically. Notwithstanding the severe cortical atrophy in scurvy diaphyseal cortical fractures are rare. In contrast fractures of the calcified cartilage in the metaphysis are common.

Subperiosteal hemorrhages may appear on any of the long bones; they are most common in the larger bones such as the femur, tibia and humerus. Occasionally subperiosteal hematomas form on the flat bones of the calvaria, orbit and shoulder girdle. The hemorrhages vary greatly in size; they are usually confined to the ends of the long bones but may extend the entire length of the shaft from one epiphyseal plate to the other. Subperiosteal hemorrhages over the epiphysis are said never to occur in scurvy. Hemarthrosis is also exceedingly rare during infancy and childhood. Large subperiosteal hemorrhages cast shadows of increased density in the soft tissues surrounding the bone and may spread apart two bones which normally lie close together and parallel, such as the tibia and fibula, and radius and ulna. The subperiosteal hemorrhage is actually not as large as it appears to be clinically and roentgenographically; much of the regional swelling is due to edema and

Fig. 8715—Early skeletal changes in scurvy. 7 months of age. A, normal; B, scorbutic bones showing generalized osteoporosis, cortical atrophy, atrophy of the spongiosa and thickening of the provisional zones of calcification. The ossification centers show marked central rarefaction with heavy ring shadows on the margins. These findings may also be found in several types of non-scurvitic chronic bone atrophy.



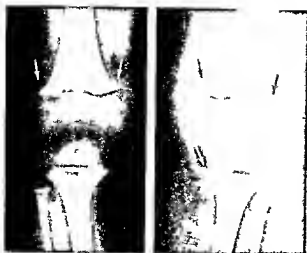


Fig 8-716—Scorbutic bones in an infant 11 months of age showing multiple spur formation in addition to the changes in Figure 8-715. The combination of spurs and bone atrophy is pathognomonic of scurvy.

hemorrhage external to the periosteum in the overlying soft tissues.

Roentgen appearance—The roentgen changes in the prodromal phase of scurvy have not been observed in humans. In two of our patients who were fed pasteurized formulas for three and five months respectively without the addition of fruit juices to the diet, we found no significant changes in the roentgenograms of the bones. The optimal sites for the detection of scurvy in the skeleton are the bones of the lower extremities; diagnostic changes may be demonstrable at the knees when minimal changes are present at the wrists.

The mildest and probably the earliest changes in human scurvy are generalized bone atrophy and thickening of the provisional zones of calcification (Fig 8-715). These findings are of course not diagnostic of scurvy because they are found in many non-scorbutic types of bone atrophy. In more severe cases several other roentgen signs may be added to the basic atrophic changes and thus give rise to a variety of pictures pathognomonic of scurvy. The combination of diffuse bone atrophy and multiple spurs at the cartilage-shaft junctions occurs only in scurvy (Fig 8-716). Subepiphyseal atrophy of the cortex and spongiosa casts a transverse band of diminished density on the shaftward border of the provisional zone of calcification (Fig 8-717) which favors the diagnosis of scurvy but is not diagnostic. The fractures through the thickened provisional zones and the deformities secondary thereto are diagnostic of scurvy (Fig 8-718) when syphilis can be excluded. The corner sign of scurvy (Fig 8-719) described by Park and his co-workers is a valuable diagnostic feature when found with generalized bone atrophy.

Subperiosteal hematomas produce regional increases in the soft tissue density. Large subperiosteal

hematomas situated between two parallel bones may displace them away from each other (Fig 8-720).

The roentgen signs in healing scurvy were described in detail by McLean and McIntosh. With the onset of healing the cortices become thicker and the spongiosa becomes more clearly defined. The transverse band of diminished density in the metaphysis regains its normal density and disappears as the terminal spongiosa and cortex become completely mineralized. As growth proceeds the thickened provisional zone of calcification is buried within the shaft as a transverse line (Fig 8-721). When a subperiosteal hematoma is present with the advent of healing the raised periosteum begins to layer the periphery of the hematoma with a new shell of subperiosteal bone (Fig 8-722). Concurrently with resorption of the hematoma, this new layer of bone thickens and shrinks down onto the shaft to become the new cortex. Residues of these cortical thickenings may persist for years, especially on the concavities of the posterior aspects of the femurs. In the event of epiphyseal displacement the longitudinal growth after healing proceeds from the displaced proliferating cartilage; the shaft and the marrow cavity shift to this new position and adapt themselves to the new axis of longitudinal growth without difficulty (Fig 8-722). This recalcification has taken place spontaneously in all

Fig 8-717—Advanced scurvy in an infant 7 months of age. Shaftward from the thickened provisional zones of calcification is a deep transverse band of diminished density so-called scurvy lines. Atrophy of the cortex and spongiosa is also evident in the proximal femurs. Small lateral spurs projected from the cartilage shaft junctions at the distal ends of the femurs and at both ends of the tibiae. This combination is pathognomonic of scurvy.





Fig. 8-718 — Advanced scurvy with fractures of thickened but the proximal zones of calcification. **A**, multiple infarctions in the proximal zone with peripheral spurting and beginning subperiosteal ossification on the terminal segment of the shaft by the externally displaced periosteum. The osteogenic layer is lifted by hemorrhage and continues to form no mat cortical

bone. The bones generally are rarefied, but the proximal zones of the femur, tibia and tibia and of the femoral and tibial ossification centers are thickened. **B**, longitudinal fractures of proximal zones and distal ends of the tibia. **C**, crushing fractures of distal proximal zones of the ends of the femurs with incomplete cupping of ends of the shafts.



Fig. 8 719 —Peripheral metaphyseal clasts in scurvy. The cortical and spongiosal defects in the angle between the provisional zone of calcification and the cortex are responsible for the roentgen change called the "corner sign" of scurvy. The peripheral segment of the provisional zone is tilted off the shaft toward the epiphyseal cartilage. A, distal end of the radius in an infant 11 months of age. B, distal end of the tibia in an infant 14 months of age.

Fig. 8 721 —Healing scurvy in an infant 6 months of age showing formation of a new cortex and its re-alignment with the displaced epiphyses of the left femur. A, acute stage: the provisional zone of calcification of the femur is fractured and the epiphyses displaced laterad. B, 14 days after administration of ascorbic acid: a heavy shell of subperiosteal bone has formed around the subperiosteal hematoma. C, 4 months after A: the shell of bone around the subperiosteal hematoma has shrunk and now

forms the new cortex. The old cortex and provisional zone are still visible (arrows); they are buried in the new shaft and are being gradually resorbed. The new shaft is now aligned with the displaced epiphyses. D, a year after A: The old cortex is barely visible (arrow) and the old provisional zone is buried deeply in the shaft as a transverse line. The new shaft is in perfect alignment with its distal epiphysis which in turn is in normal relation to the tibial epiphysis across the knee joint.



Fig. 8 720 —Fresh subperiosteal hematoma surrounding the distal half of the tibia and spreading apart the distal ends of the tibia and fibula. Transverse tractures are present in the terminal segments of the shafts of the tibia and fibula.

forms the new cortex. The old cortex and provisional zone are still visible (arrows); they are buried in the new shaft and are being gradually resorbed. The new shaft is now aligned with the displaced epiphyses. D, a year after A: The old cortex is barely visible (arrow) and the old provisional zone is buried deeply in the shaft as a transverse line. The new shaft is in perfect alignment with its distal epiphysis which in turn is in normal relation to the tibial epiphysis across the knee joint.

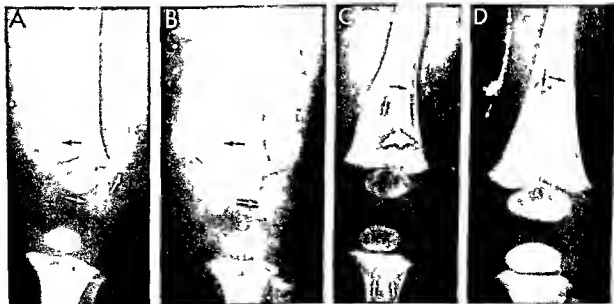


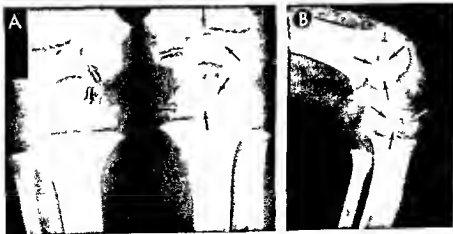


Fig 8-722—Healing scurvy showing the spur of subperiosteal bone spur around the distal femoral epiphysis. A, frontal projection; B, lateral projection. The distal femoral epiphysis is displaced laterally and dorsally.

of our cases without the application of extension or other orthopedic treatment. The healed epiphyseal ossification center may exhibit a central inset of rarefaction which persists for years after the inception of healing (Fig 8-723); these rarefied insets are identical in size and contour with the rarefied epiphyseal centers which develop during the active stage of the disease.

In the remarkable patient of Silverman, 12 months

Fig 8-723—Healing scurvy showing the epiphyseal insets of central rarefaction 20 months after the active stage of the disease.



after recovery from active scurvy epiphyseal separation at the distal end of the femur and ossification around a subperiosteal hematoma was followed by deep segmental central cupping of the metaphyses with shaftward protuberance of the enlarged epiphyseal ossification center proximally into the metaphyseal cup at 19 months. At 4 years fusion of the epiphyseal ossification center and the shaft with stoppage of longitudinal growth appeared to be imminent but at age 22 the affected femur was only slightly shortened and deformed (Fig 8-724). This careful prolonged study indicates that the metaphyseal cupping associated with scurvy should be carefully watched before the normal side is shortened to compensate for shortening of the affected side. We have seen similar cupping following traumatic injury to the femoral metaphysis and inflammation of the metaphysis (see Fig 8-654) and it has been reported as a residual of vitamin A poisoning. Cupping of this type but less in degree is a regular feature of achondroplasia during the early years (see Fig 8-306) and occurs commonly in the manual phalanges in chondroectodermal dysplasia (see Fig 8-332).

REFERENCES

- Burns R B. The unusual occurrence of scurvy in an 8 week old infant. *Am J Roentgenol* 89:923, 1963.
- Dennis J M and Mercado R. Scurvy following folic acid antagonist therapy. *Radiology* 67:412, 1956.
- Engeser A et al. Skeletal changes resembling scurvy in infantile hypothyroidism before and after therapy. *Acta radiol* 36:1, 1951.
- Jackson D and Park E A. Congenital scurvy. Case report. *J Pediatr* 7:741, 1935.
- Kato K. Cnucque of the roentgen signs of infantile scurvy. *Radiology* 18:1096, 1932.
- McLean S and McIntosh R. Healing in infantile scurvy as shown by x ray. *Am J Dis Child* 36:875, 1928.
- Park E A et al. Recognition of scurvy with especial reference to early x ray changes. *Arch Dis Childhood* 10:265, 1935.

as seen in distal ossification centers of the femurs and proximal centers of the tibiae. A, frontal projection; B, lateral projection.

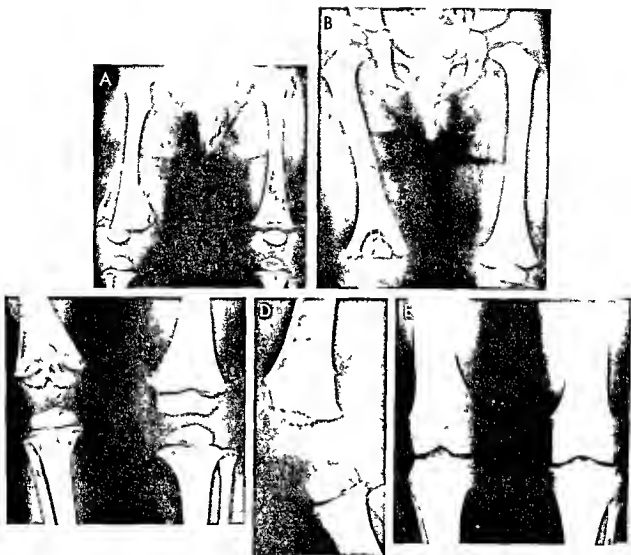


Fig 8724—Successive changes in scurvy with traumatic segmental cupping and spreading of the distal femoral metaphysis and overgrowth and extension of the epiphyseal ossification center into the metaphyseal cup. **A**, at 6 months there is laceration of the cartilage plate and lateral displacement of the epiphysis laterad. A shell of cortical bone is forming around a subperiosteal hematoma. **B**, at 19 months the femoral metaphysis is deeply cupped in its central segment; the longitudinal growth of which is retarded. The peripheral segment of the metaphysis is only slightly retarded in growth and the walls of the cup are thick. The enlarged and conoidal epiphyseal ossification center has insinuated into the cup and is almost completely buried in it.

The thick walls of the cup have failed to constrict and the distal end of the femoral shaft is splayed. **C**, at 4 years the findings are similar but relatively retardation of the longitudinal growth is not as marked as in **B**; the cup is not relatively as deep as before and the epiphyseal ossification center extends caudad well beyond the end of the shaft. A deep intercondylar notch now separates the lateral and medial femoral condyles. **D**, lateral projection of **C**. **E**, at 22 years there is surprisingly little residual deformity particularly shortening and splaying of the right femur. The intercondylar notch is deeper in the right femur and the lateral intercondylar spine is enlarged. (Courtesy of Dr. Frederic N. Silverman, Cincinnati.)

Silverman F N. Recovery from epiphyseal invagination. Sequel to an unusual complication of scurvy. *J Bone & Joint Surg* 52 A 384 1970.

HYPERVITAMINOSIS

Accurate diagnosis and successful treatment, both curative and prophylactic, of disorders caused by vita-

min deficiency stand high among the major triumphs of modern medicine. Early, the vitamins were used in natural form in foodstuffs where they occurred in such dilute concentrations that they could be safely sold without restriction for uncontrolled use at home. The belief has long prevailed and generally persists that all vitamin preparations are harmless. This belief has not been tenable for some years. Substantial

experience demonstrates clearly that prolonged feedings of excessive amounts of highly potent concentrates of fat soluble vitamins A and D are seriously and in the case of vitamin D, sometimes fatally toxic. As a result, a man made disease has appeared in man—hypervitaminosis.

The control of vitamin D poisoning presents no serious problem because excessive vitamin D ingestion is still in the hands of physicians. Almost without exception hypervitaminosis D has developed in patients who were being intentionally treated with massive doses of vitamin D to combat rheumatoid arthritis or tuberculosis—calculated risks taken by physicians. In contrast, all recorded cases of vitamin A poisoning in infants and children have resulted from prolonged daily feeding of excessive amounts of vitamin A concentrates by mothers who either increased the dose to toxic levels on their own initiative, in ignorance of the potential dangers, or misunderstood the directions of their doctors, although in each case the correct dosage was clearly stated in the manufacturer's label on the bottle.

Excepting breast fed infants there is no need for either vitamin or mineral supplements in the diets of American men, women, children or infants who are in good health. An abundance of both vitamins and minerals is supplied in the average American diet of meat, fish, poultry, milk and milk products, eggs, cereals, vegetables and fruits. Some sick persons may need supplemental vitamins, and these should be taken on the advice of a physician who should control dosage and the duration of their intake. The dishonest claims in the advertising blurbs in this field are disgraceful because they divert millions of dollars out of the pockets of parents which could be used for the improved care of their children. And scores of infants have been poisoned, some fatally. No one knows how much subclinical poisoning exists. Substantial evidence suggests that excess of vitamin D in the diet of pregnant women sensitive to vitamin D is responsible for chronic hypercalcemia, mental retardation, renal disease and cardiac malformations in the newly born infant.

VITAMIN A POISONING—*Chronic vitamin A poisoning* was first recognized in 1944 when the diagnostic significance of increased blood vitamin A was first demonstrated. Three years later a second example was recorded and the hard swellings in the extremities and bone changes detectable roentgenographically were first described. The skeletal changes were described in detail and the clinical picture was fairly well established in a single report of seven new cases in 1950 combined with the data on five cases reported earlier. There are undoubtedly many unrecognized cases of severe chronic vitamin A poisoning. What is believed to be the first case of chronic vitamin A poisoning in an adult was reported from New York City in 1951. An overenthusiastic woman on hearing from a "nutrition commentator" on a radio broadcast that vitamin A is "good for alleviating dry throats and a prophylaxis for colds" began a daily

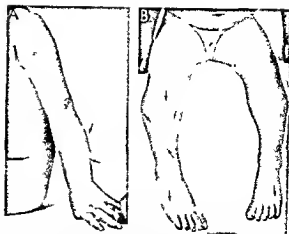


Fig. 8 725—Soft tissue swellings in hypervitaminosis A five weeks after onset. A, suprailiac swelling of the left forearm. There was a similar swelling in the right forearm. B, pretibial swelling on the right shank and symmetrical swelling over the 5th metatarsals in both feet. This girl 21 months of age had received 1 teaspoonful of alium percomorphum daily for nine months.

intake of 600 000 units of the concentrate and continued for 18 months, with occasional supplemental spoonfuls of 1–2 000 000 units when impending dry throat or colds were suspected.

In Woodward's patient who was poisoned during the first weeks of life from the administration of 70 000 I U daily from birth, the anterior fontanel bulged at 2 months of age, and he then suffered from hyperirritability, hyperesthesia, alopecia and tender hyperostoses of the clavicles and one parietal bone. This must be the youngest patient ever to be poisoned by vitamin A, and it is interesting that cranial thickenings as well as increased intracranial pressure developed. Of the three infantile patients reported by Turrell and Pierson, none had cortical hyperostoses but all had radiographic rickets.

The early clinical features in infants and children are not distinctive; they include only such common complaints as loss of appetite, itching and fretfulness. The diagnosis could probably often be established during this early phase of the poisoning by careful questioning regarding excessive intake of vitamin A and, possibly, by finding an increase of blood vitamin A content. The prevalence of mild vitamin A poisoning is unknown. Many weeks or months after the onset of these early signs, the clinical picture becomes diagnostic when hard tender lumps appear in the extremities (Fig. 8 725) and the underlying bones show cortical thickenings. At this stage the blood vitamin A content has always been increased several fold. Additional findings in some patients include fissures in the lips, loss of hair, dry skin, jaundice and enlargement of the liver. In most cases six months have elapsed between the beginning of excessive intake and the appearance of swellings in the extremities, which has occurred after the 12th month of life in all but one case. In some instances the latent period

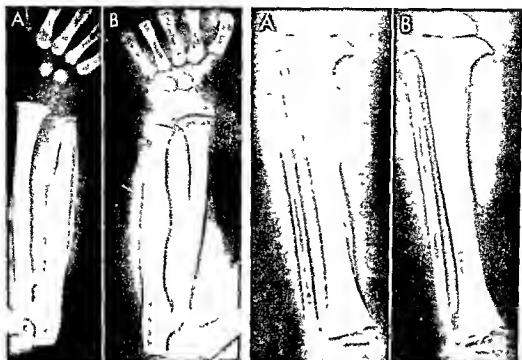


Fig. 8-726 (left) — Symmetrical cortical hyperostoses of the ulnas in poisoning due to vitamin A, five weeks after onset. Same patient as preceding. A, right; and B, left ulna. These films and the photographs in Figure 8-725 were made at the same time.

Fig. 8-727 (right) — Tibial cortical hyperostoses in the same

patient as the preceding. A, 5 weeks after onset. B, 10 weeks after onset and 5 weeks after stopping of vitamin A. The hyperostosis and spur on the medial aspect of the proximal end of the tibial shaft show increased mineralization in comparison with A. The patient had been well for four weeks.

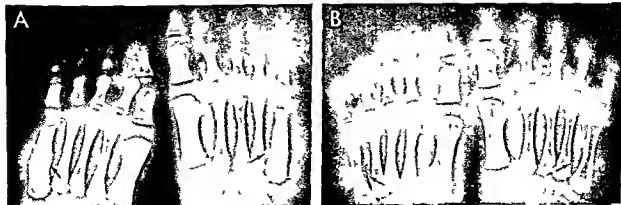
od has continued for as long as 15 months. Complete recovery follows rapidly on withdrawal of the concentrate. The clinical signs often subside within 72 hours. The high blood vitamin A level falls to normal within about six weeks. The cortical hyperostoses are gradually and slowly resorbed over a period of several months.

Roentgen changes in the skeleton have played an important role both in the recognition of vitamin A

poisoning as an entity and in the diagnosis of individual cases. In every case some of the tubular bones have been thickened (Figs. 8-726 to 8-728), both ulnas and some of the metatarsals have been consistently affected. The basic skeletal change is an external thickening of the cortical wall which is often wavy in outline when first seen. These cortical thickenings usually stop short of the ends of the shafts, the metaphyses and epiphyseal ossification centers are charac-

Fig. 8-728 — Symmetrical cortical hyperostoses in the 5th metatarsals of the same patient as preceding, with poisoning from excess of vitamin A. A, 5 weeks after onset. B, 10 weeks after onset and 5 weeks after stopping of vitamin A. The lesions in

comparison with A, have shrunk so that they are barely visible. The hyperostoses in these small bones disappeared much more rapidly after withdrawal of vitamin A than did those in the ulnas and tibiae.



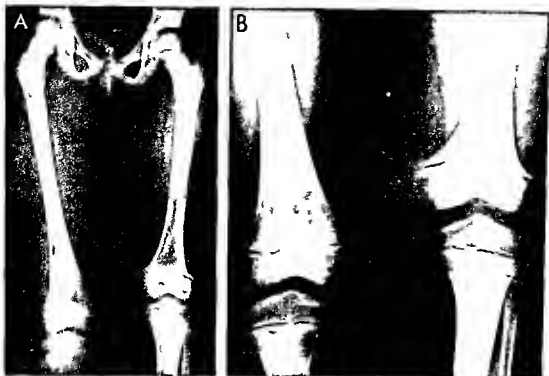


Fig. 8-729—Radiual changes from vitamin A poisoning. In A, three years after acute poisoning, the left femur is shortened several centimeters and its distal end fuses to join with a greatly enlarged epiphyseal ossification center. B, frontal projection of the knees of another patient shows enlargement of the distal

end of the femur and premature fusion of the shaft with the enlarged epiphyseal ossification center. The other bones were normal radiographically (Figs. 8-729 and 8-730, courtesy of Dr. Charles N. Pease, Chicago).

teristically normal. Microscopic structure of the cortical hyperostoses shows only an excess of normal subperiosteal bone with fibrous marrow in the neighboring spongiosa.

A permanent crippling sequel to vitamin A poisoning was found in several patients by Pease. Arrests in growth of the long bones caused severe and permanent shortenings of the affected bones, especially the femurs at their distal ends. The radiographic findings include cupping, shortening and splaying of the affected end of the shaft, hypertrophy of the contiguous epiphyseal ossification center and premature fusion of this center with its shaft (Figs. 8-729 and 8-730). In one girl who was acutely poisoned at 2 years of age the left femur was shortened 5 cm at age 18.

In two English patients described by Pickup the clinical and chemical manifestations of vitamin A poisoning were severe, but there were no radiographic changes in the skeleton, although both had pains in the arms and legs. In the first patient, a boy 6 years of age, large doses of vitamin A had been given for only six weeks; in the second, a girl 4 years of age, 350,000 IU of vitamin A had been given daily during two years in the treatment of ichthyosis. Oliver pointed out that radiographic changes in the skeleton have

been found in all infants and toddlers who had hypervitaminosis A, but in only one of nine older children and adults.

In contrast to the now numerous chronic poisonings by vitamin A concentrate, acute poisoning from this source is all but unknown. According to Bulls (cited by Caffey), children have occasionally swallowed as much as 50 cc (a whole bottle) of oleum percomorphum—3,000,000 units of vitamin A—at one sitting and without harm, save for transient nausea and vomiting. In the Arctic Eskimos and experienced travelers have long believed that livers of polar bears are toxic to man and other animals. Rodahl presented convincing experimental evidence that the toxic effect of polar bear liver is due to its richness in vitamin A. The liver of the bearded seal, the principal food of the polar bear, also has an exceedingly high vitamin A content, as does the liver of the Greenland fox. In two other species, the walrus and the snow hare, hepatic content of vitamin A is low. The highest hepatic concentrations of A were found in polar bears, and it is possible that some polar bears actually suffer from hypervitaminosis A. Kottlein (cited by Rodahl) found frequent hyperostoses in 122 bears examined by him at necropsy.

The medical facts are conclusive vitamin A concentrates are probably superfluous certainly expensive and potentially toxic preparations which should not be placed in the hands of mothers for daily feeding to healthy children. Medical control of vitamin A administration at home will be difficult because the public gets most of its information concerning the magic of vitamins from commercial advertising and too many physicians learn about the most recent vitamin advances from salesmen of pharmaceutical houses. Commercial advertising is understandably designed to create public belief that there is a wide spread need for daily supplementary intake of vitamin A that daily supplements prevent and cure a host of indefinite common complaints and that vitamin A concentrate is harmless. Physicians are almost helpless against the commercial exploitation which gushes endlessly from newspapers magazines radio broadcasts and television programs. According to

Fig 8730.—Residual changes from vitamin A poisoning in both femurs and the left tibia and fibula. In contrast the right tibia and fibula are normal as were the other bones. The ends of the shafts are splayed and cupped the ossification centers are enlarged and fusing prematurely with the shafts.



Culver the annual sale of costly high potency vitamin preparations increased 200% between 1945 and 1947 from 15 to 45 million dollars. The public has long been overstimulated on the need for and the safety of vitamin A concentrate and it will be exceedingly difficult for individual physicians to protect even their own patients from overdosage and poisoning. However until the whole truth becomes available to the public all authentic cases of vitamin A poisoning should be carefully recorded and widely published in medical literature.

REFERENCES

- Caffey J. Chronic poisoning due to excess of vitamin A. *Pediatrics* 5:672 1950 also *Am J Roentgenol* 65:12 1951.
 ———. Hypervitaminosis A. *Am J Roentgenol* 67:818 1952 [editorial].
 Josephs H W. Hypervitaminosis A and carotenemia. *Am J Dis Child* 67:33 1944.
 Knudson A G Jr and Rothman P E. Hypervitaminosis A. A review with a discussion of vitamin A. *Am J Dis Child* 85:316 1953.
 Pease C N. Focal retardation and arrestment of growth of bones due to vitamin A intoxication. *JAMA* 182:980 1962.
 Pickup J D. Hypervitaminosis A. *Arch Dis Childhood* 31:229 1956.
 Toomey J A and Morrisette R A. Hypervitaminosis A. *Am J Dis Child* 73:473 1947.
 Turrell R and Pierson B. Chronic vitamin A intoxication in infants. *Acta paediat* 50:319 1961.
 Woodward W K et al. Acute and chronic hypervitaminosis in a 4-month old infant. *J Pediatr* 59:260 1961.

Acute poisoning due to vitamin A causes acute hydrocephalus as measured by bulging of the anterior fontanel but without adequate increase in pressure of the cerebrospinal fluid to explain the conspicuous bulging. Acute poisoning usually follows a single massive dose of vitamin A of several hundred thousand units. Bulging of the fontanel is evident within 12 hours and usually has disappeared after 36 hours. Vomiting is the principal clinical disturbance. There are no residuals. Ocular fundi and cerebral electroencephalograms are normal. In one infant said to have ingested large amounts of vitamin A films of the skull showed widening of the coronal suture.

Three girls 14, 15 and 16 years of age studied by Morrice took 90 000–200 000 units of vitamin A daily for the treatment of acne and developed signs of increased intracranial pressure, bone pain, alopecia, hypomenorrhea and rhagades, all of which disappeared when vitamin A was stopped. Other examples of pseudotumor cerebri have been recorded.

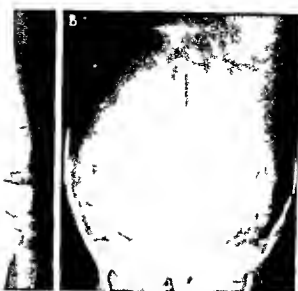
REFERENCES

- Marric J and See G. Acute hypervitaminosis A of the infant. *Am J Dis Child* 87:731 1954.
 Morrice G Jr et al. Vitamin A intoxication as a cause of pseudotumor cerebri. *JAMA* 173:100 1960.

VITAMIN D POISONING may be acute or chronic. Massive dosage (4–18 000 000 units daily) may cause death or severe or slight illness within three to nine



Fig 8-731—Fetal vitamin D poisoning in a boy 9 years of age who had diabetes mellitus and had been on a high vitamin D diet as part of his general treatment. In A, in the metaphyses of all of the bones at the knees is a series of radiolucent and radiopaque



transverse bands. The epiphyseal ossification centers are not affected. In B, Towne projection of the skull, the falx cerebri and tentorium cerebelli are affected.

days (Ruziczka). Vomiting followed by dehydration and high fever are common in the severely ill. Other manifestations in some patients include coma, convulsions, abdominal cramps, and bone pain. In chronic poisoning, the common early symptoms are lassitude, thirst, anorexia, and urinary urgency with or without polyuria. Later symptoms are vomiting, diarrhea, and abdominal discomfort. Renal damage with renal calcification is due to the excretion of increased lime through the kidneys. The urine contains albumin, casts, blood, and an excess of lime. The blood has increased calcium and phosphate. The radiologic changes include metastatic calcifications in the media of blood vessels, kidneys (especially the tubules), heart, gastric wall, alveoli of the lungs, bronchi, and adrenals. In the long bones (Fig 8-731), the initial change is an increase in depth of the provisional zones of calcification, followed by cortical thickening and later osteoporosis of the skeleton with deep zones of diminished density in the ends of the shafts, often alternating bands of increased and diminished density.

It is possible that the chronic idiopathic hypercalcemia of infants is due to the excessive ingestion of vitamin D over long periods by infants who are slightly sensitive to this vitamin. Excessive absorption of calcium from the alimentary tract is the probable causal mechanism. Creery and Neil demonstrated in Belfast that infants were actually receiving two to three times the dosages of vitamin D recommended by physicians.

The discovery of supra-aortic stenosis in association with idiopathic hypercalcemia and the

association of hypercalcemia with several different forms of vascular anomalies indicate that vitamin D excess in the mother prior to parturition may be an important cause of congenital malformations of the cardiovascular systems in the fetus. Friedman and Mills demonstrated disturbances in the development of the facial bones and calvaria (dental malocclusions, microcephaly, and premature synostosis of sutures) after an injected antirachitic substance crossed the placenta and raised the vitamin D levels in newly born rabbits.

REFERENCES

- Chaplin H, Jr, et al. Vitamin D intoxication. *Am J M Sc* 221:369, 1951.
- Christensen W R, et al. Skeletal and periarticular manifestations of hypervitaminosis D. *Am J Roentgenol* 65:27, 1951.
- Creery W and Neil D W. Intake of vitamin D in infancy. *Lancet* 1:944, 1961.
- Friedman W F and Mills L F. The relationship between vitamin D and the craniofacial and dental anomalies of the supra-aortic stenosis syndrome. *Pediatrics* 43:12, 1969.
- Ross S G. Vitamin D intoxication in infancy. *J Pediatr* 41:815, 1952.
- Rowe R D and Cooke R E. Vitamin D and craniofacial and dental anomalies of supra-aortic stenosis. *Pediatrics* 43:1, 1969.
- Ruziczka O. Injuries due to overdosage of vitamin D. *Wien. klin. Wchnschr* 64:964, 1952.
- Swoboda W. Roentgenologic symptoms of vitamin D intoxication in children. *Fortschr Röntgenstrahlen* 77:534, 1952.

VITAMIN C POISONING is believed to be a reality by Gordonoff and the overingestion of vitamin C danger



Fig 8 732.—Solitary external osteochondroma (cartilaginous exostosis). A, pedunculated osteochondroma of the femur. B, broad based (flat) osteochondroma of the humerus.

ous. He found guinea pigs especially prone to scurvy if they had been previously maintained on high intakes of vitamin C. In the siege of Leningrad those who had previously had large intakes of vitamin C developed scurvy in the greater numbers.

REFERENCE

Gordonoff T. Misused vitamin therapy. *Therapies* p 4. 1960.

BONE TUMORS

Neoplasms of bone are not so important in infants and children as they are in adults. Malignant primary

bone tumors are exceedingly rare in infants and are rare during the entire first decade of life. Many pediatricians do not encounter a single primary skeletal neoplasm in their own patients during a lifetime of busy practice. Precise and conclusive radiographic evaluation of some of the important tumors is not to be expected owing to the uncertainties of microscopic diagnosis and the frequent differences of opinion of the experts on the significance of primitive connective tissue cells. Uncertainties in the radiographic interpretation of the micropathology are the rule rather than the exception. Early biopsy is essential for early diagnosis and effective treatment. However, the biopsy findings are often not conclusive, and the diagnosis may remain in doubt as to whether the lesion is neoplastic or inflammatory, and if conclusively neoplastic whether it is benign or malignant. For authoritative and detailed information on the morbid anatomy the reader is referred to Jaffe's *Tumors and Tumorous Conditions of the Bones and Joints*.

BENIGN OSTEOLASTOMAS are rare, they are found most frequently in the spine and short tubular bones. They are made up of a varying mixture of primitive osseous tissue and osteoid in which osteoblasts are abundant. The patients are usually in the second and third decades of life. The radiographic picture is not specific; the osteoid and vascular parts are radiolucent in opaque bone.

SOLITARY BENIGN CHONDROMAS are common. They grow from proliferative cartilage cells derived from the neighboring epiphysis. When the tumor extends outside from the cortical wall it is called a *solitary cartilaginous exostosis*, and when it grows inside the cortical wall in the medullary cavity it is called a *solitary enchondroma*. The latter develop most often in the short and long tubular bones of the extremities.

Fig 8 733.—External osteochondroma of the right femur and a chondroma in the cortex of the left femur of a patient 11 years of age.



As the cartilaginous mass expands asymmetrically in the medullary cavity, it dilates the cavity and thins the cortical wall from the inside at the same level. The radiolucent tumor cartilage, the thin cortical wall and dilated medullary cavity are all evident in films (Figs 8 734, 8 733 and 8 743). Focal calcifications of variable sizes are often visible in the radiolucent mass. Malignant conversion to chondrosarcoma may occur in the larger tubular bones but is rare in the short tubular bones of the hands and feet.

Solitary cartilaginous exostosis is one of the most common of tumors in the growing skeleton. Strangely, these tumors do not develop in the fetal skeleton and are virtually nonexistent until the 2nd year of postnatal life. This suggests that some factor from the mother crosses the placenta and suppresses the growth of these tumors in the fetus, leaving the fetus with this factor before birth in high concentration which gradually diminishes after birth with advancing age until, at the 12th to 18th month its concentration is low enough to permit the tumor to begin to grow. Radiographically, the exostoses appear in a great variety of sizes and shapes—slender and bulky, pointed and blunt sessile and pedunculated rough and smooth (Figs 8 732 and 8 733). The segment of the shaft from which the exostosis grows is usually widened due to failure of constriction (Fig 8 734), the epiphyseal ossification center is not affected. The exostosis is covered with periosteum which is continuous with the periosteum of the shaft. The long axis of the exostosis is in the plane of greatest muscular pull and is always directed obliquely away from the end of the shaft. The tumor grows from a proliferative cap of cartilage on its tip, by a growth mecha-

nism similar to that at the cartilage shaft junction of a growing long bone. When the individual reaches maturity, growth ceases in the long bones and in the exostosis as well. There may be no clinical complaints, or swelling, pain and limitation of motion may be evident. When an exostosis impinges on blood vessels or nerves, it may cause secondary vascular and neural manifestations. Conversion of an exostosis to sarcoma is rare and is said to occur only after puberty. In contrast, sarcomatous conversion is common in multiple hereditary exostoses in both the young and the old. Cole and Dartre encountered benign exostoses in the sites of earlier irradiation in eight children.

PRIMARY CHONDROSARCOMA is rare before age 20, and the femur is the common site. When these tumors grow inside the cortical wall of the shaft in the medullary cavity they are called *central chondrosarcomas*, when they grow externally from the cortical wall they are called *peripheral chondrosarcomas*. The former are the more common. Microscopic diagnosis is uncertain, and their rapidity of growth and expansion may be just as important in determining their malignancy as their microscopic appearance. The cartilaginous tumor in bone produces a radiolucent image in which there are often foci of calcification to suggest a cartilaginous origin. The cortex usually bulges externally and is thinned from the inside at the site of the tumor. The peripheral chondrosarcoma is malignant conversion of a solitary cartilaginous exostosis; the radiographic examination shows the excessive growth and partial destruction by the malignant tissue. In rare cases, chondrosarcomas arise in the soft parts adjacent to the skeleton (Fig 8

Fig 8 734—Solitary broad based cartilaginous exostosis of the lower end of the femur appears as a radiolucent defect in frontal projection (A) but the cupped exostosis is visible in lateral projection (B). The ventral cortical wall only has failed to constrict and is bowed ventrad. The bowed ventral wall is also thin. This lesion could also be classified as a juxtacortical chondroma. (See Figs 8 744 and 8 747.)

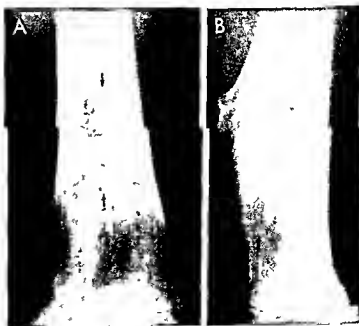
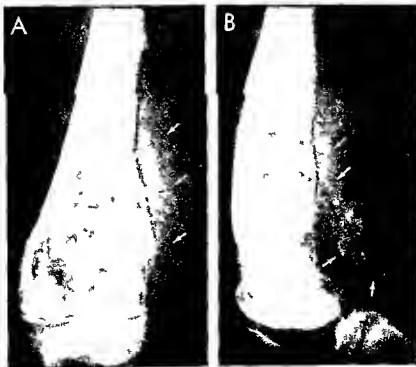




Fig 8 735 Chondrosarcoma in the medial segment of the ankle region in a boy 3 years of age. At surgical exploration a mass of bone and cartilage completely separated from the epiphyseal cartilage was found in the soft tissues outside the capsule of the tibio-talar joint. Microscopic changes were characteristic of malignant cartilaginous growth. Chondrosarcomas are rare in younger children. (Courtesy of Dr Barbara Stimson Poughkeepsie, NY.) These changes resemble those seen in some cases of dysplastic epiphyseal sarcomas (see Fig 8 347).

Fig 8 736 —Osteogenic sarcoma, osteoblastic type in a boy 11 years of age. A frontal and B lateral projection. The distal end of the femoral shaft is filled with an irregularly radiolucent multiloculated mass. The overlying cortex is partially destroyed on the medial posterior aspect where the radial artery is palpable.



735) without precedent exostosis or enchondroma.

Fibrosarcomas are rare and usually affect young or middle aged adults. The femurs and tibias are commonly involved. The basic radiographic change is a patch of diminished density in opaque bone due to the destruction and replacement of spongiosa and cortical wall by fibrous neoplasm. The medullary cavity is dilated and the cortical wall eroded on its internal edge. The radiographic diagnosis is never conclusive. Final diagnosis must be made from microscopic changes in the tumor.

Hemangiosarcomas are rare and the exact age distribution is not known to me. They produce radiographic changes similar to the fibrosarcomas and the diagnosis can be made only by microscopic study.

Osteogenic sarcoma is the most common primary malignant tumor which grows in the bones of children. Most of these neoplasms are found in patients in their second and third decades. Prior to the 6th year of life osteogenic sarcomas are very rare. In all but a few cases the femurs or tibias or humeri are affected at one of their ends. Pain of short duration followed by local swelling is the cardinal and often the only complaint. At the time of recognition of their disease the patients are in good health with normal stature and good nutrition. All laboratory findings are normal save for the serum alkaline phosphatase ac-

extends beyond the cortex into the extraosseous neoplastic mass in the soft tissues of the popliteal space is a large irregular mass of neoplastic bone. The large radiolucent segments of the tumor which dilate the medullary cavity are made up of chondroid and osteoid matrix with meager collagen content.



Fig 8 737 - Osteogenic sarcoma (macroscopic diagnosis) of the right femoral shaft in a girl 6 years of age. Above much of the tumor is external to the shaft; below replacement of compacta and spongiosa by the osteoid and chondroid matrix of the neoplasm has produced extensive irregular rarefaction. The reader will appreciate the wide variety in radiographic appearance of different osteogenic sarcomas by comparing Figures 8 736 to 8 739.

tivity which is only moderately increased in most patients. Greater increases in alkaline phosphatase usually mean a rapidly growing, highly malignant primary tumor or metastatic spread. This spread occurs by way of the blood stream. Lymphatic metastases to regional nodes are rare. Blood-borne metastases lodge in the lungs most frequently, with only occasional spread to other bones or the viscera.

The cardinal radiographic finding is calcification of the tumor tissue well beyond the normal limits of the bone in which the neoplasm is growing (Fig 8 736) with thickenings of the regional cortical wall externally (Fig 8 737). Often the extracortical tumor tissue has radial streaks of increased bone density. On the other hand, in some highly malignant osteogenic tumors the malignant osteoblasts replace bone but produce little or no bone themselves (Fig 8 738); they produce primitive osteoid. The actual radiographic picture has a wide spectrum, although most patients present a highly suggestive pattern of changes. Tissue specimens taken at biopsy usually have a high content of alkaline phosphatase but with no increase in acid phosphatase activity. The latter is high in giant cell tumors.

Juxtacortical osteogenic sarcoma grows from the external edge of the cortical wall in contrast to the standard osteogenic sarcoma which grows from inside the medullary cavity outward. Most of the juxtacortical tumors grow slowly, metastasize late, and have low malignant potentials. Patients younger than 15 years are rarely affected, and in more than half of all patients the distal end of the femur is the site of involvement. Mild pain may be felt for years before the diagnosis is made. In the film, an opaque mass of bone density in the soft tissues near the distal end of the femur fuses to the edge of the femur on a broad base. There is little or no bone destruction. The malignant lesion simulates a sessile peripheral osteochondroma radiographically. Biopsy is essential for definitive diagnosis. Malignant masses of primitive connective tissue which contain bone and cartilage may grow near bones without direct attachment to them. These are called *extraskeletal osteogenic sarcoma*.

Neuroblastomas in growing bones are usually multiple, metaphyseal in location, and associated with a primary tumor in the adrenals or sympathetic ganglia. Occasionally, however, a solitary neuroblastoma (Fig 8 739) develops in a single bone.

Multiple sclerotic osteogenic sarcomas were found

Fig 8 738 - Osteogenic sarcoma, osteoid type, in a girl 12 years of age. The spongiosa and cortex of a deep terminal segment of the shaft are extensively destroyed. The adjacent epiphysis is not affected. Absence of dilation of the shaft is noteworthy. There is some cortical thickening, but no roentgen evidence of neoplastic osteogenesis. The tumor was made up almost exclusively of osteoid and chondroid matrix.



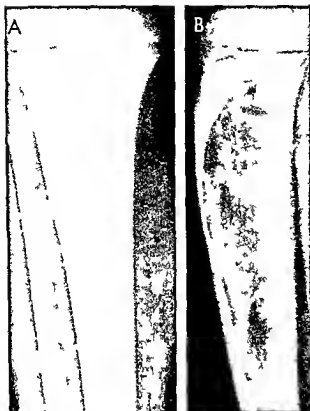
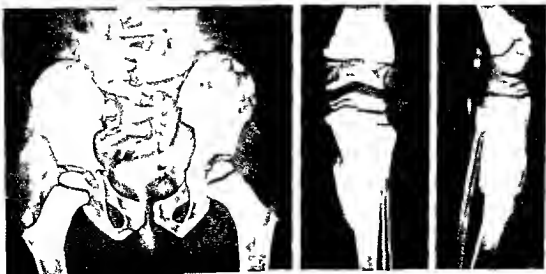


Fig. 8 739 Unusually large solitary radiolucent intramedullary neuroblastoma (macroscopic diagnosis) in the right tibia of a boy 9 years of age. The expanding tumor has dilated the medullary cavity, abraded the overlying cortical walls and replaced the more opaque bone with more radiolucent neoplasm (necrosis). A: Antal; B: late al p oject ions.

Fig. 8 740 Multiple sclerotic osteogenic sarcoma in the pelvic bones, femurs and right tibia of a 15 years of age. Sclerotic bony masses are also evident in the soft tissues behind the knee.



in a girl 5 years of age by Moseley and Bass. Multiple images of intense ivory density were scattered through flat and tubular bones (Fig. 8 740). They considered this a distinct radiographic entity because they found almost identical radiographic descriptions in three other cases: two in girls 7 and 8 years of age and one in a boy of 15. The two patients of Singleton and colleagues were a girl and a boy 6 and 5 years of age. The number, size and distribution of the sclerotic osteogenic sarcomas suggested that these lesions might be multicentric rather than metastatic.

REFERENCES

- Cole A. R. C. and Dartt J. M. M. Osteochondromata after irradiation in children. *Pediatrics* 32: 285, 1963.
- Dahlin D. C. and Coventry M. D. Osteogenic sarcoma. A study of 600 cases. *J. Bone & Joint Surg.* 49-A: 101, 1967.
- Huyes A. B. et al. Osteogenic sarcoma in children. *J.A.M.A.* 174: 1174, 1960.
- Jaffe H. L. Tumors and Tumorlike Conditions of the Bones and Joints (Philadelphia: Lea & Febiger, 1958).
- Moseley J. E. and Bass M. H. Sclerosing osteogenic sarcomatosis. Report of a case. *Radiology* 66: 41, 1956.
- Singleton E. B. et al. Sclerosing osteogenic sarcomatosis. *Am. J. Roentgenol.* 88: 483, 1962.
- Weinfeld F. S. and Dudley R. D. Jr. Osteogenic sarcoma. *J. Bone & Joint Surg.* 44-A: 269, 1962.

BENIGN NONOSTEOGENIC TUMORS - Bone cysts -

These are localized benign fibrocystic destructive lesions which have no power of bone production. The spongiosa at the end of the shaft is destroyed and replaced by a mass of fibroblasts, capillaries, macrophages and giant cells. Central liquefaction necrosis of the fibrous mass gives rise to cysts filled with serous or serohemorrhagic fluid and surrounded by a thin fibrous wall which usually contains some giant cells. Thus localized fibrocystic lesion is also called

Similar sclerotic lesions were also present in the clavicles and the tubular and round bones in the arms and hands (Redrawn from Moseley and Bass).

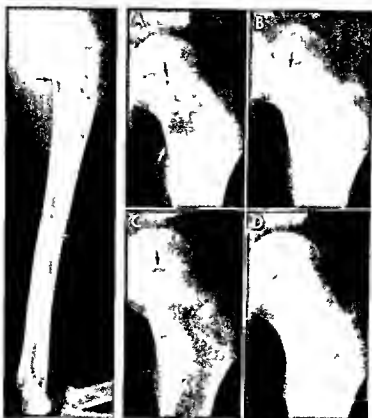


Fig 8-741 (left)—Simple bone cyst in the proximal end of the humerus of a boy 16 months of age from which 30 cc of yellowish fluid was aspirated. The overlying cortex is thinned from within and the spongiosa is destroyed and replaced by fibrous tissue and fluid. The cyst extends to the provisional zone of calcification but does not break through, and the epiphyseal ossification center is not affected. There are incomplete fractures in the thinned cortex.

Fig 8-742 (right)—Serial changes during healing of a simple

bone cyst in the femoral neck of a boy 6 years of age. **A**, the untreated cyst with a narrow zone of normal bone 3 mm deep between the proximal edge of the cyst and the provisional zone. **B**, 2 months later, after curettage and insertion of bone chips. The zone of normal bone between cyst and provisional zone has deepened to 7 mm. **C**, 5 months after **A**. The zone of normal bone has increased to 11 mm in depth and the cyst is smaller. **D**, 19 months after **A**. The zone of normal bone is now 22 mm deep and the cyst is about a fourth its earlier size.

localized osteitis fibrosa cystica. Simple bone cysts represent bone destruction caused by growing intraosseous hemangioma with local hemorrhage and bone resorption. As the lesion enlarges, the medullary cavity of the bone is dilated and its overlying cortex is eroded on the internal aspect. There is no new bone formation except in the case of pathologic fracture when callus formation causes local cortical thickening. The cyst may also elongate with increasing age until it occupies several inches of the terminal segment of the shaft. An interesting and characteristic feature of the simple bone cyst is its failure to extend into the epiphysis directly adjacent to it. As a result the proliferating cartilage remains intact and epiphyseal growth is not affected.

Jonathan Cohen in a study of the drainage of an opaque contrast agent injected into two simple bone cysts found that there was no drainage by way of the metaphyseal veins, which led him to the hypothesis

that obstruction to metaphyseal drainage may be the basic cause of formation of simple bone cysts. Cohen had shown previously that the chemical elements in the fluid in simple bone cysts are similar to those in blood serum. He pointed out that one weakness of his hypothesis is the fact that drainage from the marrow cavity of the proximal end of the humerus has not been satisfactorily demonstrated radiographically using opaque contrast agents in normal children.

Such cysts (Figs 8-741 and 8-742) are found in the metaphyses of the larger tubular bones, commonly in the proximal ends of the femur and humerus. They cast a shadow of diminished density owing to the local destruction of the spongiosa and cortex (Fig 8-743). In the case of large cysts, the end of the shaft is dilated and the surrounding cortex is eroded to paper thinness, sometimes to complete atrophy and pathologic fracture. Remnants of the spongiosa and ridges of callus may give rise to a trabeculated multilocular

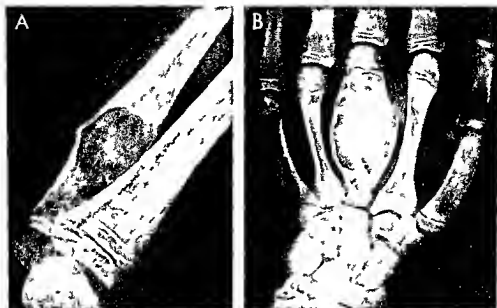


Fig 8-743—A bone cyst (macroscopic diagnosis) in the distal end of the shaft of the humerus. The medullary cavity is dilated and filled with a mass of water density in which no bone is visible. The overlying cortex is thinned due to pressure atrophy on its internal aspect. In B, the 3rd metacarpal of a girl 11 years of age

is dilated and filled with a radiolucent mass of water density which appears to be multilocular. The cortex is atrophic from internal erosion. The adjacent epiphysis is enlarged. The macroscopic nature was not proved. Bone cyst, aneurysmal bone cyst, and aneurysmal bone cyst were considered among the possibilities.

Fig 8-744—Epidermal cyst (epidermoid) of the distal phalanx of digit 4 of a girl 6 years of age. The phalanx is enlarged and dilated with internal erosion of the cortex and spongiosa. Opaque bones are replaced by a radiolucent mass which occupies more than two-thirds of the shaft. The apophyseal ossification centers are not affected. (From Hensley)



roentgen pattern. Large cysts of this type may develop in the body of the calcaneus.

Several lesions in the metaphyses may cast cystlike shadows in the ends of the shafts of tubular bones, namely physiologic cortical defects, desmoplastic fibromas of bone, bone abscesses, chondromas, osteolytic sarcomas, monostotic osteitis fibrosa cystica, eosinophilic granulomas, giant cell tumors, nonosteogenic fibromas, and parasitic cysts. The osteolytic sarcomas destroy the end of the shaft with little or no expansion of it. Giant cell tumors are rare in children and characteristically involve the epiphyses as well as the metaphyses. Eosinophilic granulomas and localized osteitis fibrosa cystica produce the same cystic rarefaction but do not usually dilate the shaft. In the early phases of all of these destructive cystic metaphyseal lesions, a conclusive roentgen diagnosis cannot be made and biopsy should be resorted to without delay. Even in biopsy specimens, which often do not represent the whole cystic lesion, the macroscopic findings may be judged differently by experienced pathologists.

Epidermoid cysts of a terminal phalanx of a digit of the hand were reported by Hensley and Byers in 1966. In Hensley's patient (Figs 8-744 and 8-745), a girl 8 years of age, pain and swelling had developed four months before radiographic study (Fig 8-744). Curettage revealed white caseous material surrounded by a cyst wall. The cortex was eroded through on the ventral aspect. Healing was prompt after insertion of bone chips in the surgical defect. The affected finger had not been injured prior to onset of pain. Hensley

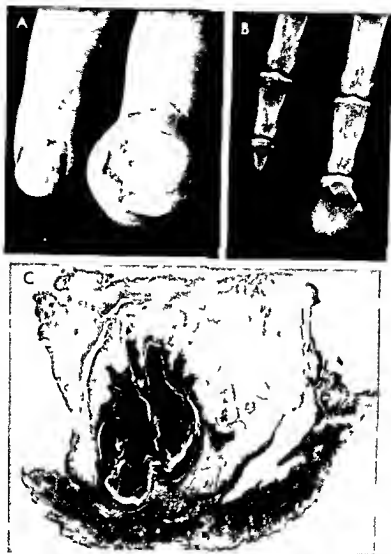


Fig 8-745—Epidermoid cyst (epidermoidoma) of the distal phalanx of digit 3 of a laborer, 32 years of age who had cut his finger on a sharp stone. The changes extended into the bone structure of the distal phalanx. The external wound healed and closed after three weeks, but the end of the finger slowly swelled and

after seven years reached the size in (A) and the destruction of the phalanx in (B). Macroscopic section (C) of the bone disclosed a well-circumscribed, multiloculated cyst lined with squamous epithelium and filled with keratin flakes (From Byers et al.)

cited this as the first example of epidermoid cyst in the long bones of a preadolescent patient. In the same year Byers and associates reported a case in an adult (Fig 8-745).

REFERENCES

- Byers P, et al: Epidermoid cysts of the phalanges. *J Bone & Joint Surg* 48-B:577, 1966
 Cohen J: Etiology of simple bone cysts. *J Bone & Joint Surg* 52-A:1493, 1970
 Cohen P and Goldenberg R R: Desmoplastic fibroma of bone. *J Bone & Joint Surg* 47 A:1620, 1965

- Carreau G J, et al: Solitary unicameral bone cyst. *J Bone & Joint Surg* 36-A:267, 1954
 Graham J: Solitary unicameral bone cyst. *Bull. Hosp Joint Dis* 13:106, 1952
 Hensley C D Jr: Epidermoid cyst of the distal phalanx occurring in an eight year-old child. *J Bone & Joint Surg* 48-A:946, 1966

Periosteal juxtacortical chondroma (Lichtenstein and Hall) develops as a slowly growing lump over one of the long bones. Some are painful and tender, while others are painless. They originate below the periosteal connective tissue and produce local cortical

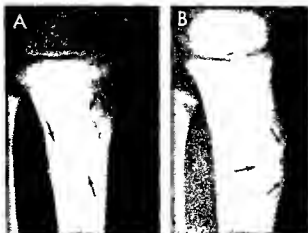
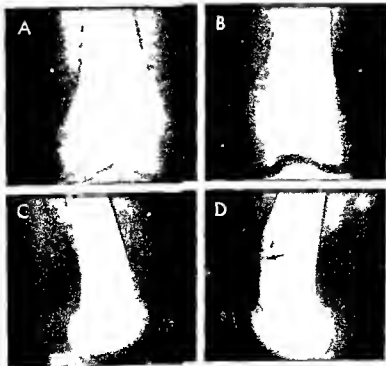


Fig 8746 — Painless periosteal juxtacortical chondroma of the tibia of a boy 20 months of age. A, frontal; and B, lateral projections. The cortex is thickened externally and sclerosed with a craterlike defect in the summit of the bony thickening. Excision disclosed a mass of cartilage nestled in the apical defect which was lobulated hyaline and basophilic.

Fig 8747 — Juxtacortical chondroma (microscopic diagnosis) of the femur of a girl 13 years of age. A and C, asymptomatic right knee; B and D, painful left knee which had been twisted one week before. The lesion is barely visible in frontal projection (B) as a poorly defined patch of diminished density, but is clearly visible in lateral projection (D). At the end of the shaft the ventral cortical wall is slightly thickened and acrotic external to which is a radiolucent mass of cartilage which sits on a thin sclerotic base and above which the cortex is thickened and sclerotized.



thickening by stimulation of the osteogenetic periosteal layer. The apex of the thickening is scooped out into a craterlike depression which is occupied by the radiolucent chondroma (Fig 8746). Lesions of this type have been found on such large tubular bones as the femur (Fig 8747), tibia and humerus and also on the shorter tubular bones of the hands and feet. Block excision of the thickening with its mass of cartilage in the summit brings permanent cure.

REFERENCES

- Jaffe H S: Juxtacortical chondromas. *Bull Hosp Joint Dis* 17:20, 1956
 Lichtenstein L and Hall J E: Periosteal chondroma. A benign cartilage tumor. *J Bone & Joint Surg* 34-A:691, 1952

Chondromyxoid fibroma of bone was reviewed in 20 children 5–10 years of age and in 57 aged 10–19 years by Feldman and colleagues. The peak age incidence is in the second and third decades. The femur and tibia are the most frequently affected bones; occasional examples were found in the fibula, the bones of the upper extremity, ribs, pelvis and feet. A vertebral lesion was found in a single patient. In children pain, swelling and limitation of motion were the common and often severe complaints; these serve to differentiate chondromyxoid fibromas from benign

lesions. In lateral projection (D), at the end of the shaft the ventral cortical wall is slightly thickened and acrotic external to which is a radiolucent mass of cartilage which sits on a thin sclerotic base and above which the cortex is thickened and sclerotized.



Fig 8-748—Benign epiphyseal osteochondroma in a boy 5 years of age. The cartilage in the medial femoral condyle of the right femur is swollen and contains several ossification centers. At 3 years of age the cartilage was already swollen but did not

contain ossification centers. The radiographic appearance resembles that of dysplasia epiphyseal hemimelica; these two conditions cannot be satisfactorily differentiated at the ends of a long bone (see Fig 8-347).

cortical defects which are consistently asymptomatic. Subperiosteal chondromyxoid fibromas produced external abrasion of the cortical wall and simulated early small fibrous cortical defects. The intramedullary lesions were characteristically sharply defined oval or round radiolucent patches which varied from pinhead size to the entire width of the medullary cavity. Grooves and ridges in the overlying cortical wall produce false trabeculations radiographically. During the later phases when the tumors are large, the contiguous cortical wall may bulge externally. The periosteum, however, remains intact. Calcification in the tumors is rare (2%) as is pathological fracture (3%). Radiographically chondromyxoid fibromas resemble several other lesions (benign fibrous cortical defects, nonosteogenic fibromas, fibrous dysplasia, enchondromas, simple bone cysts, and proliferative reticulosis eosinophilic granuloma). Satisfactory diagnosis can be made microscopically.

REFERENCE

Feldman F *et al*: Chondromyxoid fibroma of bone. *Radiology* 94:249, 1970

Epiphyseal osteochondroma is a benign overgrowth of the epiphyseal cartilage in which separate supernumerary ossifications appear with advancing age (Fig 8-748).

REFERENCE

Donaldson J S *et al*: Osteochondroma of the distal femoral epiphysis. *J Pediatr* 43:212, 1953

Benign chondroblastoma usually grows in one femur or tibia at the knee or one humerus at the shoulder. The lesion originates in the epiphyseal cartilage but may extend later to the contiguous meta-

physis. It is virtually nonexistent during the first decade of life but common during the second decade. The most common site of growth is the greater trochanter of the femur and then the greater tubercle of the humerus (Fig 8-749). The basic radiographic lesion is the replacement of bone by more radiolucent chondroid tumor tissue and blood vessels. Focal calcifications may supplant the radiolucent patch and blur its edges (Fig 8-750).

Fig 8-749—Benign chondroblastoma (microscopic diagnosis) in the humerus of a girl 12 years of age. In the humeral head is a large but poorly defined patch of diminished density. In its lateral half, in this radiolucent segment, is a large and small sclerotic patch as a result.



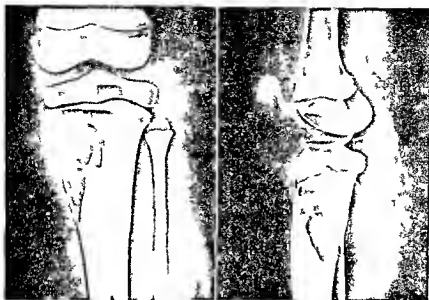


Fig 8 750 — Chondroblastoma of bone benign type (microscopic diagnosis) in the tibia of a girl 9 years of age who complained of pain in the knee for six months. Destruction limited

to the shell, although the tumor is in contact with the epiphyseal cartilaginous plate. (Redrawn from Sherman and Uzal.)

Fig 8 751 (left) — Aneurysmal bone cyst in the proximal end of the ulna of a girl 13 years of age who had complained of pain and swelling in the elbow for three months. A radiograph showing the dilated end of the ulna in which the thin shell of bone surrounds the relatively redolent tumors and many bony ridges and septa traverse the dilated medullary cavity. B, photograph of a longitudinal section of the ulna showing honeycomb of

bone surrounding the dilated vessels and vascular spaces. (From Barnes.)

Fig 8 752 (right) — Aneurysmal bone cyst of the ulna in an adolescent boy (microscopic diagnosis). The terminal segment of the ulna is dilated and contains a large redolent patch over which the cortex is thinned. The dilated segment was filled with hemorrhagic fibrous tissue. (From Lichtenstein.)

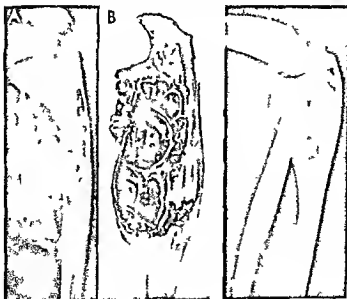




Fig 8 753 —Aneurysmal bone cyst in the body and neural arch of the C6 vertebra of a boy 10 years of age (microscopic diagnosis). He had had pain in the neck, worse at night, for two months.



Fig 8 754 —Aneurysmal bone cyst of the 4th metacarpal of a boy 10 years of age (microscopic diagnosis). The medullary cavity is dilated and the overlying cortex reduced to paper thickness. (Redrawn from Lichtenstein.)

Much of the right side of the body and the neural arch are destroyed. (Redrawn from Lichtenstein.)

Fig 8 755 —Aneurysmal bone cyst in the femur (microscopic diagnosis) of a girl 16 years of age who had had local pain and swelling for several weeks. The large defect does not extend into the epiphysis; a thin shell of bone, best seen in the caudal levels, outlines the lateral edge of the cyst.





Fig 8 756 —Aneurysmal bone cyst of the proximal end of the humeral shaft (macroscopic diagnosis). The proximal segment is dilated and the cortical walls are reduced to paper thickness. The spongy ossicles are replaced by material of water density. The metaphysis and proximal zone of calcification are slightly cupped. The epiphyseal ossification center is rarefied but not dilated and is probably not affected. The boy was 6 1/2 years of age.

REFERENCES

Jaffe H and Lichtenstein L. Benign chondroblastomas of bone. A re-interpretation of the so-called calcifying chondromatous giant cell tumor. *Am J Path.* 18:969 1942.

Fig 8 757 —Aneurysmal bone cyst of the atlas with cystic dilations of the spinous process which is surrounded by a thin shell

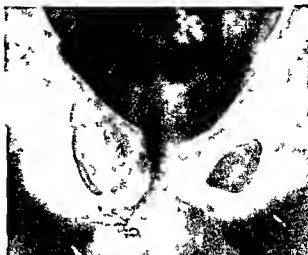


Fig 8 758 —Aneurysmal bone cyst (macroscopic diagnosis) in the right pubic bone of a boy 12 years of age. The bone is swollen and rarefied with dilatation of its medullary cavity and atrophy of its cortical walls.

Sherman R S and Uzel A R. Benign chondroblastoma of bone. Its roentgen diagnosis. *Am J Roentgenol* 76:1137 1956.

Aneurysmal bone cysts (hemangiomas) occur most frequently in children and young adults. The neural arches of the vertebrae and the shafts of the long bones are the most commonly affected sites. Jaffe suggested that the cysts result from hemorrhage followed by local resorption of bone. They consist of varying amounts of blood and connective tissue, with increase in the latter as the lesion gets older. The compacta is dilated locally by the cyst, which finally becomes limited by a thin shell of bone, which is the most characteristic radiographic finding (Figs

of bone in a girl 4 years of age who had had pain in the neck for three months (Redrawn from Taylor).



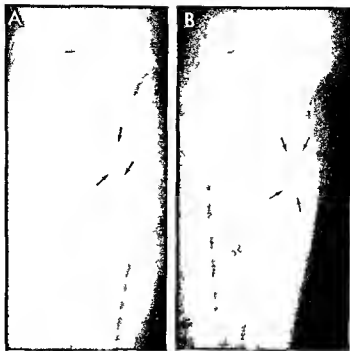


Fig 8 759—Osteoid osteoma (necrotic) in the tibia of a girl 4 years of age who had limped because of pain for eight months. A, anteroposterior projection; B, planogram focused 4 cm above the tibial top. The medial cortical wall is thickened ex-

ternally and the lesion is a small radiolucent patch in the medullary thickening—the nidus of osteoid trabecular bone. The ventral, dorsal and lateral cortical walls also show some external cortical thickening. (Proved by biopsy.)

8 751 to 8 754) In the ends of the femur and tibia aneurysmal bone cysts and benign cortical defects may be difficult to differentiate radiographically. Once diagnosed aneurysmal bone cysts should be removed immediately because of their great potential for rapid extensive destruction of bone (Figs 8 755 and 8 758). They should be looked for carefully radiographically when children have recurrent pain in the spine (Fig 8 757). We have seen a large aneurysmal cyst in the pubic bone (Fig 8 758).

REFERENCES

- Barnes R. Aneurysmal bone cyst. *J Bone & Joint Surg* 38-B 301 1956.
 Clough J R, and Price C H G. Aneurysmal bone cysts. Review of twelve cases. *J Bone & Joint Surg* 50-B 116 1968.
 Donaldson W F Jr. Aneurysmal bone cyst. *J Bone & Joint Surg* 44-A 25 1962.
 Jaffe H L. Aneurysmal bone cyst. *Bull. Hosp. Joint Dis* 11 3 1950.
 Lichtenstein L. Aneurysmal bone cyst. Observations on fifty cases. *J Bone & Joint Surg* 39-A 873 1957.
 Taylor F W. Aneurysmal bone cyst. *J Bone & Joint Surg* 38-B 293 1956.

Osteoid osteoma, according to Jaffe, is a small oval benign tumor of bone made up of osteoid and trabeculae of newly formed osseous tissue embedded in a substrate of highly vascularized osteogenic connective

tive tissue. It has been located in the spongiosa in some cases and in the corticis in others. Although the osteoid lesion itself rarely exceeds 1 cm in diameter, the reactive perifocal bone sclerosis which accompanies it may be several centimeters in its longest diameter. The characteristic roentgen findings include a small radiolucent shadow surrounded by extensive bony thickening and sclerosis (Figs 8-759 to 8-761). Heavy roentgen penetration is usually necessary for optimal visualization of the tiny osteoid osteoma encased in its heavy envelope of dense bone. Planigrams (Fig 8-762) are helpful in demonstrating the nidus more clearly, and this is essential for a satisfactory block biopsy, which must include the nidus. Planigrams should be resorted to in all cases in which the diagnosis is in doubt.

Sometimes an osteoid osteoma may appear and grow with little or no marginal hyperostosis; this is especially true in the neck of the femur, where the lesion is inside the articular cavity of the hip. At the proximal end of the femur, an intracapsular osteoid osteoma may sometimes be associated with diffuse inflammatory reaction in the neighboring synovium and other articular tissues, which includes villous hypertrophy of the synovium, dilatation of vessels and a cellular exudate of lymphocytes and plasma cells, all of which may suggest rheumatoid arthritis clinically and radiographically (Case Records of Mas-



Fig. 8-760.—Intracortical osteoid osteoma of the midshaft of the left tibia of a girl 15 years of age. A, frontal and B, lateral projections. The cortical walls are thickened and sclerotic both internally and externally. The radiolucent nidus (arrows) is located peripherally in the dorsal cortical wall (B).

sachusetts Gen. Hosp., case 36-1961. *New England J. Med.* 264:1053, 1961). Occasionally the regional hyperostosis is limited to a narrow strip in the margin of the contiguous bone, which has been called "ring sequestrum." The osteoid osteoma itself may become partially calcified and suggest a small sequestrum radiologically. This lesion occurs in children but is most common in adolescent boys and young men. The tibia and femur are most often affected and tubular bones of the hands and feet are common sites, especially the basal phalanges (Fig. 8-763) but osteoid osteoma has been found in all other bones save the ribs and calvaria. One of our patients had typical pulsating pain in the knee which worsened at night. The epiphyseal ossification center of the tibia was diffusely sclerotic in its lateral half which contained a radiolucent patch or nidus. Osteoid osteoma was not proved microscopically, but the clinical and radiographic findings were highly suggestive of an osteoid osteoma in an epiphyseal ossification center. Local pain which may be chronic and severe, is the only important clinical manifestation and this is promptly relieved by excision. The radiologist should



Fig. 8-761.—Typical osteoid osteoma (microscopic diagnosis) of the femur with a small radiolucent nidus (arrows) and regional sclerosis and thickening of the neighboring cortical wall. This boy 6 years of age had had severe pulsating pain in the right thigh for several months.

Fig. 8-762.—Osteoid osteoma in the ulna of a boy 3 years of age. A, standard film in which the sclerosis and swelling of the shaft are clearly visible but the nidus is not visible. B, planigram in which the nidus is clearly visible as well (arrow).



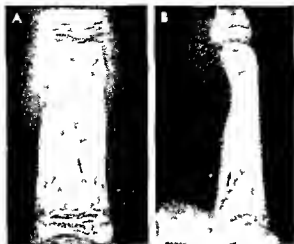


Fig. 8-763—Osteoid osteoma (intracortical) of the proximal phalanx of the index finger (macroscopic diagnosis). A, frontal and B, lateral projections. The radiolucent nidus (arrows) has a central patch of sclerosis which produces a bull's eye pattern. In B, the nidus and its surrounding segment of sclerosis is both in the ventral cortical wall of the phalanx.

remember that the clinical signs of pain may be present and persist for as long as two years before the radiographic changes become visible. Painful pseudoparalysis may cause muscular atrophy and suggest acute poliomyelitis and postpoliomyelitic muscular weakness and atrophy in some cases. The pains of osteoid osteoma often respond favorably to acetylsalicylic acid in small doses and suggest the rheumatic or rheumatoid state. It is evident that Garre's osteomyelitis sicca and osteoid osteoma are probably identical disorders.

It has become manifest with increasing experience that osteoid osteoma is not a rare disease during the first decade of life and that in many cases pain may be much less severe and much less protracted than in the first cases reported. Also it seems likely that the lesion is self limited and disappears spontaneously after variable periods. There is, for example, no case on record in which an adult had a persistent osteoid osteoma with the antecedent history suggestive of the lesion during childhood. In some cases the pain, lump and radiologic features have lasted for as long as six years.

REFERENCES

- Carroll, R. E. Osteoid osteoma of the hand. *J Bone & Joint Surg.* 35-A:888, 1953.
 Dahlin, D. C. and Johnson, E. W. Giant osteoid osteoma with report of 20 cases. *J Bone & Joint Surg.* 36-A:559, 1954.
 Freiburger, R. H. et al. Osteoid osteoma. Report of 80 cases. *Am. J. Roentgenol.* 82:194, 1959.
 Goldring, J. H. S. The natural history of osteoid osteoma with report of 20 cases. *J Bone & Joint Surg.* 36-B:218, 1954.
 Jaffe, H. L. Osteoid osteoma of bone. *Radiology* 45:319, 1945.
 Moberg, E. The natural course of osteoid osteoma. *J Bone & Joint Surg.* 33-A:166, 1951.

Purcell, H. M. et al. Osteoid osteoma in childhood. *Pediatrics* 9:290, 1952.

Seaman, W. B. The case of the painful ankle (osteoid osteoma of the calcaneus). *Hosp. Practice* p. 95, October 1968.

Sherman, F. S. Osteoid osteoma associated with changes in the adjacent joint. Report of two cases. *J. Bone & Joint Surg.* 29:483, 1947.

Fibrous dysplasia, monostotic type, may resemble neoplasms and bone cysts radiologically although it appears to be a dysplasia structurally. The medullary cavity is usually dilated with internal atrophy of the cortex at the same level in the shaft. Often the thinned cortex bulges sharply externally in compensation for the local increase in intraosseous pressure (see the involved bones in Fig. 8-396). At the site of this dilatation the medullary cavity is filled with a rubbery fibrous tissue in which are scattered innumerable newly formed trabeculae of immature bone. In some lesions islands of hyaline cartilage are also found. Actual cysts may form following local hemorrhage or degeneration which may also give rise to lipid laden macrophages and lead to the erroneous microscopic diagnosis of lipogranulomatosis of some type in some parts of some lesions so much immature

Fig. 8-764—Local radioblastic dysplasia (macroscopic diagnosis) of the femoral neck of a girl 8 years of age. The large radiolucent patch represents replacement of opaque bone by radiolucent fibrous tissue with marginal sclerosis laterally.





Fig 8-765—Multiloculated cystlike type of fibrous dysplasia. A, localized fibrous dysplasia (microscopic diagnosis) in the proximal third of the left tibial shaft of a girl 13 years of age. The irregular multiloculated cystic pattern of densities is cast by islands of hyaline cartilage mixed with opaque bone spicules and radiolucent whorls of connective tissue and radiolucent local hematomas. B, cystic type of fibrous dysplasia which has dilated the medullary cavity of the humerus and eroded the overlying cortical wall of a girl 7 years of age.

bone may form in the connective tissue that the fibrosis is largely replaced by new bone.

The radiologic changes depend on the degree to which the different elements are developed. When fibrosis predominates the radiologic image is largely radiolucent; when immature bone replaces most of the fibrotic tissue, the radiologic image is largely sclerotic with a smudged or ground glass texture (Fig 8-764). The smudged or melted textures of the cystic segment are the most characteristic radiographic changes. Coarse opaque trabeculae in the radiolucent cystic patches are cast by the calcified bony branchings in the radiolucent rubbery fibrous mass. In the bones of newborns the ground glass smudged texture may not be present in the 'cystic' areas. Large islands of hyaline cartilage whorled masses of fibrotic tissue and local hemorrhage and degeneration cast cystlike images (Fig 8-765). Coarse, curving columns of immature bone extending along the edges of the fibrous masses produce a multiloculated pattern. Masses of new bone in the connective tissue often taper off from the radiolucent segments in a flame-shaped sclerosis.

The individual basic lesions of monostotic fibrous dysplasia are identical with the single lesions of polyostotic fibrous dysplasia and also the individual

bone lesions of the McCune-Albright syndrome, which includes hyperpigmentation of the skin, accelerated maturation of the skeleton and precocious puberty as well as polyostotic fibrous dysplasia (see p 1061).

REFERENCES

- Gould D M *et al* Fibrous dysplasia of bone. *Am J M Sc* 234:590, 1957.
 Harris W H *et al* Natural history of fibrous dysplasia. Orthopedic pathological and roentgenographic study. *J Bone & Joint Surg* 44-A:207, 1962.
 Jaffe H L. Fibrous dysplasia of bone. *Bull New York Acad Med* 22:583, 1946.

Giant cell tumor of bone is virtually nonexistent in infants and is exceedingly rare before the third decade of life. This diagnosis in a prepubescent individual should be rejected until confirmed by authoritative consultations. The tumor usually grows at the ends of one of the longer tubular bones—a femur or tibia at the knee or radius at the wrist; occasionally it is encountered in the ends of other long bones and in the patella, talus and calcaneus. Local pain is the first symptom and often appears after pathologic fracture. General health is not affected. The basic radiographic change is a radiolucent patch which indicates the replacement of bone by the more radiolucent tumor.

Fig 8-766—Giant cell tumor of the humerus of a boy 4 years of age. The cystic rarefaction of the swollen proximal third of the shaft is trabeculated and has a multilocular pattern. The adjacent epiphyseal ossification center (arrow) also shows an area of cystic rarefaction. The concomitant destructive changes in the epiphyseal ossification center and in the shaft are characteristic of giant cell tumor.





Fig 8 767 — Benign cortical defect in the left femur (A and B) and a nonossifying fibroma in the left tibia (C and D) of an asymptomatic girl 13 years of age. It is probable in their early

smaller phases that nonossifying fibromas are benign cortical defects and that these two lesions represent two different phases of the same entity.

tissue. At the same level the medullary cavity is dilated and the cortical walls are thinned from the inside (Fig 8 766). This picture is, of course, not diagnostic because it can be simulated by many other lesions, notably nonosteogenic fibroma, eosinophilic granuloma, and aneurysmal bone cyst. The principal value of the radiographic examination is demonstration of a bone lesion, the nature of which must be determined on clinical and microscopic grounds.

Fig 8 768 — Thorn-induced tumor of the fibula of a boy 6 years of age. There is an extensive fusiform cortical thickening around a large radiolucent patch of destruction in the middle third of the shaft. Although there was no evidence of a puncture wound in the overlying skin, a palm thorn was found in the center of the destructive segment at surgical exploration and biopsy section (From Mayhew).

REFERENCES

- Jaffe H L et al: Giant cell tumor of bone. Its pathologic appearance, grading, supposed variants and treatment. *Arch Path* 30:993, 1940.
 Sherman M and Fabricius R: Giant cell tumor in the metaphysis of a child. Report of an unusual case. *J Bone & Joint Surg* 43-A:1223, 1961.
 Willis R A: The pathology of osteoclastoma or giant cell tumor of bone. *J Bone & Joint Surg* 31-B:236, 1949.

Nonosteogenic fibroma — According to Jaffe and Lichtenstein, there is a type of localized fibrosis of the ends of the shafts which should be differentiated microscopically at least from bone cysts, giant cell tumor, and eosinophilic granuloma. They call this fibrous tumor a nonosteogenic fibroma. It is commonly located in the lower extremities of individuals 6–31 years of age. The terminal third of the shaft is the site of predilection; the spongiosa is partially destroyed, but at some distance from the cartilage shaft junction, from 1–2 in. of normal bone is usually interposed between the epiphyseal plate and the edge of the fibroma. Small fibromas are eccentric, lying near to one side of the cortical wall; the spongiosa on the internal margin of the tumor is thickened (Fig 8 767). In the case of larger tumors, the spongiosa may be completely destroyed, the medullary cavity dilated, and the cortex thinned. Trabeculation in the mass may cast a reticulated multilocular shadow. The diagnosis is made by microscopic examination. This tumor is made up of whorled bundles of connective tis-



sue cells with relatively few vessels multinuclear giant cells are loosely interspersed through the connective tissue. The lesion disappears after curetage and does not recur.

In one of Jaffe's patients 9 years of age a benign cortical defect had converted into a nonosteogenic fibroma when the boy was 13 years old.

REFERENCES

- Goldenberg R. R. Non-osteogenic fibroma of bone. *Bull Hosp Joint Dis* 17:230, 1956.
 Jaffe H. L. Tumors and Tumorlike Conditions of Bones and Joints (Philadelphia: Lea & Febiger, 1959).
 — and Lichtenstein L. Nonosteogenic fibroma of bone. *Am J Path* 18:205, 1942.

Foreign body tumors of bone are in the experience of Maylath induced exclusively by the thorns of plants either in or near the bones (Fig. 8768). The reaction may be osteolytic or osteoblastic singly or in combination. Lesions of this type should be considered in radiologic diagnosis in communities where children are exposed to plant thorns especially where palms are common.

REFERENCE

- Maylath D. J. Thorn-induced tumors of bone. *J Bone & Joint Surg* 34-A:386, 1952.

MALIGNANT NONOSTEOGENIC TUMORS—The skeletal changes found in leukemia, reticulum cell sarcoma and Hodgkin's disease are discussed later in the section on blood and blood-forming organs. Much perhaps all of the malignant proliferation of reticulum cells in the bone marrow of leukemic patients is pri-

mary there and is not metastatic from the lymphatic structures. In this sense leukemia is by far the commonest type of primary malignant disease of the growing skeleton. In most cases of so-called leukopenic leukemia, primary malignant reticulosis of the skeleton would be a more exact designation.

During childhood Ewing's sarcoma is the only other important primary malignant neoplasm of the skeleton which is derived from the nonosteogenic tissues in bone. It is doubtful that myelomas occur prior to puberty although they are occasionally found in young adults. Fibrosarcomas and neurosarcomas are rare tumors which affect bone secondarily by extension from neighboring soft parts. Their roentgen changes are not characteristic; areas of bone destruction appear on the margins of the shaft and then extend inward. In some cases the exact diagnosis and estimate of their malignant status is uncertain even after biopsy.

Ewing's sarcoma is not common and is much less common than osteogenic sarcoma. It has been found at all ages from infancy to the seventh decade of life but the majority of cases occur during the second decade. Few cases are seen in children younger than 5 years. Almost any bone in the body may be affected but these sarcomas grow most frequently in the femur, humerus and tibia. In Dahlin's large series the tumors originated in the metaphyses more frequently than in the shafts. In contrast to most of the primary malignancies in the growing skeleton these patients are sick with fever, weakness, pallor, lassitude and leukocytosis and the sedimentation rate of their red blood cells is increased. Local pain and swelling are the dominant complaints. Radi-

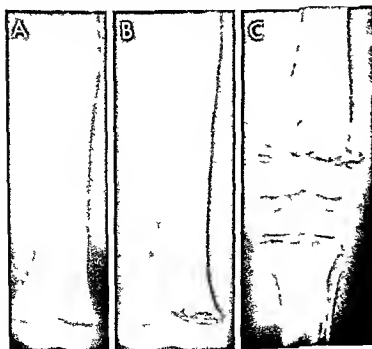


Fig. 8769—Ewing's sarcoma (macroscopic diagnosis) of the left femur which appears to be metaphyseal in the middle third only at 3 years of age (A) but which has become metaphyseal 3 months later (B) and despite roentgen therapy caused extreme destruction of the metaphyseal bone at 5 years of age (C). The continuous epiphyseal ossification on center is not affected. All the changes resemble those caused by inflammatory disease. The radiographic changes of Ewing's sarcoma are not usually diagnostic in themselves.



Fig. 8-770—Ewing's sarcoma (microscopic diagnosis) in the left tibia. A long segment of the cortical wall of the proximal half of the tibia is irregularly thickened with peripheral marginal destructions as well. These changes are not diagnostic and could be due to inflammation or trauma.

ographic findings result from the replacement of opaque spongiosa and cortical wall by more radiolucent tumor tissue. The changes are not specific and vary greatly in different patients and in the same patient at different times (Figs 8-769 to 8-774). The tumor cells cannot produce bone themselves but they do stimulate local osteoblasts to produce single and multiple sheets of cortical bone (onion skin layering) and often radial streaks of bone beyond the cortical walls. Osteogenic sarcoma, reticulum cell sarcoma, eosinophilic granuloma and even osteomyelitis mimic Ewing's sarcoma radiographically and the definitive diagnosis must be based on the clinical and microscopic findings. Metastasis is common to the lungs and to other parts of the skeleton.

REFERENCE

- Dahlin D C *et al*. Ewing's sarcoma. A critical review of 165 cases. *J Bone & Joint Surg* 43-A:185, 1961.

Fibrosarcomas primary in bone are rare at all ages; they usually develop in young and middle aged adults. The femurs and tibias are most frequently affected. The more radiolucent tumor tissue replaces compact cortex and spongiosa, erodes the cortical walls from the inside and dilates the medullary cavity. These tumors produce no bone. The radiographic picture is similar in many other neoplastic and inflammatory lesions and the diagnosis must be made on clinical and microscopic grounds.

Neural tumors—Cells from the neural sheaths do on rare occasions grow as solitary masses in bone and produce radiolucent defects in bones. These neurolemmomas are usually found in mature women.

Neurofibromatosis of Recklinghausen is associated with a wide variety of important changes in the growing skeleton. Regional hypertrophy of the soft tissues of an extremity (regional gigantism) usually a leg is nearly always associated with overgrowth of the underlying bones. Chronic hyperemia of the part induced by the hemangiomatous and lymphangiomatous elements of the neurofibromatosis causes the overgrowth. The bones themselves need not be directly involved but in some cases the periosteum is invaded by the tumor and becomes raised to produce localized external cortical thickenings. Extension into the bone itself may produce a variety of bone defects and roughenings of the cortical walls. Large parosteal neurofibromas may cause segmental thinness of the cortical wall by erosion of it from the outside (Fig 8-775) simulating nonosteogenic fibromas and benign cortical defects. In fetuses and young infants neurofibromas usually cause ventral bowing of the tibia and pseudarthrosis (see Figs 8-290 and 8-291). The clavicles may be similarly affected. Neurofibromas have been found at the sites of pseudarthroses in some cases but not in others. Slight external dimples in the cortical walls and deeper erosive pits have also been found with neurofibromas. The growth of large neurofibromas in the medullary cavity to produce large cystic defects has been claimed by some and denied by others; such defects are rare in comparison with the large external erosive lesions which they may simulate in a single projection (see Fig 8-775). McCarroll studied two interesting patients in whom the bone changes mimicked melorheostosis.

Kyphoscoliosis is frequently due to neurofibromatosis. Acute angulation at the gibbus is characteristic with multiple deformities of the vertebrae at the level of the angulation. All degrees of scoliosis are found in association with neurofibromatosis. The primary curve is commonly in the thoracic levels. Also neurofibromas may erode the edges of the intervertebral foramina (see Fig 1-407). Ribs in the same level are commonly twisted and hypoplastic. Secondary scoliosis may develop in the spine from neurofibromas which cause overgrowth of one leg.

In a review of the literature and a study of 46 infants and children with neurofibromatosis Fienman

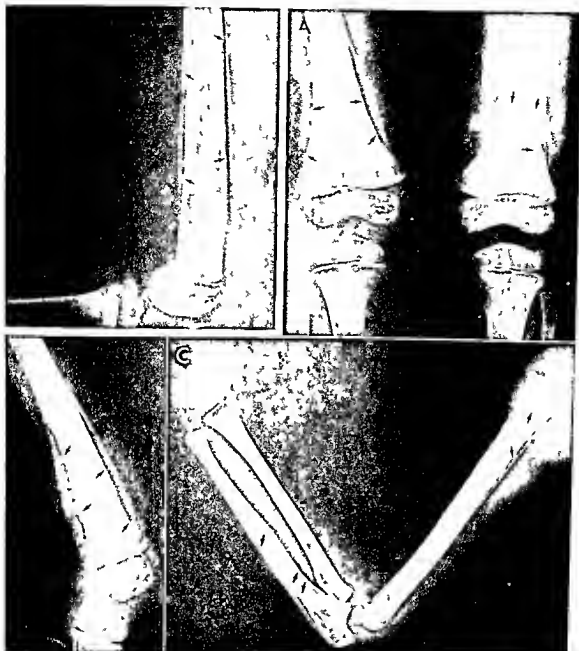


Fig. 8771 (above left) — Low grade osteomyelitis which resembles Ewing's tumor roentgenographically. In the middle third of the femoral shaft is a long segment of moth eaten destruction. The overlying cortex is thickened and lamellated.

Fig. 8772 — Polyostotic Ewing's sarcoma in a girl 2 years of age (necropsy). A, femur frontal projection. B, right femur lateral projection. C, left upper extremity. Extensive destructive and

productive changes were present in both femurs, both tibiae, both fibulae, the left humerus and ulna and the right scapula. Microscopically the neoplastic cells were so poorly differentiated that exact classification was uncertain. A majority of experts consulted favored Ewing's sarcoma, but a minority of equally expert opinion rejected this diagnosis.

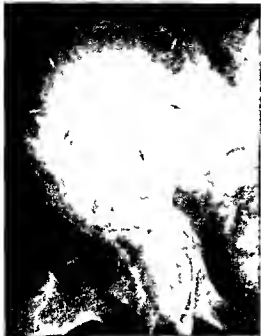


Fig 8 773 —Ewing's sarcoma of the pelvis in a girl 12 years of age (microscopic diagnosis). The entire left ilium is involved. There is a large central defect completely devoid of lime on the margins is an extensive moth eaten rarefaction.



Fig 8 774 —Ewing's neoplasm of the basal phalanx of the 2nd finger of a girl 14 months of age (microscopic diagnosis). The bone is generally sclerotic with many fine radiolucent foci and the overlying soft tissues are swollen. There is no onion peel lamellae on of the cortical walls and no Codman's triangle. Several pathologists agreed that the microscopic findings indicated Ewing's neoplasm.

Fig 8 775 —Neurofibromatosis of the right femur and tibia of a girl 8 years of age who had many café-au-lait patches on the skin and kyphoscoliosis. The large radiolucent defect in the femur is

due to a large neurofibroma which has eroded its dorsal wall and also thickened it at the same time. A similar lesion is visible in the dorsal cortical wall of the tibia in both A and B.



and Yakovac concluded that it is a chronic progressive disease which may be present at birth or appear during early infancy and childhood. The lesions are often widely spread, involving several organs and systems. The most frequent clinical manifestations are cutaneous patches and tumors of coffee-milk color. More than one member of a family were affected in about one-half the cases. Malignancy developed in 2% of patients under 30 years, but reached an incidence in older patients of 16%. Both speech and motor power were retarded in development in 11 of the 46 patients. Sexual development was normal, retarded and precocious in different patients. The mammary glands were enlarged in 6. Severe vascular disease and circulatory hypertension and gross malformation of the vascular system were associated with neurofibromatosis of the autonomic nervous system. Such patients should be examined for both decreased and increased circulatory pressures.

The incidence of neurofibromatosis is estimated to be 1 per 2500-3300 births. Inheritance is autosomal and dominant with variable penetrance and an unusually high rate of mutation. In the view of Fienman and Yakovac, neurofibromatosis is a primary proliferative disorder of the fetal neural crest which affects the supporting mesenchymal fibrous elements secondarily. It is not clear whether the neural and fibrous proliferations develop independently. Observations with the electron microscope suggest that collagenous fibrils originate in the basement membranes of the Schwann cells of the neural sheaths.

REFERENCES

- Agnewssens A. An unusual case of neurofibromatosis in an infant, *Maandschr kindereneesk* 18:347 1950.
 Fienman N L, and Yakovac, W C. Neurofibromatosis in childhood. *J Pediatr* 76:339 1970.
 Hunt, J C, and Pugh, D G. Skeletal lesions in neurofibromatosis. *Radiology* 76:1, 1961.
 McCarroll H R. Clinical manifestations of congenital neurofibromatosis, *J Bone & Joint Surg* 32-A:601 1950.

Hemangiomas often stimulate the regional soft tissues and bones to overgrowth and give rise to regional gigantism. Sometimes the bones associated with hemangiomas show irregular cortical thickenings (Fig 8-776). Parsons and Ebbs studied a girl who had multiple large skeletal defects (Fig 8-777) in the sites of large cavernous intraosseous hemangiomas.

Cystic angiomatosis of the skeleton was reported in three children by Jacobs and Kimmelstein. Both tubular and flat bones showed cystlike defects of varying sizes. In tubular bones, the defects were superficial and tended to be near the ends of the shafts. In the skull, there was no radial striation, as is the case in many solitary hemangiomas of the skull. Palpable masses were usually detected over the bone defects. The patient of Ritchie and Zeur, a boy 2½ years of age, had multiple cystic lesions widely distributed in the skeleton (Fig 8-778), save in the hands and feet



Fig 8-776—Irregular cortical thickening of the femur (arrows) of a 7 year old boy with generalized hemangiomas and gigantism of the leg. There are similar but less marked thickenings in the tibia. All of the bones show conspicuous strophy of diaphysis and there are many small shadows of calcium density in the soft tissues.

The authors pointed out that the spine is commonly affected and that the roentgen appearance varies with the bone affected. In the flat bones the lesion presents a "sunburst" radial ray pattern, the vertebrae are streaked vertically, and in the long bones the cysts tend to develop at the sites of the vascular foramina for the nutrient arteries.

Harris and Prandoni considered primary lymphangiomatosis of bone exceedingly rare. They reported widely spread multiple cavernous lymphangiomatosis of bone associated with congenital lymphedema of the forearm in a boy 20 years of age. Cystlike lesions were demonstrated radiologically in practically all bones. A conclusive diagnosis was made from microscopic study of biopsy specimens. We have seen one example of lymphangiomatosis of the radius and ulna, in which the pattern of destruction was streaked rather than cystic (Fig 8-779). Shopfner and Allen found multiple lymphangiomatosis in the skull, ribs, humeri, femurs and tibiae which cast multiple radiolucent images in radiographs (Fig 8-780). These lesions were asymptomatic. In Najman's patient, 3½ years of age, the skull, long bones and flat



Fig 8-777 —Large bony defects in the tubular bones due to multiple cavernous intrasosseous hemangiomas (necropsy). The patient's age at death was 15 years old (From Parsons and Ebbs)

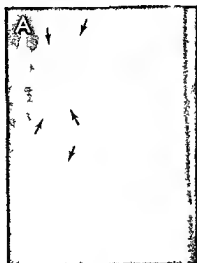
Fig 8-778 —Hemangiomas of bone in a boy 2 1/2 years of age. Long central segments of the shafts are sclerosed and contain multiple sharply defined red fluorescent patches. Similar changes were present in the left clavicle, both radiuses, the right ulna, pelvic bones and both femurs. The spleen was enlarged and riddled with large and small cystic hemangiomas. After pathologic fracture in the long bones, healing was rapid and complete (Redrawn from Ritchie and Zeier)





Fig. 8-779—Lymphangioma of the bones and soft tissues of the forearm in a girl 3 years of age. The radius and ulna are widened in the middle thirds where there are several elongated radiolucent defects which are probably the sites of intraosseous lymphangiomas. The soft tissues of the forearm and wrist are greatly swollen.

Fig. 8-780—Widely scattered lymphangiomas in the skeleton (macroscopic diagnosis). In the femur (A) multiple sharply defined radiolucent patches simulate benign cortical defects in the



bones were riddled with dozens of sharply defined radiolucent defects. Contrast agent injected into the cystic defects in the skull remained in situ for more than a month. Moseley and Starobin suggest that hamartomatous cystic vascular formation is the mechanism common to all of the vascular deformities in the skeleton and they prefer the name "cystic angiomatosis of bone."

Regional angiomatosis of both blood and lymph vessels may produce progressive massive destruction of large segments of the growing skeleton (Fig. 8-781). In their two patients, Gorham and Stout suggested that slight regional changes in the pH of the tissues might be the stimulant to rapid overgrowth of blood vessels.

Generalized lipomatosis with localized gigantism of the skeleton and local defects in the bones was studied in a girl 6 years of age by Fainsinger and Harris. They concluded that the bony defects were occupied by fatty tumors.

REFERENCES

- Bickel W H and Broders A C: Primary lymphangioma of the ileum. Report of a case. *J Bone & Joint Surg* 29:517, 1947.
- Cohen J and Craig J M: Multiple lymphangiectosis of bone. *J Bone & Joint Surg* 37A:585, 1955.
- Fainsinger M H and Harris L C: Generalized lipomatosis involving bone. *Brit J Radiol* 23:274, 1950.
- Gorham L W and Stout A P: Massive osteolysis (acute spontaneous resorption of bone phantom bone disappearing bone). *J Bone & Joint Surg* 37A:985, 1955.
- Harris R and Prandoni A G: Primary generalized lymphangiomas of bone. Report of a case associated with congenital lymphedema of the forearm. *Ann Int Med* 33:1302, 1950.
- Holt J F: Unusual bone tumors in infants and children. *Radiology* 61:749, 1953.
- Jacobs J E and Kimmelstein P: Cystic angiomatosis of the skeletal system. *J Bone & Joint Surg* 35-A:409, 1953.

cavities. (B) numerous large and small patches of reduced density were filled with lymphangiomas. (From Shopfner and Allen.)



Fig 8-781—Massive osteolysis of the left side of the pelvis in a girl 15 years of age 15 months after the appearance of limp. A: The left ilium is almost completely destroyed, as well as part of the sacrum and L5 vertebra. M. Grosskopf diagnosed this as at first primary lymphangoma of the ilium later changed to hemangioma. B: 10 years later there is complete destruction of the left ilium and practically all of the sacrum and part of destruction of L4 and L5 vertebrae, left pubic bone, ischium and femur. There was no evidence of bone regeneration in any of the sites of bone destruction. (Redrawn from Goh and Stout.)



- Koblentz P J and Bukowski M J Angiomatosis (hamartomatous hem lymphangiomatosis) Report of a case with diffuse involvement *Pediatrics* 29:65 1961
- Moseley J E and Starobin S G Cystic angiomatosis of bone Manifestation of a hamartomatous disease entity *Am J Roentgenol* 91:1114 1964
- Najman E et al Lymphangoma in the inguinal region with cystic lymphangiomatosis of bone *J Pediatr* 71:561 1967
- Parsons L G and Ebbs J H Generalized angiomatosis presenting the clinical characteristics of storage reticulosis *Arch Dis Childhood* 15:129 1940
- Ritchie G and Zeir F G Hemangiomatosis of the skeleton and the spleen *J Bone & Joint Surg* 38-A:115 1956
- Sherman M S Capillary hemangioma of bone *Arch Path* 38:158 1944
- Shopfner C E and Allen R P Lymphangoma of bone *Radiology* 76:449 1961
- Strang C and Rannus I Dyschondroplasia with hemangiomas (Maffucci's syndrome) *J Bone & Joint Surg* 32-B:376 1950
- Ward C E and Horton B T Congenital arteriovenous fistulas in children *J Pediatr* 16:746 1940

Congenital scattered fibromatosis is characterized by widely scattered fibromas and fibrous proliferations at many sites in many tissues of the body. In the fatal case of Condon and Allen with death at 3 months of age, multiple fibrous nodules were found at necropsy in a great variety of sites in the skeleton, lungs, liver, heart, brain, skin, and large and small intestines. Each nodule was believed to be primary rather than metastatic. Radiolucent patches indicative of fibromas were found in the long bones (Fig 8-782) and in the ribs, scapulas, pelvis, vertebrae, man-

dible and cranium. In the case of Holt, calcified subcutaneous fibromas were evident as well (Fig 8-783); these and the bone lesions disappeared before the infant reached his 18th month. In the unpublished case of Dr Alfred Berne of Syracuse, N.Y., multiple metaphyseal fibromatosis was progressive from the 5th to the 8th years, when large segments of the long bones had become fibrosed and dilated (Fig 8-784). Arlen reported partial erosion of the radial and ulnar shafts in localized fibromatosis of the forearm of an infant 3 months of age.

REFERENCES

- Arlen M Juvenile fascial fibromatosis of the forearm with osseous involvement *J Bone & Joint Surg* 51-A:591 1969
- Beatty E C Jr Congenital fibromatosis in infancy *Am J Dis Child* 103:620 1962
- Berne A Personal communication.
- Condon V R and Allen R P Congenital generalized fibromatosis *Radiology* 76:444 1961
- Holt J F and Wright E M The radiological features of neurofibromatosis *Radiology* 51:647 1948
- Levkoff A H et al Congenital diffuse fibromatosis: A case report *Pediatrics* 35:331 1965
- Stout A P Juvenile fibromatosis *Cancer* 7:953 1954
- Zeisel H and Hellig G Polystuche polytopefost systema tische Skeletaffektion beim Säugling *Zschr f Kinder heilk* 76:379 1955

Disseminated lipogranulomatosis (Farber) is characterized by nodular swellings around peripheral joints with regional atrophy of muscles. The ends of the tubular bones near the affected joints are rarefied



Fig. 8-782 — Multiple fibromatosis of the tubular bones of the legs and iliac bones of the pelvis of a patient 3 months of age (necropsy). The ends of the tubular bones are swollen and filled with masses of radiolucent fibrous tissue. At the proximal end of the right femur a long segment of the overlying cortex has been destroyed. The epiphyseal ossification centers are not affected. Similar patches of diminished density are scattered through the pelvic bones. (From Condon and Allen.)

Fig. 8-783 — Multiple defects in the tubular bones in the extremities of an infant 3 months of age with scattered subcutaneous fibromatosis. Large calciferous foci are also evident in the soft tissues of the thigh. (Courtesy of Dr. J. F. Holt, Ann Arbor, Mich.)



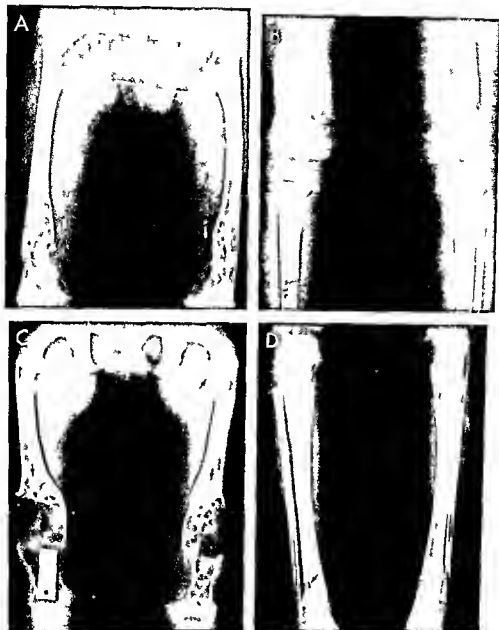


Fig. 8784—Widespread metaphyseal defects due to cystic mesenchymal proliferation and hypervascularity (Jaffe). **A** and **B** in a boy 5 years of age: multiple loculated radiolucent patches in both ends of the femoral shafts and in the proximal ends of the tibial shafts. Similar changes were present in the proximal metaphyses of the humeri, but there were no lesions in the distal metaphyses of the tibiae and humeri. Both ends of the radii and ulnae were normal. **C** and **D** the same bones 2 1/2 years

later. The distal ends of the femoral shafts are now dilated in long terminal segments which exhibit increased multilocular expansion. In the proximal ends of the tibiae similar progressive changes have developed. At the distal end of the right tibia a defect exists in the cortical wall (arrow) which is similar to a benign cortical defect found commonly in healthy children without large metaphyseal lesions.

due to disruption of their trabecular meshes. The lungs are said to contain nodules of both parenchymal and interstitial origin. Early the diagnosis should be suggested from the terminal juxta articular erosions in the bones and juxta articular swellings of the soft tissues. It is said that the terminal erosions are diagnostic in themselves. All recorded patients have died during infancy.

REFERENCE

Schance A F *et al*. Disseminated lipogranulomatosis. Early roentgenographic changes, *Radiology* 82:675, 1964.

Malignant metastatic tumors—The malignant tumors which metastasize through the blood stream to the bones of infants and children include neuroblastomas, retinoblastomas and embryonal rhabdomyosarcomas. The radiographic features of neuroblastomas have already been discussed in the sections on the adrenal glands and on the skull.

Lymphoblastomas often proliferate in several long bones and produce areas of destruction and production in the metaphyses (Fig 8-785). Both spongiosa and corticalis are partially destroyed. Segments of the overlying cortex may become thickened owing to the stimulating action of the neoplastic cells on the normal bone producing cells in the osteogenic layer of the periosteum. Such bone formation is wholly a secondary reactive phenomenon; the lymphoblastomas per se have no power of osteogenesis.

Lymphosarcoma in bone are rare. Sherman and Wolfson could find only 10 satisfactory examples of lymphosarcoma, reticulum cell sarcoma in bone in patients younger than 12 years in the huge experience of the Sloan Kettering Cancer Center in New York City during a period of 30 years. In 2 of these cases the tumors were solitary and in 8 multiple. These tumors, which are radiolucent, replace opaque bone usually in the metaphysis to produce a variable pattern of patchy radiolucencies mixed with normal and dead sclerotic bone and sometimes stimulate local osteoblasts to thicken the cortical walls locally (Fig 8-785). They rarely dilate the medullary cavity. The radiographic changes are not specific or diagnostic because they resemble many other lesions, such as benign reticulosis, infections and other neoplasms including leukemia. The metaphyseal transverse bands which are common in leukemia were not present in the patients of Sherman and Wolfson. Some long time students of these lesions maintain that there are no significant differences between Ewing's sarcoma and reticulum cell sarcoma. **Malignant lymphoma** which is said to constitute one half of all malignancies in children in some parts of Africa frequently affects the skeleton, especially the facial bones, sometimes the spine and pelvis but rarely the long bones. In the United States the incidence of lymphoid tumors in adolescent patients is much

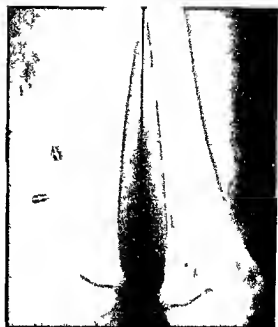


Fig 8-785—Lymphosarcoma of the tubular bone in a girl 2 years of age (necropsy). Both femurs show large and small areas of destruction in the spongiosa at the ends of the shafts. The arrows point to nontumorous thickening of the overlying corticalis. The epiphyses are not affected. The medullary cavity is not dilated. The bones of the arms also contained destructive lesions. These lesions probably result from primary malignant proliferation of the reticulum cells native to the bone marrow in these sites rather than from transport of malignant reticulum cells from germ centers in the lymphatic structures.

greater in males than in females in the ratio of about 5:1 but in the very young and very old this ratio approaches unity (Rosenberg *et al*).

REFERENCES

- O'Connor G T. Malignant lymphoma in African children. II. A pathological entity. *Cancer* 14:270, 1961.
- Rosenberg S A *et al*. Lymphosarcoma. A review of 1269 cases. *Medicine* 40:31, 1961.
- Sherman R and Wolfson S F. Roentgen diagnosis of lymphosarcoma and reticulum cell sarcoma in infancy and childhood. *Am. J. Roentgenol.* 86:693, 1961.

Hodgkin's sarcoma is rare in pediatric practice among 100,000 admissions to the Babies Hospital in New York City there were but 12 cases of Hodgkin's disease. The primary lesion is malignant proliferation of lymph nodes usually in the neck but also in the mediastinum, abdomen and pelvis. Clinical signs are due to local pressure by the swollen nodes. The spleen is usually enlarged and the lungs and bones may be affected secondarily. In skeletal Hodgkin's disease the spine is most frequently affected then the ilium, sternum and scapula; the long bones are rarely involved. The radiographic changes are not diagnostic. Radiolucent tumor tissue replaces opaque bone to



Fig 3 756 — Reticulum cell sarcoma at the distal end of the left tibia (microscopic diagnosis) in which the principal change is diffuse sclerosis due to overproduction of bone secondary to stimulation of local osteoblasts by the reticulum cells. The long standing hyperemia associated with growth of the neoplasm has stimulated overgrowth of the affected tibia. Radiographically all changes could have been caused by osteomyelitis. The tibial defect is a bony sequestrum.



Fig 3 757 — Metastatic retinoblastoma of the skeleton in a girl 9 years of age, eight years after enucleation of one eye. A, destructive and productive changes in the humerus. There is considerable cortical thickening which appears to be directly subperiosteal. B, massive sclerosis of the 3rd metatarsal. The radiolucent lesions tend to become sclerotic with advancing age.



produce a wide variety of radiolucent defects. The affected vertebral bodies may collapse to produce spinal deformities and neurologic deficits in the spinal cord. In some cases the local osteoblasts are irritated to produce ivory like sclerosis of the affected bone.

Reticulum cell sarcoma in bone can be differentiated from Ewing's sarcoma and lymphosarcoma microscopically only by the most expert pathologists, and the diagnosis may not be agreed on by a panel of experts. The diagnosis can never be made satisfactorily from the radiographic findings (Fig 8 786). Reticulum cell sarcoma does not metastasize to other bones and organs early, as is the case in Ewing's sarcoma, and usually has a longer survival time. The diagnostic uncertainties of the "malignant round cell sarcomas" are illustrated in a patient of ours, a boy 9 years of age, in whom a destructive focus first appeared in one ilium and slides for microscopy were sent to eight experienced American pathologists with special competence in bone tumors. Two of them replied that the neoplasm was a reticulum cell sarcoma, and one each reported neuroblastoma, embryonal rhabdomyosarcoma, Hodgkin's sarcoma, Ewing's sarcoma, lymphosarcoma and chronic osteitis. Four years later the patient died with several neoplastic foci in other long bones, at several levels in the spine and in the liver.

Retinoblastoma metastasizes by direct extension inside the skull and by way of the blood to distant bones in all parts of the skeleton. At first the metastases grow in the marrow of the medullary cavity and by their extension destroy spongiosa and the overlying cortical walls. Sometimes neoplastic cells grow under the periosteum and lift it so that extra shells of peripheral cortex appear. In later phases, the neoplastic cells stimulate the osteoblasts to excessive bone production, and osteoblastic reactions are common. Both destructive and productive lesions of skeletal retinoblastoma are shown in Figure 8 787. Skeletal retinoblastoma cannot be differentiated from skeletal neuroblastoma and lymphoblastoma, radiologically.

REFERENCE

- Mernam, G R Jr. Retinoblastoma. Analysis of 17 cases, Arch Ophth 44 71, 1950

Metastatic embryonal rhabdomyosarcoma frequently affects the growing skeleton, producing destructive lesions in the long bones of the extremities and the flat bones of the skull, shoulder girdle and pelvis (Figs 8 788 and 8-789). The spine is involved consistently in different patients and may be affected at several levels in a single patient. Radiographically the metastatic lesions of rhabdomyosarcoma and neuroblastoma are similar and easily confused. The diagnosis rests finally on the microscopic findings. One important differential clinical feature of these two malignancies of the growing skeleton is the site of the primary tumors in each. Primary neuroblastoma

is usually in the adrenals, or in the sympathetic nerve chains, or in the central nervous system itself. The primary tumors of the embryonal type of rhabdomyosarcoma are never found in these sites, they occur in many other parts of the body, in muscles of the orbit, chest wall, pelvis and extremities.

REFERENCE

- Caffey, J., and Andersen, D. Metastatic embryonal rhabdomyosarcoma in the growing skeleton, Am J Dis Child 95 581, 1958

Cerebellar medulloblastomas, in untreated patients, may spread by way of the cerebrospinal fluid to all levels of the spinal cord and brain, but metastases outside the central nervous system are rare. In treated patients, in contrast, after biopsies and partial excisions and radiotherapy, several examples of hematogenous spread to the skeleton, flat as well as tubular bones, have been recorded. The metastatic tumor cells cause little or no destruction of bone but rather stimulate the local osteoblasts to diffuse thickening of the spongiosa, which replaces more radiolucent marrow. The radiographic changes include regional generalized internal sclerosis (Fig 8 790), especially in the vertebral bodies. Some believe, on the basis of the reticulum stain, that these metastatic tumors are cerebellar sarcomas rather than medulloblastomas.

REFERENCE

- Black P W B and Keats, T E. Generalized osteosclerosis secondary to metastatic medulloblastoma of the cerebellum. Radiology 82 395 1964

BONE CHANGES WITH DISEASES OF THE BLOOD AND BLOOD-FORMING ORGANS

ERYTHROBLASTOSIS FETALIS (HEMOLYTIC DISEASE OF THE NEWBORN)—This disease results in most cases from isoimmunization of an Rh negative pregnant woman by Rh positive fetal erythrocytes. The maternal anti Rh agglutinins later cross the placenta to the fetal circulation and hemolyze the vulnerable fetal red blood cells. The hemolysis of fetal cells before birth is responsible for icterus, anemia, edema, erythroblastemia, splenomegaly and hepatomegaly which characterize the disease in the newborn infant. In many cases, mild and severe, there are no roentgen changes in the skeleton. In some cases, however, prenatal endochondral bone formation is interfered with and transverse bands of increased and diminished density develop in the ends of the shaft (Fig 8-791). Folks and his colleagues found diffuse sclerosis of the shaft in five cases; they attributed this to excess of spongiosa and cortices. In our cases, density of the shafts has not exceeded that found in many normal newborns.

Samuel and Cohen claimed that normal fetal kyphosis is obliterated in erythroblastosis fetalis due to

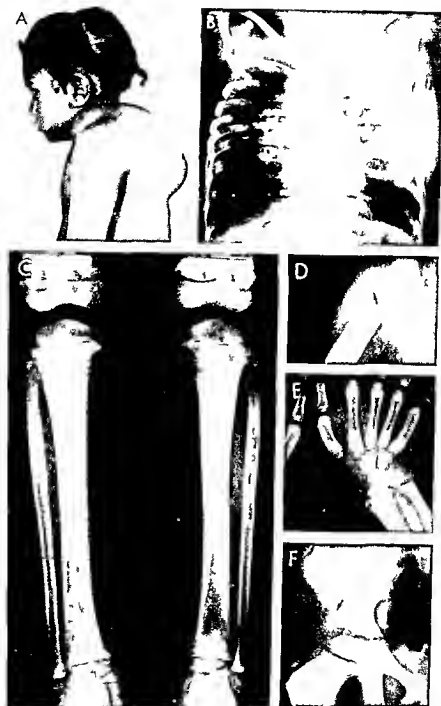


Fig 8788—Metastatic embryonal rhabdomyosarcoma of the skeleton, primary in the left thoracic wall of a girl 2 years of age. A, photograph of the head and chest, she died two weeks later. B, frontal film of the chest, showing tumorous thickening of

the left thoracic wall, with enlargement of hilar images. C, D, and E show destructive and productive changes in the metaphyses of the larger bones. In F, the base of the right humerus is partly destroyed.

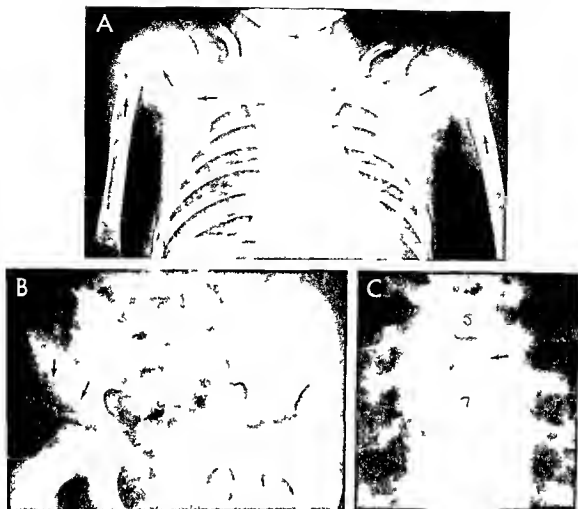


Fig 8789—Metastatic embryonal rhabdomyosarcoma of the skeleton in a boy 6 years of age, two weeks after onset of pain in the right shoulder and spine. The primary tumor was in the soft tissues above the right ankle, a swelling which was not noticed until the bone pain developed elsewhere. A, Symmetrical destruc-

tion of the proximal ends of the humeri and right scapula. B, Segmental destruction of the base of the right humerus. C, Destruction and compression of the body of the D6 vertebra and its left pedicle.



Fig 8790—Metastatic cerebellar medulloblastomas in the right femur of a boy 14 years of age. The bones are regularly sclerotic due to the reactive osteoblastic reaction to the metastatic medulloblastoma cells. In the left femur (not shown) is a large radiolucent patch representing replacement of bone by the metastatic medulloblastoma tissue. (Courtesy of Dr Edward B. Singleton, Houston, Tex.)

Fig 8791—Erythroblastosis fetalis four hours after birth. Deep transverse bands of increased density in the distal ends of the radius and ulna. The depth of these bands suggests that endochondral bone formation had been disturbed for several weeks prior to birth.



enlargement of the liver and spleen, ascites and anasarca and that this straightening of the fetal spine is an important radiologic sign of fetal hydrops. The same factors are said to cause extension of the thighs and flexion of the knees.

Fetal hydrops is the earliest and most severe form of the disease. It can be demonstrated radiographically by the obliteration of the normal black fetal fat line under the skin by subcutaneous edema fluid in the fetus as early as the fifth fetal month. Bishop thinks that the halo sign—the increase in depth of the edematous subcutaneous tissue in the scalp—is unclear in relation to the causal mechanism and of little diagnostic value.

Bowman and Friesen reported successful intrapentoneal transfusions of the fetus as early as the twenty-fourth week.

REFERENCES

- Bishop P A: The roentgenographic diagnosis of fetal hydrops. *Am J Roentgenol* 86:415, 1961
- Bowman J M and Friesen R F: Multiple intrapentoneal transfusions of the fetus for erythroblastosis fetalis. *New England J Med* 274:703, 1964
- Brenner C and Allen R P: Skeletal changes in erythroblastosis fetalis. *Radiology* 80:427, 1963
- Browne J C M: Fallibility of the radiologic diagnosis of erythroblastosis fetalis. *J Obst & Gynecol Brit Emp* 57:71, 1950
- Follis R H Jr, et al: Skeletal changes associated with erythroblastosis fetalis. *J Pediatr* 21:80, 1942
- Samuel E and Cohen J: The prenatal radiological diagnosis of hydrops fetalis. *Brit J Radiol* 23:225, 1950

FANCONI'S ANEMIA (CONGENITAL HYPOPLASTIC ANEMIA WITH MULTIPLE CONGENITAL ANOMALIES) is a pancytopenic type with hypoplastic changes in the bone marrow and peripheral blood associated with a variable complex of congenital malformations in other tissues. The skeletal anomalies include aplasia and hypoplasia of the bones in the thumbs, first metacarpals and radii; syndactyly; congenital dislocation of the hip; and occasionally deformities of some of the large tubular bones. The most frequent skeletal lesion is undergrowth of the thumbs. The nonskeletal anomalies include patchy hyperpigmentation of the skin, dwarfism, mental retardation, microcephaly, renal malformations and deafness. Although the skeletal anomalies are present at birth, the anemia is rarely recognized until after the 3rd year of life and sometimes not until the 12th year. Death usually occurs early and is often due to intracerebral and alimentary bleedings associated with thrombocytopenia. Familial disease is common. In the same family some siblings may have the full Fanconi syndrome with anemia, while other siblings have multiple congenital anomalies without anemia.

In *erythrogenesis imperfecta* the congenital anomalies and the skeletal deformities are not as frequent or as marked as in Fanconi's anemia. However, minor developmental lesions were found in 28 of 74 cases.

REFERENCES

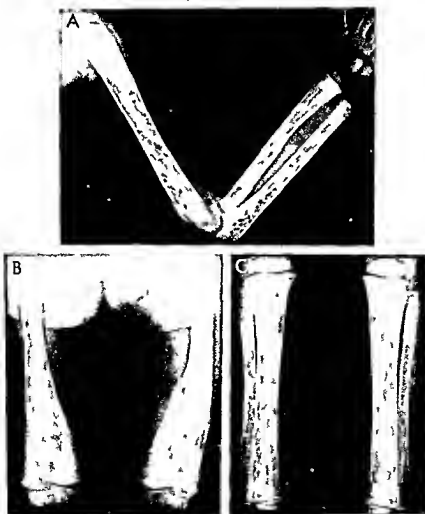
- Fanconi G. Familiäre infantile perniöseartige Anämie (pernizioses Blutbild und Konstitution). *Jahrb f Kinderh* 117:257, 1927.
- Minagi H. and Steinbach H. L. Roentgen appearance of anemias associated with hypoplastic anemias of childhood. Fanconi's anemia and congenital hypoplastic anemia (erythropoiesis imperfecta). *Am J Roentgenol* 97:100, 1968.
- Moseley J. E. Bone Changes in Hematologic Disorders (Roentgen Aspects) (New York: Grune & Stratton Inc. 1963).

CHRONIC HEMOLYTIC ANEMIAS—*Inheritable dys hemoglobinoses* comprise a group of important clinical diseases characterized by the presence of abnormal hemoglobins or fetal hemoglobin in excessive amounts. They are all determined genetically and

tend to be limited racially. The abnormal hemoglobin S was first recognized by Pauling and associates in 1947; it is responsible in the homozygous state for the chemical and hematologic entity, sickle cell anemia, limited largely to American blacks. Fetal hemoglobin F in excessive amounts is associated with Cooley's anemia (thalassemia), which occurs largely in the natives of the shores of the Mediterranean Sea and their descendants in other countries, mostly Greeks and Italians. Hemoglobin E is found in Thais and some of whom have mild anemias. Hemoglobin H has been demonstrated in Chinese and Filipinos who suffer from a Cooley-like anemia. Sometimes two abnormal hemoglobins are present and produce clinical

Fig. 6792—Mediterranean (Cooley's) anemia in an Italian boy 3 years of age. A, upper extremity; B, thigh; C, lower leg. The medullary cavities are dilated; the shafts are swollen and rectangular in outline; the cortices are thin. All of the bones are osteoporotic and present a bizarre trabeculated appearance owing to

irregular destruction of the spongiosa and irregular internal erosion of the cortices. Multiple transverse lines mark the ribs. The deformity of the left femur is secondary to a podiatric fracture.



cal diseases such as sickle cell Cooley's disease from hemoglobins A F and S which accounts for much of so-called sickle cell anemia in Caucasians and hemoglobins F and C in Cooley's hemoglobin C disease which accounts for a Cooley like disease in Blacks. Githens and colleagues found hemoglobin D in two American Indian children.

Cooley's (erythroblastic) anemia—This disease with strong familial and racial characteristics is generally limited to natives of the Mediterranean region although surprisingly it has not been identified in Spaniards or the Mediterranean French. Authentic cases have also been described in Chinese and Asian Indian children. In 1943 Dameshek reported a case in a black child and Cooley's anemia is said to have occurred in several members of a black family in Cape Town, South Africa (Herditz Olson and Woolf). Dreyfuss found a high incidence of Cooley's anemia in three families of Oriental Jews—one from Kurdistan and two from towns in the southeastern corner of Turkey. The exact mechanism of inheritance is not well understood, there is substantial evidence that the condition is transmitted to offspring by parents with a benign latent form of the disease.

The severe cases present a uniform clinical picture consisting of progressive anemia and jaundice which begin during the first two years; death usually occurs before adolescence. Splenomegaly is invariably present and is usually accompanied by hepatomegaly. In the most severe cases, mongoloid facies appears owing to swelling of the facial bones; this feature is absent in the milder forms of the disease. The blood picture is characterized by erythroblastemia and marked changes in size and shape of the red blood cells. Showers of nucleated red cells appear a feature which is aggravated by splenectomy and may persist for many months. In milder cases the clinical and hematologic manifestations are less conspicuous. Siblings of children with severe erythroblastic anemia may show only target cells and increased resistance of the red blood cells to the action of hypotonic saline solution.

The roentgen findings are diagnostic in the severe cases. The shafts of the long bones are osteoporotic and swollen; the spongiosa is partially destroyed and deformed and the corticulis is thinned from internal resorption (Fig. 8-792). The entire skeleton is affected but the changes are usually most conspicuous in the long bones which normally have deep concave external contours such as the metacarpals and the femurs. The concave surfaces become shallower, flat or convex as the superabundant marrow distends the medullary cavity and bends the corticulis outward.

In some cases the spongiosa is almost completely destroyed and the bones have a swollen, mottled appearance in contrast with the usual coarse trabeculated spongiosal pattern (Fig. 8-792). The skeletal changes are indistinct during the 1st year of life and become more clearly defined as age advances. During infancy skeletal changes similar to those found in

Cooley's anemia may be noted in some patients with proliferative reticulosis, especially Gaucher's disease (see Fig. 8-816). During late childhood and early adult life there is a tendency to sclerosis in some cases (Figs. 8-793 and 8-794); this is apparently due to the increased formation of corticulis in older age periods. We have shown that the bone lesions in the extremities begin to involute during early adolescence and may then disappear while the lesions in the bones of the trunk persist into adult life. The bone lesions disappear in the peripheral segments of the skeleton where normally red marrow is converted to yellow marrow with advancing age but they persist in the central skeletal segments where the bone marrow normally remains red throughout life. Emery and Follett found that the replacement of red marrow by fatty marrow begins in the toes before birth and is complete by the age of 1 year. The conversion from red to fatty marrow appeared to be accelerated by birth.

In the longstanding severe cases both maturation and growth of the skeleton are retarded. However, premature fusion of the epiphyseal ossification centers with their shafts occurred in 23% of patients older than 10 years in the study of Currarino and Erlandson. The proximal end of the humerus and the distal end of the femur were the only sites of these early fusions, excepting one tibia at its proximal end. Thus Cooley's anemia presents the paradox of delayed appearance time of the secondary centers in the epiphyseal cartilages with later premature fusion of these delayed secondary centers with their primary centers—the shafts. Transverse metaphyseal bands are common. Pathologic fractures of the femur have been serious complications in several of our patients in view of the frequency of extreme cortical atrophy. It is surprising that pathologic fractures are not more common. The cranial changes in Cooley's anemia are discussed in Section I on the skull.

Extramedullary hemopoiesis should be suspected according to Ross and Logan when lobulated or rounded masses of water density are found in the mediastinum contiguous to the spine in patients who have chronic hemolytic anemia or myelofibrosis. The spleen is usually enlarged but the vertebrae are not eroded by the mediastinal masses. In some of their patients, nephrograms disclosed peripelvic filling defects and myelograms demonstrated complete block to the flow of Pantopaque in the thoracic levels of the subarachnoid space.

REFERENCES

- Caffey J. Skeletal changes in chronic hemolytic anemias. *Am J Roentgenol.* 37:293, 1937.
- Cooley's erythroblastic anemia. Some skeletal findings in adolescents and young adults. *Am J Roentgenol.* 65:547, 1951.
- Cooley's anemia. A review of the roentgenographic findings in the skeleton. *Am J Roentgenol.* 78:381, 1957.
- Cooley T B, Wilmer E R, and Lee P. Anemia in children with splenomegaly and peculiar changes in the bones. *Am J Dis Child.* 34:347, 1927.



Fig 8 793 —Changes in the bones with advancing age in a long-standing case of Cooley's anemia. In A, at 11 years of age, the characteristic findings with osteoporosis are present. In B, at



19 years of age, the swollen contours persist but the osteoporosis has disappeared in large part with increased formation of corticals and spongiosa.

Fig 8 794 —Changes in the skeleton with advancing age in Mediterranean (Cooley's) anemia in a Greek girl. A, in the 3d year all of the characteristic changes are present: cortical atrophy and swollen external contours, rarefaction and coarse reticulation. B, in the 12th year all the characteristic changes have disappeared

despite the fact that severe hemolytic anemia persisted. In our experience the characteristic infantile changes always disappear completely or partially in the long bones if the patient survives childhood.



- Curran G and Erlandson E. Premature fusion of epiphyses in Cooley's anemia. *Radiology* 83:656 1964
- Emery J M and Follett G F. Regression of bone-marrow hemopoiesis from terminal digits in fetus and the infant. *Brit J Haemat* 10:485 1964
- Githens J H et al. The prevalence of abnormal hemoglobins in American Indian children. Survey of the Rocky Mountain area. *J Lab & Clin Med* 57:755 1960
- Munnich V et al. Mediterranean anemia. A study of 32 cases in Thailand. *Blood* 9:1 1954
- Nilsson J M et al. Thalassemia (Mediterranean disease) occurring in Filipinos and Chinese. *California Med* 74:195 1951
- Nutts S and Spiliopoulos G. Similarity of erythroblastic anemia and chronic or congenital malaria. *Am J Dis Child* 54:60 1937
- Ross P and Logan W. Roentgen findings in extramedullary hematopoiesis. *Am J Roentgenol*, 106:614 1969
- Smith C H. *Blood Disease of Infancy and Childhood* (St Louis: C V Mosby Company 1960)

Sickle cell anemia—Cranial changes similar to those of erythroblastic anemia have been found in many cases (see Fig 1 149). Apparently marrow hyperplasia in the long bones is much less marked than in Cooley's anemia and for this reason the bone changes secondary to overgrowth of the marrow fail to develop. At necropsies on adults hemorrhage and fibrosis of the marrow and new bone formation on the internal aspect of the cortices have been found in addition to the overgrowth of marrow. The roentgen images of the adult bones show thickening of the corticals and narrowing of the medullary cavity in contrast with the thin cortices and widened medullary

cavities in juvenile Cooley's anemia. The bone changes found in adult patients with sickle cell anemia are exceedingly rare in children (Figs 8-795 and 8-796). It was formerly believed that sickle cell anemia was confined to the Negro race, but several cases have now been described in individuals of non Negro origin.

Infarction in the bones of children with both destructive and productive changes in the roentgenogram are being found with increasing frequency. We have seen several patients in whom the changes in an epiphyseal ossification center suggested osteochondrosis juvenilis (Fig 8 797). The cuplike depressions on the edges of the vertebral bodies described by Reynolds in adults are not found in children. However cupping of the ends of the shafts of the long bones has been observed in children suffering from sickle cell anemia (Fig 8 798). This is the same causal mechanism which produces the acquired cupping of the metaphyses in long bones under a variety of other conditions. In some cases extensive focal destruction with sclerosis has simulated chronic osteomyelitis (Fig 8 799). Hodges and Holt first pointed out the high incidence of *Salmonella* infections in Negroes who carried the abnormal hemoglobin S and had sickle cell anemia. In Africa Negro carriers of the sickle cell trait are said to be especially resistant to malaria, because it is believed that this is a substantial factor in promoting the survival of carriers of the S gene. Hughes and Carroll believed that children

Fig 8 795 (left)—Sickle cell anemia in a black girl 4 years of age. The medullary canals of both femurs are obliterated in their middle thirds by internal thickening and sclerosis of the cortical wall. Changes of this type are apparently common in adults but rare in children.

Fig 8 796 (right)—Internal cortical thickenings and sclerosis of the same patient at 7 years of age. The distal part one of the femurs were not affected and the rest of the skeleton was normal roentgenographically.



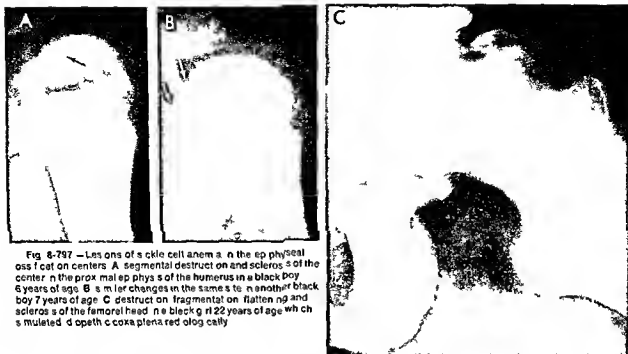


Fig 6-797 — Lesions of sickle cell anemia in the epiphyseal ossification centers. A: segmental destruction and sclerosis of the center in the proximal epiphysis of the humerus in a black boy 6 years of age. B: similar changes in the same site in another black boy 7 years of age. C: destruction, fragmentation, flattening and sclerosis of the femoral head in a black girl 22 years of age which is mutilated despite coxaplasty and allograft.



Fig 6-798 — Cupping of the distal end of the shaft in sickle cell anemia. In A at 16 months of age the central segment of the end of the shaft is partially destroyed but there is no cupping. In B at 76 months the sclerotic enlarged epiphyseal ossification center has fused with the cupped central segment of the shaft and the peripheral segments of the shaft have grown caudal around the ossification center to produce the central depression or cup. The epiphyseal ossification center and shaft have fused over a long segment at the base of the cup.



Fig 8 799—Osteomyelitis like changes in the shafts of the humerus (A) and femur (B) of a black girl 9 years of age who had sickle cell anemia. *Salmonella* was probably the causal agent from the clinical course. It was not proved bacteriologically. (Courtesy of Drs F J Hodges and J F Holt University of Michigan)

with sickle cell anemia have a special vulnerability to salmonella osteomyelitis. Radiographically it is often difficult to differentiate the basic sickle cell changes in the bones from inflammatory changes (Fig 8 800). Hook encountered four examples of salmonella osteomyelitis in 36 patients with sickle cell anemia. 1 was an infant 15 months of age. One of the most interesting bone lesions in sickle cell anemia is the transitory change found in the tubular bones of the hands and feet during infancy (Fig 8 801).

Burko and associates found destructive chondritis and osteitis in the sternum of a girl 4 years of age who had homozygous sickle cell anemia and heavy infection with *Salmonella typhimurium*; these organisms were grown from the sternal lesion. Segmental pulmonary infarcts develop occasionally and resemble pneumonic consolidations radiographically. Cholelithiasis has appeared during the 1st year of life. The heart is often enlarged in the very young

sometimes to a degree which may suggest pericarditis with effusion radiographically. In the central nervous system thrombosis is the most frequent complication and may be followed by focal spinal or cerebral bleeding, hypoxia and necrosis.

Sickle-C disease differs from typical sickle cell anemia according to Denny and colleagues by the presence of hemoglobin C in addition to hemoglobin S. Patients with sickle C disease usually have large spleens in contrast to the small spleens or absence of the spleen in juvenile classic sickle cell anemia.

In a radiographic study of 17 patients in Nigeria who had hemoglobin SC disease, Barton and Cockshott found skeletal changes of marrow hyperplasia, infection and infarction.

REFERENCES

- Barton C J and Cockshott W P: Bone changes in Hemoglobin SC disease. *Am J Roentgenol* 89:523, 1962.
 Burko H et al: Unusual changes in sickle cell anemia in childhood. *Radiology* 80:937, 1963.
 Caffey J: Skeletal changes in the chronic hemolytic anemias (erythroblastic anemia, sickle cell anemia and chronic hemolytic icterus). *Am J Roentgenol* 37:293, 1937.
 Cockshott W P: Dactylitis and growth disorders. *Brit J Radiol* 36:19, 1969.
 Hodges F J and Holt J F: *The 1951 Year Book of Radiology* (Chicago: Year Book Publishers, Inc.) p 88.
 Hook E W et al: *Salmonella osteomyelitis in patients with sickle cell anemia*. *New England J Med* 257:403, 1957.
 Hughes J et al: Involvement of the nervous system in sickle cell anemia. *J Pediatr* 17:168, 1940.
 Hughes J G and Carroll D S: *Salmonella osteomyelitis complicating sickle cell disease*. *Pediatrics* 19:184, 1957.
 Middlemiss J: Sickle cell anemia. *J Fac Radiologists* 9:18, 1958.
 Reynolds J: A reevaluation of the fish vertebra sign in sickle cell hemoglobinopathy. *Am J Roentgenol* 97:693, 1966.
 Rowe C W and Haggard M E: Bone infarcts in sickle cell anemia. *Radiology* 68:661, 1957.
 Watson R J et al: The hand foot syndrome in sickle cell anemia in young children. *Pediatrics* 31:975, 1963.

Familial hemolytic (spherocytic) anemia as defined by Smith is characterized by hemolysis, spherocytosis, increased osmotic fragility of red blood cells and splenomegaly. The hemoglobin is not abnormal. There are several reports of changes in the skull and long bones similar to those found in erythroblastic anemia. Skeletal changes, however, are absent in most cases of spherocytic anemia when present they usually are not striking and are variable. The cranial changes are commonly more marked than those in the long bones (see Figs 1 147 and 1 148). Snelling and Brown described a case in which the skeletal lesions improved following splenectomy.

REFERENCES

- Moseley J E: *Bone Changes in Hematologic Disorders* (New York: Grune & Stratton, Inc., 1963).
 Smith C H: *Blood Disease of Infancy and Childhood* (St. Louis: C V Mosby Company, 1960).
 Snelling C E and Brown A: A case of hemolytic jaundice with bone changes. *J Pediatr* 8:330, 1936.

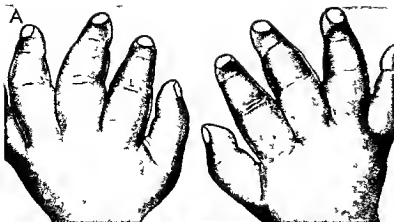
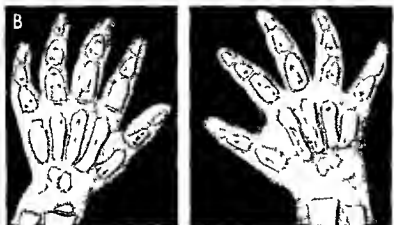


Fig 8 800 — Multiple osteomyelitis in the tubular bones of the hands and swellings of the fingers in a girl 12 months of age who had sickle cell anemia and probably had shigellosis. A, cellulitis of the fingers with diffuse swelling of the soft tissues



B, destructive and productive osteitis of the phalanges and metacarpals (Redrawn from Jevy and Howard)

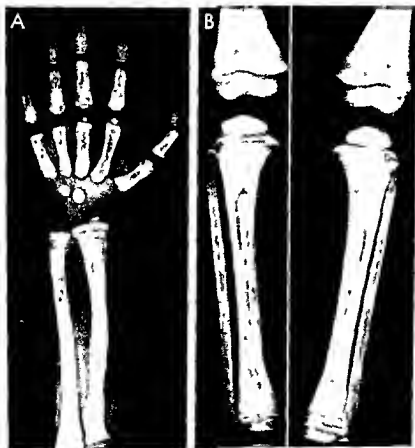
Fig 8 801 — Polyphalangeal osteitis which resembles the phalangeal changes of sickle cell anemia. This black girl 10 months of age did not have either active or latent sickle cell anemia in several tests. The soft tissues of the affected fingers are swollen and the phalanges are generally sclerotic with sequestrums at their bases. Similar changes were present in the other hand and both feet. *Streptococcus A* was cultured several times directly from the bone lesions. (Courtesy of Drs. Kenneth Haltalin and John Nelson, Dallas, Tex.)





Fig 8 802 —Leukemia in a girl 3½ years of age with terminal transverse striping of the shafts. These transverse lines of both increased and diminished density are the commonest and the earliest roentgen bone changes and may persist for weeks or months as the only changes in leukemia. The lines are usually best developed in the large metaphyses at the knees.

Fig 8 803 —Leukopenic lymphatic leukemia in a boy 2 years of age. A, hand and forearm. B, lower extremities. Irregular destruction of all of the bones is evident. Deep transverse zones of diminished density occupy the ends of the shafts. In addition to



LEUKEMIA (MALIGNANT RETICULOSIS) —The growing skeleton is the site of malignant proliferation of reticulum cells in nearly all cases of leukemia unless early death supervenes. In the course of the disease multiple areas of destruction and production appear and increase in size at variable sites in numerous bones. The roentgen changes are usually most conspicuous and appear first in the metaphyses at both ends of the femur and tibia (Fig. 8 802) and at the proximal end of the humerus and the distal end of the radius. In advanced cases spotty destruction is visible in the larger epiphyseal ossification centers and in the flat bones of the calvaria, shoulder girdle and pelvic girdle (Figs. 8 803 and 8 804). It is likely that the skeletal lesions of leukemia are due to malignant proliferation of reticulum cells originally native to the bone marrow tissues rather than to malignant proliferation of reticulum cells transported from lymphatic structures such as the spleen and lymph nodes. In this sense the disorder which has been called 'leukopenic

these destructive features there are numerous large and small irregular patches of sclerosis indicative of massive osteoblastic reaction as well.



Fig 8 B04 - Severe osteolytic leukopenic lymphatic leukemia in a girl 3 years of age. Most eaten areas of cystic reaction are scattered in the long tubular bones. Leukopenia persisted until death; the diagnosis of leukemia was proved at necropsy.

leukemia could be more accurately designated as "malignant proliferative reticulosis."

During the early stages the marrow cavity is filled with leukemic cells but there is no bone destruction and the roentgen appearance is normal. Bone pain in such cases is due to increased intraosseous pressure. Later the spongiosa is partially destroyed and replaced by masses of leukemic tissue which are responsible for metaphyseal foci of rarefaction found in the roentgenogram. Concurrently the overlying cortex is eroded on its internal aspect. Leukemic cells penetrate the overlying corticalis and lift the periosteum. The elevated periosteum produces layers of compact bone beyond the cortical margin. Occasionally cortical thickening in leukemia is residual to subperiosteal hemorrhages secondary to thrombocytopenic purpura. Callus formation following pathologic fractures may also cause regional cortical thickenings. In the most severe cases the extensive osteolytic lesions may suggest hyperparathyroidism. Rarely the reaction of the bone to the leukemic infiltration appears to be almost exclusively osteoblastic and the roentgen changes are predominantly osteosclerotic owing to the excessive formation of spongiosa.

Svab and Horak, using a magnifying lens in the study of their films, found internal abrasion of the cortical walls of the metacarpal bones of all patients with leukemia, and they concluded that the metacarpals are the optimal sites for the identification of skeletal leukemia. We have seen many examples of gross leukemic lesions in the metaphyses of the larger long tubular bones in which the metacarpals appeared normal to the unaided eye. In eosinophilic leukemia Bentley and colleagues found transverse radiolucent metaphyseal bands in the long bones.

The diagnosis of leukemia is relatively easy when the clinical and hematologic findings are characteristic. However, in the leukopenic type of lymphogenous leukemia, which is the common form in early life, the hematologic picture may be equivocal for long periods and may remain inconclusive until death. The roentgen demonstration of skeletal involvement in such cases is of great diagnostic help in differentiating leukemia from rheumatic fever and rheumatoid arthritis. Films should be made of the skeleton of children who exhibit leukopenia, splenomegaly, chronic fever, and bone and joint pain; the identification of destructive skeletal lesions in these circumstances makes the diagnosis of leukopenic leukemia a practical certainty. The roentgen appearance of leukemia of the skeleton is similar to that caused by lymphosarcoma and sympathetic neuroblastoma.

It should be remembered that meningeal involvement in leukemia is often accompanied by the development of radiographic signs of actively increased intracranial pressure. This complication is characteristically encountered after prolonged treatment with corticosteroids.

Although the pain in leukemia usually originates in the bones, Bedwell and Dawson demonstrated actual leukemic infiltrations in the synovial tissues of an 8 year old girl who died of chronic myeloid leukemia. It is possible that some of the pain in leukemia originates in articular tissues as well as bone.

Chloroma is invariably associated with myelogenous leukemia; the leukemic lesions are green and this color has been attributed to the reduction of split products in the degeneration of hemoglobin. In children the principal lesions develop in the periorbital tissues and the marrow cavities of the long bones and skull. Austin described changes in the ribs in a girl 11 months of age: swellings at the sternal ends of the ribs which simulated a rachitic rosary clinically. The ventral ends of the second through seventh ribs presented bulbous swellings where the cortical walls were thickened externally.

The bone lesions sometimes disappear completely during the long remissions induced by chemotherapy or adrenalcorticosteroids. Before the advent of such treatment remissions of the bone lesions had been observed following severe infections, especially cervical adenitis; it now seems probable that these remissions were responses to the excess adrenalcorticosteroids generated naturally by the stress of the severe infections.

Study of the offspring of women exposed to diagnostic radiologic procedures during pregnancy has not disclosed increased incidence of leukemia in the offspring.

Ulcerative lesions in the intestinal walls were demonstrated in one of five leukemic patients at necropsy by Amroman and Solomon; therapeutic adrenalcorticosteroids are probably responsible for many of these lesions.

REFERENCES

- Amromin G D and Solomon R D Necrotizing enteropathy A complication of treated leukemia and lymphoma cases JAMA 182 133 1962
- Austin J H Chloroma Report of a patient with unusual nb lesions Radiology 93 671 1969
- Bedwell C A and Dawson A M Chronic myeloid leukemia in a child presenting as acute polyarthritis Arch Dis Childhood 29 78 1954
- Bentley H P et al Eosinophilic leukemia Report of a case with review and classification Am J Med 30 310 1961
- Dennis J M and Mercado R Scurvy following folic acid antagonist therapy Radiology 67 412 1956
- Follis R H Jr and Park E A Some observations on the morphologic basis for the roentgenographic changes in childhood leukemia, Bull Hosp Joint Dis 12 67, 1951
- Karpinski F E and Martin J F Skeletal lesions of leukemic children treated with aminopterin J Pediat 37 208 1950
- Landolt R F Bone changes in juvenile leukemia Rheumatoid leukemia form Helvet paediat acta 1 146 1946
- Silverman F N Skeletal lesions in leukemia Clinical and roentgen observations in infants and children with review of the literature Am J Roentgenol 59 819 1948
- Svab V and Horak B Diagnosis of bone changes in leukemic children by aid of x rays Pediat bstr 6 335 1951
- Thomas L B et al The skeletal lesions of acute leukemia, Cancer 14 609 1961

HEMOPHILIA—Lesions in the skeleton may be due to bleeding directly into the bones or to secondary changes in the bones which result from hemorrhages into adjacent joints. Intraosseous hemorrhages into the shafts and epiphyses produce rounded defects in the spongiosa of variable size which cast cystic shadows of rarefaction in roentgenograms (Fig 8-805)

Fig 8-805—Hemophilic intraosseous hemorrhages into the medullary cavity of the calcaneus of a young adult. The large redolucent patches represent intramedullary hematomas in different stages of organization (Courtesy of Dr Bruce Ward Grand Junction Colo)

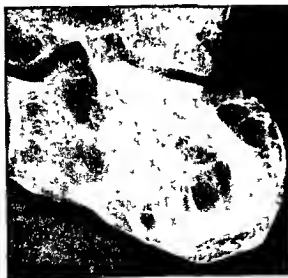


Fig 8-806—Hemophilic subchondral hemorrhages in the proximal epiphysis of the femur which are responsible for the marginal defects in the region of the femoral head. The epiphysis is flattened in its longitudinal axis and the neck of the femur is broadened. A large bony spine protrudes laterally from the root of the acetabulum.

Fig 8-807—Hemophilia in a boy 14 years of age. Old and recent subperiosteal hemorrhages have swollen the soft tissues and thickened the cortical walls of the proximal phalanx of the 3rd and 4th digits. The old cortical wall is still visible but a lace-work of bony branches extends peripherally from it. The epiphyseal ossification center at the proximal end of the phalanx of the 3rd digit is slightly displaced. The smaller and older subperiosteal hemorrhages have produced the cortical thickenings and fatty branchings in the proximal phalanx of the 4th digit and in the 2nd metacarpal.



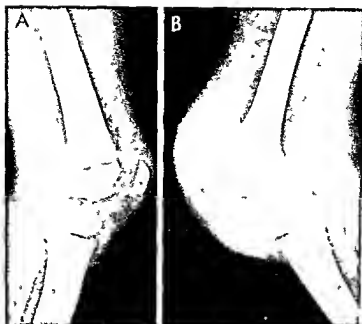


Fig 8 808 —High tension hemarthrosis (recurrent) of the left knee of a hemophilic boy 7 years of age. The suprapatellar and popliteal bursas are dilated with blood, the large amount of blood in the knee proper has obliterated the image of the tibia.

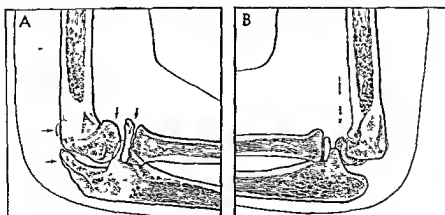
patellar fat pad. The patella is displaced ventrad. The patella and epiphyseal ossification centers of the femur and tibia are enlarged secondary to chronic hyperemia.

Subperiosteal hemorrhages in hemophilia are rare, but when they occur they are followed by external cortical thickenings in the same way that subperiosteal hemorrhages from other causes are followed by cortical thickenings. Sometimes, in the case of tension hematomas under the periosteum pressure atrophy of the underlying cortex develops. Subchondral hemorrhages are responsible for marginal bony defects on the juxta articular borders of the epiphyseal ossi-

fication centers (Fig 8 806), in the proximal epiphysis of the femur a flattening deformity which resembles coxa plana may accompany the subchondral defects. Subperiosteal hemorrhages are astonishingly rare in hemophilia at all ages but they are occasionally demonstrable in roentgenograms and have been found at necropsy. Hemophilic subperiosteal hematomas have the same roentgen appearance as those of non hemophilic origin (Figs 8 807 and 8-808).

Fig 8 809 —Accelerated maturation of the apophyses contiguous to the hemarthrotic right elbow of a hemophilic boy 10 years of age. A, hemarthrotic right elbow. B, normal left elbow tracings of roentgenograms. The secondary centers on the right side (arrows) are all hypertrophic in comparison with the normal left side. Large ossification centers are visible in the olecranon

process of the right ulna and in the trochlea of the right humerus at the same sites on the normal side. Secondary centers have not yet appeared. The shafts of the bones on the right side as well as the epiphyses are enlarged. The accelerated maturation and growth are probably due to the chronic hyperemia induced by longstanding recurrent hemarthrosis.



Bleeding into the articular spaces is much more common than bleeding into the bones. Intra articular blood may be completely resorbed after a few days or weeks without residual deformity or disability. When, however, the resorption of blood from the joint space is incomplete following a single hemorrhage or recurrent hemorrhages, the retained blood and blood clots set up a chronic inflammatory reaction in the articular tissues which results in deformities, disability and sometimes ankylosis. When there is long standing limitation of motion of the part atrophy of disuse develops in the bones adjacent to the affected joint. Chronic regional hyperemia of the neighboring epiphyseal cartilages induced by long standing continuous and recurrent hemarthrosis, is believed to be responsible for accelerated maturation and hypertrophy of the adjacent epiphyses (Fig. 8 809).

More than half of all hemophilic children are said to develop permanent deformities due to chronic hemarthrosis. During the acute phase the articular swelling increases rapidly and motion and weight bearing are prevented by severe pain. Fever is the only constitutional symptom. It may reach 104 F. In severe cases Leukocytosis commonly accompanies the fever. Local heat, at the site of the hemarthrosis, may or may not be increased. Roentgenograms in the early stages show local soft tissue swelling, and sometimes the articular space appears to be widened.

Panarthrosis develops when the resorption of blood is incomplete, and the affected joint remains swollen, tender and painful for months. After each recurrence of bleeding the picture of simple acute hemarthrosis is repeated, the signs and symptoms partially subside in the intervals between the recurrent acute exacerbations. Gradually the chronic irritation produces a permanently swollen joint with local deformity, contractures, muscular atrophy and cumulative loss of

motion. The superabundant synovial membrane becomes folded and exhibits villous hypertrophy. The subsynovial connective tissue is hyperplastic and becomes thickened into a dense fibrous layer. The swollen soft tissues are impregnated with iron containing blood pigments (Fig. 8-810). The articular space is narrowed by destruction of the articular cartilage and encroachment of the thickened synovial membrane on the cartilaginous margins, with invasion of the more central portions by connective tissue. The ends of the bones which subtend the destroyed cartilage are also invaded by connective tissue, and irregular marginal bony defects result. The roentgen appearance in long standing hemophilic panarthrosis is shown in Figure 8 811.

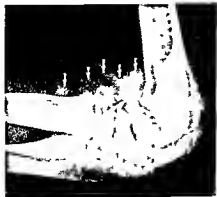
PURPURA—In contrast with hemophilia, demonstrable bleeding into bones and joints is rare in both acute and chronic thrombocytopenic purpura. Subperiosteal hemorrhage has been found at necropsy.

POLYCYTHEMIA VERA is rare during early life. No characteristic roentgen changes have been found in adult bones. Theoretically the overgrowth of the red marrow in polycythemia vera should produce the same changes in the growing skeleton as the red marrow overgrowth in Cooley's anemia.

REFERENCES

- Caffey J. and Schlesinger E. R. On certain facts of hemophilia on the growing skeleton. *J. Pediat.* 16: 549 1940.
 Dykstra, O. H., and Halbertsma T. Polycythemia vera in childhood. Report of a case with changes in the skull. *Am. J. Dis. Child.* 60: 907, 1940.
 Hodgson J. R., Good C. A., and Hall B. E. The roentgen aspects of polycythemia vera. *Proc. Staff Meet., Mayo Clin.* 21: 152 1946.
 Marlow A. A., and Fairbanks V. F. Polycythemia vera in an eleven year old girl. *New England J. Med.* 263: 950 1960.
 Schwartz E. Hemophilic pseudotumor of bone. *Radiology* 75: 795 1960.
 Smith C. H. *Blood Diseases of Infancy and Childhood* (St. Louis: C. V. Mosby Company 1960).

Fig. 8 810—Chronic hemophilic hemarthrosis of the right elbow in a boy 10 years of age. The arrows are directed at images of increased density in the periparticular soft tissues. It is probable that the heavy density is due in part to the high iron content of these tissues. Acceleration of maturation and overgrowth of the bones due to chronic regional hyperemia are also evident.



PRIMARY ERYTHROCYTOSIS is characterized by an increase in the concentration of hemoglobin in each red blood cell and an increase in the number of red blood cells which results in an absolute increase in the total circulating red cell mass and an absolute increase in the total circulating mass of hemoglobin. The numbers of leukocytes and thrombocytes are normal. The clinical course is benign. In the bones, rarefaction and coarsening of the trabecular pattern suggest overgrowth of the marrow.

REFERENCE

- Abilgaard C. F., et al. Primary erythrocytosis. *J. Pediat.* 63: 1072 1963.

PROLIFERATIVE RETICULOSES (RETICULOENDOTHELIOSIS, HISTIOCYTOSIS X)—These disorders are all characterized by granulomatous proliferation of the reticu-

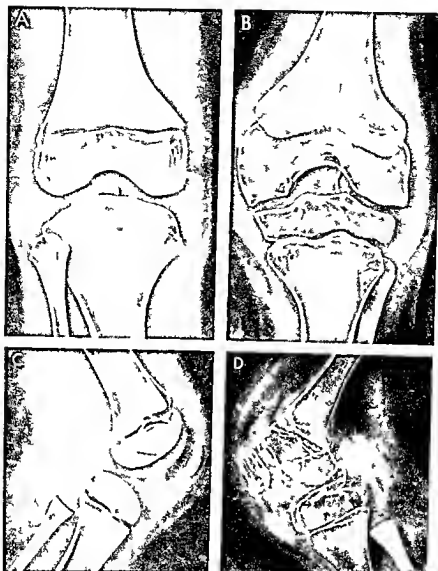


Fig 8-811 ~ Hemophilic arthropathy in a boy 7 years of age. A and C normal right knee and B and D hemarthrotic left knee frontal and lateral projections. In the left knee the soft tissues are swollen and increased in density. In addition the bone is marked generalized rarefaction of the epiphyses and shafts and atrophy

of the shafts. The epiphyseal centers and patella, however, are enlarged on the left side. The intercondylar notch is deepened and the juxta articular surfaces of the bones are ragged. In D a large intraosseous hematoma is visible in the tibial epiphysis (arrows).

lum cells at one or several sites in the reticuloendothelial system: the skeleton, lymph nodes, spleen, thymus, liver, and skin. Hemorrhage usually accompanies the proliferation. The cause of reticulosis is not established; infection appears to play a causal role in many cases. At different ages and in different stages of its evolution, reticulosis is responsible for a variety of clinical and anatomic manifestations, all of which are due to the basic hyperplasia of reticulum cells. Infants, children, adolescents, and young adults may be affected.

Nonlipoid reticulosis — When the disease develops during the first years of life, there is a diffuse general

ized proliferation in all parts of the reticuloendothelial apparatus; the course is rapid and usually fatal. The predominating clinical manifestations of this diffuse infantile type include purpura, rash, progressive anemia, splenomegaly, hepatomegaly, and skeletal defects (Fig 8-812). The outstanding microscopic feature of the diffuse infantile type is hyperplasia of reticulum cells without lipidization. The absence of lipids has given rise to the name nonlipoid reticulosis, which is further subdivided clinically into infectious and noninfectious (Letterer-Siwe disease) types.

In Fisher's patient the clinical and radiologic fea-

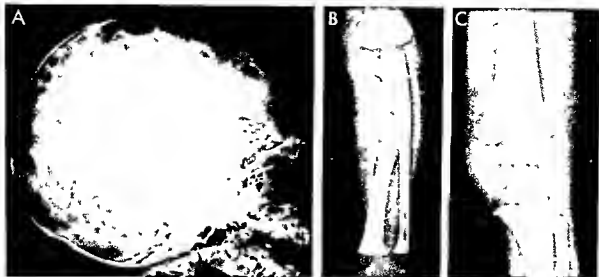


Fig 8-812—Noninfectious nonlipid infantile proliferative reticulosis (Letterer-Siwe disease) in a boy 1 year of age (necropsy). There are numerous small and large sharply defined defects in

the tubular and flat bones at necropsy nonlipid reticulosis were found in the sites of the bone defects. A, lateral projection of the skull. B, forearm.

tures and biopsy specimens were characteristic of Letterer-Siwe disease. Later lipid storage became evident in the biopsy specimen and the macroscopic diagnosis was Schuller-Christian disease. Cultures from the bone lesions and excised tissues yielded paracolon Arizona bacilli, the bone lesions and clinical manifestations regressed immediately after institution of antibiotic therapy.

Granulomatous changes in the lungs are common in young patients who have proliferative reticulosis and at first the radiologic findings may simulate hematogenous disseminated tuberculosis in both lungs. Later, infection is often superimposed and may be complicated by bronchial obstruction with secondary atelectasis and emphysema. Granulomas of the pleura may produce changes suggestive of suppurative pleurisy.

Liporeticulosis—In older children, adolescents and adults, reticulosis runs a more protracted course, the granulomatous proliferations of reticulum cells are more localized and skeletal lesions predominate. The cutaneous and lymphatic manifestations may be meager or absent. The hyperplastic reticulum cells are filled with cholesterol. Cholesterol liporeticulosis is also known as xanthomatosis or Hand-Schüller-Christian disease. In later healing stages, fibrous tissue replaces the lipid-laden reticulum cells. The localization of the disease in the orbits, base of the skull and calvaria in some cases is responsible for exophthalmos, diabetes insipidus and cranial defects which were considered to be the cardinal manifestations of lipid reticulosis in the original descriptions of the disorder. It is now evident that the first descriptions included only those cases with conspicuous clinical manifestations and that the distribution of the

lesions is much more variable and widely scattered than formerly believed. One, two or all of the so-called cardinal symptoms may be absent while there are extensive lesions in the long and flat bones, skin, spleen and thymus.

Eosinophilic granuloma—Eosinophilic infiltration of the lesions of nonlipid and lipid reticulosis occurs not infrequently, concurrent eosinophilia of the blood may also appear. The eosinophilic type of reticulosis, in the report of Jaffe and Lichtenstein was described as a separate disease and called eosinophilic granuloma. Farber and his colleagues presented convincing evidence that eosinophilic granuloma is a variant of reticulosis and not a separate entity clinically or anatomically. The eosinophilic type appears to be the most frequently localized and the mildest form of reticulosis. Solitary xanthoma of bone and solitary eosinophilic granuloma of bone are also variants of the same basic localized process of reticulum cell hyperplasia. During the proliferative phase of eosinophilic granuloma, the bone lesions are sensitive to adrenocorticosteroids.

The roentgen appearance of the skeletal lesions is identical in all types of reticulosis—nonlipid cholesterol lipid and eosinophilic. The bony changes are essentially destructive, the radiopaque spongiosa and cortex are replaced by radiolucent reticulum cell granulomas which cast cystic shadows of rarefaction (Fig 8-813). Expansion of the granulomas in the medullary cavity of long bones often dilates it and produces internal pressure atrophy of the overlying cortices. Pathologic fractures develop at the site of the lesions in some cases. Sometimes the overlying periosteum is stimulated to excessive bone production which results in regional cortical thickening. One,

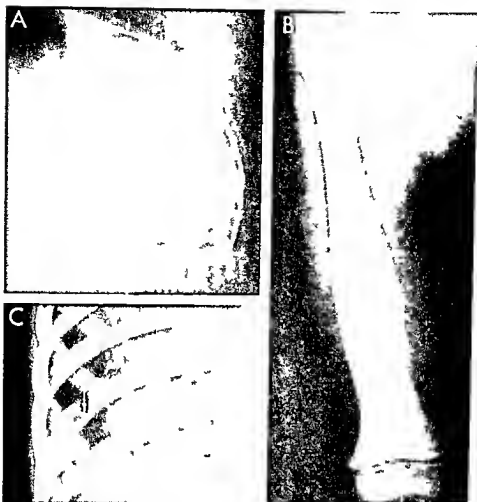


Fig 8-813—Eosinophilic cholesterol liporeticulosis (eosinophilic granuloma) in a boy 3 years of age. A: Large defect in the frontal bone. B: Cystic area with regional cortical thickening of the femur. The cortical thickening is unusual. There was no clinical or roentgenographic evidence of pathologic fracture. C: Expansion, destruction, and thickening of the 8th rib.

ng of the femur. The cortical thickening is unusual. There was no clinical or roentgenographic evidence of pathologic fracture. C: Expansion, destruction, and thickening of the 8th rib.

several or many of the bones may be involved in the skull, vertebral column, shoulder girdle, ribs, pelvis, and extremities. The cranial changes in cholesterol reticulosis are shown in Figures 1-155 to 1-157.

REFERENCES

- Avery M E, *et al*. The course and prognosis of reticuloendotheliosis (eosinophilic granuloma, Schuller-Christian disease and Letterer-Siwe disease): a study of 40 cases. *Am J Med* 22:636, 1957.
- Batson B, *et al*. Acute nonlipid disseminated reticuloendotheliosis in childhood. *J Pediatr* 38:744, 1955.
- Green W T and Farber S. Eosinophilic or solitary granuloma of bone. *J Bone & Joint Surg* 24:499, 1942.
- Gross P and Jacox H W. Eosinophilic granuloma and certain other reticuloendothelial hyperplasias of bone. *Am J M Sc* 203:673, 1942.
- Jaffe H L and Lichtenstein L. Eosinophilic granuloma of bone. *Arch. Path* 37:99, 1944.
- JAMA 135:935, 1947 (letter).
- Moseley J E. *Bone Changes in Hematologic Disorders (Roentgen Aspects)* (New York: Grune & Stratton Inc, 1963).

- Ponseti I. Bone lesions in eosinophilic granuloma, Hand-Schuller-Christian disease and Letterer-Siwe disease. *J Bone & Joint Surg* 30-A:811, 1948.
- Saenger E L and Johansmann R J. Letterer-Siwe disease. Problems in diagnosis and treatment. *Am J Roentgenol* 71:472, 1954.
- Schaeffer E L. Nonlipid reticuloendotheliosis. Letterer-Siwe's disease. *Am J Path* 25:40, 1949.
- Smith C H. *Blood Disease of Infancy and Childhood* (St. Louis: C V Mosby Company, 1960).
- Symmers W St C. Reticulosis I. Some comments on the pathology of the reticulosis. *Brit J Radiol* 24:469, 1951.
- Weinstein A, Francis H C and Sprock B F. Eosinophilic granuloma in bone and pulmonary infiltration. *Arch. Int Med* 79:176, 1947.

Gaucher's disease (keratin liporeticulosis)—There is still difference of opinion as to the exact pathogenesis of this rare disorder, but the primary disturbance appears to be an excessive proliferation of the reticulum cells in the reticuloendothelial apparatus. The principal hyperplasia is located in the lymph



Fig 8-814 (left) —Gaucher's disease in epiphyseal ossification centers. Destructive and productive changes in the distal right femoral ossification center of a girl 6 years of age. There are similar changes in the shafts of both femurs and in the ossification center in the proximal epiphyseal cartilage of the right femur.



Fig 8-815 (right) —Gaucher's disease in an infant 18 months of age showing characteristic changes in the femur. The medullary cavity is dilated, the shaft swollen, the cortex thin and the spongiosa irregularly destroyed.

phatic and hemopoietic components but hyperplasia of reticulum cells within the skeleton is conspicuous in most advanced cases. The unique feature of Gaucher's disease is the presence of the lipid called kersatin in the hyperplastic reticulum cells. Kersatin liporeticulosis and cholesterol liporeticulosis resemble each other pathogenetically but are dissimilar clinically and chemically.

The predominant clinical manifestations are a slow progressive enlargement of the spleen and a less marked enlargement of the liver and lymph nodes. Bleeding into the skin and mucous membranes is common; recurrent epistaxis, hemoptysis and hematemesis are not unusual. The hemoglobin, erythrocytes, leukocytes and platelets are diminished but there is no tendency to erythroblastemia or reticulocytosis. Bone pain is not infrequent and is usually dull and poorly localized. Severe, sharply localized pain is caused by pathologic fractures. Growth of the long bones may be retarded generally owing to the associated severe malnutrition or locally from invasion of the proliferating epiphyseal cartilages by reticulum cells. Extreme dwarfism has resulted.

There is no cure for Gaucher's disease; splenectomy may give temporary relief from abdominal discomfort. Early death is the rule when the disease becomes manifest during infancy. In the milder juvenile and adolescent cases the disease advances insidiously and life may be prolonged for many years.

The roentgenographic changes in the skeleton are due primarily to the destruction of bone and replacement of it by hyperplastic kersatin-laden reticulum cells. During infancy the skeletal changes appear

long after pallor and splenomegaly are manifest. The changes in the bones become progressively more marked with advancing age. Changes may be detected in one, several or many of the tubular bones (Fig 8-814) and flat bones. In contrast with nonlipoid reticulosis and cholesterol liporeticulosis, the cranium is

Fig 8-816 —Infantile Gaucher's disease in a patient 14 months of age showing generalized skeletal changes similar to those found in Cooley's erythroblastic anemia.



rarely affected in Gaucher's disease. The vertebral column on the other hand is often involved in juvenile and adolescent patients suffering from Gaucher's disease.

Hypertrophy of the intraosseous reticulum causes increased intraosseous pressure, expansion of the shafts, destruction of the spongiosa and pressure atrophy of the overlying cortices. In infants the earliest and most characteristic lesions are usually found in the femurs (Fig. 8-815). If the patient survives sufficiently long and the disease advances, changes similar to those in the femurs appear in several of the larger tubular bones (Fig. 8-816). The swollen appearance of the shafts, the irregular rarefaction and cortical atrophy are similar to the changes in Cooley's erythroblastic anemia. However, the tubular bones in the hands and feet are usually conspicuously involved in Cooley's anemia while they are only slightly affected in Gaucher's disease. In children and adolescents repair and overproduction of the spongiosa may produce a late sclerosis of the dilated thin-walled shafts.

REFERENCES

- Askin A. M. and Schein A. G. Aseptic necrosis in Gaucher's disease. *J. Bone & Joint Surg.* 30-A: 631, 1948.
 Relis O. and Kato K. Gaucher's disease. Clinical study with special reference to the roentgenography of bones. *Am. J. Dis. Child.* 43: 635, 1932.

Disseminated lipogranulomatosis (Farber's disease) is a rare fatal syndrome of infants in which subcutaneous nodules at the peripheral joints, muscular atrophy, hyperpigmentation of the skin over bony prominences, rickets-like rosary, patchy increases of density in the lungs, laryngeal stridor and projectile vomiting are the principal manifestations. The pararticular nodules and pulmonary lesions have been visualized radiographically. Abul Haj and associates have suggested that this disease is a mucopolysaccharidosis. The accumulated material in the central nervous system in their patient proved to be a nonsulfated acid mucopolysaccharide. Urinary excretion of mucopolysaccharides was not determined. The principal radiographic finding in Farber's disease is destruction of joint cartilage and contiguous bone.

REFERENCES

- Abul Haj S. K., et al. Farber's disease. Report of a case with observations on histogenesis and notes on the nature of the stored material. *J. Pediatr.* 61: 221, 1962.
 Farber S., et al. A lipid metabolic disorder: Disseminated "lipogranulomatosis." *Am. J. Dis. Child.* 84: 499, 1952 (abst).
 Schanche A. F., et al. Disseminated lipogranulomatosis. Early roentgenographic changes. *Radiology* 82: 675, 1964.

Niemann-Pick disease (lecithin liporeticulosis) resembles the infantile type of Gaucher's disease pathogenetically and clinically but is a distinct entity histologically and chemically. The basic pathologic

change is the diffuse proliferation of reticulum cells throughout the reticuloendothelial apparatus which gives rise to splenomegaly, hepatomegaly and destructive skeletal changes. The disease usually becomes evident during the 1st year of life and death occurs before the end of the 2nd year. A lipid composed largely of lecithin is deposited in the hyperplastic reticulum cells which have a vacuolated foamy texture in contrast with the striated fibrillar pattern of the typical Gaucher cell. The diagnosis is made by demonstration of characteristic cells in the spleen or lymph nodes and identification of the lipids lecithin and sphingomyelin in the spleen removed by splenectomy or at necropsy.

The patient usually dies before conspicuous skeletal changes develop. Poncher found focal areas of rarefaction in the tubular bones in one patient 18 months of age.

We have seen two examples of massive calcification of the adrenals (see Fig. 6-92) in fatal cases of Niemann-Pick disease. The large size of these calciferous adrenals indicated that calcification of them must have taken place before birth or during the 1st days of life before physiologic neonatal atrophy of the adrenals had occurred.

REFERENCES

- Crocker A. C. and Farber S. Niemann-Pick disease. Review of 18 cases. *Medicine* 37: 1, 1958.
 Moseley J. E. Bone Changes in Hematologic Disorders (Roentgen Aspects). (New York: Grune & Stratton Inc. 1963).

SKELETAL CHANGES IN THE ENDOCRINOPATHIES

THYROID GLAND—The growth and maturation of the skeleton are profoundly affected by the activity of the thyroid. Capps and Hipona demonstrated opacification of the normal thyroid gland and tumorous thyroids during angiocardiology.

Hypothyroidism—In this condition both growth and maturation are retarded (Fig. 8-817). The medullary cavities in the tubular and flat bones are characteristically small and narrow with corresponding internal thickenings of the overlying cortex. These features disappear with treatment. Dental development is consistently delayed. Before the onset of puberty the progress of skeletal maturation is probably the best single index of the adequacy of thyroid therapy. At birth the hypothyroid infant exhibits normal or only slightly retarded maturation owing to the effect of the maternal thyroid hormones which cross the placenta into the fetal circulation and assist in the promotion of prenatal development of the fetal skeleton. Following birth the maternal thyroid effect is lost and the infantile skeleton grows slowly; the appearance time of secondary ossification centers may be postponed for months and years. Atavistic accessory epiphyseal ossification centers frequently appear in the carti-

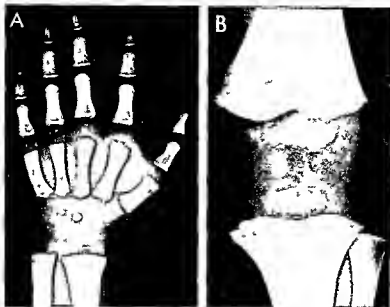


Fig 8-817—Retardation of skeletal maturation in an untreated hypothyroid girl 8 years of age. **A**, hand and forearm. **B**, knee. The epiphyseal development approximates that of a normal infant 6-12 months of age. The medial aspect of the femoral epiphysis is irregularly mineralized. See Figures 6-35 and 6-37 for comparison with normal osseous maturation.

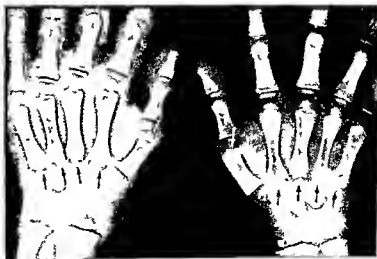
ages at the bases of the metacarpals of cretins (Fig 8-818). In some infantile cretins deep transverse bands of increased density are found both before and after treatment.

The most reliable diagnostic findings in hypothyroidism are low values for the uptake of radioactive iodine isotopes and low values for serum protein

bound iodine concentration. It should be remembered that iodine crosses the placenta from mother to fetus and that high values for protein bound iodine in the serum of newborns may result from diagnostic procedures with iodine contrast agents in the mother done as long as four years before the birth of the infant in the case of iophenoxic acid (Tendax) (Fink

Fig 8-818—Multiple accessory ossification centers at the proximal ends of the 2nd to 5th metacarpals in both hands (arrows); an accessory center is also present in the distal end of each of the 1st metacarpals. The patient was an untreated hypothyroid girl 10 years of age whose skeletal age approximated

the average for a normal child 2 years of age. At 14 years of age, after four years of thyroid medication, the bone age was normal and all of the accessory epiphyseal metacarpal centers had fused with the shafts.



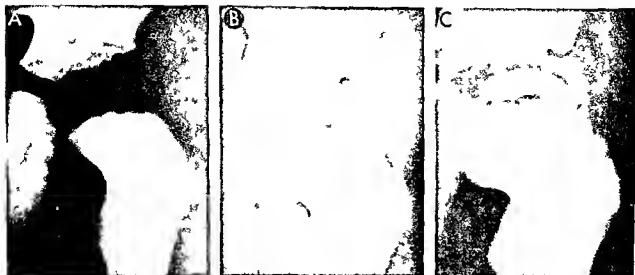


Fig. 8-819—Spotted epiphyses and epiphyseal dysgenesis in a hypothyroid girl 8 years of age. A, before treatment. The proximal femoral epiphyseal center is not visible. B, after one year of treatment at 9 years. The irregularly mineralized spotted small femoral center has appeared. C, after three years of treatment at 11 years. The femoral epiphyseal center is flattened and the femoral

neck broadened into a coxa plana deformity. A narrow, irregular strip of ossification is evident in the medial segment of the epiphyseal center. Similar changes were present in the other femur. In serial examinations, spotted epiphyses were also demonstrated in the proximal and distal epiphyses of the humeri and distal epiphyses of the femurs and both ends of the tibiae.

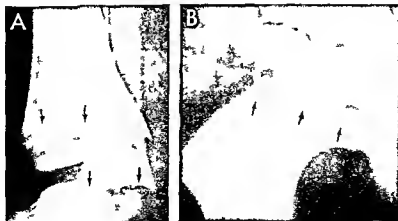
claimed to have described the first example of isolated thyrotropin deficiency in a dwarfed girl 7 years of age whose skeleton was immature. Rapid increase in stature and bone maturation followed thyroid therapy.

During early infancy, hypothyroidism and mongoloidism may coexist in a single patient. Skeletal maturation in mongoloids may be accelerated, normal, or retarded. It is likely that mongoloids with retarded skeletal development are in part hypothyroid and can be benefited by the administration of thyroid substance.

The ossification of the epiphyseal centers is spotty and irregular as well as delayed. This holds true for both untreated and treated cases. Instead of develop-

ing from a single focus of ossification followed by uniform marginal extension as in the normal, the hypothyroid epiphyseal ossification may begin in numerous small foci in the cartilage. These grow larger and finally coalesce to form a single center of uneven density with irregular margins (Fig. 8-819). This phenomenon has been called creunoid epiphyseal dysgenesis. In older untreated hypothyroids, the metaphyses are sometimes irregularly mineralized and simulate active rickets (Fig. 8-820). The appearance of the spotted epiphyses found in cretins resembles the fragmented picture of the ossification centers in juvenile ischemic necrosis (osteochondrosis juvenilis). The latter disease is usually confined to one or two

Fig. 8-820—Rickets-like irregularities in the metaphyses of an untreated cretin 8 years of age. A, distal metaphyses of the tibia and fibula. B, proximal metaphysis of the femur.



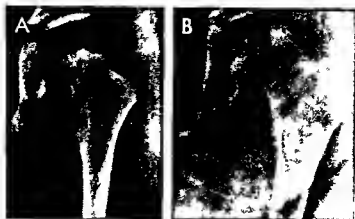


Fig 8 821.—Hypothyroidism with stenosis of the medullary cavities of the femurs at 52 months of age in an untreated patient (A) After 24 months of treatment with thyroid extract (B) the

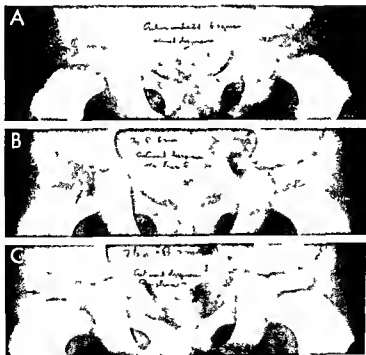
medullary cavities have enlarged and the cortical walls become thinner

ossification centers in contrast with the multiple spotted epiphyses of hypothyroidism. The proximal centers of the femurs may be flattened as well as irregularly mineralized and the neck of the femur broadened and bent into coxa vara deformity in hypothyroid children. Hypothyroidism is also one cause of

coxa plana (Fig 8 819). Spotted epiphyses are found in some cases of achondroplasia. Ollier's dyschondroplasia, Hurler's syndrome and familial spotted epiphyses: there is no convincing evidence however that there is inadequate thyroid activity in these diseases. At several sites in the growing skeleton irregular

Fig 8 822.—Cranioid dysgenesis of the right proximal femoral epiphyseal ossification center with development of asymptomatic coxa plana during administration of thyroid extract. A at 6 1/2 years and before treatment both femoral centers are small and irregularly ossified. B, at 7 years and after 6 months of thyroid

the apy both centers have increased in size but are flat and granular in texture. C at 7 1/2 years and after 12 months of treatment both centers are larger but are still too small and the right one is still granular and flattened. There were no clinical signs of Perthes' disease and thyroid treatment was effective.



spotted epiphyseal ossification is a normal physiologic variant (see Fig 8 245) This should be remembered in x ray evaluation of spotted epiphyses

Stenosis of the medullary cavities due to internal thickening of the overlying cortex in the untreated cretin and then opening up of the medullary cavity due to thinning of the overlying cortex during and following treatment are shown in Figure 8 821 The progressive development of coxa plana during treatment is depicted in Figure 8 822

In some untreated cretins deep transverse bands of increased density develop in the major metaphyses suggesting that the provisional zones of calcification are not being normally destroyed from their shaftward faces The metaphyses in the sternal ends of the ribs are curiously not affected when there are severe lesions of this type in the bones in the extremities In the round bones and in the ossification centers in the epiphyseal cartilages analogous peripheral zones of increased density may develop around the more radiolucent central portions When the bones of a cretin present signs of sclerosis as well as retarded maturation idiopathic hypercalcemia should be considered as a possible cause of the sclerosis Megavand and associates have discussed the skeletal changes in hypothyroidism comprehensively and in detail

Hyperthyroidism—This is almost nonexistent during infancy and is uncommon and usually not severe during childhood In pediatric practice toxic goiter is encountered most frequently in preadolescent and adolescent females the skeleton has appeared to be normal in our cases of this type In a girl 4 1/2 years of age with severe hyperthyroidism Beilby and Mc Clintock found skeletal maturation at a 9 year level

Fetal acceleration of skeletal maturation may occur in the offspring born of mothers suffering from severe thyrotoxicosis especially when it is uncontrolled during the last trimester of pregnancy Schlesinger and Fischer reported thyrotoxicosis and accelerated development of the skeleton in children from excessive treatment with thyroid extract one was a mongol another a cretin

REFERENCES

- Capps J H and Hipona F A Visualization of thyroid tissue by contrast angiography *Radiology* 81 619 1963
Engeset A et al Skeletal changes resembling scurvy in infantile hypothyroidism before and after thyroid therapy *Acta radiol* 36 1 1951
Fink C W Thyrotropin deficiency in a child resulting in secondary growth hormone deficiency *Pediatrics* 40 881 1967
Frensch F S and Van Wyk J J Fetal hypothyroidism, *Am J Dis Child* 64 589 1964
Megavand A et al Skeletal anomalies of calcium metabolism in infantile and juvenile thyroid deficiencies, *Tr 28th Cong French speaking Pediat Soc Vol I Hypothyroidism* (Basel S Karger AG 1961)
Schlesinger B and Fischer O D Accelerated skeletal development from thyrotoxicosis and thyroid overdosage *Lancet* 2 289 1951
Shapiro R, and Man E B Iophenoxic acid and serum bound iodine values *J.A.M.A* 173 1532, 1960

Silverberg M. and Silverberg R. Skeletal changes by combined administration of thyroxine and estrogen *Am J Path* 22 1035 1946

Wilkins L. *Hypothyroidism in Children* in Astwood E. B. (ed.) *Clinical Endocrinology* (New York Grune & Stratton Inc 1960) Vol I

PARATHYROID GLANDS—Excess of parathyroid secretion affects growing bone in two ways It leaches phosphate and calcium directly from the supporting tissues of bone and sometimes may destroy this matrix itself and it promotes abnormally rapid urinary excretion of phosphate by lowering the tubular level of excretion of phosphate and raising the tubular level of reabsorption The bones lose radiographic density in a variety of patterns with hypophosphatemia and hyperphosphaturia and hypercalcemia and hypercalciuria Deficiency of parathyroid secretion produces converse action in the kidney and the converse findings in the serum of hyperphosphatemia and hypocalcemia but strangely no consistent changes in growing bones

In hyperparathyroidism the skeleton usually shows severe generalized rarefaction (Fig 8 823) but in some cases the skeleton has been normal radiologically The degree of skeletal change depends on the severity and especially the duration of the disease Cystic rarefactions may be present but they are absent in many cases Pugh claimed that subperiosteal resorption of coracal bone is pathognomonic of primary hyperparathyroidism and renal osteodystrophy (Fig 8-824) Extraskelatal calcification should be looked for in the kidneys and walls of the arteries (see Fig 8-27)

All parts of the long bones are demineralized the epiphyseal ossification centers as well as the shafts and to the same degree The trabecular pattern is coarse owing to the disappearance of the smaller secondary trabeculae The calvaria may be normal or exhibit a granular rarefaction The lamina dura gradually lose their sclerotic density and disappear late in severe cases Vertebral bodies become more radiolucent and are weakened so that the nuclei pulposi dislocate against them and compress them into biconcave shapes In long standing cases kyphosis scoliosis and loss of stature from spinal deformity are common Multiple cystic rarefactions and pathologic fractures followed by bowing and angulation deformities may be conspicuous radiologic features Important radiologic findings in the abdomen and pelvis include stones in the kidneys renal pelvis ureters and bladder In the case of large medially placed parathyroid tumors indentation on the contiguous antrum filled esophagus has been demonstrated

Aceto and associates found severe rarefaction in the bones of an infant 5 days of age born of a mother with hypoparathyroidism they postulated that the fetus had compensatory intrauterine hyperparathyroidism secondary to the maternal hypoparathyroidism Bronsky and associates described 2 cases of intrauterine hyperparathyroidism secondary to mater

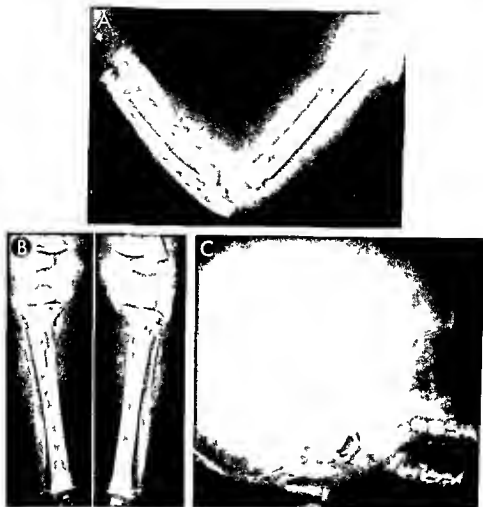


Fig 8-823 — Fetal hyperparathyroidism in an infant 12 months of age (necropsy). A and B arms and legs. The tubular bones show extreme coarse rarefaction of the cortexes and possibly the spongiosa, but the provisional zones of calcification are surprisingly well mineralized. Active rickets could not be diagnosed according to usual criteria. C lateral projection of the skull.

There is extreme generalized osteoporosis of iliac bones. The walls of the semicircular canals are conspicuous in the petrous pyramids. The well calcified teeth stand out in the poorly mineralized maxillas. The laminae in the upper maxilla and mandible are completely decalcified and invisible roentgenographically.

nal hypoparathyroidism in 1 of which severe coarse rarefactions of the bones were demonstrated on the 7th postnatal day (Fig 8-825) the bones were normal in the second patient. Du Bois and associates in 1969 found that only 10 cases of primary hyperparathyroidism reported in small infants and newborns. In their patient the skeleton was generally demineralized, particularly the ribs and the long bones in the extremities. The texture of the bones was coarsened with subperiosteal demineralization of the cortical walls. The provisional zones of calcification were intact so there were no radiographic signs of active rickets. Their findings were similar to those in Figure 8-823.

Secondary hyperparathyroidism is usually associated with renal insufficiency and causes rachitic

changes in the long bones and occasionally cystic rarefaction; this condition is called renal rickets. Parathyroid enlargement is said to be common in severe vitamin D deficiency rickets. The chemical changes hypercalcemia and hypophosphatemia with increased urinary excretion of calcium characteristic of hyperparathyroidism may also be found in other conditions associated with extensive bone destruction such as leukemia and lymphosarcoma of the growing skeleton.

Significant skeletal changes have not been described in the few authentic cases of chronic *hypoparathyroidism* reported in children. Emerson and his colleagues described some osteosclerosis in a boy 15 years of age who had congenital absence of the

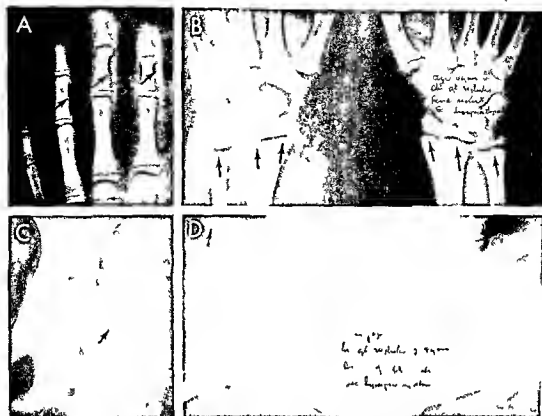


Fig 8-824—Secondary hyperparathyroidism in the renal glomerular type of juvenile rickets in a girl 10 years of age. A, Subperiosteal bone resorption on the external edge of the cortical walls of the phalanges. B, Severe rickets in the metaphyses of the radius and ulna. C, Subperiosteal bone resorption on the lateral edge of the femoral neck. A similar lesion was present in the

other femoral neck. D, Resorption on the lateral end of the clavicle. The kidneys of this patient were gradually destroyed by the back pressure from an obstruction at the bladder outlet and both tubular and glomerular functions were impaired. The general bone density is surprisingly good in view of the severe subperiosteal and metaphyseal lesions.

Fig 8-825—Prenatal hyperparathyroidism secondary to hypoparathyroidism of the pregnant mother. Coarse resorption and subperiosteal resorption of cortical bone is clearly visible in these

humeral shafts. These films were made 7 days after birth. (From Bonsky et al.)





Fig 8-826—Pseudohypoparathyroidism in a girl 19 years of age. All of the tubular bones are swollen and have thickened cortical walls. The right 4th metacarpal is disproportionately small and

short. Its secondary ossification center has nearly fused with the shaft.

parathyroids. Talbot found thickening of the cortical walls in some patients and metastatic calcification in soft tissues. In the patient of Schulman and Ratner, a girl 12 years of age, the skeleton was generally demineralized; she also had unusually low concentrations of calcium in the blood serum. The calcium content of the skeleton and the serum calcium value increased following vitamin D therapy.

Taybi and Keele reviewed the bone findings and reported two new examples in sisters 16 and 11 years of age.

Pseudohypoparathyroidism is a metabolic disease in which the clinical and chemical findings are identical to those of hypoparathyroidism but in contrast the patients are resistant to the administration of parathormone. The diagnosis is often suggested by the radiographic findings in the head and hands. The calvaria is thickened and the metacarpals are shortened unevenly (Fig 8-826). Extraskelatal calcifications have been found in the basal cerebral ganglions and in soft tissues near the distal joints. In the tubular bones of the hands, the fourth and fifth metacarpals are usually most shortened and in the feet the fourth metatarsal. In some of the shortened bones the shaft and its epiphyseal center fuse prematurely but in others the fusion time is normal.

REFERENCES

- Aceto T Jr *et al*: Intra uterine fetal hyperparathyroidism. A complication of untreated maternal hypoparathyroidism. *J Clin Endocrinol* 26:487 1966
- Andersen D H and Schlesinger E R: Renal hyperparathyroidism with calcification of the arteries in infancy. *Am J Dis Child* 63:102 1942
- Bronsky D *et al*: Intra uterine hyperparathyroidism secondary to maternal hypoparathyroidism. *Pediatrics* 42:606 1968
- Du Bois R *et al*: Primary hyperparathyroidism in a new born. *Ann radiol* 12:407 1969
- Landon J F: Parathyroidectomy in generalized osteitis fibrosa cystica. Report of a case in a child 2 1/2 years of age. *J Pediatr* 1:544 1932
- Philips R N: Primary diffuse parathyroid hyperplasia in an infant 4 months of age. *Pediatrics* 2:428 1948
- Piatt E L, Green B B and Neuhauser E B D: Hypercalcaemia and idiopathic hyperplasia of the parathyroid glands in an infant. *J Pediatr* 30:388 1947
- Pugh D G: Subperiosteal resorption of bone. A roentgenographic manifestation of primary hyperparathyroidism and renal osteodystrophy. *Am J Roentgenol* 66:577 1951
- Taybi H and Keele D: Hypoparathyroidism. A review of the literature and report of 2 cases in sisters, one with steatorrhea and intestinal obstruction. *Am J Roentgenol* 88:432 1962
- Idiopathic hypercalcemia* in infants when prolonged and severe (Fanconi type) is characterized in the skeleton by generalized sclerosis of all bones and transverse metaphyseal bands of increased and diminished density in the shafts and zonal sclerotic margins in the round bones and the epiphyseal ossification centers (Fig 8-827). The skeletal changes simulate those of vitamin D poisoning. The radiographic osteosclerosis in De Wind's patient, a boy 8 years of age who died of renal failure after taking excessive amounts of vitamin D for more than five years resembled the usual findings in idiopathic chronic hypercalcemia. Microscopic calciferous foci are found in the kidneys but these are rarely visible radiographically. In 15 cases the Daeschners reported gener-

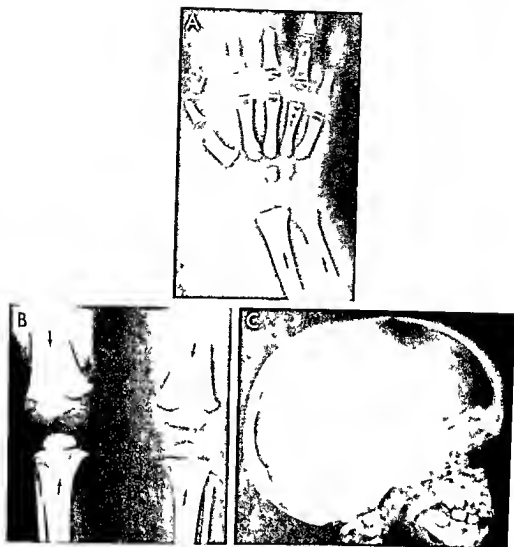


Fig 8-827—Chronic idiopathic hypercalcemia with generalized sclerosis of the skeleton and transverse bands in the metaphyses in a boy 4 years of age who had failed to grow and gain weight with retardation of motor development. Serum calcium value was 13.6 mg per 100 cc when these films were made. A: there are deep transverse radiolucent bands in the metaphyses of

the tubular bones and peripheral radiolucent zones in the round bones. B: similar changes are evident in the bones at the knees although the terminal radiolucent bands are much deeper in these larger and more rapidly growing metaphyses. C: all parts of the skull—calvaria, base and facial segment—are sclerotic. Both renal regions were stippled with fine foci of calcium density.



Fig. 8 828 — Eln faces of chronic idiopathic hypercalcemia. The epicanthal folds are broad and the nose is pinched and turned up at the tip with large nostrils and a broad base. The lips are loose with the upper lip prominent. Temples are narrow. In profile the forehead bulges and the chin recedes. (From Joseph and Parrott.)

alized osteoclerosis in all premature closure of cranial sutures and craniosostenosis in 4 and nephrocalcinosis in 2. Osteoclerosis was most marked at the base of the skull in their cases. Shuers and colleagues found extraskelatal calcifications in the kidneys, blood vessels, intermuscular septum and a variety of other structures. They also described the interesting combination of hypothyroidism and idiopathic hypercalcemia in a single infant. Chronic hypercalcemia is common in hyperphosphatemia. Bongiovanni and associates pointed out that idiopathic hypercalcemia is a distinct clinical entity of unknown cause, although it is probable that excess vitamin D plays a causal role. Individual hypersensitivity to small amounts of vitamin D may also be a causal factor. In the severe cases these authors reported craniosostenosis in 20%. An elfin facies has been present in some severe cases (Fig. 8 828). In a careful study of 3 cases of the severe type, Fellers and Schwartz found the serum vitamin D activity to be increased 20–30 times. This suggested to them that the syndrome is a congenital defect in the metabolism of vitamin D and related substances and properly belongs in the category of inherited molecular diseases or inborn errors of metabolism.

Thyroxine appeared to be effective in the three patients treated by Hooft and Vermassen, in addition to the administration of decalcified milk and prednisone. It is possible that subclinical hypothyroidism is a causal factor in some cases of hypersensitivity to vitamin D.

In the milder type of idiopathic hypercalcemia the Lightwood syndrome the bones are normal radiographically.

Aortic systolic murmurs have been present in many

patients with the severe type of hypercalcemia. Isolated supra-aortic stenosis and isolated peripheral pulmonary stenosis have been demonstrated by angiography (see vitamin D poisoning).

REFERENCES

- Bongiovanni A M *et al*: Idiopathic hypercalcemia of infancy with failure to thrive. *New England J Med* 257:951, 1957.
- Daeschner G L and Daeschner C W: Severe idiopathic hypercalcemia in infancy. *Pediatrics* 19:362, 1957.
- De Wind L: Hypervitaminosis D with osteoclerosis. *Arch Dis Childhood* 36:37, 1961.
- Fellers F X and Schwartz R: Etiology of the severe form of idiopathic hypercalcemia of infancy. *New England J Med* 259:1050, 1958.
- Fraser D: The relation between infantile hypercalcemia and vitamin D. Public health implications in North America. (Rep of Comm on Nutrition. Am Acad Pediatr.) *Pediatrics* 40:1050, 1967.
- Hooft C and Vermassen A: Hypersensitivity to vitamin D. *Acta paediatrica belg* 18:73, 1962.
- Lightwood R: Idiopathic hypercalcemia in infants with failure to thrive. *Arch Dis Childhood* 7:193, 1932.
- Lowe K G *et al*: The idiopathic hypercalcemia syndrome of infancy. *Lancet* 2:101, 1954.
- Shuers J A *et al*: Idiopathic hypercalcemia. *Am J Roentgenol* 78:19, 1957.
- Singleton E B: The radiologic features of severe idiopathic hypercalcemia. *Radiology* 68:721, 1957.

Oxalosis is a rare disorder in which there are widely and evenly spread deposits of oxalate crystals in the kidneys with progressive renal failure. The renal glomeruli are spared in contrast to the extensive degeneration in the tubules. The parathyroid glands are either normal in size or slightly enlarged. In the bones, clusters of oxalate crystals have been demonstrated in the marrow tissues, cortical walls and provisional zones of calcification. In our single case there were profound changes in the skeleton which simulated those of osteitis fibrosa cystica and hyperparathyroidism (Fig. 8 829). At necropsy, rosette-like clusters of oxalate have been found in many tissues: pericardium, myocardium, thymus, lungs, spleen and pituitary gland.

It seems likely that an inborn error of metabolism is the cause of oxalosis. Excessive amounts of oxalic acid are formed which combine with calcium to form opaque calcium oxalate, which is almost inert in the tissues.

REFERENCES

- Dunn H C: Oxalosis. Report of a case with review of the literature. *Am J Dis Child* 90:58, 1955.
- Shepard T H *et al*: Primary hyperoxaluria. *Pediatrics* 25:582, 1960.

PITUITARY GLAND — Disorders of this organ may be responsible for marked changes in the growing skeleton. Hyperactivity of the eosinophilic cells causes the excessive growth which characterizes pituitary gigantism. It has long been suspected but not proved that the atrophic type of dwarfism is due to underactivity of the anterior portion of the pituitary. Skeletal and

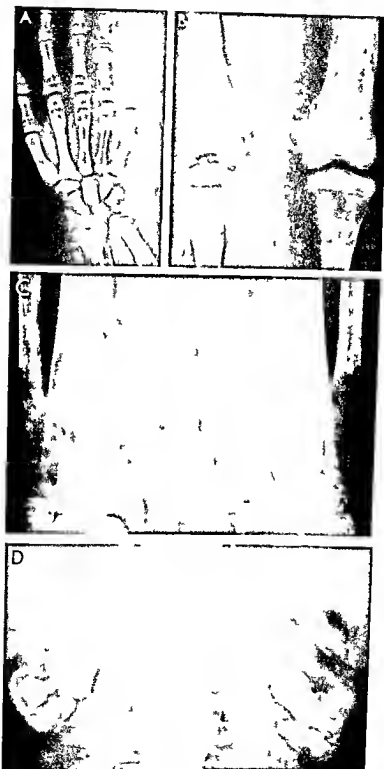


Fig. 8-829 — Oxalosis in girl 10 years of age (necropsy). A: cystic rarefaction in the tubular bones of the right hand and forearm. There were similar changes in the tubular bones in the feet. B: generalized coarse rarefaction of the shafts at the knees with subperiosteal resorption of the cortex and symmetrical Milkman's clefts in both femurs and both tibias. The epiphyseal ossi-

fication centers in the iliac crest are relatively sclerotic. C: swelling and demineralization of deep terminal segments of the shafts of the femurs and fibulas with sclerosis of the contiguous epiphyseal ossification centers. D: diffuse calcification of the kidneys with large opaque stones in both renal pelvises.

sexual infantilism and dwarfism are consistent features of the cranio-pharyngeal pouch tumors these phenomena are explained by injury to the chromophilic cells due to pressure by the growth. In a few cases of cerebral tumors and cerebral cysts of extrapituitary origin skeletal and sexual development has been accelerated supposedly by stimulation of the eosinophilic cells in the pars anterior of the pituitary.

Pituitary dwarfs are usually normal in stature at birth and may continue to grow and thrive normally for two or three years. Then the velocity of growth slows and continues indefinitely at a very slow rate. Although stature is reduced the pituitary dwarf is symmetrically small. Skeletal maturation is also retarded in about the same degree as stature is reduced in hypothyroid children. Epiphyseal cartilage plates remain visible radiographically for years after the normal age of fusion and may not close until late in adult life. Secondary sexual development is markedly delayed and secondary sex changes may fail to appear. Facial features also remain childish but in the second and third decades cutaneous elasticity is lost and the typical wrinkled appearance of oldish young develops. The patients are greatly improved by the administration of human growth hormone. Smallness of the bones and retardation of skeletal maturation are the only consistent radiographic findings. The pituitary fossa is characteristically normal.

Deprivation infantilism (*pseudohypopituitarism*) is characterized by shortness of stature, retarded skeletal maturation, voracious appetite and disturbed sleep patterns in children who have been deprived of the normal emotional and psychic experiences of infancy and childhood. Stature, weight and skeletal maturation are all presumably normal at birth and the velocity of growth remains normal for variable periods until it begins to diminish and remains reduced until treatment is given. In severe cases bizarre patterns of eating, drinking and sleeping develop; some patients drink from toilet bowls, hot water faucets, rain puddles and beer cans. These children eat two to three times as much as their siblings at one meal and frequently eat garbage and steal food from kitchens and pantries and from other children. Some of them get up from sleep at night to "roam around the house or look out the window or run out into the street. They tend to be shy and do not play with other children, even their siblings. After exposure to normal social and emotional stimuli in the hospital, weight, height and skeletal maturation increase rapidly toward normal and may reach and later exceed normal. The only significant radiographic findings are the smallness of the individual bones and delayed maturation. In some cases the cranial sutures have been widened before treatment; it is claimed that the sutures have widened during treatment in other cases (see Fig. 5-56).

REFERENCES

Powell G F et al. Emotional deprivation and growth retardation simulating idiopathic pituitarism. I. Clinical evalua-

tion of the syndrome. II. Endocrinological evaluation of the syndrome. *New England J. Med.* 276: 1271 and 1279, 1967.

Silver H K and Finkelstein M. Deprivation dwarfism. *J. Pediatr.* 70: 317, 1967.

PINEAL GLAND — Neoplasms have in some instances been associated with precocious sexual development and roentgen examinations of such patients have shown advanced maturation of the skeleton. It has not been proved that these changes are due directly to pineal hyperplasia.

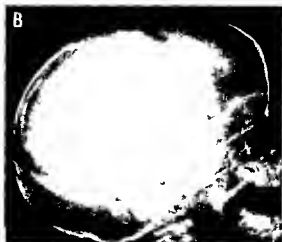
ADRENAL GLAND — *Cushing's syndrome* is rare in children and the changes in the endocrine structures are varied. In approximately one-half of one series of cases there was some type of a pituitary tumor. 31% of them were basophilic adenomas. Malignant tumors of the adrenal occur in about one-fifth of cases and benign adrenal tumors in about one-tenth. Notwithstanding the site of the tumor, the clinical picture is due to an excess of adrenal cortical hormones. Obesity of the facial and truncal type with hypertension and weakness are the outstanding clinical manifestations. The most important radiologic finding is rare-

Fig. 8-830 — Diffuse severe rarefaction of the vertebral bodies after prolonged high dosage treatment with adrenocorticosteroids for rheumatoid arthritis. All of the vertebral bodies are diffusely rarefied and weakened. The nuclei pulposi have expanded against the weakened edge of the vertebral bodies and compressed each into a biconcave disk. Each nucleus pulposus has expanded in the intervertebral disk to produce a biconvex intervertebral disk. This girl was 13 years of age.





Fig 8-831—Adrenal corticosteroid effect on the growing skull. Widening of the sutures and enlargement of fontanelles after cortisone daily in 10-20 mg doses from age 8 months (A) when the skull is normal to age 20 months (B) when all of the major su-



tures are widened and the fontanelles enlarged. The patient, a boy had congenital neutropenia. Neurologic findings were normal and the cerebrospinal fluid remained free of cells.

Fig 8-832—Severe muscular atrophy and hypoplasia in a nephrotic boy 26 months of age who had received daily doses of 20-100 mg of Prednisone for six months. The muscular bundles are reduced in volume with compensatory increase in subcutaneous and intramuscular fat.



faction of the vertebral bodies with compression fractures. The skull may also be markedly demineralized and fractures of the ribs have occurred in several cases.

The administration of corticosteroids in large doses during long periods may demineralize the spine, weaken the vertebral bodies and produce compression fractures in them (Fig 8-830). In the skull the sutures may widen and the fontanelles enlarge at the same time—changes which simulate acutely increased intracranial pressure and hydrocephalus (Fig 8-831). The long bones also become rarefied after protracted administration of corticosteroids and pathologic fractures may develop. Corticosteroids given in long uninterrupted courses to juvenile asthmatics have caused severe dwarfism and infantilism. Protracted administration produced clinical and radiographic signs of increased intracranial pressure in two children treated by Mathews and Shepard.

Muscular atrophy and weakness, most severe in the thigh and pelvic muscles (Fig 8-832) have been reported in several children after prolonged high-dose administration of adrenocorticosteroids who were suffering from collagen disease, nephrosis, asthma, and leukemia. Byers's youngest patient was two years nine months of age. Afifi and colleagues reviewed steroid myopathy in 1968.

REFERENCES

- Afifi A. K. *et al*. Steroid myopathy. Clinical, histologic and cytologic observations. *Johns Hopkins M J* 123:158, 1963.
- Byers R. K. *et al*. Steroid myopathy. Report of five cases during treatment of rheumatic fever. *Pediatrics* 29:26, 1962.
- Good R. A. *et al*. Serious untoward reactions to therapy with cortisone and adrenocorticosteroids in pediatric practice (part I). *Pediatrics* 19:95, 1957.
- Knowlton A. I. Cushing's syndrome. *Bull. New York Acad. Med.* 29:441, 1953.

Mathews, L. B. M. and Shepard R. H. Raised intracranial pressure with triamcinolone. *Lancet* 1 75 1961
 Sosman M. C. Cushing's disease—pituitary basophilism. *Am J Roentgenol* 62 1 1949

In primary chronic underfunction of the cortex (Addison's disease), which is much rarer in children than in adults, the principal clinical signs are malnutrition, muscular weakness, strikingly easy fatigability, salt craving, dehydration, vascular hypotension, regional hyperpigmentation and microcardia. Radiologic examination of the long bones may show moderate rarefaction.

In excessive chronic overfunction of the cortex, virilism is the most important clinical feature. It results from excess of androgens and is due to congenital bilateral hyperplasia or unilateral carcinoma. When this begins early during fetal life the lower genital tract is malformed with changes suggestive of hermaphroditism. Girls make up 80% of such cases. After birth the excess androgens stimulate overgrowth and accelerated maturation of many tissues. In females the clitoris hypertrophies, in boys the penis grows rapidly to adult size during childhood. In girls breast development is delayed or does not occur and menstruation does not begin during the usual time, at adolescence. Hirsutism is the rule in both sexes. Radiologic examination of the long bones always shows acceleration of maturation and of growth. Later the overgrowth may be converted into dwarfism owing to premature disappearance of the metaphyseal cartilage and early union of the shafts and their epiphyseal centers. The laryngeal and costal cartilages calcify early, the latter begin to calcify at 9–10 years instead of between the normal 18–30 years. Wagner and associates, in a study of androgenic virilism (both hyperplastic and neoplastic), found dental maturation advanced in the majority of these patients; in contrast, accelerated maturation of the teeth was exceptional in constitutional sexual precocity.

Increased medullary function is usually due to tumors of the pheochromocytoma type, which cause vascular hypertension due to excessive output of epinephrine. Changes in the long bones which resemble infarcts radiographically were found in patients with benign pheochromocytomas by Becker. Studies of the microcirculation indicated that an excess of epinephrine caused hemoconcentration with engorgement of the capillaries with red blood cells and slowing of the capillary blood due to increased viscosity to blood. Eventually microthrombi formed resulting in stasis of blood and disruption of the capillary walls. Radiographs were made originally in these patients because of ankle and knee pain. The bone changes simulated the infarcts of sickle cell anemia—triangular patches of mixed sclerosis and rarefaction with disruption of local trabeculae. After excision of the adrenal tumors the bone changes disappeared. Becker suggested that the microcirculatory changes explain

the acrodynalike clinical findings in some cases of pheochromocytoma.

Decreased medullary function has not been identified as a clinical entity and there are no known changes in the long bones due to this factor.

REFERENCES

- Becker M. H. Bone and microcirculatory changes in a child with benign pheochromocytoma. *Radiology* 88 487, 1967
 Wagner R., et al. Dental development in idiopathic sexual precocity, congenital adrenocortical hyperplasia and androgenic virilism. *J. Pediatr.* 63 566, 1963

GONADS—Underfunction of the ovaries is most often due to congenital aplasia but may also follow bilateral disease or removal surgically or by radiation. The lack of estrogen causes slight undergrowth and often inversion of the nipples and webbed (sphinx) neck. During childhood skeletal development is in the lower levels of the normal range. Later, after adolescence, there is delayed fusion of the epiphyseal centers with the shafts. Underfunction of the testes is relatively rare; there are no known abnormal changes in the long bones during infancy and childhood, after adolescence the epiphyses fail to fuse or fuse too late with their shafts.

Overfunction of the gonads is usually characterized by rapid increase in growth and an acceleration of maturation. Excessive ovarian function is usually due to granulosa cell tumor, and excessive testicular function to interstitial (Leydig) cell tumor. Radiologic examination of the long bones invariably shows acceleration of their maturation provided sufficient time has elapsed since the onset of the excess hormonal effect.

In females the pelvic viscera can be visualized to advantage by pneumopentoneum according to Kuntzler and co-workers. Tumors and cysts of the ovaries can be identified and normal and hypoplastic female pelvic organs can be seen without recourse to surgical exploration.

CHROMOSOMAL ABNORMALITIES—Cytogenic evaluation of human chromosomal patterns has demonstrated that there are several clinical syndromes which are associated with chromosomal aberrations of the sexual chromosomes as well as the somatic chromosomes. Two clinical entities, in which gonadal growth and function have been destroyed or weakened, are associated with the abnormal sexual chromosomal patterns—the XO pattern in ovarian dysgenesis and the XXY pattern in dysgenesis of semiferrous tubules. In both the phenotype is heterosexual to the nuclear chromatin patterns.

In gonadal dysgenesis (ovarian dysgenesis, Turner's syndrome, Bonneville-Ullrich) the real gonad never develops in either the fetus or the child being represented by a ridge of connective tissue, lacking germinal elements in each mesosalpinx. Functionally, this gonadal deficit operates as a fetal castration, and in the absence of gonads, the somatically male



Fig 8-833 —Edema of the foot in class c infantile gonadal dysgenesis in a boy 2 months of age. The soft tissues dorsal to the bones in the foot are swollen and increased in density with obliteration of the image of the subcutaneous fat. Gonadal dysgenesis often presents symmetrical edema of the dorsums of the feet which is marked during early infancy but disappears gradually as the infant grows older.

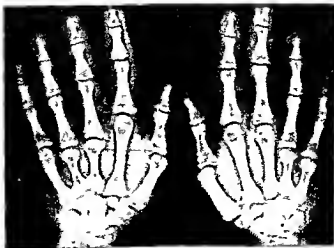
fetus and child develops as a female. True sex can be identified in such patients only by the male pattern of the nuclear chromatin. The external genitalia are feminine but remain infantile, as do the other reproductive structures and functions. At puberty the usual estrogen induced secondary sexual features do not develop or develop very weakly, except for the sexual hair, which does appear somewhat late and is sparse. The urinary gonadotropins at adolescence, increase to excessively high concentrations, owing to the attempts of the pituitary to stimulate the rudimentary gonads to normal hormonal function. During infancy and childhood the urinary gonadotropins remain at normal levels. At and after adolescence, excessively high gonadotropin concentrations provide one of the basic diagnostic findings. At all ages the number of nuclear chromosomes is 45 instead of 46, and the sexual chromosomal pattern is XO due to the absence of the male Y chromosome. Other abnormal sex chromosome patterns such as XX/XO and XXX/XX/XO are rarely present. In such cases, the female nuclear

chromatin bodies are always one less in number than the number of X chromosomes.

The patient presents a short stature, legs and ankles swollen with lymphedema, especially during infancy (Fig 8-833), and widely spaced, small, inverted nipples. Webbing of the neck, one of the hallmarks of the syndrome, is present in about one third of patients. A variety of congenital malformations, which vary in different patients, have been described. In the skeleton, the third and fourth metacarpals may be shortened (Fig 8-834). Kosowicz found the proximal ends of the tibial shafts to be widened (Fig 8-835) in 19 of 24 patients; we have not seen these lesions in infants and children. The mandible is usually abnormally small. Finby and Archibald found Madelung's ulnar deviation of the hand at the wrist, and hypoplasia of the first cervical vertebra in 33 patients, 26 of whom were older than 13 years. In our juvenile patients the skeletons have been normal except for shortness of long bones, retarded maturation and slight generalized rarefaction.

Fig 8-834 —Asymmetrical hypoplasia of the metacarpals of a girl 15 years of age with clinical and chemical gonadal dysgenesis and male nuclear chromatin. In the left hand the 3rd to 5th metacarpals are shortened and in the right hand the 4th and 5th metacarpals. In all of the shortened metacarpals the ends are

enlarged and the secondary epiphyseal ossification centers prematurely fused to their shafts. The shortened metacarpals thus exhibit the paradoxical combination of hypoplasia and accelerated maturation. In the unaffected bones maturation is delayed and approximates the average for healthy girls 11 years of age.



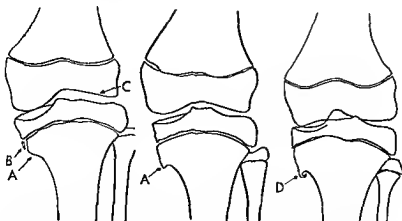


Fig. 8-835—Characteristic changes in the proximal ends of the femur and tibia in Turner's syndrome (gonadal dysgenesis) according to Kosowicz, who found them in 16 of his 24 cases. A, broad medial spur at the metaphyseal level due to failure of constriction; B, independent ossicle beyond spur; C, flattening of the

face of the medial femoral condyle; D, curved spine on the broad medial tibial spur. We have not found these changes in infants and younger children; most of Kosowicz's patients were young adults.

The reader is referred to the publications of Baker and of Palma and their colleagues for the differences and similarities in true Turner's syndrome and pseudo-Turner's syndrome.

REFERENCES

- Archibald R. M. *et al.* Endocrine significance of short metacarpals. *J. Clin. Endocrinol.* 19:1312, 1959.
 Baker D. H. *et al.* Turner's syndrome and pseudo-Turner syndrome. *Am. J. Roentgenol.* 100:40, 1967.
 Finby N. and Archibald R. M. Skeletal abnormalities associated with gonadal dysgenesis. *Am. J. Roentgenol.* 89:1222, 1963.
 Grumbach M. W. *et al.* Chromosomal sex in gonadal dysgenesis (ovarian agenesis). *J. Clin. Endocrinol.* 15:1161, 1955.
 Kosowicz J. The deformity of the medial tibial condyle in 19 cases of gonadal dysgenesis. *J. Bone & Joint Surg.* 42-A:600, 1960.
 Palma, L. D. *et al.* Skeletal development in gonadal dysgenesis, female type. *Am. J. Roentgenol.* 101:876, 1967.

In *dysgenesis of seminiferous tubules* (true Klinefelter's syndrome) feminine nuclear chromatin bodies are present in individuals who are somatically males but who have small and defective testicles. The seminiferous tubules are fibrosed and lined with Sertoli cells; the germinal epithelium is absent or deficient. Smallness or seeming absence of the testicles is the only clinical sign until puberty, when gynecomastia and a general eunuchoid constitution develop. This lesion is one of the common causes of infertility in phenotypic males and is believed to be the most frequent of all chromosomal aberrations. There are 47 diploid chromosomes in most patients, with an XXY pattern of sexual chromosomes. Other abnormal patterns such as XXXY and even XXXXY (see radioulnar synostosis) have been encountered. After puberty the urinary gonadotropins rise to high levels and

thereafter become an important diagnostic feature. During infancy and childhood there are no diagnostic radiographic changes; the diagnosis is made in the presence of 47 chromosomes with an extra X chromosome and feminine pattern of the nuclear chromatin. Orchids, acquired postnatally, may simulate the clinical picture of prenatal seminiferous tubule dysgenesis and has been called "false Klinefelter's syndrome."

REFERENCE

- Grumbach M. W. Sex chromatin pattern in seminiferous tubule dysgenesis and other testicular disorders. *J. Clin. Endocrinol.* 17:703, 1957.

The autosomal trisomies, in which the sex chromosomes are normal and the somatic chromosomes are excessive in number, have been found in three clinical syndromes: trisomy G (group 21-23) in mongoloidism or Down's syndrome and trisomy D (group 13-15) and trisomy E (group 16-18) in clinical syndromes made up of multiple variable congenital malformations and malfunctions. All three of these trisomies are characterized by a high incidence of mental retardation, malnutrition, fetal and postnatal dwarfism, abnormal dermal patterns, small mandibles, malformations of the heart and with all of them, high maternal age at the time of conception. In each of the clinical syndromes the karyotype of the affected individual is increased to 47 and the extra chromosome is located at 21-23 (G) or 13-15 (D) or 17-18 (E). The radiographic features of mongoloidism or trisomy G (21-22) are recorded elsewhere in this book.

Trisomy-E (16-18) is said to have more consistent clinical manifestations than mongoloidism, and the clinical diagnosis can be made before the chromosomal changes have been identified microscopically.

The most important clinical findings include dwarfism, mental retardation, malnutrition, hypertonia, small mandible with low set ears and small triangular mouth, highly arched palate, abnormal dermal patterns, widely spaced nipples, overlapping flexion deformities of the fingers, flat feet and hammer toes, long heels and short great toes, short sternum, anomalies of the urinary tract, and congenital malformations of the heart—usually patencies of the ductus arteriosus and of the interventricular septum. The radiographic examination is helpful in identifying shortness of the sternum and in detailed study of the anomalies of the heart and urinary tract. The supernumerary acrocentric chromosome is in a group made up of chromosomes 17-18 with the total number of chromosomes increased to 47.

REFERENCE

James A E Jr, et al. Trisomy 18. *Radiology* 92:37 1969

In trisomy D (13-15) syndrome, the principal clinical findings are psychomotor retardation, apneic episodes, deafness, psychomotor seizures, hypertonia, incomplete ossification of the calvaria, arhinencephaly, microphthalmia, frontal hemangioma, small mandible and low set ears, harelip and cleft palate, flexion deformities of fingers and toes, polydactyly, hyperconvex fingernails, simian creases in the palms, abnormal dermal patterns, malrotation of the colon, early infantile death and advanced maternal age. Radiographic examination aids in the diagnosis of malrotation of the colon, and the heart and urinary tract should be studied radiographically in the complete investigation of such patients. The karyotype is increased to 47 chromosomes and the extra chromosome is located on the group 13-15.

REFERENCES

James A E Jr, et al. Trisomy 13-15. *Radiology* 92:44 1969
Smith D W., et al. The D, trisomy syndrome. *J Pediatr* 63:326 1963

The cri du chat syndrome was first described by Lejeune in 1963 and is one of the recognized autosomal genetic syndromes. The karyotype contains a normal number of chromosomes (46), but in 1 of the B group (Denver 4-5) much of the short arm is deleted. Clinical features include mental retardation, muscular hypotonia, small and retrodisplaced tongue, low set ears, moon face, oblique palpebral fissures which extend laterad and caudad (antimongoloid) and hypertelorism. The cardinal clinical finding is a thin high plaintive cry which simulates the meowing of a frightened kitten. The diagnosis is usually made from this kittenlike cry. The radiographic findings are nonspecific and of secondary and tertiary importance in diagnosis. They include microcephaly and occipital postural flattening of the calvaria and orbital hypertelorism. In the pelvis the iliac angle has been increased in some patients. Other inconstant findings

are agenesis of the corpus callosum, horseshoe kidney and congenital malformations of the heart. The long bones are usually slender, elongated and poorly mineralized due to muscular hypotonia.

REFERENCE

James A E Jr, et al. The cri du chat syndrome. *Radiology* 92:50 1969

Idiopathic hemihypertrophy (asymmetry), in one case, was associated with diploid triploid mosaicism. In this case, described by Ferner and colleagues, cultures of the leukocytes yielded chromosomes normal in both number and pattern. However, in cultures of fibroblasts from the fascia lata and the skin, some cells had 69 chromosomes in triploid groupings. The sex chromosomes were grouped XXY. The sex nuclear chromatin pattern was normal. A minority of the fibroblasts were triploid and the majority were diploid. Clinical findings also included dolicho-oxyccephaly, antimongoloid slant to palpebral fissures, syndactyly, patchy hyperpigmentation of the trunk and thigh, and mental retardation. Benson and coworkers have pointed out the high incidence of Wilms' and adrenal tumors in congenital asymmetry, but chromosomal patterns were not reported by them.

REFERENCES

Benson P F, et al. Congenital hemihypertrophy and malignancy. *Lancet* 1:468 1963
Ferner P, et al. Congenital asymmetry associated with diploid triploid mosaicism and large satellites. *Lancet* 1:80 1964

The orodigitofacial syndrome was first recognized by Papillon Leage and Psaume in 1954. Grob is said to have named the same syndrome "dysplasia linguofacialis" in 1957. Hypertrophy of the upper and lower frenula appears to be the basic lesion, which leads to clefts in the tongue and jaws. The tongue is cleft anteriorly in the midsagittal plane and on the sides symmetrically at the levels of the lateral incisor canine teeth (Fig 8-836, A). The maxillary canine teeth are usually ectopic and the mandibular lateral incisors are commonly absent. Multiple other cranial dysplasias include median incomplete cleft of the upper lip, true cleft palate, smallness of the mandible, hypoplasia of the alar cartilages of the nose, hypoplasia of the base of the skull and orbital hypertelorism. Finger deformities are present in most cases, these include shortening, bending and fusion of the phalanges (Fig 8-836, B and C). This is another example of the developmental dependence of the tongue and the digits, which occurs in its more severe form in combined absence of the tongue and digits—the lingual aplasia-adactylia syndrome. Deformities of the toes are less common than those in the fingers. Dryness and sparseness of hair in the scalp are present in more than half of the patients. One-third to one-half of the patients are mentally retarded. In necropsies, Doege found polycystic disease of the kidneys in one

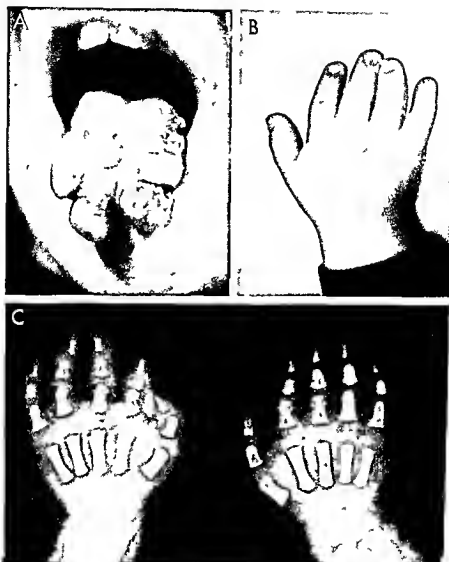


Fig. 8-536 —The orodigital facial syndrome of Papillon-Léage and Psaume. **A**, longitudinal and lateral clefts and fibrous swellings in the tongue of a girl 14 years of age. **B**, hands and fingers are broad and short, and some of the fingers are bent; the 4th and 5th fingers are relatively long in a girl 10 years of age. (**A** and

B from Gorlin and Psaume.) **C**, shortening and bending of the basal and middle phalanges of the 2nd and 3rd fingers and relative elongation of the 4th and 5th fingers, despite some deformity of the 1st basal phalanges. (**C** from Schwarz and Fish.)

case and renal polycystic disease combined with generalized cystic disease of the liver and pancreas in another. The orodigitofacial syndrome is limited to females, with one possible exception, they are usually mentally retarded.

In a few cases Reuss and Kushnick and their colleagues and Gorlin and Psaume found autosomal trisomy with a complement of 47 chromosomes and partial trisomy of the no 1 chromosome. The syndrome appears to be linked with the sex chromosomes and is lethal in the male. The nuclear chromatin pattern is female (positive) in all cases except that of Kushnick. Gorlin and Psaume pointed out that some elements of the orodigitofacial syndrome are seen in other conditions: fusion of the upper lip with the gum in the Ellis Van Creveld syndrome, hypoplasia of the alar cartilages in the Waardenberg syndrome, and hypoplasia of the malar bones in Treacher Collins disease.

The similar syndrome of Remoin is characterized by bilateral syndactyly of the great toes, genetic transmission is autosomal recessive.

REFERENCES

- Doegge, T. C., et al. Studies of a family with the oral facial digital syndrome. *New England J Med* 271 1073, 1964.
- Gorlin R. J., and Psaume J. Orodigitofacial dysostosis—a new syndrome. *J Pediatr* 61 320 1962.
- Kushnick T., et al. Orofaciodigital syndrome in a male. Case report. *J Pediatr* 63 1130, 1963.
- Remoin, D. L., and Edgerton M. T. Genetic and clinical heterogeneity in the oral facial digital syndrome. *J Pediatr* 71 94 1967.
- Reuss, A. L., et al. The oral facial-digital syndrome. *Pediatrics* 29 985 1962.
- Schwartz, E., and Fish A. Roentgenographic features of a new congenital dysplasia. *Am J Roentgenol* 84 311 1960.
- OBESITY**—For many years it was assumed that skeletal development was delayed in obese children, in the belief that hypothyroidism was a causal factor in juvenile obesity. In a careful study of a large group of excessively fat children, Bruch found that skeletal maturation and growth were advanced or normal.
- REFERENCES**
- Bruch H. Obesity in childhood. Physical growth and development of obese children. *Am J Dis Child* 58 457, 1959.
- Mossberg H. Obesity in children. *Acta paediat*, Vol. 35, supp 1, p 129 and supp 2 1948.

BONE CHANGES IN DISEASES OF THE CENTRAL NERVOUS SYSTEM

Growth and maturation of the skeleton may be retarded or normal in cerebral hypoplasia. In the extreme cases of microcephaly, dwarfism and skeletal infantilism are common. Maturation of the skeleton has been retarded, normal and rarely advanced in our cases of mongoloidism. According to Benda the slow growth in mongoloidism is due to premature degeneration of the cartilage columns in the metaphyses of

the tubular bones, a similar type of degeneration is found after ablation of the pituitary gland. The most valuable diagnostic changes in the mongoloid skeleton are in the pelvic bones, where the changes are most significant during the first weeks and months of life, when diagnosis on other grounds is most uncertain (see Fig 5-52). Koehler stated that in Little's spastic paraplegia the patellas may be displaced cephalad several centimeters in patients with longstanding rigidity and contractures of the lower extremities. In all of the chronic paralytic diseases of neural origin, regional bone atrophy develops shortly after onset of the paralysis. Papavasiliou and colleagues found widely scattered skeletal changes in their patient who had idiopathic acroosteolysis, which suggested possible widely scattered disturbances in the peripheral nerves. The skull showed remarkable bathrocephaly with irregular and incomplete ossification along both limbs of the lambdoidal suture. The skeletal changes in neurofibromatosis and sympathicoblastomas are discussed on pages 608 to 811. It has been pointed out that Len's flowing perostitis and osteodystrophia fibrosa (McCune-Albright) may be manifestations of primary disease of the peripheral nerves.

In *tuberous sclerosis* (adenoma sebaceum), Holt and Dickerson found that 40% of their adult patients had sclerotic plaques in the diploic space of the calvaria, and more than two thirds had "cystic" destruction of the phalanges and/or cortical thickenings of the metacarpals and metatarsals. Other lesions included fibrous nodules in the cerebrum, often paraventricular, which projected into the lateral ventricles. Many of these were calciferous. Retinal fibromas can be seen in many patients on fundoscopic study. Embryonal fibromas in the kidneys and renal pelvis have been found frequently. Hamartomas (cysts and fibromas) have also been present in the lungs, liver, adrenals and the myocardium. In the facial skin, small hyperemic nodules are distributed in a butterfly pattern over the nose, cheeks and chin. The cardinal components of tuberous sclerosis are mental retardation, epileptiform seizures and facial adenoma sebaceum, according to Bourneville, who first described the syndrome in 1880.

The *kinky hair syndrome*, described by Menkes in 1962, is a degenerative disease of the central nervous system characterized by failure to thrive, mental and motor retardation, clonic seizures, peculiar kinky hair and eyebrows and profound degeneration of the brain and spinal cord. Genetic transmission is sex limited, limited to males. Wesenberg and associates found spurs at the ends of the shafts of the long bones, diffuse flaring of the sternal ends of the ribs, excessive numbers of Wormian bones in the calvaria and smallness of the skulls. During the second half of the 1st year, cortical thickenings developed in the femur and humerus and to a less degree, in the bones of the forearms and shanks. These bones were not fractured, but one could raise the question of cortical

thickenings due to trauma possibly a result of severe repeated clonic seizures. The symmetrical position of the cortical thickenings is unusual for external traumatic origin. In two cases arteriograms disclosed marked malformations of the cerebral arteries.

REFERENCE

Wesenberg R L *et al*. Radiologic findings in the kinky hair syndrome. *Radiology* 92:500, 1969.

Multiple neurofibromas of the intercostal nerves may produce multiple erosions on the under edges of the ribs similar to the costal erosions of coarctation of the aorta.

In association with subdural hematoma we have found multiple lesions of the long bones in many cases. Roentgenographically these changes are multiple fractures (Fig 8-837) large subperiosteal hemorrhages usually accompany the fractures. It is highly probable that the hyperostoses and fractures are due to unrecognized simple direct trauma with the traumatic episodes denied by the parents or other custodian of the infant or young child.

In mongoloidism the facial bones are hypoplastic and mineralization of the small nasal bone may be greatly delayed or missing. Maturation of the long bones may be normal, delayed or accelerated in mongoloidism and other types of mental retardation associated with cerebral hypoplasia. The most character-

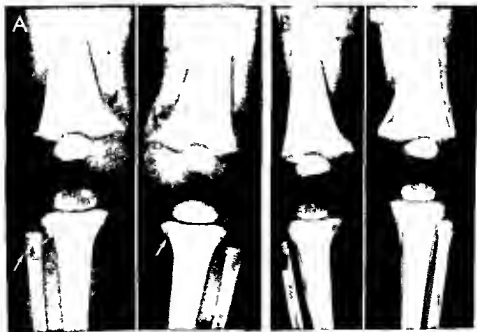
istic skeletal feature of mongoloidism during the early months of life is smallness of the acetabular angles and deepening of the acetabular cups; the wings of the ilia are large and flare laterad.

Lesions of the spinal cord which denervate the bones produce profound changes in them. The long bones become brittle and easily vulnerable to fracture by even trivial trauma. Failure of union and pseudarthrosis have followed some of these fractures. The shafts may become osteoporotic and small in caliber owing to overconstriction. In the sites of fracture the shaft may be expanded when the rest of the same shaft is overconstricted. Repeated mechanical injury to insensitive joints may produce neuropathic joints with the customary radiologic signs of sclerosis and fragmentation in the ends of the opposing bones.

Wilson's disease (hepatolenticular degeneration) may include multiple skeletal changes, among them osteochondrosis on the edges of the vertebral bodies, osteochondrosis dissecans in the femurs and talus bones, multiple osteoarthritis and generalized bone rarefaction. All of these bone lesions have been related causally to dysfunction of the renal tubules, which in turn may be due to deposition of copper in the renal tubular epithelium. The resultant damage to renal function may induce radiographic changes identical to those of classic rickets (Cavallino and Grossman). Among 38 patients Mindelzun and associates found normal skeletons in only 5. 9 had subarticular cysts

subperiosteal bone which are most conspicuous in the left femur and tibia. There are no scorbutic changes in metaphyses or epiphyses.

Fig 8-837—Subdural hematoma with changes in the long bones of an infant 8 months of age. A, multiple impacted fractures in the bones near the knee joints. B, six weeks later the periosteum is separated from the shafts and is laying down sheets of



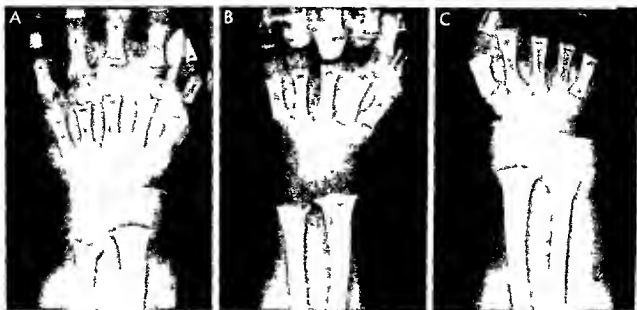


Fig 8-838—Opaque longitudinal spiculation of the metaphysis of the radius and to a lesser degree of the ulna of a boy 2 months of age who had chemically proved phenylketonuria. In A at 2 months the spicules project beyond the provisional zone of calcification into the continuous epiphyseal cartilage. In B and C at 4 and 5 months of age respectively the spiculations are buried

into the shaft as the bone grows distalward. The cupping of the ulna and slightly frayed appearance of the metaphyses are both suggestive of rickets, but the intact provisional zones of calcification negate this diagnosis. (From Feenberg and Fisch)

The bones near the joints were fragmented in 6 patients.

Phenylketonuria is due to a deficiency of the enzyme phenylalanine hydroxylase in the liver which prevents the normal conversion of phenylalanine to tyrosine. As a result, phenylketone bodies are excreted in the urine and normal tyrosine metabolism is reduced, which leads to the underproduction of melanin, which is responsible for the fair complexion of affected persons. They also suffer varying degrees of mental deficiency associated with high phenylalanine levels in the central nervous system. Incidence is about 1 per 50,000 births but is as high as 1 in 4 births in the offspring of phenylketonuric parents. Chemical diagnosis can be made after the first few weeks of life by the identification of phenylpyruvic acid in the urine and the high phenylalanine levels in blood plasma. In 5 of 10 patients younger than 13 months, Feenberg and Fisch found cupping and fraying of the distal ends of the radius and ulna but without demineralization of the provisional zone of calcification as in rickets (Fig 8-838). Murdoch and Holman found similar bone changes in 2 patients who had had low phenylalanine diets since infancy.

Homocystinuria—Similar longitudinal spiculations in the metaphyses and neighboring epiphyseal cartilages were found in four children suffering from homocystinuria by Morells and associates. In many of its features, homocystinuria simulates the Marfan syndrome and many of the patients are mentally retarded.

Cystinosis is a rare familial disease in which cystine crystals accumulate in the bone marrow, peripheral leukocytes, cornea, and conjunctiva. Children often die of renal failure during the first decade of life, in contrast to adult cystinosis which is marked by long survival. Juvenile cystinosis begins during infancy with polyuria, polydipsia, retardation of growth, and the development of classic rickets. Defective reabsorption in the renal tubules causes renal hyperphosphaturia, glycosuria, aminoaciduria, hypophosphatemia, hypokalemia, and acidosis (Fanconi syndrome).

REFERENCES

- Benda C E: Research in congenital acromicria (mongolism) and its treatment. *Quart Rev Pediatr* 8:79, 1953
- Berrey B H: Postinfantile cortical hyperostosis with subdural hematoma. *Pediatrics* 6:78, 1950
- Caffey J: Multiple fractures in the long bones of infants suffering from chronic subdural hematoma. *Am J Roentgenol* 56:163, 1946
- Cavallaro R and Grossman H: Wilson's disease presenting with rickets. *Radiology* 90:493, 1968
- Feenberg S B and Fisch R O: Roentgen findings in growing long bones in phenylketonuria. *Radiology* 78:394, 1962
- Fisch R O et al: Growth and bone characteristics of phenylketonuria. *Am J Dis Child* 112:3, 1966
- Holt J F and Dickerson W W: The osseous lesions of tuberous sclerosis. *Radiology* 58:1, 1952
- Mane J et al: Subdural hematoma in the infant associated with fractures of the limbs. *Semaine hop Paris* 30:1757, 1954
- Mandelzys R et al: Skeletal changes in Wilson's disease. *Radiology* 94:127, 1970

- Morells C L Jr *et al* Roentgenographic features of homocystinuria Radiology 90 1159 1968
- Murdoch M M and Holman G H Roentgenologic bone changes in phenylketonuria, *Am J Dis Child* 107 523 1964
- Papavasiliou C G *et al* Idiopathic nonfamilial acroosteolysis associated with other bone abnormalities *Am J Roentgenol* 83 687 1960
- Rosenoer V M and Mitchell R C Skeletal changes in Wilson's disease (hepatolenticular degeneration) *Brit J Radiol* 32 805 1959
- Schneider J A *et al* Biochemical comparisons of adult and childhood forms of cystinosis *New England J Med* 279 1253 1968
- Smith M J Subdural hematomas with multiple fractures *Am J Roentgenol* 63 342, 1950

BONE CHANGES ASSOCIATED WITH CARDIAC DISEASE

In poorly compensated heart disease which begins at birth or in the first years of life the growth and maturation of the skeleton may be conspicuously retarded. We have never seen generalized periosteal thickening of the long bones (cardiac osteoarthropathy) in numerous cases of cardiac disease with long standing and eventually fatal decompensation. In our experience clubbing of the digits is limited to thickening of the soft tissues at their distal ends; the terminal phalanges have not been significantly altered. Phalen and Ghormley found extensive scattered sclerosis of the skeleton associated with coarctation of the aorta in a woman 22 years old. Occasionally the diploic spaces of the parietal bones are widened and radially striated in infants who have cyanotic congenital heart disease (see Figs 1 153 and 1 154). Sclerotic patches in the vertebral bodies have also developed in some cyanotic patients (see Fig 9 59). This cranial lesion probably represents a local hyperplasia of the diploic red marrow in compensation for the increased need for red cells in cyanotic heart disease.

Holt Oram syndrome—In 1960 Holt and Oram described the familial transmission of combined congenital cardiac deformities and skeletal dysplasias in the arms and hands. There were no changes in the lower extremities. In their first report defects in the atrial septum were associated with dysplasias of the tubular bones of the hands principally the thumbs and first metacarpals. At least 30 examples had been reported by 1967 (Chang). Patency of the interatrial septum has been the most frequent cardiac lesion but ventricular septal defects and anomalies of the great vessels also are common. In the skeleton the thumbs are most frequently affected with three phalanges in the thumbs instead of two. The third phalanx of the thumb is located in the same plane as in the fingers and the thumbs resemble the other digits. Apposition of the phalangeal thumb and fingers is difficult and often impossible. Any segment of the upper extremity however may have skeletal and muscular anomalies. Poznanski and associates found

extra carpal bones to be the most striking abnormality in the skeletons of their patients.

REFERENCES

- Chang C H Holt Oram Syndrome Radiology 88 479 1967
- Gellis S S and Feingold M Holt Oram syndrome *Am J Dis Child* 112 465 1960
- Holt M and Oram S Familial heart disease with skeletal malformation, *Brit Med J* 22 236 1965
- Phalen G S and Ghormley R K Osteopathia condensans disseminata associated with coarctation of the aorta, *J Bone & Joint Surg* 25 693 1943
- Poznanski A K *et al* Skeletal manifestations of the Holt Oram syndrome Radiology 94 45 1970

BONE CHANGES ASSOCIATED WITH DISEASES OF ALIMENTARY TRACT

Baker and Harns found the skeleton to be normal at birth in patients who suffered from congenital absence or atresia of the intrahepatic bile ducts. With advancing age the tubular bones became rarefied and failed to constrict which produced long bones with dilated medullary cavities and thin cortical walls. Also the burrs in the extensor surfaces of the arms and legs swelled progressively. These changes were proportionate to the severity of the hepatic deficiencies. The calvaria remained normal.

Traumatic pseudocyst of the pancreas is not a common cause of lesions in the growing skeleton. Sperling found scattered changes in the bones of a girl 21 months of age who had been struck by an automobile trailer and pinned beneath it. The bones in the extremities were tender and the skin was swollen and reddened. A mass was felt in the abdomen which yielded 700 ml of bile stained fluid. A biopsy bone specimen was normal microscopically. At surgical exploration of the abdomen the peritoneal cavity was filled with bile stained fluid adhesions and calcareous plaques. The head of the pancreas was necrotic and the body and tail were hemorrhagic edematous and friable. A large pancreatic pseudocyst was present. The radiographic changes in the bones were most marked in the radius and ulna and consisted of terminal rarefactions of the epiphyseal ossification centers plus defects in cortical and cancellous bone. The changes in the distal ends of the tibia were most severe and were still marked one year after the accident.

REFERENCES

- Baker D H and Harris R C Congenital absence of the intrahepatic bile ducts *Am J Roentgenol* 91 875 1964
- Sperling M A Bone lesions in pancreatitis *Australasian Ann Med* 17 334 1968

BONE CHANGES ASSOCIATED WITH RESPIRATORY DISEASE

The growth and development of the skeleton may be retarded in severe long standing diseases of the

REFERENCES

- Altman H S and Pomerance H H. Chronic polyostotic per-
iostitis of unknown origin. *Pediatrics* 28:248 1961
- Camp J D and Scanlan R L. Chronic idiopathic hyper-
trophic osteoarthropathy. *Radiology* 50:581 1948
- Cavanaugh J J A and Holman G H. Hypertrophic os-
teoarthropathy in childhood. *J Pediatr* 66:27 1965
- Chamberlain D S et al. Idiopathic osteoarthropathy and
cranial defects in children (familial idiopathic osteoar-
thropathy). *Am J Roentgenol* 93:408 1965
- Curran G et al. Familial idiopathic osteoarthropathy.
Am J Roentgenol 85:633 1961
- Gottheb C, Sharlin H S and Feld H. Hypertrophic pul-
monary osteoarthropathy. *J Pediatr* 30:462 1947
- Grossman H et al. Hypertrophic osteoarthropathy in cystic
fibrosis. *Am J Dis Child* 107:1 1964
- Medlin V L. Hypertrophic osteoarthropathy in children.
Radiology 74:414 1960
- Remoin D L. Pachydermoperiostosis (idiopathic clubbing
and periostosis). Genetic and physiologic considerations.
New England J Med 272:923 1965

BONE CHANGES ASSOCIATED WITH
RENAL DISEASE

The growing skeleton is often profoundly affected by chronic renal insufficiency especially tubular failure of reabsorption. Renal rickets and generalized demineralization of the bones are seen in many types of chronic renal failure: renal hypoplasia, congenital polycystic disease, renal atrophy due to back pressure from bilateral obstructive lesions in the urinary tracts, idiopathic renal tubular insufficiency with and without glycosuria, and in chronic glomerulonephritis. In the nephrotic syndrome in contrast renal rickets is all but unknown. The bone changes in both primary and secondary hyperparathyroidism are also associated with chronic renal disease and renal failure. Rarefaction of the bones also may develop in the "milk drinker's" syndrome in which renal injury is the rule. The common infantile and juvenile tumor of the kidney, Wilms' tumor, rarely if ever metastasizes to the skeleton in contrast to the common secondary skeletal tumors with sympathicoblastoma of the adrenals.

Progressive bilateral resorption of the bones of the hands, wrists, forearms and upper arms began at age 2½ years in a girl studied by Torg and Steel. She had chronic hematuria and albuminuria. Focal necrosis of the bone also developed in the left clavicle, the bones at the cuneiform metatarsal junctions and their metatarsal phalangeal joints.

REFERENCES

- Burnet C H et al. Hypercalcemia without hypercalcemia or
hypophosphatemia, calcinosis and renal insufficiency.
New England J Med 240:787 1949
- Davis J G. The osseous radiographic findings of chronic
renal insufficiency. *Radiology* 60:406 1953
- Torg J S and Steel H II. Essential osteolysis with nephro-
pathy. *J Bone & Joint Surg* 50-A:1629 1968



Fig 8-839. Genua at zaid ismellated cortical hyperostosis (pul-
monary osteoarthropathy) in a girl 7½ years of age who had had
cystic fibrosis of the pancreas with severe obstructive emphyse-
ma, bronchopneumonia and cor pulmonale since the second half
of her 1st year. A: left arm. B: shanks. On both sides the humerus,
radius, ulna and ulna were affected.

lungs and bronchi especially in bronchiectasis associated with severe malnutrition. The chronic broncho-
pneumonia and emphysema of cystic fibrosis of the
pancreas are the common cause of respiratory under-
growth of the skeleton and infantile. In several pa-
tients the radiographic picture of pulmonary osteoar-
thropathy has been demonstrated (Fig 8-839) and in
some the joints have been swollen. In true hyper-
trophic pulmonary osteoarthropathy according to
Camp and Scanlan the bone changes do not appear
before puberty. Clubbing of the digits due to chronic
respiratory disease has not been associated with
thickening of the underlying phalanges in our experi-
ence. We believe that several cases of hyperphospha-
tasia have been confused with hypertrophic pulmo-
nary osteoarthropathy.

In the report of Curran and associates on fami-
lial idiopathic osteoarthropathy pachydermoperiostitis
was cited as a special type of pachydermia which has
the peculiar tendency to be associated with osteoar-
thropathy. Cutis verrucosa gyrate has been present in
some of the patients. In Curran's two patients
diffuse infantile eczema preceded and then accompa-
nied generalized external thickenings of the long
bones and preceded the onset of arthritis by many
months.

BONE CHANGES ASSOCIATED WITH CUTANEOUS DISEASE

Several intrinsic and congenital disorders have already been described in which lesions of the skeleton and of the skin and its appendages the hair nails and teeth are associated. In osteodystrophia fibrosa (McCune Albright) the skin shows excessive pigmentation in patches the nails and teeth are hypoplastic in the Ellis Van Creveld syndrome (chondroectodermal dysplasia) osteopoikilosis may be complicated by dermatofibrosis lenticularis and albinism was present in one of the two patients who had Pyle's disease (symmetrical splaying of long bones). The tetrad made up of anomalies of the nails hypoplasia of the radius (see Fig 8-841) and humerus at the elbows absence hypoplasia or dislocation of the patella with hypoplasia of the lateral femoral condyle and the presence of bilateral iliac horns is a distinct clinical and genetic entity which has been called hereditary onychodysplasia and might also be called the nail elbow knee ilium syndrome. Renal disease frequently complicates the nail patella syndrome (Leahy). At necropsy most of the glomeruli have been completely hyalinized with broad zones of tubular destruction and moderate fibrosis. In the interstitial tissues lymphocytes and plasma cells are present in large numbers. Beals and Eckhardt found albuminuria in 30% of the affected patients in their nine kindreds of osteo-onychodysplasia. Multiple skeletal defects have also been reported in association with adenoma sebaceum (tuberous sclerosis).

Follicular atrophy of the skin has been found in several dwarfed and deformed infants and children. Alopecia of the scalp and mental retardation have also been present in some of these patients. The skeletal changes simulate hypoplastic achondroplasia except that the shortening of the long tubular bones is much more marked on one side of the body.

Xanthomatosis cutis may be characterized by de-

fects in the bones underlying the fatty tumors in the skin (Fig 8-840).

In the angio-osteohypertrophy syndrome of Klippel Trenaunay Weber (triad of cutaneous hemangioma, varicose veins and hypertrophy of soft tissues and bone) Caplan and associates noted in one girl of 9 years massive edema ascites and hypoproteinemia due to exudative enteropathy.

REFERENCES

- Beals R K and Eckhardt, A L. Hereditary osteo-onychodysplasia (nail patella syndrome). A report of nine kindreds. *J Bone & Joint Surg* 51 A 505 1969.
- Burckhardt E. Ein Fall von Chondrodystrophie calcarea. *Schweiz med Wchnschr* 68 330 1938.
- Caplan, D B *et al*. Angio-osteohypertrophy syndrome with protein losing enteropathy. *J Pediatr* 74 126 1969.
- Curran G *et al*. Familial idiopathic osteoarthritis. *Am J Roentgenol* 85 633 1961.
- Duncan J C *et al*. Hereditary oncho-osteodysplasia. The nail patella syndrome. *J Bone & Joint Surg* 45-B 242, 1963.
- Leahy M S. The hereditary nephropathy of osteo-onychodysplasia nail patella syndrome. *Am J Dis Child* 112 237 1966.
- Miescher G. Atypische Chondrodystrophie Typus Morquio mit folliculäre Atrophodermie. *Dermatologica* 89 38 1944.

Scleroderma and melorheostosis have been found in conjunction in several patients the lesions are usually regional with the scleroderma overlying the sites of melorheostosis. The bones and skin in the arms and at the shoulder have usually been most severely affected. In two cases there have been associated focal sclerosis in the proximal ends of the femurs which suggested osteopoikilosis (see reference of Clement and our Fig 8-395). In Thompson's patient a girl 10 years of age one leg was affected.

REFERENCES

- Clement R and Combes-Hamelie A. Mélorheostose et sclérodémie en bandes. *Osteopécrose et hypopécrose*. *Presse med* 22 311 1943.

Fig 8-840—Xanthomatosis cutis in a girl 15 years of age (topsy). There are many defects in the basal phalanges of the fifth digits both of which were swollen by large xanthomas. The e-

were severe as in far and larger xanthomas in the feet and other portions of the extremities but none of the bones underlying these other xanthomas had defects.



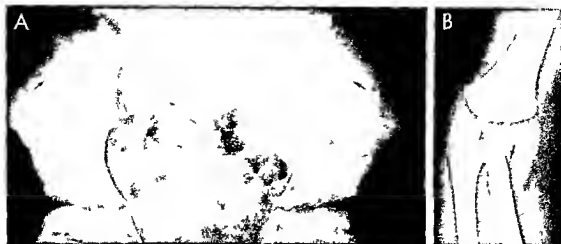


Fig 8-841 — Bilateral iliac horns (A) with hypoplasia of the radial heads (B) in a boy 6 years of age. Both radial heads were hypoplastic.

Thompson N M et al. Scleroderma and melorheostosis. Report of a case. *J Bone & Joint Surg* 33 B 430 1951

Reticulohistiocytoma is a rare disease in which the skin, joints and bones are affected. Radiographic findings include early destruction of the ends of the tubular bones followed by a slower progressive destruction of the articular cartilages. The bone changes simulate those of rheumatoid arthritis, psoriasis and gout. The disease appears first in the tubular bones of the hands and feet but later the larger joints may become involved and go on to permanent crippling deformities. Bone changes have been described in a single adult.

REFERENCE

Schwarz E and Fish A. Reticulohistiocytoma. A rare dermatologic disease with roentgen manifestations. *Am J Roentgenol* 83 692 1960

Syndrome of Rocher Sheldon has been found in patients as young as 10 years. In addition to the two most frequent manifestations, amyoplasia and stiffening of the joints, one patient had regional losses of pigmentation in the skin and hair, slate blue irises, deafness of labyrinthine origin and multiple bony dysplasias in the skull, thorax, sacrum, feet and at all of the major joints.

REFERENCE

Voluter G and Klein D. Unpublished and radiomorphologic findings in the syndrome of Rocher Sheldon. *J radiol et electrol* 38 19 1950

Cutis gyrata with pachyperiostosis was proved anatomically in the patient of Franceschetti, a woman 43 years old. The adnexal tissues of the skin, the sebaceous glands and connective tissue were hyperplastic and thickened. The long and flat bones showed multiple symmetrical external cortical hyperostoses.

REFERENCE

Franceschetti A et al. A new familial case of cutis gyrata with pachyperiostosis of the extremities, verified anatomically. *Schweiz med Wchnschr* 80 1301 1950

Osteomalacia due to bone losing nephritis is characterized by generalized hyperpigmentation of the skin with regional deficiencies of pigmentation over the bony prominences (Talbot). After proper therapy such pigmentary changes clear completely.

In pseudohypoparathyroidism, subcutaneous calcium plaques may develop in the abdominal walls and in some cases be evident at birth.

REFERENCE

Talbot N B et al. *Functional Endocrinology* (Cambridge Mass: Harvard University Press 1952) pp 94 and 113

Iliac horns (Fong's lesion) — These bony symmetrical bilateral posterior iliac processes have been found alone and in association with a variety of symmetrical anomalies of mesodermal and ectodermal origin. The cutaneous dysplasia has usually been limited to aplasia or hypoplasia of the nails of the thumbs and index fingers. The nails of the toes are normal. In some cases the ectodermal element in the irises has been widened and darkened (Lester's sign), causing an irregularly widened dark pupillary border. In the skeleton, the patellas and the radial heads are commonly hypoplastic (Fig 8-841) but many other bones at the major joints in the feet and in the skull (hyperostosis) have been involved. In the pelvis, in addition to the pelvic horns, the ilia may be short cephalocaudally, the sacrum may be bowed and coxa valga may occur in both femurs.

In one of our patients, a boy 20 years of age, independent ossification centers were still visible in the tips of the horns (Fig 8-842) which indicates that these horns are probably cartilaginous exostoses. One

Fig 8-842 — Bilateral symmetrical iliac horns in a boy 20 years of age. Secondary ossification centers crown the tips of the horns (arrows). The iliac wings are flattened transversely and their lateral edges, normally convex, are deformed into concave contours. The clinical history of this patient is unknown.

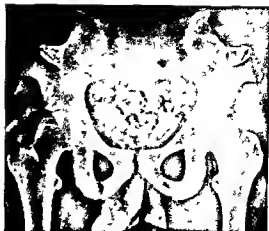
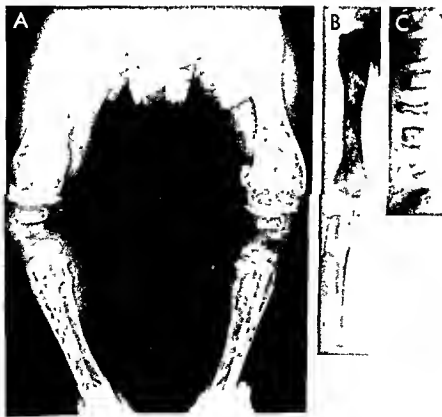


Fig 8-843 — Mastocytosis (urticaria pigmentosa) in a boy 6 months of age who had been irritable since birth with constant crying, vomiting and diarrhea. Scattered urticarial pruritic skin lesions were relieved by Benadryl. In several tests, histamine levels in the blood had been increased. The liver and spleen were enlarged and the left leg and foot paralyzed. Diagnosis was based on biopsy study of one femur. A, all long bones in the legs are widened due to dilatation of the medullary cavities. This has caused failure of normal constriction of the shafts and the nor-

mal concave contours have been converted to convex bulges by hypertrophy of the marrow due to hyperplasia of mast cells. The cortical walls have been abraded from the inside by the same causal mechanism. The external tags on the femurs are not eustatically explained. B, similar but less marked changes in the bones of the arm. C, compression fractures have flattened L3 and L5 vertebral bodies. (Courtesy of Dr. Edward B. Singleton, Houston, Texas.)



of the patients of Hawkins and Smith a girl 14 years of age also had secondary ossification centers at the tips of the horns

REFERENCES

- Fong E E. "Iliac horns (symmetrical bilateral central posterior iliac processes) A case report Radiology 47 517 1946
- Hawkins C F and Smith O E. Renal dysplasia in a family with multiple hereditary abnormalities including iliac horns Lancet 1 803 1950
- Thompson E A et al. Iliac horns (an osseous manifestation of hereditary arthrodysplasia associated with dystrophy of the fingernails) Radiology 53 88 1949

Osteopoikilosis and palmar and plantar keratomas were found associated in two sisters one of whom was 14 years of age by Aigner. The author concluded that the two disorders were related genetically and structurally

REFERENCE

- Aigner R. On osteopoikilosis associated with hereditary disseminated palmar and plantar keratomas Wien klin Wchnschr 65 860 1953

Urticaria pigmentosa (mastocytosis) is a generalized disease which involves bone marrow lymph

nodes spleen liver and other organs as well as the skin. Proliferation of mast cells in the bone marrow may cause dilatation of the medullary cavities and internal thinning of the cortical walls of the long bones with localized patches of rarefaction and sclerosis (Fig. 8-843)

REFERENCE

- Bendel W L and Race G J. Urticaria pigmentosa with bone involvement J Bone & Joint Surg 45-A 1043 1963

Familial absence of the middle phalanges (brachymesodactyly) with hypoplasia of the nails (Bass syndrome) -- In four members of a single family Bass found shortening of the fingers and toes with absence of the middle phalanges in the lateral four digits in the hands and feet duplication of the distal phalanges of the thumbs and hypoplasia of the fingernails of all digits but the thumbs. In the pedal digits the nail of the second toe was absent at birth, but the other toenails were normal. The cartilages of the ear were misshapen in one member of the pedigree

REFERENCE

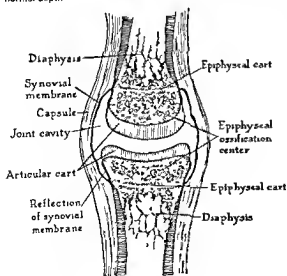
- Bass H N. Familial absence of middle phalanges with nail dysplasia. A new syndrome Pediatrics 42 318 1968

The Joints

Normal Anatomy

The joints comprise the tissues which bind together and are interposed between articulating bones. The nature of the articular tissues in different joints varies widely and is dependent principally on the type of motion at the joint. In temporary joints of little or no motion the *synarthroses*, the articular tissues gradually diminish during growth and disappear completely when growth is complete. The *sutures* and *fontanels* of the cranial vault are *synarthroses* in which the edges of the articulating bones are bound together by fibrous tissue. The *synchondroses* are *synarthroses* in which union of the articulating bones is effected by a disk or mass of hyaline cartilage, and they are found in the cartilaginous base of the skull, in the

Fig 8-844—Schematic representation of the principal structures in a typical joint. The synovial membrane is the internal layer of the articular capsule. It does not extend onto the articular cartilages. The joint cavity is suitably dilated to many times its normal depth.



innominate bones and between the primary and secondary ossification centers of the tubular bones.

The permanent joints of limited motion are called *amphiarthroses* or half joints. When their articulating bones are covered by cartilage and the bones are also bound together by fibrous tissue we call them *symphyses*. The joints between the vertebral bodies (see Fig 9-3) and between the bodies of the pubic bones are *symphyses*. *Syndesmoses* are half joints in which the articulating bones are bound together by fibrous tissue alone in the form of ligaments, sometimes ligaments between bones well removed from each other such as in the stylohyoid, costoclavicular and coracoacromial articulations.

In the joints of free motion or true joints the *diarthroses* there is a joint cavity, lined with synovial membrane and filled with synovial fluid interposed between cartilage-covered bones which are bound together by a fibrous capsule (Fig 8-844). In the healthy living joint, the opposing articular cartilages are in apposition and all parts of the capsule are closely compressed onto the bones and cartilages by the surrounding muscles and tendons. The synovial fluid is present in only small amounts for lubrication, the articular cleft and the articular cavity are potential rather than actual spaces during life.

The articular cartilage is derived from the epiphyseal cartilage. During infancy and childhood these two structures are directly continuous with each other (see Fig 8-61), with increasing age the underlying epiphyseal cartilage is progressively ossified until only the covering articular cartilage remains when growth is completed. In compound joints such as the knee a cartilaginous disk is interposed between the two articular cartilages. This disk or meniscus is attached on its periphery to the joint capsule. The free surface of the disk is covered with synovial membrane in contrast with the articular cartilages which lie naked in the joint cavity devoid of synovial covering.

The joint is enclosed in a connective tissue envelope the capsule, which rises from the periosteum near the ends of the opposing bones. The outer layer of the articular capsule is a fibrous membrane of vari-

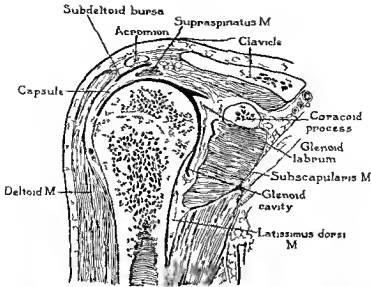


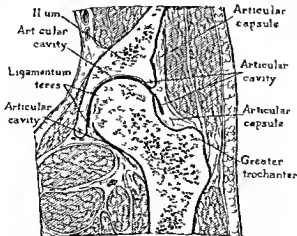
Fig 8 845 — Normal structures in the right shoulder joint, frontal section

able thickness it may contain one or several local thickenings, the capsular ligaments. Fascial and ligamentous thickenings often blend with the capsule and reinforce it. As a rule, the capsule arises from the bone near the epiphyseal line and covers all or almost all of the epiphysis. The importance of the position of the capsular attachments in metaphyseal and epiphyseal bone infections and their extension to the adjacent joint is illustrated in Figures 8-845 and 8-846. The internal layer of the joint capsule, the synovial membrane, covers all of the free surface of the articular cavity except the articular cartilages and portions of some of the intra-articular ligaments. The synovium is a delicate sheet made up of flattened connective tissue cells on a layer of loose connective tissue which form an incomplete endothelium like

lining. Internal projections of the synovial membrane—synovial folds or villi—fluctuate in size and position during motion of the part. Wherever the synovial mesothelium is defective, the lining of the articular cavity is made up of tight fibrous tissue. The subsynovial fat pads lie external to the synovial membrane but internal to the fibrous articular capsule.

Bursae are fluid-filled spaces in the periarticular connective tissue which are located at the sites of maximal frictional impact between neighboring movable structures. The bursal spaces are lined with a cellular membrane similar to the synovial covering of the articular spaces. Bursae are variable in number; they may be multilocular and often communicate with one another and also with the joint space itself.

Fig 8 846 — Normal structures in the left hip joint, frontal section (Redrawn from Morris Human Anatomy)



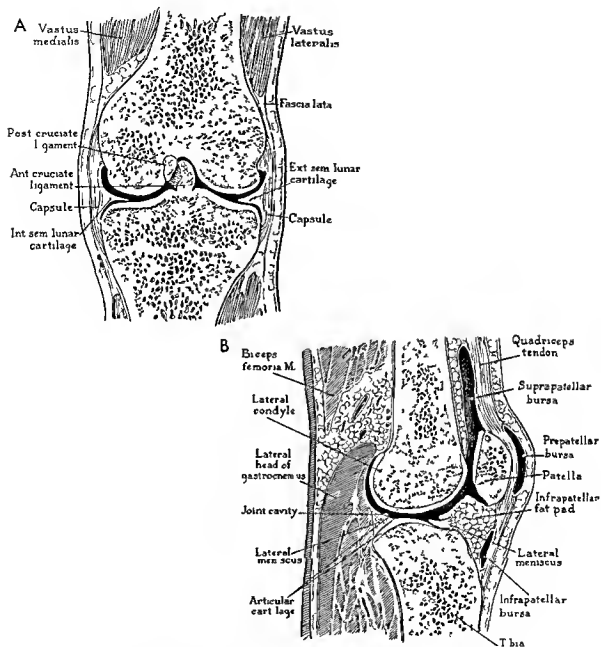


Fig 8 847 —A, frontal section of right knee posterior view B lateral projection of the knee joint (Redrawn from Sobotta and McMurrich)

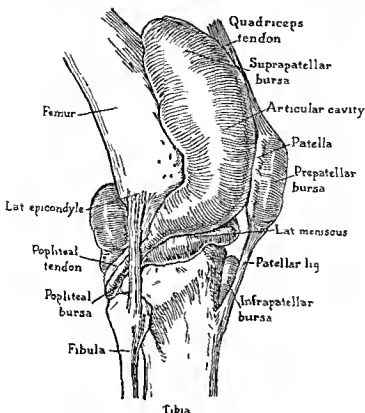


Fig. 8 848 — Normal bursas at the knee joint

The principal anatomic features of some of the larger joints and their surrounding soft tissues are shown in Figures 8 845 to 8 848

Normal Roentgen Appearance

The normal joint is composed entirely of tissues of water density and the shadows cast by the different articular components are all of a similar density. The articular shadows are also of the same density as the shadows cast by the periarticular tissues. For these reasons the shadows of the individual components of a normal joint cannot be clearly differentiated from one another or from the roentgen images of neighboring muscles, fascia, tendons, ligaments, nerves and vessels. At the knee joint several large fat pads provide a contrast density which permits satisfactory visualization of some of the articular soft tissue structures, especially in lateral projection (Fig. 8-849).

The shadow of water density which fills the space between the opposing bones is cast by the two contiguous articular cartilages and their underlying uncified epiphyseal cartilages (Fig. 8 850). The depth of this intermediate cartilage shadow varies inversely with the age of the individual (see Fig. 8-61). In compound joints the articular disk also contributes to the

interposed cartilage shadow. It should be remembered that in the healthy living joint the articular cleft and synovial fluid contribute almost nothing to the intermediate cartilage shadow.

Transitory natural pneumography is due to entrance of gases into the joint spaces following a sudden increase in intra articular volume and lowering of intra articular pressure by sudden stresses either from endogenous muscular pulls or from external traction. The gases move from the higher pressures in the contiguous tissues to the lower pressure in the suddenly expanded joint space, oxygen, carbon dioxide and nitrogen are present in the same proportions in the joint as they are in the circulating blood. The gas outlines the internal surface of the synovial layer and the articulating surfaces of the articular cartilages which are not covered by synovium. We have encountered natural pneumograms most frequently in infants, particularly in the shoulders when the arms have been suddenly and fully abducted in positioning for chest films in frontal projection and in the hip after sudden abduction of the femur (Figs. 8 851 to 8-853). In one of our patients the gas which accumulated in the knee joints in a natural hypotensive pneumoarthrogram was superimposed on the upper edge of the tibias and simulated fracture lines (Fig.

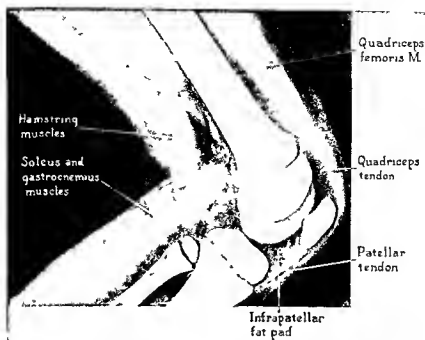


Fig 8 849 — Roentgen appearance of the normal knee: drawing of a roentgenogram

Fig 8 850 — Cartilage space between the ends of the opposing bones at the knee joint of a newborn infant. A, roentgenogram; B, schematic drawing of A. The space between the ends of the opposing bones is occupied by a shadow of water density in the roentgenogram. In the drawing, this space is shown to be filled

completely by the epiphyseal cartilages and the overlying articular cartilages. In the normal living joint, the joint cleft is exceedingly narrow and casts an insignificant shadow in the roentgenogram.

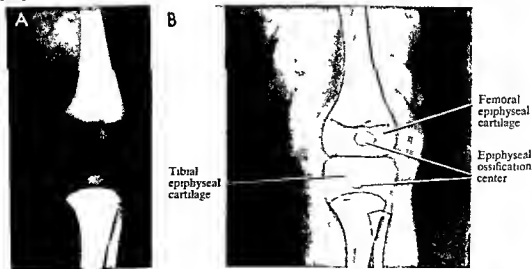
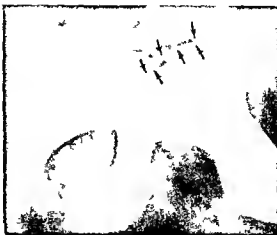




Fig. 8 851 (left).—Natural pneumogram of the shoulder following sudden full abduction of the arms in position for a frontal projection of the chest. A similar gas image was visible in the left shoulder. The patient was 3 years of age.



sudden abduction and external rotation in position for a frontal projection of the hips. In a film of the hips made a few minutes before with the femurs in adduction, there was no evidence of gas in the hips. This patient was 2 years of age.

8 854) The presence of even substantial amounts of gas in these circumstances should be recognized as a normal phenomenon. After natural pneumography the gas is rapidly replaced by fluid even if the stress and traction on the joint are maintained; replacement is complete after 10 minutes according to Nordheim. We have also seen gas accumulate spontaneously in the articular spaces of the wrists and in the diarthroses of the spine.

REFERENCE

- Fuiks D M and Grayson C Vacuum pneumography and the spontaneous occurrence of gas in joint spaces *J Bone & Joint Surg* 32-A 933 1950

Diseases of the Joints

The roentgen examination of abnormal joints is not as productive of valuable diagnostic information as in

many other organs of the body owing to the proportionately poorer visualization of much of the articular structure. Notwithstanding this general truth, important information about disease of the joints can often be gained by the careful study of good films which are placed before a strong light to bring out more detail in the soft tissues. The location and extent of articular lesions can often be identified and their involution under treatment followed to advantage. Films are nearly always essential in the study of articular disease for the identification and exclusion of associated changes in the bones. The exact cause of articular changes usually cannot be deduced conclusively from roentgen findings.

Fig. 8 854.—Transverse strips of gas (natural hypotensive pneumoarthrogram) superimposed on the edge of the tibial shaft with multiple fracture lines in the knee joint of an asymptomatic girl 8 years of age.

Fig. 8 853. Bilateral natural pneumograms of the hips of a normal infant 12 months of age. The radiolucent strips (arrows) represent intra-articular gas between the cartilaginous edge of the acetabulum and the epiphyseal cartilage of the femoral head.



CONGENITAL MALFORMATIONS

Most of the congenital articular malformations are associated with the congenital errors in segmentation of the skeleton which have already been described (see Fig 8-271). Complete absence of a joint results from local failure of segmentation of the fetal cartilaginous skeleton or fusion following segmentation. Congenital dislocations and subluxations are sometimes due primarily to congenital defects in the articular cartilages and articular capsule, congenital anterior dislocation of the head of the radius is the most common of these anomalies. Absence of the cruciate ligaments of the knee has been found in patients with congenital subluxation of the tibia. Congenital dislocation of the hip has been described (see Figs 5-35 and 5-36). The entire shoulder joint is displaced cephalad in Sprengel's deformity (see Fig 2-54).

Congenital lateral dislocation of the patella should be suspected when a persistent flexion contracture at the knee is present in the early months of life. Flexion contraction is not always present but there is almost always a loss of active extension. Early radiographic diagnosis is uncertain because the ossification center for the patella does not appear until the 3rd year. The patella is palpable when the knee is extended and is felt in lateral position when displaced. Arthrogryposis and other neuromuscular disorders should always be excluded. After the 4th year radiographs show the patella displaced laterad. The displaced patella is unusually small. The lesion is sometimes familial.

Fig 8-855 — Posterior aspect of right knee with a discoid lateral meniscus which is thickened and displaced medially and fastened to the medial condyle of the femur by a short meniscofemoral ligament.

Green J P and Waugh W. Congenital lateral dislocation of the patella. *J Bone & Joint Surg* 50-B 285 1968

Discoid cartilage of the knee is a thickening of all or a part of the meniscus (Fig 8-855) which produces a snapping or loud clicking sound when the knee is flexed and extended. Usually there is no pain or limitation of motion. Kaplan concluded after careful dissections that the meniscus becomes thickened after birth owing to defective attachments posteriorly to the tibial plateau and a continuous meniscofemoral ligament which fastens the posterior horn of the meniscus to the medial condyle of the femur. These abnormal attachments in turn cause excessive movement of the meniscus during motion at the knee. In standard radiographs of the knee, discoid meniscus is invisible. Pneumograms of the knee should demonstrate the cartilaginous thickening and pneumograms combined with plainography should theoretically demonstrate this lesion in exact detail.

REFERENCES

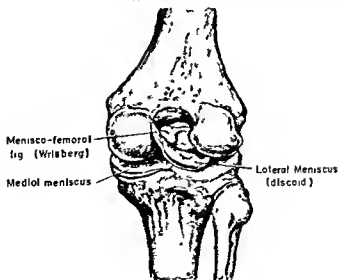
- Kaplan, E B. Discoid lateral meniscus of the knee joint. Nature, mechanism and operative treatment. *J Bone & Joint Surg* 39-A 77 1957.
 Ross J A et al. Congenital discoid cartilage. Report of a case of discoid medial cartilage with embryological note. *J Bone & Joint Surg* 40-B 262 1958.

TRAUMATIC CHANGES

Detailed descriptions of the findings in dislocations and subluxations of the joints are available in surgery.

morel ligament of Wrisberg. The posterior attachments of the thickened lateral meniscus to the opposite tibial plateau are lacking. The medial meniscus is normal. (Redrawn from Kaplan.)

KNEE EXTENDED



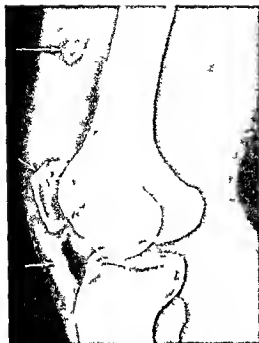


Fig. 8-856 — Laceration of the quadriceps tendon shown by deformation of the soft tissue shadows anterior to the knee. The shadow of the quadriceps tendon is obliterated. A soft tissue swelling above the patella. A small fragment of the patella is displaced cephalad. The relaxed patellar ligament is wavy. (From Lewis.)

cal texts. At the knee and ankle lacerations of tendons and deformities of the soft tissues caused by injury can sometimes be clearly demonstrated roentgenographically (Fig. 8-856). Serous and purulent arthritis and bursitis, hemarthrosis and regional extracapsular hematomas and cellulitis may all follow injuries to the joints. These traumatic swellings have the same roentgen appearances as the inflammatory swellings in infectious arthritis which are described in the following paragraphs. Traumatic opaque fixed

and loose bodies in the joints are almost nonexistent during infancy and childhood.

Stenstrom found pneumograms of the knee valuable in identifying and localizing meniscal tears in the knees. These are rare during the first decade. Arthrography also made possible the demonstration of the cartilage laceration in osteochondrosis dissecans which may be important in treatment. The extent of synovial changes in arthritis could be estimated from the irregularities on the capsular edge.

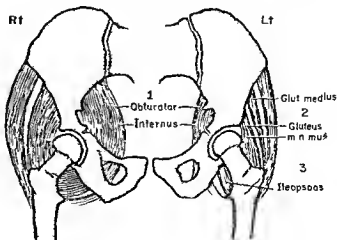
REFERENCE

- Stenstrom R. Arthrography of the knee joint in children. Roentgenologic anatomy, diagnosis and the use of multiple discriminant analysis. *Acta Radiol. supp.* 281 1968.

INFECTIOUS ARTHRITIS

Acute transitory synovitis of the hip is an entity in itself in which the inflammatory reaction is in the synovial layer only of all of the intra-articular structures. The joint capsule becomes distended and filled with excessive synovial fluid. This lesion is not so important of itself because spontaneous complete regression usually occurs within a few days. It is important in radiologic diagnosis owing to the difficulties with which it can be differentiated from more serious lesions such as tuberculosis, purulent arthritis, osteomyelitis and early coxa plana. It is believed that in most instances the reaction in the hip is due to local toxic effect or allergic effect rather than actual infection of the synovium. Children younger than 10 years are commonly affected. The principal clinical manifestations are local pain and limp; pain may also develop in the ipsilateral knee. Movement at the hip is limited in all directions because all of the muscular groups controlling the hip are spastic. The patient is most comfortable with the thigh in flexion and adduction; extension is particularly painful. Fever varies from 99 to 103 F. Laboratory studies rarely disclose evidence of positive diagnostic value. Radiologic

Fig. 8-857 — Schematic drawing showing edema of the muscles on the right side which is characteristic of transitory synovitis of the hip. The obturator internus, iliopsoas and gluteus minimus are swollen, and the radiolucent strips between them are displaced and partially obliterated. The bones are normal. (Redrawn from Dey.)



examination shows no changes in the bones, and I have never seen widening of the articular space. There is usually an increase in the volume and density of the soft tissues at the hip. Drey claimed that he could detect specific swellings of the internal obturator, gluteus minimus and iliopsoas muscles with loss of the normal radiolucent fat strips between them which he attributed to edema of the muscles (Fig 8-857). His illustrations support his claims, and films should be made for good soft tissue detail in the radiologic study of this important lesion. Drey believes his findings are pathognomonic of acute synovitis. It is possible that some of Drey's patients suffered from regional myositis rather than synovitis (see Fig 8-18, this patient had clinical signs characteristic of synovitis for several months).

Spock, on the other hand in a study of 47 cases found radiography valuable only in the exclusion of conditions other than acute synovitis. None of his patients exhibited signs of disease in the neighboring bones, and thus we agree is the major contribution of the radiographic examination. Often asymmetries of the images of the soft tissues at the hips, unrelated to synovitis, are attributed to it. These asymmetries are often due to the natural largeness of muscles on one side, to projection of the pelvis in slightly oblique positions and to the shifting of weight to one side of the pelvis—to one of the buttocks by the patient.

Neuhauser and Wittenberg estimated that in acute synovitis, radiographic signs are diagnostic in one third of cases suggestive of the lesion in one third of cases and normal in one third.

REFERENCES

- Drey L. Roentgenographic study of transitory synovitis of the hip joint. *Radiology* 60:588 1953.
 Neuhauser E B D, and Wittenberg M H. Synovitis of the hip in infancy and childhood. *Radiol Clin North America* 1:13 1963.
 Spock H. Transient synovitis of the hip joint in children. *Pediatrics* 24:1042 1959.

Foreign body arthritis is usually easily identified by the presence of a puncture wound or of an opaque image in the joint when the foreign body is metallic, as most of them are. The possibility that a nonopaque foreign body is a cause of chronic arthritis should always be considered because the perforating wounds may heal quickly and leave little or no scar. Prolonged swelling of a joint with indifferent response to antibiotics warrants surgical exploration in many cases. Karshner and Hanafec pointed out the importance of palm thorns as the cause of obscure articular effusions in children who live in tropical and subtropical regions. Some nonopaque foreign bodies might be demonstrated prior to surgical exploration by contrast arthrography.

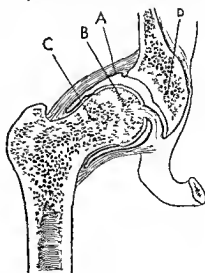
REFERENCE

- Karshner R C, and Hanafec W. Palm thorns as a cause of joint effusions in children. *Radiology* 60:588 1953.

Acute purulent hematogenous inflammations of the joints are much more common during infancy and childhood than during later life. This higher incidence in the early years is attributed to the greater flow of blood to the joints during the most active stages of growth. Purulent arthritis usually develops as a metastatic complication of bacteremias due to upper respiratory infections, pyoderma and purulent omphalitis in the newborn. At all ages there is a great diversity of infecting bacteria. During the first two years of life, *Hemophilus influenzae* is the predominant single causal agent after age 6 months and coagulase positive staphylococci before age 6 months. At all ages, staphylococci predominate in the hip and *H influenzae* in the ankle. However, at all ages a wide variety of bacteria invade the joints of children. The radiologist, of course, cannot identify the infecting organism.

The infecting organisms may invade the joint from the blood stream or by contiguous extension from hematogenous pyogenic foci in the neighboring bones (see Fig 8-646, p 1192). The adjacent bones may, on the other hand, be infected secondarily by extension from the purulent joint. In our experience, associated bone changes are common in all types of purulent arthritis in infants and children, especially in infants. The bone involvement may not become evident roentgenographically until many days and weeks after the arthritis is manifest clinically. The common local sites of origin of purulent infections of the hip joint are illustrated in Figure 8-858. Pathologic disloca-

Fig 8-858—Possible primary sites of origin from which infection may extend secondarily into the hip joint. This initial focus may be in the femoral epiphysis (A), in the synovium itself (B), in the femoral metaphysis (C) or in the innominate bone on the margins of the acetabular cavity (D). In some cases the hip joint may be infected by extension from more than one of these neighboring primary foci.



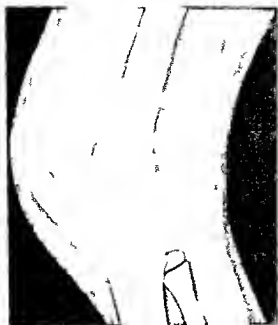


Fig. 8-859—Characteristic changes in the soft tissue of the knee joint in purulent arthritis. The suprapatellar fat pad is encroached on from behind and flattened dorsoventrally by the distended articular capsule. The patella and the tendon of the quadriceps femoris are displaced ventrad owing to distention of the underlying articular capsule and suprapatellar bursa. The soft tissue shadows beneath the quadriceps tendon are thickened for the same reasons. The popliteal space is filled with the swollen popliteal bursa. Compare these abnormal findings with the structures in the normal knee (Figs 8-847 B and 8-849).

tions at the hip are common in infants who suffer from purulent arthritis of the hip. Arthritis may be a rare complication of salmonella bacteremia, especially during the first years of life, and in some cases may resemble the onset of rheumatic arthritis. Although salmonella osteitis is frequently associated with sickle cell anemia in infants and younger children, arthritis rarely accompanies this osteitis (David and Block).

As in other tissues, inflammation in the joints is characterized by congestion, edema, and leukocytic infiltration. The capsular and pericapsular tissues are thickened, and synovial exudate accumulates in the joint cavity and distends the capsule. Extreme distention of the capsule may permit pathologic subluxation, especially in the hips and shoulders. If the bursas communicate with the affected joint, they undergo analogous inflammatory changes. The increase in joint fluid and the thickening of the articular and periarthral tissues produce a regional swelling of water density in the roentgenogram (Fig. 8-859). Owing to the fusion of contiguous shadows of equal density cast by the synovial exudate, by the thickened articular capsule, and by the swollen periarthral tissues, one usually cannot satisfactorily differentiate the intra-articular, the capsular, and the extra-articular components of the arthritic reaction. Serous fibri-

nous hemorrhagic purulent and fibrous articular exudates singly or in any combination cast similar roentgen shadows.

At the knee, the patella is displaced away from the femur as the joint becomes distended with synovial fluid (Fig. 8-859). The suprapatellar bursa often becomes distended at the same time because it often communicates with the articular cavity. Clouding of the normally radiolucent triangle in front of the Achilles tendon usually is indicative of increased synovial fluid in the ankle joint. Large high-tension articular effusions may spread apart the opposing ends of the bones and increase the depth of the soft tissue shadow interposed between them. At the shoulder and hip, pathologic subluxations may develop in severe cases; at the knee, on the other hand, spreading of the bones is uncommon except in long-standing cases in which destruction of ligaments and destruction of the articular capsule also plays a causal role.

The articular cartilages may not be significantly affected or may undergo rapid destruction. Phemister demonstrated that proteolytic enzymes are liberated by the leukocytes of purulent arthritic exudates and that the amount of destruction of the articular cartilages is directly proportional to the length of exposure of the cartilage to this enzymatic solvent action. Pressure and friction further accelerate the destruction. Destruction of the articular cartilages is measured roentgenographically by a diminution in width of the shadow interposed between the ends of the opposing bones (Fig. 8-860). The infection may extend entirely through the articular cartilage and produce destruc-

Fig. 8-860—Traumatic arthritis of the left hip joint in a patient 10 years of age, showing destruction of the articular cartilages and narrowing of the cartilage space. The underlying bone is also partially destroyed.



tive inflammatory foci on the juxta articular margin of the underlying bone. These areas of destructive osteitis appear as definite patches of rarefaction on the edges of the adjacent epiphyseal ossification centers.

During healing the intra articular exudate may be completely resorbed. In other cases the exudate persists and becomes organized into a fibrous mass which replaces the destroyed articular cartilages and causes fibrous ankylosis. Fibrous tissue shadows show water density and cannot be differentiated from those of other soft tissues roentgenographically. In some cases healing is followed by a bony bridging between the opposing bones and the cartilaginous space is obliterated by opaque shadows of bone density and texture.

REFERENCES

- David R. and Block R. L. Salmonella arthritis. *Medicine* 39:385 1960.
Nelson J. D. and Koontz W. C. Septic arthritis in infants and children. A review of 117 cases. *Pediatrics* 38:966 1968.

BURSITIS

The inflammatory changes in the bursas are analogous to those in the joints. bursitis and arthritis are often associated but may develop independently of each other. The inflamed swollen bursas cast local shadows of water density which can be recognized roentgenographically as soft tissue tumors but which

Fig 8 861 Popliteal (Baker's) cyst in a patient 5 years of age. A large rounded soft tissue mass fills the popliteal space. Drawing of a roentgenogram.

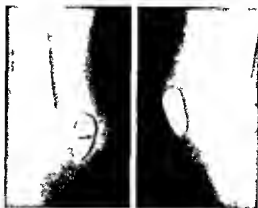


Fig 8 862 Swelling of the bursa in prepatellar bursitis in a girl 9 years of age.

cannot be satisfactorily differentiated from other soft tissue swellings such as hematomas, cellulitis, lymphangiomas, hemangiomas, and ganglions. Prior to adolescence, calcification of long standing traumatic bursal exudates is extremely rare.

At the knee joint, popliteal cysts (Baker's cysts) sometimes form owing to the accumulation of fluid within the popliteal bursas. They commonly communicate with the synovial space of the knee joint. In some cases the popliteal cyst is caused by actual herniation of the articular synovial membrane posteriorly through the articular capsule and the accumulation of fluid within the synovial hernial sac. There is considerable evidence that the accumulation of fluid is due to the mechanical closure of the channels between the knee joint and the bursas or the herniated synovial sac by muscular pressure during movement. Inflammation may also be a causal factor. Roentgenographically, Baker's cyst appears as a well-defined, rounded soft tissue tumor of variable size in the popliteal space (Fig 8 861). Air bubbles have been demonstrated in popliteal cysts after injection of air into the cavity of the knee joint.

In contrast, the soft tissues in front of the patella are swollen in the case of prepatellar bursitis (Fig 8 862) or better traumatic prepatellar hemorrhagic bursitis.

REFERENCES

- Baker W. M. Formation of synovial cysts of the leg in connection with disease of the knee joint. *St. Bartholomew's Hosp. Rep.* 13:245 1877.
Burleson, R. J. et al. Popliteal cyst. A clinicopathological survey. *J. Bone & Joint Surg.* 38-A:1265 1956.
Neyerding H. W. and Van Denmark R. E. Posterior hernia of the knee (Baker's cyst, popliteal cyst, semi-membranous bursitis, medial gastrocnemius bursitis and popliteal bursitis). *J. A. M. A.* 122:858 1943.

TUBERCULOSIS OF JOINTS

The mode of transmission of tubercle bacilli to joints is similar to that of pyogenic bacteria. The syno-

vium may be infected directly by implantation from the blood stream or secondarily by extension from a hematogenous tuberculous focus in an adjacent bone. The converse is also true, tubercle bacilli may spread from the hematogenous focus in the joint to the underlying bone. In some joints, transmission of infection in both directions—to the joint from the bone and from the joint to the bone—may take place. The proportionate frequency of these two types of spread in tuberculous arthritis is not known.

The roentgen appearance of the soft tissue swelling is identical in tuberculous and nontuberculous arthritis. The associated primary hematogenous lesions in the ends of adjacent bones are similar macroscopically in tuberculous and purulent arthritis and they cast similar roentgen shadows (see Figs. 8-660 and 8-661). For these reasons tuberculous and pyogenic arthritis derived secondarily from adjacent bone cannot be satisfactorily differentiated roentgenographically. Phemister and Hatcher stated that the hematogenous tuberculous bone foci associated with tuberculous arthritis cannot be differentiated from the arthrogenic tuberculous bone foci in some cases "even in the pathological examination of the resected joint."

In direct primary synovial tuberculosis Phemister and Hatcher observed that in joints in which the opposing articular cartilages fit accurately, the tuberculous granulation tissue first destroys the articular cartilages on the periphery where there are little or no contact and pressure. In joints like the knee, in which the opposing cartilages do not fit into each other accurately, the noncontact surfaces are not all located on the periphery and the tuberculous granulations erode the noncontact areas wherever they may be, in the center or on the margins. The destruction of articular cartilage by granulation tissue is characteristically slow in tuberculosis, even detached cartilage persists for a long time owing to the lack of proteolytic enzymes in the tuberculous exudate. For these reasons, the cartilage space between the opposing ends of the bones is well preserved for long periods in tuberculous arthritis. *Reduction in the depth or disappearance of the cartilage space is characteristically rare and late in tuberculous arthritis in contrast with early narrowing of the cartilage space in purulent arthritis.*

The destruction of bone follows the destruction of the overlying articular cartilage and begins in the same peripheral and noncontact areas, the subchondral bone is, like the articular cartilage, well preserved in the contact regions. When this noncontact marginal pattern of bone destruction can be demonstrated roentgenographically, the probability of tuberculous arthritis is increased. Such findings, however, are not pathognomonic of tuberculosis because the noncontact pattern of bone destruction may also be present in nontuberculous arthritis. *The noncontact pattern of bone destruction is limited to cases in which the tuberculous infection spreads from the joint to the bone; it is not found in cases in which*

the infection is primary in the metaphyses or epiphyses and then extends to the joint. Phemister and Hatcher found that when both of the opposing ends of the bones exhibit destructive foci in tuberculous arthritis, these foci are usually directly opposite each other. The value of this sign has been limited in our experience because bone destruction on both sides of tuberculous joints has been uncommon in infants and younger children.

In the late stages of tuberculous arthritis the entire articular cartilages are destroyed and extensive areas of subchondral bone erosion appear in both contact and noncontact areas.

There are no pathognomonic roentgen findings in tuberculous arthritis—in the capsule, in the articular cartilages or in the adjacent bones, in any stage of the disease. A conclusive diagnosis can be made only by microscopic examination of the tissues or by the demonstration of tubercle bacilli in the synovial exudate. A negative reaction to the tuberculin skin test, with few exceptions, excludes tuberculosis completely. A positive reaction demonstrates that the patient has been infected with tubercle bacilli, but it does not prove conclusively that a morbid joint in a tuberculin positive child is necessarily a tuberculous joint.

REFERENCES

- Phemister D. B. Changes in the articular surfaces in tuberculosis and pyogenic infection of joints. *Am. J. Roentgenol.* 12:1 1924.
 — Effect of pressure on articular surfaces in pyogenic and tuberculous arthritides and its bearing on treatment. *Ann. Surg.* 80:481 1924.
 — and Hatcher H. C. Correlation of pathological and roentgenological findings in the diagnosis of tuberculous arthritis. *Am. J. Roentgenol.* 29:736 1933.

RHEUMATIC FEVER

Roentgen examination of the joints provides little of positive value in the diagnosis of rheumatic polyarthritis. The regional soft tissue swellings of the affected joint appear roentgenographically as swellings of water density, the bones show no abnormalities. As the attack subsides the articular and periarthral swellings disappear, the joints are usually restored to normal roentgenographically and functionally. It is said that fibrous and even bony ankylosis of the joints may be a sequel of rheumatic arthritis in severe cases in older children and adults, but even this must be distinctly rare. Leukopenic leukemia with ostealgia may simulate rheumatic fever and rheumatic arthritis clinically and hematologically for long periods before characteristic leukemic changes appear in the blood. In such circumstances roentgen examination of the skeleton may reveal leukemic bone changes (see Figs. 8-802 and 8-803) and facilitate earlier diagnosis of leukemia.

LEUKEMIC ARTHRITIS

Bone and so-called joint pain are common in the leukopenic leukemia of infants and younger children. Ac-

tual radiologic and clinical evidence of articular involvement in leukemia is all but unknown. In the patient of Bedwell and Dawson, an older child with myeloid leukemia, there were swelling and redness and increased local heat at the interphalangeal joints, wrists, elbows, shoulders, knees and ankles. Radiologic examination showed no evidence of leukemia in the contiguous bones. At necropsy, the synovial membranes of the left knee and right elbow showed marked edema with petechial hemorrhages and extensive infiltration with leukemic cells. There was also cortical thickening in the right femur.

REFERENCE

Bedwell C A and Dawson A M. Chronic myeloid leukemia in a child presenting as acute polyarthritis. *Arch Dis Childhood* 29:78, 1954.

OSTEOARTHRITIS
(HYPERTROPHIC ARTHRITIS)

This is a degenerative disease of the articular cartilages and the bones which appears to result from prolonged use and recurrent mild trauma. Osteoarthritis is common in middle aged and elderly persons but does not occur in children.

RHEUMATOID ARTHRITIS

This, although by no means common, is by far the most important chronic disease of the joints in children. The articular lesions, subacute and chronic polyarthritis, represent but one of the tissue injuries of a

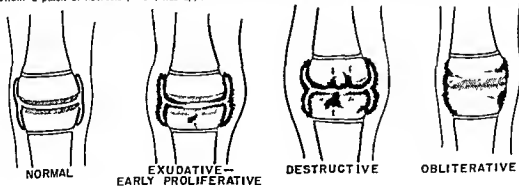
generalized and scattered inflammation which is more properly called rheumatoid disease or the rheumatoid state. In children, when polyarthritis is combined with enlargement of the spleen and lymph nodes, and sometimes adhesive pericarditis, the syndrome is called Still's disease. The conspicuous feature of Felty's syndrome in adults is leukopenia and hepatomegaly as well as polyarthritis. Widely distributed cutaneous eruptions develop in some children during the course of polyarthritis, and the eruption may persist for months after the polyarthritis has disappeared.

In most children the first clinical manifestations appear during the 3rd to 5th year. Transitory pain, swelling and stiffness of one joint, usually the knee, first make their appearance. We have seen 2 cases in which stiffness of the neck due to rheumatoid arthritis of the cervical spine (see Figs. 9-69 to 9-71) was present for several weeks before one knee became swollen. The cervical spine may be affected for months before radiographic changes become visible. In Schlesinger's study of 100 patients, the cervical spine was frequently affected, and in three cases was the site of initial involvement. Crippling deformities and ankyloses develop as the disease progresses, and the joint cartilages are destroyed and the joint capsule and regional muscles and tendons contract. Complete remissions, however, may occur in younger children even after the disease has been established in several joints.

The morbid structural changes, which determine the radiographic changes, are basically subacute and chronic inflammation of the articular and periarтику

Fig. 8-863—Gross progressive structural changes responsible for the radiographic findings in rheumatoid arthritis. The synovial layer is drawn in heavy black. In the normal, the synovium stops at the edges of the articular cartilages, which are uncovered and exposed directly to the synovial fluid and to the opposing articular cartilage. In the early exudative and proliferative stage, the synovial layer is thickened, and the articular space laterally and medially beyond the articular cartilages is dilated but the space between the cartilages themselves is not deepened. The synovium is beginning to grow over the articular cartilages from the edges and abrade the cartilage edge on which they grow. Deep in the tibial ossification center and unrelated to the overgrowth of synovium, a patch of necrosis (arrow) has appeared which

represents overgrowth of mesenchymal elements in the marrow. At this time, radiographic findings include regional swelling of soft parts and beginning irregularity of the bones with destruction in the tibial epiphyseal center. In the destructive phase, the edges of the articular cartilages (arrows) are deeply abraded with beginning destruction of subchondral bone and extension of the marrow overgrowth in the tibial center through the bone and cartilage into the joint space (arrow). In the obliterative phase, most of the articular cartilages have disappeared and there is junction by bony union. Hypertrophic synovium still grows on the side walls (arrows) of the condyles and is growing into these walls and destroying them.



lar tissues followed by progressive overgrowth of the synovium (pannus formation) which leads eventually to destruction of the underlying cartilage and then the bone underlying the cartilage when the penetration of pannus is sufficiently deep. The redundant overgrown synovium and the secondary effects on bone and cartilage are shown schematically in Figure 8-863. The connective tissue in the intraosseous

medullary cavities contiguous to the arthritis also hypertrophies and this is responsible in part for the early severe terminal rarefaction of the shafts seen in radiograms. The articular capsule also participates in the inflammatory reaction; it becomes vascularized, fibrosed and redundant in the same fashion as the synovium. These capsular changes in association with regional fibrosis of regional muscles are respon-

Fig 8-864 Early rheumatoid arthritis in the 4th finger which began clinically during the 4th month of life. A: 20 months the soft tissues overlying the base and middle phalanges are swollen with a fusiform extension contour and these two phalanges are swollen externally by external thickening of the cortical

was B: at 30 months the soft tissues are more swollen as are the phalanges externally. Cortical thickening has now begun in the distal end of the 4th metatarsal. C: swelling of the 4th finger and in the hand at the distal end of the 4th metatarsal at 30 months (Courtesy of Dr. S. G. E. R. Kshospitale, Oslo, Norway)

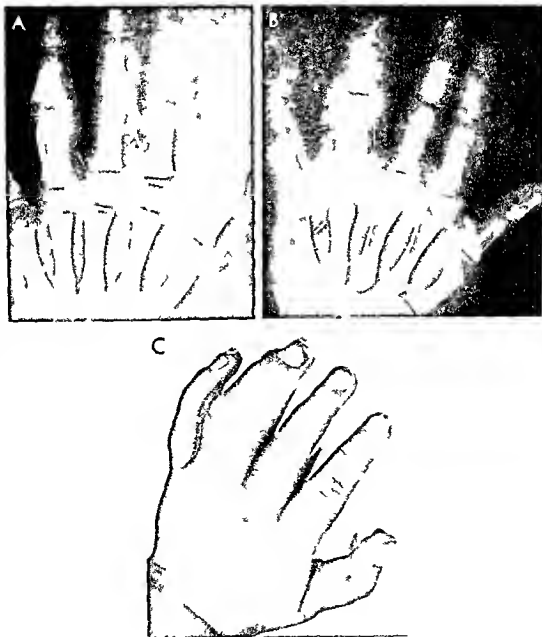




Fig. 8-865—Rheumatoid arthritis in the left knee of a girl 13 years of age, the knees in frontal and lateral projections. The swelling of the soft tissues at the left knee and atrophy of the muscles in the left thigh and shank are not visible in these films. The bones at the left knee are all diffusely rarefied, but there is no evidence of loss of articular cartilage or destruction of subchondral bone. The femoral and tibial epiphyseal ossification

centers and the patella on the left side are enlarged, owing presumably to the longstanding regional hyperemia induced by the chronic arthritis. Symmetrical series of transverse lines have formed in the femoral and tibial metaphyses on both sides. The spaces between the transverse lines are deeper on the affected side, which indicates accelerated growth on this side due to chronic hyperemia.



Fig. 6-866.—Early changes of rheumatoid arthritis at age 6 years. The cortical walls of four of the metacarpals are thickened externally before the appearance of diagnostic changes in the wrist.



sible for the late contractures. In some cases there are sufficient focal necroses in the muscles to produce focal calcifications near the affected joints. When extensive destruction of cartilage has occurred, fibrous and then bony adhesions develop between the ends of opposing bones in rigid permanent bony ankylosis from which there is no recovery.

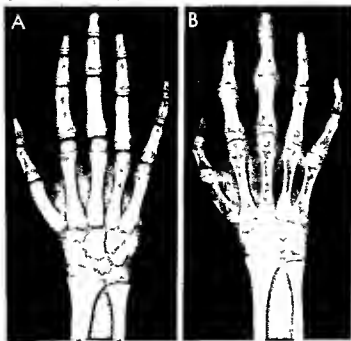
Radiographic findings depend on the stage of the disease in which the patient is examined. During the first weeks of the clinical manifestations, swellings of the articular and peritubular tissues are visible. A single joint may be affected first before polyarthritis develops. When rheumatoid arthritis appears in the joints of the fingers during the early years of life, diffuse soft tissue swelling of one finger and hypertrophy of the underlying phalanges may be the only findings for several months (Fig. 8-864). Regional rarefaction of the bones opposing at the affected joints, out of all proportion to the disease, is a common early sign. Intense local hyperemia and local overgrowth of the connective tissue in the underlying medullary cavities are believed to produce this disproportionate rarefaction. After a few months in younger children and before there is any destruction of cartilage, the local epiphyseal ossification centers enlarge and begin to differentiate too soon, thus accelerated maturation

of round bones, epiphyseal centers and sesamoids (Fig. 8-865) is also due to hyperemia. Another early change which has not been adequately emphasized, and which disappears early in the disease is the cortical thickening of the tubular bones near affected joints (Fig. 8-866); these changes are best developed in the tubular bones of the hands and are probably caused by an actual rheumatoid periostitis which lifts the bone forming layers of the periosteum off the external edge of the cortex.

During later phases the synovium thickens and grows over the face of the articular cartilages, then grows into the cartilages and then into the underlying bones to produce narrowing of the cartilage spaces and marginal irregular defects in the bones themselves (Figs. 8-867 to 8-871). At this time, the shafts have usually overconstricted to become slender tubes with narrow medullary cavities and flaring ends. At the elbows, we have seen substantial subchondral bone necrosis with the articular cartilages showed little evidence of destruction (Fig. 8-872). The focal necroses in the muscles near the joints sometimes calcify in sufficient size and degree to become visible radiographically (Fig. 8-873). The late residual shortening of the fingers of rheumatoid arthritis may simulate congenital hypoplasias (Fig. 8-874). The cervical

Fig. 8-867—Rheumatoid arthritis in a girl 6 years of age. A, 4 weeks after onset of vague pains when the radiographic findings are normal. B, 15 months later when all of the bony tissues are rarefied and the tubular bones are overconstricted. The latter is best seen in the flares at the ends of the radius and ulna with marked constriction just proximal to the flares. All of the fingers show fusiform swelling owing to the swelling of soft parts at the

interphalangeal joints. The most striking change is the loss of spaces between the carpal bones owing to destruction of the articular cartilages of the intercarpal joints and the carpal radial joint as well. The same loss of cartilage is evident at the carpometacarpal joints. Subchondral bone necrosis is beginning but is not clearly evident.



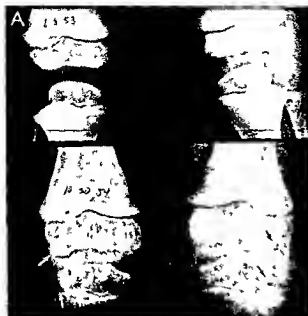


Fig 8-868—Subchondral necrosis of bone in rheumatoid arthritis. In A, in the upper part, before onset of rheumatoid arthritis the findings are normal. In the lower part, 18 months later and after onset of rheumatoid arthritis, much marginal bone is lost on the nonweight-bearing edges (lateral edges, arrows) in



the femoral and tibial ossification centers. In B, at the hip of a girl who had had rheumatoid arthritis for 7 years, there is marked loss of subchondral bone on the acetabular edge and the superior edge of the femoral ossification center. Also, bone is being destroyed in the femoral metaphysis (arrows).

Fig 8-869—Late destructive phases of rheumatoid arthritis of the hands. A, in a boy 6 years of age, generalized loss of the intercarpal cartilages which permits crowding together of the carpal bones, all of which are frayed with sclerotic edges and marginal defects due to subchondral bone necrosis. The latter is most conspicuous in the radial ossification center (arrow). Interphalangeal swelling of the periarticular and articular tissues have produced fusiform swelling of the 2nd and 3rd digits. The basal

phalanges of these two digits are enlarged from cortical thickenings which are completely fused with the shafts during this relatively late stage. B, 3 1/2 years after A, almost total destruction of articular cartilages has been followed by bony ankylosis of the carpal bones into a single bony mass, and with the metacarpal and carpal bones. The deep subchondral defects in the radial ossification center are now clearly visible.





Fig 8-870—Shallow cupping and splaying of the proximal end of the right tibial shaft with hypertrophy, uneven density and squaring of the epiphyseal ossification center in a 17-year-old



Fig 8-871—Severe rheumatoid arthritis of the left wrist of a girl 15 years of age, with extensive destruction and ankylosis of the carpometacarpal joints 2-5. The distal end of the radial shaft is deformed by a central narrow triangular depression into which the proximal edge of the enlarged epiphyseal ossification center has grown. The ends of the radius and ulna are tipped toward each other, slowing longitudinal growth in the medial segment of the radial carpal ligament and the lateral segment of the ulnar carpal plate.



age (B) which was normal when rheumatoid arthritis first became clinically evident at age 2 years (A) (Figs 8-870 and 8-871 courtesy of Dr. Fred E. Lee, Los Angeles)

spine may be the first part affected, and the late radiographic findings resemble congenital failures of segmentation (see Figs 9-69 and 9-70). Rheumatoid involvement of the temporomandibular joints often leads to severe hypoplasia and atrophy of the mandible.

Cassidy and colleagues observed rheumatoid arthritis that presented clinically as a disease in a single joint and remained monoarticular during the first four months of the illness in about 30% of their 40 patients. In 9 patients the disease remained monoarticular; in 21 the disease affected from two to four joints within the next four months to nine years, and in 10 it also became polyarticular. Bone erosion was a late radiographic manifestation. Uveitis was unexpectedly frequent, developing in 6 of the 40 patients.

In a review of juvenile rheumatoid arthritis, Calabro and Marchesano pointed to excellent functional recovery in four of five juvenile patients within 10 years of onset. They concluded that laboratory and radiographic studies are of limited diagnostic value because they lack specificity and vary greatly during different phases of the disease. In their patients, classic articular disease usually lasted more than 12 weeks in rheumatoid arthritis and less than 12 weeks in rheumatic fever. The radiologist should keep in mind that fever and pain in the joints may develop weeks, months, and years before significant structural changes are apparent in the joints.

Schlesinger and colleagues described a girl 6 years of age who suffered from rheumatoid arthritis and

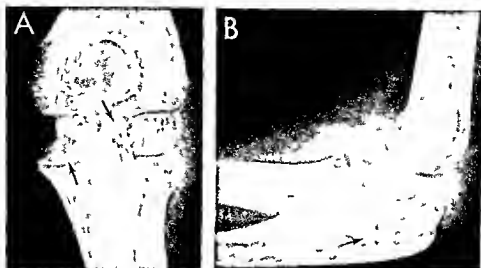


Fig 8 872.—Large subchondral defects in the juxta-articular edges of the olecranon processes (arrows) in a girl with chronic rheumatoid arthritis of the elbow

had large subcutaneous nodules in the scalp. In the underlying calvaria there were patches of diminished density. After the administration of corticosteroids the nodules as well as the radiolucent patches disappeared.

Seaman and Wells found destructive lesions in the spine in 11 of 100 patients with rheumatoid arthritis; their ages were not given. The outer ends of the clavicles were partially resorbed in 11 patients studied by Alpert and Meyers.

The great variety of rheumatoid lesions in bone, their distribution and their effects on bone growth were described and illustrated in detail by Martel and colleagues, especially the partial destruction and

sharpenings of the metacarpals in association with multiple carpal necrosis.

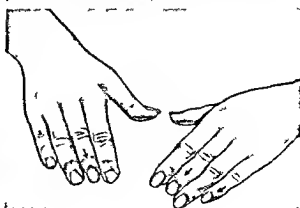
REFERENCES

- Alpert M and Meyers M. Osteolysis of the acromial ends of the clavicles in rheumatoid arthritis. *Am J Roentgenol* 86:251, 1961.
- Calabro J J and Marchesano J M. Juvenile rheumatoid arthritis. *New England J Med* 277:696 and 748, 1967.
- Cassidy J T et al. Mono-articular juvenile rheumatoid arthritis. *J Pediatr* 70:867, 1967.
- Hiltebrand H. Periostitis ossificans in rheumatic polyarthritis in children. *Fortschr geb Röntgenstrahlen* 88:68, 1957.
- Martel W et al. Roentgenographic manifestations of juvenile rheumatoid arthritis. *Am J Roentgenol* 88:400, 1962.
- Middlemiss J H. Juvenile rheumatoid arthritis (Still's disease). *Proc Royal Soc Med* 44:805, 1951.
- Schlesinger B E et al. Observations on the clinical course and treatment of 100 cases of Still's disease. *Arch Dis Childhood* 36:65, 1961.

Fig 8 873.—Rheumatoid arthritis of both hips with juxta-articular calcification in the soft tissues at the right hip (arrows) of a boy 9 1/2 years. The coxa valga is noteworthy; this lesion is common in rheumatoid arthritis of the pelvis and legs and is probably due to non-use.



Fig 8 874.—Shortening deformities of the fingers in adults secondary to the destructive rheumatoid arthritis of childhood. (Redrawn from Coss and Boos.)



Seaman W B and Wells J Destructive lesions of the vertebral bodies in rheumatoid disease. *Am J Roentgenol* 86:241 1961

Alkaptonuric arthritis develops in association with urinary excretion of homogentisic acid and ochronosis of certain tissues especially cartilage. This syndrome is apparently an inborn error of metabolism which is present at birth and continues until death. It should be suspected during infancy and childhood from blackish discoloration of the diapers and clothing. Homogentisic acid is an intermediate product in the metabolism of tyrosine and phenylalanine and is the result of incomplete oxidation of these amino acids.

Ochronosis and arthritis are rare before the third and fourth decades of life. Umber and Buerger have reported severe arthritis in four of eight alkaptonuric children whose father had alkaptonuria. The arthritis follows metabolic injury to the articular cartilages which become brittle and degenerate. Blackened cartilage fragments may become embedded in the underlying marrow spaces where they stimulate a fibrous reaction with destruction of the neighboring spongiosa. The principal radiologic findings are narrowing of the cartilage spaces and severe rarefaction of the bones. In adults the spine is usually affected conspicuously with generalized narrowing of the intervertebral spaces and massive calcification of the intervertebral disks.

REFERENCES

- Harrold A J Alkaptonuric arthritis. *J Bone & Joint Surg* 38-B:532 1956
 Sacks S Alkaptonuric arthritis. *J Bone & Joint Surg* 33-B:407 1951
 Umber F and Buerger M Alkaptonurie mit Ochronose und Osteoarthritis deformans. *Zystinurie Deutsche med Wchnschr* 39:2337 1913

Fig. 8-875—Tumoral calcinosis. A, lobulated mass of calcium density behind the elbow of a black boy 4 years of age. B, lobulated mass of calcium density below the right hip and around the

CALCIFICATION OF CARTILAGE AND JOINTS

Painful joints associated with calcification of the articular cartilages have been described in several adults. Lime is laid down in a thin plate on the joint side of the articular cartilage with a radiolucent zone between it and the underlying bone. This interesting condition has not been reported in children.

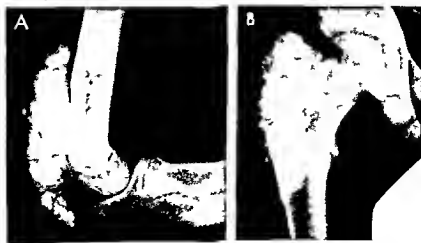
REFERENCE

- Bunje H and Cole W R Calcification of articular cartilage. Report of a case. *J Bone & Joint Surg* 38-B:874 1956

Juvenile gout is exceedingly rare. Pain and swelling of the joints first began at 5½ years of age in a patient of Middlemiss and Broband when radiographic findings were normal. At 9 years, however, the cartilage spaces at the affected joints were reduced. These authors pointed out that the diagnosis of juvenile gout should be made from the chemical findings—high levels of uric acid in the plasma or microscopic demonstration of sodium urate crystals in the skin—which are specific—rather than from the radiographic changes in the joints which are nonspecific.

Congenital hyperuricosuria (Lesch-Nyhan syndrome) develops in male infants only. They are normal at birth. After the first few months of life, however, their motor development becomes retarded; the extremities become spastic and sometimes athetoid movements appear. Mental development slows down and almost ceases. During the 2nd and 3rd years characteristic mutilations of the lips and fingers from chewing and biting present a diagnostic clinical picture. Uric acid crystals may be evident in the diapers after the first weeks of life. Stature and maturation

greater than that of a black boy 15 years of age. (From Harkness and Peters.)



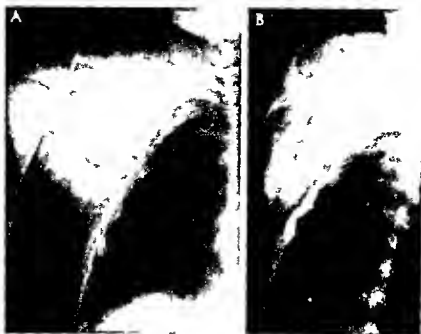


Fig 8-876—Leomyoma (microscopic diagnosis) of the right subacromial region with extensive calcification (tumoral calcinosis?). This boy 3 years of age had had progressive swelling in

the subacromial region for several weeks. The acromion was displaced laterally and dorsally by the displacement by a large calcified mass as shown in both A, frontal and B, lateral projections.

are both reduced. Convulsions develop later and hematuria may be induced by uric acid stones in the urinary tract. Most patients die of pneumonia before age 7. In older children, changes typical of gout may appear. The diagnosis depends on the demonstration of excessive uric acid in the plasma and urine. The defects in the fingers due to self-mutilation can be seen radiographically as well as delayed maturation and growth in the skeleton, subluxation at the hip and calculi in the urinary tracts. Pneumoencephalograms have shown slight cerebral abnormalities or normal findings.

REFERENCES

- Becker M H and Wallin J K. Congenital hyperuricosuria. Associated radiological features. *Radiol Clin North America* 6:239 1968.
 Lesch M and Nyhan W L. A familial disorder of uric acid metabolism and the central nervous system function. *Am J Med* 36:561 1964.
 Middlemiss J H and Broband H. Juvenile gout. *Clin Radiol* 13:149 1962.

Tumoral calcinosis (peribursal idiopathic calcification) occurs in otherwise healthy older children and young adults without associated calcification in other tissues. All but one of the patients described in the Anglo-American literature have been blacks. Painless periarthral swellings are the sole clinical manifestations. Laboratory findings are characteristically normal. The periarthral swellings cast radiographic images with lobulated patterns of calcium density (Figs 8-875 and 8-876) which are diagnostic

in themselves. Large calciferous tumors have not been reported at the knees. According to Harkness and Peters, the swellings are limited by fibroelastic capsules from which fibroelastic septa extend centrad, the spaces between the mesh of the septa are filled with fine and coarse calcium granules. There is no cartilaginous metaplasia, but osseous metaplasia was found in one tumor. Necrosis, inflammation and hemosiderosis have not been found. These authors believe that tumor calcinosis is not a neoplasm but hypertrophic proliferation similar to the keloid tumor. There is no intratrenal calcification. Recurrences are common following surgical excision and new foci of calcinosis have been induced by surgical trauma. Profound cachexia has followed infection and the development of sinus tracts. Najjar and associates reported tumoral calcinosis in association with pseudoxanthoma elasticum in a white boy 9 years of age. Viskulety and Aszodi recorded elevated serum phosphorus in a boy 8 years of age. Baldursson and colleagues found hyperphosphatemia in four siblings

REFERENCES

- Baldursson H et al. Tumoral calcinosis with hyperphosphatemia. A report of a family with incidence in four siblings. *J Bone & Joint Surg* 51-A:913 1969.
 Harkness J W and Peters H J. Tumoral calcinosis. A report of six cases. *J Bone & Joint Surg* 49-A:721 1967.
 Najjar S S et al. Tumoral calcinosis and pseudoxanthoma elasticum. *J Pediatr* 72:243 1968.
 Viskulety T and Aszodi K. Bilateral calcareous bursitis at the elbow. *J Bone & Joint Surg* 50-B:644 1968.



Fig 8 877 (left) Cyst of the lateral meniscus of the knee (Redrawn from Lewis)



Fig 8 878 (right) Cyst of the infrapatellar fat pad of the knee (Redrawn from Lewis)

INTERMITTENT HYDRARTHROSIS

In children painless symmetrical swellings of the joints commonly the knees develop and persist for varying periods. Roentgenographically hydrarthrosis shows as a local swelling of water density which has no differential diagnostic features. Syphilis (Clutton's joints) is one cause of painless hydrarthrosis. Allergy appears to play a causal role in many cases, especially when the swellings are transitory. Unrecognized trauma and mild infections may also be causal agents. There are no associated changes in the adjacent bones.

CYSTS AND NEOPLASMS

Primary tumors of the articular structures are exceedingly rare in children. In adults, synoviomias and

synovial sarcomas form tumor masses in and near the joints and cast shadows of water density. Lewis pointed out the frequency of scattered foci of calcium density in synoviomias.

Cysts of the articular and perarticular structures cast shadows of water density which ordinarily are poorly visualized because their shadows blend with surrounding soft tissues. At the knee, however, where fat pads provide adequate contrast density, some cysts can be clearly demonstrated and accurately localized (Figs 8-877 and 8-878).

REFERENCES

- Lewis R W. The roentgen recognition of synoviomias. *Am J Roentgenol* 44:170, 1940.
- . Roentgenographic soft tissue study in an orthopedic hospital. *Am J Roentgenol* 48:634, 1942.
- Swein E. Arthrograms of the hip joints in children. *Surg Gynec & Obst* 72:601, 1941.

SECTION 9

The Vertebral Column

Normal Vertebral Column

THE CERVICAL AND sacrococcygeal portions of the spine are considered in the discussions of the neck (in Section 1) and pelvis (Section 5). The thoracolumbar spine is considered here.

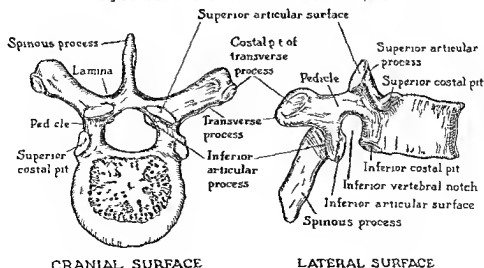
Anatomy

The vertebrae which together with the intervertebral disks constitute the spinal column, may be regarded from the developmental point of view as short tubular bones. Normally there are 12 thoracic and 5 lumbar vertebrae.

Each thoracic vertebra is composed of an anterior mass or body and a posterior ring or arch. Several appendages project from the arch: the paired transverse processes, the paired superior and inferior articular processes, and the single spinous process (Fig 9-1). In the lumbar spine there is a pair of additional small processes, the mammillary tubercles, which project posteriorly from the summits of the superior articular processes.

The spongiosa of the vertebral bodies, a delicate wide meshed reticulum, is surrounded by a thin cylindrical wall of compact bone (Fig 9-2). Amstutz and Sissons demonstrated that the vertebral spongiosa consists of a complex network of bony plates perforated by round openings of varying size. These plates were oriented preferentially in the vertical and horizontal planes, and the amount of spongiosa was greatest near the upper and lower edges of the vertebral bodies and least in their central segments. Their study was made on the third lumbar body of a young woman who died following head injuries. The upper and lower surfaces of the body are not limited by a true closing plate of compact bone as is the case at the ends of the tubular bones in the extremities. At these vertebral surfaces the trabeculae of the spongiosa are concentrated transversely into a profusely perforated plate. The perforations afford direct contact of the marrow spaces with the articular plates and permit the direct transfer of fluids from the vertebral body into the contiguous intervertebral disks.

Fig 9-1—Normal thoracic vertebra: cranial and lateral aspects



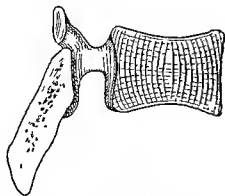


Fig 9-2.—Schematic representation of the pattern of the spongiosa in a thoracic vertebral body. The transverse trabeculae are curved and their shallow convexities are directed toward the center of the body. In the curved longitudinal trabeculae their convexities are directed toward the surface of the vertebral body.

thus serving as channels through which the disk is nourished and at times infected from the body. The neural arch and its appendages are covered with a layer of compact bone which is much thicker and stronger than the thin cortex in the cylindrical wall of the vertebral body.

Each intervertebral disk contains three components: the paired cartilaginous articular plates, the fibrous ring or annulus fibrosus, and the nucleus pulposus (Fig 9-3). In the growing spine the paired cartilaginous articular plates are merely central superficial portions of the underlying cartilaginous mass of the vertebral body and are directly continuous with them. In the adult spine the articular plate is composed of ordinary hyaline cartilage and lies between the end surface of the bony vertebral body and the annulus fibrosus. The cartilage plate does not extend peripherally to the outer margins of the disk but merges with the fibers of the annulus which completely fill the outermost zone of the intervertebral space. The annulus fibrosus is a homologue of the fibrous capsule of the freely movable joints in the extremities; it is made up of a series of connective tissue lamellae which run from one vertebral surface to the adjacent vertebral surface in wide curves. Compressed in the central portion of the disk and surrounded by the annulus is a highly elastic fluid fibrous mass, the nucleus pulposus, which plays an outstanding role in many vertebral diseases. The nuclei pulposi are segmental intervertebral remnants of the fetal notochord.

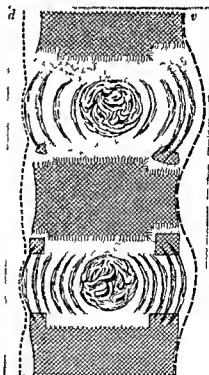
One of the most important features of the spine from a radiologic standpoint is the size of the interpediculate spaces. This space in each vertebra is measured from the inner edge of one pedicle to its counterpart in the opposite pedicle and represents the greatest internal distance between companion pedicles. The interpediculate space is increased at the

sites of spina bifida, diastematomyelia and expanding intraspinal tumors.

Growth and Development

Following the early mesenchymal stage in which the sclerotomes grow and segment into primitive connective tissue vertebrae and intervertebral disks, centers of chondrification begin to appear in the connective tissue vertebrae at approximately the seventh fetal week. Two cartilaginous centers develop in each vertebral body and one appears on each side of the incomplete vertebral arch. These four primary centers grow and fuse into a single cartilaginous vertebra. Failure of development or hypoplasia of one of

Fig 9-3.—Schematic drawing of sagittal section of the spine. Phases in progressive ossification and fusion of the vertebral rings. In the under edge of the uppermost vertebral body the vertebral ring in the peripheral notch is made up entirely of cartilage which is stippled. In the upper edge of the middle vertebral body an ossification center (cross hatched) is present in the vertebral ring front and back. In the under edge of the same body this ossification center is larger and occupies more of the cartilaginous ring. In the upper edge of the lowermost vertebral body the ossification center occupies all of the notch and has fused with the main mass of the vertebral body. In all phases of its development the vertebral ring is deeply penetrated by Sharpey's fibers. The growth and ossification of the vertebral ring appears to contribute little or nothing to the growth of the vertebral body. The anterior longitudinal ligament (heavy broken line) is attached to the vertebral bodies but skips attachment to the intervertebral disks; the converse is true for the posterior longitudinal ligament & dorsal edge & ventral edge. (From Schmorl and Junghans.)



the two chondrification centers in the vertebral body is thought to be the principal cause of hemivertebra. The open vertebral arch continues to grow posteriorly around the spinal cord until after the second fetal month, when the two sides of the cartilaginous arch unite and enclose the cord completely. The transverse, articular and spinous processes grow from edges of the arch.

Tager offered a sign of fetal death based on ventro-dorsal films of the gravid uterus with the patient recumbent and then erect. In the case of fetal death, the fetal spine collapses, with deepening of the curvature in the lumbosacral segments and sharp angulation of the neck on the thorax. The loss of normal spinal course in the dead fetus is due to loss of tone in the dead fetal muscles.

It should be emphasized that the best evidence indicates that the vertebral body grows in length exclusively from the proliferating cartilage plates at the cephalic and caudal ends, just as a long bone grows in length. The vertebral ring cartilage, long misnamed a ring epiphyseal cartilage, is outside the zone of growth and endochondral bone formation.

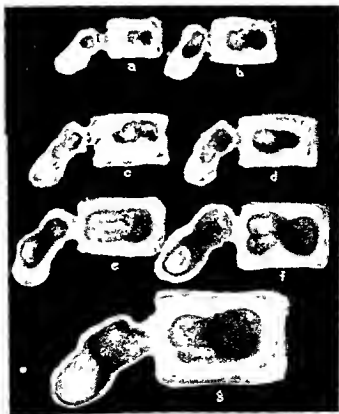
The longitudinal growth of each vertebral body and the total composite longitudinal growth of the whole spine are modified by the stress of weight bearing.

Gooding and Neuhauser demonstrated longitudinal overgrowth and transverse undergrowth of the vertebral bodies of growing children whose spines had never been subjected to the stresses of gravity and weight bearing because of neuromuscular weakness and paralysis. In the lumbar levels, where the normal stress of weight bearing is greatest, excessive longitudinal growth and transverse hypoplasia of the vertebral bodies were maximal. Their paper contains an excellent brief review of the origin, growth and development of normal vertebrae.

PRIMARY OSSIFICATION CENTERS

Ossification centers first make their appearance in the cartilaginous vertebrae at about the tenth fetal week. There are three primary centers: a single osseous nucleus in the body and two nuclei in the arch, one of which is in each pedicle. These primary ossification centers continue to extend into the cartilaginous vertebra during embryonic life but are still separated from one another by cartilaginous ridges at birth (Fig 9-4). The marginal growth zones of the proliferative cartilage in the body are located on the surfaces of the ossification center where they merge with the cartilaginous portions of the body. As growth

Fig 9-4 — Primary vertebral ossification centers from the 6th fetal week (a) to the neonatal period (g). (From Hitchcock's drawings of cleared specimens.)



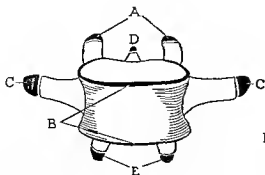
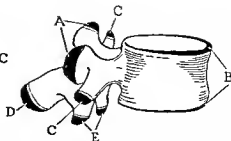


Fig 9-5—The secondary vertebral ossification centers *A* superior articular processes *C* transverse processes *D* spinous processes *E* inferior articular processes. These all appear at approximately 16 years and fuse with their respective processes



at approximately 25 years *B* the annular ossification centers these appear as early as the 7th year in females and fuse with the main mass of the body at approximately 25 years

proceeds cephalad and caudad the amount of bone increases and the amount of cartilage diminishes correspondingly until about the 16th year when growth is practically complete. At this time only the central portions of the upper and lower surface cartilage persist as the cartilaginous articular plates. The fusion of the ossification center in the body with the center in each side of the arch takes place at the neurocentral sutures between the 3rd and the 6th year. The two bony centers in the arch extend posteriorly toward the midline and complete the bony neural arch during the first two postnatal years.

SECONDARY OSSIFICATION CENTERS

Secondary ossification centers begin to appear in the annular cartilages shortly before puberty in females (Fig 9-5), in males they develop somewhat later. We have seen substantial segmental calcification of the annular cartilages in normal girls 7 years of age. Among 20 children aged 2-6 years lateral radiographs of the chest and abdomen taken for a variety of unstated clinical reasons Hindman and Poole found fine calciferous foci in the annular cartilages of 9 aged 2 and 3 years and of 11 who were 4-6 years of age. The bone ages were normal or advanced in all of these children. In the single illustration fine calciferous short strips of calcium density are visible in both superior and inferior annular cartilages of the vertebral bodies. Normally the secondary centers fuse with the vertebral body 5-10 years after their first appearance. Occasionally the secondary centers in the arch persist as separate ossicles and in case of injury may be mistaken in films for fracture fragments.

The postnatal longitudinal growth of the spine is due exclusively to the proliferation of cartilage on the upper and lower zones of the primary ossification center in the vertebral body according to Beadle there is no growth and no trace of endochondral bone formation in the annular cartilages. This ring of carti-

lage often mis-called an epiphysis ossifies independently of the primary center which constitutes the body of the vertebra and bears no direct relation to its longitudinal growth and contributes nothing to its endochondral bone formation. It merely fuses with the body when growth of the body is complete.

The principal change in the intervertebral disk during growth is the reduction of its fluid content particularly in the nucleus pulposus which at birth is a mass of mucoid gelatinous fluid dispersed through a widely meshed reticulum of mesenchymal cells derived from the notochord. With increasing age the annulus fibrosus expands centrally into the margins of the cartilaginous plates which at the same time are contracting peripherally. Physiologic calcification of the annulus and more rarely of the nucleus pulposus has been observed not infrequently in middle-aged and elderly persons but is rare in young adults and children and has not been reported in infants.

At birth the average length of the spine without the sacrum is 20 cm. during the first two years growth is rapid and the length increases to about 45 cm. The velocity of growth is greatly diminished thereafter, at puberty the longitudinal axis measures about 50 cm. The final adult length of 60-75 cm is attained between the 22nd and the 24th year. There is a significant change in the relative length of the cervical and lumbar portions during growth. At birth the cervical spine makes up one-quarter of the total length of the spinal column, the thoracic spine one-half and the lumbar spine one-quarter. In the adult the cervical spine is reduced to one-fifth or one-sixth of the total length while the lumbar segment is increased until it comprises nearly one-third of the whole (Scammon). The apparent shortness of the neck in infants is due to the fulness of the cervical soft tissues, the cervical spine is proportionately longer during infancy than in later age periods. The normal curves of the spine do not become fixed until after puberty. At birth the vertebral column forms a single long shallow curve extending from the first cervical to the fifth lumbar

segments with its concavity directed anteriorly. The cervical curve appears shortly after the head is held up during the 1st year. The lumbar curve develops when erect posture is assumed at about the beginning of the 2nd year and gradually becomes more prominent during the years of childhood.

Röntgen Appearance

The bony vertebrae cast opaque shadows of calcium density in contrast with the interposed radiolucent strips of water density cast by the intervertebral soft tissues. The spinal canal is filled with soft tissues of water density. During infancy and childhood all of the cartilaginous portions of the incompletely mineralized growing vertebrae cast shadows of water density. The intervertebral spaces appear proportionately thicker and the vertebral bodies smaller during early life owing to the radiolucent cartilage zones in the upper and lower surfaces of the vertebral body. These merge with the radiolucent shadow of the intervertebral disk and augment its width above and below. The individual components of the intervertebral disk—the paired cartilaginous articular plates, the annulus fibrosus and the nucleus pulposus—all cast shadows of water density and cannot be distinguished from one another or from the surrounding soft tissues.

Fig 9-6—The normal roentgen appearance at birth of a roentgenogram. The anterior and posterior notch shadows (arrows) in the vertebral body are noteworthy. The cartilaginous neurocentral synchondroses (arrows) between the body and the arch cast shadows of water density.



Fig 9-7—A, the neurocentral synchondroses (arrows) of the lumbar and sacral vertebrae in oblique projection. The infant was asymptomatic and 13 months of age. These longitudinal radiolucent strips and lines in older infants sometimes simulate fracture lines. B, the neurocentral synchondroses (arrows) of the upper sacral segments in frontal projection. This infant was asymptomatic and 12 months of age.

Owing to the complexity of the symmetrical neural arch with the paired processes projecting from it in three different planes, all portions of even a single vertebra cannot be satisfactorily visualized in a single projection because of superimposed shadows of the different vertebral components. Frontal, lateral and often oblique projections are essential for complete visualization. In detailed studies, stereoscopic films of the four surfaces should be made (anterior, posterior and both lateral projections) and in special cases planigrams are of great help. The vertebral bodies can be most clearly visualized in full lateral projections in which there is no superimposition of the vertebral arches on the bodies.

The vertebrae present widely different normal roentgen images at different ages. In the first weeks of life, the three opaque primary ossification centers are still separated by radiolucent cartilaginous bridges (Fig 9-6). The radiolucent neurocentral synchondroses persist as longitudinal bands and in older children as lines of diminished density at the junctions of the body and the two sides of the neural arch until the 3rd to 6th years. In oblique projections (Fig 9-7), especially they are easily mistaken for fractures. They disappear last in the lower lumbar and upper sacral levels. In a single vertebra, one neurocentral synchondrosis may remain open for months after its counterpart on the other side has closed. The opaque ossification center in the vertebral body tends to be oval. The intervertebral space is a thick biconcave radiolucent strip. In lateral projections the vertebral bodies exhibit paired notched shadow defects in the middle third of the anterior and posterior walls.

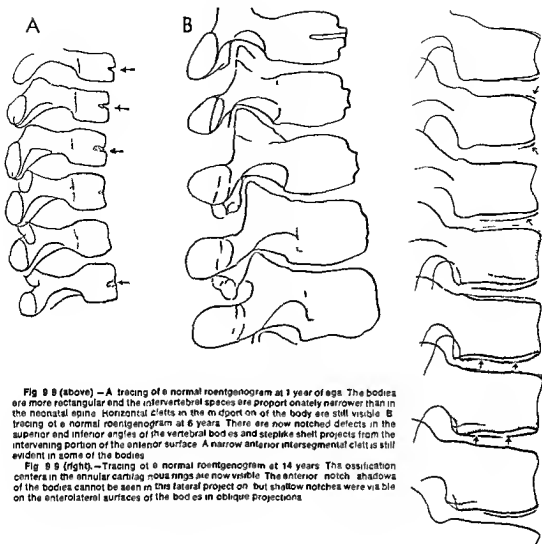


Fig 9.8 (above)—A tracing of a normal roentgenogram at 1 year of age. The bodies are more rectangular and the intervertebral spaces are proportionately narrower than in the neonatal spine. Horizontal clefts in the midportion of the body are still visible. **B** tracing of a normal roentgenogram at 6 years. There are now notched defects in the superior and inferior angles of the vertebral bodies and step-like shelf projects from the intervening portion of the anterior surface. A narrow anterior intersegmental cleft is still evident in some of the bodies.

Fig 9.8 (right)—Tracing of a normal roentgenogram at 14 years. The ossification centers in the annular cartilaginous rings are now visible. The anterior notch shadows of the bodies cannot be seen in this lateral projection, but shallow notches were visible on the anterolateral surfaces of the bodies in oblique projections.

The notches are cone shaped and resemble a pair of horizontal V's with their apexes directed toward the center of the body. Wagoner and Pendergrass showed in anatomic specimens that the radiolucent anterior notch shadow is cast by a large sinusoidal blood space within the ossification center. The posterior notch shadow, in contrast, is generated by an actual perforated indentation on the posterior wall of the body through which the posterior vertebral veins emerge and the posterior nutrient arteries enter. This posterior indentation persists throughout life but is not clearly seen in roentgen films because in lateral projections the shadows of the lateral masses are superimposed.

With advancing age the primary centers fuse; the bodies become proportionately larger and the intervertebral spaces proportionately narrower. The body

also loses its oval shape and becomes more rectangular. The anterior vascular notch shadow develops into a deep narrow horizontal radiolucent strip in the middle third of the body (Fig 9.8). This strip shadow is cast by the channels of the paired anterolateral vessels; it persists longest in the lower thoracic segments, where it usually disappears late in childhood but may persist into adult life in some cases. Throughout late childhood notched rectangular radiolucent defects are visible in the upper and lower anterior angles of the body; these are cast by the thick furrowed cartilaginous rims of the annular vertebral rings.

Secondary ossification centers develop in the annular cartilaginous rings as early as the 7th year in females. In one girl 2½ years of age and otherwise normal in all respects, we found ossification centers

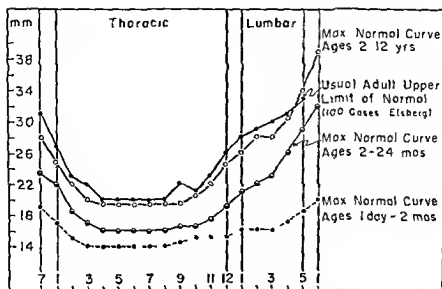


Fig 9-10—Composite graph of the normal maximal interpediculate distances for all ages (From Smith and Thurston)

in some of the rings. They appear first as multiple small opaque foci on the rims of the bodies (Fig 9-9). The small foci later fuse into solid calcareous disks; the paired upper and lower bony epiphyseal disks in turn fuse with the main mass of the body after the 20th year.

The normal values for the interpediculate spaces at different levels in the thoracic and lumbar levels of the spine at different ages are shown in Figure 9-10.

Howorth and Keillor attempted to simplify measurements of the spinal canal at all levels by the use of tracings of normal spines on transparencies which can be superimposed on the radiograph in question for direct comparison. In the belief that the usual standards for evaluating the size of the cervical spine are of little value, Hinck and his co-workers presented data for normal measurements in persons 3-18 years of age.

REFERENCES

- Amstutz H C and Sissons H A. The structure of the vertebral spongiosa. *J Bone & Joint Surg* 51 B 540 1969.
- Bailey D K. The normal cervical spine of infants and children. *Radiology* 59 212 1952.
- Bailey W. Persistent vertebral process epiphyses. *Am J Roentgenol* 42 85 1939.
- Beadle O A. The Intervertebral Discs. Special Report Series no 161. Medical Research Council (London: His Majesty's Stationery Office 1931).
- Ferguson W R. Some observations on the circulation in fetal and infant spines. *J Bone & Joint Surg* 32 A 640 1950.
- Gooding C A and Neuhauser E D B. Growth and development of the normal vertebral body in the presence and the absence of stress. *Am J Roentgenol* 93 388 1965.
- Hinck V C et al. Sagittal diameter of the cervical canal in children. *Radiology* 79 97 1962.
- Hindman B W and Poole C A. Early appearance of secondary vertebral ossification centers. *Radiology* 95 359 1970.
- Howorth J B and Keillor G W. Use of transparencies in evaluating the width of the spinal canal in infants, children and adults. *Radiology* 79 109 1962.
- Keegan J J. Alterations of the lumbar curve related to posture and seating. *J Bone & Joint Surg* 35-A 640 1953.
- Meschan I and Farber Meschan R M F. Important aspects in the roentgen study of the normal spine. *Radiology* 70 637 1958.
- Rowe C R and Roche M B. The lumbar neural arch. Roentgenographic study of ossification. *J Bone & Joint Surg* 32-A 554 1950.
- Smith W A and Thurston D. Normal interpediculate space in the spines of infants and children. *Radiology* 64 340 1955.
- Tager S N. A new roentgen sign of fetal death. *Am J Roentgenol* 67 106 1952.

Congenital Disturbances

Malformations

VARIATIONS IN THE NUMBER of the 5 lumbar and 12 thoracic vertebrae are due to oversegmentation and undersegmentation of the mesenchymal provertebrae early in fetal life. The supernumerary vertebrae may

be normal or deformed. Undersegmentation may affect two or more segments. The fusion may be complete or may be limited to portions of the arches or bodies. Errors in the number of thoracic segments are often compensated for by a reverse error in the number of lumbar segments so that the total number of

Fig 9-11—The different congenital malformations associated with congenital scoliosis. **A** hypoplasia of the vertebral body (partially wedged vertebra); **B** hemivertebra (single); **C** hemivertebra (double unbalanced); **D** hemivertebra (double balanced); **E** symmetrical failure of segmentation of bodies; **F** asymmetrical failure of segmentation (unsegmented); **G** asymmetrical failure of segmentation of the posterior elements only—the neural arch

es (unsegmented bar in anteroposterior view). **H** lateral projection of **G** showing that the bodies are normal but segmented and that fusion is limited to the posterior elements. This type is easy to separate surgically. **I** failure of segmentation of neural arches and the bodies. **J** multiple unsegmented bodies and neural arches. (From Winter et al.)

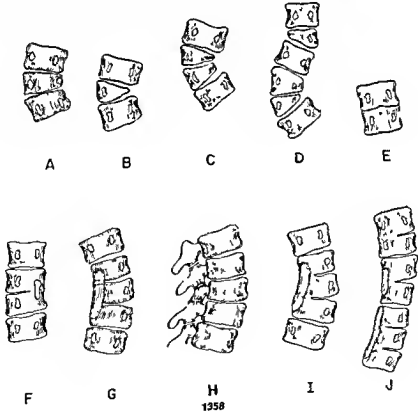




Fig 9-12 Congenital scoliosis with right-sided longitudinal bar due to failure of segmentation of the neural arches. A at 2

years when the curve was measured 54°. B at 14 years when the curvature had increased to 105°. (From MacEwan et al.)

thoracolumbar segments is unchanged. Reverse variation in number of sacral segments may also compensate for errors in number of lumbar segments.

Congenital scoliosis is caused by a variety of congenital malformations of the spine (Fig 9-11). Progressive increase in the curvature is common, especially in those caused by unsegmented bars due to asymmetrical failure of segmentation of the arches of two or more contiguous vertebral segments (Fig 9-12). Associated malformations have been found in the head and neck, thorax, abdomen, and genitourinary tract, and a variety of anomalies in the extremities. Once a curve begins to progress, it continues to do so until growth is complete. Death is rare during childhood.

Structural idiopathic infantile scoliosis in contrast recovers completely without treatment in more than 90% of cases. Faulty fetal position and intrauterine molding are believed to be the major causes. The clinical diagnosis is based on the presence of a lateral curve in the thoracic spine which does not disappear on suspension of the infant. The ribs are prominent dorsally on the convex side of the curve but are depressed on its concave side. Rotation of the head toward the convex side is limited. Head molding (plagiocephaly) is also common. Anteroposterior films with the baby in suspension disclose a lateral curve comparable to the one seen clinically. Rigidity of the curve can be demonstrated in films made during

bending of the spine. In 100 cases diagnosed by Lloyd Roberts and Pilcher, age at onset varied from birth to the 10th month.

In rheumatoid arthritis of the spine, the cartilage spaces at the articulations may be completely destroyed; these acquired lesions simulate congenital fusion of the vertebral segments, especially in the cervical portion (see Figs 9-69 and 9-70).

Variations in form are common. Many of the defects in the arches should be considered anatomic variants rather than malformations because they are found in so many healthy infants and children. This is especially true of laminar defects in the inferior lumbar levels.

Defects in the body may be due to undergrowth of one or both of the fetal chondrification centers (Figs 9-13 and 9-14). Occasionally the entire body may be absent when the arch is well developed. The asymmetrical undergrowth of one of the paired fetal chondrification centers in the body gives rise to hemivertebra, a common and sometimes disabling malformation (Figs 9-15 and 9-16). One or many spinal segments may be affected in the case of thoracic hemivertebra, errors in segmentation of the ribs are almost invariably associated. Congenital hypoplasia of one lung is often accompanied by hemivertebra (see Fig 2-121). Multiple hemivertebrae which affect the spine at many levels may cause marked dwarfism owing to shortening of the trunk when the extremities are

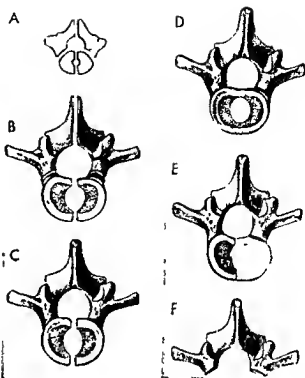
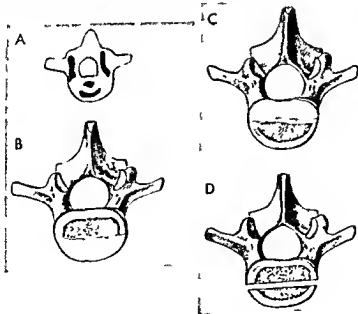


Fig 9-13 —Developmental errors in the vertebral segments in the chondrification stage. A, normal pattern during early chondrification stage. B, persistence of early midsagittal cleft. C, persistence of midsagittal cleft in the body only. D, persistence of chordal canal in the vertebral body. E, lateral hemivertebra only due to agenesis and hypoplasia of the right half of the chondrification center in the body. F, epistrophe of the vertebral body due to failure of growth of both early prevertebral masses (Figs 9-13 and 9-14 from Koehler and Zimmer).

Fig 9-14 —Malformations secondary to developmental errors during the ossification stage. A, early normal ossification centers in contrast to the two early chondrification centers in the body which are lateral to each other. These ossification centers

in the body are ventrodorsal to each other. B, dorsal transverse hemivertebra. C, ventral transverse hemivertebra. D, transverse fissure between the two tandem ossification centers of the vertebral body—coronal cleft in the vertebral body.



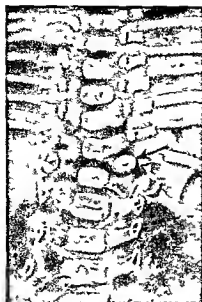


Fig 9 15 (left) — Combined hemivertebra and spine bifida in a newborn infant. The neural arches are widely open and spread apart from the upper thoracic through the lumbar levels. At the T 11 segment there is a hemivertebra deformity (arrow)

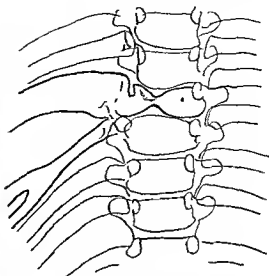


Fig 9 16 (right) — Single hemivertebra of the T 7 segment with associated errors in segmentation of the sixth, seventh and eighth left ribs of a boy 6 years of age. tracing of a roentgenogram

Fig 9 17 — Familial dwarfism in siblings due to multiple hemivertebrae. A brother and sister 10 and 8 years of age show short neck, thorax, abdomen and pelvis in contrast to normal length of the extremities. Roentgen examination revealed multiple hemivertebrae (Figs 9 18 and 9 19) at practically all levels in the spines of both children. Otherwise the skeletons were normal. The dis-

proportion in this type of dwarfism is similar to that in Morquio's disease, in which the spine is shortened owing to universal vertebral plana. In achondroplasia the extremities are short and the trunk is disproportionately long. The converse of the disproportions with multiple hemivertebrae

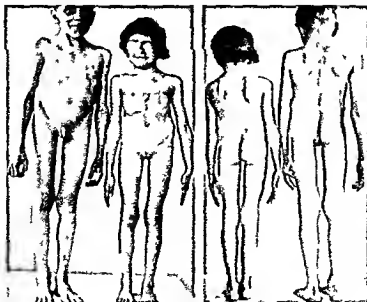




Fig 9-18 (left) — Multiple hemivertebrae in the boy shown in Figure 9-17. A, in the cervical and superior thoracic segments. B, in the inferior thoracic and lumbosacral levels. The deformed vertebral bodies occupy practically the entire spine. The errors in segmentation of the ribs are noteworthy. The other bones were a normal roentgenographically.



Fig 9-19 (right) — Multiple hemivertebrae, scoliosis and costal deformities in the dwarfed girl shown in Figure 9-17. The hemivertebra deformities are similar but not identical with those of her brother (Fig 9-18). Her other bones were a normal roentgenographically.

normally long. We have observed two such dwarfed children who were siblings (Figs 9-17 to 9-19). Multiple hemivertebrae were found by Van de Sar in a mother and her 2-year-old daughter; two other siblings were normal. We have seen multiple hemivertebrae in sibling fetuses who died soon after birth; it is possible that many of the cases of multiple hemivertebrae are never detected because the fetus dies before birth and the spine is not adequately examined. In one of our cases the multiple hemivertebrae were clearly visible in films made of the pregnant uterus several weeks before birth. Multiple hemivertebrae and short spine may be components of a syndrome which also includes alopecia of the scalp, follicular atrophy of the skin and unilateral shortening of the extremities. A great variety of defects in the vertebral body may be due to persistence of remnants of the fetal notochord in the vertebral body (Fig 9-20). When this remnant is centrally placed and extends the entire length of the vertebral body, a characteristic butterfly appearance may be visible in frontal projections (Fig 9-21).

Coronal cleft vertebral bodies were demonstrated anatomically and radiographically by Schinz and Tondury. Their study of the early fetal ossification of the vertebral body showed that the coronal cleft is merely the normal mass of cartilage between the ventral and dorsal ossification centers which have not yet fused. It is probable that the coronal clefts in the lumbar bodies in Figure 9-20 are produced by the double-center mechanism rather than notochordal remnants. Either of these mechanisms is possible. In one of the cases of Wollin and Elliot, the coronal cleft represented persistence of notochord (an axial rod of notochord) and in another case the coronal clefts were filled with cartilage. It seems likely that persistence of the notochord interferes with earlier normal fusion of the paired vertebral ossification centers. Cohen and co-workers confirmed the findings of Schinz and Tondury in three cases; microscopically their roentgen material indicated that coronal clefts are more common in association with other anomalies, especially chondrodystrophia calcificans congenita (see Fig 8-321) than in otherwise normal skeletons.

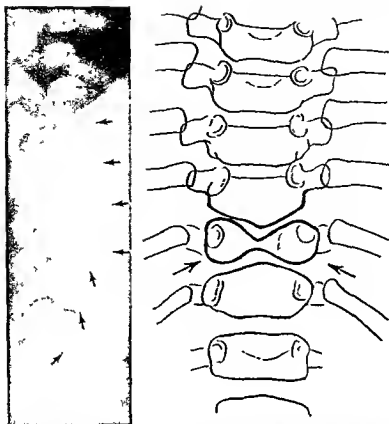


Fig 9-20 (left) - Defects in vertebral bodies at L 3, L 4 and L 5 (vertical arrows) of asymptomatic newly born infant which may be due to persistence of notochordal remnants. The defects in the ventral edges of the vertebral bodies (horizontal arrows) are cast by the normal vascular canals. The longitudinal strips of water density which separate each neural arch from its body are the normal bars of cartilage in the neurocentral synchondroses. The notochordal remnant was not proved anatomically and the

defects may well be coronal clefts between ventral and dorsal ossification centers which are delayed in fusing.

Fig 9-21 (right) - Butterfly deformity of the vertebral body due to persistence of a remnant of the fetal notochord in the vertebral body in a patient 13 months of age. There are no associated errors in segmentation of the ribs which are almost invariably present in hemivertebrae. Diagnosis was not proved anatomically.

etions One or several vertebral bodies may be affected, most commonly in the lumbar spine. Ordinarily the clefts disappear during the first weeks of life, they predominate in males in the ratio of about 10:1. Stewart and McKenzie pointed out the value of the cleft in predicting the male sex of a fetus when the clefts are visible in films of the gravid uterus. In our most severe example of this benign lesion, which is merely a retardation of the normal growth and fusion of the ventral and dorsal ossification centers, all of the lumbar bodies and most of the thoracic were affected and the clefts persisted longer than the 7th month. The patient was a girl (Fig 9-22).

Asymmetrically placed remnants of the notochord cause asymmetrical defects that resemble hemivertebra.

Congenital anomalies of the vertebral arches may be found in several sites (see Figs 9-13 and 9-14), one or more of these defects may be present in a single arch. The roentgen defect is due to absence of bone

segments in different regions (Fig 9-23), cartilaginous bridges usually fill the site of the bony defect. The importance of defects in the neural arches in the causation of spondylolisthesis is discussed in the section on the pelvis (see Fig 5-45).

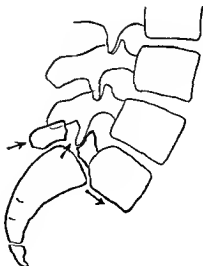
Spina bifida (rachischisis) is a congenital cleft in the neural arches (see Fig 9-13, A and B) which permits external protrusion of the soft tissues and fluid of the spinal canal. The diagnosis is manifest in the clinical examination. The sac of sacral meningocele may be superimposed on the scrotum in frontal projection and simulate hydrocele (Fig 9-24). The laminar defects in the neural arches and the spreading of the pedicles are, however, best demonstrated in the roentgen examination (Fig 9-25). Hemivertebrae are sometimes found in the same levels as the cleft. Minor defects in the laminae of the lumbar and sacral vertebrae without changes in the overlying soft tissues (spina bifida occulta, see Fig 5-29) are exceedingly common in asymptomatic infants and children.



Fig 9-22.—Multiple coronal cleft vertebrae in a girl 7 months of age who had several other congenital anomalies. In the metaphyses of the bones at the wrists and ankles, irregular and defective ossification suggested metaphyseal dysplasias. Several tubular bones in the hands were missing as well as in the right foot with hypoplasia of the right tibia and absence of the left tibia. The heart was deformed and the colon enlarged. Large extracranial clefts developed in the innominate synchondroses of the occipital bone. A: coronal clefts are present in vertebral bodies from T11 through L-4. B: frontal projection. Incomplete clefts in the mid

sagittal plane are visible in many vertebral bodies at different levels, which suggests that these bodies developed from four ossification centers in each body. The sacral lateral masses are defective on both sides. In the bodies of the lumbar vertebrae, clusters of small ossification centers which we have not seen in any other skeleton. C and D: equivalent as in ossification of the achilles tendon in the same patient at 6 weeks and 9 months of age. These irregularities probably represent the limited form of chondrodysplasia calcificans congenita.

Fig 9-23.—Separate neural arch in the L5 vertebra with forward displacement (spondylosis) of the L5 body on the sacrum (also see Fig 5-45).



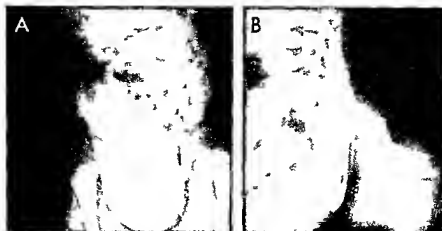


Fig 9 24 —Lumbosacral meningocele on the 1st day of life. The sac of which simulates a lateral hydrocele in the scrotum

in frontal projection (A) but is seen as a sacral meningocele which protrudes dorsally in lateral projection (B)

(Fig 9-26) Most of the midsagittal defects in the neural arches seen radiographically are image defects rather than anatomic defects and represent incomplete ossification of the neural arch at this site rather than an absence of bone and cartilage. Spina

bifida occulta is an inaccurate label for this arch bound securely by a cartilaginous bar which is radio-lucent. There is no splitting of the arch although the roentgen image appears to be split. Many of these supposed defective split arches become normal as age

Fig 9 25 (left).—Thoracolumbosacral spina bifida. There is a long wide central cleft in the neural arches which is a wide spread laterally. The film was made a few hours after birth.

Fig 9 26 (right).—Spina bifida occulta in an asymptomatic girl 10 years of age. The neural arches are probably complete ana-

tomically and the radiographic defects in them probably represent unossified cartilage which will ossify with advancing age. Persistent synchondroses is a more accurate term than spina bifida occulta.



advances Sutow and Pryde found that the incidence of spina bifida occulta (radiographic) diminished in males from 22% in the 7th year to 4% in adults and in females from 9% in the 7th year to 1% in adults

REFERENCES

- Bard P H *et al* Klippel Feil syndrome *Am J Dis Child* 113 546 1967
- Cohen J *et al* A significant variant in the ossification centers of the vertebral bodies *Am J Roentgenol* 76 469 1956
- Ingraham F D *et al* Spina Bifida and Cranium Bifidum (Cambridge Mass Harvard University Printing Office 1944)
- Knuttson F Fusion of the vertebrae following noninfectious disturbance in the zone of growth *Acta radiol* 32 404 1949
- Koehler A and Zimmer E A Borderlines of Normal and Early Pathologic and Skeletal Roentgenology (tr by J T Case) (New York Grune & Stratton Inc)
- Lloyd Roberts G C and Filcher N F Structural idiopathic scoliosis in infancy Study of the natural history in one hundred patients *J Bone & Joint Surg* 47 B 529 1965
- MacEwen G D *et al* Congenital scoliosis with unilateral bar *Radiology* 90 711 1968
- Matson D M and Ingraham F D Intracranial complications of dermal sinus *Pediatrics* 8 463 1951
- Mount L A Congenital dermal sinus as a cause of meningitis intraspinal abscess and intracranial abscess *JAMA* 139 1263 1951
- Rubin S and Stratemeyer E H Intrathoracic meningocele A case report *Radiology* 58 352 1952
- Schanz H R and Tondury G Die Frühossifikation der Wirbelkörper Fortschr Geb Röntgenstrahlen 66 253 1942
- Stewart A M, and McKenzie J A possible method of fetal sex determination *Brit M J* 1 1396 1957
- Sutow W W and Pryde A W Incidence of spina bifida occulta in relation to age *Am J Dis Child* 91 211 1956
- Van de Sar A Hereditary multiple hemivertebra, Doc de med geograph et trop 4 23 1952
- Willis T A The lumbosacral vertebral column in man its stability of form and function *Am J Anat* 32 95 1923

- Winter R B *et al* Congenital scoliosis A study of two hundred and thirty four patients treated and untreated *J Bone & Joint Surg* 50-A 1 1968
- Wolkin D G and Elliot G B Coronal cleft vertebrae and persistent notochordal derivative of infancy *J Canad A Radiol* 12 78 1961

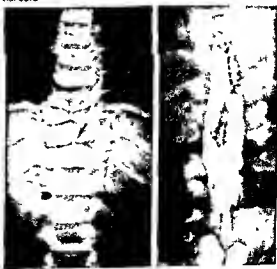
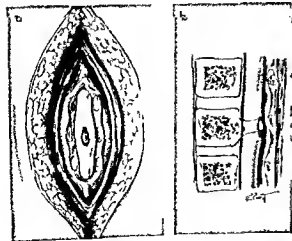
Diastematomyelia is a congenital malformation of the spinal cord and the contiguous portion of the vertebral column. The cord is widened and split into two lateral halves between which lies a longitudinal septum made up of fibrous tissue cartilage and a small spicule of bone. The septum transfixing the cord is attached to the ventral wall of the spinal canal and to the dura mater posteriorly and fixes the cord at this level so that the spinal cord cannot make its normal shift cephalad as the vertebral column lengthens with growth. As a result of this drag on the cord the cerebellum and midbrain may be pulled caudad toward the foramen magnum and sometimes into it and even partially through it to produce an Arnold Chiari malformation with blockage to the flow of cerebrospinal fluid and hydrocephalus. The structural changes are shown in Figure 9 27.

The radiologic findings (Figs 9 28 and 9 29) depend on the type and extent of the tissue changes. Diastematomyelia is most common in the lower thoracic and lumbar portions of the spine. The vertebral anomalies and dilatation of the spinal canal may ex-

Fig 9 28 (left) —Radiologic findings in diastematomyelia in plain film in frontal projection. The spinal canal is widened and the interpediculate distances are increased from T 9 through L 2. The arrow points to the transfixing ossicle superimposed on T 11. The body of T 10 is deformed in a fashion consistent with bilateral hemivertebra or a notochordal remnant.

Fig 9 29 (right) —Myelographic findings in diastematomyelia in a boy 4 years and 10 months of age. The spinal canal is dilated and the opaque subarachnoid column is split by a radiolucent septum—the fibrocartilaginous septum which also splits the spinal cord.

Fig 9 27 —Morbid anatomy of diastematomyelia exposed on surgical exploration. The spinal cord is widened and split by a transfixing ossicle which is continuous with the vertebral body ventrad and the dura dorsad (Figs 9 27 to 9 29 courtesy of Dr E D B Newhauser Boston)



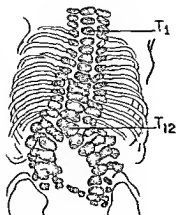


Fig 9-30.—Double lumbosacral spine or total lumbosacral rachischisis below a meningocele tracing of roentgenogram (Redrawn from Rosselet)

tend over several of the contiguous segments in the region of the split spinal cord. In the same levels the interpediculate spaces are increased the vertebral bodies flattened and the intervertebral spaces narrowed. The intraseptal ossicle is best seen in frontal projection at or near the midsagittal plane of the spinal canal. It often cannot be seen in lateral projections. This small opaque spicule can be seen in plainograms when it is invisible in standard films. In one of our patients a girl 2 years of age the diastematomyelia was double with characteristic spinal lesions at two levels—the eighth thoracic and the third lumbar and the spinal cord was split at the same levels by transfixing fibrocartilaginous septums each of which contained its own ossicle. Hemivertebra is commonly associated and spina bifida, lipoma, meningocele and meningomyelocele have been found in some cases.

Diastematomyelia should be suspected clinically

Fig 9-31.—Double lumbosacral spine with a midsagittal plane separate ossicle (arrow) between two dural sacs. The radiographic changes suggest the complete form of diastematomyelia (Redrawn from Kahn and Lemmen)



when there are weaknesses in the legs and feet with disturbances in gait, fecal and urinary incontinence, enuresis—especially when there are associated cutaneous anomalies over the lower spine. Surgical treatment is often beneficial in preventing progression of the neurologic disturbances and should be advised as soon as the diagnosis is established.

Double sacrolumbar column or total rachischisis (Fig 9-30) has been described. The case of Kahn and Lemmen presented features characteristic of double sacrolumbar column and of diastematomyelia (Fig 9-31).

REFERENCES

- Bremer J L. Dorsal intestinal fistulas. Accessory neurenteric canal. *Diastematomyelia*. Arch. Path. 54:132, 1952.
 Kahn, E. A. and Lemmen L. J. Unusual congenital anomalies of neurosurgical interest in infants and children. *J. Neurol.* 7:544, 1950.
 Matson D. D. et al. *Diastematomyelia* (congenital clefts of the spinal cord). Diagnosis and surgical treatment, *Pediatrics* 8:98, 1951.
 Neuhauser E. B. D. et al. *Diastematomyelia*. Transfixation of the spinal cord or cauda equina with congenital anomalies of the spine. *Radiology* 54:659, 1950.
 Rosselet, P. J. A rare case of rachischisis with multiple malformations. *Am. J. Roentgenol.* 72:235, 1955.
 Sands W. W. and Clark W. K. *Diastematomyelia*. *Am. J. Roentgenol.* 72:64, 1954.

Vertebral sacral meningocele is an important and not exceedingly rare congenital malformation which is usually missed unless it is identified radiologically by the characteristic defect in the sacrum as viewed in frontal projection. In Pantopaque myelograms some of the contrast agent flows from the normal subarachnoid space into the cavity of the meningocele (Fig 9-32). The principal complaint is often dysuria caused by compression of the bladder by the meningocele. Local pain and tenderness may also be present. In one of our patients, a girl 12 years of age the only complaints were weakness in the feet and legs with clumsy gait. When large the meningocele is easily felt on direct palpation. Early recognition and surgical treatment in young females are especially important owing to the serious complications during pregnancy. The meningocele may be compressed to a degree which causes increased intraspinal and intracranial pressure. Sometimes the meningocele has ruptured with sudden drop in intraspinal pressures and late infection and meningitis.

Lateral intrathoracic meningocele is characterized by a paravertebral tumor of variable size with excavation of the dorsal edges of one or more of the contiguous vertebral bodies (Brunner). These findings simulate those of neurofibromatosis but the meningoceles fill with gas after injection at the lumbar levels into the subarachnoid space.

REFERENCES

- Brunner R. Lateral intrathoracic meningocele. *Acta radiol.* 51:1, 1959.

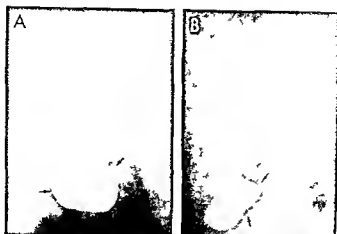


Fig 9 32 —Anterior sacral meningocele after a Pantopaque myelogram in a girl 12 years of age. At the site of the sacral de-

fect the sac of the meningocele is filled with the opaque contrast agent. A frontal and B lateral projections.

Leigh T F and Rogers J V Jr. Anterior sacral meningocele. *Am J Roentgenol* 71:808, 1954.

Sherman R M et al. Anterior sacral meningocele. *Am J Surg* 79:743, 1950.

Congenital spinal anomalies associated with other congenital malformations —Hemivertebrae

Fig 9 33 —Hypoplastic achondroplasia in a boy 4 years of age. The arrows are directed at hypoplastic, bullet-nosed bodies of the L 1 and L 2 segments which are the site of a kyphosis. The sacrum is rotated clockwise, upward and backward. The intervertebral spaces are wide.



are common in association with congenital absence of the lung and bony dysplasias in the extremities. In the lumbar segment of the spine, anomalies such as hemivertebra, malsegmentations and hypoplasias of the intervertebral disk may be associated with imperforate or ectopic anus. Coronal clefts have been found in some males with the high type of imperforate anus. Congenital sacral anomalies associated with imperforate anus include a variety of sacral dysplasias which cause shortening and scoliosis of the sa-

Fig 9 34 —Hyperplastic achondroplasia in a boy 5 years of age. The anterior edges of the bodies show deep terminal notched defects above and below, between which are large step-like anterior projections. Lamy and Maroteaux prefer to call such changes spondyloepiphyseal dysplasia (pseudochondroplastic type).



crum. In patients with an imperforate anus any anomalies in the lumbar and sacral segments of the spine are indications for excretory urography for early detection of correctable associated lesions in the urinary tract.

REFERENCE

- Berdon W E *et al*. The association of lumbosacral spine and genitourinary anomalies with imperforate anus. *Am J Roentgenol* 98 181 1960

Systemic Dysplasias

The vertebral bodies are short tubular bones and they exhibit the same changes in the skeletal dysplasias as the long tubular bones. The vertebral changes are however less marked because of the smaller amount of growth and of endochondral bone formation on the growing surfaces of each vertebra than in the growing ends of a long bone. For this reason the roentgen changes are usually less conspicuous in the spinal column and the spine is not the optimal site for the diagnosis of skeletal dysplasias of growth.

ACHONDROPLASIA

The differences between the spines in hypoplastic and hyperplastic achondroplasia are shown in Figures 9-33 and 9-34. Kyphosis is sometimes a serious and painful complication of achondroplasia. It is due to hypoplasia of a lumbar body and its neural arch at one or more levels. Kyphosis of the cervical spine is one of the most consistent changes in diastrophic dwarfism (Fig 9-35). For detailed changes in the achondroplastic spinal columns see Figures 8-309, 8-311 and 8-313. In severe cases the vertebral bodies appear as narrow sclerotic plates interposed between widened intervertebral spaces (Fig 9-36). Vertebra

plana is one of the most characteristic features of Morquio's disease.

In Ollier's dyschondroplasia the vertebrae are normal even in the presence of severe dyschondroplastic changes in all of the tubular bones and the flat bones in the pelvis and shoulder girdles.

In external chondromatosis (multiple cartilaginous exostoses) the spine usually appears normal radiologically. In one of our patients a girl 8 years of age who had dozens of large and small exostoses in the other bones, numerous exostoses were demonstrated in the lumbar segments of the spine (Fig 9-37). All of these small vertebral exostoses appeared to project off the transverse processes and the pedicles.

REFERENCE

- Vogl A. and Osborne R. C. Lesions of the spinal cord (transverse myelopathy) in achondroplasia. *Arch Neurol & Psychiat* 61 644 1949

MUCOPOLYSACCHARIDOSES

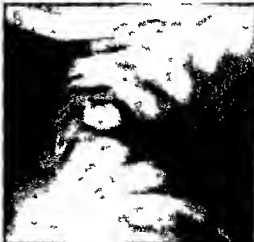
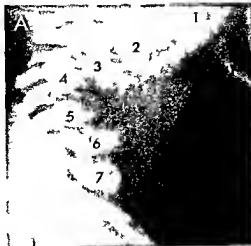
Lumbar kyphosis (Fig 9-38) is a common feature of dysostosis multiplex. Begg demonstrated at necropsy that the hook shaped vertebral body of gargoyism is caused by protrusion of the nucleus pulposus through the annulus fibrosus to impinge on the anterior longitudinal ligament which then deflects it back onto the ventral edge of the body where it produces local compression atrophy (Fig 9-39). In the lumbar levels the pedicles may be rarefied and small in caliber and the vertebral dorsal edges concave dorsad, all of which is highly suggestive of localized increased intraspinal pressure (see Fig 8-385).

REFERENCE

- Begg A. C. Nuclear herniations of the intervertebral discs. Their radiologic manifestations and significance. *J Bone & Joint Surg* 36-B 180 1954

Fig 9-35.—Sharp kyphosis and possibly spondylolyses of the cervical spine of a diastrophic dwarf. A, at 3 months of age. B, at 12 months. The 4th and 5th vertebrae are hypoplastic and

displaced dorsad to produce a sharp angle cervical kyphosis. This patient had no signs of spinal cord compression until the 12th month following an injury to the head and cervical region.



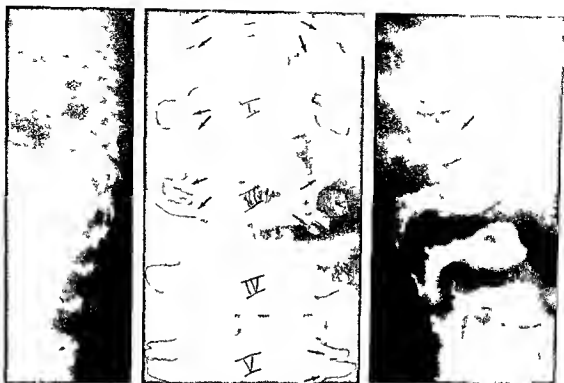


Fig 9-36 (left) — Severe hypoplastic echondroplasia in an infant 2 days of age. The intervertebral spaces are several times thicker than the flat scale of ossification centers of the vertebral bodies (compare with normal vertebral bodies in the newborn, Figs 9-313 and 9-6). Serum phosphatase activity was not studied. It is possible that the patient had hypophosphatasia rather than echondroplasia.

Fig 9-37 (center) — Multiple cartilaginous exostoses on the

lumbar segments of the spine of a girl 6 years of age, who had dozens of exostoses in other bones. In these vertebral bodies the exostoses appear to protect all the transverse processes and pedicles.

Fig 9-38 (right) — Lumbar kyphosis in *dysostosis multiplex* (Hurler's syndrome) in a patient 20 months of age. The arrow is directed at the deformed hypoplastic L2 body.

OSTEOGENESIS IMPERFECTA

As in the long bones, the characteristic finding in the vertebrae is a generalized osteoporosis due to defective cortex and spongiosa. In severe cases the weak osteoporotic bodies exhibit compression deformities near their centers with expansion of the contiguous *nuclei pulposi* (Fig 9-40). The central concavities on the upper and lower vertebral surfaces produce a deformed vertebral body which in lateral projection casts an hourglass shadow which is thinnest in the center and thickest at the anterior and posterior edges. It is possible that minute fractures contribute to the malformation of the vertebral bodies because not all of the bodies are affected and the in-

volved ones are disposed irregularly. Spinal curvatures are common in osteogenesis imperfecta.

OSTEOPETROSIS (MARBLE BONES)

The vertebrae show sclerosis similar to that found in the other portions of the skeleton. The development of the vertebrae is distinctly retarded. Infantile characteristics may persist for many years (Fig 9-41). The vascular channels which perforate the vertebral body and the vascular sinuses within the body are large and conspicuous. Often in the center of the body there is an inset of diminished density which has the approximate size and contour of a neonatal vertebral body.

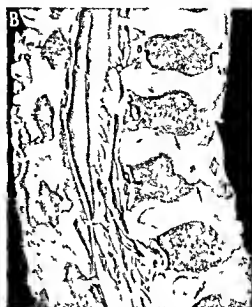


Fig 9-39—Hook shaped lumbar vertebral body of gargoylism in a boy 6 years of age. **A**, radiograph showing large defect in the body of L 1 with narrowing of the contiguous intervertebral space below. The summit of the kyphosis is at the same levels. **B**, a sagittal section of the same spine showing the intervertebral

disk thickened at the site of the vertebral body defect of L 1 which was found to be a displaced nucleus pulposus with necrosis of the contiguous vertebral body due to pressure. (Redrawn from Begg.)

Fig 9-40 (left)—Biconcave compression of the vertebral bodies in a boy 12 years of age with osteogenesis imperfecta. The intervertebral disks are deepened proportionately but are biconvex in the same degree. The bodies in the neural arches of all of the vertebrae are diffusely resorbed.

Fig 9-41 (right)—Osteopetrosis (marble bones) in a boy 4 years of age. All parts of the vertebrae are sclerotic; the bodies

retain the oval infantile contours. Within each body is a small bony nucleus which has the shape and size of a neonatal vertebral body. The large notched defects in the anterior portion of the vertebral body and the transverse strip of diminished density are due to vascular channels and persistence of the intersegmental tissues.



Traumatic Lesions

Dislocations

DISLOCATIONS ARE most common in the more flexible cervical spine and at the lumbosacral articulation. Cervical dislocations and spondylolisthesis are described in the discussion of the neck (Section 1) and the pelvis (Section 5).

Fractures

Fractures may occur at one or more sites in a single vertebra, and more than one spinal segment may be

Fig 9-42—Compression fractures of L-3 and L-4 bodies in a boy 7 years of age. There are no visible fracture lines. The edges of the broken bodies are compressed and mushroomed beyond normal limits and the heights of the two affected bodies are diminished. There is a corresponding expansion of the contiguous intervertebral spaces owing to expansion of the nucleus pulposus in each of the spaces against the weakened bodies. The greater compression of the bodies in ventral axis produces the wedge-shaped deformities. The superior edge of the wedge-shaped body is always displaced more than its inferior edge.



affected. The vertebral body is fractured more frequently than the arch. As in other bones, a simple fracture casts an irregular linear shadow of diminished density between the separated fragments. The fracture line is usually obliterated and the overlap of the edges of the fragments may produce a border of increased density (Fig 9-42). Fracture lines in the vertebral body are usually best visualized in lateral projections. Fracture lines of the vertebral bodies which are invisible with standard technique in multiple positions often can be demonstrated in planograms. In crushing fractures the body is deformed by compression; usually the body assumes the shape of a wedge. The intervertebral disks usually escape injury, but they may be lacerated and become narrow owing to collapse of the nucleus pulposus. In infants and children the normal vascular channels and persistent intersegmental cleft of the provertebrae (see Fig 9-8) should not be mistaken for fracture lines. In adolescents the secondary ossification centers in the superior and inferior annular epiphyses should not be confused with marginal chip fractures (see Fig 9-9). External callus is rarely visible during the healing of fractures in the body.

Fractures of the arch and its processes are best visualized in stereoscopic frontal, lateral and oblique projections. Planigrams are also often helpful. Fractures of the spinous processes in the cervical and upper thoracic segments (Fig 9-43) can however be clearly seen in both frontal and lateral projections when the terminal fracture fragment is displaced caudad (Zanca and Lodmell). During the second decade of life, trophic changes in the tips of the spinous processes of traumatic origin simulate those of osteochondrosis juvenilis in other bones. It is likely that these changes represent necrosis following mechanical injury. Small fractures without displacement of the fragments can be satisfactorily identified only several weeks after the injury when callus formation becomes evident. Congenital defects are common in the neural arches, especially in the inferior lumbar segments; caution should be used in the diagnosis of fractures of the arches at these levels. The normal secondary ossification centers appear in the tips of

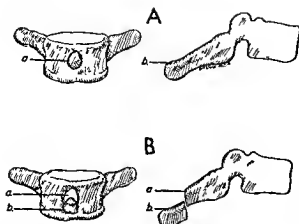


Fig 9-43—Schematic representation of fractures of the spinous processes in the cervical and upper lumbar vertebrae. A normal vertebra. B vertebra with fractured spinous process. In B the caudally displaced fragment of the spinous process (b) casts a separate image (a) in frontal projection. (From Zanca and Lod melli)

the various processes of the arch during late adolescence (see Fig 9-5). These normal epiphyseal ossicles have been mistaken for fracture fragments.

Tetanic convulsions may be responsible for compression fractures of the vertebral bodies and secondary spinal deformity (Fig 9-44). Dietrich Karshner and Stewart found compression fractures in 70% of a group of children who had recovered from tetanus. In Montevideo Bonabo and Pieroni found similar residual spinal changes in tetanus: the upper half of the thoracic spine was consistently affected in one or more segments. The fractured bodies become flattened and wedge-shaped; they may be either rarefied or sclerotic. The prognosis is usually good without serious later spinal deformity. Destruction of the spongiosa due to hemorrhage appears to be an important causal factor in weakening the vertebral body.

A specific type of distraction injury (fulcrum fractures) to the lumbar spine following injuries to persons wearing the lap type of seat belts in automobiles has been studied by Smith and Kaufer. These injuries are characterized by marked longitudinal spreading of the adjacent injured neural arches behind but with little or no anterior compression and anterior

Fig 9-44—Residual fractures and compression deformities of vertebral bodies due to tetanus in a boy 8 years of age. A, frontal; and B, lateral projections.



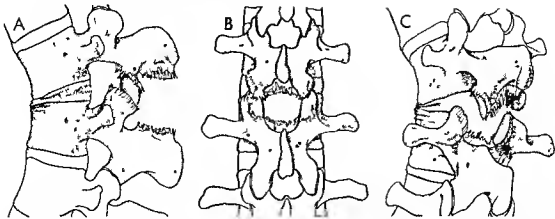


Fig 9-45—Distraction injury to two lumbar vertebrae is the outstanding pattern of seat belt injuries. **A**, the posterior elements are widely separated with slight or no anterior compression. The lumbosacral fascia, interspinous ligaments, ligamentum flavum, posterior longitudinal ligament and joint capsules are all lacerated. **B**, the neural arches of the two injured vertebrae are spread longitudinally; the intervening intervertebral foramen is

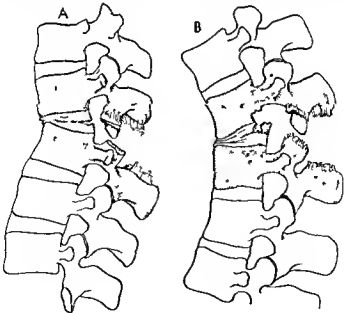
enlarged longitudinally and ventrodorsally; the intervertebral disk is broken and wedged ventrad, but the lumbar bodies themselves are intact, although tipped counterclockwise (upper vertebral body) and clockwise (lower vertebral body). **C**, the intervertebral space is shallow ventrad and deepened dorsad (Figs 9-45 to 9-47 from Smith and Kaufer).

wedging of the vertebral body (Figs 9-45 and 9-46). The causal mechanism for the fulcrum fracture is depicted in Figure 9-47. Two of seven patients with distraction injuries were 9 and 15 years of age. Three older patients, 23, 19, and 40 years of age, suffered

Chance fractures—a horizontal splitting through the vertebral bodies and their transverse processes, pedicles, laminae and spinous processes without compression of the body itself. With the expected progressive increase in the use of lap belts, the incidence of dis-

Fig 9-46—Characteristic spinal injuries associated with seat belts. **A**, drawing of lateral radiograph which shows fracture of the articular process, laceration of the dorsal segment of the intervertebral disk and posterior widening of the contiguous wider verte-

bral spaces and ligamentous damage. **B**, drawing of lateral radiograph with additional avulsion fracture of the dorsal edge of the vertebral body from stress induced by the posterior longitudinal ligament.



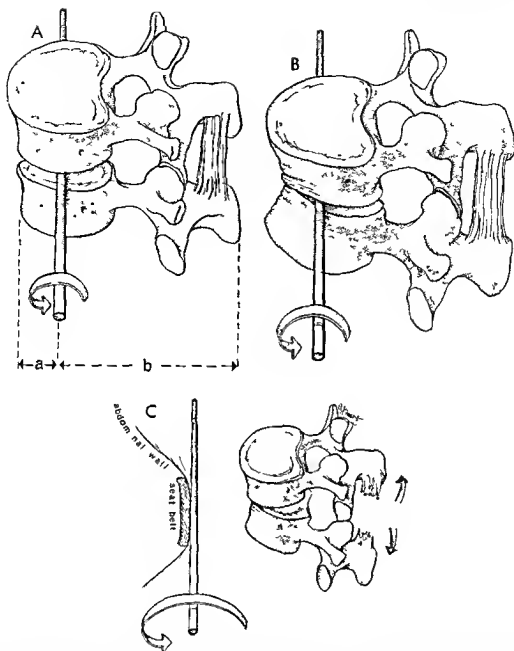


Fig. 9-47—Mechanism of distraction fracture from seat belt injury. A, in the usual flexion injury of an intact lumbar spine the active force rotates the vertebral body counterclockwise around a transverse axis which passes through the nucleus pulposus. The distance from the transverse axis of the anterior edge of the vertebral body (*a*) is one-fourth the distance from the transverse axis to the tip of the spinous process (*b*). According to the law of leverage the anterior segment of the vertebral body will be subjected to a compression force four times greater than the stretch

distraction force on the interspinous ligaments. B, hyperflexion around the normal transverse axis produces compression fracture of the anterior segment of the vertebral body without laceration of the intervertebral ligaments. C, with hyperflexion around the belt the axis of flexion is far forward at the point of contact of the belt and abdominal wall. Anterior to the spine both bodies and neural arches are subjected to tensile stress with laceration of the posterior ligaments and distraction of the neural arches and bodies but no compression.

traction fractures of the lumbar neural arches and of chronic fractures will probably increase proportionately.

In adult epileptics the incidence of fractures and compression deformities in the vertebral bodies has been reported as high as 66% and as low as 7%. I have seen no detailed data on spinal fractures in juvenile epileptics. It is probable that their incidence is considerably lower than in adult epileptics owing to the protection afforded by the encasing layer of cartilage. In male adult epileptics the incidence of spinal fracture is higher than in females owing to the stronger heavier muscles in males.

The prolonged administration of cortisone and corticotropin led to marked osteoporosis and then fractures and compression deformities of the vertebral bodies in four patients studied by Curtiss and others. One was a boy of 9 who had rheumatoid arthritis.

REFERENCES

- Sujoy E. Spinal lesions in tetanus in children. *Pediatrics* 29: 629 1962.
Zanca P. and Lodmell E. A. Fracture of the spinous processes. A new sign for the recognition of fractures of the cervical and upper dorsal spinous processes. *Radiology* 56: 627 1951.

Traumatic Lesions in the Disks

In severe compression fractures of the vertebral bodies the intervertebral disks may also be injured and the nucleus pulposus dispersed or displaced. Direct injury to the disk may be due to penetrating wounds of the vertebral column. Beadle cited a case in which a long nail was driven into the spine at the third lumbar level and the intervertebral disk split.

The commonest cause of direct injury to the disk in

Fig 9-48 — Destruction of an intervertebral disk and sclerosis of the vertebral bodies after lumbar puncture. (Redrawn from Pease.)

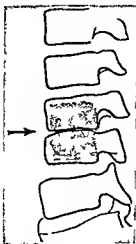


Fig 9-48 — Loss of intervertebral disk space (arrows) between T9 and T10 bodies after a boy 12 years of age had injured his back on a ramp. His back became painful. Results of tuberculin skin tests were negative. (Courtesy of Dr. Arthur Robinson, Denver, Colo.)

infants and children is lumbar puncture when the needle is pushed the entire width of the spinal canal and beyond anteriorly into the disk. During early life when the nucleus pulposus is largely fluid, much of the nucleus may be aspirated back into the needle or may leak into the surrounding tissues. Thinning or obliteration of the affected intervertebral space may follow (Fig 9-48). The adjacent vertebral bodies may be injured or infected at the same time. Symptoms of lumbar pain, limitation of motion and weakness of the back may appear immediately or as late as two weeks after the lumbar puncture. The normal lumbar lordosis is usually lost and in severe cases actual kyphosis may develop. Injuries to the intervertebral disks used to occur most frequently after repeated lumbar punctures made for the intrathecal injection of therapeutic serum in the pre-antibiotic era.

Protrusion of the nuclei pulposi through the articular plates into the spongiosa of contiguous vertebrae is discussed with adolescent kyphosis.

VERTEBRA PLANA (CALVE)

Protrusions of the intervertebral disks and their nuclei pulposi into the spinal canal and onto the spinal nerve roots have apparently not been demonstrated as a cause of back pain in infants and younger children. In older children and adolescents the typical disk syndrome has been found and demonstrated anatomically in several cases (Vahren Key Webb and MacGee). The youngest patient reported was 3 years of age. The lumbar disks have been most frequently affected. These lesions are usually in the lumbosacral level, especially at the fifth lumbar disk with compression of the root of the first sacral nerve. In such cases plain films of the spine show normal findings. Opaque myelography is helpful in diagnosis but many cases have been explored and found surgically without benefit of radiologic observations. Boys are more frequently affected than girls.

Trauma alone can result in marked thinning of the intervertebral space (Fig. 9-49).

REFERENCES

- Beadle O. A. The Intervertebral Discs. Special Report Series no. 161. Medical Research Council (London: H. M. Stationery Office, 1931).
- Begg A. C. Nuclear herniations of the intervertebral disc: their radiological manifestations and significance. *J. Bone & Joint Surg.* 36-B:180, 1954.
- Everett, A. D. Lumbar puncture injuries. *Proc. Roy. Soc. Med.* 35:208, 1942.
- Findlay L. and Kemp F. H. Osteomyelitis of the spine following lumbar puncture. *Arch. Dis. Childhood* 18:102, 1943.
- Key J. A. Intervertebral disc lesions in children and adolescents. *J. Bone & Joint Surg.* 32-A:97, 1950.
- MacGee E. E. Protruded lumbar disc in a nine year old boy. *J. Pediatr.* 73:418, 1968.
- Smith W. S. and Kaufer H. Patterns and mechanisms of lumbar injuries associated with lap-seat belts. *J. Bone & Joint Surg.* 51-A:239, 1969.
- Webb J. H. et al. Protruded lumbar intervertebral discs in children. *J. A.M.A.* 154:1153, 1954.

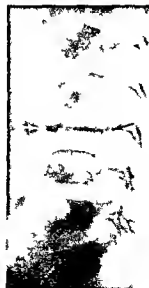
Traumatic Disorders of Growth

Trauma is undoubtedly a cause of growth disturbances in many infantile and juvenile spines. During normal activity the vertebral column is subjected to recurrent stresses of considerable magnitude. Traumatic interference with the blood supply may lead to a suppression of growth and ischemic necrosis of the vertebral body (see Fig. 8-570). Trauma to the intervertebral disks may injure the nucleus pulposus and interfere with its normal water cushion function which provides for even distribution of force to the adjacent vertebral surfaces. The post-traumatic uneven transmission of force results in vertebral and spinal deformities. The exact role played by mild repeated trauma in growth disorders of the spine is difficult to evaluate accurately because recurrent and conspicuous nevertheless significant trauma may not be recognized by the patient or his parents and may even be denied by them.

This lesion resembles coxa plana in some respects. The cause has not been proved conclusively. Antecedent trauma has been noted in some cases and infection has preceded the onset in others. Ischemic necrosis is the traditional causal mechanism for weakening and eventual collapse of the vertebral body. Usually a single vertebral segment is affected. Vertebra plana has been found in children from 2 to 15 years of age. Many believe that idiopathic vertebra plana is often due to unrecognized eosinophilic granuloma, and there is substantial evidence to support this view. It would be well to consider vertebra plana as eosinophilic granuloma in origin until proved otherwise. The spine should be examined and vertebra plana looked for in all patients with reticuloendothelial disease of all types. I have seen vertebra plana in Letterer-Siwe disease.

The diagnosis is established in the roentgen examination. The principal findings are collapse and sclerosis of the vertebral body, the adjacent intervertebral spaces are characteristically normal or increased in depth (Fig. 9-50). In severe cases the sclerotic vertebral body is flattened to a thin disk (Fig. 9-51). The pedicles on one or both sides may be partially destroyed during the destructive phase of the disease. In the patient of Weston and Goodson, destruction of the vertebral body was exceedingly fast; roentgen appearance changed from normality to almost complete destruction of body and pedicles during 15 days and the vertebral body was compressed into a thin horizontal wafer after six weeks.

Fig. 9-50. Calvé's localized osteochondritis vertebralis in a boy 4 years of age. The L3 body is flattened, sclerotic and lengthened ventrally. The intervertebral spaces in contrast are apparently not affected. Lumbar pain had been present for six months when this film was made. (From Fawcett.)



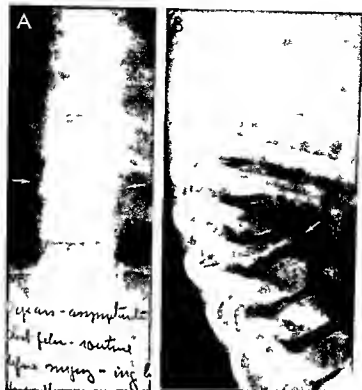


Fig 9-51 -Idiopathic vertebra plana of Calvé in the body of T 9 in a boy 7 years of age. This was a chance finding in films made of the chest because the child was coughing. The spinal lesion

caused neither signs nor symptoms. A, frontal and B, lateral projections.

Fig 9-52 -Calvé's disease (vertebra plana) on D 9 vertebral body of a boy 9 years of age who also had proved destructive eosinophilic granuloma in the temporal bone. The D-9 body has collapsed cephalocaudad into a hairline opaque strip between intervertebral disks which retain their normal depths. In the frontal projection (not reproduced) there was a spindle shaped peri-spinal image of water density which resembled the perispinal swellings of tuberculous spine. It seems probable that most if not all cases of idiopathic vertebra plana (Calvé's disease) are caused by destructive eosinophilic granuloma and not by ischemic necrosis (juvenile osteochondrosis).



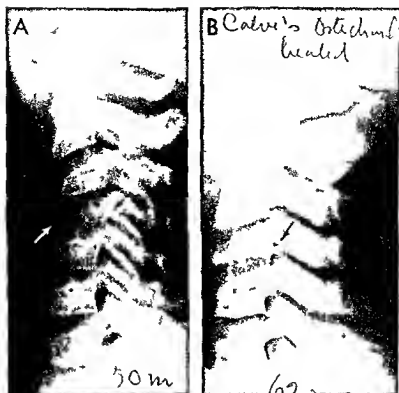


Fig 9 53 —A vertebra plana (Calve) of the body of the C4 segment of a girl 50 months of age. The body is flattened and collapsed with widening of the contiguous intervertebral spaces. B

at 60 months the affected body is still flattened but has become sclerotic and is beginning to re-expand toward its normal thickness.

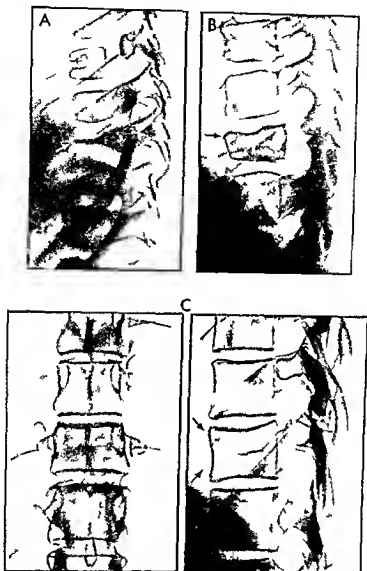


Fig 9 54 Complete healing of vertebral plana due to eosinophilic granuloma of 22 years. A marked vertebra flattened at 3V years. B part a

residual at 7 years. C complete healing at 25 years (Redrawn from Frapp)

Vertebra plana resembles tuberculosis of the body except that sclerosis is uncommon in the latter. In *eosinophilic granulomas of the spine* there may be large and small perispinal swellings which simulate the perispinal abscesses of tuberculosis of the spine (Fig 9 52).

Restoration of the body may begin after several months (Fig 9 53) but the deformity may persist for years. Frapp made long follow up studies of vertebra plana and found that the diseased vertebral bodies were restored to nearly normal shape and density after periods of 12-22 years (Fig 9 54). None of his patients received radiation therapy or corticosteroids.

REFERENCES

- Calvé J. Localized affection of the spine suggesting osteochondritis of the vertebral body with the clinical aspects of Pott's disease. *J Bone & Joint Surg* 7:41, 1925.
- Compere E. L. et al. Vertebra plana (Calvé's disease) due to eosinophilic granuloma. *J Bone & Joint Surg* 36-A:969, 1954.
- Dickey L. E. et al. Vertebra plana and the histiocytoses. Report of a case with involvement of 5 vertebrae. *J Bone & Joint Surg* 37-A:126, 1955.
- Frapp A. T. Vertebra plana. *J Bone & Joint Surg* 40-B:378, 1958.
- Wes on W. J. and Goodson G. M. Vertebra plana (Calvé). *J Bone & Joint Surg* 41-B:477, 1959.

ADOLESCENT KYPHOSIS (SCHEUERMANN SCHMORL DISEASE)

Scheuermann called attention, in 1921, to kyphosis in adolescents associated with fragmentation of the epiphyseal ring, flattening and wedging of one or more vertebral bodies in the lower thoracic and lumbar levels and progressive deformity of the spine. He called this syndrome *kyphosis deformans juvenilis* in the belief that it was similar pathogenetically to Perthes' disease in the femur and Kohler's disease in the tarsal scaphoid. Scheuermann hypothesized that the primary cause of the lesion was a disturbance in epiphyseal growth due to injury and ischemic necrosis of the marginal epiphyseal cartilaginous rings which rim the cartilaginous plates on the upper and lower edges of each vertebral body. The disorder has become known as Scheuermann's disease.

In Schmorl's comprehensive studies of the spine, adolescent kyphosis was found to be due to an entirely different mechanism—protrusion of the nuclei pulposi into the marrow cavities of the neighboring vertebral bodies with narrowing of the intervertebral space or spaces between the affected bodies (Fig. 9-55). According to Schmorl, the onset and progression of vertebral destruction and wedging are caused by excessively heavy stresses on the articular plates

which permit the nuclei pulposi to break through these plates and extend into the vertebral body itself. During adolescence, these traumatic stresses are due to vigorous athletic exercises, heavy manual labor and habitual bending postures which weaken and break healthy cartilaginous plates. In many cases, however, these lesions develop in children who have undergone only normal activity, and in them it is believed that the cartilaginous plates are congenitally weak. Schmorl expressed doubt that the so-called epiphyseal rings had anything to do with longitudinal growth of the vertebral body.

The work of Ehrenhaft and of Bick and Copel confirmed Schmorl's view that longitudinal growth of the vertebra is exclusively the function of the cartilaginous plates, which are the counterparts of the proliferating cartilage and the provisional zones of calcification in the tubular bones. Actually the "epiphyseal rings" lie outside the zones of growth in the vertebral bodies, external to the growing cartilaginous plates. Ehrenhaft concluded that in adolescent kyphosis nuclear prolapses into the body may occur at several sites in different bodies or in a single body, and thus produces the uneven growth and marginal defects. It also causes a shift in the load on the vertebral body toward the ventral segment of the cartilaginous plate where growth is disproportionately retarded and wedging followed by kyphosis, develops. Fragmentation of the "epiphyseal" ring is a secondary compression phenomenon according to this hypothesis.

In careful roentgen studies Begg found Schmorl's nodes common in adolescent spines in the lower dorsal and lumbar segments. He concluded that these nodes develop owing to congenital weaknesses in the cartilage plates at the sites of the notochordal canals. Following herniation the loss of the nuclear material impairs the normal cushioning effects of the disk so that the stresses of weight bearing are not evenly distributed over the faces of the opposing vertebral bodies. The resulting abnormal pressures become greatest on the anterior segments of the bodies because the posterior segments are protected by the articular joints which maintain the intervertebral spaces posteriorly and at the same time promote excessive pressures and compression deformities ventrad. It is the anterior compression wedging which leads to juvenile kyphosis or Scheuermann's disease. Plaingrams of the spine will disclose nuclear herniations which are invisible in standard films when the herniations are centrally located. Begg's article should be read in detail by those interested in the radiologic study of the adolescent spine.

Bick and Copel in their study of normal spines found that longitudinal growth of the vertebral body is similar to that in the long tubular bones. They concluded that the "epiphyseal" ring is a cartilaginous ring which ossifies and fuses with the body but does not contribute to longitudinal growth in much the same way as an apophysis fuses with a long bone but does not increase its length. They implied that "epi-

Fig. 9-55—Anatomic changes in adolescent kyphosis (Schmorl type). The disks are deformed and the vertebral bodies wedge-shaped. Schmorl's nodes, protrusions of the nuclei pulposi into the spongiosa of the adjacent bodies, are seen at several levels. (From Beadie.)



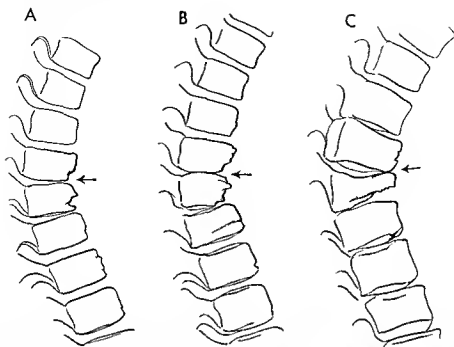
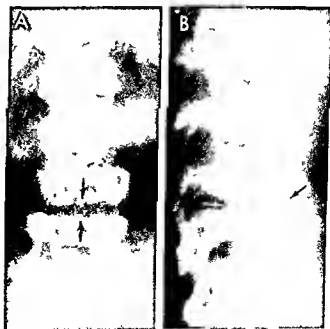


Fig 9 56 —Adolescent kyphosis (Scheuermann type) which developed in a nontuberculous child in the absence of recognized trauma. **A** at 11 years the intervertebral spaces are narrowed and the bodies of T 6 and T 7 vertebrae show notched deformities on their anterior margins. kyphosis is evident. **B** and

C progressive changes at 13 and 15 years respectively. All of the changes can be explained on the basis of anterior herniation of the intervertebral disks followed by local compression atrophy of contiguous vertebral bodies.

Fig 9 57 —Marginal destruction of vertebral bodies of L 3 and L 4 with narrowing of the intervertebral space in an infant 14 months of age, four months after a fall from a high chair. Repeated tuberculin tests in increased dosage gave negative results. There is no kyphosis. The radiologic changes are similar to those of Scheuermann's disease in adolescents, before the appearance of kyphosis. **A** frontal and **B** lateral projections.



physal ring is a misnomer and should be changed to vertebral ring

Brauer studied the spines of contortionists and found changes similar to those in Scheuermann's disease in them which he attributed to traumatic injury to the intervertebral disks without herniation of the nuclei pulposi. He believed that juvenile kyphosis is due to congenital defects in the intervertebral disk.

The pathogenesis of adolescent kyphosis is still controversial. There is little evidence to sustain Scheuermann's hypothesis of injury to the epiphyseal ring as the primary causal factor. Many cases are surely due to injury to the intervertebral disk and herniation of the nucleus pulposus. There are also however many cases in which there is no radiologic evidence of injury to the cartilaginous ring or to the intervertebral disk. It is probable that Scheuermann's syndrome can develop from more than one pathogenetic mechanism. Ferguson believes that persistence of the anterior vascular grooves makes individuals susceptible to progressive collapse of the vertebral bodies.

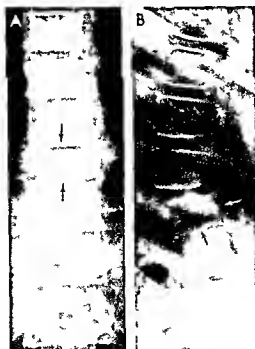
The principal radiologic findings include progressive narrowing of the intervertebral space, deep irregularities on the edges of the vertebral body, sometimes even on the ventral edge. Schmorl's nuclei in the vertebral body wedging and kyphosis (Fig 9-56). These changes are usually located in the lower dorsal and upper lumbar segments. Knutson found that

actual fusion of the edges of the affected bodies in their ventral aspects with complete obliteration of the intervertebral space was a late complication in some cases. It should be emphasized that similar changes in the spine may be found long before adolescence during earlier childhood and even during infancy (Fig 9-57). The lesion may also be demonstrated radiologically without kyphosis especially when a single vertebra is involved (Fig 9-58). The vertebral rings during adolescence usually calcify in irregular segments and these normal marginal irregularities should not be used as evidence of osteochondritis juvenilis of the spine.

REFERENCES

- Bendall O. The Intervertebral Discs. Special Report Series no 161. Medical Research Council (London: H M Stationery Office, 1931).
- Berg A C. Nuclear herniations of the intervertebral disc. Their radiological manifestations and significance. *J Bone & Joint Surg* 36-B:180, 1954.
- Bick E M and Copel J W. Longitudinal growth of the human vertebra. *J Bone & Joint Surg* 32 A:803, 1950.
- Brauer W. On the cause of juvenile kyphosis. *Fortschr Geb Röntgenstrahlen* 83:839, 1955.
- Ehrenhaft J L. Development of the vertebral column as related to certain congenital and pathological changes. *Surg Gynec & Obst* 76:282, 1943.
- Scheuermann H. Kyphosis dorsalis juvenilis. *Zschr orthop Chir* 41:4, 1921.
- Kyphose juvenis. *Arch med belges* 81:353, 1928.
- Schmorl K. Die Pathogenese der juvenilen Kyphose. *Fortschr Geb Röntgenstrahlen* 41:359, 1929, 30.
- Williams H J and Pugh D G. Vertebral epiphysitis: A comparison of the clinical and roentgen findings. *Am J Roentgenol* 90:1236, 1963.

Fig 9-58—Adolescent kyphosis (Scheuermann's disease). A 11 years of age. The body of T9 vertebra is flattened and wedge shaped with deep marginal defects on its superior edge. The intervertebral spaces above and below T9 are narrowed and early kyphosis is evident. A, frontal and B, lateral projection.



HABITUAL IDIOPATHIC SCOLIOSIS

This is an exceedingly important disorder of the growing spine which we cannot discuss adequately owing to the limitations of space. The reader is referred to orthopedic texts for more comprehensive and detailed descriptions. There are four basic changes in the radiologic findings: transverse shift of vertebral segments, contracture of the entire spine, unilateral compression of the vertebral bodies on the inside and at the apex of the curve or curves, and rotation of vertebral segments. Muscular imbalance is an important causal factor. Many so-called idiopathic cases are due to unrecognized postpoliomyelitic muscular paralyses and weaknesses. During infancy hemivertebra is a common cause of habitual scoliosis.

Scoliosis which begins during childhood usually progresses to severe and disabling deformities; in contrast the scoliosis which begins during adolescence often remains moderate.

CHRONIC HYPOXIA

The entire skeleton, especially the calvaria, may be thickened and dense as a result of long standing hypoxia due to cardiac failure. In one patient we found



Fig 9-59 — Segmental sclerosis of the vertebral bodies of a boy 10 years of age due to the chronic hypoxia of a single-ventricle heart with transposition of the great arteries. The sclerotic segment in each body surrounds the canal of the nutrient artery.

The calvaria and ribs were generally sclerotic and other bones slightly sclerotic generally (Courtesy of Dr. Marvin Daves, Denver, Colo.)

a peculiar patchy sclerosis of the vertebral bodies (Fig 9-59).

Scoliosis is associated with congenital heart disease in substantially higher incidence than in the general juvenile population. Scoliosis has a higher incidence in cyanotic congenital heart disease than in congenital acyanotic heart disease. The causal mechanism of the scoliosis is not known. Thoracotomy of course

may be responsible for scoliosis in patients treated surgically.

REFERENCES

- Collis D. K. and Ponseti, I. V. Long term follow up of patients with idiopathic scoliosis not treated surgically. *J Bone & Joint Surg* 51 A: 425, 1969.
- Luke M. J. and McDonnell E. J. Congenital heart disease and scoliosis. *J Pediatr* 73: 725, 1968.

Calcification of Intervertebral Disks

CALCIFICATION of intervertebral disks is not uncommon in adults and is usually considered a sign of degeneration with calcification, due to normal aging without specific clinical or anatomical significance. The incidence in infants and children is relatively small, although calciferous disk lesions are being detected in them with increasing frequency. Melnick and Silverman found 48 examples in the literature and added five personal cases. There are, of course, countless cases which have not been recorded. Usually, excepting the neck, there are no associated local clinical signs. Calcifications have been found in all of the components of the disk—in the cartilage plates, the nucleus pulposus and the annulus fibrosus (Fig 9-60). The lesions may be single or multiple at different levels of the spine, with the highest incidence in the midthoracic levels. Disk calcifications have been most extensive in alkaptonuric ochronosis. Transitory disk calcifications have been reported in poisoning due to vitamin D.

Radiologic examination shows images of calcium

density in the normally radiolucent intervertebral tissues (Fig 9-61). In two projections one can differentiate central and peripheral calcifications (Fig 9-62), but one cannot identify accurately the exact components of the disk which carry the lime. The edges of the vertebral bodies adjacent to the calcified mass are usually bent into the vertebral body. In two of our patients, 22 months and 5 years of age, the prevertebral tissues were calcified in a peculiar "bull's eye" pattern (Fig 9-63). The clinical signs of fever, and pain and stiffness in the neck disappeared after two to three weeks and the calcifications after several months. The lesions may be permanent or transitory. The latter are in the cervical spine and are usually associated with local pain.

REFERENCES

- Melnick, J. C., and Silverman, F. N. Intervertebral disk calcification in childhood. *Radiology* 80:399, 1963.
Morns, J., and Niebauer, J. Calcification of cervical intervertebral disc. *Am J Dis Child* 106:295, 1963.

Fig. 9-60—Schematic drawings of the normal intervertebral disk. A, before the appearance of ossification centers in cartilaginous vertebral rings. B, after ossification of the vertebral rings

and the fusion with the vertebral body (Courtesy of Dr. Frederic N. Silverman, Cincinnati.)

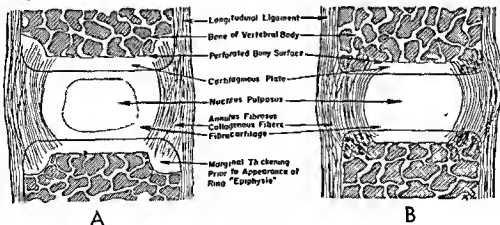




Fig 9 51—Calcification of the nucleus pulposus in the third and fourth intervertebral disks of an asymptomatic girl 11 years of age. **A**, frontal; and **B**, lateral projections.

Fig 9 63—Idiopathic transitory focal calcifications in the prevertebral ligaments and ventral segments of the intervertebral disks of the cervical spines of two young children who had fever and painful tender necks. In both, the clinical signs disappeared after a few weeks and the calcifications after several months. **A**, in a boy 22 months of age most of the calcification is in front of the spine, and one must assume that the spinal ligaments and possibly the disks protrude forward to these levels. In the upper mass of calcification there is a distinct "bull's eye" pattern. **B**, in

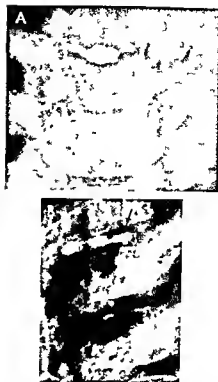
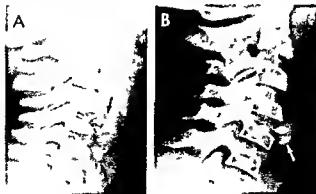


Fig 9 62—Calcification of the intervertebral disk between T-4 and T-5 of an asymptomatic boy 5 years of age. In **A**, frontal projection, the central nucleus pulposus appears to be solidly calcified, with two lateral calcified wings which extend laterally into the fibrocartilage of the disk. In **B**, lateral projection, the wings extend ventrad and dorsad into the fibrocartilage.

a boy 5 years of age there is a single focus of calcification with a "bull's eye" pattern which seems to fit into the ventral segment of the intervertebral disk. In both cases the calciferous masses were in or near the midsagittal plane of the spine, and reacted on the tuberculin skin test were negative. There is a notable lack of thickening of the soft tissues at the levels of the calcifications. It is possible that this benign disease is a calcific tendinitis, or it may represent calcifications in the front end of the intervertebral disks as well.

Diseases Involving Vertebrae

Infections

NONTUBERCULOUS

NONTUBERCULOUS INFECTIONS of the spinal column are rare during infancy and childhood age periods when osteomyelitis occurs most frequently in the long bones. When one or more of the long bones are infected during staphylococcal and streptococcal bacteremias the spine almost invariably escapes concurrent infection. In rare instances however the vertebrae are affected and a wide variety of organisms may be the causal agent: staphylococcus, streptococcus, *Bacillus typhosus* and paratyphosus, pneumococcus, meningococcus, *Brucella melitensis* and other organisms. Infection of the vertebrae produces the same basic changes as in other bones, namely bone destruction and bone production singly or in combination and in a variety of patterns. During the early stage of the acute infections destructive changes predominate; later productive changes appear. In the low grade chronic infections productive changes are the rule throughout the course of the disease. Either the margins of the bodies or their central portions may be infected first and collapse of the body or the intervertebral disk may occur early or late during the infection. The perispinal soft tissues may be thickened from abscess formation or fibrosis. The roentgen findings in the different kinds of spondylitis are similar and a differential etiologic diagnosis from the roentgen findings alone is uncertain.

Spondylarthritis in children was described as a special entity by Saenger; it includes low grade fever and infection of the intervertebral disk and contiguous vertebrae. This entity has not been proved bacteriologically or anatomically but was presumed because of the constitutional signs of infection. All patients complained of pain in the lumbar region or one hip and the lumbar spine was stiff and tender to palpation. Three of Saenger's four patients had suffered trauma. It is possible that trauma served to localize the infection in the lumbar spine. Collapse of the intervertebral disk is said to be much more rapid in

these cases than in Scheuermann-Schmorl disease. Diagnosis depends on the radiologic findings which include narrowing of the intervertebral space and marginal destruction of the contiguous vertebral bodies. Sclerosis of the affected bodies is common later (Fig 9-64). Jamison and colleagues concluded that these lesions are self-limited; complete recovery occurred in their six patients treated with antibiotics although narrowing of the disk spaces persisted. Menelaus in contrast found fusion of the contiguous bodies to be a common sequel. Milone and co-workers cultured material obtained by needle biopsy of the spinal lesions in five patients and recovered staphylococci in all five. In Moes's cultures from five patients two yielded staphylococci. Brucellosis has been neither proved nor satisfactorily excluded as a cause. Lascari and associates found the disease to be self-limited and recommended antibiotics and bed rest for treatment.

REFERENCES

- Jamison R. C. et al. Nonspecific spondylitis of infants and children. *Radiology* 77:355 1961.
Lascari, A. D. et al. Intervertebral disc infection in children. *J. Pediatr* 70:751 1967.
Menelaus M. B. Discitis: An inflammation affecting intervertebral discs of children. *J. Bone & Joint Surg.* 46-B:16 1964.
Milone F. P. et al. Infections of the intervertebral disk in children. *J.A.M.A.* 181:89 1962.
Moes C. A. F. Spondylarthritis in childhood. *Am. J. Roentgenol* 91:578 1964.
Smith R. F. et al. Inflammatory lesions of the intervertebral discs in children. *J. Bone & Joint Surg.* 49-A:1508 1967.

TUBERCULOUS SPONDYLITIS

Tuberculosis of the vertebrae is by far the commonest vertebral infection. It may become manifest during the early stages of the primary pulmonary infection or years later after the primary infection has subsided in the lungs. One or several segments may be involved at any level of the spine; the cervical and sacral portions are least commonly affected. Tubercu-



Fig 9 64 (left) — Sclerosis and marginal destruction of the vertebral body with narrowing of the intervertebral disk in a girl 14 years of age. The lumbar segment of the back was stiff and tender but there was no deformity. The patient had a low grade fever. The clinical and radiologic findings are suggestive of spondyloarthritis but the diagnosis was not proved anatomically or bacteriologically.

Fig 9 65 (center) — Tuberculosis of the spine, marginal type in a boy 3 years of age. Drawing of a roentgenogram. The bodies

of the T 11 and T 12 vertebrae show destruction and compression of the lower and upper margins. The intervening intervertebral space is obliterated.

Fig 9 66 (right) — Tuberculosis of L 3, L 4 and L 5 vertebrae in a patient 2 years of age. The intervertebral space is narrowed between the L 3 and L 4 vertebrae; the space between L 4 and L 5 is much wider notwithstanding collapse of the contiguous vertebral bodies above and below. Drawing of a roentgenogram.

losis is characteristically limited to the bodies, but on rare occasions the neural arches may be infected.

The macroscopic anatomic and the roentgen findings in tuberculosis are characterized by destructive changes in the vertebral bodies, destruction of neighboring intervertebral disks and formation of paraspinal abscesses. Osteoblastic changes are rare early in the disease but may appear later. Usually the destructive changes first appear on the upper and lower margins of the vertebral bodies and the adjacent intervertebral spaces are narrowed or obliterated (Fig 9 65). Less commonly destruction and collapse of the body develop before the intervertebral space becomes narrow (Fig 9 66). When the infection enters the vertebral body through the anterolateral arteries the anterior portion of the body is destroyed first. The anterior margins of the bodies may also be destroyed from secondary extension by contiguity from an overlying paraspinal abscess whose infection originated in bodies one or more segments distant. The paraspinal abscess itself casts a fusiform or rounded shadow of water density which is best visualized in the thoracic levels where the air-filled lungs provide contrast density (Fig 9 67). The shadow of the paraspinal ab-

scess may become visible before the destructive changes in the vertebral bodies are evident. In long-standing cases, paraspinal and psoas abscesses may become calcified (Fig 9-68 and see Fig 4-9).

The roentgen findings of tuberculosis of the spinal column resemble those of nontuberculous infections and of several noninfectious spinal diseases. There are no pathognomonic roentgen changes in tuberculous spondylitis and a conclusive diagnosis cannot be made from the roentgen findings alone. Destruction and deformities of the bodies, narrowing and obliteration of the intervertebral spaces and paraspinal swelling of the soft tissues are all common to many spinal disorders. In particular, narrowing of the intervertebral space is not produced by tuberculous inflammation alone but is also characteristic of purulent spondylitis, fracture, protrusions of the nuclei pulposi (Schmorl's disease), juvenile and adolescent kyphoses and spinal injuries due to lumbar puncture. The compression deformities in tuberculosis do not differ from the compression deformities found in other conditions. Sclerosis is rare early in tuberculosis but is also rare in adolescent kyphosis and fracture. Paraspinal abscess is common in tuberculosis but paraspinal soft tissue

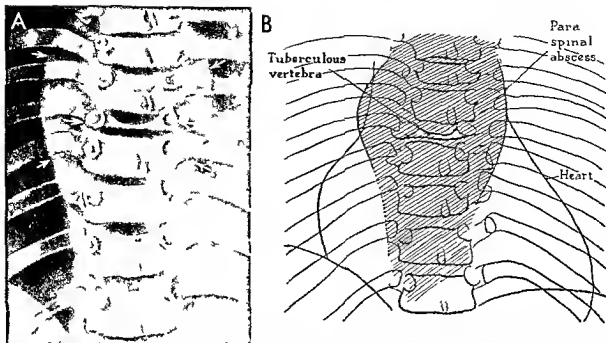
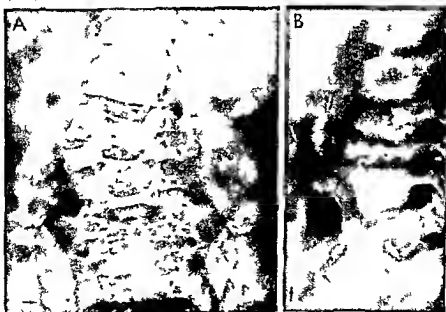


Fig 9-67—Tuberculous paraspinal abscess in a boy 4 years of age. **A**, drawing of a roentgenogram. **B**, diagrammatic sketch of **A**. A fusiform soft tissue mass surrounds the lower portion of the thoracic spine and has displaced the posterior portions of the

lungs away from each side of the spine. The body of the T7 vertebra is collapsed and the adjacent intervertebral spaces are obliterated.

Fig 9-68—Destructive tuberculous and part of collapse of the vertebral bodies of L3 to L5 and the intervertebral disks with calcifying bilateral paraspinal abscesses and ossification of

some of the mesenteric lymph nodes in the right side. **A**, frontal and **B**, lateral projections. This boy was 5 years of age.



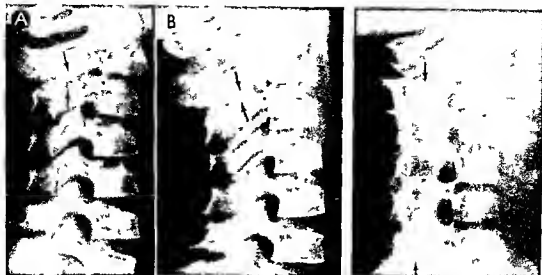


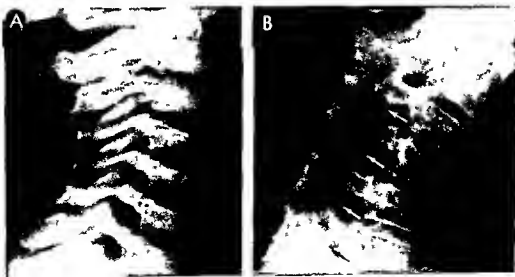
Fig 9 69 (left)—Rheumatoid arthritis of the cervical spine. **A**, at 6 years of age, early destruction of the articular cartilages between the articular processes of C-2 and C-3 is already evident but the cartilaginous spaces are still visible roentgenographically. **B**, at 8½ years, with complete destruction of the same cartilages and bony fusion of the articular processes between the C-2 and C-3 vertebrae. The findings now simulate congenital failure of segmentation of the neural arches. The intervertebral disks between the affected vertebrae are, in contrast, normal roentgenographically.

Fig 9 70 (right)—Bony fusion of all the articular processes of the cervical spine of a girl 9 years of age who had had rheuma-

toid arthritis and a painful cervical spine for over two years. The cartilaginous joint spaces between the articular processes have been obliterated by bony ankylosis following complete destruction of the articular cartilages between the articular processes. Without the history, these acquired rheumatoid fusions of the neural arches might be mistaken for congenital failure of segmentation of the arches. It is noteworthy that the synchondroses between the vertebral bodies, the intervertebral disks are not affected. This is a clear demonstration of the special vulnerability of the tissues of the true joints to rheumatoid disease in the presence of apparent immunity of the tissues of the synchondroses.

Fig 9 71—Rheumatoid arthritis of the cervical spine. **A**, at 2 years of age, when asymptomatic. **B**, at 9 years of age and after six years of clinical cervical arthritis, all of the diarthroses be-

tween the neural arches are fused; the fixed joints between the bodies, the synchondroses, are not affected.



swellings also are found in purulent spondylitis neoplasms vertebra plana and leukemia

✓ RHEUMATOID ARTHRITIS

Spinal lesions are not uncommon in juvenile rheumatoid arthritis especially in girls Barkin and colleagues found radiographic evidence of spinal involvement in 70% of juvenile arthritis. In our experience rheumatoid lesions are common at the cervical levels of the spine in younger children and lesions and clinical signs at the sacroiliac levels are rare. The cervical spine is often the first site affected before there is any evidence of the disease in the more peripheral joints of the extremities. The true joints between the articular processes show the most marked roentgen changes in contrast the synarthroses and particularly the intervertebral disks show surprisingly little roentgen change even in the presence of complete destruction of the articular cartilages of the articular processes.

As in the other true joints rheumatoid disease produces in the spine soft tissue swellings destruction and obliteration of the articular cartilages and their cartilage spaces visible in the roentgen film generalized rarefaction of bone and localized subchondral necrosis of bone. After complete destruction of the cartilages and bony fusion of the articular processes the rheumatoid changes in the cervical spine may resemble congenital failure of segmentation of the neural arches (Figs 9 69 and 9 70). In Figure 9 71 the cervical spine is normal at 2 years of age before the onset of cervical rheumatoid arthritis at 9 years of age and after six years of rheumatoid disease the diarthroses are fused and suggest congenital failure of segmentation.

Baggenstoss found that the inflammatory granulomas of rheumatoid arthritis sometimes break through the walls of the vertebral bodies and weaken and partially destroy them so that compression deformities develop which cannot be differentiated radiologically from destructive lesions of tuberculosis and neoplasms. All of his four patients were adults.

REFERENCES

- Baggenstoss A H et al Rheumatoid granulomatous nodules as destructive lesions in vertebrae J Bone & Joint Surg 34-A 601 1952
Barkin R E et al The spondylitis of juvenile arthritis New England J Med 253 1107 1955
Coss J A and Boots R H Juvenile rheumatoid arthritis J Pediat 29 143 1946

✓ SYPHILIS

In early infantile syphilis McLean found zones of increased and diminished density in the upper and lower margins of the vertebral bodies which resembled syphilitic osteochondritis in the long tubular bones. However he described no destructive changes in the vertebral bodies. The apparent immunity of the

infantile spine to destructive syphilitic changes when extensive destructive changes are present in several other portions of the skeleton is a striking feature of early infantile syphilis and is in marked contrast to the vulnerability of the vertebral column to infantile and juvenile tuberculosis.

REFERENCES

- Doub H P and Badgley C E Roentgen signs of tuberculosis of the vertebral body Am J Roentgenol 27 827 1932
Harris H J Brucellosis Problems in diagnosis and treatment Bull New York Acad Med 22 147 1946
McLean S III Correlation of the roentgenologic picture with the gross and microscopic examination of pathologic material in congenital osseous syphilis Am J Dis Child 41 607 1931

Hypovitaminoses

✓ VITAMIN D

During the early phases and in the milder cases of rickets the vertebral changes are limited to a slight generalized osteoporosis. In more severe cases the osteoporosis is more marked the vertebral bodies are thin and the intervertebral spaces are widened. Compression deformities of the bodies are rare and do not appear until late in severe cases. During healing marginal lines of increased density appear on the upper and lower surfaces of the vertebral bodies which are analogous to the posttraumatic transverse lines in the long tubular bones.

Spinal curvatures develop only in the more severe cases and are due primarily to muscular weakness and relaxation of ligaments deformities of the thoracic cage are often associated with the spinal deformities. Kyphosis is the commonest spinal deformity usually several segments in the lower thoracic and upper lumbar levels are affected. Rachitic kyphosis which appears after the infant begins to sit erect forms a long shallow curve in contrast with the narrow deep angulation of Pott's disease. Rachitic scoliosis is associated with and is secondary to rachitic deformities in the pelvis and lower extremities.

VITAMIN C

In scurvy there is rarely any clinical evidence of spinal involvement and the roentgen signs in the vertebral column have not been adequately described. Inasmuch as scurvy interferes with endochondral bone formation at all sites in the skeleton where it has been studied it is probable that a similar interference operates in the growth zones in the vertebrae. I have seen spinal rigidity and regional spinal tenderness in a scorbutic infant which were promptly cured by the administration of orange juice. Roentgenograms of the spine unfortunately were not made.

REFERENCE

- Oppenheimer A Rickets of the spinal column Internat. Radiol. Rev 8 332, 1939

Marginal Lines

Bands of increased density form on the upper and lower edges of the growing vertebral body under the same conditions in which Parks's transverse lines appear in the ends of growing long bones. In the vertebral body however the line formation is not as rapid or as marked owing to the limited slow growth in each segment of the spine. In experimental bismuth poisoning heavy marginal lines have been produced in the vertebral bodies of young dogs.

REFERENCE

Caffey J. Changes in the growing skeleton after the administration of bismuth. *Am J Dis Child* 53:56, 1937.

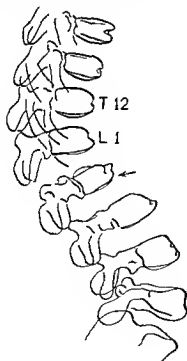
Endocrine Disorders

The maturation of the spine may be delayed or accelerated by endocrine dysfunction in the same way that the maturation of the long bones is affected. In

hypothyroidism the development of the spine is retarded and individual vertebral bodies may be deformed (Figs. 9-72 and 9-73). In some of our cretins the spinal kyphosis persisted after treatment when there were good results in all other parts of the skeleton. In the adrenogenital syndrome and in hypergonadism the maturation of the spine is accelerated.

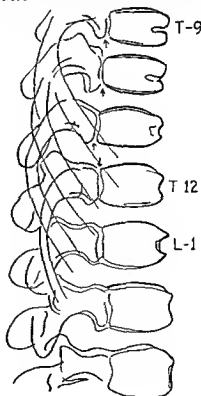
In Cushing's adrenohypophyseal syndrome the vertebrae are conspicuously and disproportionately demineralized and often show mechanical compression deformities common to all types of weakened vertebrae. Expansion of the nucleus pulposus in the contiguous intervertebral disks compresses the vertebral body between them so that the central segment of the body is narrower than its edges—the so-called codfish vertebra which casts an hourglass-shaped shadow in lateral projection. In some cases the nucleus pulposus may actually break through the vertebral plate and protrude into the vertebral body and form a Schmorl node in it. Curtiss et al. found multiple fractures and compression deformities in patients given prolonged courses of cortisone and corticotropin. One

Fig. 9-72 (left)—The vertebral column of a hypothyroid black boy 3 years of age. Maturation of the vertebrae is retarded and the L1 body is hypoplastic. There are compensatory hyperplasia and deformity of the anterior portion of the L2 body. The kyphotic deformity persisted despite long continued and otherwise effective thyroid therapy. In the 12th year marked kyphosis supervened.



dyolysis and vertebral deformity were at the level of the 5th (Fig. 9-50).

Fig. 9-73 (right)—Infantile form of the vertebral column in an untreated hypothyroid girl 8 years of age. The vertebrae have the oval, only notched bodies characteristic of the 1st year of life. The arrows are directed at an open neurocentral synchondrosis.



of their patients was a boy 9 years of age. Growth of the long bones is retarded or ceases in advanced cases. Opaque renal stones are not uncommon in Cushing's syndrome.

Hyperparathyroidism produces essentially the same basic changes in the vertebral bodies as in the long bones. The decalcified and weakened bodies usually show the compression deformities characteristic of all weakened vertebral bodies. During infancy and before weight bearing by the spine there may be no compression deformities even in the presence of marked demineralization of the vertebrae and the long tubular bones (see Fig. 8-823).

REFERENCES

- Chute A. L., Robinson G. C., and Donohue W. L. Cushing's syndrome in children. *J. Pediatr.* 34:20 1949.
Curtiss P. H. Jr., et al. Vertebral fractures resulting from the prolonged use of cortisone and corticotropin therapy. *J.A.M.A.* 156:467, 1954.
Evans P. R. Deformity of the vertebral bodies in cretinism. *J. Pediatr.* 41:706 1952.
Swoboda, W. Angular dorsolumbar kyphosis as an unrecognized skeletal sign of congenital myxedema. *Fortschr. Geb. Röntgenstrahlen* 73:740 1950.

Reticulosis

One or more of the vertebrae may be affected in cholesterol reticulosis (Schuller-Christian), eosinophilic granuloma (Fig. 9-74) and Gaucher's kersin reticulosis. The hyperplastic granulomatous tissue replaces bone and produces vertebral defects in roentgenograms. Collapse of the vertebral bodies and spinal curvature may result. The intervertebral spaces usually retain their normal width, even in the presence of extensive destruction in contiguous vertebrae.

REFERENCES

- Compere E. L., et al. Vertebral plana (Calvé's disease) due to eosinophilic granuloma. *J. Bone & Joint Surg.* 36-A:869 1954.
Dicke L. E., et al. Vertebra plana and the histiocytoses. Report of a case with involvement of 5 vertebrae. *J. Bone & Joint Surg.* 37-A:126, 1955.
Jaffe H. L. and Lichtenstein I. Eosinophilic granuloma of the bone. *Arch. Path.* 37:98 1944.
Reiss O. and Kato K. Gaucher's disease. A clinical study with special reference to the roentgenography of the bones. *Am. J. Dis. Child.* 43:365 1932.

Hemolytic Anemias

Sickle cell anemia in adults often causes changes in the vertebral bodies, compression deformities with corresponding widenings of the intervertebral disks develop owing to demineralization and weakening of the vertebral bodies. The lower thoracic and lumbar segments are most frequently affected. Legant and Ball observed necrosis of lumbar bodies, presumably caused by infarction and ischemic necrosis, in a black patient 30 years of age who had sickle cell anemia. Vertebral lesions have not been reported in



Fig. 9-74—Eosinophilic granuloma of the spine of a girl 2 years of age who had multiple eosinophilic granulomas in the skull, ribs, pelvic bones and in the bones in the extremities. The bodies of T2, T6 and T8 show massive destruction with compression deformities.

the roentgen studies of juvenile sickle cell anemia, so far as I know.

Cooley's erythroblastic anemia—All parts of the vertebrae become osteoporotic and coarsely reticulated. The vertebral bodies tend to be hypoplastic with a relative elongation of their cephalocaudal axes. Compression deformities are surprisingly rare. However, in one case we did find multiple destructions and compressions of vertebral bodies in the lower dorsal and lumbar levels of a girl 17 years of age. She had enormously enlarged liver and spleen and suffered from chronic hemochromatosis. It was believed that the excessive drag of the heavy liver and spleen may have been a causal factor in the vertebral fractures in this case.

REFERENCE

- Legant O. and Ball R. P. Sickle-cell anemia in adults. Roentgenographic findings. *Radiology* 51:665 1948.

Leukemia

Disruptive and productive changes similar to those found in the long bones, may also develop in the spinal column in leukemia. In the case of severe de-

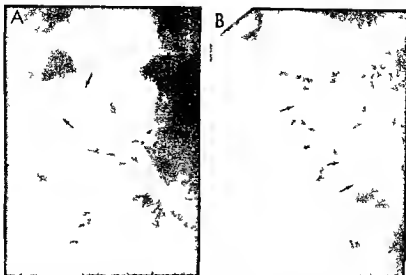
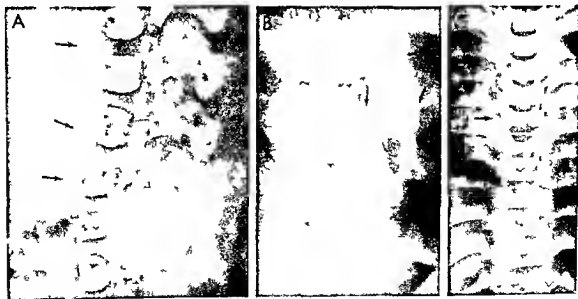


Fig 9.75 —Osteoid osteoma (macroscopic diagnosis) of the right pedicle lamina superior and inferior articular processes and the transverse process of the L3 vertebra of a girl 10 years of age who had had severe low back pain at night for two months. A: frontal and B: lateral projections. The scale of

changes (arrows) are continued to the right side of the neural arch and are better demonstrated in lateral projection (B). The spinous process is not affected. The nodus was not demonstrable radiographically.

Fig 9.76 —Destruction of vertebrae by intraspinal neuroblastoma. A: extensive destruction of neural arches of the vertebral bodies of L3 to L5 with collapse of the body of L5 of an infant 5 months of age. B: partial destruction and collapse (arrows) with sclerosis of the left side of the vertebral body of a child 6

years of age. The lateral arrow points to a parasagittal swelling of soft tissue at the same level. C: bilateral collapse and sclerosis of T6 vertebral body of a boy 5 years of age without parasagittal soft tissue swelling.



struction and weakening of the bodies they collapse and assume wedge-shaped or biconcave contours. According to Hildebrand leukemic changes in the spine may be visible radiologically months before clinical manifestations become evident.

REFERENCES

- Epstein B S. Vertebral changes in childhood leukemia. *Radiology* 68:65 1957.
Gouglens K. *et al*. Spinal changes during leukemia in children. *Fortschr Geb Röntgenstrahlen* 88:309 1958.
Hildebrand H. Leukemia of the spine in children. *Fortschr Geb Röntgenstrahlen* 72:709 1950.

Cysts

Extradural cysts in the lumbosacral levels are a rare cause of low back pain in children. They are characterized radiographically by defects in the dorsal segments of the contiguous vertebral bodies which produce local expansions of the spinal canal. The studies of Elsberg indicated that most of the extradural cysts in the midthoracic levels occur in patients younger than 20 years.

REFERENCES

- Elsberg C A. *et al*. Symptoms and diagnosis of extradural cysts. *Bull Neurol Inst* 3:395 1934.
Schurr P H. Sacral extradural cysts. An uncommon cause of low back pain. *J Bone & Joint Surg* 37 B:601 1955.

Neoplasms

PRIMARY LESIONS

Primary tumors of the vertebrae are rare in infants and children. Osteogenic sarcomas cause extensive destruction of the bodies and neural arches; fragmentation and collapse of the body and spinal curvature may follow. A paraspinal neoplastic mass may cast a paraspinal shadow of water density which resembles the shadow cast by a paraspinal tuberculous abscess. Chordomas, which arise from the primitive notochord or its remnants, destroy the intervertebral disks and later may extend into and destroy adjacent vertebral bodies. Chordomas are exceedingly rare in infants and children, in view of the fact that they represent the persistence of the embryonic tissues of the primitive notochord. The rare sacrococcygeal chordoma or chordoblastoma is characterized by rapid growth and rapid destruction of the coccyx and lower sacral segments. This tumor is usually palpable per rectum and later may become visible as a swelling in the buttock and back. Although enlargement by direct extension is rapid, metastasis by blood or lymph is rare. Several have occurred at the base of the skull in older children.

Hemangiomas are probably the commonest tumors of the spine; many of them produce no symptoms. Angiomas are characterized roentgenographically by a spongy or honeycomb osteoporosis. The intervertebral spaces are normal in width.

Giant cell tumors may produce massive destruction of the vertebral body and collapse of the adjoining intervertebral spaces.

Osteoid osteoma should be suspected when back pain is worse at night than during the day and associated with regional muscular spasm, paravertebral tenderness and localized scoliosis. Aspirin often gives substantial relief from this pain. Such patients should have carefully made stereoscopic films of the spine in multiple projections; planigrams should be made when the conventional methods give negative results. The radiographic findings are similar to those in other parts of the skeleton and consist of a sclerotic patch with a central radiolucent nidus located most often in the laminae (Fig. 9-75). Surgical excision of the nidus usually results in immediate and permanent relief from the pain.

REFERENCES

- Freyberger R H. Osteoid osteoma of the spine. A cause of backache in children and young adults. *Radiology* 75:232 1960.
Wood E H Jr and Humadi G M. Chordomas. A roentgenologic study of 16 cases previously unreported. *Radiology* 54:706 1950.

SECONDARY NEOPLASMS

Secondary vertebral neoplasms are also rare in infants and children. Metastases from sympathicoblastomas may lodge in the spine and produce destruction and deformity. The primary growth of a paraspinal sympathicoblastoma may impinge on or grow into the spine and the neighboring ribs and cause necrosis by direct pressure. Metastatic adrenal sympathicoblastoma may cause vertebral deformities at several levels (Fig. 9-76).

In myelogenous leukemia, lymphatic leukemia and lymphoblastomas, destruction and compression of the vertebrae have been observed. The intervertebral spaces may be narrowed, widened or normal.

The spine is a common site of metastasis by embryonal rhabdomyosarcoma; spinal segments at several levels may be affected (Fig. 9-77).

REFERENCE

- Caffey J and Andersen D. Metastatic embryonal rhabdomyosarcoma in the growing skeleton. *Am J Dis Child* 95:581 1958.

TUMORS OF THE SPINAL CORD

Tumors of the spinal cord may develop and grow without producing detectable roentgen changes in the adjacent vertebrae. Not infrequently, however, valuable diagnostic vertebral changes do appear. Local pressure may cause erosions in the contiguous portions of the vertebrae in the arches or on the posterior surface of the bodies. Extensive destruction of the body may go on to pathologic fracture and compression deformities. One of the most helpful diagnostic

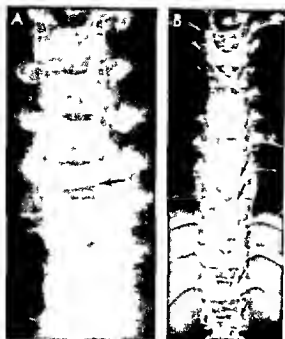


Fig 9 77—Metastatic embryonal rhabdomyosarcoma of the spine. A, destruction and collapse of the vertebral body and left pedicle of the D 6 vertebra of a boy 8 1/2 years of age whose primary neoplasm was in the muscles above one ankle with metastases to flat and long bones as well as the single vertebral body. B, metastases in several vertebrae (arrows) with compression deformities in the T 2, T 4, T 6 and T 12 segments and L 1 of a boy 52 months of age whose primary neoplasm was in the orbit. There were multiple skeletal metastases in several round and flat bones.

changes is the regional widening of the interpediculate spaces which produces a fusiform widening of the spinal canal at the level of the intraspinal tumor (Fig 9 78). At the same levels the medial edges of the pedicles are flattened or in severe cases bent into concave contours on their medial aspects. Primary intraspinal tumors often project externally through the spaces between the vertebrae. In the thoracic levels these neoplastic paraspinal masses cast a shadow which resembles that of Pott's abscess. Leukemic paraspinal masses which originate from intraspinal leukemic growths cast similar paraspinal shadows. Tumors of the spinal cord rarely cause productive changes in the adjacent vertebrae and seldom contain sufficient calcium for roentgen visualization, although microscopic calciferous foci are frequently found in many of them. Myelography with Pantopaque as the contrast substance is the most accurate



Fig 9 78—Intraspinal neuroblastoma (microscopic diagnosis) in which the interpediculate spaces are increased and the pedicles eroded and elongated. Large portions of the pedicles of L 2 and L 3 are destroyed. In A, frontal projection, the numbers on the right pedicles represent measurements in millimeters of the maximal interpediculate distances; they are all elongated. B, lateral projection.

roentgen method for the identification and localization of intraspinal tumors and inflammatory obstructive lesions in the spinal subarachnoid space.

REFERENCES

- Anderson F M, and Carson M G. Spinal cord tumors in children. *J Pediatr* 43:190, 1953.
- Bucy P C, and Capp C S. Primary hemangioma of bone with special reference to the roentgenologic diagnosis. *Am J Roentgenol* 23:1, 1930.
- Chambers W R. Intraspinal tumors in children resembling anterior poliomyelitis. *J Pediatr* 41:288, 1952.
- Elsberg C A, and Dyke C G. Diagnosis and localization of tumors of the spinal cord by means of measurements made on x ray films of the vertebrae and correlation of clinical and x ray findings. *Bull Neurol Inst New York* 3:359, 1934.
- Sussman M L, and Kugel M A. The roentgen diagnosis of spinal deformities. *Am J Roentgenol* 30:163, 1933.
- Wood E H, Jr. An Atlas of Myelography (Washington D C: American Registry of Pathology, 1946).

SECTION 10

The Neonate and Young Infant

Special Procedures in Diagnosis

THE SEPARATE GROUPING of special procedures in pediatric radiology is admittedly artificial since their use is repeatedly illustrated elsewhere in these volumes. The highly refined techniques of cardiac and neurologic investigation are omitted as are discussions of bronchography and such rarely used methods as sialography. We have tried to view methods of arteriography, venography, lymphangiography and nuclear scanning in terms of risk to the patient weighed against the information gained in the hope that the pediatric patient will benefit from their intelligent application. Some portions of this discussion may

DRS WALTER E. BERDON and DAVID H. BAKER have written Section 10, THE NEONATE AND YOUNG INFANT

Fig 10-1 —A, ascites secondary to cytomegalic inclusion disease. The ascitic fluid lateral to the medially displaced liver and small bowel loops is lucent. Liver density and small bowel wall opacification parallel each organ's content of opacified blood.

soon be obsolete. Ultrasound offers great hope. Nuclear medicine will emerge as a separate discipline, although the radiologist will continue to use it as part of his evaluation with films and scans (heat sound isotopes) of normal and abnormal structures and functions.

Total Body Opacification

The recognition and utilization of total body opacification represent a major advance in radiographic diagnosis. Most satisfactory in infants, it can be utilized at any age if sufficient contrast material is used. It is part of and supplementary to intravenous pyelography and the two studies are done at the same time.

(Courtesy of Dr. J. F. O'Connor, Boston.) B, ascites secondary to perforation of the colon in an infant with cystic fibrosis and meconium peritonitis. Arrows indicate calcifications. Small bubbles of free air are present lateral to the liver.





Fig 10-2—Wilms tumor. A: total body opacification shows a lucent mass contiguous with and part of the right renal outline. B: right renal and left lower pole nephrograms demonstrate functioning renal tissue. The mass had been noted for several months



and thought to be spleen. B: excretory phase of the same study shows calyceal dilatation and slight dilatation of left lower pole. A large partly necrotic and cystic Wilms tumor was found in the upper two-thirds of the left kidney on surgical exploration.

O'Connor and Neuhauser were the first to point out that when the dose of triiodinated urographic contrast agents approaches 2 cc/kg, all vascularized tissues such as the liver are rendered opaque in proportion to their vascularity. Even the walls of the hollow viscera become visible (Fig 10-1 A). This phenomenon precedes and for a short time overlaps the renal excretory phase. It does not reflect vicarious excretion by the liver in the usual case. This then is a simple intravenous method of evaluating masses of water density in plain films. The seeming subsequent loss of density during the total body opacification phase relates directly to the relative decrease of blood content of the mass. Conversely, the degree of increased density reflects the relatively greater content of opacified blood. The method is comparable to the late capillary phase of aortography.

Caution must be used to avoid serious errors of interpretation. Thus lucency means relatively reduced blood content and not necessarily cystic or benign. Both benign and malignant hepatic tumors (such as hemangioma, hepatoma) and renal tumors (malignant Wilms, benign hamartoma) and adrenal tumors (neuroblastoma, ganglioneuroma, cortical carcinoma) have been seen with varying degrees of

lucency, often mottled, reflecting cystic and necrotic and avascular areas (Figs 10-2 and 10-3) and exact diagnosis requires histologic examination. Examples of the methods' usefulness are so numerous that only a few can be given here.

Ascites with medial hepatic displacement is seen as a lucent (relatively black) space contrasted with the dense (relatively white) liver (see Fig 10-1). An intra-splenic posttraumatic epidermoid cyst appears as a lucent circular mass surrounded by dense splenic parenchyma (Fig 10-4).

The problem of the newborn with an abdominal mass lends itself to this technique. The nonfunctioning multicystic kidney is visualized as a lucent mass without subsequent excretion (Fig 10-5). In contrast the hydronephrotic kidney is a lucent mass (representing the urine-filled renal pelvis) with delayed films showing the opacified dilated renal collecting system (Fig 10-6). Adrenal hemorrhage in the newborn is seen as a lucent suprarenal mass with downward and lateral renal displacement (Fig 10-7). Renal vein thrombosis in the newborn may present a large kidney-shaped mottled blackish image according to the degree of engorgement with blood and decreased renal function (Fig 10-8). A cystic coccygeal



Fig 10-3 —Giant hepatic hemangioma with congestive heart failure in a newborn. A: total body opacification shows vascular (dense) and avascular (lucent) areas in the right lobe of the liver. The kidneys were normal in later films. The patient died of the

effects of arteriovenous shunting. B: postmortem aortogram shows regular vascular spaces in the hemangioma surrounding the cystic necrotic areas. Note the huge draining hepatic vein. (From Berdon *et al*.)

Fig 10-4 (left) —Infected epidermoid cyst of the spleen demonstrated in nephrotomogram. The apparently gas-filled left upper quadrant space is actually the avascular center of the spleen surrounded by the normally dense splenic tissue. (Courtesy of Drs. H. Grossman and P. Winchester, New York.)

Fig 10-5 (right) —Right cystic dysplastic kidney in a newborn.

The intravenous pyelogram shows a nonfunctioning flank mass which is actually a group of cysts, the largest of which is seen as a lucent space surrounded by dense images of the liver and other viscera. The left kidney despite odd appearance and anatomy of the collecting system functioned well. (Courtesy of D. G. Currar, no Dallas, Tex.)





Fig 10-6—Hydronephrosis secondary to ureteropelvic obstruction of the left kidney of a newborn infant with a left flank mass. **A** Total body opacification phase shows a large lucent renal pelvis with opaque left renal parenchyma (arrows). The



right kidney is normal. **B** At 24 hours there is gradual opacification of the contents of the partly blocked renal pelvis. The kidney was saved by resection of the ureteropelvic junction and part of the renal pelvis and reconstructive pyeloplasty.

teratoma appearing as a lucent presacral internal extension (Fig 10-9) required a combined abdominoperineal excision.

The total body opacification phenomenon may not be as dose-related as assumed. It can be noted in retrospect in pyelograms made in the 1950s when doses were far below those now used. Also, it is not always

produced when high doses are used. Its safety requires that the following precautions be taken: (1) The patient should not be dehydrated; (2) The dose (3–5 cc/kg for the newborn, 1–2 cc for the older child and adult) should be injected intravenously over 1–2 minutes and not as a rapid high pressure injection through a large catheter. In the older child and adult

Fig 10-7 (left)—Bilateral adrenal hemorrhage in a newborn infant who had bilateral masses and jaundice from hemoglobin breakdown with adrenals. Total body opacification shows the lucent hemorrhagic adrenals with dense liver above and kidney below. Calcifications developed as the masses shrank in the following weeks and months.

Fig 10-8 (right)—Renal vein thrombosis. A right flank mass developed in a 2-week-old infant with hematuria, casts, and proteinuria. Hypertension was marked. Total body opacification shows a lucent kidney-shaped mass in the right renal area. Nephrectomy for suspected renal tumor reveals an infarcted right kidney due to major and minor renal vein thrombosis.

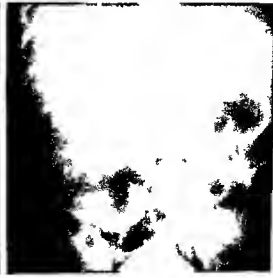
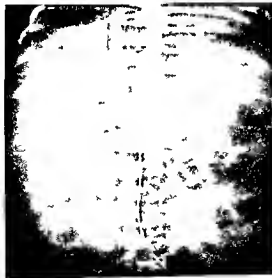




Fig 10-9—Sacrococcygeal teratoma with presacral extension. Intravenous pyelogram, lateral projection, shows both bladder (B) and rectum (A) displaced anteriorly with a lucent area (not apparent in plain films) reflecting avascular components. An operation on a cystic hygomatous element was removed from the presacral space.

1 cc/lb of 90% sodium Hypaque can be used and with tomography of the kidneys, liver or spleen depending on the region of interest.

REFERENCES

- Berdon W E et al. Giant hepatic hemangioma with cardiac failure in the newborn infant. Value of high dosage intravenous urography and umbilical angiography. *Radiology* 92:1523 1969.
- Kurlander C J et al. Total body opacification in diagnosis of Wilms tumor and neuroblastoma. *Radiology* 89:1075 1967.
- O'Connor J F and Neuhauser E B D. Total body opacification in conventional and high dose intravenous urography in infancy. *Am J Roentgenol* 90:63 1963.

Arteriography

The Seldinger method of percutaneous catheterization of the aorta allows visualization of the aorta and its branches. With meticulous technique and adequate sedation the method can be applied to children and even infants. Underlying the use of such angiographic studies is the belief that the demonstrated vascular findings reflect the primary pathologic processes

though these are not of themselves of vascular nature. Thus tumors have been studied in many children and it is this area that is emphasized here.

The initial angiographic experience with tumors was in adults. The masses were mainly renal and were usually either clear cell carcinoma or benign cysts. Since the former were commonly quite vascular and the latter avascular, a logical conclusion seemed to be that vascular meant malignant and avascular meant benign. It is now well recognized that some highly malignant tumors are avascular and some benign lesions (abscesses, infected hydronephrotic kidneys) are vascular. The vessels within and around malignant tumors tend to have a bizarre appearance with tortuosity and microaneurysms, normal tapering and branching are lacking. Arteriovenous shunts are observed. These findings reflect an abnormal vascular supply but do not of themselves mean malignancy. It is important to emphasize that angiographic study cannot replace histologic study in the establishment of malignancy. With this background, certain conclusions can be drawn regarding the value of angiography in the study of abdominal tumors in infants and children.

Wilms tumor—Extremely rare during the newborn period (when renal tumors are usually benign fetal hamartomas), Wilms tumor is the commonest renal neoplasm from about 6 months of age through the next decade, with most patients less than 5 years of age. Occasionally bilateral, the tumor commonly replaces only a part of the kidney and distorts the remaining collecting system. Usually there is some residual renal function. The tumor may totally replace kidney or extend into the renal vein with absence of visualization in the intravenous pyelogram.

Aortography and selective renal arteriography have been applied to the study of Wilms tumor. Some tumors are highly vascular (Fig 10-10 A) with intertwining patterns of neovascularity resembling strands of spaghetti. In others the only signs are indistinct or broken nephrographic outlines (Fig 10-10 B) with sparse, if any, neovascularity. A rare patient has congestive heart failure, the tumor acting as an arteriovenous shunt with flooding of the inferior vena cava and right side of the heart (Fig 10-11). Rarely does the arteriogram identify a tumor when the intravenous pyelogram has not led to the same diagnosis. Use of selective arteriography to study the opposite normal kidney may aid in diagnosing small contralateral foci of tumor.

Obviously the arteriogram will indicate that the mass is a tumor and not a benign cyst; this should have been apparent from the intravenous pyelogram. Similarly, the intravenous pyelogram should exclude a hydronephrotic blocked area by the absence of calyces and crescents. The arteriogram cannot reliably distinguish Wilms tumor from renal hamartoma (benign) or from renal carcinoma of the adult clear cell type, both of which occur in children. As noted later in the comments on bronchial arteriography

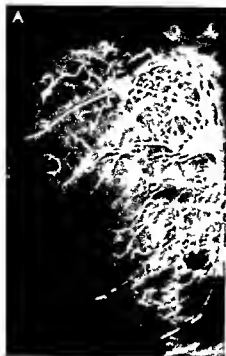


Fig 19-10—Wilms tumors. A: arteriogram showing a huge tumor with intertwining patterns of neovascularity involving the right kidney which is virtually replaced by the tumor. (A: courtesy of Dr. H. Grossman, New York.) B: defect in the nephrogram

of a small tumor of the upper pole of the right kidney containing few vessels. The renal axis is displaced from the midline by the tumor. (B: courtesy of Dr. C. H. Meng, New York.)

Fig 19-11—Highly vascular Wilms tumor of the left kidney of a child with congestive heart failure. A: arteriogram demonstrates the vascularity. B: venous phase shows massive arterio-

venous shunt into the dilated inferior vena cava. Resection of the tumor relieved the congestive heart failure. (Courtesy of Dr. K. L. Bron, Pittsburgh.)



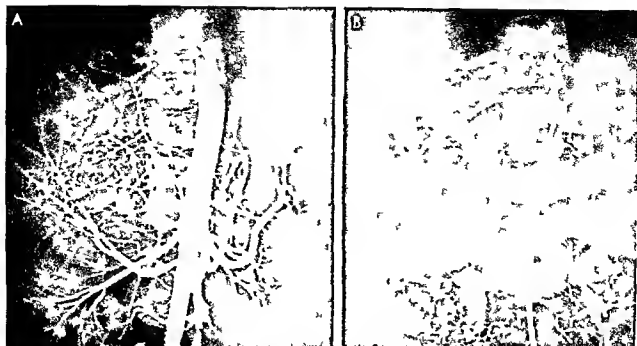


Fig. 10-12.—Right adanal neuroblastoma. A: midstream aortogram demonstrating displacement of the right anal artery and hyperplastic supra-anal vessels. B: venous phase shows intact

though displaced right anal outline and neovascular pattern within the tumor. (Courtesy of Dr. M. K. Ng, New York from Baron and Baker.)



Fig. 10-13. Left retroperitoneal neuroblastoma. A: midstream aortogram shows stenosis of the left renal artery. Spasm of tumor vascularity develops from abdominal and lumbar arteries. B: venous phase shows little if any persistent neovascularity. The upper pole of the left kidney has an indistinct outline while the lower pole is invaded by the tumor. (Courtesy of Dr. G. Debrun, Paris.)

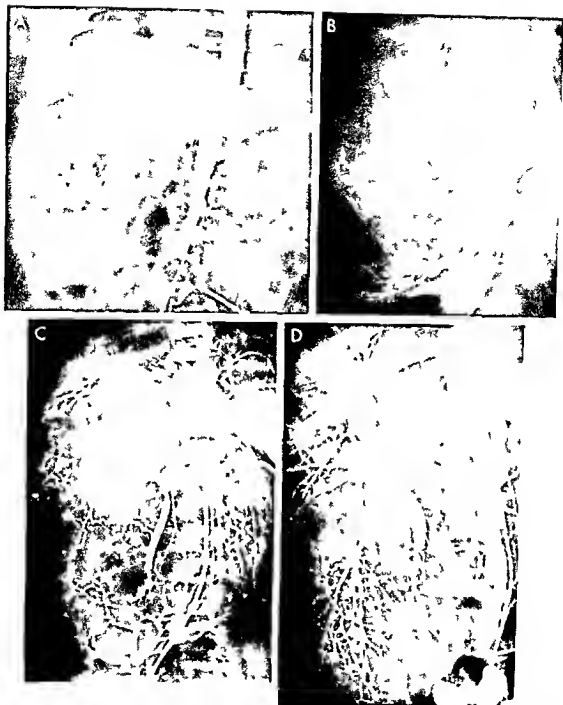


Fig 10-14 A in a newborn with congestive heart failure from arteriovenous shunting in a giant right hepatic hemangioma the umbilical aortogram demonstrates regular vascular pooling. The venous phase (see Fig 10-16) showed equally massive venous shunting. B in an infant 4 months of age with huge right hepatoblastoma the selective celiac arteriogram shows displacement of hepatic arterial feeders to the tumor. Central avascular areas contained hemorrhage and necrosis. C in a child with benign

hepatic hamartoma, the celiac arteriogram delineates a regular arterial surrounding avascular areas in the right hepatic lobe (C courtesy of Dr D. Darling, Boston, Mass.). D in an adolescent patient with adult type carcinoma of the right hepatic lobe, the selective celiac arteriogram demonstrates extensive neovascularity of the inferior aspect of the right lobe (D courtesy of Dr J. C. Leonard, New York).

metastases of Wilms' tumor in the lung can be studied in terms of the bronchial blood supply. Selective arteriography of each kidney may aid in planning surgery for gross bilateral Wilms' tumor.

Neuroblastoma—This other common retroperitoneal tumor of childhood has angiographic patterns ranging from marked vascularity (Fig 10-12) to avascularity (Fig 10-13). The experience of Debrun and colleagues in Paris has been that the avascular pattern is the more common. To establish a correct radiographic diagnosis, the demonstration of renal displacement by a mass must be correlated with the clinical history. Hypertension might suggest pheochromocytoma and osteoporosis and glycosuria a cortical adenoma or carcinoma. With neuroblastoma (or the more benign ganglioneuroblastoma and benign ganglioneuroma) there may be elevated urinary catecholamine excretion, diarrhea, or signs of cerebellar ataxia. Arteriography has little value in establishing the diagnosis since the well-performed intravenous pyelogram clearly shows the extent of renal displacement. The infant with calcifications, displaced kidneys and ureters, and a mass usually has a neuroblastoma regardless of the vascular pattern seen on arteriography.

Hepatic tumors—Though rare, hepatic tumors lend themselves to arteriographic study even in the neonate. Both benign (hemangioma, hepatocellular carcinoma) and malignant tumors (hepatoblastoma, hepatoma) may be encountered. The tumors derive their blood supply from the hepatic artery, splenoportography usually shows the tumor as an area devoid of vas-

cularity, and liver scanning shows a cold area. The arteriographic pattern may be similar in benign and malignant tumors. Histologic, not radiologic findings, establish the benignity or malignancy. Benign hemangioma (Fig 10-14 A) may kill by arteriovenous shunting. Hepatoblastoma (Fig 10-14 B) can metastasize to lung and bone and is lethal. Benign hamartoma (Fig 10-14 C) may be very vascular in arteriograms mimicking malignancy. Adult-type hepatoma (Fig 10-14 D) may show neovascularity, although this per se does not indicate malignancy. Arteriography may disclose anomalies of blood supply such as a right hepatic lobe supplied by a superior mesenteric branch, thereby assisting the surgeon in planning for excision.

BRONCHIAL ARTERIOGRAPHY—The bronchial arteries arise in varying fashion to supply the lung and anastomose with pulmonary arteries. They can be visualized by midstream aortography (Fig 10-15) or selective catheterization (Fig 10-16). The bronchial arteries largely supply metastases in the inner half of each lung field; an example is shown in Figure 10-15 of a Wilms' tumor. Peripheral lung metastases may derive their blood supply solely from the pulmonary arteries. Repeated pulmonary infections cause enlargement of the bronchial arteries (Fig 10-16). It is possible that some of the ill-defined radiographic findings described as prominent bronchopulmonary markings or prominent hilar images represent some bronchial artery prominence as well as lymph node enlargement.

Trauma—bleeding—Selective arteriography is well

Fig 10-15 (left)—Large right middle lobe metastases from Wilms' tumor. Midstream aortogram demonstrates its bronchial arterial blood supply. Other films revealed some lesser supply from inferior phrenic and intercostal arteries. The mass disappeared after radiotherapy and chemotherapy.



Fig 10-16 (right)—Selective right-sided arteriogram showing prominent anastomosing bronchial arteries in an infant with right hepatic tumor and frequent respiratory infections (same patient as in Fig 10-14 B). No tumor developed in the right lung although the child died of left-sided metastases.



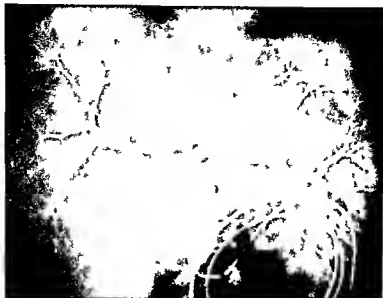


Fig 10-19—Transumbilical venous demonstration of the portal vein in an infant 9 months of age with type I glycogen storage disease and massive hepatomegaly. The veins are normal except for stretching to encompass the liver, which contains extensive

glycogen deposits. The catheter was passed by extraperitoneal umbilical vein cutdown with dilatation of the collapsed vein. The left lobe extends well into the left upper quadrant to the left flank. (Courtesy of Dr. R. P. Timmen, Vancouver, Canada.)

many patients and thus can be dilated by an extraperitoneal approach. Portography and portal pressure recording are possible. For example, a 9-month-old infant with type I glycogen storage disease had hepato-

megaly. Umbilical venography showed the splaying of otherwise normal intrahepatic branches of the portal vein (Fig 10-19).

Fig 10-20—In a premature infant with a huge right renal tumor, intravenous pyelography demonstrated slight residual function and the total body opacification phase delineated mottled vascularity (not shown). The umbilical aortogram shows two renal arteries supplying the rather vascular benign renal tumor. Pathologic diagnosis was fetal renal hamartoma.



Umbilical aortography—The paired umbilical arteries can be catheterized to visualize the thoracic and abdominal aorta and branches. Aortic injection is midstream. It is even possible to pass the catheter through the ductus arteriosus into the pulmonary artery or into the brachiocephalic vessels. Selective catheterization of the abdominal branches in the newborn is possible, but has not been accomplished. A prime use of this method is in study of vascular masses such as neonatal hepatic (Fig 10-18 B and C) and renal tumors (Fig 10-20) for assessment of the blood supply and degree of vascularity. Our illustrations demonstrate that both hepatic and renal masses were highly vascular, both were benign, the hepatic mass being a giant cavernous hemangioma, the renal mass a benign renal hamartoma of the fetal type, not to be confused with Wilms tumor. Angiographic signs of hypervascularity are no substitute for histologic evidence of malignancy.

Kaufmann has used failure to visualize the renal arteries as a confirmatory sign of renal agenesis (Fig 10-21). It is possible that this could be mimicked by layering and streaming of contrast material in such a way that the renal artery, though present, is not opacified. Similarly, a hypoplastic renal artery might be mistaken for a lumbar artery.

Umbilical arteriovenous fistula formation and congestive heart failure—The fetus normally utilizes the low resistance placenta as an organ of respira-



Fig 10 21 —Umbilical aortogram of an infant with renal agenesis. Note pneumomamastium and the small pelvic bony outlet. No renal arteries are seen in this anuric newborn — a confirmatory sign of renal agenesis. (Courtesy of Dr. H. J. Kaufmann, Basel, Switzerland.)

Fig 10 22 —Umbilical arteriovenous malformation in a newborn with congestive heart failure. A, umbilical aortogram shows huge arterial feeders including epigastric arteries and early venous filling. B, venous phase demonstrates a huge umbilical

vein and communicating portal branches. Heart failure was cured by ligation of epigastric and umbilical artery feeders and excision of the umbilical region. (Courtesy of Dr. D. E. Murray and associates, San Mateo, Calif.)



tion (fetal lung) and waste elimination (fetal kidney) with oxygenated blood returned through the umbilical vein to the ductus venosus. When the latter is open, flow passes to the right heart and almost completely through the foramen ovale to the left side of the heart. The paired umbilical arteries return the body's mixture of right and left sided blood for oxygenation and waste removal.

After birth, congestive heart failure can result if there is a patent major direct communication between the umbilical arteries and the vein. The anatomy was well worked out in Murray's case with multiple epigastric arterial feeders identified (Fig. 10-22). Ligation of the feeders and excision of the umbilical region cured the heart failure. The nature of the failure is identical to that seen in cerebral arteriovenous malformations (vein of Galen malformation) and cutaneous or hepatic giant hemangioma with shunting.

Prolonged neonatal therapeutic canalization of the umbilical vessels can lead to an acquired arteriovenous connection. This resulted in Reagan's case in

a buzzing belly button with aortography at age 6 weeks demonstrating direct arterial venous connections (Fig. 10-23). The fistula spontaneously closed in this case.

Safety of umbilical catheterization and angiography in the newborn—At present there are no serious problems in short-term catheterization for angiography. Unfortunately, catheterization of the umbilicus is attended by thrombotic problems; this may well relate to its principal use in sick newborns with respiratory distress syndrome. Frequently there are shock and intravascular clotting examples have been encountered of hepatic and renal infarction secondary to arterial thrombosis. Some may have been worsened by introduction of highly alkaline solutions into catheters inadvertently wedged into peripheral areas in the liver or into a renal artery blocked by the catheter. Although the umbilical arteries commonly go into spasm from catheterization, actual aortic thrombosis has not complicated short-term catheterization or angiography. In fact, a case of idiopathic aortic thrombosis was diagnosed by umbilical aortog-

Fig. 10-23—Umbilical arteriovenous fistula in a 6-week-old infant with buzzing belly button and history of umbilical venous catheterization for 72 hours in the newborn period. Heart failure was not present, but central findings led to aortography. A, frontal view shows direct connection of umbilical artery (ua) and umbilical vein (uv). B, lateral view shows umbilical artery leading to umbilical vein, which ascends and passes posteriorly to join the portal vein. Cardiac murmur diminished and buzzing belly button disappeared without surgery. (Courtesy of Dr. L. C. Reagan and associates. C, neonatal.)





Fig 10-24 -Idiopathic aortic thrombosis suspected because of pulseless, cold left leg led to umbilical aortography. A shows a filling defect in the saddle area of the aorta and failure to fill the

left iliac and femoral arteries. B demonstrates flow to the left leg reconstituted by collateral vessels. (Courtesy of Dr D Bowdler Sydney Austral a)

raphy (Fig 10-24). Umbilical venous catheterization for exchange transfusions or introduction of alkaline solutions has occasionally led to portal thrombosis with later portal hypertension and esophageal varices. The radiologist and pediatrician must then weigh the slight risk of such catheterization with the great advantages. These include avoidance of femoral puncture or cutdown with danger of spasm, thrombosis, bleeding, or even introduction of serious infection into the adjacent hip joint. The method should not be abused. It should never be a substitute for properly performed intravenous pyelography. It should be reserved for cases in which additional information will benefit the present patient or future patients with similar disorders. It would be wise for the procedure to be performed by pediatricians skilled in such umbilical catheterization.

REFERENCES

- Berdon, W. E. et al. Giant hepatic hemangioma with cardiac failure in the newborn infant. Value of high dosage intravenous pyelography and umbilical angiography. *Radiology* 92:1323, 1969.
- Emmanouilides, G. C. et al. Transumbilical aortography and selective arteriography in newborn infants. *Pediatrics* 39:337, 1967.
- Gonzalez Carbalhaes, O. Hepatoportography through the umbilicus. *Rev. Saude. Milet. Mexico* 12:38, 1959.
- Kaufmann, H. J. et al. Transumbilical aortography and selective arteriography in the newborn infant. *Fortschr. Röntgenstrahlen* 98:699, 1963.
- Kessler, R. E. et al. Umbilical vein angiography. *Radiology* 87:841, 1966.
- Murray, D. E. et al. Congenital arteriovenous fistula causing congestive heart failure in the newborn. *JAMA* 209:770, 1969.
- Reagan, L. C. et al. Umbilical artery vein fistula. *Am J Dis Child* 119:363, 1970.

Salerno, F. G. et al. Transumbilical abdominal aortography in the newborn. *J. Pediatr. Surg.* 5:40, 1970.

INFERIOR VENACAVOGRAPHY -The inferior vena cava can be opacified at the time of intravenous pyelography. Methods range from single or bilateral ankle vein injection to transfemoral catheterization of the inferior vena cava. Use of a serial film changer (preferably biplane) improves visualization. The opacified vein is inspected for intraluminal filling defects, obstruction, extrinsic pressure effects, and anomalous development. The catheter method offers greater accuracy and is preferred. Catheter injection in an infant without a tumor but actively crying at the time of injection may even reveal the rich anastomotic network between the vena cava and the retroperitoneal paravertebral and lumbar veins that drain into the azygos vein (Fig 10-25).

Solid abdominal tumors -The hope that detection of inferior vena caval obstruction would help in determining resectability of Wilms' tumor and neuroblastoma has not been realized because crying, the size of the mass in a small infant's abdomen, and so on can produce apparent obstruction (Fig 10-26). Furthermore, the vena cava may be patent in the presence of a tumor that cannot be resected because of encasement of major arteries (Fig 10-27). Intraluminal masses (Fig 10-28) may be encountered so the study as part of the initial intravenous pyelogram seems worthwhile. For practical purposes, therefore, the leg injection (with all its drawbacks) is used. Venacavography by catheter is however superior.

Lymphoma -We have given up inferior venacavography in evaluating lymphoma since lymphangiography is much more satisfactory.

Benign caval anomalies -Anomalous development

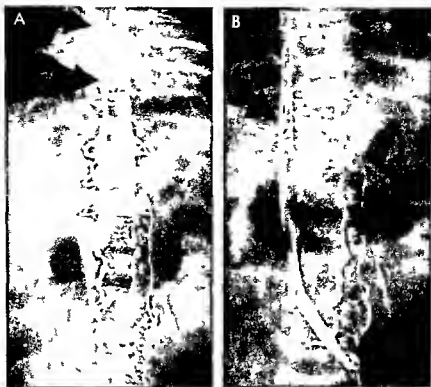


Fig. 10-25—Spurious obstruction of the inferior vena cava noted in an infant who had urologic studies after colostomy for complicated imperforate anus. A: intravenous pyelogram with injection through the asphenous vein catheter with the patient crying shows virtually complete blockage of the inferior vena cava

and massive filling of retroperitoneal ascending lumbar veins leading to the dilated azygos vein (arrows). The kidneys are delineated from an aortic injection. B: repeat injection without movement of the catheter but with the infant asleep demonstrates a normal inferior vena cava and a few collateral vessels.



Fig 10 28.—Right ganglioneuroma demonstrated by downward lateral displacement of the right kidney. A, inferior vena cavagram, frontal projection, shows apparent obstruction and displacement at the level of the right kidney with nearly all flow through retroperitoneal collateral vessels to the azygos system. B, lateral projection with horizontal beam and patient supine, shows the extent of collateral flow. The tumor was resected; the inferior vena cava was not intrinsically involved though draped over the tumor. The patient was well 5 years later.

Fig 10-27 — Displaced though widely patent inferior vena cava in a child with left ganglioneuroma. Multiple biopsies and two laparotomies revealed no signs of malignancy; the tumor so encased major structures and vessels that it could not be removed and did not respond to radiotherapy. The patient was well five years later.



Fig 10-28 — Tumor thrombus in the inferior vena cava extending into the right atrium in a patient with partially resected left Wilms tumor (note clips). The patient died of metastatic disease. (Courtesy of Dr. C. H. Meng, New York.)



Fig 10.29 A Right metastatic mass (upper arrow) between the right masseteric bone and the thoracic spine. An asymptomatic chondrosarcoma of the right mandible mass. No evidence of a mass in the right upper quadrant and no other abnormalities. Lower arrow indicates the mass extending into the right



medial with posterior displacement. B In the venacavogram showing mass to be the dilated azygos venous arch in a patient with azygos continuation of the inferior vena cava. No calcifications were present, though many such patients have the polysplenic syndrome.

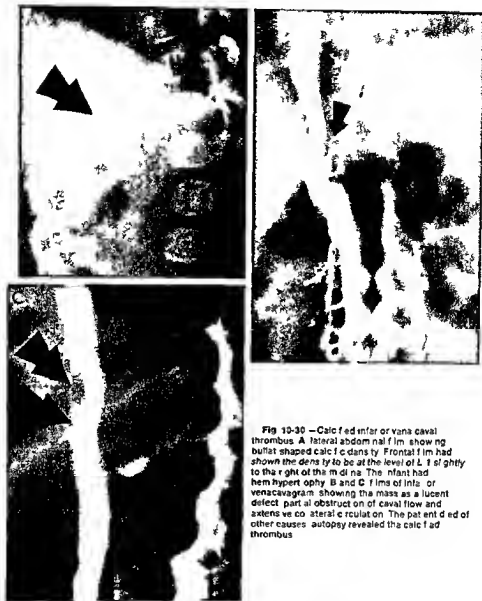


Fig 10-30 —Calcified inferior vena caval thrombus. **A** Lateral abdominal film showing bullet shaped calcific density. Frontal film had shown the density to be at the level of L1 slightly to the right of the midline. The infant had hemihypertrophy. **B** and **C** films of inferior venacavagram showing the mass as a lucent defect, partial obstruction of caval flow and extensive collateral circulation. The patient died of other causes; autopsy revealed the calcified thrombus.

of the hepatic portion of the inferior vena cava is also called azygos continuation of the inferior vena cava. Single or multiple channels lead directly from the lower vena cava into the azygos vein. This would seem to be of little interest except that the azygos arch may be so large as to present as a chest mass (Fig 10-29 A). In such patients inferior venacavography is diagnostic and can save the patient from exploratory thoracotomy (Fig 10-29 B).

The rare but interesting calcified inferior vena caval thrombus is seen as a bullet shaped density in the

right posterior abdomen (Fig 10-30 A). Venacavography shows the degree of obstruction and the collateral channels (Fig 10-30 B and C). Most of such cases have been in infants.

Renal vein thrombosis has been studied occasionally by venacavography. Lack of renal vein washout into the inferior vena cava is considered a diagnostic feature. Since renal vein thrombosis usually occurs in a neonate, selective renal vein injection does not now seem feasible. Thrombus extension into the cava might be seen.

REFERENCES

- Berdon, W. E., et al. Plain film findings in azygos continuation of the inferior vena cava. *Am J Roentgenol* 104:452, 1968
- , et al. Factors producing spurious obstruction of the inferior vena cava in infants and children with abdominal tumors. *Radiology* 88:111, 1967
- Ferris E., et al. Venography of the Inferior Vena Cava and Its Branches (Baltimore: Williams & Wilkins Company, 1969)
- McDonald P., et al. Angiography in abdominal tumors in childhood with particular reference to neuroblastoma and Wilms' tumor. *Clin Radiol* 19:1, 1968
- Silverman N. R., et al. Thrombus calcification in the inferior vena cava. *Am J Roentgenol* 106:97, 1969
- Singleton E. B., et al. Intraluminal calcification of the inferior vena cava. *Am J Roentgenol* 86:556, 1961
- Tucker A. S. The roentgen diagnosis of abdominal masses in children. Intravenous urography vs. inferior vena cavography. *Am J Roentgenol* 95:76, 1965

Lymphangiography

Pedal lymphangiography is a technically difficult procedure in infants and children. Although of interest in many conditions, its principal use is in staging Hodgkin's disease, a relatively rare disease in children with sufficient cure potential to make the study worthwhile.

Pedal lymphangiography involves the injection into the dorsum of one or both feet of iodized oil (Ethiodol) by the method of Knemuth, with subsequent opacification

of lower extremity and retroperitoneal lymphatics and lymph nodes. The former clear in several hours, but the nodes remain opacified for weeks to months, the pediatric patient traps contrast medium in lymph nodes for less time than the adult. The young patients may require heavy sedation or even general anesthesia, successful studies have been performed in infants as young as 7 weeks and in young children. In the older child successful studies are the rule. The method has been mainly applied to study of tumors (lymphoma, neuroblastoma), but also in study of lymphatic anomalies (including chylous ascites, chylous mesenteric cysts).

Since the oily material reaches the lung in the form of small opaque oil emboli (Fig. 10-31) via the thoracic duct, film or fluoroscopic monitoring of the injection is useful, with the injection terminated when the thoracic duct starts to fill. Postinjection cough and fever are not uncommon, eosinophilic pneumonitis (Loeffler's syndrome) may occur but has not been a serious problem.

Lymphoma—Pedal lymphangiography for staging of Hodgkin's disease is superior to inferior venaography and intravenous pyelography. The diagnostic criteria for a "positive" study include the presence of enlarged retroperitoneal nodes that appear to be foamy and may have discrete filling defects (Fig. 10-32). By combining delayed films with an intravenous pyelogram, it is apparent that some involved nodes are above the ureters, which may appear to be normal. However, the pyelogram may show ureteral abnormality caused by involved lymph nodes not filled in the lymphangiogram (Fig. 10-33). Other nodes may be so involved as not to fill at all. Nodes that look normal may actually be involved, while others looking abnormal may be free from disease. The accuracy of the study seems to be reasonably good but the need for accurate staging requires laparotomy, especially to check on involvement of a normal size spleen. Failure to make the diagnosis of abdominal involvement could lead to failure to irradiate the area, with subsequent loss of the patient. **Lymphosarcoma** (Fig. 10-34) can yield similar radiographic results. The outlook here is grim since most patients die of their disease, some with leukemic dissemination.

Solid retroperitoneal tumors—Lymphangiography of Wilms' tumor yields little information other than evidence of blockage by the sheer size of the mass. Actual nodal involvement is rare so that the study is not used in preoperative evaluation.

Neuroblastoma commonly occurs as a matted tumor of the retroperitoneum, total surgical excision is impossible in most patients. It is not surprising that lymphangiograms are positive. Enlarged nodes, both foamy and with filling defects, are encountered (Fig. 10-35), with obstruction of contrast flow being common. The obstructed lymphatics may drain by collateral lymph and venous channels, oil embolization to

Fig. 10-31—Close-up of the left lower lobe one day after pedal lymphangiography in a child 8 years of age with Hodgkin's disease. Small opacities represent multiple oil emboli, a picture regularly seen after such studies, especially in children.





Fig 10 32 (above left) — Enlarged toamy nodes as well as part a y replaced nodes in padal lymphang ogram, nd cat ng retroperitoneal spread of Hodgk n s d saase. Nota lack of cor elat on w th the u eteral cours the great range of no mal var at on makas eva uat on of the ureters uncertain

Fig 10 33 (above) — In a pat ant w th Hodgk n s d saase and lymphang og aph c ev denca of retroperitoneal node nvolvement the intravenous pyelogram w th pat ant p ona shows d sc etc u eta al ndantat on by nonopact ad nodes (ar ow) on the left

Fig 10 34 (left) — Lymphoma coma l ke Hodgk n s d saase may ba cha actenized by toamy or detect ve nodes as n th s lymphang og am Some renal ena gement is also present nd cat ng w despread lymphoma coma n th s 12 year o d pat ent who d ed of leukem c d ssem nat on

the liver which is unusual in adult lymphangiograms has been seen in several children with neuroblastoma (Fig 10-36) Whether the flow to the liver is by lymphatic or venous channels is not clear The basic mechanism is obstruction at the mesenteric root In view of the time and effort required it is unlikely the lymphangiography in children with neuroblastoma is worth while No other study however is so useful in mapping the extent of disease after the

initial usually diagnostic intravenous pyelogram is obtained

Congenital lymphedema is difficult to study since the initial injection of dye into the dorsum of the foot causes diffuse dermal backflow and the lymph channels are virtually impossible to find

In *chylous ascites* the cause may be obstruction of the retroperitoneal lymph pathways although the actual site may be impossible to identify in a 7 week

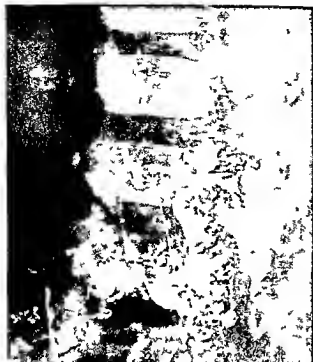


Fig. 10-35 (left) —Neuroblastoma may cause foamy nodes and nodal replacement. In this lymphangiogram this pattern extends well below the iliacs revealed by intravenous pyelography. The tumor was not resectable.



lymphangiography in a patient with neuroblastoma is evidence of marked obstruction of retroperitoneal lymph channels. This sign has been noted in adults with retroperitoneal node metastases from seminoma and cervical carcinoma, although rare in all age groups.



Fig. 10-37 In an infant 7 weeks of age with chylous ascites, the lymphangiogram shows striking abnormalities with partial pelvic inlet obstruction and retroperitoneal extravasation on the left into the peritoneal cavity and possibly by the small bowel lumen. (Courtesy of Dr. C. E. Craven, Galveston, Tex.)

old infant the Ethiodol passed by bizarre collateral channels into the peritoneum and bowel lumen (Fig 10 37) Such a condition can be treated medically by a diet rich in medium chain triglycerides which reduces the load on lymph absorptive routes and is mainly absorbed into the portal venous circulation Surgical exploration may be needed to search for congenital bands around the root of the mesentery Chyle filled mesenteric cysts are part of the same picture representing a lymphocele In one patient injection of Ethiodol into the exteriorized cyst revealed flow both antegrade to the thoracic duct and retrograde to retroperitoneal lymph nodes and pedal lymphangiography (Fig 10 38) filled the cyst as well as showing flow to the thoracic duct

Lymphangioma of bone—Lytic processes in bone may reflect lymphangiomatous malformations Pedal lymphangiography opacifies the bones proving the relative role of the lymphatic system in malformations that may have hemangiomatous components as well (Fig 10 39)

REFERENCES

- Altman D *et al* Lymphangiography in children *Am J Dis Child* 104 335 1962
 Bray D A *et al* Loeffler's syndrome as a complication of bipedal lymphangiography *JAMA* 214 369 1970
 Craven C E *et al* Congenital chylous ascites Lymphangiographic demonstration of obstruction of the cisterna chyli and chylous reflux into the peritoneal space and small intestine *J Pediatr* 70 340 1967

Fig 10 38—Mesenteric chyle filled cyst studied by both cyst injection and pedal lymphangiography which demonstrates interconnecting lymph channels and cyst with contrast medium flowing in both directions (Courtesy of Dr J C Leonard New York)



Fig 10 39—Diffuse lymphomatous malformation of the spinal column and ribs demonstrated by pedal lymphangiography Contrast medium opacifies the vertebrae Opacification in the five areas further evidence of congenital anomaly of the lymph channels (Courtesy of Dr G Curran Dallas Tex)

- Gasquet C *et al* Lymphangiography in malignant diseases of childhood *Am J Roentgenol* 103 1 1968
 Grossman H *et al* Roentgenographic changes in childhood Hodgkin's disease *Am J Roentgenol* 108 354 1970
 Hecht H *et al* Hepatic oil embolization following lymphangiography in a child with neuroblastoma *Am J Roentgenol* 104 860 1968
 Kinnmouth J B Lymphangiography in man Method of outlining lymphatic trunks at operation *Clin Sci* 11 13 1952
 Leonidas J *et al* Mesenteric cyst associated with protein loss into the gastrointestinal tract Study with lymphangiography *Am J Roentgenol* 112 150 1971
 Lowenbraun S *et al* Diagnostic laparotomy and splenectomy for staging Hodgkin's disease *Ann. Int. Med.* 72 655 1970

Nuclear Medicine Isotopic Scanning

The diagnostic as well as therapeutic uses of radioactive isotopes are making nuclear medicine an emerging separate specialty The following discussion will briefly illustrate some of the uses of organ scanning with various isotopes The method is easily carried out and can be used repeatedly with a low total radiation exposure from the tracer doses



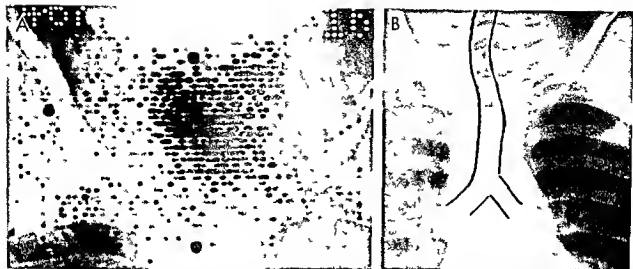


Fig. 10-40 — Masses adjacent to the organ being scanned may suggest intrinsic involvement of the organ. A, thyroid scan of a child with a mass in the left side of the neck shows diminished activity in the left lobe. Diagnosis was probable thyroid lesion on an adenoma or carcinoma. B, frontal tracheal view shows curvilinear

ear tracheal deviation by a mass. The mass moved with swallowing and an experienced thyroid surgeon was sure it was of thyroid origin. At surgery a branchial cleft cyst extrinsic to the left lobe of the thyroid was excised.

Essential in the use of such scans is the recognition of inherent limitations. Peripheral involvement of an organ by a mass cannot accurately be distinguished from pressure effects on the organ by an adjacent mass. Thus a large resectable Wilms tumor may so deform the adjacent liver on liver scan as to mimic invasion or metastasis. Similarly, a branchial cleft cyst can simulate involvement of the ipsilateral thyroid lobe (Fig. 10-40). Present physical limitations of the scanning equipment preclude detection of masses less than 2 cm in diameter; thus a liver may be ridged with small abscesses or metastases and seem

homogeneous on scanning. These are not errors in interpretation of scans but rather disease involvement beyond the physical resolving characteristics of the method. In addition, the isotopes depend for their concentration within an organ both on the integrity of the organ and on the blood flow to it. Thus total nonvisualization of an organ could be due to a block in its blood supply, total replacement of the organ function, diversion of flow or a combination of processes. This is best illustrated in the lung (see below) where air trapping, tumor or massive pneumonia can cause a pattern of nonperfusion resembling to some degree that seen in congenital obstruction to flow or acquired embolic or thrombotic obstruction to flow.

The isotopes outline normal rather than diseased tissue in most areas; the cold areas reflecting a gross finding that must be analyzed in relation to physical and laboratory evidence as well as that of other radiographic studies.

Lung—The unilateral nonperfused lung (Fig. 10-41, A) can be due to many causes including congenital absence of the ipsilateral pulmonary artery with

the lung supplied by a ductus or bronchial arteries (Fig. 10-41, B and C). Massive cardiomegaly as with a large ventricular septal defect, can lead to functional diversion of flow to the opposite lung; usually this is due to air trapping on the left from pressure on bronchi and increased flow to the right lung (Fig. 10-42).

Bronchial obstruction, as from a foreign body, can be most confusing if the air trapping is not noted and a lung scan shows nonperfusion (Fig. 10-43, A). The angiocardiogram of such a patient shows that the scan faithfully reflects the diminished slow flow through the obstructed side (Fig. 10-43, B). Similar findings in adults with bronchogenic carcinoma have been erroneously attributed to invasion of the pulmonary artery when in fact they reflect endobronchial obstruction. The unilateral hyperlucent lung seen after radiation therapy, kerosene ingestion and adenoviral pneumonia reflects similar diversion of flow, usually secondary to obliterative bronchial and bronchiolar disease (Fig. 10-44). Pneumonia acts as a focus of nonperfusion on lung scans. This creates confusion in adult radiology in separating it from pulmonary infarction. Patients with both bacterial and lipid pneumonia have shown this picture (Fig. 10-45). Areas of diminished perfusion in cystic fibrosis correlate well with diminished ventilation on ventilation scanning.

Such chronic diseases as cystic fibrosis and immunologic disorders with pulmonary manifestations (e.g., agammaglobulinemia) can be followed by chest films and lung scans to study sequential bronchial obstruction or chronic pneumonia. The scans may show more severe involvement than is apparent in

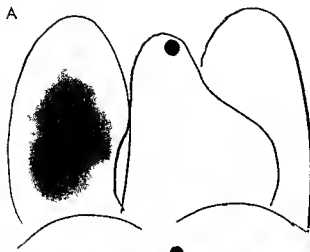


Fig 10-41 — **A** total nonperfusion of the left lung on a radioactive albumin lung scan. The picture cannot be interpreted without knowledge of the history and chest films. **B** chest film of the same patient shows overcirculation in the right lung and slight left-sided shift of the mediastinum. Barium delineates an indentation of the right aortic arch in this child with congenital absence of the central segment of the left pulmonary artery. **C**, pulmonary angiogram shows all flow to the right lung. Branch stenoses of the right pulmonary artery and right ventricular hypertension were present. Right aortic arch with left innominate artery was vented in later films of the left side of the heart and aorta.

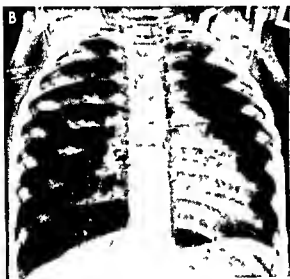




Fig. 10-42—Film of an infant with total nonperfusion of the right lung on lung scan shows cardiomegaly and overcirculation of the right. The hyperlucent left lung reflects trapping of a contrast medium by the heart (especially the large left ventricle) on the left.

angiogram. Angiogram also demonstrated deviation of the right lung with a patent though small left pulmonary artery. A large ventricular defect was the principal cardiac lesion.

Fig. 10-43—A combined lung scan with chest film shows significant shift of the right and total nonperfusion of the left lung. The pattern is typical when the large lung is trapped by airways with endobronchial obstruction. Granulation tissue was found in the left main stem bronchus with edema and narrowing. The history suggested aspiration of a peanut. B: venous angiogram shows gate, hyperlucency and increased volume on the left with slow flow through the patent left pulmonary artery. In the right lung, contrast medium has already passed through the arteries to the pulmonary veins with filling of the left atrium, ventricle and aorta. (Courtesy of Dr. D. P. Neri, New Rochelle, N.Y.)



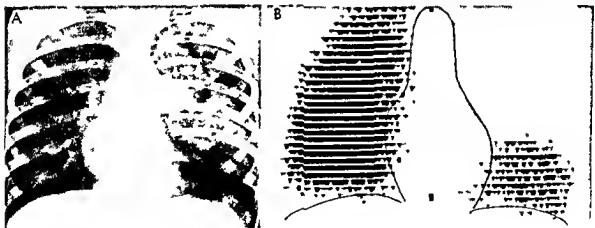


Fig 10-44 — This 5-year-old child at age 2 had ingested kerosene. A: chest film shows air trapping in the right lower lobe magnified by exposing the film during expiration. B: lung scan shows pronounced right basilar underperfusion again reflecting

redirection of flow due to air trapping. This is presumably due to hydrocarbon pneumonia leading to obstructive bronchiolitis. Similar changes have been seen after adenoviral pneumonia.

Fig 10-45 — This child 9 years of age suffered from weight loss and hemoptysis. A: chest film shows massive densities in the upper lobe of the left lung. Diagnosis was infected cystic mass possibly congenital. B: lung scan demonstrates almost total non-

perfusion of the area. Anomalous blood supply was considered. Surgery revealed normal blood supply to the left upper lobe which was involved by extensive lipid pneumonia. Later a history was obtained of chronic use from age 2 to 4 of oily nose drops.



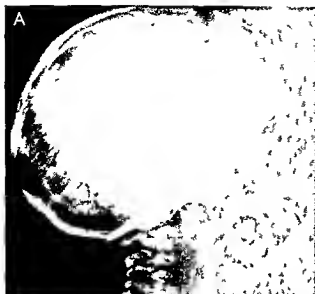
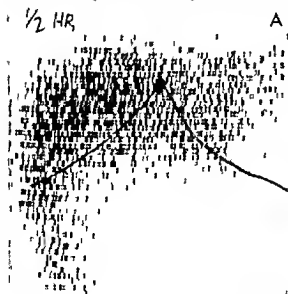


Fig 10-46—This 9 year old girl had a bone age of 2 years, short stature and severe cyanotic heart disease. Growth failure was attributed to the heart disease. **A**, skull film shows prominent sutures, wormian bones in the lambdoid area, prominent sella turcica and dense base of the skull—all signs of unrecognized



severe hypothyroidism. **B**, lateral thyroid scan shows a slight amount of functioning tissue after priming by thyroid-stimulating hormone. The tissue is at the base of the tongue and represents lingual undescended thyroid remnant causing severe hypothyroidism.

Fig 10-47—In a girl with a large, right upper quadrant mass, arteriography had shown draping of hepatic vessels but no conclusive evidence of tumor. History of intermittent fever suggested choledochal cyst. **A**, scan 30 minutes after administration of rose bengal shows a large cold area in the region of the porta hepatis.



B, scan at 17 hours with filling of the cold area by rose bengal bile mixture shows the mass to be compatible with the clinical impression of choledochal cyst. Anastomosis to the intestine led to decompression of the partially obstructed extrahepatic biliary system. (Courtesy of Dr. D. Darling, Boston, from Williams et al.)

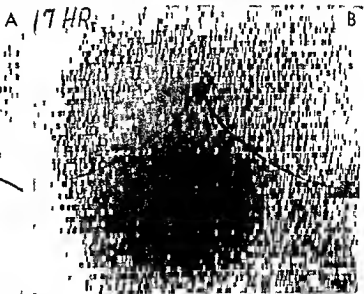




Fig 10-48—Chronic granulomatous disease of childhood due to defective neutrophil function. **A**, plain film shows liver calcifications surrounding an abscess in the right lobe of the liver in a boy with history of recurring infections. Note the bilateral chronic pneumonia infiltrates. **B**, liver scan with radioactive gold (before

technetium sulfur colloid was available) shows large cold areas in the right hepatic lobe corresponding to the area of calcifications in **A**. On surgical exploration multiple abscess cavities were found. In the following four years recurring abscesses led to further liver damage and calcifications shifted laterally.

Fig 10-49—Epidermoid cyst of the spleen. **A**, scan shows a large cold area in a left upper quadrant mass with normally functioning splenic tissue below it. Intravenous pyelography had demonstrated a lucent area in the spleen, leading to a diagnosis of intrasplenic cyst, probably epidermoid. **B**, celiac arteriogram

capillary phase shows normal vascularization in the lower pole of the spleen, correlating perfectly with the scan. The center of the spleen, which is lucent, contained 1100 cc of fluid and hemosiderin-laden macrophages were present in the cyst wall, suggesting traumatic etiology of such cysts.



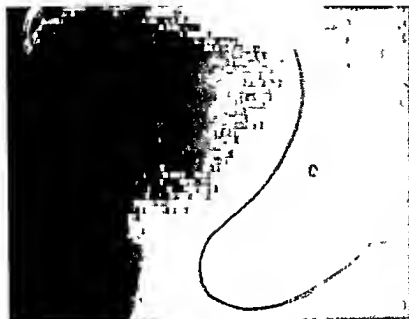


Fig 10 50 — S C hemoglobinopathy with functional asplenia. Technetium sulfur colloid scan shows no sign of splenic uptake in a patient with greatly enlarged spleen. Reversion to normal followed transfusions. This represents functional asplenia. Most such cases have been of S-S anemia.

chest films. At an age when evaluation of the function of each lung is impossible by bronchspirometry, lung scanning plus inspiration-expiration chest films is of great value.

Thyroid—In the thyroid gland both benign and malignant masses can be studied. The cold nodule may be due to either cause, some thyroid tumors are so differentiated as to trap the isotope while the metastases in the lung can also pick up the tagged iodine, especially if the normal thyroid gland has been removed. Scanning of the thyroid gland should include the base of the tongue. Some patients with undescended lingual thyroid tissue may in childhood have hypothyroidism with years elapsing before the true diagnosis is made. During this time there is growth failure, with permanent damage to the child's normal development (Fig 10-46).

Liver—Two basic scanning agents are used. The first, rose bengal, is eliminated through hepatic function into the bile, so it can be used in study of biliary obstructive disease. Choledochal cysts, which represent dilatation of the common bile duct, may fill on delayed scans (Fig 10-47) although seeming cold in early scans. The cold area might indicate anything from a tumor to an abscess, but its later filling points to choledochal cyst. The method has little if any value in the jaundiced neonate with biliary atresia. The second group of agents go to the reticuloendothelial system; technetium sulfur colloid is generally used. This group outlines abscesses, tumors, and infarction which replace normal reticuloendothelial tissue (Fig 10-48). Care must be taken to avoid misinterpreting peripheral cold areas as meaning intrinsic disease, otherwise liver pathology is read into scans of renal

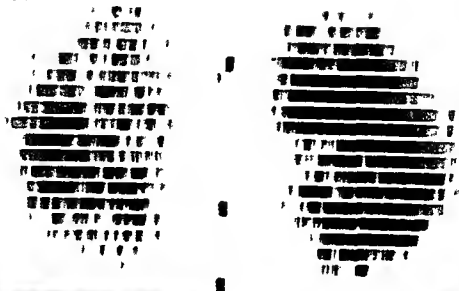
masses (tumors, cysts) that indent but do not invade the adjacent liver.

Spleen—Technetium sulfur colloid outlines the normal spleen and reveals the intrasplenic mass of an epidermoid cyst (Fig 10-49) or the nonvisualized enlarged spleen in sickle hemoglobinopathy of the S-C type (Fig 10-50). The latter is a paradox and apparently reflects arteriovenous shunting and splenic engorgement that is reversed by transfusions. It behaves as a case of functional asplenia; the peripheral blood smear may show Howell-Jolly bodies as signs of circulating aged red cells that should normally be sequestered by the spleen.

Kidney—The former limited use of renal scanning for diagnosis was due largely to the limitations of scans done with radioactive mercury. They showed gross filling defects from trauma or with tumors such as lymphoma (Fig 10-51), but scanning was time consuming and insufficient scanning agent was released in a short enough period to allow observation of ureteral anatomy. Newer agents such as technetium DTPA allow both visualization of renal homogeneity or heterogeneity in terms of masses and rapid flow into and recording (with Anger cameras or similar rapid scanning devices) of ureteral and bladder dynamics. For example, the dilated but really nonobstructed hydronephrotic ureters in cases of congenital absence of the abdominal musculature (Eagle-Barrett syndrome) can now be studied (Fig 10-52). Hypertension has been evaluated in adults by renography, using comparison of vascular secretory and excretory phases with varying results. Such studies in pediatric patients are limited although used in some centers.

Central nervous system—Brain tissue may pool

A



B



Fig. 10.51—Lymphosarcoma, right kidney. A: renal enlargement led to ^{201}Tl scanning, which shows heterogeneity and renal enlargement. B: intravenous pyelography delineates stretched calyces and lucent defects from intrarenal lymphomatous masses.

With response to chemotherapy the intravenous pyelogram and scan returned to normal, but the patient died of leukemic dissemination 6 months later.



Fig 10-52.—Absence of abdominal musculature and hydronephrosis (Eagle-Barrett syndrome) in a male infant. Technetium DTPA scan 45 minutes after injection shows rapid filling of the ureter indicating the nonobstructive nature of ureteral dilatation in this syndrome (Courtesy of Dr G S Freedman New Haven Conn)

isotopes in diseased areas unlike most other sites in which coldness indicates disease Tumors infarct and abscesses are grossly outlined but differential diagnosis requires further study and often exploration The ease of scanning and safety of repeated use make it useful in study of brain abscesses in patients with cyanotic heart disease Isotope cisternography and ventriculography are used in the study of hydrocephalus and the efficacy of shunting procedures

Heart—Pericardial effusion can be outlined by blood pool scans (as with radioactive Cholegrafin) combined lung scanning accentuates the cold area surrounding the blood pool However as with CO₂ angiocardiology such methods are being replaced by echocardiographic studies

REFERENCES

- Charles N D Limitations of scintillation scanning J Pediatr 77 350 1970
 Fellows K E et al Abdominal masses simulating metastatic disease Am J Roentgenol 104 678 1968
 Freeman L M et al Diagnosis of hepatic hemangioma with combined scanning technique Radiology 95 118 1970
 Glasauer F E et al Isotope cisternography and ventriculography evaluation of hydrocephalus in children Am J Dis Child 120 109 1970
 Pearson H A et al Transfusion reversible functional asplenia in young children with sickle cell anemia New England J Med 283 333 1970
 — et al The binary spleen A radioisotope scan sign of splenic pseudocyst J Pediatr 77 216 1970

- Pendarvis B et al Lung scanning in the assessment of respiratory disease in children Am J Roentgenol 107 313 1969
 Williams L E et al Preoperative diagnosis of choledochal cyst by hepatoscintigraphy New England J Med 283 85 1970

Ultrasound

The use of ultrasound will be of great value in the diagnosis of masses and their effect on normal organs and in the study of motion of normal structures. Two types of scans can be obtained A scans recording the amplitude and site of reflection of the pulse scans and B scans the stored multiple reflections with a moving scanning head the end result being a cross section of scanned areas

Scans which delineate the midline of the cranial cavity and can be used to detect shifts from the midline are especially helpful when the pineal is not displaced The posterior myocardium gives a separate motion that of the pericardium when there is pericardial effusion Cardiac valve motion can be studied and masses cause a multitude of bizarre echo spikes measured to the anterior and posterior tracings with a filter obtained from a cystic structure The latter types are seen with benign cysts as well as cystic uterine tumors such as necrotic neuroblastoma (Fig 10-53 A and B) The tracings cannot differentiate between malignant masses but they do show that a mass is not solid In an infant with abdominal masses hydronephrosis caused a clear central space between the anterior and posterior walls of the dilated renal pelvis (Fig 10-53 C) whereas Wilms tumor caused irregular multiple tracings between the anterior and posterior limits (Fig 10-53 D) Ultrasound has great promise especially when combined and correlated with radiographic procedures

REFERENCES

- Freimanis A K Echographic exploration of abdominal structures Critical Rev Radiol 1 207 1970
 LeFebvre J et al Use of ultrasound and its diagnostic value in internal medicine Ann radiol 13 619 1970

Carbon Dioxide Contrast Studies

Carbon dioxide (100%) is a safe contrast agent for the investigation of pericardial effusion and outlining of pleural and peritoneal borders It can also be used for retroperitoneal gas studies Its rapid diffusion allows its use within the vascular system

Pericardial effusion—Rapid intravenous injection of CO₂ in about 1 cc/lb volume outlines the thickness of the right atrial region in study of suspected pericardial effusion With the patient on his left side the right atrium acts as a trap for the CO₂ which outlines the inner wall of the right atrium and allows estimation of the thickness of the atrial wall (The presence of a right pleural effusion would render this estimate inaccurate as it too would layer in the area of the

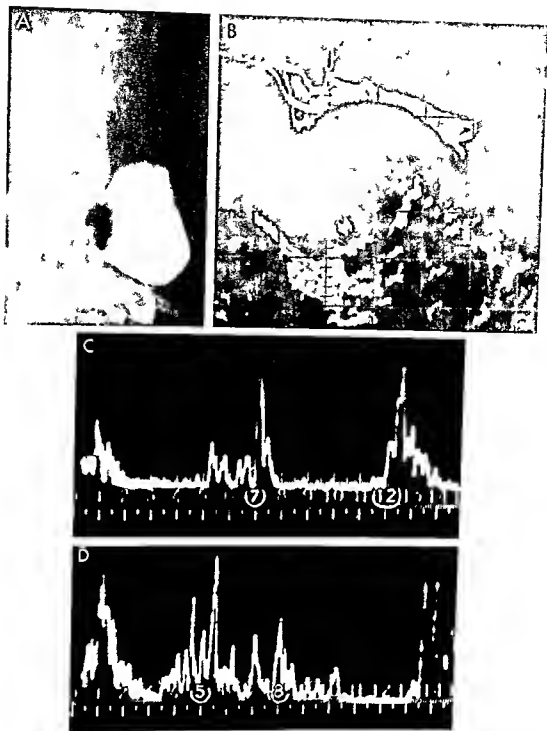


Fig. 10-53 —A and B studies in a newborn with marked right orbital proptosis secondary to retrobulbar cystic necrotic neuroblastoma. A: water-soluble contrast medium injected into the mass delineates a slightly irregular wall superiorly. The black area represents a nodule of tissue. B: echo B scan from above shows anterior and posterior curved near reflections with clear centers suggesting the cystic nature of the lesion. Chest films and

intravenous pyelograms showed no abnormalities, but bone marrow contained neuroblastoma cells. (Courtesy of Dr. L. Polak, New York.) C: in hydronephrosis, an A scan shows sharp deflections by the anterior and posterior walls of the dilated renal pelvis at 7 and 12 cm. D: in Wilms' tumor, an A scan shows multiple echoes from within the large tumor between 5 and 8 cm. (C and D courtesy of Dr. J. LeFebvre, Paris.)



Fig 10 54 During an upper respiratory infection in an otherwise healthy infant 8 weeks of age a chest film demonstrated a flask shaped consolidation. There was the question of pleural effusion despite no malformation on chest film, electrocardiogram and heart sounds. The false positive CO₂ study shown here indicated an apparent right atrial wall thickness of 10 mm demonstrating that the thymus can extend to the diaphragm in a healthy infant.

Fig 10 55 (left) A question of hampercardium was raised in a 4 month old infant with ventricular septal defect corrected transposition of great vessels and congenital heart block. The CO₂ study shows a normal right atrial wall thickness. A pacemaker catheter is in the right atrium.

Fig 10 56 (right) A premature infant with transposition of the

great vessels had cardiac catheterization required retrocardiac demonstration of epinephrine. Signs of cardiac tamponade led to the CO₂ study that demonstrates 11 mm thicknesses of the right atrial wall. Autopsy revealed hemopericardium secondary to rupture of the right coronary artery by the epinephrine injection.

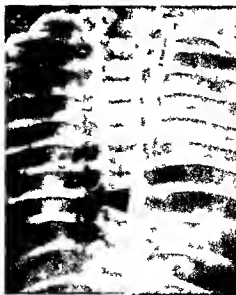




Fig 10 57 —A patient 2½ years of age with neurofibromatosis and optic glioma had a routine chest film that showed abnormal cardiac shape suggestive of congenital absence of the left pericardium. To prove the diagnosis left pneumothorax was induced with CO₂. This film shows gas passing through the combined left pleuroparicardial defect to outline the diaphragmatic and remaining right pericardium.

Fig 10 58 —An infant 6 weeks of age who was being placed for adoption had a routine chest film that showed a large right paracardiac anteromedial mass. To verify the radiographic impression of partial eventration of the right diaphragm pneumo-

right atrial wall with the patient lying on his left side.) Although pediatric measurements are lacking we have used 1–2 mm as a normal wall thickness in the infant, 2–3 mm in the young child and 5 mm in the older child. A wall of more than 10 mm would be abnormal and an effusion the most likely diagnosis. A false positive result can be caused by a large thymus (Fig 10-54), but films eliminating a diagnosis of possible pericardial effusion (Fig 10-55) or confirming it (Fig 10-56) are readily obtained even at the patient's bedside. The technic has largely been replaced by echocardiography. The A (for amplitude) scan will show separation of the posterior myocardium from the pericardium by fluid.

Pleuroparicardial defects—In the evaluation of major absence of the left pericardium the injection of CO₂ is safer and as accurate as air and can be diagnostic. Since there is commonly an associated pleural defect an induced left pneumothorax will show the CO₂ passing through the combined pleuroparicardial defect into the remaining pericardium. The gas passes around the heart and with the patient in the left lateral decubitus position, outlines the pericardium adjacent to the right atrium (Fig 10-57). The diagnosis should be established since the abnormal appearance of the heart in the chest film and the possible finding of arrhythmias and murmurs could lead to an incorrect diagnosis of heart disease in an otherwise healthy child.

Pneumoperitoneography—Induced CO₂ pneumoperitoneum is useful in outlining the diaphragmatic part of the peritoneal cavity. With the patient in erect position the paper thin outline of diaphragmatic eventration (Fig 10-58) can be demonstrated in some infants whose chest films suggested a chest mass or peritoneum was induced by CO₂. In the erect film of the abdomen the bulbous elevation of a portion of the liver fits into the thin area of diaphragmatic eventration accounting for the chest mass.



enlarged heart. The high position of the liver is readily revealed by the procedure, and CO₂ has replaced air for this study. Since the normal liver and spleen fall as the CO₂ rises, damage to these organs can also be demonstrated by CO₂ pneumoperitoneum. Trauma, hepatic abscesses and subphrenic abscesses with pleural effusions have been studied, failure of normal hepatic or splenic descent is considered to be indicative of subdiaphragmatic disease.

Pneumomediastinography—Carbon dioxide does not remain long enough in the mediastinum to be of help in distinguishing a prominent thymus from an enlarged heart. We have not used air although, with care, air could serve to float the thymus free of the heart.

REFERENCES

- Asch, T. Case of pneumoperitoneum in the diagnosis of inflammatory disease about the diaphragm. *Radiology* 86: 60, 1966.
- Baker, D. H., et al. Use of pneumoperitoneum in differential diagnosis of paracardiac masses in children. *Arch Surg* 79: 63, 1959.
- Elbs, K., et al. Congenital deficiency in the parietal pericardium. *Am J Roentgenol* 82: 125, 1959.
- Shuford, W. H., et al. A comparison of carbon dioxide and radiopaque angiocardigraphic methods in the diagnosis of pericardial effusion. *Radiology* 86: 1064, 1966.
- Viamonte, M., Jr. Carbon dioxide angiocardigraphy, improved technique and results. *Am J Roentgenol* 88: 31, 1961.

The Chest

RADIOGRAPHIC INTERPRETATION of chest films of the newborn is difficult at best. The radiologist is hampered by not knowing, in many cases, the nature of the infant's respiratory problem. The films are taken during a period of rapid adaptation to extrauterine life, with replacement of the fluid-filled fetal lung by the aerated newborn lung. The first hours of life are a transitional state with varying degrees of persistence of the fetal circulation (elevated pulmonary vascular resistance and potential bidirectional shunts at the ductus arteriosus and foramen ovale). Avery's book is a major contribution to the correlation of physiologic knowledge and medical problems in this age group.

Rarely are films taken under direct medical supervision. Crying opacifies the lung fields, and a film obtained directly after a cry may show evidence of deep gasp (simulating air trapping) and the heart may enlarge as the blood rushes into it. Thymic and cardiac images are difficult to separate. The radiologist feels inadequate in many instances to define what is going on in the infant's chest at the moment the film was obtained. He should realize that his inadequacies are shared not only by the pediatricians but by the neonatologists (a growing subspecialty of pediatricians) armed with blood gas analyses and direct observation.

The following discussion is based on the radiologist's knowledge of certain minimal facts. These include the gestational age and weight of the infant, the time of onset and nature of the symptoms and pertinent acid-base data. No attempt is made to give an encyclopedic listing of causes of respiratory distress in the newborn. The references are selected for their freshness and their bibliographies. Historical references not included here will be found in previous editions of *Pediatric X-ray Diagnosis*.

It is worth stating (and this will be repeated throughout the discussion) that the findings in any single radiograph could be either pulmonary or cardiac (or both) in origin and that only time, clinical observation and repeat chest roentgenograms lead to a specific diagnosis. In some patients one can only conclude that whatever the infant recovered from

was "transient" and benign. The admission of ignorance is to be encouraged when indicated. To us, this is more factual than giving a specific nonprovable name to observations from a single film, such as "transient tachypnea due to retention of fetal lung fluid."

Radiographic Technique

The initial chest study of the distressed newborn should include frontal and lateral views with much of the abdomen deliberately included. This is important since coexistent serious abdominal abnormality may be present, also the chest signs may actually reflect abdominal disease. Collimation to screen the extremities should be used. Immobilization is most important in obtaining a good film; the use of diapers or sand bags or simply holding the arms and legs assures well-centered films if care is taken. Mechanical restraining devices have not proved valuable in our experience.

There is no need to take chest films with the newborn erect; the position is not physiologic and usually results in a sagging infant and distortion of the chest and lung detail. The frontal and lateral projections may be supplemented when needed by oblique, lateral decubitus or cross-table lateral views, especially when pneumomediastinum or pneumothorax is questioned.

Since portable radiographic equipment is usually used to examine sick newborns, it is important that films can be taken with at least 60 ma and $\frac{1}{200}$ second exposures; more rapid exposure is obviously desirable. The 750 and 1000 ma generators with 0.3 mm focal spot tubes allow rapid exposures with sharp definition and also offer the option of magnification radiography. A 14x14 in. chest film of a newborn provides a unique opportunity to observe details previously not appreciated. It is a superb teaching tool, the cost is increased radiation exposure. The major disadvantage of such equipment has been that, in general, the infant must come to the machine rather than vice versa.

The ideal neonatal intensive care unit (a better

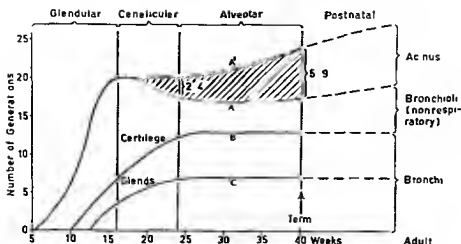


Fig 10-59—Comparison of prenatal and postnatal relative growth of alveoli and bronchi. Bronchial growth is virtually complete in utero; alveolar growth continues after birth. (From Bucher and Avery.)

term than premature nursery) would include the above equipment possibly with option for television fluoroscopy and tape recording. This and an adjacent blood gas laboratory possibly automated for immediate readout would give meaning to radiographs since they could be instantly correlated with the patient's current status.

Factors Determining Fetal Lung Growth

The fetus breathes through the placenta. Ten to 15% of the blood reaching the right heart perfuses the fetal lung; the remainder is diverted in utero by large right-to-left shunts at the foramen ovale and ductus arteriosus. Serious cardiorespiratory malformations incompatible with extrauterine survival are well tolerated in utero.

The tracheobronchial tree forms as an outpouching of the primitive foregut at about the 3½ week stage by subsequent branching; the primary and secondary bronchi appear. This development continues from the 4th to 16th week when bronchial generation is largely complete. Simultaneously the diaphragm, gastrointestinal tract and kidneys are developing and any major malformations of these organ systems may be associated with pulmonary hypoplasia. The associated clinical respiratory distress syndrome in such a patient may divert attention from the real abnormality and delay the diagnosis until it is revealed at autopsy. Bronchial cartilage deposition begins at about 10 weeks and continues until the 24th week. The alveoli grow at a steady rate throughout gestation; however, unlike the cartilage and bronchi, alveolar growth continues into postnatal life. This is well demonstrated in Figure 10-59. Surface active agent (surfactant), the lipoprotein which prevents total collapse of the postnatal alveoli on expiration, begins to be formed in the alveolar lining cells in the second and beginning of the third trimester.

The fetal lung is not a tiny totally collapsed structure but is partially expanded by fluid formed within the lung, probably from the alveolar lining cells. It has a different composition from that of amniotic fluid. Fetal lung fluid probably contributes to the amniotic fluid as it is constantly being formed in the lung. There is speculation that it may be in part retained in the lung by spasm of the laryngeal muscle. That the fetal lung is partially expanded by fluid has been demonstrated both in fetal animal surgery and in radiographs of human fetuses after inadvertent

Fig 10-60—The fetal lung partly expanded by fetal lung fluid. This radiograph taken during attempted intrauterine transfusion shows inadvertent intrapleural injection of the contrast medium. The fetal lung is seen as a filling defect.



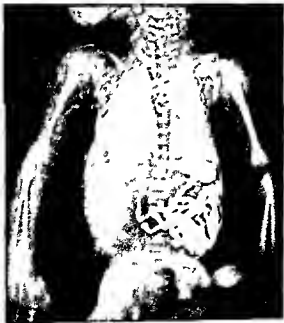


Fig 10-61—Lungs of a normal newborn in the first minutes of life show fissural thickening, streaky radiating densities and slight enlargement of the central mediastinal image. The infant was in no distress. Unanswerable questions include: is this transient stasis of fetal lung fluid ordinarily taken up by the lymphatics and veins; is there slight cardiac dilatation; is this a mild congestive change; and finally is this normal?

injection of contrast material in the pleural space during intrauterine transfusion for erythroblastosis. The fetal fluid-filled lung is seen to occupy a significant portion of the hemithorax (Fig. 10-60).

Cineradiographic studies at the time of delivery have demonstrated almost total aeration of the lungs

Fig 10-62—Thorotrast in the gastrointestinal tract and lungs of an aborted fetus; the contrast medium was injected into the amniotic cavity the day before abortion. The lung opacification is now thought to reflect fetal gasping and aspiration rather than in utero respiration, as formerly believed. (From Davis and Potter.)



in the first breath or breaths in the few infants studied. The actual fate of the pulmonary fluid is not known, although its extraordinarily rapid removal through the trachea and bronchial tree secondary to thoracic compression during delivery seems to be the main mechanism. Capillaries and lymphatics probably also remove some of the fluid. Films taken in the delivery room of normal newborns have occasionally shown streaky radiating pulmonary densities, thickened fissures and even minimal pleural reaction (Fig. 10-61). The pattern resembles pulmonary edema and the heart may be slightly enlarged. The infants were subsequently well. This may be evidence of transient cardiorespiratory distress that was self-limited and related to impaired resorption of the fluid. Harris stated that abnormal pulmonary densities may be found in chest films of newborn infants who have no clinically apparent respiratory difficulties. He considered these fleeting densities to be the result of physiologic disturbances which, in a given infant, are not sufficient to produce clinically recognizable signs.

The fetus does not normally respire in utero unless it is hypoxic and gasping. Physiologic studies in primate fetuses have suggested that Davis and Potter's films showing Thorotrast (injected into the amniotic space before abortion) in the lungs of the aborted fetus reflected fetal distress and not "breathing" (Fig. 10-62).

REFERENCES

- Avery M. E., et al. *Lung and Its Disorders in the Newborn Infant* (2nd ed. Philadelphia: W. B. Saunders Company, 1968).
- Davis M. E., and Potter E. L. Intrauterine respiration of the human fetus. *J.A.M.A.* 131:1194, 1946.
- Harris, G. B. C. *Progress in Pediatric Radiology* (Basel: S. Karger, 1967) Vol. 1, p. 138.
- James L. S., and Adamson K. Jr. Respiratory physiology in the fetus and newborn. *New England J. Med.* 271:1352, 1964.
- Lind, J. et al. *Human Foetal and Neonatal Circulation* (Springfield, Ill.: Charles C. Thomas Publisher, 1964).
- et al. Roentgenologic studies of the size of the lungs of the newborn baby before and after aeration. *Ann. pediat. fennae* 12:20, 1965.

The Newborn with Respiratory Distress

Fetal lung development requires a normal cushion of amniotic fluid (as well as an intact diaphragm) to prevent undue internal pressure by the huge fetal liver and external pressure by the uterus on the developing lung. In a patient with oligohydramnios and respiratory distress, severe renal malformations or chronic amniotic leakage should be considered. Any condition leading to major oligohydramnios may be manifested by lethal pulmonary hypoplasia. A few gasps may be made or the infant may live a few hours. The lungs are stiff and readily rupture, causing interstitial emphysema which may lead to pneumomediastinum and pneumothorax (airblock). Misshapen ears and a receding chin (Potter's facies) may be

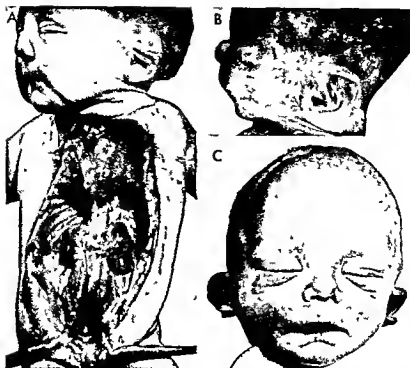


Fig 10-63 — Potter's faces characteristic of bilateral agenesis. In A the bilateral retroperitoneal masses are large fetal adrenal glands. There is a facial resemblance in all three infants: flat

nose, receding chin and large, flattened, distorted ears. C shows the abnormal distance between the eyes and prominent apical nasal fold. (From Potter.)

noted as well (Fig 10-63). Conversely, respiratory distress in an infant after hydramnios has been observed should alert the physician to the possibility of esophageal or duodenal obstruction (the usual absorption of swallowed amnion in the small bowel cannot occur) or cervical obstructions (such as teratoma) which prevent swallowing. Meconium staining of a distressed infant suggests fetal hypoxia and prenatal defecation with aspiration of meconium. This must be suctioned out before resuscitation and oxygen administration. Purulent amniotic fluid may be associated with fetal and neonatal pneumonia and sepsis; the placenta should be examined and cultures taken.

Some surgical causes of respiratory distress (lobar emphysema, cystic lung disease) are apparent after the first few hours of life. Others, such as diaphragmatic hernia and eventration, cause symptoms immediately to the degree that there is pulmonary hypoplasia (both on the side of the anomaly and on the opposite "normal" side). Hyaline membrane disease, preferably called respiratory distress syndrome, usually does not cause acute symptoms immediately after birth, although on careful observation, respiratory abnormalities are detectable. Abnormalities of the thoracic cage may be associated with severe respiratory distress such as that seen with severe infantile osteogenesis imperfecta or with the tiny unyielding thorax of the asphyxiating dystrophy of Jeune.

Some such patients survive, and the thoracic cage must be assessed in the infant with early respiratory distress.

Some infants with severe postnatal respiratory distress have unrecognized cervical cord damage or even transection. The neurologic deficit may not be recognized and the patient is considered to have respiratory distress syndrome. Radiographic demonstration of marked narrowing of the trachea during inspiration (Fig 10-64) should not be confused with or called "tracheomalacia." This term is poorly defined and places the blame for clinical findings on an abnormally soft collapsing trachea. Once it is realized that the infant's trachea normally is markedly responsive to transmural transmission of intrathoracic and extrathoracic pressures and straining, it is not surprising to see extreme ranges in caliber. The same comment could be applied to the somewhat older infant with noisy stridorous breathing. (This too has been called tracheomalacia, although it is almost always merely noise in an otherwise healthy infant with floppy aryepiglottic folds that partially collapse over the glottic airway during inspiration.)

The physician confronted with a distressed newborn in the delivery room should promptly obtain a chest film to distinguish remediable surgical conditions from nonsurgical or nontreatable causes of respiratory distress.

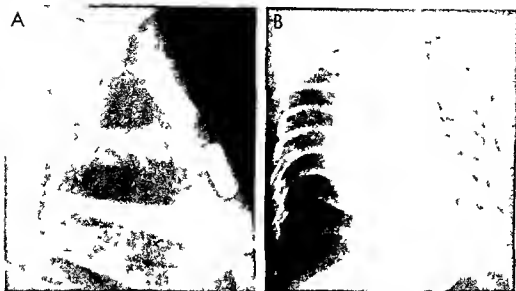


Fig 10 64—A marked tracheal narrowing in an infant with obstructive C5 and C6 cord transection. Autopsy showed complete tracheobronchial cartilaginous rings, no definite *from* those seen in other infants dying at the same age of nonrespiratory causes. B In a desperately ill infant, a very narrow trachea in the lateral chest film (not shown) could have been confused with

primary tracheomalacia. The frontal projection shows the cause of respiratory distress to be the tiny thorax with restrictive rib motion, termed *Jeune's thoracic esophy* at *ng dystrophy*. Radiographically (and sometimes clinically) this is similar to the Ellis-van Creveld dwarfism seen in the Amish; some patients with this syndrome survive, but the chest remains small.

Fig 10 65—Bilateral choanal atresia secondary to fibrous septa between the back of the nasal and the nasopharynx. A Lateral view: the infant is ectopic on his back with the x-ray beam horizontal and the head hyperextended. Bilateral broncho-

graphic contrast agents can be used for this study. B: the patient in the same position but with the x-ray beam vertical, resulting in a submentovertex projection to show bilateral obstruction.



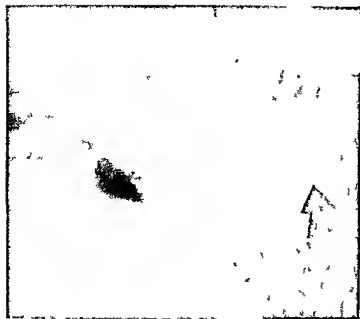


Fig 10-66—Cervical teratoma in a newborn infant with respiratory distress and marked maternal hydramnios. The large cervical mass contains calcifications (arrow). The thyroid scan suggested a mass of thyroid origin, but the extrathyroidal teratoma was removed with relief of the airway obstruction.

MECHANICAL AIRWAY OBSTRUCTION—Upper airway obstruction is harmless in utero, although sometimes accompanied by hydramnios if swallowing is also obstructed. It may endanger life after birth since the newborn is virtually an obligatory nose-breather due to the horizontal position of the large neonatal tongue. Bilateral choanal atresia therefore may be a critical emergency. The diagnosis is suspected when covering of the mouth causes cyanosis and dyspnea. Nasal catheters cannot be advanced and the diagnosis is readily confirmed by the instillation of contrast material into each nostril with the infant in the horizontal position (Fig 10-65). Submental vertex and lateral views confirm the presence of obstruction; usually in the posterior nasal cavity. Fibrous or bony septa may be present but are very difficult to identify in plain films. Immediate treatment is insertion of an oral airway through which the infant can both breathe and swallow. Gastrostomy is occasionally needed. The second possible site of obstruction is the nasopharynx, which may be blocked by tumor, for example a teratoma. Such tumors are visualized as large soft tissue masses obstructing the nasopharyngeal airway in the lateral projection. Children born with hypoplastic mandible and a large posterior tongue (Pierre Robin syndrome) may have airway obstruction. Prevertebral soft tissue masses may compress the airway. Hemangiomas around the glottis, prevertebral neuroblastomas, cervical hygromas and teratomas and goiter can all cause obstruction (Fig 10-66). In each case the plain film shows the level of the obstruction; instillation of contrast material into the airway is occasionally needed to confirm the diagnosis.

Atresia of a portion of the trachea may be present,

with air entering the lung through a fistula between the esophagus and the bronchi. Death is the usual outcome, although the potential for cure exists. Roentgen studies show the nasotracheal tube and the nasogastric tube to be in the esophagus, and to overlap each other in the lateral projection (Fig 10-67, A and B). In contrast study of the esophagus the material fills the bronchi through the esophageal fistula (Fig 10-67, C).

The tracheobronchial tree may be obstructed by mediastinal mesodermal tumors, hemangiomas or bronchogenic cysts (Fig 10-68). In these instances the lungs may show unilateral or bilateral air trapping or retention of fetal fluid (Fig 10-69). Varying degrees of mediastinal shift may be present. Specific diagnosis may not be possible; however, mechanical mediastinal obstruction can be identified as the cause of the respiratory distress by conventional and barium studies of the esophagus.

Although the commonest causes of respiratory difficulty in the neonate are related to medical conditions, it must be repeatedly emphasized that surgically correctable conditions may mimic medical respiratory distress.

REFERENCES

- Capitano M A et al: Upper airway tract obstruction in infants and children. *Radiol Clin North America* 6:265 1968
- Dunbar J S: Upper airway obstruction in infants and children. *Am J Roentgenol* 107:1 1970
- Jeune M et al: Dystrophie thoracique asphyxiante de charactère familial. *Arch franc pediat* 12:866 1955
- Joshi V V: Tracheal agenesis. *Am J Dis Child* 117:341 1969
- Köhler E et al: Dystrophic thoraces and infantile asphyxia. *Radiology* 94:55 1970

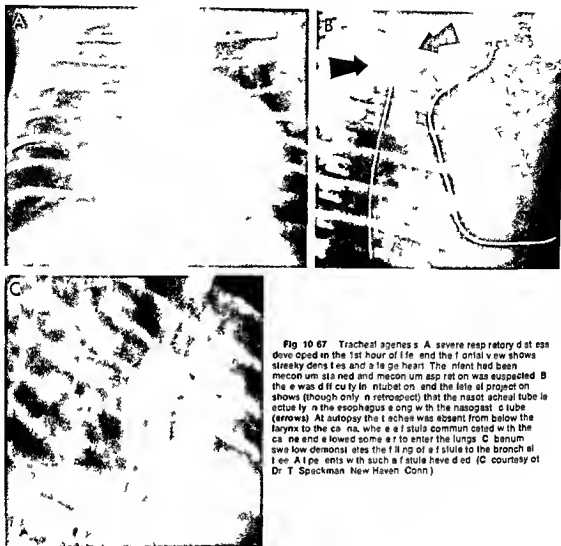
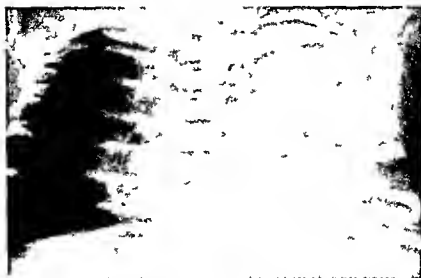


Fig 10-67 Tracheal agenesis. A: severe respiratory distress developed in the 1st hour of life, and the frontal view shows streaky densities and a large heart. The infant had been meconium stained and meconium aspiration was suspected. B: there was difficulty in intubation, and the lateral projection shows (though only in retrospect) that the nasogastric tube is actually in the esophagus along with the nasogastric tube (arrows). At autopsy the trachea was absent from below the larynx to the caudal, where a fistula communicated with the caudal end, allowing some air to enter the lungs. C: barium swallow demonstrates the filling of a fistula to the bronchus. All patients with such a fistula have died. (C courtesy of Dr T. Speckman, New Haven, Conn.)



Fig. 10-68 (above) —A huge and ultimately lethal mediastinal mesodermal sarcoma in a 2-week-old infant. The trachea is shifted to a curvilinear fashion since the thymus does not shift the trachea; this suggests the possibility that the mediastinal widening is due to tumor, not thymus.

Fig. 10-69 (below) —A mediastinal bronchogenic cyst in a



newborn has caused left bronchial obstruction with retention of fetal lung fluid. Thus the opaque left side of the chest is actually an emphysematous left lung filled with fluid rather than air. Films after a barium swallow should be obtained in such a patient to search for esophageal deviation before attempting thoracentesis. (Courtesy of Dr. N. T. Grasmann, Boston.)

Taybi H. Congenital malformations of the larynx, trachea, bronch, and lungs. *Prog Pediat Radiol* 1:231, 1967.

Wittenberg M H et al. Tracheal dynamics in infants with respiratory distress: stridor and collapsing trachea. *Radiology* 88:653, 1967.

TRANSIENT TACHYPNEA OF THE NEWBORN—Tachypnea alone has been observed in a small group of infants 1 or 2 days of age whose films show streaky densities, thickened fissures and slight cardiomegaly. Avery has called this uncommon occurrence of self limited tachypnea without other signs or symptoms transient tachypnea of the newborn (Fig. 10-70).

Fig. 10-70—Tachypnea for the first 48 hours of life in a patient with mild respiratory distress. A, at 6 hours shows mild cardiomegaly, fissural thickening, streaky radiating densities, this represents fetal fluid, mild congestive failure, not a failure of expansion. Neonatal atelectasis, meconium aspiration, or total anomalous pulmonary venous return below the diaphragm? B, 2 days later, heart and lungs are normal and the infant recovered without specific therapy. It is this sequence rather than the initial findings which allows consideration of the transient respiratory distress syndrome.

other terms are transient respiratory distress syndrome, transition syndrome, and wet lung of the newborn. The pathogenesis is unclear. Avery speculated that it could be a delay in venous and lymphatic removal of fetal lung fluid. The diagnosis requires knowledge of the course as well as correlation with the clinical and laboratory studies. The major difficulty in assigning a cause of such tachypnea is that all infants recover. It seems to be a self limited minor derangement in adaptation to extrauterine life. During this period the following must occur: fetal lung fluid must be resorbed or expelled through the tracheobronchial tree; all segments of lung must aer-

lous pulmonary venous return below the diaphragm? B, 2 days later, heart and lungs are normal and the infant recovered without specific therapy. It is this sequence rather than the initial findings which allows consideration of the transient respiratory distress syndrome.

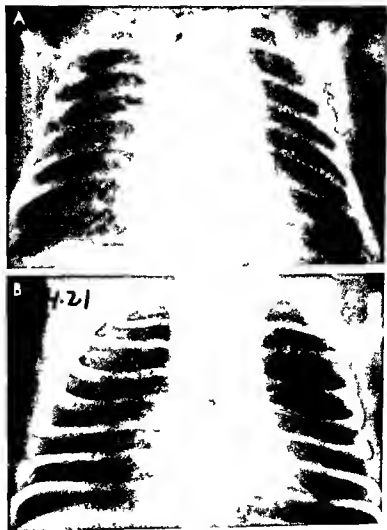




Fig 10-71 — Chest film of an infant with typical respiratory distress syndrome. Fine granular densities surround a rilled bronchus. The mediastinal image is wide (it is not known whether this is due to failure of thoracic shrinkage or to cardiac dilatation). (Courtesy of Dr R. C. Ablow, San Francisco.)

ate and stay inflated. Central respiratory centers must function normally. Intracardiac and extracardiac shunts are present with the direction of flow determined by the fluctuating relationships of pulmonary and systemic arterial pressure. To attribute the clinical and radiographic findings to a single factor such as fetal lung fluid is attractive but unwarranted. Abnormal pulmonary densities in the chest films of newborn infants without clinically apparent respiratory difficulties may be the result of physiologic disturbances not sufficient to produce clinically recognizable signs. They should not be dismissed as normal.

REFERENCES

- Avery M. E. *et al*. Transient tachypnea of the newborn. Possible delayed resorption of fluid at birth. *Am J Dis Child* 111:380, 1966.
- Fletcher B. D. *et al*. Radiographic demonstration of postnatal fluid in the lungs of newborn lambs. *Pediatrics* 252, 1970.
- Kuhn J. P. *et al*. Roentgen findings in transient tachypnea of the newborn. *Radiology* 92:751, 1969.
- Swischuk, L. E. Transient respiratory distress of the newborn (TRDN). A temporary disturbance of a normal phenomenon. *Am J Roentgenol* 108:557, 1970.

RESPIRATORY DISTRESS SYNDROME (HYALINE MEMBRANE DISEASE)—This frequently fatal disease is largely confined to newborn infants weighing less than 2000 Gm. It has however been seen in larger infants in the macrosomatic infants of diabetic mothers and in infants born by cesarean section. The old concept of primary failure of lung expansion is not an acceptable diagnosis for such newborns with respiratory distress; rather it reflects the onset of progressive atelectasis in previously expanded lungs leading to respiratory and cardiac failure, although usually not clinically detected for several hours. Radiographs at this time may look normal or show a mini-

mal granular pattern. With progression of the atelectasis granular densities become more apparent; these represent overlapping collapsed areas (Fig 10-71). The air-filled bronchi stand out, causing an air bronchogram. They are particularly distended and therefore well seen when the patient is receiving assisted ventilation. In fact both granular densities early in the course and the air bronchogram vary with the phase of ventilatory assistance. Some of these peripheral dilated air spaces perhaps reflect mild interstitial pulmonary emphysema (Fig 10-72).

Fig. 10-72 — Hyaline membrane disease. Close-up of right lower lobe shows a rilled bronchus in relief against innumerable granular densities causing the air bronchogram sign. The small peripheral lucencies probably represent developing foci of interstitial pulmonary emphysema.



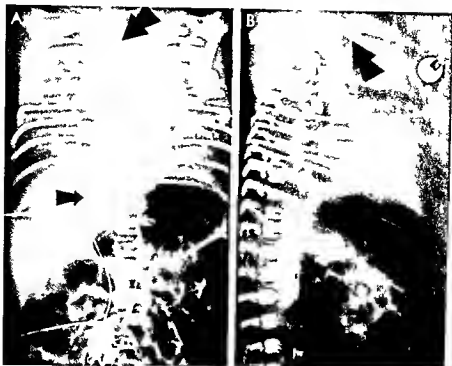


Fig 10-73—Hyaline membrane disease with nasotrachea (upper arrow) and umbilical arterial and venous catheters (lower arrows) in place. A frontal projection shows the venous catheter in the liver below the ductus venosus and the arterial catheter improperly placed near the origins of the major abdominal

aortic branches. B lateral projection easily separates the posterior and anterior venous catheters. Note the aortic bifurcation and the esophagus and trachea contrasted with opaque lungs secondary to severe hyaline membrane disease.

Avery and others have stressed the importance of the lipoprotein surfactant (surface active agent) in this syndrome. It is manufactured in the fetus from 20 weeks on, probably in the alveolar lining cells, and its continued production prevents total collapse of the lungs on expiration. Its production apparently is inadequate in the lungs of these distressed newborns, presumably in response to pulmonary damage from hypoperfusion and hypoxia in utero. The lungs thus initially expand, then foci of collapse begin to develop, usually in the lower lobe. The substance is apparently able to regenerate, as it is found in the lungs of infants dying of this condition after the 3rd day of life. Management of the respiratory distress syndrome includes assisted ventilation and monitoring of blood gases. Endotracheal intubation is usual with assisted ventilation, and the tube may inadvertently enter major bronchi with a potential for obstruction of a portion of or an entire lung. Clinicians must be alerted to the position of the tube. Blood gas analysis is commonly monitored by arterial and/or venous arterial catheters. The arterial catheter must be away from major aortic ostia, and the catheter's location should be noted. Lateral views clearly demonstrate the distal extent of the nasotracheal airway and easily separate the posterior umbilical arterial catheter from the

anterior venous catheter (Fig 10-73). The venous catheter should lie in the inferior vena cava or right atrium. One that is inadvertently twisted may come to lie in a mesenteric vein or within the liver. If concentrated alkali solutions are injected in these sites, major necrosis is likely to develop (Fig 10-74). The aortic catheter should lie above the diaphragm away from the brachiocephalic vessels or major ostia and well below the ductus arteriosus (Fig 10-75).

Respiratory distress syndrome follows one of three courses. The first is relentless progression to a totally atelectatic lung with collapsed chest wall (bell thorax) and death. The second is mild, with rapid recovery both clinically and radiographically. The third course is more protracted, with recovery or death ensuing after or in spite of vigorous respiratory assistance and repeated correction of acid base imbalance, which may last for weeks to months. During this time the lungs demonstrate persistence of radiographic abnormalities. Large confluent densities develop adjacent to areas of overexpanded lung, and in this phase the patient is particularly subject to interstitial pulmonary emphysema, pneumomediastinum and pneumothorax (airblock). The lungs are stiff and do not fully collapse. The mediastinum may not shift even though there is a tension pneumothorax in

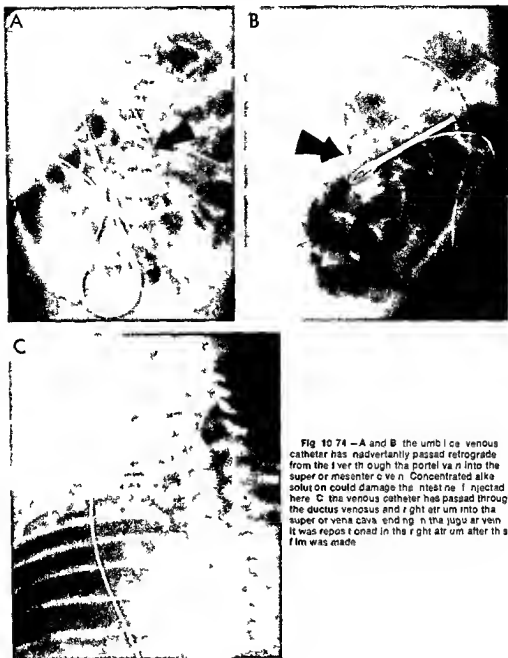


Fig 10-74 —A and B: the umbilical venous catheter has inadvertently passed retrograde from the liver through the portal vein into the superior mesenteric vein. Concentrated alkaline solution could damage the intestine if injected here. C: the venous catheter has passed through the ductus venosus and right atrium into the superior vena cava, ending in the jugular vein. It was repositioned in the right atrium after this film was made.



Fig 10.75—Severe hyaline membrane disease with an air bronchogram and opaque lungs. The arterial catheter was inadvertently passed into the innominate artery. The best sites for the catheter are low in the thorax well below the ductus arteriosus

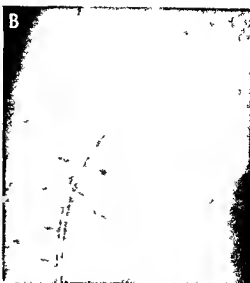
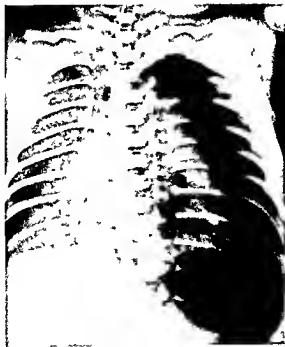


Fig 10.76—Severe hyaline membrane disease in a patient treated by positive pressure assisted ventilation. There is tension pneumothorax on the left. The inversion of the left diaphragm rather than a marked mediastinal shift is due to extreme loss of compliance in both lungs.

Fig 10.77 (right)—Chronic hyaline membrane disease in a patient treated for two months by positive pressure ventilation

and low in the abdomen well below the major aortic branches. Marked pulmonary hemorrhage was also present at autopsy on this patient.

end high oxygen concentration. The bubbly areas indicate emphysema adjacent to atelectatic and normal areas. This has been termed bronchopulmonary dysplasia oxygen toxicity lung and respiratory lung. Note the nephrothiasis (arrow) presumably due to prolonged acidosis and episodes of renal hypoperfusion secondary to systemic hypotension.



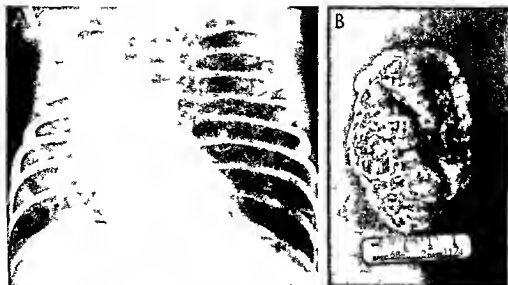


Fig 10-78—A chest film of a survivor of hyaline membrane disease treated with oxygen and assisted ventilation shows an emphysematous left upper lobe containing many reticular densities that simulate lobar emphysema. B thoracotomy specimen shows blebs and contains many dilated lymphatics. Pathologic

considerations included lobar emphysema as well as coexistent lymphangectasia; the changes are probably due to the original disease and to the therapy. (Courtesy of Dr. H. Burko, Nashville, Tenn.)

stead the diaphragm inverts (Fig 10-76). The lungs in chronic hyaline membrane patients are a bizarre combination of emphysematous areas and areas of collapse (Fig 10-77). Air trapping is common at the bases. Rarely a lobe is so involved as to simulate congenital lobar emphysema (Fig 10-78).

In infants who die the hyaline membranes may be

Fig 10-79—Total collapse of the right lung in hyaline membrane disease. The cleared rapidly with suction, and the chest was virtually normal two days later. Ductal secretions from the major bronchus can cause alarming radiographic findings in patients with nonlethal respiratory distress syndrome.

seen to be surrounded by histiocytes that ingest and remove them; surfactant returns. Marked fibroblastic proliferation possibly due to the toxic effects of oxygen therapy is noted throughout the interstitium. It is difficult to separate the individual contribution of oxygen toxicity, healing hyaline membrane disease, and assisted ventilation (especially positive pressure) in such a damaged lung. Also, the infant's ability to expel mucus is impaired by the drying effects of the oxygen; atelectasis of entire lobes occurs (Fig 10-79). Nasotracheal intubation impairs expulsion of secretions as ciliated epithelium is replaced by squamous metaplasia of the trachea and bronchi.

REFERENCES

- Ablow R. C. *et al*: Advantages of direct magnification technique in the newborn chest. *Radiology* 92:745, 1969.
- Avery M. E. *et al*: Lung and Its Disorders in the Newborn Infant (2nd ed). Philadelphia: W. B. Saunders Company, 1968.
- Baker D. H. *et al*: Proper localization of umbilical arterial and venous catheters by lateral roentgenograms. *Pediatrics* 43:34, 1969.
- Campbell R. E.: Intrapulmonary interstitial emphysema: A complication of hyaline membrane disease. *Am. J. Radiol.* 110:449, 1970.
- Gregory C. A. *et al*: Gas embolism in hyaline membrane disease. *New England J. Med.* 282:1141, 1970.
- Harris C. C. B.: The newborn with respiratory distress. Some roentgenographic features. *Radiol. Clin. North America* 1:497, 1963.
- Kuterman J. A. *et al*: Catheterization of the umbilical vein in newborn infants. *Pediat. Clin. North America* 17:895, 1970.
- Nelson N. M.: On the etiology of hyaline membrane disease. *Pediat. Clin. North America* 17:943, 1970.



- Reynolds E O R *et al* Hyaline membrane disease respiratory distress and surfactant deficiency *Pediatrics* 42: 758 1968
- Robertson B *et al* Late stage of pulmonary hyaline membrane of the newborn *Acta Paediatr* 53: 433 1964
- Rosengren K Hyaline membrane disease *Acta radiol* suppl. 62 1967
- Singleton E B Respiratory Distress Syndrome in Kaufmann H J (ed) *Progress in Pediatric Radiology* (Chaucer Year Book Medical Publishers Inc 1967) Vol 1 p 109

PULMONARY HEMORRHAGE—The incidence of pulmonary hemorrhage increases with the degree of prematurity and is a common finding in small premature infants. It is often associated with hyaline membrane disease with infection and especially with hypoxia. At autopsy many patients with pulmonary hemorrhage are also found to have intracranial hemorrhages. Whether pulmonary hemorrhage is a cause or an accompanying event is not settled. Radiographically pulmonary hemorrhage cannot be distinguished from other causes of respiratory distress. Indeed as noted they frequently coexist (see Fig 10-75). Clinically according to Avery most of these patients have blood in the upper airway and larynx. This finding is used by her group as an indication to treat for pulmonary hemorrhage.

MIKITY WILSON SYNDROME (PULMONARY DYSMATURITY)—In a few infants usually weighing below 1500 Gm mild symptoms of respiratory distress develop insidiously in the 1st week of life. In most severe respiratory distress syndrome has not been present. Chest radiographs at this time show small bubbly

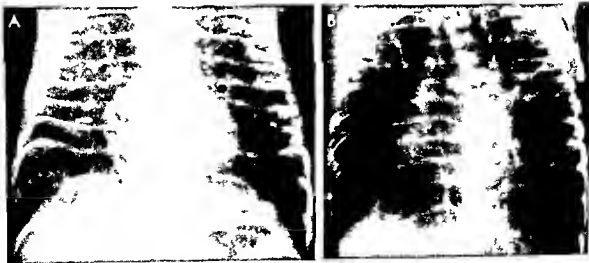
areas of focal hyperaeration (Fig 10-80 A). The clinical course is protracted with severe pulmonary disease and occasionally death. In patients who survive pulmonary abnormalities may be present for months (Fig 10-80 B). The bubbly pattern is replaced with the passage of time by large confluent densities again more commonly seen in the upper lobes associated with large areas of overaeration in the lower lobes. This may gradually recede centrally and the patient may recover fully. Oxygen is widely used (and needed) in supportive treatment of most of these infants as it is in the treatment of respiratory distress syndrome so the question of oxygen toxicity has again been raised to explain the pulmonary abnormalities. However signs of focal hyperinflation have been observed before oxygen was given and the initial cause of this syndrome is as unknown now as it was in 1960 when first described by Mikity and Wilson. We believe that the later stages so similar to those in survivors of chronic hyaline membrane disease probably again reflect the noxious effects of oxygen and assisted ventilation. This has been called bronchopulmonary dysplasia by Northway although it is an acquired disease not a true congenital dysplasia.

REFERENCES

- Burnard E D The pulmonary syndrome of Wilson and Mikity and respiratory function in very small premature infants *Pediatr Clin North America* 13: 999 1966
- Hodgman J E *et al* Chronic respiratory distress in the premature infant *Pediatrics* 44: 179 1969

Fig. 10-80—Focal diaphragmatic hyperaeration in a premature infant (delayed pulmonary maturation of Mikity and Wilson bubbly lung syndrome). A This infant weighing 1400 Gm had tachypnea and cyanosis and needed oxygen at 5 days of age. Fine bubbly changes were present in the initial film prior to oxygen therapy. B Three months later there are larger basal emphysematous areas with large coarse streaky densities in the middle and upper lung

fields. Gradually the infant was weaned from oxygen and over the next year the lungs returned to normal appearance. Not all patients recover. Some patients develop pulmonary hypertension and some die of pulmonary insufficiency. B shows the noxious effects of oxygen therapy. This patient also received positive pressure assisted ventilation.



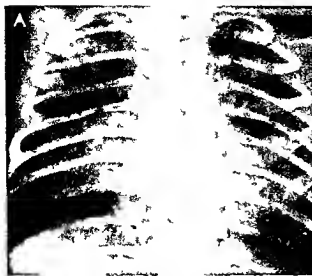


Fig 10-81.—Meconium aspiration syndrome—a full-term infant who had fetal distress during labor and was meconium-stained at delivery. Laryngoscopy revealed sticky meconium in the airway which was suctioned. A, frontal and B, lateral projections show an overexpanded chest with flat diaphragm and retrosternal lucency. The lungs contain patchy and dense

areas with large clear areas and clear periphery indicating that there is airway obstruction at multiple sites with peripheral atelectasis and emphysema. Pneumothorax (chemical from the effects of meconium or secondary to superimposed infection) may be present but cannot be diagnosed from these films.

Mikity V G, et al. The Radiologic Findings in Delayed Pulmonary Maturation in Premature Infants. In Kaufmann H J (ed) Progress in Pediatric Radiology (Chicago: Year Book Medical Publishers Inc 1967) Vol 1 p 149
 Thibeault D W, et al. Radiologic findings in lungs of premature infants. J Pediatr 74:1 1969

MECONIUM ASPIRATION SYNDROME—The hypoxic fetus may defecate meconium in utero or during delivery and aspirate considerable amounts of it. The thick tenacious meconium acts as a mechanical block to the airway producing radiographic changes quite different from those of the respiratory distress syndrome. The roentgen manifestations of severe me-

conium aspiration syndrome consist of large irregularly distributed densities usually centrally placed and extending toward the periphery in an uneven fashion and considerable peripheral and overall overaeration (Fig 10-81). The findings vary from mild to severe. Patients with the most severe changes are likely to have had assisted ventilation prior to adequate suctioning. Treatment of the aspiration syndrome initially therefore is preventive with adequate suctioning to remove the meconium prior to the institution of ventilation. Once the meconium has reached the small airways treatment is supportive with repeated suctioning. Oxygen administration may

Fig 10-82.—Extensive interstitial emphysema. A, frontal projection shows many small radiolucencies in both lungs; these are in the interstitium, a though difficult to distinguish from over-

distended alveoli. B, autopsy specimen shows the multiple small bubbles to be interstitial, surrounded by totally collapsed lung tissue. (Courtesy of D. B. D. Fletcher, Montreal)



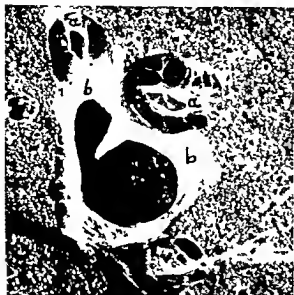
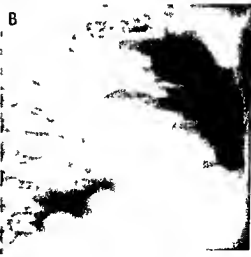


Fig 10 83 —Photomicrograph of the cut surface of lung of a cat in which interstitial emphysema had been induced by intra tracheal air insufflation. Interstitial air surrounds the branches of the pulmonary artery (a) and a vein (v) but not the bronchus (b) except where it sheaths the vessels. (From Macklin and Macklin.)



Fig 10 84 —Localized interstitial emphysema secondary to meconium aspiration. Frontal projection shows coalescence of many small bubbles into several large ones in the right lower lobe. These are easily mistaken for congenital cysts if the sequence is not appreciated. The interstitial air was rapidly resorbed and the infant thrived.

Fig 10 85 —A block syndrome. In A frontal projection on the pneumothorax elevates the thymus and shifts the left mediastinal pleura laterally. In newborns with this syndrome the air tends to collect and remain in this area, whereas in older children and adults it rapidly dissects in the neck. B lateral projection



tion shows both the anterior collection elevating the thymus and the inferior extension below the lung and the diaphragmatic pleura simulating subpulmonary pneumothorax. (Courtesy of Dr H Morgan New York.)

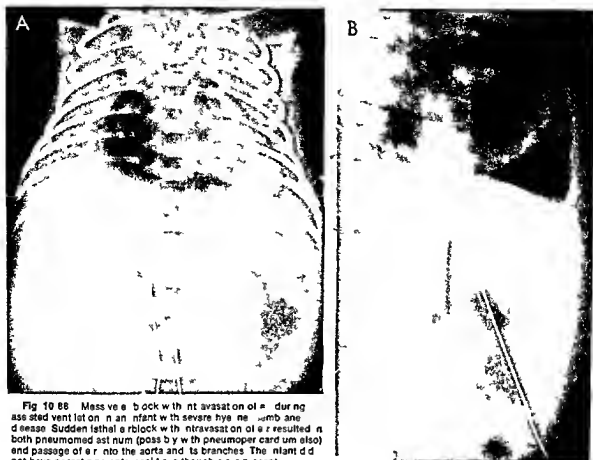


Fig 10-88 Massive air block with intravasation of air during assisted ventilation in an infant with severe hyaline membrane disease. Sudden lethal air block with intravasation of air resulted in both pneumomediastinum (possibly with pneumopericardium also) and passage of air into the aorta and its branches. The infant did not have necrotizing enterocolitis although air is present throughout the portal venous system. A, frontal and B, lateral projections. (Courtesy of Dr C. A. Gregory, San Francisco.)

be necessary. Antibiotics are commonly given and occasionally steroids to prevent chemical pneumonia. Meconium aspiration has been the most common cause of the airblock syndrome in the Babies Hospital neonatal service.

AIRBLOCK—Any condition in which there is expiratory airway obstruction (as with meconium aspiration) or a stiff lung (as in respiratory distress syndrome, pulmonary hypoplasia with renal agenesis, diaphragmatic hernia) may lead to the sequence of events termed airblock by the Macklins. They believed that such airblock occurs when air exit is obstructed. A pressure differential develops during expiration between overdistended blocked alveoli and the adjacent interstitium; alveolar rupture occurs into this interstitium. Pulmonary interstitial emphysema develops as fine bubbles within the lung parenchyma (Fig 10-82). It may if not decompressed, block pulmonary venous return and cause death with pulmonary edema. The air may pass along perivascular sheaths (Fig 10-83) to the mediastinum. In other cases the small foci in the lung coalesce into cysts that may be mistaken for congenital lung cysts (Fig

10-84). Once the pulmonary interstitial emphysema leaks to the mediastinum, pneumomediastinum develops. Usually the air stays in the anterior mediastinum; if extensive it is anterior and well seen in lateral films as a bubble of air elevating the thymus (Fig 10-85). It may be difficult in frontal projections to distinguish pneumomediastinum from pneumopericardium (Fig 10-86).

A left superior mediastinal bulge (ductus bump) seen in frontal chest radiographs of some newborn infants on the 1st or 2nd day of life represents the ductus arteriosus and main pulmonary artery (Fig 10-87). It is caused by the straight line tubular connection of these structures (Figs 10-88 and 10-89). Pneumomediastinum by pressing the pulmonary artery downward further exaggerates the straight line connection; the largest ductus bumps seen have been in patients with pneumomediastinum (Fig 10-90). It should not be confused with a mediastinal tumor. By the 3rd day it is gone. It can only be seen in frontal projections; barium swallow studies are normal (see Fig 10-87).

Another spurious mass may be seen in lateral chest

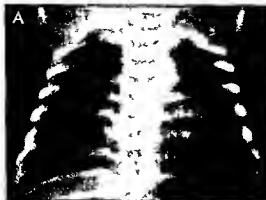


Fig 10 87 —A, frontal projection on day 1 shows a ductus bump—a left superior mediastinal bulge adjacent to the aortic knob. Presumably it represents dilatation of the ductus arteriosus and main pulmonary artery. The lateral view was normal. B, on



day 2 after a barium swallow shows no esophageal mass effect and the bulge is smaller. A radiograph the following day was normal.

Fig 10 88 (above) —A, a frame from a cine angiogram in left ventricular systole. The umbilical venous catheter has passed through the ductus venosus and right atrium into the left atrium. Arrows indicate that the arch of the aorta within the mediastinal contours is not the cause of the ductus bump. The letter does not till as pulmonary and systemic circuits have similar systolic pressures. B, a frame in left ventricular diastole. The ductus bump fills because the higher end diastolic aortic pressure causes left to right shunting to the ductus arteriosus and pulmonary artery. (Courtesy of Dr L S James.)

Fig 10 89 (below) —A, a frame from a cine angiogram

shows that the umbilical aortic catheter has passed into the aortic arch. Contrast medium delineates the arch and descending aorta within the mediastinal contour. Left to right shunting now opacifies the ductus bump made up of the ductus arteriosus and pulmonary artery. In B, lateral projection of an umbilical aortogram, the arrows indicate filling from the aorta through the horizontally aligned ductus arteriosus and main pulmonary artery to the level of the pulmonary valves. It is probably this tubular confluence of the ductus and pulmonary artery seen in this lateral view that appears as the ductus bump in frontal views. (Courtesy of Dr L S James.)

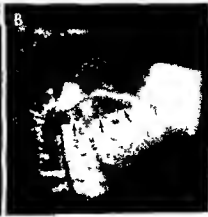
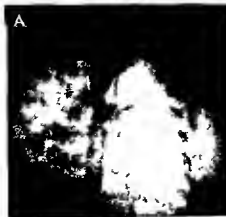
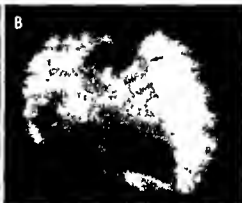




Fig 10-90—A large ductus bump in an infant with a large mediastinum (extending subpleurally into the left diaphragm), a small right pneumothorax and meconium aspiration. These findings disappeared but the lungs remained abnormal with red atelectases and the infant remained cyanotic. At autopsy on day 12, total anomalous pulmonary venous return below the diaphragm entering the portal vein was found. When an infant does not respond in the usual time to the suspected cause of respiratory distress, other causes should be considered.

Fig 10-92—In an infant with a bilateral pneumothorax, note the dense lung (due to engorgement, atelectasis, bleeding, hyaline membrane disease or whatever combination has led to a large block). There is probably some pneumomediastinum as well. Subcutaneous emphysema is distinctly uncommon in newborns with a large block, although it does occur.



Fig 10-91—A pseudoposterior mediastinal mass due to the scapulae overlaying the posterior chest, commonly seen in lateral projections of the chest of newborns. Should this mass be seen in lateral views of an infant whose frontal film showed a ductus bump, it could lead to the erroneous diagnosis of a posterior mediastinal tumor and even to thoracotomy.

Fig 10-93—Skull fold simulating pneumothorax. It is long and curved, extending above and below the lung (arrows), lung medial to the folds of normal density. This can occur on one or both sides and has led to unexpected air collections and surgeons to tap a non-existent pneumothorax.

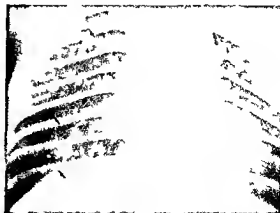




Fig 10-94—Mediastinal emphysema (with elevation of the trachea) and marked subcutaneous emphysema. An attempt to use the internal jugular vein for blood analysis resulted in accidental puncture of the trachea (not lung) so that expiration against the

closed glottis during crying forced air through the puncture site. Pneumothorax never developed and the infant recovered uneventfully.

films of newborns as a posterior density. It is an illusion made up of trachea and bronchi anteriorly and under surface of the scapula inferiorly. It is not visible after a barium swallow because there is no mass. Rarely a ductus bump is noted in frontal films while this seeming posterior mass is observed in lateral films of an infant who then is subjected to unnecessary thoracotomy (Fig 10-91).

With sufficient pressure the pneumomediastinum ruptures through the mediastinal parietal pleura leading to unilateral or bilateral pneumothorax (Fig 10-92). Such pneumothorax in the neonate must be differentiated from the common observation of skin folds in infants of low birth weight in the neonatal chest radiograph (Fig 10-93). Collapsed lung is usually considerably denser than aerated lung due both to compression and to the presence of foreign material in the airway. In questionable cases oblique and decubitus projections are helpful.

In the newborn mediastinal air tends to remain in the anterior mediastinum or to go on to pneumothorax; it does not commonly dissect into the cervical subcutaneous tissues or into the abdomen. Attempts at jugular puncture for blood samples have resulted in accidental nicking of the trachea, followed by pneumomediastinum and extensive subcutaneous emphysema (Fig 10-94). Air in the mediastinum may dissect down between the parietal pleura and the diaphragm and collect extrapleurally causing a picture easily confused with subpulmonary pneumothorax (Fig 10-95). In such instances decubitus films help to

differentiate intrapulmonary pneumothorax from extrapleural mediastinal air. The pressure of the pneumothorax may be because of inability of the lungs to expand and deflate severely limit gas exchange (see Fig 10-76).

Fortunately the airblock syndrome is usually secondary to meconium aspiration and is self-limited. The usual treatment is supportive. While this condition is much more common in full-term postmature infants than in premature infants, the possible danger to the eyes if 100% oxygen is given must be borne in mind.

REFERENCES

- Avery M E et al: Lung and Its Disorders in the Newborn Infant (2nd ed). Philadelphia: W B Saunders Company, 1968.
- Berdon W E et al: The ductus bump. *Am J Roentgenol* 95:91, 1965.
- Chernick V et al: Spontaneous alveolar rupture at birth. *Pediatrics* 32:816, 1963.
- et al: Pneumothorax and chylothorax in the neonatal period. *J Pediatr* 76:624, 1970.
- Fletcher B D et al: Pulmonary interstitial emphysema in the newborn. *J Canad A Radiologists* 21:273, 1970.
- Lillard R L et al: Extrapleural air signs in pneumomediastinum. *Radiology* 85:1093, 1965.
- Macklin M T and Macklin C C: Malignant interstitial emphysema of the lung and mediastinum as an important occult complication in many respiratory diseases and other conditions. *Medicine* 23:281, 1944.
- Matthieu J et al: Pneumopericardium in the newborn. *Pediatrics* 46:117, 1970.
- Rudhe U et al: Pneumomediastinum and pneumothorax in the newborn. *Acta radiol (diag)* 4:193, 1966.

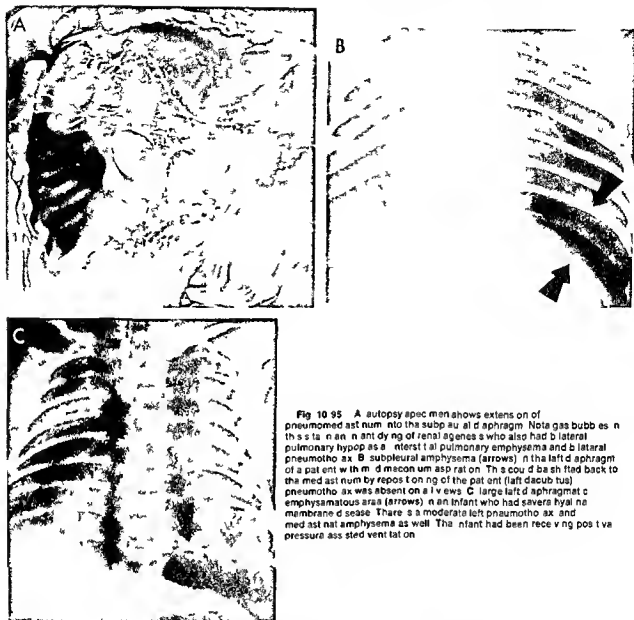


Fig 10-95 A: Autopsy specimen shows extension of pneumothorax into the subdiaphragmatic space. Note gas bubbles in the subdiaphragmatic space. B: Autopsy specimen shows bilateral pulmonary hypoplasia, interstitial pulmonary emphysema, and bilateral pneumothorax. C: Autopsy specimen shows subpleural emphysema (arrows) in the left diaphragm of a patient with meconium aspiration. The could be shifted back to the mediastinum by repositioning of the patient (left decubitus). Pneumothorax was absent on all views. C: Large left diaphragmatic emphysematous areas (arrows) in an infant who had severe hyaline membrane disease. There is a moderate left pneumothorax and mediastinal emphysema as well. The infant had been receiving positive pressure assisted ventilation.

CARDIOVASCULAR LESIONS SIMULATING PULMONARY DISEASE—Congenital cardiac malformations are not dealt with here but mention must be made of some that closely resemble lung disease. The clinical picture including respiratory distress and its response to treatment may strikingly simulate lung disease. Total anomalous venous return usually below the diaphragm to the portal vein is one example. The diagnosis may be suspected in an infant with reticular patterns of interstitial edema or radiating vascular engorgement and a normal size heart in plain films but is proved only by angiocardiography which shows

both failure of normal filling of the left atrium and the anomalous trunk going to its junction with the systemic venous return (Fig 10-96). Lymphatic malformations of the lung may be primary (termed pulmonary lymphangectasis) (Fig 10-97) or associated with pulmonary venous anomalies such as total anomalous venous return below the diaphragm (see Fig 10-96) or atresia of the distal common pulmonary vein or may be part of a more generalized lymphatic abnormality possibly involving viscera and bones and associated with a protein losing enteropathy.

Infants born with any of these malformations may

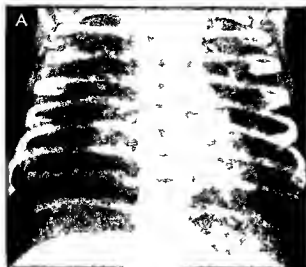


Fig 10-96—Two infants with the same lethal entity (total anomalous venous return below the diaphragm to the portal vein) have totally differing plain film patterns. **A** shows a diffuse reticular pattern probably due to the secondary problem of en-

gorged edematous lymphatic. **B** shows more radial lung vasculature engorgement due to obstruction of the anomalous channel by a combination of its small diameter, its length, possible narrowing at diaphragmatic passage and high portal venous pressures.

have stiff lungs and respiratory distress that simulates lung disease. The primary diagnosis may not be made, and resuscitative efforts can produce airblock. Generally the diagnosis of obstructed venous return is not considered until days have gone by during which time the usual patient with meconium aspiration would have recovered. Since the heart may be of

normal size, cardiac causes are considered late. Survival is rare.

The large cardiophymic image (a thickset of words shielding the radiologist from being precise as to which is heart and which is thymus) has generally proved to be a large heart in most of the ill newborns in whom this image has been seen. In the 1st days of

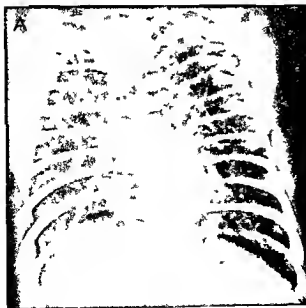


Fig 10-97—Primary lethal lymphangectasia of the lung. In **A**, note the great similarity to the pattern in Figure 10-96. **A** is with total anomalous venous return below the diaphragm. This is to be expected because lymphatic dilates with venous obstruction. **B**, autopsy specimen shows dilated lymphatic on the lung surface. Some patients with the more generalized lymphatic anomalies that include bone and mediastinum have less severe clinical manifestations but similar pulmonary radiographic findings at a later age. (Courtesy of Dr V. G. M. Kety, Los Angeles.)

life such enlargement may be due to extracardiac shunts such as hepatic hemangioma and umbilical or cerebral arteriovenous malformations. In the infant with a hypoplastic left heart syndrome such as that seen with mitral or aortic atresia the radiographic picture may range from normal to that of gross cardiomegaly and engorged lungs. Determining factors are the size of the left-to-right shunt at the foramen ovale and the size and patency of the vital right-to-left shunt at the ductus arteriosus.

These cardiac problems are dealt with in detail elsewhere in this book. Hepatic hemangioma with heart failure alluded to earlier in this section (see Fig 10-3) is diagnosed by total body opacification during intravenous pyelography with confirmation by umbilical aortography and venography.

REFERENCES

- Avery M E *et al*. Lung and Its Disorders in the Newborn Infant (2nd ed). Philadelphia: W B Saunders Company 1968).
- Case Records of Mass Gen Hosp. Total anomalous pulmonary venous drainage into portal vein. New England J Med. 268 1354 1963.
- Cooley D A *et al*. Correction of total anomalous pulmonary venous drainage. Surgery 42 1014 1957.
- Murray D E. Congenital arteriovenous fistula causing congestive heart failure in the newborn. JAMA 209 770 1969.
- Noonan J A. Congenital pulmonary lymphangectasis. Am J Dis Child 120 314 1970.
- O'Hara A E *et al*. Congenital pulmonary lymphangectasis. Am J Radiol 103 119 1968.
- Rudolph A M. Cardiac failure in children. A hemodynamic overview. Hosp Practice July 1970.

CHYLOUS PLEURAL EFFUSION—Effusion of pleural fluid in the neonate is rare. Thoracentesis should be performed to see if chylous effusion is present. Pathogenesis is obscure; actual organic obstruction to the thoracic ducts is not usually found. Clinically tachycardia, retractions and cyanosis develop (similar to respiratory distress syndrome). The chest radiograph shows pleural effusion which is usually unilateral and more common on the right (Fig 10-98). Chylous fluid is clear before the infant is given milk feedings because there is insufficient ingestion of long chain triglycerides to result in milky chyle. As part of the treatment a diet of medium chain triglycerides can be used since it depends on portal venous absorption and spares the lymphatic system until the leak seals. Since sepsis and pneumonia can lead to neonatal pyothorax the tapping of neonatal effusions for gram stain, fat analysis and culture is important because the treatment depends on the proper diagnosis.

REFERENCES

- Chernick V *et al*. Pneumothorax and chylothorax in the neonatal period. J Pediatr 76 624 1970.
- Gwinn J L. Chylothorax in the newborn. Am J Dis Child 115 59 1968.
- Hashim S A *et al*. Treatment of chylothorax and chylothorax with medium chain triglycerides. New England J Med 270 756 1964.

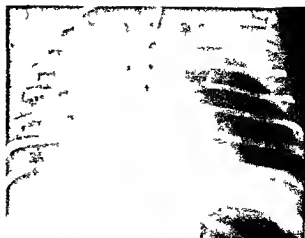


Fig 10-98 Chylous effusion in the newborn. This may be on the left (as shown) on the right or rarely bilateral. The initial diet of newborns may be too poor in long chain triglycerides to cause the fluid to become obviously chylous. Repeated tapping usually is the only therapy needed until the presumed leak from the thoracic duct seals off. Medical management can include a medium chain triglyceride diet that spares the lymphatic transport system. (Courtesy of Dr H S Goldman, New York.)

Yancy W S *et al*. Spontaneous neonatal pleural effusion. J Pediatr Surg 2 313 1967.

PNEUMONIA—Pneumonia is a clinically significant neonatal problem that is virtually impossible to distinguish radiographically from many noninfectious processes. Prolonged rupture of the membranes, prolonged labor and excessive obstetric handling are all related to neonatal infection. Transplacental passage of organisms can occur or the amnion itself can be infected. Neonatal pneumonia has been reported as being due to bacterial, spirochetal, fungal and viral agents.

Immune defects, interference with body defense mechanism and isolated areas of immune deficiency all reported in children are generally not neonatal problems.

REFERENCES

- Avery M E *et al*. Lung and Its Disorders in the Newborn Infant (2nd ed). Philadelphia: W B Saunders Company 1968).
- Munif G R. Congenital bacterial pneumonia with intact fetal membranes. Pediatrics 45 865 1970.
- Willch E. The Roentgenological Appearance of Pulmonary Listeriosis in Kaufmann H J (Ed.) Progress in Pediatric Radiology (Chicago: Year Book Medical Publishers Inc 1967) Vol. 1 p 161.

Surgical Conditions of the Newborn Chest

As noted earlier, tachypnea, cyanosis, retractions and acid-base balance disturbance are the hallmarks in the newborn of medical respiratory distress syndrome. Similar signs and symptoms may occur from aspiration of meconium with airway obstruction or as

TABLE 10-1 --DIFFERENTIAL DIAGNOSIS OF RESPIRATORY DISTRESS IN THE NEWBORN*

Analysis of Chest Film in Terms of Mediastinal Shift

- 1 Shift away from abnormal side
 - A Cystic lung (adenomatoid malformation)
 - B Lobar emphysema
 - C Bronchial atresia
 - D Diaphragmatic hernia, eventration
 - E Effusion (empyema, chylothorax)
 - F Origin of left pulmonary artery from right pulmonary artery (pulmonary sling)
 - G Duplication (neurenteric) cyst
- 2 Shift toward abnormal side
 - A Agenesis of the lung
 - B Massive atelectasis
- 3 No significant shift
 - A Meconium aspiration
 - B Pulmonary hemorrhage
 - C Hyaline membrane disease
 - D Mikity-Wilson syndrome
 - E Transient tachypnea of Avery
 - F Pneumonia
 - G Upper airway obstruction (choanal atresia)
 - H Abnormal thoracic cage (osteogenesis imperfecta, asphyxiating dysplasia, etc.)
- 4 Variable patterns of shift/no shift
 - A Vascular rings
 - B Mediastinal tumors (bronchogenic cysts)
 - C Pneumatoceles

*Modified from Caplan and Kirkpatrick

a secondary manifestation of intracranial hemorrhage with fetal anoxia. The radiologist has a crucial role in establishing the diagnosis of conditions that can be treated surgically since they may cause identical clinical signs and symptoms in the newborn period. A useful approach for considering these conditions appears in Caplan and Kirkpatrick's review (Table 10-1).

The following discussion is centered on respiratory distress due to mechanical compression of the lung (as in lobar emphysema, diaphragmatic hernia, duplication cyst) or of the trachea and bronchi (as with mediastinal vascular rings). Oscar Wilde said: Experience is the name we give our mistakes, and we can add nothing to his comment.

DIAPHRAGMATIC HERNIA AND EVENTRATION—Both true defects in the diaphragm (hernia) and the paper-thin intact diaphragm (called eventration or hernia with intact sac) are important surgical conditions which cause respiratory distress in the newborn. The wide range of signs and symptoms reflects the degree of coexistent pulmonary hypoplasia. There is the infant who is stillborn, the one who makes a few feeble gasps and dies (Fig. 10-99) and the infant who on the 3rd or 4th day of life is found to have bowel sounds in the chest or is suspected of having dextrocardia (Fig. 10-100) since most hernias are left-sided and shift the

mediastinum to the right. The defects are often large and usually posterolateral or involve the entire hemidiaphragm. Although termed Bochdalek defects, they actually represent persistent pleuropertoneal canals. As the left side is four to five times more commonly involved than the right, the midgut as well as the stomach, spleen, left lobe of the liver, and kidney may be in the chest.

The mortality rate for the child whose diagnosis is made at 3–4 days of age is very low compared to the nearly 100% mortality in the infant whose defect is detected at 30 minutes of age. This reflects the prime role in the prognosis of the coexistent pulmonary hypoplasia (Fig. 10-101 and see Fig. 10-99) not only on the side of the hernia but in the opposite normal lung. Apparently slight differences in the timing in utero when the herniation occurs result in either arrest of pulmonary bronchial growth at a stage that will not allow viability or reasonable lung development with good prospect for survival. The group between these extremes may survive with proper operative and especially postoperative care.

The very sick infants are commonly referred with the clinical diagnosis of respiratory distress syndrome (Fig. 10-102). The very depressed infant may not have swallowed air, and the herniated midgut appears as a water-density mass within the chest (see Fig. 10-99 A). Mediastinal shift is marked. In a patient with such a mass density diaphragmatic hernia is one diagnostic possibility (see Fig. 10-99 A and C) air in small amounts makes an excellent contrast material and is to be favored over barium in this instance. Severe eventration is radiographically and clinically indistinguishable from a true hernia (see Fig. 10-101).

Some infants with Erb's palsy may also have transitory or permanent paralysis of the diaphragm. A radiograph of such a patient obtained during deep inspiration will show paradoxical elevation of the affected side and can be confused with eventration (Fig. 10-103).

The hypoplastic lung, always worse on the side of the hernia but a bilateral phenomenon, may take considerable time to fully expand. These immature lungs rupture very easily and therefore both pneumothorax and pneumomediastinum and pneumothorax may develop on either side in the postoperative period (Fig. 10-104) especially if forceful attempts are made to expand the lungs either by the operating surgeon or by assisted breathing techniques. Since the involved bronchial tree is abnormal in number as well as in structure, the hypoplastic lung may eventually overinflate and become emphysematous (Fig. 10-105).

The diagnosis of diaphragmatic hernia thus may be extremely easy with a gasless scaphoid abdomen and obvious bowel loops in the left chest, or extremely difficult in an infant believed clinically to have severe respiratory distress syndrome. Unfortunately it must be accepted that the earlier the diagnosis is made, the worse the prognosis. Hopefully some patients with

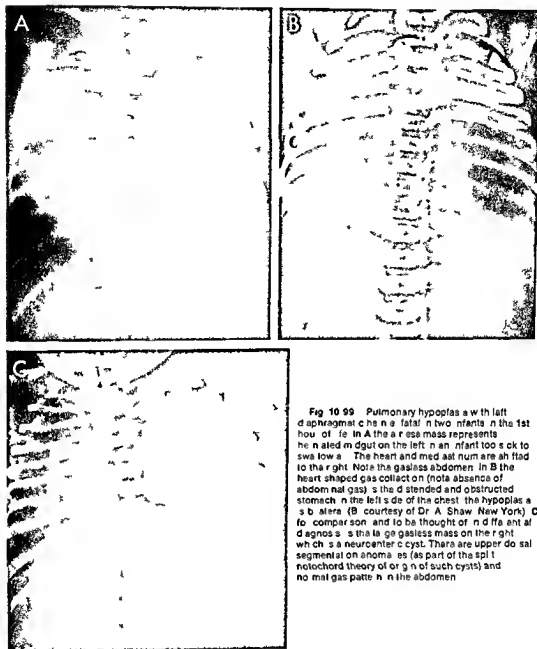


Fig 10-99 Pulmonary hypoplasia with left diaphragmatic hernia in two infants in the 1st hour of life. In A the large mass represents the enlarged lung on the left in an infant too sick to swallow. The heart and mediastinum are shifted to the right. Note the gasless abdomen. In B the heart-shaped gas collection (note absence of abdominal gas) is the distended and obstructed stomach in the left side of the chest; the hypoplasia is bilateral (B courtesy of Dr A. Shaw, New York). C for comparison and to be thought of in differential diagnosis is the large gasless mass on the right which is a neuroenteric cyst. There are upper abdominal segmental anomalies (as part of the split notochord theory of origin of such cysts) and no malgas pattern in the abdomen.

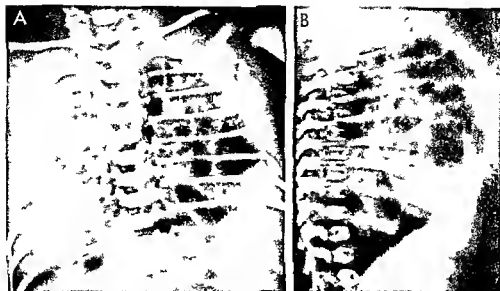


Fig 10-100—Typical radiographic appearance of a congenital diaphragmatic hernia. **A**, frontal projection; **B**, lateral projection. Heart sounds were heard on the right (due to left-sided hernia). Intestinal gas was present in the chest; the chest film was obscured because of

respiratory distress. Gas-filled small bowel is the left side of the chest. The abdomen is moderately scaphoid in the lateral view although the abdominal location of noninvolved right hepatic lobe prevented clinical detection.

Fig 10-101—**A**, left-sided eventration (with paper-thin, intact diaphragm above the displaced midgut) in a neonate who died following repair of severe bilateral pulmonary hypoplasia. Symptomatic eventration in this newborn should be treated the same

way as symptomatic congenital diaphragmatic hernia. **B**, bronchogram of the excised lungs shows the tiny distorted left lung bronchus. The right bronchus looks normal, although the right lung was a so small in weight and size.

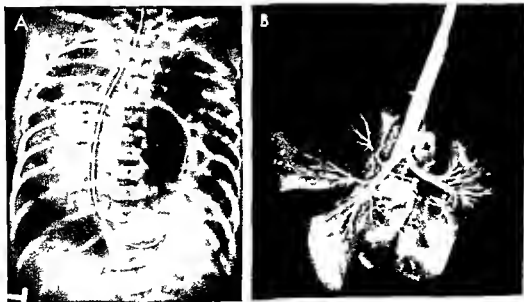




Fig 10-102 — A, frontal projection of the chest of a 4-hour-old infant with severe respiratory distress. The abnormally high position of the liver was not appreciated. B, lateral projection at 12

hours shows the right diaphragm at the level of the cardiac shadow due to the right eventration. The patient was operated on but died of bilateral pulmonary hypoplasia.

Fig 10-103. Benign diaphragmatic eventration due to right Erb's palsy with phrenic nerve involvement. Frontal projection during inspiration shows deep descent of the normally rising and paradoxical rise of the paralyzed right diaphragm. The infant recovered totally in a few months.



Fig 10-104. Right pneumothorax developed in an infant who had a left diaphragmatic hernia had been repaired (note chest deformity). This resulted from attempts to expand forcibly the left lung. This film shows the stiffness of the right lung and demonstrates that both lungs are hypoplastic.



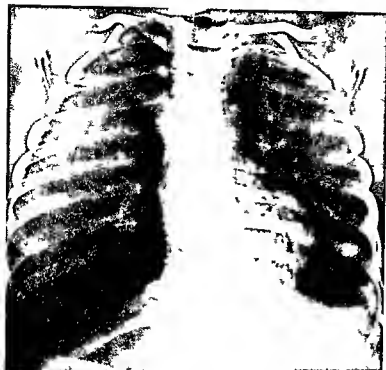


Fig 10-105 — Emphysema of the right lower lung of an infant who survived right diaphragmatic hernia repair and whose right lung was hypoplastic. The basal segments are the most hypoplastic. This can lead to a picture of overdistention of the area on delayed studies. There were no symptoms when this study was made; however, the lung scan showed no perfusion of the right lower lung.

hypoplastic lungs with early diagnosis can survive. Their inclusion because of earlier diagnosis and attempted repair increases the mortality rate in recent surgical series.

REFERENCES

- Areechon W *et al*: Hypoplasia of lung with congenital diaphragmatic hernia, *Brit M J* 1:230 1963
 Baffes T B: Diaphragmatic Hernia, in Mustard W T *et al* (ed): *Pediatric Surgery* (2nd ed, Chicago Year Book Medical Publishers Inc 1969) Chap 27
 Berdon W E *et al*: Role of Pulmonary Hypoplasia in the prognosis of infants with diaphragmatic hernia and even trancon Am J Roentgenol 103:413 1968
 Capitanio M A and Kirkpatrick J A: Roentgen examination in evaluation of the newborn infant with respiratory distress J Pediatr 75:896 1969

MEDIASTINAL SHIFT SECONDARY TO EMPHYSEMA TOUS LOBES — This condition is called congenital lobar emphysema. The incomplete cartilage rings of the trachea and major bronchi of the infant readily collapse on expiration with a normal mild tendency to air trapping. In some babies this is extreme and massive emphysema develops with collapse of adjacent lobes and mediastinal shift. Resultant tachypnea, retractions and cyanosis mimic respiratory distress syndrome. This condition is commonly confined to a lobe. Upper lobes and the right middle lobe are those usually involved (Figs 10-106 and 10-107 B). Occasionally all lobes are involved to a lesser degree and surgery cannot be undertaken (Fig 10-108). The

condition develops with varying rapidity in different patients. If seen in the first hours or day of life, streaky densities (possibly dilated lymphatics) or even fluid may fill the distended lobe (Fig 10-107 A).

Bronchography fails to demonstrate bronchial obstruction or stenosis (see Fig 10-106) even though dynamic studies show apparent marked expiratory

Fig 10-108 — Congenital lobar emphysema of the left upper lobe seen in part of a bronchogram. Note that the bronchus fills. Cause of obstruction is not found in most cases, though some patients seem to have even less cartilaginous rings in the involved bronchus than the normally incomplete cartilage genea. This may act as an obstruction during expiration.

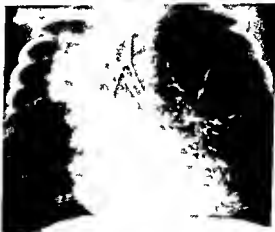




Fig 10-107—Congenital lobar emphysema of the right upper and middle lobes. A demonstrates a largely fluid-filled density on day 1. Note the mediastinal shift to the left. B, angiogram done a week later to exclude an anomalous left pulmonary artery arising from the right pulmonary artery as possible cause of the emphysema. The fluid has been resorbed (or perhaps expelled

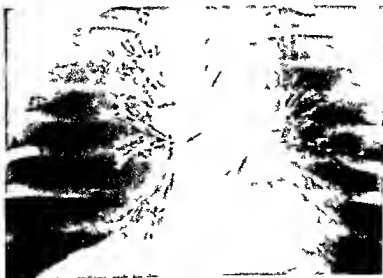
through the bronchial tree). As in any emphysematous lobe, the vessels are displaced away from the segment. Part of the right lung has herniated across the anterior mediastinum and the pulmonary vessels also cross the mediastinum. (Courtesy of Dr J. A. Kirkpatrick, Philadelphia.)

collapse (Fig 10-108). Some pathologists believe that defects in cartilage, especially at the level of saddle bronchi, predispose to lobar emphysema. If the emphysematous lobe continues to grow, surgical removal may be necessary. In some patients the same process then develops in other lobes. In still others the process seems to arrest itself; distention gradually disappears and the mediastinum returns to normal

position. The ultimate result in such a case may be a normal lung or a relatively avascular lobe with poor perfusion detected on lung scanning. Angiocardography in lobar emphysema shows redirection of flow to other lobes and stretching of vessels within the lobes (see Fig 10-107 B). It serves mainly to exclude compressive vascular anomalies. Barium swallow also aids in this differentiation and also demon-

Fig 10-108—Pentobar emphysema. Multiple episodes of trapping are seen during expiration, with resultant emphysema. The arrows indicate collapsing saddle bronchus during expiration. There was involvement of the right middle lobe, left main stem and lingular bronchus. The left lower and right lower lobe bronchi

show crowding and small volume. Surgery was not undertaken and the patient was relatively symptom-free several years later. Persistence of the abnormalities was demonstrated on chest radiographs, bronchography, studies and lung scans.



strates mediastinal masses such as bronchogenic cysts that can interpose themselves between esophagus and trachea and cause tracheal or bronchial obstruction

REFERENCES

- Allan R P *et al* Congenital lobar emphysema with dilated septal lymphatics *Radiology* 86 929 1966
 Campbell P E Congenital lobar emphysema, *Australian Paediatr J* 5 226 1969
 Franken E A *et al* Infantile lobar emphysema Report of two cases with unusual roentgen manifestations *Am J Roentgenol* 98 354 1966
 Griscom N T *et al* Fluid filled lung due to airway obstruction in the newborn *Pediatrics* 43 383 1969
 Mellins R B *et al* Obstructive disease of the airways in cystic fibrosis *Pediatrics* 41 3 1968
 Staple T W *et al* Angiographic findings in four cases of infantile lobar emphysema *Am J Roentgenol* 97 195 1966
 Talner L B The syndrome of bronchial mucocoele and regional hyperinflation of the lung *Am J Roentgenol* 110 675 1970

BRONCHIAL ATRESIA—Bronchial atresia is a rare cause of emphysema affecting part or all of a lobe that may be encountered in the newborn period although most cases have been seen in adults. The left upper lobe is most commonly affected although other lobes may be involved (Fig 10 109 A). The lobe is hyperlucent and presumably derives its air from collateral ventilatory channels. At birth it may be distended by retained fetal lung fluid rather than air. A nodule representing mucus in a dilated bronchus (Fig 10 109 B) is often noted near the site of normal bronchial origin and the intralobar bronchi are present. The atresia affects the connection of the lobe or major subsegments to the main stem bronchi. Bronchography may show this but it is difficult to distinguish bronchial atresia from lobar emphysema and

even congenital cystic adenomatoid malformation. In all three fluid may fill the involved lobes or streaky septums can be seen. The differential diagnosis is not critical since treatment is similar: the ill patient should have surgical exploration and the thriving infant can be watched.

REFERENCES

- Booth J B *et al* Unilateral pulmonary agenesis, *Arch Dis Childhood* 42 361 1967
 Guscom N T *et al* Fluid filled lung due to airway obstruction in the newborn *Pediatrics* 43 383 1969
 Litt R Congenital stenosis of the right mainstem bronchus, *Am J Roentgenol* 89 1007 1963
 Simon G *et al* Atresia of an apical bronchus of the left upper lobe *Brit J Dis Chest* 57 124 1963
 Talner L B The syndrome of bronchial mucocoele and regional hyperinflation of the lung *Am J Roentgenol* 110 675 1970

CONGENITAL CYSTIC ADENOMATOID MALFORMATION—Part of or all of a lung may be involved with a hamartomatous malformation termed congenital cystic adenomatoid malformation. The cysts may be gas-filled or fluid filled or contain elements of both. They may be small or large, single or multiple (Figs 10 110 and 10 111). Rarely they are associated with renal cysts. Cystic adenomatoid malformation probably accounts for most congenital cystic disease of the lung. The diagnosis is based on pathologic detection of distorted areas of glandlike structures and of bronchial structures lacking cartilage. The air when present enters through collateral pathways; bronchography usually fails to demonstrate any communication with a normal tracheobronchial tree and there is no histologic evidence of a normal bronchus. The cysts are easily mistaken for bowel loops and the diagnosis of diaphragmatic hernia has frequently been made

Fig 10 109—Bronchial atresia involving the left upper lobe. A at 1 day of age shows mainly a white density mass representing the enlarged left upper lobe. B at 8 later date air has replaced

the fluid. The nodule is a mucoid impact on in the enlarged bronchus with an atelectasis between the end of the main stem bronchus. (Courtesy of Dr John Dorst, Baltimore)



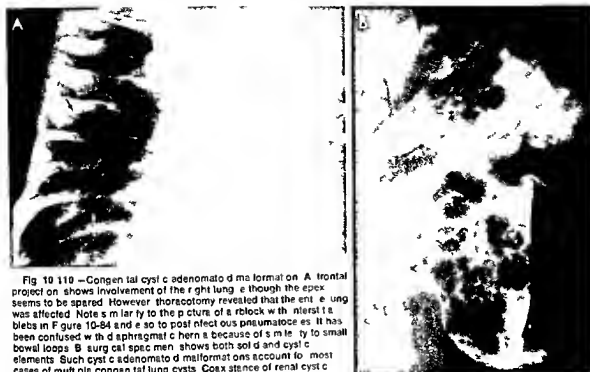


Fig 10-110—Congenital cystic adenomatoid malformation. A: Frontal projection shows involvement of the right lung, although the apex seems to be spared. However, thoracotomy revealed that the entire lung was affected. Note similarity to the picture of a ribcage with interstitial blebs in Figure 10-84 and also to postinfectious pneumatoceles. It has been confused with diaphragmatic hernia because of similarity to small bowel loops. B: Surgical specimen shows both solid and cystic elements. Such cystic adenomatoid malformations account for most cases of multiple congenital lung cysts. Coexistence of renal cystic disease is extremely rare.

In such cases if the attempted repair was performed transthoracically no great harm would be done. If however a transabdominal approach is used to correct the hernia serious problems may follow.

Since the cystic masses occasionally have anomalous arterial blood supply from the aorta either above or below the diaphragm exact differentiation of this group of anomalies from the group of pulmonary sequestration is not always possible. Perhaps these enti-

ties are actually part of a spectrum ranging from bronchogenic cysts through cystic adenomatoid malformation to sequestration and represent similar embryologic abnormalities which occurred at slightly different times in utero.

Acquired cystic disease (see below) in the form of postinflammatory pneumatoceles may be difficult to separate radiographically from the foregoing anomalies although pneumatoceles are uncommon in the

Fig 10-111—Cystic adenomatoid malformation. A: Frontal projection with the patient supine was originally misinterpreted as demonstrating lobar emphysema of the left upper lobe. In B with the patient erect a single large air-fluid level is apparent with small cysts in the area. The left upper lobe was removed. The

left lower lobe then developed the same picture and a portion of the left lung was removed. Diagnosis was congenital cystic adenomatoid malformation. This is usually a unilateral disease although rarely bilateral involvement is seen.



1st week of life tend to enlarge very rapidly and are frequently accompanied by pleural effusion or pleural thickening. Large air cysts as part of interstitial pulmonary emphysema seen in airblock can also cause confusion (see Fig 10 84)

REFERENCES

- Aslam P A *et al* Congenital cystic adenomatoid malformation with anasarca JAMA 212 622 1970
 Birdsell D L *et al* Congenital cystic adenomatoid malformation in the lung Canad J Surg 9 350 1966
 Craig M *et al* Congenital cystic adenomatoid malformation in the lung of infants Am J Roentgenol 76 516 1956
 Merenstein G B Congenital cystic adenomatoid malformation of the lung Am J Dis child 118 772 1969

DUPLICATION CYSTS (NEUROENTERIC CYSTS WITH OR WITHOUT MENINGOCELE)—Large sometimes multiple posterior mediastinal masses may be seen in the newborn infant. Respiratory distress when present, is due to pressure on the bronchial tree causing either collapse or air trapping. The diagnosis of duplication of the neuroenteric variety is suggested when a posterior mass is present usually in association with vertebral anomalies including hemivertebrae malsegmentation and block vertebrae (Fig 10-112 A and see Fig 10-99 C). Air myelography occasionally reveals a direct connection with the subarachnoid space and hence a thoracic meningocele (Fig 10-112, B) but in most cases the connection is a fibrous cord that does not have a lumen. Intra abdominal duplica-



Fig 10 112—Neuroenteric cyst A Plain film radiograph showing a large common cyst on the right with air in the vertebral segmental anomalies B Air myelogram shows an air fluid level demonstrating that in addition to the gastrointestinal and central nervous system components the lesion is ante vertebral meningocele. This is important to know preoperatively to alert the surgeon to possible need of neurosurgical help (Courtesy of Dr W McAlester St Louis)

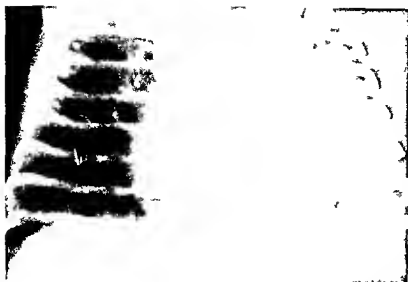


Fig 10-113—Bilateral poststaphylococcal pneumatoceles. These may attain enormous size at a time when the infant is no longer ill. They spontaneously regress in most cases and do not require excision or drainage. They should not be confused with congenital cyst of lung disease.

tions may coexist; they may be noted later with the onset of gastrointestinal bleeding as the acid-producing cysts discharge their contents into the intestine or as an increasing mass if the cyst is not in communication with the intestine. Barium swallow is helpful in showing the posterior nature of the masses. Rarely is there communication with the esophagus.

REFERENCES

- Bentley J F R, et al. Developmental posterior enteric remnants and spinal malformations. *Arch Dis Childhood* 35:76, 1960.
- Elliott G B, et al. The notochord as an abnormal organizer in production of congenital intestinal defect. *Am J Roentgenol* 110:628, 1970.
- Thoracic sequestration cysts of fetal bronchogenic and esophageal origin. *Canad J Surg* 4:522, 1961.
- Gerle R D, et al. Congenital bronchopulmonary foregut malformations. *Arch Dis Childhood* 35:87, 1960.

POSTINFECTIONOUS PNEUMATOCELE—Staphylococcal pneumonia was a great killer of infants at one time with the development of empyema and sepsis. Rapid enlargement of air spaces to giant size (pneumatoceles) probably reflected a check valve internal rupture of air into the lung interstitium. In many cases complete clearing developed with prolonged chemotherapy; others required drainage because of increasing size and respiratory embarrassment. Pneumatoceles are seen occasionally in the 1st week of life (Fig 10-113). The process is more common later in infancy when pneumonic infiltrations are followed by rapidly developing and enlarging pneumatoceles which on occasion may be bilateral.

A long argument has existed as to whether such pneumatoceles are infected congenital lung cysts or are acquired after pneumonia. There are enough cases in which early radiographs show an evolving pneumonia with subsequent formation of pneumato-

celes to point strongly to acquired disease. As Caffey noted in long term studies, the natural life history of such lung cysts as regression with surgery rarely being needed. Often the cysts enlarge to enormous proportions at a time when the infant has become asymptomatic and is thriving.

REFERENCE

- Caffey J. On the natural regression of pulmonary cysts during early infancy. *Pediatrics* 11:49, 1953.

UNILATERAL PULMONARY APLASIA OR MARKED HYPOPLASIA Any diagnosis of emphysema of a lung (from cysts, lobar emphysema or mediastinal bronchogenic cyst with airway obstruction) must be made after it has been proved that the smaller, collapsed contralateral lung is actually present. To put it in reverse, the large emphysematous lung may be the only lung. Although published reports of such pulmonary aplasia or marked hypoplasia mention the presence of vertebral anomalies as a helpful sign, these are not invariably present (Fig 10-114 A). Lung scanning would provide interesting information since it might show excellent uptake in the large lobe whereas an airtrapping or cystic lobe would not be perfused. Bronchography in pulmonary hypoplasia discloses either absence or marked hypoplasia of the bronchial tree on the involved side (Fig 10-114 B). In patients with primary agenesis of the lung, which is more common on the left than on the right, the main stem bronchus seems to be directly in line with the trachea on bronchoscopy. Survival is related to the severity of other existing anomalies such as complicated congenital heart disease. In vascular anomalies such as congenital absence of a pulmonary artery with a systemic blood supply to the lung or the scimitar syndrome of anomalous venous return from the small right lung to the inferior vena cava, the degree of

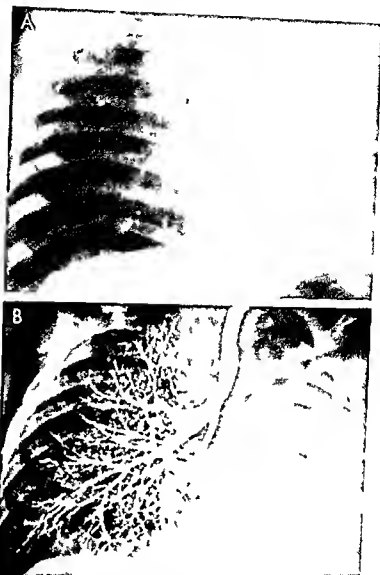


Fig 10-114 — A, marked left pulmonary hypoplasia is seen to be the cause of the small opaque left hemithorax and large lucent right lung. There were no vertebral anomalies or heart disease. B, bronchogram shows a normal right lung with the right main stem bronchus as large as, and a direct extension of, the trachea. There is a filling of a hypoplastic left lung bronchus. The right lung has been inflated across the anterior mediastinum, accounting for apparent aerated lung to the left of the midline.

pulmonary hypoplasia is slight and would not normally be confused with aplasia of a lung. In some cases, however, definitive diagnosis requires angiocardiology and bronchography.

REFERENCES

- Booth J B *et al*: Unilateral pulmonary agenesis. *Arch Dis Childhood* 42:361, 1967.
Wexels P: Agenesis of the lung. *Thorax* 6:171, 1951.

VASCULAR RINGS AND TRACHEAL COMPRESSION —

The soft trachea of the infant may be dangerously compressed by vascular anomalies, and this must be thought of in any infant with respiratory distress with or without stridor. A clue is that the infant is more

comfortable and the signs abate when the patient is prone with head hyperextended. Congenital laryngeal stridor should be a diagnosis of exclusion after plain film and barium swallow studies have shown a normal trachea and lack of aberrant vessels (Fig 10-115). The infant trachea normally buckles to a right angle merely from flexion or rotation of the head. Sharp local narrowing or curvilinear indentation is more ominous and demands a search for adjacent sources of encirclement or compression. Finally, the trachea indents the thymus; the thymus does not impinge on the trachea. Sad to say, some infants still receive radiotherapy for stridor due to thymic pressure on the airway.

The two commonest vascular rings—double aortic



Fig 10-115—Normal lateral view of a barium filled esophagus showing a trachea of normal caliber

arch (Fig 10-116 A) and right aortic arch with a left ductus arteriosus (Fig 10-116 B)—characteristically cause tracheal deviation to the left with a sharp localized indentation. They also displace the right mediastinal pleura since the aorta usually descends on the right in these patients. Unfortunately these two signs are very difficult to appreciate in most radiographs of the infant chest and, although useful, will not be stressed in the diagnosis of a vascular ring (Fig 10-116, C). The use of high kilovoltage technique or the development of short exposure tomography could improve visualization of these two findings. However, it is the encroachment by the ring on the esophagus and trachea seen in lateral projection after barium, that is the basis for the diagnosis.

In the evaluation of vascular rings it should be realized that each life endangering anomaly can also be seen in an asymptomatic adult. The signs in early life may relate to coexistent defects in tracheal growth (including stenosis) and to superimposed infections in older infants, the edema further narrowing the lumen. Stridor, atelectasis and, most seriously, apneic episodes are the respiratory signs of vascular anomalies in infants. The adult may have dysphagia from the esophageal component but the infant's signs reflect the tracheal embarrassment.

Angiocardiology has not been routinely used in the study of vascular rings at Barnes Hospital. The cardiologic and surgical point of view has been to explore the infants with signs compatible with a vascular ring and roentgen evidence of an aberrant bronchopulmonary vessel. This has led occasionally to fruitless surgery because the symptoms and signs were unrelated to the radiographic findings. The possible

combinations of aberrant vessels and persistent ligamentous ductus arteriosus are almost endless. Four major patterns have emerged that have proved helpful in the vast majority of cases. No simple scheme can be 100% accurate, and advocates of angiocardiology have a valid point in saying that the more information gained before surgery, the more accurate the surgical approach and treatment.

Posterior esophageal anterior tracheal indentation (secondary to double aortic arch or right aortic arch with left ligamentous ductus arteriosus)—With either of these anomalies the trachea is caught in a ring created by both anterior and posterior encircling vessels. The posterior esophageal indentation is large and due to either part of the aortic arch or a broad based origin of the left subclavian artery (Fig 10-116 A and B). Anteriorly, either the arch or the carotid arteries press on the trachea and stridor results. The ductus adds to the tension. The patient with a double aortic arch (Fig 10-116, A) and the patient with a right aortic arch and anomalous left subclavian artery and a left ligamentous ductus arteriosus (Fig 10-116, B) present the foregoing radiographic pattern (Fig 10-117, A). The double aortic arch more commonly causes symptoms in early infancy. At the time of left thoracotomy the ductus can be divided in one case or the smaller of the doubled arches in the other, to relieve the anterior compression of the trachea. The esophageal defect persists postoperatively (Fig 10-117, B). Occasionally the tracheal narrowing and clinical picture may continue or increase in severity after surgery, necessitating tracheostomy. This reflects mediastinal edema and bleeding and what may be an actual growth disturbance of the trachea, with stenosis or excessive collapsibility present.

Unfortunately, any simple scheme has its defects. For example, although angiocardiology is neither needed nor helpful in diagnosing the usual vascular ring, it is essential in the exceptional case in which barium swallow delineates a retroesophageal indentation resembling a double arch. This represents the very rare left ascending aorta with a transverse retroesophageal arch and right descending aorta. A right sided ductus tightens and closes the ring (Fig 10-118). Angiocardiology is diagnostic and a right thoracotomy, not used to approach the usual vascular ring, is needed to divide the ductus.

Anterior esophageal posterior tracheal indentation (secondary to anomalous left pulmonary artery)—An anomalous left pulmonary artery (pulmonary sling) is another vascular cause of respiratory distress (Fig 10-119 A). The left pulmonary artery arising from the right pulmonary artery crosses through the mediastinum to the left lung, passing over the right main stem and right middle lobe bronchus then coursing between the trachea and esophagus. Any of the components of the tracheobronchial tree with which the anomalous left pulmonary artery comes in contact may be impinged on. Right sided

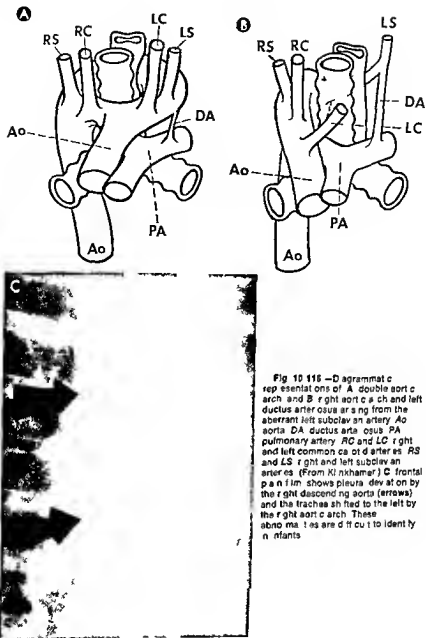


Fig 10-116—Diagrammatic representations of **A** double aortic arch and **B** right aortic arch and left ductus arteriosus arising from the aberrant left subclavian artery. **Ao**, aorta; **DA**, ductus arteriosus; **PA**, pulmonary artery; **RC** and **LC**, right and left common carotid arteries; **RS** and **LS**, right and left subclavian arteries. (From Kinkhamer.) **C**, frontal plain film shows pleural deviation on the right descending aorta (arrows) and the trachea shifted to the left by the right aortic arch. These abnormalities are difficult to identify in infants.

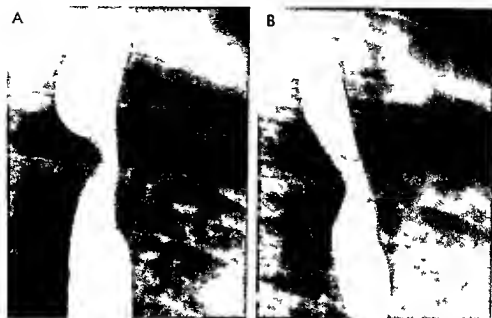


Fig 10-117—Vascular ring. A lateral view of an infant with stridor shows evidence of a large aberrant retroesophageal vessel and anterior tracheal indentation (arrow) representing a vascular ring due to a double aortic arch. Stridor continued for sev-

eral months after surgery. B repeat postoperative radiograph shows the aberrant vessel with slight tracheal narrowing (arrow). The symptoms finally disappeared.

emphysema is the most common result (Fig 10-119 B). One or more lobes may be affected. Barium swallow may be diagnostic (Fig 10-119 C). This anomaly if suspected should be confirmed by angiocardiography. Why the barium swallow is inconsistently diagnostic in this anomaly is not known. Surgical division of the left pulmonary artery from its source re-establishing communication anterior to the trachea is the treatment of choice. This rare though important anomaly must be thought of in any infant with massive areas of overinflation collapse or both in the first weeks of life. Right thoracotomy without preoperative angiocardiography has several times led to confusion and delayed correct diagnosis because the anomalous vessel was hidden from sight by the azygos vein and superior vena cava. A small mediastinal bronchogenic cyst at or near the carina may cause the same radiographic appearance as the pulmonary sling with overinflation or collapse of the lungs or elements of both. An anomalous right subclavian artery (see below) rarely if ever goes between the trachea and the esophagus but rather passes *behind* the esophagus.

Anterior tracheal narrowing normal esophagus (secondary to compression by the innominate artery)—In the crowded superior mediastinum of the infant the innominate artery (or a truncus formation of the innominate and left carotid artery) may press on the anterior tracheal wall and cause the signs and symptoms of vascular rings although there

is no aberrant retroesophageal vessel (Fig 10-120 A). A constant anterior tracheal curvilinear narrowing seen in lateral projection is the sign of this anomaly (Fig 10-120 B). Surgery may be required when apnea or recurrent atelectasis complicates the clinical stridor. Stridor alone has not been an indication for repair in our series. Intercurrent respiratory infection with edema of the trachea makes this relatively common anomaly symptomatic in patients whose narrowing was *inconstant*. Surgery has not alleviated the symptoms. Angiocardiography does not prove this diagnosis since the appearance of the innominate artery does not differ from that of the normal infant. Skilled bronchoscopic examination in infants with stridor due to this anomaly has disclosed a pulsating bulge on the anterior tracheal wall.

Normal trachea oblique retroesophageal indentation (secondary to anomalous subclavian artery)—This is the most common anomaly of the aortic arch representing either the usual aberrant right subclavian artery with left aortic arch or the much rarer aberrant left subclavian artery with right aortic arch. Barium swallow delineates a small oblique retroesophageal indentation (Fig 10-121 A and B). It is rarely a cause of any respiratory signs or symptoms unless the trachea is also compressed anteriorly by a common trunk of the carotids (truncus anomaly) (Fig 10-121 C). In this case both an anterior tracheal narrowing and a posterior esophageal indentation is visualized. Surgery has not been helpful in patients with an aber-

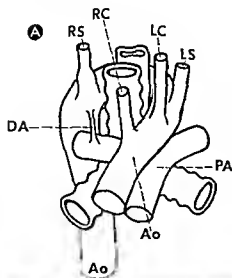


Fig 10-118 —Vascular ring A, diagram of rare vascular ring due to a left aortic arch which extends retroesophageally and a right descending aorta. The ring is completed by a right ductus arteriosus (DA) Ao aorta PA pulmonary artery RC and LC right and left common carotid arteries RS and LS right and left subclavian arteries (From Klunkhamer) B, frontal view after barium swallow in a patient with such an anomaly plus large ventricular septal defect, shows prominent indentation on the left side of the esophagus which is then displaced to the left by the right descending aorta C, lateral projection demonstrates a large retroesophageal vessel, erroneously thought to be an aberrant left subclavian artery or part of a double aortic arch Angiocardiography provided the correct diagnosis The patient died after thoracotomy and division of the right ductus arteriosus A sibling died of the same complex of anomalies.



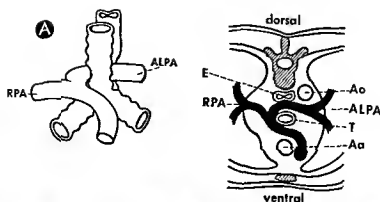


Fig 10-119—Aberrant pulmonary artery. **A**, diagram of aberrant left pulmonary artery (ALPA) arising from the right pulmonary artery (RPA) and crossing between the esophagus (E) and trachea (T) to the left lung. (From Kinkhimer.) **B**, frontal view of an infant 2 weeks of age with severe bilateral air trapping and respiratory distress reveals marked overinflation of the right lung with mediastinal shift to the left. Barium swallow revealed no abnormality. **C**, right thoracotomy was performed with right middle lobectomy; the surgical specimen was interpreted as showing

congenital lobar emphysema. Signs and symptoms continued unabated. **C**, at age 6 months, barium swallow reveals an aberrant pulmonary artery passing between the esophagus and trachea. This had been missed at surgery because the azygos vein and superior vena cava cover the area when approached through the right chest. At surgery the left pulmonary artery was separated from the right pulmonary artery and reanastomosed to the main pulmonary artery. Recovery was uneventful and symptoms were alleviated.

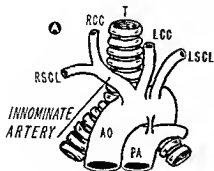


Fig 10 120—Tracheal compression by the innominate artery. A, diagram of the innominate artery arising in a common trunk with the left common carotid (LCC) and crossing over the trachea (T). This crossing per se is a normal variant, not an anomaly, and is found in at least 25% of angiograms of infants. AO, aorta; PA, pulmonary artery; RCC, right common carotid; RSCL,

and LSCL, right and left subclavian arteries. B, lateral projection after barium of an infant with stridor and apneic episodes reveals a normal esophagus and fixed reproducible curvilinear anterior tracheal narrowing (arrow) due to the innominate artery. Symptoms cleared dramatically after the artery was sutured to the back of the sternum.

Fig 10 121—Aberrant right subclavian artery. A, lateral projection after barium of an infant with stridor demonstrates a small oblique retroesophageal indentation due to an aberrant right subclavian artery. The trachea is normal. Stridor continued after division of the artery since no sign of a true obstruction had been demonstrated. B, diagram of the usual aberrant right

subclavian artery (ARS) which causes no symptoms. C, diagram of aberrant right subclavian artery (ARS) with a common trunk for both carotids (RC and LC) in front of the trachea. This can cause the same signs and symptoms as innominate artery compression of the trachea. (B and C from Klinkhamer.)

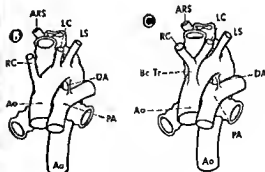


Fig.

rant subclavian artery, unless the trachea is impinged on

REFERENCES

- Bayford D. An account of a singular case of obstructed deglutition, *Mem Med Soc London* 2:275, 1794.
- Berdon, W. E., *et al*. Innominate artery compression of the trachea in infants with stridor and apnea, *Radiology* 92:272, 1969.
- Clarkson, P. M. Aberrant left pulmonary artery, *Am J Dis Child* 113:373, 1967.
- Fein, B. T., *et al*. Diagnosis and treatment of congenital vascular anomalies causing bronchial asthma, *South Med J* 52:551, 1959.
- Jue, K. I., *et al*. Anomalous origin of the left pulmonary artery from the right pulmonary artery, *Am J Roentgenol* 95:595, 1965.
- Kale K. K., *et al*. Aberrant left pulmonary artery presenting as a mediastinal mass, *Arch int med* 125:121, 1970.
- Klinkhamer, A. C. Esophagography in Anomalies of the Aortic Arch System (Baltimore: Williams & Wilkins Company, 1969).
- Lincoln, J. C. R. Vascular anomalies compressing the esophagus and trachea, *Thorax* 24:259, 1969.
- Murthy K., *et al*. Vascular ring due to left aortic arch, right descending aorta and right patent ductus arteriosus, *J Pediatr Surg* 5:550, 1970.
- Neuhauser E. B. D. The roentgen diagnosis of double aortic arch and other anomalies of the great vessels, *Am J Roentgenol* 56:1, 1946.
- Stewart J. R., *et al*. An Atlas of Vascular Rings and Related Malformations of the Aortic Arch System (Springfield, Ill: Charles C Thomas Publisher, 1964).

The Gastrointestinal Tract

Problems involving the gastrointestinal tract of the newborn encompass a large part of pediatric radiology and surgery. Failure to appreciate the maternal and immediate neonatal history often leads to delay in diagnosis and consequently a high mortality among infants with correctable lesions. In some cases of obstruction the diagnosis is known before radiographic study which is carried out to confirm the diagnosis; in others the radiologist is the first to appreciate the existence of an obstruction or finds a second level of

obstruction distal to the clinically presenting lesion. The following discussion is therefore directed to early radiographic detection based on suggestive elements in the history and physical examination.

The Fetal Gastrointestinal Tract

The fetal gastrointestinal tract functions efficiently through the second and third trimesters. The fetus swallows great amounts of amniotic fluid and absorbs

Fig. 10-122.—In A, the fetus is surrounded by opacified amnion as part of the intrauterine transfusion procedure. In B, 24 hours later, there is excellent delineation by the water-soluble medium demonstrating the water-absorptive role of the jejunum

and ileum (arrows). The radiograph is reproduced as if viewing the erect fetus from behind. (Courtesy of Dr. R. Fleming Stamford, Conn.)



the fluid, part of which is recirculated as fetal urine (Fig 10-122). Any major disturbance of either swallowing or absorption of the fluid may be reflected in the maternal history. Failure to swallow leads to hydrops and excessive weight gain of the mother. Although more commonly related to disturbances outside the gastrointestinal tract, hydrops may be caused by gastrointestinal obstruction such as esophageal atresia. Inability of the small bowel to absorb the fluid can occur with high obstruction such as duodenal atresia. Hydrops is rare with low small bowel obstructions such as meconium ileus.

At birth the intestinal tract contains meconium, the fetal feces, which is a mixture of bile salts, swallowed amnion, gastric and small bowel juice and desquamated cells. Fetal defecation is not normal (Fig 10-123) and usually is secondary to fetal distress. An obstetric history of meconium-stained fluid should alert the pediatrician to meconium aspiration. As far as the gastrointestinal tract and meconium are concerned, interest centers on the presence of meconium in the small bowel and colon distal to sites of atresia, proof that fetal swallowing occurred normally well after the embryologic events that were previously invoked in the pathogenesis of such atresia.

EMBRYOLOGIC DEVELOPMENT—Any disturbance during separation of the primitive foregut into the upper gastrointestinal tract and tracheobronchial tree can lead to anomalies of sequestered gastrointestinal or respiratory tissue, or both, in immediate relation to the esophagus. These are variously called neuroenteric cysts, duplications, foregut duplications and se-

questration. They are of true embryologic derivation and are found in the chest or abdomen or both.

The midgut leaves the fetal coelomic cavity, rotates and returns to complete the process of rotation that culminates in a well-based small bowel mesentery and fixed right colon. Any delay or arrest in this process can cause omphalocele (exomphalos), the midgut outside the coelomic cavity) or those anomalies classified as malrotations, which are often obstructive. The hindgut, originally a primitive cloaca draining meconium and fetal urine, separates into bladder and rectum. Failure of this separation leads to anomalies of the anus and rectum of the "imperforate anus" group. Finally, failure of the abdominal wall to form normally can lead to defects that may be high, although away from the umbilicus (gastroschisis), or low in the abdomen with bladder exstrophy or combined bladder and gastrointestinal exstrophy (exstrophy of the cloaca). The embryologic events are discussed in greater detail elsewhere in these volumes and in our appended references.

Gastrointestinal Tract in the First Hours of Life

At birth, swallowing continues, with air replacing and displacing fluid. Meconium is passed by most normal newborn infants within a day, rarely as long as two days. Bacteria propagate rapidly, being found in the small bowel and colon as soon as eight hours after birth. Swallowing can be disordered for days, raising questions of tracheoesophageal fistula. It is noteworthy that infants with functional swallowing abnormalities have no history of hydrops, which leads to speculation on transitory central nervous system disturbances perhaps induced by hypoxia before or during delivery. Radiographic study of such anomalies as imperforate anus (with which gas distribution is of interest) should be delayed until gas fills the colon, usually six to eight hours after birth.

Fig 10-123—Lateral view of the rectum of a newborn infant demonstrates retention of swallowed water-soluble agent from intravenous transfusion. Fetal defecation would have been a sign of fetal distress.



Radiographic Evaluation of Newborns with Gastrointestinal Obstruction

The usual clinical manifestations that lead to radiologic study are vomiting and distention. The radiologist and surgeon should think in common terms and always ask certain key questions, including whether the obstructed infant has an incarcerated inguinal hernia (Fig 10-124) and whether the vomitus is bile-stained. Bile staining of the vomitus eliminates supra-ampullary lesions such as pyloric obstruction (atresia or stenosis), hiatal hernia and esophageal obstruction. Clinical distention may be generalized (suggesting low small bowel or colonic obstruction, ascites or massive pneumoperitoneum) or localized to the epigastrium (with high small bowel obstruction) or low (as with a dilated bladder).

The radiographic examination, to be helpful, must be correlated with the physical findings and clinical



Fig 10-124 Small bowel obstruction secondary to incarcerated right inguinal hernia. The small gas collection in the right inguinal area (arrow). Although rare in the neonatal period such a hernia must be considered and excluded in the obstructed child before investing in the many congenital causes of intestinal obstruction.

history One must remember that nasogastric suctioning will remove air and fluid so that the subsequent plain film might look normal. Similarly in an infant with colonic distention and vomiting from Hirschsprung's disease, rectal examination or passage of a rectal tube can lead to compensation, loss of colonic air fluid levels and a normal appearing plain film. The first thing to be done when an infant is distended and vomiting is to obtain a radiographic obstruction series.

INITIAL PLAIN FILM EXAMINATION—The basic obstruction series used at Babies Hospital consists of prone supine frontal erect and left lateral recumbent views. A single supine film is almost always inadequate to define intestinal obstruction. It fails to localize findings and to distinguish the large from the small bowel free air unless massive is readily missed. Additional information is obtained from a prone film, the prone position allowing free air if present to collect in the flanks (Figs 10-125 and 10-126). Small bowel gas will remain centrally located, whereas colonic gas shifts from the transverse and sigmoid loops to the right and left colon and rectum because of their dorsal orientation (Fig 10-127). Lateral films taken with the infant erect are helpful if

air fluid levels are sought particularly in posterior structures such as the duodenum and rectum. The left lateral recumbent position allows gas to rise and demonstrate the duodenum to advantage. Erect films (for air fluid levels and free air) can be obtained. Some radiologists add decubitus views as well. The left lateral decubitus position allows analysis of the right side of the abdomen for free air (which rises to the right flank and displaces the liver). Portal vein air if present is well seen in this position. Inverted frontal and lateral views show how far distally colonic gas has extended. They also demonstrate the level of duodenal or high jejunal obstruction. Air can be introduced through nasogastric tubes to outline further the distal extent of high obstruction such as duodenal or jejunal atresia.

POSITIVE CONTRAST MATERIALS—Barium is well known for its excellent coating of the mucosa. Non-fluoculent preparations are the agents of choice for the usual upper gastrointestinal or enema study. In the infant with low small bowel obstruction when an enema is used to reveal microcolon, the colon may be ruptured by the hydrostatic effects of the enema. Some radiologists prefer to use water soluble agents for this kind of investigation. When positive contrast agents are used only two groups of compounds should be considered: the various barium preparations and the water soluble agents. The latter are the flavored though very bitter Gastrografin and the extremely bitter urographic agents Hypaque Renografin or Conray. Lipiodol is of historical interest only and has no place in pediatric gastrointestinal radiology. Given by mouth the material cannot be swallowed normally and it may be gummed by the infant until aspirated.

Water soluble agents are very hypertonic and may pull large amounts of body fluids into the lumen of the intestinal tract. This leads in the small bowel to marked dilation and loss of detail on the films. Hypovolemic shock and collapse in the infant are also possibilities. In the colon however this property can be used to help evacuate sticky meconium in the meconium plug syndrome and has been utilized in meconium ileus to evacuate masses of inspissated meconium.

There is virtually no place for water soluble agents in upper gastrointestinal studies unless perforation is suspected and confirmation of its site desired. In the patient with esophageal fistula, the amount of contrast medium rather than the type is what usually causes difficulties. Very small amounts of water soluble agents are tolerated by the lung if aspirated although the infant may react with violent coughing to their presence in the trachea. Larger amounts aspirated into the lungs can cause pulmonary edema. Some gastrointestinal absorption of water soluble contrast material is normal and visualization of the bladder therefore does not mean perforation. Some radiologists prefer to use water soluble contrast agents to investigate the colon. Unfortunately the

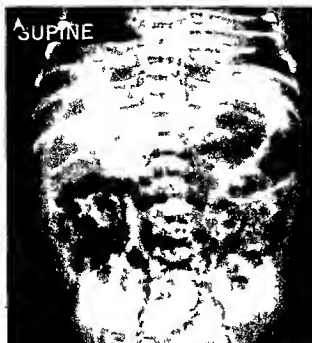
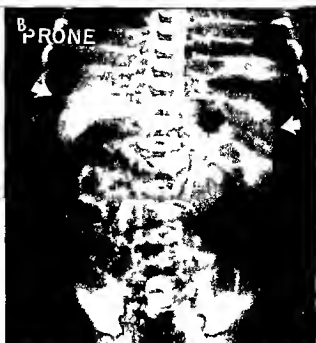


Fig 10-125—Pneumoperitoneum. A, radiograph with the patient supine visualizes a vague oval lucency over the upper abdomen with the fetal form ligament outlined by air. This could be due to perforation in many places but in this infant was secondary to the mother's perforation of the rectosigmoid. Free air can be



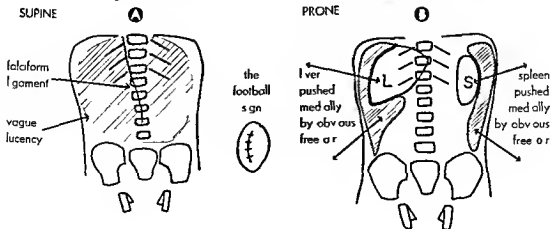
diagnosed from the supine film only if large amounts of air are present. In B, with the patient prone, free air pushes the liver and spleen medially as it collects in the lateral peritoneal recesses. Even small amounts of free air are readily diagnosed from the prone film (Figs 10-125 to 10-127 from Be don et al.)

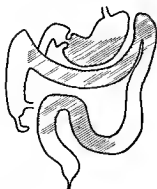
hydroscopic effects of water soluble agents can lead to diarrhea, and the radiographic signs of Hirschsprung's disease can be missed in infants lacking a true transition zone because of total evacuation of the water soluble compounds. Thus radiologists differ as to which agents are superior. We feel strongly that nonflocculent barium should be the basic positive contrast agent. The radiologist, not the surgeon, should select the proper contrast material.

A few aphorisms are relevant here. Many surgeons will read the films if the radiologist does not know the diagnostic problems well. The surgeon will dictate the choice of films and contrast agents unless the radiologist knows exactly what to do in a given case. The surgeon who does his own radiology gets the radiology he deserves, but his patient does not.

TECHNIC OF CONTRAST ENEMA—Foley catheters should not be used for enemas in neonates. The colon

Fig 10-126 Schematic drawings A, of Figure 10-125 A, B of Figure 10-125 B



A SUPINE
AIR RISES VENTRALLY

FILLS GASTRIC
ANTRUM
TRANSVERSE
COLON
SIGMOID
COLON
B PRONE
AIR RISES DORSALLY

FILLS GASTRIC
FUNDUS
DUODENAL
BULB
RIGHT, LEFT
COLON
RECTUM


Fig 10 127 — **A**, diagram showing localization of gastric and colonic air in the supine projection. Small bowel gas centrally situated can simulate transverse and sigmoid colon gas and vice versa. **B**, diagram showing localization of gastric and colonic air in the prone projection. Localization of colonic vs small bowel gas is facilitated as gas in the transverse and sigmoid colon shifts to the rectum and posteriorly placed right and left colon. **C**, supine film of an infant with bile-stained vomitus, distention and air fluid levels in the erect projection. Large centrally placed loops are present. Barium enema study was requested to verify the clinical suspicion of low small bowel obstruction. **D**, with the patient prone, proves that the gas is colonic as the sigmoid gas shifts to fill the rectum and transverse colon gas shifts to fill the right and left colon. Diagnosis was gastroenteritis; the patient recovered.

is readily perforated in this age group even a thermometer or a straight catheter can cause perforation but inflated balloons have been more often causal. The peritoneal reflection of the rectosigmoid is only 3-4 cm away from the anal orifice and perforation is usually intra-abdominal (see Fig. 10-125).

A no. 8 nasogastric tube is passed into the rectum with fluoroscopic confirmation of position. The buttocks are bound tightly together over the tube with adhesive tape. This nearly always suffices, however on occasion it may be necessary with great care to use a syringe with the baby in prone position when hydrostatic filling in the supine position results in continued leakage.

TECHNIQUE OF UPPER GASTROINTESTINAL STUDY—For upper gastrointestinal series and esophagrams two schools of thought exist. The bottle approach offers a physiologic method of analyzing swallowing as a coordinated act from mouth and tongue through out deglutition. The major disadvantages are obvious: air swallowing, failure to drink, and so much drinking that the areas of interest may be obscured. The tube school uses the no. 8 (or no. 5 for undersized infants) nasogastric tube. The lower esophagus and stomach can be selectively studied: the stomach first, then with the catheter pulled back, injections into the esophagus can be made at varying levels for H₂ fistulae. Finally barium can be instilled into the oropharynx to analyze swallowing or a bottle given at that point. The tube approach is popular at the Babies Hospital.

REFERENCES

- Barnard C N et al: The genesis of intestinal atresia, *Minnesota Med* 39:745 1956
- Berdon W E: Gastrointestinal Activity and Water Absorptive Capacity of the Fetus: Diagnosis and Treatment of Fetal Disorders (New York: Springer Verlag 1968) p 250
- et al: Microcolon in newborn infants with intestinal obstruction. *Radiology* 90:878 1968
- Berman C Z et al: The use of water soluble urographic contrast media in pediatric gastrointestinal series. *Brit J Radiol* 33:92 1960
- Capitano M A et al: Roentgenographic evaluation of intestinal obstruction in the newborn infant. *Pediatr Clin North America* 17:983 1970
- Greenbaum E I: Rectal thermometer induced pneumoperitoneum in the newborn. *Pediatrics* 44:539 1960
- Harris P D et al: Osmotic effects of water soluble contrast media on circulating plasma volume. *Am J Roentgenol* 91:694 1964
- Hays D M: Intestinal Atresia and Stenosis (Current Problems in Surgery) (Chicago: Year Book Medical Publishers Inc 1969)
- Miller R E: Perforated viscous in infants. New roentgen sign. *Radiology* 74:65 1960
- Parker J J et al: Traumatic pneumoperitoneum in the newborn. *Am J Roentgenol* 95:203 1965
- Reich S B: Production of pulmonary edema by aspiration of water soluble non absorbable contrast media. *Radiology* 92:367 1969
- Santulli T V et al: Perforation of the rectum or colon in infancy due to enema. *Pediatrics* 23:972 1959
- et al: Congenital atresia of the intestine: Pathogenesis and treatment. *Ann. Surg.* 154:939 1961
- Singleton E B: Radiologic evaluation of intestinal obstruction in the newborn. *Radiol. Clin North America* 1:571 1963
- Staple T W et al: Perforation of the atretic colon during barium enema examination. *Am J Roentgenol* 101:325 1967
- Wagner M L et al: Neonatal defects associated with abnormal malices of amnion and amniotic fluid. *Radiol Clin North America* 6:279 1968
- Wolffson J J et al: Hazard of barium enema studies in infants with small bowel atresia. *Radiology* 95:341 1970

Esophagus

Clinical signs of esophageal obstruction include excessive salivation, drooling, choking with feedings and dyspnea. A nasogastric tube may seemingly pass into the stomach with return of fluid, although it is actually coiled in the dilated proximal pouch. Postoperative swallowing defects are common in newborns with repaired esophageal anomalies. Aspiration and gastroesophageal reflux occur despite excellent anatomic repair. This may reflect inherent neuromuscular abnormalities of peristalsis.

ESOPHAGEAL ATRESIA WITH FISTULA TO DISTAL ESOPHAGUS—In about 80% of cases there is a communication near or at the carina with the distal esophagus (Fig. 10-128). The dilated pouch of the proximal esophagus because of gaseous distention can often be demonstrated in plain chest films. It terminates at varying distances above the carina. This structural pattern allows air to reach the stomach via the trachea.

Fig. 10-128—Distention of the commonest form of esophageal atresia as a oblique projection. The dilated proximal pouch is filled with barium (too much was used and could have been as rated). Arrows are directed to the air filled distal esophagus extending from carina to stomach.

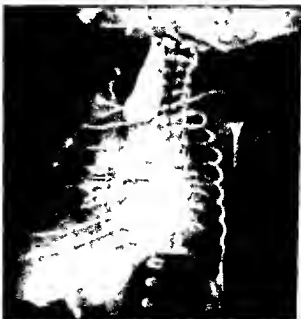




Fig 10-129—Esophageal atresia with distal fistula. A, radiograph with patient erect in which the proximal pouch is outlined by use of a catheter and small amount of barium (even less could be used). B, frontal and C, lateral projections show a rare unusually long pouch which facilitates repair.



al fistula and allows regurgitation of gastric juice into the lungs adding chemical pneumonitis to the aspiration pneumonia related to the obstructed proximal esophagus. The level of the pouch can be identified by putting small amounts of barium through a nasogastric tube with the patient erect (Fig 10-129 A). Rarely the pouch is very long (Fig 10-129 B and C) which facilitates repair. An unusual coexistent fistula from the proximal pouch to the trachea may be identified by this method as well if fluoroscopy is added to the

study. To allow an infant with tracheoesophageal fistula to drink barium from a bottle is dangerous because of massive aspiration (Fig 10-130). Further more water soluble contrast materials are hydroscopic and, if aspirated in quantity may cause pulmonary edema (Fig 10-131). A right aortic arch which severely complicates surgical repair is extremely difficult to identify before operation. Prematurity or congenital heart disease or both with esophageal atresia considerably lowers the survival rate.

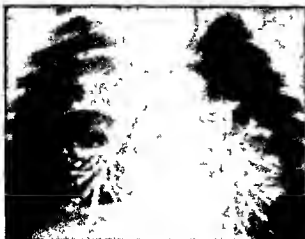


Fig 10-130—Esophageal atresia with distal fistula. An excess of barium was given by bottle and has been aspirated outlining the tracheobronchial tree. The barium was well tolerated and virtually gone in radiographs obtained an hour later.

The radiographic findings in these patients permit easy classification. Plain film studies show a dilated air-filled proximal pouch. The presence of abdominal gas indicates a fistula. Preoperative studies of the abdominal gas pattern are important because they may reveal coexisting duodenal obstruction (Fig 10-132). Anomalies of the lumbar spine may also be present, as well as imperforate anus.

ESOPHAGEAL ATRESIA WITHOUT FISTULA—About 15% of patients with esophageal atresia have no fistula with the trachea. Symptoms resemble those with fistula, hydramnios is almost always present. Plain films show a gasless abdomen. The esophageal pouch can be outlined by either air or contrast material; the latter preferably injected through a tube (Fig 10-133). The distal esophagus is present but is usually short and extends a few centimeters above the esodoesophageal junction. The distal esophageal segment can be identified and its length estimated after injection of contrast material via the gastrostomy tube with gastroesophageal reflux (Fig 10-134). Gastrostomy is performed for feeding purposes; definitive repair is not done until later.

Most patients with esophageal atresia without fistula require the interposition of small bowel or colon, although successful attempts to stretch the proximal and distal segments to achieve primary repair have been reported. The stretching is accomplished by use of mercury-weighted tubes from above and bougies from below via the gastrostomy (Fig 10-135).

The patient with esophageal atresia without fistula may also have intra-abdominal abnormalities such as duodenal obstruction (Fig 10-136) which cannot be suspected from preoperative plain films. Meconium peritonitis secondary to fetal midgut volvulus can be detected from its calcifications (Fig 10-137). The

examiner must be aware that the clinical and plain film pictures of esophageal atresia can be totally mimicked in the depressed infant with central nervous system damage and a gasless abdomen (Fig 10-138).

TRACHEOESOPHAGEAL FISTULA WITHOUT ATRESIA—This abnormality accounts for a small percentage of cases. Although such infants usually have symptoms in the newborn period, the diagnosis is difficult and may be delayed for months. Recording of esophagrams on cine or television tape offers the best possibility of diagnosis. A tube is passed into the esophagus, starting at the level of the carina; several injections of contrast material via the nasogastric tube are made and recorded. Observations are made at progressively ascending levels because these fistulas may be anywhere from carina to larynx, and may be multiple. Recording is started prior to each injection so that if contrast material appears in the trachea, playback can ascertain if it went directly through a fistula or was aspirated via the larynx. These studies are best done with the patient prone and with horizontal beam, lacking the necessary equipment, a steep recumbent oblique view with vertical beam is satisfactory (Fig 10-139). Fistulas may recur after primary repair, or multiple fistulas may have been present.

Fig 10-131—Demonstration of the danger of aspiration of large amounts of water-soluble contrast agents. This patient with esophageal atresia and distal fistula had gastrostomy. Surgeons instilled a water-soluble agent into the stomach to check on gastric emptying. The agent refluxed up the distal esophagus through the fistula (arrow) into the tracheobronchial tree causing choking (allowing contrast to fill the pharynx) and moderately severe pulmonary edema due to hyperosmolarity of the agent.





Fig 10-132.—**A**, preoperative demonstration of esophageal atresia with duodenal atresia (arrow). Excessive barium given by bottle caused tracheobronchial aspiration. Gas in the stomach testifies to the existence of tracheoesophageal fistula and a second duodenal obstruction. The infant had clinical features of 21 trisomy proved by chromosomal study. **B**, postop-

erative study in another patient following end-to-end esophageal anastomosis demonstrating unsuspected duodenal stenosis. The trachea is narrowed as it passes between the distal esophagus posteriorly and the innominate artery anteriorly. Some of these patients have brassy cough and even epistaxis related to a tracheal compression.

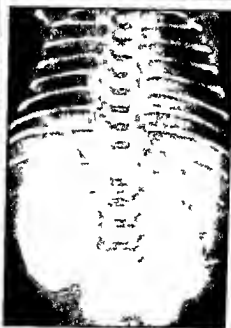
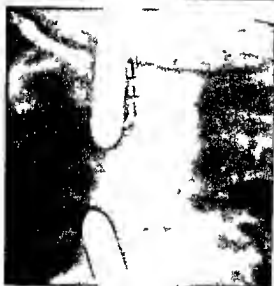


Fig 10-133 (upper left) —Esophageal atresia without fistula. Lateral projection shows a dilated proximal pouch with air or tracheal displacement and absence of abdominal gas in a newborn infant. Less contrast material should have been used.

Fig 10-134 (upper right) —Esophageal atresia without distal fistula. The short distal esophageal segment is identified by reflux from the stomach during gastrostomy study of the stomach and small bowel.

Fig 10-135 (lower left) —Esophageal atresia without fistula.

Spot film taken during stent procedure. Mercury weighted tube in the proximal segment and bougie in the distal segment, introduced via gastrostomy, show the gap to be demonstrated. Repair was satisfactory.

Fig 10-136 (lower right) —Esophageal atresia without fistula after gastrostomy which was not functioning. Contrast study reveals an unsuspected marked duodenal stenosis. Radiolucency overlying the upper dorsal segments is created by the dilated air-filled proximal pouch.



Fig 10 137 (left) —Esophageal atresia without fistula. Lateral film with the pouch filled with barium reveals the gasless abdomen and a so-called mass (arrow) indicating that the patient had an in utero volvulus with infarction.



Fig 10 138 (right) —Lateral film of a patient with high spinal cord transection who was too depressed to swallow. The gasless scaphoid abdomen simulates esophageal atresia without fistula.

Fig 10 139 —Tracheoesophageal fistula without esophageal atresia. Spot film taken during fluoroscopy shows an H-fistula. The fistula actually runs up 1½ cm from the esophagus to the trachea as an H-fistula is usually in the low cervical or high dorsal area.





Fig 10-140—S mulet on ot esophageal ates a w th d staf f s tula Th s ntent had swa low ng problems attempts elsewhere to pass a large tube were unsuccessful A, L p odo swallow shows a blind pouch w th several pockets thought to represent p o x mal d lated at et c esophagus w th d staf f stule B follow up film

Fig 10-141—Th s rad ograph appea ed n e e l e d tions as an example of congen tel pharyngeal d vert culum Th s newborn patient had swa low ng problems attempts to pass a nasogastric tube were unsuccessful Follow up roentgen studies and phys cal exam net on fa led to show any abno mal ty and the n tant recovered w thout surgery other than neonatal gastrostomy at the tme of the presumed perforat on (that s mutated pharyngeal d vert culum)



shows a patent bar um fl ed esophagus w th res dual L p odo n false passages n the med est num Th s r s represents pr or perfo a tion of ether the hypopharynx or the esophagus w th a false passage s mutat ng esophageal atres a The patient recovered w thout surgery

and not noted at the time of primary repair These events convert any of a number of types of esophageal atresia into the so-called H type of fistula Barium has been safely used in these examinations Some radiologists prefer Dionosil or even water soluble agents The amount aspirated into the lungs could be dangerous with the latter (see Fig 10-131) The signs and symptoms of the H fistula can be mimicked by a persistent esophagotrachea (posterior laryngeal cleft) Diagnosis is made by endoscopy the radiographs showing only marked aspiration

ACQUIRED ESOPHAGEAL OBSTRUCTION—Some infants have spasm of the pharyngeal musculature or swallowing incoordination Overzealous attempts to pass nasogastric tubes in such infants to ascertain if the esophagus is patent have resulted in perforations in the pharynx and upper esophagus and created false passages Passages thus created may almost mimic esophageal atresia with tracheoesophageal fistula, both clinically and radiographically (Fig 10-140) Patients who in the past, had the diagnosis of pharyngeal diverticulum or esophageal diverticulum or esophageal duplication in all likelihood had traumatic perforation of the pharynx or the esophagus or both (Fig 10-141)

HIATUS HERNIA CHALASIA—In the United States symptomatic hiatus hernia and total cardioesophageal

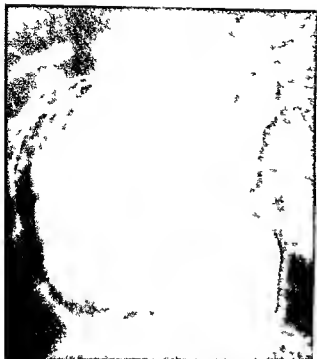


Fig 10 142 (left) — Huge asymptomatic hiatus hernia in a new born infant who had the clinical features of 13-15 trisomy although the chromosomes were normal. Gastroesophageal reflux was not demonstrated on fluoroscopic study.

Fig 10 143 (right) — Sliding hiatus hernia in an asymptomatic newborn infant with nonbilious vomiting. Gastroesophageal reflux was pronounced on fluoroscopic study. Narrowing above the hernia disappeared with thickened feeding and propping of the infant in semi-erect position. At 1 year of age the hernia was no longer demonstrable though moderate reflux persisted.



Fig 10 144 — Pulmonary sequestration communicating with the foregut. A, plain film shows a mass resembling a hiatal hernia pouch. B, barium swallow demonstrates an esophageal connection to the mass which contained both pulmonary and gastrointestinal tissue as a form of sequestered foregut. (Courtesy of D. T. Spackman, New Haven, Conn.)

to the mass which contained both pulmonary and gastrointestinal tissue as a form of sequestered foregut. (Courtesy of D. T. Spackman, New Haven, Conn.)



incompetence are uncommon in the neonate whereas in Great Britain many are seen in the large medical centers

Some of the largest hiatus hernias cause no symptoms and are discovered incidentally (Fig 10-142). Others may cause such serious complications as reflux esophagitis, repeated aspiration pneumonia, bleeding, severe anemia, and stricture formation. The patients with symptoms reflect the high degree of gastric acidity of the neonate (Fig 10-143).

Congenital short esophagus is very rare. If the concept is correct, the thoracic stomach should have a separate aortic blood supply. In fact, virtually all thoracic parts of the stomach associated with cases of hiatus hernia have a subdiaphragmatic celiac axis supply and the short esophagus is secondary to peptic esophagitis.

Chalasia (massive cardioesophageal incompetence) is best considered with hiatus hernia. Either can cause severe peptic esophagitis which, if chronic, can lead to esophageal stricture. Esophagitis per se is never radiographically demonstrable in the acute phase. Surgery is limited to the very few patients who do not respond to standard medical treatment.

ESOPHAGEAL-BRONCHIAL COMMUNICATION INCLUDING SEQUESTERED FOREGUT—Rarely there is a congenital esophageal bronchial fistula with signs similar to the H type of tracheoesophageal fistula. In some infants a mass made up of sequestered lung and gas-trontestinal tissue is present and fills with barium. Radiographically this may simulate a hiatus hernia both in plain films and in contrast studies (Fig 10-144).

Spontaneous perforation of the esophagus in the

neonate described by Boerhaave is usually manifested as hydropneumothorax. It is very rare and the cause is speculative.

REFERENCES

- Altman D H *et al*: Esophageal atresia. Simple radiologic technique to facilitate surgical management. *Radiology* 86:1112, 1966
- Eckstein H B *et al*: Tracheoesophageal fistula without esophageal atresia. 23 cases. *Ztschr Kinderchir* 9:43, 1970
- Frech R S *et al*: Comparison of barium sulfate and oral 40% diatrizoate injected into the trachea of dogs. *Radiology* 95:299, 1970
- Gerle R D *et al*: Congenital bronchopulmonary foregut malformation. *New England J Med* 278:1413, 1968
- Girdany B R *et al*: Traumatic pseudodiverticula of the pharynx in newborn infants. *New England J Med* 280:237, 1969
- Griscom N T: Persistent esophagotrachea. *Am J Roentgenol* 97:211, 1968
- Gwinn J L: Tracheo-esophageal fistula with and without Esophageal Atresia. *Special Aspects in Kaufmann H J (ed) Progress in Pediatric Radiology (Chicago: Year Book Medical Publishers Inc, 1969) Vol 2 p 170*
- Haight C: Congenital Esophageal Atresia and Tracheoesophageal Fistula. In Mustard W T *et al* (ed): *Pediatric Surgery* (2nd ed. Chicago: Year Book Medical Publishers Inc, 1969)
- Hays D M *et al*: Esophageal atresia and tracheoesophageal fistula. Management of the uncommon types. *J Pediatr Surg* 1:240, 1966
- Humphreys A C *et al*: Esophageal hiatus hernia in infants and children. *Pediatrics* 36:1, 1965
- Kirkpatrick J A *et al*: Motor activity of the esophagus in association with esophageal atresia and tracheoesophageal fistula. *Am J Roentgenol* 88:884, 1961
- Marun L W: Management of esophageal anomalies. *Pediatrics* 36:342, 1965
- Roe B B: Congenital tracheoesophageal fistula. *Am J Dis Child* 106:101, 1963

Fig 10-145—A, plain film of a newborn infant with non-tussive vomiting and epigastric peristaltic waves shows an active stomach and no distal gas. B, contrast study confirms the impression

of total gastric obstruction. An antropyloric imperforate membrane was found at surgery.



Sauvegrain J. Esophageal atresia with fistula at the upper end. *Ann Radiol* 12:145, 1969.

Waterston D. Hiatus Hernia. In: Mustard W T, *et al* (ed). *Pediatric Surgery* (2nd ed). Chicago: Year Book Medical Publishers Inc, 1969; p 392.

Stomach

GASTRIC OBSTRUCTION—In the immediate neonatal period gastric obstruction is rare and usually due either to hypertrophic pyloric stenosis or to antral webs and membranes (Fig 10-145). Total obstruction suggests atresia or a tight pyloric stenosis. Partial obstruction is more likely to represent hypertrophic pyloric stenosis or severe pyloric spasm. As one would anticipate, these patients vomit nonbilious material, have hyperactive peristalsis, and therefore may have visible peristaltic waves. They rapidly become alkalotic.

Plain film studies may show a large stomach, usually

with evidence of peristaltic activity (Fig 10-146 A) and either no gas or very little gas beyond the stomach. Gastrointestinal series could be performed with air as a contrast medium, but barium is more commonly used (Fig 10-146 B and C). To facilitate control, the contrast study is performed via nasogastric tubes. This also allows aspiration of stomach contents prior to the study.

Hypertrophic pyloric stenosis is included here although it is not commonly diagnosed until after the immediate neonatal period. The infant with hypertrophic pyloric stenosis may have a readily palpable olive and not require radiologic study; a mass is never felt in a small percentage of cases, and roentgen study is necessary to establish the diagnosis. The number of times the olive becomes palpable after radiographic demonstration of hypertrophic pyloric stenosis is impressive. Hypertrophic pyloric stenosis is a combination of intermittent pyloric and antral spasm.

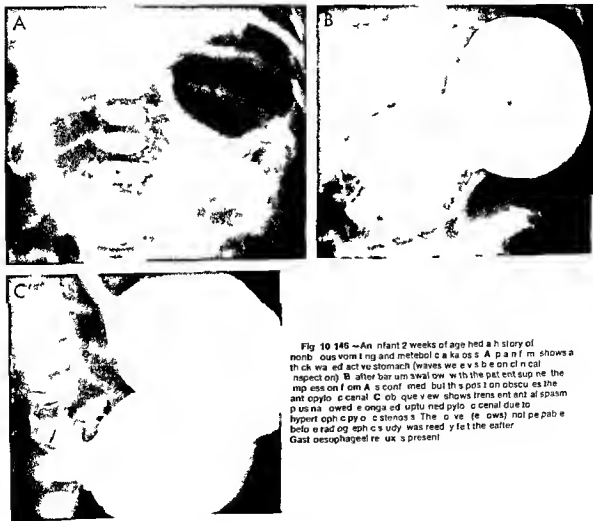


Fig 10-145—An infant 2 weeks of age had a history of nonbilious vomiting and metabolic alkalosis. A, plain film shows a thick-walled active stomach (waves were visible on clinical inspection). B, after barium swallow with the patient supine, the impression on film is confirmed, but the position obscures the antral pyloric canal. C, oblique view shows transient antral spasm plus narrowed elongated pyloric canal due to hypertrophic pyloric stenosis. The olive (olive) not palpable below radiographic study was readily felt thereafter. Gastroesophageal reflux is present.



Fig 10 147—Gastric perforation. **A**, plain film shows free gas from complete rupture of the gastric wall. Both inner and outer walls of the small bowel are outlined as well as the falciform ligament. **B** demonstrates free gas from complete gastric perforation

in an infant who also had left diaphragmatic hernia. This led to the unique combination of pneumoperitoneum and pneumothorax (**B** courtesy of Dr B. Eerenberg, Suffern, NY).

Fig 10 148—Incomplete rupture of the gastric wall. **A**, plain film reveals unexplained gastric dilatation in an infant in whom the nasogastric tube was left in place. The following day the patient had a gasless abdomen and obstructive signs. **B**, contrast study at this time shows the gas filling defect in the distal portion

of the stomach and a most total obstruction. Surgery revealed rupture of the serosa and muscle, although the mucosa was intact. The filling defect was thought to represent a combination of the distorted retracted muscle and the edematous, although intact mucosa.



in an infant with a hypertrophied pyloric muscle. The stomach is alternately quiet without peristalsis and hyperperistaltic with obstruction at the pylorus. Radiographic findings reflect these two patterns. The string sign of an elongated, upturned pyloric canal can be mimicked by spasm. Fluoroscopic evidence of hyperperistalsis, the string sign with indentation of the base of the elevated duodenal bulb and chemical evidence of metabolic alkalosis in an infant several weeks old usually indicate hypertrophic pyloric stenosis. Errors are made, probably related to marked pylorospasm. Barium injected via nasogastric tube into the stomach after removal of its contents with the infant on his right side allows early visualization of the area without overlapping by large amounts of swallowed barium. Delayed gastric emptying is a poor sign on which to base the diagnosis.

Some patients may continue to vomit postoperatively and radiographic studies show continued narrowing of the elongated pyloric channel. Therefore radiographic study is not the method of choice in evaluating the success of surgery. The channel in the postoperative state is either horizontal or directed downward.

GASTRIC PERFORATION—This is a catastrophic event with the infant going into sudden shock and becoming lethargic and markedly distended. Films show varying degrees of free peritoneal gas. This is by no means pathognomonic since perforation of the rectum by a thermometer (see Fig. 10-125) or perforation from any other cause can lead to an identical clinical and radiographic picture (Fig. 10-147). Such gastric perforation was formerly attributed to congenital

absence of the gastric musculature since no muscle was found on biopsy study of tissue around the rent. Occasionally a nasogastric tube had been passed and was blamed for the defect. Surgeons now believe that it is an acquired lesion either caused by hypoxia and ischemic perforation or secondary to acute gastric dilatation. In experimental acute gastric dilatation in puppies, Shaw and colleagues were able to produce absence of the gastric musculature around the rent. This reflected perforation first of the serosa, then of the muscularis with lateral retraction of the musculature away from the rent. The mucosa finally perforated and biopsy specimens from around the defect contained no muscle. One patient has been encountered with gastric obstruction after a period of acute distention in whom exploration revealed disruption of serosa and muscularis. The intact edematous mucosa was ready to perforate (Fig. 10-148).

GASTRIC MASSES IN THE NEWBORN—Gastric intramural teratoma and also duplication may be encountered. There may be gastrointestinal bleeding with shock or an asymptomatic mass may be felt or these lesions may be identified on abdominal films obtained for other reasons. Calcium, bone and fat content in such a mass suggest a teratoma, whereas a mass of water density may indicate a duplication (Fig. 10-149).

In the stomach as well as the small bowel and colon a duplication may reflect a true embryologic failure of normal delamination or of vacuolization and failure of recanalization. Other duplications may be within the involved organ's mesentery and reflect a persistent connection to the primitive notochord. It is

Fig. 10-149—Gastric duplication. On intravenous pyelography in a 3-week-old infant because of failure to thrive, the supine film showed no abnormality, but the prone film (A) shows a rounded mass protruding into the gastric mucosa (arrows). An upper gas-

trointestinal series was performed immediately. Prone postnatal oblique retrogastric curved diaphragm representing two gastric duplications containing pancreatic and gastric tissue. No vertebral anomalies were noted.



with this group that segmentation anomalies of the spine have been noted

REFERENCES

- Atwell, J. D., *et al*. Teratoma of the stomach in the newborn. *J Pediatr Surg* 21:197, 1967
- Beardmore, H. E., *et al*. Vertebral anomalies and alimentary tract duplication. *Pediatr Clin North America* 5:457, 1958
- Bentley, J. F. R., *et al*. Developmental posterior enteric remnant and spinal malformations. *Arch Dis Childhood* 35:76, 1960
- Cremin, B. J. Congenital pyloric antral membranes in infancy. *Radiology* 92:509, 1969
- Elliott, G. G., *et al*. The notochord as an abnormal organizer in the production of congenital intestinal defects. *Am J Roentgenol* 110:628, 1970
- Grossfeld, J. L., *et al*. Duplication of the pylorus in the newborn. *J Pediatr Surg* 5:365, 1970
- Gwinn, J. L., *et al*. Gastric volvulus. *Am J Dis Child* 120:551, 1970
- Kramer, R. M., *et al*. Duplication of the stomach. *J Pediatr Surg* 5:360, 1970
- Lloyd, A. Jr., *et al*. Etiology of gastrointestinal perforation in the newborn. *Harper Hosp Bull* 22:224, 1964
- Mellus, G. M., *et al*. Congenital hypertrophic pyloric stenosis. *J Pediatr* 66:649, 1965
- Sarach, T., *et al*. Rupture of the stomach in the newborn infant. *Clin Pediatrics* 5:583, 1967
- Shew, A., *et al*. Spontaneous rupture of the stomach in the newborn. A clinical and experimental study. *Surgery* 58:561, 1965
- Shopfner, C. E. The pyloric dot sign in hypertrophic pyloric stenosis. *Am J Roentgenol* 91:679, 1964
- Soper, R. T. Tubular duplications of the colon and distal ileum. *Surgery* 83:998, 1968

Duodenum

Duodenal obstruction may be intrinsic (atresia or stenosis), extrinsic (malrotation with or without volvulus), or both, in the same patient. Intrinsic duodenal obstruction is usually manifested during the 1st day of life by bile vomiting. Accumulation of excessive bile-tinged gastric secretions may be noted if the stomach is aspirated. Rarely the obstruction is above the ampulla, in which case bile is not present in either vomitus or gastric aspirate. Typically, these patients do not seem distended.

One third of the patients with duodenal atresia have 21 trisomy (Down's syndrome). Anomalies of the esophagus, anus, lumbosacral spine or extremities may be present. Maternal hydramnios is common. In plain films of the typical case there is a "double bubble" with a gasless abdomen below. The double bubble is only an indication of a high degree of duodenal obstruction but not of its cause (Fig 10-150).

Plain film evaluation should include prone, erect and left lateral exposures. Lateral decubitus or inverted films may also be added. Barium enema study should be made to assess cecal position if any delay in surgery is proposed, because of the possible confusion and/or association of duodenal atresia with midgut malrotation and volvulus. With incomplete obstruction there is, of course, gas beyond the duodenum.



Fig 10-150—Total duodenal obstruction in a newborn due to atresia. The double bubble (not specific for this condition) represents air fluid levels in the stomach and duodenum. This patient had 21 trisomy (one third of patients with duodenal atresia have Down's syndrome).

The duodenum in either case is dilated. If the stomach and duodenum are fluid filled, nasogastric aspiration and replacement by air facilitates radiographic diagnosis. Air is the preferred contrast medium for high, complete or almost complete obstructions. Very rarely, because of a presumed anomaly of the bile ducts, one entering above and one below the site of obstruction, air may reach the distal bowel, even with complete atresia (Fig 10-151).

MALROTATION AND VOLVULUS—Duodenal obstruction, even on the 1st day of life, may be due to malrotation and associated volvulus. This is the critical emergency in the obstructed newborn because the entire midgut may become infarcted. Clinically, 80% of these patients are seen during the 1st month of life, as reflected in the Babies Hospital statistics: 59 of 77 seen in the 1st month, 30 of the 59 in the 1st week (10 of these 30 died). There is bile vomiting, which may be intermittent. Soft distention is usually present. These patients, however, may appear to be quite well after the initial bile emesis, so that the critical nature of their illness is not appreciated.

Malfixation is a better term than malrotation because the usual broad mesenteric fixation from the left upper quadrant to the right lower quadrant is absent (Fig 10-152), and the entire midgut hangs on a narrow pedicle, at the base of which is the superior mesenteric artery. For reasons that are not clear some patients with this anomaly are asymptomatic. Those

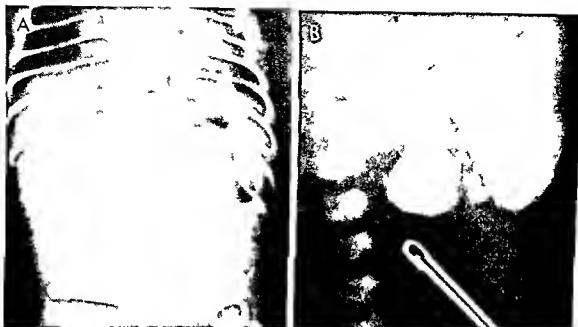
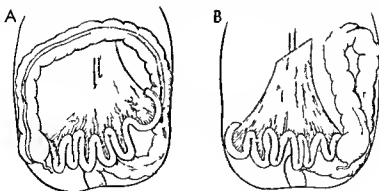


Fig 10-151—Total duodenal obstruction. A: plain film, apparently no me. The es m n mel duodenal dilatation and deg no e of malrotation volvulus was considered. B: part of the gas t on test nel ee es demonstrates total duodenal obstruction. Surgery disclosed complete separation of the duodenum. The

only explanation for the radiographic findings was bifurcating bile ducts (one above and one below the atri a) which allowed swallowed air to pass from the proximal to distal duodenum by way of the anteroposterior junction of the ducts.

Fig 10-152—A: schematic drawing of the normal broad fan-shaped mesentery fixation of the midgut from the left upper to right lower quadrant. B: schematic drawing of failure of adequate

fixation in malrotation with a narrow attachment for the midgut around the superior mesenteric artery. (From Snyder.)



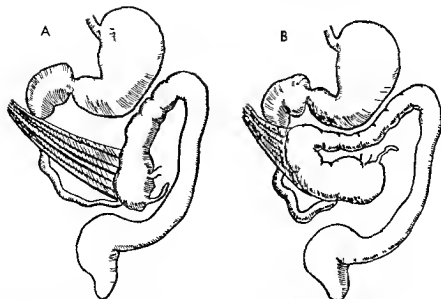


Fig. 10 153 — Ladd's bands with duodenal compression in patients with malrotation. The left sided (A) and midline (B) cecum has dense pentoneal bands crossing over the duodenum. These

must be divided after reduction of the volvulus in order to relieve the obstruction.

seen in the neonatal period have the midgut twisting around the superior mesenteric artery. As this occurs the initial symptoms are due not to the volvulus of the midgut but to obstruction of the duodenum by the dense bands, so-called Ladd's congenital pentoneal bands that extend from the cecum over the duode-

num to the right gutter and liver. Ladd discovered that reduction of the volvulus was insufficient to relieve the obstruction in these patients and that the bands had to be divided to permit total recovery (Fig. 10-153). Compromise of the vascular supply may cause necrosis of the entire small bowel. Less severe con-

Fig. 10 154 — Total duodenal obstruction in an infant 5 days of age who took normal feedings for four days, then began to vomit bile. A demonstrates obstruction; this could be due to intrinsic or extrinsic causes. B, after barium enema, delineates the malrotat-

ed cecum (arrow). Surgery revealed Ladd's bands crossing the duodenum and 360° volvulus of the midgut (Figs. 10-154 and 10-155 from Berdon et al.).



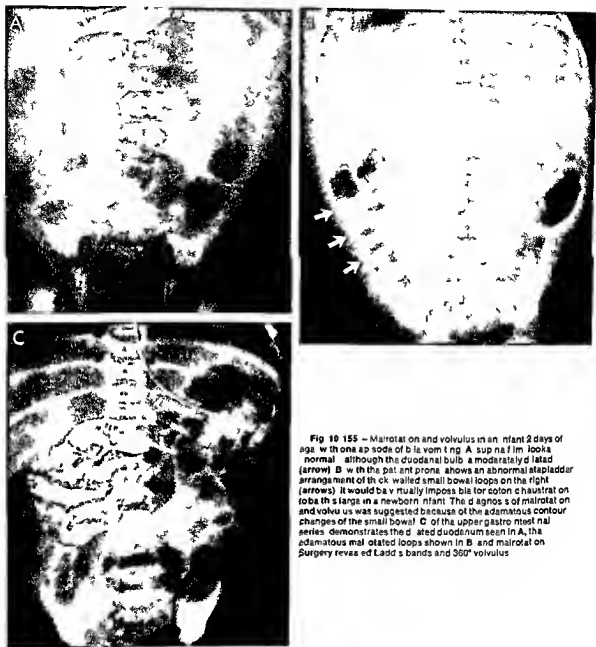


Fig 10-155 — Malrotation and volvulus in an infant 2 days of age with one episode of bilious vomiting. **A**, supine film looks normal, although the duodenal bulb is moderately dilated (arrow). **B**, with the patient prone, shows an abnormal ladder-like arrangement of thick-walled small bowel loops on the right (arrows). It would be virtually impossible for colon haustra to rotate this large in a newborn infant. The diagnosis of malrotation and volvulus was suggested because of the abnormal contour changes of the small bowel. **C**, of the upper gastrointestinal series demonstrates the dilated duodenum seen in **A**, the abnormal malrotated loops shown in **B**, and malrotation surgery revealed Ladd's bands and 360° volvulus.

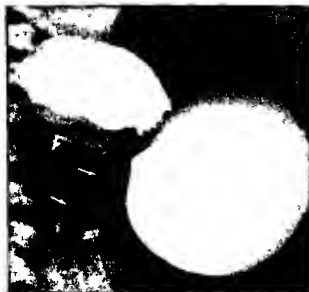


Fig 10-155 — Nearly complete duodenal obstruction in an infant with volvulus, with the upper gastrointestinal series demonstrating the diagnostic corkscrew pattern of twisting loops of jejunum (arrows) descending around the superior mesenteric artery. This is evidence of absence of a ligament of Treitz and of volvulus of the midgut.

struction may result in venous engorgement with leakage of blood into the intestinal tract and melena. Rarely the obstruction is principally lymphatic, and the distended lacteals rupture, producing chylous ascites.

Two major groups of patients with malrotation and volvulus can be defined. In some infants total duodenal obstruction is visualized in plain films (Fig 10-154, A). Originally, the obstruction series would be similar to that of a patient with duodenal atresia. If surgery is to be undertaken immediately regardless of the cause of the duodenal obstruction, no further studies are indicated. If, however, a delay of surgery is contemplated (for fluid replacement, improved anesthetic assistance, and so on) it is mandatory to exclude the presence of malrotation. Emergency barium enema is then indicated (Fig 10-154, B), even though some patients with actual duodenal atresia have associated asymptomatic malrotation. Malposition of the cecum in an infant with duodenal obstruction means associated volvulus until proved otherwise and is an indication for immediate surgery. In the second group of patients with malrotation and volvulus, plain film findings either appear to be normal or indicate minimal duodenal dilatation (Fig 10-155) reflecting the intermittency of the obstruction or the fact that the patient has either vomited or had suction immediately before the films were obtained. Infants who vomit bile and have "normal" plain films must be studied if the 33% mortality in newborns with this condition is to be lowered. It has been customary in this situation to use a barium enema. This plus barium given by mouth in cases of suspected obstruction allows assessment of other possible causes of the same clinical picture. Use of the upper gastrointestinal series has great appeal in these cases. It is rapid and easily performed, defines both presence and de-

gree of duodenal obstruction and identifies the duodenojejunal junction and the right-sided location of the jejunum. It has even been possible to demonstrate venous engorgement of the jejunum with signs of edema and bleeding into the bowel walls (Figs 10-155, C, and 10-156).

An intrinsic obstruction may be present in 10-15% of patients with malrotation and volvulus. After correction of the extrinsic obstruction, the duodenal web, or diaphragm, may stretch and give rise to varying degrees of duodenal obstruction and to the "wind sock" duodenum (Fig 10-157, A and B). In all likelihood this is what used to be called intraluminal duodenal diverticulum (Fig 10-157, C). By running a large catheter from the stomach into the jejunum, the intrinsic obstruction, coexisting with the extrinsic one, can be identified and both corrected at the initial procedure.

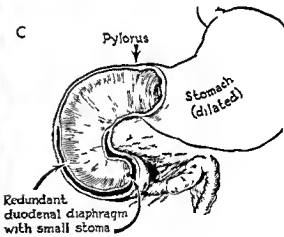
Some conditions in the newborn—diaphragmatic hernia, omphalocele and gastroschisis—are always associated with malrotation. Volvulus may therefore develop in any of these circumstances following repair of the primary anomaly (Fig 10-158). Gastrointestinal anomalies, especially malrotation, are found in patients with anomalous situs, as in asplenia and polysplenia syndromes (Fig 10-159, A). These include malrotation and volvulus as well as duodenal diverticular formation and pyloric obstruction by a prepyloric portal vein (Fig 10-159, B).

REFERENCES

- Astley R. Duodenal atresia with gas below the obstruction. *Brit J Radiol* 42:351 1969.
- Berdon W E, et al. Midgut malrotation and volvulus. *Radiology* 96:375 1970.



Fig 10-157 —A from a gastrointestinal series shows total duodenal obstruction in an infant 7 days of age. At surgery a 360° volvulus was reduced and Ladd's bands were divided. Five days later the patient was again obstructed. B at this time demonstrates the lucent curve near outline of an internal duodenal diaphragm (arrows) that was missed at the first operation. C, schematic drawing of the internal duodenal windsock diaphragm. This is the same as the intraluminal duodenal diverticulum. (From Berdon et al. C courtesy of Dr. A. H. Bill, Seattle, Wash.)



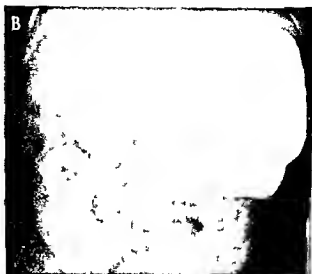


Fig 10-158—Omphalocele. **A** shows a huge ventral defect involving the umbilicus (if the umbilicus is not involved the defect is termed gastroschisis); the liver and midgut are out of the abdominal cavity with obligatory lack of normal midgut fixation. **B**, after repair it is not unusual for blood to ooze from the turgid

previously exteriorized loops of midgut; the radiograph shows irregular thickened walls of the malrotated midgut. Volvulus was not present, and the patient recovered (**B**, courtesy of Dr. A. Shaw, New York).

Fig 10-159—**A**, anomalous situs with midgut volvulus. Although volvulus was present, luminal obstruction of the duodenum was minimal, and venous engorgement of the midgut was the striking finding at operation, which also disclosed multiple spleens (polysplenia syndrome). **B**, anomalous situs with priapic

long portal vein causing gastric obstructive signs similar to those of pyloric stenosis. On the left is a large, asymptomatic duodenal diverticulum containing both gas and barium (arrow). The patient had asplenia syndrome. (From Bardon *et al*.)



- Free E A *et al* Duodenal obstruction in the newborn due to annular pancreas *Am J Roentgenol* 103 321 1968
- Houston C S *et al* Roentgen evaluation of anomalies of rotation and fixation of the bowel in children, *Radiology* 84 1 1965
- Kirkpatrick, J A A complex of anomalies associated with tracheoesophageal fistula and esophageal atresia *Am J Roentgenol* 95 208 1965
- Lynn H B Duodenal Obstruction in Mustard W T *et al* (ed.) *Pediatric Surgery* (2nd ed Chicago Year Book Medical Publishers Inc 1969) p 800
- Richardson, W R *et al* Pitfalls in the surgical management of the incomplete duodenal diaphragm *J Pediatr Surg* 4 303 1969
- Rowe M I *et al* Windsock web of the duodenum *Am J Surg* 116 444 1968

Small Bowel

ATRESIA AS A FETAL VASCULAR INSULT—All intestinal atresia was formerly thought of as an embryologic failure of normal canalization and vacuolization. This had never been demonstrated except in the duodenum but was accepted as the explanation for jejunal and ileal atresia. The true cause would have been realized had it been appreciated that swallowed squamous cells, lanugo and bile pigments are usually present in the distal bowel. This is evidence that the fetus swallowed and had an intact gastrointestinal tract long after the occurrence of the embryologic events supposed to be responsible for atresia. It remained for surgeons and pathologists to produce atresia by fetal surgery on pregnant ewes with ligation of the blood supply to the fetal bowel. Barnard and Louw in South Africa and Blanc and Santulli in the United States were able to do this without cause.

Fig 10-160—A schematic drawing of uncomplicated meconium ileus. Pellets of inspissated meconium fill the terminal ileum above a microcolon. Several loops of more proximal ileum contain thick tenacious meconium. B, schematic drawing of the pos-

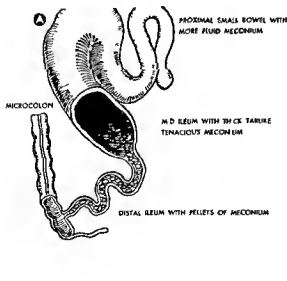


Fig 10 160 — A schematic drawing of uncomplicated meconium ileus. Pellets of inspissated meconium fill the terminal ileum above a microcolon. Several loops of more proximal ileum contain thick tenacious meconium. **B** schematic drawing of the pos-

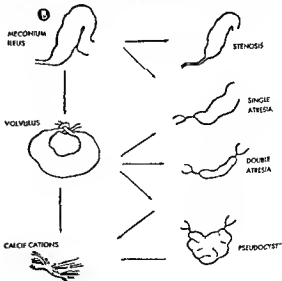
ing fetal death or miscarriage. Depending on the duration of the ischemia and the site they could produce single or multiple stenoses or atresias. Since about three-quarters of the infants born with such atresias have no obviously demonstrable fetal vascular compromise the skeptic might doubt the relevance of such experimental studies. For this reason it is proper to turn to infants with cystic fibrosis of the pancreas 10% of whom are born with intestinal obstruction in the form of meconium ileus (Fig. 10-160 A). The common occurrence of atresia or segmental volvulus and stenosis in such patients may justify the ischemic theory for the causation of jejunal and ileal atresias in human infants (Fig. 10-160 B).

REFERENCES

- Berdon W E *et al* Microcolon in newborn infants with intestinal obstruction. *Radiology* 90 878 1968
- Cross V F Giant Meckel's diverticulum in a premature infant. *Am J Roentgenol* 108 591 1970
- Louw J H, and Barnard C N Congenital intestinal atresia. Observations on its origin. *Lancet* 2 1065 1955
- Santulli T V *et al* Congenital atresia of the intestine. Pathogenesis and treatment. *Ann Surg* 154 939 1961
- Singleton E B Radiologic evidence of intestinal obstruction in the newborn. *Radiol Clin. North America* 1 571 1961
- Widman W D Gastrochisis with antenatal evisceration. *Am J Dis Child* 110 478 1970

MECONIUM ILEUS—The infant with inspissation of the abnormal ileal meconium secondary to cystic fibrosis may be totally or partially obstructed. Distention and bile emesis are common. The rectal examination shows a tiny rectum barely admitting a finger.

sible effect when volvulus occurs above the inspissated meconium. Ischemic changes may occur leading to stenotic strictures, perforation, meconium peritonitis and pseudocyst formation (Figs. 10.160 to 10.163 A and B Leonides et al.)



sible effect when volvulus occurs above the inspissated meconium. Ischemic changes may occur leading to stenotic strictures, perforation, meconium peritonitis and pseudocyst formation (Figs. 10.160 to 10.163 A and B Leonides et al.)

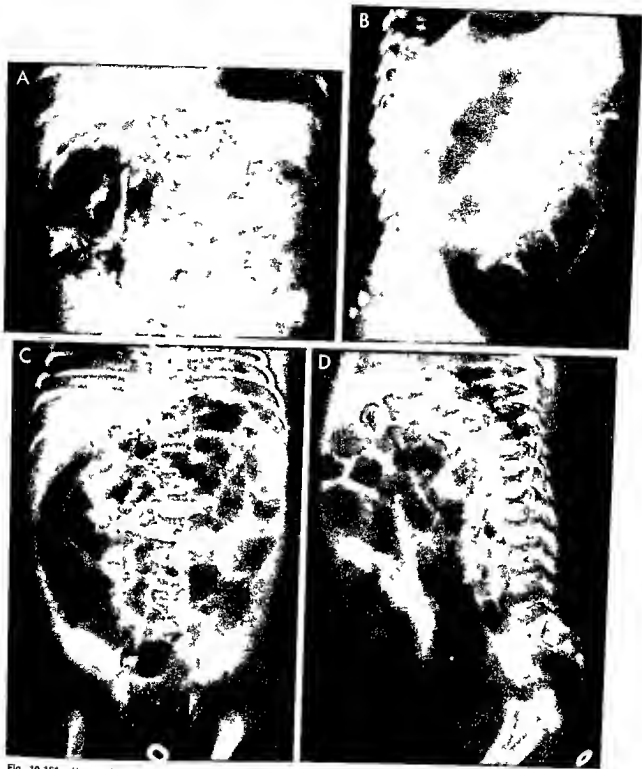


Fig 10-161—Uncomplicated meconum ileus. A, plain film erect position shows a bubbly pattern reflecting admixture of gas and meconium (not specific for meconum ileus). Note lack of air-fluid levels—a helpful sign of meconum ileus. B, lateral view of another patient shows the ability of dilated small bowel loops to simulate colon. Rectosigmoidal gas is absent. The problem of differentiating small from large bowel can be solved by

obtaining upsidedown lateral views. C, frontal and D, lateral views of a patient with clinical diagnosis of imperforate anus; the examiner thought he felt an occluding membrane in the tiny rectum. The lack of air-fluid levels in C and presence of the small lumen rectum in D proves that the obstruction is above the colon, causing its small caliber. Sweat test was positive for cystic fibrosis.



Fig 10-162 — Meconium ileus. Barium enema shows an incompletely opacified microcolon. Arrows indicate the bubbly inspissated small bowel pattern. The huge loop crossing the upper abdomen resembles transverse colon but is small bowel.

and sometimes erroneously considered to be a form of anorectal malformation. Hydramnios, which is relatively common with duodenal or high jejunal obstruction, is rare, with meconium ileus. The cause of the ileal obstruction is unsettled, pancreatic achylia and abnormality of the intestinal mucosa per se are popular explanations.

In uncomplicated meconium ileus the terminal ileum is full of dried pellets resembling deer droppings (Fig 10-160 A). Proximal to this are one or two distended loops filled with tenacious tarlike contents. In erect films there is a paucity or absence of air fluid levels (Fig 10-161) first noted in 1948 by Zimmer and in 1956 by White. Distention is uneven, with several large loops while others are normal in size or slightly dilated. The small bowel loops in meconium ileus have an amazing ability to mimic colonic loops in both size and location. Frequently only the contrast enema, by demonstrating a "microcolon" (Fig 10-162), can give the answer. In addition some gas gets into the tarlike meconium, creating a bubbly pattern in the right lower quadrant. This is not specific for meconium ileus, it resembles the gas-fecal mixture seen in the cecum in older patients and in infants with low sigmoid obstruction such as Hirschsprung's disease.

Obstruction in uncomplicated cases may be relieved by cleansing enemas. Formerly hydrogen peroxide was used before and during surgery for this purpose with considerable success, but reports of gas

embolism associated with this method led to its abandonment. Evidently the peroxide is irritating and the bowel mucosal integrity is lost, gas from both the peroxide and the bowel lumen penetrates the wall and gram negative bacteria follow. The gas in portal radicles goes to the liver, and shock probably secondary to gram negative sepsis develops. If water soluble agents such as Gastrografin are employed as an enema to disimpact uncomplicated meconium ileus, this should be done with surgical cooperation and consent. Intravenous fluid will be needed to counteract the powerful hydropic effect of the hypertonic contrast enema.

Less than 50% of cases of meconium ileus are of the uncomplicated type, the majority being complicated meconium ileus (Fig 10-160 B). The usual complication is segmental volvulus. Proximal to the volvulus, there may be atresia (single or multiple) or stenosis. Obviously with ischemia and secondary atresia air fluid levels in the dilated segment above the atresia will be found (Fig 10-163 A and B). The fact that about 25% of cases of jejunal and ileal atresia at the Babies Hospital have been secondary to cystic fibrosis has led to performance of a sweat test on all survivors of small bowel atresia.

Should perforation occur in utero in such patients a chemical peritonitis occurs accompanied by the formation of dense adhesions. Calcification may be evidence of such meconium peritonitis (Fig 10-163 C). Although commonly found on the peritoneal sur-

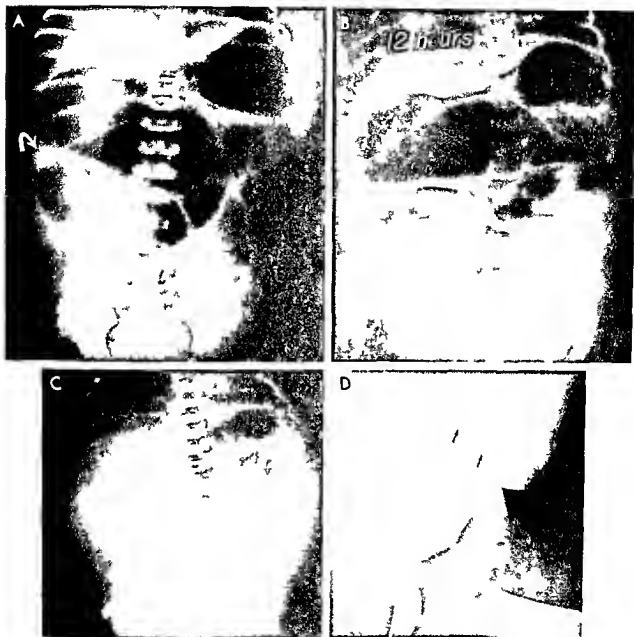


Fig 10 163 A and B compounded meconium eus with ea
a es above an ea of pena vou us n a sup n m the e
a es ma c a c a o n s (a row) w h d a e d ea oops es m
b n g co o n c oops n b o h s w e d and loca n b e e c t m
flud eves a es seen s nce a es a s p e n t (A and B om
Leon d e a e) C compounded meconium eus w h e x e n s v e

mecon um pe on s The ca c ca ons a e on the surface of the
vo vu a e oops above nss paa de mecon um h e e m na
eum D ac es sress nes n a pa ent w h mecon
eum and pe on s No a ways p esent n mecon um pe on s.
hey may e a e o s y e m c s t e s s of the vo vu u on the fetus
Pen oney ca c ca ons ma k the eft ank

face, it may also be intramural or even intraluminal. Wolffson and associates concluded that meconium peritonitis can be suspected (Fig 10-163, D), in the absence of calcification, by the detection of iliac crest and long bone stress lines that they had not found in uncomplicated meconium ileus or other types of obstruction such as Hirschsprung's disease. Unfortunately the stress lines date the insult rather than indicating its exact cause, and cases of meconium peritonitis without stress lines or calcifications will continue to be seen.

Microcolon in meconium ileus and relations to level of obstruction—If a contrast enema is given a patient with meconium ileus a microcolon is demon-

strated (see Fig 10-162), that is a colon of normal length but tiny caliber. The colon contains lanugo squamous cells and bile tinged meconium. Its small size is related to loss, probably relatively late in utero, of continued passage of small bowel contents to the colon, where water absorption leaves a meconium residue. Following surgical decompression and anastomosis in meconium ileus, the 'microcolon' regains normal size. Microcolon is seen whenever an obstruction is so low in the small bowel as to prevent a significant amount of small bowel contents from reaching the colon. A long period of time need not elapse between the insult and birth, because it occurs with meconium ileus, a presumed third trimester event.

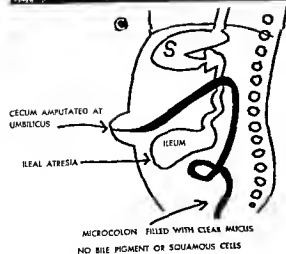


Fig 10-164 — Malrotated cecum with microcolon. A, frontal and B, lateral projections after barium enema, show distended loops of ileum, the right colon and malrotated cecum end at the umbilicus, as does the distal distended small bowel. Prenatal amputation of this portion of midgut created ileal atresia as the intestine was returning to the abdominal cavity. C, schematic drawing of the condition (C, from Berdon et al.)

Rarely it is associated with a true embryologic vascular amputation of the part of the midgut that can be caught at the umbilical ring during extracoeleomic intestinal rotation and return to the coelomic cavity. The microcolon leads to a malrotated cecum which is seen in the lateral view after barium enema to go to the umbilicus (Fig 10-164). The pathologist may find tiny unfarcted bowel loops in the umbilical cord of such a patient.

Patients with esophageal and duodenal atresia have normal caliber colons indicating that swallowed amniotic fluid, gastric juice and bile pigments are not necessary for development of a colon of normal caliber. What determines colon caliber is the amount of succus entericus and the amount of small bowel left in continuity with the colon plus the ability to propel the succus entericus into the colon.

REFERENCES

- Berdon, W. E. *et al*: Microcolon in newborn infants with intestinal obstruction. *Radiology* 90: 878, 1968.
- Denis, R. K. *et al*: Danger of hydrogen peroxide as a colon irrigation solution. *J. Pediatr. Surg.* 2: 131, 1967.
- French, R. S. *et al*: Meconium ileus relieved by 40% water soluble contrast enemas. *Radiology* 94: 341, 1970.
- Grossman, H. *et al*: Gastrointestinal findings in cystic fibrosis. *Am. J. Roentgenol.* 97: 227, 1966.
- Leonidas, J. *et al*: Meconium ileus and its complications. *Am. J. Roentgenol.* 108: 593, 1970.
- Neuhauser, E. B. D.: Roentgen changes associated with pancreatic insufficiency in early life. *Radiology* 46: 319, 1946.
- Noblett, M. R. *et al*: Treatment of uncomplicated meconium ileus by Gastrografin enema. *J. Pediatr. Surg.* 4: 190, 1969.
- Santulu, T. V.: Meconium ileus. In Mustard, W. T. *et al* (ed): *Pediatric Surgery* (2nd ed). Chicago: Year Book Medical Publishers, Inc. 1969. Chap. 54.
- Shaw, A. *et al*: Gas embolism produced by hydrogen peroxide. *New England J. Med.* 277: 238, 1967.
- Wagget, J.: Nonoperative treatment of meconium ileus by Gastrografin enema. *J. Pediatr.* 77: 407, 1970.
- White, H.: Meconium ileus. *New roentgen sign.* *Radiology* 66: 567, 1956.
- Wolffson, J. J. *et al*: Anticipating meconium peritonitis from metaphyseal bands. *Radiology* 92: 1055, 1969.
- Zimmer, J.: Microcolon with report of two cases. *Acta radiol.* 29: 228, 1948.
- PRENATAL VOLVULUS AND PSEUDOCYSTS**—In some patients with jejunal or ileal obstruction prenatal intestinal gangrene with calcification of the loop may be evident on pelvimetry or newborn films (Fig 10-165 B). Depending on the time of onset and tightness of the involved loops the ischemic bowel may be matted together into a cystlike mass or pseudocyst (Fig 10-165 A). With time this can separate from the dilated proximal bowel and the collapsed lower ileal loops to resemble a duplication cyst. The pathologist may be able to give the real diagnosis by finding meconium and bowel loops within the cyst. Wilham Blanc (N.Y. Babies Hospital pathologist) concluded that about one-half of the cases of such pseudocysts were secondary to cystic fibrosis.
- The distended patient with such a pseudocyst may show evidence of apparent high small bowel obstruction on plain films (Fig 10-165 C) even though the flanks are bulging. Barium enema reveals a microcolon. The total body opacification phase of the intravenous pyelogram has shown evidence of lucent unfarcted loops within the volvulus or pseudocyst (Fig 10-165 D). To confuse the diagnosis further the pseudocyst may rupture and ascites may be present as well.
- COLON PERFORATION IN CYSTIC FIBROSIS**—Five infants in the Babies Hospital series of newborns with intestinal obstruction from cystic fibrosis had distention, bilious vomiting and massive ascites with small amounts of free intra abdominal gas (Fig 10-166). Contrast enema showed colon perforation. There was no particular site of predilection; the hepatic flexure and various sites in the left colon were involved. There was no evidence at operation of meconium ileus *per se*. The lower ileum showed no signs of inspissated obstructing contents. All patients gave a positive response to the sweat test. The cause for this complication of fibrocystic disease is unknown, although speculation has centered on stercoral ulceration by meconium contents.
- MECONIUM PERITONITIS WITHOUT OBSTRUCTION IN CYSTIC FIBROSIS**—One infant with an intact gastrointestinal tract had soft bilateral scrotal masses thought to be hydroceles at birth and firm masses in the scrotum at 6 weeks of age. Roentgen study revealed calcification and meconium peritonitis within the scrotum and abdominal cavity (Fig 10-167). The patient had a positive response to the sweat test and later developed typical pulmonary findings. The precise in utero event leading to such perforation is not known. This sequence is rare and most reported cases of calcified scrotal masses as a sign of meconium peritonitis with an intact gastrointestinal tract were in infants without cystic fibrosis. Meconium enters the scrotum via the patent processus vaginalis, apparently being sufficiently fluid to flow and to mimic soft hydroceles. Perforation may be secondary to hypoxia shortly before birth and in nearly all cases there is a delay of several weeks before the masses solidify and are palpable.
- DUPPLICATION OF THE SMALL BOWEL**—Tubular or cystic masses may be observed in the small bowel. Some are parallel to and within the serosa of the normal small bowel and probably reflect embryologic errors in normal canalization. Others of varying size are found within the mesentery or on the mesenteric side. Vertebral segmentation anomalies are sometimes present. The latter group includes neuroenteric cysts as part of the split notochord syndrome (Fig 10-168) presumably due to persistence of the embryologic connection between the developing gut and neural tubes. Both types of duplication may contain gastric and pancreatic tissue. They may communicate with the ileum and cause ulceration and bleeding or obstruction from adhesions.
- MICKEL'S DIVERTICULUM**—A tubular mass with

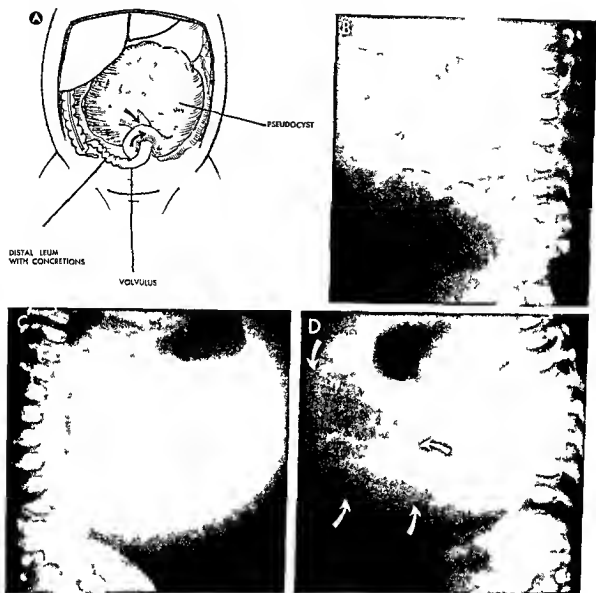


Fig 10-165 — A schematic drawing showing how a pseudocyst (representing matted volvulated loops) forms in meconum ileus. B prenatal volvulus with calcification of the intussuscepted bowel and proximal dilatation as a secondary to distal meconum ileus. C, apparent high small bowel obstruction secondary to a pseudocyst

above the meconum ileus. D total body bipartite cal on an intra-venous pyelography delineates adjacent matted volvulated loops in the pseudocyst above the distal meconum ileus. This study was requested because the mass (pseudocyst) was palpated (C and D from Leonard et al.)



Fig 10-166—Colon perforation in cystic fibrosis. There was a clinical impression of an abdominal mass. Total body osteocalcin on intravenous pyelography shows the dense liver shifted medially by ascites and meconium peritonitis (arrows). Note bubbles of free gas lateral to the liver. Surgery revealed perforation at the hepatic flexure without terminal ileal meconum ileus. (From Leonard *et al*.)

Fig 10-167—Meconium peritonitis without gastrointestinal obstruction manifested as hard scrotal masses in an infant subsequently proved to have cystic fibrosis. Presumably the prenatal

perforation sealed; however, the perforation allowed liquid meconium to flow through the patent processus vaginalis into the scrotum, where it solidified and calcified. (From Berdon *et al*.)



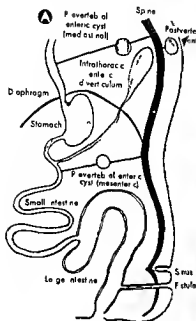


Fig 19 168 —A schematic drawing of developmental posterior enteric remnant, the so-called neuroenteric forms of duplication are included as part of the split notochord syndrome. They are often associated with missegmentation of the vertebral column, although not necessarily at the same level as the mass. B: huge communicating gas-filled neuroenteric cyst with vertebral mal-

segmentation. The only clinical sign was mild g-bbuss at the site of the abnormal vertebrae. Barium could not be introduced into the cyst despite obvious communication with the intestine, as shown by its gas content. Such masses are mesenteric in location (A: courtesy of Dr J F R Bentley Glasgow, Scotland)

Fig 19 169 —Giant Meckel's diverticulum in an infant 6 days of age. In A, the mixture of gas and meconium in the giant diverticulum simulates the plain film picture of meconium ileus. Obstructive signs were minimal. Such masses are entmesenteric in

location. B: surgical specimen shows the entmesenteric site of the diverticulum. The afferent ileum (on right) is dilated and the efferent ileum (on left) is normal. (Courtesy of Dr V F Cross Albany, NY)





Fig 10-170—Patent omphalomesenteric duct. A tiny orifice was noted after cleansing of an asymptomatic crusted umbilicus. Water-soluble contrast medium injected into the orifice fills the ileum, demonstrating the patent duct. Meckel's diverticulum is an incomplete internal remnant of this duct. (Courtesy of Dr G. Van Syckle, Danbury, Conn.)

areas simulating gastric and pancreatic tissue may be found on the antimesenteric border in some normal infants and adults at autopsy. This is the persistence of the inner part of the omphalomesenteric duct and is called Meckel's diverticulum. Clinical signs and symptoms may be present in the newborn, such

as bleeding and obstruction from adhesions secondary to diverticulitis. Rarely the diverticulum enlarges as it fills with meconium and feces and simulates intestinal obstruction from meconium ileus (Fig 10-169).

The entire omphalomesenteric duct may be patent. This may cause no symptoms or lead to fecal umbilical drainage on the abdominal wall. Injection of contrast medium demonstrates a fistula to the ileum (Fig 10-170).

REFERENCES

- Bentley J F R *et al*: Developmental remnants and spinal malformations. *Arch Dis Childhood* 35:76, 1960.
 Cross V F *et al*: Meckel's diverticulum in a premature infant. *Am J Roentgenol* 108:591, 1970.
 Elliott G B *et al*: The notochord as an abnormal organizer in production of congenital intestinal defects. *Am J Roentgenol* 110:628, 1970.

Colon

Colonic obstruction may be functional (Hirschsprung's disease, meconium plug syndrome) or organic (congenital anorectal malformations, colon atresia). These obstructions are not usually reflected in fetal growth disturbances, and hydramnios is rare.

HIRSCHSPRUNG'S DISEASE (AGANGLIONOSIS)—Full-term infants with distention, bile emesis, and initial difficulty in passing meconium show the neonatal signs of aganglionic stenosis, first noted in 1887 by Hirschsprung. The nursery records of older children with megacolon usually also reveal this history. The diagnosis is made in the newborn by relating the clinical and radiographic findings (Fig 10-171).

Premature infants rarely have this condition. Males

Fig 10-171—Plain films in aganglionic megacolon. A, supine film shows gaseous distention of multiple intestinal loops; the gas-filled appendix (arrow) is a clue that the colon shares in the

distention. B, lateral inverted film is helpful in showing that distention is due to the colon and that the rectum is not large. Gas-fluid levels are present.



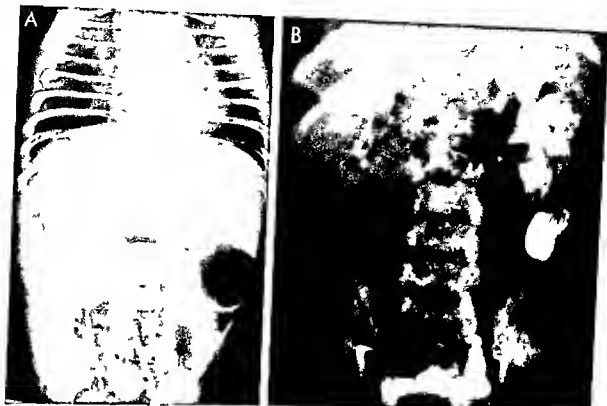


Fig 10-172—Aganglionosis. **A**, frontal projection of a patient with levocardia, transverse liver, cyanotic heart disease and asplenia as well as aganglionosis. Autopsy disclosed malrotated right colon. This is one of a very few patients who have had congenital anomalies in addition to Hirschsprung's disease. **B**, intravenous pyelogram delineates a left hydronephrotic (without reflux

or infection) in a patient with aganglionosis of the low sigmoid and rectum. Usually the intravenous pyelogram shows no abnormality in aganglionosis. The possibility of compression of the ureter by the distended bowel as the cause of hydronephrosis was considered. Aganglionosis of the ureter is not an acceptable diagnosis to most pediatric pathologists.

predominate 4:1 in the usual type, which involves the low sigmoid and rectum, 75% of cases are of this type. In another 10–15% the entire colon and terminal ileum are involved and there is a greater incidence of family history of the condition and an equal male-female ratio. The remaining cases involve varying lengths of colon, on occasion the entire midgut and colon have been aganglionic.

In the most common form, skip areas (alternating normal and aganglionic segments) are not present despite sporadic reports. Thus, 'transition in the mid sigmoid' means that the entire distal bowel to the lowest portion of the rectum lacks ganglion cells. This disease is usually not associated with other anomalies (Fig 10-172 **A**), although there is a slightly greater incidence with 21 trisomy. Genitourinary anomalies are not usually associated with aganglionosis. There is no support for the concept of aganglionic ureter (Fig 10-172 **B**). The occasional example of a dilated ureter probably reflects compression of the ureter by the distended colon in utero. These ureters have improved or returned to normal following colostomy.

Initial plain films taken when the patient first has

clinical signs of obstruction usually show corresponding patterns of distended loops with air-fluid levels (Fig 10-171 **A**). The appendix may be air-filled and distended and in some cases free air occurs secondary to appendiceal or cecal perforation (Fig 10-171 **B**). The diagnosis of Hirschsprung's disease can be firmly established if barium enema studies are made at this time of 'decompensation' (Figs 10-173 and 10-174). The findings, best seen in lateral projection, include normal caliber of the rectum and lower sigmoid colon (Fig 10-174 **B**) and dilated proximal sigmoid and remainder of the colon. The dilated loops filled during the enema correspond to those seen in plain films. The paradox of Hirschsprung's disease is that the dilated portion of the bowel is normal while the normal appearing bowel (rectum) lacks ganglion cells. This results in sustained spastic tone in these areas with functional bowel obstruction. Spastic irregular contour changes are occasionally seen in the involved rectum and sigmoid (Fig 10-175). Unfortunately this sign, described by Hope and associates, may be present in normal infants as a form of spasm and absent in some patients with Hirschsprung's dis-

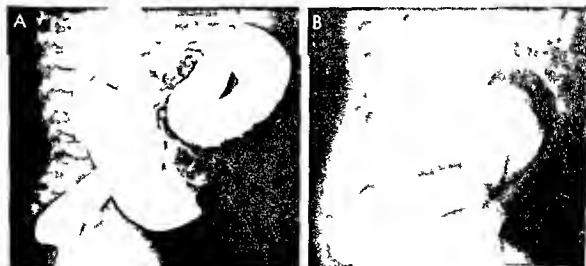


Fig 10-173—Aganglioneosis. A frontal view after barium enema, is valuable in showing that the bag loops seen in plain films are colon c but is a poor projection for visualizing the normal rectum and dilated sigmoid colon—diagnostic features in the

usual case. B eight days later clearly demonstrated marked emptying of the colon and discrepancy in caliber between rectum and sigmoid colon.

Fig 10-174—Aganglioneosis. A lateral view after barium enema demonstrates a normal rectum and dilated sigmoid and descending colon. The change is subtle, there being no actual sig-

moid megacolon or sharp transition. B 95 hours after repeat barium enema and indicates the diagnosis.



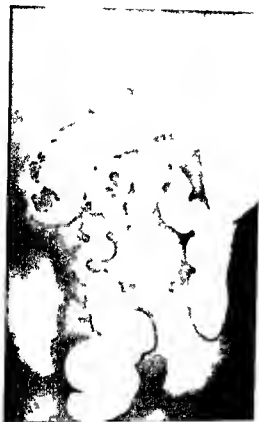


Fig 10-175—Aganglionicosis. The saw-toothed spastic contour irregularities in the sigmoid colon appear here as a heaped-up mass though not always present. They are thought to reflect irregular and abnormal tonics in the aganglionic bowel. Transition to normal ganglionocytes is at the splenic flexure.

ease. Use of a Foley catheter is to be avoided in general and in particular in the evaluation of Hirschsprung's disease. It merely obscures the normal caliber of the rectum. One infant in the Babies Hospital series died of unrecognized colonic perforation by the catheter (Fig 10-176).

Delayed films (especially lateral views) at 24-48 and even 96 hours after the enema will show retention of barium so long as cleansing enemas are not given after the barium (Figs 10-173 B and 10-174 B). Even some compensated patients maintain this valuable evidence of delayed evacuation. Any patient with colonic distention in the newborn period should have a biopsy to exclude Hirschsprung's disease before discharge from the nursery. Should the patient be compensated (by rectal examination or cleansing enemas) he may seem normal for weeks or months. Some do not come to clinical attention until megacolon develops at 1-2 years of age. In others, tragically fulminating enterocolitis appears with foul diarrhea, shock and death (Fig 10-177). This can be prevented by early diagnosis and a diverting colostomy

until the infant is old enough to undergo a definitive procedure.

The next most common form, total colonic and terminal ileal aganglionicosis, may be difficult to diagnose. The severity of the obstructive symptoms does not parallel the length of involvement and adults have been found with this form of the disease. The vast majority have died early in life without the correct diagnosis having been made. The plain films (depending on the state of compensation) may show varying degrees of distention of small bowel origin, although this is difficult if not impossible to determine in plain films. Barium enema study shows a surprising picture in the context of such small bowel distention: the colon looks normal in length and caliber (Fig 10-178 A). In time, some patients show a shortened appearance of the colon and disappearance of the usual redundant sigmoid loop (Fig 10-178 B-D). This "normal" barium enema picture in the suspected case of small bowel obstruction in the newborn is unacceptable and demands search for aganglionicosis. Rectal biopsy will at least show whether the basic disease is present, although not its proximal extent. When nothing is found on surgical exploration of the newborn with clinical small bowel obstruc-

Fig 10-176—Tragic fatal use of a Foley catheter in aganglionicosis. The catheter, both obscured as the rectum (in distension in which diagnosis is based on discrepancy in caliber between rectum and sigmoid) and has caused an unrecognized perforation (note barium below the sigmoid obscuring the catheter balloon) that led to death.





Fig 10-177 Lateral enterocolitis in aganglionosis in a boy 12 days of age whose diagnosis was missed in the immediate newborn period. Barium enema (given because of severe abdominal distention and fever) demonstrates dilated bowel to the

low sigmoid with edematous mucosa of this ganglionic bowel that had severe enterocolitic involvement. The film accompanied the patient, who was dead on arrival at the hospital.

tion biopsy at the peritoneal reflection or in the rectum should be performed to establish the presence or absence of this form of aganglionosis.

Marked sacral deformity in an infant with meconium and fecal impaction points to a neurogenic cause rather than aganglionosis (Fig 10-179). Lateral views after contrast enema in such patients show fecal distention down to the puborectalis sling, whereas in Hirschsprung's disease the dilatation stops above the sling with a normal rectum below the distended bowel.

Caution is necessary if water-soluble enemas are used. These may compensate the patient since they act as hydrogogue cathartics and the evacuation may be complete and the diagnosis missed. The patient may thus be discharged as normal only to return with enterocolitis and die.

REFERENCES

- Berdon W E *et al*. Radiographic diagnosis of Hirschsprung's disease in infancy. *Am J Roentgenol* 93:432, 1965.
- *et al*. Diagnosis of colonic and terminal ileal aganglionosis. *Am J Roentgenol* 91:680, 1964.
- Chandler N W *et al*. Reflux of the small bowel in total colonic Hirschsprung's disease. *Radiology* 94:335, 1970.
- Fleisch R S. Aganglionosis involving the entire colon and variable length of the small bowel. *Radiology* 90:249, 1968.
- Gerald B. Aganglionosis of the colon and terminal ileum. *Am J Roentgenol* 95:230, 1965.

Hope J W *et al*. Radiologic manifestations of Hirschsprung's disease in infancy. *Am J Roentgenol* 95:217, 1965.

Kilcoyne R F *et al*. Conditions associated with congenital megacolon. *Am J Roentgenol* 108:615, 1970.

MECONIUM PLUG SYNDROME—In 1956 Clatworthy and colleagues described a group of infants with colonic obstruction, sometimes necessitating colostomy, whose condition resembled aganglionic megacolon but the colon contained normal ganglion cells. Others had lesser obstruction and passed a 'plug' of sticky meconium. The term 'meconium plug syndrome' is unfortunate because the meconium is normal and the patients basically have a functional colonic inertia that responds to enemas. The diagnosis of meconium plug syndrome requires exclusion of cystic fibrosis by sweat test and of aganglionosis by rectal biopsy (Fig 10-180). The truly obstructed patients with meconium plug syndrome have left-sided microcolon with transverse and right colonic distention. In this they differ from patients with Hirschsprung's disease in whom aganglionic bowel looks normal. Evacuation may be impaired as in Hirschsprung's disease with retention of barium at 24 and 48 hours. The cause of the syndrome is unknown. An occasional patient has a history of maternal diabetes, hypotonia or fetal distress. Several have had areflexia and hypermagnesemia as a result of magnesium sulfate treatment of the mother for toxemia. It has been speculated that



Fig 10-178 — A aganglionsis of the entire colon and terminal ileum in an infant 3 days of age. The colon has normal caliber and evidence of inspissated meconium mixed with the small bowel and dilated loops suggest low small bowel obstruction (mccolon would be expected). Autopsy revealed multiple foci of neuroblastoma (these are several cases of associated neuroblastoma and long segment aganglionsis). B of a 3-week-old infant shows a short sigmoid loop but normal caliber of the colon. Note the poor technique in use of the Fekety barium and also the dilated small bowel loops. Mccolon rather than no mal-

ccolon caliber would be expected and the normal caliber of the terminal ileum requires muscle biopsy of rectal or other colon sections to exclude aganglionsis. C, example of the value of the Chassard-Lapina view to demonstrate shortening of the sigmoid. This is progressive and rarely seen in the neonate although common in infants several weeks or months of age. D for comparison, the barium enema picture of a normal newborn to show the usual redundant sigmoid (often swinging into the right abdomen) (A and D from Berdon et al).

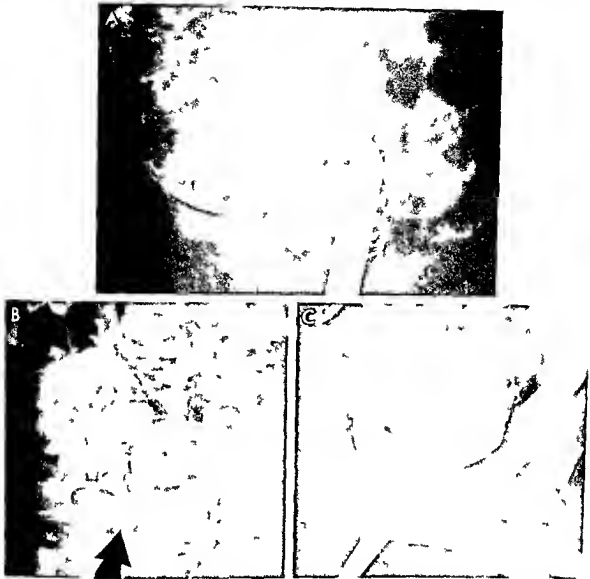


Fig 10-179—in an infant with constipation, barium enema suggested aganglionosis of the megacolon. **A**, frontal view obscures the change in caliber between rectum and sigmoid; the diagnostic hallmark of the usual type of aganglionosis of the megacolon. **B**, anteroposterior view reveals markedly abnormal sacrum (arrow) and

abnormal position of the right kidney (arrow). Such sacral and renal anomalies are most unusual in aganglionosis and suggest neurogenic abnormality. **C**, lateral view after barium enema shows the large rectum down to the levator ani, signifying no transition. Rectal biopsy revealed ganglion cells.



Fig 10-180 —Pseudo Hirschsprung's disease (meconium plug syndrome) in a full term infant with obstructive signs and failure to pass meconium. A: Barium enema reveals left-sided megacolon with dilated transverse and right colon. B: 24 hours later much of the barium is retained raising the question of aganglionosis.

gionosis. Normal ganglion cells were found both in the rectum and around the transition zone at the splenic flexure. The tiny left colon would be most rare in aganglionosis in which involved bowel loops appear to be normal while normal bowel is dilated. (From Beaton et al.)

the relaxing effects of hypermagnesemia on smooth muscle may be linked to the meconium plug syndrome in these patients.

REFERENCES

- Clatworthy H W Jr et al: The meconium plug syndrome. *Surgery* 39:131, 1956
 Ellis D G et al: Meconium plug syndrome revisited. *J Pediatr Surg* 1:54, 1966
 Mikity V G: Meconium blockage. *Radiology* 88:740, 1970

NECROTIZING ENTEROCOLITIS—Some infants usually below 2000 Gm may present signs and symptoms suggesting either colonic obstruction (confused with Hirschsprung's disease) or small bowel obstruction. Reports of appendicitis, colitis, or ileitis in the newborn or spontaneous perforation of the colon describe the same group of patients. The condition is now generally called necrotizing enterocolitis. The cause is unknown, although it is probably of ischemic origin and related to splanchnic underperfusion during periods of prenatal or perinatal distress. There is a high percentage of breech deliveries. There is usually a period of several days of apparent well-being, then apnea, blood-streaked stools, distention, and bile emesis develop. Sepsis or volvulus may be suspected in others; the apneic episodes and illness lead to suspicions of pulmonary or cardiac disease.

Plain films (of the chest, if this is the area of clinical interest) show distention of loops. Free intra-abdominal gas may be present or appear in follow-up

films. The right lower quadrant is commonly the site of intramural gas collections, either as bubbles or linear strips. This is most ominous and not to be confused with benign 'pneumatosis cystoides intestinalis' (Fig 10-181). Gas may be present in the intrahepatic branches of the portal vein in the form of arborizing collections going toward the hepatic periphery and reflecting portal venous flow (Fig 10-182). This should not be confused with the extremely uncommon finding in the newborn of gas in the biliary tree (Fig 10-183). Gas has been demonstrated on a few occasions within the bile ducts of infants with duodenal obstruction and an incompetent sphincter of Oddi. Biliary gas tends to be centrally located, sparing the hepatic periphery and reflecting bile flow toward the gut. Gas in the portal vein is an ominous sign when associated with gram-negative sepsis, and most patients die soon. Air accidentally introduced into the portal vein by umbilical venous catheters is well tolerated.

Some patients survive this initial insult without surgical exploration and go on to develop small bowel obstruction secondary to colonic stricture. Review of enema studies of these infants during the initial illness (when Hirschsprung's disease was suspected) has shown irregular mucosal outline in the area of subsequent stricture formation (Fig 10-184 A). Atresia of the ileum developed in one 6-week-old patient who also had a perirenal abscess from associated septic involvement. Another manifestation of colonic involvement was a roentgen appearance virtually

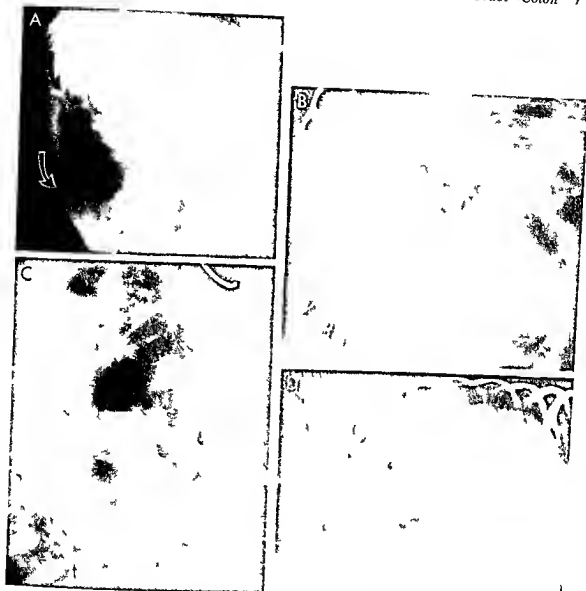


Fig 10-181—Necrotizing enterocolitis. **A**, in a 6-day-old premature infant, intramural bubbles are seen in the right lower quadrant (arrow) and small bowel distention. Multiple perforations of the appendix, right colon and terminal ileum were found at surgery. The patient died. **B**, frontal and **C**, lateral views of a 5-day-old premature infant, in which the linear pattern of intraluminal gas (arrow) is well seen. Gas was also present in the intrahe-

patheal spaces of the porta hepatis, though not well visualized here. **D**, left lateral decubitus projection of the abdomen of a 4-day-old infant, demonstrates free gas distention of small bowel loops and intraluminal gas in the right lower quadrant. This is an excellent projection for follow-up study of such patients because the right side of the abdomen is well seen and free gas readily noted.

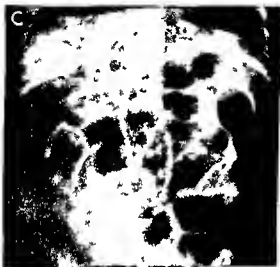


Fig 10 162 —A nt ahepat c portal ve n aneurysm (note gas n necrotizing enterocolitis combined w th gast c involvement) (note gast c intramural gas) B nt ahepat c portal ve n gas plus nt amural duodenal gas na mongolo d w th duoden stenosis and ph egmonous gast oduoden t s (B courtesy of Dr B J Ral ly To onto Canada) C marked nt ahepat c portal ve n gas plus sma bowel stent on a postmortem radiograph revealed free gas due to ileal perforations (B from Mek n and R ay)

Fig 10 163 In a patient w th Down s syndrome and duodenal stenosis an incompetent sph ncter s demonstrated both by et rograde air (A) and subsequently by barium lining of the bile

ducts (B) The e was no cl ncl s gns of necrotizing enterocolitis (Courtesy of Dr E Go d New Yo k)



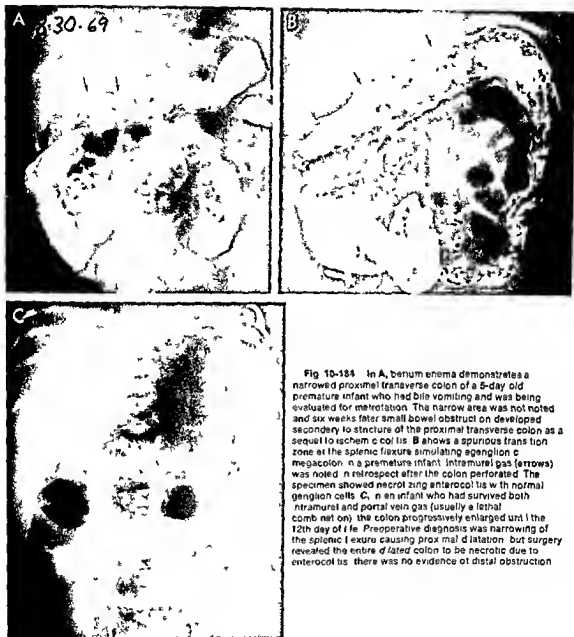


Fig 10-184 In A, barium enema demonstrates a narrowed proximal transverse colon of a 5-day old premature infant who had bile vomiting and was being evaluated for malrotation. The narrow area was not noted and six weeks later small bowel obstruction developed secondary to stricture of the proximal transverse colon as a sequela to ischemic colitis. B shows a spurious transposition zone at the splenic flexure simulating aganglionic megacolon in a premature infant. Intramural gas (arrows) was noted in retrospect after the colon perforated. The specimen showed necrotizing enterocolitis with normal ganglion cells. C, in an infant who had survived both intramural and portal vein gas (usually a lethal combination), the colon progressively enlarged until the 12th day of life. Preoperative diagnosis was narrowing of the splenic flexure causing proximal dilatation, but surgery revealed the entire dilated colon to be necrotic due to enterocolitis; there was no evidence of distal obstruction.

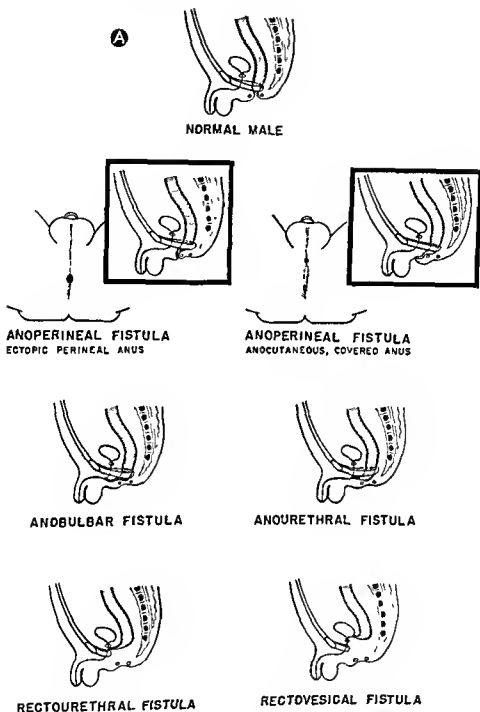


Fig 10 185 — A, schematic diagram of common sites of ectopic termination of the hindgut in the male

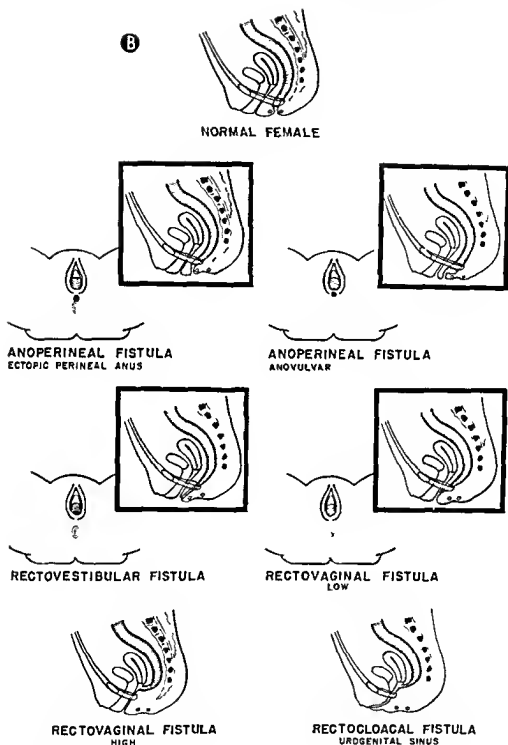


Fig. 10-185 —B, schematic diagram of common sites of ectopic termination of the hindgut in the female (Figs 10-185 and 10-186 from Santulli)

identical to that of Hirschsprung's disease involving the splenic flexure (Fig 10-184 B). The presence of intramural gas and the low birth weight were against the diagnosis of Hirschsprung's disease although the proper diagnosis was not made until after perforation and death. Toxic dilatation of the involved colonic segments similar to that in older patients with ulcerative colitis has been seen (Fig 10-184 C).

Treatment is controversial. Free intra abdominal gas is an obvious indication for exploration. Reports of more aggressive surgery have emphasized clinical deterioration as an indication. Claims have been made of higher survival rates with this approach. Cecal or ileal perforation has been found in a few such patients even when free gas was not present.

Although premature infants account for most cases of necrotizing enterocolitis in the newborn it should not be thought of as a premature or newborn illness per se. Similar radiologic pathologic changes have been found in patients with perforation of the colon after exchange transfusion and in a large series of older infants with infectious diarrhea, usually due to pathogenic *Escherichia coli*.

REFERENCES

- Bardon W E et al. Necrotizing enterocolitis in the premature infant. *Radiology* 83:879 1964.
 Coello-Ramirez P et al. Pneumatosis Intestinalis. *Am J Dis Child* 120:3 1970.
 Denes J et al. Necrotizing enterocolitis in the premature infant. *Acta paediatr (Budapest)* 9:237 1968.
 Hilgartner M W. Perforation of large and small intestine following exchange transfusions. *Am J Dis Child* 120:79 1970.
 Hopkins C B. Necrotizing enterocolitis in premature infants. *Am J Dis Child* 120:229 1970.
 Lifshitz F et al. Monosaccharide intolerance and hypoglycemia in infants with diarrhea. *J Pediatr* 77:595 1970.
 Miskin M et al. Gas in the intestinal wall and portal venous system in infants. *Canad M A J* 101:129 1969.
 Rabinowitz J et al. Colonic changes following necrotizing enterocolitis in the newborn. *Am J Roentgenol* 103:359 1968.
 Rossier A et al. Ulcerating necrotic enterocolitis of the premature. *Ann paediatr* 34:1425 1959.
 Stevenson J K et al. Neonatal necrotizing enterocolitis. *Am J Surg* 118:260 1969.
 Swain T J et al. Hepatic portal venous gas in infants with out subsequent death. *Radiology* 94:343 1970.
 Thelander H E. Perforation of the gastrointestinal tract of the newborn infant. *Am J Dis Child* 58:371 1959.
 Touloukian R J et al. Surgical experience with necrotizing enterocolitis in the infant. *J Pediatr Surg* 2:389 1967.
 Waldhausen J A et al. Necrotizing colitis of the newborn. Common cause of perforation of the colon. *Surgery* 54:365 1963.
 Wolfe J N et al. Gas in the portal vein of the liver in infants. *Am J Roentgenol* 74:486 1965.

ANORECTAL MALFORMATIONS (IMPERFORATE ANUS)

The formerly held concept of imperforate anus is attributable to the pioneer descriptions of Ladd and Gross. Actually of their four types only type III includes the usual patient with imperforate anus. Their remaining types were as follows:

Their type I was anal stenosis, type II was imperforate anal membrane, a very rare lesion treated by incision, and type IV was colonic atresia with a normal rectum below and dilated bowel above an acquired atretic segment. This discussion will center on the patients with congenital anorectal malformations in which the rectum fails to empty normally into an anatomically normal anus in the usual site (Fig 10-185).

At an international pediatric surgical meeting in Melbourne in 1970 a classification was adopted that will be used here. As noted by the participants, no single classification of these anomalies is ideal. Each falls short as a pure anatomic, embryologic, therapeutic or prognostic classification. We believe that the classification will best serve all of these interests and form a basis of common language for these anomalies. It is presented as a suggested classification for international use. Three basic groupings emerged which classified the patients: male and female with high, intermediate or low anomalies based on the relationship of the rectum and anus to the puborectalis sling of the levator ani group of pelvic muscles.

1. High (supralevator). With the bowel above the puborectalis sling, such patients would be severely damaged from blind probing of the perineum by inexperienced surgeons trying to "reach" the rectum. The colon usually terminates in the urinary tract in the male (rectoposterior urethral fistula, rarely rectovesical) or the vagina in the female (rectovaginal fistula). In some females the urethra also opens into the vagina with a narrow common urogenital sinus and the rectovaginal fistula contributing meconium and feces. This combination is termed the cloacal anomaly. The distended vagina filled with urine, gas and meconium may reach enormous size.

2. Intermediate. This less well defined group may include the bowel ending in or just below the puborectalis sling. There may be a low vaginal fistula in the female, rarely the male has a fistula to the bulbar urethra.

3. Low (translevator). Here the bowel has gone through the puborectalis sling of the levator ani group. Among the anomalies are the anocutaneous and the anovulvar fistula. In nearly all cases there is visible evidence of meconium leaking from a perineal orifice.

This is a great simplification of the 27 anomalies discussed and adopted in the 1970 classification of imperforate anus. The radiologist should be aware that the high and intermediate groups commonly need colostomy. This assignment of category must be based on the physical findings and not on radiographic evidence that the distended bowel is several centimeters from a penny taped to the anus.

The plain films of patients with congenital anorectal malformations, whether inverted or not, must be read with knowledge of the sex of the patient. The physician must also take into consideration the results of physical examination of the perineum (a

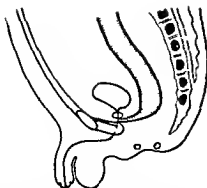


Fig. 10-186—Schematic drawing of the usual site of rectourethral fistula in the high male form of imperforate anus. The rectum ends in the prostatic urethra without passing through the puborectalis sling. Note the urethra passing through the pubourethral component of the same sling.

perineal orifice would automatically put it in a low classification).

Finally, complete urologic evaluation of all patients with congenital anorectal malformations should be done before discharge from the newborn nursery. This includes analysis of lumbosacral segmentation; it is the presence, not necessarily the severity, of the anomalies that has led to detection of urologic abnormalities, whether structural (missing or dysplastic kidneys, ectopia) or functional (reflux, neurogenic bladder), or both.

Radiologic findings in high and intermediate anomalies—In the male with no visible perineal opening there is usually a fistula. Commonly located in the posterior urethra (Fig. 10-188) it is responsible for evidence in plain films of gas in the bladder (Fig. 10-187, A and B), although with the rarer rectovesical fistula gas may also be seen in the bladder. Lateral projections are best for demonstrating this. The fistula can also be delineated on voiding cystograms (Fig. 10-187, C and D). Another method, after double barrel colostomy, is to inject contrast material into the distal loop.

Rarely, the male has either no fistula or a fistula to the bulbar urethra (Fig. 10-187, E). In the latter group distal colostomy study shows the bowel to "beak" as it goes through the puborectalis sling and to pass anteriorly to enter the bulbar urethra. Since the bowel is below the sling and enters the urethra below the external sphincter, no gas is seen in the bladder in plain films of this unusual anorectal malformation.

Of females without visible fistula, 90% have an internal communication between rectum and vagina (see Fig. 10-185, B). Vesical or urethral fistulas are very rare in females because of interposition of Mullerian structures between rectum and urinary tract. The fistula is often large enough so that there is no distention. Gas does not collect in the vagina without associated outlet stenosis. Distal colostomy injection demonstrates the vaginal fistula (high or low),

as does flush injection of the vagina or catheterization of the fistula through the vagina. Again, the classification of high or intermediate in the female is based on absence of a perineal orifice.

Rarely, the female has both the rectum (with air and meconium) and the urethra (with urine) entering a common cloacal chamber (see Fig. 10-185, B). This is actually a dilated vagina above a narrow common urogenital sinus (see p. 1556). Vaginal distention by air mixed with urine (pneumovagina) can be seen in plain films (Fig. 10-188). Voiding cystograms show the bladder emptying into the vagina, and distal colostomy injections show contrast material from the rectum filling the huge vagina.

Radiologic findings in low anomalies (visible perineal orifice)—If a terminal orifice of the colon is visible anterior to the normal anus, even as a tiny pinhole within thickened midline perineal tissue, the clinical diagnosis should be a low anorectal malformation. Synonyms include "anterior perineal anus," "ectopic perineal anus" and "covered anus" (see Fig. 10-185, B). Since contrast medium injected into this opening must fill the rectum, this procedure is of little value to the surgeon (Fig. 10-189). Obviously plain films of such patients in the inverted position only confuse the issue, showing gaps of varying degree related to crying, gas content of the rectum and motion up and down of the rectum. There are fewer lumbosacral and genitourinary anomalies with the low anomalies, with more in the male than in the female. Nevertheless full genitourinary studies should be made, including voiding cystography.

Value of inverted films in "imperforate anus"—This has been intentionally left to the end of the discussion because it should be clear that the basic concept has inherent flaws that can be most misleading. At worst, a high lesion can be mistaken for low if crying and increased intra abdominal pressure cause the rectum to descend toward the anal marker (Fig. 10-190). Perineal exploration in such a patient can destroy any hope of continence if the puborectalis sling is damaged or bowel is brought to the skin behind the sling. At the other end is the chance of a surgeon's performing an unnecessary colostomy in a low anomaly in which there seems to be a gap of several centimeters between the anal marker and the termination of the rectum (Fig. 10-191). It may not be realized that the bowel is through the puborectalis sling and that the "fistula" is actually the end of the rectum in an ectopic location. The only treatment needed here is dilatation after a cut back to the external sphincter. No greater handicap can be induced in a child than fecal incontinence because of erroneous diagnosis and consequent ill planned surgery for "imperforate anus." Any infant without a visible orifice should be treated for a high anomaly and only by a surgeon knowledgeable in the varieties of anorectal malformations.

COLONIC DUPLICATION—Long tubular duplications of part or all of the colon may be complex, combined

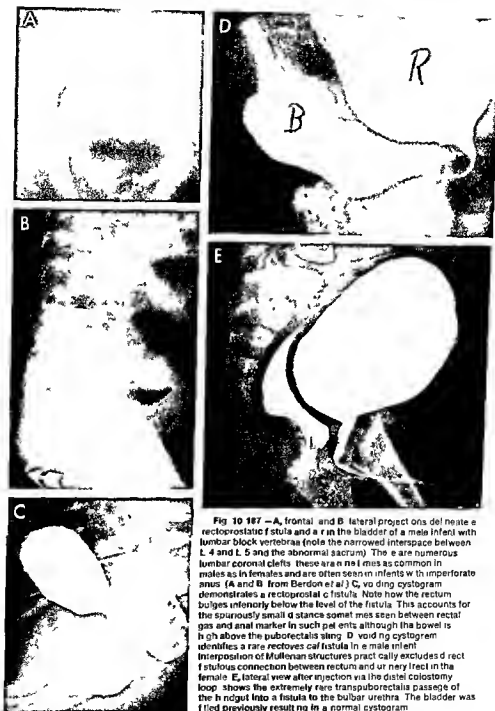


Fig 10-187 —A, frontal and B, lateral projections of neonate with rectoprostatic fistula and a rectum in the bladder of a male infant with lumbar block vertebrae (note the narrowed interspace between L4 and L5 and the abnormal sacrum). There are numerous lumbar coronal clefts; these are anomalies as common in males as in females and are often seen in infants with imperforate anus (A and B, from Berdon et al). C, voiding cystogram demonstrates a rectovesical fistula. Note how the rectum bulges inferiorly below the level of the fistula. This accounts for the spuriously small distance sometimes seen between rectal gas and anal marker in such patients although the bowel is high above the puborectalis sling. D, voiding cystogram identifies a rare rectovesical fistula in a male infant. Interposition of Mullerian structures practically excludes a rectofistulous connection between rectum and urinary tract in the female. E, lateral view after injection via the distal colostomy loop shows the extremely rare transpuborectalis passage of the hindgut into a fistula to the bulbar urethra. The bladder was filled previously resulting in a normal cystogram.

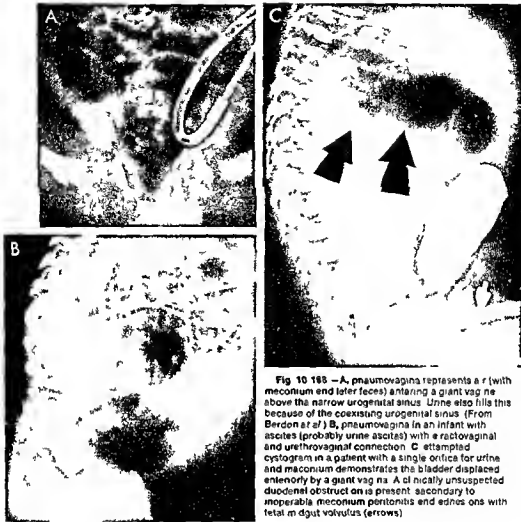


Fig 10188—A, pneumovagina represents a r (with meconium and later feces) entering a giant vagina above the narrow urogenital sinus. Urine also fills this because of the coexisting urogenital sinus. (From Berdon *et al*.) B, pneumovagina in an infant with ascites (probably urine ascites) with a rectovaginal and urethrovaginal connection. C, attempted cystogram in a patient with a single orifice for urine and meconium demonstrates the bladder displaced anteriorly by a giant vagina. A clinically unsuspected duodenal obstruction is present secondary to inoperable meconium peritonitis and adhesions with fetal midgut volvulus (arrows).



Fig. 10-189 — **A**, injection of contrast medium into the perineal fistula is of little help to the surgeon. It shows a spurious long narrow fistula that is actually contrast medium channeling through impacted meconium. The fistula is the end of the colon and needs only dilatation for cure. **B** demonstrates that the

rectum has passed through the puborectalis sling and along the pelvic perineal floor under the skin to open on the under surface of the penile urethra. Usually such a long covered anus seals off once the normal anorectal opening is established. (**B** courtesy Dr. H. S. Goldman, NYC.)

Fig. 10-190 — High anomaly (rectourethral fistula) in an infant who also had esophageal atresia and distal fistula. There was no perineal orifice. **A**, lateral inverted plain film shows thick presacral space due to impacted meconium. Gas terminates almost 5 cm above the anal skin. The lateral sacral segment is stubby. Transperineal injection shows rise (**B**) and descent (**C**) of the rectum with contraction and relaxation of the puborectalis muscle.

The bowel ended above this muscle sling in a fistula to the prostatic urethra. If the picture in **C**, showing the bowel descended were taken to indicate the true fixed end of the rectum near the anal skin and the rectum was then approached surgically from below, permanent damage to the puborectalis could result in lifelong fecal incontinence. (Figs. 10-189 and 10-191 from Berdon *et al.*)

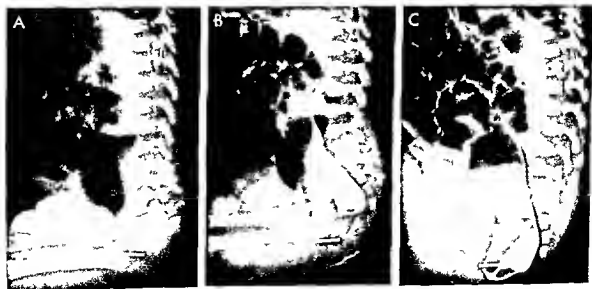




Fig 10.191—Low anomaly in an infant with visible thin imperforate anal membrane. **A**, lateral inverted plain film, shows gas terminating well above the anal skin, the thick presacral spaces due to impacted meconium. The distance of almost 5 cm from anal skin to gas erroneously suggested a severe surgical problem

with the rectum ending well above the pelvic floor. Transperineal injection of contrast medium through the membrane into the rectum then demonstrated rectal rise (**B**) and descent (**C**) on contraction and relaxation of the puborectalis muscle. Cutting of the membrane was curative.

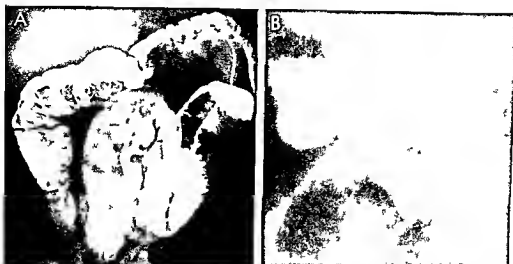


Fig 10-192.—Colon duplication. A, after barium enema shows a long parallel duplication involving the left colon, sigmoid and rectum. B shows one of the two rectums ending in the

form of a rectoprostatic urethral fistula. Partially obstructing post-anal urethral valves caused moderate dilatation of the posterior urethra. (Courtesy of Dr. G. Curranno, Dallas, Tex.)

with duplicated bladder or genitalia. In some cases there are two anal orifices. In others, one rectum ends blindly and is evident as an obstructing meconium and feces filled mass. Occasionally the duplicated rectum ends as a fistula to the prostatic urethra (Fig 10-192).

ANAL STENOSIS—Considered as type I imperforate anus in the Ladd and Gross classification, anal stenosis is not really imperforate anus since the rectum ends by joining a normally placed anus. Some pa-

tients also have anterior sacral meningocele and lipoma. The usual case is never seen by the pediatric surgeon since the initial problem, inability to pass meconium, is inadvertently treated. This is accomplished by the mere taking of rectal temperature or by deliberate distal dilatation (Fig 10-193).

COLONIC ATRESIA—Although formerly classified in imperforate anus type IV, patients with colonic atresia actually have a rectum below and dilated colon above an area of atresia. The distal segment contains

Fig 10-193.—Anal stenosis is usually adequately treated by inadvertent dilatation with a thermometer. A, lateral film shows gas outlining impacted meconium in a slightly distended new-

born who had not defecated. B, after barium enema, an impacted meconium mass is demonstrated. Gentle manual dilatation of the rectum was curative.

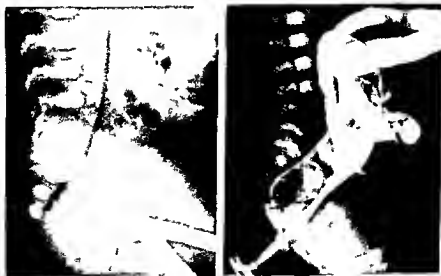




Fig 10-194—Colonic atresia. A huge gas-filled loop represents the sigmoid colon with microcolon of the rectum and distal sigmoid. Labeled squamous epithelial cells and bile stained meconum in the distal bowel indicated that the colon had once been patent. Radiographic study could be confused with meconum ileus if it was assumed that the microcolon was completely filled.

lanugo bile salts and swallowed squamous cells indicating that there had been an intact fetal colon well beyond the embryologic disturbances discussed earlier.

Colonic atresia is rare and therefore is seldom thought of in an infant with intestinal obstruction. The most experienced radiologist may miss it. Plain films show distention resembling either small bowel obstruction (from meconum ileus) or colonic obstruction as in Hirschsprung's disease. Barium enema reveals a microcolon to the point of obstruction and there is a tendency to consider the bowel incompletely filled and thus to render an erroneous diagnosis of meconum ileus or ileal atresia, not realizing that the entire distal colon has been opacified (Fig 10-194). Reported series, although small, show a poor survival rate reflecting delays in diagnosis.

REFERENCES

- Berdon W E *et al* Association of lumbosacral spine and genitourinary anomalies in imperforate anus. *Am J Roentgenol* 98:181, 1968
- *et al* Radiographic evaluation of imperforate anus: An approach correlated with current surgical concepts. *Radiology* 90:468, 1968
- Erskine J M Colonic stenosis of the newborn. *J Pediatr Surg* 5:321, 1970
- Gans S L Classification of anorectal anomalies. *J Pediatr Surg* 5:511, 1970 (editorial)
- Louw J H Congenital Abnormalities of the Rectum and Anus (Current Problems in Surgery) (Chicago: Year Book Medical Publishers Inc, May 1965)
- Ravitch M M Duplications of the Alimentary Canal in Mustard W T *et al* (ed.) *Pediatric Surgery* (2nd ed) (Chicago: Year Book Medical Publishers Inc, 1969)
- Rudhe U Roentgenologic examination of anal and rectal anomalies in the newborn male infant. *Ann radiol* 11:429, 1968
- Santulli T V Malformations of the Anus and Rectum in Mustard W T *et al* (ed.) *Pediatric Surgery* (2nd ed) (Chicago: Year Book Medical Publishers Inc, 1969)
- *et al* Anorectal anomalies: A suggested international classification. *J Pediatr Surg* 5:281, 1970
- Shopfner C E Roentgenographic demonstration of the ectopic anus. *Radiology* 84:464, 1965
- Gallbladder Bile Ducts Liver**
- NEONATAL JAUNDICE, LIVER DAMAGE AND BILIARY ATRESIA**—Infants with jaundice, biopsy evidence of liver damage and surgical diagnosis of extrahepatic biliary atresia may actually have acquired ischemic or inflammatory fetal damage to the bile ducts with subsequent failure of these structures to grow. Tiny ducts may be found at autopsy in the porta hepatis of such patients after exploratory laparotomy had failed to disclose any extrahepatic bile ducts. This is a tragic condition because there is increasing evidence that even careful surgical dissection further destroys the blood supply to any ducts that may be present and converts a bad situation to a hopeless one. The usual story is of an infant with jaundice persisting beyond the newborn period whose liver biopsy and function tests have not been sufficient to diagnose medical disease (neonatal hepatitis, giant cell hepatitis and so on). Since obstruction cannot be excluded, laparotomy is performed to allow open liver biopsy and operating room cholangiography.
- There is usually no bile in the gallbladder (this must be known if the radiologist is to interpret the cholangiogram intelligently) and the gallbladder leads to a tiny cystic and distal common bile duct with filling of the duodenum. No contrast agent is present in the intrahepatic branches of the biliary tree (Fig 10-195). There is no surgical help for these patients who account for almost all cases of extrahepatic biliary atresia.
- A few patients have bile in the gallbladder and evidence on cholangiography of filling of the gallbladder, cystic duct and intrahepatic biliary tree, the distal common bile duct and duodenum do not fill. This group occasionally benefits from anastomosis of small bowel to the gallbladder (Fig 10-196). Some patients suspected of having obstructive jaundice have bile in the gallbladder which, with the cystic and common bile ducts, fills on cholangiography. Thus there is no evidence of anatomic obstruction when the clinical and x-ray findings are combined. These patients have been thought to have biliary sludge syndrome, neonatal hepatitis and so on (Fig 10-197).
- CONGENITAL BILIARY BRONCHIAL FISTULA—A true**



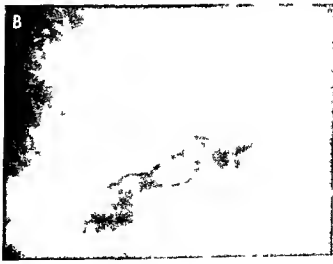
Fig 10 195 (left) —Typical picture of extrahepatic biliary atresia in the operative cholangiogram. No bile is present in the gall bladder. Contrast material leads from the gall bladder through the tiny cystic and common bile ducts to the duodenum; no intrahepatic bile ducts are visible.

Fig 10 195 (right) —Rare remnant type of extrahepatic biliary atresia in the operative cholangiogram. Bile is present in the gall bladder; contrast medium fails to fill the common bile duct or to enter the duodenum but does pass retrograde to fill the rather slightly dilated intrahepatic ducts. Anastomosis was possible between the patent portion of the extrahepatic biliary tree and the small bowel.



Fig 10 197 —A: Operative cholangiogram shows bile in the gall bladder. Contrast medium fills the cystic and common bile ducts and duodenum. A tiny amount flows retrograde into the right and left hepatic ducts. B: On temporary pressure on the

sphincter of Oddi, shows sudden massive retrograde filling of normal intrahepatic ducts, proving that a presumed surgical cause of jaundice was mechanical obstruction.



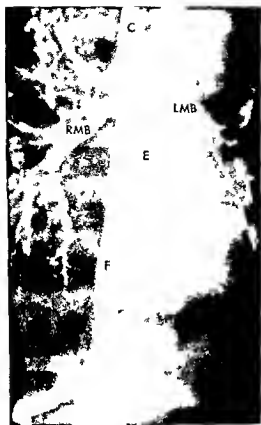


Fig 10-198—Congenital bilateral bronchial fistula. B. onchogram shows both right and left major bronchus (RMB, LMB) outlined with good filling of a large fistulous tract (F) to the left lobe of the liver. Since the fistula is really the drainage of that portion of the liver, it causes bile pneumonia. Ligation of the fistula resulted in atrophy of the portion of the liver drained by it. C, carina; E, esophagus. (Courtesy of Dr. B. G. R. Pitts, Pittsburgh, Pa.)

anomaly exists in the biliary tree in the rare infant with a congenital biliary bronchial fistula. Clinical signs and symptoms include recurring respiratory infections with bile-tinged sputum or hemoptysis. Bronchography shows the fistula communicating with the bronchial tree in or around the carina (Fig 10-198). Surgery is directed to thoracic ligation of the fistula. These fistulas in some cases represent an anomalous duct that drains its portion of the liver. Ligation stops the flow of irritating bile into the lung at the expense of some shrinkage of the involved lobe. This is said to be an example of defective foregut differentiation between upper gastrointestinal tract biliary tree and bronchial tree.

LIVER MASSES—Diagnostic studies of the neonate with liver disturbances should include plain films to search for calcification and for estimation of liver size. Radioisotope scanning with technetium and total body opacification during intravenous pyelography are used to visualize liver substance. A gastrointestinal series is occasionally useful in demonstrating

displacement by hepatic masses. Both umbilical aortography and venography are possible and easy to perform in the newborn and frequently yield valuable information. Ultrasonography may separate solid and cystic masses.

The liver may be involved with tumors in the newborn (or fetus) which include malignant hepatomas, hemangiomas (giant or multiple) and hamartomas. The hemangioma is of critical interest because of the possible association of massive arteriovenous shunting and congestive heart failure. If giant and localized resection is possible. Calcification may be present. The diagnosis is based on the total body opacification phase of intravenous pyelography that shows lakes of contrast agent surrounding cystic and avascular areas (Fig 10-199 A and B). The areas of involvement can be further studied by umbilical aortography (Fig 10-199 C and D) and the normal liver tissue outlined by either liver scanning or umbilical venography (Fig 10-199 E). Some hepatic hemangiomas are associated with platelet trapping, severe thrombocytopenia and bleeding; others rupture into the peritoneal cavity. Benign hepatic hamartomas and malignant hepatoblastomas are rare in the newborn, both may appear to be hypervascular on arteriography. Specific diagnosis requires microscopic examination. It should be realized that massive left hepatic enlargement by such masses can displace the stomach medially, mimicking splenomegaly (Fig 10-200 A). Lateral views showing posterior gastric displacement help to define their hepatic nature (Fig 10-200 B).

Other causes of hepatomegaly include diffuse metastatic neuroblastoma in which calcification may be present. Here liver scanning shows marked heterogeneity. Storage diseases are usually diagnosed later in infancy and are discussed elsewhere, as are lymphoma and leukemia.

HEPATIC CALCIFICATION WITHOUT MASSES OR ENLARGEMENT—Calcifications are occasionally seen in the newborn's liver, particularly in the subcapsular segment of the left lobe (Fig 10-201). They are manifestations of calcified portal vein thrombi. Most patients are premature and these calcifications are seen more commonly in stillborns. This is another cause of abdominal calcification in the neonate that can be confused with meconium peritonitis.

ASCITES—Ascites have many causes. As mentioned in the genitourinary section that follows, rupture of bladder and ureters or kidney can cause urinary ascites. In this discussion of gastrointestinal causes of neonatal ascites, primary attention is directed to exclusion of bowel and colonic perforation.

Chylous ascites in the newborn may be due to intestinal lymphatic obstruction (Fig 10-202). The fluid is clear at birth but turns milky as the usual diet of the newborn is given, with its high content of long-chain triglycerides. These are absorbed into the intestinal lymphatic system and any block can cause lacteal distention, local rupture (with mesenteric cysts) or

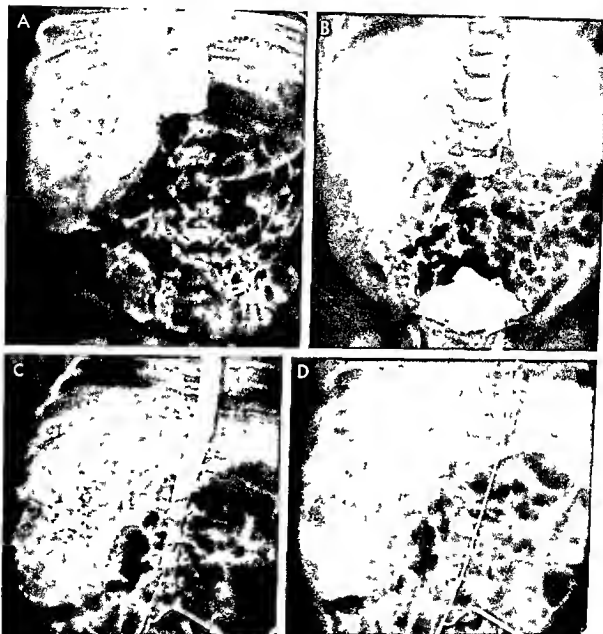


Fig 10-199 — Giant right hepatic hemangioma. At 3 day of age this infant with a right upper quadrant mass was given a clinical diagnosis of neuroblastoma. **A**, total body opacification phase of the intravenous pyelogram shows lucent areas in the right hepatic lobe surrounded by hypervascular areas. Lakes of contrast medium persisted for several minutes. **B**, excretory phase of the intravenous pyelogram shows normal kidneys and diagnosis

was a vascular hepatic tumor, probably hemangioma. **C**, transumbilical aortogram, arterial phase, shows the right lobe filled with irregular dilated hepatic artery feeders to a hemangioma. **D**, capillary and venous phase of the aortogram shows large draining hepatic veins and large subcapsular spaces pooling contrast agent around central cystic and necrotic areas. (Cont. next)



Fig 10-199 (cont.) - E transumbilical venogram shows normal left portal branching (left) and hepatogram defining the limits of uninvolved hepatic tissue (right). Heart failure developed that was cured by right hepatic resection. (From Bergeron et al.)

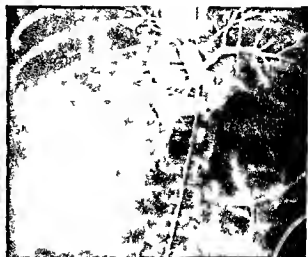
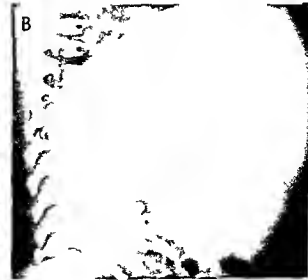


Fig 10-200 - Hamartoma of the left lobe of the liver. In A, the left upper quadrant mass displaces the stomach medially. Absence of abnormality in the right aortogram excluded renal or adrenal tumor as the cause. B, lateral film shows the mass to be entirely anterior to the stomach, thus excluding the spleen. The left hepatic lobe was totally replaced by a huge benign hamartoma. Surgical excision on the 3rd day of life was curative.



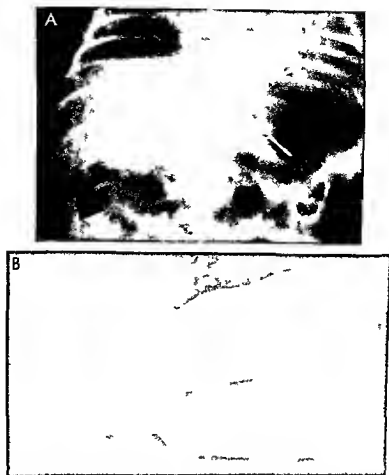


Fig 10.201—Intracalcified portal vein thromboembolism in a newborn infant. In **A**, arrows point to the loci of calcification. There was no liver necrosis in surrounding areas. The predominant

ferential consideration was meconium peritonitis. **B**, specimen (after death of sepsis) shows the peripheral subcapsular locations of the calcifications.



Fig 10 202 —In an infant with chylous ascites the lymphangiogram shows striking abnormalities with partial pelvic inlet obstruction and retroperitoneal extravasation on the left into the peritoneal cavity and possibly the small bowel lumen (Courtesy of Dr C E Craven Galveston Tex)



Fig 10 203 —Spontaneous bile peritonitis in the newborn. Ascites developed in the first days of life. Paracentesis revealed bilious fluid. Cholangiography during exploratory laparotomy shows perforation of the nonobstructed bile ducts. The patient recovered following drainage.

Fig 10 204 —Presumed in utero liver damage causing jaundice and portal hypertension in a newborn (who later had ascites). Splenoportogram shows no evidence of intrahepatic portal vein branches other than the small channel in the area of the ductus venosus. There was massive hepatofugal filling of gas, and esophageal varices with mediastinal venous return to azygos system.



free rupture (with chylous ascites). Protein losing enteropathy may be present. The ascitic fluid may have sufficient fat content to appear lucent when compared to the liver density. Repeated paracentesis and a diet rich in medium chain triglycerides (which utilize the portal venous absorptive route) diminish the protein loss that would otherwise occur. Many surgeons explore such patients in a search for mechanical obstruction as by plaques of meconium peritonitis or adhesions from congenital or inflammatory causes.

Ascites due to extrahepatic biliary perforation is rare but important in diagnosis since bile peritonitis can lead to extensive adhesions. Although strictures are sought to explain this, some cases appear to be spontaneous (Fig 10-203). Some surgical discussion of the pathogenesis of choledochal cyst has related it to a walled off perforation of the bile ducts with the closed space in continuity with the bile duct forming the cyst. Liver disease and portal hypertension can also lead to ascites. Even ascites with diffuse cirrhosis

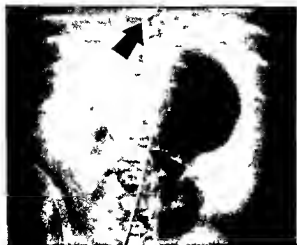


Fig 10-205 — Hemoperitoneum in a hydropic newborn with Rh incompatibility. A supine film shows ascites secondary to rupture of the spleen. The spleen can rupture spontaneously in this disease, although in this infant the intruterine transfusion needle caused the rupture. Arrows indicate tips of umbilical vein (upper arrow) and umbilical artery (lower arrow) catheters.

has been present at birth secondary to fetal infection (both toxoplasmosis and rubella) (Fig 10-204). Medical causes of ascites related to liver disease in the

newborn include syphilis, cytomegalic disease, and hydrops fetalis, all of which may be manifested by massive ascites. Some such patients have had bloody ascites secondary to rupture of the enlarged spleen or liver associated with the hydrops (Fig 10-205).

REFERENCES

- Berdon W E *et al*: Giant hepatic hemangioma with cardiac failure in the newborn infant. *Radiology* 92:1523, 1969.
- Cywes S, *et al*: The roentgenologic features of hemoperitoneum in the newborn. *Am J Roentgenol* 106:198, 1969.
- Hays D M *et al*: The relative accuracy of percutaneous liver biopsy. *J Pediatr* 79:598, 1967.
- Hyde G A: Spontaneous perforation of the bile ducts in infancy. *Pediatrics* 35:453, 1965.
- Pickett L K: Obstructive Jaundice. In Mustard W T *et al* (ed): *Pediatric Surgery* (2nd ed). Chicago: Year Book Medical Publishers Inc., 1969; Chap 48.
- Ruckham P P *et al*: Tumors of the liver in childhood. *Zschr Kinderchir* 7:447, 1969.
- Selke A C *et al*: Infantile hepatic hemangioendothelioma. *Am J Roentgenol* 106:200, 1969.
- Snyder W H Jr: Fetal Ascites. In Mustard W T *et al* (ed): *Pediatric Surgery* (2nd ed). Chicago: Year Book Medical Publishers Inc., 1969; Chap 54.
- Teybi H: The Roentgenology of the Biliary Tract in Children. In Margulis A R. and Burhenne H J (ed): *Alimentary Tract Roentgenology* (St. Louis: C V Mosby Company, 1967) Vol 2 p 1099.
- Waggett J *et al*: Congenital bronchobiliary fistula. *J Pediatr Surg* 5:566, 1970.

The Genitourinary Tract

THE HUMAN KIDNEYS function in utero from about 14 weeks on, their output contributes significantly to amniotic volume. The placenta acts as a kidney and removes most fetal nitrogenous waste products. Birth is a change of degree in this biologic system that is important in utero to normal fetal growth and survival and whose integrity is essential for extrauterine life.

The following discussion of genitourinary abnormalities in the newborn will stress those whose recognition in the first weeks of life leads to proper therapy and salvage of renal function. No attempt is made to review all the anomalies of form and position of the kidney since these are commonly not encountered until later in life and are well covered in Section 6. The current controversy regarding the intertwining roles of infection, vesicoureteral reflux and obstruction in the urinary tract is approached with caution.

The relative safety of modern urologic investigative procedures, even in newborn and premature infants, has allowed many observations to be made that have solved some renal problems that would have caused death in previous years.

REFERENCES

- Johnston, J. H. Neonatal Surgery (New York: Appleton Century Crofts, Inc., 1969).
Kjelberg S. V. et al. The Lower Urinary Tract in Childhood (Chicago: Year Book Medical Publishers, Inc., 1957).
Stephens, F. D. Congenital Malformations of Rectum, Anus and Genitourinary Tract (Edinburgh: E & S Livingstone Ltd., 1963).
Williams D. I. Urology in Childhood. Vol. 15 of Encyclopedia of Urology (Berlin: Springer Verlag, 1958).
— (ed.) Pediatric Urology (New York: Appleton Century Crofts Inc., 1968).

Renal Function in Fetus and Newborn

EMBRYOLOGIC DEFECTS—If the kidneys fail to develop in utero and they do not contribute adequate fetal urine to the amniotic volume, oligohydramnios occurs. When this is marked, there is almost always coexistent pulmonary hypoplasia. This has been noted in stillborns and newborns dying of bilateral polycystic disease, in those with severe fetal obstructive

uropathy from posterior urethral valves and nearly always in those with renal agenesis. The less the amniotic volume, the more abnormal the fetus. The facies is often characterized by flattened ears, receding chin, depressed nose, and the elderly, wizened appearance termed Potter's facies (Fig. 10-206). Not every infant with severe lethal renal malformations has such facies. The hands may seem unduly large. There is a high incidence of club feet as well. These are called oligohydramnios deformities. The hypoplastic lungs are stiff, neonatal respiratory distress is common, with interstitial pulmonary emphysema, pneumomediastinum and pneumothorax (Fig. 10-207). Infants with such signs of airblock (and lack of adequate history of meconium aspiration, depression at birth or respiratory distress syndrome) should be evaluated in terms of serious urologic malformations. The presence of one unaffected kidney (so that fetal urine output is adequate) prevents the sequence of oligohydramnios deformities, including Potter's facies.

Currarino has shown that in some cases of renal agenesis plain films reveal a very small pelvic bony outlet. Proof that this is not invariably so is the finding of an identical small bony pelvic outlet in an infant with virtual sacral agenesis, neurogenic bladder of tiny capacity and normal kidneys (Fig. 10-208). The small pelvic outlet nevertheless is worth looking for especially when there is also pneumomediastinum (Fig. 10-207, B).

RADIOGRAPHIC VISUALIZATION OF THE FETAL URINARY TRACT—It is not yet possible to perform excretory pyelography on fetuses. The amount of absorption through the fetal gastrointestinal tract of the triiodinated urographic compounds used for amniography does not permit visualization of the fetal kidneys. Accidental direct puncture of the kidney during attempted fetal transfusion (as for erythroblastosis fetalis) has allowed good visualization of ureter and bladder (Fig. 10-209). This indicates that the functioning kidney can pass the compounds via glomerular filtration into the fetal collecting system. The future possibility is not far fetched that by radiographic

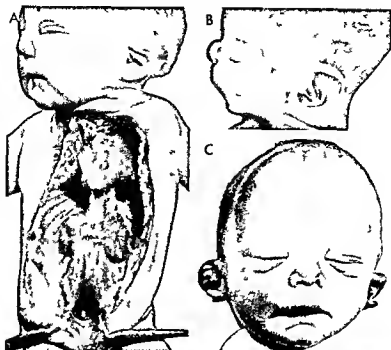


Fig. 10-208 —Potter's facies: characteristic of bilateral agenesis of the kidneys. In A the bilateral retroperitoneal masses are large fetal adrenal glands. The face is facies resemblance in all three infants flat

nose, receding chin and large flattened distorted ears. C shows the abnormal distance between the eyes and prominent epicanthic fold. (From Potter.)



Fig 10-207 A bilateral renal agenesis the specimen providing pathologic evidence of emphysema of the mediastinum and subcutaneous extensions into the diaphragm B umbilical aortogram of an infant with renal agenesis Note pneumomediastinum and the small pelvic outlet. No renal arteries are seen in this aortic newborn a confirmatory sign of renal agenesis. (Courtesy of Dr H J Kaufmann Basel Switzerland)

Fig 10-208 T-type pelvic bony outlet in an infant with virtual absence of sacrum and neurogenic bladder A cystogram shows the tiny bladder B intravenous pyelogram shows no marked

hydronephrosis indicating that size of the pelvic outlet may be related to a small bladder from any cause not specifically renal agenesis



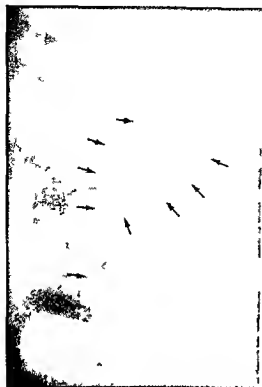


Fig 10-209—Urographic visualization of fetal kidney following accidental puncture of the kidney during intrauterine transfusion. Calyces, ureter and bladder are well seen, presumably owing to the higher dose injected directly into the kidney. (Courtesy of Drs. A. T. Fort and W. R. Gage, Memphis, Tenn.)

or other methods (possibly ultrasound) fetal genitourinary malformations may one day be detected and diverted by fetal surgical procedures with maintenance of pregnancy until fetal maturation is compatible with extrauterine survival.

RETENTION IN IMMEDIATE NEWBORN PERIOD—The bladder at birth may contain $\frac{1}{2}$ to $1\frac{1}{2}$ oz of dilute urine. Although most newborns void in the first hours, an occasional infant requires a day or more before beginning urination. This is worrisome and has led to radiographic studies. Cystograms have shown exaggerated trabeculation (Fig 10-210) resembling that of a neurogenic bladder in an older patient. Since the newborn has a neurogenic bladder in that he has retention and periodic incontinence, this picture is not surprising. Further, there is no reason why all vital sphincters should work normally at birth. Certainly swallowing and defecation can be disordered in some infants for days or longer.

REFERENCES

Blanc W A et al. Pathology of the newborn and of the placenta in oligohydramnios. *Bull. Sloane Hosp Women* 8: 51, 1962.

- Curran G. Association of congenital small pelvic outlet with hypoplasia of bladder and urethra and absent kidneys. *Am J Roentgenol* 109:399, 1970.
- Edelmann C M Jr et al. The maturing kidney. A modern view of well balanced infants with imbalanced nephrons. *J Pediatr* 75:509, 1969.
- Fort A T et al. Urographic prenatal sex determination during intrauterine fetal transfusion. *J Urol* 100:699, 1968.
- Kaufman H et al. Angiographic evaluation of the renal artery in the newborn. *Australasian Radiol* 14:64, 1970.
- Isberman M M et al. Association between pneumomediastinum and renal anomalies. *Arch Dis Childhood* 44:471, 1969.
- Potter E L. *Pathology of the Fetus and Infant* (2nd ed). Chicago: Year Book Medical Publishers Inc, 1961.
- Strauss J. Fluid and electrolyte composition of the fetus and newborn. *Pediatr Clin North America* 13:1077, 1966.

Uroradiologic Procedures

INTRAVENOUS PYELOGRAPHY—More accurately called excretory urography, this is the basic radiologic diagnostic procedure in the newborn. The child and adult. Problems of visualization of even normal kidneys in the newborn are related to the maturing kidney and its total effective glomerular filtration of contrast agent and tubular reabsorption of water. The triiodinated contrast mediums are handled at least in terms of radiographic visualization totally by glomerular filtration. The dose used in most pediatric centers is 3 cc/kg of the 50–60% sodium or meglumine agents.

Fig 10-210. Radiologic bladder studies in a newborn male who did not void for more than 72 hours. Upper tracts were normal on intravenous pyelography. The cystogram (done via suprapubic route) shows exaggerated bladder base, irregularities during voiding. The prominent postvoid bar at the level of the bladder neck is seen in normal infants. The bladder neck was resected and the pathologic report was normal bladder neck.





Fig 10.211.—Intravenous pyelogram with patent pylorus. This position shifts gas away from the kidneys and allows better filling of the renal pelvis and ureters. The left kidney shows no major dilation, while the right kidney shows some dilation. Many infants

or 10 cc for a full-term newborn. Infants of low birth weight are given 6–8 cc; some institutions use as much as 5 cc/kg for all newborns with strikingly few ill effects.

Despite these large amounts (equal to 200 cc in an adult), it is not uncommon to fail to obtain adequate

delineation of calyces or ureter in newborns studied on the 1st or 2nd day of life whose follow-up intravenous pyelograms at the age of 1 week show no abnormality. This is poorly understood, and the loose terms "glomerulotubular imbalance" and "need for renal maturation" cover rather than explain the finding. The clinical import is that screening or elective pyelography should be deferred until age 1 or 2 weeks. Obviously, emergency pyelography is performed as needed.

The usual dose is safe when injected intravenously and not rapidly. 90–120 seconds is a typical time for injection through a no. 23 scalp vein needle. Dehydration is avoided. The dose used is a significant osmotic diuretic in such small infants, and early (first 10 minutes) films commonly show a dilute, slightly dilated collecting system and a large bladder filled with low-density contrast agent. The infant frequently voids, and films at 1 hour show better opacification of the upper tracts that have lost their slight dilation (thanks to the brisk early diuresis). The improved detail in late films is not specific to the newborn period; the same phenomenon is seen in adults given 1 cc/lb of 90% contrast agent for nephrotomography. It is primarily dose-related with the diuresis fading even though the blood levels of contrast agent are not diminished to 50% for 45–60 minutes.

There seems to be a theoretical and perhaps slight clinical superiority of sodium over meglumine agents in terms of visualization. Bennes in animal studies showed that this may be due to greater milligrams of iodine per cubic centimeter of urine for the sodium salts than for an equal dose of the meglumine compounds. This might reflect renal sodium (and water) absorption with the sodium compounds while the meglumine agents pass, pulling water with them, resulting in more dilute, less opaque urine. Though

Fig 10.212.—A, frontal and B, lateral views of bladder exstrophy. The images show the bladder and surrounding structures. The caption notes that the patient has a large extraperitoneal herniation of the bladder, and since an inguinal hernia may also be present, it is apparent why

surgeons occasionally catch a portion of the bladder in resecting the hernial sac.

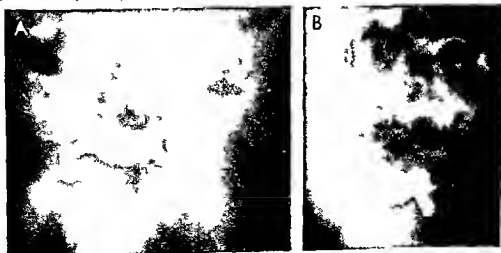




Fig 10-213—A dysmorphic sacrum in a patient with imperforate anus. The patient had neurogenic bladder and severe genitourinary infection despite presence of more than two sacral segments (indicating that presence rather than severity of sacral defects is related to genitourinary abnormalities). B lateral view

of a patient with rectourethral fistula (note gas in the bladder) and imperforate anus. The S4 and S5 segments are fused and stubby indicating significant sacral defect. This is easily obscured by feces and air in frontal views (From Berdon et al.)

proved in the laboratory animal, these differences are not great enough to warrant a specific recommendation of sodium compounds and rejection of meglumine agents.

Prone positioning offers many advantages over supine (Fig 10-211). These include displacement of obscuring small bowel gas and better filling of renal pelvis and ureter. Supplemental use of an inflated pneumatic paddle (Nogarty technique) beneath the prone infant's abdomen further aids in visualization. Gas insufflation of the supine infant's stomach by tube or with carbonated beverage may reveal part of the left kidney, but accidental eructation or passage of gas into the small bowel frequently negates its value.

The infant's bladder may show signs of extraperitoneal herniation in the form of unilateral or bilateral bladder ears (Fig 10-212). Its significance relates to the coexistence in some infants of an inguinal hernia. Resection of part of the bladder at the time of herniorrhaphy can be tragic.

The lumbar spine and sacrum should be carefully examined since apparent primary urologic disturbances may be related to neurogenic deficit; the dysmorphic or partly formed sacrum may be a clue (Fig 10-213 and see discussion of imperforate anus on p 1524).

CYSTOGRAPHY—Voiding cystography is the preferred term since the study is incomplete without films during voiding for determination of vesicoureteral reflux and possible urethral obstruction. Urethral catheterization is the usual method of instillation, though suprapubic puncture or intravenous pyelography to fill the bladder has its advocates. In the newborn, Foley catheters of small enough size may not be

available; no 5 or no 8 nasogastric tubes can be used although they frequently fall out or the infants void around them. Contrast agents used for intravenous pyelography are the preferred opaque compounds diluted by 3 to 4 parts of 5% glucose/water since they are so opaque. The use of agents now discarded for intravenous administration (such as sodium acetate)

Fig 10-214 In an infant radiographed with diagnosis of left ureteropelvic obstruction the additional distention of the left renal pelvis secondary to bilateral mass vessel reflux without distal obstruction. The left kidney shows no distal reflux of contrast material to the surface of the kidney.





Fig 10-215—Retrograde pyelogram of an infant with right renal vein thrombosis; there was no excretion on intravenous pyelography. The calyces in the enlarged infarcted kidney are stretched.

zoate) has been criticized because of their irritating effects and a slight potential danger if large amounts are intravasated. Antibiotics such as neomycin should not be added; massive vesicoureteral reflux can lead to an intravasation of urine and contrast

agent into the kidney parenchyma (Fig 10-214) and neomycin in such situations has led to autonomic blockade and respiratory arrest with death narrowly averted.

A minimal study includes films of the bladder with a small volume with a full volume (determined by onset of voiding or suprapubic palpation of the enlarging bladder) and films during and after voiding. The choice of 70 or 90 mm spot films, conventional spot films, television tape recording or cine or overhead films is usually determined by the preference of an individual institution or radiologist. Overhead films give the greatest anatomic detail, whereas cine studies give the greatest exposure.

We believe that vesical reflux into the ureter or kidneys is always abnormal, though this has never been proved. Iannoccone felt that occasionally as a "para-physiologic" phenomenon a transient reflux can occur. What has become clear is that reflux per se may not harm the kidney if not massive and if infection is eradicated.

MISCELLANEOUS STUDIES—Retrograde pyelography is difficult to perform in the male neonate for technical reasons, although skilled urologists have used it. It is of value when a kidney is not visualized (Fig 10-215) as in massive renal vein thrombosis or when the site of obstruction in a hydronephrotic kidney cannot be determined by intravenous pyelography or voiding cystography.

Antegrade cystography (translumbar approach) is accomplished by percutaneous puncture of a hydro-

Fig 10-216—Translumbar antegrade pyelography. A: In an infant with a hydronephrotic left kidney manifested as a flank mass, no reflux was noted in the voiding cystogram and the left ureter was not seen in the intravenous pyelogram. The antegrade pyelogram demonstrates the tiny left ureter, proving the ureteropelvic site of obstruction. Surgery included pyeloplasty with salvage of kidney. B and C: In an infant with left ectopic ureter, occlusion of the left upper renal collecting system but showed an intravesical lucent mass. Direct puncture of the left upper pole demonstrates hydronephrosis leading to partially obstructed ureter, which partly collapsed at the time of study. (B: courtesy of Dr. P. F. Boms, Philadelphia.)

phrotic kidney. The procedure is performed under fluoroscopic guidance. The needle is inserted into the left upper renal collecting system but showed an intravesical lucent mass. Direct puncture of the left upper pole demonstrates hydronephrosis leading to partially obstructed ureter, which partly collapsed at the time of study. (B: courtesy of Dr. P. F. Boms, Philadelphia.)



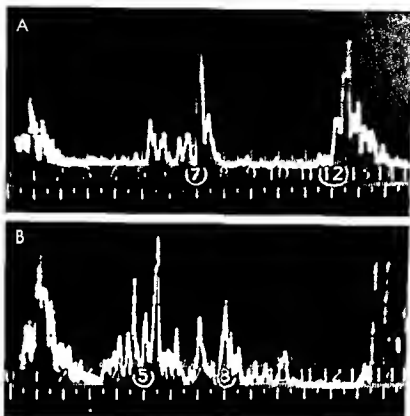
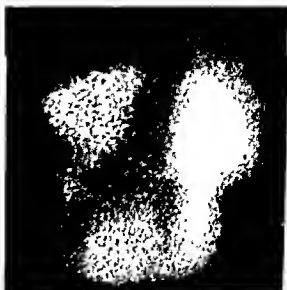


Fig 10 217 —Ultrasound A, in hydronephrosis an A scan shows sharp deflections by the anterior and posterior walls of the dilated pelvis at 7 and 12 cm B, in Wilms' tumor an A scan

shows multiple echoes from within the large tumor between 5 and 8 cm (Courtesy of Dr J LeFebvre Paris)

Fig 10 218 —Absence of abdominal atherosclerosis and hydronephrosis (Eagle-Barrett syndrome) in a male infant Technetium DTPA scan 45 minutes after injection shows rapid filling of the ureters indicating the nonobstructive nature of ureteral dilatation in this syndrome (Courtesy of Dr G S Freedman New Haven Conn)



nephrotic renal pelvis and is facilitated by image intensified fluoroscopy. The 50–60% urographic medium is hand injected without undue pressure and films are obtained. Ureteropelvic obstruction (Fig 10-216, A) can be studied with visualization of the tiny proximal ureter, in renal duplication with ectopic ureterocele, direct injection into the nonfunctioning dilated upper pole delineates filling of the ureter and its terminal dilated segment (Fig 10-216, B and C).

Transillumination and ultrasound can both be used to determine whether masses are fluid filled or solid (Fig 10-217). Both have the advantage of "going to the patient" and of safety.

Isotopic scanning had rather limited value from the static scans performed with radioactive mercury (Chlormerodrin), which allowed tubular fixation and demonstration of filling defects and the like. The newer more rapidly excreted mediums combined with rapid recording (as with the Anger camera or similar scanning devices) allow visualization of ureters and evaluation of the degree of obstruction in a dilated system. For example, technetium DTPA scanning in a "prune belly" infant (Fig 10-218) showed rapid nonobstructive activity in the dilated ureters. This procedure has promise and could be used when iodinated contrast agents are contraindicated. At present these studies are being used in conjunction with rather than in place of, contrast studies.

UMBILICAL ANGIOGRAPHY—Aortography via the umbilical artery is valuable in studying newborns with renal malformations. Aortography should follow adequate dose pyelography since the latter's 10 cc dose provides detail not available with the 1 cc/kg dose of the aortogram. The two dose schemes should not be confused; rapid injection of 10 cc through an umbilical catheter could be dangerous.

Neonatal anuria and azotemia are indications for renal artery visualization by aortography. Kaufmann, studying a newborn group, concluded that the renal artery always can be seen and that failure to visualize it in cases of anuria and azotemia is most meaningful and strongly suggests renal agenesis (see Fig 10-207, B). It is conceivable, however, that the supine position could allow streaming and layering of contrast medium with spurious nonvisualization of the renal arteries when they were actually present.

REFERENCES

- Allen R. P., et al. Transient extraperitoneal hernia of bladder in infants (bladder ears). *Radiology* 77:979, 1961.
Baghdassarian O., et al. Neonatal urography. *Radiol Clin North America* 3:139, 1965.
Bennett G. T. Urographic contrast agents: A comparison of sodium and methylglucamine salts. *Clin Radiol* 21:150, 1970.
Berdon W. E., et al. Prone positioning in GI and GU roentgenologic studies in infants and children. *Am J Roentgenol* 103:444, 1968.
Carrano G., et al. Congenital Anomalies of the Upper Urinary Tract. In Kaufmann, H. J. (ed.) *Progress in Pediatric Radiology* (Chicago: Year Book Medical Publishers, Inc. 1970) Vol. 3 p. 179.

Iannoccone, G. Ureteral reflux in normal infants. *Ann. radiol.* 9:31, 1966.

Nogrady, M. B., et al. Delayed concentration and prolonged excretion of urographic contrast medium in the first months of life. *Am J Roentgenol* 104:289, 1968.

O'Connor, J. F., et al. Total body opacification in conventional and high dose intravenous urography in infancy. *Am J Roentgenol* 90:63, 1963.

Genitourinary Causes of Abdominal Masses

It has been amply demonstrated in large reviews, such as Gnscom's, of abdominal masses in the neonate, that genitourinary abnormalities account for at least one-half of such masses. For this reason, if no other, the screening examination in any newborn with a mass must include intravenous pyelography if the plain films fail to show gas filled bowel as the cause of the mass. Total body opacification is thus available to outline the opacified blood content of the mass while the excretory films show whether the kidney is involved.

Hydronephrosis (usually due to ureteropelvic obstruction) and unilateral multicystic disease account for most abdominal masses of genitourinary origin. Less common genitourinary causes include tumors of the adrenal or kidney, renal vein thrombosis with renal infarction and retroperitoneal teratomas and hygromas. Even perirenal and retroperitoneal abscesses may occur in the neonatal period as complications of sepsis. Thus the common and uncommon may be encountered in the study of a newborn with a mass in the abdomen and pelvis. Radiographic diagnosis is usually correct since the majority of masses in the urinary tract are either hydronephrotic or multicystic kidneys.

Hydronephrosis

RELATION OF URINARY TRACT INFECTION AND REFLUX.—In general, the older child with hydronephrosis (pyelectasis and caliectasis) has both infection and vesicoureteral reflux; the hydronephrosis is not due to organic obstruction. The dilating effects of reflux and endotoxin on ureteral smooth muscle (hypotonia) respond to medical management of the infection without need for surgical relief of "obstruction."

In the newborn, however, obstruction may exist without infection. The following discussion will focus on those repairable causes of obstruction seen early in life before infection supervenes. If the hydronephrotic kidneys are not infected early, they will become so later, once foreign bodies such as nephrostomy or cystostomy catheters are left in place.

The role of prenatal infection in the pathogenesis of such "obstruction" is difficult to prove. However, there seems to be definite evidence of organic prenatal obstruction in such lesions as renal dysplasia accompanying ureteropelvic stenosis, ectopic ureteroceles and urethral valves. Serious disease of the urinary tract in the newborn may be hidden by seeming

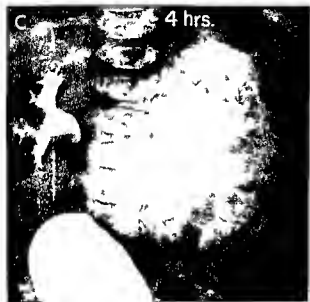


Fig 10-219 — Hydronephrosis man tested as a flank mass in a newborn infant. **A**, total body opaque cat on effect in the 1 minute film of the intravenous pyelogram. **B**, view of the lucent renal pelvis that contains unexpected urine. **C**, at 10 minutes the renal pelvis (arrows) is dilated collecting tubules that have been distended and turned 90° so that they appear as the greatly dilated renal pelvis and calyces. **C**, at 4 hours with full filling of contrast agent and urine, ureteropelvic obstruction is seen. Intravenous pyelogram was found on nephrectomy. The kidney had good parenchyma, was uninfected and potentially could have been repaired. (From Berdon, *et al*.)

signs of alimentary tract disease such as vomiting and distention. Once infection occurs, these may be increased, and even jaundice may appear (possibly from the cholestasis accompanying gram-negative endotoxemia), and the diagnosis may be missed entirely. As previously noted, the signs of pulmonary hypoplasia may so dominate the clinical appearance that the primary lesion is not found prior to death. The young male infant has about the same involvement with reflux and infection as does the female, whereas infection, reflux, and nonobstructive hydronephrosis in the older child is much more common in the female than in the male.

GENERAL CONSIDERATIONS — Hydronephrosis (i.e., abnormal dilatation of the pelvicalyceal system) may

be unilateral or bilateral. These large masses are palpable, and their contents may represent 5–10% of the total body weight. In the usual case, treatment depends on the demonstration of the obstruction and its site and the decision whether a nephrectomy or attempted repair is required.

The diagnostic procedure starts with plain films. These reveal that the mass (or masses) is not gas-filled intestinal loops. Lateral views may show a posterior position of the mass, confirming that it is probably renal.

Intravenous pyelography is performed next, using 3 cc/kg, though up to 15 cc can be injected in a 3.5 kg full-term infant without ill effects so long as the infant is well hydrated and the injection is not made too

rapidly. On total body opacification the mass is lucent (Fig 10-219, A) since the huge renal pelvis is surrounded by more opaque vascularized liver, spleen and residual renal tissue. The parenchymal "rim" slowly fades as crescent shaped collecting tubules fill (Fig 10-219, B). Finally, the dilated calyces fill, initially, because of the weight of the contrast medium, it collects along the side and posterior wall of the renal pelvis. With motion and time, full mixing of the urine and contrast occurs to the point of obstruction (Fig 10-219, C), this may be at the ureteropelvic junction, at the ureterovesical junction or at the urethra.

The next procedure is usually cystography (including voiding films) to determine the presence and degree of reflux, and, in the male urethra, presence of valves. The balloon shaped defect of a ureteroceles may be observed in either sex. In an occasional patient percutaneous antegrade pyelography via the dilated renal pelvis may be helpful, particularly when there is no visualization of the ureter in the intravenous pyelogram or voiding cystogram and retrograde cystography is not possible due to the small size of the infant.

LOCATION AND ETIOLOGY—Ureteropelvic—This site accounts for most examples of giant hydronephrosis in the newborn (Fig 10-219). The junction is narrowed by an intrinsic dysplasia, there is little inflammatory reaction. There is some speculation that this might be a growth disturbance secondary to ischemia, analogous to small bowel stenosis. In a study

of older children with ureteropelvic obstruction, Johnston found one-third to have periureteral kinks and adhesions possibly secondary to prior infection. Rarely, an aberrant artery crosses and compresses the ureter, in others there may be so-called "high insertion" of the ureter into the renal pelvis, with the pelvis distending and causing stasis. Regardless of cause, treatment must provide drainage before infection supervenes, otherwise, further renal damage renders nephrectomy the only procedure. Infection and hypertension are considered contraindications to repair by some urologists.

A voiding cystogram should be obtained to exclude reflux. Antegrade or retrograde pyelography may be used to visualize the tiny ureter (see Fig 10-218, A).

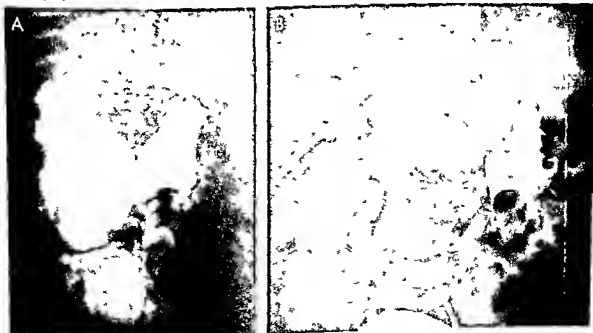
Ureterovesical—This site may be involved on one or both sides. Masses representing dilated ureters as well as kidneys may be palpable. A voiding cystogram is needed to exclude reflux and infection as the cause of obstruction, it also discloses obstructing urethral valves if present.

Proper treatment for ureterovesical hydronephrosis is controversial, even in the newborn. Some patients are vigorously treated by ureteral "tailoring" with removal of redundant loops and reimplantation into the bladder. In others, antibiotics and suprapubic drainage of the more involved kidney lead to amazing restoration of the kidneys and ureters to normal function with renal growth (Fig 10-220).

Bladder neck—Primary bladder neck obstruction, if it exists, is not felt to be a lesion that can be diag-

Fig 10-220—A, In a newborn female with right flank mass massive right and lesser left hydroureteronephrosis is evident. No reflux was seen in the voiding cystogram, urine was sterile. B, in travenous pyelogram several months later after therapy limited to

antibiotics and right nephrostomy shows amazing recovery of both sides with good renal growth and normal function. The patient has recovered from seeming neonatal ureterovesical obstruction following conservative medical and surgical therapy.



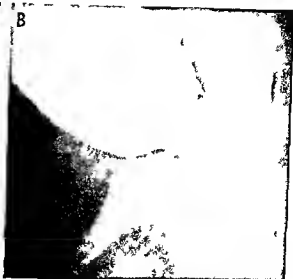


Fig 10-221—Simple adult type of ureteroceles in a newborn male with ascites. A, cystogram shows reflux into the spiraling left ureter and left perirenal extravasation. The intravenous pyelogram had shown no signs of either kidney. Ascites is present with medial displacement of liver. B, voiding film shows vesicoureteral

neck lucent defect—ureteroceles. At autopsy the right kidney was tiny and dysplastic and the left kidney was cystic with a single ureter leading to a simple ureteroceles and the left ureter orifice in no malposition.

Fig 10-222—Ectopic ureteroceles. A, typical picture (in this case bilateral) with the lower collecting system pushed down and laterally by nonvascularized upper pole hydronephrosis. A rim of parenchyma surrounds the upper pole pelvis. Filling

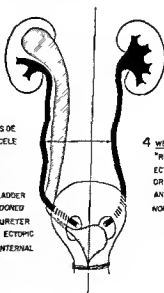
defects in the bladder are terminal dilated ureteral segments from the upper poles and nonvascularized ureteroceles. B, diagrammatic representation. (From Bardon et al.)



B
1. DROOP OF LOWER CALYCES

2. LOWER POLE URETER ON SIDE OF URETEROCELE DISPLACED Laterally

3. "MASS" IN BLADDER DUE TO BALLOONED UPPER POLE URETER WITH ORIFICE ECTOPIC IN ZONE OF INTERNAL SPHINCTER



4. WEGERT MEYER "RULE" — ECTOPIC URETERAL ORIFICE MEDIAL AND CAUDAL TO NORMAL ORIFICE

nosed radiographically in infants (or children) with reflux hydronephrosis and infection. The vesical outlet can be obstructed by congenital anomalies and ureterocele. These can be searched for. These can be simple adult draining nonduplicated kidneys (Fig 10-221) or part of a complex anomaly of renal duplication with the ectopic ureter (Fig 10-222 A) from the upper pole ending in the ureterocele. Then the intravenous pyelogram shows the 'drooping lily' deformity of the lower pole calyces depressed by the hydronephrotic upper pole.

This diagnosis is made in the intravenous pyelograms that show a balloonlike intravesical filling defect (Fig 10-222 B) in combination with poor or no visualization of part or all of either kidney. As with urethral valves, rupture of the bladder or of the kidney may occur and be confirmed during cystography and pyelography by leakage of contrast medium into the perirenal space. Sometimes there is flow into the peritoneal cavity with urine ascites (see Fig 10-221 A).

Treatment if there is salvageable renal tissue consists of heminephrectomy and ureterectomy (for the case of ectopic ureterocele with renal duplication) or of nephroureterectomy (for the simple adult type of ureterocele).

REFERENCES

- Berdon W E *et al*. Ectopic ureterocele. *Radiol Clin North America* 6:205 1968
 — *et al*. Hydronephrosis in infants and children. Value of high dosage excretory urography in predicting renal salvageability. *Am J Roentgenol* 109:380 1970
 Dunbar J S *et al*. The calyceal crescent. A roentgenographic sign of obstructive hydronephrosis. *Am J Roentgenol* 110:530 1970

- Ginscom N T. The roentgenology of neonatal abdominal masses. *Am J Roentgenol* 93:447 1965
 Hartman G W. The duplex kidney and related abnormalities. *Clin Radiol* 20:387 1969
 Johnston J H. Experience with ectopic ureteroceles. *Brit J Urol* 41:61 1969
 —. The pathogenesis of hydronephrosis in children. *Brit J Urol* 41:724 1969
 Lundin E. Upper urinary tract duplication associated with ectopic ureterocele. *Acta radiol (diag)* 7:13 1968
 Usón A C *et al*. Giant hydronephrosis in children. *Pediatrics* 44:209 1969

Urethral Obstruction

POSTERIOR URETHRAL VALVES—The infant in whom posterior urethral valves are identified during the first weeks of life has a poor prognosis. This reflects the serious damage done to the kidneys in utero in terms of both obstructive effects and coexistent renal dysplasia. Pulmonary hypoplasia may be incompatible with survival.

The valves consist of membranes originating from the verumontanum which descend to divide and insert at the level of the external sphincter in the form of an inverted V. They balloon out during voiding (Fig 10-223) acting like sails and encroaching on the urethral lumen to impede flow. Unfortunately the clinically observed urinary stream may seem normal though some patients exhibit dribbling.

Some patients have in utero rupture of the bladder (Fig 10-224 A) or even of a kidney secondary to obstruction with development of perirenal urinoma (Fig 10-224 B) and urinary ascites. Others have pneumothorax and pneumomediastinum presumably related to stiff lungs accompanying diminished fetal urinary output (Fig 10-225).

there may be marked reflux (B) although again urterovesical obstruction is common.

Fig 10-223—Two cases of posterior urethral valves with bilateral hydronephrotic dysplastic kidneys. The bladder may be tiny (A) without reflux with secondary ureterovesical obstruction. Or

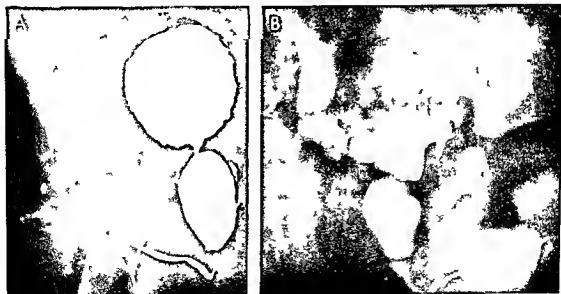




Fig 10-224 A urinary ascites in a newborn infant from rupture of the bladder secondary to obstructing posterior urethral valves. The kidneys were virtually normal, raising the question of helpful decompression from long-standing in utero bladder leak.

age (Courtesy of Dr J. C. Leonard, New York.) B perirenal extravasation combined with urinary ascites in an infant with posterior urethral valves (B, courtesy of Dr R. Moncada, Chicago.)

The bladder may be either small and thick walled (Fig 10-223) or huge (Fig 10-225). Reflux may be massive (Figs 10-223 B and 10-224 B). The serious problem of establishing urinary drainage has led to many methods of decompression. Since the kidneys show bilateral hydronephrosis with tortuous ureters (with or without reflux), secondary points of obstruction may be present at several levels in the ureters, especially at the ureterovesical junction. Suprav vesical diversion therefore may be needed. Most pediatric urologists use some type of diversion above the bladder, such as cutaneous loop ureterostomies. These have the advantage of being tubeless and avoid the foreign body reaction in the urinary tract that inevitably introduces infection. Resection of the valves may have to be delayed until the kidneys recover from the secondary obstruction and infection.

The infants may have had such severe fetal obstruction that marked secondary renal cystic dysplasia has developed. The kidneys may be unable to reabsorb water, and a diabetes insipidus-like picture has been identified in some male infants with posterior ureth-

ral valves. In some cases hematuria may be gross.

The usual infant with posterior urethral valves has no other anomalies, although Curranno had encountered several cases of posterior urethral valves associated with duplication of the coxal with one coxal entering the obstructed urethra (Fig 10-226). A few male infants with congenital absence of the abdominal musculature ('prune belly syndrome') have associated urethral valves.

MEATAL STENOSIS—This is not considered to be a radiographic entity and has unclear significance at any age as a cause of genitourinary infection and associated reflux.

ANTERIOR URETHRAL OBSTRUCTION—Rarely the obstruction in the male infant is secondary to anterior urethral diverticulum (Fig 10-227). Its effect is similar to that of a valve in that it fills on voiding, obstructing the urinary stream. The bladder may be small and thick walled or large and thin walled. Reflux may be present as well as secondary ureterovesical obstruction. Treatment, aside from repair of the urethra, is decompression of the upper tracts.



Fig 10-225 —Pneumomediastinum elevating the thymus in a newborn with posterior urethral valves and large bladder. There was a history of polyhydramnios.

Fig 10-226 —Duplication of the colon. One colon ends normally while the second enters the distal posterior urethra above the level of the external sphincter. Obstructing valves caused the dilatation. (Courtesy of Dr. G. Curran, Dallas, Tex.)



Fig 10-227 —Massive bladder wall thickening with urethral dilatation secondary to enterourethral diverticulum in a newborn infant. As the diverticulum filled it ballooned out, obstructing the anterior urethra and causing urinary retention. (Courtesy of Dr. K. Walehouse, New York.)



REFERENCES

- Garrett R A *et al* Neonatal ascites perirenal urinary extravasation with bladder outlet obstruction *J Urol* 102 627 1969
- Johnston J H Posterior Urethral Valves in Neonatal Surgery (London Butterworth & Co Ltd 1969) Chap 41 p 532
- Leonidas J C *et al* Congenital urinary tract obstruction presenting with ascites at birth *Radiology* 96 111 1970
- Moncada R *et al* Neonatal ascites associated with urinary outlet obstruction (urine ascites) *Radiology* 90 1165 1968
- Waldbaum R S *et al* Posturethral valves Evaluation and surgical management *J Urol* 103 801 1970
- Waterhouse K Anomalies of the Urethra, in *Encyclopedia of Urology* (Berlin Springer-Verlag 1966) Vol 7 p 242

Triad Syndrome (Prune Belly or Eagle Barrett Syndrome)

This syndrome is characterized by undescended testes dilated ureters and dysplastic kidneys and absence of abdominal musculature (Fig 10-228). Males by definition have this syndrome although a rare female has a similar syndrome. Some patients survive into adult life after cosmetic surgery for the abdominal wall others are stillborn or die in infancy of

azotemia. The renal insufficiency is due in severe cases to cystic renal dysplasia presumably from renal damage in utero. Pulmonary hypoplasia, Potter's facies and club feet all signs of oligohydramnios have been encountered (Fig 10-229).

The kidneys may not be hydronephrotic but have only huge atonic ureters with small bizarre nondilated calyces as signs of renal dysplasia (Fig 10-230). Some authors consider the ureteral dilatation dysplastic and not secondary to distal obstruction. This reflects the failure in the usual case to find vesical or urethral obstruction at necropsy although a few examples of urethral valves have been recorded. The urachus may be patent (Fig 10-231 A) and the posterior urethra elongated. Occasionally a dilated utricle (or vagina masculinus) is seen arising high in the posterior urethra (Fig 10-231 B). Imperforate anus and rotational anomalies of the gut occasionally coexist.

Treatment is controversial since infection is introduced by placement of any tube. Some favor diversion such as cutaneous pyelostomy or ureterostomy. The natural life history of the anomaly is impossible to define since it encompasses such a wide range of renal dysplasia plus the superimposed effects of infection and surgical drainage.

Fig 10-228 (left) —Typical prune belly showing wrinkled abdomen. The testes were undescended and flank masses representing huge ureters were easily palpated.

Fig 10-229 (right) —A newborn infant with prune belly syn-

drome also had involvement of the diaphragm. Hypoplastic lungs led to death. Interstitial pulmonary emphysema pneumomediastinum and bilateral pneumothorax were found at autopsy.





Fig 10.230 — Prune belly syndrome. A, an early intravenous pyelogram shows a normal renal pelvis but not hydronephrosis of upper tracts. B, good ureteric trochanter and there was no

infection. B, a later film shows giant ureters that were virtually atonic on fluoroscopic cavitation.

Fig 10.231 — Voiding cystourethrograms in the prune belly syndrome. A shows a partially patent urachus (upper arrow) and long, slightly dilated but unobstructed posterior urethra. Vaginas

are very rare in these patients. B, of another patient shows a small vagina masculinized (arrow), a not infrequent finding in these patients (b, bladder; u, urethra).



Fig 10-232 — Contrast medium instilled into a giant vagina in an infant with the cloacal type of imperforate anus (i.e., rectum and bladder drain into the vagina above a narrow common urogenital sinus).



REFERENCES

- Burkholder G V *et al*: Congenital absence of the abdominal muscles. *Am J Clin Path* 53:602, 1970
 Williams D I *et al*: The prune belly syndrome. *J Urol* 98:244, 1967

Vaginal Obstruction

Rarely a female infant is born with a giant fluid distended vagina. The fluid includes secretions stimulated by maternal estrogens. Since such infants often have an anomaly other than a simple obstructing diaphragm, cases of imperforate vaginal membrane

(producing hydrocolpos) are joined in this discussion with those of female infants born with a common stenotic urogenital sinus with urine draining into the vagina (Fig 10-232). Attempts at catheterization in the latter type usually result in filling of the vagina, since the urethra enters the vagina high and behind the symphysis and is difficult to catheterize. In many of these girls the rectum also enters the vagina above the stenosis so that meconium mixes with urine and vaginal secretions. This is termed the cloacal type of imperforate anus since it is a common chamber for the excreted contents of the intestinal and urinary tracts.

Fig 10-233 — Estrogen effect causing vaginal enlargement. A, in this otherwise normal newborn there is anterior displacement of the bladder and posterior displacement of the rectum. No ob-

struction was noted on gynecologic examination; the vagina and uterus were boggy on palpation. B, a year later the space between rectum and bladder is normal.



Radiographically the huge vagina may contain gas if there is a rectovaginal fistula. Total body opacification may show the vascularized wall to light up with the contents seeming lucent. The intravenous pyelogram shows dilated ureters displaced to the flanks by the central vaginal mass. If severe enough the obstruction may produce oligohydramnios deformities including hypoplastic lungs and death.

Do not confuse the mild vaginal enlargement in some normal newborns with hydrocolpos (Fig 10-233). One commonly sees mild posterior displacement of the rectum and anterior displacement of the bladder by a boggy vagina and uterus; this has been attributed in the newborn to the maternal estrogen effect which causes gynecomastia in the newborn. Physical examination shows a normal vaginal introitus and the enlargement recedes in the weeks following birth.

REFERENCES

- Brinto E H. Hydrocolpos. *Mayo Clin Proc* 45:505 1970
 Tank E S et al. Urogenital sinus outlet obstruction. *J Urol* 104:769 1970

Vascular Disturbances of the Neonatal Kidney and Adrenal

The kidneys and adrenals of the fetus and newborn may be the site of infarction, hemorrhage and necrosis. The involvement may cause rapid death or recovery may ensue with calcification in the involved re-

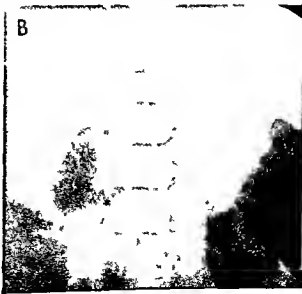
gion as the only sign of the previous events. Some infants have a prolonged stormy course including shock, pallor, hematuria and azotemia, some of whom survive and recover. In this group radiologic studies aid both in the diagnosis and in follow up observations.

RENAL CORTICAL AND TUBULAR NECROSIS—These are best considered together since the effect of renal ischemia is most marked in the cortical and pyramidal circulation. Causes include fetal anemia, shock or intravascular clotting as part of sepsis. "Lower nephron nephrosis of the newborn" is an older term for the tubular necrosis that may develop. Patients who recover may have a permanent concentrating defect.

In the acute phase the intravenous pyelogram shows faint or non visualization of the calyces. A patchy or dense prolonged nephrogram indicates that there is continuing glomerular filtration. The contrast material accumulates in tubules that may be blocked by precipitation of urinary glycoprotein of Tamm and Horsfall. This dense nephrogram in mild cases persists for several days (Fig 10-234). Follow up intravenous pyelograms are usually normal although the more severely affected infants exhibit papillary cavities as a sign of necrosis. The kidneys may be slightly enlarged. The combination of such enlargement and the streaky nephrogram may cause confusion with infantile polycystic disease. The rapid recovery in the group with tubular stasis differentiates the two conditions.

Fig 10-234—A dense nephrogram (lasting several days) during the acute phase of lower nephron obstruction in a neonate 2 days of age who recovered. Follow up films were normal. Some such infants excrete large amounts of Tamm-Horsfall urinary glycoprotein once diuresis commences. In others permanent papillary necrosis is present. In follow up intravenous pyelograms. (Courtesy of Dr J. Foley, Burlington, Vt., from Berdon et

al.) B. In the chronic phase of renal cortical and tubular necrosis several weeks after birth, marginal calcifications surround both kidneys and both adrenals are calcified. Neonatally there had been disseminated intravascular clotting and adrenal hemorrhage developed. The infant died after azotemia, urine concentrating defects and polyuria. (Courtesy of Dr J. Leonard, NYC.)



Cortical necrosis may lead to marginal cortical calcifications within as little as two to three weeks after birth. The proposed causal mechanism is cortical ischemia with necrosis and calcification; the corticomedullary and medullary regions maintain their blood supply by corticomedullary shunting (Trueta effect) (Fig. 10-234 B).

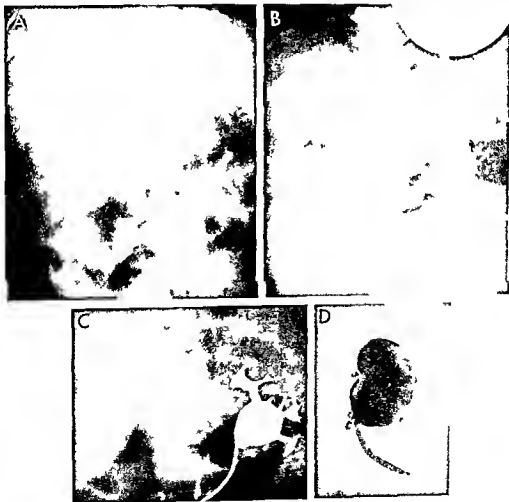
REFERENCES

- Berdon W. E. *et al.* Tamm-Horsfall proteinuria: Its relationship to prolonged nephrogram in infants and children and to renal failure following intravenous pyelography in adults with multiple myeloma. *Radiology* 92:714, 1969.
- Crispin A. R. *et al.* Renal tubular necrosis and papillary necrosis after gastroenteritis in infants. *Brit. Med. J.* 1:410, 1970.
- Eskeland G. *et al.* Bilateral cortical necrosis of the kidney in infancy. *Acta paediatrica Scandinavica* 48:278, 1959.
- Jaenke J. R. Micropuncture study of methemoglobin-induced renal failure in the rat. *J. Lab. & Clin. Med.* 73:459, 1969.
- Jonsson, B. Lower nephron nephrosis in asphyxia neonatorum. *Acta paediatrica Scandinavica* 40:401, 1957.
- Mauer S. M. *et al.* Renal papillary and cortical necrosis in an infant. *J. Pediatr.* 74:750, 1969.
- Tan K. *et al.* The excretion of cells in urine following perinatal asphyxia. *Pediatr. Res.* 3:228, 1969.
- Whelan, J. G. *et al.* Antemortem roentgen manifestation of bilateral renal cortical necrosis. *Radiology* 89:682, 1967.

RENAL VEIN THROMBOSIS—The manifestations of renal vein thrombosis range from marked hematuria

Fig. 10-235—Renal vein thrombosis. A. In the acute phase intravenous pyelogram shows a kidney-shaped lucency in an area of enlarged though nonfunctional right kidney. Hematuria, proteinuria, and hypertension were present. In B. retrograde pyelogram the calyces in the large infarcted kidney are stretched. C. retrograde pyelogram shows small but otherwise normal kidney. Thrombosis developed shock in the newborn period. B. lateral ad-

renal calcifications were noted. Repeat biopsy showed renal vein thrombosis. The child was a ve. though azotemic at age 8 years. D. resected specimen shows multiple calcifications in a small kidney from an infant in the chronic phase of renal vein thrombosis. Hypertension present initially had disappeared then reappeared late, leading to nephrectomy. (D. courtesy of Dr. H. Nohum, Paris.)



and azotemia with bilateral flank masses to the discovery of a mass with no function on intravenous pyelography (Fig 10-235, A and B) or a small, unperfused, poorly functioning kidney on retrograde pyelography (Fig 10-235, C). Later arborizing calcifications may be seen within the affected kidney (Fig 10-235, D). Recovery is possible, though late onset of hypertension has been noted.

In the acute phase intravenous pyelography may demonstrate an enlarged kidney-shaped lucency in the total body opacification phase with little if any function (Fig 10-235, A). Retrograde pyelography delineates stretched calyces (Fig 10-235, B) that mimic polycystic disease, contrast material readily extravasates since the kidney may be virtually destroyed by the infarction. Treatment is usually nephrectomy in unilateral cases and heparinization or even clot removal in bilateral cases.

The cause of the thrombosis is unknown. Maternal diabetes was emphasized in the past, but recent investigations suggest fetal and neonatal shock, disseminated intravascular clotting, marked dehydration and altered glomerular filtration. It is possible that the clotting is secondary to altered intrarenal dynamics rather than the cause. Although rarely diagnosed in life, renal vein thrombosis is not so rare in necropsies of the newborn.

REFERENCES

- Belman, A. B., et al. Nonoperative treatment of unilateral renal vein thrombosis in the newborn. *JAMA* 241:1160-1170, 1970.
- Karash, L., et al. Renal vein thrombosis in children. *J Urol* 92:91, 1964.
- Nahum, H., et al. Unilateral renal vein thrombosis in the newborn. *Ann. radiol.* 12:293, 1969.
- Takeuchi, C. W., et al. Renal vein thrombosis of newborn and its relation to maternal diabetes. *Biol. neonat.* 3:23, 1961.
- Trystad, C. W., et al. Renal vein thrombosis and the nephrotic syndrome. *J. Pediatr.* 79:861, 1970.

Adrenal Hemorrhage and Calcifications

The huge fetal adrenal gland (one-third to one-half the size of the kidney) involutes normally without event. Occasionally massive hemorrhage occurs either from traumatic breech delivery or from intravascular clotting. Sepsis has occasionally been associated with such clotting. The hemorrhage either unilateral or bilateral, may lead to exsanguinating retroperitoneal or intraperitoneal hemorrhage. However, the blood may be contained within the gland and the breakdown of hemoglobin to bilirubin has led to pronounced jaundice in the first 5-10 days of life. Jaundice, when combined with unilateral or bilateral palpable abdominal masses, should raise the clinical suspicion of intra-adrenal hemorrhage.

The radiographic diagnosis can be made without waiting for peripheral or central triangular calcifications to form. The total body opacification phase of

the intravenous pyelogram during the acute phase shows a homogeneously lucent round mass above one or both kidneys (Fig 10-236, A) sharply contrasted with the dense liver, spleen and kidneys. The kidneys are depressed and flattened and their calyces, in the excretory film, are tilted down and laterally in a "drooping lily" deformity (Fig 10-236, B and C). Renal tubular stasis is present in some patients with a prolonged nephrogram that may last for a day (Fig 10-236, A and B).

In the following weeks peripheral or central flocculent calcifications may develop, several months later the glands have shrunk to a triangular calcified mass (Fig 10-236, D). A major therapeutic problem for these patients is the common clinical (both pediatric and surgical) diagnosis of neuroblastoma or Wilms' tumor. Surgical exploration does not solve the problem since the adrenal and kidney are bound together and the surgeon often thinks he is dealing with a renal tumor and performs an adrenonephrectomy. In one case the tail of the pancreas and spleen were included in an attempt at en bloc resection of a suspected neuroblastoma.

The diagnosis of adrenal hemorrhage is easy if peripheral calcifications are noted in the initial film (Fig 10-237) and shrinkage rapidly follows.

Neonatal adrenal hemorrhage is much more common than neonatal adrenal neuroblastoma, which is rarely bilateral. If the diagnosis cannot be made preoperatively aspiration of the hemorrhagic adrenal and biopsy should be done and interpreted before the kidney and adrenal are removed. Results of urine catecholamine studies were normal in two patients with adrenal hemorrhage but are not, unfortunately, always positive in patients with neuroblastoma. Also to be thought of, mainly because of the renal distortion, not the physical findings, is unilateral or bilateral renal duplication with hydronephrotic upper poles depressing the lower calyces. Most such duplications have lucent intravesical signs of ureteroceles and the nephrogram is not complete, showing this mass to be intrarenal (see Fig 10-222, A), whereas with adrenal hemorrhage or neuroblastoma the nephrogram is intact though flattened and distorted (Fig 10-236, A).

The largest triangular adrenal calcifications occur in the rare cases of familial xanthomatosis, described in 1956 from Israel and now called *Wolman's disease* (Fig 10-238). The example of such giant adrenal calcifications illustrated in previous editions was called Niemann-Pick disease but has been proved to be Wolman's disease. On restudy of the tissues large amounts of cholesterol and its esters and triglycerides have been found in the liver, spleen, lymph nodes and adrenals.

Infants with Wolman's disease die in weeks or months after a stormy course of diarrhea, failure to thrive and infections. It is possible that treatment with low cholesterol diets and modifications in the intake of triglycerides may alter the course.

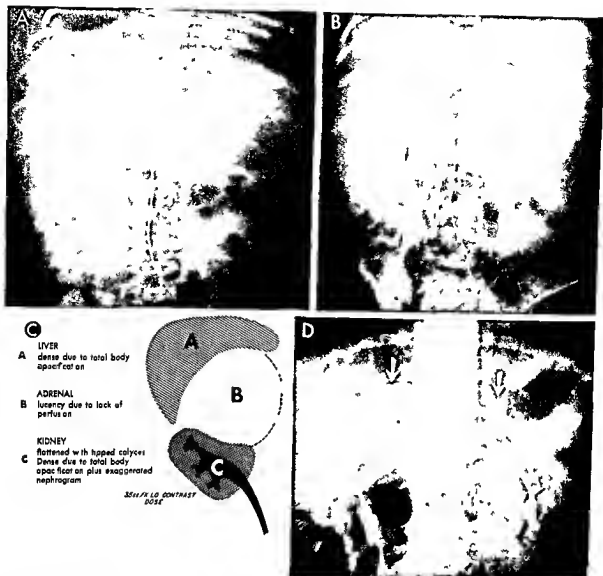


Fig 10-236 —Adrenal hemorrhage. **A** total body opacification reveals a lucent mass above both kidneys (best seen on the right). The displaced kidneys are somewhat enlarged with dense nephrogram. (Large amounts of Tamm Horsfall glycoprotein have been collected in such patients once diuresis has commenced.) **B**, at one hour, there is calyceal distortion with downward and

lateral displacement, the drooping pattern of a mass effect either from the upper pole of the kidney or from the adrenal area. **C** diagrammatic summation of both early and late intravenous pyelographic findings. **D** several months later there are flocculent adrenal calcifications. The kidneys have returned to normal. (From Rose et al.)

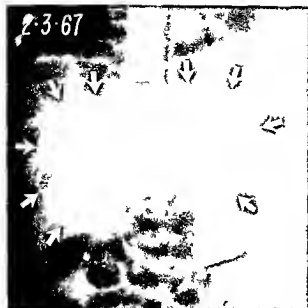


Fig 10-237—Adrenal hemorrhage. Films 24 days apart show peripheral calcifications surrounding large adrenal glands. As the glands shrink, calcifications increase and assume a triangular shape.



Fig 10-238—Adrenal hemorrhage. Films 24 days apart show peripheral calcifications surrounding large adrenal glands. As the glands shrink, calcifications increase and assume a triangular shape. There was no evidence of adrenal insufficiency (From Beaton and Baka).

REFERENCES

Abramov A. et al. Generalized xanthomatosis with calcified adrenals. *Am J Dis Child* 91:282, 1956.

Fig 10-238—Wolman's disease. Intravenous pyelogram of an infant with adrenomegaly shows huge calcified adrenal glands. This is a familial xanthomatosis with cholesterol in the involved organs, although the adrenals alone calcify. Previously confused with Hurler-Pick disease, this case was so illustrated in earlier editions on the basis of diagnosis at autopsy. Review of radiated pathological specimens led to the present diagnosis of Wolman's disease.

Brown B. St. J. et al. The radiologic features of acute massive adrenal hemorrhage of the newborn. *J Canad A Radiologists* 13:100, 1962.

Favara B. E. et al. Adrenal abscess in a neonate. *J Pediatr* 77:681, 1970.

Gross M. et al. Neonatal adrenal hemorrhage. *J Pediatr Surg* 2:308, 1967.

Rose J. et al. Prolonged jaundice as presenting sign of massive adrenal hemorrhage in newborn. Radiographic diagnosis by intravenous pyelography with total body opacification. *Radiology* 98:262, 1971.

Van de Water J. M. et al. Adrenal cysts in infancy. *Surgery* 60:1267, 1966.

Waggoner A. C. Bilateral hemorrhagic pseudocysts of the adrenal gland in a newborn. *Am J Roentgenol* 86:540, 1961.

Wolman M. et al. Primary familial xanthomatosis with involvement and calcification of the adrenal. *Pediatrics* 28:742, 1961.

Renal and Adrenal Tumors

Both the kidney and adrenal gland may be the site of tumors during the newborn period. Diagnostic procedures include plan films (for calcifications), intravenous pyelography with total body opacification, ultrasonography, and occasionally umbilical aortography. Knowledge of the natural history of these tumors is important in planning therapy.

RENAL TUMORS—A detailed search of the literature on renal tumors in newborns (including stillborns) fails to reveal a metastasizing tumor. The overwhelming number of these renal tumors, although called Wilms' tumor, are benign and represent a form of fetal renal hamartoma. Some function usually remains in the involved kidney (bilateral involvement is incompatible with life due to lack of sufficient function).





Fig 10-239—Benign fetal renal hematoma. In a premature infant, intravenous pyelography demonstrated a right renal pelvis and the total body opacification phase demonstrated mottled vascularity. A. Umbilical aortogram shows two renal arteries supplying this huge, rather vascular benign tumor.

ing renal tissue) and total body opacification during excretory urography reveals mottled avascular and peripheral compressed vascular areas. Umbilical aortography outlines the blood supply to the tumor with the density differing from case to case (Fig 10-239).

Because true Wilms tumor is rare in the newborn period and most neonatal renal tumors are benign, there is no need to operate on an infant with tumor during the first days of life. The infant may be premature although weighing due in part to the tumor more than 2000 or 2500 Gm. Difficulties of temperature regulation at this age have led to death at the time of surgical removal of what was a benign tumor. Furthermore, postoperative radiotherapy with the potential for damage to the spine and growth centers of the infant should be withheld until competent pathologic studies have revealed the exact diagnosis.

Renal displacement like that with Wilms tumor has been observed with retroperitoneal abscess (Fig 10-240) and hygroma (see Fig 10-243 A) which is a form of lymphangioma.

NEUROBLASTOMA.—As mentioned in the discussion of differential diagnosis of adrenal hemorrhage, neuroblastoma can be present in the newborn period. The adrenal may be the primary site, but the disease may arise first from any level in the sympathetic chain and be midline or presacral or paravertebral (Fig

B pathologic specimen of the large fleshy tumor with some normal parenchyma draped over the superior pole of the right kidney. Pathologic diagnosis was benign fetal renal hematoma. (B courtesy of D. J. H. Wigger, New York.)

Fig 10-240—Retroperitoneal abscess secondary to bowel perforation from necrotizing enterocolitis. Mass effect below the left kidney suggests renal tumor.



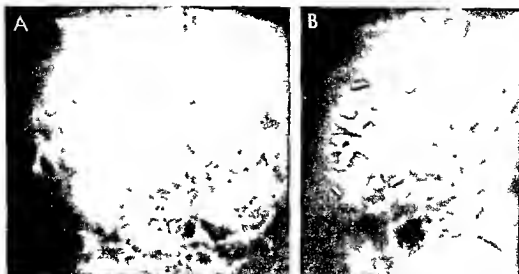


Fig 10-241. Neonatal neuroblastoma. In A, a right paravertebral mass is medial to the right kidney, partially obstructing collecting system. Cerebral calcifications are faint at this time. This tumor in a 3-day-old infant could not be resected. Radiotherapy and

chemotherapy led to shrinkage. B, three months later, shows shrinkage and further calcification of the mass. The patient weighed one and one-half years later, all calcifications had disappeared and repeat laparotomy failed to disclose residual tumor.

10-241 A) even cervical neuroblastoma has been recorded with airway obstruction.

With radiotherapy and time, the tumor may progressively calcify and shrink (Fig 10-241 B). Survival data in the newborn indicate a salvage of 40% or

less. This may not be because of metastases themselves, since many of the survivors had exophthalmos, liver enlargement, and cutaneous nodules. This type of lesion has been followed by transformation to benign ganglioneuroma in some cases and disappear

Fig 10-242. A, a right flank mass in a newborn infant, representing fetus in fetu, the most complete form of teratoma. B, specimen shows abortive extremities and trunk with bony structures.

les. Central nervous system and gastrointestinal elements were also present.



ance of all tumors in others. Most surprising is the finding of microscopic foci of neuroblastoma in 0.5-1.5% of careful studies of the adrenal glands of stillborns and infants up to the age of 3 months by Beckwith and associates. This suggests that this tumor is more common than is recognized but is rejected by antigenic processes of infancy. The clinical incidence of neuroblastoma is only a tiny percentage of Beckwith's incidence in necropsy studies.

Diagnostic investigation includes intravenous pyelography with total body opacification. The tumor may be slightly lucent although would rarely be as lucent as a hemorrhagic adrenal gland. Gastrointestinal series may show bowel displacement. Liver scans identify mottling of disseminated liver involvement. A bone survey should be made because skeletal metastases are common. Pulmonary metastases though found at necropsy are rarely seen in life. Cranial metastases may cause apparent widening of cranial sutures in the absence of increased intracranial pressure. Urine studies may reveal elevated catecholamine levels.

The maternal history may include sweating, palpitations and tingling of the hands and feet in the last weeks of pregnancy suggestive perhaps of catecholamines crossing the placenta from the affected fetus to mother. Voute suggested that such history should lead to a careful search in the newborn for a neural

tumor including urine vanillyl mandelic acid studies and possibly intravenous pyelography and chest films.

RETROPERITONEAL TERATOMA—Masses containing bone cartilage teeth central nervous system tissue fat and muscle may be found in the abdomen of newborns. Termed teratomas, they are defined as fetus-in-fetu (Fig. 10-242) if there is a recognizable trunk and limbs seemingly an abortive twinning. Although rare, they should be removed because of the potential effect on normal renal function and the slight malignant potential. Plain films may delineate the fat and bone structures; intravenous pyelography demonstrates the site of the teratoma. If above the kidney the kidney is shifted down and laterally as by adrenal neuroblastoma. The correct diagnosis should be possible from analysis of the plain film densities.

RETROPERITONEAL HYGROMAS (LYMPHANGIOMA CYSTIC MESODERMAL TUMORS)—Huge cystic masses with lymph-filled spaces as the major component are found in the retroperitoneum. Depending on their site they simulate Wilms' tumor or neuroblastoma. They may extend down into the pelvis and even into the inguinal area, simulating inguinal hernia. The cystic extrarenal nature can be appreciated on total body opacification when opacified septums surround the avascular cystic lucent spaces (Fig. 10-243). Surgical biopsy should be attempted for exact diag-

Fig. 10-243—Hygroma of the left retroperitoneum simulating left renal tumor. In A, septums run through the cystic tumor showing effects of the total body opacification on phase of intravenous pyelography. The base of the bladder is shifted; this would

be most unusual with renal tumor. In B, the specimen, the lower pole (arrow) fits into the area of bladder displacement; part of the tumor filled the left inguinal area mimicking hernia.

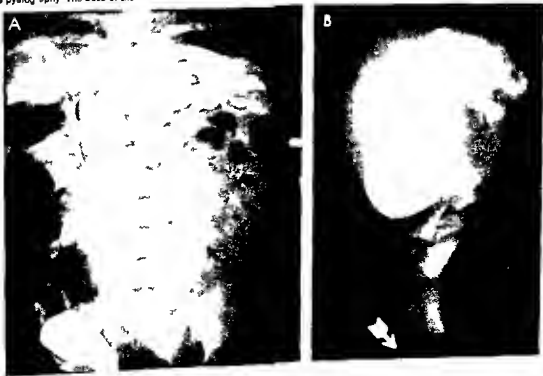




Fig 10-244—Sacrococcygeal teratoma. In A, the external component contains fat and calcifications. In B, intravenous pyelogram lateral projection, the bladder (B) and rectum (R) are

displaced anteriorly with a lucent area (not apparent in plain films). At operation, a cystic hygromatous element was removed from the presacral area.

nosis. Preoperative radiotherapy should be avoided since Wilms tumor is extremely rare in the newborn and the radiographic findings should differentiate hygroma from neuroblastoma and benign fetal hamartoma.

SACROCOCYGEAL TERATOMA—Huge clinically obvious sacrococcygeal teratoma in the newborn is a mixture of solid and cystic elements that may be 20–30 cm in diameter originating from the presacral area and extending down between the infant's legs (Fig 10-244 A). Containing fat, bone, teeth, central nervous system and gastrointestinal elements, they have a low but real chance of malignant dissemination. Most are benign and readily removed. Some, however, have a serious presacral and retroperitoneal extension. Those that extend above the 3rd sacral segment cause neurogenic bowel and bladder dysfunction.

Radiographic evaluation includes plain films in frontal and lateral projections. The rectum is opacified to outline the extent of presacral extension (Fig 10-244 B). Cystography can be used to see if the mass is behind the rectum and bladder or between them (as with ovarian teratoma). The total body opacification phase of the intravenous pyelogram outlines the cystic/lucent nature of the presacral and retroperitoneal extension (Fig 10-244 B).

REFERENCES

- Beckwith J B *et al*. In situ neuroblastoma. A contribution to the natural life history of neural crest tumors. *Am J Clin Pathol* 43:1089, 1963.
- Bolande R P *et al*. Congenital mesoblastic nephroma of infancy. *Pediatrics* 40:272, 1967.
- Dillard B M *et al*. Sacrococcygeal teratoma in children. *J Pediatr Surg* 5:53, 1970.
- Favara B E *et al*. Renal tumors in the neonatal period. *Cancer* 22:845, 1968.
- Gunn C H *et al*. Incidental neuroblastoma in infants. *Am J Clin Pathol* 51:126, 1969.
- Kafka V *et al*. Multicystic retroperitoneal lymphangioma in an infant appearing as an inguinal hernia. *J Pediatr Surg* 5:873, 1970.
- Macpherson R I *et al*. Sacrococcygeal tumors. *J Canad Assoc Radiologists* 21:131, 1970.
- Ramesh Pai K *et al*. Foetus-in-foetu. *Australian & New Zealand J Surg* 35:177, 1966.
- Richmond H *et al*. Neonatal renal tumors. *J Pediatr Surg* 5:413, 1970.
- Schneider K M *et al*. Neonatal neuroblastoma. *Pediatrics* 36:359, 1965.
- Voite P A. Congenital neuroblastoma. Symptoms in the mother during pregnancy. *Clin Pediatr* 9:206, 1970.
- Waisman J *et al*. Renal neoplasms of the newborn. *J Pediatr Surg* 5:407, 1970.
- Wigger J H. Fetal hamartoma of the kidney. *Am J Clin Pathol* 51:323, 1969.

Renal Cystic Disease

Several recent attempts at pathologic-radiologic correlation of renal cystic disease have emphasized the confusing and overlapping classifications. Radiologists should read these and acquaint themselves with the four types proposed on the basis of microscopic pathology and adoption of any one



Fig 10-245—A retrograde pyelogram showing dysplastic left kidney and absence of the right kidney. The clinical syndrome was secondary to respiratory compensatory efforts for unsuspected (and ultimately lethal) renal hypoplasia. Autopsy revealed a blind ending right ureter and two cysts in the hypoplastic left kidney with cystic dysplasia. B function of hypoplastic left kidney and a minor change in the lower pole of the right kidney in an infant with hypoplastic left heart syndrome secondary to aortic coarctation. Autopsy revealed cystic dysplasia.

system of classification is best avoided in this area where pathologists differ. One approach is offered largely derived from the work of Elkin and Bernstein since it seems most helpful clinically.

UNILATERAL MULTICYSTIC DISEASE—When renal dysplasia is associated with total replacement of the involved kidney by large and small cysts it is termed unilateral multicystic disease. This seems to correspond to type II of Potter. Elkin and Bernstein pointed out that it represents only part of a spectrum of cortical medullary dysplasia that also includes the aplastic and hypoplastic kidney (Fig 10-245). The clinical involvement of this type is unilateral since symmetrical bilateral involvement is incompatible with life. Such bilateral involvement is not uncommon in pathologic studies of stillborns. The proximal ureter is usually atretic or severely stenosed. It has been suggested that this might be the sequel to a prenatal vascular insult to the ureter with the kidney destroying itself from the obstruction. The kidney is a mass of grapelike cysts ranging from a few millimeters to many centimeters in size (Fig 10-246 A). The intravenous pyelogram shows no function as such, but total body opacification may reveal multiple lucent defects (Fig 10-246 B and C). The opposite kidney may seem normal; however, several patients have developed obstruction at the ureteropelvic junction that required pyeloplasty (Fig 10-247).

RENAL CYSTIC DYSPLASIA SECONDARY TO PRENATAL URINARY TRACT OBSTRUCTION—Prenatal obstruction of urine flow, as in some cases of urethral valves or of

urethral atresia with patent urachus (seen in severe examples of absent abdominal musculature syndrome) is associated with dysplastic kidneys and varying degrees of cortical and medullary cystic change. The kidneys are small or of normal size. Similar changes are present in some infants with complicated forms of imperforate anus and accompanying urologic malformations.

The cysts, type IV of Potter, occasionally are outlined in the intravenous pyelogram. Early films show lucent defects within the parenchyma during the nephrogram stage (Fig 10-248 A). Late films have shown filling of the cysts with contrast material (Fig 10-248 B) and in voiding cystograms reflux has on occasion filled these small cysts. Survival depends on the amount of functioning parenchyma, though the kidneys tend to be hypoplastic.

We should add here that renal dysplasia possibly associated with prenatal reflux or obstruction accounts for most of the tiny or small kidneys seen in infants. Renal artery stenosis itself is not the cause; the renal artery will be small when the kidney is small, reflecting the demand. The size of the renal artery ostia in a newborn, of course, will be small so that one cannot distinguish an acquired small from a congenitally small kidney in the newborn by such proposed criteria as the size of the renal artery ostia.

INFANTILE POLYCYSTIC DISEASE—Pathologists encounter polycystic disease as an entity largely confined to stillborn infants with huge bilateral spongelike kidneys. The thousands of cysts represent dilated

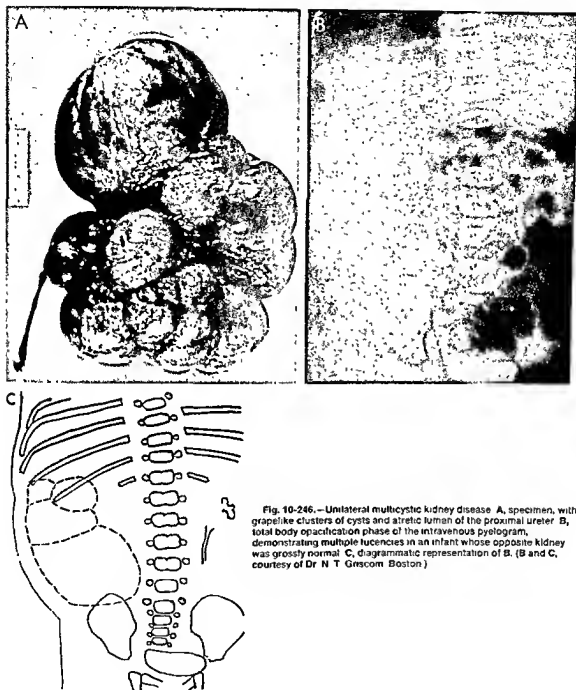


Fig. 10-246.—Unilateral multicystic kidney disease. A, specimen, with grape-like clusters of cysts and atretic lumen of the proximal ureter. B, total body opacification phase of the intravenous pyelogram, demonstrating multiple lucencies in an infant whose opposite kidney was grossly normal. C, diagrammatic representation of B. (B and C, courtesy of Dr N. T. Gnscom, Boston.)



Fig 10-247—A. Intravenous pyelogram, supine position, of a 3-week old infant whose left multicystic kidney was removed on the 1st day of life. Calyces filled by contrast material surround

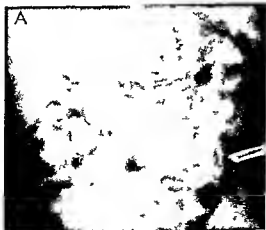


the enlarged right renal pelvis. B. prone position shows significant uretero-pelvic obstruction that responded to pyeloplasty (From Be don *et al*)

ed collecting tubules. Osathanondh and Potter termed this type I and considered it incompatible with survival for more than a few days. The effect on fetal urine output must be profound in view of the high association with oligohydramnios and pulmonary hypoplasia.

What is the relation of this infantile polycystic disease to the newborn who survives and even more confusing to the older infant or child with less renal enlargement but with the same radiographic evidence of dilated collecting tubules? The radiographs merely show that the kidneys are enlarged not by large noncommunicating cysts but by hundreds or thousands of dilated tubules that fill with contrast material which may linger for a week (Fig 10-249).

Fig 10-248—Cystic kidneys in an infant with posterior urethral valves. A. Small radiolucencies are seen in the nephogram early film. The hydrophrotic collecting system is readily identified



shows good excretion. B. at six hours shows the cysts now filled with contrast material. After effective urethral decompression intravenous pyelograms no longer demonstrate cysts.

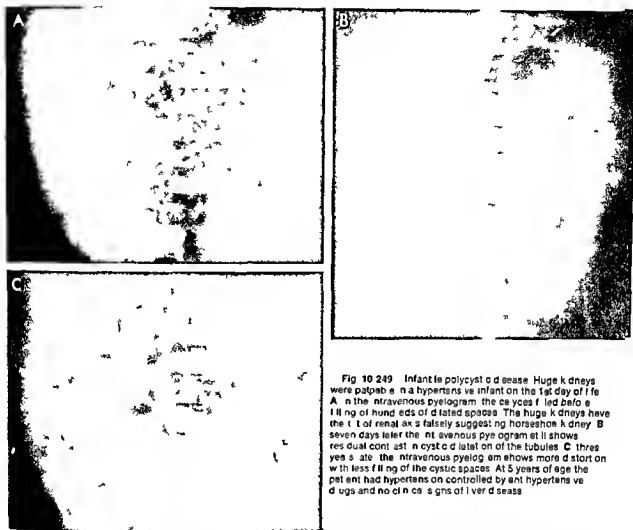


Fig 10-249 Infantile polycystic disease. Huge kidneys were palpable in a hypertensive infant on the 1st day of life. **A** In the intravenous pyelogram the calyces filled before filling of hundreds of dilated spaces. The huge kidneys have the tilt of renal axis falsely suggesting horseshoe kidney. **B** Seven days later the intravenous pyelogram still shows residual contrast in cystic dilatation of the tubules. **C** Three years later the intravenous pyelogram shows more distention with less filling of the cystic spaces. At 5 years of age the patient had hypertension on controlled antihypertensive drugs and no clinical signs of liver disease.

azotemic and die of renal failure. Still others have adequate renal function but portal hypertension appears and they may bleed to death. This reflects coexistent congenital hepatic fibrosis.

Finally lung cysts and renal cysts are so rarely seen in the same individual that they are best separated. It is legitimate to speculate that some of the cysts found in the lungs of newborns dying with polycystic renal disease may actually be signs of airblock and dilated interstitial emphysematous blebs.

MISCELLANEOUS CYSTIC CHANGES—Cystic changes are found in patients with trisomies 13, 15, and 17, 18 and with tuberous sclerosis (in addition to hamartomatous change) but have not been studied radiographically in the newborn period. Simple cysts, single or multiple, are occasionally seen in older children as is medullary sponge kidney (seemingly a mild form of type I of Potter by radiographic description but a form of type III by Potter's microdissections). The combi-

nation of such sponge kidney and azotemia with death in the first two decades has been called juvenile nephronophthisis—cystic disease of the renal medulla. These are not newborn diagnostic problems.

REFERENCES

- Edlin M, and Bernstein J. Cystic diseases of the kidney. Radiological and pathological considerations. *Clin. Radiol.* 20:65, 1969.
- Fauci C. Cystic maladies of the kidney in the infant. *J. Can. and A. Radiologists* 18:356, 1970.
- Gleason D C, et al. Cystic disease of the kidneys in children. *Am. J. Roentgenol.* 100:135, 1967.
- Gwynn J L, et al. Cystic diseases of the kidneys in infants and children. *Radiol. Clin. North America* 6:191, 1968.
- Ivemark B I, et al. Roentgenologic diagnosis of polycystic kidney and medullary sponge kidney. *Acta radiol. (diag)* 10:225, 1970.
- Osathanondh V., and Potter E. L. Pathogenesis of polycystic kidneys. Historical survey. *Arch. Path.* 77:459, 1964.

Screening Intravenous Pyelograms in Newborns with Anomalies

If a "screening IVP" is performed in infants with congenital anomalies the yield ranges from high (as with imperforate anus of the high type, Turner's syndrome, congenital absence of the radius) to moderate (imperforate anus of the low type, complex congenital heart disease) to poor (anomalies of fingers or toes, single umbilical artery in normal appearing infant, aganglionosis, undescended testes)

Screening intravenous pyelography should be deferred until the infant is 1 or 2 weeks old or longer because of occasional failure of visualization of normal kidneys on the 1st or 2nd day of life. This has occurred despite doses of 10 cc for a 3 kg infant, the equivalent of over 200 cc in an adult. This may be due to glomerulotubular imbalance in the immediate postnatal period.

In the infant with anomalies that seemingly predispose to neoplasia (such as the association of anuria or hemihypertrophy to Wilms' and other tumors), a single normal intravenous pyelogram does not indicate that Wilms' tumor will not subsequently develop, and such patients must be followed, perhaps with a single film after injection of contrast material, every 6-12 months for the period of risk (at present not

known). Infants with undescended testes and hypospadias have shown a very low yield on screening intravenous pyelography. The 8-12% of abnormalities cited includes anomalies of form such as partial duplication, the percentage of serious anomalies is very, very low. It is the policy at the Babes Hospital to screen patients with any type of imperforate anus by intravenous pyelography and voiding cystography in the first week of life, there is such a high association of serious genitourinary defects that their discovery, prior to superimposed infection, warrants this routine. However, in this group, as in those with aganglionosis, the unilaterally or bilaterally dilated ureters in infants without infection may spontaneously improve after colonic decompression. Structural renal malformations such as crossed ectopia and unilateral agenesis may be found alone or with reflux in as many as one-half of the patients with the high type of imperforate anus. Reflux alone may exist with or without infection, neurogenic bladder may also be present.

In some pediatric institutions a film of the abdomen is obtained on completion of angiocardigraphic investigations of infants with congenital heart disease. This yields some positive information, although the dose (usually 1 cc/kg of 75% contrast material) is rather low for good pyelography.

SECTION 11

*Artifacts and
Natural Misleading Images*

Artifacts and Natural Misleading Images

THE WORD "ARTIFACT" is derived from the Latin *factum*, something made or done, and *arti*, by art or skill. It was introduced into the English language in 1829* to designate an object such as a tool or ornament that showed evidence of human workmanship or modification, as distinguished from a natural object. When the word was later applied in the biological sciences, the concept of human modification predominated. The connotation was that an extraneous modification had distorted the natural appearance or performance of the tissue or organism studied. In microscopy, for example, an artifact may result from death, manipulation or reagents, and is not indicative of the actual structural relationship during life.

Itself a product of human workmanship, a roentgenogram is, strictly speaking, an artifact. In medical roentgenology, however, the term is usually used to designate an image that is not an accurate reproduction of the normal or abnormal structures examined. Thus a foreign body within a patient, whether it be a radiopaque pill, a surgical sponge or a graphite pencil in the thigh (Fig 11-1), is not truly an artifact. Neither is a radiopaque dressing, whether it lies on or extends beneath the patient's skin (Fig 11-2).

In general use, however, any density that may be mistaken for a structural lesion is usually considered an artifact. Such densities contribute some of the more interesting problems in diagnostic roentgenology. Sometimes they are normal structures, readily recognized on most roentgenograms, that are projected on the specific film so as to create an unusual

and disturbing shadow. For example, the penis may be shown on end, simulating a pelvic tumor (Fig 11-3). When the aurial pinna is bent forward, air caught between it and the scalp may suggest intracranial air (Fig 11-4). Even the shadow of the umbilical cord may confuse those not accustomed to viewing roentgenograms of infants. And a residuum of the silver nitrate that was used to cauterize the umbilical cord may simulate the calcifications of meconium peritonitis (Fig 11-5).

Internal structures may also be projected so as to cause diagnostic error. On a frontal chest roentgenogram if the patient is rotated slightly to the left the

Fig 11-1 Graphite (lead) pencil in the soft tissues of the thigh. Because the wood of the pencil is relatively more radiolucent than either the graphite core or the surrounding muscle, it appears as two radiolucent stripes (arrows). The graphite (lead) core is of water density. (Courtesy of Dr Eugene Blank, Pittsburgh.)



DR. JOHN DORST has written Section 11 ARTIFACTS AND NATURAL MISLEADING IMAGES

* Although the word 'artifact' is a relatively recent addition to the English language, related words from the same roots date from the late fourteenth century. The Oxford English Dictionary dates *artificer*, meaning *one who makes by art or skill* from 1393. The original meaning of *artificial-made or resulting from art contrived not natural*—is dated slightly earlier, 1382.

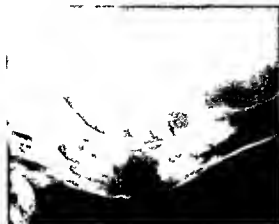


Fig 11-2—Iodoform gauze with a nuchal abscess. The surgeon who incised and drained the high nuchal abscess in this 9-month-old girl was disturbed by its proximity to the occipital



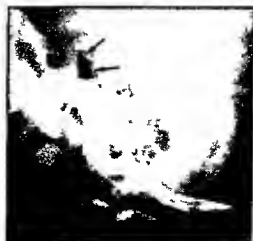
Fig 11-3—When the penicillin syringes (arrows) lay on the pelvic mass. Two examples are shown (Figs 11-3 and



11-4 courtesy of Drs. Thomas P. Coburn and F. Edwin Silverman Cincinnati.)



Fig 11-4—Traumatic pneumocephalus was initially suspected in this 13-month-old infant. Air that appears to be within the interpeduncular cistern (arrows) is actually caught between the scalp and the pinnas, which was bent forward.



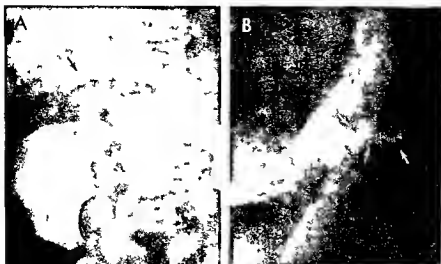


Fig 11-5 — In A, frontal projection, silver nitrate on the umbilical cord (arrow) of a newborn infant simulates meconium peritonitis. B, lateral projection shows the red density to be outside

of the peritoneal cavity and on the umbilical cord (arrows) (Courtesy of Dr. Hooshang Teybi, Oakland, Calif.)

sternal manubrium may simulate an enlarged aortic knob (Fig 11-6). Almost any elongated structure is difficult to identify when it is projected axially. In the case of the clavicle, this may occur on a frontal chest roentgenogram when an infant is only slightly turned (see Fig 11-33, A). A more important example is the uvula, which has been misinterpreted as a foreign body in the pharynx on Waters' projection of the face (Fig 11-7). In one 15-year-old boy, the short and unusually wide twelfth ribs simulated adrenal calcifications (Fig 11-8).

Among the surface structures that are likely to be misinterpreted, hair is a common offender. Practically every medical student learns to differentiate disease in the pulmonary apexes from "pigtails" over-

hanging the apexes. Yet when the pigtail is thin and secured by an elastic band, the experienced observer may misinterpret it as parenchymal disease with apical or hilar calcification (Fig 11-9). Occasionally brads extending down the back of the neck cast a shadow reminiscent of the nuchal ossification of fibrodysplasia ossificans progressiva (Fig 11-10).

Fig 11-7 — Axial projection of the uvula. In Waters' projection, which simulates a mass or foreign body in the pharynx of a 4-year-old girl.



Fig 11-6 — With the patient, a boy 8 years of age, rotated slightly to the left, the prominent manubrium simulates an enlarged aortic knob (Figs 11-6 to 11-8, courtesy of Drs. Thomas P. Coburn and Frederic N. Silverman, Cincinnati).

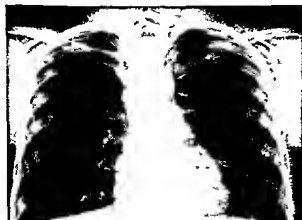




Fig. 11.8 —Unusually formed 12th ribs (arrows) that simulate adrenal or renal calcifications in a 15-year-old boy

Fig. 11.9 —A: oval densities (arrows) cast by an elastic band on the end of a hair band that cast a faint density within the curve of the first rib (A: courtesy of Dr. Andrew K. Poznanski, Ann Arbor, Mich.) B: a longer projection in the 10-year-old girl suggests

gas disease to the left of the superior mediastinum (white arrows). The rubber band securing the pigtail manometer calcification (black arrow). (Courtesy of Drs. Thomas P. Coburn and Frederick N. Silverman, Cincinnati.)





Fig 11 10 — A, nuchal ossifications in a 6 year old boy with fibrodysplasia ossificans progressiva. The zygapophysial joints are fused. B, hair braids on the back of the neck in an older girl. In the original roentgenograms, both the ossifications and the

hair braids could only be clearly discerned when viewed with a bright light. They had a similar appearance. The true nature of the shadows is well brought out in these logEtronic prints.

Fig 11 11 — Multiple hair braids on a 14 month old boy





Fig 11 12.—A pigtail (white arrows) that simulates an intracranial calcification on Waters projection of the skull of a 5 year old girl. It is secured by an elastic band (black arrow). (Courtesy of Drs Thomas P Coburn and Frederic N Silverman Cincinnati)



that simulates an intracranial calcification. The white arrows point to a line made with indelible ink on the original roentgenogram by one of the referring physicians. This type of artifact will not occur if physicians use grease pencils to mark roentgenograms. (Courtesy of Dr Andrew K Poznanski Ann Arbor Mich)

Intracranial calcifications may be mimicked by many shadows formed partly or completely by hair. Pigtails are usually readily identified on a lateral skull roentgenogram (Fig 11 11). They may more easily be confused with intracranial calcifications when they are shown only on frontal roentgenograms (Fig 11 12). The chewing gum a 13-year old girl stored in her hair before a pneumoencephalogram simulated an intracranial mass, such as an ependymoma (Fig 11 13).

The elaborate hair arrangement on a mentally retarded 3-year old girl caused considerable concern, particularly since the referring physicians anticipated that she might have intracranial calcifications (Fig 11 14 A). Inspection of her skull roentgenograms with a bright light, however, showed that the disturbing radiodensities extended beyond the confines of the skull. They were cast by a surprisingly radiopaque hair dressing that simulated intracranial calcifications on both frontal and lateral roentgenograms. The dressing proved quite tenacious. Four shampoos only redistributed it (Fig 11 14 B), three days and many shampoos later, some of the hair dressing was still present (Fig 11 14 C).

The classic example of extracranial radiodensities that simulate intracranial calcifications is the opaque paste used to fasten electroencephalographic electrodes to the scalp (Livingston and Paul). The resultant densities show on all standard roentgenographic projections (Fig 11 15). While their true nature

Fig 11 13.—This 13 year old girl placed her chewing gum in her hair for safekeeping before a pneumoencephalogram. The resultant shadow (arrow) suggested an intraventricular mass, possibly an ependymoma. (Courtesy of Drs Thomas P Coburn and Frederic N Silverman Cincinnati)



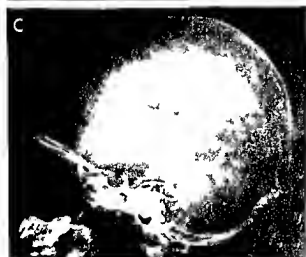
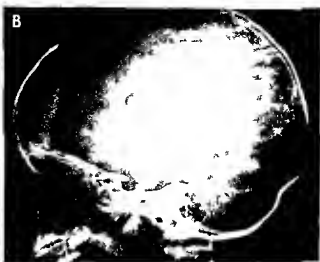


Fig 11-14 — A 3 year old moderately mentally retarded girl had an elaborate coiffure secured by a surprisingly radioopaque hair dressing. **A**, original study. **B**, 24 hours and four shampoos later. The curved radiodensity in the frontal region is caused by the pad of the head clamp. **C**, 3 days later. (See text for details.)

Fig 11-15 — Multiple dabs of electroencephalographic electrode paste on the scalp simulating multiple intracranial calcifications.

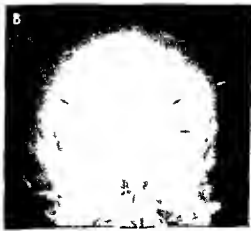
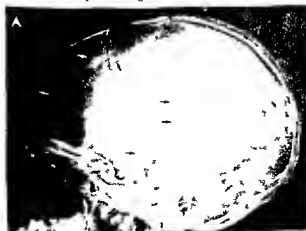


Fig 11-15 — Multiple dabs of electroencephalographic electrode paste on the scalp simulating multiple intracranial calcifications in a 6 year old girl studied because of seizures. **A**, lateral and **B**, frontal projections.

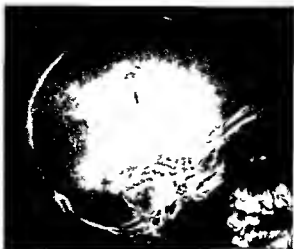


Fig 11 16 — Electrode paste distributed so as to suggest two calvarial defects with sclerotic margins in a 9-year-old male.

photograph (Courtesy of Drs. Thomas P. Coburn and Frederick N. Silverman, Cincinnati).

may be surmised from their position on the skull, the possibility that at least one of the radiodensities is cast by an actual intracranial calcification can often be ruled out only by roentgenograms repeated after a thorough shampoo. Rarely electrode paste may be distributed on the scalp and hair so that it simulates a cranial defect with sclerotic margins (Fig 11 16).

Such common external foreign bodies as earrings and metallic ornaments on a radiolucent necklace usually are easily identified. Confusion may occur, however, when the situation is unusual, such as an earring on either a boy or an infant (Fig 11 17) or when the ornament is positioned so that it appears to be within the trachea or esophagus (Fig 11 18). Commonly in such situations two roentgenograms will have been obtained at right angles. The object usually is seen readily only on one of the films. Frequently, however, it can be detected clearly outside of the patient. If the second film is viewed with a bright spot light. When the object has been moved between the

two exposures so that it superimposes the same part of the child on each roentgenogram, additional roentgenograms often are necessary to be certain that it is not within the child (Fig 11 19).

When the arm of a doll which she had clutched tightly to her side slipped under a 5-year-old girl, an artifact was created that was particularly appropriate to pediatric radiology (Fig 11 20). Similarly appropriate are the images of a pacifier handle projected over the mediastinum (Fig 11 21) and the staple in the spine of a comic book a lad placed beneath his abdomen for safekeeping (Fig 11 22).

The devices used to restrain infants and young children during filming frequently show on the roentgenograms. Occasionally they cause confusion or consternation, especially when the devices have not been

Fig 11 17 — Perced ear and earring in a 6-month-old infant.

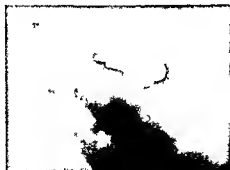


Fig 11 18 — Key hung around the neck on a string simulating a foreign body in the esophagus of an 8-year-old girl.



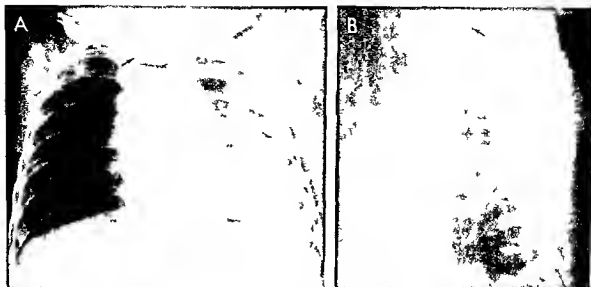
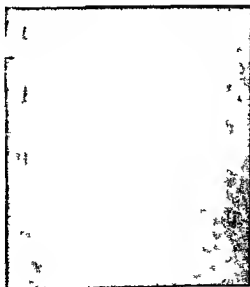


Fig 11 19 —A 5-month-old boy had fever, severe cough, and upper airway congestion. Both A, frontal, and B, lateral projections raised the possibility of a coin within the hypopharynx (arrows) that changed position with coughing. Actually the coin was

hung around the neck on a string that should have been removed. Instead the technician carefully positioned the coin away from the lungs, moving the coin between the two exposures.

Fig 11 20 — Security is a doll. This 5-year-old girl was willing to have an x-ray examination if she could keep her doll by her

side. The doll's arm slipped beneath her during the study and is shown superimposed on the left side of the abdomen.



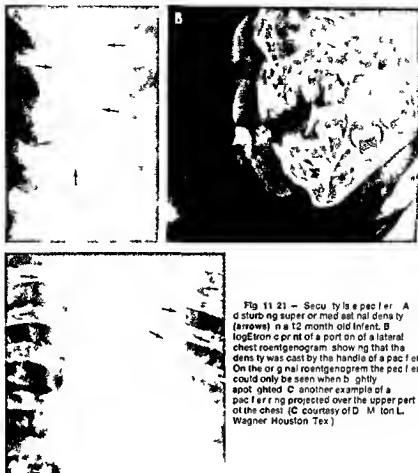


Fig 11-21 — Secu ty is a pac ier. A d sturb ng super or med iat nal dens ty (arrows) n a 12 month old Infant. B logEtron c p rnt of a port on of a lateral chest roentgenogram show ng that the dens ty was cast by the handle of a pac ier. On the o g nal roentgenogram the pac ier could only be seen when b ghtly spot ghted. C another example of a pac ier r ng projected over the upper part of the chest (C courtesy of D M ton L. Wagner Houston Tex.)

correctly used properly maintained or both (Fig 11 23) A disturbing example occurred in examining a 10-week old infant who had fallen from a bed The head clamp was so tightly applied that the posterior sponge indented the occiput which is normally fairly soft at that age and suggested a depressed skull fracture (Fig 11 24) Once the clamp was released the calvaria resumed its normal contour and a repeat roentgenogram showed no fracture

Drops of opaque roentgenographic contrast material located on a restraining band on the x ray table or on the child's clothing or wraps may simulate pathologic calcifications (Fig 11 25) Sometimes contrast material administered for a previous roentgenographic examination causes confusion Residual barium in the appendix was thought to represent a fecalith in a 7 year old girl with fever and abdominal pain for two weeks (Fig 11 26) Only after the density had disappeared on films made the next day could her physician elicit a reluctant confession from the par-

ents Three days earlier they had taken their child to another doctor who had performed a barium enema.

We encountered an unusual artifact while monitoring an excretory urogram of an infant Because the urinary tract was not opacified in 20 minutes we thought the contrast material might inadvertently have been injected subcutaneously A frontal roentgenogram of the injection site was made that showed an opacity suggestive of subcutaneous contrast material (Fig 11 27 A) The margin of the density was surprisingly regular however so a lateral roentgenogram was made that showed no contrast material in the arm (Fig 11 27 B) The technician explained the artifact Because the light in the localizing collimator had burned out she hung a crude plumb bob made from adhesive tape from the center of the collimator The swinging tape made the disturbing radiodensity This technician was considerably more helpful than the one who failed to remove the blouse when making skull roentgenograms of a 2 year-old girl. On the



Fig 11 22 (above left) —Staple within the spine of a comic book that this 4-year-old boy slipped beneath him for safekeeping as pyelography progressed (Courtesy of Drs Thomas P. Coburn and Frederic N. Silverman, Cincinnati.)

Fig 11 23 (above) —This infant was incorrectly positioned on the special wooden restraining board. Had he been placed higher on the board, the slots (white arrows) used in immobilizing the legs would not have shown. The multiple radiopaque lines and bands (black arrows) were caused by barium embedded in the board.

Fig 11 24 (left) —Fracture (horizontal arrow) simulated by compression of the occiput by tightly applied sponge of the head clamp (vertical arrows) (logEtron c print). Examination later after the clamp was removed showed normal occipital contour and no fracture. This infant was 10 weeks old. (Courtesy of Drs Thomas P. Coburn and Frederic N. Silverman, Cincinnati.)



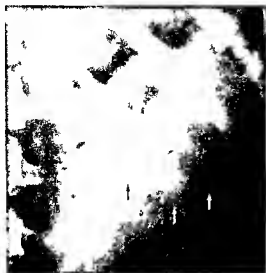


Fig 11 25—Left upper quadrant abdominal cysts with calcified walls simulated by droplets of water: so subtle radiographic contrast material that had dried on the top of the x-ray table. (Courtesy of Dr Andrew K. Poznanski, Ann Arbor, Mich.)



Fig 11 26—Barium in the appendix that simulates a fecalith. (See text for details.) (Courtesy of Drs Thomas P. Coburn and Frederick N. Silverman, Cincinnati.)

Fig 11 27—A, frontal projection shows apparent extravasation of contrast material into subcutaneous tissues of the arm.



during injection for an intermittent pyelogram. **B**, lateral projection proves the density to be an artifact. (See text for details.)





Fig 11 28 — Button on the blouse of a 2 year old girl projected within the foramen magnum on Towne's projection of the skull

(Courtesy of Drs Thomas P Coburn and Frederick N Silverman Cincinnati)

Towne projection the top button of the blouse was projected exactly within the foramen magnum (Fig 11 28). Another technician completely filled the concavity of a pectus excavatum with barium paste for the frontal as well as the lateral chest roentgenogram (Fig 11 29). A urethral stricture was simulated during a voiding cystourethrogram when a 7 year old boy was instructed to press the urethral tightly against his perineum (Fig 11 30).

Premature infants should be disturbed as little as possible. Particularly when ill they are best left in the incubator during filming. In this situation one roentgenographic artifact often occurs. The small hole in the incubator top is magnified by the diverging x ray beam and when projected over the lung or abdomen simulates an air containing cyst (Fig 11 31).

One of the most difficult problems in pediatric

roentgenology is mild pneumonia. Minimal respiratory motion may blur the normal vascular shadows sufficiently to mimic the early peribronchial consolidation of bronchopneumonia (Fig 11 32). Slightly greater motion may obscure early consolidation and falsely suggest that the chest is clear. Incorrect positioning may also confuse the diagnosis. During chest roentgenography an erect infant sometimes slouches into a lordotic position so that consolidation in the posterior portion of the lung base is hidden by the diaphragm (Fig 11 33).

Although not artifacts, optical illusions may similarly confuse the radiologist. The Mach effect can be particularly troublesome (Eaglesham). It is a thin radiolucent strip at the edge of a radiodensity. If this radiolucent strip falls over a bone as when the fingers are partly superimposed, it simulates a fracture

Fig 11 29 — A, unusual radiodensity on a frontal chest roentgenogram created by barium paste within the concavity of a pectus excavatum in an 8 year old girl. B, lateral projection from the

same examination. Our usual practice is to outline the deformity with a thin line of barium paste applied for the lateral chest roentgenogram only.

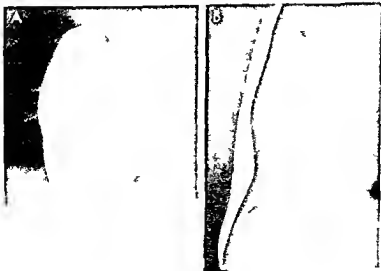


Fig 11 30 —A a 7 year old boy clamped the urethra (margin indicated by double arrow) tightly against his perineum during a voiding cystourethrogram simulating a urethral stricture (single arrow) B three months later the urethra is normal (Courtesy of Drs Thomas P Coburn and Frederic N Silverman Cincinnati)



Fig 11 31 —An 18 hour old boy was examined because of tachypnea grunting external retractions and mild cyanosis In A, the radiologist pointed out that the apparent lung cyst (arrows) was the shadow of the hole in the top of the Isolette magnified

by the diverging beam of x rays B a repeat roentgenogram obtained three hours after A, was necessary to stay the surgeon's hand (Courtesy of Dr Charles E Shoptner University of Alabama School of Medicine)

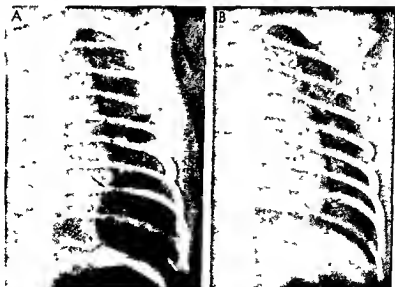




Fig 11-32 Slight respiratory motion blurs the vessels in a 7-day-old infant, making easily perceptible bronchial consolations. A repeat roentgenogram showed the lungs to be clear.

Fig 11-33 — A pneumonia in the left lower lobe is hidden behind the diaphragm on a lordotic projection of the chest. Arrow points to the right clavicle, which is projected axially because the shoulders are turned slightly to the right. B, left lower-lobe pneumonia with pneumatoceles (arrows) is clearly shown in lateral projection. (Courtesy of Drs. Thomas P. Coburn and Frederick N. Silverman, Cincinnati.)



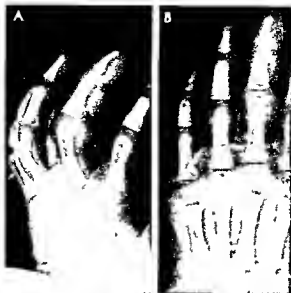


Fig 11-34—Pseudofractures. **A**, Mach bands simulating fractures (arrows) of the proximal phalanges of the 4th and 5th fingers. The Mach band simulating a fracture in the 4th finger (closed arrow) is adjacent to the skin of the anterior surface of the 5th finger. That simulating fracture in the 5th finger (white

arrow) is adjacent to the posterior surface of the 4th finger. Both of the pseudofracture lines could also represent air trapped between the fingers. **B**, frontal projection shows no fracture in either phalanx. (Courtesy of Dr Thomas Hendrick, San Diego, Calif.)

Fig 11-35—Shadow of a skin fold projected on the upper abdomen suggesting pneumoperitoneum or a lateral defect in the diaphragm of a 16 day old infant. (Courtesy of Drs Thomas P. Coburn and Fredrick N. Silverman, Cincinnati.)



line (Fig 11-34). Skin folds create similar confusion in part due to adjacent Mach effects. On a chest roentgenogram a skin fold may simulate pneumothorax while on a film of the abdomen it may suggest a pneumoperitoneum or a defect in the diaphragm (Fig 11-35).

Numerous artifacts may attend special roentgenographic procedures. One example is pertinent. With tomography, an extremely dense natural structure or foreign body is shown in planes other than the one it occupies. In these other planes it is distorted by the tomographic motion to create a confusing shadow often referred to as a "parasite shadow" (Fig 11-36).

Many artifacts relate to film handling and processing. These include chemical spots, pressure marks and crimping marks (Fig 11-37), as well as the effects of static electricity and of the transport systems of automatic film processors. Defects in the intensifying screens are common and especially disturbing. The right lower quadrant density shown in Figure 11-38 was initially interpreted as a fecalith. On reappraisal it was recognized that the density had exactly the same position on all three roentgenograms obtained, each of which was exposed in the same cassette. Such an analysis suggests that the radiodensity is an intensifying screen artifact. The supposition may be confirmed without additional irradiation of the patient by exposing another film in the same cassette. This technique proved particularly helpful in re-



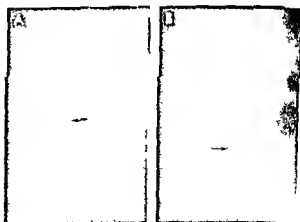
Fig 11-36 —A: parasitic shadow (arrows) of a metallic foreign body in the orbit on a linear tomogram. B: plain roentgenogram showing multiple metallic fragments. The fragment marked

with the arrow cast the parasitic shadow in A. (Courtesy of Dr. Andrew K. Poznanski, Ann Arbor, Mich.)

Fig 11-37 —Artifacts due to both crimping of the unexposed x-ray film (double arrow) and excessive pressure on the exposed film before it was processed (single arrows). The arrow points to only a few of the multiple artifacts.



Fig 11-38 —Apparent fecalith in a 1-month-old infant admitted because of constant crying and occasional vomiting. The density was first thought to represent a fecalith. Analysis of the original three roentgenograms (two of which are reproduced) indicated that it was a screen artifact. (See text.) (Figs 11-38 and 11-39 courtesy of Drs. Thomas P. Coburn and Frederic N. Silverman, Cincinnati.)



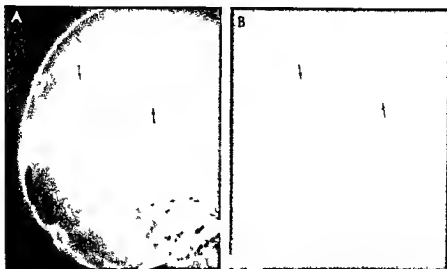


Fig 11-39 — A, skull artifact simulating intracranial calcification produced by glue that poorly attached the intensifying screen to the cassette B, roentgenogram of the intensifying

screen showing the disturbing redensities to be caused by the defective screen. Arrows point to corresponding screen artifacts.

evolving the artifacts on a skull roentgenogram that resulted when defective glue failed to hold an intensifying screen firmly in the cassette (Fig 11-39). Zimmer prepared a detailed catalogue of artifacts that are caused by faults in handling and processing x-ray films.

REFERENCES

- Eaglesham D C Visual illusions affecting radiographic interpretation *J Canad A Radiologists* 19:95 1968
- Livingston S and Paul L L Opaque areas on cerebral roentgenography simulating intracranial calcification caused by disease *J Pediatr* 64:772 1964
- Zimmer E A *Artifacts in Handling and Processing Faults on X-ray Films* (New York: Grune & Stratton Inc 1960)

Index

[An asterisk (*) following a page number indicates a reference to an illustration]

A

ABDOMEN 541-556
 after insufflation of perirenal spaces 816*
 masses genitourinary causes 1547
 muscle (see Muscle abdominal)
 musculature congenital deficiencies 545*
 in nephrosis 547*
 pain (see Pain abdominal)
 surface projection of organs 541*
 upper 542*
 in tracheoesophageal fistula, 590*
 tumors solid venacavography 1413
 urography of excretory 542*
 vessels of 556
 wall
 calcifications 546
 calcifications in myositis ossificans progressiva, 545*
 diseases 543-556
 ganglioneuroma of congenital 546*
 hypoplasia, and urinary tract dilatation 544
 thickenings of 545
 tuberculous abscess 546*
ABSCESSES
 brain 196-197*
 Brodie's 1197*
 cecum (see Cecum abscess)
 cold of hand 1201*
 intraperitoneal due to perforated appendix, 707*
 kidney 800-801
 metaphysis, 1192*
 nuchal gauze in 1574*
 penitendiceal, in perforated appendix, 703*
 penitendiceal, in pain in appendix 703*
 pulmonary 372-373
 hematogenous 374*
 retropharyngeal, 234*
 spine
 mediastinum and 443
 tuberculous 1389*
 subdiaphragmatic 548*
 thigh, 849*
 in tuberculosis (see Tuberculosis abscess in)
 in ulcerative colitis 704*

ACETABULUM
 normal 750*
 normal irregular margins 729*
 normal supra acetabular plicae of rarefaction 722*
 os acetabuli marginalis superior in cartilaginous rim 722
 protrusion, 749 750
ACHALASIA cncopharyngeal nasopharynx in 586*
ACMEIRIA 979*
ACHILLES TENDON
 ossification of 859
 visualization of 928*
ACHONDROPLASIA 56 57 255 257 998 1000
 calcifications congenita 1007*
 extremities in lower 1004
 femur in 1000* 1001*
 humerus in 1000*
 hyperplastic 1000 1370*
 hyperplastic flaring 1005* 1006*
 hypoplastic 999 1368*
 malacic form 1000
 pelvis in 740 741 1002
 comparison normal pelvis 740*
 roentgen features of 1000
 (in rat) 999*
 spine in 1003* 1004*
 tibia in 1000* 1001*
 ulna in 1000* 1001*
 vertebra in 1369
ACROMIUS hyperchloremic and calculi 796*
ACROSIS tarsoepiphyseal 1030*
ACROMIAL PROCESS 276*
ACTH
 in rheumatoid arthritis vertebra after 1310*
 skull after 1311*
ACTINOMYCOSIS lungs in 420
ADACTYLIA 979*
 incomplete 980*
ADDISON'S DISEASE 1312
ADENOCARCINOMA colon 711*
ADENOMAS
 enlargement, 233*
 obstructive hypertrophy 232* 233*
ADENOMA
 bronchial 374
 sebaceous extremities in 1317

ADENOMATOID ANOMALIES congenital cystic 1466-1468
ADRENAL(s) 813-818
 agenesis 1439*
 calcification 814*
 in newborn, 1559-1561
 rib stimulating 1576*
 after sepsis and convulsions in newborn 813*
 in Wolman's disease 815*
 cortex
 overfunction excessive chronic 1312
 underfunction primary chronic 1312
 corticosteroids (see ACTH)
 dysfunction skull in 82
 hemorrhage (see Hemorrhage adrenal)
 hyperplasia, in female pseudohermaphroditism, 817*
 insufficiency 818
 medullary function
 decrease 1312
 increase 1312
 neuroblastoma (see Neuroblastoma, adrenal)
 pituitary changes due to 1310-1312
 sympathoblastoma, 815*
 tumors 816-818
 classification 816
 in newborn 1561-1565
 vascular disturbances in newborn 1557-1559
ADRENOCORTICOSTEROIDS causing thymic atrophy 447*
ADENOGONITAL SYNDROME
 in female pseudohermaphroditism, 817*
 skull in 84*
AGAMMAGLOBULINEMIA lungs in, 365
AGANGLIONOSIS 1511-1515 1516*
 enterocolitis in 1515*
 Foley catheter in 1514*
 pyelography in 1512* 1517*
 rectal 684* 694*
 megacolon due to 690*
 megacolon and neurogenic 689*
AGENESIS
 corpus callosum, 208-210
 lung 315*

AGYRIA 206-207

AIR

- as artifact 1574*
- between fingers simulating fracture 695*
- simulating humeral fracture 909*
- subdural 163-166
- during pneumoencephalography 164*

AIRBLOCK 1453-1456

syndrome 1452*

AIRWAY OBSTRUCTION

- mechanical, 1441
- upper and pulmonary hypertension 529

ALBERS SCHÖNBERG DISEASE 57-56*

1035-1037

ALBUMIN lung scan 1424*

ALDRICH SYNDROME lungs in 364

ALIMENTARY TRACT

- disease extremities in 1320
- duplications 443
- fetal 578-580

ALKALPTONURIC ARTHRITIS 1346

ALLANTOIC STALK 543*

ALLERGY

- lung reactions 368-369
- milk allergy pneumonia, 368

ALVEOLI

- growth comparison of prenatal and postnatal 1437*
- in microthanas 379-380
- in proteinosis pulmonary 380

AMEBIC COLITIS 701

AMELIA 979*

AMNIOTIC FLUID intrauterine

- aspiration, 297

AMPHIBARTHROSIS 1326

AMPUTATION Incomplete congenital, 992*

AMYOPLASIA CONGENITA 668-669*

- knee and patella in 669*

AMYOTONIA CONGENITA

- muscular atrophy in 670*
- paralytic thorax and 253*

ANAPHYLACTOID PURPURA, 669

ANASTOMOSIS

- in esophageal atresia with tracheoesophageal fistula, 566*
- of esophageal segments 566*

ANDRÉ VON ROSEN METHON in hip

- dislocation 737*

ANDROGENS and intersex, 625

ANEMIA

- aplastic and moniliasis 599*
- cardiac enlargement in 475-476*
- Cooley's (see Mediterranean below)
- erythroblastic 1284
- esophageal ulcer and 604*
- Fanconi's 1252-1283
- hemolytic 86-90
- biliary calculi in 567*
- chronic 1283*
- familial 1288
- spherocytic 1288
- vertebra in, 1393
- hypoplastic congenital, 1282-1283
- iron deficiency 90-91*
- calvaria in 91*
- cranium in, 91*
- Mediterranean 87*-89* 1283*
- 1284-1285*
- differential diagnosis 1298*
- maxillary sinuses in, 110*

nbs in 282*

vertebra in 1393*

sickle cell (see Sickle cell, anemia)

spherocytic 89*-90*

trichobezoar and 624*

vertebra in 1393*

ANEURYSM (s)

arteriovenous pulmonary 325

carotid angiography of 214*

intracranial, 214-215

mycotic 216

vein of Galen 215-216

ANEURYSMAL BONE CYST 1259*-1262

ANGIOCARDIOGRAPHY

cardiothymic image 451*

ciné of ductus bump in newborn

1454*

in corrected transposition of great

vessels 512*

heart 465

in tricuspid atresia, 516*

of ventricular defect, 1425*

ANGIOGRAPHY

brachial 168*

carotid 169*

aneurysm 214*

arachnoid cyst and corpus callosum

absence 209*

ependymoma, cystic 188*

bead enlargement 201*

hematoma, subdural 201*

vein of Galen aneurysm 216*

cerebral, 167-170

in abscess 197*

kidney 769-770

in lung total nonperfusion, 1424*

in newborn safety of 1412-1413

selective 465-466

umbilical 1408-1413 1547

ANGIOMA spinal cord 221*

ANGIOMATOSIS regional, 1273

ANKLE

in arthritis after bacteremia, 1011*

in battered child syndrome 1141*

chondrosarcoma, 1251*

foreign body in soft tissues of 864*

in osteosclerosis 1066*

rhabdomyosarcoma, 1281*

ANOMALIES

anus

- congenital 1524-1531
- tracheoesophageal fistula and 591
- aorta, right sided branches of 485*
- aortic arch (see Aortic arch anomalies)
- Arnold Chian (see Arnold Chian malformation)
- arteries
- left coronary 491 492*
- subclavian 484 1471 1476*
- subclavian esophagus bx, 1473
- associated with scoliosis congenital, 1358*
- bladder congenital, 782-785
- bones congenital 978-998
- brain (see Brain, anomalies)
- bronchi, congenital, 305
- bronchopulmonary foregut 321*-322*
- "butterfly" deformity of vertebral body 1363*
- cerebral, congenital, 202-210
- cystic adenomatoid, congenital, 1466-1468

Dandy Walker 177-179

cyst in 178*-179*

Einstein's of tricuspid valve 518 520

esophagus cervical congenital 230-231

extremities congenital, O Rahilly

classification 979*

heart (see Heart anomalies)

hemivertebra, 684*

intestine

large 678-686

small, congenital 635-637

jejunum 639*

joints congenital 1332

kidney (see Kidney anomalies congenital)

Kimer's deformity 1074*

lungs congenital, 314 323

mediastinum congenital, 431

nose

external, 99

internal 101

omphalomesenteric duct persistence

causing 543*

ostalocalcaneum 927*

pelvis congenital, 730-740

pericardium, congenital 509

pharynx congenital 230-231

pulmonary venous return 504-508

anomalous vertical vein 506

left superior vena cava and 506

partial, 506-507*

total 505* 506*

rectum congenital, 1524-1531

rib (see Rib anomalies)

spine (see Spine anomalies)

stomach, congenital 612-613

stress deformities of epiphyses round

bones and metaphyses 1148-

1165

trachea, congenital 305

ureter congenital 777-782

urethra, congenital 784-785

urinary tract congenital, 770-785

veins total anomalous venous return

1458*

vena cava, 1413-1418

ventricle angiocardiology of

1425*

vertebra, congenital, 1358-1369

ANUS

- anomalies 1524 1531
- tracheoesophageal fistula and, 591
- atresia, 681* 682-684
- duplication causing 685*
- fistulas in 683*
- rectal distention after surgery 696*
- ectopic 835-839
- clinical types of 837*
- embryology of 836*
- in posterior fourchette 839*
- Imperforate 683* 835-839 1524-1525
- dysmorphic sacrum and 1544*
- giant vagina and 1556*
- hypospadias and, third-degree 837*
- inverted films in 1525
- rectourethral fistula and, 1544*
- in syndrome of multiple anomalies 771*
- type III fistulas in, 682*
- stenosis 681* 682-684 1530*
- structure in syndrome of multiple anomalies, 771*

- AORTA**
(See also Aortic)
cervical 485
coarctation (see Coarctation of aorta)
convergence with inferior vena cava
in asplenia, 481
right sided anomalies of branches
485*
- AORTIC** (see also Aorta)
- AORTIC ARCH**
anomalies 484
diagrammatic representations
1472*
- esophagus and trachea in 1471
double 485 486* 1471
right 484
tracheography 485*
- AORTIC ATRESIA** 1566
- AORTIC KNOR** manubrium simulating
1575*
- AORTIC STENOSIS** (see Stenosis aortic)
- AORTIC THROMBOSIS** umbilical
aortography in 1413*
- AORTIC VALVE** 528
bicuspid 491 495
disease cardiac shadow in, 525*
insufficiency in rheumatic heart
disease 528*
- AORTICOPULMONARY SEPTAL DEFECT**
494 495
arteriography in retrograde left
brachial, 495
- AORTICOPULMONARY WINDOW** 494
495
arteriography in retrograde left
brachial, 495
- AORTOGRAPHY**
in hamartoma, fetal renal 1410*
in hemangioma, hepatic 1406*
1409*
- in neuroblastoma, 809*
adrenal 1405*
retropentoneal, left 1405*
umbilical, 1410
in arteriovenous malformation
1411*
in renal agenesis 1411* 1541*
in thrombosis aortic 1413*
urinary tract, 769 770
Wilms tumor metastases 1407*
- APLASIA**
bones congenital 978-988
digits 980*
extremities 978 981
femur 989
fibula, 988 989
forearm, 980*
hand 980*
kidney 774
lung 314 316*-317*
in newborn 1469-1470
metacarpals 980*
phalanges, 980*
radius 989
tibia, 989
- APPOPHYSIS OF ISCHIUM** avulsion
fracture 745* 746*
- APPENDICEAL COPROLITH** 702*
- APPENDICITIS** 702-707
appendicolith and bowel dilation in
706*
- APPENDICOLITH** 703*
calcifying in appendicitis 706*
- APPENDIX**
foreign body in, metallic 703*
invaginated stump causing cecal
filling defect 706*
- PERFORATED** 703*
intraperitoneal abscess due to 707*
peritonitis and 548*
- PN** in 703*
- RETROCECAL** 705*
- COILED** 704*
- RETROCECAL** 705*
- AQUEDUCTAL STENOSIS** (see Stenosis
aqueductal)
- ARACHNOIDACTIVELY** 1058* 1059*
- ARACHNOID CYSTERN** 152*
- ARACHNOID CYSTS**
congenital 196
corpus callosum absence and 209*
- ARACHNOIDITIS** and meningitis 179*
- ARM**
(See also Forearm)
in dwarfism, diastrophic 1020*
emphysema of interstitial, 868*
in enchondromatosis 1027*
fractures in osteogenesis imperfecta,
1040*
in macropolysaccharidosis 1 1047*
1054*
in Ollier's chondromatosis 1024*
in osteodystrophy fibrosa 1061*
in osteogenesis imperfecta, 1043*
in Pyle's disease 1068*
upper soft tissues of 847*
- ARNOLD-CHIARI MALFORMATION** 179-
181
aqueductal stenosis and 180*
meningomyelocele and 180*
- ARRHENOTECHELY** 207 208
trisomy 13 15 and 207*
- ARTERIES**
brain anomalies 212 213
bronchial anastomosing
arteriography of 1407*
carotid looping 216
coronary (see Coronary artery)
ectopic compression tracheal
compression 308*
great, transposition of 384* 509
corrected 512*
hypoxia due to 1384*
septectomy in thymus after 450*
innominate tracheal compression by
1473 1476*
intracranial occlusions 217 218
pulmonary
absence 317*
anomalies 1475*
anomalies esophagus and trachea
in 1471 1477
left, ectopic 486*
poststenotic dilatation, 502* 503*
slung 485 488
stenosis 504*
subclavian
anomalies 484 1471 1476*
anomalies esophagus in, 1473
arteriography 486*
ectopic right 484*
- ARTERIOGRAPHY**
bronchial 1407 1408
bronchial arteries anastomosing
1407*
in carcinoma, hepatic 1406*
carotid in Menke's syndrome 217*
in hamartoma, liver 1406*
- hemorrhage and 1407 1408
in hepatoblastoma, 1406*
in hypertension, 1408
in neuroblastoma, 1407
in newborn, 1403 1419
in pulmonary artery slung 487*
renal in laceration 799*
retrograde left brachial in
aorticopulmonary septal defect
495
splenic cyst 1428*
splenic trauma, 1408*
subclavian artery 486*
trauma and 1407-1408
vein of Galen aneurysm 215*
- ARTERIOSCLEROSIS** upper extremity
and hyperparathyroidism 861*
- ARTERIOVENOUS**
aneurysms pulmonary 325
fistula (see Fistula, arteriovenous)
shunt 1404*
- ARTHRALGIA** in adrenal
neuroblastoma, 808*
- ARTHRITIS**
alkaptonuria 1346
after bacteremia, 1010 1011*
foreign body 1334
hip traumatic, 1335*
hypertrophic 1338
infectious 1333-1336
knee 1200* 1335*
leukemic 1337 1338
purulent knee in 1335*
rheumatoid (see Rheumatoid
arthritis)
spondylarthritis 1387
tuberculous 1337
joints in 1202
- ARTHOCHALASIS MULTIPLEX**
CONGENITA 855
- ARTHOGRAPHY** in labrum infolding in
hip dislocation 733*
- ARTHOGRYPHOSIS CONGENITA** (see
Amyoplasia congenita)
- ARTICULAR TISSUES** calcifications in
extremities 863
- ARTIFACTS** 1573 1590
- A SCAN** 1432*
in hydronephrosis 1546*
in Wilms tumor 1546*
- ASCARIS** in ileum 671*
- ASCENDING LIPIODOL** in
cystourethrography 769*
- ASCITES**
bladder rupture causing in newborn
1552*
chylous 1537*
lymphangiography in 1420-1422
colonic perforation and 1399*
cytomegalic inclusion disease and
1399*
in newborn, 1533 1538
pneumovagina and 1527*
ureterocele and, in newborn 1550*
- ASPERGILLIOSIS** pulmonary 420
- ASPLENIA**
convergence of aorta and inferior
vena cava in, 481
syndrome 1501*
technetium scan in 1429*
- ASTHMA**
atop c 254*
bronchial, 309 311
atelectasis in 310*

ASTHMA (Cont)

- emphysema of 254* 255* 333*
- microcardia and 477*
- ASTROCYTOMA
 - calcification in 133*
 - cerebellar 190*
- ASYMMETRY 1315
- calvaria, 98*
- ATAKIA TELANGIECTASIA
 - lymphoma in, 571
 - pancreatic sarcoma in 571*
- ATLECTASIS
 - in asthma, bronchial, 310*
 - in bronchiectasis 313*
 - compensatory 326
 - compression marginal, 326*
 - cystic fibrosis of pancreas and, 361*
 - laryngeal polyps and 237*
 - obstructive 328-332
 - causal mechanism 327*
 - massive 327*
 - massive foreign body study 328*
 - in tuberculosis pulmonary 413*
 - pneumonia and lobar 343*
 - simulating double diaphragm 287*
 - in tuberculosis pulmonary 403*
- ATLAS aneurysmal cyst 1261*
- ATRESIA
 - anus (see Anus atresia)
 - aortic 1566
 - biliary 659* 1531 1532*
 - cholangiography in 563* 1532*
 - bronchial in newborn 1466
 - choanal 102* 1440*
 - colon 681* 1530-1531*
 - duodenum (see Duodenum atresia)
 - esophagus (see Esophagus atresia)
 - as fetal vascular insult 1502
 - ileum 650*, 1503*
 - intestine
 - development of 638*
 - large 681-682
 - pulmonary 520
 - pulmonary vein common 506
 - rectum, 681* 682-684
 - fistula in 683*
 - stomach 613-614
 - tricuspid 515*, 516
- ATRIOVENTRICULAR CANAL 499*
- ATRIUM
 - interatrial septum
 - defect 498*
 - defect high 497
 - patency of 497-501
 - left superimposed on right atrium 470*
- ATROPHY
 - bone 964-965
 - cerebral 202-203
 - unilateral 204*
 - muscular
 - of extremities 870-872
 - after poliomyelitis 872*
 - in rickets 1225*
 - skin follicular 1322
 - thoracic wall, 265*
 - (thymus (see Thymus atrophy))
- AURICULO-OSTEODYSPLASIA 50
- AUTOMOBILE SEAT BELT INJURIES (see Seat belt injuries)
- AUTONOMIC DYSFUNCTION familial, lungs in 364 365
- AVITAMINOSIS 1222-1243

AVULSION

- epicondyle 1105* 1106*
- femoral epiphysis 1126*
- femoral trochanter 1170*
- fracture of trochanter 1126*
- ossification centers traumatic 1170
- AXIS MALFORMATION in dysmelia, 979-981
- AYERZA'S SYNDROME lungs in 380
- AZOTEMIA and pulmonary edema, 323*
- AZYGOS LOBE 318-319
- AZYGOS VEIN arch of 426-428

B

BACILLUS INFECTION gas in fetus 579*

BACK

- hair braid superimposed on, 263*, 266*
- in myositis ossificans progressiva, 545*
- straight back syndrome 249-250 480
- BACKWASH ILIITIS* in ulcerative colitis, 609* 700*
- BACTEREMIA arthritis after 1010-1011*
- BACTERIA arterial channels for invasion of bone 1192*
- BAKER'S CYST 1336*
- BANDS
 - as artifacts 1576*
 - bone 972-976
 - bismuth 974-975
 - lead 972-974
 - phosphorus 721* 975-976
 - after plumbism 974*
 - radium, 975
- BANTI'S SYNDROME 625
- esophageal varices in 600*
- gastric varicosities in, 601*
- BARIUM
 - esophagography of aberrant subclavian artery 484*
 - paste as artifact 1585*
 - peritonitis 554-556
- BASIPHARYNGEAL CANAL persistent 120*
- BASS SYNDROME 1325
- BATHROCEPHALY 14*
- BATTERED CHILD SYNDROME 1132-1148
- "BATTERED" INFANT ribs in 283*
- BCC VACCINE and calcification in tuberculosis 418 419*
- BILE IN GALLBLADDER 1531
- BILIARY ATRESIA 659* 1531 1532*
 - cholangiography in 563*, 1532*
- BILIARY BRONCHIAL FISTULA 1531-1533
- BILIARY CALCULI in hemolytic anemia, 567*
- BILIARY DUCT
 - congenital cystic dilatations 564*
 - in newborn 1531-1538
- BILIARY PERITONITIS in newborn, 1537*
- BILIARY TRACT 562-567
 - diseases 563-567
 - normal, schematic drawings 562*
 - tracheobiliary fistula, 566*
- BIOPSY injury causing tubulation

failure of femur 967*

BIRD-HEADED FETAL DWARFISM 1075*

BISMUTH BANDS 974-975

BLADDER

- anatomy normal 756
- anomalies congenital 782-785
- calculi in 795*
- oxalate stone 796*
- diverticula, 782-783
- Hutch, 783*
- duplication 685*
- ears 760* 1543*
- ectrophy 731*, 783-784 839-844
- clinical types 841*
- construction of vagina in 843*
- embryology 839-840*
- gentiography in 842*
- pyelonephritis and 802*
- hermia, transitory 780*
- hypertrophy in meatal stenosis 792*
- neck, 1549-1551
- neurogenic 1541*
- obstruction, 788-790
 - of neck in newborn 1542*
 - of outlet 789-790
 - in syndrome of multiple anomalies 771*
- rupture in newborn ascites due to 1552*
- trabeculated and reflux 790*
- urography of excretory 758*
- BLASTOMYOSIS lungs in 420
- BLEEDING (see Hemorrhage)
- BLOCK
 - airlock 1453-1456
 - syndrome 1452*
 - heart congenital, 1433*
- BLOOD
 - clot, ureteral shadow due to 798*
 - diseases 86-96
 - bone changes in 1279-1299
 - supply of growing bone 874-878
- BLOUNT'S TITIA VASA, 1172-1175*
- BODY total body opacification in newborn 1399-1403
- BONE(S)
 - (See also Skeleton)
 - anomalies congenital, 978-998
 - aplasia, congenital, 978-988
 - arterial channels through which bacteria invade 1192*
 - atrophy 964-965
 - bands (see Bands bone)
 - blood supply of 874-878
 - carpal necrosis 1178* 1179*-1180
 - constriction 966-969
 - cyst aneurysmal, 1259*-1262
 - development, alterations in 976-977
 - electrical potential in stress effects of 1062
 - electrical trauma to 1082
 - of extremities (see Extremities bones)
 - facial fibrous dysplasia of 86*
 - frontal dermoid cyst of 225*
 - growth
 - alterations in 976-977
 - effects of excessive heat on, 1083*
 - of hand (see Hand bones of)
 - hypertrophy 965
 - hypoplasia, congenital, 978-988
 - innominate appearance of secondary ossification centers in, 718*

interparietal, 12° 15° 16° 31°
 normal 11°
 ossification center in 13°
 intrasutural 12°
 ischial retarded ossification of 724°
 islands scleroses of 961-963
 long
 (See also tubular below)
 bowing of prenatal (see Bowing
 prenatal, of long bones)
 modeling of failure 885°
 modeling of normal 885°
 nutrient canals in 876°
 ossification centers in appearance
 of 879°
 splicing of 1066-1071
 lymphangioma, lymphangiography
 of 1422
 lymphosarcoma, 1277
 marble (see Osteopetrosis)
 marrow (see Marrow)
 occipital
 at birth 10°
 at eleven years 26°
 in paralytic disorders 1129
 parietal 15° 28°
 bilobed bilateral 18°
 congenital defects drawings of 39°
 in epidermoids 96°
 fracture 70° 71° 72°-73°
 in osteogenesis imperfecta 1041°
 rubber band superimposed on 225°
 in syphilis 80°
 veins of 27° 28°
 in visceral larva migrans 81°
 pelvic
 normal vascular markings 721°
 ostetis 747°
 pubic (see Pubic bones)
 rarefaction 964-965
 round stress fractures and
 deformities of 1148-1185
 sclerosis 885
 spheonod 120-121
 fibrous dysplasia of 88°
 synchondrosis of 120°
 spotted 1059-1061
 supraoccipital accessory bones of
 18°
 suprasternal in adult 268°
 sutural juvenile 23 32, 35
 tarsal (see Tarsal bones)
 temporal 111-120
 anatomy normal 111-113
 curved section of 112°
 diseases of 115-117
 neonatal, 113°
 pneumatization 113-115
 roentgenographic features 112°
 surface projection 111°
 thoracic wall, 267-285
 transverse lines of Park (see
 Transverse lines of Park)
 in tuberculosis 1199-1202
 tubular
 (See also long above)
 lamellar arrangement in cortex of
 873°
 macroscopic components of 875°
 tumors (see Tumors bone)
 wormian 13°-14° 31° 32° 33°
 ossification center in 11°
 wrist (see Wrist bones)
 BONNEVILLE-ULRICH DISEASE causing

skeletal changes 1312-1314
 BOWLING
 dilation in appendicitis 706°
 in mentis stenotic regional 667°
 lymphosarcoma, 702°
 pseudoseparation of loops 547°
 small
 duplication 1507 1510°
 gas 1482°
 in newborn 1502-1511
 obstruction in newborn 1480°
 BOWLING PRENATAL OF LONG BONES
 994-998
 schematic drawing of pressure and
 tension in 996°
 schematic drawing of probable faulty
 fetal positions in 995°
 BOWLING 1185 1189
 conversion to knock knee 1187°
 BRACHIAL ANGIOGRAPHY 168°
 BRACHMAN DE LANGE SYNDROME
 1072-1073 1074°
 BRACHYMELODACTYLY 1325
 BRAIDS OF HAIR as artifacts 1576°-
 1577°
 BRAIN 151-219
 abscess 196-197°
 anomalies
 corpus callosum absence and 210°
 vessels 212-219
 enlargement in Canavan's spongy
 degeneration 185°
 growth of 143-149
 metastases 187°
 scanning (see Scanning brain)
 tumors calvaria in 148°
 ventricles
 age dependent changes in, 160°
 anatomy 152-160
 cyst of 193°
 pneumoencephalography 156°
 vessels anomalies 212 219
 BRANCHIAL ARCHES cervical structures
 derived from 231°
 BRANCHIAL CLEFT CYST thyroid 1423°
 BREAST
 adolescent superimposed on thoracic
 wall 261° 262°
 pigeon 252
 BREACH DELIVERY hydrocephalus
 after 182°
 BRODIE'S ABSCESS 1197°
 BRONCHI
 adenoma, 374
 anomalies congenital 305
 arteries anastomosing arteriography
 of 1407°
 arteriography 1407-1408
 asthma 309 311
 atelectasis in 310°
 atresia in newborn 1466
 esophageal communication 1491
 growth comparison of prenatal and
 postnatal 1437°
 during inspiration and expiration
 298°
 lesions in pulmonary tuberculosis
 404°
 neoplasms 314
 normal 297
 obstructions 325 326-339
 pneumatocele due to 339°
 pathologic changes 308-314
 tracheal 307°

wall in pulmonary tuberculosis 403°
 BRONCHIAL-BILIARY FISTULA 1531-
 1533
 BRONCHIECTASIS 311-314
 alelectatic compensatory 313°
 bleb of Hodson and France in
 cystic fibrosis of pancreas 364°
 cavities in 373°
 compensatory in pulmonary
 tuberculosis 413°
 cylindrical, 311°
 honeycombing of 310°
 sacculus 312°
 bronchography in 313°
 segmental congenital, 305 306°
 BRONCHIOLITIS thymus after 445°
 BRONCHOSOPHAGEAL FISTULA, 317-
 318
 BRONCHOGENIC CYST 378° 440°
 BRONCHOGRAPHY 309°
 of biliary bronchial fistula, 1533°
 in bronchiectasis sacculus 313°
 emphysema 1464°
 in respiratory distress syndrome
 1448°
 tracheobiliary fistula, 566°
 BRONCHOPNEUMONIA
 chronic 360
 interstitial, 355-360
 nitrogen dioxide 371-372
 BRONCHOPULMONARY COMMUNICATION
 322°
 BRONCHOPULMONARY DYSPLASIA 1448°
 BRONCHOPULMONARY FOREGUT
 ANOMALY 321°-322°
 BUCKET HANDLE DEFORMITY OF
 TIBIA 1137°-1138°
 BULL-EYE PATTERN in vertebral
 calcification 1388°
 BURKITT'S TUMOR mandible in 128-
 127
 BURSA normal structures 1329°
 BURRITIS 1336
 BUTTERFLY DEFORMITY OF
 body 1363°
 BUTTOCKS
 calcium gluconate in 864°
 pencil in soft tissues of 865°
 BUTTON as artifact 1585°
 BUZZING RALLY BUTTON 1412°

C

CAPÉ AU LAIT PATCHES and
 neurofibromatosis 1270°
 CAFFEY KEMPE SYNDROME 1132-1148
 CALCANEOVALGUS FOOT 988
 CALCANEUS 918 922
 apophyses 918°-919°
 in Brodie's abscess 1197°
 coalition with cuboid 986°
 epiphysis stress compression of 1171
 fracture 1110°
 false 920°
 ossification centers double 920°
 pseudocystic circle in normal 922°
 roentgen appearance normal, 919°
 sclerosis and 919° 920° 963°
 secundarius 920° 921°
 CALCIFICATION
 (See also Calculi)
 abdominal wall, 546
 in myositis ossificans progressiva,
 545°

CALCIFICATION (Cont.)

- adrenal (see Adrenal(s) calcification)
- appendicolith in appendicitis 706*
- in astrocytoma, 133*
- of cartilage 1346-1347
- cerebrum (see Cerebrum calcification)
- choroidal plexuses 131*
- cranium (see Cranium calcification)
- in dermatomyositis 858*
- disks 1385-1386
- in ductus arteriosus dilatation 495
- of extremities (see Extremities calcifications)
- eye 140-141
- falx cerebri normal 131*
- in hematoma, suprarenal 814*
- in histoplasmosis 422*
- of joints 1346-1347
- kidney nb simulating 1576*
- larynx 308*
- cartilages 230
- ligaments
- interclunoid 132*
- petroclunoid 133*
- stylohyoid 229*
- stylohyoid physiologic 229-230
- liver
- in granulomatous 559*
- in newborn 1533
- in visceral larva migrans 559*
- lymph nodes, abdominal 576*-577*
- in lymphadenitis 409*
- in lymphangitis 409*
- after measles encephalomyelitis 857
- mesenteric cyst 575*
- of muscle after poliomyelitis 857
- neck physiologic 229-230
- in neuroblastoma, renal 807*
- nucleus pulposus, 1386*
- overcalcification (see Overcalcification)
- Pachionian bodies 131*
- pancreas in dwarfism, 572*
- peribulbar idiopathic 1347
- in pericarditis constrictive 531*
- pineal body 130*
- in polyp, intracardiac 534*
- severe traumatic fragmentation of provisional zones at 8 months 1135*
- in Sturge Weber syndrome 134*
- of teeth (see Schematic representation 122*)
- thyroid cartilage 229*
- trachea, 308*
- in tuberculoma intracerebral 134*
- tuberculosis (see Tuberculosis calcification)
- undercalcification (see Undercalcification)
- CALCINOSIS
- circumscripta, 852*
- interstitialis 852*
- of kidney 796*
- tumoral 1346*-1347*
- universalis 851-852* 853*
- CALCIUM GLUCONATE
- in buttocks 864*
- in soft tissues at elbow 864*
- for tetany in newborn 863*
- CALCULI
- (See also Calcification)

- biliary in hemolytic anemia, 567*
- bladder 795*
- oxalate stone 796*
- intrapelvic 795*
- kidney 796*
- pelvis 797*
- nb hypoplasia resembling 798*
- staghorn 795*
- ureteral shadow due to, 798*
- urinary 795-798
- CALIX normal, 758*
- CALVARIA
- asymmetry of 98*
- in brain tumor 148*
- in cephalhematoma 63*
- defect electrode paste simulating 1580*
- depressions congenital 67-69
- drug reactions in 96
- in dystrophy polyostotic fibrous 85*
- in Engelmann's disease 1064*
- in epilepsy after Dilantin 97*
- fractures (see Fractures calvaria)
- granuloma, eosinophilic 95*
- in hyperphosphatasemia, 1233 1234*
- in iron deficiency anemia, 91*
- in Kenny dwarf 1079*-1080*
- in neuroblastoma, adrenal 806*
- osteomyelitis hematogenous 78*
- in osteopetrosis tarda, 1038*
- in polycythemia, 92*-93*
- relationship to great sutures 34*
- symostosis of premature 41* 43*
- in tuberculosis 79*
- CALVE
- osteochondritis vertebralis 1377*
- vertebra plana (see Vertebra plana, Calve)
- CAMPOTODACTYLY 1181
- CANAVAN'S SPONGY DEGENERATION
- ventriculography in, 183*
- CANCER
- extremities 1267-1279
- ovarian metastatic to lung 378*
- CANNON'S LEVEL in normal colon 677*
- CAPITELLUM 907*
- humerus osteochondrosis of 1176-1177
- CAPUT SUCCEDANEUM 61
- CARIEAT SELF INJURIES (see Seat belt injuries)
- CARBOHYDRATE METABOLISM
- ABNORMALITY and dwarfism 572*
- CARBON DIOXIDE contrast studies in newborn 1431-1435
- CARBUNCLE 800 801
- CARCINOMA
- colon 710-711
- liver arteriography in 1406*
- CARDIAC (see Heart)
- CARDIOANGIOGRAPHY (see Angiocardiography)
- CARDIODIAPHRAGMATIC ANGLE right in pericardial effusion 531
- CARDIOMEGALY
- fistulous 472*
- fistula and intracranial arteriovenous 476*
- fusion of thymic and cardiac images to suggest 470*
- gutter and 477*
- lung scan in, 1425*

- pleural effusion and tachycardia, 475*
- pulmonary edema and 324*
- thymus and 451*
- CARDIOMYOPATHY 532*
- obstructive 532
- in diastole 533*
- CARDIOSPASM 597 598*
- CARDIOTHORACIC INDEX 470-473
- CARDIOTHYMIC IMAGE 451*
- CAROTIDOCRAVENOUS SINUS FISTULA, 213
- CAROTID ANEURYSM 214*
- CAROTID ANGIOGRAPHY (see Angiography carotid)
- CAROTID ARTERY looping 216
- CARPAL BONES necrosis 1178* 1179*-1180
- CARTILAGE
- in arthritis rheumatoid 1338*
- calcification of 1346-1347
- disoid of knee 1332
- epiphyseal of metacarpals 898*
- in exostosis (see Exostosis cartilaginous)
- hair hypoplasia of McKusick 1035
- plate 875*
- epiphysis and metaphysis of 876*
- injuries 1129
- injuries classification by Salter and Harris 1130*
- injuries of femur 1125-1126 1131*
- longitudinal section 876*
- longitudinal section (in puppy) 877*
- normal structure 874*
- of ulna, 903*
- CAT
- in osteomyelitis muscular atrophy after 872*
- plaster body in scoliosis diaphragmatic obstruction after 860*
- CAT SCRATCH FEVER 1204*
- CATHETER
- Foley in anguilliosis 1514*
- in respiratory distress syndrome 1446*-1447*
- CATHECTERIZATION
- cardiac 465
- umbilical safety of 1412-1413
- CAUDA EQUINA lipoma, 221*
- CAVUM
- septipellucidi 157*
- veli interpositi 158-160
- vergae 158*
- CAVUS FOOT 988
- CIRCUM
- abscess
- in pin in appendix 703*
- in ulcerative colitis 704*
- in colonic rotation failure 636*
- failure of fixation 680
- fecal mass in 713*
- filling defect
- coiled retrocecal appendix causing 704*
- due to invaginated appendiceal stump 706*
- Heocecal intussusception (see Intussusception Heocecal)
- Heocecal tuberculosis 670*
- Heocecal valve implanted on 678*
- lymphoma, 702

- malrotation 1506*
in midgut rotation errors 680*
volvulus 680
- CELIAC DISEASE**
megacolon of 697-698
tibia and fibula undercalcification and rarefaction in 964*
- CELL(s)**
giant cell tumors of bone 1265-1266
sickle (see Sickle cell)
- CELLULITIS pyogenic 857**
- CENTERS OF CHONDRIPLICATION 1352**
- CENTRAL NERVOUS SYSTEM (see Nervous system central)**
- CEPHALHEMATOMA, 58-61**
anatomic changes in 59*
calvarial thickening due to 63*
cystlike residues of 64*
deformans 61
parietalis 65*
double 61*
forceps causing 64*
internal and hyperostosis 67*
parietal bilateral 59*
subperiosteal ossifying 63*
- CEREBELLUM**
astrocytoma, 190*
hypoplasia, 204-206
medulloblastoma, 181* 189* 191* 1279
metastatic 1282*
synchondrosis Towne projection 16*
tumors 139*
- CEREBROSPINAL FLUID**
flow after calvarial fracture 67*
normal production 173
obstruction of flow 175-178
overproduction 173
reabsorption impairment 182-183
- CEREBRUM**
angiography 187-170
in abscess 197*
anomalies congenital 202-210
atrophy 202-203
unilateral 204*
calcification
after prenatal rubella 138*
in toxoplasmic encephalitis 135*
giantism 978-977
hemihypoplasia, 69*
traumatic 206*
hypoplasia 202-203*
unilateral 204 205*-206*
Moyamoya vascular disease 217*
tuberculoma, 134*
- CERVICAL PEDICLE congenital absence 241**
- CERVICAL RIB SCALENE SYNDROME 241-242**
- CHALASIA**
of esophagus 600-601
in newborn 1489-1491
- CHEMICAL POISONS pulmonary reactions to 370-371**
- CHEMISM 128*-129***
- CHEST (see Thorax)**
- CHewing GUM in hair as artifact 1578***
- CHICKENPOX pneumoma complicating 359***
- CHILADITIS SYNDROME 558***
- CHILDREN granulomatous disease liver scan in 1428***
- CHLOROMA, 1291***
- CHOANA atresia, 102* 1440***
- CHOLANGIOGRAPHY**
in bile in gallbladder 1532*
in biliary atresia 1532*
hepatitis and 563*
- CHOLECYSTITIS 566***
- CHOLECYSTOGRAPHY normal 563***
- CHOLEDOCHAL CYSTS 565* 1427***
- CHOLESTATOMA 118***
- CHOLESTEROL**
liporeticulosis 1297*
reticulosis 94*
- CHONDRIPLICATION CENTERS 1352**
- CHONDROBLASTOMA benign 1258-1261**
- CHONDRODYSPLASIA CALCIFICANS CONGENITA 1008 1012**
feet in 1009*
femur in 1009*
hands in 1009*
neck in 1010*
patella in 1009*
pelvis in 1010*
thorax in 1010*
tibia in 1009*
vertebra in 1010*
- CHONDROECTODERMAL DYSPLASIA (see Ellis Van Creveld syndrome)**
- CHONDROBLASTOMA B SULFATURIA 1055 1057**
heparatin and 1055
- CHONDROMA**
benign solitary 1249 1253
perosteal juxtaarticular 1256 1257
- CHONDROMATOSIS 1018-1025**
external 1018 1025
exostoses in 1021*
ulna in 1022*
hereditary 281*
internal 1024* 1025 1026* 1028*
- CHONDROMYXOID FIBROMA 1257 1258**
- CHONDROSARCOMA**
central 1253*
peripheral 1250
primary 1250-1253
- CHONDROSTERNAL PROMINENCE congenital 252**
- CHORIORETINITIS 137***
- CHOROID FLEXUS**
calcification 131*
papilloma ventriculography of 192*
ventricular puncture injuring 166*
- CHROMOSOME**
aberrations causing skeletal changes 1312 1317
sex pattern of XY XO 843*
trisomy (see Trisomy)
- CHYLE FILLO NESPENTERIC CYST lymphangiography of 1422**
- CITYLOPENTONEUM 549**
- CITYLOPNEUMOTHORAX 396***
- CITYLOTHORAX 396-397**
tension 396*
- CITYLOUS**
ascites 1537*
lymphangiography in 1420 1421
pleural effusion in newborn 1459*
- CINE ANGIOCARDIOGRAPHY of ductus bump in newborn 1454***
- CINECTOURTHROGRAPHY in medial stenosis in girl 792***
- CINEFLUOROGRAPHY**
of heart 463 464
in pulmonary sling 487*
- CIRCULATION**
in coarctation of aorta, 489*
in Eisenmenger's syndrome 518*
lungs disturbances 323-325
- CIRRHOSIS splenoportography in 570***
- CISTERN 160-163**
fluid origin pathways and direction of flow 162*
interventricular 158-160
subarachnoid
anatomy of 161*
schematic drawing 162*
- CLAMP for head sponge as artifact, 1583***
- CLAVICLE, 270-275**
bony spurs in rheumatoid disease 275*
in cleft sternum 269*
fracture 272*-273*
in hyperparathyroidism 1305*
in infantile cortical hyperostosis 274* 1214*
in mucopolysaccharidosis 1 1052*
ossification centers in 272*
in Pyle's disease 1070*
rhomboid fossa in 271*
supernumerary left 272*
- CLEFTS**
branchial cyst thyroid 1423*
coronal cleft vertebral bodies 1362 1364*
Milkman's 1309*
sternum 269*
- CLEIDOCANAL DYSOSTOSIS 53 54 85* 1059**
- CLINODACTYL 1181**
- CLOTS blood ureteral shadow due to, 798***
- CLUBBING**
feet
congenital 988
in dwarfism diastrophic 1019*
in syndrome of multiple anomalies 790*
hand 980*
- CNS (see Nervous system central)**
- COARCTATION OF AORTA 488-494**
circulation in collateral arterial 489*
costal erosions in 490*
postcoarctectomy syndrome 537
- COCCIDIOIDOMYCOSIS pulmonary 421**
- COCKAYNE'S SYNDROME 1073 1075***
- CON**
as artifact 1581*
in esophagus 235*
- COLD excessive causing bone lesions 1082-1083**
- COLITIS**
amebic 701
neurogenic megacolon and 689*
sigmoid 701*
ulcerative
abscess and pericecal and
pericolic 704*
advanced 689*
backwash ileitis and 700*
nonspecific chronic 689-701
pseudopolyposoid and backwash
ileitis in 689*
pseudopolyposoid and
retroperitoneal fibrosis 700*
- COLLAGEN DISEASE lungs in 369 370**
- COLLIMATOR in excretory urography 762***

COLON

adenocarcinoma, 711*
air in diagram showing localization of 1482*
ascending failure of fixation 680
atresia, 681* 1530 1531*
carcinoma, 710 711
in Crohn's disease 668*
descending normal filling of intestinal glands in 678*
dilatation segmental 697* 698
diverticula, 698 699
duplications 684 685* 714* 1525-1530 1553*
fecal mass in 713*
filling defects and
dysgammaglobulinemia, 712*
hyperplasia, lymphoid 711 712*
ingested dirt in 708*
in leukemia 702*
malrotation causing duodenal obstruction 654*
in newborn, 1511 1531
normal, 674*
Cannon's level in 677*
delineated by barium enema, 675*
juvenile 674*
neonatal 674*
structural components of 676*
normal variation of 679*
perforation
ascites and 1399*
in cystic fibrosis 1507 1509*
polyp in 709*
polyposis 710*
in siblings 708*
rotation failure jejunum and cecum in 636*
sigmoid (see Sigmoid)
surgical graft in mediastinum 434*
swallowed air normal distribution in newborn 578*
in tuberculosis ileocecal 670*
Colostomy in colitis and neurogenic megacolon 689*
Comic book staple as artifact 1583*
Condylar canals 19*
Constipation
in ingestion dirt in colon 708*
megacolon and neurogenic 688*
Contrast material dried on x ray table as artifact 1584*
Contrast visualization of heart 465
Convulsions neonatal adrenal calcification after 813*
Cooley's anemia (see Anemia, Mediterranean)
Coproolith appendiceal 702*
Cox
pulmonale 528 529
triatrium 508
trilocular biventricular 497
Coracoid process 276*
Cord (see Spine cord Umbilical)
Cornea in mucopolysaccharidosis 11047*
Coronal suture
falciform widening of 33*
superimposed on occipital squamosa, 17*
synostosis of premature 40* 47*
Coronary
arteriovenous fistula, 491 493*
artery

left, anomalies 491 492*
rupture by epinephrine injection 1433*
sinus fistulous communication with right ventricle 493*
Corpus callosum
absence 208*
arachnoid cyst and 209*
complete and brain abnormalities 210*
agenesis 208 210
lipoma, 138* 139 209*
Cortical thickenings traumatic 1129 1131
Corticospinoids
adrenal (see ACTH)
thymic atrophy due to 447*
Coxa
in dwarfism diastrophic 1020*
 plana
acquired 1165*
anterior segmental involvement 1158*
early dislocation phase 1152*
early fracture stage 1155*
early radiographic findings in 1153*
essential early fracture stage 1154* 1155*
essential retarded skeletal maturation in 1150*
essential sclerosis and flattening in, 1155*
familial, in three generations 1151*
frog position 1158*
after hip dislocation treatment 734* 735*
hypothyroidism and 1301* 1302*
idiopathic differential diagnosis, 1287*
intraepiphyseal gas 1158* 1159*
metaphyseal defects 1159 1161
Perthes 1161*
sclerosis and flattening in 1155*
valga, 748 750
in Brachman de Lange syndrome 1074*
of femur 730*
rheumatoid arthritis and 1345*
schematic drawing of 748*
vara, 748 750 990*
acquired 1165*
bilateral, 749*
rachitic 749*
schematic drawing of 748*
Craniolacunia 35 37*
Craniopharyngioma, 148* 150*
pneumography of 193*
Cranioclinosis (see Cranium bifidum)
Craniostenosis
brachycephalic type 42*
head and face in, 41*
microcephalic type 46*
oxycephalic type 45*
scaphocephalic type 44*
Craniostynosis
generalized "mollification" operation for 47*
premature 40 50
brachycephalic type 42
dolichocephalic type 42
Cranium
adult, compared with newborn 3*
left, anomalies 491 492*
rupture by epinephrine injection 1433*
sinus fistulous communication with right ventricle 493*
Corpus callosum
absence 208*
arachnoid cyst and 209*
complete and brain abnormalities 210*
agenesis 208 210
lipoma, 138* 139 209*
Cortical thickenings traumatic 1129 1131
Corticospinoids
adrenal (see ACTH)
thymic atrophy due to 447*
Coxa
in dwarfism diastrophic 1020*
 plana
acquired 1165*
anterior segmental involvement 1158*
early dislocation phase 1152*
early fracture stage 1155*
early radiographic findings in 1153*
essential early fracture stage 1154* 1155*
essential retarded skeletal maturation in 1150*
essential sclerosis and flattening in, 1155*
familial, in three generations 1151*
frog position 1158*
after hip dislocation treatment 734* 735*
hypothyroidism and 1301* 1302*
idiopathic differential diagnosis, 1287*
intraepiphyseal gas 1158* 1159*
metaphyseal defects 1159 1161
Perthes 1161*
sclerosis and flattening in 1155*
valga, 748 750
in Brachman de Lange syndrome 1074*
of femur 730*
rheumatoid arthritis and 1345*
schematic drawing of 748*
vara, 748 750 990*
acquired 1165*
bilateral, 749*
rachitic 749*
schematic drawing of 748*
Craniolacunia 35 37*
Craniopharyngioma, 148* 150*
pneumography of 193*
Cranioclinosis (see Cranium bifidum)
Craniostenosis
brachycephalic type 42*
head and face in, 41*
microcephalic type 46*
oxycephalic type 45*
scaphocephalic type 44*
Craniostynosis
generalized "mollification" operation for 47*
premature 40 50
brachycephalic type 42
dolichocephalic type 42
Cranium
adult, compared with newborn 3*
aneurysms 214 215
arteriovenous fistula and cardiomegaly 476*
bifidum 35
encephalocele and 35
intrafrontal and interparietal 36*
occulum, 37*
at birth 4*
calcification
elastic band simulating 1578*
electrode paste simulating 1579*
glue as artifact, 1590*
hair braid mistaken for 225*
pathologic 133 141
physiologic 130-133
depressions congenital 68*
enlargement in Canavan's spongy degeneration 185*
extracranial structures 224 225
growth of 143 149
hemorrhages associated with closed head injuries 198*
hypertension benign intracranial 141 183
ventriculography in 183*
increased intracranial pressure 141 143
Individual structures 99-129
intracranial structures 130 150
in iron deficiency anemia, 91*
mineralization, normal irregularities 962*
sutures and fontanels as synarthroses 1325
in syphilis 79 80* 81*
teratoma, 137*
tumors 149 150 188 196
CRESCENT SIGN in hydronephrosis 787*
CRETINISM
extremities in 1301* 1302*
hip dislocation in 732*
skull in 84*
spondylolisthesis in 740*
CRICOPHARYNGEAL ACTHARIAL nasopharynx in 586*
CRI DU CHAT SYNDROME extremities in 1315
CRISTA CALLI fibrous dysplasia of 85*
CROHN'S DISEASE 667 668
CROUZON'S DISEASE, 48*
CRYPTOCOCCOSIS lungs in 420
CRYPTORCHIDISM and abdominal muscle congenital absence 793*
CUROID 925
coalition with calcaneus 986*
mineralization 926*
Cuneiforms 925-927
fusions congenital, 984*
irregular densities 927*
irregular growth and ossification of 1171*
CUPPING OF METAPHYSES traumatic 1129 1131*
CUSHING'S SYNDROME
extremities in, 1310-1312
vertebra in 1392 1393
CUTIS CYRATA, 1323
CYAMELLA, 940*
CYANOSIS and congenital heart disease 509-524
CYST(s)
arachnoid congenital, 196

corpus callosum absence and 209*
 Baker's 1336*
 biliary duct, 564*
 bone
 aneurysmal, 1259* - 1262
 of extremities 1253-1256
 bronchogenic 378* 440*
 choledochal 565* 1427*
 Dandy Walker 178* - 179*
dermoid
 frontal bone 225*
 nose 101 103*
 duplication 1468-1469
 femur 1254*
 aneurysmal, 1260*
 fibula, 1255*
 aneurysmal 1261*
 postfracture 1132*
 gastric 595
 hemangiomas 1261-1262
 humerus 1254*
 joints 1348
 kidney (see Kidney cystic disease)
 knee 1348*
 leptomeningeal pulsating 74* - 76*
 lung 338-339
 congenital 319-320
 hydatid 380
 mandible 125-126*
 mediastinum 438-441
 in newborn, 1443*
 mesenteric 574*
 calcification of 575*
 chyle-filled lymphangiography of 1422
 metacarpals 1255*
 aneurysmal 1260*
 neurenteric 642-644
 gas-filled 1510*
 meningocele and 1468-1469
 nose dermoid 101 103*
 pericardial celomic 443
 phalanges 1255* - 1258*
 pharyngeal pouch persistence causing 231*
 pneumatocoele resembling 337*
 popliteal 1336*
 postfracture of fibula, 1132*
 retention and maxillary sinusitis 109*
 septum pellucidum, 157*
 spleen, 1428*
 nephrotomography of 1401*
 after trauma, 569*
 suprasellar 149*
 thymus 456
 thyroid branchial cleft, 1423*
 trigonal 784
 urachus 782*
 ventricle of brain 193*
 vertebra 1395
 aneurysmal 1260*
 CYSTIC ADENOMATOID ANOMALIES
 congenital 1466-1468
 CYSTIC DISEASE renal congenital 774* 775
 CYSTIC FIBROSIS (see Fibrosis cystic)
 CYSTINOSIS extremities in 1319
 CYSTITIS 801
 cystica, 804
 CYSTOGRAPHY 766-768
 in abdominal muscle congenital absence 794*

of fistula, rectoprostatic 1526*
 of hymen imperforate 833*
 in newborn 1544-1545
 patent urachal remnant 782*
 retrograde 767*
 in trabeculated bladder and reflux 790*
 in urinary infections 803*
 of vagina giant 1527*
 CYSTOURETHROGRAPHY
 artifacts in 1586*
 Ascending Lipodol in 768*
 in Eagle-Barrett syndrome 1555*
 of genital tract 822
 of vaginal foreign body 822*
 voiding in Hutch diverticulum with reflux 783*
 CYTOMEGALIC INCLUSION DISEASE 136 137*
 ascites in 1399*

D

DANDY WALKER SYNDROME 177-179
 cyst in 179* 179*
 DEFORMITIES (see Anomalies)
 DEHYDRATION and intravenous pyelography 1543
 DENTAL ARCH growth of 104*
 DERMAL SINUS congenital 50
 DERMATOMYOSITIS 858 859
 chronic progressive recurrent 859*
 DEVELOPMENT OF BONES alterations in 976 977
 DEXTROARCH 481*
 extrinsic 481
 intrinsic 481
 situs inversus and complete 480*
 DIABETES
 insipidus and pinealoma 195*
 mellitus
 cystic fibrosis and 572
 vitamin D poisoning and 1248*
 DIAPHRAGM 285 296
 abscess subdiaphragmatic 548*
 bulge congenital 286*
 defect, skinfold simulating 1588*
 displacements 289-299
 duplication 286*
 atletaxis simulating 287*
 emphysema 1457*
 eventration 289* 442* 443
 CO, contrast studies in 1434*
 in newborn 1460 1464
 hernia (see Hernia diaphragmatic)
 hypertrophic individual muscular bundles 287 288*
 movement causing cardiac shadow changes 465*
 mucosal esophageal obstruction due to 594*
 paralysis and elevation 288*
 pathologic congenital defects
 schematic representation 290*
 scallop 288*
 tenting 288*
 windsock 1500*
 DIAPHYSEAL DYSPLASIA progressive 1063 1066
 DIAPHYSEAL SCLEROSIS hereditary multiple 1066
 DIAPHYSIS
 growth units of 874*
 normal structure 873

DIAPHYSITIS
 in syphilis in infant 1206-1208 1209*
 tuberculous 1201* 1202
 DIARRHEA
 chronic abdomen in 659*
 in Crohn's disease 668*
 DIARTHROSES 1326
 DIASTOMATOMYELIA 1366
 morbid anatomy of 1366*
 myelography in, 1366*
 radiologic findings in 1366*
 DIASTOMYELIA complete form of 1367*
 DIENCEPHALIC SYNDROME OF RUSSEL, 50
 DIGESTIVE TRACT 578-714
 fetal function, 578-580
 DIGIT(s)
 aplasia, 980*
 after door injury 1146*
 in Ellis-Van Creveld syndrome 1017*
 fractures 1087*
 giantism and lipomatosis of 851*
 in hyperphosphatasemia, 1234*
 hypertrophy 982*
 hypoplasia, 980*
 orodigitofacial syndrome extremities in 1315-1317
 oversegmentation 983*
 segmentation failure 983*
 in spina ventosa, 1202*
 DIGITAL-OTO-PALATAL SYNDROME, 50
 DILANTIN in epilepsy calvaria after 97*
 DIMELIA ulnar 989-991
 DIPHENHYDANTOIN in epilepsy calvaria after 97*
 DIPLOIC SPACE
 in microcephaly 144*
 sarcoidosis 79 80*
 DIRT ingested in colon 708*
 DISKS
 calcification 1385-1386
 destruction after lumbar puncture 1376*
 loss of space after trampoline injury 1376*
 normal schematic drawing 1385*
 trauma, 1376-1377
 DISLOCATION
 - fracture at elbow 1098*
 hip (see Hip dislocation)
 patella, 1123*
 congenital lateral 1332
 phase of coxa plana 1152*
 radial head partial 1095 1102
 vertebra 1372
 DIVERTICULUM 640*
 bladder 782 783
 Hutch 783*
 calyceal urography of 777*
 colon 698-699
 duodenal intraluminal 1500*
 esophagus 599
 gangrenous 613*
 Meckel's 635 637* 1507 1510* - 1511
 pharyngoesophageal 593*
 ureter in pyuria, 779*
 urethra, 784
 in newborn 1553*
 ventricle left 509
 DOLL'S ARM as artifact, 1581*

- DOUBLE BURBLE SIGN** in duodenal atresia, 1495*
- DOWN'S SYNDROME** 144-145 741-742
duodenal atresia and 639*
duodenal stenosis and 1520*
megacolon and aganglionosis 687*
pelvic changes in 741*
pelvic measurements in 742*
- DRAINAGE TUBE**
hyperostosis after 284*
rib lesions after 284*
- DRUG REACTIONS** in calvaria, 98
- DUCTUS ARTERIOSUS**
anomalies esophagus and trachea in, 1471
dilatation calcification in 495
patency of 494-495
in Eisenmenger's syndrome 518*
mediastinal widening and 511*
- DUCTUS BUMP** in newborn, 1453-1455*
- DUHAMEL OPERATION** in megacolon 694* 695
- DUHAMEL'S TECHNIC** in esophageal atresia with tracheoesophageal fistula, 588*
- DUODENOJEJUNAL FLEXURE** 636*
- DUODENOJEJUNOSTOMY** in duodenal obstruction 534*
- DUODENUM**
anatomy normal 608*
at 4 years 610*
atresia
Down's syndrome and, 639*
in newborn 1488* 1495*
course variations in 638*
diverticulum intraluminal, 1500*
foreign body in 672*
in ileitis terminal, 667*
malrotation in newborn 1495-1499
malrotation in newborn 1495-1499
in newborn, 1495-1499
normal roentgen appearance 627-628
obstruction 654*
annular pancreas causing 650*
complete 655*
complete due to volvulus and colonic malrotation, 654*
incomplete 634* 638*
incomplete after plaster body cast for scoliosis 660*
incomplete due to volvulus 654*
pancreatic hematoma causing 661*
third portion incomplete 648*-649*
third portion transitory and intermittent 634-635
total 1500*
total, in newborn 1496* 1497*
polyposis 672*
position variations in, 636*
stenosis and Down's syndrome 1520*
trichobezoar in, 623*
ulcer 621* 622
wall, traumatic hematoma of 660*
in Whipple's disease 634*
- DUST** pulmonary reactions to 372
- DWARFISM** 976
carbohydrate metabolism abnormality and 572*
diastrophic 1018 1019*-1020*
- kyphosis and spondyloarthrosis** in 1369*
- Elbs Van Creveld 1440***
familial hemivertebra causing 1361*
fetal, 1073-1076
"bird headed" type 1075*
intrinsic muscellaneous 1071-1082
in Jansen's metaphyseal dysostosis 1031*
Kenny dwarf 1076 1078-1080*
mesomelic 1007-1008
metatrophic 1003-1005 1006*
pituitary 1310
Robinow Silverman Smith 1081-1082
Rubinstein Taybi 1076 1077*-1078*
senile 1071-1072
S.L.O. 1076*
thanatophonic 1081
twisted 1018
- DYKE-DAVIDOFF MASSON SYNDROME** 205*
- DYSAUTONOMIA**
Kochler's disease and 1166*
lungs in 364-365
- DYSCEPHALIC SYNDROME OF FRANÇOIS** 49
- DYSCHONDROPLASIA**
hereditary deforming 741
Olier's 1024* 1025 1026*-1028*
- DYSCHONDROSTEOSIS** 1007
- DYSCHONDROSTEOSIS** 1007-1008
- DYSCHAMCLOBLULINEMIA** and colonic filling defects 712*
- DYSGENESIS**
gonadal causing skeletal changes 1312-1314
ovarian causing skeletal changes 1312-1314
semiferous tubules 1314
- DYSHEMOGLOBINOTIC** inheritable 1283-1284
- DYSMELIA** 979
- DYSOSTOSIS**
cleidocranial, 53-54 55* 1059
Crouzon's hereditary craniofacial 48
face (see Face dysostosis)
metaphyseal, 1364*
hands in 1032*
head in 1032*
of Jansen 1030-1035
of Jansen dwarfism in 1031*
of Jansen ricketslike deformities in 1031*
of Kozlowski and Zychowicz 1034*
legs in, 1033*
ricketslike deformities in 1033*
wrist in, 1032*
- multiple (see Gargoyles)**
peripheral 1012-1013
feet in, 1012*
hands in 1012*
spondylometaphyseal 1007
- DYSPLASIA**
bronchopulmonary 1448*
cartilaginous congenital, 998-1037
chondroectodermal (see Elbs-Van Creveld syndrome)
craniofacial 46 48
diaphyseal, progressive 1063-1066
epiphyseal multiple 1025 1029*
epiphyseal hemimeles, 1030*
- Fairbank, 1030***
fibrous
bone localized or monostotic 1062-1063
of crista galli 85*
in extremities 1264-1265
of facial bone 86*
polyostotic 1061-1062
skull in 85-86
of sphenoid bone 86*
of squamosa, frontal 85*
tibia, 993*
hereditary ectodermal mandible in 127*
hip dislocation and 731*
intrinsically congenital, 998-1071
kidney 1566*
pyelography in newborn 1401*
uterine ectopia in vas deferens and 780*
maxillomaxillary, 48
Meyer's femoral head, 1161-1167
occipital, congenital 40
pulmonary familial fibrocystic 380
skeletal congenital skull in, 53-58
skull congenital 35-58
spondyloriphyseal, 1006-1007
pseudochondroplastic type 1368*
tarda, 776*
systemic vertebral in 1369-1371
teeth in Elbs-Van Creveld syndrome 1016*
- DYSTROPHY**
chondrodystrophy (see Chondrodystrophy)
muscular
of extremities 868-870
pseudohypertrophic 871*
peroneal congenital, 1037-1044
polyostotic fibrous 82-85
calvaria in 85*
skeletal, intrinsic generalized 740-742
syphilitic 1205
- E**
- EAGLE-BARRATT SYNDROME**
1554-1556
cystourethrography in 1555*
scanning in 1431*
technetium 1546*
- EAB**
bladder ears "760" 1543*
in dwarfism diastrophic 1019*
in Rubinstein Taybi dwarfism, 1077*-1078*
- EARRING AS ARTIFACT**, 1580*
- EBSTEIN'S ANOMALY** of tricuspid valve 518-520
- ECHO-B-SCAN** in neuroblastoma 1432*
- ECHROENCEPHALOGRAPHY** 172-173
abnormal 173*
in hydrocephalus 175*
normal, 172*
- ECTASIA** renal tubular in newborn 774*
- EDEMA**
pulmonary 323-325
Kerley B lines 480*
pulmonary vein stenosis causing 506*
thigh 849*
- EGG SHELL** in larynx, 236*

EHLERS DANLOS SYNDROME, 854-855
EISENMENGER'S SYNDROME circulation in, 518*
ELASTIC BAND as artifact, 1576*
ELBOW
 accessory ossicles at, 909*
 in arthritis, rheumatoid, 1345*
 bones of, anatomic variations, 904-912
 calcium gluconate in soft tissues at, 864*
 in dwarfism, diastrophic, 1019*
 fat pads, displacement of, 1095
 fracture-dislocation, 1098*
 frontal projections, 907*
 hemangioma of, 850*
 in hermarthrosis, 1293*-1294*
 ossification centers, 906*
 secondary, 893*
ELECTRICAL POTENTIAL, in bone, stress effects of, 1082
ELECTRICAL TRAUMA to bone, 1082
ELECTRODE PASTE as artifact, 1579*-1580*
ELECTROENCEPHALOGRAPHY
 electrode paste
 stimulating calvarial defect, 1580*
 stimulating cranial calcification, 1579*
 images from paste on scalp, 225*
ELLIS VAN CREVELD DWARFISM, 1440*
ELLIS VAN CREVELD SYNDROME, 1014*-1018
 chest in, 1017*
 dental dysplasia in, 1018*
 external appearance in, 1014*
 hand in, 1017*
 polydactyly in, 1015*
 radius in, 1016*
 shank in, 1018*
 syndactyly in, 1015*
 ulna in, 1016*
EMACIATION SYNDROME, 50
EMBOLISM
 hepatic oil, after lymphangiography, 1421*
 pulmonary fat, 373-374
EMBRYOLOGY
 of anus, ectopic, 836*
 bladder exstrophy, 839-840*
 of gastrointestinal tract, 1479
 in intersex, 825-828
EMBRYOMA dental, 126*
EMPHYSEMA
 of asthma, 254*, 255*, 333*
 bronchography of, 1464*
 chest in, 254*, 255*
 compensatory, 326
 complicating pneumoencephalography, 164*
 cystic, 338*
 cystic fibrosis of pancreas and, 361*
 diaphragmatic, 1457*
 after hernia, diaphragmatic, 1464*
 interstitial, 867-868
 of arm and forearm, 868*
 (in cat), 1452*
 extensive, 1451*
 localized after meconium aspiration, 1452*
 mediastinal, 1541*
 subcutaneous, 1456*
 after tracheotomy, 432*
 mediastinal shift secondary to, 1464*-

1466
 obstructive 332 337
 causal mechanism 327*
 corn kernel causing 332*
 film near end of expiration, 335*
 inspiratory and expiratory films in, 334*
 localized 336*
 pneumothorax causing 333*
 of single lobe 335*
 in tuberculosis primary 413*
 subpleural, 1457*
ENCEPHALITIS TOXOPLASMIC 136*
 137*
 calcification in, 135*
ENCEPHALOCYCLIX 210 212
 cranium bifidum and 35
 frontal, 211*
 sphenocephalic after removal 211*
ENCEPHALOMYELITIS measles calcification after 857
ENCHONDROMA
 hand 1027*
 solitary, 1249
ENCHONDROMATOSIS
 arm in, 1027*
 chest in, 1027*
 generalized 1026-1028*
 legs in, 1027*
 metacarpals in 1028*
 pelvis in 1027*
 phalanges in, 1028*
ENDOCARDITIS 524
ENDOCARDIUM
 cushion defects, 497 499*
 fibroelastosis 482
ENDOCRINE
 disease, skull in, 82
 disorders and vertebra, 1392-1393
ENDOCRINOLOGY skeletal changes in, 1299-1317
ENGELMANN-CAMURATI DISEASE, 1063-1066
ENTERIC FISTULAS formation, schematic drawings of 643*
ENTERITIS
 gastroenteritis, and ileus due to potassium depletion, 658*
 regional
 acute, 669
 stenotic, 667*
 segmental, 667-668
 tuberculous, 670*
ENTEROCOLITIS
 in aganglionosis 1515*
 necrotizing, 669, 1518-1524 1562*
EOSINOPHILIC GRANULOMA (see Granuloma, eosinophilic)
EPENDYMOA
 chewing gum in hair as artifact in, 1578*
 cystic, 188*
EPICARDIUM fat shadows in pericardial effusion, 529
EPICONDYLE
 avulsion, 1105*, 1106*
 fractures, 1105*, 1106*
EPIDERMOIDOMA, 1255*-1256*
 parietal bone in, 96*
EPITHELIOMATOUS BULLOSA DYSTROPHICA, 597, 599*
EPITELIOTIS
Hemophilus influenzae, 236*

after lye ingestion, 596*
EPILEPSY diphenylhydantoin in, calvaria after, 97*
EPIPLUNATUM, 900*
EPINEPHRINE
 injection, hemopericardium after, 1433*
 in urticaria after urography, 765*
EPiphyseometaphyseal junction, 876*
EPIPHYSIS
 in cartilage plate, 878*
 deformities of, 1148-1185
 dysplasia, multiple, 1025, 1029*
 femoral (see Femur, epiphysis) fractures, 1111, 1148-1185
 growth units of, 874*
 in hemophilia, 1293*
 normal structure, 874
 ossification centers, 875*
 of phalanges, 896*
 secondary, time schedule for appearance, 882*-883*
 plates, thickness of, 963
 tibia
 intercondylar spines, stress fracture and sclerosis, 1176
 ossification center, stress sclerosis, 1176
EPITHELIOMA, 1202, 1194*, 1199
 pyogenic, 1199*
 tuberculous, 1200*
EAS & PASTER, 1463*
ERUPTION OF TEETH schematic representation, 122*
ERYSIPELOTHRIX RHUSIOPATHIA
 arthritis after, 1011, 1012
ERYTHROBLASTIC ANEMIA, 1284
 vertebra in, 1393*
ERYTHROBLASTOSIS FETALIS, 1279-1282
ERYTHROCYTOSIS primary, 1294
ESOPHAGITIS, 603-604
ESOPHAGOGASTRIC JUNCTION structure of, 582*
ESOPHAGORAPHY
 bariatric, of aberrant subclavian artery, 484*
 normal, 583*
ESOPHAGUS, 580-609
 (See also Gastroesophageal junction)
 anastomosis of segments, surgical, 588*
 anatomy, normal, 580-581
 anomalies, congenital, 587-596
 in aortic arch anomalies, 1471
 atresia, 587-590
 complete, with blind pouch, 587*
 morphologic varieties, 586*
 in newborn, 1483-1488
 stenosis after anastomosis, 588*
 tracheoesophageal fistula and, 588*-589*
 during belching, 582*
 bronchial communication, 1491
 bronchoesophageal fistula, 317-318
 cervical, 230-235
 anomalies congenital, 230-231
 inflammation, 231-234
 neoplasms, 234-235
 chafasia, 600-601
 coils in, 235*
 compression defects due to aorta, 485*

Esophagus (Cont)

- dilation and mediastinum 443
 - diseases 584 609
 - diverticulum 599
 - pharyngoesophageal 593*
 - duplication 442* 594-595
 - examination methods 581-584
 - filling defects in, 601*
 - foreign bodies in (see Foreign bodies esophagus)
 - hernia, hiatus 619*
 - hiatus dilatation 295*
 - hypertrophy congenital muscular 590
 - invagination and gastric hiatus
 - hernia, 607*
 - lumen during swallowing 584*
 - in newborn, 1483-1492
 - normal semischematic drawing 581*
 - obstruction
 - acquired, 596-597 1489
 - mucosal diaphragm causing 594*
 - perforation, in newborn 1491
 - pin in open safety 599*-600*
 - in pulmonary artery anomalies 1471-1477
 - in pulmonary artery sling 487*
 - short 604-607
 - congenital, 1491
 - stenosis (see Stenosis esophagus)
 - stricture 606*
 - in subclavian artery anomalies 1473
 - tracheoesophageal fistula (see Fistula, tracheoesophageal)
 - ulcer 603-604 606*
 - varices 600
 - splenoportography in 570*
 - venous drainage 626*
- ESTROGEN** causing vaginal enlargement 1556*
- ETHMOID SINUSES** 111
- EVENTRATION**
- diaphragm (see Diaphragm eventration)
 - liver 293*
 - peritoneum, 292 293*
- EWING'S SARCOMA** (see Sarcoma, Ewing's)
- EXOSTOSIS**
- cartilaginous 281* 1022*
 - humerus 967*
 - pelvis 1023*
 - solitary 1249 1250
 - spine in, 1370*
 - tibia, 1023*
 - tibial shaft 968*
 - in chondromatosis external, 1021*
 - femur shaft, 849*
 - tibia, 938* 968* 1023*
- EXPIRATION** effect on mediastinal silhouette 469*
- EXSTROPHY** (see Bladder exstrophy)
- EXTREMITIES** 845 1348
- anomalies, O'Rahilly classification, 979*
 - aplasia, 978-981
 - atrophy of muscles of 870-872
 - bones 873-1325
 - anatomic variations 895 963
 - anatomic variations local, 895-960
 - anatomic variations multiple generalized and scattered, 960

- 963
- changes due to alimentary tract diseases 1320
- changes in blood diseases 1279-1299
- changes due to CNS diseases 1317-1320
- changes due to heart disease 1320
- changes due to renal disease 1321
- changes due to respiratory disease 1320-1321
- changes due to skin diseases 1322-1325
- constriction 885
- cyst 1253-1256
- development of appraisal methods 885 886
- development of velocity of 885-895
- diseases 963-1082
- growth 879 894
- growth appraisal methods 685-886
- growth in limbs 881
- growth, velocity of 885-895
- infections 1192-1222
- lesions due to excessive cold, 1082-1083
- lesions due to excessive heat 1083
- lesions due to physical agents 1082-1222
- marrow cavity 881
- maturation, 879-894
- medullary canal, 881
- modeling of 885
- normal structure of 873-878
- ossification centers (see under Ossification centers)
- ossification, velocity of 888 894
- ossification velocity of fetal and neonatal, 886-889
- ossification velocity of postnatal 889-894
- meningographic appearance 878 879
- spongiosa of 878-879
- calcifications 851-863
- of articular tissues 863
- of fat subcutaneous 851 855
- of lymphoid tissues 861
- muscular 860 861
- in neural tissues 862-863
- of periauticular tissues 863
- vascular 862
- cancer 1267-1279
- in cretinism 1301* 1302*
- in Cri-du-chat syndrome 1315
- dystrophies muscular 868 870
- fibrosarcoma, 1268
- foreign bodies in, 863-867
- in Gaucher's disease 1297-1299
- hemangioma, 1271-1274
- in hemophilia, 1292-1294
- hyperplasia, 981-988
- hypoplasia, 978 981
- inflammations 849-850
- in leukemia, 1290 1292
- lower
 - in achondroplasia, 1004*
 - bowing of prenatal, 994*
 - dysostosis of metaphyseal, 1033*
 - in enchondromatosis 1027*
 - fibromatosis of 862*
 - fractures 1103-1125

- giantism 1271*
- in Ollier's chondromatosis 1024*
- in osteodystrophy fibrosa, 1061*
- in Pyle's disease 1068*
- venous insufficiency 861
- neural tumors 1268
- ring contractions 991* 992
- sarcoma, Ewing's 1267-1268
- soft tissues of 847-872
- tumors (see Tumors of extremities)
- upper arteriosclerosis and hyperparathyroidism, 861*

EYE

- calcification, 140 141
- hypertelism 52 53

F

FARELLA, 939*-940

FACE

- adult, compared with newborn, 3*
 - bones fibrous dysplasia of 86*
 - in craniostenosis 41*
 - in dwarfism diastrophic 1019*
 - dysostosis
 - Treacher Collins mandibular 48-49
 - Weyers mandibular 124 125
 - in mucopolysaccharidosis 1 1045*
 - orodigitofacial syndrome extremities in 1315-1317
 - in Pyle's disease 1070*
- FACIES**
- in Brachman-de Lange syndrome 1072*
 - elfin in idiopathic hypercalcemia, 1308*
 - in hyperostosis cortical, infantile 1212* 1213*
 - Potter's 1439* 1540*
 - in trichorhinophalangeal syndrome 1013*

FAHRER'S DISEASE 134

FAIRBANK DYSPLASIA, 1030*

FALLOT'S TETRAD 513 518

- brain abscess and 197*
- schematic drawing of malformations in, 513*

SURGERY

Jungs after 300*

thymus after 448*

FALLOT'S TETRALOGY (see Fallot's tetrad)

FALKENBERG

calcification, normal 131*

in vitamin D poisoning 1248*

FANCONI ANEMIA, 1282-1283

FANCONI SYNDROME, 994

FARBER'S DISEASE 1299

FARBER'S LIPOCRANULOMATOSIS 1015

1274 1277

FAT

- embolism, pulmonary 373-374
- necrosis, subcutaneous in newborn, 852 854

PAD

- at elbow displacement, 1095
- olecranon, displacement, 1002*
- subcutaneous
 - calcifications, of extremities 851-855
 - water density shadows of vessels in, 848*

FATIGUE FRACTURES 1118-1123

- stress, of metatarsal, 1109*
- FEET**
- impaction, 711-714
- in sigmoid, 713*
- mass
- in cecum, 713*
- in colon, 713*
- simulating polyposis, 710*
- FEET**
- bones of, anatomic variations, 912-928
- calcaneovalgus, 988
- cavus, 988
- clubbing (see Clubbing, feet)
- in dysostosis, peripheral, 1012*
- "exaggerated fetal position foot," 988
- flat (see Flatfoot)
- fractures in, 1105
- glass in, simulating fracture, 867*
- in gonadal dysgenesis, 1313*
- lateral oblique projection, 921*, 926*
- maturation of bones of, 892*
- in mucopolysaccharidosis 1, 1048*
- ossicles, common accessory, 927-928
- ossification centers
- in bones of feet, 884*
- secondary, 893*
- in osteosclerosis, benign familial
- idiopathic, 1065*
- oversegmentation, 943*
- pronated, 986*
- varicosities, and phleboliths, 862*
- in xanthomatous cuts, 1322*
- FEMORA VARIA, 1189***
- FEMUR**
- in chondroplasia, 1000*, 1001*
- anatomic variations, 943-960
- in anemia, sickle cell, 1287*, 1288*
- aplasia, 989
- in arthritis, rheumatoid, 1340*, 1343*
- in battered child syndrome, 1141*-1143*
- biopsy injury causing tubulation
- failure, 967*
- bowing, prenatal, 900*, 996*
- in bowleg, 1188*-1189*
- calcifications of subcutaneous fat in
- front of, 882*
- cartilage plate injuries, 1125-1126, 1131*
- after cat scratch fever, 1204*
- in chondrodysplastic calcifications
- congenita, 1009*
- chondroma, 1249*, 1257*
- in chondromatosis, Ollier's, 1024*
- condyle
- irregularities, 945*
- popliteal groove in, 946*
- rough edge of, 944*
- contusion
- juvenile, 1145*
- neonatal, 1144*
- cortical defects, 936*, 937*
- benign, 1266*
- in dorsal and medial walls, 954*
- fibrous, 948-955
- large multilocular, 951*
- lateral wall, 950*
- medial wall, 952*, 954*
- oval, 952*
- ventral wall, 950*
- cortical thickening, 1145*
- of dorsomedial wall of distal end, 956*
- in prematurity, 961*
- in coxa plana, essential, 1154*
- coxa valga, 730*
- in cretinism, 1301*, 1302*
- cyst, 1254*
- aneurysmal, 1260*
- after cystic fibrosis, 1321*
- double canals through medial cortical
- wall of, in newborn, 879*
- in dwarfism, diastrophic, 1020*
- dysplasia
- epiphyseal, 1029*
- fibrous, 1264*
- epiphysis
- anterior segment, 946*
- avulsion, 1126*
- capital, slipping of, 1127-1129
- intracapsular, 1158*-1159*
- nutrient foramen, shadow of, 947*
- in exostosis, cartilaginous, 1250*
- fractures (see Fractures, femur)
- in Gaucher's disease, 1298*
- head
- factitious splitting, 959*
- Meyer's dysplasia of, 1161-1167
- in hemophilia, 1292*
- hyperostosis, 1218*
- cortical infarct, 1219*
- in hyperparathyroidism, 1305*
- in hypophosphatasemia, 1233*
- hypoplasia, 989*, 990*
- in hypothyroidism, 1300*, 1301*, 1302*
- irregular condylar ridges, normal, 956*
- in liporeticulosis, 1297*
- lymphangioma, 1273*
- lymphosarcoma, 1277*
- marginal irregularities, 948
- medulloblastoma, 1282*
- metaphysis
- cupping after poliomyelitis, 968*
- defect in, 950*
- proximal, irregular ossification, 958*
- mineralization of, normal irregular, 944*
- in mucopolysaccharidosis 1, 1050*
- neurofibromatosis of, 1270*
- normal companion image of lateral
- wall of femurs, 848*
- ossification centers extra, 946*, 949*
- fusion of, 948*
- osteitis, staphylococcal, 1165*
- osteochondroma, 1249*, 1258*
- in osteochondritis dissecans, 1183*
- in osteogenesis imperfecta, 1042*, 1043*
- osteolysis, 1274*
- osteoma, osteoid, 1263*
- in osteomyelitis, 1185*, 1197*
- cupping after, 1196*
- low grade, 1269*
- in osteopetrosis, 1036*
- in osteopikilosis, 1060*
- osteosclerosis, 1067*
- normal fetal, 960*
- proximal end, normal irregularities
- 958*
- pseudoarthrosis, 990*
- in Pyle's disease, 1068*
- radiolucent fatty stripping muscular
- mass contiguous to, 848*
- in rickets, 1225*, 1227*
- in rubella syndrome, 1210*
- sarcoma
- Ewing's, 1267*, 1268*
- osteogenic, 1251*, 1252*
- in scurvy, 1241*, 1242*, 1243*
- shaft
- exostosis, 949*
- transverse lines of Park, 969*
- short, congenital, 990*
- striations, longitudinal, 955-960
- superior foramina for nutrient
- arteries, 957*
- trochanter (see Trochanter of femur)
- in tuberculous diaphysitis, 1201*
- in urticaria pigmentosa, 1324*
- in vitamin A poisoning, 1246*, 1247*
- FERRUCALCINOSIS cerebrovascular,**
- idiopathic functional, 134
- FETUS**
- aborted, Thorotrast in, 1436*
- alimentary tract of, 578-580
- death in utero, radiographic signs,
- 580
- gas bacillus infection, 579*
- gastrointestinal tract of, 1478-1479
- meconium peritonitis, 552-554
- respiration, 297
- FEVER**
- Q pneumonia complicating, 359
- rheumatic (see Rheumatic fever)
- FIBRODYSPLASIA OSSIFICANS**
- PROGRESSIVA
- microdactyls and, 855-857*
- nuchal ossifications in, 1577*
- FIBROELASTOSIS endocardial, 482**
- FIBROGENESIS IMPERFECTA, 1071**
- FIBROMA**
- chondromyxoid, 1257-1258
- mesenteric, 574*
- nonosteogenic, 1268-1267
- FIBROMATOSIS**
- congenital scattered, 1274
- of leg, 862*
- multiple, 1275*
- FIBROSARCOMA, 1251**
- extremities, 1268
- FIBROSIS**
- cystic, 360-364, 572*
- colonic perforation in, 1507, 1509*
- extremities in, 1321*
- meconium ileus and, 652*-653*
- meconium peritonitis and, 1389*
- jaws, familial, 128*-129*
- lungs diffuse idiopathic interstitial,
- 360
- peritumeric, 789
- progressive, of vastus intermedius,
- 859
- retroperitoneal, and ulcerative colitis,
- 700*
- FIBROUS DEFECTS of femur 948-955**
- FIBROUS DYSPLASIA (see Dysplasia,**
- fibrous)
- FIBULA**
- anatomic variations, distal end, 928-932
- aplasia, 988-989
- after boots with tight laces, 1145*
- bowing of, prenatal, 995*
- in chondromatosis Ollier's, 1024*
- cortical defect, 936*
- in cretinism, 1301*
- cyst (see Cyst(s), fibula)

FIBULA (Cont)

- in diaphysitis ephyliotic 1209°
 in Ellis Van Creveld syndrome 1016°
 fractures (see Fractures fibula)
 hemangiomas 1271°
 in hyperostosis cortical infantile 1219°
 hypoplasia, 988 989
 inset accessory center in 929°
 malleolus of 929°
 normal fibular notch in tibia, 930°
 ossicles of accessory 931° 933°
 in osteodystrophy fibrosa, 1061°
 in osteopetrosis 1036°
 in oxalosis 1309°
 in rubella syndrome 1210°
 sarcoma Ewing's 1268°-1269°
 in scurvy 1241°
 tumor thorn induced 1266°
 undercalcification in cellulose disease 964°
 in vitamin A poisoning 1247°
FILARIA BANCROFTI 861
FILM CLIPPING as artifact 1589°
FINGER(s)
 air between simulating fracture 895°
 amputation incomplete congenital 992°
 in arthritis rheumatoid 1339° 1345°
 after door injury 1146°
 in dwarfism diastrophic 1020°
 fist swelling of terminal segment 1180°-1181°
 osteomyelitis 1289°
 in Rubinstein Taybi dwarfism 1077°-1078°
FISTULA
 arteriovenous
 coronary 491 493°
 intracranial and cardiomegaly 476°
 pulmonary 325 379° 523°-524°
 umbilical 1410 1412°
 in atresia, anorectal type III 683°
 biliary bronchial 1531 1533°
 bronchoesophageal, 317-318°
 carotidocavernous sinus 213°
 enteric formation schematic drawings of 643°
 esophageal atresia and in newborn 1483 1488°
 in imperforate anus type III 682°
 pharyngeal pouch persistence causing 231°
 rectoprostatic 1526°
 rectourethral 1525° 1528° 1544°
 tracheobiliary 566°
 tracheoesophageal 590-591°
 esophageal atresia and 588° 589°
 in newborn 1485-1489°
 stenosis after anastomosis 588°
FISTULOUS COMMUNICATION between
 pancreatic duct and gastric
 duplication 641°
FLATFOOT 986° 1190° 1191°
 plantar flexion of talus in 987°
 spastic congenital 981-986°
FLUOROGRAPHY pericardial effusion 463°
FLUOROSCOPY
 gastroesophageal junction normal 602°
 heart 463-464°

- in herma, hiatus 604°
FOLY CATHETER in aganglionosis 1514°
FONG & LEECH 1323 1325°
FONTANELLS
 accessory 4°
 anterior 33°
 at birth 4°
 constant 4°
 interparietal 15°
 persistent 38°
 ossification center in 10° 11°
FOOD simulating gastric bezoar 623°
FOOT (see Feet)
FORAMEN
 intraorbital dilatation of 110°
 intervertebral, enlargement due to neurofibroma, 245°
 of Luschka, congenital obstruction 377°
 of Magendie congenital obstruction 177°
 of midclavicular canals 271°
 of Morgagni hernia, 294°
 optic 194°
 parietal 38°
 symmetrical 35 39 40°
 rotunda 107°
 superior of femur 957°
FORCERS causing cephalhematoma, 64°
FOREARM
 (See also Arm)
 amputation incomplete congenital, 992°
 aplasia 980°
 bones of anatomic variations 904°
 emphysema of interstitial 868°
 fracture 1085 1090 1102°
 glass in 863°
 hemangioma of 850°
 in hypomelosis cortical infantile 1213° 1217°
 in hyperphosphatasemia, 1234°
 hypoplasia, 984°
 in hypothyroidism 1300°
 in Letterer Siwe disease 1296°
 lymphangioma, 1273°
 sclerosis of bone 1066°
FOREGUT
 bronchopulmonary anomaly 321°
 322°
 sequestered, 1491°
FOREIGN BODY(ies)
 in ankle soft tissues 864°
 in appendix, metallic 703°
 arthritis 1534°
 atelectasis due to 328°
 in duodenum 672°
 emphysema due to obstructive 332°
 in esophagus 599 600°
 cervical 234°
 key simulating 1580°
 in extremities 863 867°
 in heart 532 534°
 in intestine small 672°
 iron 672°
 nose 101°
 orbit 1589°
 pharynx, 234°
 axial projection of uvula
 simulating 1575°
 "tumors of bone 1267°
 in vagina (see under Vagina)

- Fossa**
 pituitary
 anatomic features 121°
 in craniohypopharyngioma, 150°
 normal 120°
 rhomboid in clavicle 271°
FOVEA CAPITIS FEMORIS 959°
FRACTURES 1083 1126°
 air between fingers simulating 895°
 arm, in osteogenesis imperfecta, 1040°
 calcaneus 1110°
 false 920°
 calvaria
 in battered child syndrome 1137°
 CSF flow after 67°
 scalp wrinkles mistaken for 224°
 classification according to course and
 nature of fracture line 1084°
 clavicle 272° 273°
 diacondylar 1104°
 digits 1087°
 dislocation at elbow 1098°
 epicondyle 1106°
 medial 1105°
 extremities lower 1105 1126°
 fatigue 1118 1123°
 stress of metatarsal 1109°
 of feet 1105°
 femur 980° 1125°
 in battered child syndrome 1136°
 1137° 1140°
 epiphyseal capital, 1128°
 epiphyses ossification center 1162°
 false 948° 949°
 head Legg's stress 1150 1159°
 impacted 1125°
 proximal half 1124°
 shaft 1125°
 shaft fatty strip simulating 866°
fibula
 carlignous plate distraction
 transverse 1122°
 chip 1122°
 diaphyseal, varices of 1116°
 epiphyses 1111°
 false 933°
 postfracture cyst 1132°
 Salter injury type I 1122°
 shaft, 1111 1118 1123°
 shaft transverse comminuted 1120°
 torus 1118°
 forearm 1085 1090 1102°
 Freiberg's 1181° 1182°
 glass in foot simulating 867°
 hand, 1085-1089°
 humerus 277° 1102 1105°
 in battered child syndrome 1140°
 distal end different patterns of 1104°
 false 908° 909° 911°
 proximal end 1105 1107°
 supracondylar 1102°-1103°
 1107°
 supracondylar morbid anatomy of 1102°
 transverse of surgical neck, 1108°
 thumb 744°
 avulsion, 745°
 ischium apophysis 745°-746°
 mandible 125°
 march, 1118 1123°

of metatarsal 1109*
 metacarpals 1088*
 metatarsals 917* 1108 1109*
 Monteggia's 1098*
 navicular 1088* - 1089*
 false 926*
 nose
 commuted 101*
 external, 99
 olecranon ossification center
 simulating 907*
 olecranon synchondrosis simulating
 906*
 orbit blowout, 73*
 parietal bone 70* 71* 72* - 73*
 patella, 1123 1125
 ventral superior edge 1123*
 pathologic 1131 1132
 pelvis 743
 displacement and protrusion of
 ischium after 744*
 examples of 744*
 multiple 743*
 phalanges 1086* - 1087*
 false 896*
 pedal 1105 - 1108
 spurious 896* 897*
 radius
 distraction of distal third 1090
 1091
 impacted 1097*
 impacted of distal third 1091
 1095
 impacted greenstick, 1094*
 middle third 1097*
 midshaft 1095 1097*
 postfracture cyst 1132*
 proximal and 1099*
 proximal third 1095
 shaft distal third 1096*
 shaft, transverse 1091*
 torus 1097*
 transverse through cartilage plate
 1099*
 transverse compacted 1096*
 transverse of distal third 1090*
 1191* 1192*
 transverse invisible 1094*
 transverse of shaft 1091*
 ramus 123* 744*
 nb in Pierre-Robin syndrome 283*
 sacrum 744*
 sesamoids
 false 918*
 on metacarpals simulating 904*
 skull, 70 78
 frontal bone depressed 72*
 metopic suture and 70* 71*
 in newborn 70
 spine avulsion 744*
 stress 1118 1123
 fatigue of metatarsal 1109*
 focal of epiphyses round bones
 and metaphyses 1148 - 1185
 Legg's of femoral head 1150
 1159
 marginal, 1182 1185
 sites of 1149*
 talus 1185*
 tibial epiphyseal intercondylar
 spines 1176
 tarsal bones 1108 - 1111
 thumb 1083*
 tibia, 1084*

in hattered child syndrome 1136*
 1137*
 diaphyseal variances of 1116*
 epiphyses 1111 1113*
 epiphyses proximal 1123
 false 931* 938* 939*
 gas layer simulating 867*
 impacted 1117*
 invisible 1119*
 long oblique spiral 1116*
 malleolus 1110* 1113*
 pathologic 955*
 shaft, 1111 - 1118
 shaft, commuted oblique spiral
 1115*
 shaft, compacted torus 1118*
 shaft long oblique unstable 1120*
 shaft, rubber band causing 866*
 shaft transverse 1120*
 stress 1121*
 toddler's 1119* 1120*
 toes false 913* 915*
 torus
 fibula, 1118*
 radius 1097*
 tibia, 1118*
 trochanter 1126*
 ulna, 1090*
 false 905*
 middle third, 1097*
 proximal end 1099*
 proximal third 1095
 shaft, 1093*
 shaft distal third 1096*
 transverse of distal third 1091*
 transverse of proximal third 1096*
 transverse of shaft 1091* 1092*
 vertebra 1372 1376
 compression of L-3 and L-4 bodies
 1372*
 distraction from seat belt injury
 1375*
 residual after tetanus 1373*
 schematic representation 1373*
 FRANCOIS DYSCEPHALIC SYNDROME 49
 FREDERICK'S FRACTURE, 1181* - 1182*
 FROG POSITION and coxa plana, 1158*
 FRONTAL SINUSES 110
 FROSTBITE of phalanges 1083*
 FUCOSIDOSIS 1058
 FUNGUS CAUSING OSTEITIS 1204
 FUNNEL CHEST 250* 253*

G

GALLBLADDER
 bile in 1531
 in newborn 1531 1538
 GANGLIOMYOSARCOMA, 810*
 VERTEBRATOGRAPHY of 1415*
 GANGLIOMYOMA
 congenital of abdominal wall 546*
 mediastinum, 437*
 vena cava in 1416*
 GANGLIOMYOSARCOMA, 613*
 GASTROENTERITIS 56-57* 742 1045 1055
 kyphosis lumbar 1370*
 pelvis in 742*
 ribs in 282, 283*
 vertebra in 1371*
 GAZER'S DISEASE 1197* 1198
 GAS
 bacillus infection, fetal, 579*
 femoral intracapsular, 1158* -

1159*
 GASOLINE INGESTION lungs after 371*
 GASTRIC (see Stomach)
 GASTRITIS
 chemical, 620 621
 necrotizing due to zinc chloride 620*
 GASTROENTERITIS and ileus due to
 potassium depletion 658*
 GASTROENTEROSTOMY in
 granulomatous disease 620*
 GASTROESOPHAGEAL JUNCTION
 disorders at 602 - 603
 hernia at hiatus 603*
 normal valvular mechanism 602*
 schematic drawing, 602*
 GASTROINTESTINAL OBSTRUCTION
 radiographic evaluation in
 newborn 1479 - 1483
 GASTROINTESTINAL TRACT 539 - 714
 embryology 1479
 examination 611 612
 fetal 1478 1479
 in first hours of life 1479
 in newborn 1478 1538
 GAUCHER'S DISEASE extremities in,
 1297 - 1299
 GAUZE iodiform in nuchal abscess
 1574*
 GENETIC INDUCTION in sexual
 differentiation 824
 GENITAL TRACT 819 - 844
 cystourethrography of 822
 examination methods 821 - 823
 in newborn 1539 - 1570
 obstruction 833 - 835
 physiology of intravenous 822
 tumors 833 835
 GENITALIA
 external ambiguous in infants 822*
 in S-L-O dwarfism 1076*
 tumors 805 812
 secondary 811
 GENITOGRAPHIC ANATOMY
 classification, 828 832
 six types of 827*
 type I 828*
 type II 828*
 type III 829*
 type IV 829*
 type V 830*
 type VI 830*
 GENITOGRAPHY 823
 in bladder ectrophy 842*
 GENITOURINARY (see Tumors
 genitourinary)
 GEOPHYGIA, 707 708
 GERMINOMA, 195*
 mediastinum 435*
 GIANT CELL TUMORS of bone 1265
 1266
 GIANTISM 976 - 977
 cerebral, 976 - 977
 of digits 851*
 of leg 1271*
 GLASS
 in foot, simulating fracture 867*
 in forearm 863*
 GLIOMA
 optic 194*
 neurofibromatosis and, 1434*
 pontine 191*
 GLOMERULONEPHRITIS
 heart in, 474 475*

GLOMERULONEPHRITIS (Cont)

- dilatation 528
 pleural effusion in 475*
- GLUCOSE TOLERANCE TEST and cystic fibrosis 572
- GLYCOGEN STORAGE DISEASE 481-482*
 type 1 and hepatomegaly 1410*
- GLYCOGENOSIS cardiac 481 482*
- GOITER and cardiomegaly 477*
- GOLDBLOOM HYPEROSTOSIS 1222
- GONADS
 dysfunction skull in 82
 dysgenesis causing skeletal changes 1312 1314
 overfunction causing skeletal changes 1312
 skeletal changes due to, 1312
- GOUT juvenile 1346
- GRAFTS colonic surgical, in mediastinum 434*
- GRANULOMA
 eosinophilic 1296 1297
 of lungs thymus and lymph nodes 383*
 of skull, 94 96
 spine 1393*
 mediastinum 441*
- GRANULOMATOSIS
 disseminated, 1299
 septic
 hepatic calcifications in 559*
 progressive lungs in 365
- GRANULOMATOUS DISEASE
 of childhood liver scan in, 1428*
- GASTRIC ANTRUM in 620*
- GREAT SUTURES relationship to calvaria, 34*
- GAOIN testes in, and hypospadias 831*
- GUM chewing in hair as artifact, 1578*
- GUT
 foregut (see Foregut)
 hindgut ectopic termination 1522* 1523*
 midgut (see Midgut)
- GYNECOLOGIC DISORDERS amenable to radiography 823
- GYNECOMASTIA in boy 262*

H

HAGLUND'S DISEASE 1177*

HAIR

- in Brachman de Lange syndrome 1073*
- braids
 as artifacts 1576*-1577*
 mistaken for intracranial calcifications 225*
 superimposed on back 263* 266*
 cartilage hypoplasia of McKusick, 1035
 chewing gum in, as artifact, 1578*
 dressing as artifact, 1579*
 kinky hair syndrome 216, 217*
 extremities in 1317 1318
- HALLUX metatarsals in irregularities of tips 916*
- HAMARTOMA
 kidney 811*
 fetal 1410*
 in prematurity 1562*
 liver 1535*
 arteriography in, 1406*

- lung 320 321 375*
 circular 320*
- tuber cinereum 189*
- HAMMIE book of 901*
- HAMMAN RICH SYNDROME, 360
- HAND
 abscess cold 1201*
 in anemia Cooley's 1285*
 aplasia, 980*
 in arthritis rheumatoid 1343*
 bones of
 accessory 902*
 anatomic variations 898-904
 maturation of in boys 890*
 maturation of in girls 891*
 ossification centers extra and false 898-904
 in chondrodystrophy calcificans congenita, 1009*
 clubbing of 980*
 in dwarfism diastrophic 1020*
 in dysostosis
 metaphyseal, 1032*
 peripheral 1012*
 in Ellis Van Creveld syndrome 1017*
 enchondromas 1027*
 fractures 1085 1089*
 in gonadal dysgenesis 1313*
 hemangioma, 862*
 in hyperphosphatasemia, 1234*
 hypertrophy 982*
 hypoplasia, 984*
 in hypothyroidism, 1300*
 injuries due to insensitivity to pain 1146*
 in mucopolysaccharidosis 1 1048* 1054*
 in orodigitofacial syndrome 1316*
 ossification centers 898 904
 in bones of 884*
 secondary 893*
 osteomyelitis 1289*
 in osteopetrosis 1060*
 in osteosclerosis benign familial idiopathic 1065*
 in pseudohypoparathyroidism 1306*
 in sarcoidosis 1203*
 sesamoids 904*
- HAVESIAN CANALS 873*
- HAVESIAN SYSTEMS 873*
- HEAD
 clamp sponge as artifact, 1583*
 in craniostenosis 41*
 in dysostosis metaphyseal, 1032*
 injuries closed intracranial hemorrhages associated with 196*
 mesial sagittal section structures of 226*
- HEART 459 537
 anatomy normal 461 462
 angiocardiology 465
 anomalies congenital 478 524
 intrinsic 483 524
 pulmonary vessels in 479
 in syndromes 482-483
 block, congenital 1433*
 cardioangiography selective 465-466
 cardiothoracic index, 470 473
 catheterization 465
 chambers
 enlargement, congenital 479*
 size and position, schematic

- representation, 462*
- cine fluorography 463 464
 contrast visualization, 465
 development 462 463
 dilatation, 474
 generalized in anemia, 476*
 generalized in rheumatic fever 474*
 in glomerulonephritis 528
 in newborn 474*
- disease
 acquired 524 535
 congenital acyanotic 484 509
 congenital, cyanotic 509 524
 congenital radiologic-clinical correlation 483*
 cyanotic and kyphosis of sternum, 270*
 extremities in 1320
 rheumatic and aortic insufficiency 528*
 displacement into hemithorax 316*
 enlargement
 in anemia, 475 476*
 chambers congenital 479*
 generalized, 474 477
 examination types of 463 466
 failure
 congestive total body opacification in newborn, 1401*
 congestive umbilical arteriovenous fistula and 1410 1412
 congestive Wilms tumor and 1404*
 hypoplastic left heart syndrome causing 522*
 pulmonary edema and 324*
 fluoroscopy 463 464
 foreign bodies in 532 534
 fusion of thymic and cardiac images to suggest cardiomegaly 470*
 in glomerulonephritis 474 475* 528
 glycogen storage disease 481 482*
 glycogenosis 481 482*
 growth, 462 463
 in hypertension, 474
 hypertrophy 474
 hypoplastic left heart syndrome 496 520, 522 1566
 cardiac failure due to 522*
 lesions simulating pulmonary disease 1457 1459
 malpositions
 with intrinsic disease 481
 without intrinsic disease 480 481
 myxoma, 532
 pathology 474-535
 polyp 532
 calcifying 534*
 position, 467 470
 postoperative changes 535 537
 after left right shunt surgery 535*
 after transplantation, 536* 537
 after ventricular septal defect surgery 535*
 radiographic appearance 466 473
 extracardiac intrathoracic factors 469-470
 lateral type thoracic cavity 467
 linear type thoracic cavity 467
 position 467-470
 shape, 467-470
 size 470
 radiography

- conventional 463
conventional positions of patient.
464*–465*
- RHABDOMYOMA**, 532
- SCANS** 1431
- SHADOWS**
in aortic valvular disease 525*
changes due to movement of
diaphragm 468*
decrease in generalized 477–478
in mitral disease 524*
normal structures diagrams
showing relations 467*
shape 467–470
size normal 470
surface projection normal heart.
461*
transplantation changes after
536* 537
tumors 532
- HEAT EXCESSIVE**
bone lesions due to 1083
effects on growing bones 1083*
- HZELS** lateral projections 916*
- HEINER'S SYNDROME** 368
- HEMANGIOMA**
calcification in 134*
cavernous congenital 644–645
of jejunum with phleboliths 644*
of elbow and forearm 850*
extremities 1271–1274
of hand 802*
ilium 1274*
liver giant
aortography of 1406* 1409*
right 1534*
total body opacification in
newborn 1401*
venography of 1409*
lung 374*
mediastinum 442* 443
peritoneum 546*
of wrist 862*
- HEMANGIOMASARCOMA** 1251
- HEMANGIOMATOSIS** fibula 1271*
- HEMANGIOMATOUS CYSTS** 1261–1262
- HEMARTHROSIS**
elbow in 1293*–1294*
knee in 1293*
- HEMATHEMESIS** and esophageal ulcer
604*
- HEMATOMA** 197–202
epidural ossifying 66*
extradural 201–202
intrapertoneal 661*
pancreas causing duodenal
obstruction 661*
subdural 60* 76–78
bilateral 199*
infantile 197–201
long bones in 1318*
morbid anatomy 199*
pathogenesis 198*
superficial 60*
ossifying 62*
supraparietal, schematic drawing
68*
suprarenal calcification in 814*
thoracic wall traumatic 265*
- HEMATOMA** hematoma after 814*
- HEMIDYSPHROTHY** 977
- IDIOPATHIC** extremities in 1315
- HEMISTOPHASIA CEREALIS** 69*
traumatic 206*
- HEMIMELIA** 979*
incomplete 980*
- HEMIPLEGIA**, 217–218
- HEMITHORAX**
heart and mediastinum displacement
into 316*
in newborn 1470*
paramedian section, 286*
- HEMIVERTebra** 242, 1358*
- ANOMALIES** 684*
multiple 612*
combined and spina bifida in
newborn 1361*
lung hypoplasia and 315*
multiple 241* 1362*
familial dwarfism due to 1361*
single of T 7 segment, 1361*
in syndrome of multiple anomalies
771*
- HEMOGLOBINOPATHY** sickle cell,
technique scan in 1429*
- HEMOLYTIC ANEMIA** (see Anemia,
hemolytic)
- HEMOLYTIC DISEASE OF NEWBORN**
1279–1282
- HEMOPERICARDIUM**
after epinephrine injection 1433*
traumatic 530*
stimulating pericarditis 529
- HEMOPERITONEUM**
after pyloromyotomy 618*
Rh incompatibility and 1538*
- HEMOPHILIA**
epiphysis in 1293*
extremities in 1292–1294
parathyrus in 1295*
- Hemophilus influenzae* epiglottitis
236*
- HEMOPHYTIS** lung scan in 1426*
- HEMORRHAGE**
adrenal
in newborn 1559–1561
total body opacification in
newborn 1402*
arteriography and 1407–1408
intracranial associated with closed
head injuries 198*
pulmonary 325–340*
in newborn 1450
supraparietal 67
traumatic into scalp in newborn
58–61
- HEMOSTASIS** pulmonary 380–381
- HEMOTHORAX** 396
- HEPARIN SULFATRIA** 1055
- HEPATIC FLEXURE**
hyperplasia at lymphoid 711*
in ileocecal tuberculosis 670*
- HEPATITIS**
cholangiography in 563*
mononucleosis and, 599*
- HEPATOMASTOMA** arteriography in
1406*
- HEPATOODUODENAL LIGAMENT** 636*
- HEPATOULCERULAR DEGENERATION**
extremities in 1318–1319
- HEPATOMEGALY** and glycogen storage
disease type I 1410*
- HEPATOSPLENOMEGALY** and
cystic meckel inclusion disease
137*
- HEMAPHRODITISM** true 843*
- HENNA**
bladder transitory 760*
- diaphragmatic congenital 289–296
in anterior segment of right side
291*
bronchopulmonary communication
and 322*
left at birth 294*
pericardial 291*
through pleuropertoneal canal
left, 290*
through pleuropertoneal canal
right 291*
residual pleuropertoneal air sac
after surgery 292*
- diaphragmatic gastric 619
- diaphragmatic in newborn 1460–
1464
- foramen of Morgagni 294*
- HIATUS**
esophageal 618*
gastric 606*
gastric esophageal invagination
and 607*
gastric and esophageal stenosis —
605*
at gastroesophageal junction 603*
in newborn 1489–1491
sliding 604 607
inguinal causing ileal obstruction
659*
Morgagni, 560*–561*
- HERNIAL SAC** 551*
- HERNIORGRAPHY** of hydrocele and
hernial sac 551*
- HIATUS HERNIA** (see Hernia, hiatus)
- HIGHCHAIR FALL** vertebral body
destruction after 1382*
- HILAR SHADOWS** 297–298
- HILGRENHINER'S METHOD** in hip
dislocation 736*
- HIP**
in arthritis
rheumatoid 1343* 1345*
traumatic 1335*
in battered child syndrome 1140*
in calcinosis tumoral 1346*
dislocation acquired
in neuromuscular disease 734*
traumatic 734
dislocation congenital 731–737
Andren von Rosen method in,
737*
bilateral 732*
coxa plana after therapy 735*
Hilgenreiner's method in 736*
labrum infolding in 733*
Martin's method in 736*
in newborn 734–735
small ilium in 733*
unilateral 731*
unilateral coxa plana after
treatment, 734*
dislocation and dysplasia, 731*
dislocation repeated examinations
in 732*
dislocation, unilateral, in cretinism
732*
normal structures in 1327*
ossification centers secondary 893*
pneumography natural, 1331*
pyarthrosis of 1165*
synovitis transitory 1333*–1334
- HIRSCHSPRUNG'S DISEASE** (see
Aganglionosis)
- HISTIOCYTOSIS X**, 1294–1299

HISTOPLASMOSIS

- lymph nodes in 423*
- pulmonary 421-423*

HODGKIN'S DISEASE

- lymphangiography in 1419* 1420*
- thorax in 435*

HODGKIN'S SARCOMA 1277-1279

HOLOPROSEPHALY 207 208

- alobar and trisomy 13-15 207*

HOLT ORAM SYNDROME extremities in 1320

HOMOCYSTINURIA extremities in 1319

HONEYCOMB PATTERN in osteogenesis imperfecta 1041*

HORSZHOV KIDNEY 771* 772*

HOURGLASS CHEST 252-255

HUMERUS

- in achondroplasia 1000*
- in anemia, sickle cell 1287* 1288*
- bicipital groove shadow of 911*-912*
- bicipital ridges stimulating spur 912*
- capitulum, osteochondrosis of 1176-1177
- chondroblastoma, benign 1258*
- cyst 1254*
- after cystic fibrosis 1321*
- in dysplasia
- epiphyseal 1029*
- fibrous 1265*
- fractures (see Fractures humerus)
- in Garre's disease 1197*
- in hyperostosis cortical infantile 1218*

- in hyperparathyroidism 1305*
- in hypothyroidism 1301*
- in melorheostosis 1080*
- in mucopolysaccharidoses 1 1050* 1054*

ossification centers

- faciotoxic shift 911*
- stimulating fractures 908*
- osteochondroma 1249*
- in osteogenesis imperfecta, 1041*
- rhabdomyosarcoma 1281*
- sarcoma, Ewing's 1269*
- sclerosis 963*

shaft

- construction failures 967*
- exostosis cartilaginous 967*
- supracondylar process on anterior surface 910*
- tumors giant cell 1265*

HUNTER'S SYNDROME

- (MUCOPOLYSACCHARIDOSIS 2) 1055

HURLER'S SYNDROME (see

- Mucopolysaccharidosis 1)

HUTCH DIVERGICULUM of bladder 783*

HYALINE MEMBRANE DISEASE (see

- Respiratory distress syndrome)

HYDATID CYSTS pulmonary 380

HYDRANENCEPHALY 203-204*

HYDRARTHROSIS intermittent 1348

HYDROCELE

- hermography of 551*
- scrotum myelomeningocele stimulating 1365*

HYDROPHALUS 173-178

- clover leaf 183*
- communicating 182-187
- after breech delivery 182*
- protein elevation causing 184*
- echocardiography in 175*

encephalitis and 135*

external 174*

hypertension 173 176

hypotensive 173

internal noncommunicating 177*

macrocrania due to 145*-146*

obstructive 176-181

sagittal suture synostosis and 147*

HYDROMA

subdural 76-78

subepicranial 61-67

HYDRONEPHROSIS 1547-1551

A scan in 1432

bladder neck 1549-1551

crescent sign in 787*

etiology 1549 1551

general considerations 1548-1549

location of 1549-1551

pyelography in 1545*

teratoma and 835*

total body opacification in

newborn 1402*

ultrasound in 1546*

ureteropelvic 1549

ureterovesical 1549

urethral valves and 1551*

HYDROURETER scan of 1431*

technetium 1546*

HYGROMA

cystic of mediastinum 438*

retroperitoneal 1564-1565

HYMEN imperforate 833*

HYPERCALCEMIA IDIOPATHIC

chronic 1248

splanchnic in 1308*

extremities in 1306-1308

in supravalvular aortic stenosis 495

HYPERCHLOREMIC ACIDOSIS and ceculi 796*

HYPERGLOBULINEMIA lungs in 365

HYPEROSTOSIS

cortical 1222

cortical idiopathic 1222

cortical, infantile 1210-1222

chronic 1218 1222

clavicles in 274*

diaphragm in 289*

distribution of skeletal lesions

schematic drawing 1214*

facies in 1212* 1213*

mandible in 125* 1214* 1219*

1221*

residual bony bridges in 1220*

ribs in 281 282*

scapula in 279*

cortical lamellated extremities in

1321*

cortical traumatic serial changes in

formation of 1134*

costal 1217*

craniofacial 146*-147*

femur 1218*

Goldblum 1222

infantile traumatic sequential

changes in 1135*

internal and cephalosmatoma 67*

ipsilateral 1214*

mandibular 1216*

after pleurisy and intercostal

drainage 284*

skull 83*

HYPERARTHROIDISM

arteriosclerosis of upper extremity

and 861*

extremities in 1303-1304

secondary 1304 1305*

vertebra in 1393

HYPERPHOSPHATEMIA

calvaria in 1233 1234*

familial chonic 1231-1237

HYPERPIGMENTATION

of lip and intestinal polyposis 673*

in osteodystrophy fibrosa 1061*

HYPERPLASIA

in achondroplasia, 1370*

adrenal in female

pseudohermaphroditism 817*

extremities 981-988

lymphoid

colon 711 712*

at hepatic flexure and rectum 711*

in rickets 1224*

HYPERTELORISM

ocular 52 53

orbital in diastrophic dwarfism

1019*

in Pyle's disease 1070*

HYPERTELESION

arteriography in 1408

heart in 474

in hydrocephalus 173-178

intracranial benign 141 183

ventriculography in 183*

portal in newborn 1837*

pulmonary 501* 528 529

in Eisenmenger's syndrome 518*

primary 508-509

ventricular septal defect

transformation to 501*

HYPERTHYROIDISM extremities in

1303

HYPERTRICHOSES in

mucopolysaccharidosis 1 1047*

HYPERTRICHOSES

adrenoids 232* 233*

in arthritis 1338

bladder in urethral stenosis 792*

bones 965

diaphragm 287-289*

digits 982*

esophagus congenital muscular 550

hand 982*

heart 474

rib 284*

in stenosis

pyloric (see Stenosis pyloric

infantile hypertrophic)

subacute idiopathic 496

tonsils palatine 227* 232*

in tuberculosis 409*

ventricle left 479

verrucciform 790

HYPERURICEMIA congenital 1346-

1347

HYPERVITAMINOSIS 1243-1249

HYPOCHONDROPLASIA 1000-1003

HYPOPHARYNGEAL DYSPLASIA 1304 1306

intracranial pressure increase in

142*

HYPOPHOSPHATASIA 1230 1231

HYPOPLASIA

abdominal wall, and urinary tract

dilatation 544

in achondroplasia 1368*

bones congenital 978-988

bronchiectasis and 306*

cartilage hair of McKusick, 1035

cerebellar 204-206

- cerebral 202-203*
 unilateral 204 205*-206*
 digits 980*
 extremities 978-981
 femur 980* 990*
 fibula, 988-989
 forearm 984*
 hand 984*
 bernihypoplasia 69*
 traumatic 206*
 kidney 774 1566
 lung 314-317*
 in newborn 1461* 1462* 1469-1470
 mandible 124*
 metacarpals 980* 983*
 muscular after poliomyelitis 872*
 nails 1325
 phalanges 983*
 radius 989
 ribs 280*
 resembling renal stone 798*
 in rickets, 1225*
 sacrum 724* 730*
 thoracic wall 264*
 tibia 989 1364*
 vertebra
 body 1358*
 cervical 242*
HYPOPLASTIC LEFT HEART SYNDROME, 496 520 522
 cardiac failure due to 522*
HYPOSPADIAS
 third-degree
 imperforate anus and 837*
 testes in groin and 831*
 urethral orifice at base of phallus and 831*
HYPOTENSION in hydrocephalus 173
HYPOTHYROIDISM
 coxa plana and 1301* 1302*
 extremities in 1299-1303
 femur in 1300* 1301* 1302*
 thyroid scan in 1427*
 vertebra in 1392*
HYPOTYROSINEMIA 81-82, 747-748
 vertebra in 1391
HYPOTYROSINEMIA 1383-1384
- I**
ICTERUS familial hemolytic 89*-90*
ILEITIS
 "backwash," in ulcerative colitis 699* 700*
 terminal 667*
ILEOCECAL INTUSSUSCEPTION (see Intussusception ileocecal)
ILEOCECAL TUBERCULOSIS 670*
ILEOCECAL VALVE
 implanted cecum 678*
 normal schematic drawing 677*
ILEUM
 atresia, 650* 1505*
 in Crohn's disease 668*
 duplication 640*
 normal roentgen appearance 628-632
 mucosal patterns 631*
 terminal ileum 630*
 obstruction due to inguinal hernia, 650*
 round worm in 671*
 surface view 627*
 volvulus 650*
ILEUS
 meconium (see Meconium ileus)
 potassium depletion causing and gastroenteritis 658*
ILIUM
 crest normal marginal scalloping 729*
 fracture 744*
 avulsion 745*
 horns 1323-1325
 in hyperostosis cortical infantile 1215* 1218*
 in mucopolysaccharidosis I 1050*
 normal secondary epiphyseal center in 720*
 in Ollier's chondromatosis 1024*
 ossification centers in apophyseal cartilage 721*
 osteitis pyogenic 747*
 osteolysis 1274*
 in rhabdomyosarcoma, 1280* 1281*
 in rubella syndrome 1210*
 sarcoma of Ewing's 1270*
 small in congenital hip dislocation 733*
IMAGES natural misleading 1573 1590
IMPERFORATE ANUS (see Anus imperforate)
INDEX cardiopulmonary 470-473
INFANT 1397-1570
 battered ribs in 283*
 diagnosis special procedures 1399-1435
 scoliosis structural idiopathic 1359
 young 1397-1570
INFECTIONS
 skull 78-81
 vertebra and 1387-1391
INFECTIOUS ARTHRITIS 1333 1336
INFECTIOUS MONONUCLEOSIS lungs in 366 367*
INGUINAL HERNIA ileal obstruction due to 659*
INJURIES (see Trauma)
INSPIRATION effect on mediastinal silhouette 469*
INTERATRIAL SEPTUM (see Atrium interatrial septum)
INTERFEDICULATE DISTANCES normal roaximal composite graph 1357*
INTERSEX 823-832
 androgens and 825
 embryology in, 825-828
 phallus with single perineal opening at base 825*
 sequential changes in anatomy in sexual development, 826*
INTERVENTRICAL DISK (see Disks)
INTESTINE
 (See also Gastrointestinal)
 atresia development of 638*
 distention obliterating hepatic shadow 558*
 duplication development of 638*
 large (see below)
 obstruction
 complete diagnostic gas patterns in 656*
 complete and meconium peritonitis in newborn 554*
 in newborn, 578*
 radiographic evaluation, in newborn 1479-1483
 small (see below)
 Thorotrast in in aborted fetus 1438*
INTESTINE LARGE, 673-686
 anatomy
 normal 673-674
 variant 678-680
 anomalies congenital 678-686
 atresia 681-682
 development 674
 distention in perforated appendix 703*
 growth 674
 inflammations 699-707
 roentgen appearance normal 674-678
 rotation errors 680
 failure of fixation 680
 failure of rotation 680
 partial rotation 680
 reversed rotations 680
 stenosis 681-682
INTESTINE SMALL, 626-673
 diseases 632-673
 duplications 639-642
 transdiaphragmatic 642
 varieties of 640*
 in enteritis tuberculous 670*
 foreign bodies in 672
 iron 672
 functional disturbances 632-635
 lymphangiectasia 633*
 lymphosarcoma 873*
 neoplasms 673
 normal 626-632
 in longitudinal section 627*
 mucosal relief 628*-629*
 roentgen appearance 627-632
 obstructions acquired 657-670
 high 658*
 high organic 657*
 obstructions congenital, 637-639
 extrinsic types 837
 failure of recanalization, 637-639
 intrinsic types 637-639
 segmental defect and 639*
 obstructions extrinsic 645 649
 obstructions multiple 650*
 obstructions roentgen findings in 653 656
 obstructions traumatic 661
 parasites 670-671
 polyposis 672-673
 lip hyperpigmentation and 673*
 reticulendotheliosis 673
 segmental defect and obstruction 639*
 surface projection, 541*
 swallowed air normal distribution in newborn 578*
 tuberculosis 670
INTRACRANIAL PRESSURE increased 141-143
INTRATENTORIAL TRANSFUSION (see Transfusion intratentorial)
INTUSSUSCEPTION 661-666
 colonic fecal mass simulating 713*
 common types in longitudinal section 662*
 ileocecal 662*
 acute 663*
 "bedspring shadow in 663*
 chronic 663*
 hydrostatic reduction, ileocecal

INTUSSUSCEPTION (cont.)

- valve during 665*
- hydrostatic reduction late crucial phase in 665*
- hydrostatic reduction progressive changes during 664*
- ileocolic 666*
- jejunum 637*
- transitory multiple 635*

IRON

- deficiency anemia (see Anemia iron deficiency)
- foreign bodies in small intestine 672

ISCHEMIC NECROSIS 1148

sites of 1149*

ISCHIAL BONES retarded ossification of 724*

ISCHIAL TUBEROSITY IRREGULARITIES

in density 725*

marginal 727*

ISCHIOFEMORAL OSTEOCHONDROSIS

JUVENILIS 743-747

deminalization of 723*

early closure at two years 723*

mineralization of irregular 722*

ossification center 723*

swelling of 722* 723*

ISCHURM

apophyseal center on 720*

apophyseal avulsion fracture 745*-746*

displacement and protrusion after fracture 744*

irregularities in 725*

marginal 724*

osteitis tuberculous 747*

osteolysis 1274*

in rubella syndrome 1210*

sharply defined patch in 726*

soap bubble rarefaction of 724*

ISLANDS bone sclerosis of 881 963

ISOLATE HOLE as artifact 1586*

ISOTOPE SCANNING (see Scanning)

J

JANSEN'S DISEASE (see Dysostosis metaphyseal of Jansen)

JAUNDICE 659*

cholangiography in 563*

cytomegalic inclusion disease and 137*

papilla of Vater filling defect and 566*

in newborn, 1531

thrombosis causing 1537*

JAWS

fibrosis familial, 128*-129*

range of condylar motion 124*

JEJUNUM

anomaly of 639*

in colonic rotation failure 636*

duplication, 641*

transdiaphragmatic schematic drawing 642*

in enteritis stenotic regional, 667*

gas-filled loops of 632*

hemangioma cavernous with phleboliths 644*

intussusception 637*

normal roentgen appearance 628-632

obstruction 655*

sudden segmentation and changes in

mucosal relief 632*

surface view 637*

trichobezoar in 623*

in Whipple's disease 634*

JIT PHENOMENON during excretory

urography 764*

JOINTS 1326-1348

anatomy normal 1326-1329

anomalies congenital 1332

calcification of 1346-1347

coalition familial congenital 985*

cysts 1348

diseases 1331-1348

inflammations purulent

hematogenous 1334-1336

neoplasms 1348

principal structures schematic

representation, 1326*

roentgen appearance normal 1329

1331

temporomandibular normal 123*

traumatic changes in 1332-1333

tuberculosis 1336 1337

in tuberculous arthritis 1202

K

KARTAGENER'S SYNDROME 480

KENNY DWARF 1076 1078-1080*

KERASIN LIPORETICULOSIS 1297-1299

KERATOMA palmar and plantar 1325

KERATOSULFATURIA, 1053-1057

KERKING'S PROGRESS 19*

KIRLEY'S LINES 479

in pulmonary edema, 480*

KROENKE'S INGESTION lung scan after

1426*

KEY as artifact, 1580*

KIDNEY

abdomen after insufflation of

perirenal spaces 816*

abscess 800-801

absence right 1566*

agenesis 1541*

aerography in umbilical 1411*

1541*

anatomy normal macroscopic in

longitudinal section 754*

angiography 769 770

anomalies congenital 771-778

of form 771 772

of number 771

of position 772-774

of structure 774-777

aplasia, 774

calcification, nonstimulating 1576*

calcosinosis 796*

calculus (see Calculi kidney)

calyx

deformities in pyelonephritis 804*

dilatation of 788*

diverticulum urography of 777*

caruncle 800 801

changes in pyelonephritis 802*

cystic disease 1565 1569

congenital 774* 775

pyelography of in newborn, 1401*

tubules 776*

unilateral multicystic 1568 1567*

duplication, 1559

dysfunction, extremities in 1321

dysplasia (see Dysplasia, kidney)

ectopic 772*

crossed 773*

embryologic defects 1539

failure and pulmonary edema, 323*

function

in fetus 1539-1542

in newborn 1539 1542

hamartoma (see Hamartoma, kidney)

hematoma, calcification in 814*

hooveshoe 771* 772*

hypoplasia 774 1566

infection 800-805

laceration 799*

masses bilateral 775

necrosis 1557-1558

in neuroblastoma, 807* 809* 810*

normal difference in appearance on

left and right, 761*

outline comparison in infant and

adult, 753*

pelvis

anatomy normal, 755 756

anomalies congenital 777-782

branching variations 755*

dilation in posterior urethral valves,

791*

duplications of 778*

duplications of ureteroceles and

781*

duplications of walled flower'

appearance in 779*

form variation in Wilms tumor

806*

size variations 755*

stone in, 797*

urography of excretory 758*

pelvicocystic visualization prone

and supine positions in 773*

polycystic 214* 775*-778* 1568-

1569

rickets renal, 796*

roentgenographic appearance

normal, 758*

scanning 770 1429

in sclerosis, tuberosus 811*

shadow lymph nodes superimposed

on calcifying abdominal, 577*

sinus comparison in infant and

adult, 753*

soft tissues in longitudinal section

754*

solitary in syndrome of multiple

anomalies 771*

in teratoma, 811*

trauma, 798-800

tubules

dilatation of 776*

ectasia, in newborn 774*

tumors in newborn 1561-1565

vascular disturbances, in newborn,

1557-1559

vein thrombosis (see Thrombosis

renal vein)

KINKY HAIR SYNDROME 216, 217*

extremities in, 1317 1318

KIRNER'S DEFORMITY in Brachman-de

Lange syndrome 1074*

KIRNER'S DISEASE 1180* 1181

KLEIN'S METHOD in slipping of femoral

head 1128*

KLINEFELTER'S SYNDROME true 1314

KLIPPEL-FEIL SYNDROME, 242*-243

KNEE

in arthritis 1200*

after bacteremia, 1011*

purulent, 1335*

rheumatoid 1340*
 cartilage
 discoid 1332
 space between opposing bones 1330*
 cysts 1348*
 hemarthrosis 1293*
 in hypothyroidism 1300*
 knock (see Knock knee)
 normal structures 1328*
 ossification centers secondary 893*
 in panarthrosis hemophilic 1295*
 in rickets 1227*
 roentgen appearance normal 1330*
 in vitamin A poisoning 1246*
 in vitamin D poisoning 1248*
 webbing in myopathy 869*
KNOCK KNEE 1189-1191
 conversion of bowleg to 1187*
 rickets and 1227*
 tibia in 1190*
KOHLER'S DISEASE 1167-1169
 progressive 1168*
KOZŁOWSKI AND ZYCHOWICZ
 METAPHYSAL DYSOSTOSES 1034*
KYPHOSCOLIOSIS and
 neurofibromatosis 1270*
KYPHOSIS 1368*
 adolescent 1381-1383
 anatomic changes in 1381*
 in dwarfism, diastrophic 1369*
 lumbar in Hurler's syndrome 1370*
 mucopolysaccharidosis I and 1046*
 spine cervical and
 neurofibromatosis 245*
 sternum 270*

L

LABRUM FOLDING In congenital hip
 dislocation 733*
LABYRINTH ethmoid 105*
LACUNAR SKULL in newborn 35 37*
LADD'S BANDS 1497*
LAMARCA SUTURE
 ossification center in 11*
 premature closure 45*
LAMELLAR ARRANGEMENT in cortex of
 tubular bone 873*
LAMY MAROTEAUX
 MUCOPOLYSACCHARIDOSIS 1057
LAMY MAROTEAUX PYKNODYSOSTOSIS
 1066
LARYNX 235-237
 calcification 308*
 cartilage 230
 egg shell in 236*
 papilloma, 237
 polyps and atelectasis 237*
LEAD
 bands 972-974
 poisoning
 radiographic changes after 973*
 underconstriction after 966*
LECITHIN LIPORETICULOSIS 382 1299
LEG (see Extremities lower)
LEGG-PERTHES CALVE DISEASE 1150
 1159
LEIOMYOMA 1347*
LEPTOMENINGEAL CYST pulsating
 74*-76*
LEPTOSPIRAL CHANGES in lungs 381
LERI MELORRHOESTOSIS 1042-1044
LESCH NYHAN SYNDROME 1346-1347

LETTERER SIWE DISEASE, 382* 1296*

LEUKEMIA 92
 arthritis and 1337-1338
 colon in 702*
 extremities in 1290-1292
 leukopenic 92*
 leukopenic lymphatic 1290*
 osteolytic 1291*
 lungs in 382 383*
 ribs in 285*
 vertebra in 1393-1395
LIGAMENTS (see Calcification
 ligaments)
LILIEQUIST MEMBRANE 163*
LIP HYPERPIGMENTATION and
 intestinal polyposis 673*
LIPIDOL Ascending in
 cytiourethiography 768*
LIPOGRANULOMATOSIS
 disseminated 1274-1277
 Farber's 1015 1274-1277
LIPOMA
 cauda equina 221*
 corpus callosum 138*-139 209*
 medastinum 436*
 of thigh 850*
LIPOMATOSIS
 of digits 851*
 generalized 1273
LIPORETICULOSIS 1296
 cholesterol 1297*
 keratin, 1297-1299
 lecithin 382 1299
LISSENCEPHALY 206-207
Listeria microcytogenes arthritis
 after 1011-1012
LIVER 557-561
 (see also Hepatic flexure)
 calcification (see Calcification, liver)
 carcinoma, arteriography in 1406*
 damage in newborn, 1531
 evagination 293*
 gas in portal vein branches 557*
 hamartoma, 1535*
 arteriography in, 1406*
 hemangioma (see Hemangioma,
 liver)
 masses in newborn 1533
 in newborn 1531-1538
 oil embolism after
 lymphangiography 1421*
 scanning 1429
 in granulomatous disease of
 childhood 1428*
 shadow obliterated by distended
 intestine 558*
 in tuberculosis 558*
 tumors arteriography in 1407
LONG BONES (see Bone(s) long Bone(s)
 tubular)
LORDOSIS in dwarfism diastrophic
 1019*
LUCAYA TECHNIC in urethrography
 769*
LÜCKENSCHÄDEL 35 37*
LUMBAR PUNCTURE disk destruction
 and sclerosis after 1376*
LUMPOSACRAL (see Spine lumbosacral)
LUNATE FUSION with triangularis 900*
LUNG(S) 298 302
 abscess, 372-373
 hematogenous 374*
 accessory lobe 321*
 in actinomycosis 420

aeration disturbances 325-338
 in agammaglobulinemia, 365
 agenesis 315*
 in Aldrich syndrome 364
 allergic reactions 368-369
 aneurysms arteriovenous 325
 anomalies congenital 314-323
 aplasia, 314 316*-317*
 in newborn 1469-1470
 arteries (see Arteries pulmonary)
 aspergillosis 420
 in Ayer's syndrome 380
 in blastomycosis 420
 bronchopulmonary communication
 322*
 bronchopulmonary foregut anomaly
 321*-322*
 circulatory disturbances 323-325
 coccidioidomycosis 421
 in collagen diseases 369-370
 collapse
 lower lobe schematic
 representation 331*
 middle lobe schematic
 representation 331*
 in respiratory distress syndrome
 1449*
 upper lobe schematic
 representation 331*
 congestion passive 323-325
 contusion 339-340
 in cryptococcosis 420
 cyst (see Cyst(s) lung)
 cystic disease 338-339
 in cystic fibrosis of pancreas 360-
 364
 disease cardiovascular lesions
 stimulating 1457-1459
 dysmaturation 1450
 dysplasia familial fibrocystic 380
 edema, 323-325
 Ketterly's lines in 480*
 embolism fat 373-374
 fibrosis diffuse idiopathic interstitial
 360
 fistulas arteriovenous 325 379*
 523*-524
 after gasoline ingestion 371*
 in geotrichosis 420
 granuloma, eosinophilic 383*
 in granulomatosis progressive septice
 365
 growth fetal factors determining
 1437-1438
 hamartoma, 320-321 375*
 circular 320*
 hemangioma, 374*
 hemorrhage 325 340*
 in newborn 1450
 hemosiderosis 380-381
 histoplasmosis 421-423*
 honeycomb 338-339
 in bronchiectasis 310*
 in hyperglobulinemia 365
 hypoplasia 314-317*
 in newborn 1461* 1462* 1469-
 1470
 in infectious mononucleosis 366
 367*
 inflammations 340-360
 insufficiency due to trauma and
 shock, 341
 leptospiral changes in 381
 in leukemia, 382 383*

LUNG(s) (cont)

- lycoperdonosis 420
- lymphangectasia, 1458*
 - congenital 378
- after mercury fumes inhalation 371
- metastases hematogenous 375-378
- metrolithiasis alveolar 379 380
- in moniliasis 420
- mycoses 420-423
- necrosis 372-373
- neoplasms 374-378
- in newborn 1438*
- nocardiosis 424
- nonperfusion of total 1424*-1425*
- normal
- lobes and fissures of 301*
 - lower lobe 303*
 - lower lobe bronchial distribution in 302*
 - middle lobe 302*
 - at 3 years 300*
- osteochondroplasty extremities in 1321*
- oxygen toxicity 1448*
- Paragonimiasis 424*
- in polycythemia vera, 380
- in protomiasis alveolar 380
- rare diseases 378-384
- reactions
 - to chemical poisons 370-371
 - to dust 372
 - to water 370
- respiratory 1448*
- in reticuloendotheliosis 382
- in rheumatoid arthritis 366
- right middle lobe syndrome 368 369
- right protrusion of apex 249*
- in Riley Day disease 364-365
- in sarcoidosis 418-420
- scan (see Scanning lung)
- in scleroderma 384
- sequestration congenital 321-323
 - extralobar 321*
- sequestration in newborn 1490*
- sporotrichosis 420
- surface projections of posteromedial limits 304*
- systemic diseases 360 374
- after tetralogy of Fallot surgery 300*
- Thorotrast in aborted fetus 1438*
- torsion 335
- traumatic lesions 339-340
- in tuberculosis (see Tuberculosis pulmonary)
- in uremia, 370
- LYCOPERDONOSIS pulmonary 420
- LYE INGESTION
- esophageal stenosis after 597*
- nasopharynx and epiglottis after 596*
- LYMPH NODES
- abdominal 576 577
- calcifying 576*-577*
- enlarged 409*
- granuloma eosinophilic 383*
- in histoplasmosis 423*
- hypertrophy in tuberculosis 409*
- mediastinal normal, 426*
- peribronchial 298
- tuberculosis 230* 419*
- LYMPHADENITIS CALCIFYING 409
- tuberculous 576*
- LYMPHANGECTASIA
- intestinal 633*

- lung 1458*
 - congenital 378
- LYMPHANGIOGRAPHY
- in ascites chylous 1537*
- bepatic oil embolism after 1421*
- in newborn 1419-1422
- LYMPHANGIOMA 65*
 - bone lymphangiography of 1422
 - forearm 1273*
 - mediastinum 438*
 - retroperitoneal 1564-1565
 - widely scattered 1273*
- LYMPHANGITIS calcifying 409*
- LYMPHEDEMA congenital
 - lymphangiography in 1420
- LYMPHOMASTOMA 1277
 - mediastinum 435 436*
- LYMPHOID HYPERPLASIA (see Hyperplasia lymphoid)
- LYMPHOID TISSUES calcifications in extremities 861
- LYMPHOMA
- in ataxia telangiectasia, 571
- cecum 702
- lymphangiography in 1419
- malignant, 1277
- multifocal nonleukemic mandible in 126-127
- venacavography 1413
- LYMPHOSARCOMA
- bone 1277
- bowel 702*
- lymphangiography in 1419 1420*
- mediastinum 436*
- pyelography in 1430*
- scanning in 1430*
- of small intestine 673*
- tubular bones 1277*

M

- MACH EFFECT 1585 1588*
- MACRORHEALTY pneumography in 148*
- MACROCRANIA 145 149
- hydrocephalus causing 145*-146*
- MADELUNG'S DEFORMITY in mesomelic dwarfism, 1006*
- MAFFUCCI'S SYNDROME 1025
- MALFORMATIONS (see Anomalies)
- MALLEOLUS
- of fibula 929*
- fracture 1110* 1113*
- of tibia, 928* 929*
- MANDIBLE 121 129
- anatomy normal 121 124
- in Burkitt's tumor 126-127
- cysts 125-126*
- diseases 124-125
- in dysplasia, hereditary ectodermal 127*
- fractures 125
- in hyperostosis 1216*
- infantile cortical 125* 1214*
- 1219* 1221*
- hypoplasia, 124*
- neoplasms 125 126
- osteomyelitis 125
- in Pyle's disease 1070*
- in rheumatoid arthritis 127-128
- in Weyers facial dysostosis 124-125
- MANOSIDIOSIS 1057
- MANUVERUM simulating aortic knob, 1575*
- MARBLE
- bones (see Osteopetrosis)
- in vagina 832*
- MARCH FRACTURES 1118 1123
- of metatarsal 1109*
- MARFAN'S SYNDROME 1058
- chest in 254*
- MARROW
- cavity of bones of extremities 881
- oxalate crystals in 796*
- MARTIN'S METHOD in hip dislocation, 736*
- MASTOIDITIS 115*-117* 118*
 - in Towne projection 117*
- MASTOPECTOMY 1324* 1325
- MAXILLA
- in dwarfism diastrophic 1019*
- growth of 104*
- in hyperostosis cortical infantile 1219*
- osteomyelitis 129
- MAXILLARY SINUSES 106-110
- factitious eluding 109*
- growth of 104* 105*
- inflammation 106-110
- lateral view 107*
- in Mediterranean anemia 110*
- variants of 107*
- in Water's projection 106*
- McCUNE-ALBRIGHT SYNDROME 1061-1063
- differential diagnosis 1233
- McKUSICK HYPOPLASIA cartilage-hair 1035
- MEASLES ENCEPHALOMYELITIS
- calcification after 857
- MEATAL STENOSIS 792-793 1552
- in girl cuneystourethography of 792*
- MEATOTOMY in stenosis 792*
- MECEL'S SPINTEGULUM 635 637*
 - 1507 1510*-1511
- MECONIUM
- aspiration syndrome 1451* 1453
- emphysema after 1452*
- flexus 651*-653* 1502-1507
- complicated 1504 1505*
- cystic fibrosis of pancreas and 652*-653*
- "equivalent, 652*
- pseudocysts in 1507 1508*
- uncomplicated 1502*-1503*
- peritonitis (see Peritonitis meconium)
- plug
- obstructive 679* 680
- syndrome 1515 1518
- pyopneumoperitoneum 553*
- MEDIASTINUM 425 443
- anatomy normal 425
- anomalies congenital 431
- change in newborn 429*
- colonic surgical graft in 434*
- cross-section 425*
- cysts 430-441
 - in newborn, 1443*
- diseases 431 443
 - rubber band simulating 1576*
- displacement into hemithorax, 316*
- effect of inspiration and expiration on silhouette 469*
- ephysema (see Emphysema, mediastinal)
- esophageal dilation and 443

- ganglioneuroma 437*
 germinoma, 435*
 granuloma, eosinophilic 441*
 hemangioma, 442* 443
 hygroma cystic 438*
 hypertrophy in tuberculosis 409*
 inflammations 431 434
 lateral projection 426*
 lipoma 438*
 lymphoblastoma, 435 436*
 lymphosarcoma, 436*
 mass, right venacavography of 1417*
 meningocele 443
 mesenchymoma 438*
 neurofibroma, 437*
 neuroma, 436 438
 reticulosis proliferative 441*
 roentgen appearance 425 431
 sarcomas 419*
 sarcoma 1443*
 shadow
 large and sudden death 454 456
 supracardiac (see supracardiac shadow below)
 variations due to thymus 452*
 shift secondary to emphysema, 1464 1466
 shrinkage in newborn 429*
 spinal abscess and 443
 subdivisions schematic representation, 425*
 supracardiac shadow
 influence of patient position on width, 430*
 influence respiration on width 430*
 rotation of thorax causing widening 430*
 width diminution in newborn 429*
 teratoma, 439*
 tumors 434 443
 widening and patent ductus arteriosus 511*
 MEDITERRANEAN ANEMIA (see Anemia Mediterranean)
 MEDULLARY CANAL of bones of extremities 881
 MEDULLOBLASTOMA CEREBELLAR, 161*
 189* 191* 1279*
 roetastatic 1282*
 MEGACOLON 686 698
 aganglionic 686 695 1511*
 comparison of radiographic findings and ganglion cell counts 692*
 Down's syndrome and, 687*
 Duhamel operation on, 694* 695
 long segmental type 690* 693*
 saccular regional, 692*
 segmental patterns in schematic drawings, 691*
 typical 686*
 of celiac disease 697 698
 functional 696* 697
 mechanical 695 697
 myenteric plexus absence in, 686*
 neurogenic 688* 691* 695*
 colons and 689*
 rectal aganglionosis and 689*
 neuromuscular (see aganglion c)
 psychogenic 696* 697*
 rectal aganglionosis causing 690*
 in syndrome of multiple anomalies 771*
- MEGARECTUM 695 697
 MELENA and ulcer 621*
 MELODONDROSTOSIS of Lén 1042 1044
 osteopoikilosis and 1060*
 MENETRIER'S DISEASE, 624 625*
 MENINGITIS and arachnoiditis 179*
 MENINGOCELE, 35 37*
 intramedullary 443
 intrathoracic lateral 1367
 neuroenteric cyst and 1468-1469
 rachischisis below total lumbosacral 1367*
 sacral
 anterior 1368*
 ventral 1367
 in syndrome of multiple anomalies 790*
 MENINGOENCEPHALITIS and cytomegalic inclusion disease 137*
 MENINGOENCEPHALOCELE 36*
 MENINGOMYELOCELE Arnold Chiari malformation and 180*
 lumbosacral in newborn, 1365*
 MENKE'S SYNDROME, 216 217*
 MENTAL RETARDATION in S-L-O dwarfism 1076*
 MENSTRUAL ABSORBENT image of 719*
 MERCURY FUMES INHALATION lungs after 371
 MELFENYCHOMA of mediastinum 438*
 MESENTERY 574 575
 cysts (see Cyst(s) mesenteric)
 defects 639* 649
 fibroma, 574*
 vascular occlusion, 666 667
 METACARPALS aplasia, 980*
 in arthritis rheumatoid 1341*
 in Brachman-de Lange syndrome 1073*
 cuticular walls thickening in newborn 900*
 cupping of 900*
 cysts 1255*
 aneurysmal, 1260*
 in Ellis Van Creveld syndrome 1017*
 in enchondromatosis 1028*
 epiphyseal cartilages of ossification centers of 698*
 flattening and cupping of 898*
 fractures 1088*
 giantism and lipomatosis of 851*
 in gonadal dysgenesis 1313*
 in hyperphosphatasemia, 1234*
 hypoplasia, 980* 983*
 in hypothyroidism 1300*
 irregular segmentation 983*
 in mucopolysaccharidosis I 1054*
 osteitis 1289*
 in osteopetrosis 1035*
 tarda, 1039*
 in spina ventosa 1202*
 METAPHYSIS(ES) abscess 1192*
 bands normal primary zones of calcification 964*
 in cartilage plate 878*
 clefts in scurvy 1241*
 cupping of traumatic 1129 1131*
 defects in coxa plana, 1159*-1161
- defects cystic mesenchymal proliferation and hypervascularity causing 1276*
 dysostosis (see Dysostosis roetaphyseal)
 femur (see Femur metaphysis)
 growth units of 874*
 normal structure 874
 of phalanges uneven cupping 897*
 radius (see Radius metaphysis)
 in rickets 1226*
 saw tooth, in syphilis in infant 1207*
 spongiosa, longitudinal striations 955*
 spread of infection into articular space 1198*
 stress fractures and deformities of 1148 1185
 in syphilis in infant, 1204* 1207*
 METAPHYSITIS 1194* 1202
 in syphilis infantile 1205-1206
 tuberculous 1200*
 METASTASES to bones of extremities 1277
 brain 187*
 lungs hematogenous 375-378
 medulloblastoma cerebellar 1282*
 neuroblastoma, 97*
 adrenal 808*
 ovarian cancer to lung 378*
 retinoblastoma of skeleton 1278*
 rhabdomyosarcoma embryonal 1279 1280*-1281*
 spine 1396*
 sarcoma, Ewing in lung 376*-377*
 teratoma mediastinum 439*
 Wilms tumor (see Wilms tumor metastases)
 METATARSALS anatomic variations 912 918
 apophysis 921*
 in arthritis rheumatoid 1339*
 cleft in cortical wall 916*
 depression in cortical wall, 916*
 in diaphysis syphilitic 1208*
 distal end, osteochondrosis dissecans 1184-1185
 fractures 917* 1108 1109*
 Freiberg's 1181*-1182*
 fusions congenital 984*
 irregularities in tps 916*
 in lateral oblique projection 917*
 oversegmentation 983*
 synchondrosis 914*
 in Vitamin A poisoning 1245*
 METATARSUS VARUS 988*
 METOPIC SUTURE 32*
 skull fracture and 70* 71*
 MEYER FEMORAL HEAD DYSPLASIA, 1161-1167
 METYERING'S CLASSIFICATION in spondylolisthesis 739*
 MICRORHINIA 143* 1580*
 pneumoencephalography in, 144*
 MICROCARDIA, 478
 asthma and 477*
 MICROCEPHALY in Cockayne's syndrome 1075*
 diplotic space in 144*
 encephalitis and 135*
 pneumoencephalography in 202*
 MICROCRANIAL 698 1506 1507
 MICROCRANIA, 143 145
 pneumoencephalography in, 144*

MICRODACTYL and fibrodysplasia ossificans progressiva 855-857*
MICROGASTRIA 613 614*
MICROLITHIASIS pulmonary alveolar 379-380
MICROPHTHALMIA right sided 140*
MICTURITION in newborn period 1542
MINDUT
 fixation normal 1496*
 malrotation
 nonobstructive 649*
 preduodenal portal vein and 650*
 rotation
 errors 680*
 normal schematic representation 646*
 reversed schematic drawing 647*
 volvulus 647* 649* 1501*
MIXITY WILSON SYNDROME 1450
MILK ALLERGY PNEUMONIA 368
MILKMAN & CLEFTS 1309*
MILKMAN'S SYNDROME 1229-1230
MINERALIZATION
 focal irregularity of 961
 normal irregularities common sites for 962*
 patella irregular 1176*
MITRAL VALVE 526-528
 disease
 cardiac shadow in 524*
 combined with tricuspid disease 525*
 insufficiency 508 527*
 rheumatic fever and 528*
 stenosis
 congenital 508
 rheumatic fever and 526*
MODELING 966-969
MOLAR third ectopic 108*
MONGOLISM (see Down's syndrome)
MONILIAL INFECTIONS 597 599*
MONILIASIS pulmonary 420
MONONUCLEOSIS infectious lungs in 366 367*
MONTEGGIA'S FRACTURE 1098*
MORCELLATION operation for craniostomias 47*
MORCAGIN HERNIA 560*-561*
MORQUIO'S DISEASE
 (mucopolysaccharidosis 4)
 1055-1057
MOYAMOYA CEREBRAL VASCULAR DISEASE 217*
MPS (see Mucopolysaccharidosis)
MUCOPOLYSACCHARIDOSIS 1044-1057
 1 (Hurler's syndrome) 56-57*
 1045-1055 1370*
 2 (Hunter's syndrome) 1055
 3 (Sanfilippo syndrome) 1055
 4 (Morquio's disease) 1055-1057
 5 (Schrieffer's disease) 1057
 6 (Lamy-Marcoileux) 1057
 rheumatoid type 1057
 vertebra in 1369
MUCOVISCIDOSIS 360-364
MULTANGULAR normal irregular mineralization of 901*
MUSCLE
 abdominal absence of
 congenital 793*-794*
 scan of 1431*
 scan of technetium 1546*
 atrophy (see Atrophy muscle)
 calcification

of extremities 860-861
 after poliomyelitis 857
 defects in stomach 613
 dystrophy of (see Dystrophy muscular)
 pectoralis major absence 264*
 postpoliomyelitic 872*
 triceps defect in head of 867*
Mycosis
 in aneurysms 216
 in osteomyelitis 81
 pulmonary 420-423
MYOLOGRAPHY
 in diastematomyelia, 1366*
 meningocele anterior sacral 1368*
 spinal cord angioma 221*
 spondylolisthesis second degree 222*
MYELOMENINGOCELE (see Meningocele)
MYENTERIC PLEXTUS absence in megacolon 686*
MYOCARDIOPATHY (see Cardiomyopathy)
MYOCARDITIS 524
MYOCARDIUM TUBERCULOSIS
 pneumopneumocardiography in 531*
MYOPATHY
 knee and patella in 869*
 Werdnig Hoffmann 870*-871*
MYOTIS
 calcifying acute idiopathic 857-658
 ossificans
 acute idiopathic 858*
 circumscripta 659-860
 local 858*
 progressive, 845* 855-857*
 traumatic localized 859-860
 pyogenic 857
MYXOMA heart 532

N

NAILS hypoplasia 1325
NASAL SEPTUM deviation 101 104
NASOGASTRIC TUBE 583*
NASOPHARYNX
 after barium study of swallowing 585*
 in cricopharyngeal achalasia, 586*
 lateral wall 100*
 after lye ingestion 596*
 nasogastric tube in place in 585*
NAVICULAR, 923* 924 925*
 fractures 1088*-1089*
 false 926*
NECK, 226-245
 anatomy 226-230
 calcifications physiologic 229-230
 in chondrodystrophy calcificans congenita, 1010*
 hygroma cystic 438*
 lateral projection normal 227*
 at 2 days 228*
 at 10 years 228*
 in myositis ossificans progressiva, 545*
 soft tissue pathology 230
 structures derived from branchial arches 231*
NECROSIS
 carpal bones 1178* 1179*-1180
 in enterocolitis 669 1518-1524
 1562*
 fat subcutaneous in newborn 852-854
 focal aseptic miscellaneous 1177-1178
 gastritis and zinc chloride 620*
 ischemic 1148
 sites of 1149*
 kidney 1557-1558
 metatarsal head ischemic 1182
 pulmonary 372-373
NEONATE (see Newborn)
NEOPLASMS (see Tumors)
NEPHRITIS
 cardiac dilatation in 528
 osteomalacia due to 1323
NEPHROGRAPHY 758*
 in nephron obstruction 1557*
 in Wilms tumor 1404*
NEPHRON OBSTRUCTION nephrography in 1557*
NEPHROSIS
 abdomen in, 547*
 Prednisone for extremities after 1311*
NEPHROTOMOGRAPHY 770
 of spleen cyst 1401*
NERVES
 calcification in tissues of extremities 862-863
 infraorbital neurofibromatosis of 110*
NEUROUS SYSTEM CENTRAL
 diseases extremities in 1317-1320
 scanning 1429-1431
NEURAL TUMORS of extremities 1268
NEURILENTIC CYSTS 642-644
NEURILENTIC REMNANT schematic drawings of 643*
NEUROBLASTOMA 808-811 1252 1253*
 adrenal 815* 1405*
 calvaria in 808*
 metastases in 808*
 in newborn 1559
 aortography in 809*
 retroperitoneal left 1405*
 arteriography in 1407
 ganglioneuroblastoma 810*
 venacavography of 1415*
 kidney in, 807* 809* 810*
 lymphangiography in 1419-1420 1421*
 metastatic 97*
 in newborn, 1562-1564
 proptosis and, orbital 1432*
 retroperitoneal left 1405*
 spine 1394* 1396*
NEUROCENTRAL SYNCHONDOSES 1355*
NEUROENTERIC CYST
 gas-filled 1510*
 with meningocele 1468-1469
NEUROFIBROMA, 245*
 mediastinum 437*
NEUROFIBROMATOSIS
 glioma and optic 1434*
 of infraorbital nerve 110*
 hypophysis of cervical spine and 245*
 of Recklinghausen 1268-1271
NEUROGENIC BLADDER, 1541*
NEUROGENIC UROPATHY in syndrome of multiple anomalies 790*
NEUROLYPHOSIS pneumography in, 206*

NEUROMA mediastinum 436-438
 NEUROMUSCULAR DISEASE hip
 dislocation in 734*
 NEUTROPHIL DEFECT liver scan in
 1428*
 NEWBORN 1397-1570
 angiography
 safety of 1412-1413
 umbilical 1408-1413
 arteriography 1403-1419
 bile ducts of 1531-1538
 bismuth hands in 975*
 bowel of small 1502-1511
 carbon dioxide contrast studies in
 1413-1435
 chest of 1436-1477
 surgical conditions of 1459-1477
 colon of 1511-1531
 diagnosis special procedures 1399-
 1435
 ductus bump 1453-1455*
 duodenum of 1495-1499
 esophagus of 1483-1492
 gallbladder of 1531-1538
 gastrointestinal tract of 1478-1538
 genital tract of 1539-1570
 hemivertebra combined 1361*
 hemolytic disease of 1279-1282
 liver of 1531-1538
 lung of 1438*
 lymphangiography 1419-1422
 meningomyelocele lumbosacral,
 1365*
 micturition of 1542
 osteosclerosis of normal 960*
 pyelography of screening
 intravenous 1570
 respiratory distress (see Respiratory
 distress, of newborn)
 scanning of 1422-1431
 spine bialia, 1361*
 stomach in (see Stomach in
 newborn)
 tachypnea transient 1444-1445
 temporal bone in 113*
 ultrasound and 1431
 urinary tract of 1539-1570
 venacavography 1413-1419
 NIEMANN PICK DISEASE 382 1299
 NITROGEN DIOXIDE
 BRONCHOPNEUMONIA 371-372
 NOCARDIOSIS pulmonary 424
 Nose, 99-104
 cysts dermoid 101 103*
 external
 diseases of 99-100
 fractures 99
 malformations congenital, 99
 foreign bodies 101
 fossa
 frontal section 99*
 lateral wall 100*
 fractures comminuted 101*
 internal
 diseases of 101-104
 malformations congenital 101
 in mucopolysaccharidosis 1 1047*
 1053*
 neoplasms of 101
 normal 99
 in Rubenstein Taybi dwarfism
 1077*-1078*
 NUCAL ABSCESS gauze in 1574*
 NUCLEAR MEDICINE and newborn

1422 1431
 NUCLEUS PULPOSUS calcification
 1386*

O

OAKSITY skeletal maturation in 1317
 OCCIPITAL OSSICLES symmetrical 19*
 OCCIPITAL SQUAMOSA 30* 115*
 flattening of 45*-46*
 ODONTOID PROCESS 239*
 absence 240-241
 ODONTOMA 126*
 OLECRANON
 fatpad displacement 1102*
 ossification center simulating
 fracture 907*
 process 905*
 in rheumatoid arthritis 1345*
 synchondrosis of 906*
 OLIGOMEGALOPHRONIE 774-775
 OLLIER'S DYSCHONDROPLASIA 1024* -
 1025 1026*-1028*
 OMENTUM 574-575
 OMPHALOCLE 544* 1501*
 OMPHALOCENTRIC DUCT 543*
 patent 1511*
 persistence anomalies due to
 schematic drawings 543*
 ONDINE'S CURSE, 529
 OPACIFICATION total body in newborn
 1399-1403
 OPPENHEIM'S DISEASE, 870*
 OPTIC FORAMEN 194*
 OPTIC GLIOMA 194*
 neurofibromatosis and 1434*
 O'RABBY CLASSIFICATION OF
 ANOMALIES OF EXTREMITIES 979*
 ORBIT 105*
 foreign body 1589*
 fracture blowout, 73*
 proptosis 1432*
 ORONOTOPICAL SYNDROME
 extremities in 1315-1317
 Os
 acetabuli marginale superior 722*
 supranaviculare 925 926*
 supratolare 923*
 talocalcaneum, anomalies 927*
 tibiale externum 924 925*
 trigonum 923*
 vesibulum 917*
 OSOOD-SCHLATTER LESION 1168*
 1170*
 OSSIFICATION of Achilles tendon 859
 OSSIFICATION CENTERS
 avulsion traumatic 1170
 of bones of extremities 879*-881
 secondary 881 885
 secondary epiphyseal time
 schedule for appearance 882*
 883*
 calcaneus double 920*
 at different months of age 893
 elbow 906*
 secondary 893*
 in feet 884*
 femur
 accessory 946* 949*
 accessory fusion of 948*
 epiphyseal fracture 1162*
 epiphyseal Meyer's dysplasia of
 1164*
 in fetal skeleton 887*

hand (see Hand ossification centers)
 humerus (see Humerus ossification
 centers)
 of metacarpals 898*
 in newborn by race sex and birth
 weight 888
 olecranon simulating fracture 907*
 patella (see Patella ossification
 centers)
 pelvis accessory secondary 722*
 phalanges (see Phalanges
 ossification centers)
 rib 279*
 scapula, 275*
 shoulder 893*
 talus 922*
 double 924*
 of tarsal bones appearance of 879*
 tibia 933*
 epiphysis stress sclerosis 1176
 toes 917*
 great, 915*
 trochlea, 906*
 vertebra (see Vertebra, ossification
 centers)
 of wrist 893* 898-904
 OSTIITIS
 femur staphylococcal 1165*
 fungal 1204
 ilium pyogenic 747*
 ischium tuberculous 747*
 metacarpals 1289*
 pelvic bones 747
 phalanges 1289*
 pubic bones and tibia, 746*
 pyogenic 1209*
 sickle cell anemia and 1289*
 in styphus 81*
 overcalcification 965*
 viral 1203-1204
 OSTEOARTHRITIS 1338
 OSTEOARTHRITIS pulmonary
 extremities in 1321*
 OSTEOBLASTOMA benign 1249
 OSTEOCHONDROSIS vertebrae of Cervé
 1377*
 OSTEOCHONDROMA
 epiphyseal 1258*
 solitary external 1249*
 OSTEOCHONDROSIS
 dissecans 1182-1185
 metatarsal distal end 1184-1185
 Freiberg's 1181*-1182*
 humerus capitulum 1176-1177
 ischopubic juvenilis 743-747
 juvenilis 1148
 contrasted with normal
 cuneiforms 927*
 sites of 1149*
 pubic bones and tibia, 746*
 radial head 1177
 OSTEOIDYPLASIA auriculo- 50
 OSTEOIDYSTROPHY fibrosa 1061-1062
 OSTEOGENESIS IMPERFECTA, 54-56
 1037-1042
 arm in 1043*
 fractures of 1040*
 bowing in 1041*
 femur in 1042* 1043*
 honeycomb pattern in, 1041*
 humerus in, 1041*
 parietal bones in 1041*
 pelvis in 740
 phosphorus bands and 975*

OSTEOGENESIS IMPERFECTA (cont.)
 tubia in 1039* 1043*
 vertebra in 1370 1371*
 OSTEOID OSTEOMA, 1262-1264
 vertebra 1394*
 OSTEOLYSIS pelvis 1274*
 OSTEOMA
 osteoid 1262-1264
 vertebra, 1394*
 ramus 128*
 OSTIOMALACIA nephritis causing 1323
 OSTIOMYELITIS
 cast in muscular atrophy after 872*
 hands 1289*
 hematogenous
 of calvaria 78*
 pyogenic (see pyogenic
 hematogenous below)
 infantile 1198-1199
 complications 1198-1199
 low grade 1269*
 mandible 125
 maxilla, 129
 mycotic 81
 patella 1199
 pyogenic hematogenous 1192-1199
 healing 1194*
 localized 1196-1198
 penicillin in 1195-1196
 roentgen findings 1194-1196
 sclerosing 1197* 1198
 sicca 1198
 OSTIOPATHIA STRIATA 1025 1028*
 OSTIOTRISIS 57-58*
 congenita 1035-1037
 rickets and healing 1037*
 overcalcification in 965*
 tarda 1036* 1037 1038*
 metacarpals in 1039*
 underconstruction in 966*
 vertebra in 1370-1371
 OSTIOPOROSIS 1059-1061 1325
 melorheostosis and 1060*
 OSTIOPOROSIS and
 mucopolysaccharidosis 1 1046*
 1050*
 OSTEOSCLEROSIS
 benign idiopathic familial 1065*
 1066
 of newborn normal 960*
 OTO-PALATAL-DIGITAL SYNDROME 50
 OTTO'S PELVIS 749-750
 OVARIES
 cancer metastases to lung 378*
 dysgenesis causing skeletal changes
 1312-1314
 teratoma cystic 834*
 underfunction causing skeletal
 changes 1312
 OVERCALCIFICATION
 focal, 966
 generalized 965
 OVERCONSTRUCTION 967-969
 OVERGROWTH
 generalized 976-977
 localized 977
 OVERSEGMENTATION of digits and
 metatarsals 983*
 OVOTESTES bilateral 843*
 OXALATE
 crystals in marrow 796*
 stone in bladder 796*
 OXALOSIS 1309*
 OXYGEN toxicity lung 1448*

P

PACCHIONIAN BODIES
 calcification 131*
 PACCHIONIAN DEPRESSION 29*-30*
 PACHTER
 as artifact 1582*
 PAIN
 abdominal 621
 in Crohn's disease 668*
 in retrocecal and retrocolic
 appendix 705*
 insensitivity to congenital 1135*,
 1146*
 sensitivity to diminished and
 Koehler's disease 1166*
 PALATAL OTO-DIGITAL SYNDROME 50
 PALATINE TONSILS (see Tonsils
 palatine)
 PALSY Erb's 1463*
 PANARITRITIS hemophytic 1295*
 PANCREAS 571-573
 annular 649-651
 duodenal obstruction due to 650*
 calcifications in dwarfism, 572*
 cystic fibrosis (see Fibrosis cystic)
 duct fistulous communication with
 gastric duplication 641*
 hematoma causing duodenal
 obstruction 661*
 pseudocyst 571*
 traumatic 1320
 sarcoma reticulum cell 571*
 PANNE'S DISEASE 1176-1177
 PANOSTEITIS syphilitic 1205*
 PAPILLOE OF VATER filling defect and
 jaundice 566*
 PAPILOMA
 choroid plexus ventriculography of
 192*
 larynx 237
 PAPILLON LEAGH AND PSAUNE
 ORODIGITOPALATIAL SYNDROME
 1315-1317
 PARACONDYLAR PROCESS 20*
 PARAGONIMIASIS pulmonary 424*
 PARALYSIS
 bone injuries associated with 1129
 diaphragm 288*
 pes cavus after poliomyelitis 1191*
 PARANASAL SINUSES 252-255
 PARANASAL SINUSES 104-111
 in dorsoventral projection 105*
 frontal section 99*
 PARASITE SHADOW 1588 1589*
 PARASITIC MUSCULAR CALCIFICATIONS
 860
 PARATHYROID
 dysfunction, skull in 82
 skeletal changes due to 1303-1308
 PARENT INFANT TRAUMA SYNDROME
 1132-1148
 PARIETAL BONE (see Bone(s) parietal)
 PARK'S TRANSVERSE LINES (see
 Transverse lines of Park)
 PARS ARTICULARIS DEFECT in
 spondyloarthrosis 738*
 PATELLA
 anatomic variations 940-943
 in arthritis rheumatoid 1340*
 in chondrodysostrophic calcifications
 congenita, 1009*
 dislocation 1123*
 congenital lateral 1332
 in dysplasia, epiphyseal 1029*

fractures 1123-1125
 ventral superior edge 1123*
 in hyperostosis cortical infantile
 1213*
 marginal segmentation of 942*
 mineralization irregularities 1176*
 ossification centers
 absence and myopathy 869*
 extra, 942*-943*
 osteomyelitis 1199
 sclerosis stress 1174 1176
 PATANT
 ductus arteriosus (see Ductus
 arteriosus patency of)
 omphalomesenteric duct 1511*
 PATHOLOGIC FRACTURES 1131-1132
 PECTUS CARINATUM 252
 PELVIS 715-750
 (See also Ureteropelvic)
 achondroplastic 740-741 1002*
 comparison with normal pelvis
 740*
 anomalies congenital 730-740
 bones (see Bone(s) pelvis)
 calculi in 795*
 in chondrodysostrophic calcifications
 congenita, 1010*
 diseases 740-750
 in dwarfism diastrophic 1020*
 in enchondromatosis 1027*
 in Engelmann's disease 1064*
 exostosis cartilaginous 1023*
 fibromatosis 1275*
 fractures (see Fractures pelvis)
 in gargolism 742*
 mass axial projection of penis
 mimicking 1574*
 menstrual absorbent hygiene 719*
 mineralization normal irregularities
 962*
 in mongoloidism 741*
 measurements 742*
 normal 717-718 740*
 girl at 10 years 717*
 measurements 742*
 variations 719-730
 ossification centers accessory
 secondary 722*
 in osteogenesis imperfecta, 740
 osteolysis 1274*
 in osteopikilosis 1060*
 in osteosclerosis 1067*
 Otto's 749-750
 phosphorus bands in bones 721*
 in Pyle's disease 1070*
 renal (see Kidney pelvis)
 roentgen appearance 718-719
 abnormal soft tissues 718-719
 normal at different ages 720*
 normal skeleton 719
 normal soft tissues 718
 sarcoma of Ewing's 1270*
 shadow
 cast by penis 719*
 in midpelvic plane due to
 overlapping buttocks 719*
 PENCIL
 in soft tissues of buttocks 865*
 in thigh, 1573*
 PENICILLIN in osteomyelitis 1195-
 1196
 PENIS
 axial projection mimicking pelvic
 mass 1574*

PNEUMOMEDIASTINUM (cont.)

- airblock and, 1453*
- autopsy specimen 1457*
- complicating
 - pneumoencephalography 164*
 - falciform due to air in lungs 278*
 - loculated 433*
 - in newborn 471*
 - urthral valves and in newborn 1553*
- PNEUMONIA 340-360 1587*
 - alveolar 341
 - granulomatous and progressive septic 365
 - massive localized (see lobar below)
 - retrocardiac 351*
 - scattered 354 355*
 - aspiration, 366 367*
 - emphysema due to obstructive 333*
 - interstitial 341
 - bronchopneumonia 355-360
 - bronchopneumonia, chronic 360
 - complicating chickenpox, 359*
 - desquamative 359
 - left upper lobe 358*
 - regional or local, 357*
 - right middle lobe 358*
 - rubella complicated by 360
 - whooping cough and 359*
 - lipoid 366-367*
 - lobar 341-354 355*
 - left lobe 353*
 - left lobe lower 349-351* 354*
 - left lobe upper 345 349*
 - multiple 351 354*-355*
 - right lobe lower 345 346*-349* 352*
 - right lobe middle 343-345*
 - right lobe upper 342*-344* 353*
 - milk allergy 368
 - mixed type 341
 - in newborn 1459
 - plasma cell, 368-368
 - Pneumocystis carinii* 368-368
 - pulmonary artery sling and 487*
 - Q fever complicated by 359
 - smallpox 359
 - thymic atrophy after in newborn 446*
 - tuberculous 408*
 - varicella, 356*
 - viral 355*
 - respiratory syncytial 359-360
- PNEUMONITIS rheumatic 365 366
- PNEUMOPERICARDIOGRAPHY in
 - tuberculosis of myocardium and pericardium 531*
- PNEUMOPERITONEOGRAPHY 1434 1435
- PNEUMOPERITONEUM 549 552
 - gas in scrotum and 550*
 - generalized free in newborn, 550*
 - in newborn 1481*
 - skinfold simulating 1588*
- PNEUMOTHORAX 340* 397-398
 - bilateral 1455*
 - after tracheotomy tube 398*
 - cystic fibrosis of pancreas and 362*-363*
 - right, 1463*
 - skinfold simulating 1453*
 - superimpositions resembling 259*
 - tension 397*
 - transitory in newborn 399*
- PNEUMOVAGINA, 1527*

POISONING

- chemical, pulmonary reactions to 370 371
- lead
 - radiographic changes after 973*
 - underconstriction after 966*
 - vitamin A 1244-1247
 - vitamin C 1248-1249
 - vitamin D 1247-1248
- POLIOMYELITIS
 - fatty replacement and stripping of muscles after 872*
 - femoral cupping after 968*
 - muscular calcification after 857
 - overconstriction of radius and ulna after 968*
 - pes cavus after paralytic 1191*
- POLIOMYELOSLIS CONGENITAL ANTERIOR, 868
 - knee and patella in, 869*
- POLYCYSTIC KIDNEY 214* 775*-776* 1566-1569
- POLYCYTHEMIA 92*-93*
 - secondary due to heart disease 92-93
 - vera 92
 - lungs in 360
- POLYDACTYLY in Ellis-Van Creveld syndrome 1015*
- POLYP(s)
 - in colon 709*
 - intracardiac 532
 - calcifying 534*
 - laryngeal and atelectasis 237*
 - in sigmoid 710*
 - urethra 790
- POLYPOSIS 708-714
 - colon 710*
 - in siblings 708*
 - duodenum 672*
 - fecal masses simulating 710*
 - intestine small 672 673
 - lip hyperpigmentation and, 673*
 - rectal 710*
 - sigmoid 710*
- POMPE'S DISEASE 481 482*
- PONS GLIOMA 191*
- PONTICULUS PONTICUS 240*
- PONTITAIL* as artifact, 1578*
- POPULITEAL CYST 1336*
- PORECEPHALY 203*
 - after ventriculography 165*
- POSTOCALFEE transumbilical 1408
- POSITIVE PRESSURE VENTILATION in
 - respiratory distress syndrome 1448*
- POSTARREST LINEA 971
- POSTCAECTECTOMY SYNDROME 537
- POSTOPERATIVE CHANGES OF HEART (see Heart, postoperative changes)
- POSTPERICARDIOTOMY SYNDROME, 529 537
- POTASSIUM DEPLETION causing ileus 658*
- POTTER'S PACIES 1439* 1540*
- PROLAPSUS PUPILLARY and hamartoma, 189*
- PROLAPSUS IN NEPHROSIS extremities after 1311*
- PREMATURITY
 - cortical thickening of 960-961
 - femur 961*
 - diffuse thickening in, 960*
 - enterocolitis and, necrotizing 1519*

- hamartoma and renal, 1562*
- metaphysis in syphilis 1206*
- Mikity Wilson syndrome and 1450*
- rickets and 1229
- PRAPYLORIC LEVEL transverse filling defect at 614*
- PRAPYLORIC MEMBRANE congenital incomplete 614*
- PROCTITIS ulcerative 701*
- PROGERIA, 1071-1072
- PROPTOSIS orbit 1432*
- PROSTATE rectoprostatic fistula, 1526*
- PROTEIN elevation causing
 - hydrocephalus 184*
- PROTEINOSIS pulmonary alveolar 380
- PROTRUSIO ACETABULI 749 750
- PRUNE BELLY (see Eagle-Bartlett syndrome)
- PSEUDARTHROSIS
 - congenital
 - early primary fibrous lesion 993*
 - tibia, 993*
 - femur 990*
- PSEUDORHONDROPLASIA 1006-1007
- PSEUDOCYST 491
- PSEUDOCYST
 - in meconium ileus 1507 1508*
 - pancreas 571*
 - traumatic 1320
- PSEUDOPHYSEMA chronic obstructive 337-338
- PSEUDOFRACTURES 1588*
 - of phalanges 898*
- PSEUDORHAPHRODITISM female 817
- PSEUDO-HIRSCHSPRUNG'S DISEASE 1516*
- PSEUDOHYPOTHRYROIDISM 1323
- SKIDSIDES IN, 1306
- PSEUDOPOLYPOSIS in ulcerative colitis 699* 700*
- PSEUDOSCLEREMA, 852 854
- PSEUDOTRUNCUS ARTERIOSUS 520 521*
- PSEUDOTUMOR
 - cerebrum, 183
 - ventriculography in, 183*
 - sigmoid fecal impaction causing 713*
- PUBERTY precocious and hamartoma, 189*
- PUBIC BONES
 - in bladder exstrophy 731*
 - cyst, aneurysmal 1261*
 - osteochondroma 746*
 - osteolysis 1274*
 - retarded ossification of 724*
- PULMONARY VALVE
 - absence 523* 524
 - stenosis (see Stenosis pulmonary)
- PULMONARY VEINS (see Veins pulmonary)
- PULMONARY VESSELS (see Vessels pulmonary)
- PUSULA
 - anaphylactoid 669
 - thrombocytopenic 1210*
- PYARTHROSIS of hip 1165*
- PYELECTASIS 767*
- PYELOGRAPHY
 - in aganglionosis 1512* 1517*
 - cystic kidney in newborn 1401*
 - ectorecty 767*
 - in gastric duplication, 1494*
 - in hamartoma, fetal renal 1410*

- in hydronephrosis 1545* 1549*
 intravenous
 artifact in 1584*
 bladder neck obstruction in newborn 1542*
 of genital tract 822
 in hamartoma renal 1562*
 of hymen imperforate 833*
 multicystic kidney 1568*
 in newborn 1542-1544
 screening in newborn 1570
 teratoma cystic ovarian 834*
 Wolman's disease 1561*
 of kidney laceration 799*
 in lymphosarcoma 1430*
 retrograde 767*
 in diverticulum of ureter in pyuria 779*
 in kidney dysplasia 1566*
 in thrombosis renal vein 1545* 1558*
 splenic cyst 1428*
 staple from comic book as artifact in 1583*
 in teratoma sacrococcygeal 1403*
 in ureteroceles 1545*
 urinary infections and 803*
 vena caval obstruction 1414*
PYLONEPHRITIS 800
 chronic 801-804
 bladder exstrophy and 802*
 calyceal deformities in 804*
 renal changes in 802*
PYCNODYSTOSIS 1066
PYLE'S DISEASE 1086-1071
PYLOMYOTOMY
 hemoperitoneum after 618*
 incomplete 618*
PYLORUS
 antrum contraction simulating stenosis 617*
 obstruction incomplete 614*
 stenosis (see Stenosis pyloric)
PYLORENIC
 cellulitis 857
 epiphysitis 1199*
 hematogenous osteomyelitis (see Osteomyelitis pyogenic hematogenous)
 myositis 857
 osteitis 1209*
 of ileum 747*
PROPERITONEUM 548-549
PROPEMOPROPERITONEUM 552
 generalized free 552*
 meconium 553*
PROPEMOPROTHORAX 398-399
 generalized 399* 400*
 multiloculated 400*
PYRAMIDS petrous 117 119*
PYURIA
 cystography in 767*
 diverticulum of ureter and 779*
 sacral hypoplasia and 730*
- Q**
Q FEVER pneumonia complicating 359
- R**
RACHISCHISIS lumbosacral total, 1367*
RACHITIC CHEST 255
 morbid changes in 256*
RACHITIC COXA VARA 749*
RADIATION
 diagnostic
 of chest in newborn 1436 1437
 film cramping as artifact 1589*
 gastrointestinal obstruction in newborn 1479-1483
 gynecologic disorders amenable to 823
 heart appearance (see Heart radiographic appearance)
 heart conventional 463 464*-465*
 during intrauterine transfusion 1437*
 vertebra normal appearance 1355-1357
 therapeutic thymus after 455*
RADIOISOTOPE SCANNING (see Scanning)
RADIUM HANDS 975
RADIUS
 absence of congenital 980*
 aplasia 989
 in arthritis rheumatoid 1342* 1344*
 in battered child syndrome 1140*
 bowing prenatal 994*
 in Brachman-de Lange syndrome 1073*
 contusion infantile 1144
 cyst postfracture 1132*
 in diaphysitis syphilitic 1207*
 dislocation partial of head 1095 1102
 in dwarfism diastrophic 1020*
 in dysplasia
 epiphyseal 1029*
 fibrous 1062*
 in Ellis Van Creveld syndrome 1016*
 in erythroblastosis fetalis 1282*
 fractures (see Fractures radius)
 head osteochondrosis 1177
 in hyperostosis coronal infantile 1220*
 in hyperparathyroidism 1305*
 hypoplasia 989
 in insensitivity to pain, congenital 1135*
 lymphangioma 1273*
 massive sequestration in situ 1195*
 in melorheostosis 1060*
 metaphysis
 defect in cellist 902*
 physiologic wavy irregularities in 903*
 in mucopolysaccharidosis 1 1054*
 in Ollier's chondromatosis 1024*
 overconstriction after polyomyelitis 968*
 in phenylketonuria 1319*
 in Pyle's disease 1068*
 synostosis 984*
RAMUS
 fracture 123* 744*
 marginal irregularities 724* 727*
 mineralization of
 irregular and retarded 728*
 irregular serial changes in 726*
 osteoma, 126*
 in Pyle's disease 1070*
 soap bubble rarefaction of 724*
 strip defect in 727*
RAREFACTION bone 964-965
- RECKLINGHAUSEN NEUROFIBROMATOSIS** 1268-1271
RECTOURTHRAL FISTULA 1525*
 1528* 1544*
RECTUM
 aganglionosis (see Aganglionosis rectal)
 anomalies 1524-1531
 atresia 681*-684
 fistulas in 683*
 distention enormous after anal atresia surgery 696*
 gas in ureteroceles simulating 781*
 hyperplasia, lymphoid 711*
 after intrauterine transfusion, 1479*
 polypoid 710*
 pull through of fecaloid vaginal discharge after 838*
 stenosis 681* 692-684 701*
 swallowed air normal distribution, in newborn 578*
REFLUX
 Hutch diverticulum and 783*
 trabeculated bladder and 790*
 urinary tract infection and 1547
RESPIRATION fetal 297
RESPIRATORY
 disease extremities in 1320-1321
 distress in esophageal duplication 595*
 distress of newborn 1438-1459
 chest film at 4 hours 1483*
 chest film at 12 hours 1463*
 differential diagnosis 1460
 tachypnea in 1444*
 teratoma and cervical 1441*
 tracheal agenesis in 1442*
 typical chest film in 1445*
 distress syndrome 1445-1450
 at birth in 1453*
 bronchography in 1448*
 positive pressure ventilation in 1448*
 lung 1448*
 tract 297-304
 infection thymus after 445*
RESTRAINING BOARD as artifact 1583*
RETICULOENDOTHELIOSIS 1294-1299
 lungs in 382
 of small intestine 673
RETICULOHISTIOCYTOMA, 1323
RETICULOSIS 93 339*
 cholesterol 94*
 lungs in 382*
 malignant 1290-1292
 mediastinum 441*
 nonhypoid 1295-1296
 proliferative 1294-1299
 vertebra in 1393
RETICULUM CELL SARCOMA (see Sarcoma, reticulum cell)
RETINOBLASTOMA, 138 1279
 skeleton metastatic 1278*
RETROPERITONEAL
 hygrota, 1564-1565
 teratoma, in newborn 1563* 1564
 tumors 1564
 solid lymphangiography in, 1419
RH INCOMPATIBILITY and
 hemoperitoneum 1538*
RHABDOMYOMA of heart 532
RHABDOMYOSARCOMA
 embryonal metastatic 1279 1280*-1281*

RHABDOMYOSARCOMA (cont)
 spine 1396*

RHEUMATIC FEVER 524-526 1337
 mitral stenosis and insufficiency and 526*

recurrent generalized cardiac dilatation in 474*

RHEUMATIC PNEUMONITIS AND PLEURISY 365-366

RHEUMATOID ARTHRITIS 1338-1347
 ACTH in vertebra after 1310*
 early changes in hands 1341*
 femur in 1340* 1343*
 lungs in 366
 mandible in, 127 128
 moniliasis and 599*
 of spine cervical 1390* 1391
 structural changes in 1338*

RHEUMATOID DISEASE bony spurs of clavicle in 275*

RHEUMATOID
 MUCOPOLYSACCHARIDOSIS 1057

RHEUMATOID STATE 81

RHINITIS 101 104*

RIB 279 285
 anomalies
 congenital 280
 lymphangomatous 1422*
 in battered infant 283*
 cervical 241-242
 in exostoses cartilaginous 281*
 fractures in Pierre-Robin syndrome 283*
 in gargoyism 282 283*
 in hyperostosis infantile cortical 281 282, 1215* 1220*
 hypertrophy 284*
 hypoplasia, 280*
 resembling renal stone 796*
 lesions after drainage tube 284*
 in leukemia, 285*
 in liporeticulosis 1297*
 in Mediterranean anemia, 282*
 in mucopolysaccharidosis 1 1051*
 ossification centers 279*
 resection changes after 280*
 in rickets 257*

RISING SCLEROSIS 1066

RICKETS 91 89* 1229 1229

advanced hyperplastic 1224*
 atrophic 1225*
 healing 1225*
 osteopetrosis congenita and 1037*
 overcalcification in 965*
 underconstruction in 966*
 hyperparathyroidism and 1305*
 hypoplastic 1225*
 juvenile 1226 1228
 like deformities in Jansen's metaphyseal dysostosis 1031* 1033*
 mild early 1222*
 pathogenesis of curvature deformities in 1227*
 prematurity and 1229
 refractory, active 1227*
 renal, 796*
 ribs in 257*
 roentgen findings 1223 1226
 sequelae 1226

RIGHT MIDDLE LOBE SYNDROME of lungs 368-369

RILEY DAY SYNDROME

Koeber's disease and, 1166*

hinges in 364-365

RING CONTRACTIONS of extremities 991* 992

ROBINSON-SILVERMAN SMITH DWARFISM 1081 1082

ROCHER SHELDON SYNDROME 1323

ROENTGENOGRAPHY (see Radiation)

ROUNDWORM in ileum 671*

RUBBER BAND
 as artifact 1576*
 superimposed on parietal bone 225*
 tibial shaft fracture due to 866*

RUBEKIA
 intrauterine and peripheral pulmonary stenosis 502
 pneumonia complicating 360
 prenatal, cerebral calcification after 133*
 syndrome neonatal transplacental 1210

RUBENSTEIN-TAYBI DWARFISM, 1076 1077*-1078*

RUPTURE coronary artery by epinephrine injection 1433*

RUSSEL DIENCEPHALIC SYNDROME, 50

S

SACRALIZATION of vertebra, 728*

SACROCOCYGEAL TERATOMA (see Teratoma, sacrococcygeal)

SACRUM
 absence 1541*
 appearance of secondary ossification centers in 718*
 dysmorphic 1544*
 fracture 744*
 hypoplastic 724* 730*
 osteolysis 1274*
 spina bifida
 occulta, 729*
 vara, in syndrome of multiple anomalies 790*

SAFETY PIN in pharynx 234*

SAGITTAL SINUS venography 183*

SAGITTAL SUTURE
 ossification center in 11*
 superimposed on occipital squamosa, 17*
 synostosis of 147*
 premature 40* 43*

SALTER AND HARRIS classification of cartilage plate injuries 1130*

SALTER INJURY TYPE I 1124* 1140*
 of fibula, 1122*

SAPHYLOPOD SYNDROME (MUCOPOLYSACCHARIDOSIS 3) 1055

SARCOCYSTIS 418 420 1202-1203*
 of diaphragm space 79 80*
 mediastinum 419*

SARCOMA
 Ewing's 1270*
 extremities 1267 1268
 lung metastases in 376* 377*
 polyostotic 1269*
 Hodgkin's 1277 1279
 mediastinal, 1443*
 osteogenic 1251-1252
 extracranial 1252
 osteoblastic type 1251*
 osteoid type 1252*

sclerotic multiple 1252 1253
 reticulum cell, 1279
 of pancreas 571*
 tibia, 1278*
 Wilms 252*

SCALP
 traumatic bleeding into in newborn, 58 61
 wrinkles mistaken for fractures of calvaria, 224*

SCANNING 170 172 1547
 A scan (see A scan)
 brain 171*
 in abscess 197*
 ependymoma, cystic 188*
 metastases 187*
 central nervous system 1429 1431
 in Eagle-Barrett syndrome 1431* 1546*
 echo B scan in neuroblastoma, 1432*
 heart 1431
 kidney 770 1429
 liver 1429
 in granulomatous disease of childhood 1428*
 lung
 albumin 1424*
 in cardiomegaly 1425*
 in hemoptysis 1428*
 after kerosene ingestion, 1426*
 in lymphosarcoma, 1430*
 newborn and 1422 1431
 spleen 1429
 in S-C hemoglobinopathy and asplenia, 1428*
 technetium in Eagle Barrett syndrome 1431* 1546*
 thyroid 1429
 in hypothyroidism 1427*
 in newborn 1423*

SCAPHOCEPHALY 44*

SCAPHOID TARSAL
 fracture 1109*
 stress compression 1187 1169

SCAPULA, 275-279
 in battered child syndrome 1140*
 descent failure 277* 278*
 in hyperostosis
 infantile cortical 279*
 ipsilateral, 1214*
 in mucopolysaccharidosis 1 1052*
 ossification centers 275*
 rhabdomyosarcoma, 1281*
 sarcoma, Ewing's 1269*
 winged 278*

SCHEER-GARY RINGS 583 584

SCHIEF'S DISEASE (MUCOPOLYSACCHARIDOSIS 5), 1057

SCHUERMANN-SCHMORL DISEASE, 1381-1383

SCHMORL TYPE ADOLESCENT RYTHOIS 1381*

SCHOENLEIN-HENOCH SYNDROME, 669

SCHULLER-CHRISTIAN DISEASE, 94* 382

SCIATIC NOTCHES with sclerotic edges, 727*

SCIMITAR SYNDROME 507

SCLERODERMA lungs in 384

SCLEROSIS (es)
 bone 965
 calcaneus and 919* 920* 963*
 epiphysis of 1171
 in coxa plana, 1155*

- diaphyseal hereditary multiple 1066
 forearm, 1066*
 humerus 963*
 multiple focal irregular 1178
 in osteomyelitis 1197* 1198
 in osteopetrosis 1036*
 tarda, 1038*
 patella stress 1174-1176
 phalanges
 ossification centers 1178-1179
 physiologic 899*
 Ribbing 1066
 in sarcoma, osteogenic 1252-1253
 of sciatic notch edges 727*
 of spongiosa, 961-963
 talus 1171
 tarsal 1170 1171
 scaphoid focal 1167-1169
 tibial epiphyseal stress sclerosis
 intercondylar spines 1176
 ossification center 1176
 tuberos 189*
 extremities in 1317
 kidney in 811*
 twin symmetrical focal, 39*
 ulna, 905*
 vertebra, 1388*
 hypoclia causing 1384*
 after lumbar puncture 1376*
- SCOLIOSIS**
 appendicitis and 706*
 congenital 1339*
 anomalies associated with 1358*
 in dwarfism, diastrophic 1019*
 habitual idiopathic 1383
 hemivertebra and 1362*
 lung hypoplasia and 315*
 structural idiopathic infantile 1359
 in syndrome of multiple anomalies 790*
- SCROTUM**
 gas in, and pneumoperitoneum 550*
 hydrocele meningomyelocele
 simulating 1365*
- SCUARY 82**
 healing 1241* 1242*
 overcalcification in 965*
 infantile 1237-1243
 advanced 1240*
 corner sign 1241*
 metaphyseal clefts in 1241*
 roentgen appearance 1239-1242
 successive changes in 1243*
- SEAT BELT INJURIES**
 distraction fracture from
 mechanism of 1375*
 spine in 1374*
 vertebra in lumbar 1374*
- SELLA TURCICA** in craniopharyngioma,
 193*
- SEMINIFEROUS TUBULES** dysgenesis
 1314
- SEPSIS** neonatal, adrenal calcification
 after 813*
- SEPTAL DEFECT**
 aorticopulmonary 494 495
 arteriography in retrograde left
 brachial, 495
 interatrial, 498*
 high 497
 ventricular 497-501 1433*
 effect of surgical management
 335*
 in Eisenmenger's syndrome 518*
- large 500*
 small 499*
 spontaneous transformation 500*
 spontaneous transformation to
 pulmonary hypertension 501*
- SEPTOTOMY** in transposition of great
 arteries thymus after 450*
- SEPTOSTOMY** balloon atrial in
 transposition of great vessels 511
- SEPTUM PELLUCIDUM** 158*
 absence of 169*
 cyst 157*
- SESAMOID** 904* 939 940
 bipartite normal 918*
 fractures (see Fractures sesamoids)
SEVER'S DISEASE 1171
- SEX**
 chromosomal pattern of XY XO 843*
 variable components of 823
- SEXUAL DEVELOPMENT** sequential
 changes in anatomy in 826*
- SEXUAL DIFFERENTIATION**
 errors studies utilized in evaluation
 of 824
 indicators
 primary (genetic) 824
 secondary 824
 tertiary 824 825
 normal 824
- SHINGLOSIS** 1289*
- SHOCK** causing pulmonary
 insufficiency 341
- SHOULDER**
 normal structures in 1327*
 ossification centers secondary 893*
 pneumography natural 1331*
- SHREWSBURY MARK** 985
- SHUNT**
 arteriovenous 1404
 left right effect of surgical
 managemen 333
 in transposition of great arteries 509*
- SICKLE CELL**
 anemia, 90*
 extremities in 1286 1288
 femur in 1287* 1288*
 fibula in 1286*
 hand in, 1289*
 humerus in 1287 1288
 osteitis and 1289
 technetium scan in 1429*
 vertebra in 1393
 hemoglobinopathy technetium scan
 in 1429*
- SICMOP**
 colitis 701*
 fecal impaction in 713*
 normal filling of intestinal glands in
 678
 polyp in 710*
 polyposis 710*
 stenosis 701*
 volvulus 680 681
- SILICOILLERS DISEASE** 371 372
- SILVER NITRATE** simulating meconium
 peritonitis 1575*
- SILVER'S SYNDROME**, 1075-1076
- SINUSES**
 craniocavernous fistula, 213
 ethmoid 110
 frontal 110
 maxillary (see Maxillary sinuses)
 paranasal (see Paranasal sinuses)
 sagittal venography 183*
- sphenoid 105*, 111
 in submentovertical projection
 106*
 sphenoparietal 30*-31*
 venous defects 497
- SINUSITIS** maxillary 106-110
- SINUS**
 anomalous 1501*
 inversus complete and dextrocardia,
 480*
- SKELTON**
 (See also Bone(s))
 changes in endocrinopathy 1299-
 1317
 dystrophy intrinsic generalized
 740-742
 fetal ossification centers in 887*
 maturation of 977-978
 acceleration generalized 977
 acceleration localized, 977-978
 retardation, in essential coxa plana,
 1150*
 retardation generalized 977
 retardation, localized 978
 pelvic normal 719
 retinoblastoma, 1278*
 rhabdomyosarcoma, embryonal
 metastatic 1280*-1281*
- SKIN**
 atrophy follicular 1322
 disease extremities in 1322-1325
- SKINFOLD**
 simulating pneumoperitoneum
 1588*
 simulating pneumothorax 1453*
- SKULL** 1-98
 after ACTH 1311*
 in adrenogenital syndrome 84*
 adult, compared with newborn 3*
 anatomy 3 6
 neonatal 3-6
 artifact 1590*
 in cretinism 84*
 development, 6-21
 dysplasia
 congenital 35-58
 fibrous 85-86
 in endocrine disease 82
 flattening acquired postural 69-70
 fractures (see Fractures skull)
 granuloma, eosinophilic 94-96
 growth, 6-21
 hyperostosis 83*
 infections 78-81
 lacunar in newborn 35 37*
 in Letterer-Siwe disease 1296*
 normal 3-35
 normal juvenile
 convolutional markings 21
 digital markings 21
 duplex markings 21 23
 normal variations 21
 roentgenographic appearance of
 21-35
 sutural bones 23, 32, 35
 sutures 23 32, 35
 vascular markings 21 23
 normal, newborn
 anteroposterior projection 8*
 lateral projection 5*
 posteroanterior projection 6*
 normal at six years 24*
 convolutional markings 26*
 normal, at three years 25*

SKULL (cont)

- normal at two years 22*
- in osteosclerosis 1067*
- benign familial idiopathic 1065*
- traumatic lesions 58-78
 - in newborn 58 70
- tumors of 96-98
- vessels 29*
- SLIPPING** of capital femoral epiphysis 1127-1129
- S L-O DWARFISM** 1076*
- SMALLPOX PNEUMONIA** 359
- SOAP BUBBLE RAREFACTION** of ramus and ischium 724*
- SOFT TISSUES**
 - of arm upper 847*
 - of extremities 847-872
 - of pelvis normal and abnormal, 718 719
 - perineal, in longitudinal section 754*
- SPASTIC FLAT FEET** congenital 981-986
- SPHENOID BONES** (see Bone(s) sphenoid)
- SPHENOID SINUSES** 105* 111
 - in submentovertical projection, 106*
- SPHENOPARIETAL SINUSES** 30*-31*
- SPINA BIFIDA**
 - cervical 240
 - hemivertebra and in newborn, 1361*
 - occulta, 1365
 - sacral, 729*
 - thoracolumbosacral 1365*
 - vara, sacral in syndrome of multiple anomalies 790*
- SPINA VENTROSA** 1202*
- SPINE**
 - abscess (see Abscess spine)
 - in achondroplasia, 1003* 1004*
 - anomalies
 - associated with other congenital anomalies 1368 1369
 - cervical, congenital 240 243
 - lymphangiomatous 1422*
 - in battered child syndrome 1141*
 - cervical 237-245
 - anomalies congenital, 240-243
 - infections 244
 - kyphosis and neurofibromatosis 245*
 - neoplasms 244-245
 - normal mobility 243*
 - rheumatoid arthritis of 1390* 1391
 - segmentation errors 242
 - traumatic lesions 243-244
- cord** 219-223
 - angioma, 221*
 - tumors of 1395-1396
 - in exostosis cartilaginous 1370*
 - fracture avulsion 744*
 - granuloma, eosinophilic 1393*
 - lumbosacral
 - double 1367*
 - meningomyelocele in newborn, 1365*
 - neuroblastoma, 1394* 1396*
 - normal, at 9 months, 739*
 - rhabdomyosarcoma, 1396*
 - sagittal section schematic drawing 1352*
 - in seat belt injuries 1374*
 - tuberculosis 1388*

SPINOUS PROCESS cystic dilatation 1261*

- SPRAYING** of long bones 1066-1071
- SPLIEN** 568 570
 - cyst (see Cyst(s) spleen)
 - in cystic fibrosis 572*
 - normal visualization 568*
 - scans 1429
 - in S C hemoglobinopathy and asplenia, 1429*
 - trauma, arteriography of 1408*
 - in tuberculosis 558*
 - venous drainage 626*
- SPLENOMEGALY**
 - esophageal varices in 600*
 - hypertensive gastric varicosities in 601*
- SPLENOPOCTOGRAPHY** in cirrhosis and varices 570*
- SPLIT NOTOCHORD SYNDROME** 219
- SPONDYLAESTHISIS** 1387
- SPONDYLITIS** tuberculous 1387 1391
- SPONDYLOEPHYSAL DYSPLASIA** (see Dysplasia, spondyloepiphyseal)
- SPONDYLOLISTHESIS** 737-740 1364*
 - in dwarfism, diastrophic 1369*
 - juvenile
 - early slight, 738*
 - late marked, 738*
 - above lumbosacral junction in cretinism 740*
 - Meyerding's classification, 739*
 - pars interarticular defect in 738*
 - second degree myelography of 222*
- SPONDYLOLYSIS**
 - pars interarticular defect in 738*
 - at 10 years 739*
- SPONDYLOMETAPHYSAL DYSOSTOSIS** 1007
- SPONGE** of head clamp as artifact 1583*
- SPONGIOSA**
 - central roentgen appearance of 876-879
 - peripheral roentgen appearance 879
 - sclerosis of 961 963
 - structural changes which cast transverse band shadows 972*
 - in vertebra thoracic 1352*
- SPOROTRICHOSIS** pulmonary 420
- SPOTTED BONES** 1059-1061
- SPRENGEL'S DEFORMITY** 277* 278*
- SQUAMOSA**
 - frontal fibrous dysplasia of 85*
 - occipital 30* 115*
 - flattening of 45*-46*
- STAGHORN CALCULI** 795*
- STAPHYLOCOCCAL INFECTION**
 - osteitis of femur 1165*
 - pneumatocele after 1469*
- STAPLE** from comic book as artifact, 1583*
- STEINMANN PIN** migration of 865*
- STENOSIS**
 - after anastomosis in esophageal atresia with tracheoesophageal fistula, 588*
 - anus 681* 682-684 1530*
 - aortic 495-497
 - subaortic 496
 - subaortic idiopathic hypertrophic 496
 - supraaortic 496*
 - supraaortic in idiopathic

hypercalcemia 495

- aqueductal
 - Arnold Chiari malformation and, 180*
- ventriculography of 175* 176* 177
- calcaneus and 919* 920* 963*
- colon in adenocarcinoma, 711*
- duodenal and Down's syndrome 1520*
- in enteritis regional, 667*
- esophagus 592*-593* 594*
- gastric hiatus hernia and 605*
- low ring 583*
- after lye ingestion 597*
- large intestine 681-682
- in Kennedy dwarf 1079*-1080*
- meatal 792-793 1552
- in girl, cinecystourethrography in 792*
- mitral congenital 508
- in mucopolysaccharidosis 1 1051*
- pulmonary 502* 503*
- artery branch 504*
- isolated 501 503
- peripheral and intrauterine rubella, 502
- solitary schematic drawings of different types 502*
- valvulotomy for thymus after 449*
- veins producing edema 506*
- pyloric infantile hypertrophic 614-619 1492-1494
- classic findings in 617*
- hemoperitoneum after pyloromyotomy in 618*
- incomplete pyloromyotomy in 618*
- morbid anatomic changes in 615*
- pyloric antrum contraction simulating 617*
- pyloric canal elongation in 616*
- ulcers and channel 618*
- rectum 681* 682 684 701*
- sigmoid 701*
- subaortic 496
- idiopathic hypertrophic 496
- trachea, 307*
- STERNUM** 267-270
 - clef, 269*
 - development 270*
 - in dysplasia, epiphyseal 1029*
 - kyphosis 270*
 - ossification patterns at different ages 268*
 - suprasternal bones in adult 268*
- STEROIDS** causing thymic atrophy 447* 448*
- STOMACH** 509-626
 - (See also Gastrointestinal)
 - air in, diagram showing localization of 1482*
 - anatomy normal 608* 609 611
 - anomalies congenital, 612 613
 - antrum, in granulomatous disease 620*
 - atresia, 613 614
 - bezoar food simulating 623*
 - cysts 595
 - diseases 611-626
 - duplication 612* 640*
 - complete embedded in gastric wall 613*
 - fatalous communication with pancreatic duct, 641*

incomplete 613*
 large intrathoracic 612*
 pylorography of 1494*
 esophagogastric junction structure of 582
 extragastric factors 624-626
 failure of rotation 613 614*
 fundus filling defects in 601*
 hernia
 diaphragmatic 619
 hiatus (see Hernia, hiatus gastric)
 book* normal 610*
 inflammation 620-621
 ingested materials 622-623*
 masses in newborn 1494-1495
 muscular defects 613
 neoplasms 622
 in newborn 1492-1495
 obstruction 1492-1494
 obstruction radiographic evaluation 1479-1483
 perforations 549*
 in newborn 1493* 1494
 roentgen appearance normal 609
 shift of gaseous and liquid contents with position change 611*
 swallowed air normal distribution in newborn 578*
 thoracic partial 295* 604-607
 Thorotrast in in aborted fetus 1438*
 ulcer 622
 perforated prepyloric 549*
 varices 625 628
 splenoportography in 570*
 varicosities in hypertensive splenomegaly 601*
 venous drainage 628*
 wall incomplete rupture 1493*
STONE (see Calculi)
"STRAIGHT BACK SYNDROME" 249-250
480
STREPTOCOCCIC PLEURISY 389*
STRESS
 compression
 epiphysis of calcaneus 1171
 talus bones 1171
 tarsal bones 1170-1171
 tarsal scaphoid 1167-1169
 tibia, proximal end 1172-1175*
 deformities
 of epiphyses round bones and metaphyses 1148 1185
 sites of 1149*
 effects of electrical potential in bone 1082
 fractures (see Fractures stress)
 lines of Park (see Transverse lines of Park)
 sclerosis (see under Sclerosis)
STRIDOR and pulmonary artery sling 487*
"STRIP DEFECT" in ramus 727*
STURGE WEBER SYNDROME 213-214
calcification in 134*
STYLOID PROCESS
 calcifications physiologic 229-230
 ossification centers in shaft 229*
SUBACROMIOID SPACES anatomy 160-163
SUBCLAVIAN ARTERY (see Arteries subclavian)
SUBDURAL AIR, 163-166
 during pneumoencephalography 164*

SULCI 160-163
 age-dependent differences in 161*
 superimposition of 30*
SULFATURIA, CHONDROITIN B 1057
 heparatin and 1055
SUPRACONDYLAR PROCESS 910*
SUPRANAVICULAR, 923*
SWALLOWING
 disorders of 585-587
 esophageal lumen during 584*
 nasopharynx after barium study of 585*
 problems 1489*
SYMPATHICOBLASTOMA (see Neuroblastoma)
SYMPHYSEAL ANGIOSIS 985*
SYMPHYSEAL 1326
 pubis in bladder exstrophy 731*
SYNARTHROSES 1326
SYNCHONDROSIS 1326
 cerebellar Towne projection 16*
 ischiopubic (see Ischiopubic synchondrosis)
 metatarsal 914*
 neurocentral 1355*
 normal 34*
 of olecranon 906*
 sphenoid bone 120
 talus 922*
SYNDACTYL in Ellis Van Creveld syndrome 1010
SYNDESMOSSES 1326
SYNOSTOSIS
 premature
 calvaria 41* 43
 coronal suture 40* 4*
 sagittal suture 40* 4*
 radioulnar 984*
 sagittal suture 147
SYNOVITIS hip transition 1333*-1334
SYNOVIUM in rheumatoid arthritis 1338*
SYPHILIS
 cranium in 79 80 81
 infantile 1204 1209
 diagnosis 1208
 diaphysitis in 1206 1208 1209*
 healing 1208
 metaphysitis in 1205 1206
 roentgen appearance 1205
 small bones in 1208
 juvenile 1208 1209
 osteitis in B1*
 overcalcification and 965*
 parosteitis 1205*
 parietal bone in 80*
 vertebrae in 1391

T

TACHYCARDIA cardiomegaly and pleural effusion, 475*
TACHYPNEA transient, of newborn, 1444-1445
TALIPES EQUINOVARUS 988
 in dwarfism diastrophic 1019*
TALONAVICULAR COALITION congenital 984*
TALUS 922-924
 in flatfoot 1190*-1191*
 fractures stress 1185*
 lesions 1184
 ossification center 922*

double 924*
 in osteochondrosis dissecans 1185*
 plantar flexion in flatfoot 987*
 roughening of superior edge
 facituous 924*
 stress compression 1171
 sustentaculum 921*
 synchondrosis 922*
 vertical congenital 986*
TARSAL BONES
 anatomic variations 918-922
 in flat foot, 986*
 fractures 1108-1111
 navicular 924 925*
 ossification centers in appearance of 879*
 scaphoid (see Scaphoid tarsal)
 stress compression 1170-1171
TARSOEPHYPHYSEAL ACLASIS 1030*
TECHNETIUM 984M
 in Eagle-Barrett syndrome 1431*
 1540*
 of S-C hemoglobinopathy and asplenia 1429*
TEETH
 dysplasia in Ellis Van Creveld syndrome 1016*
 eruption and calcification schematic representation 122*
 in mucopolysaccharidosis 1 1046*
TELANGECTASIA (see Ataxia telangiectasia)
TELORADIOGRAPHY in cardiopulmonary index measurements 472*
TEMPORAL BONES (see Bone(s) temporal)
TEMPOROMANDIBULAR JOINT normal 123*
TENDON
 Achilles (see Achilles tendon)
 quadriceps laceration 1333*
TERATOMA
 cervical in newborn 1441*
 cranial 137*
 hydronephrosis and 835*
 kidney in 811*
 mediastinum 439*
 ovarian, cystic 834*
 pineal 195*
 retroperitoneal 811
 in newborn 1563* 1564
 sacrococcygeal
 in newborn 1565*
 pyelography in 1403*
 testes 843*
TESTES
 in groin, and hypospadias 831*
 in hydrocele 551*
 teratoma 843*
 underfunction causing skeletal changes 1312
TETANUS vertebral fractures and compression deformities due to 1373*
TETANY calcium gluconate for in newborn 863*
TETRAD OF FALLOT (see Fallot's tetrad)
TETRALOGY OF FALLOT (see Fallot's tetrad)
THEMANN'S DISEASE 1178-1179
 differential diagnosis 1083
THIGH
 abscess 849*

- THIGH (cont.)**
 edema of 849*
 lipoma of 850*
 pencil in 1573*
 phosphorus bands in bones 721*
- THORAX 247-457**
 cardiothoracic index 470 473
 in chondrodysplasia calcificans congenita 1010*
 cross-sections of 304*
 in Ellis Van Creveld syndrome 1017*
 emphysematous chest 254* 255
 in enchondromatosis 1027*
 external contour 249 257
 external deformities 249
 floor (see Diaphragm)
 funnel chest 250*-253*
 in Hodgkin's disease 435*
 hourglass chest 252-255
 in Marfan's syndrome 254*
 nasogastric tube in place in 565*
 in newborn 1436-1477
 surgical conditions of 1459-1477
 paralytic chest 252-255
 pathologic changes 305-401
 rachitic chest 255
 morbid changes in 256*
 in rhabdomyosarcoma, embryonal 1280*
 thoracic stomach partial 295*
 in tracheoesophageal fistula 590*
 wall 253-269
 atrophy 265*
 bones 267-285
 hematoma traumatic 265*
 hypoplasia 264*
 manubria superimposed on 261*-262*
 normal posterior 267*
 normal retrosternal shadow 263*
 normal shadows of axillary folds 259*
 soft tissue 258-267
 superimpositions resembling pneumothorax 259*
- THORN INDUCED TUMOR of fibula 1266***
- THOROTRAB in aborted fetus 1438***
- THROMBOEMBOLISM portal vein calcified in newborn 1536***
- THROMBOPHLEBITIS and venous insufficiency in legs 861**
- THROMBOSIS**
 aortic umbilical aortography in 1413*
 jaundice due to 1537*
 renal vein 1558* 1559
 pyelography in 1545* 1558*
 total body opacification in 1402*
- THROMBOSIS IN VENA CAVA**
 urinary tract infection and 556*
 in Wilms tumor 1418*
- THUMB**
 absence of congenital 990*
 fractures 1085*
- THYMOMA 456***
- THYMUS 443-457**
 anatomy normal 443 452
 atrophy 445*
 after pneumonia in newborn 446*
 steroid provoked 447*-448*
 cardiomegaly and 451*
 changes during respiratory cycle 453*
 cysts 456
- after Fallot's tetrad surgery 448*
 fusion of thymic and cardiac images to suggest cardiomegaly 470*
 granuloma, eosinophilic 363*
 increase during body weight increase 450*
 inflammations 456
 mediastinal shadow variations due to 452*
 neoplasms 456
 normal 454*
 in lateral projection 453*
 position variations 444*
 after pulmonary stenosis valvulotomy 449*
 after radiotherapy 455*
 after respiratory infection 445*
 shape variations 444*
 size
 sex and 452
 variations in 444*
 transposition of great arteries after septectomy 450*
 wave sign 434*
- THYROID**
 cartilage calcification in 229*
 cyst branchial cleft 1423*
 disease skull in 82
 scan (see Scanning thyroid)
 skeletal changes due to 1299-1303
- TIBIA**
 absence 1364*
 in achondroplasia, 1000* 1001*
 anatomic variations
 distal end 928-932
 proximal end 932 940
 in anemia Cooley's 1283*
 anterior process
 irregular ossification 935*
 size and configuration normal variations 935*
 aplasia 989
 in arthritis rheumatoid 1340*
 1343* 1344*
 in battered child syndrome 1141*
 bowing of prenatally 995* 996* 997*
 998*
 in bowleg 1189*
 in Brodie's abscess 1197*
 "bucket handle deformity 1137* 1138*
 chondroblastoma benign 1259*
 chondroma, 1257*
 in chondromatosis Oliver's 1024*
 confusion of neonatal, 1143*
 cortical defect 936* 937* 952*
 benign 950*
 cortical wall thickening 934*
 in cretinism 1301*
 in diaphysis apylitic 1209*
 in dysplasia
 epiphyseal 1029*
 fibrous 993* 1265*
 in Ellis Van Creveld syndrome 1016*
 epiphysis
 intercondylar spines stress fracture and sclerosis 1176
 ossification center stress sclerosis of 1176
 exostosis 938*
 cartilaginous 1023*
 fibroma, nonossifying 1266*
 fibromatosis 1275*
- fractures (see Fractures tibia)
 growth
 with advancing age 885*
 progressive stages in 880*
 hemangiomas 1271*
 in hyperostosis cortical infantile 1219*
 hypoplasia 989 1364*
 in hypothyroidism 1301*
 in knock knee 1190*
 laceration of cartilage plate 1111 1112* 1115*
 longitudinal section of 875*
 malleolus of 928* 929* 933*
 metaphyseal defect 938*
 multiloculated defects 954*
 neuroblastoma 1253*
 neurofibromatosis of 1270*
 notch in
 anterior surface shadow of 933*
 normal fibular 930*
 in Osgood Schlatter lesion, 1168*-1170*
 ossification centers 933*
 deformity 889*
 osteochondrosis 746*
 in osteodysplasia fibrosa 1061*
 in osteogenesis imperfecta 1039* 1043*
 osteoma, osteoid 1262* 1263*
 in osteomyelitis 1193*
 in osteopetrosis 1036*
 in exostosis 1309*
 in panarthrosis hemophilic 1295*
 proximal end stress compression 1172 1175*
 psudarthrosis congenital 983*
 in Pyle's disease 1068*
 rarefaction of intercondylar spine 939*
 in rickets 1225* 1227*
 in rubella syndrome 1210*
 sarcoma
 Ewing's 1269*
 osteogenic 1253*
 reticulum cell 1278*
 sclerosis (see Sclerosis tibial epiphyseal)
 in scurvy 1241* 1242*
 shaft
 constriction failure 968*
 cortical defect in 934*
 transverse lines of Park, 969*
 tenon of mortise of 930*
 transverse line of Park in incomplete 970*
 in tuberculous epiphysitis 1200*
 in tuberculous metaphysitis 1200*
 tunnels through cortical wall 931*
 in Turner's syndrome 1314*
 undercalcification in celiac disease 964*
 vara Blount's 1172-1175*
 in vitamin A poisoning 1247*
- TIEZKE'S SYNDROME 285**
- TISSUES (see Soft tissues)**
- TODDLER'S FRACTURE 1119*-1120***
- TOE**
 amputation incomplete congenital 992*
 fractures false 913* 915*
 great, 913*
 frontal projection 913* 914*
 ossification centers 915*

- ossification centers 917*
in Rubenstein Taybi dwarfism 1077*–1078*
- TOMOGRAPHY** artifacts in 1588 1589*
- TONGUE** in orodigitofacial syndrome 1316*
- TONSILS PALATINE**
enlarged 232* 233*
hypertrophic 227*
obstructive 232*
- TORTICOLLIS** muscular 230
- TORUS FRACTURES** (see *Fractures torus*)
- TOTAL BODY OSMIFICATION** in newborn 1399–1403
- TOWNE PROJECTION**
cerebellar synchondrosis 16*
in mastoiditis 117*
- TOXOPLOSMIC ENCEPHALITIS** 136*, 137*
calcification in 135*
- TRACHEA** 235–237
agenesis 1442*
anomalies congenital, 305
in aortic arch anomalies 1471
calcification 308*
compression, 1470–1477
defects due to aorta, 485*
by ectopic arteries 308*
in innominate artery compression 1473 1476*
- narrow** comparison with tracheomalacia, 1440*
normal, 297 1471*
pathologic changes 305–308
in pulmonary artery anomalies 1471–1477
stenosis 307*
- TRACHEAL BRONCHUS** 307*
- TRACHEOBILARY FISTULA** 566*
- TRACHEOBRONCHIAL BRANCHES** 299*
- TRACHEOBRONCHOMEGALY** 305–307*
- TRACHEOESOPHAGEAL FISTULA** (see *Fistula tracheoesophageal*)
- TRACHEOGRAPHY** of aortic arch 483*
- TRACHEOMALACIA** comparison with narrow trachea, 1440*
- TRACHEOTOMY** mediastinal emphysema after 432*
- TRAMPOLINE INJURY** disk space loss after 1376*
- TRANSFUSION INTRAUTERINE**
effects of 1478*
radiography during 1437*
rectum after 1479*
- TRANSILLUMINATION** 1547
- TRANSPLANTATION** heart, changes after 536* 537
- TRANSPOSITION**
of great arteries (see *Arteries great, transposition*)
of great vessels (see *Vessels great, transposition*)
- TRANSVERSE LINES OF DIMINISHED DENSITY** 976
- TRANSVERSE LINES OF PARK** 969–972
generation of 971*
3-dimensional view of 970*
- TRAUMA**
arteriography and 1407–1408
in evulsion of ossification centers 1170
cartilage plate (see *Cartilage plate injuries*)
- cortical thickenings 1129–1131
cupping of metaphyses 1129 1131*
disks 1376–1377
electrical to bone 1082
hematoma
of duodenal wall 660*
of thoracic wall 265*
hemihypoplasia, cerebral 206*
in hip arthritis 1335*
hip dislocation due to 734*
intestinal obstruction due to 661
joint changes due to 1332–1333
kidney 798–800
lungs 339–340
in myositis ossificans 859 860
in Osgood Schlatter lesion 1168*–1170*
parent infant trauma syndrome 1132–1148
pseudocyst of pancreas 1320
pulmonary insufficiency due to 341
spine cervical 243–244
spleen, arteriography of 1408*
splenic cyst after 569*
vertebra 1372–1384
- TRACHER COLLINS MANDIBULAR FACIAL DYSOSTOSIS** 48 49
- TREVOY'S DISEASE** 1030*
- TRIAD SYNDROME** (see *Eagle-Bairdett syndrome*)
- TRIANGULARIS** fusion with lunate 900*
- TRICEPS MUSCLE** defect in head of 867*
- TRICHOZOAR** 623*
anemia and 624*
- TRICHOHINOPHALANGIAL SYNDROME** 1013–1014
facies in 1013*
phalanges in 1013*
- TRICUSPID VALVE** 528
atresia 515* 516
disease combined with mitral disease 525*
Ebstein's anomaly 518 520
- TRIGONAL CYSTS** 784
- TRIGONOCYPHALY** 50 52
in newborn, 51*
- TRISOMY**
13–15 1315
holoprosencephaly and alobar 207*
16 18 1314–1315
autosomal 1314
D 1315
E 1314–1315
- TROCHANTER OF FEMUR**
avulsion 1126* 1170*
fracture 1125*
fragmentation 1170*
normal irregularities in density 957*
- TROCHLEA** 907*
ossification center 906*
- TRUNCUS ARTERIOSUS** 520 521*
calvaria in 93*
- TUBER CINERUM** 183*
hamartoma of 189*
- TUBERCULOMA** cerebral 134*
- TUBERCULOSIS**
abscess in
abdominal wall 546*
paraspinal 1389*
bone in, 1199–1202
calcification in
lymph node 230*
- pulmonary 408*, 410*
pulmonary BCG vaccine and 418 419*
calvaria in 79*
ileocecal, 670*
intestine small 670
joints 1336–1337
liver in 558*
lymph nodes 230*
myocardium
pneumopneumocardiography in 531
pericardium in 529 531*
pleura, 412*
pneumonia and 408*
pulmonary primary 402–418
anatomic changes in 402–406
atelectasis in 403*
atelectasis in obstructive 413*
bronchial lesions in 404*
in bronchial wall 403*
bronchiectasis in, compensatory 413*
bronchogenic spread 416*
calcification in (see *calcification in above*)
diagnostic value of roentgen exam 416
emphysema in obstructive 413*
entry portal 402
extrapulmonary primary foci, 418
healing patterns in 410*
hematogenous spread 417–418
hypertrophy of lymph nodes and mediastinum in 409*
lateral projection in value of 415*–416*
local complications 418–417
lymph nodes in 419*
lymphogenic spread 405*
pleurisy and 411*
primary focus position of 402
primary tuberculous complex 402
primary tuberculous complex
schematic drawings of components of 405*
primary tuberculous complex, schematic representation, 403*
roentgen appearance 406–416
spine 1388*
spleen in 558*
urinary 804
vertebra 1388* 1389*
- TUBERCULOUS**
arthritis 1337
joints in 1202
diaphysitis 1201* 1202
enteritis 670*
epiphysitis 1200*
lymph nodes calcifying 576*–577*
metaphysitis 1200*
osteitis of ischium 747*
spondylitis 1387–1391
- TUBEROUS SCLEROSIS** (see *Sclerosis tuberosus*)
- TUBULAR BONES** (see *Bone(s) tubular*)
- TURULUM** 966 969
- TUMORAL CALCINOSIS** 1346*–1347*
- TUMORS**
abdomen, solid venacavography 1413
adrenal (see *Adrenal(s) tumors*)
bone
of extremities (see *of extremities below*)

TUMORS (cont.)

- foreign body 1267
 - giant cell 1265-1266
 - brain calvaria in 148*
 - bronchi 314
 - Burkitt's mandible in 126-127
 - cerebellum 139*
 - cranium 149-150 188-196
 - esophagus cervical 234 235
 - of extremities
 - bone 1249-1279
 - malignant nonosteogenic 1267-1279
 - neural 1268
 - of soft tissues 850-851
 - fibula (thorn induced) 1266*
 - genital tract 833 835
 - genitalia 805-812
 - secondary 811
 - genitourinary 805 812
 - mucosal epithelial 811
 - secondary 811
 - heart 532
 - humeral giant cell 1265*
 - intestine small 873
 - intracranial 188-196
 - joints 1348
 - kidney in newborn 1561-1565
 - liver arteriography in, 1407
 - lung 374-378
 - malignant (see specific types)
 - mandible 125-128
 - mediastinum 434-443
 - nose 101
 - pharynx 234-235
 - pleura 399 401
 - retroperitoneal 1564
 - solid lymphangiography in 1419
 - skull 96 98
 - spine
 - cervical 244-245
 - cord 1395 1398
 - stomach 822
 - subtentorial 139*
 - thymus 456
 - urinary tract (see genitourinary above)
 - vertebra, 1395 1396
 - Wilms (see Wilms tumor)
- TURNER'S SYNDROME
- skeletal changes due to 1312-1314
 - tibia in 1314*

U

ULCER

- channel and pyloric stenosis 618*
 - duodenal 621* 622
 - esophagus 603-604 606*
 - gastric 622
 - perforated prepyloric 549*
 - peptic 621*
- ULCERATIVE COLITIS (see Colitis ulcerative)

ULCERATIVE PROCTITIS 701*

ULNA

- in achondroplasia 1000*-1001*
- in arthritis rheumatoid 1342* 1344*
- cartilage of 903*
- in chondromatosis
 - external 1022*
 - Oliver's 1024*
- contusion infantile 1144*
- cyst aneurysmal 1259*

- in diaphysitis syphilitic 1207*
 - dimelia 989-991
 - in Ellis-Van Creveld syndrome 1018*
 - in erythroblastosis fetalis 1282*
 - fractures (see Fractures ulna)
 - in hyperostosis cortical infantile 1214* 1216* 1220*
 - in hyperparathyroidism 1305*
 - in insensitivity to pain congenital 1135*
 - lymphangioma 1273*
 - in melorheostosis 1060*
 - metaphysis physiologic wavy irregularities in, 903*
 - in mucopolysaccharidosis I 1054*
 - nutrient canal in 878* 905*
 - osteoma osteoid 1263*
 - in osteomyelitis 1193*
 - overcontraction after poliomyelitis 968*
 - in phenylketonuria, 1319*
 - in Pyle's disease 1068*
 - sarcoma Ewing's 1269*
 - sclerosis 905*
 - synostosis 984*
 - in vitamin A poisoning 1245*
- ULTRASOUND
- in hydronephrosis 1546*
 - newborn and 1431
 - urinary tract 770
 - in Wilms tumor 1546*
- UMBILICAL
- angiography 1408-1413 1547
 - aortography (see Aortography umbilical)
 - arteriovenous fistula, 1410-1412
 - catheterization, safety of 1412-1413
 - lesions 543-545
 - transection obstetric 1440*
 - vein injections 1408
- UMBILICUS
- buzzing belly button, 1412*
- UNDERCIFICATION
- focal 965-966
 - generalized 964 965
- UNDERCONSTRUCTION 966*-967
- UNDERGROWTH
- generalized 976
 - localized 977
- URACIUS
- anomalies congenital, 782
 - cyst, 782*
 - patency of 782*
- UREMIA
- lungs in 370
- URETER
- anatomy normal, 756
 - anomalies congenital, 777-782
 - dilatation
 - in Hutch diverticulum, 783*
 - in posterior urethral valves 791*
 - diverticulum in pyuria, 779*
 - duplications of 778*
 - diverticulumlike 779*
 - "wilted flower" appearance in, 779*
 - ectopia in vas deferens 780*
 - fibrosis 789
 - jet phenomenon" in urography and 764*
 - obstruction, 788-789
 - in syndrome of multiple anomalies 771*
 - shadow in excretory urography 798*
 - urography of excretory 758*

- URETERECTASIS 767* 789
 - URETERITIS 804
 - cystica 804
 - URETEROCLE 1551
 - ascites and in newborn 1550*
 - ectopic 1550*
 - diagram of 780*
 - stimulating gas in rectum 781*
 - pyelography in 1545*
 - URETEROPELVIC JUNCTION
 - indentation at deep localized, 788*
 - obstruction at 785-788
 - URETEROPELVIC OBSTRUCTION 1544* 1568*
 - stone causing 797*
 - total body opacification in in newborn 1402*
 - URETEROSTOMY teratoma and hydronephrosis 835*
 - URETEROVESICULAR JUNCTION
 - diagram of 756*
- URETHRA
- anatomy normal, 758-757
 - anomalies congenital, 784 785
 - dilation in meatal stenosis 792*
 - diverticulum 784*
 - in newborn 1553*
 - duplication 784*
 - normal mucosal folds in male 791*
 - obliterations congenital 790
 - obstruction, 784* 790-793
 - anterior 1552
 - in newborn, 1551-1554
 - orifice at base of phallus and hypospadias 831*
 - polyps 790
 - rectourethral fistula 1525* 1528* 1544*
 - valves 1551-1552
 - pneumomediastinum and 1553*
 - posterior 783* 790 1551-1552 1568*
 - variations in, normal, 757*
- URETHROGRAPHY
- retrograde Lucaya technic 789*
 - voiding 765*
 - in abdominal muscle congenital absence 794*
 - diverticulum of urethra, 784*
 - erect lateral position for 765*
 - normal 765*
 - in posterior urethral valves 791*
- URINARY CALCULI 795 798
- URINARY INFECTIONS 800-805
- serial studies in 803*
- URINARY OBSTRUCTION 785 793
- at different levels roentgen appearance 785-793
 - schematic representation of obstructions 786*
 - at ureteropelvic junction, 785-788
- URINARY TRACT 753-812
- anatomy normal 753 757
 - anomalies congenital, 770 785
 - aortography 769-770
 - dilatation, and abdominal wall hypoplasia, 544
 - fetal radiographic visualization, 1539 1542
 - infection
 - reflux and 1547-1548
 - vena caval thrombus and 556*
 - in newborn, 1539-1570
 - obstruction

- prenatal 1566
schematic representation 786*
roentgen appearance normal 757-770
tumors (see Tumors genitourinary) ultrasound 770
- URINARY TUBERCULOSIS 804
- URINE transport of 759-760
- UROGENITAL SINUS in female
pseudohernaphroditism 817*
- UROGRAPHY 1542
excretory
of abdomen 542*
in abdominal muscle congenital absence 794*
calyceal diverticulum 777*
collimator in 762*
in diverticulumlike duplication of ureter 779*
Hutch diverticulum of bladder 783*
jet phenomenon during 764*
liquids after contrast material 763*
normal 758*-766
in prone position 764*
after renal laceration surgery 799*
stone in renal pelvis 797*
in supine position 764*
ureteral ectopia in vas deferens 780*
ureteral shadow 798*
intravenous reaction to 765*
retrograde 768-769
- UROGRAPHY neurogenic in syndrome of multiple anomalies 790*
- UROGRAPHIC PROCEDURES in newborn 1542-1547
- URTICARIA
pigmentosa, 1324* 1325
after urography 765*
- UVULA axial projection simulating pharyngeal foreign body 1575*

V

- VAGINA
cloth and drinking straw in 832*
constriction in bladder exstrophy 843*
enlargement due to estrogen 1556*
fecaloid discharge after pull through of rectum 838*
foreign body cystourethrography of 822*
giant, 1527* 1556*
marble in 832*
menstrual absorbent image 719*
obstruction 1556-1557
- VAGINITIS 832 833
- VAGINOGRAPHY 822-823
demonstrating cloth and drinking straw 832*
in female pseudohernaphroditism 817*
- VALVES
aortic (see Aortic valve)
ileocecal (see Ileocecal valve)
mitral (see Mitral valve)
multiple lesions 528
pulmonary (see Pulmonary valve)
tricuspid (see Tricuspid valve)
urethral (see Urethra valves)
- VALVULOTOMY in pulmonary stenosis
thymus after 449*
- VARICELLA pneumonia 356*
- VARICES
esophageal 600
splenoportography in 570*
gastric 625-626
splenoportography in 570*
- VARIOSITIES
in foot and phlebotomy 862*
gastric in hypertensive splenomegaly 601*
- VAS DEFERENS ureteral ectopia in 780*
- VASTUS INTERMEDIUS fibrosis of 859
- VEINS
anomalies total anomalous venous return 1458*
azygos arch of 426-428
brain anomalies 212-213
duplex 22*
space 27*
spider 27*
emissary 115*
esophageal 626*
of Galen aneurysm 215 216
insufficiency in legs 861
portal
gas in liver 557*
preduodenal and midgut malrotation 650*
thromboembolism in newborn 1536*
- pulmonary
anomalies (see Anomalies pulmonary venous return)
common atresia 506
stenosis causing edema 506*
renal (see Thrombosis renal vein)
spleen 626*
stellate 27*
stomach 626*
umbilical injections 1408
- VENA CAVA
anomalies benign 1413 1418
in ganglioma, 1416*
inferior
convergence with aorta in asplenia, 481
thrombus of (see Thrombus in vena cava)
left superior and anomalous pulmonary venous return 506
obstruction pyelography in, 1414*
- VENACAVOGRAPHY
ganglioma, 1415*
inferior in newborn 1413 1419
- VENOGRAPHY
hemangioma, hepatic 1409*
sagittal sinus 183*
umbilical 1408-1410
- VENTILATION positive pressure in respiratory distress syndrome 1448*
- VENTRICLES
anomalies angiocardiography of 1425*
atrioventricular canal 499*
brain (see Brain ventricles)
left
dilatation 479
diverticulum 509
hypertrophy 479
puncture choroid plexus injury due to 166*
right
double outlet 501 516 518
- ventriculoarterial communication with coronary sinus 493*
septal defects (see Septal defect ventricular)
single 520
hypoxia due to 1384*
- VENTRICULOGRAPHY
in Canavan's spongy degeneration 185*
contrast 166-167
papilloma, choroid plexus 192*
potencephaly after 165*
in pseudotumor cerebri 183*
in stenosis aqueductal 175* 176*-177
- VERTEBRA 1349-1396
in achondroplasia, 1369
after ACTH in rheumatoid arthritis 1310*
anatomy normal 1351-1352
in anemia, 1393
anomalies congenital 1358-1369
bodies
butterfly deformity 1363*
compression deformities due to tetanus 1373*
coronal cleft 1362 1364*
defects at L-3 L-4 and L-5 1363*
destruction of L-3 and L-4 after high chair fall 1382*
hypoplasia, 1358*
cervical
developmental components 236*-239*
hypoplasia and fusion of 242*
sixth elongation of tubercle 244*
in chondrodystrophy calcific congenita, 1010*
column 443 1349-1396
in Cushing's syndrome 1392-1393
cysts 1395
aneurysmal, 1260*
development normal 1352-1355
developmental errors
in chondrodystrophy stage 1360*
in ossification stage 1360*
diseases involving 1387-1396
disks (see Disks)
dislocations 1372
in dysplasia
epiphyseal 1029*
systemic 1369-1371
endocrine disorders and 1392-1393
form variations in, 1359
fractures (see Fractures vertebrae)
in gargoyle 1371*
growth
normal 1352-1355
traumatic disorders 1377-1384
in hyperparathyroidism 1393
in hypothyroidism, 1392*
in hypovitaminoses 1391
infections and 1387-1391
L-5 separate neural arch in 1364*
in leukemia, 1393-1395
lumbar in seat belt injuries 1374*
marginal line 1392
in mucopolysaccharidosis 1369
1 1051* 1052*
in neuroblastoma, 1394*
normal, 1351-1357
ossification centers
primary 1353-1354
secondary 1354*-1355

VERTEBRA (cont.)

- in osteogenesis imperfecta, 1370
 - 1371*
 - osteolysis 1274*
 - osteoma osteoid 1394*
 - in osteopetrosis 1370-1371
 - plana Calve 1377-1380
 - in C 4 1379*
 - complete healing of 1380*
 - in D 9 1378*
 - in T 9 1379*
 - in Pyle's disease 1069*
 - reticulosis and 1393
 - rhabdomyosarcoma 1281*
 - roentgen appearance 1355-1357
 - at 1 year 1356*
 - at 14 years 1356*
 - at birth 1355*
 - sacralization of 728*
 - sclerosis (see Sclerosis vertebra)
 - in syphilis 1391
 - thoracic
 - normal 1351*
 - spongiosa in 1352*
 - trauma, 1372-1384
 - tuberculosis 1388* 1389*
 - tumors 1395-1396
 - in urticaria pigmentosa 1324*
- VERUMONTANUM hypertrophy 790
- VESICAL (see Bladder)
- VESSELS
- abdominal 556
 - adrenal disturbances in newborn 1557-1559
 - brain anomalies 212-219
 - calcifications in extremities 862
 - cerebral Moyamoya disease 217*
 - great
 - anomalies congenital intrinsic 483-524
 - normal surface projection 461*
 - great transposition 509-513
 - corrected 501 512-513 1433*
 - corrected angiocardigraphy in 512*
 - septostomy in, balloon atrial 511
 - ventricular septal defect and 500*
 - kidney disturbances in newborn 1557-1559
 - lesions simulating pulmonary disease 1457-1459
 - mesentery occlusion 666-667
 - omphalomesenteric 543*
 - of pelvic bones normal markings 721*

- pulmonary 298
- congestion 479
- engorgement in
- glomerulonephritis 475*
- in heart congenital anomalies 479
- ring 484 1470-1477
- skull 99*
- water density shadows cast by in subcutaneous fat 846*

VIRUSES

- osteitis due to 1203-1204
- pneumonia due to 355*
- respiratory syncytial virus 359-360

VISCERAL LARVA MIGRANS 81

- liver calcification in 559*
- parietal bone in, 81*

VITAMIN

- A poisoning 1244-1247

C

- poisoning 1248-1249
- vertebra and 1391

D

- poisoning 1247-1248
- vertebra and 1391

K 82

VOLVULUS 680-681

- cecum 680
- duodenal obstruction due to
- complete 654*
- incomplete 654*
- ileum 650*
- midgut 647* 649* 1501*
- in newborn 647* 1495-1499
- prenatal 1507 1508*
- sigmoid 680-681

W

WAARDENBERG'S SYNDROME 53

WATER

- density shadows of vessels in subcutaneous fat 846*

pulmonary reactions to 370

WEARDING-HOFFMANN MYOPATHY 870*-871*

WEYERS MANDIBULAR FACIAL

DYSOSTOSIS 124-125

WHIFFLE'S DISEASE duodenum and

jejunum in 634*

WHOOPING COUGH and

bronchopneumonia 359*

WILMS SARCOMA 252*

WILMS TUMOR 187* 805*-808

arteriography of in newborn 1403-

- 1404* 1407
 - A scan in 1432*
 - bilateral 805*
 - heart failure and congestive 1404*
 - lymphangiography in 1419
 - metastases
 - angiography of 1407*
 - lung 375* 376*
 - prognosis in 807
 - renal pelvis form variations in, 806*
 - thrombus in vena cava in 1416*
 - total body opacification in
 - newborn 1400*
 - ultrasound in 1546*
- WILSON'S DISEASE extremities in 1318-1319
- "WILTED-FLOWER" APPEARANCE in uteroperipelic duplication 779*
- "WINDSOCK" DIAPHRAGM 1500*
- WOLMAN'S DISEASE
- adrenal calcification in 815*
 - pyelography in 1561*
- WOOLMAN BONES 13*-14* 31*, 32* 33*
- ossification center in 11*

WRIST

- in arthritis
 - after bacteremia 1011*
 - rheumatoid 1344*
 - bones
 - anatomic variations 888-904
 - ossification centers extra and false 888-904
 - round disparity in maturation 889*
 - in dysostosis metaphyseal 1032*
 - hemangioma 862*
 - lymphangioma 1273*
 - in mucopolysaccharidosis I 1048*
 - ossification centers secondary 893* 898-904
 - in osteosclerosis 1066*
- WAYNECK 230

X

- XANTHOGRAULOMA juvenile 382 384
- XANTHOMATOSIS 94*
- cutis 1322
- X RAY (see Radiation)
- XY XO SEX CHROMOSOME PATTERN 843*

Z

- ZINC CHLORIDE necrotizing gastritis due to 620*